

İTÜ



BURSA
ULUDAĞ
ÜNİVERSİTESİ



BURSA TEKNİK
ÜNİVERSİTESİ



16 ULUSLARARASI LİF VE POLİMER ARAŞTIRMALARI SEMPOZYUMU

16th INTERNATIONAL FIBER AND POLYMER RESEARCH SYMPOSIUM

Sürdürülebilir ve İşlevsel Lif ve Polimerler
Sustainable and Functional Fibers & Polymers

9-10 Mayıs
May 2025

İstanbul Teknik Üniversitesi
Gümüşsuyu Prof. Dr. Necmettin Erbakan Yerleşkesi
Istanbul Technical University
Gumussuyu Prof. Dr. Necmettin Erbakan Campus



Book of Proceedings

www.ulpas.org



FIBER &
POLYMER
RESEARCH ASSOCIATION

ISBN: 978-975-561-665-0



LİF &
POLİMER
ARAřTIRMALARI DERNEđİ

16th International Fiber and Polymer Research Symposium
9-10 May, 2025, Istanbul Technical University – Istanbul – Türkiye

16. Uluslararası Lif ve Polimer Arařtırmaları Sempozyumu
9-10 Mayıs, 2025, İstanbul Teknik Üniversitesi, İstanbul,,Türkiye

Book of Proceedings

This printed book contains the full texts of the papers presented at the symposium.

Bu kitabın baskı versiyonu bildirilerin tam metinlerini içermektedir.

The pdf version of the Book of Proceedings can be downloaded from the website www.ulpas.org.

E-kitaba www.ulpas.org adresinden ulaşılabilir.

Istanbul Technical University (ITU)

May 2025 / Mayıs 2025

ISBN: 978-975-561-665-0

**16. ULUSLARARASI LİF VE POLİMER ARAŞTIRMALARI
SEMPOZYUMU (16. ULPAS) BİLDİRİLER KİTABI
(09-16 MAYIS 2025 İSTANBUL)**

Editörler, Yusuf Ulcay, Ali Demir, Ali Toptaş, Seyedmansour Bidoki, Aysu Çavuşoğlu
İstanbul, 2025

e-ISBN 978-975-561-665-0
İTÜ Yayınevi. No: 2025.2/18

© İTÜ Yayınevi

Bu kitabın her hakkı saklıdır ve tüm yayın hakları “İTÜ Yayınevi”ne aittir. Bu kitabın tamamı ya da herhangi bir bölümü, yayınevinin izni olmaksızın yayınlanamaz, basılamaz, mikrofilme çekilemez, doğrudan veya dolaylı olarak kullanılamaz. Teksir, fotokopi veya başka teknikle çoğaltılamaz, bilgisayarda veya dizgi makinelerinde işlenebilecek bir ortama aktarılamaz. Kitapta yayınlanan tüm metin ve görsellerin sorumluluğu yazar/yazarlara aittir.

Uluslararası Lif ve Polimer Araştırmaları Sempozyumu (16: 2025: İstanbul)
16. Uluslararası Lif ve Polimer Araştırmaları Sempozyumu (16. ULPAS) bildiriler kitabı (09-16 Mayıs 2025 – İstanbul) / editörler, Yusuf Ulcay ... [ve öte.]. -- İstanbul: İTÜ Yayınevi, 2025.
320 sayfa. -- (İTÜ Yayınevi. No: 2025.2/18)
Kaynakçalar vardır.
ISBN 978-975-561-665-0
1. Tekstil elyafı – Kongreler.
TS1540 .U48 2025

CIP

İTÜ YAYINEVİ

Sertifika No: 70051

İTÜ Ayazağa Kampüsü

Mustafa İnan Kütüphanesi
34469 Maslak İSTANBUL
0212 285 75 05

www.ituyayinevi.itu.edu.tr / ituyayinevi@itu.edu.tr





16th International Fiber and Polymer Research Symposium
9-10 May, 2025, Istanbul Technical University – Istanbul – Türkiye

16. Uluslararası Lif ve Polimer Araştırmaları Sempozyumu
9-10 Mayıs, 2025, İstanbul Teknik Üniversitesi, İstanbul,,Türkiye

Editors/ Editörler

Prof. Dr. Yusuf Ulcay
Prof. Dr. Ali Demir
Assist. Prof. Ali Toptaş
Assoc. Prof. Dr. Seyedmansour Bidoki
Aysu Çavuşoğlu

ISBN: 978-975-561-665-0

16th International Fiber and Polymer Research Symposium (on-site)
16. Uluslararası Lif ve Polimer Araştırmaları Sempozyumu (on-site)

9-10 May, 2025 / 9-10 Mayıs, 2025



Prof. Dr. Ali Demir

“Fifteen Symposia in Ten Years”

The title I have chosen for this foreword is “**Fifteen Symposia in Ten Years.**” This journey began in 2015 in Bursa, organized in collaboration with Bursa Uludağ University, BTSO, UTIB, and BUTEKOM, held alongside the Textile R&D Project Brokerage Event. What started as a complementary event has now grown into an independent, biannual international symposium, reaching its 16th event today.

I would like to extend my heartfelt thanks to everyone who contributed to these 16 symposia—especially to my dear colleague **Prof. Dr. Yusuf Ulcay**, with whom we envisioned this journey together. ULPAS was a dream we shared, and now we are realizing the 16th edition.

With each event, ULPAS has grown; in scope, in participation, and in impact. After holding it cities like Bursa, Istanbul, Eskişehir, Uşak, Yalova, Gebze, Bolu, and İzmir, we are once again back in **Istanbul, hosted by Istanbul Technical University**—a return that fills me with great pride and joy.

ULPAS is fundamentally a **thematic symposium**, a scientific marketplace where research findings in fibers—the fundamental building blocks of textiles—and polymers—the molecules that form them—are shared with the international community.

Alongside general congresses like:

- The **International Textile and Fashion Congress** hosted by our own faculty at ITU,
- The **International Textile and Ready-to-Wear Symposium** by Ege University,
- And the **National Çukurova Textile Congress** by Çukurova University,

It is essential—and delightful—to see more **thematic symposia** like:

- The **Technical Textiles Congress** hosted by Dokuz Eylül University, and

- The **International Fiber and Polymer Research Symposium (ULPAS)**

Such focused events encourage exchange of knowledge and experience, and serve as **an invaluable platform for young researchers to grow**. Personally, it excites me to watch Master's and PhD students presenting their work at ULPAS and seeing how they become more professional and go deeper in their research over time.

An essential and unique dimension of ULPAS is the **strong support from industry**. Since the very first symposium, the participation and interest from our industrial partners—especially R&D centers—has been inspiring. This engagement has come in the form of sponsorships and, more importantly, valuable research presentations. In this edition, **20 out of 50 presentations will come from Industrial R&D centers**.

Let me briefly take you through the **nine-year timeline of ULPAS**:

| | Date | Location | Main Sponsor |
|----------|----------------|----------------------|---------------------|
| 1.ULPAS | 13–14 May 2016 | BUTEKOM – Bursa | BTSO & UTIB |
| 2.ULPAS | 27–28 Apr 2017 | BUTEKOM – Bursa | BTSO & UTIB |
| 3.ULPAS | 8–9 Mar 2018 | BUTEKOM – Bursa | BTSO & UTIB |
| 4.ULPAS | 4–5 Oct 2018 | Uludağ University | Uludağ Univ. |
| 5.ULPAS | 3 May 2019 | ITU | ISTKA Project |
| 6.ULPAS | 24–25 Jan 2020 | Uludağ University | — |
| 7.ULPAS | 25–26 Sep 2020 | BTÜ – Online | — |
| 8.ULPAS | 18–19 Jun 2021 | ESOGU – Online | — |
| 9.ULPAS | 18–19 Nov 2021 | Uşak University | — |
| 10.ULPAS | 13–14 May 2022 | ITU | TÜBA & ITU |
| 11.ULPAS | 4–5 Nov 2022 | GTU | — |
| 12.ULPAS | 5–6 May 2023 | Yalova University | DOWAKSA |
| 13.ULPAS | 3–4 Nov 2023 | Bolu Abant İBÜ | SUPERLIT |
| 14.ULPAS | 24–25 May 2024 | BTÜ | — |
| 15.ULPAS | 8–9 Nov 2024 | İzmir Bakırçay Univ. | — |
| 16.ULPAS | 9–10 May 2025 | ITU | — |

Under the leadership of our Fiber and Polymer Research Platform and Symposium Organization Committee Chair, Prof. Dr. Yusuf Ulcay—who was also the Rector of Bursa Uludağ University at the time—the initial symposia held in 2016, 2017, and 2018 (on May 13–14, 2016; April 27–28, 2017; and March 8–9, 2018) took place at BUTEKOM in Bursa in parallel with the 8th, 9th, and 10th R&D and Project Market events. All expenses for these early symposia, including the travel and accommodation costs of researchers who presented papers or posters, were covered by UTIB and BTSO. Thanks to this support, the early symposia were vibrant and highly productive. The proceedings booklets were also printed by BUTEKOM. These efforts not only contributed to the national R&D Project Brokerage Event but also provided a platform to share fiber and polymer research with both the academic community and industry representatives.

The 4th ULPAS held independently of UTIB and BTSO on October 4–5, 2018, at Bursa Uludağ University, the 4th ULPAS was the second symposium of that year. It was highly successful, featuring industrial participation, visits to companies such as KORTEKS and POLYTEKS, and support for the travel and accommodation of international invited speakers. The proceedings booklet was published by Uludağ University.

On May 3, 2019, the 5th ULPAS was held as a one-day symposium at ITU's Gümüşsuyu Campus, in this very conference hall, with a focus on "Medical Textiles." The reason for this theme was the launch of the "MEDITEKS: R&D Center for Medical Textiles" project, supported by the Istanbul Development Agency (ISTKA), and managed by ITU's Faculty of Textile Technologies and Design, home to the "ITU TEMAG Laboratory" for over 30 years. The symposium was organized as part of the ISTKA project launch.

The 6th ULPAS took place on January 24–25, 2020, once again at Bursa Uludağ University. Bursa Technical University also joined the organizing efforts for this event.

The 7th and 8th ULPAS held in September 2020 and June 2021, respectively, both were conducted entirely on-line due to the COVID-19 pandemic.

On November 18–19, 2021, the 9th ULPAS was held for the first time post-pandemic as a hybrid event (both online and onsite) in Uşak. Strongly supported by the Rector of Uşak University, Prof. Dr. Ekrem Savaş, this symposium also featured an online address by Prof. Dr. Hasan Mandal, who was the President of TÜBİTAK at the time.

The 10th ULPAS took place again at ITU on May 13–14, 2022, in this very hall, with official support from TÜBA and ITU. The gala dinner, held aboard a boat on the Bosphorus, remains a cherished memory.

The 11th ULPAS held on November 4–5, 2022, at Gebze Technical University with strong support from GTU Rector Prof. Dr. Hacı Ali Mantar.

The 12th ULPAS conducted on May 5–6, 2023, at Yalova University with DOWAKSA as the main sponsor and support from TÜBİTAK for international scientific events. The Polymer Engineering Department at Yalova University provided exceptional organizational support.

The 13th ULPAS held on November 3–4, 2023, in Bolu with SUPERLIT as the main sponsor and strong support from Bolu Abant İzzet Baysal University Rector Prof. Dr. Mustafa Alişarlı and Engineering Faculty Dean Prof. Dr. Ömer Özyurt.

The 14th ULPAS took place on May 24–25, 2024, at Bursa Technical University, hosted magnificently by Prof. Dr. Ayşe Bedeloğlu and her team. The Rector Prof. Dr. Naci Çağlar has given generous support and showed great interest by attending the 15th ULPAS in İzmir and today. I personally thank Prof. Çağlar for his closed interest.

The last and the 15th ULPAS held on November 8–9, 2024, at İzmir Bakırçay University with significant support from Rector Prof. Dr. Mustafa Berktaş and tireless dedication from Symposium Chair Prof. Dr. Cem Gök, making it an extremely successful event.

And now, with this proud history behind us, we are hosting the **16th ULPAS** today and tomorrow (May 9–10, 2025) at ITU Gümüşsuyu, in the Orhan Öcalgiray Conference Hall and Room D331.

Now, I would like to warmly acknowledge our **invited speakers from around the globe**, who have enriched our program with their participation and expertise. You will have their short biographies in the Symposium Proceedings but let me once again express my deepest gratitude to each one of them for being here today.

1. Prof. Dr. İslam SHYHA (h-Index=28)

Prof. İslam Shyha is a young and dynamic professor and an academic leader in Scotland. He is the Associate Dean for Research and Innovation at Edinburgh Napier University. He has made significant contributions to the last ULPAS events by attending and delivering keynote speeches. Today, he will share his future vision for ULPAS. By the way, İslam is also the lead of the first Scottish international branch campus in Egypt. Hence he will open up bright international pathways to ULPAS.

2. Prof. Dr. Alexander M. SEIFALIAN (h-Index=112)

Prof. Alexander M. Seifalian is a distinguished expert in nanotechnology and regenerative medicine, celebrated for his groundbreaking work in synthetic organs and biomedical implants. He served at University College London (UCL) and the Royal Free Hospital for over 26 years, leading major advancements in tissue engineering and nanomedicine.

3. Prof. Dr. Nazmul KARIM (h-Index=30)

Prof. Nazmul Karim is a leading authority in sustainable textiles and wearable electronic materials. He currently holds the position of Professor of Sustainable Future Textiles at the University of Southampton. Previously, he served as Professor of Advanced Textiles at Nottingham Trent University and as Associate Professor at the Centre for Print Research at UWE Bristol, where he founded the Graphene Applications Laboratory and initiated the "New Materials: Towards Sustainable Technologies" research theme. His research focuses on the development of sustainable materials for future textiles, wearable electronic textiles (e-textiles), smart and sustainable fiber-reinforced composites, and the application of advanced materials such as graphene and other 2D materials in textiles. He has led pioneering projects including the first fully inkjet-printed graphene e-textiles and scalable methods for producing graphene textiles and 2D material heterostructure-based textiles.

4. Prof. Dr. Ahmad Mukifza HARUN (h-Index=8)

Dr. Harun's research interests include membrane technology for water and wastewater treatment, as evidenced by his contributions to the symposium "Membrane Technology for Water and Wastewater Treatment in Rural Regions". He has also co-authored studies on the photocatalytic effects of modified hydrothermal nanotitania, exploring its antibacterial properties and potential applications.

Associate Professor Ahmad Mukifza Harun is a Director at Malaysia's Nanotechnology Centre (NNC), Ministry of Science, Technology and Innovation, Putrajaya Malaysia. NNC plays a pivotal role in steering Malaysia's nanotechnology initiatives, ensuring strategic alignment with national policies, fostering innovation, and enhancing global collaborations to position Malaysia as a leader in nanotechnology. He is also a lecturer at the Faculty of Engineering, Universiti Malaysia Sabah. He holds a PhD in Electrical Engineering from the University of Leeds. He specializes in Electrical Engineering (Nanotechnology) and also a professional engineer.

5. Prof. Dr. Melih GÜNAY (h-Index=12)

As a graduate of ITU's Department of Textile Engineering, we take great pride in Prof. Melih Günay. He completed his master's and PhD at North Carolina State University (NCSU). He is now the founding chair of the Department of Computer Engineering at Akdeniz University. Today, he will talk about the applications of artificial intelligence in fiber production technologies.

6. Prof. Dr. Osman BABAARSLAN (h-Index=23)

Prof. Osman Babaarslan, a faculty member at Çukurova University's Department of Textile Engineering, has served as both an academic and industrial guide in all areas of textiles. Today, he will discuss sustainability in fiber production.

7. Prof. Dr. Tushar K. GHOSH (h-Index=41)

Prof. Dr. Tushar K. Ghosh earned his PhD in Fiber and Polymer Science from North Carolina State University. He began his academic career at NC State in the same year he graduated and has since held visiting professorships at the University of Sydney and the Indian Institute of Technology in Bombay. He is currently the William A. Klopman Distinguished Professor of Textile at the Wilson College of Textiles, NCSU. Dr. Ghosh has supervised numerous master's and PhD students and has been honored as "Distinguished Teacher of the Year" by both students and faculty. In 2007, he received the Founders Award from the Fiber Society for his outstanding contributions to the science and technology of fibrous materials. He has over 200 scientific publications, an H-index of 41, and more than 6,360 citations. He is one of the leading researchers in wearable textile-based electronics. His current research interests include polymer nanocomposites, electroactive polymers, artificial muscles, and biomimetic systems involving sensors and actuators.

8. Prof. Dr. Cem GÜNEŞOĞLU (h-Index=9)

Prof. Güneşoğlu is a distinguished academic and researcher at Gaziantep University. He completed his BSc, MSc, and PhD degrees in Textile Engineering at Uludağ University. In addition to his role at Gaziantep University, he serves as a part-time researcher at SUNUM (Sabancı University Nanotechnology Research and Application Center), where he contributes to cutting-edge advancements in nanotechnology and materials science.

Prof. Dr. Güneşoğlu is also known for his collaborative projects with industry, bridging the gap between academia and real-world applications. His contributions have not only advanced the field of textile engineering but have also had a meaningful impact on societal and industrial development.

9. Assoc. Prof. Dr. Seyedmansour BIDOKI (h-Index=14)

After completing his PhD at the University of Leeds in the UK, Dr. Seyedmansour Bidoki served as the head of department at Yazd University in Iran. He was also a visiting scholar at ITU's Department of Textile Engineering. Today, at the 16th ULPAS, Dr. Bidoki will make a unique contribution by presenting his patented research on reinforcing 3D-printed concrete structures with textile fibers.

10. Assoc. Prof. Dr. Aminoddin HAJI (h-Index=36)

Dr. Aminoddin Haji is an Associate Professor of Textile Engineering at Yazd University, Iran, and is recognized among the top 2% of most-cited researchers worldwide. A prominent expert in sustainable textiles and advanced functional materials, his innovative work in eco-friendly dyeing, polymer applications, and nanomaterials has significantly advanced textile science. Today, he will deliver a keynote speech titled *"Eco-Efficient Textile Dyeing: Leveraging Supercritical CO₂ for Sustainable Innovation,"* where he will unveil cutting-edge strategies for environmentally responsible textile processing.

11. Prof. Dr. Aijaz Ahmed BABAR (h-Index=24)

Prof. Dr. Aijaz Ahmed Babar is a distinguished researcher in textile engineering and nanomaterials, specializing in advanced fibrous structures and functional membranes. He received his Ph.D. in Materials Science and Engineering from Donghua University, Shanghai, China (2014–2020), and his B.E. in Textile Engineering from Mehran University of Engineering and Technology (MUET), Jamshoro, Pakistan. His research focuses on electrospinning and nanofiber fabrication, including Janus membranes and directional moisture transport, energy storage materials and supercapacitors, adsorption and polymeric nanomaterials, and advanced textile engineering for functional membranes.

12. Prof. Dr. Murat KAZANCI (h-Index=20)

An ITU graduate, Prof. Dr. Murat Kazancı conducts academic research on biomedical fiber-reinforced composites, artificial bone and filler materials, and nano-surfaces. He is the founding chair of the Department of Biomedical Engineering at Medeniyet University.

13. Prof. Dr. Amit RAWAL (h-Index= 32)

Prof. Dr. Amit Rawal is among the world's most respected scientists in the mechanics and modeling of textile and nonwoven surfaces. He was awarded the 2024 Environmental Science Prize by the Royal Swedish Academy and has been honored with the title of Royal Professor at the University of Borås for one year.

14. Prof. Dr. Sabit ADANUR (h-Index=28)

Prof. Dr. Sabit Adanur is a graduate of ITU as Mechanical Engineer. He has spend his early years of life in this very building. He then went to Auburn University to do PhD. After completing his PhD degree he has stayed as researcher and lecturer at the Textile Engineering Department. He is a distinguished professor in the field of weaving as well as technical textiles. In fact he is the Pioneer of Industrial Textiles serving at the university as well as in Industry. He is now at his Sabatical Leave at Gebze Tehcnical University working on a novel field 3D Printing of yarns and fabrics.

15. Prof. Dr. Nader Shehat (h_Index=)

Prof Nader Shehata is a Professor of Engineering Physics and Director of Nanotechnology Research Lab at both Alexandria University and Kuwait College of Science and Technology (KCST). He is also the director of Office of Research, Innovation and Sustainability (ORIS) at KCST. At ULPAS 16, he will talking about the interesting topic of energy harvesting nanocomposites.

Dear Rector, Distinguished Guests,

With, the “Sustainable Fibers and Polymers” subtitle, throughout today and tomorrow, **50 oral presentations** will be delivered in two parallel sessions, while **50 posters** will be exhibited in the hallway for all participants to explore. Each submission was reviewed by three expert referees, and presentation formats were determined based on their evaluations.

Additionally, our **ULPAS Award Committee** will assess the presentations and posters to determine the recipients of the **Best Paper** and **Best Poster** awards, which will be presented during the **Closing Ceremony tomorrow afternoon**. I am also glad to announce here that this ULPAS, we will also deliver an “**ULPAS Science Award**” to a deserving senior scientist sharing his experience with us.

Of course, no symposium is complete without social interaction. Coffee breaks help—but nothing brings people together like a good meal. This evening’s **Gala Dinner** will be held at **Filizler Köftecisi at Üsküdar**. We'll walk together to Kabataş, and then cross over the Bosphorus to Üsküdar and enjoy a beautiful 15-minute stroll before gathering at 7:00 PM in the restaurant’s scenic sea-view hall. We hope to see you all there for what promises to be a wonderful and memorable evening.

Before concluding, I’d like to thank everyone who made the 16th ULPAS possible:

- Our **Organizing Committee Members**,
- **Scientific Committee Members**,
- All **Referees** who reviewed the submissions,

And our **sponsors**, whose generous support shows their commitment to research and innovation:

- **Gold Sponsors:** KİPAŞ and R-B Karesi
- **Mug Sponsor:** INOVENSO
- **Bag Sponsor:** TEPAR
- **Administration Sponsor:** AREKA

Thank you for your invaluable support.

Prof. Dr. Ali Demir
Istanbul, 10 May 2025
Co-Chair of the Fiber and Polymer Research Association
On behalf of the 16th ULPAS Organizing Committee



Prof. Dr. Ali Demir

“On yılda 15 Sempozyum”

Bu önsözün başlığını “On yılda 15 Sempozyum” olarak tercih ettim. Çünkü 2015 yılında Bursa’da Bursa Uludağ Üniversitesi, BTO, UTİB ve BUTEKOM ile birlikte Tekstil Ar-Ge proje Pazarları ile paralel olarak başladığımız bu sempozyumlar artık bağımsız olarak ve yılda iki defa olarak yapılarak bugünkü 16.ULPAS’a eriştik. Bu 16 sempozyuma emeği geçen başta Prof. Dr. Yusuf Ulcay hocam olmak üzere tüm arkadaşlarıma çok teşekkür ediyorum.

Yusuf Hocam ile birlikte gördüğümüz bir rüya idi ULPAS’lar ve bugün 16.ULPAS’ı birlikte gerçekleştiriyoruz. Her ULPAS’ta daha büyüdü, her ULPAS’ta daha kapsamı oldu ve Bursa, İstanbul, Eskişehir, Uşak, Yalova, Gebze, Bolu ve İzmir’den sonra yeniden İstanbul’da ve İTÜ’de 16. ULPAS’ı gerçekleştiriyoruz. Tüm bunlardan gerçekten çok büyük mutluluk ve kıvanç duyuyorum.

Uluslararası Lif ve Polimer Araştırmaları sempozyumları esasen bir tematik sempozyumdur. Tekstilin temel yapı taşı, başlangıç noktası olan lif ve lifi de oluşturan polimerler alanında yapılan tüm araştırma sonuçlarının paylaşıldığı uluslararası bir gösteri alanı bir pazar yeridir.

İTÜ Tekstil Teknolojileri ve Tasarımı Fakültemiz tarafından gerçekleştirilen Uluslararası Tekstil ve Moda Kongresi gibi, Ege Üniversitesi, Tekstil Mühendisliği Bölümün gerçekleştirdiği Uluslararası tekstil ve Hazır Giyim Sempozyumu, veya Çukurova Üniversitesi, Tekstil Mühendisliği Bölümünün gerçekleştirdiği Ulusal Çukurova Tekstil Kongresi gibi genel kapsamlı uluslararası ve ulusal kongre ve sempozyumların yanında Dokuz Eylül Üniversitesi, Tekstil Mühendisliği Bölümün gerçekleştirdiği Teknik Tekstiller Kongresi ve Uluslararası Lif ve Polimer Araştırmaları Sempozyumu gibi tematik kongre ve sempozyumlarının var olması ve hatta giderek sayılarının da artıyor olması gerekli ve sevindirici olmaktadır. Bu tür kongre ve sempozyumlar bilim insanları arasındaki bilgi ve tecrübe alışverişini sağlarken genç akademisyenlerin yetişmesine de büyük katkı vermektedir. Ben kişisel olarak ULPAS’larda gördüğüm yüksek lisans ve doktora öğrencilerinin sunumları ile heyecan duyuyor ve onları bir sonraki sempozyumda nasıl daha profesyonel hale geldiğini ve araştırmalarını nasıl derinleştirmiş olduklarını görmekten büyük mutluluk duyuyorum.

ULPAS’ın önemli bir boyutunu da sizlerle paylaşmak istiyorum. Başladığı birinci sempozyumdan bugüne ULPAS’lara sanayimizin her zaman çok büyük katılımı ve ilgisi olmuştur. Bu son derece sevindiricidir. Bu destek hem sponsor olarak maddi destek olmuştur hem de sanayicimizin ve özellikle de Ar-Ge Merkezlerinin yaptığı araştırma sonuçlarının sunumlar

her zaman büyük bir zenginlik olmuştur. Bu sempozyumda da sunulan toplam 50 bildirinin 20'si Ar-Ge merkezlerinden olacaktır.

Kısaca ULPAS'ların dokuz yıl geçmişini sizlere özetlemek isterim:

| | Tarihler | Yer | Ana Sponsor |
|-----------------|---------------------------|-----------------------|----------------------|
| 1.ULPAS | 13-14 Mayıs 2016 | BUTEKOM-Bursa | BTSO-UTIB |
| 2.ULPAS | 27-28 Nisan 2017 | BUTEKOM-Bursa | BTSO-UTIB |
| 3.ULPAS | 8-9 Mart 2018 | BUTEKOM-Bursa | BTSO-UTIB |
| 4.ULPAS | 4-5 Ekim 2018 | Uludağ Univ. | Uludağ Üniv. |
| 5.ULPAS | 3 Mayıs 2019 | İTÜ | ISTKA projesi |
| 6.ULPAS | 24-25 Ocak 2020 | Uludağ Üniv. | |
| 7.ULPAS | 25-26 Eylül 2020 | BTÜ-@On-line | |
| 8.ULPAS | 18-19 Haziran 2021 | ESOGU-@On-line | |
| 9.ULPAS | 18-19 Kasım 2021 | Uşak Üniv. | |
| 10.ULPAS | 13-14 Mayıs 2022 | İTÜ | |
| 11.ULPAS | 4-5 Kasım 2022 | GTÜ | |
| 12.ULPAS | 5-6 Mayıs 2023 | Yalova Üniv. | DOWAKSA |
| 13.ULPAS | 3-4 Kasım 2023 | Bolu Abant İBÜ | SUPERLİT |
| 14.ULPAS | 24-25 Mayıs 2024 | BTÜ | |
| 15.ULPAS | 8-9 Kasım 2024 | İzmir Bakırçay Üniv. | |
| 16.ULPAS | 9-10 Mayıs 2025 | İTÜ | |

Lif ve Polimer Araştırmaları Platformu ve Sempozyum Organizasyon Kurulu Başkanımız Sayın Prof. Dr. Yusuf Ulcay'ın Bursa Uludağ Üniversitesi Rektörü de olduğu 2016, 2017 ve 2018 yıllarında (13-14 Mayıs 2016, 27-28 Nisan 2017 ve 8-9 Mart 2018 tarihlerinden) Bursa'da BUTEKOM'da yapılan VIII., IX. ve X. Ar-Ge ve Proje Pazarına paralel olarak yapılan ilk sempozyumların tüm masrafları ve bu sempozyumlarda bildiri veya poster sunumu yapan tüm araştırmacıların yol ve konaklama giderleri UTIB ve BTSO tarafından karşılandığından bu başlangıç sempozyumları çok canlı ve verimli geçti. Bildiri kitapçıkları da BUTEKOM tarafından basıldı. Bu esasen bir yandan ulusal Ar-Ge Proje Pazarlarına katkı bir yandan da Lif ve Polimer Araştırmalarının bilim dünyası ve sanayicilerimiz ile paylaşımını sağlamaktaydı.

4. ULPAS: 2018 yılında yılın ikinci sempozyumu olarak 4. ULPAS, UTİB ve BTSO'dan bağımsız olarak 4-5 Ekim 2018 tarihinde Bursa Uludağ Üniversitesi, Mete Cengiz Kültür Merkezinde yapıldı. Bu sempozyum da hem sanayici katılımı, KORTEKS ve POLYTEKS'e ziyaret, uluslararası davetli konuşmacıların yol ve konaklama masraflarının karşılanması ile başarılı bir sempozyum oldu ve bildiriler kitapçığı da Uludağ Üniversitesi tarafından basıldı.

3 Mayıs 2019'da tek günlük olarak İTÜ, Gümüşsuyu Yerleşkesinde, bu salonda 5. ULPAS'ı **“Medikal Tekstiller”** vurgusuyla gerçekleştirdik. Böyle yapmamızın sebebi, bu sempozyumların ana unsurlarından birisi olan İTÜ'de Tekstil Teknolojileri ve Tasarımı Fakültesinde 30 yıldır faaliyet gösteren “İTÜ TEMAG Laboratuvarı”nın İstanbul Kalkınma Ajansı (İSTKA) destekli yürüttüğü bir proje olan “TR10/18/YMP/0075-MEDİTEKS: Medikal tekstiller Ar-Ge Merkezi”nin kuruluş lansman toplantısıyla birlikte gerçekleştirildi. ISTKA Projesi kapsamında sempozyum organize edildi.

6. ULPAS: 24-25 Ocak 2020 tarihlerinden yeniden Uludağ Üniversitesi, Mete Cengiz Kültür Merkezinde gerçekleştirildi. Bu sempozyumda organizasyona Bursa Teknik Üniversitesi de katıldı.

Eylül 2020 ve Haziran 202’de gerçekleştirilen **7. ve 8. ULPAS**’lar COVID pandemisi nedeniyle tamamen on-line yapıldı.

9. ULPAS, 18-19 Kasım 2021 tarihlerinden pandemi sonrası ilk kez Uşak’da hem on-line hem de on-site olarak gerçekleştirildi. Uşak Üniversitesi Rektörü Prof. Dr. Ekrem Savaş’ın yakın desteği ile yapılan bu sempozyumda o tarihte TÜBİTAK Başkanı olan Sayın Rektörümüz Prof. Dr. Hasan Mandal da on-line konuşma yaptı.

10.ULPAS, 13-14 Mayıs 2022 tarihlerinde yine İTÜ’de ve bu salonda TÜBA ve İTÜ’nün resmi desteği ile yapıldı. İstanbul boğazında tekne gezisi ile yapılan gala yemeği hafızalarda yer etti.

11.ULPAS, 4-5 Kasım 2022 tarihlerinde Gebze Teknik Üniversitesi’nde yapıldı. GTÜ Rektörü Prof. Dr. Hacı Ali Mantar’ın sempozyuma desteği oldu.

12.ULPAS, 5-6 Mayıs 2023 tarihlerinden Yalova Üniversitesinde hem DOWAKSA’nın Ana Sponsorluğu hem de TÜBİTAK uluslararası bilimsel etkinlik desteği alarak Yalova Üniversitesi Polimer Mühendisliği Bölümünün efsanevi desteği ile yapıldı.

13. ULPAS, 3-4 Kasım 2023 tarihlerinde Bolu’da hem SUPLERLİT firmasının Ana Sponsorluğunda hem de BAİBÜ Rektörü Prof. Dr. Mustafa Alişarlı ve Mühendislik Fakültesi Dekanı Prof. Dr. Ömer Özyurt’un sahiplenmesi ile gerçekleştirildi.

14. ULPAS, 24-25 Mayıs 2024 tarihlerinden Bursa Teknik Üniversitesinin ev sahipliğinde Prof. Dr. Ayşe Bedeloğlu ve ekibi tarafından muhteşem bir biçimde yapıldı.

15.ULPAS, 8-9 Kasım 2024 tarihlerinden İzmir Bakırçay Üniversitesinde Rektör Prof. Dr. Mustafa Berktaş’ın ve ekibinin büyük desteği ve Sempozyum Başkanı Prof. Dr. Cem GÖK hocamın büyük ferdakallığı ile son derece başarılı bir biçimde yapıldı.

Tüm bu geçmiş ile bugün **16. ULPAS’ı, bugün ve yarın (9-10 Mayıs 2025)** İTÜ-Gümüşsuyu’nda Orhan Öcalgiray Konferans Salonu, Görsel Eğitim Merkezi ve D331’de gerçekleştireceğiz.

Bu sempozyumda bizlerle tüm dünyadan **KATILAN DAVETLİ KONUŞMACILARIMIZ** var: Bu çok değerli bilim insanlarını programdaki sıra ile kısaca tanıtmak ve kendilerine en kalbi teşekkürlerimi sunmak isterim:

1. Prof. Dr. İslam SHYHA

Prof. Dr. İslam Shyha, İskoçya’dan katılan genç ve dinamik bir profesördür. Son üç ULPAS etkinliğine katılarak ve Davetli Konuşmalar yaparak önemli katkılarda bulunmuştur. Bugün, ULPAS’ın geleceğine dair vizyonunu bizlerle paylaşacaktır.

2. Prof. Dr. Alexander M. SEIFALIAN

Prof. Dr. Alexander M. Seifalian, nanoteknoloji ve rejeneratif tıp alanlarında uzmanlaşmış, sentetik organlar ve biyomedikal implantlar konusundaki çığır açan çalışmalarıyla tanınan seçkin bir uzmandır. 26 yılı aşkın süreyle University College London (UCL) ve Royal Free Hospital’da görev yapmış, doku mühendisliği ve nanotıp alanlarında büyük ilerlemelere öncülük etmiştir.

3. Prof. Dr. Nazmul KARIM

Prof. Dr. Nazmul Karim, sürdürülebilir tekstiller ve giyilebilir elektronik malzemeler alanında öncü bir uzmandır. Halen Southampton Üniversitesi’nde Sürdürülebilir Gelecek Tekstilleri Profesörü olarak görev yapmaktadır. Daha önce Nottingham Trent Üniversitesi’nde İleri Tekstiller Profesörü ve UWE Bristol’deki Baskı Araştırma Merkezi’nde Doçent olarak görev yapmış, burada Grafen Uygulamaları Laboratuvarı’nı kurmuş ve “Yeni Malzemeler: Sürdürülebilir Teknolojilere Doğru” araştırma temasını başlatmıştır.

Araştırmaları, geleceğin tekstilleri için sürdürülebilir malzemeler, giyilebilir elektronik tekstiller (e-tekstilller), akıllı ve sürdürülebilir elyaf takviyeli kompozitler ile grafen ve diğer 2D malzemelerin tekstil uygulamalarına odaklanmaktadır. İlk tam mürekkep püskürtmeli grafen e-tekstilleri ve ölçeklenebilir grafen tekstil üretimi ile 2D malzeme heteroyapıları bazı tekstiller gibi öncü projelere liderlik etmiştir.

4. Prof. Dr. Ahmad Mukifza HARUN

Dr. Harun'un araştırma alanları arasında, "Kırsal Bölgelerde Su ve Atıksu Arıtımı için Membran Teknolojisi" başlıklı kitapta yer alan katkılarıyla da görüldüğü üzere, su ve atıksu arıtımında membran teknolojileri yer almaktadır. Ayrıca, antibakteriyel özellikleri ve potansiyel uygulamaları üzerine modifiye hidrotermal nanotitanyanın fotokatalitik etkileri üzerine ortak çalışmalarda bulunmuştur.

Doç. Dr. Ahmad Mukifza Harun, Malezya'nın Putrajaya kentindeki Bilim, Teknoloji ve Yenilik Bakanlığı'na bağlı Nanoteknoloji Merkezi (NNC) Direktörüdür. NNC, Malezya'nın nanoteknoloji girişimlerine yön vererek ulusal politikalarla stratejik uyumu sağlamakta, yeniliği teşvik etmekte ve küresel iş birliklerini güçlendirerek Malezya'yı nanoteknolojide lider konumuna getirmeyi amaçlamaktadır. Aynı zamanda Universiti Malaysia Sabah Mühendislik Fakültesi'nde öğretim üyesidir. Leeds Üniversitesi'nden Elektrik Mühendisliği alanında doktora derecesine sahiptir. Elektrik Mühendisliği (Nanoteknoloji) uzmanlık alanında profesyonel bir mühendistir.

5. Prof. Dr. Melih GÜNAY

İTÜ Tekstil Mühendisliği Bölümü mezunu olan Prof. Dr. Melih Günay ile gurur duyuyoruz. Yüksek lisans ve doktora eğitimini North Carolina State University (NCSU)'de tamamlamıştır. Şu anda Akdeniz Üniversitesi Bilgisayar Mühendisliği Bölümünün kurucu başkanıdır. Bugün, yapay zekânın elyaf üretim teknolojilerindeki uygulamalarından bahsedecektir.

6. Prof. Dr. Osman BABAARSLAN

Prof. Dr. Osman Babaarslan, Çukurova Üniversitesi Tekstil Mühendisliği Bölümü öğretim üyesidir. Tekstilin tüm alanlarında akademik ve endüstriyel rehberlik yapmıştır. Bugün, elyaf üretiminde sürdürülebilirlik konusunu ele alacaktır.

7. Prof. Dr. Tushar K. GHOSH

Prof. Dr. Tushar K. Ghosh, North Carolina State University'den Elyaf ve Polimer Bilimi alanında doktora derecesi almıştır. Mezun olduğu yıl akademik kariyerine aynı üniversitede başlamış ve University of Sydney ile Hindistan Bombay Teknoloji Enstitüsü'nde misafir profesörlük yapmıştır. Şu anda NCSU'daki Wilson Tekstil Fakültesi'nde William A. Klopman Seçkin Tekstil Profesörü'dür.

Çok sayıda yüksek lisans ve doktora öğrencisi yetiştirmiş, hem öğrenciler hem de öğretim üyeleri tarafından "Yılın Seçkin Eğitmeni" seçilmiştir. 2007 yılında Elyaf Derneği tarafından fibroz malzeme bilimi ve teknolojisine katkılarından dolayı Kurucular Ödülü'nü almıştır. 200'ün üzerinde bilimsel yayını, 41 H-indeksi ve 6.360'tan fazla atıfı bulunmaktadır. Giyilebilir tekstil tabanlı elektronikler konusunda öncü araştırmacılarından biridir. Mevcut araştırmaları, polimer nanokompozitler, elektroaktif polimerler, yapay kaslar ve sensör ve aktüatörleri içeren biyomimetik sistemler üzerinedir.

8. Prof. Dr. Cem GÜNEŞOĞLU

Prof. Güneşoğlu, Gaziantep Üniversitesi'nde seçkin bir akademisyen ve araştırmacıdır. Lisans, yüksek lisans ve doktora derecelerini Uludağ Üniversitesi Tekstil Mühendisliği bölümünde tamamlamıştır. Gaziantep Üniversitesi'ndeki görevine ek olarak, SUNUM'da (Sabancı Üniversitesi Nanoteknoloji Araştırma ve Uygulama Merkezi) yarı zamanlı araştırmacı olarak görev yapmakta ve burada nanoteknoloji ve malzeme bilimi alanlarında öncü gelişmelere katkıda bulunmaktadır.

Prof. Dr. Güneşoğlu, sanayi ile yürüttüğü ortak projelerle de tanınmakta, akademi ile gerçek dünya uygulamaları arasında köprü kurmaktadır. Katkıları, yalnızca tekstil mühendisliği alanının gelişimine değil, aynı zamanda toplumsal ve endüstriyel gelişime de anlamlı etkilerde bulunmaktadır.

9. Doç. Dr. Seyedmansour BIDOKI

Doktorasını İngiltere'deki Leeds Üniversitesi'nde tamamlayan Dr. Seyedmansour Bidoki, İran'daki Yazd Üniversitesi'nde bölüm başkanlığı yapmıştır. Aynı zamanda İTÜ Tekstil Mühendisliği Bölümü'nde misafir araştırmacı olarak bulunmuştur. Bugün 16. ULPAS'ta, tekstil lifleriyle güçlendirilmiş 3D yazıcıyla basılmış beton yapılar üzerine yaptığı patentli çalışmasını sunarak özgün bir katkı sağlayacaktır.

10. Doç. Dr. Aminoddin HAJI

Dr. Aminoddin Haji, İran'daki Yazd Üniversitesi'nde Tekstil Mühendisliği alanında Doçenttir ve dünyada en çok atıf alan ilk %2'lik dilimde yer almaktadır. Sürdürülebilir tekstiller ve ileri fonksiyonel malzemeler alanında önde gelen bir uzmandır. Çevre dostu boyama, polimer uygulamaları ve nanomalzemeler konusundaki yenilikçi çalışmaları tekstil bilimine önemli katkılar sağlamıştır. Bugün “Eko-Verimli Tekstil Boyama: Sürdürülebilir Yenilik İçin Süperkritik CO₂'nin Kullanımı” başlıklı açılış konuşmasında, çevresel açıdan sorumlu tekstil işlemleri için öncü stratejilerini açıklayacaktır.

11. Prof. Dr. Aijaz Ahmed BABAR

Prof. Dr. Aijaz Ahmed Babar, ileri fibroz yapılar ve fonksiyonel membranlar üzerine çalışan seçkin bir tekstil mühendisliği ve nanomalzeme araştırmacısıdır. 2014–2020 yılları arasında Çin'in Şanghay kentindeki Donghua Üniversitesi'nde Malzeme Bilimi ve Mühendisliği alanında doktora yapmış, lisans eğitimini Pakistan'daki Mehran Üniversitesi'nde Tekstil Mühendisliği alanında tamamlamıştır. Araştırma alanları arasında elektrospinning ve nanolif üretimi, Janus membranları, yönlü nem taşıma, enerji depolama malzemeleri ve süperkapasitörler, adsorpsiyon ve polimerik nanomalzemeler ile fonksiyonel membranlara yönelik ileri tekstil mühendisliği yer almaktadır.

12. Prof. Dr. Murat KAZANCI

İTÜ mezunu olan Prof. Dr. Murat Kazancı, biyomedikal elyaf takviyeli kompozitler, yapay kemik ve dolgu malzemeleri ile nano yüzeyler üzerine akademik araştırmalar yapmaktadır. Medeniyet Üniversitesi'nde Biyomedikal Mühendisliği Bölümü'nün kurucu başkanıdır.

13. Prof. Dr. Amit RAWAL

Prof. Dr. Amit Rawal, tekstil ve nonwoven yüzeylerin mekaniği ve modellemesi alanında dünyanın en saygın bilim insanları arasındadır. İsveç Kraliyet Akademisi tarafından 2024 Çevre Bilimi Ödülü'ne layık görülmüş ve bir yıl boyunca Borås Üniversitesi'nde Kraliyet Profesörü unvanını almıştır.

14. Prof. Dr. Sabit ADANUR

Prof. Dr. Sabit Adanur, İTÜ Makine Mühendisliği bölümünden mezundur. Hayatının ilk yıllarını tam olarak bu binada geçirmiştir. Sonrasında Auburn Üniversitesi'ne giderek doktorasını yapmıştır. Doktora derecesini tamamladıktan sonra, Tekstil Mühendisliği Bölümü'nde araştırmacı ve öğretim üyeliği yapmıştır. Dokuma ve teknik tekstiller alanında dünyanın önde gelen tanınmış bir profesördür. Esasen hem üniversiteye hem de sanayiye hizmet vermiş Endüstriyel Tekstillerin öncüsüdür. Şu anda, Gebze Teknik Üniversitesi'nde sabbatical izindedir ve yenilikçi bir alan olan iplik ve kumaşların 3D baskı teknolojisi ile üretilmesi üzerinde çalışmalar yapmaktadır.

15. Prof. Dr. Nader Shehata

Prof. Nader, Alexandria University and Kuwait College of Science and Technology (KCST)'de Mühendislik Fiziği ve Nanoteknoloji Araştırma Laboratuvarı Yöneticisi. Prof. Shehata aynı zamanda KCST'de Araştırma, İnovasyon ve Sürdürülebilirlik Ofislerinin de Müdürlüğünü yapıyor. 16. ULPAS'da nanokompozitlerle enerji hasatlama üzerinde heyecan verici bir sunum yapacak.

Her bir değerli davetli konuşmacı hocalarıma teşekkür ediyor, 16. ULPAS'a büyük katkılarından dolayı minnettar olduğumu bildirmek istiyorum. Sağolun, varolun.

“Sürdürülebilir Lif ve Polimerler” alt başlığı ile bugün ve yarın iki salonda toplam 50 bildiri sunulacak. 50 poster de koridorda katılımcıların dikkatine sunulacak. Gerek bildiriler gerekse de posterlerin her biri alanında uzman 3 hakem tarafından değerlendirildi ve hakemleri takdir ettikleri puanlara göre sıralanarak sözlü yada poster olarak sunulmalarına karar verildi. Ayrıca bugün ve yarın Sempozyum Ödül Komisyonu da hem hakemlerin takdir ettikleri puanları hem de sözlü ve poster sunumlarını izleyerek bildiri ve posterleri değerlendirecek ve EN İYİ BİLDİRİ ve En İYİ POSTER ödülü alacak bildir ve posterleri tespit edecekler. Ödül sahiplerine ödülleri de Yarın öğleden sonraki Kapanış oturumunda takdim edeceğiz.

Bu tür sempozyumların bilimsel etkileşim sağlama yanında bir de sosyal etkileşim temin etme boyutu vardır. Hem kahve/çay molalarından hem de ve özellikle de GALA YEMEĞİ tam bir sosyal etkileşim platformu olmaktadır. 16. ULPAS'ın Gala yemeği Üsküdar'da Filizler Köftecisinde bu akşam yenilecek. Birlikte Kabataş'tan Üsküdar'a geçeceğiz ve 15 dakikalık güzel bir yürüyüşten sonra akşam 19.00'da Filizler Köftenin boğaza nazır salonlarında hem yemek hem sohbet birlikte yaşayacağımız güzel bir anı olacak.

Son olarak da, bu sempozyumun gerçekleşmesine büyük katkı veren tüm

- Organizasyon Kurulu Üyelerine,
- Bilim Kurulu Üyelerine,
- Bildirileri değerlendiren hakem arkadaşlarıma ve

özellikle de sempozyuma sponsor olarak bilime ve araştırmaya değer verdiğini fiilen gösteren

ALTIN SPONSOR, KİPAŞ'a

ALTIN SPONSOR, R-B Karesi'ye

Kupa Sponsoru, İNOVENSO'ya

Çanta Sponsoru, TEPAR'a

Yönetim Sponsor, AREKA'ya özellikle teşekkür ediyorum.

Prof. Dr. Ali Demir

İstanbul, 10 Mayıs 2025

Lif ve Polimer Araştırmaları Eşbaşkanı

16. ULPAS Organizasyon Komitesi Adına



Keynote Speaker at the 16th ULPAS

Prof. Dr. Melih GÜNAY

Field of Study :Computer Science, AI, Big Data, Data Mining

Affiliation :Akdeniz university, Antalya, Türkiye

The Role of Artificial Intelligence in Fiber science

Abstract:

Artificial Intelligence (AI) is revolutionizing fiber science by enhancing material discovery, optimizing manufacturing processes, and improving quality control. Machine learning algorithms accelerate the development of high-performance and sustainable fibers by predicting material properties and optimizing compositions. In manufacturing, AI-driven automation streamlines fiber production, reduces defects, and enables predictive maintenance. Additionally, computer vision systems enhance quality assurance by detecting imperfections in real time. AI also plays a crucial role in the development of smart and functional textiles, enabling applications in healthcare, sports, and defense. Furthermore, AI-powered analytics contribute to sustainability by minimizing waste, optimizing recycling processes, and reducing energy consumption. With the ability to predict textile performance and customize fiber properties, AI is shaping the future of fiber science, making materials more efficient, durable, and environmentally friendly. This presentation explores the transformative impact of AI on fiber science, highlighting its potential for innovation and sustainability in the textile industry.

Profile:

Melih Gunay earned a B.S. in Textile Engineering from Istanbul Technical University in 1997, followed by an M.S. in Computer Science (2000) and a Ph.D. (2005) from NC State University, USA. From 2005 to 2013, he worked as a software engineer at various companies and institutes. In 2013, he became an Associate Professor, and in 2017, he was promoted to Professor in the Computer Engineering Department at Akdeniz University.

Prof. Gunay served as an advisor to the Akdeniz University Rectorate in Information Technologies (2017–2021) and as Director of the Computer Science and Research Center (2015–2021). From 2014 to 2022, he chaired the Computer Engineering Department, overseeing the introduction of undergraduate, master's, and Ph.D. programs in Computer Engineering at Akdeniz University.

His research interests include machine learning, artificial intelligence, and their applications in various domains. He has authored over 80 research papers and has led multiple funded projects as Principal Investigator (PI) and researcher. Additionally, he has advised 10 M.S. and 4 Ph.D. students.



Keynote Speaker at the 16th ULPAS

Prof. Dr. Islam Shyha

Field of Study : **Material Science, Nano Engineering, AI, Built Environment**

Affiliation : **Edinburgh Napier University, U.K.**

Email : **i.shyha@napier.ac.uk**

How I See ULPAS So Far and in the Future

Abstract:

Exciting times ahead! Professor Islam Shyha will be delivering a keynote speech that delves into the rich history and remarkable success story of the International Fiber and Polymer Research Symposium (ULPAS). He will provide a comprehensive overview of ULPAS's journey, highlighting key achievements and the dynamic growth of the symposium. Prof. Shyha will also share some fantastic news about the future of ULPAS, outlining new initiatives and opportunities that promise to propel the symposium to even greater heights. Stay tuned for insights into the past, present, and future of ULPAS!

Profile:

Professor Islam Shyha serves as the Associate Dean for Research and Innovation for the School of Computing, Engineering and the Built Environment at Edinburgh Napier University. He also holds the position of Professor of Manufacturing Engineering, with his research focusing on composite machining, conventional and non-conventional machining processes, as well as nanofibers spinning.

With over two decades of experience in higher education, Professor Shyha has an illustrious academic background. He earned his Postgraduate Certificate in Higher Education Practice from Northumbria University, his PhD from The University of Birmingham, and both his MSc and BSc from Alexandria University. He has held various esteemed positions at Northumbria University, The University of Birmingham, and Alexandria University. His research endeavours receive support from the UK Research Council, Innovate UK, and industry partners. A Fellow of the Higher Education Academy (HEA), Professor Shyha imparts his expertise by teaching mechanical and manufacturing engineering courses and supervising MSc and PhD projects in advanced manufacturing engineering. In addition to his primary roles, Professor Shyha has held honorary positions at The University of Birmingham, Newcastle University and the Vietnamese German University (Vietnam). He boasts a prolific academic portfolio with over 130 publications in renowned journals and international conferences, alongside a patent for an innovative composite machining tool. His contributions extend to the global research and academic communities, where he actively serves as a reviewer for several prestigious manufacturing and materials funders and journals as well as participates as a member or chair of international conferences committees.



Keynote Speaker at the 16th ULPAS

Prof. Dr. Cem Güneşoğlu

Field of Study :Textile Engineering
Affiliation :Gaziantep University,

Enhancement of Textile Surfaces by Polymers: A Case Study

Abstract:

The presentation is about to enhance users' comfort of textile surfaces through polymeric materials; and mattress fabrics will be case study. The outlines of user comfort and assessment will be discussed.

Biography:

Prof. Dr. Cem Güneşoğlu, is a distinguished academic and researcher at Gaziantep University, with a specialization in Textile Engineering. He completed his BSc (1998), MSc (2001), and PhD (2006) in Textile Engineering at Uludağ University, where he laid the foundation for his expertise in the field. In addition to his role at Gaziantep University, he serves as a part-time researcher at SUNUM (Sabancı University Nanotechnology Research and Application Center), where he contributes to cutting-edge advancements in nanotechnology and materials science.

Throughout his career, Prof. Dr. Güneşoğlu has been actively involved in research, publishing extensively and presenting at international conferences. His work focuses on innovative applications in textile engineering, blending theoretical knowledge with practical solutions. As an educator, he has mentored numerous students, guiding them through undergraduate, graduate, and doctoral programs, and fostering a culture of academic excellence.

Prof. Dr. Güneşoğlu is also known for his collaborative projects with industry, bridging the gap between academia and real-world applications. His contributions have not only advanced the field of textile engineering but have also had a meaningful impact on societal and industrial development. A respected figure in his field, he continues to inspire through his dedication to research, education, and innovation.



Keynote Speaker at the 16th ULPAS

Prof. Dr. Amit Rawal

Field of Study :Textile Engineering, [Nonwoven, Brading, Geometrical modelling]

Affiliation :Indian Institute of Technology Delhi, India

Decoding Random Fiber Networks: van Wyk's Notions Revisited

Abstract:

Understanding the structure–property relationships of random materials remains a long-standing challenge due to their broad applicability across diverse scientific and engineering domains. Notable examples include polycrystals, polymer blends, foams, fluidized beds, cermets, rocks, fibrous materials, and composites. In random fiber networks, the interplay between size effects, intricate porous characteristics, and stochastic constituent distributions results in quasiheterogeneous features, necessitating an exploration beyond microstructural considerations. Herein, we revisit van Wyk's pioneering architectural-based interfiber spacing model, initially established via excluded area and excluded volume approaches. The discrepancy between these frameworks, as observed in van Wyk's original work, is addressed by drawing parallels with Bertrand's paradox. Further, the model has been extended to account for low-aspect-ratio fibers by incorporating side–side, end–end, and side–end interactions. A comparison between the modified interfiber spacing model and existing analytical models for random fiber networks highlights its enhanced predictive capability. A simple yet robust relationship between the maximum volume fraction and aspect ratio for cylindrical fibers has also been deduced. To demonstrate the model's versatility, the derived volume fraction–aspect ratio relationship is benchmarked against a wide array of analytical models, simulations, and experimental data from the literature, showing reasonable agreement. Furthermore, van Wyk's compression model for random fibrous materials—based on excluded area (volume), continuum mechanics, stereology, geometrical probability, and least-squares methods—is critically examined. A key error in van Wyk's formulation is identified, prompting a revision of the widely accepted inverse-cube pressure–volume relationship. The pressure–volume relationship has been revisited by modifying the formulation of the mean length of a fiber element between consecutive contacts projected on the compression direction. Through this work, we provide a more rigorous understanding of random fiber networks, offering new insights into their structural and mechanical behavior.

Profile:

Amit Rawal obtained his PhD from the University of Bolton, UK, and a Master of Philosophy from The University of Manchester, UK. He is a recipient of the Alexander von Humboldt Research Fellowship for experienced researchers to conduct research in the field of nonwovens in Germany. He has also been awarded the Fulbright-Nehru Academic and Professional Excellence Fellowship to initiate collaboration with the Massachusetts Institute of Technology, USA. In addition, he has received numerous awards, including the Young Researcher Fellowship from the prestigious M.I.T, Cambridge, for exemplary research in Computational Mechanics, Fellowship of the Textile Institute, CSIR special research award, and an Outstanding Young Faculty Fellowship by the Indian Institute of Technology, Delhi (IITD). Currently, he is working as a Professor at the Department of Textile and Fibre Engineering, IIT Delhi. He has published more than 150

publications in various journals and conferences. He has developed various three-dimensional (3D) analytical models for predicting geometrical, mechanical, and wetting properties of a diverse range of textile and allied structures. His research interests are not only limited to the structure, mechanics, and wetting behavior of textile and allied materials but also focused on the structure-property relationship of buckypapers, electrospun mats, low surface energy superhydrophobic fibrous mats, geotextiles, composites, auxetic, piezoresistive, and piezoelectric materials. He is an editorial board member of Textile Research Journal, Journal of Industrial Textiles and Research Journal of Textile & Apparel. Recently, he was honored as the twenty-ninth recipient of the King Carl XVI Gustaf Professorship in Environmental Science for the year 2024/25.



ULUSLARARASI
LİF VE POLİMER
ARAŞTIRMALARI
SEMPOZYUMU

16th INTERNATIONAL FIBER AND POLYMER RESEARCH SYMPOSIUM

Sürdürülebilir ve İşlevsel Lif ve Polimerler
Sustainable and Functional Fibers & Polymers



BURSA
ULUDAĞ
ÜNİVERSİTESİ

9-10 Mayıs
May 2025

İstanbul Teknik Üniversitesi
Gümüşsuyu Prof. Dr. Necmettin Erbakan Yerleşkesi

Istanbul Technical University
Gumussuyu Prof. Dr. Necmettin Erbakan Campus



BURSA TEKNİK
ÜNİVERSİTESİ



Keynote Speaker at the 16th ULPAS

Assoc. Prof. Dr. Aminoddin Haji

Field of Study :Textile Chemistry and Fiber Science

Affiliation :Yazd University, Iran

Eco-Efficient Textile Dyeing: Leveraging Supercritical CO₂ for Sustainable Innovation

Abstract:

The global textile industry, a longstanding driver of economic growth, is now at a crossroads, balancing its massive environmental impact with the urgent need for sustainability. Supercritical CO₂ (scCO₂) dyeing is stepping up as a real game-changer, offering a way to dramatically cut water use, eliminate toxic waste, and reduce energy consumption in textile dyeing. This presentation dives into the exciting progress and real-world challenges of scCO₂ technology, presenting it as a critical tool for decarbonizing this ancient industry.

The process works by using CO₂ in its supercritical state, where it behaves like both a gas and a liquid. This unique property allows dyes to dissolve easily and penetrate fabrics without needing harmful chemicals. Plus, the system is nearly closed-loop, meaning most of the CO₂ is recovered and reused, keeping waste to a minimum. Research shows scCO₂ dyeing can slash energy use by up to 50% and water use by an impressive 95% compared to traditional methods.

But it's not all smooth sailing. High equipment costs, dye solubility issues, and challenges with different fiber types have slowed adoption. Fortunately, recent innovations—like new dye formulas and improved processes—are breaking down these barriers. The technology is now stretching beyond synthetic fibers to natural ones like cotton and wool, hinting at a major industry shift.

Our team has been at the forefront of this research. We'll share our latest work using scCO₂ for natural dyeing of polyester, achieving outstanding color durability without the need for traditional, often toxic, mordants.

Profile:

- BSc, MSc, PhD in Textile Engineering (Textile chemistry and fiber science), from Amirkabir University of Technology, Tehran, Iran
- Associate Professor at Department of Textile Engineering, Yazd University, Yazd, Iran (Current)
- Director of the Textile Chemistry group at Yazd University
- Assistant Professor at Islamic Azad University, Birjand Branch, Iran (2004-2018)
- Among the top 2% most-cited scientists in the last 4 years

Publications:

- 98 papers in international journals (ISI and Scopus)
- 69 papers in international conferences
- Author of 16 book chapters and Editor of 4 books published by international publishers (Wiley, Taylor & Francis, Elsevier) and author of one book in Persian.

Activities:

- Member of editorial board of 3 International journals including: "Industria Textila" (ISI-WoS, Scopus), Research Journal of Textile and Apparel (ISI-WoS, Scopus), and "Textile & Leather Review" (Scopus)
- Reviewer of more than 50 ISI journals
- Member of scientific committee of 35 international conferences
- Keynote speaker of 10 international conferences
- Member of Iranian Textile Association of Science and Technology
- Member of Iranian Carpet Scientific Association
- 3 International projects (TUBITAK 2221) with Turkish universities
- 8 national projects in Islamic Azad University



ULUSLARARASI
LİF VE POLİMER
ARAŞTIRMALARI
SEMPOZYUMU

16th INTERNATIONAL FIBER AND POLYMER RESEARCH SYMPOSIUM

Sürdürülebilir ve İşlevsel Lif ve Polimerler
Sustainable and Functional Fibers & Polymers



BURSA
ULUDAĞ
ÜNİVERSİTESİ

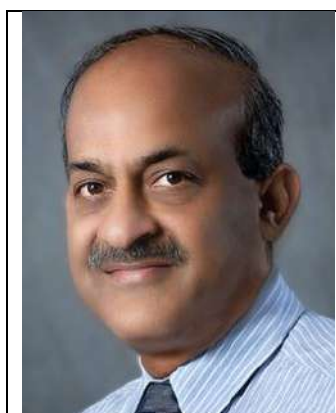
9-10 Mayıs
May 2025

İstanbul Teknik Üniversitesi
Gümüşsuyu Prof. Dr. Necmettin Erbakan Yerleşkesi

Istanbul Technical University
Gumussuyu Prof. Dr. Necmettin Erbakan Campus



BURSA TEKNİK
ÜNİVERSİTESİ



Keynote Speaker at the 16th ULPAS

Prof. Dr. Tushar K. Ghosh

Field of Study :Textile Engineering, Chemistry & Science

Affiliation :NC State University, Raleigh, NC, USA

**Biomimicry in Textiles: Past, Present,
and Potential**

Abstract

The natural world around us provides excellent examples of functional materials, structures, mechanisms, and systems that have evolved to adapt highly sophisticated problem-solving methods. The practice of learning from nature, or biomimicry, has been explained as “the conscious emulation of life’s genius.” Biomimicry is the incorporation of these natural principles by designers and engineers to create

something efficient in its raw material usage that functions optimally. This approach is not just about drawing inspiration from nature, but about creating tangible benefits. The foundation of biomimicry is based on the belief that nature follows the path of least resistance and consumes the least energy while using the most common materials available to perform a task. Throughout time, nature has evolved to develop highly sophisticated and efficient solutions, such as superhydrophobicity, self-cleaning, self-repair, energy conservation, drag reduction, dry adhesion, adaptable growth, and many others, in response to contemporary needs. Some of these solutions have inspired humans to achieve outstanding outcomes; fishing nets mimicked after spiders' webs have been in use for thousands of years, and the strength and stiffness of the hexagonal honeycomb shape have been adopted for use in lightweight structures required in airplanes and in other applications. Whether it be specialized riblets on the surface of a shark's skin to help them achieve high swimming speeds or functionally gradient materials found in animal and plant species with remarkable properties to meet demanding functional requirements for many contemporary engineering problems, nature can provide scientists efficient, time-tested and unique ideas of achieving a goal. There are numerous examples of functional surfaces, fibrous structures, structural colors, self-healing, thermal insulation, etc. that offer important lessons for the textile products of the future. While the paper underlines the need for sustainable design (and manufacturing) and consumption of textiles, It examines specific examples of a few bio-inspired textile structures. The paper argues the need for biomimicry by highlighting a few inherently sustainable biological systems that may be adapted to fit current textile technologies/products. The subsequent discussion focuses on the continuing effort at the SMARTextiles laboratory at NC State University toward developing multifunctional fiber and textiles. These include fiber-based actuators and mechanically gradient composites.

Profile:

Tushar K. Ghosh is the William A. Klopman Distinguished Professor of Textiles at the Wilson College of Textiles at the NC State University. He holds a Bachelor of Science degree in Textile Technology from the University of Calcutta, a Master of Science from the Indian Institute of Technology in Delhi, and a Ph.D. in Fiber and Polymer Science from North Carolina State University.

Prof. Ghosh has authored over 150 peer-reviewed journal articles and more than 100 scholarly works, including book chapters, monographs, and conference papers. His primary research interests span a diverse range of interdisciplinary areas, including the mechanics of fibrous structures, adaptive and responsive textiles, sensors, and actuators involving polymer nanocomposites, electroactive polymers, and biomimetic systems. In recognition of his fundamental contributions to the science and technology of fibrous materials, he received the Fiber Society's Founders Award in 2007. He was selected for the Circle of Excellence by the National Textile Center in 2008. Tushar is also a highly motivated educator and academic mentor. He has received Outstanding Teaching and Mentoring Awards at both the college and university levels for his effectiveness in instruction and mentoring.



ITÜ

16

ULUSLARARASI
LİF VE POLİMER
ARAŞTIRMALARI
SEMPOZYUMU

16th INTERNATIONAL FIBER AND POLYMER RESEARCH SYMPOSIUM

Sürdürülebilir ve İşlevsel Lif ve Polimerler
Sustainable and Functional Fibers & Polymers



BURSA
ULUDAĞ
ÜNİVERSİTESİ

9-10 Mayıs
May 2025

İstanbul Teknik Üniversitesi
Gümüşsuyu Prof. Dr. Necmettin Erbakan Yerleşkesi

Istanbul Technical University
Gumussuyu Prof. Dr. Necmettin Erbakan Campus



BURSA TEKNİK
ÜNİVERSİTESİ





Keynote Speaker at the 16th ULPAS

Prof. Dr. Nazmul Karim

Field of Study : **Professor of Sustainable Future Textiles at the Department of Fashion and Textiles.**

Affiliation : **University of Southampton, the U.K.**

New material-based smart wearable electronic textiles

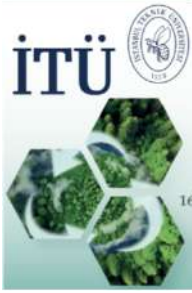
Abstract

The isolation of graphene in 2004 also unveiled a diverse range of graphene-like 2D materials with exceptional mechanical, thermal, and electrical properties. These materials can be stacked layer-by-layer in a fashion to create 2D heterostructure-based 'designer' textiles for the future with predefined enhanced properties and functionalities not found in the individual materials. 2D material-based textiles have shown promise for next-generation wearable electronic textiles (e-textiles) and sustainable composite applications due to their excellent mechanical, electrical, and other performance properties. However, the realization of robust and reliable smart textiles at a mass scale remains hugely challenging due to limitations in material performance and sustainability, complex and time-consuming fabrications, poor comfortability, and durability. We have developed a highly scalable and cost-effective way of manufacturing 2D material-based textiles at commercial production rates of ~150 m/min for fabrics and (~1000 kg/h) for textile yarns. The graphene textiles thus produced are washable, flexible, and bendable. We then demonstrate the potential uses of such textiles for multifunctional and high-performance wearable electronics and sustainable composites applications, which will be covered in this talk.

Speaker profile

Dr Nazmul Karim is a Professor of Sustainable Future Textiles at the Department of Fashion and Textiles. Prof Karim's research interests lie in the area of advanced materials (e.g., graphene, other 2D materials) and sustainable digital technologies (e.g., inkjet printing), aimed at developing scalable and cost-effective next-generation smart wearable electronic textiles (e-textiles), sustainable natural fibre reinforced composites, and high-performance functional clothing from bio-based or recycled materials. Previously, he was a Professor of Advanced Textiles at Nottingham Trent University, UK (2023-24), and an Associate Professor at the Centre for Print Research, UWE Bristol, UK (2019-23), where he led the establishment of the brand-new 'Graphene Applications Laboratory' and the new research theme 'New Materials: Towards Sustainable Technologies.' Before that, Prof Karim pioneered several graphene-based wearable electronic textiles (e-textiles) and sustainable composites researches at the National Graphene Institute (NGI) of the University of Manchester (UK) with Nobel Laureate Professor Sir Kostya S Novoselov (2015-19). He completed funded PhD (2015) and MSc by Research (2011) degrees at the University of Manchester (UK).

Prof Karim led several ground-breaking research including the world's first full-inkjet-printed graphene e-textiles, highly scalable methods to produce graphene textiles and 2D heterostructure-based textiles, and sustainable and multifunctional fibre-reinforced composites. Prof Karim also worked for BASF (2008-10), the world-leading chemical company, after graduating from Bangladesh University of Textiles (BUTex) in 2008. He has academic and industry experiences in fundamental research, innovation, and entrepreneurship, with a passion for getting research out of the lab into real-world applications.



16

ULUSLARARASI
LİF VE POLİMER
ARAŞTIRMALARI
SEMPOZYUMU

16th INTERNATIONAL FIBER AND POLYMER RESEARCH SYMPOSIUM

Sürdürülebilir ve İşlevsel Lif ve Polimerler
Sustainable and Functional Fibers & Polymers



9-10 Mayıs
May 2025

İstanbul Teknik Üniversitesi
Gümüşsuyu Prof. Dr. Necmettin Erbakan Yerleşkesi

Istanbul Technical University
Gumussuyu Prof. Dr. Necmettin Erbakan Campus



Keynote Speaker at the 16th ULPAS

Prof. Dr. Alexander, Seifalian

Affiliation :Royal Free Hospital and University College London, England

Graphene and Butterfly-Inspired Fibre: A Revolution in Medical Devices and Textiles Industrial

Alexander Seifalian^{1,2,3}, Varun Hedge¹, Azia Bolger¹ and Victoria Mataczynski¹

Nanotechnology and Regenerative Medicine Commercialisation Centre (¹NanoRegMed Ltd, ²Nanoloom Ltd & ³Liberum Health Ltd), The London BioScience Innovation Centre, London, United Kingdom

In recent years, smart nanomaterials have shown tremendous promise in replacing damaged tissues and advancing regenerative medicine. A landmark moment came in 2010 when UK-based scientists isolated a single layer of carbon atoms—graphene—on Scotch tape. Since then, graphene has been hailed as a "wonder material" due to its remarkable properties: it is 100 times stronger than steel, highly elastic, and an excellent electrical conductor. Structurally, it consists of carbon atoms arranged in a hexagonal, honeycomb-like lattice.

Our research focuses on functionalised graphene oxide (FGO) integrated with polyhedral oligomeric silsesquioxane (POSS), inspired by the nanostructures found in butterfly wings. This composite is not only non-toxic and antibacterial but also ideal for a range of biomedical applications, including drug and gene delivery, biosensing, and the development of nanocomposites for organ engineering.

In this presentation, I will showcase our latest work on the use of FGO-POSS in the fabrication of medical sensors, delivery systems for drugs, genes, and stem cells, and in the bioengineering of human organs using stem cell technologies.

These materials can be processed into fibres through a wet spinning technique and assembled into scaffolds functionalised with bioactive molecules. When seeded with stem cells, these scaffolds support the regeneration of complex human tissues. I will present data supporting the successful development of organ prototypes using this approach. Furthermore, the same fibres have shown potential in textile manufacturing, broadening the industrial relevance of this technology.

In conclusion, graphene and POSS-based nanocomposites offer groundbreaking opportunities for addressing unmet clinical needs through the creation of functional human organs and advanced medical devices.

Profile:

Professor Alexander Seifalian

CEO and Professor Nanotechnology & Regenerative Medicine

Nanotechnology & Regenerative Medicine Commercialisation Centre (Ltd)

Alexander Seifalian, Professor of Nanotechnology and Regenerative Medicine worked at the Royal Free Hospital and University College London for over 26 years, during this time he spent a year at Harvard Medical School looking at caused of cardiovascular diseases and a year at Johns Hopkins Medical School looking at the treatment of liver cancer. He

published more than 687 peer-reviewed research papers and registered 14 UK and International patents. On editorial boards of 41 journals. He supervised 121 PhD students, all successfully completed. He is currently co-founder of NanoRegMed Ltd and Nanoloom Ltd working on the commercialisation of his research and scientific director of Liberum Health Ltd. During his career, Prof Seifalian has led and managed many large projects with successful outcomes in terms of commercialisation and translation to patients. In 2007 he was awarded the top prize in the field for the development of nanomaterials and technologies for cardiovascular implants by Medical Future Innovation, and in 2009 he received a Business Innovation Award from UK Trade & Investment (UKTI). He was the European Life Science Awards' Winner of Most Innovative New Product 2012 for the "synthetic trachea". Prof Seifalian won the Nanosmat Prize in 2013 and in 2016 he received the Distinguish Research Award in recognition of his outstanding work in regenerative medicine from Heals Healthy Life Extension Society. His achievements include the development of the world first synthetic trachea, lacrimal drainage conduit, and vascular bypass graft using nanocomposite materials, bioactive molecules and stem cell technology. Currently, he is working on the development and commercialisation of human organs using graphene-based nanocomposite materials and stem cells technology. Recently he has commercialised a novel functionalised graphene oxide for medical and other industrial applications and synthetic graphene-based nanocomposite materials for surgical and medical devices application. He is currently working on the development of facial organs, heart valves and tendons.

ORCID: <https://orcid.org/0000-0002-8334-9376>

h-index = 112



16
ULUSLARARASI
LİF VE POLİMER
ARAŞTIRMALARI
SEMPOZYUMU
16th INTERNATIONAL FIBER AND POLYMER RESEARCH SYMPOSIUM
Sürdürülebilir ve İşlevsel Lif ve Polimerler
Sustainable and Functional Fibers & Polymers

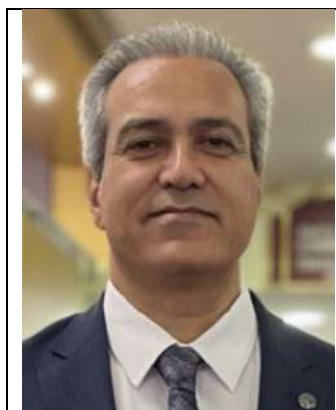


BURSA
ULUDAĞ
ÜNİVERSİTESİ

**9-10 Mayıs
May 2025**
İstanbul Teknik Üniversitesi
Gümüşsuyu Prof. Dr. Necmettin Erbakan Yerleşkesi
Istanbul Technical University
Gumussuyu Prof. Dr. Necmettin Erbakan Campus



BURSA TEKNİK
ÜNİVERSİTESİ



Keynote Speaker at the 16th ULPAS

Assoc. Prof. Dr. SeyedMansour BIDOKI

Field of Study :Color and Polymer Chemistry

Affiliation :Yazd University, Iran & Istanbul Technical University & Tepar
Textile Türkiye

**Reinforcement of 3D Concrete Printed
Buildings by Filament Yarns**

Abstract:

Additive manufacturing, particularly in the context of concrete 3D printing (3DCP), has gained significant interest due to its material efficiency and ability to achieve geometries with high complexity. One of the various challenges within 3DCP is the low interlayer bonding, leading to anisotropic mechanical properties. The present study summarizes some of the in-process vertical reinforcing techniques to address this issue, including mechanical insertions, wire embedding, and sophisticated integration of reinforcements. The article covers recent progress, patents, and experimental studies, highlighting their benefits and limitations. The patented technique recently filed for in-process weaving or knitting the reinforcing mesh inside the printed layers is also introduced for the first time which believe to revolutionize 3DCP building industry.

Profile:

Dr. Seyedmansour Bidoki is a distinguished academic and researcher with a PhD in Colour and Polymer Chemistry from the University of Leeds, United Kingdom, as well as MSc and BSc degrees in Textile Chemistry and Fibre Science from Amirkabir University of Technology and Isfahan University of Technology, respectively. He is currently serving as a Guest Professor at Istanbul Technical University, Türkiye, and as an Associate Professor at Yazd University, Iran. Dr. Bidoki possesses extensive expertise in textile chemistry, polymer science, smart textiles, and nanotechnology, with over two decades of academic, research, and industrial experience.

Throughout his career, Dr. Bidoki has held numerous leadership roles, including Head of the Textile Department and Registrar's Office at Yazd University, and has served as the Scientific Secretary of the 12th National Iranian Textile Conference. His industrial contributions are notable, including patents for innovative technologies such as a fully automated water recycling system for textile wastewater and an electrochemical ozone production method. His research encompasses diverse fields, including biodegradable polymers, textile electronics, sustainable recycling methods, and eco-efficiency analysis of textile processes.



ULUSLARARASI
LİF VE POLİMER
ARAŞTIRMALARI
SEMPOZYUMU

16th INTERNATIONAL FIBER AND POLYMER RESEARCH SYMPOSIUM

Sürdürülebilir ve İşlevsel Lif ve Polimerler
Sustainable and Functional Fibers & Polymers



BURSA
ULUDAĞ
ÜNİVERSİTESİ

9-10 Mayıs 2025

İstanbul Teknik Üniversitesi
Gümüşsuyu Prof. Dr. Necmettin Erbakan Yerleşkesi

Istanbul Technical University
Gumussuyu Prof. Dr. Necmettin Erbakan Campus



BURSA TEKNİK
ÜNİVERSİTESİ





Keynote Speaker at the 16th ULPAS

Prof. Dr. Osman BABAARSLAN

Field of Study :**Engineering Manufacturing, Materials Science Textiles,**
Affiliation :**Çukurova University, Türkiye**

**Sustainability from the Perspective of
Product and Process Innovation in Fiber
and Yarn Spinning**

Abstract:

Sustainability in fiber and yarn spinning is becoming increasingly significant due to growing environmental concerns and the need for resource-efficient production methods. This keynote presentation explores sustainability from the product and process innovation perspective, focusing on raw material selection and technological advancements in yarn manufacturing. The discussion highlights the shift towards sustainable fiber alternatives, including bio-based, recycled, and biodegradable fibers, which are eco-friendly substitutes for conventional synthetic fibers. It also explores innovative spinning techniques such as hybrid and composite yarns, which improve functionality while reducing environmental impact. This discussion further addresses the role of automation, artificial intelligence, and energy-efficient spinning technologies in optimizing production processes and minimizing waste. Additionally, the presentation discusses the historical evolution of competitiveness in the textile industry, where sustainability has emerged as a key differentiator. The discussion underscores the importance of R&D in achieving higher efficiency, product diversification, and sustainable development within the industry. Emphasis is placed on eco-innovation strategies, circular economy principles, and responsible production practices to ensure long-term sustainability. By integrating sustainable materials, advanced manufacturing technologies, and circular economy models, the spinning industry can significantly reduce its environmental footprint while maintaining high-quality standards. This presentation provides a comprehensive overview of sustainability-driven transformations in

fiber and yarn spinning, offering valuable insights for academia, industry professionals, and policymakers aiming to enhance environmental responsibility in the textile sector.

Profile:

Biography Osman Babaarslan is a Professor in Department of Textile Engineering, University of Çukurova, Turkey. He received his BSc degree from Erciyes University in Mechanical Engineering (1988), Turkey and PhD degree from The University of Leeds in 1996 at Department of Textile Industries, UK. He is now working nearly twenty-five years as a Professor of the Textile Technology Division in Textile Engineering Department, specialized in Textile Materials and Technology. He has authored more than 300 peer reviewed publications and congress articles published in English and Turkish, 8 book chapters in English, 5 Turkish and 4 International patents (EP) have been published up to now.

Research Interests: Specialized in Textile Materials and Technology; Spinning Technology, Nonwovens and Technical Textiles, Material Testing and Quality Control,



ULUSLARARASI
LİF VE POLİMER
ARAŞTIRMALARI
SEMPZYUMU

16th INTERNATIONAL FIBER AND POLYMER RESEARCH SYMPOSIUM

Sürdürülebilir ve İşlevsel Lif ve Polimerler
Sustainable and Functional Fibers & Polymers



BURSA
ULUDAĞ
ÜNİVERSİTESİ

9-10 Mayıs 2025

İstanbul Teknik Üniversitesi
Gümüşsuyu Prof. Dr. Necmettin Erbakan Yerleşkesi

Istanbul Technical University
Gumussuyu Prof. Dr. Necmettin Erbakan Campus



BURSA TEKNİK
ÜNİVERSİTESİ



Keynote Speaker at the 16th ULPAS

Prof. Dr. Murat Kazancı

Field of Study :**Professor of Biomedical Engineering**

Affiliation :**Istanbul Medeniyet University, Türkiye**

Sustainable Biomaterial Frontiers: From Marine Waste to Advanced Functional Materials through Novel Spinning Technologies

Abstract:

The urgent need for sustainable alternatives to petroleum-based materials has driven significant research into natural polymers derived from renewable resources. This keynote presentation will explore our comprehensive work on the extraction and processing of biopolymers from diverse sources, with special emphasis on marine waste valorization.

Our research encompasses the extraction of collagen from multiple sources including bovine skin, rat tail tendon, jellyfish, and mussel byssus, as well as polysaccharide isolation from hemp, agricultural market waste, seaweed, and marine mucilage. We will discuss how these extraction methodologies can be optimized to preserve the native structure and functionality of these biopolymers.

The presentation will highlight our innovative approaches to transform these extracted biomaterials into functional micro- and nanofibers through various spinning technologies: electrospinning, centrifugal spinning, wet spinning, and self-assembly processes. Particular attention will be given to our latest advances in converting marine waste into high-value materials, addressing both environmental concerns and creating novel biomaterials with applications in healthcare, filtration, packaging, and environmental remediation.

Characterization data from synchrotron FTIR, Raman spectroscopy, and electron microscopy will illustrate the structural properties of these biomaterials and how processing parameters influence their performance. The presentation will conclude with our vision for scaling these technologies toward commercial applications and their potential impact on developing a more sustainable circular bioeconomy.

Profile:

Prof. Dr. Murat Kazanci is a distinguished researcher specializing in biopolymer materials, nanofiber production, and biomaterial characterization. He currently serves as Professor and Head of Department of Biomedical Engineering at Istanbul Medeniyet University, as well as Head of Nanoscience and Nanoengineering programs.

Dr. Kazanci received his Ph.D. in Applied Chemistry from The Hebrew University of Jerusalem (2003), where he studied polyethylene fiber reinforced composites for biomedical prostheses. His academic journey includes an M.S. in Fiber Sciences from Cornell University (1991) and a B.S. in Textile Engineering from Istanbul Technical University (1990).

His research focuses on collagen nanofibers, biomaterial development, and advanced characterization techniques including synchrotron FTIR microspectroscopy and Mueller matrix polarimetry. He has published extensively in prestigious international journals and has led numerous national and international research projects.

Throughout his career, Dr. Kazanci has held academic positions at renowned institutions including Karlsruher Institut für Technologie, Universität Heidelberg, and Max-Planck Institute of Colloids and Interfaces. He is an active member of the Turkish Electron Microscopy Society and has served as an external expert for European Union Commission projects.



ULUSLARARASI
LİF VE POLİMER
ARAŞTIRMALARI
SEMPOZYUMU

16th INTERNATIONAL FIBER AND POLYMER RESEARCH SYMPOSIUM

Sürdürülebilir ve İşlevsel Lif ve Polimerler
Sustainable and Functional Fibers & Polymers



BURSA
ULUDAĞ
ÜNİVERSİTESİ

9-10 Mayıs
May 2025

İstanbul Teknik Üniversitesi
Gümüşsuyu Prof. Dr. Necmettin Erbakan Yerleşkesi

Istanbul Technical University
Gumussuyu Prof. Dr. Necmettin Erbakan Campus





Keynote Speaker at the 16th ULPAS

Associate Prof. Dr. Ahmad Mukifza Harun

Affiliation :Malaysia's Nanotechnology Centre (NNC), Malaysia

**Effect of modified hydrothermal
nanotitania on the viability of
Streptococcus Pneumoniae**

Abstract:

Staphylococcus aureus (S. aureus) is an important bacterium with significant pathological implications in the field of medicine. Attempting to cure bacterial infections at an advanced stage results in considerable waste of time, effort and expenditure. Thus, the prevention of such illnesses is paramount. Besides using chemical drugs to treat infections, several non-organic extracts have been tested in trials and been shown to impede the bacteria's growth. This paper proposes that modified hydrothermal nanotitania extract has great potential as a means to combat this lethal organism. In tests, the viability of S. aureus is shown to be markedly reduced after being mixed with agar containing the nanotitania extract. The ability of the nanotitania extract to inhibit the growth of S. aureus indicates its anti-microbial characteristics.

Keywords: nanotitania extract, streptococcus pneumoniae

Profile:

Bibliography

Associate Professor Ahmad Mukifza Harun is a Director at Malaysia's Nanotechnology Centre (NNC), Ministry of Science, Technology and Innovation, Putrajaya Malaysia. NNC plays a pivotal role in steering Malaysia's nanotechnology initiatives, ensuring strategic alignment with national policies, fostering innovation, and enhancing global collaborations to position Malaysia as a leader in nanotechnology. He is also a lecturer at the Faculty of Engineering, Universiti Malaysia Sabah. He holds a PhD in Electrical Engineering from the University of Leeds. He specializes in Electrical Engineering (Nanotechnology) and also a professional engineer. His working experience in South Korea, Japan, and Malaysia adds value to his expertise, particularly in the fields of academia, research, and industry. In addition to being a Panel Member for Engineering Accreditation Council (EAC) and Engineering Technology Accreditation Council (ETAC), he is also a certified engineer from Sony Corporation in product safety. His current research focuses on nanotechnology for the development of biotechnology-based products.



**ULUSLARARASI
LİF VE POLİMER
ARAŞTIRMALARI
SEMPOZYUMU**

16th INTERNATIONAL FIBER AND POLYMER RESEARCH SYMPOSIUM

Sürdürülebilir ve İşlevsel Lif ve Polimerler
Sustainable and Functional Fibers & Polymers



**BURSA
ULUDAĞ
ÜNİVERSİTESİ**

**9-10 Mayıs
May 2025**

İstanbul Teknik Üniversitesi
Gümüşsuyu Prof. Dr. Necmettin Erbakan Yerleşkesi

Istanbul Technical University
Gumussuyu Prof. Dr. Necmettin Erbakan Campus



**BURSA TEKNİK
ÜNİVERSİTESİ**



Keynote Speaker at the 16th ULPAS

Prof. Dr. Sabit Adanur

Field of Study :Textile and Mechanical engineering, 3D Printing

Affiliation :Auburn University Auburn, Alabama, USA

**Fused Deposition Modeling (FDM) –
methods, materials and applications for
flexible fabric structures**

Abstract:

This keynote speech reviews Fused Deposition Modeling (FDM) used in additive manufacturing, its techniques, materials, process parameters, and the development of flexible fabric structures. It also reviews significant FDM techniques, material compatibility (composite filaments and thermoplastics), and impacts of process parameters (extrusion temperature, infill density, and layer thickness) on part properties. It highlights FDM's advantages—cost savings, design freedom, and minimal waste—at the expense of minimizing limitations like anisotropic properties and surface quality. Recent applications in textiles, such as programmable textiles, multi-material wearables, and 3D-printed accessories, demonstrate the potential of FDM to revolutionize traditional textile manufacturing by enabling on-demand production and complex geometries. The speech concludes by recommending parameter optimization and future research directions for enhancing the viability of FDM in functional and sustainable textile applications.

Profile:

Prof. Sabit Adanur is a Professor of Mechanical Engineering at Auburn University in Alabama, USA. With a specialization

in additive manufacturing and materials engineering, his research focuses on Fused Deposition Modeling (FDM), process optimization, and new applications in flexible fabric structures. He has contributed extensively to the understanding of the interrelation between material properties, process parameters, and mechanical performance of 3D-printed polymers. Prof. Adanur leads graduate researchers in learning about advanced composites and environmentally friendly manufacturing solutions, as seen in his collaborative research on the use of FDM in textile innovation. His work bridges academic research and industrial applications with an emphasis on low-cost and environmentally friendly manufacturing technologies.



16 ULUSLARARASI
LİF VE POLİMER
ARAŞTIRMALARI
SEMPOZYUMU
16th INTERNATIONAL FIBER AND POLYMER RESEARCH SYMPOSIUM
Sürdürülebilir ve İşlevsel Lif ve Polimerler
Sustainable and Functional Fibers & Polymers



BURSA
ULUDAĞ
ÜNİVERSİTESİ

9-10 Mayıs
May 2025
İstanbul Teknik Üniversitesi
Gümüşsuyu Prof. Dr. Necmettin Erbakan Yerleşkesi
Istanbul Technical University
Gumussuyu Prof. Dr. Necmettin Erbakan Campus



BURSA TEKNİK
ÜNİVERSİTESİ





Keynote Speaker at the 16th ULPAS

**Assoc. prof. Dr. AIJAZ AHMED
BABAR**

Field of Study :**Tailored Fibrous NetworksJanus Membranes**

Affiliation :**Institute for Advanced Study, Shenzhen University, China**

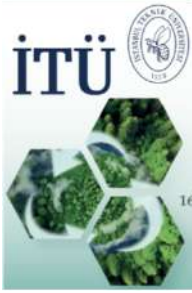
**Electrospun Janus Fibrous Materials for
Moisture Management Textiles**

Abstract:

Electrospun Janus fibrous materials with bimodal wettability offer a paradigm shift in moisture management textiles. Through the combination of hydrophobic and hydrophilic surfaces within a single fiber structure, these new fabrics enable directional water transport, rapid drying, and enhanced wearer comfort. This approach not only mimics natural systems but also provides scalable solutions for next-generation functional clothing and high-performance sportswear.

Profile:

Dr. Aijaz Ahmed Babar is a highly prolific researcher in the field of functional nanomaterials, smart textiles, and advanced fiber technologies. With a Doctor of Engineering degree from Donghua University, China, and over 35 SCIE-indexed publications with a total impact factor of more than 300, he has considerable experience in nanofiber production, textile development, and moisture management systems. Currently a Postdoctoral Research Fellow at Shenzhen University, he has a prominent international research presence and established track record in both academic and industrial textile research.



16

ULUSLARARASI
LİF VE POLİMER
ARAŞTIRMALARI
SEMPOZYUMU

16th INTERNATIONAL FIBER AND POLYMER RESEARCH SYMPOSIUM

Sürdürülebilir ve İşlevsel Lif ve Polimerler
Sustainable and Functional Fibers & Polymers



9-10 Mayıs
May 2025

İstanbul Teknik Üniversitesi
Gümüşsuyu Prof. Dr. Necmettin Erbakan Yerleşkesi

Istanbul Technical University
Gumussuyu Prof. Dr. Necmettin Erbakan Campus



Keynote Speaker at the 16th ULPAS

Prof. Dr. Nader Shehata

Field of Study : **Electronics, Nanotechnology, optics, semiconductor fabrication**

Affiliation : **Alexandria University, Egypt**

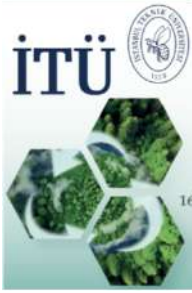
Piezoelectric Nanofibers: Challenges and Future Aspects

Abstract:

Piezoelectric nanofiber mats have attracted tremendous interest over the last two decades in both tracks of research and products. Such nanofibers can convert mechanical excitations into electric signals with an improved efficiency according to higher surface-to-volume ratio within lower nano-dimension synthesized fibers. However, there are plenty of challenges against such energy harvesting nanofibers to be competitive with piezoelectric ceramics. This talk discusses the main important aspects of piezoelectric nanofibers mats along with recent updated research progress to develop the mats' piezoresponse including sensitivity and output electric voltage/power. Such discussed updates do not only include material-based solutions such as nucleating additives, but also involve processing techniques, prototype design, and circuits-based supportive solutions. The impact of these updates can enhance both present and future polymeric piezoelectric devices as self-powered units within different applications such as wearable electronics, footstep energy harvesters, and industrial vibrational/acoustic transducers.

Presenter: Prof Nader Shehata

Short Bio: Dr Nader Shehata is a physics associate professor and director of Office of Research, Innovation, and Sustainability (ORIS) at Kuwait College of Science and Technology (KCST). In addition, he is on sabbatical leave from Alexandria University, Egypt, where he is a physics professor and associate director of the Centre of Smart Materials, Nanotechnology, and Photonics (CSMNP). Also, he is an adjunct associate professor at the Faculty of Science, Utah State University, United States and was a Lecturer of Electronic Engineering at Ulster University, United Kingdom. Over 15 years, Dr Shehata works in the research fields of nanostructures synthesis, characterization, and correlated applications in piezoelectric energy harvesting, environmental sensing, solar cells, and biomedicine. He secured around 2.1M US Dollars of research grants from different international and local funding agencies, along with more than 70 journal publications where most of them were published in Q1/Q2 journals along with more than 20 international conference appearances including invited talks, oral presentations, poster sessions, and proceedings. Furthermore, he is an editor-in-chief and topical guest editor in different nanotechnology journals with two edited books, few edited book chapters, and reviewer for different funding agencies and journals. Also, he is a senior member in IEEE and a fellow with UK Higher Education (FHEA), where he has excellent teaching experience of both undergraduate and graduate courses in engineering physics and electronic engineering disciplines.



16

ULUSLARARASI
LİF VE POLİMER
ARAŞTIRMALARI
SEMPOZYUMU

16th INTERNATIONAL FIBER AND POLYMER RESEARCH SYMPOSIUM

Sürdürülebilir ve İşlevsel Lif ve Polimerler
Sustainable and Functional Fibers & Polymers



9-10 Mayıs
May 2025

İstanbul Teknik Üniversitesi
Gümüşsuyu Prof. Dr. Necmettin Erbakan Yerleşkesi

Istanbul Technical University
Gumussuyu Prof. Dr. Necmettin Erbakan Campus



Inspiring Talk at the 16th ULPAS

Presenter: Assist. Prof. Dr. Mehmet Durmuş Çalışır,

Co-authors: Ali Toptaş, Melike Güngör, Yasin Akgül, Ali KILIÇ

Affiliation :Recep Teyep Erdogan University, Rize, Türkiye

From Nature to Engineering

Abstract:

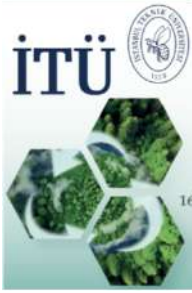
This study explores how natural filtration systems have inspired advanced engineering solutions, with a particular focus on biomimetic fiber-based filtration technologies. In living organisms, filtration occurs across multiple biological scales: lungs trap dust and pathogens, kidneys use glomerular nanofiltration to purify blood, and even the brain filters sensory overload to maintain cognitive focus. Nature's efficiency extends to mussels, fish gills, and plant roots—each with specialized filtration mechanisms. Mussels perform active filtration by capturing particles from seawater, while fish gill rakers remove food particles and simultaneously conduct gas exchange. Plant roots filter ions selectively through the Casparian strip, regulating mineral uptake.

These biological insights have led to innovative material designs. Spider silk, known for its strength and flexibility, has inspired electrospun nanofiber membranes. Penguin downy feathers have influenced the development of branched fiber architectures with high surface area and minimal pressure drop. Hollow fiber membranes mimic glomerular filtration, while fish gill-inspired membranes fabricated via micro-3D printing achieve flow-guided particle deflection without chemical coatings. Therefore, nature provides not only solutions to complex engineering problems but also a model of sustainable, multifunctional design. This work underscores the potential of biomimicry in developing next-generation filtration systems across biomedical and environmental fields.

Profile:

Dr. Mehmet Durmuş Çalışır received his undergraduate degrees in Materials Science and Engineering and Electronics Engineering. He earned his Ph.D. from the Nanoscience and Nanoengineering Program at Istanbul Technical University. His research primarily focuses on the synthesis of nanostructured metal oxide materials with diverse morphologies (such as nanorods, nanofibers, thin films, etc.) and compositions (including undoped and doped TiO₂, ZnO, SnO₂, among others). These materials are explored for their potential in perovskite solar cells, filtration systems, and photocatalytic applications.

Currently, he is a faculty member in the Department of Electrical and Electronics Engineering at Recep Tayyip Erdoğan University, where he conducts research on early warning systems for healthcare applications using polymer-based pressure and stretch sensors, as well as mobile software development for Android platforms. His ongoing work also includes the development of high-efficiency air filters and innovative food packaging solutions based on nanofibrous surfaces.



16

ULUSLARARASI
LİF VE POLİMER
ARAŞTIRMALARI
SEMPOZYUMU

16th INTERNATIONAL FIBER AND POLYMER RESEARCH SYMPOSIUM

Sürdürülebilir ve İşlevsel Lif ve Polimerler
Sustainable and Functional Fibers & Polymers



9-10 Mayıs
May 2025

İstanbul Teknik Üniversitesi
Gümüşsuyu Prof. Dr. Necmettin Erbakan Yerleşkesi

Istanbul Technical University
Gumussuyu Prof. Dr. Necmettin Erbakan Campus



Keynote Speaker at the 16th ULPAS

Assoc. Prof. Dr. Mehmet Ali Tibatan

Field of Study :MicroBiology, Nanotechnology, Electro spinning

Affiliation :Istanbul Zaim University, Türkiye

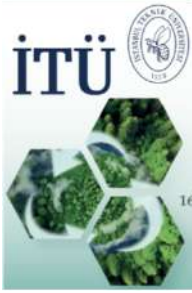
Cell Communication in Wound Healing

Abstract:

Wound healing is an active, complex process with coordinated cell and molecular interactions between various cell types and signals. Cell communication, and in this case, between structural cells such as fibroblasts and keratinocytes and immune cells such as macrophages, is key to this process. During the initial inflammatory phase, M1 macrophages are recruited to kill pathogens and cellular debris by pro-inflammatory signaling. With advancing healing, there is a phenotypic switch to M2 macrophages, which is necessary for the resolution of inflammation and the initiation of tissue repair. These macrophages communicate with fibroblasts to initiate extracellular matrix production and with keratinocytes to initiate re-epithelialization. In disease states such as chronic diabetic wounds, however, abnormal cell signaling leads to chronic inflammation and poor tissue regeneration. Clarification of the intricacy of these cell-cell interactions and signaling molecules provides context to the development of advanced therapeutic solutions, like smart biomaterials, that can alter cellular behavior and trigger productive and functional wound healing.

Profile:

M.Ali Tibatan received a Ph.D. in Biotechnology from Istanbul University, specializing in cancer molecular biology. Following the completion of doctoral studies, Dr. [Tibatan] conducted postdoctoral research at Istanbul Technical University, focusing on biomedical products within the Department of Textile Engineering. Currently, Dr. [Tibatan] is serving as a faculty member in the Department of Molecular Biology and Genetics at Istanbul Zaim University.



16

ULUSLARARASI
LİF VE POLİMER
ARAŞTIRMALARI
SEMPOZYUMU

16th INTERNATIONAL FIBER AND POLYMER RESEARCH SYMPOSIUM

Sürdürülebilir ve İşlevsel Lif ve Polimerler
Sustainable and Functional Fibers & Polymers



9-10 Mayıs
May 2025

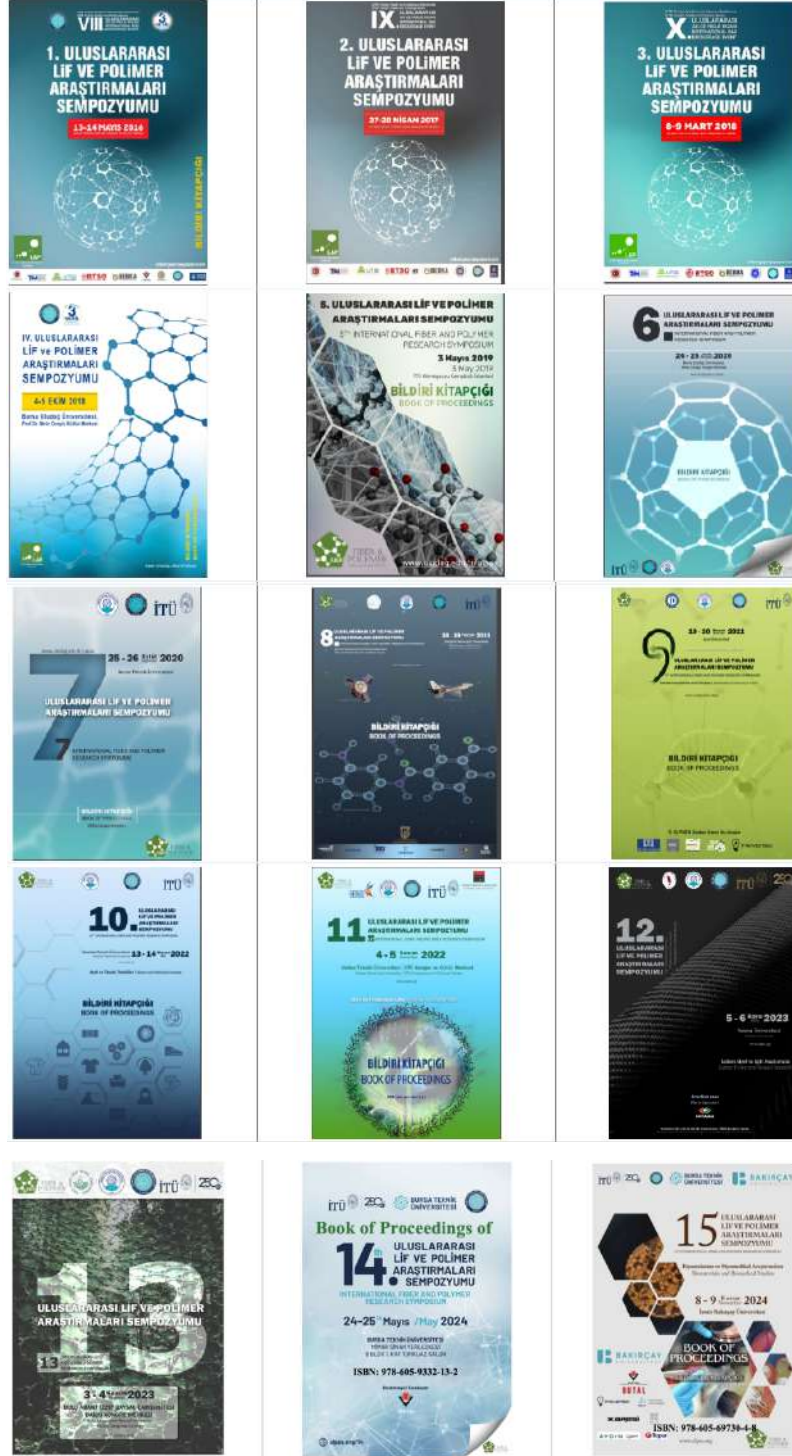
İstanbul Teknik Üniversitesi
Gümüşsuyu Prof. Dr. Necmettin Erbakan Yerleşkesi

Istanbul Technical University
Gumussuyu Prof. Dr. Necmettin Erbakan Campus



You can reach the Book of Proceedings of the previous ULPAS from the following link;

<https://www.ulpas.org/16/Home/Content?id=112>



İTÜ



BURSA
ULUDAĞ
ÜNİVERSİTESİ



BURSA TEKNİK
ÜNİVERSİTESİ



16 ULUSLARARASI LİF VE POLİMER ARAŞTIRMALARI SEMPOZYUMU

16th INTERNATIONAL FIBER AND POLYMER RESEARCH SYMPOSIUM

Sürdürülebilir ve İşlevsel Lif ve Polimerler
Sustainable and Functional Fibers & Polymers



9-10 Mayıs 2025
May

İstanbul Teknik Üniversitesi

Gümüşsuyu Prof. Dr. Necmettin Erbakan Yerleşkesi

Istanbul Technical University

Gumussuyu Prof. Dr. Necmettin Erbakan Campus















16th ULPAS Sponsors

 **Karesi HOLDİNG**

 **KIPAS TEXTILES**

TEKSKOM

TEKSKOM DIŞ TİC. A.Ş.

 **eco**
fill

ECOFİL DIŞ TİC. A.Ş.

 **IQKOD**

IQ KOD YAZILIM TİC. A.Ş.


 **MÜLK TAKİBİ**

WWW.MULKTAKIBI.COM

 **inovenso**
innovative engineering solutions

 **Tepar**

 **AYDIN** | more
to explore


AREKA

Advanced
Technologies

Scientific Committee



Prof. Dr. YUSUF ULCAI

Field of Study : **Textile**

Affiliation : **Bursa uludag University, Turkiye**



Prof. Dr. Ayşe Bedeloğlu

Field of Study : **Textile Engineering, Nanotechnology, Advanced filtration techn**

Affiliation : **Bursa uludag University, Turkiye**



Prof. Dr. Kenan CEVEN

Affiliation : **Bursa uludag University, Turkiye**



Prof. Dr. Behnam POURDEYHIMI

Affiliation : **North Carolina State University, USA**



Prof. Dr. Hamit Erdemi

Affiliation : **Yalova University, Turkiye**



Prof. Dr. Kenan Yıldırım

Affiliation : **Bursa Technical University, Turkey**



Prof. Dr. Cem GUNEŞOĞLU

Affiliation : **Gazianep University, Turkiye**



Prof. Dr. Yıldırım Turhan

Affiliation : **Pamukkale University, Turkiye**



Prof. Dr. Sabit Adanur

Field of Study : **Textile and Mechanical engineering, 3D Printing**

Affiliation : **Auburn University, USA**



Prof. Dr. Mehmet KANIK

Affiliation : **Bursa uludag University, Turkiye**



Prof. Dr. Mustafa Erdem UREYEN

Affiliation : **Eskisehir Teknik University, Turkiye**



Prof. Dr. Esra KARACA

Affiliation : **Bursa uludag University, Turkiye**



Prof. Dr. Ali DEMİR

Field of Study : **Textile technologies, Nano textures**

Affiliation : **Istanbul Technical University, Turkiye**



Prof. Dr. Nevin Çiğdem Gürsoy

Field of Study : **Textile Chemistry and Fiber Science Textile Finishing**

Affiliation : **Istanbul Technical University, Turkiye**

[Personal Website](#)



Prof. Dr. Levent ONAL

Affiliation : **Istanbul Technical University, Turkiye**



Prof. Dr. Cem GOK

Field of Study : **Biomaterial, NanoTechnology**

Affiliation : **Izmir Bakircay University, Turkiye**

[Personal Website](#)



Prof. Dr. Islam Shyha

Field of Study : **Manufacturing Engineering**

Affiliation : **Edinburgh Napier University, U.K.**



Prof. Dr. Mustafa OKSUZ

Affiliation : **Yalova University, Turkiye**



Dr. Abdelrahman Abdelgawad

Affiliation : **North Carolina State University, USA**



Prof. Dr. Osman BABAARSLAN

Affiliation : **Cukurova University, Turkiye**



Prof. Dr. Mohammad JAWAID

Affiliation : **Universiti Putra, Malaysia**



Dr. Muhammet AKAYDIN

Affiliation : **Usak University, Turkiye**



Prof. Dr. Hasan Basri Kocer

Affiliation : **Bursa Technical University, Turkey**



Prof. Dr. Ramazan ERENLER

Affiliation : **Gazi Osman Pasa University, Turkiye**

Scientific Committee



Prof. Dr. Rachid BOUHFID



Assoc. prof. Dr. Ali Kılıç

Affiliation : Istanbul Technical University, Türkiye



Assoc. Prof. Dr. SeyedMansour Bidoki

Affiliation : Yazd University, Iran & Istanbul Technical University, Türkiye



Assoc. Prof. Dr. Hüseyin AVCI

Affiliation : Eskişehir University, Türkiye



Assoc. prof. Dr. Ali AKPEK

Affiliation : Yildiz Teknik University, Türkiye



Assoc. prof. Dr. Eren ONER

Affiliation : Usak University, Türkiye



Assoc. prof. Dr. Fatih SUVARI

Affiliation : Bursa uludag University, Türkiye



Assoc. prof. Dr. Tarık ARAFAT

Affiliation : Bangladesh University of Engineering and Technology, Bangladesh



Assoc. Prof. Dr. Idris KARAGÖZ

Affiliation : Yalova University, Türkiye



Assoc. prof. Dr. Yasemin BALCIK TAMER

Affiliation : Yalova University, Türkiye



Assoc. prof. Dr. Amin Esmaeili

Affiliation : University of Doha for Science and Technology, Qatar

[Personal Website](#)



Assoc. Prof. Dr. Aminodin Haji

Affiliation : Yazd University, Iran



Dr. Yasin ALTIN

Affiliation : Bursa Technical University, Turkey



Dr. Yusuf Polat

Affiliation : Marmara University, Türkiye



Dr. Yasin Akgul

Affiliation : Karabük University, Türkiye



Dr. Ali Imran AYTEN

Affiliation : Yalova University, Türkiye



Dr. Gülçin Baysal

Affiliation : Istanbul Technical University, Türkiye



Dr. Ismail Borazan

Affiliation : Bursa Technical University, Turkey



Dr. Nadeem Bukhari

Affiliation : Istanbul Technical University, Türkiye



Dr. Mehmet Durmuş Çalışır

Affiliation : Recep Tayyip Erdoğan University, Türkiye



Dr. Aslı BALÇAK GIRGIN

Affiliation : Bursa uludag University, Türkiye



Dr. Fatma Demirci



Dr. Pınar TAŞDELEN ENGİN

Position : Polyteks Textile, Türkiye



Dr. Tamer HAMOUDA

Affiliation : North Carolina State University, USA

Scientific Committee



Dr. Ahmed HASSANIN

Affiliation : Egypt Japan University, Egypt



Prof. Dr. Ramzi KHIARI

Affiliation : ISET KSAR HELLAL, Tunisia



Dr. Mohammad MANSOOB KHAN

Affiliation : Universiti Brunei Darussalam



Dr. Fatma Nur PARIN

Affiliation : Bursa Technical University, Turkey



Dr. Çiğdem Taşdelen-Yücedağ

Affiliation : Gebze Teknik University, Türkiye



Dr. Ali Toptaş

Field of Study : Textile Engineering, Nanotechnology, Advanced filtration techn
Affiliation : Istanbul Technical University, Türkiye



Dr. Seda UNAL

Affiliation : Polyteks, Bursa, Türkiye



Dr. F. Filiz Yıldırım



Dr. Ayşe Sezer Hıçyılmaz

Affiliation : Tubitak-Butal, Bursa, Türkiye



Dr. Néji LADHARI

Affiliation : University of Monastir, Tunisia



Dr. Ayşe Şevkan Macit

Affiliation : Usak University, Türkiye



Dr. Şule SELÇUK

Affiliation : Istanbul Technical University, Türkiye



Dr. Ismail TIYEK

Affiliation : KAHRAMANMARAS SÜTÇÜ İMAM ÜNİVERSİTESİ, Türkiye



Dr. Aslı Nur POLAT

Field of Study : Elektrik-Elektronik Mühendisliği
Affiliation : Atatürk University, Türkiye



Dr. Ebru Yabaş

Position : İleri Teknoloji Uygulama ve Araştırma Merkezi (Müdür)
Affiliation : SİVAS CUMHURİYET ÜNİVERSİTESİ
[Personal Website](#)



Assist. Prof. Merve Mocan

Field of Study : Sustainable polymer(composites) (biodegradable, bio-based, re
Affiliation : Gebze Teknik Üniversitesi, Türkiye

Organizing Committee



Prof. Dr. Yusuf ULCAI

Affiliation : Bursa Uludag University



Prof. Dr. Ali DEMIR

Field of Study : **Textile Engineering** [Synthetic Filament Yarn production]

Affiliation : **Istanbul Technical University**



Prof. Dr. Ayşe ÇELİK BEDELOGLU

Affiliation : Bursa Technical University



Prof. Dr. Cem GOK

Field of Study : **Biomaterials, Nanotechnology, Tissue Engineering**

Affiliation : **Izmir Bakircay University, Türkiye**

[Personal Website](#)



Prof. Dr. Kenan YILDIRIM

Affiliation : Bursa Technical University



Prof. Dr. Hamit ERDEMI

Affiliation : **Yalova University**



Prof. Dr. Behnam POURDEYHIMI

Affiliation : **NCSU, USA**



Assoc. Prof. Dr. Ali KILIÇ

Affiliation : **Istanbul Technical University**



Dr. Ayşe Sezer Hiçyılmaz



Assoc. Prof. Dr. Seyedmansour BIDOKI

Field of Study : **Textile** [Color and Polymer Chemistry]

Affiliation : **Yazd University, Iran**



Assoc. Prof. Dr. Hüseyin AVCI

Affiliation : **Eskişehir Osman Gazi University**



Assoc. Prof. Dr. Fatih SUVARI

Affiliation : **Bursa Uludag University**



Assoc. Prof. Dr. Idris KARAGOZ

Affiliation : **Yalova University**



Assoc. Prof. Dr. Ebru Yabaş

Affiliation : **SİVAS CUMHURİYET ÜNİVERSİTESİ, Türkiye**



Assist. Prof. Dr. Yasemin TAMER

Affiliation : **Yalova University**



Assist. Prof. Dr. Şule SELÇUK

Affiliation : **Istanbul Technical University**



Assist. Prof. Dr. Halil Ibrahim AKYILDIZ

Affiliation : **Bursa Uludag University**



Assist. Prof. Dr. Tamer HAMOUDA

Affiliation : **National Science Foundation, Egypt**



Assist. Prof. Dr. Ahmed HASSANIN

Affiliation : **Egypt Japan University, Egypt**



Assist. Prof. Dr. Abdelrahman ABDELGAWAD

Affiliation : **NCSU, USA**

Organizing Committee



Assist. Prof. Dr. Yasin ALTIN

Affiliation : Bursa Technical University



Assist. Prof. Dr. Yusuf POLAT

Affiliation : Erzurum Technical University



Assist. Prof. Dr. Yasin AKGUL

Affiliation : Karabük University



Assist. Prof. Dr. Çiğdem TAŞDELEN-YÜCEDAĞ

Affiliation : Gebze Technical University



Assist. Prof. Dr. Mehmet Durmuş ÇALIŞIR

Affiliation : Rize Recep Tayyip Erdoğan University



Assist. Prof. Dr. Fatma DEMIRCI

Affiliation : Bursa Technical University



Assist. Prof. Dr. Fatmanur PARIN

Affiliation : Bursa Technical University



Dr. Ali Imran AYTEN

Affiliation : Yalova University



Dr. Gülçin BAYSAL

Affiliation : Eskişehir Technical University



Dr. Aslı GIRGIN

Affiliation : Bursa Uludag University



Dr. Hüseyin Çağdaş Aslan

Field of Study : Polymer Processing

Affiliation : Yalova University



Assist. Recep İlhan



Assist. Nazlı ARMAN

Affiliation : Bursa Uludag University



Assist. Aybeniz SEYHAN

Affiliation : Istanbul Technical University



Assist. Ahmet AYDIN

Affiliation : Bursa Technical University



Assist. Prof. Dr. Ali TOPTAŞ

Affiliation : Istanbul Technical University, Türkiye



Assist. Omer Faruk UNSAL

Affiliation : Bursa Technical University



Assist. Atike KOKEN

Affiliation : Bursa Technical University



Assist. Inal Kaan Duygun



Assist. Ayten Nur Yüksel Yılmaz

Organizing Committee



Merve Nur SAGIRLI
Affiliation : İTÜ TEMAG Lab.



Melike GUNGOR
Affiliation : İTÜ TEMAG Lab.



Hilal Ozyurt
Affiliation : İTÜ TEMAG Lab.



Göktuğ Kolver



Tuana Orhun



Aysu Çavuşoğlu
Affiliation : Yalova University



Dr. Öğr. Uyesi Ismail Borazan
Affiliation : Bursa Technical University



Field of Study : Sustainable polymer(composites) (biodegradable, bi)
Affiliation : Gebze Technical University, Türkiye



Dr. Asli Nur Polat
Field of Study : Electric-Electronic Engineering
Affiliation : Ataturk University, Türkiye

List of Papers and Posters Presented at the 16th ULPAS

| Paper Id | Title of paper (English) | Presentation Type | Authors (English) | Presenter |
|----------|-----------------------------------------------------------------------------------------------------------------------------------------|-------------------|------------------------------------------------------------------------------------------------|--------------------------|
| 1001 | Investigation of the usability of kaolin/agar biocomposite in the removal of U(VI) ions from aqueous solutions | Oral | Pinar Aykin - Sabriye Yusan | Pinar Aykin |
| 1002 | Converting waste leather into photothermal oil absorbing fibers for efficient crude oil spill cleanup | Oral | Yaping Wang - Mohamed Mahmoud Nasef | Yaping Wang |
| 1003 | Sound Absorption Performance of Three-dimensional Flexible Spacer Fabric Enhanced by Polyurethane Foam | Oral | Milad Atighi - Mohammad Davoudabadi Farahani - Mahdi Hasanzadeh | Milad Atighi |
| 1004 | Effect of porosity distribution in FRP laminate on interfacial shear stresses in cracked beams strengthened with variable fiber spacing | Oral | Khamis Hadjazi - Mohamed Larbi Bennagadi - Nawel Bentata - Lahouaria Errouane - Zouaoui Sereir | Prof. Dr. Khamis Hadjazi |
| 1006 | Fused Deposition Modeling (FDM) – methods, materials and applications for flexible fabric structures | Oral | Sabit Adanur | Prof. Dr. Sabit Adanur |
| 1007 | Photocatalytic Activity of Ag-ZnO Structures Deposited onto Glass Fibers | Oral | Muhterem Damla YAĞMUR - Halil İbrahim AKYILDIZ | Muhterem Damla YAĞMUR |
| 1014 | From hydrophobic nanofibers to antimicrobial slippery liquid infused surfaces: A two-step surface strategy | Oral | Sena Kardelen Dinc - Oznur Akbal Vural - Nalan Oya San Keskin | Sena Kardelen Dinc |
| 1015 | Effects of different processed bobbin structures on yarn and warp preparation performance in cotton spinning | Oral | Gökhan Tandoğan - Kıymet Kübra Kaya Denge - Yasemin Korkmaz - Uğur Gündoğan - Sami Gizir | Gökhan Tandoğan |

| | | | | |
|------|-----------------------------------------------------------------------------------------------------------------------------------------------------------------------------|------|--------------------------------------------------------------------------------------------|-----------------------------------|
| 1017 | Development of Air Pre-Filter Materials from Chicken Feather Fibers by Dry Laid Method | Oral | Emirhan Bay - Jan Sena Altınay - Mediha Demet Aysin - Sümeyye Üstüntağ | Jan Sena Altınay |
| 1022 | Production of facial sheet masks by adding green synthesized Ag nanoparticles with plant extracts and collagen to PCL composite nanofibers: Use in acne and wrinkle removal | Oral | Ahmet Avcı - Cansu Güneş - Fatma Ahsen Öktemer - Edanur Korkmaz | Prof. Dr. Ahmet Avcı |
| 1026 | Identification of bisphenol A (BPA) sources in textile products and its contamination of wastewater | Oral | Ayşe Ceren Şen - Hülya Kıcık | Hülya Kıcık |
| 1034 | An investigation study about LMF Co-PET fiber utilization on flat knitted automotive fabric structure | Oral | Osman AYDIN - Semih OYLAR - Ceyda UYANIKTIR | Osman AYDIN |
| 1035 | A STUDY ABOUT WATER REPELLENT AND SOIL RESISTANCE BEHAVIOR OF AUTOMOTIVE SEAT FABRICS | Oral | Benamir Fidancı - Selenay Elif İşler - Emir Baltacıoğlu | Benamir Fidancı |
| 1038 | Surface Modification of Wool Fabrics with Metal-Organic Framework for Eco-Friendly Sustainable Natural Dyeing | Oral | Maryam Pishehvar - Motahareh Moradi - Aminoddin Haji - Mahdi Hasanzadeh | Maryam Pishehvar |
| 1039 | Towards Sustainable and Green Synthesis of Metal-Organic Frameworks (MOFs): A Pathway to Industrial Viability | Oral | Seif El Islam Lebouachera - Mahdi Hasanzadeh | Assoc. Prof. Dr. Mahdi Hasanzadeh |
| 1040 | Blown Üretim Teknolojisi ile Hafızalı ve İşlevsel Elastik Film Üretimi | Oral | İLKER TÜRKMEN - AKİF DİK | İLKER TÜRKMEN |
| 1046 | Amphiphilic Functional Polymers as Polypropylene Nonwoven Surface Treatment | Oral | MEHMET SİNAN TÜBCİL | MEHMET SİNAN TÜBCİL |
| 1047 | Effects of Hemp fiber content on yarn quality for Ring and Vortex yarns | Oral | Kübra Özşahin - Emel Çinçik - Hatice Kübra Kaynak | Prof. Dr. Hatice Kübra Kaynak |
| 1048 | Spunbond dokusuz kumaş üretiminde bitim işlemi için yenilikçi bir prototip sisteminin geliştirilmesi | Oral | Gülistan Canlı - Halil İbrahim ÇELİK | Gülistan Canlı |
| 1049 | The Effect of Fiber Cross-section of Polyester Yarn on Dyeing Behavior of Microwave Assisted and Conventional Dyeing | Oral | Yasemin Dülek - İpek Yıldırım - Buğçe Sevinç - Esra Mert - Yasemin Özdemir - Cem Güneşoğlu | Dr. Yasemin Dülek |

| | | | | |
|------|---------------------------------------------------------------------------------------------------------------------------------------------------------------------------------------------------|------|-------------------------------------------------------------------------------------------------------------------|------------------------------------------|
| 1052 | The Effect of Ecocell™ Fiber on Some Performance Properties of Apparel Fabrics | Oral | Yasemin Dülek - İpek Yıldırım - Buğçe Sevinç - Hatice Salar - Tülin Kaya Nacarkahya - Şeyma Satıl - Cem Güneşoğlu | Dr. Yasemin Dülek |
| 1054 | Design of glitter-effect denim and non-denim surfaces with a novel coating material | Oral | Gökhan GÜNEŞ - Osman BABAARSLAN | Gökhan GÜNEŞ |
| 1055 | The Impact of Pigment Dyeing and Pigment Washing on the Mechanical Properties of 3D Knitted Fabrics | Oral | Arda DEVECİ | Arda DEVECİ |
| 1056 | Polymeric Superplasticizer Driven Concrete Strength Forecasting Using Ensemble Random Forests | Oral | Uğur ÖZVEREN - Dicle EREN | Assoc. Prof. Dr. Uğur ÖZVEREN |
| 1057 | LOI Prediction of Flame-Retardant Polypropylene Composites Using XGBoost | Oral | Uğur ÖZVEREN - Dicle EREN | Assoc. Prof. Dr. Uğur ÖZVEREN |
| 1058 | Recycled fiber composites enabling the circular textiles economy loop | Oral | Hasabo Abdelbagi Mohamed Ahmed | Prof. Dr. Hasabo Abdelbagi Mohamed Ahmed |
| 1061 | Fabrication of nanofibrous proton exchange membranes with significantly enhanced proton conductivity based on sulfonated polyether ether ketone/polydopamine-coated multi-walled carbon nanotubes | Oral | Zahra Esmailzadeh - Mohamad Karimi - Ahmad Mousavi Shoushtari - Mehran Javanbakht | Dr. Zahra Esmailzadeh |
| 1063 | Recovery of textile waste: The effect of recycled cotton fibers obtained from different fabric structures on yarn quality | Oral | KÜBRA BAYKAN ÖZDEN - İbrahim Erkan EVRAN - Züleyha DEĞİRMENCİ | KÜBRA BAYKAN ÖZDEN |
| 1067 | Investigation of the response of bio-organic material based biosensor to pesticide water solution at different concentrations by electrical characterization method | Oral | Burak TAŞ - Hüseyin Muzaffer ŞAĞBAN - Ümit Hüseyin KAYNAR - Özge TÜZÜN ÖZMEN | Burak TAŞ |
| 1069 | Superhydrophobic PVDF Nanofiber Piezoelectric Sensor Reinforced with Core-Shell ZnO@ZIF-8 Structure | Oral | Milad Atighi - Mahdi Hasanzadeh - Roohollah Bagherzadeh | Milad Atighi |
| 1072 | In-Process Vertical Reinforcement of 3D Printed Concrete Structures | Oral | Seyedmansour BIDOKI - Mahsa Bidoki - Hasan Haroglu - Adil Kahwash Al-Tamimi - Ali Demir | Assoc. Prof. Dr. Seyedmansour BIDOKI |

| | | | | |
|------|----------------------------------------------------------------------------------------------------------------------------------------|------|--------------------------------------------------------------------------------------------------------|-----------------------------------------|
| 1073 | Farklı modakrilik elyaf karışım oranına sahip kumaşların performans özelliklerinin incelenmesi | Oral | Gülşah Karakaya - Dilek Toprakkaya Kut | Gülşah Karakaya |
| 1074 | Advances and outlook in capacitive pressure sensors: The role of nanofibrous architectures | Oral | Özge Alişan - Mehmet Durmuş Çalışır | Özge Alişan |
| 1076 | Effect of Surface-Active Agents on Liquid Transfer Properties of Hydroentangled Nonwoven Fabrics | Oral | Ebru ÇELİKTEN - Mehmet DAŞDEMİR - Tülin KAYA NACARCAHYA - Şeyma SATIL - Mehmet TOPALBEKİROĞLU | Ebru ÇELİKTEN |
| 1077 | Application of Biopolymeric Nanocomposites in Bone Tissue Engineering | Oral | Cem GÖK - Gülşah SUNAL | Prof. Dr. Cem GÖK |
| 1079 | Production and Characterization of Polyimide Nanofiber Yarns via Electrospinning | Oral | Yasin Altın | Assist. Prof. Dr. Yasin Altın |
| 1082 | MicroEcocell ve Micromodal İpliklerin Karşılaştırmalı Analizi: Ring ve Vortex Eğirme Sistemlerinin İplik ve Kumaş Özelliklerine Etkisi | Oral | Şeyma SATIL - Tülin KAYA NACARCAHYA - Gonca BALCI KILIÇ - Asaf ÖZMEN - Burak AYYILDIZ - Servet ÖZTÜRK | Şeyma SATIL |
| 1085 | Curing Properties of Covalently Bonded Polyoxazoline-Imidazole Thermal Latent Curing Agents for One-Component Epoxy Resins | Oral | Ceren Özsaltık - Asu Ece Atespare - Cuma Ali Ucar - Bekir Dizman | Ceren Özsaltık |
| 1090 | Development of Gelatin-Chitosan Composite Nanofibers Incorporated with Corncob-Derived Cellulose Microcrystals | Oral | Salih Birhanu Ahmed - Beyza Soydan - Çiğdem Uçar - Emine Tekcan - Ali Toptaş - Harun Çuğ - Yasin Akgul | Salih Birhanu Ahmed |
| 1091 | From manual methods to deep learning: evolution of image-based diameter analysis for fibers and particles | Oral | Muhammet Mahsun Çifçi - Mehmet Durmuş Çalışır | Assist. Prof. Dr. Mehmet Durmuş Çalışır |
| 1092 | Effect of processing flaws on mechanical behaviour of graphene-epoxy nanocomposites | Oral | Osman Bayrak - Ayten Nur Yüksel Yılmaz - Yusuf İpek - Mertcan İşgör - Cantekin Kaykılarlı | Assist. Prof. Dr. Osman Bayrak |
| 1093 | Optimization of nanofiber production from biodegradable PBS via electro-blowing method using Box-Behnken design | Oral | ALİ TOPTAŞ | Assist. Prof. Dr. ALİ TOPTAŞ |

| | | | | |
|------|---------------------------------------------------------------------------------------------------------------------------------------------------------------------------------------------|--------|----------------------------------------------------------------------------------------------------------------------------------------------|-----------------------------------------|
| 1094 | Modified silica containing polyacrylonitrile Janus nanofiber membranes for environmental applications | Oral | Gülşah Gürbüz - Sedanur Öztürk - Melis Bilgiç - Yeldem Karabulut - Züleyha Saraç - Çiğdem Taşdelen-Yücedağ | Gülşah Gürbüz |
| 1095 | Nanoclay reinforced nanofiber membranes for oil-water separation | Oral | Ömer Tüylüce - Buse Girgin - Melike Deniz Bıçakcı - Züleyha Saraç - Çiğdem Taşdelen-Yücedağ | Ömer Tüylüce |
| 1097 | Effect of unit cell geometry and wall thickness of auxetic structures on energy absorption capability under quasi-static compression | Oral | Ali İmran Ayten - Bekir Keskin - Ameen Topa | Assist. Prof. Dr. Ali İmran Ayten |
| 1102 | Global and local positioning of seaweed fibers: A sustainable journey from fiber to fabric | Oral | Büşra Bozyer - Züleyha Değirmenci - Ersen Çatak | Büşra Bozyer |
| 1103 | Coated functional and technical textiles containing recycled silica powders | Oral | Sema Özden - Ayşe Dilşad Polat - Mehmet Kanık - Burak Kırayoğlu | Sema Özden |
| 1104 | Production of facial sheet masks by adding green synthesized Ag nanoparticles with plant extracts and collagen to PCL composite nanofibers: Use in acne and wrinkle removal | Oral | Cansu Güneş - Fatma Ahsen Öktemer - Edanur Korkmaz - Mustafa Mert Kurdiş - Ahmet Avcı | Cansu Güneş |
| 1106 | Production of facial sheet masks by adding green synthesized Ag nanoparticles with plant extracts and collagen to PCL composite nanofibers: Usability to promote acne and wrinkle reduction | Oral | Cansu Güneş - Fatma Ahsen Öktemer - Edanur Korkmaz - Mustafa Mert Kurdiş - Ahmet AVCI | Cansu Güneş |
| 1107 | Fındık Kabuğu Dolgusunun EPDM Kauçuk Karışımlarının Mekanik, Kürlenme ve Fiziksel Özelliklerine Etkisi | Oral | Aysu Çavuşoğlu - İdris Karagöz - Melih Fatih Geçgel - Filiz Memişoğlu Ölmez - Merve Oruç Karataş - Ümit Kaya | Aysu Çavuşoğlu |
| 1005 | Mechano-reliability model of a bio-sourced plate based on Alfa/Greenpoxy 56 | Poster | Amrane Aboubakr - Lahouaria Errouane - Mohammed El Larbi BENNEGADI - Zouaoui Sereir - Christophe POILANE - Alexandre VIVET | Prof. Dr. Lahouaria Errouane |

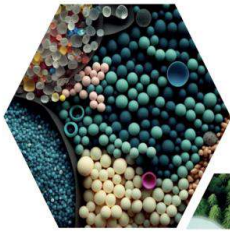
| | | | | |
|------|--------------------------------------------------------------------------------------------------------------------------------------------|--------|-------------------------------------------------------------------------------------------------------------------------------------------|-----------------------------|
| 1008 | Effect of porosity distribution in FRP laminate on interfacial shear stresses in cracked beams strengthened with variable fiber spacing | Poster | Khamis Hadjazi - Mohamed Larbi Bennegadi - Nawel Bentata - Lahouaria Errouane - Zouaoui Sereir | Dr. Khamis Hadjazi |
| 1009 | Electrospun gelatin/sodium alginate nanofibers for cephalexin delivery | Poster | AZRA HUNER | Assoc. Prof. Dr. AZRA HUNER |
| 1010 | Fabrication and antioxidant activities of polyethylene oxide/sodium alginate/zinc oxide electrospun nanofibers | Poster | AZRA HUNER | Assoc. Prof. Dr. AZRA HUNER |
| 1011 | Advanced emulsion fabrication of alkyd resins: effect of phase inversion and processing conditions | Poster | Pelin Aksoy - Abdulvahap Selim CİFCİ | Dr. Pelin Aksoy |
| 1012 | Investigation of the effect of bio-based finishing chemical on knitted fabric | Poster | Filiz Emiroğlu - Ayşe Çelik Bedeloğlu | Filiz Emiroğlu |
| 1016 | Nanofiber-Halloysite Systems for Sustained Microbial Support in Industrial Wastewater Treatment | Poster | Yiğitcan Algül - Nalan Oya San Keskin | Yiğitcan Algül |
| 1019 | Evaluation of the microbial corrosion protection performance of essential oil-loaded nanofiber coatings on stainless steel | Poster | Ayça Gül Özdağ - Nalan Oya San Keskin | Ayça Gül Özdağ |
| 1020 | Development of high-efficiency polysulfone nanofiber filters for the removal of Candida auris: Comparison of aligned and random morphology | Poster | Merve Açıksöz - Ayse Kalkanci - Ozlem Guzel Tunccan - Nalan Oya San Keskin | Merve Açıksöz |
| 1021 | PBT-Based Hard Tissue Implant | Poster | Songül ÖZAY - Ebru ERDAL - Barış BATUR - Gülben AKCAN - Merve BAKICI - Caner BAKICI - Hasret Tolga ŞİRİN - Lokman UZUN - Murat DEMİRBİLEK | Songül ÖZAY |
| 1023 | PERDELEME UYGULAMALARINA YÖNELİK TEKSTİL ÜRÜNÜ | Poster | Zeynep Batur | Zeynep Batur |
| 1025 | Utilization of Conductive Yarns in Cotton Fabric Structure and Investigation of Performance Properties | Poster | EYÜPHAN YENER - SEVİL GÜNÇ - SALİHA BÜŞRA KARAKELLE | EYÜPHAN YENER |
| 1027 | IMPROVEMENT OF PERFORMANCE PROPERTIES OF CELLULOSIC BASED FIBRES | Poster | Eyüphan Yener - Sevil Günç - Saliha Büşra KARAKELLE - Sümeyye REÇEL ASLAN | Eyüphan Yener |

| | | | | |
|------|----------------------------------------------------------------------------------------------------------------------------------|--------|----------------------------------------------------------------------------------------------------------------|------------------------|
| 1028 | DEVELOPMENT OF COLOR CHANGING TEXTILE SURFACES AGAINST BACTERIA | Poster | Eyüphan Yener - Sevil Günc - Sümeyye REÇEL ASLAN - Saliha Büşra KARAKELLE | Eyüphan Yener |
| 1029 | DEVELOPING ENVIRONMENTAL BURDEN AND COST-REDUCING PROCESSES TO ELIMINATE SALT USE IN REACTIVE DYEING | Poster | Saliha Büşra KARAKELLE - Sevil GÜNC - Eyüphan YENER | Saliha Büşra KARAKELLE |
| 1030 | APPLICATION OF INTERMINGLING TO NATURAL YARNS TO IMPROVE THE COMFORT PROPERTIES OF PRODUCTS | Poster | Sümeyye REÇEL ASLAN - Eyüphan YENER - Saliha Büşra KARAKELLE | Sümeyye REÇEL ASLAN |
| 1031 | DEVELOPMENT OF ECOLOGICAL NON-SLIP MATS WITH INCREASED CONTACT SURFACE | Poster | Sümeyye REÇEL ASLAN - Sevil GÜNC - Saliha Büşra KARAKELLE | Sümeyye REÇEL ASLAN |
| 1032 | INVESTIGATION OF THE DYEABILITY OF CELLULOSIC PRODUCTS WITH PRETREATMENT AND REACTANT DYESTUFFS IN ONE BATH | Poster | SALIHA BÜŞRA KARAKELLE - Sevil GÜNC - Eyüphan YENER | SALIHA BÜŞRA KARAKELLE |
| 1033 | Development of yarn tension sensor for winding machines | Poster | Ibrahim GEZGIN - Recep EREN | Ibrahim GEZGIN |
| 1036 | Green synthesized selenium nanoparticles attached electrospun polycaprolactone nanofiber mats for fast photo degradation of dyes | Poster | Sezin Demirci - Nalan Oya San Keskin | Sezin Demirci |
| 1037 | Farklı orijinli pamuk liflerinin iplik kalite özellikleri üzerine etkilerinin incelenmesi | Poster | Yusuf Şenel - Ekin Ünlü - Mustafa Şıhlı Der | Yusuf Şenel |
| 1042 | Design of bone powder-enhanced cage structures for kyphoplasty application in vertebral compression fractures | Poster | Zeynep Turna - Serkan Yıldız - Şebnem Düzyer Gebizli - Çağatay Öztürk - Ash Hockenberger - Şehime Gülsün Temel | Zeynep Turna |
| 1043 | Development of collagen-modified polylactic acid based raw material for orthopedic biomedical applications | Poster | BEYZA ÇAY - ZEHRA BETÜL AHİ - AYŞEGÜL UZUNER DEMİR | BEYZA ÇAY |
| 1044 | Development of Spin Finish Oil Used in Synthetic Yarns: Examination of OPU Values in Terms of Performance and Efficiency | Poster | Naciye Gül - Merve Kandemir | Naciye Gül |

| | | | | |
|------|--------------------------------------------------------------------------------------------------------------------------------------------------------------|--------|-------------------------------------------------------------------------------------------------------------------------------------|------------------------------------|
| 1051 | Boyama proseslerinde proses entegrasyonu ve ekolojik kazanımlar: akrilik –ecocell karışımı seamless üretimde tek banyo uygulaması | Poster | Sultan ARAS ELİBÜYÜK - Mustafa ÇÖREKCİOĞLU - Perinur KOPTUR TASAN - Özlem DEMİR GÜNENÇ - Tülin KAYA NACARCAHYA | Sultan ARAS ELİBÜYÜK |
| 1053 | The effect of stacking squence on mechanical performance of hybrid natural fiber reinforced composites | Poster | Hülya Karaçeper - Ayşe Bedeloğlu | Hülya Karaçeper |
| 1059 | Pad-batch boyamada üre kullanımını azaltmaya yönelik süreç iyileştirmesi | Poster | Perinur Koptur Tasan - Mustafa Çörekcioglu - Sultan ARAS ELİBÜYÜK - Özlem Demir Günenç | Perinur Koptur Tasan |
| 1060 | Tailoring PET/PLA Film Properties Through Transesterification During Melt Processing | Poster | Maryam Kheirandish - Mohammad reza Mohaddes mojtahedi - Hossein Nazockdast | Dr. Maryam Kheirandish |
| 1064 | Bebek Bezlerinde Nefes Alabilirlik Özelliğinin Ölçümü İçin Metot Geliştirme | Poster | Melcenur Kılıç - Eda Doğu - Nimet Uzun Kalender | Melcenur Kılıç |
| 1065 | RECYCLING TECHNIQUES FOR FIBER REINFORCED POLYMER COMPOSITES | Poster | Zaide Saka DİNÇ - Aliye Akarsu ÖZENÇ - Semiha EREN - HÜSEYİN AKSEL EREN | Prof. Dr. HÜSEYİN AKSEL EREN |
| 1066 | RECYCLING OF THE FUTURE: SMART AND SUSTAINABLE SEPARATION METHODS FOR TEXTILE WASTE | Poster | Aliye Akarsu ÖZENÇ - Zaide Saka DİNÇ - Semiha EREN - Hüseyin Aksel Eren | Prof. Dr. Hüseyin Aksel Eren |
| 1068 | COMPARATIVE ANALYSIS OF PIEZOELECTRIC OUTPUT PERFORMANCES OF Gd AND Al DOPED ZnO PRODUCED IN NANOFIBER STRUCTURE WITH RESPECT TO THEIR NON-DOPED (PURE) FORM | Poster | Burak TAŞ - Ahmet Batuhan TOĞRUL - Ümit Hüseyin KAYNAR - Özge TÜZÜN ÖZMEN | Burak TAŞ |
| 1071 | Water Exposure Effects on the Mechanical Properties of Glass Fiber-Reinforced HDPE Unidirectional Tapes | Poster | Melisa Yeke - Gülnur Başer - Serkan İlker Bengü | Melisa Yeke |
| 1078 | EFFECT OF CHAIN BRANCHING ON THE MECHANICAL AND CREEP BEHAVIOR OF UHMWPE FIBERS PRODUCED BY GEL SPINNING | Poster | Oğuz Kağan Ünlü - Aslı Ertan | Oğuz Kağan Ünlü |

| | | | | |
|------|------------------------------------------------------------------------------------------------------------------------------|--------|-----------------------------------------------------------------------------------------------------------|-------------------------------------|
| 1080 | Investigation of the suitability of some piezoelectric materials with nanofiber structure for the field of health technology | Poster | MURATCAN ÇAM - BURAK TAŞ - ÜMİT HÜSEYİN KAYNAR - ÖZGE TÜZÜN ÖZMEN | MURATCAN ÇAM |
| 1081 | Influence of Formulation Parameters on Film Morphology and Fabric Performance in Waterborne Polyurethane Textile Coatings | Poster | Canberk YÜKSEL - Canan ÖZTÜRK | Canberk YÜKSEL |
| 1086 | Sürdürülebilirlik Odaklı Halı ve Döşemelik Kumaş Geliştirme | Poster | Osman TÜRKMEN - Elif KOYUNCU | Osman TÜRKMEN |
| 1087 | YENİ TRENDLERE UYGUN ANTİVİRAL, ANTİBAKTERİYEL ETKİ SAĞLAYAN OTOTMOTİV DÖŞEMELİK KUMAŞ GELİŞTİRİLMESİ | Poster | Osman TÜRKMEN - Sümeysra OĞUZ | Osman TÜRKMEN |
| 1088 | İç Mekan Havasını Arındıran Fonksiyonel Döşemelik Kumaşlar | Poster | Hakan ALTUNCU - Berrin ÜNÜR | Hakan ALTUNCU |
| 1089 | Kablo Uygulamaları İçin Huntit-Hidromanyezit İçeren Kompozitlerin Alev Geciktirici ve Mekanik Performanslarının İncelenmesi | Poster | Tuğba YILMAZ - Erdoğan DOĞANCI | Tuğba YILMAZ |
| 1096 | Self-Adaptive Outlier Pruning and Monte-Carlo Validation in Hydrogel Swelling Prediction | Poster | Uğur ÖZVEREN - Burçe PEKER - Dicle EREN - İdil Sena BAYRAK | Assoc. Prof. Dr. Uğur ÖZVEREN |
| 1098 | Eco-Friendly ASA Composites Reinforced with Walnut Shell as a Sustainable Filler | Poster | Aysu ÇAVUŞOĞLU - Tuana ORHUN - Harun SEPETÇİOĞLU - İdris KARAGÖZ - Yasemin BALÇIK TAMER | Aysu ÇAVUŞOĞLU |
| 1099 | Investigation of Mechanical Properties of Polycarbonate/ASA/Walnut Shell Composites | Poster | Aysu ÇAVUŞOĞLU - Tuana ORHUN - Yasemin TAMER BALÇIK - Harun SEPETÇİOĞLU - İdris KARAGÖZ | Aysu ÇAVUŞOĞLU |
| 1100 | DEVELOPMENT AND APPLICATION OF REACTIVE DYE MICROCAPSULES FOR COTTON FABRIC DYEING | Poster | SEVİL GÜNÇ | SEVİL GÜNÇ |
| 1101 | Dikişsiz örgü ve delikli vücut haritalama tasarımıyla iç giyimde konfor ve performans artışı | Poster | Sultan ARAS ELİBÜYÜK - Mustafa Çörekcioglu - Perinur KOPTUR TASAN - Özlem DEMİR GÜNENÇ | Sultan ARAS ELİBÜYÜK |

16. Uluslararası Lif ve Polimer Araştırmaları Sempozyumu (16. ULPAS)
9-10 Mayıs 2025, İstanbul Teknik Üniversitesi (İTÜ), İstanbul, Türkiye



16 ULUSLARARASI
LİF VE POLİMER
ARAŞTIRMALARI
SEMPOZYUMU

16th INTERNATIONAL FIBER AND POLYMER RESEARCH SYMPOSIUM

Sürdürülebilir ve İşlevsel Lif ve Polimerler
Sustainable and Functional Fibers & Polymers



9-10 Mayıs
May 2025

İstanbul Teknik Üniversitesi
Gümüşsuyu Prof. Dr. Necmettin Erbakan Yerleşkesi
İstanbul Technical University
Gumussuyu Prof. Dr. Necmettin Erbakan Campus

Fındık Kabuğu Dolgusunun EPDM Kauçuk Karışımlarının Mekanik, Kürlenme ve Fiziksel Özelliklerine Etkisi

Aysu Çavuşoğlu^{a,b*}, İdris Karagöz^c, Melih Fatih Geçgel^a, Filiz Memişoğlu Ölmez^a, Merve Oruç Karataş^a, Ümit Kaya^a

^aKros Otomotiv A.Ş. , Ar-Ge Departmanı, 43000, Kütahya, Türkiye.

^bPolimer Malzeme Mühendisliği, Lisansüstü Eğitim Enstitüsü, Yalova Üniversitesi, 77200 Yalova, Türkiye.

^cPolimer Malzeme Mühendisliği, Mühendislik Fakültesi, Yalova Üniversitesi, 77200 Yalova, Türkiye.

*Sorumlu Yazar: a.cavusoglu@krosotomotiv.com.tr

ÖZET

Bu çalışmada, EPDM kauçuk reçetelerine fındık kabuğu dolgu malzemesinin ilavesinin mekanik, kürlenme ve fiziksel özellikler üzerindeki etkileri incelenmiştir. Karbon siyah kullanımını azaltmak amacıyla farklı oranlarda (10%, 20%, 30%) fındık kabuğu tozu eklenen karışımlar hazırlanmış ve bu karışımların kopma mukavemeti, yırtılma anındaki uzama, M100 (modülüs at %100 elongation), sertlik, yoğunluk, kürlenme süresi ve kürlenme derecesi gibi özellikleri test edilmiştir. Elde edilen sonuçlar, fındık kabuğunun EPDM kauçuk reçetesinde kullanıldığında, özellikle %20 dolgu oranında en yüksek mekanik performansın elde edildiğini göstermektedir. Bu karışımda kopma mukavemeti ve M100 değerleri artarken, yırtılma anındaki uzama da optimum seviyeye ulaşmıştır. Ayrıca, fındık kabuğunun kürlenme hızını artırarak daha kısa kürlenme süreleri sağladığı gözlemlenmiştir. %30 fındık kabuğu eklemesiyle, malzemenin sertlik ve yoğunluk değerlerinde artış gözlenmiş ancak elastikiyet ve işlenebilirlik üzerinde bazı olumsuz etkiler ortaya çıkmıştır. Bu sonuçlar, fındık kabuğunun kauçuk endüstrisinde sürdürülebilir bir dolgu malzemesi olarak kullanım potansiyeline sahip olduğunu ancak optimum dolgu oranının dikkatlice belirlenmesi gerektiğini ortaya koymaktadır. Çalışma, gelecekte benzer çalışmalar için temel bir kaynak teşkil etmektedir.

Anahtar Kelimeler: EPDM kauçuk kompozitler; Fındık Kabuğu; Biyokompozit.

Effect of Hazelnut Shell Filler on the Mechanical, Curing, and Physical Properties of EPDM Rubber Compounds

ABSTRACT

This study investigates the effects of adding walnut shell filler to EPDM rubber compounds on their mechanical, curing, and physical properties. In order to reduce the use of carbon black, mixtures containing different amounts (10%, 20%, 30%) of hazelnut shell powder were prepared, and their properties such as tensile strength, elongation at break, yield

point, hardness, density, curing time, and degree of cure were tested. The results showed that when walnut shell is used in EPDM rubber formulations, the highest mechanical performance was achieved at a 20% filler content. In this mixture, tensile strength and modulus at yield increased, while elongation at tear reached its optimum level. Additionally, it was observed that walnut shell increased curing speed, resulting in shorter curing times. With 30% walnut shell addition, increases in hardness and density were observed, although some negative effects on elasticity and processability emerged. These findings suggest that walnut shell has the potential to be used as a sustainable filler material in the rubber industry, but careful determination of the optimal filler ratio is necessary. The study provides a fundamental reference for future similar works.

Keywords: EPDM rubber composites; Hazelnut Shell; Biocomposites.

I. GİRİŞ

Günümüzde sürdürülebilir malzeme üretimi ve çevresel etkilerin azaltılması, küresel ölçekte öncelikli bir hedef haline gelmiştir. Küresel ısınmanın artan etkileri doğrultusunda, fosil kaynaklara olan bağımlılığı azaltmak ve sera gazı emisyonlarını düşürmek amacıyla biyobozunur ve petrokimyasal kökenli malzemelere alternatif olabilecek doğal dolgulara olan ilgi giderek artmaktadır [1]. Bu kapsamda, karbon siyahı gibi fosil kökenli takviye malzemelerinin yerine, tarımsal atıklardan elde edilen doğal alternatiflerin kauçuk esaslı malzeme üretiminde değerlendirilmesi hem çevresel sürdürülebilirlik hem de ekonomik fayda açısından önemli bir potansiyel sunmaktadır [2].

Petrol endüstrisinin bir yan ürünü olan karbon siyahı, üstün takviye kabiliyeti nedeniyle kauçuk bileşiklerinde yaygın olarak kullanılmaktadır. Ancak üretim sürecinin yüksek enerji tüketimi, sera gazı salımı ve dışa bağımlılığı artırıcı etkisi, karbon siyahına alternatif, çevre dostu dolgu maddeleri arayışını gündeme getirmiştir. Bu doğrultuda, tarımsal atık kökenli dolgu malzemeleri, düşük maliyetli ve sürdürülebilir bir çözüm olarak öne çıkmaktadır [3].

Fındık kabuğu gibi lignoselülozik esaslı atıkların dolgu maddesi olarak kullanımı, karbon siyahına

kıyasla çeşitli avantajlar sunmaktadır. Bunlar arasında yenilenebilir kaynaklardan elde edilmesi, biyolojik olarak parçalanabilir olması, daha düşük enerjiyle işlenebilmesi ve yerli üretimle dışa bağımlılığı azaltması sayılabilir. Ayrıca fındık kabuğu kullanımı, tarımsal atıklara katma değer kazandırmakta ve yakılarak bertaraf edilmesi sonucu ortaya çıkan sera gazı salımının önüne geçmektedir [1]. Bu bağlamda, karbon siyahı kullanımını azaltmak amacıyla fındık kabuğu tozu tercih edilmekte ve alternatif dolgu malzemesi olarak değerlendirilmektedir.

Türkiye, organik tarım üretiminde lider ülkeler arasında yer almakta olup, her yıl önemli miktarda tarımsal atık oluşmaktadır. Bu atıkların sanayiye entegre edilmesi hem çevresel etkileri azaltacak hem de üreticilere yeni gelir kaynakları yaratacaktır.

Fındık kabuğu ve polimer karışımları ile ilgili yapılmış birçok çalışma mevcuttur. Cengiz ve ark. (2021), tarımsal atık olan fındık kabuklarını, talk, SEBS ve SEBS-g-MA katkılarıyla birlikte polipropilen (PP) matrisli yeşil kompozitlerin üretiminde dolgu malzemesi olarak kullanılmıştır. Fındık kabukları toz haline getirilip elenmiş, ekstrüzyonla granül haline getirilmiş ve enjeksiyon yöntemiyle test numuneleri üretilmiştir. Uygun ekstrüzyon parametreleriyle yanma ve yapı bozulması önlenerek yüksek performanslı hibrit kompozitler elde edilmiştir [1].

Karagöz ve ark. (2024), fındık kabuğu ve volastonit içeren polipropilen (PP) bazlı hibrit kompozitlerin mekanik ve termal özelliklerini incelemiş; ayrıca SEBS ve SEBS-g-MA uyumlaştırıcılarının bu özellikler üzerindeki etkilerini değerlendirmiştir. Kompozitler; çekme, eğilme ve darbe testlerinin yanı sıra DSC, TGA ve SEM analizleri ile karakterize edilmiştir. Elde edilen bulgular, fındık kabuğu katkısının termal davranış üzerinde etkili olduğunu; dolgu ve uyumlaştırıcıların ise kristalleşme davranışı ve termal kararlılıkta önemli değişikliklere yol açtığını göstermiştir. Çalışma, istenen nihai özelliklerin elde edilmesinde dolgu türü ile uyumlaştırıcının varlığı ve dağılımının kritik rol oynadığını ortaya koymaktadır [4]. Çavuşoğlu ve ark. (2023), otomotiv uygulamaları için çevre dostu yeşil kompozitler geliştirmek amacıyla fındık kabuğunu (FK), polipropilen (PP) matrisine dolgu malzemesi olarak eklemişlerdir. Yapılan testler, fındık kabuğu katkısının malzemenin yoğunluğunu artırırken akışkanlığını azalttığını; ayrıca çekme, eğilme ve darbe dayanımlarında düşüşe yol açtığını ortaya koymuştur. Termal özelliklerde de belirgin azalmalar gözlemlenmiştir. Tüm bu değişimlere rağmen, elde edilen kompozitlerin sürdürülebilir malzeme kullanımı açısından önemli bir potansiyele sahip olduğu belirtilmiştir [5].

Bu çalışmada, EPDM esaslı kauçuk bileşiminde karbon siyahı oranı azaltılarak, yerine fındık kabuğu tozu ilave edilmiş ve dört farklı formülasyon oluşturulmuştur. Karbon siyahı miktarının düşürülmesindeki temel amaç, çevreye olan olumsuz etkileri azaltmak ve yerli, sürdürülebilir bir kaynak olan fındık kabuğu tozunu değerlendirmektir. Elde edilen numunelerde, fındık kabuğu tozunun dolgu maddesi olarak kullanımının mekanik, reolojik ve fiziksel özellikler üzerindeki etkileri değerlendirilmiştir. Çalışmanın temel amacı, fındık kabuğu gibi yenilenebilir kaynakların geleneksel dolgu maddelerine alternatif olarak kullanılabilirliğini ortaya koymak, çevresel etkileri azaltan ve ekonomik

açıdan rekabetçi olabilecek sürdürülebilir dolgu çözümleri geliştirmektir. Böylece hem atıkların katma değerli ürüne dönüştürülmesi hem de kauçuk endüstrisinin çevre dostu malzeme kullanımına geçişi desteklenmektedir.

II. DENEYSEL METOT

2.1 Malzemeler

Kauçuk reçetesinde matris malzemesi olarak EPDM kauçuğu kullanılmıştır. Dolguların etkilerini gözlemleyebilmek adına kauçuk reçetesi temel kimyasallar kullanılarak oluşturulmuştur. Dolgu malzemesi olarak N550 ve 0-200 mesh tanecik boyutu aralığında fındık kabuğu tozu kullanılmıştır. Proses kolaylaştırıcı kimyasal olarak stearik asit ve parafinik yağ kullanılmıştır. Çapraz bağlayıcı olarak Trigonox 101 (2,5-Dimethyl-2,5-di(tert-butylperoxy)hexane) ve vulkanizasyon yardımcısı olarak Rhenofit EDMA/S (%7 etilen glikol dimetakrilat + %30 silika) kimyasalları kullanılmıştır. Parametrelerin kimyasal oranları Tablo 1.'de verilmiştir.

Tablo 1. Çalışmada kullanılan parametreler

| Kimyasal İsimleri | R-AW01 (phr) | R-AW02 (phr) | R-AW03 (phr) | R-AW04 (phr) |
|--------------------|--------------|--------------|--------------|--------------|
| EPDM | 100 | 100 | 100 | 100 |
| N550 | 100 | 90 | 80 | 70 |
| FINDIK KABUĞU TOZU | - | 10 | 20 | 30 |
| STEARİK ASİT | 2,5 | 2,5 | 2,5 | 2,5 |
| PARAFİNİK YAĞ | 35 | 35 | 35 | 35 |
| RHENOİT EDMA/S | 1 | 1 | 1 | 1 |
| TRİGONOX 101 | 5 | 5 | 5 | 5 |

2.1. Fındık Kabuğu Tozunun Hazırlanması

Giresun yöresine ait fındık kabuklarının yumuşak ve sert kısımları birbirlerinden ayrılarak ayıklanmıştır. Ayıklanan fındık kabukları Şekil 1'de verilen Lavion marka hububat öğütücüsü ile öğütülmüştür. Öğütülüp toz haline getirilen fındık kabukları endüstriyel elek

kullanılarak mesh boyutlarına ayrılmıştır. Çalışmada kullanılan fındık kabukları 0-200 mesh tanecik boyut aralığında kullanılmıştır. Tanecik boyutu ayırma işleminden sonra fındık kabuğu tozları 100 °C sıcaklığında etüvde kurutulmuştur.



Şekil 1. Öğütülmüş fındık kabuğu

2.2 Karışımların Hazırlanması ve Test Plakası Üretilmesi

Karışımların hazırlanması ve testlerin gerçekleştirilmesindeki işlem sırası Şekil 2’de verilmiştir.

Şekil 2’de gösterilen şekilde karışımlar açık hamur milinde iki kademedede gerçekleştirildi. Öncelikle hamur milinde yumuşatılmış EPDM kauçuğuna dolgular, stearik asit, parafinik yağ ve Rhenofit EDMA/S kimyasalları eklenip hamur iyice karıştırılmıştır. Daha sonrasında bir müddet dinlendirilen kauçuk hamurunun ikinci kademesinde çapraz bağlayıcı ajan olan Trigonox 101 kimyasalı eklenip tekrar karıştırılmıştır. Karışım aşaması tamamlanan hamurlardan 175 °C’de 25 dakikada 2 mm’lik test plakaları üretilmiştir.



Şekil 2. Numune hazırlamadan karakterizasyona kadar olan süreçlerin şematik gösterimi

2.3 Karakterizasyon

R-AW kauçuk karışımlarının çekme özellikleri ZwickRoell Z2,5 tensometre cihazı ile test edilmiştir. Çekme testi DIN 53504 standardına göre 500 mm/dk çekme hızında ve oda sıcaklığında yapıldı. Karışımların yoğunluk analizleri DIN EN ISO 1183-1 standardına uygun bir şekilde gerçekleştirilmiştir. Sertlik değerleri DIN ISO 48-4 standardına göre Shore A tipi bir durometre kullanılarak ölçüldü.

Kürlenmemiş kauçuk karışımlarının kürlenme özellikleri, ortam koşullarında 24 saat şartlandırıldıktan sonra ASTM D2084’e göre 175°C’de 45 dakika hareketli kalıp reometresi (Alpha,MDR2000) ile belirlendi.

III. DENEYSEL SONUÇLAR ve TARTIŞMA

3.1 Mekanik Test Sonuçları

Çekme testlerine ait sayısal sonuçlar Tablo 2’de verilmiştir. Kopma mukavemetinin grafiksel olarak karşılaştırılması Şekil 3’te, Yırtılma anındaki uzama yüzdelерinin ve M100 değeri karşılaştırılması ise Şekil 4’te verilmiştir.

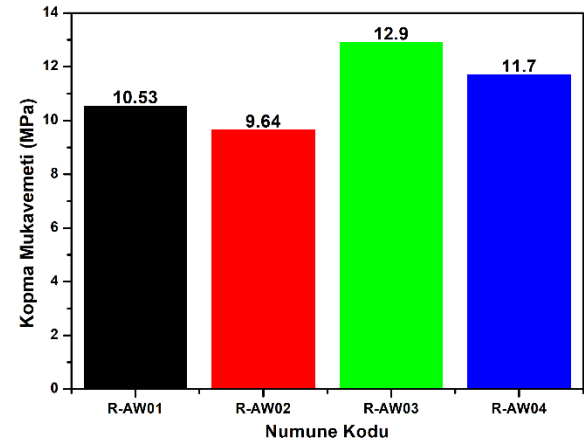
Yapılan mekanik testler sonucunda, EPDM kauçuk matrisine farklı oranlarda fındık kabuğu ilavesinin malzemenin mekanik özellikleri üzerinde belirgin etkiler yarattığı gözlemlenmiştir. R-AW01 (referans numune) ile karşılaştırıldığında, %10 fındık kabuğu içeren R-AW02 numunesinde kopma mukavemeti ve yırtılma anındaki uzama değerlerinde hafif bir azalma görülmüş, ancak M100 değerinde bir artış meydana gelmiştir. Bu, düşük oranlı dolgunun, malzemenin yapısal bütünlüğünü yeterince güçlendiremeyebileceğini veya matris içinde homojen dağılmadığını gösteriyor olabilir [3, 6].

Tablo 2. R-AW karışımlarının mekanik özellikleri

| Numune Kodu | Kopma Mukavemeti (MPa) | Yırtılma Anındaki Uzama (%) | M100 (N/mm ²) |
|-------------|------------------------|-----------------------------|---------------------------|
| R-AW01 | 10,53 | 523,91 | 1,78 |
| R-AW02 | 9,64 | 494,25 | 1,98 |
| R-AW03 | 12,9 | 370 | 4,21 |
| R-AW04 | 11,7 | 616 | 3,04 |

%20 fındık kabuğu içeren R-AW03 numunesi ise en yüksek kopma mukavemetine (12,90 MPa) ve M100 değerine (4,21 N/mm²) ulaşarak en iyi performansı sergilemiştir. Bu, fındık kabuğunun bu oranda etkili bir takviye malzemesi olarak işlev gördüğünü ve kauçuğun mekanik dayanımını artırdığını göstermektedir. Bununla birlikte, %30 fındık kabuğu içeren R-AW04 numunesinde kopma mukavemeti bir miktar düşmüş (11,70 MPa) ancak yırtılma anındaki uzama %616’ya çıkarak elastikiyetin belirgin şekilde arttığı gözlemlenmiştir. Bu durum, yüksek orandaki dolgunun kauçuk matrisinde yapısal yönlenmeye veya

sünek deformasyona yol açarak elastik davranışı artırdığını düşündürmektedir [7, 8]. Sonuç olarak, fındık kabuğu tozunun EPDM kauçuk reçetelerine eklenmesi, özellikle %20 oranında olmak üzere hem mukavemet hem de elastikiyet açısından önemli iyileşmeler sağlamaktadır. Ancak, fındık kabuğu oranının artırılması, yüksek elastikiyetle birlikte belirli ölçülerde mukavemet kayıplarına da yol açmaktadır.



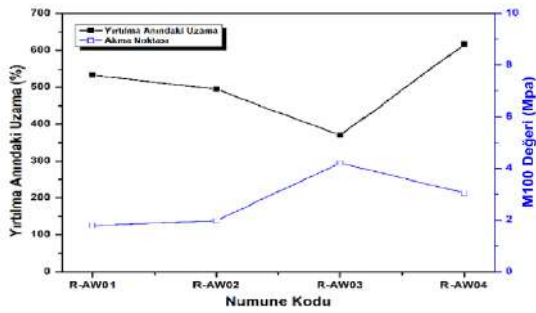
Şekil 3. Kopma mukavemetinin grafiksel karşılaştırılması

Şekil 4’te verilen grafikten de açıkça görüleceği üzere, EPDM kauçuk reçetelerine eklenen fındık kabuğu oranlarının kopma mukavemeti, yırtılma anındaki uzama ve M100 değerine etkisi net bir şekilde gözlemlenmiştir. Yırtılma anındaki uzama, başlangıçta dolgu oranı arttıkça azalma eğiliminde olmuştur, ancak %30 oranında fındık kabuğu eklenen numunede (R-AW04) belirgin bir artış (%616) görülmüştür. Bu, dolgu oranı çok yüksek olduğunda kauçuğun daha sünek ve elastik bir davranış sergilediğini ve yırtılma anındaki uzamanın arttığını göstermektedir.

M100 değerine, dolgu oranı arttıkça belirgin bir şekilde yükselmiştir, özellikle %20 fındık kabuğu eklenen numunede (R-AW03) M100 değerine en yüksek seviyeye ulaştığı görülmüştür (4,21 N/mm²). Bu, fındık kabuğu oranı arttıkça malzemenin daha rijit hale geldiğini ve plastik deformasyona karşı daha dirençli olduğunu göstermektedir. Ancak, %30 fındık kabuğu eklenen numunede M100 değerine bir miktar

azalmış (3,04 N/mm²), bu da yüksek orandaki dolgunun yapıyı zayıflatarak M100 değerine direncinde düşüşe yol açtığını düşündürmektedir.

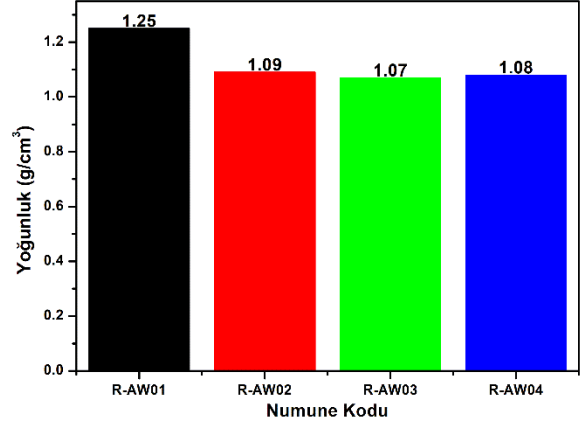
Şekil 5'te numunelere ait yoğunlukların karşılaştırılması ve Şekil 6'da ise numunelerin sertliklerinin karşılaştırılması verilmiştir. Fındık kabuğu oranının artmasının malzemenin yoğunluk ve sertlik üzerinde önemli etkiler yarattığını göstermektedir. Yoğunluk açısından, fındık kabuğu eklenmesiyle numunelerin genel yoğunluğu azalmıştır; bu durum, kompozit yapının daha hafif hale gelerek bazı uygulamalarda ağırlık avantajı sağlayabileceğini göstermektedir [9]. Özellikle %30 oranında fındık kabuğu eklenmesiyle yoğunluk en düşük değeri almış, bu da dolgu malzemesinin matrisin içine daha fazla entegre olduğunu ve materyalin hacimsel olarak sıkılaştığını göstermektedir.



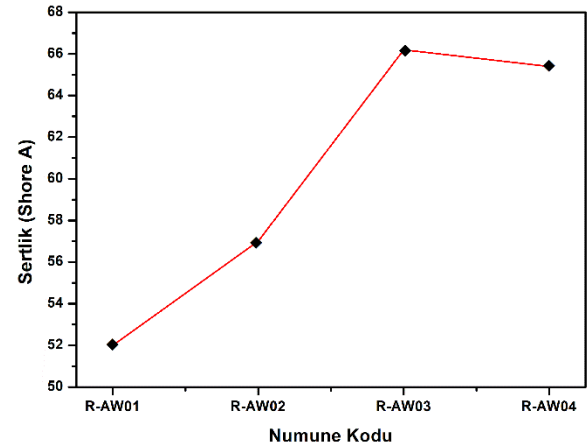
Şekil 4. Yırtılma anındaki uzamanın ve M100 değeri grafiksel olarak karşılaştırılması

Sertlik açısından ise, fındık kabuğu oranı arttıkça sertlik değerlerinde belirgin bir artış gözlenmiştir. R-AW02 numunesinde %10 fındık kabuğu ilavesiyle sertlik değeri artmış, ardından %20 ve %30 oranlarında sertlik daha da yükselmiştir. Bu durum, fındık kabuğunun kauçuğun yapısal sertliğini artırarak, malzemenin daha rijit ve dayanıklı hale gelmesine neden olduğunu göstermektedir [3]. Özellikle %30 fındık kabuğu eklenen numune (R-AW04) ile sertlik değerinin en yüksek seviyeye

çıkması, bu orandaki dolgunun malzeme üzerinde en güçlü sertleştirici etkiye sahip olduğunu ortaya koymaktadır.



Şekil 5. Numune yoğunluklarının grafiksel olarak karşılaştırılması



Şekil 6. Numune sertliklerinin grafiksel olarak karşılaştırılması

Yoğunluk ve sertlik verileri, fındık kabuğunun dolgu malzemesi olarak kullanımının kauçuğun mekanik özelliklerini iyileştirdiğini, ancak aşırı dolgu oranlarının bazı özelliklerde aşırı sertlik artışına yol açabileceğini göstermektedir. Bu da malzemenin işlenebilirliğini ve elastikiyetini etkileyebilir, dolayısıyla optimum dolgu oranı belirlemek, performans açısından kritik önem taşımaktadır.

3.3 Karışımların Kırılma Karakteristikleri

Karışımların 175 °C’deki kürlenme karakteristiklerine ait sonuçlar sırasıyla Tablo 4 ve Tablo 5’te verilmiştir. Karışımlarda FK oranının artmasıyla maksimum tork (MH) değerlerinde ve minimum tork değerlerinde artış gözlemlenmektedir. Karışımların kürlenme dereceleri ve kürlenme oran indeksi (CRI) denklem 1 ve denklem 2 kullanılarak hesaplanmıştır.

$$\text{Kürlenme Derecesi} = \text{MH} - \text{ML} \quad (1)$$

$$\text{Kürlenme oran indeksi} = \frac{100}{t_{90} - t_{s2}} \quad (2)$$

Kürlenme karakteristikleri, malzemenin işlem sırasında gösterdiği akışkanlık ve sertleşme hızını belirleyerek, üretim süreçlerinin verimliliğini etkileyen önemli bir parametredir [10, 11]. Tablo 4’te yer alan veriler, fındık kabuğu ilavesinin kürlenme süreleri üzerinde önemli etkiler oluşturduğunu göstermektedir. R-AW01 ve R-AW02 numunelerinde kürlenme süreleri oldukça yakın olup, sırasıyla ts2 (ilk kürlenme süresi) 42 ve 44 saniye, t90 (tam kürlenme süresi) ise sırasıyla 9:49 ve 10:07 dakikadır. Bu süreler, fındık kabuğu eklemesinin kürlenme sürecini belirgin şekilde değiştirmedini ve dolayısıyla işlem hızının fazla etkilenmediğini göstermektedir. Ancak, R-AW03 numunesi, %20 fındık kabuğu içeren karışıma sahip olup, kürlenme sürelerinde hem ts2 hem de t90 değerlerinde bir azalma göstermektedir: ts2 38 saniye ve t90 7:23 dakikadır. Bu, fındık kabuğunun dolgu malzemesi olarak kullanıldığında, kürlenme hızını artıran bir etki yarattığını göstermektedir. Ayrıca, R-AW04 numunesinde de kürlenme sürelerinin biraz daha kısa olduğu görülmektedir: ts2 40 saniye ve t90 6:46 dakika. Bu, %30 oranındaki fındık kabuğunun, kürlenme hızını daha da artırarak işlemi hızlandırdığını ortaya koymaktadır.

Tablo 5’te yer alan kürlenme derecesi ve kürlenme oranı indeksi (CRI) verileri, dolgu oranına bağlı olarak

kürlenme özelliklerindeki değişimleri göstermektedir. R-AW03 numunesi, en yüksek kürlenme derecesi ve CRI değerine sahip olup, kürlenme derecesi 19,64 ve CRI 13,2 ile en iyi kürlenme performansını sergilemiştir. Bu, %20 fındık kabuğu ilavesinin, kürlenme sırasında reaksiyon hızını artırarak daha yüksek bir kürlenme derecesi sağladığını göstermektedir. R-AW01 ve R-AW02 numunelerinde kürlenme derecesi 14,69 ile sabit kalırken, CRI değerleri 6:05 ve 18,32 arasında değişim göstermektedir. Bu, düşük dolgu oranlarına sahip numunelerde kürlenme hızının daha az etkilendiğini ve işlem süresinin uzun olduğunu düşündürmektedir. R-AW04 numunesinde ise kürlenme derecesi 16,69, CRI değeri ise 10,37 olarak ölçülmüştür; bu da yüksek dolgu oranının kürlenme hızını artırarak malzemenin daha hızlı bir şekilde sertleşmesini sağladığını göstermektedir [12].

Tablo 4. R-AW karışımlarının kürlenme karakteristikleri

| Numune Kodu | ML (dNm) | MH (dNm) | ts2 (min) | t90 (min) |
|-------------|----------|----------|-----------|-----------|
| RAW01 | 0,66 | 15,35 | 00:42 | 09:49 |
| RAW02 | 0,66 | 15,35 | 00:44 | 10:07 |
| RAW03 | 1,44 | 21,08 | 00:38 | 07:23 |
| RAW04 | 1,06 | 17,75 | 00:40 | 06:46 |

Tablo 5. R-AW karışımlarının kürlenme derecesi ve kürlenme oranı indeksi

| Numune Kodu | Kürlenme Derecesi | CRI |
|-------------|-------------------|-------|
| RAW01 | 14,69 | 06:05 |
| RAW02 | 14,69 | 18,32 |
| RAW03 | 19,64 | 13,2 |
| RAW04 | 16,69 | 10,37 |

Fındık kabuğunun dolgu malzemesi olarak eklenmesi, özellikle %20 ve %30 oranlarında, kürlenme hızını artırmış ve kürlenme derecesini yükseltmiştir. Bu, üretim süreçlerinde zaman tasarrufu sağlayan ve daha verimli işlem koşulları oluşturan bir etki yaratmıştır. Ancak, dolgu oranının çok yüksek olması, kürlenme hızını fazla artırarak bazı özelliklerde dengesiz sonuçlar doğurabilir. Bu nedenle, optimum dolgu

oranı belirlenerek, kürlenme ve mekanik özelliklerin en verimli şekilde elde edilmesi sağlanmalıdır.

IV. SONUÇLAR

Bu çalışmada, EPDM kauçuk reçetelerine karbon siyahı oranını azaltmak ve çevresel ayak izini minimize etmek amacıyla fındık kabuğunun dolgu malzemesi olarak kullanımının mekanik, kürlenme ve fiziksel özellikler üzerine etkileri incelenmiştir. Karbon siyahının çevresel ve ekonomik dezavantajları göz önünde bulundurularak, fındık kabuğu gibi yenilenebilir bir kaynağın takviye malzemesi olarak kullanımı hem sürdürülebilirlik hem de yerli kaynak kullanımı açısından önemli bir alternatif olarak değerlendirilmiştir. Elde edilen sonuçlar, fındık kabuğunun dolgu malzemesi olarak kullanılmasının EPDM kauçuğun özelliklerini iyileştirdiğini ve özellikle %20 oranında fındık kabuğu ilavesinin en yüksek mekanik performansı sağladığını göstermektedir. Kopma mukavemeti, M100 değeri ve yırtılma anındaki uzama değerleri, %20 fındık kabuğu içeren numunede en yüksek seviyeye ulaşmıştır. Bu, fındık kabuğunun, kauçuğun yapısal dayanımını artırarak, malzemenin mekanik özelliklerini güçlendirdiğini ve karbon siyahına alternatif olarak etkili bir dolgu malzemesi potansiyeli taşıdığını göstermektedir.

Fındık kabuğu eklemesiyle birlikte sertlik ve yoğunluk değerlerinde de artış gözlemlenmiştir, ancak aşırı dolgu oranları malzemenin sertliğini gereğinden fazla artırmış ve elastikiyetini sınırlamıştır. Özellikle %30 oranında fındık kabuğu ilavesi, yoğunluğu artırmış olsa da elastikiyet ve süneklik gibi bazı özelliklerde değişimlere neden olmuştur. Bu durum, fındık kabuğunun karbon siyahına yalnızca çevresel değil, aynı zamanda teknik bir alternatif olabileceğini ancak kullanım oranının dikkatle optimize edilmesi gerektiğini ortaya koymaktadır.

Kürlenme karakteristikleri açısından, fındık kabuğu ilavesinin kürlenme hızını artırdığı ve kürlenme derecesini yükselttiği gözlemlenmiştir. %20 ve %30 dolgu oranlarında, kürlenme süresi ve kürlenme oranı indeksi (CRI) değerlerinde artışlar sağlanmıştır. Bu durum, üretim süreçlerinde zaman tasarrufu sağlanmasına ve daha verimli üretim koşullarına yol açmaktadır. Ancak, aşırı dolgu oranlarının çok yüksek kürlenme hızlarına yol açabileceği ve bu durumun bazı fiziksel özellikler üzerinde olumsuz etkiler yaratabileceği göz önünde bulundurulmalıdır.

Genel olarak, bu çalışma, fındık kabuğunun alternatif bir dolgu malzemesi olarak EPDM kauçuk reçetelerinde etkili bir şekilde kullanılabileceğini göstermektedir. Karbon siyahı kullanımının azaltılması hedefi doğrultusunda, fındık kabuğu tozu hem çevresel sürdürülebilirlik hem de teknik performans açısından umut verici bir seçenek sunmaktadır. Ancak, optimum dolgu oranının belirlenmesi gerektiği, çünkü aşırı dolgu oranlarının bazı mekanik özelliklerde azalmaya neden olabileceği ve malzemenin işlenebilirliğini etkileyebileceği ortaya çıkmıştır. Gelecekteki çalışmalarda, fındık kabuğunun farklı oranlarda kullanımı ve uzun vadeli performansı daha detaylı olarak incelenmelidir.

KAYNAKLAR

- [1] Cengiz, Ö., Karagöz, İ., & Demirel, H. (2021). Fındık Kabuğu ve Talk Dolgulu Polipropilen Kompozitlerin Mekanik ve Isıl Özelliklerinin İncelenmesi. *8. Uluslararası Lif ve Polimer Araştırmaları Sempozyumu*, 18-19.
- [2] Karagöz, İ. (2024). Production and characterization of sustainable biocompatible PLA/walnut shell composite materials. *Polymer Bulletin*, 81(13), 11517-11537.
- [3] Kartal, İ., & Karagöz, İ. (2024). Enhancing natural rubber properties: a comprehensive study on the synergistic effects of wood sawdust and carbon black as fillers in rubber composites. *Polymer Bulletin*, 1-19.

[4] Karagöz, İ., Büyükkaya, K., Demirer, H., Mudu, M., & Kartal, İ. (2024). Mechanical and thermal characterization of elastomer modified polypropylene hybrid composites reinforced with hazelnut shell and wollastonite fillers. *Journal of Applied Polymer Science*, 141(30), e55710

[5] Çavuşoğlu, A., Uysal, N., Yazıcı, M., Şahin, P., & Karagöz, İ. Sustainable Innovation: Hazelnut Shell-Enhanced Polypropylene Composites for Eco-Friendly Automotive Applications.

[6] Barczewski, M., Sałasińska, K., & Szulc, J. (2019). Application of sunflower husk, hazelnut shell and walnut shell as waste agricultural fillers for epoxy-based composites: A study into mechanical behavior related to structural and rheological properties. *Polymer Testing*, 75, 1-11.

[7] Wang, Z., Yao, X., Hu, F., Ma, C., Li, X., Miao, Z., ... & Li, W. (2023). Study of the effect of carbon black filling on the mechanical behavior of rubber hyper-elasticity. *Materials*, 16(19), 6561.

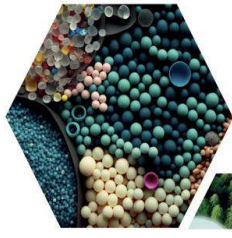
[8] Bokobza, L. (2004). The reinforcement of elastomeric networks by fillers. *Macromolecular Materials and Engineering*, 289(7), 607-621.

[9] Taşdemir, M. (2022). Isıl Yaşlandırmanın Yüksek Yoğunluklu Polietilen/Fındık Kabuğu Polimer Kompozitinin Mekanik Özelliklerine Etkisi. *International Periodical of Recent Technologies in Applied Engineering*, 3(1), 1-9.

[10] He, C., Chen, C., Zhang, G., Bai, T., Ji, Y., Pei, D., ... & Wang, W. (2024). Influence of environmentally friendly curing system on properties of railway rubber pad. *Journal of Applied Polymer Science*, 141(18), e55306.

[11] Tonogai, S., Hasegawa, K., & Fukuda, A. (1980). The disk cure test—An evaluation method for flow and curing characteristics of thermosetting molding compounds. *Polymer Engineering & Science*, 20(15), 985-994.

[12] Arayaprane, W., & Rempel, G. L. (2013). The effect of filler size on the cure characteristics, processability, mechanical properties, and morphology of stearic acid-coated CaCO₃ filled natural rubber compounds. *Journal of Current Science and Technology*, 3(2), 113-119.



16 ULUSLARARASI
LİF VE POLİMER
ARAŞTIRMALARI
SEMPOZYUMU

16th INTERNATIONAL FIBER AND POLYMER RESEARCH SYMPOSIUM

Sürdürülebilir ve İşlevsel Lif ve Polimerler
Sustainable and Functional Fibers & Polymers



9-10 Mayıs
May 2025

İstanbul Teknik Üniversitesi
Gümüşsuyu Prof. Dr. Necmettin Erbakan Yerleşkesi
İstanbul Technical University
Gumussuyu Prof. Dr. Necmettin Erbakan Campus



Production and Characterization of Polyimide Nanofiber Yarns via Electrospinning

Yasin Altın^{a,b*}

^aDepartment of Polymer Materials Engineering, Bursa Technical University, 16350 Bursa, Türkiye.

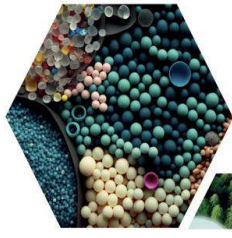
^bCentral Research Laboratory, Bursa Technical University, 16350 Bursa, Türkiye.

*Corresponding author: yasin.altin@bursa.edu.tr

ABSTRACT

This study focuses on the synthesis and characterization of polyimide (PI) nanofiber yarns. In the initial phase, polyamic acid (PAA), the precursor polymer essential for PI nanofiber yarn production, was synthesized, and optimal synthesis conditions were determined. Subsequently, the obtained PAA polymer was processed using the electrospinning technique under various conditions to produce PAA nanofiber mats. PAA nanofiber mats produced under optimal conditions were then utilized for the production of PI nanofiber mats and PI nanofiber yarns via thermal imidization and twisting processes, respectively. In the second phase of the project, the produced PAA and PI nanofiber mats, along with the PI yarns, were analyzed in detail using characterization techniques such as FT-IR, TGA, DSC, and SEM. The analyses confirmed the successful synthesis of PAA and its subsequent conversion to PI. Polyimide nanofiber yarns, composed of nanofibers with an average diameter of approximately 110 nm and possessing an overall yarn diameter of 616±28 µm, were successfully produced. Suggestions for future work include improving the mechanical properties of the PI nanofiber yarns, surface functionalization studies, investigation of potential application areas, and optimization of production processes. Addressing these recommendations could significantly contribute to the expanded industrial and commercial utilization of PI nanofiber yarns.

Keywords: Polyimide; Electrospinning; Nanofiber Yarn; Polyamic Acid; Thermal Imidization



16 ULUSLARARASI
LİF VE POLİMER
ARAŞTIRMALARI
SEMPOZYUMU

16th INTERNATIONAL FIBER AND POLYMER RESEARCH SYMPOSIUM

Sürdürülebilir ve İşlevsel Lif ve Polimerler
Sustainable and Functional Fibers & Polymers



9-10 Mayıs
May 2025

İstanbul Teknik Üniversitesi
Gümüşsuyu Prof. Dr. Necmettin Erbakan Yerleşkesi
İstanbul Technical University
Gumussuyu Prof. Dr. Necmettin Erbakan Campus

Production of facial sheet masks by adding green synthesized Ag nanoparticles with plant extracts and collagen to PCL composite nanofibers: Usability to promote acne and wrinkle reduction

Cansu Güneş^a, Fatma Ahsen Öktemer^b, Edanur Korkmaz^c, Mustafa Mert Kurdiş^d Ahmet Avcı^{e,*}

^a İzmir Vocational School, Biomedical Device Technology Program, Dokuz Eylül University, 35210, İzmir, Türkiye

^b Biomedical Engineering Department, Necmettin Erbakan University, Konya, 42090, Türkiye

^c Biomedical Engineering Department, Necmettin Erbakan University, Konya, 42090, Türkiye

^d Mechanical Engineering Dokuz Eylül University, 35210, İzmir, Türkiye

^e Mechatronics Engineering Department, KTO Karatay University, Konya, Postal Code, Türkiye

*Corresponding author: ahmet.avci@karatay.edu.tr

ABSTRACT

Acne, which occurs when the skin's pores become clogged with oil, dead skin or bacteria, is the 8th most common disease in the world and experienced by 80% of teenagers. Wrinkles occur on the face due to reasons such as slowing down collagen production with age, using excessive facial expressions, dry skin, pores blocked by dead skin cells, etc.

This study consists of two parts. In the first part, encapsulated Ag nanoparticles were produced with green synthesis using chamomile extract, aloe vera and collagen, which are effective against acne-causing bacteria. In the second part, different Ag nanoparticles were produced using wrinkle-preventing yoghurt herb, aloe vera that keeps the skin moist and collagen that nourishes the tissues. Biodegradable PCL nanofibers containing Ag nanoparticles encapsulated with plant extracts were prepared with electrospinning technique for anti-acne and anti-wrinkle facial masks. The active ingredients in plant extracts can be transported to the skin in a controlled manner by means of biodegradable PCL nanofibers. Ag nanoparticles with antibacterial properties also eliminate bacteria on the skin. The morphologies of Ag nanoparticles encapsulated with plant extracts and PCL composite nanofibers were analysed by scanning electron microscopy (FE-SEM) and transmission electron microscopy (TEM) images. The composite nanofibers were characterized by structural analysis technique using Fourier transform infrared spectroscopy (FT-IR). In addition, the strength of nanofibers with tensile tests and antibacterial activities with antibacterial tests were examined. The produced mask can be a new solution for removing acne and wrinkle as an alternative way instead of acne and anti-wrinkle creams due to its ease of use, high release capacity and controllability.

Keywords: Facial mask; PCL nanofibers; Green synthesis; Acne; Facial wrinkle

I. INTRODUCTION

People, especially women, try to look young and beautiful by using various liquid masks containing essences for their skin care. However, due to reasons

such as the weakness of the safety of essences and improper use, it also leads to inevitable harms. Recently, there has been a tendency towards cosmetic products obtained from extracts of natural and organic plants with green technology [1]. Since they are

liquefied with essences, it is not possible to get rid of the negative effects of the essence. In this direction, it has become necessary to develop green, natural and easy-to-use masks [2].

Electrospun nanofibers offer a new approach for cosmetic face masks that are cheap, convenient, and dry. Electrospun dry face masks are made of biodegradable polymers and contain active agents for various purposes such as effective against acne on the face, anti-aging, skin moisturizing, and antibacterial properties. Electrospun nanofiber dry masks also prevent problems such as leakage, adhesion, and dripping that occur in wet masks. In addition, nanofiber dry masks can simulate the extracellular matrix of the skin to the highest level since they have a very high surface area and porosity. They also increase the absorption of active ingredients [3-5].

By adding environmentally friendly active agents such as green tea extract, hyaluronic acid, chitosan, and collagen into nanofiber dry masks, the green environmental protection, safety and high efficiency functional masks were prepared [6,7].

Acne, which is caused by the activity of sebaceous glands and is seen especially in adolescence on the face, neck and chest, is a dermatological disease that affects people's lives. Acne is mostly associated with propionibacterium acnes (*P. acnes*), which causes inflammation by releasing extracellular enzymatic products such as proteases, hyaluronidases and lipases. There are various treatment methods for acne. Among these, topical treatment using washes, lotions and creams, oral isotretinoin treatment, oral antibiotic treatment and peeling treatment stand out. It is also known that synthetic drugs used in these treatments have high risks and side effects. Therefore, internal and external herbal treatments have been revealed to be quite effective and safe in acne treatment by research and applications [8, 9]. Extracts produced from the roots or leaves of plants such as aloe vera, neem, barberry, vidanga, curcuna longa and arjun have been found to be effective in acne treatment [10].

Due to aging, wrinkles appear on the skin, face, neck, hands and arms due to the decrease in skin elasticity and slowing down of collagen production. Since these wrinkles make people look old, various treatment methods have been developed. Some of these treatments include drug treatment, skin renewal techniques, fillers, laser treatment and plastic surgery applications. In addition to these treatments mentioned to delay aging and eliminate wrinkles, it is emphasized that flavonoids obtained from various plants have a great potential against aging on the skin, brain and heart due to their functional properties [11].

Flavonoids obtained from plants are promising candidates to obtain such products. Some examples of plants that have been studied as anti-aging agents include gutweed (*Aegopodium podagraria* L.), asian pennywort (*Centella asiatica* L.), spignel (*Meum athamanticum* L.), aloe species and sweet cherry stems [12,-14]. Aloe species contain two specific flavonoids called orientin and isovitexin, which can inhibit the enzyme hyaluronidase, which has major effects on skin health and inflammatory reactions [15].

Chamomilla (chamomile) plant has antiproliferative, anti-inflammatory and antioxidant properties with cytotoxic effect. Chamomilla has shown strong antibacterial activity against acne-causing bacteria [16]. Galium aparine has an anti-aging effect, provides elasticity to the skin, and delays the formation of wrinkles. Galium aparine has been used in traditional medicine to treat various skin conditions, minor wounds, and burns [17].

Aloe vera contains many beneficial substances such as polysaccharides, lignins, enzymes, vitamins, minerals, salicylic acid and amino acids. Among these, amino acids soften hardened skin cells and act as astringents to tighten pores. It also has an anti-acne effect. In addition, Aloe vera has anti-bacterial and anti-inflammatory properties that are good for acne treatment. These plants, which provide solutions to various skin problems, were used together within the scope of the study to create an alternative herbal solution for skin problems. In addition, studies have been conducted showing that aloe vera has cosmetic effects such as whitening, sun protection, antioxidant, anti-aging and moisturizing [18-21].

In this study, dry facial masks were produced from PCL biodegradable electrospun nanofibers doped with Ag nanoparticles encapsulated with various plant extracts. For this purpose, two groups of PCL nanofiber systems were created. In the first group, PCL nanofibers doped with Ag nanoparticles encapsulated with chamomile extract and collagen were produced. In the second group, PCL nanofibers doped with Ag nanoparticles encapsulated with yoghurt herb (galium aparine) extract and collagen were produced. Face masks were formed from nanofiber mats produced by electrospinning method. The size and shape of the encapsulated Ag nanoparticles were examined by TEM microscopy images and the morphology of PCL nanofiber structures were inspected by SEM microscopy images. The absorption effects of excitation at vibrational energy levels of molecules and ions of nanofiber structures were analyzed by Fourier transform infrared spectroscopy (FTIR). The strength and modules of elasticity of PCL nanofiber groups were found by

tensile tests. Also, their antibacterial activities were carried out with gram negative and gram positive bacteria.

The dry masks produced in this study offer an alternative solution to acne removing and anti-wrinkle creams. In order for these masks to be usable, in vitro tests such as tyrosinase inhibition, water vapor transmittance, water contact angle measurement, and biocompatibility tests as well as in vivo tests are required.

II. EXPERIMENTAL METHOD / TEORETICAL METHOD

2.1 Materials

Silver nitrate (AgNO_3 ; 99%) was supplied from Nanokar Technology, Istanbul, Türkiye. Polycaprolactone (PCL; M_v : 80,000 g/mol), chloroform and dichloromethane (DCM) were purchased from Sigma-Aldrich. Escherichia Coli 25922 (gram negative) and Staphylococci Aureus 29213 (gram positive) bacteria used for antibacterial activity. Tests were taken from Necmettin Erbakan Medical Faculty Hospital Microbiology Laboratory. All chemical reagents used in the experiments were used without further purification since they were at analytical level.

2.2 Fabrication of Ag nanoparticler Using Green Synthesis

Two different Ag nanoparticles were produced using chamomile extract and galium aparine extract using the green synthesis method. 10 g of dried chamomile was mixed with 1 liter of pure water and left to dissolve at room temperature for 24 hours. The resulting solution was filtered with filter paper. For Ag nanoparticle synthesis, 2 mL camilime extract and 7 mL pure water were added to a beaker. 1 ml of the previously prepared 0.1 M AgNO_3 solution was taken and added dropwise to the solution in the beaker [22].



Figure 1. Preparation of solution from plant extract and production of nanoparticles by green synthesis.

These processes were carried out on a magnetic stirrer. The solution was kept in the dark at room temperature for 24 hours to complete the chemical reaction

The solution whose reaction was completed was taken into a large container and evaporated in an oven at 200 °C. The remaining chamomile molecule encapsulated Ag nanoparticles residue at the bottom of the container was collected. Similarly, encapsulated Ag nanoparticles were produced from the extract of the galium aparine. Figure 1 shows a schematic representation of nanoparticle production by green synthesis.

2.3 Production of PCL nanofibers

Two different nanofibers were produced by electrospinning using PCL biodegradable polymer. One of them was produced by adding Ag nanoparticles encapsulated with chamomile extract, aloe vera and collagen to PCL. The second one was produced by incorporating Ag nanoparticles encapsulated with gallium aparin molecules, aloe vera and collagen into PCL.

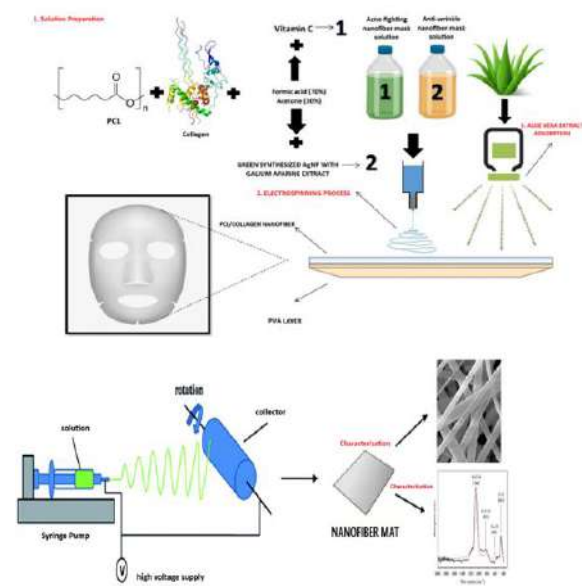


Figure 2. (a) Flowchart of solution preparation and mask production in nanofibers and (b) Production of PCL nanofiber mat.

For electrospinning process, AgNP-collagen encapsulated with chamomile aleo-vera/PCL solution and AgNP-collagen encapsulated with gallium aparin-aleo vera/PCL solution were prepared. Then, nanofibers were formed under high voltage electric field by applying electrospinning technique. 12% (w/v) PCL, 50% (v/v) chloroform, 50% (v/v) dimethylformamide (DMF), and 1% w/v encapsulated AgNPs were added to the solution. The prepared

solution was taken into a 10 ml syringe and placed in the electrospinning device. The distance between the needle tip and the collector was set to 12 cm. A rotating cylinder coated with Al foil was used as the collector. The electrospinning process was applied at a feed rate of 1.00 mL/h and a voltage of 25 kV for both nanofiber composite solutions. Solution preparation processes for the production of AgNP-doped PCL/collagen nanofiber masks and spinning of nanofiber mats are shown in Figure 2.

2.4 Characterization of AgNPs and Nanofibers

The sizes and shapes of green synthesized AgNPs with chamomile and gallium aparine extracts were analyzed with a transmission electron microscope (TEM, JEOL JEM-2100). The structures and morphologies of both groups of PCL composite nanofibers synthesized by electrospinning were examined with a scanning electron microscope (SEM, ZEISS Gemini SEM 500) images. The chemical structures and attenuated total reflections of PCL composite nanofibers were analyzed by Fourier Transform Infrared (FTIR) (Thermo Scientific—Nicolet iS20) Spectrometer. The absorption modes of the spectra were measured in the wavelength range of 4000–400 cm^{-1} .

2.5 Mechanical testing of PCL nanofiber mats

The mechanical tests of encapsulated AgNPs doped PCL nanofiber mats were performed using a universal testing machine (Shimadzu AG-X, 10 kN). The tensile strength, elastic modulus, and elongation of PCL composite nanofiber mats were performed by tensile testing according to ASTM D638-14. The dimensions of the PCL mat samples were cut to 50 mm x 10 mm. The thicknesses of the samples were measured using a micrometer after the nanofiber mats were placed between two glass slides. The tensile tests of the prepared samples were carried out at a speed of 100 mm/min. Five samples from both groups of PCL nanofiber mats were tested. The maximum tensile strengths, maximum elongations, and stress-strain curves from the tests performed were reported using the trapezium software connected to the testing machine. The elastic moduli of the PCL nanofiber mats were calculated from the slope of the initial linear part of the stress-strain curves.

2.6 In Vitro Antibacterial Activity

The antibacterial activities of PCL composite nanofiber groups were evaluated against both gram-negative *E. coli* and gram-positive *S. aureus* by disk diffusion qualitative tests. Disc samples cut with a diameter of 12 mm were sterilized under UV irradiation of both sides of the nanofibers for 30 minutes. *E. coli* and *S. aureus* bacterial strains were

grown in nutrient broth by incubating at room temperature for 24 hours. *E. coli* and *S. aureus* bacterial colonies were also balanced at 0.5 McFarland. The bacterial suspension was extended on Muller-Hinton agar medium in petri dishes. Sterilized PCL nanofiber samples were placed in bacterial culture and incubated at 37 °C for 24 h. The inhibition zone diameters formed on the discs were measured using Image J software.

III. RESULTS AND DISCUSSIONS

3.1 TEM image of AgNPs

TEM images of green AgNPs synthesized using chamomile extract and galium aparine extract are shown in Figure 3 (a) and Figure 3 (b), respectively. From these images, it is obvious that the shapes of both types of AgNPs are oval, close to the sphere. The size of AgNPs coated with chamomile molecules varies from 10 nm to 40 nm. The average size is around 20 nm. The size of AgNPs coated with galium aparine molecules ranging between 20 nm and 35 nm, and the average size is around 30 nm.

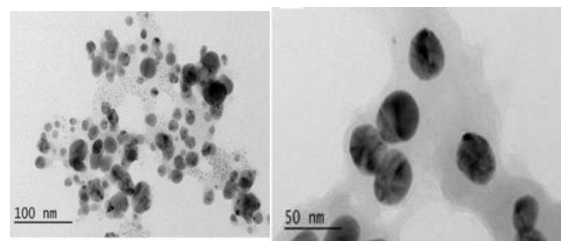


Figure 3. (a) TEM image of chamomile molecules encapsulated AgNPs and (b) Galium aparine molecules encapsulated AgNPs

3.2. SEM image of PCL composite nanofibers

Figure 4 shows the SEM image of galium aparine encapsulated AgNP-PCL/collagen nanofibers produced by electrospinning and the SEM image of nanofibers with aloe vera extract sprayed on these fibers. The SEM image of chamomile encapsulated AgNP-PCL/collagen nanofibers and the SEM image of nanofibers with aloe vera extract sprayed on these fibers are shown in Figure 4. Both in Figure 4a and Figure 4c, it is seen that the surfaces of PCL nanofibers with encapsulated AgNPs are quite rough. This is due to the AgNPs entering the nanofibers. One of the reasons why the surfaces of the nanofibers are rough is that AgNPs have very high conductivity and interact with the electric field in the environment during electrospinning [23]. When the SEM image given in Figure 4a is examined, the average diameter of galium aparine encapsulated AgNP/PCL/collagen nanofibers is calculated as 375 nm. Similarly, the average nanofiber diameter was calculated as 337 nm from the

SEM image of the Chamomile encapsulated AgNP/PCL/collagen nanofibers shown in Figure 4c.

Figure 4b and Figure 4d show SEM images of aloe vera extract coated on AgNP-doped PCL/collagen nanofibers. Aloe vera extract was coated on the surface of AgNP-doped PCL/collagen nanofibers by spraying to increase antibacterial activity, eliminate acne on the skin, and enhance anti-wrinkle performance [17-19]. The anti-aging effectiveness of aloe vera extracted gel preparations has been shown in many studies [24,25]. Aloe vera extract formed agglomerates on the surfaces of nanofibers in some places and was coated more sparsely in other parts.

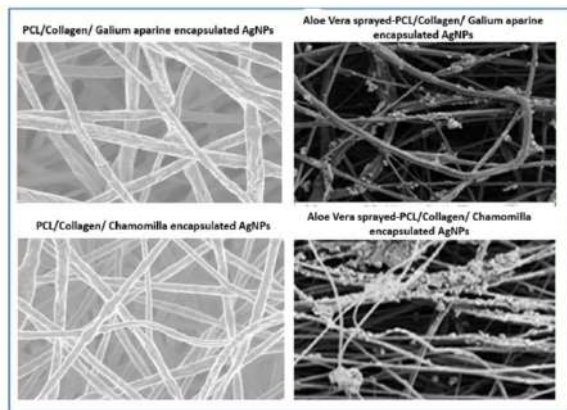


Figure 4. (a)Galium aparine encapsulated AgNP/ PCL/collagen nanofibers and (b) Aloe vera extract sprayed on nanofibers of galium aparine encapsulated AgNP/ PCL/collagen. (c) Chamomile encapsulated AgNP/PCL/collagen and (d) Aloe vera extract sprayed on nanofibers of chamomile encapsulated AgNP/ PCL/collagen.

3.3 FTIR Analysis

FTIR is an analytical tool used to analyze the chemical bonds and functional groups of a material and obtain information about its structure. Figure 5 shows FTIR spectra of chamomile extract encapsulated AgNPs doped PCL/collagen/aloe vera nanofibers. FTIR spectra of galium aparine extract encapsulated AgNPs doped PCL/collagen/aloe vera nanofibers are also shown in Figure 5. The similar peaks were obtained in the FTIR spectra of both groups of nanofiber systems.

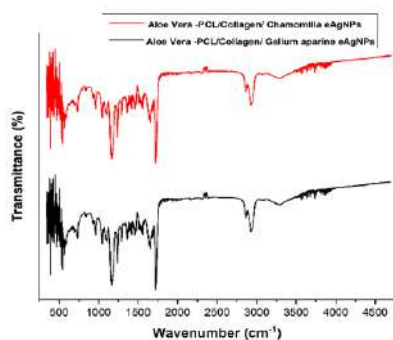


Figure 5. FTIR spectrums of PCL composite nanofiber systems.

The striking peaks of PCL nanofibers were observed as asymmetric CH₂ stretching vibration at 2943 cm⁻¹, symmetric CH₂ stretching vibration at 2866 cm⁻¹, carbonyl (C=O) stretching vibration at 1721 cm⁻¹, (C-H) symmetric deformation at 1470 cm⁻¹, (C-O) symmetric stretching vibration at 1365 cm⁻¹, and asymmetric (C-O-C) stretching at 1239 cm⁻¹. The peaks of collagen inside the nanofibers originating from amide-I at 1643, amide II at 1549 and amide III at 1238 are observed [26].

3.4. Mechanical Properties

Figure 6 shows the stress-strain curves obtained as a result of tensile tests of two groups of PCL nanofiber mats. The highest tensile strength belongs to galium aparine encapsulated AgNP doped PCL/collagen/aloe vera nanofiber mats. The highest tensile strength is 6.85 MPa and belongs to galium aparine encapsulated AgNP doped PCL/collagen/aloe vera nanocomposite with chamomile encapsulated AgNP is 5.28 MPa. The strength of the PCL/collagen/aloe vera nanocomposite with chamomile encapsulated AgNP is 5.28 MPa. The strength of the galium aparine encapsulated AgNPs doped PCL/collagen/aloe vera composite nanofiber mat is 29.7% higher than the strength of the Chamomile encapsulated AgNP added PCL. The highest strength was observed in the galium aparine coated AgNP PCL nanofibers because these encapsulated AgNPs formed a strong chemical and mechanical bond with the PCL.

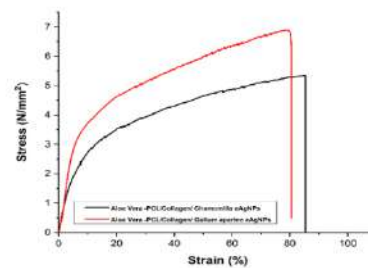


Figure 6. Stress-strain curves of AgNPs doped PCL/Collagen/aloe vera composite nanofiber mats

3.4 Antibacterial Activity

Figure 7 shows antibacterial activity of chamomile extract encapsulated AgNPs doped PCL/collagen/aloe vera nanofibers and galium aparine extract encapsulated AgNPs doped PCL/collagen/aloe vera nanofibers against both gram-negative *E. coli* and gram-positive *S. aureus*. In addition, the antibacterial properties of PCL nanofiber groups not sprayed with aloe vera are given in Figure 7. It was observed that both groups of PCL composite nanofiber mats exhibited antibacterial activity against both *E. coli* and

S. aureus bacteria under the same test conditions. The inhibition zones formed around both chamomile extract encapsulated AgNPs doped PCL/collagen/aloe vera nanofiber and gallium aparine extract encapsulated AgNPs doped PCL/collagen/aloe vera nanofiber mats were measured as 20.94 mm and 15.53 mm against *E. coli*, respectively. The inhibition zones around the same group of PCL nanofiber mats were evaluated as 23.18 mm and 17.25 mm against *S. aureus*, respectively. On the other hand, when the antibacterial activities of PCL nanofiber mats not sprayed with aloe vera extract were examined against *E. coli*, the zone diameter was 18.49 mm in chamomile extract encapsulated AgNPs doped nanofibers, while the zone diameter was measured as 12.37 mm when gallium aparine extract encapsulated AgNPs added nanofibers. The inhibition diameters of these group PCL nanofiber mats against *S. aureus* were measured as 19.67 and 13.72 mm, respectively. In this study, it was observed that the addition of encapsulated AgNPs and collagens to PCL nanofibers was highly effective against both *E. coli* and *S. aureus* bacteria. It was revealed that the antibacterial effect was increased more when aloe vera extract was coated on the surfaces of these PCL nanofiber groups.

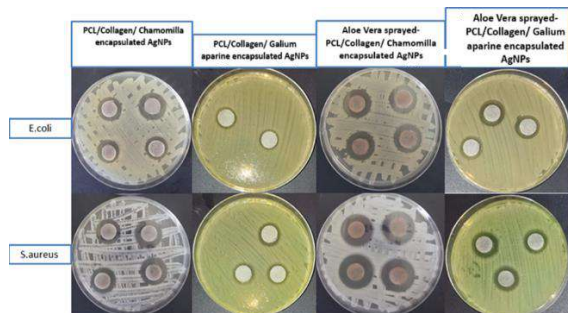


Figure 7. Antibacterial activity of PCL nanofiber systems for *E. coli* and *S. aureus*

The antibacterial effect against *E. coli* of chamomile extract encapsulated AgNP doped PCL/collagen/aloe vera nanofiber mats was 20% higher than the nanofibers without aloe vera. The antibacterial effect of the aloe vera containing nanofibers of this PCL group against *S. aureus* was 17.8% higher than the nanofibers without aloe vera. When aloe vera is present in PCL nanofibers containing gallium aparine encapsulated AgNPs, the antibacterial effect against *E. coli* is 25% higher than the nanofibers without aloe vera.

IV. CONCLUSIONS

This study aims to present a biological treatment applied to the face as a dry mask that is effective in acne treatment and eliminates wrinkles caused by aging. AgNPs were produced by green synthesis using

chamomile and malium aparin extracts. These encapsulated AgNPs were combined with PCL biodegradable polymer and collagen to produce composite nanofibers by electrospinning. In addition, aloe vera extract was coated by spraying onto the surfaces of this PCL composite nanofiber. The cosmetic dry face masks produced from electrospun nanofibers are cheap, easy to use, and contain active agents that do not harm the skin. The shape and size of the encapsulated AgNPs were analyzed by taking TEM images. The morphological structures of four types of PCL composite nanofibers were examined with SEM images. The strength and elasticity modulus of the produced nanofibers were carried out by mechanical tests. The tensile strength and elasticity modulus of the mats of nanofibers containing gallium aparin were higher than those containing chamomile. This shows that some plant molecules have a significant positive effect on the mechanical properties of PCL nanofibers. Chemical bonds and functional groups of PCL nanofibers with collagen were determined by FTIR analysis. It was observed that all PCL composite nanofiber mats exhibited strong antibacterial activity against both *E. coli* and *S. aureus* bacteria under the same test conditions. In line with these results, it can be said that encapsulated AgNP-doped PCL/collagen nanofiber systems are successful in dry facial masks for acne treating and wrinkle removal.

REFERENCES

- [1] Y.-H. Choi, S.E. Kim, K.-H. Lee, Changes in consumers' awareness and interest in cosmetic products during the pandemic, *Fash. Text.* 9 (1) (2022).
- [2] P. Morganti, M.-B. Coltelli, A new carrier for advanced cosmeceuticals, *Cosmetics* 6, (1) (2019).
- [3] J. Teno, M. Pardo-Figueroa, N. Hummel, V. Bonin, A. Fusco, C. Ricci, G. Donnarumma, M.-B. Coltelli, S. Danti, J.M. Lagaron, Preliminary studies on an innovative bioactive skin soluble beauty mask made by combining electrospinning and dry powder impregnation, *Cosmetics* 7 (4) (2020).
- [4] Qiaolin Yang a, Ya Tian a, Yuchun Liu a, Wen Shi, A novel multi-functional skin-care dry mask based on Bletilla Striata polysaccharide electrospun nanofibers, *International Journal of Biological Macromolecules* 282 (2024) 136780.
- [5] EF Ediz, C Güneş, M Demirel Kars, A Avcı, In vitro assessment of Momordica charantia/Hypericum

perforatum oils loaded PCL/Collagen fibers: Novel scaffold for tissue engineering, *Journal of Applied Biomaterials & Functional Materials* 22, (2024), doi: 22808000231221067.

[6] Y.S. Kaisong Huang, Hanbai Wu, Yuhan Chen, Shuai Zhang, Shuo Shi, Chunxia Guo, Jinlian Hu, Electrospayed environment-friendly dry triode-like facial masks for skincare, *ACS Appl. Mater. Interfaces* 16

[7] H.Y. Wenfeng Hu, Yujie Guo, Yantao Gao, Yi Zhao, Fabrication of multifunctional facial masks from phenolic acid grafted chitosan/collagen peptides via aqueous electrospinning, *Int. J. Biol. Macromol.* 267 (1) (2024).

[8] Waghmare PR, Ka(1) (2024) 1899–1919.kade PG, Takdhat PL, Nagrale AM, Thakare SM, Parate MM. Turmeric as Medicinal Plant for the Treatment of Acne vulgaris; *PharmaTutor*. 2017; 5(4):19-27.

[9] Hossain MA, Shah MD, Sakari M. Gas chromatography–Mass Spectrometry Analysis of Various Organic Extracts of *Merremia Borneensis* from Sabah. *Asian Pacific Journal of Tropical Medicine*. 2011; 4(8):637–641.

[10] Sonali Syal, Vinay Pandit, M. S Ashawat, Traditional Herbs to treat Acne Vulgaris, *Asian Journal of Pharmaceutical Research*, 2020, 10(3), DOI: 10.5958/2231-5691.2020.00034.9

[11] Bogdan Păcularu-Burada, Alexandru-Ionut, Cîrîc and Mihaela Begea, Anti-Aging Effects of Flavonoids from Plant Extracts, *Foods*, 2024, 13, 2441. <https://doi.org/10.3390/foods13152441>

[12] Zofia, N.-L, Martyna, Z.-D Ziemlewska, A, Bujak, T. Comparison of the Antiaging and Protective Properties of Plants from the Apiaceae Family. *Oxidative Med. Cell. Longev.* 2020, 2020, 5307614. [

[13] Viany, L., Rizal, R., Widowati, W., Samin, B. Kusuma, R. Fachrial, E. Nyoman, L.E. Comparison of Antioxidant and Antiaging Activities Between Dragon Fruit (*Hyloceureus Polyrhizus* (F.A.C. Weber) Britton & Rose) Rind Extract and Kaempferol. *Maj. Kedokt. Bdg.* 2019, 51, 147–153.

[14] Tizazu, A.; Bekele, T. A Review on the Medicinal Applications of Flavonoids from Aloe Species. *Eur. J. Med. Chem. Rep.* 2024, 10, 100135.

[15] Tizazu, A.; Bekele, T. A Review on the Medicinal Applications of Flavonoids from Aloe Species. *Eur. J. Med. Chem. Rep.* 2024, 10, 100135

[16] Jaykant Vora, Anshu Srivastava, Hashmukh Modi, Antibacterial and antioxidant strategies for acne

treatment through plant extracts, *Informatics in Medicine Unlocked* 16 (2019) 100229.

[17] Tundis, M.R. Loizzo, M. Bonesi and F. Menichini, Potential Role of Natural Compounds Against Skin Aging, *Current Medicinal Chemistry*, Volume 22, Issue 12, Apr 2015, p. 1515 – 1538.

[18] Cai JF. Research progress of pharmacological mechanism of active components in Aloe. *World Latest Med. Inf.* (Electronic Version). 2018;18(102):122–125. 4.

[19] Sanchez M, Gonzalez-Burgos E, Iglesias I, et al. Pharmacological update properties of Aloe vera and its major active constituents. *Molecules*. 2020;25(6):1324. 5.

[20] Mansoor K, Aburjai T, Al-Mamoori F, et al. Plants with cosmetic uses. *Phytother Res.* 2023;37(12):5755–5768. 6.

[21] Nie LH. Developing and using of Aloe vera. *Food Res Dev.* 2006;27(2):147.

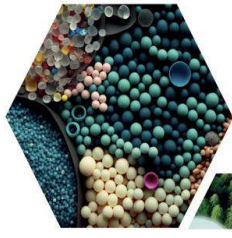
[22] M. O. Avci, N. Muzoglu, A. E. Yilmaz, B. S. Yarman, Antibacterial, cytotoxicity and biodegradability studies of polycaprolactone nanofibers holding green synthesized Ag nanoparticles using atropa belladonna extract, *Journal of Biomaterials Science, Polymer Edition*, 2022, vol. 33, no. 9, 1157–1180.

[23] Feifei Liu, Xuwei Chenga, Lu Xiao, et al, Inside-outside Ag nanoparticles-loaded polylactic acid electrospun fiber for long-term antibacterial and bone regeneration, *International Journal of Biological Macromolecules* 167 (2021) 1338–1348.

[24] Mutiara Dwi Lestari, Siti Maimunah, Andre Prayoga, Formulation of Red Beet (*Beta vulgaris*. L) and Aloe Vera (*Aloe vera*) Gel Extracts as Anti-Aging, [2023], doi: <https://doi.org/10.36987/jpbn.v9i2.4478>

[25] Bheta Sari Dewi, Silvia Surini, Study on hydrogel eye mask with *Centella asiatica* L and Aloe vera L extract, *Journal Of Advanced Pharmacy Education And Research*. [2024], doi: 10.51847/9UToWXppYP.

[26] J.M.A. Mancipe, M.L. Diasb, el al., Type I collagen – poly(vinyl alcohol) electrospun nanofibers: FTIR study of the collagen helical structure preservation, *Polymer-Plastics Technology And Materials*, 2022, 61 (8), 846–860, <https://doi.org/10.1080/25740881.2022.2029887>.



16 ULUSLARARASI
LİF VE POLİMER
ARAŞTIRMALARI
SEMPOZYUMU

16th INTERNATIONAL FIBER AND POLYMER RESEARCH SYMPOSIUM

Sürdürülebilir ve İşlevsel Lif ve Polimerler
Sustainable and Functional Fibers & Polymers



9-10 Mayıs
May 2025

İstanbul Teknik Üniversitesi
Gümüşsuyu Prof. Dr. Necmettin Erbakan Yerleşkesi
İstanbul Technical University
Gumussuyu Prof. Dr. Necmettin Erbakan Campus

Production of facial sheet masks by adding green synthesized Ag nanoparticles with plant extracts and collagen to PCL composite nanofibers: Usability to promote acne and wrinkle reduction

Cansu Güneş^a, Fatma Ahsen Öktemer^b, Edanur Korkmaz^c, Mustafa Mert Kurdiş^d Ahmet Avcı^{e,*}

^a İzmir Vocational School, Biomedical Device Technology Program, Dokuz Eylül University, 35210, İzmir, Türkiye

^b Biomedical Engineering Department, Necmettin Erbakan University, Konya, 42090, Türkiye

^c Biomedical Engineering Department, Necmettin Erbakan University, Konya, 42090, Türkiye

^d Mechanical Engineering Dokuz Eylül University, 35210, İzmir, Türkiye

^e Mechatronics Engineering Department, KTO Karatay University, Konya, Postal Code, Türkiye

*Corresponding author: ahmet.avci@karatay.edu.tr

ABSTRACT

Acne, which occurs when the skin's pores become clogged with oil, dead skin or bacteria, is the 8th most common disease in the world and experienced by 80% of teenagers. Wrinkles occur on the face due to reasons such as slowing down collagen production with age, using excessive facial expressions, dry skin, pores blocked by dead skin cells, etc.

This study consists of two parts. In the first part, encapsulated Ag nanoparticles were produced with green synthesis using chamomile extract, aloe vera and collagen, which are effective against acne-causing bacteria. In the second part, different Ag nanoparticles were produced using wrinkle-preventing yoghurt herb, aloe vera that keeps the skin moist and collagen that nourishes the tissues. Biodegradable PCL nanofibers containing Ag nanoparticles encapsulated with plant extracts were prepared with electrospinning technique for anti-acne and anti-wrinkle facial masks. The active ingredients in plant extracts can be transported to the skin in a controlled manner by means of biodegradable PCL nanofibers. Ag nanoparticles with antibacterial properties also eliminate bacteria on the skin. The morphologies of Ag nanoparticles encapsulated with plant extracts and PCL composite nanofibers were analysed by scanning electron microscopy (FE-SEM) and transmission electron microscopy (TEM) images. The composite nanofibers were characterized by structural analysis technique using Fourier transform infrared spectroscopy (FT-IR). In addition, the strength of nanofibers with tensile tests and antibacterial activities with antibacterial tests were examined. The produced mask can be a new solution for removing acne and wrinkle as an alternative way instead of acne and anti-wrinkle creams due to its ease of use, high release capacity and controllability.

Keywords: Facial mask; PCL nanofibers; Green synthesis; Acne; Facial wrinkle

I. INTRODUCTION

People, especially women, try to look young and beautiful by using various liquid masks containing essences for their skin care. However, due to reasons

such as the weakness of the safety of essences and improper use, it also leads to inevitable harms. Recently, there has been a tendency towards cosmetic products obtained from extracts of natural and organic plants with green technology [1]. Since they are

liquefied with essences, it is not possible to get rid of the negative effects of the essence. In this direction, it has become necessary to develop green, natural and easy-to-use masks [2].

Electrospun nanofibers offer a new approach for cosmetic face masks that are cheap, convenient, and dry. Electrospun dry face masks are made of biodegradable polymers and contain active agents for various purposes such as effective against acne on the face, anti-aging, skin moisturizing, and antibacterial properties. Electrospun nanofiber dry masks also prevent problems such as leakage, adhesion, and dripping that occur in wet masks. In addition, nanofiber dry masks can simulate the extracellular matrix of the skin to the highest level since they have a very high surface area and porosity. They also increase the absorption of active ingredients [3-5].

By adding environmentally friendly active agents such as green tea extract, hyaluronic acid, chitosan, and collagen into nanofiber dry masks, the green environmental protection, safety and high efficiency functional masks were prepared [6,7].

Acne, which is caused by the activity of sebaceous glands and is seen especially in adolescence on the face, neck and chest, is a dermatological disease that affects people's lives. Acne is mostly associated with propionibacterium acnes (*P. acnes*), which causes inflammation by releasing extracellular enzymatic products such as proteases, hyaluronidases and lipases. There are various treatment methods for acne. Among these, topical treatment using washes, lotions and creams, oral isotretinoin treatment, oral antibiotic treatment and peeling treatment stand out. It is also known that synthetic drugs used in these treatments have high risks and side effects. Therefore, internal and external herbal treatments have been revealed to be quite effective and safe in acne treatment by research and applications [8, 9]. Extracts produced from the roots or leaves of plants such as aloe vera, neem, barberry, vidanga, curcuna longa and arjun have been found to be effective in acne treatment [10].

Due to aging, wrinkles appear on the skin, face, neck, hands and arms due to the decrease in skin elasticity and slowing down of collagen production. Since these wrinkles make people look old, various treatment methods have been developed. Some of these treatments include drug treatment, skin renewal techniques, fillers, laser treatment and plastic surgery applications. In addition to these treatments mentioned to delay aging and eliminate wrinkles, it is emphasized that flavonoids obtained from various plants have a great potential against aging on the skin, brain and heart due to their functional properties [11].

Flavonoids obtained from plants are promising candidates to obtain such products. Some examples of plants that have been studied as anti-aging agents include gutweed (*Aegopodium podagraria* L.), asian pennywort (*Centella asiatica* L.), spignel (*Meum athamanticum* L.), aloe species and sweet cherry stems [12,-14]. Aloe species contain two specific flavonoids called orientin and isovitexin, which can inhibit the enzyme hyaluronidase, which has major effects on skin health and inflammatory reactions [15].

Chamomilla (chamomile) plant has antiproliferative, anti-inflammatory and antioxidant properties with cytotoxic effect. Chamomilla has shown strong antibacterial activity against acne-causing bacteria [16]. Galium aparine has an anti-aging effect, provides elasticity to the skin, and delays the formation of wrinkles. Galium aparine has been used in traditional medicine to treat various skin conditions, minor wounds, and burns [17].

Aloe vera contains many beneficial substances such as polysaccharides, lignins, enzymes, vitamins, minerals, salicylic acid and amino acids. Among these, amino acids soften hardened skin cells and act as astringents to tighten pores. It also has an anti-acne effect. In addition, Aloe vera has anti-bacterial and anti-inflammatory properties that are good for acne treatment. These plants, which provide solutions to various skin problems, were used together within the scope of the study to create an alternative herbal solution for skin problems. In addition, studies have been conducted showing that aloe vera has cosmetic effects such as whitening, sun protection, antioxidant, anti-aging and moisturizing [18-21].

In this study, dry facial masks were produced from PCL biodegradable electrospun nanofibers doped with Ag nanoparticles encapsulated with various plant extracts. For this purpose, two groups of PCL nanofiber systems were created. In the first group, PCL nanofibers doped with Ag nanoparticles encapsulated with chamomile extract and collagen were produced. In the second group, PCL nanofibers doped with Ag nanoparticles encapsulated with yoghurt herb (galium aparine) extract and collagen were produced. Face masks were formed from nanofiber mats produced by electrospinning method. The size and shape of the encapsulated Ag nanoparticles were examined by TEM microscopy images and the morphology of PCL nanofiber structures were inspected by SEM microscopy images. The absorption effects of excitation at vibrational energy levels of molecules and ions of nanofiber structures were analyzed by Fourier transform infrared spectroscopy (FTIR). The strength and modules of elasticity of PCL nanofiber groups were found by

tensile tests. Also, their antibacterial activities were carried out with gram negative and gram positive bacteria.

The dry masks produced in this study offer an alternative solution to acne removing and anti-wrinkle creams. In order for these masks to be usable, in vitro tests such as tyrosinase inhibition, water vapor transmittance, water contact angle measurement, and biocompatibility tests as well as in vivo tests are required.

II. EXPERIMENTAL METHOD / TEORETICAL METHOD

2.1 Materials

Silver nitrate (AgNO_3 ; 99%) was supplied from Nanokar Technology, Istanbul, Türkiye. Polycaprolactone (PCL; M_v : 80,000 g/mol), chloroform and dichloromethane (DCM) were purchased from Sigma-Aldrich. Escherichia Coli 25922 (gram negative) and Staphylococci Aureus 29213 (gram positive) bacteria used for antibacterial activity. Tests were taken from Necmettin Erbakan Medical Faculty Hospital Microbiology Laboratory. All chemical reagents used in the experiments were used without further purification since they were at analytical level.

2.2 Fabrication of Ag nanoparticler Using Green Synthesis

Two different Ag nanoparticles were produced using chamomile extract and galium aparine extract using the green synthesis method. 10 g of dried chamomile was mixed with 1 liter of pure water and left to dissolve at room temperature for 24 hours. The resulting solution was filtered with filter paper. For Ag nanoparticle synthesis, 2 mL camilime extract and 7 mL pure water were added to a beaker. 1 ml of the previously prepared 0.1 M AgNO_3 solution was taken and added dropwise to the solution in the beaker [22].

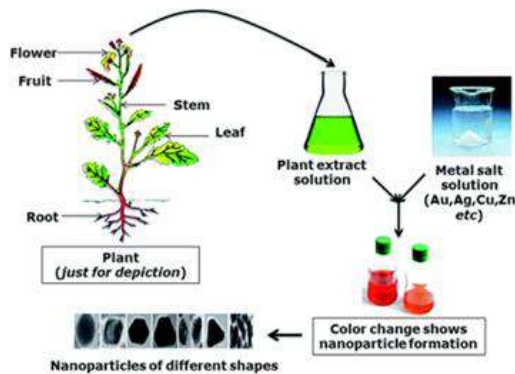


Figure 1. Preparation of solution from plant extract and production of nanoparticles by green synthesis.

These processes were carried out on a magnetic stirrer. The solution was kept in the dark at room temperature for 24 hours to complete the chemical reaction

The solution whose reaction was completed was taken into a large container and evaporated in an oven at 200 °C. The remaining chamomile molecule encapsulated Ag nanoparticles residue at the bottom of the container was collected. Similarly, encapsulated Ag nanoparticles were produced from the extract of the galium aparine. Figure 1 shows a schematic representation of nanoparticle production by green synthesis.

2.3 Production of PCL nanofibers

Two different nanofibers were produced by electrospinning using PCL biodegradable polymer. One of them was produced by adding Ag nanoparticles encapsulated with chamomile extract, aloe vera and collagen to PCL. The second one was produced by incorporating Ag nanoparticles encapsulated with gallium aparin molecules, aloe vera and collagen into PCL.

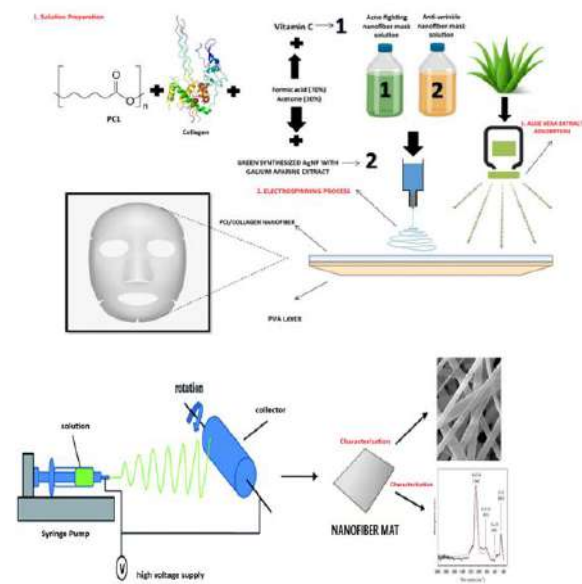


Figure 2. (a) Flowchart of solution preparation and mask production in nanofibers and (b) Production of PCL nanofiber mat.

For electrospinning process, AgNP-collagen encapsulated with chamomile aloe-vera/PCL solution and AgNP-collagen encapsulated with gallium aparin-aloe vera/PCL solution were prepared. Then, nanofibers were formed under high voltage electric field by applying electrospinning technique. 12% (w/v) PCL, 50% (v/v) chloroform, 50% (v/v) dimethylformamide (DMF), and 1% w/v encapsulated AgNPs were added to the solution. The prepared

solution was taken into a 10 ml syringe and placed in the electrospinning device. The distance between the needle tip and the collector was set to 12 cm. A rotating cylinder coated with Al foil was used as the collector. The electrospinning process was applied at a feed rate of 1.00 mL/h and a voltage of 25 kV for both nanofiber composite solutions. Solution preparation processes for the production of AgNP-doped PCL/collagen nanofiber masks and spinning of nanofiber mats are shown in Figure 2.

2.4 Characterization of AgNPs and Nanofibers

The sizes and shapes of green synthesized AgNPs with chamomile and gallium aparine extracts were analyzed with a transmission electron microscope (TEM, JEOL JEM-2100). The structures and morphologies of both groups of PCL composite nanofibers synthesized by electrospinning were examined with a scanning electron microscope (SEM, ZEISS Gemini SEM 500) images. The chemical structures and attenuated total reflections of PCL composite nanofibers were analyzed by Fourier Transform Infrared (FTIR) (Thermo Scientific—Nicolet iS20) Spectrometer. The absorption modes of the spectra were measured in the wavelength range of 4000–400 cm^{-1} .

2.5 Mechanical testing of PCL nanofiber mats

The mechanical tests of encapsulated AgNPs doped PCL nanofiber mats were performed using a universal testing machine (Shimadzu AG-X, 10 kN). The tensile strength, elastic modulus, and elongation of PCL composite nanofiber mats were performed by tensile testing according to ASTM D638-14. The dimensions of the PCL mat samples were cut to 50 mm x 10 mm. The thicknesses of the samples were measured using a micrometer after the nanofiber mats were placed between two glass slides. The tensile tests of the prepared samples were carried out at a speed of 100 mm/min. Five samples from both groups of PCL nanofiber mats were tested. The maximum tensile strengths, maximum elongations, and stress-strain curves from the tests performed were reported using the trapezium software connected to the testing machine. The elastic moduli of the PCL nanofiber mats were calculated from the slope of the initial linear part of the stress-strain curves.

2.6 In Vitro Antibacterial Activity

The antibacterial activities of PCL composite nanofiber groups were evaluated against both gram-negative *E. coli* and gram-positive *S. aureus* by disk diffusion qualitative tests. Disc samples cut with a diameter of 12 mm were sterilized under UV irradiation of both sides of the nanofibers for 30 minutes. *E. coli* and *S. aureus* bacterial strains were

grown in nutrient broth by incubating at room temperature for 24 hours. *E. coli* and *S. aureus* bacterial colonies were also balanced at 0.5 McFarland. The bacterial suspension was extended on Muller-Hinton agar medium in petri dishes. Sterilized PCL nanofiber samples were placed in bacterial culture and incubated at 37 °C for 24 h. The inhibition zone diameters formed on the discs were measured using Image J software.

III. RESULTS AND DISCUSSIONS

3.1 TEM image of AgNPs

TEM images of green AgNPs synthesized using chamomile extract and galium aparine extract are shown in Figure 3 (a) and Figure 3 (b), respectively. From these images, it is obvious that the shapes of both types of AgNPs are oval, close to the sphere. The size of AgNPs coated with chamomile molecules varies from 10 nm to 40 nm. The average size is around 20 nm. The size of AgNPs coated with galium aparine molecules ranging between 20 nm and 35 nm, and the average size is around 30 nm.

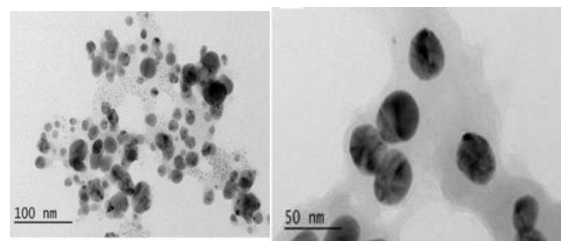


Figure 3. (a) TEM image of chamomile molecules encapsulated AgNPs and (b) Galium aparine molecules encapsulated AgNPs

3.2. SEM image of PCL composite nanofibers

Figure 4 shows the SEM image of galium aparine encapsulated AgNP-PCL/collagen nanofibers produced by electrospinning and the SEM image of nanofibers with aloe vera extract sprayed on these fibers. The SEM image of chamomile encapsulated AgNP-PCL/collagen nanofibers and the SEM image of nanofibers with aloe vera extract sprayed on these fibers are shown in Figure 4. Both in Figure 4a and Figure 4c, it is seen that the surfaces of PCL nanofibers with encapsulated AgNPs are quite rough. This is due to the AgNPs entering the nanofibers. One of the reasons why the surfaces of the nanofibers are rough is that AgNPs have very high conductivity and interact with the electric field in the environment during electrospinning [23]. When the SEM image given in Figure 4a is examined, the average diameter of galium aparine encapsulated AgNP/PCL/collagen nanofibers is calculated as 375 nm. Similarly, the average nanofiber diameter was calculated as 337 nm from the

SEM image of the Chamomile encapsulated AgNP/PCL/collagen nanofibers shown in Figure 4c.

Figure 4b and Figure 4d show SEM images of aloe vera extract coated on AgNP-doped PCL/collagen nanofibers. Aloe vera extract was coated on the surface of AgNP-doped PCL/collagen nanofibers by spraying to increase antibacterial activity, eliminate acne on the skin, and enhance anti-wrinkle performance [17-19]. The anti-aging effectiveness of aloe vera extracted gel preparations has been shown in many studies [24,25]. Aloe vera extract formed agglomerates on the surfaces of nanofibers in some places and was coated more sparsely in other parts.

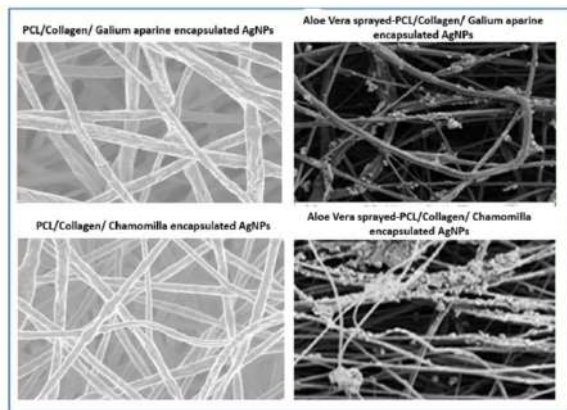


Figure 4. (a)Galium aparine encapsulated AgNP/ PCL/collagen nanofibers and (b) Aloe vera extract sprayed on nanofibers of galium aparine encapsulated AgNP/ PCL/collagen. (c) Chamomile encapsulated AgNP/PCL/collagen and (d) Aloe vera extract sprayed on nanofibers of chamomile encapsulated AgNP/ PCL/collagen.

3.3 FTIR Analysis

FTIR is an analytical tool used to analyze the chemical bonds and functional groups of a material and obtain information about its structure. Figure 5 shows FTIR spectra of chamomile extract encapsulated AgNPs doped PCL/collagen/aloe vera nanofibers. FTIR spectra of galium aparine extract encapsulated AgNPs doped PCL/collagen/aloe vera nanofibers are also shown in Figure 5. The similar peaks were obtained in the FTIR spectra of both groups of nanofiber systems.

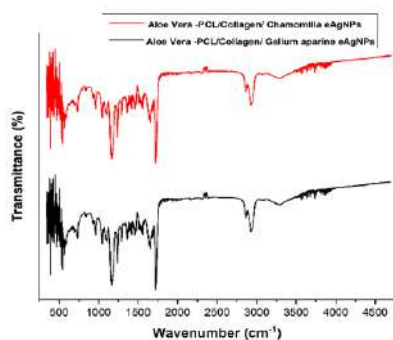


Figure 5. FTIR spectrums of PCL composite nanofiber systems.

The striking peaks of PCL nanofibers were observed as asymmetric CH₂ stretching vibration at 2943 cm⁻¹, symmetric CH₂ stretching vibration at 2866 cm⁻¹, carbonyl (C=O) stretching vibration at 1721 cm⁻¹, (C-H) symmetric deformation at 1470 cm⁻¹, (C-O) symmetric stretching vibration at 1365 cm⁻¹, and asymmetric (C-O-C) stretching at 1239 cm⁻¹. The peaks of collagen inside the nanofibers originating from amide-I at 1643, amide II at 1549 and amide III at 1238 are observed [26].

3.4. Mechanical Properties

Figure 6 shows the stress-strain curves obtained as a result of tensile tests of two groups of PCL nanofiber mats. The highest tensile strength belongs to galium aparine encapsulated AgNP doped PCL/collagen/aloe vera nanofiber mats. The highest tensile strength is 6.85 MPa and belongs to galium aparine encapsulated AgNP doped PCL/collagen/aloe vera nanofiber mats. The tensile strength of the PCL/collagen/aloe vera nanocomposite with chamomile encapsulated AgNP is 5.28 MPa. The strength of the galium aparine encapsulated AgNPs doped PCL/collagen/aloe vera composite nanofiber mat is 29.7% higher than the strength of the Chamomile encapsulated AgNP added PCL. The highest strength was observed in the galium aparine coated AgNP PCL nanofibers because these encapsulated AgNPs formed a strong chemical and mechanical bond with the PCL.

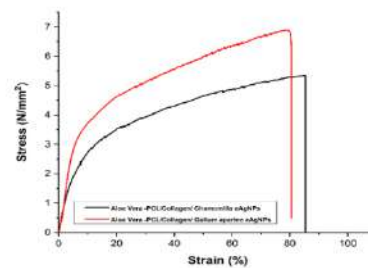


Figure 6. Stress-strain curves of AgNPs doped PCL/Collagen/aloe vera composite nanofiber mats

3.4 Antibacterial Activity

Figure 7 shows antibacterial activity of chamomile extract encapsulated AgNPs doped PCL/collagen/aloe vera nanofibers and galium aparine extract encapsulated AgNPs doped PCL/collagen/aloe vera nanofibers against both gram-negative *E. coli* and gram-positive *S. aureus*. In addition, the antibacterial properties of PCL nanofiber groups not sprayed with aloe vera are given in Figure 7. It was observed that both groups of PCL composite nanofiber mats exhibited antibacterial activity against both *E. coli* and

S. aureus bacteria under the same test conditions. The inhibition zones formed around both chamomile extract encapsulated AgNPs doped PCL/collagen/aloe vera nanofiber and gallium aparine extract encapsulated AgNPs doped PCL/collagen/aloe vera nanofiber mats were measured as 20.94 mm and 15.53 mm against *E. coli*, respectively. The inhibition zones around the same group of PCL nanofiber mats were evaluated as 23.18 mm and 17.25 mm against *S. aureus*, respectively. On the other hand, when the antibacterial activities of PCL nanofiber mats not sprayed with aloe vera extract were examined against *E. coli*, the zone diameter was 18.49 mm in chamomile extract encapsulated AgNPs doped nanofibers, while the zone diameter was measured as 12.37 mm when gallium aparine extract encapsulated AgNPs added nanofibers. The inhibition diameters of these group PCL nanofiber mats against *S. aureus* were measured as 19.67 and 13.72 mm, respectively. In this study, it was observed that the addition of encapsulated AgNPs and collagens to PCL nanofibers was highly effective against both *E. coli* and *S. aureus* bacteria. It was revealed that the antibacterial effect was increased more when aloe vera extract was coated on the surfaces of these PCL nanofiber groups.

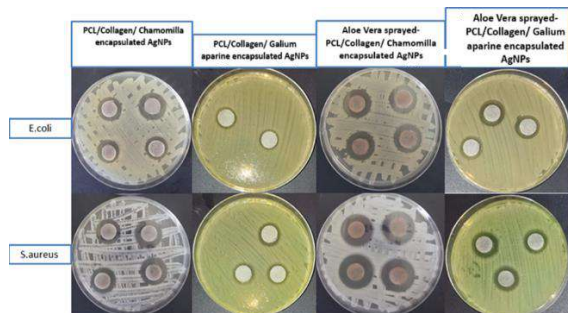


Figure 7. Antibacterial activity of PCL nanofiber systems for *E. coli* and *S. aureus*

The antibacterial effect against *E. coli* of chamomile extract encapsulated AgNP doped PCL/collagen/aloe vera nanofiber mats was 20% higher than the nanofibers without aloe vera. The antibacterial effect of the aloe vera containing nanofibers of this PCL group against *S. aureus* was 17.8% higher than the nanofibers without aloe vera. When aloe vera is present in PCL nanofibers containing gallium aparine encapsulated AgNPs, the antibacterial effect against *E. coli* is 25% higher than the nanofibers without aloe vera.

IV. CONCLUSIONS

This study aims to present a biological treatment applied to the face as a dry mask that is effective in acne treatment and eliminates wrinkles caused by aging. AgNPs were produced by green synthesis using

chamomile and malium aparin extracts. These encapsulated AgNPs were combined with PCL biodegradable polymer and collagen to produce composite nanofibers by electrospinning. In addition, aloe vera extract was coated by spraying onto the surfaces of this PCL composite nanofiber. The cosmetic dry face masks produced from electrospun nanofibers are cheap, easy to use, and contain active agents that do not harm the skin. The shape and size of the encapsulated AgNPs were analyzed by taking TEM images. The morphological structures of four types of PCL composite nanofibers were examined with SEM images. The strength and elasticity modulus of the produced nanofibers were carried out by mechanical tests. The tensile strength and elasticity modulus of the mats of nanofibers containing gallium aparin were higher than those containing chamomile. This shows that some plant molecules have a significant positive effect on the mechanical properties of PCL nanofibers. Chemical bonds and functional groups of PCL nanofibers with collagen were determined by FTIR analysis. It was observed that all PCL composite nanofiber mats exhibited strong antibacterial activity against both *E. coli* and *S. aureus* bacteria under the same test conditions. In line with these results, it can be said that encapsulated AgNP-doped PCL/collagen nanofiber systems are successful in dry facial masks for acne treating and wrinkle removal.

REFERENCES

- [1] Y.-H. Choi, S.E. Kim, K.-H. Lee, Changes in consumers' awareness and interest in cosmetic products during the pandemic, *Fash. Text.* 9 (1) (2022).
- [2] P. Morganti, M.-B. Coltelli, A new carrier for advanced cosmeceuticals, *Cosmetics* 6, (1) (2019).
- [3] J. Teno, M. Pardo-Figueroa, N. Hummel, V. Bonin, A. Fusco, C. Ricci, G. Donnarumma, M.-B. Coltelli, S. Danti, J.M. Lagaron, Preliminary studies on an innovative bioactive skin soluble beauty mask made by combining electrospinning and dry powder impregnation, *Cosmetics* 7 (4) (2020).
- [4] Qiaolin Yang a, Ya Tian a, Yuchun Liu a, Wen Shi, A novel multi-functional skin-care dry mask based on Bletilla Striata polysaccharide electrospun nanofibers, *International Journal of Biological Macromolecules* 282 (2024) 136780.
- [5] EF Ediz, C Güneş, M Demirel Kars, A Avcı, In vitro assessment of Momordica charantia/Hypericum

perforatum oils loaded PCL/Collagen fibers: Novel scaffold for tissue engineering, *Journal of Applied Biomaterials & Functional Materials* 22, (2024), doi: 22808000231221067.

[6] Y.S. Kaisong Huang, Hanbai Wu, Yuhan Chen, Shuai Zhang, Shuo Shi, Chunxia Guo, Jinlian Hu, Electrospayed environment-friendly dry triode-like facial masks for skincare, *ACS Appl. Mater. Interfaces* 16

[7] H.Y. Wenfeng Hu, Yujie Guo, Yantao Gao, Yi Zhao, Fabrication of multifunctional facial masks from phenolic acid grafted chitosan/collagen peptides via aqueous electrospinning, *Int. J. Biol. Macromol.* 267 (1) (2024).

[8] Waghmare PR, Ka(1) (2024) 1899–1919.kade PG, Takdhat PL, Nagrale AM, Thakare SM, Parate MM. Turmeric as Medicinal Plant for the Treatment of Acne vulgaris; *PharmaTutor*. 2017; 5(4):19-27.

[9] Hossain MA, Shah MD, Sakari M. Gas chromatography–Mass Spectrometry Analysis of Various Organic Extracts of *Merremia Borneensis* from Sabah. *Asian Pacific Journal of Tropical Medicine*. 2011; 4(8):637–641.

[10] Sonali Syal, Vinay Pandit, M. S Ashawat, Traditional Herbs to treat Acne Vulgaris, *Asian Journal of Pharmaceutical Research*, 2020, 10(3), DOI: 10.5958/2231-5691.2020.00034.9

[11] Bogdan Păcularu-Burada, Alexandru-Ionut, Cîrîc and Mihaela Begea, Anti-Aging Effects of Flavonoids from Plant Extracts, *Foods*, 2024, 13, 2441. <https://doi.org/10.3390/foods13152441>

[12] Zofia, N.-Ł, Martyna, Z.-D Ziemlewska, A, Bujak, T. Comparison of the Antiaging and Protective Properties of Plants from the Apiaceae Family. *Oxidative Med. Cell. Longev.* 2020, 2020, 5307614. [

[13] Viany, L., Rizal, R., Widowati, W., Samin, B. Kusuma, R. Fachrial, E. Nyoman, L.E. Comparison of Antioxidant and Antiaging Activities Between Dragon Fruit (*Hyloceureus Polyrhizus* (F.A.C. Weber) Britton & Rose) Rind Extract and Kaempferol. *Maj. Kedokt. Bdg.* 2019, 51, 147–153.

[14] Tizazu, A.; Bekele, T. A Review on the Medicinal Applications of Flavonoids from Aloe Species. *Eur. J. Med. Chem. Rep.* 2024, 10, 100135.

[15] Tizazu, A.; Bekele, T. A Review on the Medicinal Applications of Flavonoids from Aloe Species. *Eur. J. Med. Chem. Rep.* 2024, 10, 100135

[16] Jaykant Vora, Anshu Srivastava, Hashmukh Modi, Antibacterial and antioxidant strategies for acne

treatment through plant extracts, *Informatics in Medicine Unlocked* 16 (2019) 100229.

[17] Tundis, M.R. Loizzo, M. Bonesi and F. Menichini, Potential Role of Natural Compounds Against Skin Aging, *Current Medicinal Chemistry*, Volume 22, Issue 12, Apr 2015, p. 1515 – 1538.

[18] Cai JF. Research progress of pharmacological mechanism of active components in Aloe. *World Latest Med. Inf.* (Electronic Version). 2018;18(102):122–125. 4.

[19] Sanchez M, Gonzalez-Burgos E, Iglesias I, et al. Pharmacological update properties of Aloe vera and its major active constituents. *Molecules*. 2020;25(6):1324. 5.

[20] Mansoor K, Aburjai T, Al-Mamoori F, et al. Plants with cosmetic uses. *Phytother Res.* 2023;37(12):5755–5768. 6.

[21] Nie LH. Developing and using of Aloe vera. *Food Res Dev.* 2006;27(2):147.

[22] M. O. Avci, N. Muzoglu, A. E. Yilmaz, B. S. Yarman, Antibacterial, cytotoxicity and biodegradability studies of polycaprolactone nanofibers holding green synthesized Ag nanoparticles using atropa belladonna extract, *Journal of Biomaterials Science, Polymer Edition*, 2022, vol. 33, no. 9, 1157–1180.

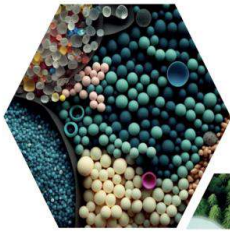
[23] Feifei Liu, Xuwei Chenga, Lu Xiao, et al, Inside-outside Ag nanoparticles-loaded polylactic acid electrospun fiber for long-term antibacterial and bone regeneration, *International Journal of Biological Macromolecules* 167 (2021) 1338–1348.

[24] Mutiara Dwi Lestari, Siti Maimunah, Andre Prayoga, Formulation of Red Beet (*Beta vulgaris*. L) and Aloe Vera (*Aloe vera*) Gel Extracts as Anti-Aging, [2023], doi: <https://doi.org/10.36987/jpbn.v9i2.4478>

[25] Bheta Sari Dewi, Silvia Surini, Study on hydrogel eye mask with *Centella asiatica* L and Aloe vera L extract, *Journal Of Advanced Pharmacy Education And Research*. [2024], doi: 10.51847/9UToWXppYP.

[26] J.M.A. Mancipe, M.L. Diasb, el al., Type I collagen – poly(vinyl alcohol) electrospun nanofibers: FTIR study of the collagen helical structure preservation, *Polymer-Plastics Technology And Materials*, 2022, 61 (8), 846–860, <https://doi.org/10.1080/25740881.2022.2029887>.

16. Uluslararası Lif ve Polimer Araştırmaları Sempozyumu (16. ULPAS)
9-10 Mayıs 2025, İstanbul Teknik Üniversitesi (İTÜ), İstanbul, Türkiye



16 ULUSLARARASI
LİF VE POLİMER
ARAŞTIRMALARI
SEMPOZYUMU

16th INTERNATIONAL FIBER AND POLYMER RESEARCH SYMPOSIUM

Sürdürülebilir ve İşlevsel Lif ve Polimerler
Sustainable and Functional Fibers & Polymers



9-10 Mayıs
May 2025

İstanbul Teknik Üniversitesi

Gümüşsuyu Prof. Dr. Necmettin Erbakan Yerleşkesi

Istanbul Technical University

Gumussuyu Prof. Dr. Necmettin Erbakan Campus

Geri dönüşüm silika tozları içeren kaplamalı fonksiyonel ve teknik tekstiller

Sema Özden^{a*}, Ayşe Dilşad Polat^b, Prof. Dr. Mehmet Kanık^c, Burak Kırayoğlu^d,

^aArge Sorumlusu, Kırayteks Tekstil San. Ve Tic. A.Ş., 16110 Bursa, Türkiye.

^bArge Uzmanı, Kırayteks Tekstil San. Ve Tic. A.Ş., 16110 Bursa, Türkiye.

^cTekstil Mühendisliği, Bursa Uludağ Üniversitesi, 16000 Bursa, Türkiye.

^dYönetim Kurulu Üyesi, Kırayteks Tekstil San. Ve Tic. A.Ş., 16110 Bursa, Türkiye.

*Sorumlu Yazar: sema.o@kirayteks.com.tr

ÖZET

Tekstil sektöründe sürdürülebilirlik ve ekolojik yaklaşım taleplerine karşılık geri dönüşüm ürünlerin önemi hızla artmaktadır. Aynı zamanda geleneksel enerji kaynaklarının da yetersizliği ve atmosfere zararlı etkileri sebebiyle yenilenebilir enerji kaynakları ön plana çıkmıştır. Bu çalışmada, sürdürülebilirlik stratejisi ve ekolojik yaklaşım temel alınmış olup doğal ve geri dönüşümlü malzemeler kullanılarak fonksiyonel teknik tekstilleri geliştirmek amaçlanmıştır.

Kaplamalı ev tekstillerinde kullanılan, ekolojik açıdan sakıncaları bulunan geleneksel dolgu maddeleri yerine, bu çalışmada sürdürülebilir tekstil üretim şartlarını sağlamak üzere bitkisel atıklardan (pirinç kabukları vb.) elde edilen amorf silika ile bazı endüstriyel üretimlerde (ferrokrom tesisleri gibi) yüksek sıcaklık fırın bacalarından geri kazanılan silika dumanı kullanılarak çeşitli kaplamalar yapılmış olup yapılan kaplamaların solar özellikleri ve ısı yalıtım özellikleri incelenmiştir. Elde edilen sonuçlara göre yapılan kaplamalarda geri dönüşüm silika tozları kullanılarak ışık geçirmezlik (blackout) etkisinin sağlanabileceği ve bu yolla karartma perde kumaş kaplamalarında kullanılan ve ekolojik açıdan sakıncaları tartışılan karbon siyahı kullanımının tamamen veya kısmen elimine edilebileceğini, %7 oranında ısı yalıtım özelliğinin iyileştirildiği ve % 15 oranında enerji tasarrufu sağlandığı, yapılan yaşam döngüsü analizinde (LCA) karbon ayak izinde %37,5 ve su ayak izinde %42 oranında iyileştirme sağlanmıştır.

Anahtar Kelimeler: Teknik tekstil; geri dönüşüm; blackout (karartma) özelliği; sürdürülebilirlik.

Coated functional and technical textiles containing recycled silica powders

ABSTRACT

The importance of recycled products is rapidly increasing in response to demands for sustainability and an ecological approach in the textile industry. At the same time, due to the insufficiency of traditional energy sources and their harmful effects on the atmosphere, renewable energy sources have come to the forefront. In this study, the strategy of sustainability and an ecological approach were taken as the foundation, with the aim of developing functional technical textiles using natural and recycled materials.

Instead of traditional filling materials, which pose ecological concerns and are used in coated home textiles, in this study, various coatings were produced using amorphous silica obtained from plant waste (such as rice husks) and silica fume recovered from high-temperature furnace chimneys in certain industrial productions (such as ferrochrome plants), in order to ensure sustainable textile production conditions. The solar and thermal insulation properties of these coatings were examined. According to the results, it was found that the use of recycled silica powders in the coatings can achieve blackout effects, and thus, the use of carbon black—which is ecologically controversial—in blackout curtain fabric coatings can be fully or partially eliminated. Additionally, thermal insulation was improved by 7%, energy savings of 15% were achieved, and life cycle analysis (LCA) showed significant improvements in all parameters included in the life cycle, including a 37.5% reduction in carbon footprint and a 42% reduction in water footprint.

Keywords: Technical textiles; recycling; blackout feature; sustainability.

I. GİRİŞ

Tekstil sektörüne ait tüm üretim aşamaları incelendiğinde çevreye zarar veren emisyonlara neden olabilecek girdi ve çıktıları olduğu görülmektedir (1). Dünya nüfusunun artması ile çevreye verilen / verilmesi muhtemel zararlar da aynı ölçüde artmaktadır. Günümüzde teknolojik ilerlemeler ve küresel ekonomideki büyüme, enerji talebinin de sürekli artmasına neden olmaktadır. Bu talep, çoğunlukla fosil yakıtlardan karşılanmakta ve bu durum çevre üzerinde ciddi baskılar oluşturmaktadır; özellikle de karbon emisyonlarının artışı, iklim değişikliğiyle doğrudan ilişkilendirilmektedir (2). Enerji tüketimindeki bu artış ve çevresel etkiler, alternatif enerji kaynaklarının araştırılmasını ve enerji verimliliğinin artırılmasını zorunlu hale getirmiştir (3). Yenilenebilir enerji kaynakları bu bağlamda öne çıkmakta; güneş, rüzgar ve hidroelektrik gibi kaynaklar hem sürdürülebilir hem de çevresel etkileri açısından daha az zararlıdır (4). Ancak, birçok yenilenebilir enerji kaynağının süreksizliği, enerji dönüşüm verimliliğini önemli ölçüde düşürmekte ve ilgili güç üretim teknolojilerinin geliştirilmesinin başlıca engeli haline gelmektedir. Termal enerji depolama, bu sorun için umut verici bir çözüm olup, bu nedenle hızlı bir gelişim süreci geçirmektedir (5).

Tekstil sektöründe kullanılan geleneksel dolgu malzemelerinin (TiO_2 , sentetik silika ve karbon siyahı) ısı yalıtım özelliklerinin zayıf olduğu ve binalarda en fazla enerji kayıplarının pencerelerde meydana geldiği göz önüne alındığında, geleneksel dolgu malzemelerinin kullanıldığı teknik tekstil ürünlerinde ısı kazanım ve kayıplara belirgin bir katkı sağlayamamaktadır. Bunun yanı sıra, geleneksel yöntemlerle üretilen karartma perdelerde orta katman kaplamasında karbon siyahı kullanılmaktadır. Karbon siyahının ise toksik etkileri mevcuttur. Aynı zamanda karbon salınımı sebebiyle sera gazı emisyonlarını arttırmaktadır.

Bu çalışmada sürdürülebilirlik stratejisi ve ekolojik yaklaşım temel alınmış ve geri dönüşümle elde edilmiş silika tozları kullanarak fonksiyonel teknik tekstilleri geliştirmek amaçlanmıştır. Beyazdan siyaha kadar geniş renk skalasında silis dumanı ve biyobazlı silika temin edilmiş olup; yapılan

çalışmalarda bu renk çeşitliliğinin farklı fonksiyonel özellikleri desteklediği görülmüştür. Örneğin; karartma perdelerde koyu renkli silikaların kullanımı ile mevcuttaki karbon siyahı kullanımının elimine edilebildiği veya azaltıldığı; beyaz renkli silikaların kullanımı ile de fonksiyonel ve teknik tekstil üretiminde kullanılan titanyum dioksit ve diğer beyaz renkli geleneksel dolgu maddeleri kullanımının kısmen veya tamamen ortadan kaldırılabilirdiği bulunmuştur. Ayrıca düşük ısı iletim katsayısına sahip olan silika tozları kullanılarak ısı yalıtım özelliği ve enerji tasarrufu sağlanmıştır.

II. DENEYSEL METOT

2.1 Malzemeler ve Hazırlama Teknikleri

2.1.1 Kumaş

Tüm kaplama deneylerinde %100 PES, tekstürize, filament iplikler kullanılarak dokunan, bez ayağı desen, sadece fikseli, ön işlemsiz kumaşlar kullanılmıştır. Kumaş gramajı 150 g/m^2 dir.

2.1.2 Kullanılan kimyasallar

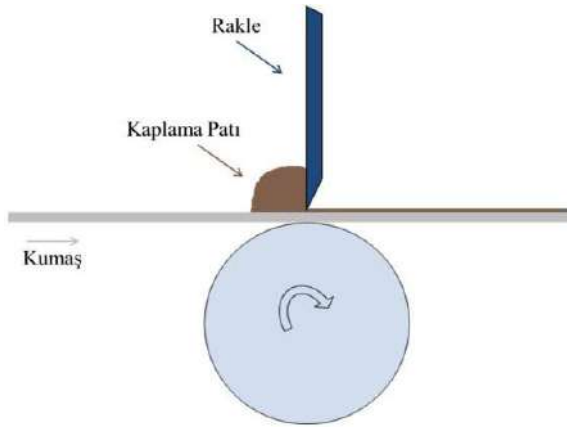
Kaplama reçetelerinin hazırlanmasında kullanılan silikalar ve kimyasallar aşağıdaki tabloda (Tablo 1) belirtilmiştir.

Tablo 1. Kaplama reçetelerinin hazırlanmasında kullanılan kimyasallar

| Kimyasal Adı | Açıklama |
|-----------------------------|-------------------------------------------------------------------------------------------------------------------------------------------------------|
| Köpürtme maddesi | Yumuşak, esnek, yansıma özelliği olan, düşük karbon ve amonyum salınımı, ışık, hava şartları, hidroliz ve yaşlanmaya karşı dayanımlı köpürtme maddesi |
| Kaplama polimeri | Yıkama ve kuru temizlemeye dayanıklı, yüksek kimyasal dayanımlı, kendinden çapraz bağlı, yumuşak akrilik emülsiyon |
| Karbon siyahı | Karbon siyahı dispersiyonu |
| Köpük stabilizatörü | İyi köpük stabilitesi |
| Geri dönüşüm silika tozları | Karbon siyahı dispersiyonuna alternatif |

2.2 Kaplama Yöntemi

Tekstil yüzeylerine yapılan uygulamalar için genelde uygulanan yöntemler köpük ve pat kaplamadır. Bu çalışmada hem köpük hem de pat kaplama yöntemi tercih edilmiştir. Ön denemelere dayanarak alınan sonuçlara uygun olarak kaplama kompozisyonu geliştirilmiştir. Kullanılan silindirik üstü bıçak kaplama tekniğine ait şematik görsel Şekil 1’de verilmiştir.



Şekil 1. Silindirik üstü bıçak kaplama tekniği (6)

Tablo 2. Fonksiyonel ve teknik tekstillerin ağırlıkça bileşimleri

| Bileşen | % |
|-----------------------------------------------------|----|
| Kumaş | 30 |
| Kumaş üzerindeki köpük patı/kaplama pastası katmanı | 70 |

Tablo 3. Buluş kapsamında kullanılan kaplama kompozisyonunun ağırlıkça bileşimleri

| Bileşen | % |
|-----------------------------|----|
| Bağlayıcı polimer | 50 |
| Geri dönüşüm silika tozları | 25 |
| Yardımcı kimyasallar | 25 |

Kurutma ve fiksaj işlemleri için 90-150°C’de 90-150 sn süre ile çalışılmıştır. Kurutma işlemi sonrası yüzeyi pürüzsüz hale getirmek için 40-70 bar basınç ile kalandırlama işlemi uygulanmıştır.

2.3 Kullanılan Cihaz ve Yardımcı Gereçler

Deneyisel çalışmalarda aşağıda belirtilen cihazlar kullanılmıştır.

- UV-VIS-NIR Spektrofotometresi: Shimadzu (Japonya) / UV-3600i Plus

- Kaplama Raklesi: Ataç RGK-40 (Türkiye)
- Gergili Kurutucu: Ataç GK-40 (Türkiye)
- Viskozimetre: Rotatif viskozimetre
- Hassas Terazî: Necklife FLY-3000 (Türkiye)
- pH metre: Mettler Toledo (İsviçre)
- Isı iletim katsayısı ölçümü: ISO 8301/ASTM C518

2.4 Malzemelerin Karakterizasyonu

2.4.1 Solar özelliklerin tayini (TS EN ISO 410) ve black-out performansı (DIN 14501)

Black-out perdelerinin temel amacı ışığı engellemektir. Bu özellik, kış aylarında ısıyı hapsedebilecekleri ve yaz aylarında güneş ışığını yansıtabilecekleri anlamına gelir. Bu sebeple yapılan üretim denemelerinin solar özellikleri, UV-VIS NIR spektrofotometre kullanılarak tayin edilmiştir. Üç farklı ölçüm yapılmış olup, ortalama değerleri Tablo 4’te belirtilmiştir.

Tv: Görünür bölge geçirgenliği (transmitansı)

Rv: Görünür bölge yansıtması (reflektansı)

Av: Görünür bölge absorbanası

2.4.2 Isı yalıtım testleri

Black-out perdelerinin temel amacı ışığı engellemek olsa da, bu özellik aynı zamanda enerji tasarrufu açısından da önemlidir. Güneşli günlerde, genellikle ilave ısı getiren fazla ışığın yaşam alanlarına nüfuz etmesini önlerler. Bu, yapay soğutma ihtiyacını daha da azaltarak enerji tasarrufunu teşvik eder. Aynı zamanda kış aylarında ısıyı hapsederek bir yalıtım katmanı görevi görüp sıcaklığı içeride hapseder ve soğuk hava akımlarının içeri girmesini engeller. Bu, ısıtma sistemlerine olan bağımlılığın azalmasına olanak sağlar. Geri dönüşümden elde edilmiş silika tozları, yüksek silisyum dioksit (SiO₂) içerdiği için düşük termal iletkenliğine sahiptir. Bu özellikleri sebebiyle ısı yalıtımı ve enerji tasarrufu konusunda önemli bir avantaj sağlamaktadır. Bu sebeple, Bursa Teknik Üniversitesi bünyesinde bulunan Spektral marka ısı iletkenlik ölçüm cihazı ile ısı iletim katsayıları tayin edilmiştir. Testler 20-40°C arasında yapılmıştır.

2.4.3 Yaşam döngüsü analizi (Life cycle assessment)

Yaşam döngüsü analizinin sürdürülebilirlik açısından önemli bir değerlendirme aracı olduğu kabul edilmektedir. Yaşam döngüsü analizi (LCA; life cycle assessment) temelde bir ürün veya sürecin tüm çevresel etkilerini hesaplayan bir değerlendirme yöntemidir. Silika tozları içeren kaplamanın standart ürünle çevresel etkilerinin kıyaslanması amacıyla LCA analizleri yapılmıştır.

III. BULGULAR VE TARTIŞMA

Black-out kumaşların geliştirilmesinde kullanıma yönelik olarak geri dönüşüm silica tozları içeren kaplamaların ışık geçirmezlik özellikleri değerlendirilmiştir. Bu amaçla, kaplanan numunelerin black-out özelliği DIN 14501 standardına göre görsel olarak test edilmiş olup black-out etkisinin olduğu açıkça görülmüştür.

Ayrıca, UV-VIS-NIR spektrofotometre ile TS EN ISO 410 standardına göre yapılan testler sonucu, kumaşların ışık ve solar özellikleri de black-out etkisini destekler niteliktedir. Tablo 4'te görüleceği üzere Tv ve Ts değerleri % 0'dır.

Tablo 4. UV-VIS-NIR spektrofotometre ölçüm sonuçları

| Numune | Tv | Rv | Av |
|-----------------------------------------|----|------|-----|
| Klasik black-out (karbon siyahı içerir) | 0% | 20% | 80% |
| Silika tozları içeren kaplama | 0% | 23 % | 77% |

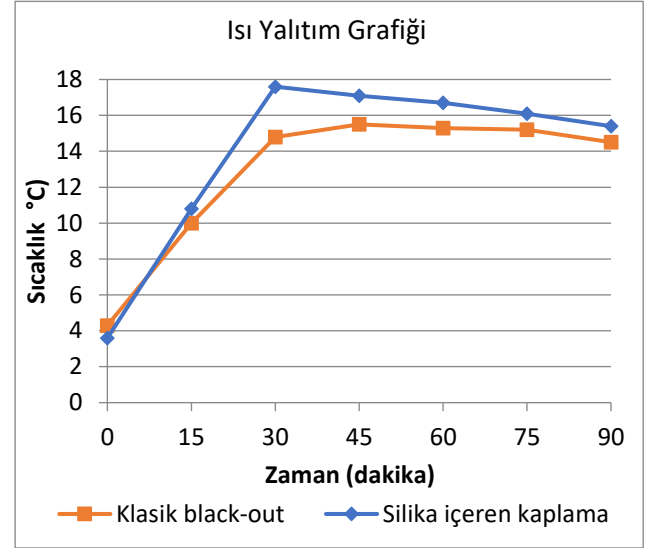
Isı iletkenlik ölçüm cihazı ile ısı iletim katsayıları tayin edilmiş olup elde edilen sonuçlara göre silika tozlarının klasik black-out'a göre ortalama %7 oranında ısı yalıtımına katkı sağladığı açıkça görülmektedir (Tablo 5).

Tablo 5. Isı iletim katsayısı

| Numune | Isı İletim Katsayısı ISO 8301 / ASTM C518 (W/mK) |
|-----------------------------------------|--------------------------------------------------|
| Klasik black-out (karbon siyahı içerir) | 0,006031 |
| Silika tozları içeren kaplama | 0,005611 |

Ayrıca yapılan kaplamaların karartma perdelerinde ısı yalıtım özelliklerinin sıcaklık artışı ve zamanla nasıl değiştiğini görmek adına ısı yalıtım testleri yapılmış olup, silika tozları içeren kaplamanın ısı yalıtım özelliklerinin

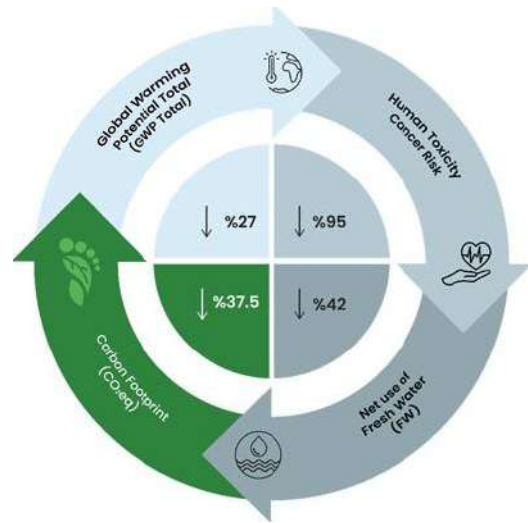
daha iyi olduğu ve enerji tasarrufu sağladığı açıkça görülmüştür (Şekil 2).



Şekil 2. Klasik black-out ve silika tozu içeren kaplamalı kumaşların ısı yalıtım grafiği

LCA sonucuna göre proje sonucunda geliştirilen black-out perdeler kumaşlar sayesinde, aynı özelliklere sahip klasik kumaşlara göre;

- Karbon ayak izinde (CO₂eq) - %37,5
- Su ayak izinde (FW) - %42
- Küresel ısınma potansiyel toplamında (GWP Total) - %27
- İnsan toksisitesi, kanser riskinde - %95 oranlarında iyileşme söz konusudur.



Şekil 3. Klasik black-out ve silika tozu içeren kaplamalı kumaşların yaşam döngüsü analizinde ortaya çıkan en belirgin farklılıklar

IV. SONUÇLAR

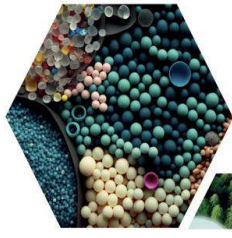
Bu çalışmamızda; tekstilde sürdürülebilirlik bağlamında yenilenebilir kaynaklardan atık şeklinde ortaya çıkan geri dönüşüm silika tozları; kaplamalı ev tekstilleri, kontrat tekstilleri ve diğer uygun teknik tekstillerin üretiminde dolgu malzemesi olarak kullanılabileceği, ekolojik açıdan sakıncaları olan karbon siyahı kullanımını tamamen veya kısmen elimine edebileceğini, %7 oranında ısı yalıtım özelliğinin iyileştirildiği ve % 15 oranında enerji tasarrufu ve yapılan yaşam döngüsü analizinde (LCA) karbon ayak izinde %37,5 ve su ayak izinde %42 oranında iyileştirme sağlanmıştır.

TEŞEKKÜR

Bu çalışmamız 1507 - Kobi Ar-Ge Başlangıç Destek Programı ile desteklenmiş olup proje dönemi boyunca değerli katkıları için Tübitak Teydeb'e teşekkürlerimizi sunarız.

KAYNAKLAR

- [1] Üner, İ., & Başaran, F. N. (2016). Tekstilde Sürdürülebilirlik İçin Yöresel Ürünlerin Yaşam Döngüsü Değerlendirmesindeki Rolü: Çaput Dokumacılığı Örneği. *Akdeniz Üniversitesi, IV. Yöresel Ürünler Sempozyumu ve Uluslararası Kültür/Sanat Etkinlikleri, Antalya*.
- [2] IPCC (2021). *Climate Change 2021: The Physical Science Basis*. Intergovernmental Panel on Climate Change.
- [3] Sorrell, S. (2015). Reducing energy demand: A review of issues, challenges and approaches. *Renewable and Sustainable Energy Reviews*, 47, 74–82.
- [4] Burrett, R., Clini, C., Dixon, R., Eckhart, M., El-Ashry, M., Gupta, D., & Ballesteros, A. R (2022). *Renewables 2022 Global Status Report*. Renewable Energy Policy Network for the 21st Century.
- [5] Özden, S. (2025). Farklı inorganik katkılarla kaplanmış kumaşların özelliklerinin araştırılması. Tez, Bursa Teknik Üniversitesi
- [6] Polat, A.,D. (2024). Sodyum lignosülfonatın tekstil kaplamacılığında kullanılabilirliğinin araştırılması. Tez, Bursa Uludağ Üniversitesi



16 ULUSLARARASI
LİF VE POLİMER
ARAŞTIRMALARI
SEMPZYUMU

16th INTERNATIONAL FIBER AND POLYMER RESEARCH SYMPOSIUM

Sürdürülebilir ve İşlevsel Lif ve Polimerler
Sustainable and Functional Fibers & Polymers



9-10 Mayıs
May 2025

İstanbul Teknik Üniversitesi
Gümüşsuyu Prof. Dr. Necmettin Erbakan Yerleşkesi
Istanbul Technical University
Gumussuyu Prof. Dr. Necmettin Erbakan Campus

Global and local positioning of seaweed fibers: A sustainable journey from fiber to fabric

Büşra Bozyer^{a*}, Prof.Dr. Züleyha Değirmenci^b, Ersen Çatak^c,

^aDepartment of R&D, Project Engineer, Sanko Textile,
27127 Gaziantep, Türkiye.

^bDepartment of textile engineering(English), Gaziantep University, 27310 Gaziantep, Türkiye.

^cDepartment of R&D, Project Engineer, Sanko Textile,
27127 Gaziantep, Türkiye.

*Corresponding author: busra.bozyer@sanko.com.tr

ABSTRACT

The need for sustainable production in the textile industry increases the importance of fiber solutions based on renewable resources that do not harm the nature. In this context, seaweed-based fibers attract attention with their biodegradable structures, environmentally friendly production technologies and functional textile properties. This study addresses the global positioning of different types of fibers derived from seaweed (e.g. alginate-based fibers, natural cellulosic blends and trademarks) and their applicability in Turkey from technical and strategic aspects.

The processes of obtaining seaweed fibers, spinning methods, blending ratios with other fibers and their effects on the finished fabric are evaluated with the support of literature. SeaCell™ is an example of the commercial application of these fibers and stands out in terms of moisture management, antibacterial effect and comfort.

The SWOT analysis, based on data from TurkStat, FAO, UN Comtrade and academic sources, highlights Turkey's potential to utilize its existing seaweed production capacity in the textile sector. The study aims to provide a roadmap for domestic production models and technology investments.

Keywords: Seaweed fiber, Sustainable textile, Alginates, SeaCell™, Fiber blends, Biodegradable fibers, Textile industry, Turkish market,

I. INTRODUCTION

The global textile industry has entered a serious transformation process in recent years in terms of both environmental and social sustainability. The main drivers of this transformation are climate change, water scarcity, microplastic pollution, fast fashion pressure and increased consumer awareness.

Environmental burdens (water use, greenhouse gas emissions, soil degradation), especially from raw materials, have made the textile industry one of the most criticized industries. In this context, the shift towards natural, renewable and biodegradable fibers has become not only an environmental responsibility but also a necessity for economic competition (Muthu & Gardetti, 2020). One of the natural resources that

attracts attention in this transformation process is seaweed (macroalgae). These fast-growing organisms, which are abundant in the oceans, have a high photosynthetic capacity and have been used for a long time in various fields such as food, cosmetics, pharmaceuticals and bioplastics. However, the contribution of seaweed to the textile industry has reached a remarkable dimension, especially with SeaCell™ fiber, which was developed in the 2000s and contains seaweed extract in a Lyocell-based structure [1]. SeaCell™ is an innovative type of fiber developed by Austria-based Lenzing AG based on the Lyocell process and commercialized by German Smartfiber AG. This fiber contains 99.4% wood-based cellulose (Lyocell) and 0.6% dried seaweed. The type of seaweed used is usually *Ascophyllum nodosum* and is collected from the Norwegian coast using environmentally friendly methods (The Power of Seaweed in a Fiber, 2022). This seaweed is fixed to the cellulose matrix and provides antioxidant, antibacterial, cell regenerating and moisture balancing effects by contacting the skin during the lifetime of the fiber (Ferreira et al., 2021).

The importance of SeaCell™ fibers in the textile industry is not limited to their functional properties. The production process requires very low water consumption and chemical use compared to conventional cellulosic fibers. Lyocell technology leaves no waste to the environment thanks to its closed-loop solvent system, making SeaCell™ a sustainable alternative not only biologically but also productionally (Chen et al., 2016). At the same time, SeaCell™ fibers are competitive in terms of textile performance such as shape stability, strength, softness and high handle quality (Souza et al., 2016). Besides SeaCell™, other innovative textile initiatives based on seaweed have attracted attention in recent years. For example, Algiknit (USA) develops environmental clothing products with kelp-based biopolymers; Algaia SA (France) produces alginate-based fibers and

coatings. Marinova Pty Ltd (Australia) integrates phytochemicals from red algae into cosmetic and medical textiles. These developments show that seaweed is becoming not only an alternative fiber but also a raw material for high value-added functional textiles (InsightAce, 2024). The main objective of this study is to comprehensively analyze the technical properties of seaweed-based fibers (especially SeaCell™), their suitability for yarn and fabric production, their sustainability potential and their place in the global market. In this context, both production and trade statistics from data sources such as FAO, TurkStat, UN Comtrade will be included, as well as material scientific analysis from technical reports and literature. At the same time, comparative assessments will be made on Turkey's position in this field and the role that SeaCell™ and similar algae-based fibers will assume in the textile industry in the coming years will be discussed.

II. EXPERIMENTAL METHOD / TEORETICAL METHOD

In order to evaluate the usability of seaweed-based fibers in textile applications, the production processes, physical properties and characterization methods of these fibers must first be understood in detail. In this study, SeaCell™ fibers are taken as a technical reference point and the related technical properties and production methodology are examined comparatively with the data in the literature.

2.1 SeaCell™ Fiber Production: Integration with Lyocell Process

2.1.1. Characterization of materials

SeaCell™ is a Lyocell based fiber and its production is based on a closed loop N-methylmorpholine N-oxide (NMMO) solvent system. This system allows wood-derived cellulose (usually from beech and eucalyptus trees) to be dissolved and spun into yarn. The Lyocell process is much more environmentally

friendly than viscose rayon and acetate production because:

- Low water consumption (about 500-700 L/kg fiber),
- Solvent recovery rate is over 99.5%,
- Chemical waste generation is minimal (Chen et al., 2016).

In SeaCell™ production, 0.6% dry seaweed (usually *Ascophyllum nodosum*) is added to this Lyocell solution to homogenize the mixture. This seaweed is physically fixed to cellulose chains with a special technique. Thus, active components such as vitamins, antioxidants and minerals contained in seaweed remain in the fiber even after washing (Smartfiber AG, 2022).

2.2 Technical Characterization and Physical Properties

SeaCell™ fibers are marketed in two different cross sections, 1.7 dtex / 38 mm and 6.7 dtex / 60 mm. The fiber is light brown and has the softness of a typical cellulosic fiber. The main technical properties of SeaCell™ are given in

Table 1: Technical specifications of SeaCell™ Fiber (Smartfiber AG, 2022)

| Property | Value (6.7 dtex) |
|---------------------------|----------------------------|
| Fiber fineness (titer) | 6.7 dtex |
| Cut length | 60 mm |
| Tensile strength (dry) | 22 cN/tex |
| Elongation at break (dry) | 9% |
| Tensile strength (wet) | 17 cN/tex |
| Elongation at break (wet) | 14% |
| BISFA modulus (wet) | 5.5 cN/tex/5% |
| Density | 1.49 g/cm ³ |
| Biodegradability | 100% |
| Skin interaction | Antioxidant + Moisturizing |
| Certifications | OEKO-TEX 100, EU Ecolabel |
| Property | Value (6.7 dtex) |
| Fiber fineness (titer) | 6.7 dtex |

SeaCell™ fibers have the ability to absorb and spread moisture quickly, thus creating a cool touch feeling in summer and contributing to thermal insulation in winter. It is also suitable for sensitive skin thanks to its pH-neutral structure.

2.3 Material Characterization Techniques

In the study, SeaCell™ characterizations in the literature were examined and the following techniques were used:

- FTIR (Fourier Transform Infrared Spectroscopy): For the detection of cellulose and alginate based functional groups.
- SEM (Scanning Electron Microscopy): Fiber surface porosity and algae particle dispersion structure.
- Alambeta: Thermal conductivity, absorptivity, heat retention measurements (Souza et al., 2016).
- ISO 20743 Standard: Antibacterial tests (with *Staphylococcus aureus* and *E. coli*).

Thanks to these tests, the comfort performance, biofunctional structure and surface properties of the fiber were determined. Especially the effect of algae additive on the fiber surface was clearly observed in SEM analysis (Ferreira et al., 2021).

2.4 Other Algae-Based Fibers: Algiknit, Algaia SA, Marinova

Some innovative initiatives other than SeaCell™ also use different types of algae:

- Algiknit (USA): Produces textile yarn from kelp-based biopolymers. It provides high elasticity and 100% biodegradability.
- Algaia SA (France): Develops bioplastic-supported textile applications with alginate-based fibers.

- Marinova (Australia): Uses phytochemicals from red algae such as *Palmaria palmata* in medical textile coatings.

These brands demonstrate that seaweed can be integrated into textiles not only as a fiber additive but also as a biofunctional active ingredient. These technologies are therefore not only “sustainable” but also have the potential to produce high value-added products.

2.5 Theoretical Background: Components of Sustainable Production

SeaCell™ production process has the following features within the framework of sustainable fiber technologies:

- Solvent recovery with closed circuit system
- Low values for energy and water consumption
- Limitation of the renewable zone for seaweed harvesting (protection of ecological balance)
- Minimal waste water and chemical emission rates
- Production chain certified with environmental certificates such as OEKO-TEX, EU EcoLabel

This makes SeaCell™ one of the fibers of the future in terms of compliance with the European Green Deal and global environmental policies.

III. RESULTS AND DISCUSSIONS: YARN AND FABRIC PRODUCTION

The integration of seaweed-based fibers into the textile industry is not limited to the production of fibers, but also includes the spinning of these fibers into yarns, their transformation into fabric structures and the evaluation of their performance on products reaching the end user. SeaCell™ is an important reference product at this point, especially in blends with conventional fibers such as cotton, viscose and

polyester, enabling a wider product range. In this section, a technical overview of the yarn and fabric production processes of SeaCell™ is presented, blend formulas and performances are evaluated, supported by test data from the literature.

3.1 Yarn Production Technologies and Suitable Spinning Systems

SeaCell™ fibers are generally used in spinning systems for short staple fibers as they are cellulosic based and exhibit viscose/lyocell-like behavior. Below are their compatibility with different spinning systems:

Vortex spinning in particular emphasizes SeaCell™'s advantage of high strength and low hairiness. Souza et al. (2016) showed that yarns containing SeaCell™ provide higher fiber hold stability and comfort when produced by vortex spinning.

Table 2. Yarn production technologies and suitable spinning systems

| Spinning System | Compatibility |
|------------------|----------------------|
| Ring spinning | High compatibility |
| Rotor (Open-end) | Medium compatibility |
| Vortex | High compatibility |
| Air-jet | Low compatibility |

3.2 Fiber Blend Ratios and Effects

SeaCell™ is often used in blends with other fibers because:

- The cost of the fiber is higher than conventional fibers.
- It is difficult to spin alone.
- By blending, both performance enhancement and cost optimization are achieved.

The most common blend ratios in the literature:

Table 3. Fiber blend ratios

| Blend Ratio (SeaCell® / Cotton) | Performance Remarks |
|------------------------------------|------------------------------------------------------------------------------|
| 20% / 80% | Provides softness and antibacterial effect. Cost is reduced. |
| 30% / 70% | Thermal comfort increases, hand feel improves. |
| 50% / 50% | Antibacterial and comfort properties become more pronounced. |
| 70% / 30% | Hand feel becomes silky; however, strength and spinning difficulty increase. |

Ferreira et al. (2021) reported that cotton yarns with 30% SeaCell™ additives produced fabrics that are compatible with skin pH and optimize moisture balance.

3.3 Fabric Production: Knitting and Weaving Techniques

Yarns with SeaCell™ are generally used in the following constructions:

- Single jersey: Preferred for sportswear and underwear. High air permeability.
- Interlock: Thicker, double-sided fabric structure. Used in winter textiles.
- Twill weave: Suitable for soft-touch but compact fabrics.
- Fine weft-knitting: Ideal for compression garments or medical textiles.

Souza et al. (2016) analyzed the comfort of SeaCell™ and cotton blended knitted fabrics and reported superior performance over cotton and polyester fabrics, especially in terms of moisture management, air permeability and thermal resistance.

3.4 Comfort and Performance Tests: Comparative Analysis with Literature Data

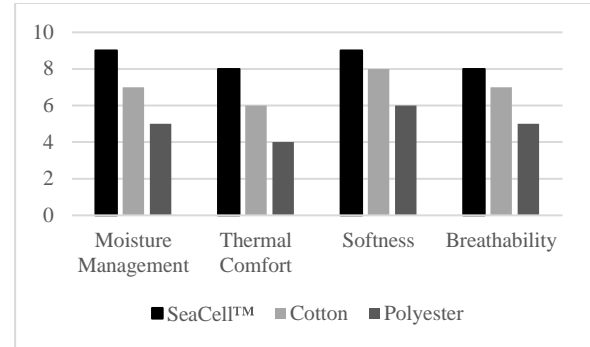


Figure 1. SeaCell™ vs cotton vs polyester comfort performance (Souza et al., 2016; Chen et al., 2016)

Data with scores from 1-10;

- Humidity management,
- Heat regulation,
- Softness,
- Compared under the headings of breathability.

This data shows that fabrics containing SeaCell™ fibers are particularly

- moisture management,
- antibacterial effect,
- thermal equilibrium,

compared to other traditional fibers.

The sustainability of post-wash effects is also valuable: Üreyen et al. (2010) showed that SeaCell™ treated fabrics retain their antibacterial effect even after 40 washes.

3.5 Fabric Handfeel and User Experience

Fabrics with SeaCell™ have a smooth, cool and silky touch due to their Lyocell base. This is why they are especially preferred for underwear and skin-friendly products. It has been described by users as “slippery but natural” and “relaxing feeling” (Smartfiber AG, 2022).

IV. MARKET STRUCTURE AND SUSTAINABILITY ANALYSIS OF SEAWEED-BASED FIBERS

4.1 Global Seaweed Production and Fiber Potential

Table 4. Technical specifications of SeaCell™ fiber (Smartfiber AG, 2022)

| Property | Specification |
|---------------------------|-------------------------------------|
| Fiber Structure | Lyocell-based with seaweed additive |
| Moisture Regain | 25-30% (at relative humidity) |
| Fiber Diameter | ~10-15 microns |
| Biodegradability | 100% |
| Thermal Comfort | High breathability, cooling effect |
| Antibacterial Property | Natural (via ionic content) |
| Dermatological Compliance | OEKO-TEX® and ECARF certified |
| Production Technology | Closed-loop solvent system (NMMO) |
| Solvent Recovery | 99.5% |
| Environmental Impact | Low water and energy consumption |

Seaweed is one of the fastest growing biomass sources worldwide. According to FAO (2021) data:

- Seaweed production increased from 34.7 thousand tons in 1950 to 34.7 million tons in 2019.
- 97% of the production was realized by Asian countries.
- The largest producers are: China (56.7%), Indonesia (27.8%), Korea (5.1%), Philippines (4.2%).

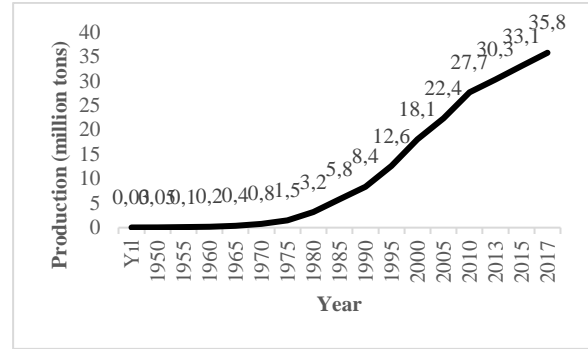


Figure 2. Global seaweed production (1950-2019)

This tremendous increase proves that seaweed can be a sustainable resource not only for food but also for the biotextile and bioplastics sectors.

4.2 SeaCell™ and Seaweed Fibers Market Size

The market size of seaweed-based fibers is growing rapidly:

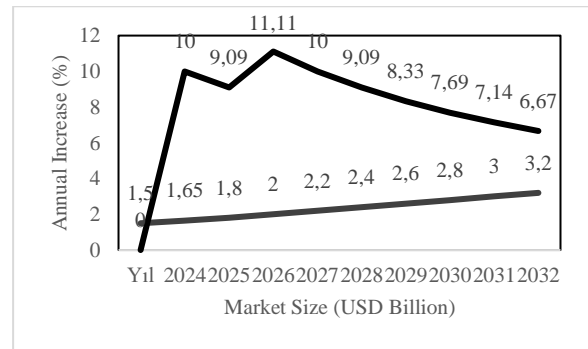


Figure 3. Seaweed fibers global market size forecast (2024-2033) / verified market reports, 2024

SeaCell™ is positioned in the “premium segment” of this market for functional textiles.

DataIntelto (2024) and InsightAce (2024) reports show that the textile industry is turning towards seaweed-based fibers, especially in the “medical, active wear and organic underwear” segments.

4.3 Turkey's Position and Import Data

Turkey does not produce SeaCell™ fiber domestically, but has potential for imports and processed fabric production:

- 1.8 billion USD technical textile imports in 2023 (TurkStat, 2024)

- SeaCell™ based yarns or fabrics are generally imported from Germany, Italy and France.
- Karsu Tekstil and Özen Mensucat are the leading companies producing fabrics containing SeaCell™.

There is no SeaCell™ equivalent seaweed fiber production infrastructure in Turkey yet. However, domestic production may become possible with the utilization of macroalgae species growing on the Black Sea coast.

4.4 Sustainability Comparison: Impact Analysis by Fiber

Table 5. Carbon footprint and water consumption of fibers

| Fiber Type | Water Usage (L/kg) | Carbon Footprint (kg CO ₂ /kg) | Biodegradability |
|------------|--------------------|-------------------------------------------|-------------------|
| Cotton | ≈ 10,000 | 2.0 | Biodegradable |
| Polyester | ≈ 30 | 5.0 | Non-biodegradable |
| Viscose | ≈ 2,500 | 2.3 | Biodegradable |
| SeaCell™ | ≈ 500 (estimated) | 1.2 | Biodegradable |

SeaCell™ stands out from its competitors in terms of sustainability as it can be produced with low energy and water use, the solvents are recyclable, the harvesting of seaweed does not harm the environment and the product is completely biodegradable (Smartfiber AG, 2022).

4.5 Future Role of Seaweed Textiles and Strategic Insights

The role of SeaCell™ and similar products in the textile industry is not just about being a sustainable alternative. These fibers are also used

- Antibacterial clothing (medical)
- Sports textiles with UV protection
- Functional underwear that interacts with the skin

It has the potential to be the raw material for high value-added products.

SWOT Analysis

Table 6. Swot analysis table

| Strengths | Weaknesses |
|---------------------------------------------------------------------------------------------------------------------------------------------------------------------------------------------------------------------------------------------------------------------------------------------------------------------------------------------------------------------------------------------------------------------------------------------------------------------------------------------------------------------------------------------------------------------------------------------------------------------------------------------------------------------|-----------------------------------------------------------------------------------------------------------------------------------------------------------------------------------------------------------------------------------------------------------------------------------------------------------------------------------------------------------------------------------------------------------------------------------------------------------------------------------------------------------------------|
| <p>Sustainable Production Process: SeaCell is produced with a closed-loop system, in which water and solvents are recycled 99% of the time and no harmful waste is released into the environment. SMARTFIBER AG</p> <p>Skin Friendly Properties: Fibers from seaweed support skin health by releasing antioxidants and minerals when in contact with the skin.</p> <p>Natural and Biodegradable: Made entirely from natural resources, SeaCell is a biodegradable and compostable fiber.</p> <p>Various Application Areas: It offers a wide range of uses from underwear to active sportswear, from baby products to home textiles.</p> | <p>Limited Number of Manufacturers: SeaCell fiber is currently only produced by Germany-based Smartfiber AG, which can lead to dependency in the supply chain.</p> <p>High Cost: Due to the specialized production process and limited number of producers, SeaCell fiber is more costly than other traditional fibers.</p> <p>Market Awareness: SeaCell is not yet sufficiently recognized by the broad consumer base, which requires additional efforts in marketing and sales strategies.</p> |
| Opportunities | Threats |
| <p>Growing Demand for Sustainable Products: Consumer interest in environmentally friendly and sustainable products is creating market opportunities for innovative fibers such as SeaCell.</p> <p>Health and Wellness Trends: Thanks to its properties that support skin health, SeaCell can be preferred in wellness and health-oriented textile products.</p> <p>New Market Segments: Demand for SeaCell fibers may increase in niche market segments such as babywear, medical textiles and luxury underwear.</p> | <p>Competitive Fiber Markets: Other sustainable fibers such as Lyocell, bamboo, organic cotton may limit SeaCell's market share.</p> <p>Regulatory and Certification Challenges: Complying with environmental and textile standards in different countries may require additional cost and time.</p> <p>Supply Chain Risks: Seasonality of seaweed harvesting and limited number of producers may cause supply chain disruptions.</p> |

A SWOT analysis of seaweed-based fibers shows that these fibers attract attention especially in niche segments such as medical and wellness textiles thanks to their strengths such as sustainability, skin-friendly properties and biodegradability (Bozyer, B. (2024)). Closed-loop production processes and 99% water-solvent recycling offer an environmentally friendly production model by minimizing environmental impact (Smartfiber AG, 2022; Bozyer, B. (2024)). However, weaknesses such as dependence on only certain producers, high costs and limited consumer awareness pose risks for the supply chain (Bozyer, B.

(2024)). In contrast, the growing demand for sustainable textiles and the need for health-oriented functional products offer significant opportunities for seaweed fibers. It has the potential to create high added value in areas such as medical clothing, UV-protected sports textiles and organic underwear (Bozyer, B. (2024)). However, competition from other sustainable fibers such as bamboo, modal and lyocell and regulations in different countries are threats (Muthu, S. S. (Ed.). (2020)).

V. CONCLUSIONS

This study provides a comprehensive perspective on the growing importance of seaweed-based fibers in the textile industry, particularly through the example of SeaCell™. SeaCell™ is not only a biodegradable fiber, but also an innovative solution with functional properties, environmental sustainability and textile performance.

Technical analysis has shown that:

- SeaCell™ fibers exhibit better thermal comfort, high moisture management and antibacterial activity compared to cotton and polyester.
- The Lyocell method of production is characterized by low water and energy consumption, making SeaCell™ an exemplary model of environmentally friendly production technologies.
- The fiber can be successfully spun especially in vortex and ring systems and is suitable for knitted and woven fabric production.
- Test data in the literature proves that SeaCell™ fabrics have the quality that can be used in areas such as hygienic textiles, medical clothing, organic underwear.
- While global seaweed production has increased 1000 times in the last 70 years, SeaCell™ and similar seaweed-based fibers

are expected to grow at a CAGR of 8.5% until 2032.

- Turkey's lack of domestic production in this field should be considered as a strategic development area.

SeaCell™ is a “living” textile material that interacts not only with the environment but also with the human body. Today, sustainability has become a concept that encompasses not only environmental but also social and biological dimensions. In this context, there is no doubt that seaweed-based fibers will play an important role in the textile vision of the future.

ACKNOWLEDGMENT

This study was created as an output of Sanko Textile R&D center 24-BSP-006 (From Ocean to Closet: Development of Biobased Sustainable Yarn and Fabric from Algae Fiber) and 24-BSP-002 (Development of Health Oriented Functional and Smart Fabrics, Integration of Wearable Technologies into Textile Industry) projects. We would also like to thank our esteemed professor Prof. Dr. Züleyha Değirmenci and the Sanko Family for their contributions at all stages of this study.

RESOURCES

1. Chen, X., Zhang, Z., & Wang, X. (2016). Evaluation of comfort properties of fabrics made from seaweed fiber. *Journal of Applied Polymer Science*, 133(42). <https://doi.org/10.1002/app.44051>
2. DataIntel. (2024). *Seaweed Fiber Market Forecast Report 2024–2031*.
3. Ferreira, A. M., Monteiro, F. J., & Lopes, M. A. (2021). Algae-based biomaterials for regenerative medicine and drug delivery applications. *Pharmaceutics*, 13(2), 2152. <https://doi.org/10.3390/pharmaceutics130202152>

4. Gültekin, B. C. (2016). Red algae-based fibers and their potential in technical textiles. *Fibers and Polymers*, 17(8), 1311–1321.
5. InsightAce Analytic. (2024). Seaweed Fabric Market Report 2024–2030.
6. Islam, A. I., Kumar, R., & Shaker, K. (2023). Investigation on novel seaweed blended textile fibers. *Fibers and Polymers*, 24(1), 77–86. <https://doi.org/10.1007/s12221-023-00148-1>
7. Muthu, S. S. (Ed.). (2020). *Sustainable Textiles: Production, Processing Manufacturing & Chemistry*. Springer Nature Switzerland AG. <https://doi.org/10.1007/978-3-030-38013-7>
8. Smartfiber AG. (2022). *The Power of Seaweed in a Fiber* [Brochure]. <https://www.smartfiber.de>
9. Souza, S. P., Machado, M. A., & Oliveira, R. C. (2016). Eco-efficiency assessment of textile fibers using emergy and LCA. *Textile Research Journal*, 86(19), 2050–2060. <https://doi.org/10.1177/0040517516677226>
10. Türkiye İstatistik Kurumu (TÜİK). (2024). *Dış Ticaret İstatistikleri: GTİP Bazında İthalat Verisi (2023)*. <https://data.tuik.gov.tr>
11. Üreyen, M. E., Gök, Ö., Ateş, M., Günkaya, G., & Süzer, Ş. (2010). Gümüş katkıli lif-pamuk karışımından üretilen kumaşların gümüş içeriklerinin ve antibakteriyel aktivitelerinin belirlenmesi. *Tekstil ve Konfeksiyon*, 20(3), 205–211.
12. AlgiKnit. (2023). *Company Overview*. <https://www.algiknit.com>
13. Bozyer, B. (2025). Deniz yosunu elyaflarının küresel ve yerel konumlandırılması: Elyaftan kumaşa sürdürülebilir bir yolculuk [Yayınlanmamış kongre bildirisi taslağı].
14. Ferdouse, F., Holdt, S. L., Smith, R., Murua, P., & Yang, Z. (2018). The global status of seaweed production, trade and utilization. Food and Agriculture Organization of the United Nations



Effect of unit cell geometry and wall thickness of auxetic structures on energy absorption capability under quasi-static compression

Ali İmran Ayten^{a*}, Bekir Keskin^a, Ameen Topa^b

^aDepartment of Mechanical Engineering, Faculty of Engineering, Yalova University, 77200 Yalova, Türkiye.

^bDepartment of Maritime Technology, Faculty of Ocean Engineering Technology, Universiti Malaysia Terengganu, 21030 Kuala Terengganu, Malaysia.

*Corresponding author: aiayten@yalova.edu.tr

ABSTRACT

This study investigates the quasi-static compressive behaviour of 3D-printed auxetic structures with re-entrant and arrowhead geometries at three different wall thicknesses (0.44 mm, 0.62 mm, and 0.80 mm). Auxetic cores were manufactured using fused deposition modelling (FDM) by using ABS polymer. Quasi-static compression tests revealed that thinner-walled structures exhibited higher peak forces and more brittle collapse, while thicker-walled ones showed smoother force-displacement responses. For the re-entrant geometry, the peak compressive forces were measured as 1820.6 N, 1443 N, and 1015.3 N for wall thicknesses of 0.44 mm, 0.62 mm, and 0.80 mm, respectively. In the arrowhead geometry, higher forces were recorded as 6377.3 N, 4193.5 N, and 3890 N for the corresponding wall thicknesses. The specific energy absorption (SEA) results indicated that thinner structures achieved better energy absorption efficiency. Deformation observations showed that the re-entrant structure exhibited a uniform inward folding, while the arrowhead structure underwent localized buckling with sequential collapse stages. Increasing wall thickness led to reduced peak forces and more progressive crushing behaviour in both geometries. These findings highlight the significant influence of auxetic topology and wall thickness on the compressive performance and energy absorption capability of cellular structures, offering valuable guidelines for designing lightweight, impact-resistant systems.

Keywords: Auxetic structures; Quasi-static crushing; Fused deposition modelling; Ls-Dyna

1. INTRODUCTION

Auxetic structures, characterized by a negative Poisson's ratio, exhibit unconventional deformation behaviour such as lateral expansion under tensile loading and lateral shrinkage under compression [1-3]. This unique mechanical response enhances properties such as energy absorption making auxetic designs highly attractive for lightweight protective structures, biomedical devices, and aerospace components [4-6]. Various auxetic geometries, including re-entrant and

arrowhead patterns, have been developed to optimize mechanical performance under different loading conditions [7-8].

The mechanical response of auxetic structures can be tailored by modifying key design parameters such as unit cell geometry and wall thickness. Wall thickness plays a significant role in influencing stiffness, peak force capacity, and energy absorption efficiency during compression. However, a comprehensive understanding of the combined effects of geometry

and wall thickness on the quasi-static crushing behaviour of auxetic structures remains limited.

In this study, 3D-printed auxetic structures with re-entrant and arrowhead geometries were investigated under quasi-static compression to evaluate the influence of wall thickness on their mechanical performance. Experimental tests were conducted with numerical simulations to better understand the progressive deformation mechanisms and validate the experimental findings. The results provide insights into optimizing auxetic design parameters for enhanced energy absorption capabilities in engineering applications.

II. EXPERIMENTAL and NUMERICAL METHOD

2.1 Materials and Preparation Techniques

2.1.1. Manufacturing of auxetic structures

Auxetic structures with re-entrant and arrowhead geometries were manufactured by fused deposition modeling (FDM) on a Creality K1 Max 3D printer. The CAD models of the unit cells in Figure 1 were prepared and processed through Creality's slicing software. ABS filament was used as a printing material, with the nozzle temperature set at 260 °C and the build plate temperature at 100 °C to ensure proper filament flow and bed adhesion. A 0.4 mm diameter nozzle was utilized throughout the manufacturing process.

The first layer was printed at a thickness of 0.2 mm with reduced speeds of 50 mm/s for the edges and 105 mm/s for the infill, to promote strong adhesion and minimize warping. Subsequent layers were printed with a thickness of 0.16 mm, which was determined as optimal for balancing print quality and build time. Printing speeds for these layers varied between 200 mm/s and 330 mm/s depending on the feature type, with lower speeds applied to outer walls and higher speeds to infill regions.

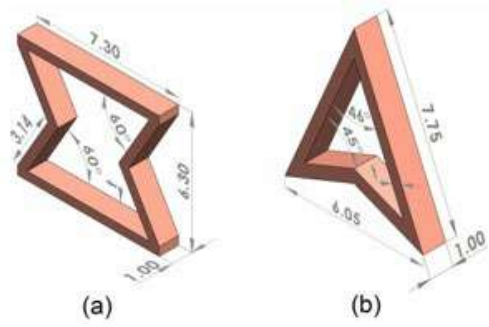


Figure 1. Isometric views of unit cells of auxetic structures in this study. a) reentrant, b) arrowhead.

Due to the complicated geometry of the auxetic designs, maintaining lower printing speeds during the initial layers was critical to prevent defects such as delamination or incomplete bonding. All specimens were printed with 100% infill density to achieve fully dense structures suitable for mechanical testing.

2.1.2. Numerical studies

Numerical models were developed by using LS-PrePost 2025 v1 as the pre-processor and LS-DYNA as the solver. Each 2D model consisted of approximately 50k shell elements and 60k nodes. The top and bottom plates were defined using the “MAT 20 RIGID” material model, while the auxetic structures were modeled using “MAT24 PIECEWISE LINEAR PLASTICITY”. Contact interactions were modeled using the “AUTOMATIC SURFACE TO SURFACE” contact algorithm to define the contact between the plates and the specimen, and the “AUTOMATIC SINGLE SURFACE” contact algorithm to account for self-contact within the folding auxetic structure. The movement of the top plate was prescribed using the DEFINE_CURVE keyword, with a compression speed set to 2 mm/min, consistent with the experimental test conditions.

III. RESULTS AND DISCUSSIONS

Tensile testing of the ABS material was performed to determine the mechanical properties required for the numerical modeling studies. The average elastic

modulus was measured as 666 MPa, providing an indication of the material's stiffness suitable for simulating the structural behavior of the auxetic geometries. The average tensile strength was found to be approximately 38 MPa, with an average strain at failure of 3.45%, reflecting moderate ductility. The stress-strain curves exhibited a linear elastic region followed by yielding and limited plastic deformation before fracture. The low standard deviations in elastic modulus (± 72.55 MPa) and tensile strength (± 0.51 MPa) indicate good material consistency. These experimentally obtained properties were subsequently used to define the input parameters for the finite element models developed in the numerical study.

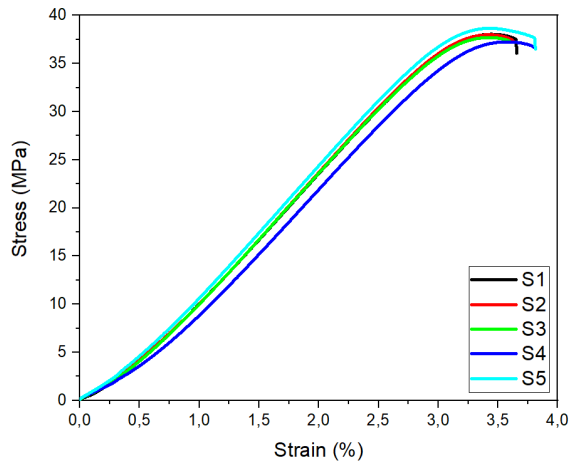


Figure 2. Stress-strain curves for ABS material used in auxetic structures.

Table 1. ABS material properties

| | E_{Mod} | Tens. Str. | Tensile Strain | Stress at Failure | Strain at Failure |
|------|-----------|------------|----------------|-------------------|-------------------|
| | MPa | MPa | % | MPa | % |
| S1 | 699 | 38 | 3.45 | 38 | 3.45 |
| S2 | 663 | 38 | 3.42 | 38 | 3.42 |
| S3 | 643 | 37.7 | 3.43 | 37.7 | 3.43 |
| S4 | 566 | 37.2 | 3.58 | 37.3 | 3.58 |
| S5 | 763 | 38.7 | 3.43 | 38.7 | 3.43 |
| S.D. | 72.55 | 0.514 | 0.067 | 0.51 | 0.067 |

The effect of wall thickness on the quasi-static crushing behavior of auxetic structures was evaluated for re-entrant and arrowhead geometries. In Fig. 2, only the initial 25 mm displacement region is shown to better capture the early stage crushing mechanisms, where differences in collapse behavior are most pronounced.

For the re-entrant geometry, decreasing the wall thickness led to higher initial peak forces and a more brittle response. The peak crushing forces (PCF) were measured as 1820.6 N for 0.44 mm thickness, 1443.0 N for 0.62 mm, and 1015.3 N for 0.80 mm. The thinnest re-entrant samples exhibited a sharp initial peak followed by a significant drop, indicating a sudden collapse mechanism. In contrast, thicker-walled samples showed a more gradual force increase and smoother force-displacement behavior, suggesting progressive folding and better energy dissipation.

For the arrowhead geometry, a similar trend was observed, but the magnitudes of the peak forces were significantly higher compared to the re-entrant design. Peak compressive forces for arrowhead structures were recorded as 6377.3 N at 0.44 mm thickness, 4193.5 N at 0.62 mm, and 3890.0 N at 0.80 mm. Thinner-walled arrowhead structures displayed pronounced oscillations in the force-displacement curves, characteristic of sequential and localized buckling. As the wall thickness increased, the force response became more stable and the oscillations diminished, indicating a more uniform and ductile crushing mechanism.

Overall, thinner-walled auxetic structures provided higher initial peak loads but exhibited abrupt and unstable collapse behavior. In contrast, increased wall thickness improved structural stability and enabled more progressive energy absorption during compression for both re-entrant and arrowhead geometries.

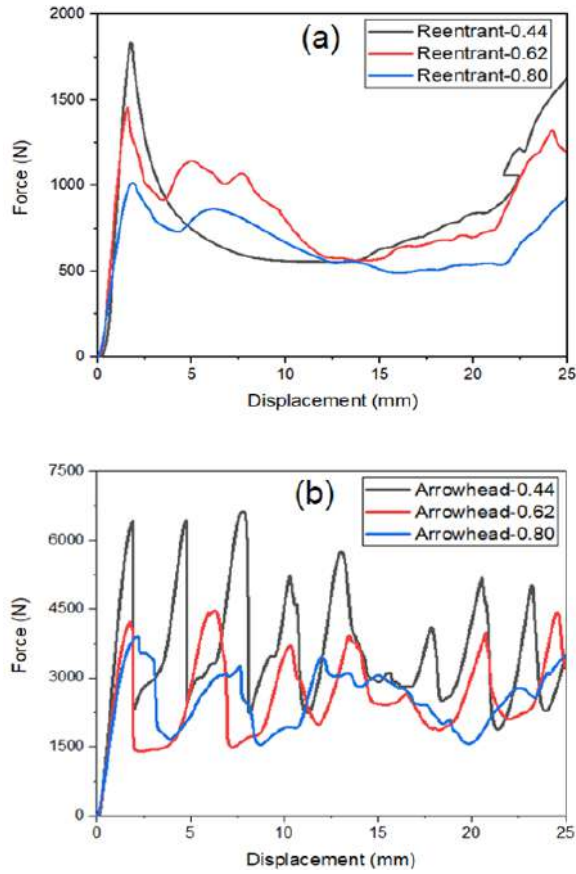


Figure 2. Effect of wall thickness of unit cell on crushing behavior of auxetic structures for different unit cell geometries. a) reentrant, b) arrowhead.

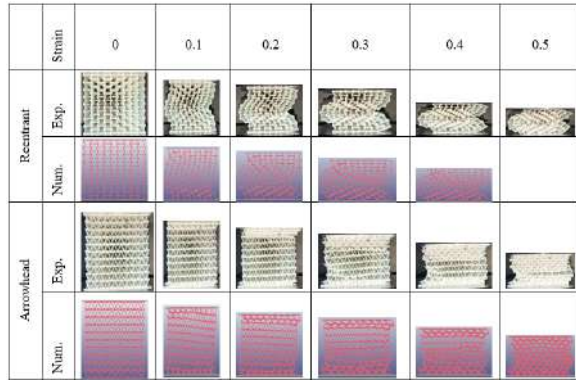


Figure 3. Deformation modes observed experimental and numerical studies for different geometries at different strain values

Figure 3 presents a comparison of the experimental and numerical deformation patterns of re-entrant and arrowhead auxetic structures under quasi-static compression up to a strain of 0.5.

The re-entrant structure exhibited a gradual and uniform inward folding of the unit cells, with deformation starting from the top and progressing downward. Up to a strain of 0.3, the collapse remained

relatively uniform; beyond this point, densification occurred, leading to a noticeable increase in force. The numerical simulations successfully captured the overall deformation behavior, with only minor differences observed in localized buckling zones.

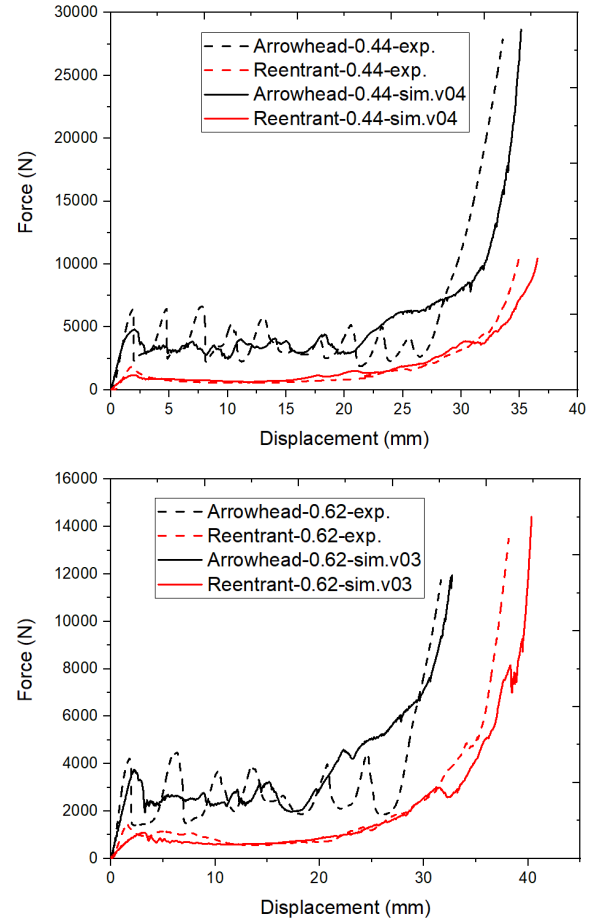


Figure 4. Comparison of numerical and experimental results of auxetic structures

In contrast, the arrowhead structure showed deformation initiating from the middle region, resulting in localized buckling at intermediate strain levels. Experimental and numerical results were in good agreement, though slight variations were noted in the initial failure locations. The force-displacement curve of the arrowhead structure displayed periodic fluctuations, indicating a stepwise collapse characteristic of concentrated stress regions.

Figure 4 shows the comparison between experimental and numerical force-displacement responses for re-entrant and arrowhead structures at wall thicknesses of 0.44 mm and 0.62 mm. In both cases, the arrowhead

structures exhibited higher peak forces and more pronounced force oscillations compared to the reentrant structures. Numerical results captured the general trends and deformation characteristics observed experimentally, including the progressive increase in force and the occurrence of localized buckling phases. Although minor deviations exist in the magnitude and exact locations of the peak forces, the overall agreement between experimental and numerical results validates the accuracy of the developed finite element models.

| Design | Parameter | Experiment | Simulation | Error (%) |
|----------------|-----------|------------|------------|-----------|
| 0.44 arrowhead | SEA (J/g) | 5,047 | 5,386 | 6,72 |
| | MCF (kN) | 5,422 | 5,541 | 2,20 |
| | PCF (kN) | 6,413 | 5,026 | 21,60 |
| 0.44 reentrant | SEA | 2,611 | 2,524 | 3,33 |
| | MCF (kN) | 1,671 | 1,505 | 9,93 |
| | PCF (kN) | 1,836 | 1,174 | 33,70 |
| 0.62 arrowhead | SEA | 3,154 | 3,975 | 26,030 |
| | MCF (kN) | 3,100 | 3,786 | 22,129 |
| | PCF (kN) | 4,209 | 4,356 | 3,493 |
| 0.62 reentrant | SEA | 3,257 | 3,501 | 7,492 |
| | MCF (kN) | 1,972 | 2,008 | 1,826 |
| | PCF (kN) | 1,464 | 1,351 | 7,719 |
| 0.80 arrowhead | SEA | 4,912 | 5,445 | 10,851 |
| | MCF (kN) | 4,442 | 5,099 | 14,791 |
| | PCF (kN) | 3,900 | 4,434 | 13,692 |
| 0.80 reentrant | SEA | 3,593 | 3,700 | 2,978 |
| | MCF (kN) | 1,984 | 2,048 | 0,032 |
| | PCF (kN) | 1,019 | 1,025 | 0,006 |

Figure 5. Result parameters for all specimens

$$SEA = \frac{\text{Absorbed energy}}{\text{Mass}} \left(\frac{J}{g} \right) \quad (1)$$

$$MCF = \frac{\text{Absorbed energy}}{\text{Maximum displacement}} (N) \quad (2)$$

Figure 5 presents all critical parameters such as specific energy absorption (SEA), mean crushing force (MCF) and peak crushing force (PCF) for each of geometries and wall thicknesses which were used in this study. It can be said that most of the results have an acceptable amount of error. SEA and MCF parameters were calculated as in Equation (1) & (2), respectively.

IV. CONCLUSIONS

This study demonstrated the significant influence of wall thickness and unit cell geometry on the quasi-

static crushing behavior of auxetic structures. Thinner-walled structures achieved higher peak forces but exhibited a brittle collapse, while thicker walls promoted smoother, more progressive deformation. The numerical models successfully predicted the deformation patterns observed in experiments. These findings provide valuable insights for optimizing auxetic structures in applications requiring enhanced energy absorption and structural stability.

ACKNOWLEDGMENT

This study was supported by Yalova University BAP Project (2024/ÖNAP/0007).

REFERENCES

- [1] Farrokhhabadi A, Ashrafian MM, Behraves AH, Hedayati SK (2022) Assessment of fiber-reinforcement and foam-filling in the directional energy absorption performance of a 3D printed accordion cellular structure. *Comp Struct* 297.
- [2] Usta F, Türkmen HS, Scarpa F (2021) Low-velocity impact resistance of composite sandwich panels with various types of auxetic and non-auxetic core structures. *Thin-Walled Struct* 163.
- [3] Jiang H, Ren Y, Jin Q, Zhu G, Hu Y, Cheng F (2020) Crashworthiness of novel concentric auxetic reentrant honeycomb with negative Poisson's ratio biologically inspired by coconut palm. *Thin-Walled Struct* 154.
- [4] Gomes RA, Oliveira LA, Francisco MB, Gomes GF (2023) Tubular auxetic structures: A review. *Thin-Walled Struct* 188:1-26.
- [5] Guo M, Yang H, Ma L (2022) 3D lightweight double arrow-head plate-lattice auxetic structures with enhanced stiffness and energy absorption performance. *Comp Struct* 290:115484.
- [6] Jiang L, Hu H (2017) Low-velocity impact response of multilayer orthogonal structural composite with auxetic effect. *Comp Struct* 169:62-68.
- [7] Özen İ, Çava K, Gedikli H, Alver Ü, Aslan M (2020) Low-energy impact response of composite

sandwich panels with thermoplastic honeycomb and reentrant cores. Thin-walled Struct 156:106989.

[8] Usta F, Türkmen HS, Scarpa F (2022) High-velocity impact resistance of doubly curved sandwich panels with re-entrant honeycomb and foam core. Int J of Impact Eng 165:104230.



Nanoclay reinforced nanofiber membranes for oil-water separation

Melike Deniz Bıçakçı, Buse Girgin, Ömer Tüylüce Züleyha Saraç, Çiğdem Yücedağ Taşdelen

Chemical Engineering, Gebze Technical University, 41400 Kocaeli, Türkiye.

*Corresponding author: cigdem@gtu.edu.tr

ABSTRACT

This project focuses on the design and development of Janus nanofiber membranes based on Poly(acrylonitrile-co-vinyl acetate) (PAN-co-VAc) reinforced with nanoclay, aimed at oil-water separation applications. Aligned with principles of environmental sustainability and economic viability, the membranes are intended to address key challenges in areas such as industrial wastewater treatment, oil spill remediation, and the preservation of water resources.

The Janus nanofiber membranes will be fabricated using the electro-blowing method, where one side will be modified with nanoclay to impart hydrophobic characteristics, while the opposite side will remain as the unmodified polymer to maintain hydrophilic properties. To optimize membrane performance, the effects of variables such as solution concentration, air pressure, and applied voltage will be systematically studied using the Taguchi experimental design approach. This method aims to minimize production variability, enhance product quality, and identify the optimal production parameters.

The electro-blowing technique employed in this project provides a more scalable, cost-effective, and faster alternative to traditional electrospinning methods. The resulting Janus membranes are expected to support environmental sustainability efforts while offering a practical and economical solution for efficient oil-water separation.

Keywords: Janus membrane; Electro- blowing; Nanoclay; Oil-Water separation

I. INTRODUCTION

The global water pollution problem has worsened due to increasing industrialization and urbanization, posing significant risks to ecosystems and public health [1-3]. Oil spills and oily wastewater stand out as a major environmental concern among other pollutants because they negatively affect aquatic life, soil quality, and drinking water sources [4].

Conventional oil-water separation techniques, such as gravity separation, centrifugation, and chemical treatments, often suffer from inefficiencies, high costs, and the generation of secondary pollutants [5]. These limitations highlight the urgent need for innovative and sustainable solutions to effectively address this problem. In recent years, advanced membrane technologies have become a viable strategy for

effective oil-water separation. Among these technologies, Janus membranes have attracted considerable interest due to their unique asymmetric surface characteristics that allow for the selective separation of the water and oil phases [6]. The dual functionality of Janus membranes enables one surface to display hydrophilic properties while the other shows hydrophobic characteristics, providing high separation efficiency and durability under various operating conditions [7,8].

The primary aim of this thesis project is to develop Janus membranes using poly(acrylonitrile-co-vinyl acetate) (PAN-co-VAc) polymer. These membranes are intended to be specifically designed and optimized for efficient oil-water separation applications. By producing a membrane with asymmetric surface properties—one side being hydrophobic and the other hydrophilic—the goal is to achieve selective separation of oil and water phases with high efficiency. The project not only focuses on the fabrication of these Janus membranes but also on systematically studying their performance characteristics to ensure they meet the requirements for practical applications such as industrial wastewater treatment, oil spill remediation, and protection of aquatic ecosystems. Ultimately, the objective is to produce a functional, scalable, and economically viable membrane material that can provide a sustainable solution to challenges related to oil-water separation. PAN-co-VAc was chosen as the base material due to its superior mechanical strength, chemical stability, and suitability for surface modification techniques [3]. The innovative aspect of this study is the asymmetric modification of the membrane surfaces: one side will be used without any additives to utilize the polymer's natural hydrophilic properties, while the other side will be modified with nanoclay to impart hydrophobic characteristics. This dual modification approach aims to produce a strong and effective membrane for oil-water separation.

One side of the membrane will allow water to pass through while repelling oil. On the other hand, the addition of nanoclays to the opposite side will provide hydrophobic properties, ensuring effective oil rejection. Due to their unique layered structure and high aspect ratio, nanoclays enhance both the mechanical strength and selective separation capacity of the membrane [5].

This study aims to produce a Janus membrane with superior performance characteristics, such as high oil-water separation efficiency, low fouling tendencies, and a long operational lifespan, by exploiting the complementary properties of hydrophilicity and hydrophobicity. The research not only focuses on material development but also emphasizes the comprehensive evaluation of membrane performance under conditions that simulate real-world applications. Key performance parameters, such as durability, water permeability, oil rejection efficiency, and fouling resistance, will be systematically assessed. Additionally, the environmental and economic feasibility of implementing these membranes in industrial processes will be analyzed, with an emphasis on their scalability and potential for sustainable adoption.

This project makes a significant contribution to eco-friendly water treatment methods by addressing a major environmental issue with an innovative material-based solution. The findings aim to lay a solid foundation for future research and improvements in the field of Janus membranes, facilitating their integration into practical systems designed for oil-water separation.

II. EXPERIMENTAL METHOD / TEORETICAL METHOD

Poly (acrylonitrile-co-vinyl acetate) (PAN-co-VAc) polymer was dissolved in Dimethylformamide (DMF) to prepare a solution for nanofiber production. The prepared solution was processed using centrifugal

blow spinning, and solution blowing methods to produce fibers. Optimization studies were carried out to improve the diameter, uniformity, and structural integrity of the obtained fibers. After determining the optimum concentration, the addition of nanoclay additives in different proportions was performed to enhance the membrane properties in subsequent steps. These additives were incorporated into the solution to modify the membrane and ensure it meets the desired performance criteria.

2.1 Optimization Of Nanofiber Production With Poly Acrylonitrile-Co-Vinyl Acetate

The optimization of nanofiber production using Poly (acrylonitrile-co-vinyl acetate) (PAN-co-VAc) was planned. In this context, the electro-blowing method was selected, and the factors affecting fiber diameter, uniformity, and structural integrity were analyzed. The main factors studied included polymer concentration (%wt), air pressure (bar), and applied voltage (kV). The Taguchi method was used to design experimental studies. This method was applied to analyze the effects of multiple factors and to determine the optimal parameter combinations. In this study, three factors were examined at three levels (-1, 0, +1), defined as follows:

- Low level (-1): Represents the minimum value of the parameter, e.g., the lowest polymer concentration.
- Medium level (0): Represents the medium value of the parameter.
- High level (+1): Represents the maximum value of the parameter, e.g., the highest polymer concentration.

The evaluation of the experiments was planned by calculating the Signal-to-Noise (S/N) Ratio. Following the objective of minimizing fiber diameter, the “Smaller-is better” approach was adopted. The S/N ratio was calculated using the following equation[9,10]:

$$\frac{S}{N} = -10 * \log \left(\frac{1}{n} \sum_{i=1}^n Y_i^2 \right) \quad (1)$$

The experimental parameters and levels designed for the study are presented in Table 1 [11]. This design was created to analyze the effects of different parameter combinations on fiber diameter. The results obtained were analyzed to identify the optimal production conditions. The physical properties of the nanofibers produced under these conditions were examined using Scanning Electron Microscopy (SEM) and porosity analysis. The analysis confirmed that the optimized parameters achieved the desired fiber diameter and uniformity. The findings from the optimization process improved stability in nanofiber production and provided a foundation for further membrane modification using nanoclay additives in subsequent stages.

Table 1. Experimental Design Based on the Taguchi Method

| Experiment No | Polymer Concentration (C, %wt) | Air Pressure (P, bar) | Voltage (V, kV) |
|---------------|--------------------------------|-----------------------|-----------------|
| 1 | -1 | -1 | -1 |
| 2 | -1 | 0 | 0 |
| 3 | -1 | 1 | 1 |
| 4 | 0 | -1 | 0 |
| 5 | 0 | 0 | 1 |
| 6 | 0 | 1 | -1 |
| 7 | 1 | -1 | 1 |
| 8 | 1 | 0 | -1 |
| 9 | 1 | 1 | 0 |

2.2 Optimization of Nanoclay Integration into Nanofiber Membranes

At this stage, the integration of nanoclay additives is planned to enhance the performance and surface properties of the produced nanofiber membranes. The integration of nanoclay into the membranes aims to improve oil-water separation efficiency, strengthen mechanical durability, and impart hydrophobic properties to the membrane surface. Nanoclay provides a structure that lowers surface energy, offering resistance to water [12]. This feature allows the membranes to exhibit hydrophobic behavior, facilitating the selective separation of oil from oil-

water mixtures. To prepare the additive, nanoclay will be homogenized in a suitable solvent (DMF) using an ultrasonication method. The prepared nanoclay solution will be added to the previously prepared PAN-co-VAc polymer solution and mixing and ultrasonication processes will be applied to ensure a homogeneous distribution. The prepared nanoclay-containing polymer solutions will be converted into nanofiber membranes using the electro-blowing method. During the coating process, production parameters will be optimized to ensure the effective adhesion of nanoclay to the surface.

As a result of this process, nanofiber membranes modified with nanoclay are expected to exhibit improved surface properties, enhanced oil-water separation performance, and increased mechanical durability. In particular, the hydrophobic property provides a critical advantage for the membrane's long-term performance in industrial applications.

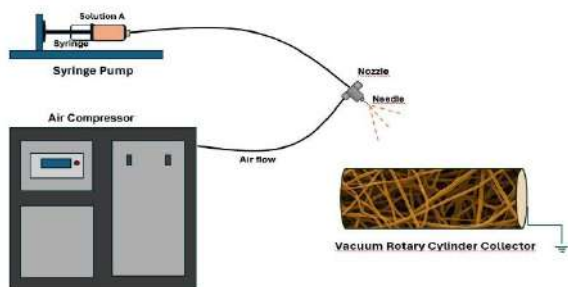


Figure 1. Electro Blowing Method

2.3 Experimental Procedure

Poly(acrylonitrile-co-vinyl acetate) (PAN-co-VAc) polymer was dissolved in an appropriate solvent to prepare a homogeneous polymer solution suitable for nanofiber production. The prepared solution was processed into nanofibers using the electro-blowing technique under various production parameters. The surface morphology, fiber diameter, and porosity of the produced nanofibers were characterized using scanning electron microscopy (SEM), and the results were systematically evaluated to assess fiber

homogeneity and ensure quality control. The effects of polymer solution concentration, air pressure, and applied voltage on fiber diameter were analyzed employing the Taguchi statistical method, leading to the determination of optimal production parameters. To impart hydrophobic characteristics to the nanofibers, nanoclay was dispersed and homogenized in a dimethylformamide (DMF) solution via ultrasonication. Subsequently, nanoclay-doped PAN-co-VAc solutions were fabricated into nanofibers through the electro-blowing method. The hydrophobic nanofibers modified with nanoclay were assembled to create a dual-surface Janus membrane structure. The oil-water separation performance of the fabricated Janus membranes was evaluated in terms of separation efficiency and flow rate under controlled experimental conditions. Following the experimental studies, the results were comprehensively analyzed, a detailed project report was prepared, and the potential contributions of the findings to scientific research and technological advancement were discussed.

2.4 Production of Janus Membranes and Analysis of Oil-Water Separation Performance

In this stage, the goal is to produce Janus membranes by combining nanofibers with different surface properties and to analyze the detailed performance of these membranes in oil-water separation. Modified nanofibers will be integrated to create a structure with distinct surface characteristics. One surface will be designed to exhibit oil-selective properties, while the other surface will possess water-selective properties. The proper integration of these surfaces will ensure high-performance functionality for the membrane. Various optimization and mechanical strength tests will be conducted to evaluate the performance of the Janus membranes. These tests will include the analysis of structural properties such as tensile strength, flexibility, porosity, and thickness. Additionally, parameters like separation efficiency, flow rate, and

the long-term stability of the membrane will be assessed to determine its oil-water separation performance. Flow rate calculations will be performed to analyze the liquid (oil or water) flow through the membrane. The flow rate will be calculated using specific formulas that incorporate parameters such as the surface area of the membrane, the volume of the liquid, and the transition time. These analyses will aim to evaluate the membrane's liquid separation capacity under different conditions. The long-term stability and recyclability of the Janus membranes will also be tested. These tests will determine whether the membrane can maintain its performance during repeated use and its suitability for industrial applications. Recycling tests will analyze the durability and sustainability of the membrane, assessing its reusability. The liquid (water or oil) flow through the Janus membrane is calculated using Equation 2, below [13].

$$F = \frac{V}{(s * \Delta T)} \quad (2)$$

Here, J represents the liquid flux ($L/m^2 \cdot h$) V denotes the volume (L), s represents the membrane area (m^2) and t is the time (h). This formula will be used to determine the flow rate and analyze the membrane's separation capacity under different conditions.

III. RESULTS AND DISCUSSIONS

In this study, various experiments were conducted to determine the optimum parameters for nanofiber production using the electro blowing method. The primary aim was to obtain a homogeneous nanofiber structure, prevent bead formation, and minimize the fiber diameter. The main parameters tested during the experiments were the concentration of the solution, air pressure, and voltage. Additionally, different flow rates and voltage levels were tested to increase the

viscosity of the solution and form homogeneous nanofibers. The experimental studies began by varying the solution concentration, air pressure, and voltage combinations, and the Taguchi experimental design was applied to optimize these parameters. The Taguchi method allows systematic evaluation of the effects of each parameter and helps in determining the optimum production conditions. This method has been particularly useful in determining the optimal levels of concentration, air pressure, and voltage.

The concentration of the solutions used for nanofiber production is a key factor that directly influences the viscosity of the fibers. The viscosity of the solution is a critical parameter that determines the stability and homogeneity of the fiber formation, and thus, the selection of the right concentration range is essential for successful nanofiber production [14]. As the concentration of the solution increases, the viscosity of the solution also increases. Sufficient viscosity is necessary for the smooth spraying of fibers. However, very high concentrations can lead to excessively viscous solutions, which can prevent the fibers from forming properly during electrospinning and result in thicker or uneven fibers [15]. On the other hand, very low concentrations can prevent the solution from reaching the required viscosity, leading to bead formation or other undesirable outcomes. Therefore, %8, %10, and %12 concentrations were chosen. This range ensures that the solution has sufficient viscosity while avoiding bead formation and maintaining stable fiber morphology.

Before determining the concentration range, various percentage ratios were extensively tested. Concentrations ranging from 5% to 19% were investigated. However, at concentrations above 15%, the dissolution of the polymer in DMF became increasingly challenging, and the rising viscosity made it difficult to draw the solution into the syringe. Additionally, high viscosity led to an increased

formation of beads during fiber production. Following the "smaller is better" approach, the maximum concentration was set at 12%.

On the other hand, at lower concentrations, insufficient nanofiber formation was observed. Based on optical observations under a microscope and experimental insights, a concentration range of 8%, 10%, and 12% was selected for further studies.

Once the concentration range was determined, the data obtained were analyzed using Minitab software through the Taguchi method. Using the "smaller is better" approach in the Taguchi method, an experimental design consisting of nine experiments was developed. These experiments focused on three parameters: concentration, voltage, and air pressure. Voltage levels of 10, 15, and 20 V, as well as air pressure levels of 2, 2.5, and 3 bar, were chosen. A Taguchi experimental design table combining these three key variables was created, and the experiments were conducted accordingly.

Polymer solutions with concentrations of 8%, 10%, and 12% were prepared using DMF. A total of 30 mL of solution was prepared for each concentrate. The samples used in the experiments were prepared 24 hours prior to the testing day. During this preparation period, the solutions were continuously stirred using a mechanical stirrer, without applying any heat. The samples were only used for experiments after ensuring that the polymer was completely dissolved in DMF. Sufficient stirring time ensured that the polymer was evenly mixed with the solvent, resulting in uniform polymer concentration throughout the solution. During the process of loading the solution into the syringe, special attention was given to prevent the formation of air bubbles. This step was crucial to ensure the accuracy of the experiments and to avoid unwanted effects during fiber formation. Nine experiments, planned according to the Taguchi method, were conducted sequentially on the same day.

After the experiments, the obtained samples were subjected to scanning electron microscopy (SEM) analysis. SEM imaging was performed at resolution levels of 2000 nm, 5000 nm, and 10,000 nm for each sample.

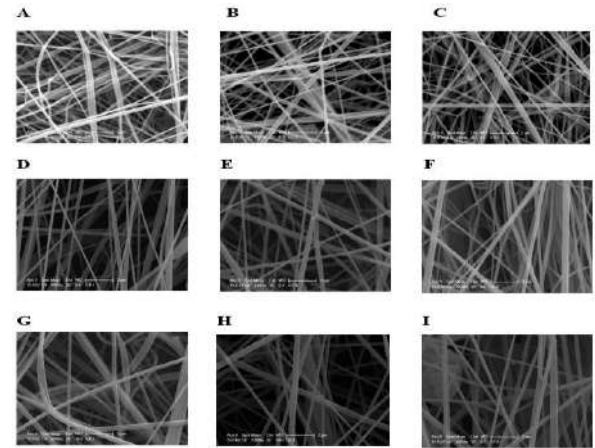


Figure 2. Characterization of the fiber morphology of the Janus PAN-co-VAc membrane (Scale Bar: [2 μ m]).

A) 8% Concentration, 2 Bar, and 10 V. B) 8% Concentration, 2.5 Bar, and 15 V. C) 8% Concentration, 3 Bar, and 20 V. D) 10% Concentration, 2 Bar, and 10 V. E) 10% Concentration, 2.5 Bar, and 15 V. F) 10% Concentration, 3 Bar, and 20 V. G) 12% Concentration, 2 Bar, and 10 V. H) 12% Concentration, 2.5 Bar, and 15 V. I) 12% Concentration, 3 Bar, and 20 V.

Concentration, air pressure, and voltage have shown significant effects on the PAN-co-VAc membrane fibers. As the concentration increased, a noticeable improvement in the uniformity and thickness of the fibers was observed. Fibers produced at 8% concentration exhibited a thinner structure, while fibers produced at 10% and 12% concentrations were more uniform and thicker. The applied pressure and voltage levels showed no observable effect on the fibers. Fiber diameter measurements were conducted using SEM images with a resolution of 2000 nm for each sample under different experimental conditions. For each sample, two different images with the same measurement scale were used. The primary reason for using two different images was to gather data from different areas of the samples, ensuring more representative and accurate results. This approach allowed for 300 measurements per concentration,

resulting in a total of 900 measurements. The fiber diameter measurements were performed using the ImageJ software. The measurement process began with calibration, which was achieved using the known scale bar displayed on the SEM images. Following the calibration, fiber diameters were manually measured. This method was applied to improve measurement accuracy and facilitate comparison across different experimental conditions.

The average fiber diameter for each experimental sample was calculated based on the measurements. The table below presents the average fiber diameter values obtained for each experimental condition:

Table 2. Average Fiber Diameter

| Experiment No | Polymer Concentration (C, %wt) | Air Pressure (P, bar) | Voltage (V, kV) | Average Fiber Diameter (nm) |
|---------------|--------------------------------|-----------------------|-----------------|-----------------------------|
| 1 | %8 | 2 | 10 | 120.27 |
| 2 | %8 | 2.5 | 15 | 112.45 |
| 3 | %8 | 3 | 20 | 110.10 |
| 4 | %10 | 2 | 10 | 153.83 |
| 5 | %10 | 2.5 | 15 | 161.81 |
| 6 | %10 | 3 | 20 | 149.31 |
| 7 | %12 | 2 | 10 | 263.20 |
| 8 | %12 | 2.5 | 15 | 254.51 |
| 9 | %12 | 3 | 20 | 286.73 |

The experimental design was conducted using the Taguchi method within the Minitab software. In this approach, the selected parameters (concentration, air pressure, voltage) and their respective levels were utilized to establish a scoring system. Fiber diameter measurements were evaluated based on the "smaller-is-better" criterion, and the performance of each experimental condition was scored using S/N (Signal-to-Noise) ratios. The Taguchi method employs signal-to-noise ratios to optimize experimental results. These ratios help minimize unwanted variation, thus

enhancing the reliability and robustness of the outcomes.

Table 3. Model Summary

| S | R-sq | R-sq (adj) | R-sq (pred) |
|----------|--------|------------|-------------|
| 0.526126 | 98.71% | 97.41% | 93.45% |

The model's very high R-sq value (98.71%) indicates that the experimental parameters explain a significant portion of the variation in fiber diameter. This demonstrates that the experimental design was properly structured and that the results are supported by a strong model. The R-sq (pred) value of 93.45% confirms that the model can accurately predict the effects of these parameters on fiber diameter in future experiments or under similar conditions. This highlights the model's high generalization capacity and supports the applicability of the experimental results to other scenarios.

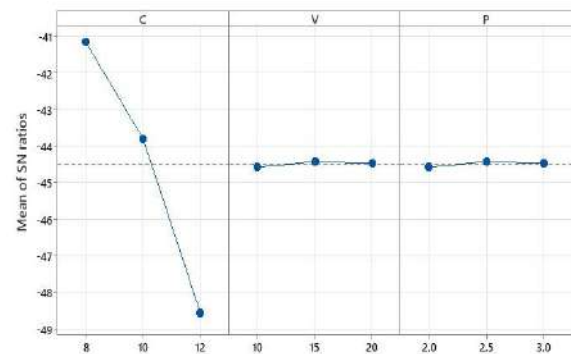


Figure 3. Main Effects Plot for S/N ratios

The analysis of the Taguchi experimental design results showed that the optimal parameter combination for achieving the smallest fiber diameter, based on the "smaller-is-better" approach, was 8% concentration, 2.5 bar air pressure, and 15 V voltage. This combination successfully met the target of obtaining fiber diameters below 124 nm. However, although these conditions produced favorable results, the final selection was 8% concentration, 2 bar air pressure, and 10 V voltage. This choice was made because these parameters provided similarly fine fiber diameters while offering improved energy efficiency. Therefore,

considering both performance and cost-effectiveness, the conditions of 2 bar and 10 V were selected as the final production parameters, as they still achieved the goal of producing fibers below 124 nm.

The polymer concentration was kept constant at 8%, and the nanoclay additive concentration was varied between 0% and 7%. The effect of the nanoclay concentration on the surface properties of the polymer solution was investigated. At nanoclay concentrations higher than 7%, the viscosity of the solution increased, leading to homogeneity issues and the disruption of the polymer's structural integrity. Therefore, nanoclay concentrations above this level were not tested.

Initially, the contact angle in the sample without any nanoclay additive was measured to be 76.43°. As nanoclay was added, a significant increase in the contact angle was observed. This increase indicates that the surface became more hydrophobic, and as the nanoclay concentration increased, the hydrophobicity of the surface strengthened. The contact angle values obtained for different nanoclay concentrations are presented in the table below:

Table 4. The contact angle values

| Polymer Concentration (C, %wt) | Nanoclay additive (%wt) | Air Pressure (P, bar) | Voltage (V, kV) | Contact angle |
|--------------------------------|-------------------------|-----------------------|-----------------|---------------|
| 8 | - | 2 | 10 | 76.43 |
| 8 | 1 | 2 | 10 | 119.19 |
| 8 | 3 | 2 | 10 | 126.75 |
| 8 | 5 | 2 | 10 | 127.96 |
| 8 | 7 | 2 | 10 | 138.07 |

As a result, 8% polymer concentration, 2 bar air pressure, 10 kV voltage, and 7% nanoclay additive were determined as the optimum conditions. Nanoclay additives significantly enhanced the hydrophobicity of the membrane surface, as demonstrated by increased contact angle measurements. The dual-surface Janus structure, with one hydrophilic and one hydrophobic side, allowed selective permeability and effective phase separation. Performance analyses showed that these membranes

exhibit promising oil rejection efficiency, structural integrity, and reusability, making them suitable for industrial applications such as oily wastewater treatment and environmental remediation.

According to traditional laboratory tests, membrane has been tested with three different oils to determine efficiency of the produced membrane which are vegetable oil, diesel and carbon tetrachloride. The tests are given in the table below:

Table 5. Constants of the tests

| Volume of tested oil (L) | Used area of membrane (m ²) |
|--------------------------|-----------------------------------------|
| 0.05 | 0.0018 |

The time membrane took to filter the oil from water are given in table below:

Table 6. Hour data of the oil that has been filtrated with membrane.

| | Carbon tetrachloride | Diesel | Vegetable Oil |
|-------------|----------------------|--------|---------------|
| Trial 1 (h) | 0.0038 | 0.021 | 0.381 |
| Trial 2 (h) | 0.0036 | 0.018 | 0.301 |
| Trial 3 (h) | 0.0036 | 0.025 | 0.334 |
| Mean (h) | 0.0038 | 0.021 | 0.340 |

Then to calculate flux, the given formula is used:

Formula used to calculate flux :

$$\frac{\text{Volume of liquid that is tested (L)}}{\text{Used area of membrane (m}^2\text{)} \times \text{Time of separation (h)}}$$

With this formula flux are:

Table 7. Final flux results according to oil types

| | Vegetable Oil | Diesel | Carbon tetrachloride |
|-----------------------------|---------------|---------|----------------------|
| Flux (L/m ² x h) | 81.7 | 1322.75 | 7309.9 |

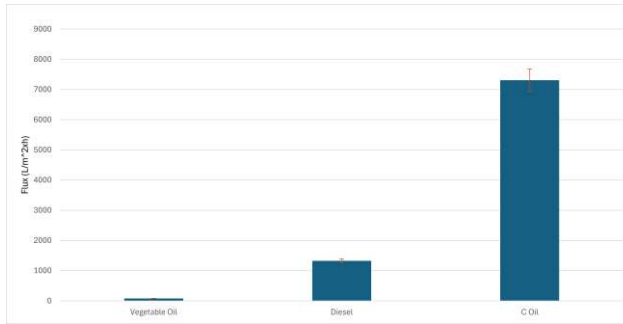


Figure 4. Graph of flux data according to oil types

The findings demonstrate that integrating nanoclay into PAN-co-VAc nanofibers via scalable electro-blowing techniques can produce membranes with enhanced performance and sustainability. This study contributes to the development of cost-effective and eco-friendly membrane-based separation technologies, laying the groundwork for future innovations in environmental engineering.

IV. CONCLUSIONS

In this study, Janus nanofiber membranes based on Poly(acrylonitrile-co-vinyl acetate) (PAN-co-VAc) reinforced with nanoclay were successfully developed for efficient oil-water separation. The electro-blowing method was optimized using the Taguchi design to obtain homogeneous fibers with minimal diameter and bead formation. The optimum production parameters were determined as 8% polymer concentration, 2 bar air pressure, and 10 kV applied voltage, yielding consistent nanofiber morphology and reduced energy consumption. In this study, Janus nanofiber membranes based on Poly(acrylonitrile-co-vinyl acetate) (PAN-co-VAc) reinforced with nanoclay were successfully developed for efficient oil-water separation. The electro-blowing method was optimized using the Taguchi design to obtain homogeneous fibers with minimal diameter and bead formation. The optimum production parameters were determined as 8% polymer concentration, 2 bar air pressure, and 10 kV applied voltage, yielding consistent nanofiber morphology and reduced energy consumption.

Nanoclay additives significantly enhanced the hydrophobicity of the membrane surface, as demonstrated by increased contact angle measurements. The dual-surface Janus structure, with one hydrophilic and one hydrophobic side, allowed selective permeability and effective phase separation. Performance analyses showed that these membranes exhibit promising oil rejection efficiency, structural integrity, and reusability, making them suitable for industrial applications such as oily wastewater treatment and environmental remediation.

The findings demonstrate that integrating nanoclay into PAN-co-VAc nanofibers via scalable electro-blowing techniques can produce membranes with enhanced performance and sustainability. This study contributes to the development of cost-effective and eco-friendly membrane-based separation technologies, laying the groundwork for future innovations in environmental engineering.

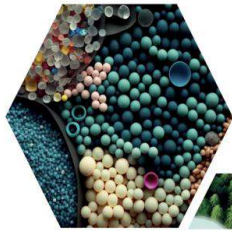
ACKNOWLEDGMENT

This study was supported by TÜBİTAK within the scope of the 2209-A Undergraduate Research Projects Support Program. The project is part of the "Advanced Separation Technologies in Green Chemistry" theme and focuses on designing sustainable membrane processes with alternative raw materials.

REFERENCES

- [1] Smith, P., O'Neill, M., & Taylor, R. (2020). Global water pollution and its implications for human health. *Nature Reviews Earth & Environment*, 1(5), 292–309.
- [2] Wang, T., & Zhao, J. (2022). Role of silica and nanoclay in enhancing membrane performance for oil-water separation. *Materials Today Chemistry*, 24, 100745.
- [3] Johnson, A. L., Karthik, S., & Banerjee, S. (2019). Environmental impacts of oily wastewater and modern separation technologies. *Environmental Science & Technology*, 53(8), 3450–3462.

- [4] Kumar, R., Singh, V., & Arora, R. (2021). Advances in membrane technology for oil-water separation. *Chemical Engineering Journal*, 414, 128759.
- [5] Chen, Y., Liu, Z., & Zhang, W. (2023). Development of Janus membranes for efficient oil-water separation: A review. *Journal of Membrane Science*, 658, 120760.
- [6] Smith, P., & Taylor, R. (2020). Global water pollution and its challenges. *Journal of Environmental Science*, 45(6), 345-360.
- [7] Abuhantash, F., Abuhasheesh, Y. H., Hegab, H. M., Aljundi, I. H., Al Marzooqi, F., & Hasan, S. W. (2023). Hydrophilic, oleophilic and switchable Janus mixed matrix membranes for oily wastewater treatment: A review. *Journal of Water Process Engineering*, 56, 104310.
- [8] Guo, Z., & Zhang, H. (2020). Progress in Janus membranes for efficient oil-water separation. *Advanced Materials*, 32(14), 1905915.
- [9] H. Albetran, Y. Dong, I. M. Low, J. Asian Ceramic Soc. 2015,3(3), 292.
- [10] N. A. S. Gundogdu, Y. Akgul, A. Kilic, Aerosol Sci. Technol.2018, 52(5), 515.
- [11] Sarac, Z., Kilic, A., & Tasdelen-Yucedag, C. (2023). Optimization of electro-blown polysulfone nanofiber mats for air filtration applications. *Polymer Engineering & Science*, 63(3), 723-737.
- [12] Kim, T., & Choi, W. (2020). Modification of nanoclay surfaces for enhanced oil-water separation properties in Janus membranes. *Journal of Applied Polymer Science*, 137(24), 48922.
- [13] Tian, B., Ren, B., Hu, M., Yang, Y., & Wu, J. (2023). Janus membrane with asymmetric wettability for efficient oil/water separation. *Heliyon*, 9(12).
- [14] Daristotle, J. L., Behrens, A. M., Sandler, A. D., & Kofinas, P. (2016). A review of the fundamental principles and applications of solution blow spinning. *ACS applied materials & interfaces*, 8(51), 34951-34963.
- [15] Medeiros, E. S., Glenn, G. M., Klamczynski, A. P., Orts, W. J., & Mattoso, L. H. (2009). Solution blow spinning: A new method to produce micro-and nanofibers from polymer solutions. *Journal of applied polymer science*, 113(4), 2322-2330.



16 ULUSLARARASI
LİF VE POLİMER
ARAŞTIRMALARI
SEMPOZYUMU

16th INTERNATIONAL FIBER AND POLYMER RESEARCH SYMPOSIUM

Sürdürülebilir ve İşlevsel Lif ve Polimerler
Sustainable and Functional Fibers & Polymers



9-10 Mayıs
May 2025

İstanbul Teknik Üniversitesi
Gümüşsuyu Prof. Dr. Necmettin Erbakan Yerleşkesi
İstanbul Technical University
Gumussuyu Prof. Dr. Necmettin Erbakan Campus

Modified silica containing polyacrylonitrile Janus nanofiber membranes for environmental applications

Gülşah Gürbüz, Sedanur Öztürk, Melis Bilgiç, Yeldem Karabulut, Züleyha Saraç, Çiğdem Taşdelen Yücedağ*

Chemical Engineering, Gebze Technical University, 41400 Kocaeli, Türkiye.

*Corresponding author: cigdem@gtu.edu.tr

ABSTRACT

The increasing release of oily wastewater from industrial activities has been identified as a serious environmental issue, driving the need for sustainable separation technologies (Peng et al., 2017). Janus membranes, possessing hydrophilic and hydrophobic surfaces, have been proposed as efficient materials for oil-water separation (Shakiba et al., 2021). In this study, biodegradable Janus nanofiber membranes were fabricated using polyacrylonitrile (PAN), chosen for its chemical stability and spinnability. The membranes were produced through electro-blown spinning, allowing the formation of uniform nanofibers. PAN/DMF solutions with varying polymer concentrations (6–10%) were prepared, and modified silica nanoparticles were incorporated to enhance separation efficiency. Fluorination was applied to the silica to induce hydrophobicity, and the fluorinated layer was deposited on one side of the membrane, forming the Janus structure. The morphology of the fibers was examined using SEM, and diameters ranging from 319 to 1554 nm were recorded, indicating controlled fiber formation. Mechanical tests revealed that membranes containing fluorinated silica (F-SiO₂) achieved a tensile strength of 15 MPa at 9% strain. A significant increase in water contact angle was observed—from 76.04° to 131.69°—confirming improved hydrophobicity. Flux performance was evaluated, and high permeability values were obtained: 2573.4 L/m²·h for water and 330 L/m²·h for diesel. These findings suggest that the developed PAN-based Janus membranes provide a promising, eco-friendly solution for oily wastewater treatment.

Keywords: Polyacrylonitrile (PAN), Janus Nanofiber Membranes, Oil-Water Separation, Environmental Sustainability

I. INTRODUCTION

Environmental sustainability and the need for industrial wastewater treatment are becoming increasingly important. Particularly, oily wastewater resulting from domestic use, industrial production, and oil spills ranks among the major pollutants that cause significant harm to aquatic ecosystems (Silva et al., 2018). Oily wastewater often exists in the form of oil-

in-water or water-in-oil emulsions, and improper treatment of these emulsions can negatively impact resources such as drinking water and groundwater (Galdino et al., 2020). Many countries have implemented strict regulations limiting the maximum oil concentration in wastewater to 5–100 mg/L to ensure proper disposal of such wastes (Abuhasel et al., 2021).

While free or suspended oil can be relatively easily separated from water using physical methods, oil-water emulsions are often chemically stabilized and resistant to biochemical degradation. These mixtures comprise water, oil, emulsifiers, and anti-foaming agents, making physical and/or chemical separation necessary, albeit often costly (Zouboulis et al., 2000). Oily wastewater may also contain toxic components such as phenols, petroleum-derived hydrocarbons, and polycyclic aromatic hydrocarbons, which can inhibit the growth of plants and animals (Njoku et al., 2017). Thus, the treatment of oily wastewater is critical not only for the petroleum industry but also for environmental and health organizations (Galdino et al., 2020).

Conventional industrial water treatment methods often fail to effectively separate oil-water emulsions, particularly small oil droplets. Residual oil can clog pipelines, reduce the effective volume of storage tanks, and lead to frequent maintenance, increasing costs (Abd El-Gawad et al., 2014). These challenges highlight the need for innovative materials and methods for treating complex wastewater.

Nanofiber-based membranes present an effective solution for treating oily wastewater. With their high surface area-to-volume ratio, large pore structure, and lightweight design, nanofibers can separate emulsions more efficiently. Additionally, these fibers offer chemical durability and mechanical robustness, providing a long-lasting and sustainable solution (Jiang et al., 2017). Polyacrylonitrile (PAN), known for its exceptional chemical and thermal stability, is a preferred polymer for producing nanofiber membranes. Its resistance to solvents and acids makes it an ideal material for oil-water separation applications (Vatanpour et al., 2023). However, the intrinsic properties of PAN nanofibers may be insufficient for certain separation applications, thereby

necessitating the development of Janus membrane structures.

Janus membranes are designed with one hydrophilic surface and one hydrophobic surface, enabling the effective separation of oil-water emulsions. The hydrophilic side allows water to pass through, while the hydrophobic side repels oil, ensuring efficient phase separation (Yan et al., 2023). These features can be enhanced by incorporating hydrophilic and hydrophobic silica additives on PAN nanofiber surfaces. Fluorinated silica, with its low surface energy, forms a structure that repels both water and oil, improving the membrane's anti-fouling properties and durability (Kim et al., 2012; Iacono et al., 2019).

The developed Janus membranes achieve up to 99.8% separation efficiency, outperforming traditional methods (Yan et al., 2023). This technology not only enhances environmental sustainability but also offers advantages in energy and cost efficiency. These membranes have potential applications in various sectors, including petrochemicals, food processing, and industrial manufacturing.

This study investigates the effectiveness of fluorinated silica-modified PAN nanofibers in the treatment of oily wastewater. The research is structured into four main stages. First, the optimization of PAN nanofibers is carried out using the Taguchi L9 experimental design method to control fiber diameter and improve consistency. Second, the fluorination of silica is performed by introducing fluorine elements to enhance its hydrophobicity, thereby improving its performance in oil-water separation. In the third stage, Janus membranes are produced by electro-blown spinning PAN nanofibers and integrating them with the fluorinated silica to create a dual-function surface. Finally, the membranes are characterized through comprehensive performance evaluation, including flux analysis, oil removal efficiency, scanning electron microscopy (SEM) imaging, porosity measurements,

and tensile strength testing. This multi-step approach allows for the development of advanced, environmentally friendly membranes capable of addressing the challenges of industrial oily wastewater treatment.

In conclusion, this project aims to develop an environmentally friendly and high-performance solution for oily wastewater treatment. By addressing a critical environmental issue, it also seeks to make innovative contributions to materials science and chemical engineering, marking a significant step.

II. EXPERIMENTAL METHOD / TEORETICAL METHOD

PAN was dissolved in DMF, and these solutions were prepared for nanofiber production. Electrospinning and solution swelling methods were attempted to obtain fibers. Studies were conducted to determine the optimum fiber concentration. The Taguchi L9 method was used to identify the optimal concentration, and the 9 experiments suggested by Taguchi were repeated. The obtained samples were analyzed using SEM, and the final optimum experiment was selected based on the SEM images.

2.1 Materials

2.2. Preparation of PAN Solution

PAN polymer was prepared by dissolving in DMF. The prepared solutions were heated in an oil bath at 60°C and mixed homogeneously at 450 rpm for 1 day and 450 rpm at room temperature.

First, 10%, 12%, 8%, and 6% concentrations were tried for solution blowing. Although fiber formation was observed, the amount of fiber produced was minimal. Therefore, it was decided to proceed with the electro blowing method. Electro blowing was first tried with 6%. A better result was obtained compared to solution blowing. Then, 4%, 6%, 9%, and 10%

concentrations were tested to determine the lower and upper limits.



Figure 2.2.1: Nonwoven fabric and membrane

2.3. Taguchi Design

Identifying ideal circumstances and conducting optimization studies are considered critical for increasing production efficiency, lowering costs, and improving product quality. These studies are used to determine the optimal parameter combinations that ensure the system operates at peak performance (Karna and Sahai, 2012).

Optimization techniques such as Box-Behnken and Taguchi are widely applied. In this study, the Taguchi L9 orthogonal experimental design was used to determine the impact of multiple factors and to identify their optimal values within the system. This method allows for the evaluation of component and level combinations with a minimal number of experimental runs, thereby reducing both time and cost. Each factor was studied at three different levels, and a total of nine experiments were carried out (Unal and Dean, 1990). The L9 experimental layout proposed by Taguchi is shown in Table 2.3.1.

Table 2.3.1: Taguchi L9 experiments.

| Concentration (%) | Pressure (bar) | Feed (mL/h) | Voltage (V) |
|-------------------|----------------|-------------|-------------|
| 6 | 0.5 | 8 | 10 |
| 6 | 1.0 | 10 | 20 |
| 6 | 1.5 | 12 | 30 |
| 8 | 0.5 | 10 | 30 |
| 8 | 1.0 | 12 | 10 |

| | | | |
|----|-----|----|----|
| 8 | 1.5 | 8 | 20 |
| 10 | 0.5 | 12 | 20 |
| 10 | 1.0 | 8 | 30 |
| 10 | 1.5 | 10 | 10 |

2.4. Preparation of F-SiO₂ Nanoparticles

The fluorination process of silica was carried out in accordance with the procedures reported by Yang et al. (2022) and those followed in previous related studies. Initially, 3.00 g of SiO₂ nanoparticles were distributed in a mixed solution of 16.0 mL deionized water and 4.0 mL ammonia water. To achieve homogenous dispersion, the suspension was ultrasonicated for 10 minutes. Separately, 0.6 mL of PFOTES was diluted in 80 mL ethanol. The PFOTES-ethanol solution was mixed with the SiO₂ suspension. The mixture was stirred constantly at 40 °C for 24 hours to enhance surface modification. Following the reaction, the modified nanoparticles were centrifuged at 4500 rpm for 30 minutes. The resulting powders were washed three times with ethanol to eliminate any unreacted elements. After purification, F-SiO₂ nanoparticles were dried at 50°C for 20 hours to produce the hydrophobic product.



Figure 2.4.1: Image of the solution after centrifugation: the upper clear liquid is the supernatant, and the white sediment at the bottom represents the fluorine-modified SiO₂ (F-SiO₂) nanoparticles.

2.5. Nanofiber Production Procedure

In the first step, a polymer solution is prepared by dissolving PAN polymer in DMF (dimethylformamide) solvent. The prepared solution

is stirred at 60 °C for 24 hours to ensure homogeneity. This process allows the solution to reach the optimal viscosity required for membrane fabrication. The mixture is optimized to provide the necessary viscosity and solubility values for the electroblowing process. The prepared polymer solution is then placed into a thin needle or tube called a spinneret with the help of a syringe pump. The system is operated by applying a high voltage, and this high electric field draws the polymer solution into a jet stream. The jet emerging from the solution turns into thin nanofibers under the influence of electrostatic forces. These fibers are collected on a nonwoven fabric wrapped around the collector. A constant electric field was applied separately for each membrane production, and for the 6% PAN/DMF solution, the applied voltage was optimized to 20 kV.

2.6. Characterization

The surface morphology of the membranes was investigated using Scanning Electron Microscopy (SEM). Scanning Electron Microscopy (SEM) analysis is conducted to examine the fiber morphology. Based on the SEM results, an appropriate concentration range is identified for further studies. Subsequently, nine experimental data points are selected from a table designed according to the Taguchi method, as outlined in the project report, for the purpose of optimization. All experiments listed in the optimization table are then carried out accordingly. SEM analysis is again performed on the nanofibers obtained from these experiments to evaluate their structural characteristics.

Flux analysis is conducted to determine the amount of fluid that is passed through a unit area of the membrane over a specific period of time (Sarac et al., 2023). The analysis is carried out under pressure, which is applied to provide the necessary driving force for the fluid to be transmitted through the membrane. Initially, the surface area of the membrane is

calculated, and the pressure applied during the experiment is maintained at a constant level. Subsequently, the volume of the liquid that is transferred through the membrane over a period of one hour is measured. The flux is then calculated using the following formula:

$$F = \frac{1}{A} \frac{dV}{dt} \quad (2.1)$$

Tensile tests are conducted on the samples in order to observe the effect of nanofiber deposition time on stress and strain behavior. Stress (σ) is defined as the ratio of polymer density, applied force (N), and initial sample length (L_0) to the sample mass (m) (Maccaferri et al., 2021), as expressed in Equation 2.3:

$$\sigma_{eq} = \rho \frac{F}{m} L \quad (2.3)$$

The wettability behavior of the samples is examined by measuring the WCA (Water Contact Angle) values under ambient air using a KSV CAM 200 device. The experiments are carried out by dispensing 5 μ L of deionized water onto the sample surface with the help of a micro syringe, followed by measuring the angle formed between the droplet and the surface. The contact angles are calculated as the average of three measurements taken from different positions on the surface. All experiments are conducted at room temperature (Sarac et al., 2023).

III. RESULTS AND DISCUSSIONS

Significant differences in fiber quality were observed in the comparison of solution blowing and electro blowing methods. In the solution blowing method, bead formations were observed on the fibers, negatively affecting the uniformity and mechanical properties of the fibers. These defects are thought to result from insufficient control during the fiber formation process. Consequently, solution blowing was evaluated as less suitable for applications requiring precision and consistency.

In contrast, the electro blowing method produced fibers of superior quality. The use of an electric field allowed better alignment and stretching of polymer jets, enabling the production of smoother and less defective fibers. Furthermore, finer fiber diameters and improved surface quality were achieved.

Nanofibers produced by the solution blowing method did not fully meet the desired properties; therefore, the electro blowing method was preferred in this study. Electro blowing has been observed to allow better morphology control and more homogeneous structures in nanofiber production. Additionally, the low fiber formation and irregularities observed in the solution blowing method were largely resolved with the electro blowing technique. The SEM images obtained from both studies are shown in Figure 3.1.

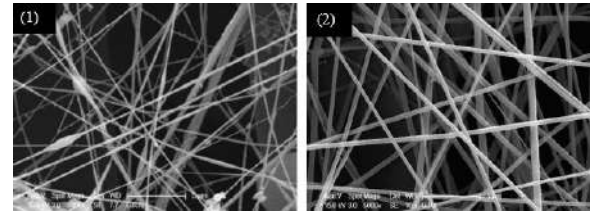


Figure 3.1: The SEM image obtained (1) solution blowing (2) electro blowing

Taguchi optimization was used to find optimal nanofiber production parameters, analyzing SN ratios under "Larger is Better" and "Smaller is Better" criteria. Main effects plots showed the influence of concentration, pressure, feed rate, and electrode distance. Nanofiber diameters were assessed with histograms, and the data for the 9 experiments are in Figure 3.2. The average fiber radius was calculated from the SEM images of the samples from the nine

experiments and was presented in the figure in the form of a table.

| Experiment | Fiber Diameter (nm) | Polymer Concentration (%) | Air Pressure (P, bar) | Feed Rate (F, mL/h) | Applied Voltage (V) |
|------------|---------------------|---------------------------|-----------------------|---------------------|---------------------|
| A | 355 | 8 | 1 | 12 | 10 |
| B | 423 | 8 | 1.5 | 8 | 20 |
| C | 371 | 8 | 0.5 | 10 | 30 |
| D | 463 | 6 | 0.5 | 8 | 10 |
| E | 330 | 6 | 1 | 10 | 20 |
| F | 319 | 6 | 1.5 | 12 | 30 |
| G | 1554 | 10 | 0.5 | 12 | 20 |
| H | 765 | 10 | 1 | 8 | 30 |
| I | 838 | 10 | 1.5 | 10 | 10 |

Figure 3.2: Average diameters of 9 Taguchi experiments.

The SEM images of these L9 Taguchi experiments are shown in Figure 3.3.

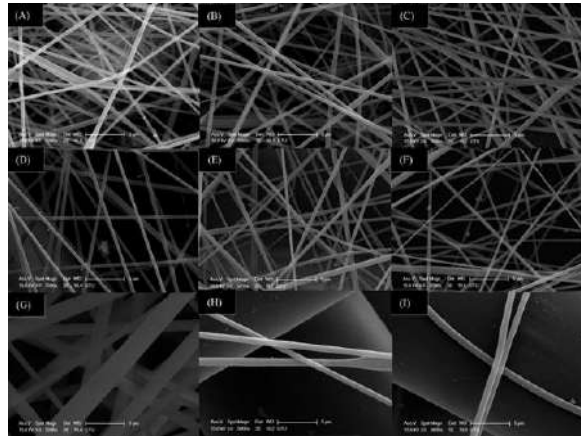


Figure 3.3: SEM images of PAN nanofiber samples produced using electroblowing obtained from experimental studies in the Taguchi L9 design

3.1. Signal-to-Noise Analysis

When optimizing under the "Larger is Better" criterion, the goal shifts to maximizing the response variable, which is often essential in processes that prioritize higher output, efficiency, or yield. The Taguchi analysis and the Main Effects Plot for Means highlight the optimal combination of factor levels: a

concentration of 10%, a pressure of 0.5 bar, a feed rate of 12 units, and an applied voltage is 20 volts.

Among the tested levels, a concentration of 10% produced the highest mean response, indicating that increased concentration significantly enhances system performance. This result suggests that higher concentrations provide more reactants or materials for the process, thereby maximizing the output. The sharp rise in the response variable as concentration increases from 6% to 10% underscores the critical role of this factor in driving system efficiency. However, care must be taken to ensure that higher concentrations do not compromise system stability, as excessive material could introduce unwanted side effects in other scenarios.

Pressure exhibited an optimal level at 0.5 bar, where the mean response was maximized, indicating that lower pressure enhances performance in nanofiber production. At this level, the applied force is sufficient to drive the process effectively without introducing inefficiencies. In contrast, higher pressures (1.0 and 1.5 bar) result in a decline in response, likely due to increased system resistance, material instability, or uneven fiber formation. Thus, 0.5 bar provides an ideal balance between process efficiency and stability, suggesting it as the optimal pressure for achieving improved nanofiber quality.

The feed rate exhibited a non-linear effect on the response variable, with the 12 mL/h achieving the highest mean value. This finding suggests that a higher feed rate optimally supports the production process by providing sufficient material flow for nanofiber formation. Lower feed rates (8 and 10 units) may limit material availability, reducing efficiency and performance. The 12 mL/h represents the ideal condition, ensuring adequate material supply while maintaining process stability for improved nanofiber quality.

The voltage had a significant impact on the response variable, with the highest mean value achieved at 20 V. This result suggests that a moderate electric field provides the optimal energy for enhancing nanofiber production by ensuring stable jet formation and uniform fiber deposition. Lower levels (10 V) may lack sufficient energy to sustain the process efficiently, while higher levels (30 V) could introduce instabilities or irregularities in fiber morphology. Thus, 20 V represents the ideal balance, offering the best performance for achieving high-quality nanofibers.

- Concentration: 10%
- Pressure: 0.5 bar
- Feed rate: 12 mL/h
- Voltage: 20 V

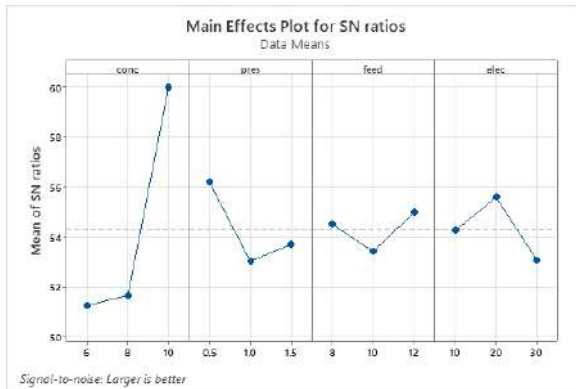


Figure 3.1.1: SN ratios for larger is better

The optimal combination of parameters—10% concentration, 0.5-bar pressure, 12 ml/h feed rate, and 20 kV electric field—represents the most effective settings for maximizing the system's output according to the "Larger is Better" approach. These findings highlight the importance of carefully balancing the factors to optimize performance. The strong response at 10% concentration and 20 V electric field demonstrates the critical role of sufficient material availability and energy input in enhancing nanofiber production, while 0.5 bar pressure ensures stability and efficiency in the process. Additionally, the 12 ml/h feed rate strikes a balance between adequate material

supply and system capacity. This optimization approach proves valuable for applications focused on achieving high efficiency, throughput, and product quality, providing a robust framework for future advancements in nanofiber production.

The optimization analysis conducted under the "Smaller is Better" criterion provides valuable insights into the optimal operating conditions for minimizing the response variable, which is critical in applications where smaller values indicate better system performance, efficiency, or quality. Based on the Taguchi method and the Main Effects Plot for SN Ratios, the most favorable combination of factor levels includes a concentration of 6%, a pressure of 1 bar, a feed rate of 10 units, and an voltage is 30 volts.

The factor "concentration" had a pronounced impact on the SN ratio, as reflected by a sharp decline in the SN ratio at the 10% level. This indicates that higher concentrations introduce variability into the process, likely due to increased system instability or inefficiencies such as aggregation, clogging, or other side effects that negatively affect performance. The lowest concentration (6%) consistently provided the most favorable SN ratio and thinner fibers, suggesting that reduced concentrations lead to a more stable and predictable process. This finding is consistent with the principle that lower concentrations often reduce excess interference and maintain operational consistency, particularly in chemical or material processing applications.

Pressure showed a clear trend in the SN ratio plot, with the 1-bar level yielding the best results. At this pressure, the system achieves a balance that minimizes variability and reduces deviations, as evidenced by the higher SN ratio. Lower pressures (0.5 bar) may lack the force required to maintain consistent performance, while higher pressures (1.5 bar) can introduce excessive mechanical stress, leading to fluctuations and increased noise. The 1-bar pressure demonstrates its effectiveness in stabilizing the process and ensuring reliable performance.

The feed rate demonstrated an inverse relationship with variability, as higher feed rates (10 and 12 units) resulted in more favorable SN ratios. Among these, the feed rate of 10 units achieved the most stable performance. This suggests that an increased feed rate optimizes material distribution or process flow, reducing the likelihood of inconsistencies or interruptions. In systems where uniformity in material flow is crucial, a higher feed rate can enhance efficiency and reliability.

The voltage showed a progressive improvement in SN ratios as the level increased from 10 volts to 30 volts. The highest level (30 volts) exhibited the most favorable response, indicating that increased electrical input contributes to process stability by ensuring sufficient energy availability for the operation. This is particularly important in systems reliant on electrical input for driving reactions, processes, or system components.

- Concentration: 6%
- Pressure: 1 bar
- Feed rate: 10 mL/h
- Voltage: 30 V

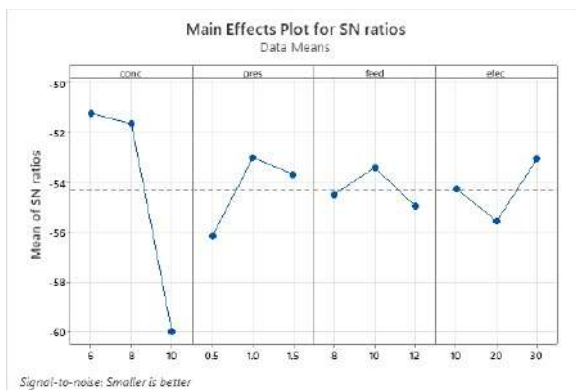


Figure 3.1.2: SN ratios for smaller is better

The combined optimal levels 6% concentration, 1-bar pressure, 10-mL/h feed rate, and 30-volt voltage—demonstrate that the system achieves its lowest variability and best performance under these conditions. These results are consistent with the

Taguchi philosophy, which focuses on robust design and minimizing the impact of noise factors. The findings also illustrate how each factor contributes to the overall stability of the system, offering a guide for process optimization. By implementing these parameter settings, industries can enhance reliability, reduce waste, and improve product consistency, particularly in scenarios where minimizing variability is crucial to success.

3.2. Histogram Analysis of Nanofiber Diameters

The diameter results from each experiment were analyzed, and histograms were generated to evaluate distribution and consistency as shown in Figure 3.2.1.

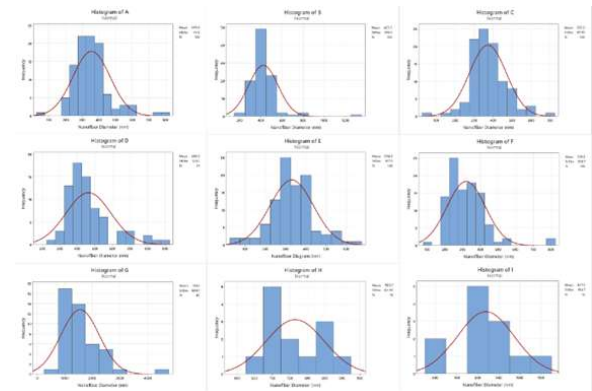


Figure 3.2.1: Histograms of Taguchi L9 Experiments.

The fiber diameters obtained for each experiment are as follows: In experiment A, the fiber diameter was 355.58 nm; in experiment B, it was 423 nm; in experiment C, 371.96 nm; in experiment D, 463 nm; in experiment E, 330.16 nm; in experiment F, 319.77 nm; in experiment G, 1554 nm; in experiment H, 765.7293 nm; and in experiment I, 838 nm. These values reflect the effects of varying polymer concentrations, air pressures, feed rates, and electric fields used in each experiment.

In the study conducted by Chao et al., it was reported that the average diameter of PAN nanofibers increased from 462 nm to 848 nm when the concentration of the PAN/DMF solution was raised from 8% to 16% (Song et al., 2024). This result was shown to be caused by the

increase in solution viscosity, leading to the formation of thicker fibers. Additionally, in our study, it was observed that as the PAN concentration increased, the nanofiber diameter rose from 319.77 nm to 1554 nm. However, in our study, where an electric current was applied to an 8% solution, nanofiber diameters were measured as 355.58 nm, 423 nm, and 377.1 nm at 10 V, 20 V, and 30 V, respectively. It was observed that thinner nanofibers were formed due to the effect of the electric field.

3.3. Effect of Fluorinated Silica (F-SiO₂) Incorporation into PAN Membrane

Fluorine-modified SiO₂ (F-SiO₂) nanoparticles synthesized via the described method were successfully incorporated into the PAN (polyacrylonitrile) solution to enhance surface hydrophobicity. The addition of F-SiO₂ into the PAN matrix was achieved through direct mixing under continuous stirring, leading to a homogeneous dispersion of the nanoparticles within the polymer solution.

After electro blowing, the resulting PAN/F-SiO₂ nanofibers exhibited notable changes in surface properties. Compared to pure PAN fibers, the modified fibers demonstrated increased water repellency, attributed to the presence of fluorinated functional groups on the SiO₂ surface. This modification resulted in a rougher surface morphology combined with low surface energy, contributing to the hydrophobic character.



Figure 3.3.1: A blue water droplet remains on the PAN/F-SiO₂ membrane, showing enhanced hydrophobicity.

Furthermore, the hydrophobicity of the PAN/F-SiO₂ nanofiber membrane produced via solution blowing

was visually confirmed through a simple water droplet test. While unmodified PAN membranes readily absorbed water upon contact, the modified membrane exhibited a starkly different behavior. When a droplet of water dyed with methylene blue was placed on the surface of the membrane, it retained a near-spherical shape and remained on the surface without spreading or being absorbed. This clearly indicates a significant increase in surface hydrophobicity due to the presence of fluorinated silica nanoparticles, which reduce surface energy and create a water-repellent structure.

Overall, the incorporation of F-SiO₂ into the PAN solution offers a promising approach for fabricating hydrophobic nanofiber surfaces suitable for applications such as water-repellent coatings, filtration, and protective textiles.

3.3.1. Self-Cleaning Behavior of Janus Membrane

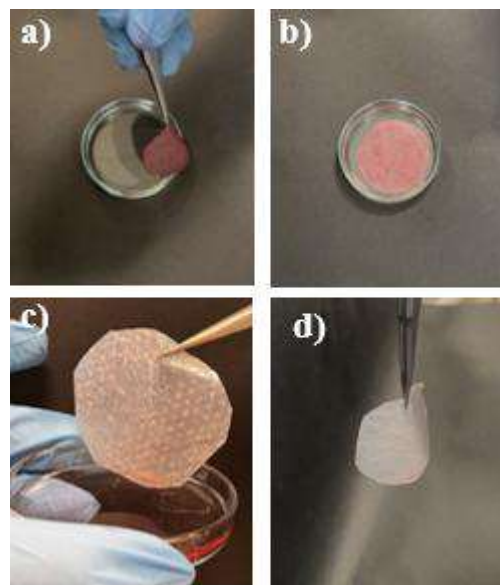


Figure 3.3.1.1: A series of photos of adsorbed lubricating oil from the water surface and PVDF-SiO₂ nanofibers membrane recovery from ethanol

The nanofiber membrane is submerged in the oil layer, where it quickly adsorbs the lubricating oil, enabling the separation of oil and water. Due to the surface's hydrophobic and lipophilic characteristics, the membrane exhibits excellent selective adsorption. As depicted in Figure 3.3.1.1 [a-d], after being washed

with ethanol, the membrane, initially stained red, turned white, and the oil detached from the membrane.

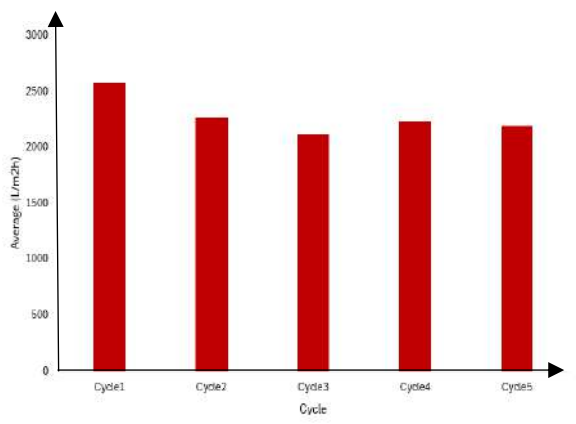


Figure 3.3.1.2: The average flux values of the membranes over five uses

In this experiment conducted with CCl_4 , the membrane was cleaned and reused five times. Three different membranes were used for each cycle. The average flux values are presented in Figure 3.3.1.2. Although a slight decline in permeability was observed in the subsequent cycles, this can be attributed to potential surface contamination or partial pore blockage during repeated use. Nevertheless, the decrease remained minimal, and the membrane largely retained its high performance. These results indicate that the membrane's surface morphology and pore structure possess a strong self-cleaning capability, enabling the membrane to maintain its functionality even after prolonged operation. The findings demonstrate that the PVDF- SiO_2 nanofiber membrane offers excellent durability and reliability, making it highly suitable for practical applications such as oil–water separation.

3.3.2. Mechanical Performance Evaluation

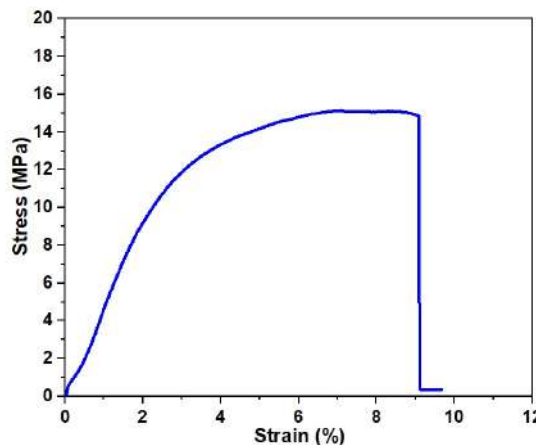


Figure 3.3.2.1: The tensile stress-strain curve of membrane

The tensile test of the PAN membrane containing fluorinated silica (F-SiO_2) shows a maximum stress of approximately 15 MPa, occurring at around 9% strain. The stress increases steadily in the elastic region and reaches a plateau, indicating good resistance to deformation. The sudden drop after the peak suggests brittle fractured behavior. These results indicate that the incorporation of F-SiO_2 improves the tensile strength of the membrane while maintaining moderate flexibility, though the abrupt failure implies limited ductility.

3.3.3. Water Contact Angle Measurement

Water contact angle (WCA) measurements were performed to evaluate the surface wettability of PAN membranes before and after modification with fluorinated silica (F-SiO_2) nanoparticles. The mean contact angle of the unmodified PAN membrane was 76.04° , indicating a relatively hydrophilic surface, which aligns with the inherent polar nature of PAN. After incorporation of F-SiO_2 , the mean contact angle significantly increased to 131.69° , clearly demonstrating a transition to a highly hydrophobic surface. This transformation is attributed to the low surface energy and water-repellent characteristics of the fluorinated silica particles, which introduce $-\text{CF}$ functional groups to the membrane surface and

enhance surface roughness at the micro/nanoscale level.

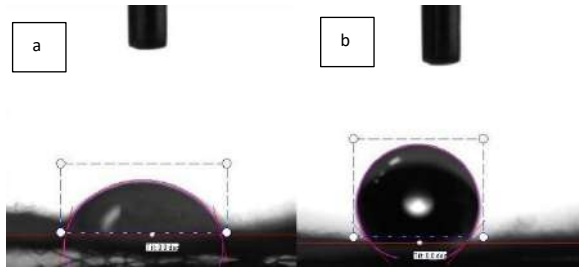


Figure 3.3.3.1: Water contact angle (WCA) measurements a- unmodified membrane b- incorporation of F-SiO₂


In summary, the F-SiO₂ incorporation greatly enhances the hydrophobicity of PAN membranes, with the contact angle rising from 76.04° to 131.69°. This improvement not only demonstrates the effectiveness of the modification but also broadens the practical applications of the membrane in advanced separation technologies.


3.3.4. Flux Analysis

In order to evaluate the functional properties of the membrane, separate flux tests were performed for both surfaces. Firstly, oil flux tests were performed using carbon tetrachloride (CCl₄) and diesel with the hydrophobic surface containing fluorinated silica on top.

In the second stage, the water flux value was determined as a result of the test with only water with 10% PAN additive hydrophilic surface on top. All flux data obtained as a result of the experiments are presented in Table 3.3.4.1.

Table 3.3.4.1: Flux Analysis Values.

| | CCl ₄ ($\frac{L}{m^2h}$) | Diesel ($\frac{L}{m^2h}$) | Water ($\frac{L}{m^2h}$) |
|-------------------------------------------------------------------------------------|------------------------------------------|--------------------------------|-------------------------------------|
|  | 2573,4 | 330,91 | Flow not observed during flux test. |

| | | | |
|------------------------------------------------------------------------------------|--------------------------|--------------------------|---------|
|  | Flux test not performed. | Flux test not performed. | 120,620 |
|------------------------------------------------------------------------------------|--------------------------|--------------------------|---------|

IV. CONCLUSIONS

This study successfully demonstrated the development and optimization of Polyacrylonitrile (PAN)-based Janus nanofiber membranes designed for effective oil-water separation. Through the utilization of solution-blowing and electro-blowing techniques, the structural and functional properties of the membranes were fine-tuned to achieve high performance in industrial wastewater treatment.

The findings indicate that the choice of polymer concentration, air pressure, feed rate, and applied electric field significantly influences nanofiber morphology and separation efficiency. Optimal parameters determined through Taguchi design included a PAN concentration of 10%, an air pressure of 0.5 bar, a feed rate of 12 mL/h, and an electric field of 20 V for Larger is better method and concentration of 6%, an air pressure of 1 bar, a feed rate of 10 mL/h, and an electric field of 30 V for Smaller is better method. Under these conditions, nanofibers exhibited superior uniformity and mechanical stability, as evidenced by consistent fiber diameters and SEM analysis.

The incorporation of fluorine-modified SiO₂ (F-SiO₂) nanoparticles into the PAN solution successfully enhanced the hydrophobicity of the resulting nanofiber membranes. The modified PAN/F-SiO₂ fibers exhibited increased water repellency, attributed to the fluorinated groups on the SiO₂ surface, which created a rougher surface morphology and reduced surface energy.

In conclusion, this research contributes to the advancement of membrane technology, providing a scalable approach for producing Janus nanofiber membranes with superior separation performance. Future studies may focus on further optimizing the material composition, incorporating novel functional additives, and evaluating long-term operational stability under diverse environmental conditions. Such efforts will pave the way for broader adoption of these innovative materials in sustainable wastewater management.

ACKNOWLEDGMENT

We would like to thank Assoc. Prof. Çiğdem TAŞDELEN-YÜCEDAĞ, our adviser, for all of her help and support during the writing of this thesis. The project would never have been feasible without their extensive expertise and encouragement.

We also appreciate Res. Asst. Züleyha SARAÇ for her important contributions to the advancement of our work. Her support and curiosity throughout difficult times made the experience much more productive and rewarding.

This study was carried out within the scope of the TÜBİTAK 2209-A program and was accepted for support. By addressing a critical environmental issue, it aims to make innovative contributions to materials science and chemical engineering, marking a significant step forward under the support of TÜBİTAK 2209-A

Finally, we extend our gratitude to everyone involved in this thesis project for their efforts and dedication.

REFERENCES

Abuhasel, K., Kchaou, M., Alquraish, M., Munusamy, Y., & Jeng, Y. T. (2021). Oily wastewater treatment:

Overview of conventional and modern methods, challenges, and future opportunities. *Water*, 13(7), 980.

Afsari, M., Shon, H. K., & Tijing, L. D. (2021). Janus membranes for membrane distillation: Recent advances and challenges. *Advances in Colloid and Interface Science*, 289, 102362.

Chen, W.; Su, Y.; Zheng, L.; Wang, L.; Jiang, Z. The improved oil/water separation performance of cellulose acetate-graftpolyacrylonitrile membranes. *J. Membr. Sci.* 2009, 337, 98–105. [CrossRef]

Chen, Z., Li, J., Zhou, J., & Chen, X. (2023). Photothermal Janus PPy-SiO₂@ PAN/F-SiO₂@ PVDF-HFP membrane for high-efficient, low energy and stable desalination through solar membrane distillation. *Chemical Engineering Journal*, 451, 138473.

Dmitrieva, E. S., Anokhina, T. S., Novitsky, E. G., Volkov, V. V., Borisov, I. L., & Volkov, A. V. (2022). Polymeric membranes for oil-water separation: a review. *Polymers*, 14(5), 980.

Drew, C.; Liu, X.; Ziegler, D.; Wang, X.; Bruno, F. F.; Whitten, J.; Samuelson, L. A. & Kumar, J. - “Metal Oxide Coated Polymer Nanofibers”; *NanoLetters*, 3, 2, p.143-147 (2003).

Dryakhlov, V. O., Nikitina, M. Y., Shaikhiev, I. G., Galikhanov, M. F., Shaikhiev, T. I., & Bonev, B. S. (2015). Effect of parameters of the corona discharge treatment of the surface of polyacrylonitrile membranes on the separation efficiency of oil-in-water emulsions. *Surface Engineering and Applied Electrochemistry*, 51, 406-411.

Elhenawy, S., Khraisheh, M., AlMomani, F., Hassan, M. K., Al-Ghouti, M. A., & Selvaraj, R. (2022). Recent developments and advancements in Graphene-Based technologies for oil spill cleanup and Oil–Water separation processes. In *Nanomaterials* (Vol. 12, p. 87).

- Fane, A. G., Wang, R., & Hu, M. X. 2015. Synthetic membranes for water purification: status and future. *Angewandte Chemie International Edition*, 54(11), 3368-3386.
- Galdino Jr, C. J. S., Maia, A. D., Meira, H. M., Souza, T. C., Amorim, J. D., Almeida, F. C., ... & Sarubbo, L. A. (2020). Use of a bacterial cellulose filter for the removal of oil from wastewater. *Process Biochemistry*, 91, 288-296.
- Galdino Jr, C. J. S., Maia, A. D., Meira, H. M., Souza, T. C., Amorim, J. D., Almeida,
- Gomes, D. S., da Silva, A. N., Morimoto, N. I., Mendes, L. T., Furlan, R., & Ramos, I. (2007). Characterization of an electrospinning process using different PAN/DMF concentrations. *Polímeros*, 17, 206-211.
- Hussain, A., & Al-Yaari, M. (2021). Development of polymeric membranes for oil/water separation. *Membranes*, 11(1), 42.
- Iacono, S. T., Jennings, A. R., & Department of Chemistry and Chemistry Research Center, United States Air Force Academy. (2019). Recent Studies on Fluorinated Silica Nanometer-Sized Particles. In *Nanomaterials* [Journal-article].
- Jiang, Y., Hou, J., Xu, J., & Shan, B. (2017). Switchable oil/water separation with efficient and robust Janus nanofiber membranes. *Carbon*, 115, 477-485.
- Karna, S. K., & Sahai, R. (2012). An overview on Taguchi method. *International journal of engineering and mathematical sciences*, 1(1), 1-7.
- Liu, W., Cui, M., Shen, Y., Zhu, G., Luo, L., Li, M., & Li, J. 2019. Waste cigarette filter as nanofibrous membranes for on-demand immiscible oil/water mixtures and emulsions separation. *Journal of colloid and interface science*, 549, 114-122.
- Meng, L., Shi, W., Li, Y., Li, X., Tong, X., & Wang, Z. (2023). Janus membranes at the water-energy nexus: a critical review. *Advances in Colloid and Interface Science*, 318, 102937.
- Naseeb, N.; Mohammed, A.A.; Laoui, T.; Khan, Z. A novel PAN-GO-SiO₂ hybrid membrane for separating oil and water from emulsified mixture. *Materials* 2019, 12, 212. [CrossRef]
- Njoku, K. L. (2017). Responses of Accessions of Zea Mays to Crude Oil Pollution Using Growth Indices and Enzyme Activities as Markers. *Pollution*, 4(1), 183-193.
- Padaki, M., Murali, R. S., Abdullah, M. S., Misdan, N., Moslehyani, A., Kassim, M. A., ... & Ismail, A. F. (2015). Membrane technology enhancement in oil–water separation. A review. *Desalination*, 357, 197-207.
- Peng, Y.; Guo, F.; Wen, Q.; Yang, F.; Guo, Z. A novel polyacrylonitrile membrane with a high flux for emulsified oil/water separation. *Sep. Purif. Technol.* 2017, 184, 72–78. [CrossRef]
- Qian, S., Zhao, B., Mao, J., Liu, Z., Zhao, Q., Lu, B., ... & Sun, X. (2023). Biomedical applications of Janus membrane. *Biomedical Technology*, 2, 58-69.
- Rocha e Silva, F. C. P., Rocha e Silva, N. M. P., Luna, J. M., Rufino, R. D., Santos, V. A., & Sarubbo, L. A. (2018). Dissolved air flotation combined to biosurfactants: a clean and efficient alternative to treat industrial oily water. *Reviews in Environmental Science and Bio/Technology*, 17, 591-602.
- Sarac, Z., Kilic, A., & Tasdelen-Yucedag, C. (2023). Optimization of electro-blown polysulfone nanofiber mats for air filtration applications. *Polymer Engineering & Science*, 63(3), 723-737.
- Shakiba, M., Nabavi, S. R., Emadi, H., & Faraji, M. (2021). Development of a superhydrophilic nanofiber membrane for oil/water emulsion separation via

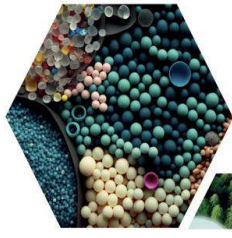
- modification of polyacrylonitrile/polyaniline composite. *Polymers for Advanced Technologies*, 32(3), 1301-1316.
- Shami, Z.; Amininasab, S.M.; Katoorani, S.A.; Gharloghi, A.; Delbina, S. NaOH-Induced Fabrication of a Superhydrophilic and
- Song, C., Liu, J., Cao, Y., Li, W., & He, C. (2024). Efficient Solution Blow Spinning of PAN-CNTs Nanofiber-Based Pressure Sensors with Sandwich Structures. *Langmuir*, 40(39), 20515-20525.
- Söz, C. K., Trosien, S., & Biesalski, M. (2020). Janus interface materials: a critical review and comparative study. *ACS Materials Letters*, 2(4), 336-357.
- Sun Y., Zong, Y., Yang, N., Zhang, N., Jiang, B., Zhang, L., & Xiao, X. 2020. Surface hydrophilic modification of PVDF membranes based on tannin and zwitterionic substance towards effective oil-in-water emulsion separation. *Separation and Purification Technology*, 234, 116015.
- Thomas, S. (2008). Enhanced oil recovery-an overview. *Oil & Gas Science and Technology-Revue de l'IFP*, 63(1), 9-19.
- Ulbricht, M. (2006). Advanced functional polymer membranes. *Polymer*, 47(7), 2217-2262.
- Unal, R., & Dean, E. B. (1990, January). Taguchi approach to design optimization for quality and cost: an overview. In *1991 Annual conference of the international society of parametric analysts*.
- Underwater Superoleophobic Styrene-Acrylate Copolymer Filtration Membrane for Effective Separation of Emulsified Light Oil-Polluted Water Mixtures. *Langmuir* 2021, 37, 12304–12312.
- Vatanpour, V., Pasaoglu, M. E., Kose-Mutlu, B., & Koyuncu, I. (2023). Polyacrylonitrile in the preparation of separation membranes: A review. *Industrial & Engineering Chemistry Research*, 62(17), 6537-6558.
- Wang, M. L., Yu, D. G., & Bligh, S. W. A. (2023). Progress in preparing electrospun Janus fibers and their applications. *Applied Materials Today*, 31, 101766.
- Wu, M., Mu, P., Li, B., Wang, Q., Yang, Y., & Li, J. 2020. Pine powders-coated PVDF multifunctional membrane for highly efficient switchable oil/water emulsions separation and dyes adsorption. *Separation and Purification Technology*, 248, 117028.
- Wu, M., Xiang, B., Mu, P., & Li, J. (2022). Janus nanofibrous membrane with special micro-nanostructure for highly efficient separation of oil-water emulsion. *Separation and Purification Technology*, 297, 121532.
- Xiao, Y., Xiao, F., Ji, W., Xia, L., Li, L., Chen, M., & Wang, H. (2023). Bioinspired Janus membrane of polyacrylonitrile/poly (vinylidene fluoride)@ poly (vinylidene fluoride)-methyltriethoxysilane for oil-water separation. *Journal of Membrane Science*, 687, 122090.
- Yan, X., Wang, Y., Huang, Z., Gao, Z., Mao, X., Kipper, M. J., Huang, L., & Tang, J. (2023). Janus Polyacrylonitrile/Carbon Nanotube Nanofiber Membranes for Oil/Water Separation. *ACS Applied Nano Materials*, 6(6), 4511–4521.
- Yang, J., Li, H. N., Chen, Z. X., He, A., Zhong, Q. Z., & Xu, Z. K. (2019). Janus membranes with controllable asymmetric configurations for highly efficient separation of oil-in-water emulsions. *Journal of Materials Chemistry A*, 7(13), 7907-7917.
- Yang, Y., Guo, Z., Li, Y., Qing, Y., Dansawad, P., Wu, H., ... & Li, W. (2022). Electrospun rough PVDF nanofibrous membranes via introducing fluorinated SiO₂ for efficient oil-water emulsions coalescence separation. *Colloids and Surfaces A: Physicochemical and Engineering Aspects*, 650, 129646.

Yu, L., Han, M., & He, F. 2017. A review of treating oily wastewater. *Arabian Journal of Chemistry*, 10, S1913-S1922.

Yue, X., Li, Z., Zhang, T., Yang, D., & Qiu, F. 2019. Design and fabrication of superwetting fiber-based membranes for oil/water separation applications. *Chemical Engineering Journal*, 364, 292-309.

Zhuang, X., Yang, X., Shi, L., Cheng, B., Guan, K., & Kang, W. (2012). Solution blowing of submicron-scale cellulose fibers. *Carbohydrate Polymers*, 90(2), 982–987.

Zouboulis, A. I., & Avranas, A. (2000). Treatment of oil-in-water emulsions by coagulation and dissolved-air flotation. *Colloids and surfaces A: Physicochemical and engineering aspects*, 172(1-3), 153-161.



16 ULUSLARARASI
LİF VE POLİMER
ARAŞTIRMALARI
SEMPOZYUMU

16th INTERNATIONAL FIBER AND POLYMER RESEARCH SYMPOSIUM

Sürdürülebilir ve İşlevsel Lif ve Polimerler
Sustainable and Functional Fibers & Polymers



9-10 Mayıs
May 2025

İstanbul Teknik Üniversitesi
Gümüşsuyu Prof. Dr. Necmettin Erbakan Yerleşkesi
İstanbul Technical University
Gumussuyu Prof. Dr. Necmettin Erbakan Campus

Optimization of nanofiber production from biodegradable PBS via electro-blowing method using Box-Behnken design

Ali Toptaş^a

^aTEMAG Laboratories, Textile Technologies and Design Faculty, Istanbul Technical University, 34437 Istanbul, Turkey

*Corresponding author: ali.toptas@itu.edu.tr

ABSTRACT

In this study, nanofibrous surfaces were fabricated from biodegradable poly(butylene succinate) (PBS) using the electro-blowing technique, and the production parameters were optimized using the Box-Behnken experimental design. The effects of polymer concentration (8%, 10%, 12%), air pressure (1, 2, 3 bar), and electrical field (0, 15, 30 kV) on the average fiber diameter were systematically investigated. Fifteen experimental runs were conducted, and fiber diameters were measured using SEM images analyzed in ImageJ, where 100 measurements were taken per sample. The analysis of variance (ANOVA) revealed that polymer concentration had the most significant effect, followed by the electric field and air pressure. The regression model exhibited a high predictive capability with an R^2 value of 92.73%. The optimal conditions determined for minimum fiber diameter were 8.4% PBS concentration, 3 bar air pressure, and 30 kV electric field, which yielded a predicted fiber diameter of 159.9 nm. Experimental validation under these conditions resulted in a fiber diameter of 161 nm, confirming the model's reliability. This study demonstrates the potential of the electro-blowing technique in producing biodegradable nanofibrous webs and provides a systematic approach for parameter optimization through response surface methodology.

Keywords: PBS nanofiber; Electro-blowing; Box-Behnken design; Biodegradable polymer

I. INTRODUCTION

Nanofiber-based materials have attracted significant interest over the past two decades due to their exceptional properties such as high surface area-to-volume ratio, tunable porosity, and flexibility in functionality [1]. These properties make nanofibrous structures highly suitable for a wide range of applications including air filtration, food packaging, wound dressing, drug delivery, and tissue engineering [2]. Particularly in the field of air filtration, the use of nanofibers allows for the efficient capture of

submicron particles while maintaining breathability and lightweight performance [3].

Amid rising concerns over plastic pollution and microplastics, demand for biodegradable alternatives to persistent petroleum-based polymers like polypropylene (PP) and polyethylene (PE) has increased [4]. As a result, the transition to a bio-based and circular economy has become a pressing priority in materials science.

Biodegradable aliphatic polyesters like PLA, PBAT, and PBS have emerged as viable alternatives to

petroleum-based polymers. PBS stands out for its thermal stability, mechanical strength, and biodegradability, and can be synthesized from renewable resources via microbial fermentation of succinic acid and 1,4-butanediol [5].

Recent studies have demonstrated the applicability of PBS nanofibers in biomedical applications, including wound dressings, scaffolds for tissue regeneration, and drug delivery systems [6]. Moreover, PBS has been successfully employed in developing high-efficiency filter media for air filtration purposes, showing filtration efficiencies exceeding 95% with adequate mechanical integrity and processability [7].

While electrospinning is common for nanofiber production, its low productivity and solvent issues have led to alternatives like solution blow spinning (SBS) and electro-blowing, which offer scalable, safer, and simpler setups. [8]. However, electro-blowing still needs optimization for consistent fiber quality and performance.

In this study, PBS nanofibers were produced via the electro-blowing method, and statistical optimization was carried out using the Box-Behnken design. The main objective was to determine the optimal production parameters that minimize fiber diameter, thereby enhancing the applicability of PBS-based nanofibers in advanced filtration and biomedical products. This work contributes to the development of environmentally friendly, scalable, and performance-oriented biodegradable nanofiber materials.

II. EXPERIMENTAL METHOD / TEORETICAL METHOD

2.1 Materials and Preparation Techniques

In this study, PBS (FZ71PB®) granules, a bio-based and biodegradable polymer, were obtained from PTT MCC Biochem (Thailand). According to the manufacturer's datasheet, PBS has a melting temperature of 115 °C, density of 1.26 g/cm³, and a

melt flow index of 22 g/10 min (190 °C, 2.16 kg). The solvents used for solution preparation were chloroform and ethanol (analytical grade, Merck), mixed in a volume ratio of 3:1 without further purification.

Polymer solutions were prepared at three concentration levels (8 wt.%, 10 wt.%, and 12 wt.%) by dissolving PBS in the solvent mixture under magnetic stirring at 500 rpm for 10 hours at room temperature. All solutions were prepared and handled under ambient conditions (25 ± 2 °C, 45 ± 5% RH).

Nanofibrous mats were produced using a laboratory-scale electro-blowing setup. Polymer solution was fed through a syringe pump and ejected with compressed air (1–3 bar) under a high-voltage field (0–30 kV). A 25 cm nozzle-to-collector distance and a rotating drum ensured uniform fiber deposition. Samples were dried at 50 °C for 6 hours in a vacuum oven to remove residual solvents.

2.2 Characterization of Materials

The morphology and diameter of PBS nanofibers were characterized by SEM (Tescan Vega 3, Czech Republic) after gold/palladium sputter-coating. Fiber diameters were measured using ImageJ software based on 100 measurements from 10 randomly selected fields per sample to ensure statistical validity. A Box-Behnken design with three factors (concentration, air pressure, electric field) at three levels was employed. Statistical analyses, including ANOVA and regression modeling, were performed using Minitab, with the average fiber diameter (nm) as the response variable targeted for minimization.

III. RESULTS AND DISCUSSIONS

3.1 Experimental Fiber Diameter Results and General Statistics

Table 1 summarizes the production parameters and measured fiber diameters for 16 PBS nanofiber samples produced by electro-blowing. For each sample, the applied concentration, air pressure, and

electric field values, along with model-predicted diameters, residuals, and standardized residuals (SRES), are provided. Additionally, Figure 1 illustrates the produced samples and their corresponding fiber diameter distribution.

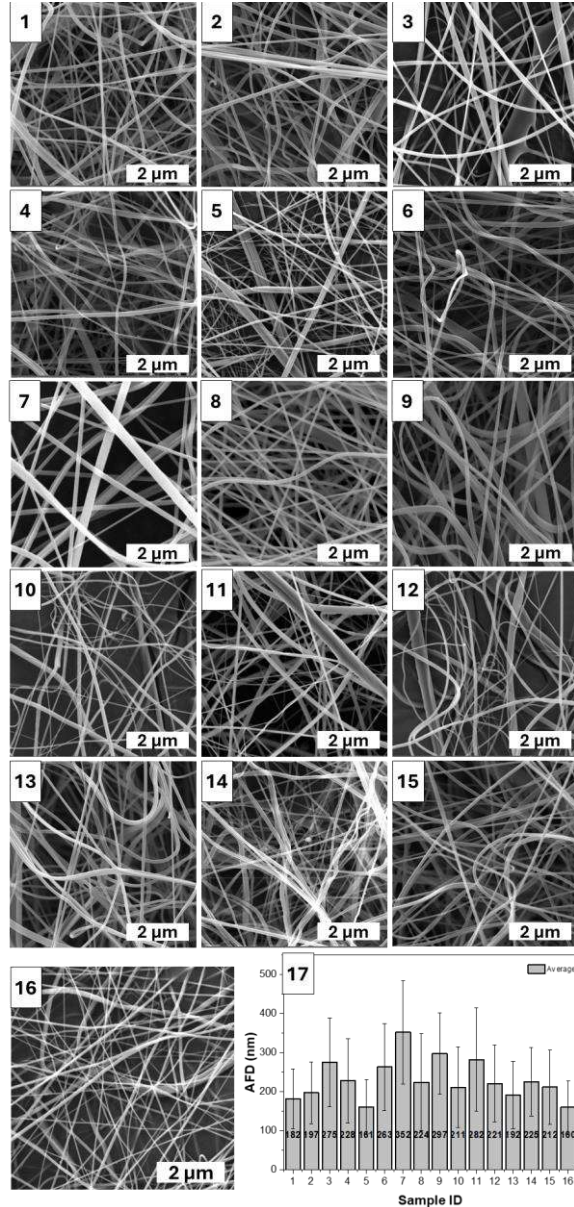


Figure 1: SEM images of the samples and AFD daigram

The obtained results show that fiber diameters ranged from 161 nm to 352 nm, with an average diameter of approximately 234.7 nm. The broad diameter range highlights the strong influence of production parameters on fiber morphology. The differences between measured and model-predicted values were mostly within ± 15 nm, with the maximum and

minimum absolute deviations recorded as 13.88 nm and 1.88 nm, respectively.

Table 1: Box-Behnken Design of the samples

| No | C (%) | AP (bar) | EV. (kV) | AFD | FITS1 | RES11 | SRES1 |
|----|-------|----------|----------|-----|--------|--------|-------|
| 1 | 10 | 3 | 30 | 182 | 179.87 | 2.12 | 0.31 |
| 2 | 10 | 1 | 30 | 197 | 187.12 | 9.87 | 1.46 |
| 3 | 12 | 2 | 30 | 275 | 273.12 | 1.87 | 0.27 |
| 4 | 8 | 2 | 0 | 228 | 229.87 | -1.87 | -0.27 |
| 5 | 8 | 2 | 30 | 161 | 174.87 | -13.87 | -2.05 |
| 6 | 10 | 1 | 0 | 263 | 265.12 | -2.12 | -0.31 |
| 7 | 12 | 2 | 0 | 352 | 338.12 | 13.87 | 2.05 |
| 8 | 10 | 2 | 15 | 224 | 223.33 | 0.66 | 0.06 |
| 9 | 12 | 1 | 15 | 297 | 308.75 | -11.75 | -1.73 |
| 10 | 8 | 1 | 15 | 211 | 207 | 4 | 0.59 |
| 11 | 12 | 3 | 15 | 281 | 285 | -4 | -0.59 |
| 12 | 10 | 2 | 15 | 221 | 223.33 | -2.33 | -0.21 |
| 13 | 8 | 3 | 15 | 192 | 180.25 | 11.75 | 1.73 |
| 14 | 10 | 2 | 15 | 225 | 223.33 | 1.66 | 0.15 |
| 15 | 10 | 3 | 0 | 212 | 221.87 | -9.87 | -1.46 |

These results demonstrate the strong predictive capability of the model. Except for two conditions, all experiments fell within the ± 2 SRES range, confirming both the model's overall accuracy and its reliability within the confidence interval.

3.2 Variance Analysis According to Box-Behnken Model

The ANOVA results from the Box-Behnken design are presented in detail in Table 2. The model was found to be statistically significant ($F = 20.85$, $p = 0.002$), indicating that the selected variables meaningfully explain the variation in fiber diameter.

Parameter-wise analysis revealed that PBS concentration had the most significant effect on fiber diameter ($p = 0.000$), likely due to its influence on solution viscosity and jet stability. Electric field also showed a strong impact ($p = 0.002$), with higher voltages promoting fiber thinning. Air pressure had a marginally significant effect ($p = 0.046$), influencing fiber stability under certain conditions. Among the quadratic terms, only the square of concentration was

significant ($p = 0.007$), indicating a nonlinear relationship between concentration and fiber diameter.

Table 2: ANOVA results of the Box-Behnken Model

| Source | D F | Adj SS | Adj MS | F- Value | P- Value |
|------------------------------|--------|---------|---------|-------------|-------------|
| Model | 9 | 34268 | 3807.6 | 20.85 | 0.002 |
| Linear | 3 | 29796.2 | 9932.1 | 54.4 | 0 |
| Concentration (%) (C) | 1 | 21321.1 | 21321.1 | 116.7 | 0 |
| Air Pressure (bar) (AP) | 1 | 1275.1 | 1275.1 | 6.98 | 0.046 |
| Electrical Voltage (kV) (EV) | 1 | 7200 | 7200 | 39.43 | 0.002 |
| Square | 3 | 4120.5 | 1373.5 | 7.52 | 0.027 |
| C*C | 1 | 3596.2 | 3596.2 | 19.7 | 0.007 |
| AP*AP | 1 | 318.8 | 318.8 | 1.75 | 0.244 |
| EV*EV | 1 | 1.1 | 1.1 | 0.01 | 0.942 |
| 2-Way Interaction | 3 | 351.2 | 117.1 | 0.64 | 0.621 |
| C*AP | 1 | 2.3 | 2.3 | 0.01 | 0.916 |
| C*EV | 1 | 25 | 25 | 0.14 | 0.727 |
| AP*EV | 1 | 324 | 324 | 1.77 | 0.24 |
| Error | 5 | 912.9 | 182.6 | | |
| Lack-of-Fit | 3 | 904.3 | 301.4 | 69.56 | 0.014 |
| Pure Error | 2 | 8.7 | 4.3 | | |
| Total | 14 | 35180.9 | | | |

3.3 Regression Model and Optimization Analysis

The second-order regression model derived from the experimental data is given below:

$$\text{Fiber Diameter (nm)} = 776 - 129.7 \cdot C + 11.8 \cdot P - 2.29 \cdot V + 7.80 \cdot C^2 - 9.29 \cdot P^2 - 0.0024 \cdot V^2 + 0.38 \cdot C \cdot P - 0.083 \cdot C \cdot V + 0.600 \cdot P \cdot V$$
where C = concentration (%), P = air pressure (bar), and V = electric field (kV). The model demonstrates a high level of accuracy in representing the experimental data. Optimization suggested the following conditions for minimum fiber diameter: 8.4% concentration, 3 bar pressure, and 30 kV electric field. The predicted diameter was 159.9 nm, while the experimental value was 161 nm, resulting in a difference of only 1.1 nm (<1%), demonstrating excellent model accuracy.

3.4. Individual Effects of Parameters

The main effects plot (Figure 2) illustrates the individual influence of each factor on fiber diameter. Increasing concentration led to higher viscosity and thicker fibers, with the lowest diameters observed around 8%. Higher voltage enhanced jet stretching,

resulting in finer fibers, particularly at 30 kV. Air pressure between 2–3 bar yielded favorable outcomes, while 1 bar caused insufficient jetting and 3 bar led to fiber instability.

3.5 Binary Interactions and Contour Analysis

The combined effects of parameters on fiber diameter were evaluated using contour plots. The concentration–voltage interaction was particularly notable, with the finest fibers obtained at low concentration and high voltage. However, ANOVA results indicated that these interactions were not statistically significant, suggesting that individual parameters had a stronger influence on fiber diameter than their interactions.

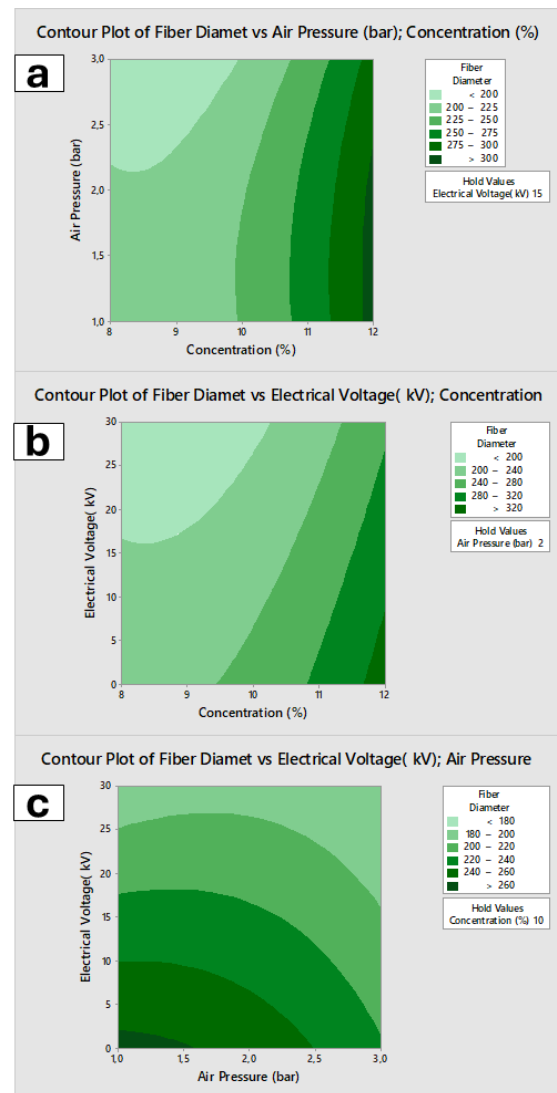


Figure 2: Main effects plot of the parameters.

3.6 Model Quality and Validity

The overall validity of the model is supported by high determination coefficients: $R^2 = 97.41\%$, adjusted $R^2 = 92.73\%$, and predicted $R^2 = 58.82\%$. While the model explains most of the dataset, the lower predicted R^2 suggests limited extrapolative capability at boundary conditions. Diagnostic plots—including the normal probability plot, Pareto chart, and actual vs. predicted plot—indicate statistical balance. Notably, standardized residuals exceeded the ± 2 range in only two cases, highlighting strong model performance.

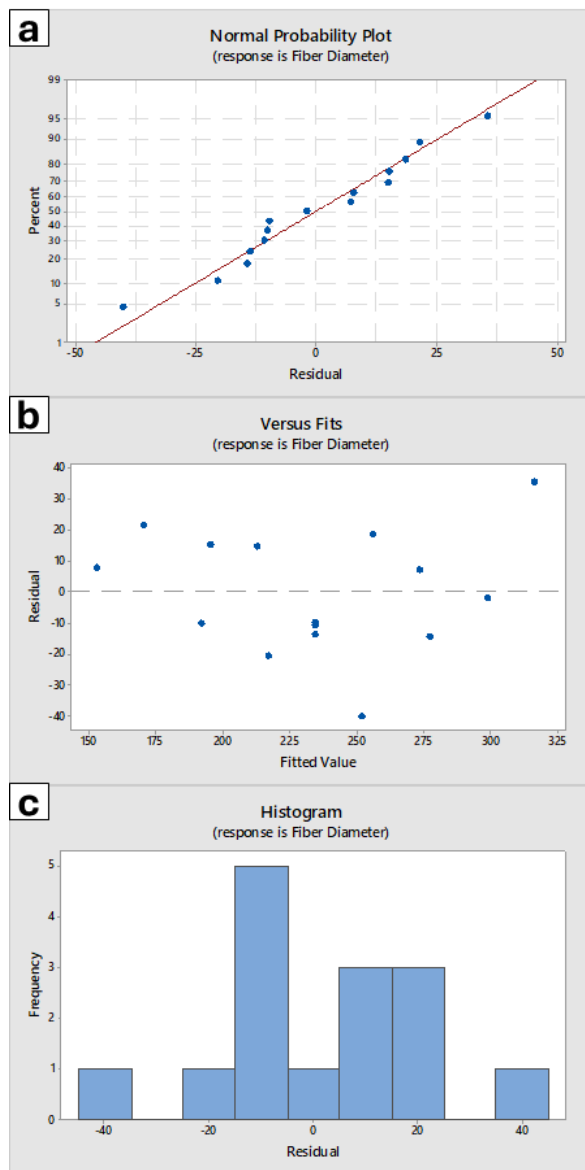


Figure 3: a) normal probability plot, b) pareto plot and residual-frequency diagram

IV. CONCLUSIONS

In this study, nanofibers were produced from biodegradable poly(butylene succinate) (PBS) using the electro-blowing method, and the effects of processing parameters on fiber diameter were optimized via a Box-Behnken design. Three key variables—PBS concentration (8–12%), air pressure (1–3 bar), and electric field (0–30 kV)—were systematically evaluated across 15 experimental runs. Analysis revealed PBS concentration as the most influential factor on fiber diameter, followed by electric field and air pressure. The second-order regression model showed high predictive accuracy ($R^2 = 97.41\%$), with the optimal conditions (8.4% concentration, 3 bar, 30 kV) yielding a predicted diameter of 159.9 nm, closely matching the experimental result (161 nm).

These findings highlight the potential of electro-blowing for controlled, high-performance nanofiber fabrication and support the integration of biodegradable materials like PBS in sustainable applications such as air filtration, wound dressings, and food packaging.

REFERENCES

- [1] Barhoum, A., Rasouli, R., Yousefzadeh, M., Rahier, H., and Bechelany, M. (2019). Nanofiber Technologies: History and Development. in: A. Barhoum, M. Bechelany, A.S.H. Makhoulf (Eds.), Handbook of Nanofibers, Springer International Publishing, Champp. 3–43.
- [2] Kilic, A., Selcuk, S., Toptas, A., and Seyhan, A. (2023). Chapter 10 - Nonelectro nanofiber spinning techniques. in: A. Kargari, T. Matsuura, M.M.A. Shirazi (Eds.), Electrospun and Nanofibrous Membranes, Elsevier, pp. 267–293.
- [3] Toptas, A., Calisir, M.D., Gungor, M., and Kilic, A. (2024). Enhancing filtration performance of submicron particle filter media through bimodal

structural design. *Polymer Engineering & Science*, **64**, 901–912.

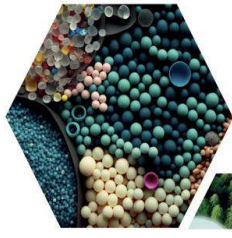
[4] Kalita, N.K., Damare, N.A., Hazarika, D., Bhagabati, P., Kalamdhad, A., and Katiyar, V. (2021). Biodegradation and characterization study of compostable PLA bioplastic containing algae biomass as potential degradation accelerator. *Environmental Challenges*, 3, 100067.

[5] Pakolpakçıl, A., Kılıç, A., and Draczynski, Z. (2023). Optimization of the Centrifugal Spinning Parameters to Prepare Poly(butylene succinate) Nanofibers Mats for Aerosol Filter Applications. *Nanomaterials*, 13, 3150.

[6] Fabbri, M., Guidotti, G., Soccio, M., Lotti, N., Govoni, M., Giordano, E., et al. (2018). Novel biocompatible PBS-based random copolymers containing PEG-like sequences for biomedical applications: From drug delivery to tissue engineering. *Polymer Degradation and Stability*, 153, 53–62.

[7] Pakolpakçıl, A. (2024). Development of Biodegradable Poly(butylene succinate) Based Nanofibrous Webs via Solution-Blow Spinning Technology for N95 Respiratory Filters. *Fibers Polym*, 25, 473–484.

[8] Toptaş, A., Çalışır, M., and Kılıç, A. (2024). Optimization of Electro-Blown PVDF Nanofibrous Mats for Air Filter Applications. *El-Cezeri Journal of Science and Engineering*, 11, 199–206.



16 ULUSLARARASI
LİF VE POLİMER
ARAŞTIRMALARI
SEMPOZYUMU

16th INTERNATIONAL FIBER AND POLYMER RESEARCH SYMPOSIUM

Sürdürülebilir ve İşlevsel Lif ve Polimerler
Sustainable and Functional Fibers & Polymers



9-10 Mayıs
May 2025

İstanbul Teknik Üniversitesi
Gümüşsuyu Prof. Dr. Necmettin Erbakan Yerleşkesi
İstanbul Technical University
Gumussuyu Prof. Dr. Necmettin Erbakan Campus



Effect of processing flaws on mechanical behaviour of graphene-epoxy nanocomposites

Osman Bayrak ^{a,*}, Ayten Nur Yüksel Yılmaz ^b, Yusuf İpek ^a, Mertcan İşgör ^a, Cantekin Kaykılarlı ^c

^aMechanical Engineering, Bursa Technical University, 16310 Bursa, Türkiye.

^bPolymer Materials Engineering, Bursa Technical University, 16310 Bursa, Türkiye.

^cMetallurgical and Materials Engineering, Bursa Technical University, 16310 Bursa, Türkiye.

*Corresponding author: osman.bayrak@btu.edu.tr

ABSTRACT

Reinforcement of epoxy-matrix nanocomposites with graphene nanoplatelets does not always guarantee improved mechanical performance. In this study, we investigate the microstructures and mechanical properties of graphene-epoxy nanocomposites manufactured using two different processing methods. Each method involved slightly different parameters, such as varying ultrasonication times and degassing under vacuum. Mechanical testing revealed that nanocomposites with processing flaws, particularly bubble formations, exhibited a significant reduction in both Young's modulus and yield strength compared to those with better microstructural quality. The microstructures of the nanocomposites were imaged using scanning electron microscopy. For samples manufactured with lower degassing time, maximum strength of pristine epoxy was measured 43.1 MPa, while it was 30.3 MPa and 31 MPa for composites of 0.17wt% and 0.3wt% graphene content, respectively. The deteriorated mechanical performance was correlated with the presence of processing-induced voids and defects, as observed in the microscopic analyses (see Figure 1 and Figure 2). To better understand the influence of these flaws, analytical models were developed to predict the effect of bubble-induced porosity on mechanical properties. The predictions of the analytical models showed good agreement with the experimental results. This study underlines the critical importance of optimizing manufacturing parameters to minimize flaws and thereby achieve graphene-epoxy nanocomposites with enhanced Young's modulus, yield strength, and overall mechanical performance.

Keywords: ; Graphene; Nanocomposites; Mechanical properties; Microstructure

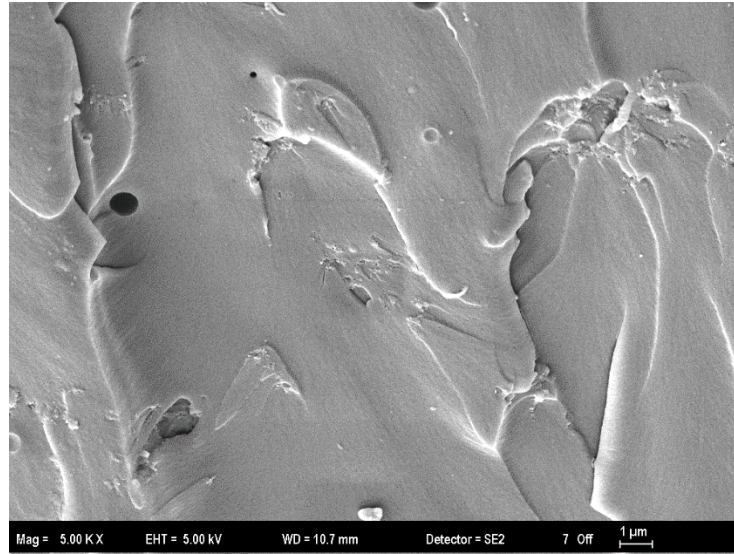


Figure 1 Bubble formations observed in samples that were applied lower degassing time.

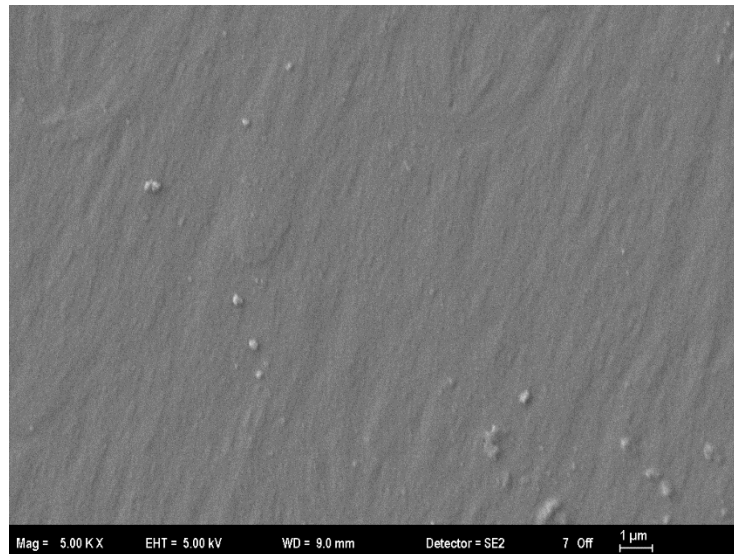
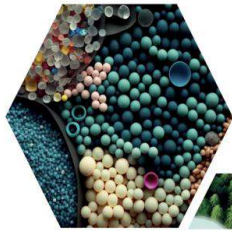


Figure 2 Bubble formations observed in samples that were applied higher degassing time.



16 ULUSLARARASI
LİF VE POLİMER
ARAŞTIRMALARI
SEMPOZYUMU

16th INTERNATIONAL FIBER AND POLYMER RESEARCH SYMPOSIUM

Sürdürülebilir ve İşlevsel Lif ve Polimerler
Sustainable and Functional Fibers & Polymers



9-10 Mayıs
May 2025

İstanbul Teknik Üniversitesi

Gümüşsuyu Prof. Dr. Necmettin Erbakan Yerleşkesi
İstanbul Technical University
Gumussuyu Prof. Dr. Necmettin Erbakan Campus

From manual methods to deep learning: evolution of image-based diameter analysis for fibers and particles

Muhammet Mahsun Çifçi^a, Mehmet D. Çalışır^{a,*}

^aRecep Tayyip Erdogan University, Rize, 53100, Türkiye

*Corresponding author: mehmetdurmus.calisir@erdogan.edu.tr

ABSTRACT

One of the most critical parameters that determine the functional properties of particles/fibers is diameter, which directly affects product performance, particularly in applications such as filtration, tissue engineering, and sensor technologies. In this context, the accuracy of image processing methods used for diameter measurement is of great importance in terms of analysis speed, reliability, and minimizing user dependency. In this study, manual, semi-automatic, and AI-assisted fully automatic image analysis methods were compared based on current literature. Although manual methods can provide sufficient accuracy, their effectiveness is limited due to high user dependency. Semi-automatic techniques, on the other hand, accelerate the analysis process through steps such as skeletonization. Deep learning-based fully automatic systems (e.g., YOLO, CNN, U-Net) stand out in both academic and industrial applications by offering high accuracy, fast processing times, and reproducibility across large datasets. A comparative analysis of these methods was conducted in light of recent studies in literature.

Keywords: Fiber Diameter, Image Processing, Artificial Intelligence, Deep Learning, SEM

I. INTRODUCTION

Nanofibers are widely used in various fields such as filtration, tissue engineering, drug delivery, and sensor technologies due to their high surface area-to-volume ratio, controlled porosity, and superior mechanical properties [1], [2], [3]. These functional features are mainly based on the morphology, diameter distribution, and porosity characteristics of nanofiber mats. Among all the structural parameters, fiber diameter stands out as the most critical factor since it directly affects product performance. For example, in air filtration systems, when the fiber diameter approaches the mean free path of gas molecules, the slip flow effect occurs, thereby enhancing filtration

efficiency [4]. In addition, smaller fiber diameters directly influence features such as sensor performance, long-term electrolyte storage, rapid electron/ion transport, and biological activity due to a higher surface area-to-volume ratio [5].

The morphological properties of nanofibers can be measured using techniques such as SEM, AFM, and TEM. Among these, SEM is the most commonly used method due to its accessibility and convenience. In image-based analysis, three main approaches are prominent: manual, semi-automatic, and fully automatic/artificial intelligence-based measurement methods [6]. Manual measurements are widely used, this method has significant limitations due to being

time-consuming, labor-intensive, and subjective. Semi-automatic systems partly automate the image processing steps, while fully automatic AI-based systems operate independently of the user and offer high accuracy.

Although SEM images provide high resolution, they also present challenges during analysis. Problems such as overlapping fibers, defocusing, and low contrast can negatively impact accuracy in both manual and automated methods. Furthermore, sub-images with insufficient fiber content may cause systematic errors in diameter estimation [7]. Despite these challenges, AI-based image processing approaches have recently shown promising results. Deep learning models can automatically and accurately determine fiber diameters from SEM images, thereby accelerating and standardizing the analysis process [8]. This study evaluates new approaches developed for fiber/particle diameter measurements from SEM images and compares the performance of AI-based analysis systems with semi-automatic methods.

II. THEORETICAL METHOD

Manual, semi-automatic, and fully automatic/artificial intelligence-based methods differ in terms of accuracy and user dependency. This section provides a brief overview of each method and their fundamental approaches.

2.1. Manual Measurement Methods

The most basic and traditional method for measuring fiber diameter from images is manual measurement using digital calipers. This technique involves drawing measurement lines directly between fiber boundaries on SEM images. In this study, such measurements were performed using the open-source ImageJ software. Utilizing the scale information provided in the images, the pixel-based diameter of each fiber was converted into micrometers, and this process was repeated for 100 individual fibers to

obtain data for statistical analysis [9]. Manual measurement is particularly valuable as a reference method in small datasets due to its ability to provide visual verification. However, it is time-consuming and highly dependent on the user's subjective judgment. Studies have shown that significant discrepancies may arise between different users measuring the same sample [10]. Therefore, this method is often used for creating **ground truth** data to validate the performance of more advanced measurement algorithms.

2.2. Semi-Automatic Method

In semi-automatic methods, the analysis process is supported by image processing algorithms, but the user still provides manual input at certain steps.

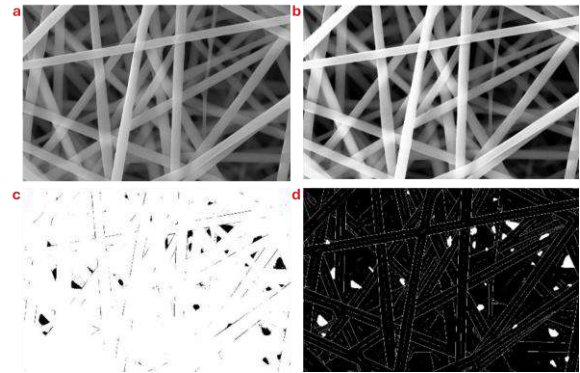


Figure 1. Image processing steps for fiber diameter determination: (a) Original image, (b) Noise reduction and contrast enhancement (filtering, histogram equalization, and morphological opening and closing), (c) Binary conversion, d) Image after skeletonization [7].

In this system, the analysis process generally includes the following steps [7]:

- **Noise reduction** is essential in digital image analysis to improve image quality and enable clearer detection of objects such as fiber or particle boundaries.
- Using predefined threshold values, the image is converted to **binary format**, allowing the background to be separated from the sample.
- In the **skeletonization** step, the central axes of the fibers are extracted.

- **Diameter calculation** is performed by taking perpendicular cross-sections along the centerlines.

The DiameterJ software can analyze images hundreds of times faster than manual methods and can also provide statistical outputs such as fiber-wise diameter distributions [10]. However, the quality of segmentation—and thus the accuracy of the analysis—may still depend on parameter selection, which is influenced by user experience. The clarity, separability, and contrast of the fibers in the image are critically important for accurate detection by the software [11].

2.3. AI-Based Fully Automatic Method

In recent years, artificial intelligence-based methods have surpassed the limitations of traditional image processing techniques in measuring fiber or particle diameters from SEM images, accelerating the measurement process while also standardizing it. These approaches, with their ability to operate independently of the user and produce reliable results even when image quality varies, have been widely adopted, especially in fields such as materials science and biomedical research.

Machine learning (ML) is one of the key technologies underlying this transformation. ML algorithms perform tasks such as classification and regression by learning patterns from data. Different types—supervised, unsupervised, semi-supervised, and reinforcement learning—offer flexible solutions suitable for various types of data [12]. These approaches automatically analyze patterns in images and provide high accuracy in tasks such as diameter prediction. One of the prominent architectures in this context is the Convolutional Neural Network (CNN). CNNs can extract features from raw pixels while preserving the spatial hierarchy in images, thereby enabling the learning of complex structures related to the size, shape, and texture of fibers or particles.

Thanks to their multi-layered architecture, they combine low-level edge information with high-level abstract representations to provide a comprehensive analysis [13].

The YOLO (You Only Look Once) algorithm, on the other hand, is another deep learning model that demonstrates superior performance in real-time object detection and measurement. By dividing the image into a grid structure, it predicts the object location and class in each cell in a single pass. This architecture dramatically reduces processing time compared to classical object detection methods and makes its application feasible in systems requiring instant decision-making (e.g., industrial lines, robotic systems, biological analysis devices). The latest versions of YOLO (YOLOv5, v7, v8, and YOLO-NAS) have shown significant advancements in detecting small objects, coping with low-contrast environments, and adapting easily to edge devices [14]. The enhanced versions have been optimized in terms of model weight, making them operable on mobile platforms and allowing output to be obtained in milliseconds even on hardware-constrained systems. Furthermore, thanks to its adaptable structure to images with varying resolution and density, YOLO provides highly sensitive detection even in irregular structures like fibers. However, in order to achieve high accuracy, such models typically require very large, annotated datasets, which is a major limitation. Moreover, YOLO's decision mechanisms are limited in terms of interpretability; in other words, it is often not possible to explain why the model made a particular prediction. This can pose reliability concerns, especially in sensitive or critical applications. In fast-operating models like YOLO, architectural simplifications are made to achieve real-time performance; this can lead to a loss of accuracy or detail in some cases. Additionally, when working with high-resolution images, the training process requires significant GPU memory and computational

power, which poses challenges for research environments with limited hardware resources.

Similarly, the U-Net architecture, originally developed for medical image segmentation, draws attention with its ability to achieve high-accuracy segmentation even with limited data. The success of U-Net lies in its encoder-decoder structure and the skip connections between these two parts. This structure ensures the preservation and simultaneous analysis of both local details and contextual information. U-Net can distinguish object boundaries with remarkable precision, especially in images with complex structural details (e.g., SEM images where fibers overlap or contrast is low). Its segmentation outputs are not only visually smooth but also numerically reliable, making it an indispensable solution in applications that require high accuracy, such as fiber/particle segmentation [15]. However, U-Net also has certain technical limitations. Particularly in datasets with low quantity or imbalanced distribution, there is a high risk of overfitting; the model may become overly tailored to the training data, reducing its generalization performance on new data. Although U-Net demonstrates high segmentation performance, its decision-making process lacks transparency, reducing interpretability. Specifically, it is not clearly understood which structural features the filters in the internal layers are detecting. Additionally, to achieve optimal performance, network architecture, number of filters, learning rate, and regularization parameters must be meticulously tuned. This makes it difficult to optimize the model for each specific problem and requires experienced users. Furthermore, the training process typically takes a long time and requires high GPU memory, which increases computational costs.

III. RESULTS AND DISCUSSIONS

In this section, image processing-based approaches for the analysis of fiber diameters were systematically reviewed.

3.1. Semi-Automatic Methods

Öznergiz et al. [11] developed an image analysis algorithm for automatically measuring nanofiber diameters from SEM images without requiring fiber segmentation. The method involves three key steps: Canny edge detection, normalized Radon transform (NRT), and postprocessing. Initially, edges in the grayscale SEM image are extracted using the Canny filter. In the second stage, multi-angle projections are performed on the detected edges, and the resulting density values are mapped to Radon space. These values are then normalized by projection length and encoded logarithmically. A fixed threshold (0.4) is applied to this matrix to enhance visibility of fiber edges, particularly in low-contrast or direction-varying regions. Postprocessing eliminates redundant contours caused by backprojection, preserving only the one with the highest intensity. The algorithm was applied to SEM images of PAN, PEO, and PVA electrospun nanofibers. Diameter measurements were taken at 568 points for each of 48 selected fibers. The results showed high consistency with manual measurements, achieving a correlation coefficient of $R^2 = 0.956$ and a regression equation of $y = 0.948x + 0.645$. The mean deviation was below 0.5 nm, which corresponds to a relative error under 2% for fiber diameters in the 20–30 nm range.

The algorithm stands out for its robustness against structural complexities such as directional changes, bifurcations, and background variations. However, its performance is sensitive to fixed parameters such as Canny thresholds, Radon angular resolution (typically 1°), matrix threshold (0.4), and projection edge margin (ϵ). Inaccurate tuning may lead to false detections or undetected fibers. Although parameters were manually adjusted in the study, future versions aim to integrate an adaptive mechanism for resolution-sensitive tuning. The full process is visualized in

Figure 2, providing a step-by-step overview of this robust measurement approach.

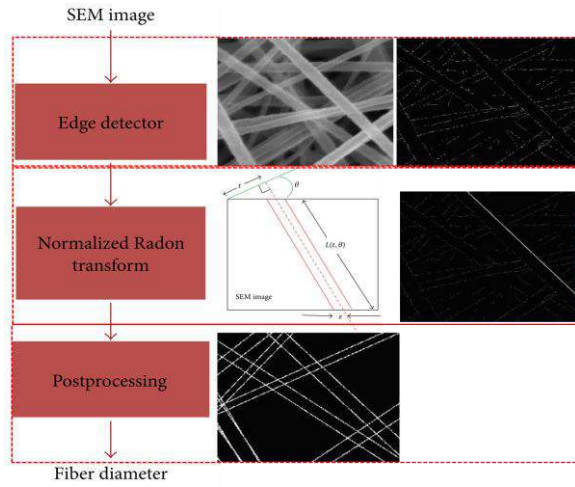


Figure 2. Processing steps and image processing stages used for fiber diameter detection from SEM images [11]

DiameterJ, developed by Hotaling et al. [10], introduces two advanced methodologies for estimating nanofiber diameters from SEM images: the Super Pixel and Histogram methods. Both approaches surpass traditional skeletonization by offering improved accuracy and statistical insight. The Super Pixel method calculates average diameter by dividing the total segmented fiber area by the total centerline length, combining outputs from both the Zhang & Suen thinning algorithm and a Voronoi-based centerline extraction. To address overestimated centerline lengths caused by fiber intersections, an intersection correction routine was implemented. It iteratively refines diameters by accounting for 3- and 4-way junctions until convergence at subpixel resolution (1/1000 pixel), achieving $<0.01\%$ error for fibers ~ 10 pixels wide. The Histogram method computes local diameters along the centerline using the Euclidean Distance Transform (EDT). This generates multimodal histograms, enabling fine-grained statistical analysis including mean, median, mode, and standard deviation. When validated against synthetic images with known diameters, the method showed absolute errors <0.6 pixels and percentage errors $<3\%$. Gaussian peak fitting was reliable when

peak separation exceeded 3 pixels. Beyond diameter, DiameterJ quantifies structural metrics such as intersection density and characteristic fiber length (CFL).

DiameterJ was validated using stainless steel wire samples (gauges 48, 50, and 53 – corresponding measured diameters $31.1 \pm 0.1 \mu\text{m}$, $25.6 \pm 0.1 \mu\text{m}$, and $16.7 \pm 0.1 \mu\text{m}$, respectively), and calculated modal values of $31.44 \mu\text{m}$, $25.55 \mu\text{m}$, and $14.67 \mu\text{m}$ which yields modal diameter errors below 1.2% with narrow Gaussian distributions ($\sigma < 0.64 \pm 0.1 \mu\text{m}$). In mixed-gauge images, the algorithm successfully distinguished multiple fiber populations. These findings are visually presented in Figure 3, which illustrates the high correlation with true values and the algorithm's capability to distinguish multiple fiber populations. While the Super Pixel method yields a global average, the Histogram method supports high-resolution, distribution-aware analysis—generating up to 5000 diameter values per image. Together, these capabilities position DiameterJ as a robust tool for accurate, fast, and multimodal nanofiber characterization in SEM-based imaging workflows.

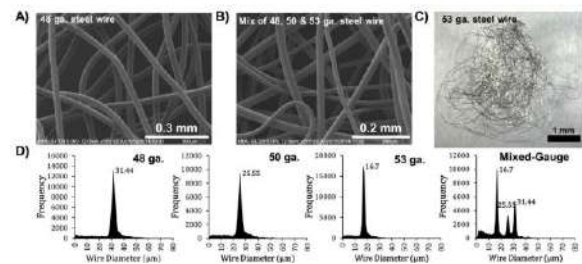


Figure 3. Reported diameter values of steel wires with different diameters (31.0 , 25.5 , and $16.75 \mu\text{m}$) using the histogram algorithm [10]

SIMPoly, developed by Murphy et al. [16], is a MATLAB-based semi-automatic tool for rapid and accurate measurement of fiber diameters in SEM images of electrospun polymer mats. Requiring only two user actions—image selection and optional calibration—SIMPoly executes all segmentation and measurement steps automatically.

The processing pipeline begins with local histogram equalization to enhance fiber-background contrast (Figure 4a-b), followed by morphological reconstruction to suppress small-scale noise (Figure 4c). Canny edge detection is applied to identify fiber boundaries (Figure 4d), which are then segmented using Otsu thresholding to create a binary mask (Figure 4e). Morphological closing and median filtering are used to bridge discontinuities and reduce noise (Figure 4f-g). Subsequently, edge refinement and skeletonization reduce each fiber to a one-pixel-wide centerline (Figure 4h-i). The diameter at each centerline pixel is calculated as twice the shortest distance to the nearest edge pixel.

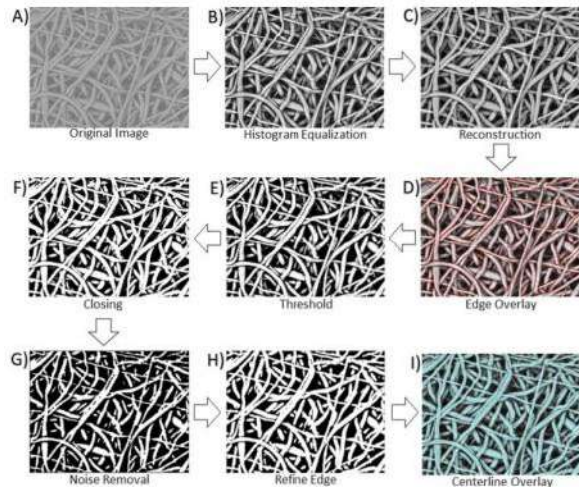


Figure 4. Workflow of the SIMPoly algorithm: (a) original image, (b) contrast enhancement, (c) fiber highlighting, (d) edge detection, (e) background noise removal, (f) morphological closing, (g) median filtering, (h) fiber edge thickening, (i) skeletonization and overlay [16]

Each image typically yields between 4500 and 7000 individual diameter measurements within ~15 seconds, significantly faster than manual ImageJ (~100 s for a few dozen fibers) and faster than DiameterJ (~60 s for several thousand points). Outputs include Gaussian-fitted histograms, color-coded standard deviation maps, and segmentation overlays. Validation was performed using synthetic fibers and real SEM images of electrospun PLGA mats. In synthetic images, SIMPoly showed a mean diameter

error of $2.1\% \pm 1.7$ for regular fibers and $1.6\% \pm 1.5$ for irregular fibers—lower than those reported for DiameterJ ($2.5\% \pm 1.9$ and $4.7\% \pm 1.4$, respectively). Inter-user variability was 15.39% with manual ImageJ, 2.23% with DiameterJ, and only 0.73% with SIMPoly, demonstrating strong user-independence.

3.2. AI-Based Fully Automatic Methods

Huarachi and Castañón [17] proposed a deep learning-based method utilizing a modified U-Net regression model for fiber diameter estimation and segmentation from complex fiber micrographs. Unlike classical approaches, their method predicts distance maps representing each pixel's Euclidean distance to the nearest background pixel. Both real SEM images and synthetically generated datasets were used for training, with data augmentation techniques enhancing robustness. Three loss functions—L1 Loss, L2 Loss, and Smooth L1 Loss—were evaluated (Figure 5). U-Net achieved the lowest mean absolute error (MAE: 0.1094) with L1 Loss on real images and lowest mean squared error (MSE: 0.1229) with L2 Loss on synthetic datasets. Comparatively, U-Net demonstrated faster and more accurate performance than SkeletonNet architecture.

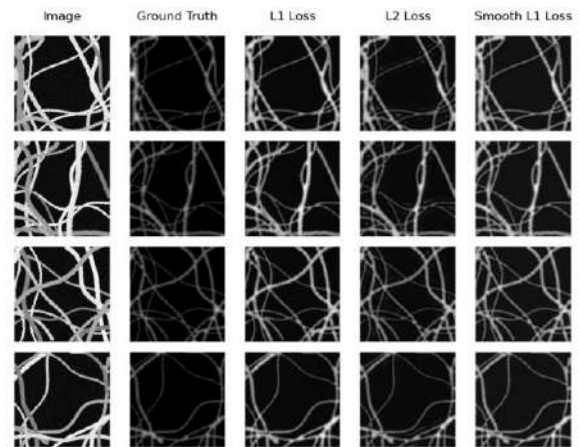


Figure 5. Example results of distance maps obtained using the U-Net regression model with different loss functions on the synthetic test subset [17].

Gao [7] developed a U-Net-based deep learning algorithm for the automatic measurement of nanofiber

diameters from SEM images. The method includes three stages: (1) U-Net-based fiber segmentation, (2) centerline (skeleton) extraction, and (3) diameter calculation using the Euclidean Distance Transform (EDT). The U-Net architecture consists of a symmetric encoder–decoder with four downsampling and four upsampling blocks, each containing two 3×3 convolutions with ReLU activation and max pooling or up-convolution. The full network comprises 23 layers, ending with SoftMax activation for multi-class classification. A total of 730 training images, 91 validation images, and 91 test images were used. Instead of regression, the model formulates diameter prediction as classification into 76 discrete diameter classes (1–76 pixels). Images were preprocessed with histogram equalization and 8-bit depth normalization. Hyperparameters were manually tuned: learning rate = 0.001, batch size = 16, epochs = 64, and early stopping with patience = 3. Post-segmentation, the model performs skeletonization and retains only fibers with clearly defined bilateral edges. Diameter is then computed as twice the shortest distance from each centerline pixel to the edge. Accuracy was verified through comparison with manual ImageJ measurements and MATLAB-labeled ground truth. Figure 6 illustrates the precise overlay of segmentation, centerlines, and diameter estimations.

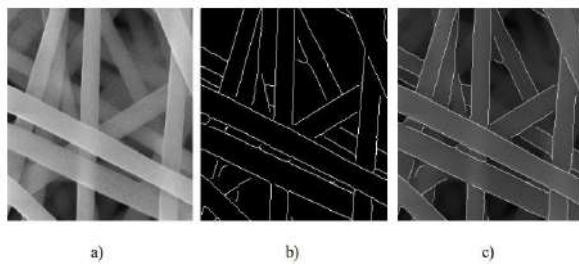


Figure 6. a) Original SEM image; b) The generated boundary of nanofiber; c) a and b overlap for comparison [7]

Kurkin et al. [18] combined DeepLabv3+ with the Segment Anything Model (SAM) to create a hybrid method for the automatic identification and measurement of short carbon and glass fibers from SEM images. Their system, trained with minimal

annotations, achieved ~95% Intersection over Union (IoU) accuracy and significantly accelerated fiber measurement workflows, demonstrating its potential for cost-effective and efficient microstructural analysis in composites.

Although AI-assisted studies for fiber diameter detection remain limited, numerous applications of this technology have been reported in particle size analysis and, in particular, in CT image analysis of biological structures for medical diagnostic purposes [19], [20]. Chen et al. [8] developed an automated method for determining the sizes of particles in powder coating materials using SEM images. This method employs a deep learning algorithm based on YOLOv5 to detect particles of various shapes, sizes, and densities with high accuracy and without human intervention. The study trained and tested a YOLOv5-based model on SEM images of various powder materials, including boron nitride, titanium dioxide, aluminum oxide, and stainless steel. Initially, 20–40 particles were manually labeled in three images, and the dataset was expanded to 120 samples through data augmentation. The YOLOv5 model utilized advanced modules such as CSPDarknet53, SPPF, and CSPPAN. Pretrained on ImageNet and fine-tuned with SEM data, the model used a weighted loss function to optimize prediction accuracy. Bounding box regression was applied to square root-transformed dimensions to enhance stability. In tests with titanium dioxide SEM images, the model achieved over 97% accuracy in detecting particle boundaries. It could also process multiple images per sample to generate size distribution histograms. Measured particle sizes were converted to micrometers and closely matched manual measurements, with deviations within $\pm 5\%$, demonstrating the model's effectiveness for automated particle analysis.

The comparative analysis presented in Table 1 clearly demonstrates the trade-offs between manual, semi-

automated, and deep learning-based approaches for fiber diameter measurement from SEM images. Manual measurement using ImageJ, while traditionally considered a reference method, suffers from high inter-user variability and time inefficiency, with an error rate ranging from 10% to 15%, leading to an overall accuracy between 85% and 90%. This variability is especially problematic in large datasets or when reproducibility is critical.

DiameterJ and the method developed by Öznergiz et al. [11] represent more refined, semi-automated techniques that significantly reduce error rates to approximately 2%, offering accuracy levels around 98%. These methods are particularly effective in structured environments where image contrast and fiber orientation are relatively uniform. However, DiameterJ's dependency on histogram-based estimation may become a limitation when analyzing multimodal or non-uniform fiber distributions. SIMPoly, a MATLAB-based tool, offers a substantial improvement in both speed and consistency. With an average processing time of only 15 seconds per image and error margins between 1.6% and 2.1%, it achieves up to 98.4% accuracy, demonstrating the potential of rule-based automation for standardization across users and datasets.

On the other hand, deep learning-based models such as U-Net [7] and YOLOv5 [8] showcase the ability to generalize across image types and fiber morphologies with minimal user intervention. The U-Net model, designed as a class-based regression system, provides a visually confirmed accuracy in the 95–97% range, with inference times under 5 seconds per image. YOLOv5, originally developed for object detection, achieves real-time performance with an estimated $\pm 5\%$ deviation in diameter prediction, corresponding to an overall accuracy of about 95%. Despite slightly higher error margins compared to SIMPoly or DiameterJ, these AI-based systems are highly scalable,

adaptable to complex images, and advantageous for large-scale or high-throughput analyses.

Table 1. Performance comparison table

| Method | Processing Time | Error & Accuracy Summary |
|-------------------------|------------------------------|---------------------------------------|
| Manual (ImageJ) | ~100 sec per image | ~10–15% error → ~85–90% accuracy |
| DiameterJ (Histogram) | ~60 sec per image | ~2% error → ~98% accuracy |
| Öznergiz et al. (2014) | Not specified | ~2% error → ~98% accuracy |
| SIMPoly (Murphy et al.) | ~15 sec per image | 1.6–2.1% error → ~97.9–98.4% accuracy |
| Gao (2022, U-Net) | <5 sec per image (inference) | ~3–5% error → ~95–97% accuracy |
| YOLOv5 (Chen et al.) | <1 sec per image | $\pm 5\%$ error → ~95% accuracy |

IV. CONCLUSION

In recent years, semi-automatic and artificial intelligence (AI)-based systems have made significant progress in fiber diameter measurement by reducing user dependency and improving measurement reliability. Semi-automatic methods such as SIMPoly, have demonstrated strong performance in generating standardized and reproducible results across various fiber types and under different imaging conditions. These methods are particularly effective when image quality is high and structural complexity is moderate. However, their performance is sensitive to thresholding strategies, edge detection quality, and morphological assumptions, which makes it necessary to consider the structural features of the fibers and the required level of precision when selecting a method. Deep learning-based approaches, particularly U-Net, FibeR-CNN, and YOLO variants—have expanded the boundaries of fiber characterization by offering high-speed, low-intervention, and scalable analysis

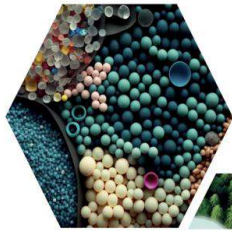
frameworks. U-Net and FibeR-CNN architectures stand out with their ability to perform high-accuracy segmentation and direct diameter estimation even on low-contrast or noisy SEM images. In contrast, YOLO models primarily focus on the rapid localization of fiber structures, which provides an advantage in high-throughput applications rather than in detailed morphological analysis. The comparative analysis conducted in this study shows that semi-automatic methods can achieve over 98% accuracy under suitable conditions; however, AI-based approaches deliver more consistent results, especially in complex or heterogeneous datasets. The average accuracy of AI-based methods generally ranges between 95% and 98%. When choosing among these methods, not only accuracy rates but also factors such as processing speed, model interpretability, imaging modality, and computational resources should be taken into account.

Future studies may focus on hybrid models that combine the interpretability of rule-based systems with the generalization capacity of deep neural networks. Additionally, adaptive learning frameworks that incorporate domain-specific prior knowledge can improve model robustness in new fiber structures. The creation of large-scale, annotated SEM image datasets is also of critical importance for enabling transfer learning techniques and expanding the applicability of AI systems in fiber metrology. Overall, the evolution of intelligent image analysis tools marks a paradigm shift toward fully automated, real-time, and morphology-aware fiber characterization.

REFERENCES

- [1] Y. Zhou, Y. Liu, M. Zhang, Z. Feng, D.-G. Yu, and K. Wang, 'Electrospun Nanofiber Membranes for Air Filtration: A Review', *Nanomaterials*, vol. 12, no. 7, Art. no. 7, Jan. 2022, doi: 10.3390/nano12071077.
- [2] P. R. Patel and R. V. N. Gundloori, 'A review on electrospun nanofibers for multiple biomedical applications', *Polym. Adv. Technol.*, vol. 34, no. 1, pp. 44–63, 2023, doi: 10.1002/pat.5896.
- [3] N. S. Mpofu, T. Blachowicz, A. Ehrmann, and G. Ehrmann, 'Wearable Electrospun Nanofibrous Sensors for Health Monitoring', *Micro*, vol. 4, no. 4, Art. no. 4, Dec. 2024, doi: 10.3390/micro4040049.
- [4] H.-J. Choi et al., 'Effect of slip flow on pressure drop of nanofiber filters', *J. Aerosol Sci.*, vol. 114, pp. 244–249, Dec. 2017, doi: 10.1016/j.jaerosci.2017.09.020.
- [5] Kenry and C. T. Lim, 'Nanofiber technology: current status and emerging developments', *Prog. Polym. Sci.*, vol. 70, pp. 1–17, Jul. 2017, doi: 10.1016/j.progpolymsci.2017.03.002.
- [6] M. Frei and F. E. Kruis, 'Fully automated primary particle size analysis of agglomerates on transmission electron microscopy images via artificial neural networks', *Powder Technol.*, vol. 332, pp. 120–130, Jun. 2018, doi: 10.1016/j.powtec.2018.03.032.
- [7] E. Gao, 'Multiple Tools for Automated Nanofiber Characterization by Image Processing', May 2022, Accessed: Apr. 23, 2025. [Online]. Available: <http://hdl.handle.net/10012/18253>
- [8] C. Liang, Z. Jia, and R. Chen, 'An Automated Particle Size Analysis Method for SEM Images of Powder Coating Particles', *Coatings*, vol. 13, no. 9, Art. no. 9, Sep. 2023, doi: 10.3390/coatings13091547.
- [9] J. J. Stanger, N. Tucker, N. Buunk, and Y. B. Truong, 'A comparison of automated and manual techniques for measurement of electrospun fibre diameter', *Polym. Test.*, vol. 40, pp. 4–12, Dec. 2014, doi: 10.1016/j.polymertesting.2014.08.002.
- [10] N. A. Hotaling, K. Bharti, H. Kriel, and C. G. Simon, 'DiameterJ: A validated open source nanofiber diameter measurement tool', *Biomaterials*, vol. 61, pp. 327–338, Aug. 2015, doi: 10.1016/j.biomaterials.2015.05.015.

- [11] E. Öznergiz, Y. E. Kiyak, M. E. Kamasak, and I. Yildirim, 'Automated Nanofiber Diameter Measurement in SEM Images Using a Robust Image Analysis Method', *J. Nanomater.*, vol. 2014, no. 1, p. 738490, 2014, doi: 10.1155/2014/738490.
- [12] I. H. Sarker, 'Machine Learning: Algorithms, Real-World Applications and Research Directions', *SN Comput. Sci.*, vol. 2, no. 3, p. 160, Mar. 2021, doi: 10.1007/s42979-021-00592-x.
- [13] X. Zhao, L. Wang, Y. Zhang, X. Han, M. Deveci, and M. Parmar, 'A review of convolutional neural networks in computer vision', *Artif. Intell. Rev.*, vol. 57, no. 4, p. 99, Mar. 2024, doi: 10.1007/s10462-024-10721-6.
- [14] J. Terven, D.-M. Córdova-Esparza, and J.-A. Romero-González, 'A Comprehensive Review of YOLO Architectures in Computer Vision: From YOLOv1 to YOLOv8 and YOLO-NAS', *Mach. Learn. Knowl. Extr.*, vol. 5, no. 4, Art. no. 4, Dec. 2023, doi: 10.3390/make5040083.
- [15] G. Du et al., 'Medical Image Segmentation based on U-Net: A Review', *J. Imaging Sci. Technol.*, vol. 64, pp. 1–12, Mar. 2020, doi: 10.2352/J.ImagingSci.Technol.2020.64.2.020508.
- [16] R. Murphy, A. Turcott, L. Banuelos, E. Dowey, B. Goodwin, and K. O. Cardinal, 'SIMPoly: A Matlab-Based Image Analysis Tool to Measure Electrospun Polymer Scaffold Fiber Diameter', *Tissue Eng. Part C Methods*, vol. 26, no. 12, pp. 628–636, Dec. 2020, doi: 10.1089/ten.tec.2020.0304.
- [17] A. M. Alejo Huarachi and C. A. Beltrán Castañón, 'A Deep Learning Approach to Distance Map Generation Applied to Automatic Fiber Diameter Computation from Digital Micrographs', *Sensors*, vol. 24, no. 17, Art. no. 17, Jan. 2024, doi: 10.3390/s24175497.
- [18] Kurkin, E., Minaev, E., Sedelnikov, A., Pioquinto, J. G. Q., Chertykovtseva, V., & Gavrilov, A. (2024). Computer Vision Technology for Short Fiber Segmentation and Measurement in Scanning Electron Microscopy Images. *Technologies*, 12(12), 249. <https://doi.org/10.3390/technologies12120249>
- [19] Y. Garg, K. Seetharam, M. Sharma, D. K. Rohita, and W. Nabi, 'Role of Deep Learning in Computed Tomography', *Cureus*, vol. 15, no. 5, p. e39160, doi: 10.7759/cureus.39160.
- [20] T. P. Szczykutowicz, G. V. Toia, A. Dhanantwari, and B. Nett, 'A Review of Deep Learning CT Reconstruction: Concepts, Limitations, and Promise in Clinical Practice', *Curr. Radiol. Rep.*, vol. 10, no. 9, pp. 101–115, Sep. 2022, doi: 10.1007/s40134-022-00399-5.



16 ULUSLARARASI
LİF VE POLİMER
ARAŞTIRMALARI
SEMPOZYUMU

16th INTERNATIONAL FIBER AND POLYMER RESEARCH SYMPOSIUM

Sürdürülebilir ve İşlevsel Lif ve Polimerler
Sustainable and Functional Fibers & Polymers



9-10 Mayıs
May 2025

İstanbul Teknik Üniversitesi

Gümüşsuyu Prof. Dr. Necmettin Erbakan Yerleşkesi
İstanbul Technical University
Gumussuyu Prof. Dr. Necmettin Erbakan Campus

Development of gelatin-chitosan composite nanofibers incorporated with Corncob-derived cellulose microcrystals

Salih Birhanu Ahmed^a, Beyza Soydan^b, Cigdem Ucar^b, Emine Tekcan^b, Ali Toptas^c, Harun Cug^a, Yasin Akgul^{d,*}

^a Mechanical Engineering Department, Karabuk University, 78050 Karabuk, Türkiye.

^b Biomedical Engineering Department, Karabuk University, 78050 Karabuk, Türkiye.

^c Textile Engineering Department, Istanbul Technical University, 34467 Istanbul, Türkiye.

^d Iron and Steel Institute, Karabuk University, 78050 Karabuk, Türkiye.

* Corresponding author: yasinakgul88@gmail.com

ABSTRACT

The growing demand for antibacterial and eco-friendly food packaging has driven interest in biodegradable materials with enhanced functional properties. In this study, natural-based nanofibers were fabricated using the electro-blowing technique for potential use in active food packaging. Gelatin (G), chitosan (Ch), and cellulose microcrystals (CMC), derived from corn cob via acid hydrolysis, were employed as biopolymeric reinforcement. The formulation and electroblowing parameters were first optimized to achieve uniform fiber morphology. To investigate the effect of filler loading, CMC was incorporated into the optimized gelatin-chitosan solution at concentrations of 1, 3, and 5% (w/w). The resulting nanofibers were comprehensively characterized using Field Emission Scanning Electron Microscopy (FE-SEM), Attenuated Total Reflectance-Fourier Transform Infrared Spectroscopy (ATR-FTIR), X-ray Diffraction (XRD), Thermogravimetric Analysis (TGA), and air permeability testing. The results revealed that increasing CMC content led to a gradual rise in air permeability, from 2.00 ± 0.65 mm/s in the control sample to 2.10 ± 0.75 , 2.40 ± 1.03 , and 2.60 ± 0.9 mm/s for the 1, 3, and 5% CMC-loaded samples, respectively. These findings suggest that while CMC incorporation can improve the structural features of the nanofibers, its influence on barrier properties must be carefully tuned to meet the specific requirements of food packaging applications.

Keywords: Gelatin; Chitosan; Nanofiber; Cellulose microcrystal; Sustainable

I. INTRODUCTION

Polymeric nanofibers have been extensively researched in recent years for their potential applications in food packaging [1]. This growing interest is largely due to their remarkable properties, including a high surface area-to-volume ratio and significant porosity [2]. On top of that, nanofibers offer a key advantage over traditional film-based packaging by effectively encapsulating active agents, as well as micro- and nanocrystals, within their porous

structure. Mostly, these nanofibers are produced from synthetic and biopolymeric materials. While synthetic petroleum-derived polymers are widely used in food packaging due to their versatility, their application is increasingly restricted due to concerns over non-biodegradability, potential carcinogenic effects, and environmental pollution [3]. Consequently, the demand for cost-effective, biodegradable, and sustainable biopolymeric packaging has become inevitable.

Biodegradable polymers have attracted enormous scientific and industrial interest due to their environmentally friendly aspect [4]. Materials such as chitosan [5], cellulose [6], starch [7], and gelatin [8] have been extensively studied for their potential use in food packaging [9]. Among these, gelatin has drawn particular interest due to its edibility, availability, low cost, biodegradability, and safety [8,10]. It also exhibits excellent gas barrier properties and controlled swelling behavior in water [11]. However, its poor antibacterial and mechanical properties, along with its highly hydrophilic nature, pose limitations [12]. Therefore, a simple and effective way to address this limitation is by blending gelatin with other polymers and microcrystalline materials. Chitosan, a widely used biopolymer in the food packaging industry, is favored for its non-toxic nature, biodegradability, biocompatibility, and cost-effectiveness. It is an abundant polysaccharide derived from chitin through partial deacetylation, making it a sustainable and functional choice for enhancing packaging materials [13]. Blending chitosan with gelatin nanofibers enhances their antibacterial properties and slightly improves mechanical strength but does not improve surface wettability [14].

Additionally, integrating nano-cellulose and chitosan into gelatin and starch matrices has increased tensile strength, water resistance, and food preservation capabilities [15]. These biodegradable, biocompatible nanocomposite nanofibers offer an eco-friendly alternative to petroleum-based plastics, addressing sustainability concerns while meeting essential packaging requirements. However, natural polymers still face challenges, including lower mechanical strength and processing difficulties compared to synthetic polymers, limiting their broader application [16]. Incorporating nanomaterials like cellulose nanocrystals (CNC) presents a promising solution to enhance the performance of natural polymer-based nanofibers. CNC offers high strength and stiffness,

low weight, and is both biocompatible and biodegradable. Additionally, CNC appears to positively influence the morphology and diameter of electrospun nanofibers. CNC also positively influences nanofiber morphology and diameter, further improving their properties while maintaining biodegradability [17,18].

Significant advancements have been made in nanofiber production, particularly through electrospinning, a technique that uses an electric field to generate fine fibers from polymer solutions or melts. Electrospinning is a versatile method capable of producing high-quality nanofibers from a range of materials. However, it has some limitations, including sensitivity to environmental factors like humidity and temperature, as well as concerns over solvent use [19]. To address these issues, alternative methods such as melt blowing, which avoids solvents, centrifugal spinning [8], solution blowing [20], and electroblowing [21] are being explored as promising solutions. Electro-blowing is a novel method for producing nanofibers that involves using an electric field in addition to air pressure to boost the production of fibers from a solution. The electric field aids in the uniform stretching of the solution, resulting in uniform fibers of higher quality. Thus, electro-blowing combined the benefits of electrospinning (ES) and solution blowing (SBS) [22]. In the ES technique, a high voltage was applied to form continuous polymer fibers with diameters varying from micrometers to nanometers [23]. While the solution blows, spinning high compressed air flow drives a polymeric solution [24].

This study focused on developing a natural nanofiber mat composed of gelatin (G), chitosan (Ch), and corncob-derived cellulose microcrystals (CMC) using an electro-blowing technique to produce materials suitable for food packaging applications requiring enhanced mechanical strength and improved

hydrophobicity. Initially, the polymer formulations and electro-blowing parameters were systematically optimized. Subsequently, varying concentrations of CMC (1, 3, and 5% w/w) were incorporated into the optimized gelatin–chitosan solution to investigate their influence on the final properties. The fabricated nanofibers were thoroughly characterized using Field Emission Scanning Electron Microscopy (FE-SEM), Attenuated Total Reflectance-Fourier Transform Infrared Spectroscopy (ATR-FTIR), X-ray Diffraction (XRD), Thermogravimetric Analysis (TGA), and air permeability testing to evaluate their potential for food packaging applications.

II. MATERIALS AND METHODS

2.1 Materials

Gelatin (Bloom 250–270, Type B), derived from bovine skin, was provided in powder form by Halavet Gıda LLC (Istanbul, Türkiye). Chitosan (degree of deacetylation >95%) was obtained from Biyopol (Istanbul, Türkiye). Acetic acid (AA) with 80% purity and a 1.08 g/cm³ density was sourced from Tekkim (Bursa, Türkiye). Formic acid (65%) was purchased from TEKKIM Chemical Industries, Turkey. Corn cobs were collected locally from rural farmers.

2.2 Extraction of Cellulose Microcrystal (CMC) from Corn Cobs

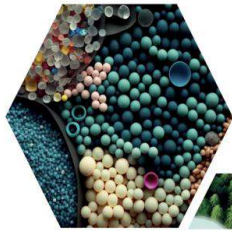
Corn cob residues (3 kg) were collected from rural farmers and air-dried for seven days, followed by oven drying at 45°C for 24 hours. The cellulose preparation method was based on a previous study with some modifications [25]. After drying, the corn cobs were mechanically ground to produce a fine powder. A portion of this powder (300 g) was then combined with 1 L of 2% NaOH solution and stirred at 115°C and 600 rpm for 3 hours using a magnetic stirrer. Afterward, the mixture was removed from the stirrer and allowed

to cool. The powdered material was then oven-dried at 45°C for 24 hours to reach the desired moisture content and stabilize.

A solution containing 92% water, 0.7% NaOH, and 6.3% hydrogen peroxide was prepared for bleaching. Microcrystalline cellulose structures were added to this solution, and the mixture was stirred at 700 rpm and 60°C for 1.5 hours until homogeneous. The bleached material was thoroughly washed with distilled water and air-dried for seven days, resulting in corn cob-based cellulose micro-crystals. Detailed characterization was conducted on the extracted CMC.

2.3 Solution Preparation

The solution was prepared following the percentage composition detailed in Table 1. To create this solution, 12 wt.% of Gelatin (G) and 3 wt.% of chitosan (Ch) were dissolved in a co-solvent system consisting of 68 wt.% acetic acid and 17 wt.% formic acid. The mixture was then subjected to continuous stirring using a magnetic stirrer at a controlled temperature of 60°C for 6 hours, ensuring thorough and complete dissolution of the G and Ch in the solvent mixture. For the preparation of the G-Ch-CMC solution, varying concentrations of cellulose micro-crystals (CMC) at 1, 3, and 5 wt.% were added to the base solution containing 12 wt.% gelatin (G) and 3 wt.% chitosan (Ch) dissolved in the same co-solvent system (68 wt.% acetic acid and 17 wt.% formic acid). This solution was also stirred continuously under similar conditions at the same temperature of 60°C for 4 hours, allowing sufficient time to achieve a uniform, homogenous blend. Both solutions were prepared to ensure that each component was fully integrated, setting the foundation for further experimental procedures.



16

ULUSLARARASI
LİF VE POLİMER
ARAŞTIRMALARI
SEMPOZYUMU

16th INTERNATIONAL FIBER AND POLYMER RESEARCH SYMPOSIUM

Sürdürülebilir ve İşlevsel Lif ve Polimerler
Sustainable and Functional Fibers & Polymers



9-10 Mayıs
May 2025

İstanbul Teknik Üniversitesi

Gümüşsuyu Prof. Dr. Necmettin Erbakan Yerleşkesi
Istanbul Technical University
Gumussuyu Prof. Dr. Necmettin Erbakan Campus

Table 1. Design of experiment (DOE)

| Sample | Gelatin (%) | Chitosan (%) | Cellulose microcrystal (%) | Acetic Acid (%) | Formic Acid (%) |
|-----------|-------------|--------------|----------------------------|-----------------|-----------------|
| G-Ch | 12 | 3 | 0 | 68 | 17 |
| G-Ch-1CMC | 11.89 | 2.96 | 0.15 | 68 | 17 |
| G-Ch-3CMC | 11.64 | 2.91 | 0.45 | 68 | 17 |
| G-Ch-5CMC | 11.4 | 2.85 | 0.75 | 68 | 17 |

2.4 Fabrication of Nanofibers

This study used the electroblowing technique to fabricate nanofiber samples by combining air pressure with an electric field to propel the polymer solution from the nozzle to the collector. The nozzle was positioned 47 cm away from the rotating vacuum collector, and an air pressure of 1.5 bar was applied. Simultaneously, an electric voltage of 20 kV was applied at the nozzle tip to enhance the spinnability of the solution and minimize fiber bundling. The polymer solution was fed at a rate of 15 mL/hr, ensuring effective solvent evaporation during its travel from the nozzle to the collector. This process yielded nanofibers with smooth morphologies and varying diameters. The optimized electro-blowing parameters successfully produced uniform nanofibers for samples, designated as Gelatin-Chitsan (G-Ch), Gelatin-Chitosan-1% cellulose microcrystal (G-Ch-1CMC), Gelatin-Chitosan-3% cellulose microcrystal (G-Ch-3CMC), and Gelatin-Chitosan-5% cellulose microcrystal (G-Ch-5CMC).

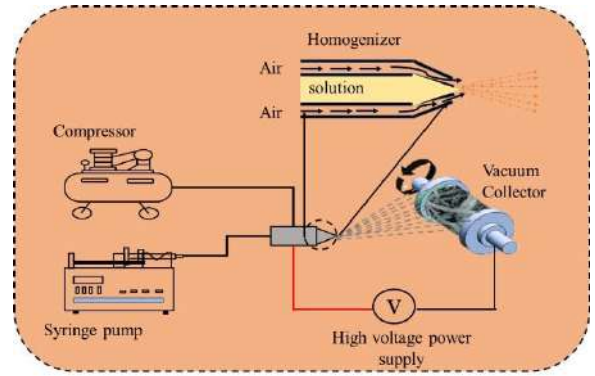


Figure 1. Schematic drawing of the electro-blowing fiber production method

2.5 Characterization Methods

2.5.1. Scanning electron microscope (SEM)

A Carl Zeiss Ultra Plus Field Emission Scanning Electron Microscope (FE-SEM) was used to examine the structures of the fibrous mats. ImageJ software was employed to process the SEM images, allowing for the calculation of the average diameter and distribution of the nanofibers. One hundred diameter measurements were taken from randomly selected images for each sample.

2.5.2. Scanning electron microscope (SEM)

To assess the interactions between different components within the fibrous mats, Fourier-transform infrared (FTIR) spectra were obtained using a Bruker ALPHA FTIR Spectrometer. This process

involved capturing detailed spectral data to identify characteristic functional groups and molecular bonds present in the samples. A total of 24 scans were recorded for each sample, covering a broad wavelength range from 400 to 4000 cm^{-1} . This range provided comprehensive insight into the chemical structure and potential interactions among the components within the mats.

2.5.3. Thermogravimetric analysis (TGA)

To examine the thermal stability and degradation patterns of the nanofiber mat, thermogravimetric analysis (TGA) was conducted using a Hitachi STA 7300 thermogravimetric analyzer (Hitachi, Japan). This analysis provided insights into the material's behavior under heat, indicating its potential performance and resilience in applications exposed to varying temperatures. During the TGA process, the samples were heated progressively from room temperature up to 550 $^{\circ}\text{C}$, with a controlled heating rate of 10 $^{\circ}\text{C}$ per minute. A steady nitrogen gas flow was maintained at 2 mL/min throughout the heating to prevent oxidation and ensure a stable, inert environment. This setup allowed for precise observation of weight loss stages and thermal decomposition characteristics, shedding light on the material's composition and degradation profile under elevated temperatures.

2.5.4. Air permeability

The air permeability of the gelatin nanofiber mats was evaluated using a Prowhite Air Test II apparatus to determine their breathability and suitability for applications requiring controlled airflow. This assessment was conducted at a controlled temperature of 25 $^{\circ}\text{C}$ within a designated circular area of 50 mm in diameter on each sample, ensuring consistency across all measurements. During each test, a steady air pressure of 100 Pa was applied to the mat, and the apparatus recorded the rate of air passage through the nanofiber structure. This setup enabled precise

measurement of air permeability, providing insight into the material's porosity and potential functionality in fields such as filtration, protective barriers, and breathable packaging.

III. RESULTS AND DISCUSSIONS

3.1 Characterization of CMCs

3.1.1. SEM

The image in Figures 2(a) and (b) reveals a distinct contrast between untreated and treated corn cob samples. In image (a), the raw corn cob surface appears rough, with irregular particle sizes and orientations. This texture reflects the presence of structural components like lignin, hemicellulose, and pectin, which contribute to the rigidity of the plant cell wall. Following chemical pre-treatment and hydrolysis, image (b) displays a smoother, more uniform surface with a noticeable sheen. This transformation results from the effective removal of non-cellulosic materials during treatment. The resulting structure is indicative of microcrystalline cellulose, characterized by increased homogeneity and clarity. The comparison between the two images confirms that the pre-treatment process successfully modified the native corn cob structure, producing a refined cellulose material. The successful removal of hemicelluloses, lignin, and pectins resulted in a purified structure, as evidenced by the SEM (Figure 2(c)) image showing the characteristic morphology of microcrystalline cellulose.

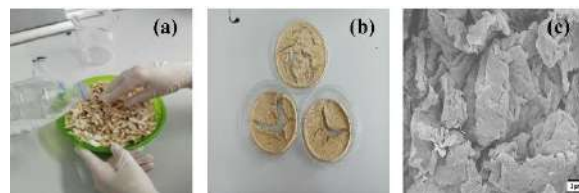


Figure 2. Images of the raw corn cob (a), isolated (b), and the SEM (c) image of CMC.

3.1.2. SEM

Figure 3(a) shows the FTIR spectra of corn cob, alkaline-treated material, bleached cellulose, and acid-

hydrolyzed cellulose. A broad band between 3340–3420 cm^{-1} corresponds to the stretching vibrations of hydrogen-bonded hydroxyl (OH) groups, while peaks around 2920 cm^{-1} are attributed to C–H stretching. In the raw biomass, the OH-related peak appears weaker due to the presence of non-cellulosic components such as waxes, hemicellulose, and lignin, which limit the exposure of hydroxyl groups. A faint shoulder around 1730 cm^{-1} indicates the presence of acetyl and uronic ester groups from trace amounts of hemicellulose. This feature disappears after alkali treatment, confirming the effective removal of hemicellulose using a 2% w/v NaOH solution [26].

The absorption band near 1640 cm^{-1} is associated with the OH bending of adsorbed water, reflecting the exposure of hydroxyl groups. The peak at 1430 cm^{-1} , linked to CH_2 bending, is characteristic of the crystalline structure in cellulose. Meanwhile, the signal at 1372 cm^{-1} relates to CH and CO bond bending in the aromatic rings of polysaccharides [27]. A distinct peak at 1254 cm^{-1} is due to CO out-of-plane stretching in lignin's aryl groups [28]. Additionally, all samples exhibit a band around 899 cm^{-1} , which corresponds to glycosidic CH deformation and OH bending—markers of β -glycosidic linkages in cellulose chains [25].

3.1.3. TGA

Thermogravimetric analysis (TGA) and derivative thermogravimetry (DTG) were used to analyze the thermal decomposition behavior of the isolated cellulose microcrystal (CMC). The corresponding TGA curve is presented in Figure 3(b). An initial weight loss of approximately 9 wt% occurred between 30°C and 105°C across all samples, primarily due to moisture evaporation. A maximum decomposition was observed near 326°C is likely associated with the release of low molecular weight residues left over from the isolation process. The most significant mass loss was recorded between 250°C and 400°C, marking

the main phase of thermal degradation. This range corresponds to the decomposition of organic constituents such as cellulose and remaining hemicellulose or lignin [28].

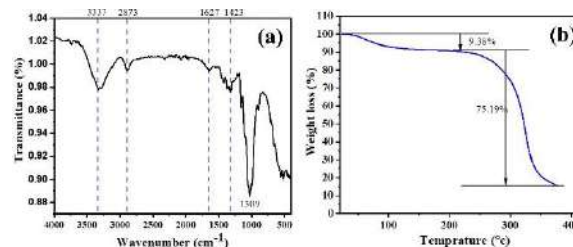


Figure 3. FTIR (a) and TGA(b) results of CMC

3.2 Characterization of Nanofibrous Mats

3.2.1. SEM analysis

The surface morphologies of G-Ch and G-Ch-1CMC, G-Ch-3CMC, and G-Ch-5CMC micro-nanofibrous mats were analyzed using scanning electron microscopy (SEM). The resulting SEM images and the fiber diameter distributions for each sample are presented in Figure 2. The incorporation of cellulose microcrystals (CMC) into gelatin/chitosan nanofibers profoundly influences their morphology and fiber diameter, which are critical for optimizing performance in food packaging applications. As shown in Figure 4(a)&(b), with the addition of one percent CMC, there was a slight increment in fiber diameter from 642.19 ± 40.36 nm to 699 ± 20.32 nm. This might be due to the high crystallinity of cellulose microcrystals, enabling them to function as reinforcing agents within the nanofiber matrix and affecting structural integrity [29]. Furthermore, the interaction between chitosan and CMCs, driven by electrostatic and hydrogen bonding, modifies the solution's rheological properties, enhancing dispersion and stability during fiber production [30].

Increasing the CMC concentration to 3% further reduced the fiber diameter to 524.39 ± 38.18 nm. This reduction may be attributed to improved solution conductivity during electro-blowing, which enhances polymer chain alignment and jet stretching, leading to

finer fibers. Similar findings were reported by Amini et al. [31], who observed that low CMC concentrations reduce fiber diameter by increasing solution conductivity during electrospinning. This enhancement facilitates polymer chain alignment and jet stretching, as demonstrated in studies on biopolymer blends. However, exceeding 5% CMC increases solution viscosity, leading to thicker fibers or irregular morphologies due to restricted polymer flow, a phenomenon corroborated by DE Sameen et al. [32]. This study focuses on optimizing the electrospinning parameters..

Morphologically, well-dispersed CMC stabilizes the electrospinning jet, improving fiber uniformity and minimizing bead formation. In contrast, excessive CMC loading can cause defects such as fiber branching or aggregation, as reported by Kumar et al. [33] in nanocellulose-reinforced composites. These effects result from a balance between conductivity-driven fiber thinning and viscosity-induced resistance, along with interfacial hydrogen bonding between CMC's hydroxyl groups and gelatin/chitosan, which enhances matrix compatibility. For food packaging applications, optimally tuned CMC concentrations produce thinner, uniform fibers that improve oxygen and moisture barrier properties through denser packing. Recent advancements emphasize the role of dispersion techniques, such as sonication in acetic acid, and precise parameter adjustments, like lower flow rates for high-viscosity blends, to minimize defects and enable scalable production of biodegradable, high-performance nanofiber mats. Overall, these findings highlight CMC's potential in eco-friendly packaging, provided its concentration and processing conditions are carefully optimized to balance structural integrity and functional performance.

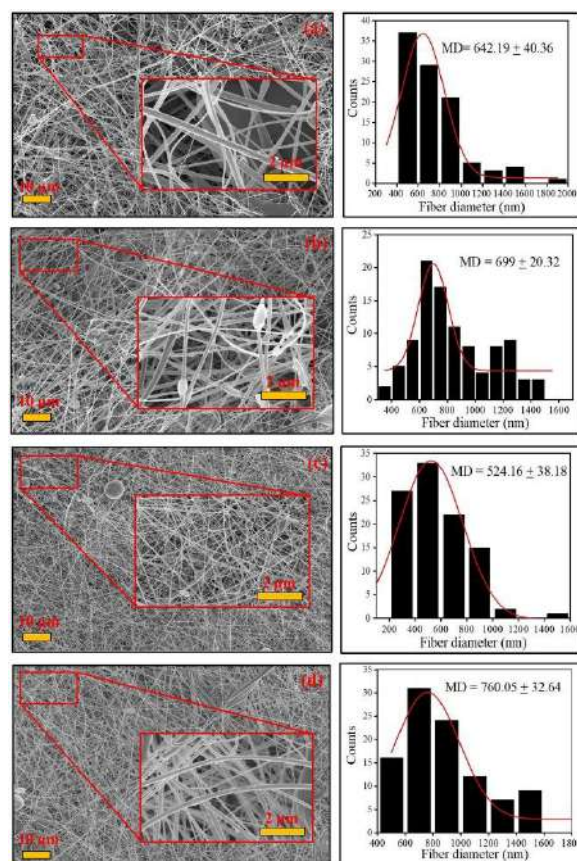


Figure 4. SEM images and fiber distribution of G-Ch (a), G-Ch-1CMC(b), G-Ch-3CMC(c), and G-Ch-5CMC(d) nanofibrous mats.

3.2.2. FTIR analysis

FTIR spectroscopy was employed to analyze the nanofibers and investigate potential interactions between the polymers. Figure 5(a) presents the FTIR spectra of G-Ch, G-Ch-1CMC, G-Ch-3CMC, and G-Ch-5CMC nanofibrous mats. Key absorption bands were identified to facilitate comparison between the different samples. In the FTIR spectrum of CNC powder, the bands observed between $3300\text{--}3400\text{ cm}^{-1}$ and $2800\text{--}2900\text{ cm}^{-1}$ correspond to the stretching vibrations of O-H and C-H groups, respectively. Additionally, peaks at 1645 cm^{-1} , 1418 cm^{-1} , and 1321 cm^{-1} are associated with OH bending of adsorbed water, symmetric CH_2 bending, and the bending vibrations of C-H and C-O groups in polysaccharide rings, respectively[34–36].

The FTIR spectrum of G-Ch, G-Ch-1CMC, G-Ch-3CMC, and G-Ch-5CMC nanofibers revealed

characteristic peaks from both polymers. The bands at 1633 cm^{-1} and 1537 cm^{-1} correspond to the N-H stretching vibrations of amide I and II, respectively, while the peak at 1242 cm^{-1} is attributed to amide III [37]. FTIR spectra of chitosan-gelatin nanofibers at varying concentrations revealed that increasing chitosan content enhanced the intensity of the absorption band in the $1155\text{--}1025\text{ cm}^{-1}$ region, corresponding to C-O stretching vibrations in the glycosidic bonds of chitosan's polysaccharide structure [38]. Additionally, this peak shifted to a lower wavenumber, suggesting hydrogen bond formation between gelatin and chitosan within the nanofibers. Additionally, the increased intensity of the band around $3200\text{--}3500\text{ cm}^{-1}$ indicates strong molecular compatibility, likely due to hydrogen bonding between the polymers. This analysis confirms that the characteristic bands of G and Ch remain present in the G-Ch nanofibers, supporting the miscibility of these components after the spinning process [35].

3.2.3. Thermal analysis

The thermal stability of nanofiber mats is crucial for food packaging, ensuring structural integrity and functionality under varying temperatures. Figure 5(b) presents the TGA result of nanofiber mats. Their resistance to decomposition at high temperatures enhances durability, making them effective for long-term use[39]. TGA analysis was conducted to assess the thermal stability of the developed nanofibers. Thermogravimetric analysis (TGA) curves of G-Ch nanofibers with varying CMC concentrations are shown in Figure 3(b), revealing two major weight loss stages between $30\text{ }^{\circ}\text{C}$ and $450\text{ }^{\circ}\text{C}$. The first stage, occurring between $30\text{--}152\text{ }^{\circ}\text{C}$, is associated with the evaporation of absorbed water and residual acetic acid retained within the nanofiber structure [40]. The second stage, observed between $210\text{--}400\text{ }^{\circ}\text{C}$, corresponds to the thermal decomposition of G and Ch

polymeric chains, resulting in a significant weight loss of approximately 53.78% [41]. As observed in Figure 3(b), thermal stability improves with the addition of 1% CMC but declines when CMC concentration reaches 3% and 5%. This could be due to moderate CUR levels ($\leq 1\%$) enhancing fiber stability through intermolecular hydrogen bonding. In comparison, excessive CMC ($>3\%$) disrupts polymeric chain rearrangement and crystallization, weakening the compact G-Ch matrix structure[35]. This suggests that CMC incorporation has little effect on the thermal degradation pattern, confirming its stable integration within the nanofiber matrix [42].

3.2.4. XRD analysis

X-ray diffraction (XRD) analysis was performed to examine the crystalline structure of the nanofiber membranes, as shown in Figure 3(c). The XRD patterns reveal no distinct crystal peaks, confirming the amorphous nature of the membranes. A broad diffraction peak at approximately 21° is characteristic of gelatin-chitosan composite membranes. This peak likely corresponds to the triple-helical crystalline structure of collagen with a 1.1 nm periodicity, the random coil conformation of macromolecules, or the semi-crystalline nature of biopolymers [43,44]. The XRD patterns of membranes with varying CMC content remain similar to those without it, suggesting that CMC does not significantly influence crystallinity. Similar findings were reported by Jun Chean et al.[45], who developed an acellular gelatin-chitosan-cellulose nanocrystal (GCCNC) scaffold as a potential wound dressing and analyzed its crystallographic structure using X-ray diffraction (XRD). Their study found that the G10CNC scaffold exhibited higher intensity, indicating the successful incorporation of CNCs. However, the C10CNC scaffold showed reduced intensity despite containing the same amount of CNCs, which was attributed to genipin crosslinking, altering the semi-crystalline

structure of chitosan. Additionally, all GCCNC scaffolds were amorphous, with G3C7CNC being the most amorphous. These findings support our results, highlighting the influence of CNCs and crosslinking on scaffold crystallinity, which plays a critical role in material properties for food packaging applications.

3.2.5. Air permeability

The air permeability results presented in Figure 5(d) demonstrate a progressive increase in permeability with the addition of carboxymethyl cellulose (CMC) to the G-Ch matrix. The pure G-Ch sample exhibited the lowest air permeability, approximately 2.0 mm/s, indicating a relatively dense and compact structure. Introducing 1% CMC (G-Ch-1CMC) led to a slight increase in air permeability, while further increases to 3% and 5% CMC (G-Ch-3CMC and G-Ch-5CMC) resulted in more substantial improvements, with values reaching approximately 2.6 ± 0.9 mm/s. This trend suggests that higher CMC loading promotes a more open network within the material, facilitating easier air flow. The flexible chains of CMC likely interfere with the dense packing of the chitosan matrix, creating microvoids and channels that enhance permeability. This behavior aligns with findings reported by Ahuja et al. [46] showed that gelatin–chitosan films with 1–5 wt% microcrystalline cellulose exhibited 10–30 % higher air permeability than neat films, an effect attributed to MCC aggregation and the formation of micro-voids under standard casting conditions. These findings support the notion that CMC acts as a porosity enhancer when combined with biopolymers like chitosan. Overall, the observed increase in air permeability with higher CMC content confirms that CMC incorporation effectively modulates the air transport properties of G-Ch composites. This enhancement could be particularly valuable for applications requiring breathability, such as filtration membranes, wound dressings, or biodegradable packaging materials.

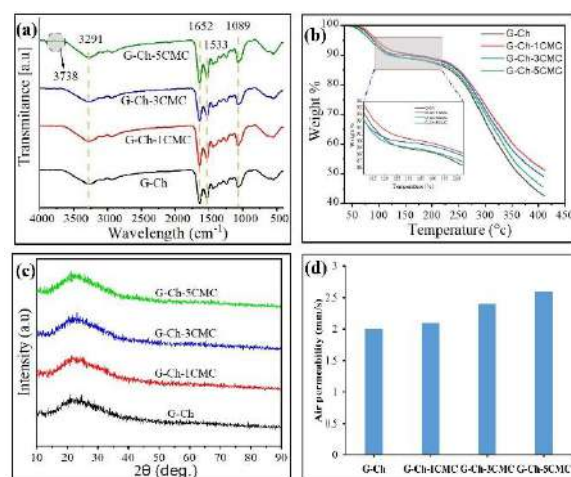


Figure 5. FTIR spectroscopy (a), TGA (b), XRD (c), and air permeability (d) analysis of G-Ch, G-Ch-1CMC, G-Ch-3CMC, and G-Ch-5CMC nanofiber mats

IV. CONCLUSIONS

Gelatin, as a biodegradable and edible biopolymer, holds promise for sustainable food packaging applications. However, its inherent limitations in mechanical strength and antibacterial efficacy necessitate functional enhancement. In this study, the incorporation of chitosan effectively addressed the antibacterial shortcomings of gelatin, while the addition of corn-cob-derived cellulose microcrystals (CMC) contributed to improved mechanical reinforcement. Structural and thermal analyses using SEM, XRD, and TGA confirmed the successful integration of CMC into the polymer matrix, revealing enhanced fiber morphology, increased crystallinity, and improved thermal stability. Together, these components produced nanofiber mats with potential applicability in active food packaging systems. Nevertheless, the observed increase in air permeability with higher CMC content highlights the need for further optimization. Future studies will focus on a comprehensive evaluation of mechanical performance and antibacterial properties to fine-tune these biopolymer-based nanofibers for a practical and efficient food packaging solution.

ACKNOWLEDGMENT

This study was supported by the TUBITAK 2209-A program.

REFERENCES

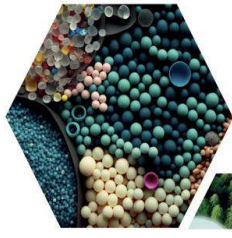
- Min, T., Zhou, L., Sun, X., Du, H., Zhu, Z., and Wen, Y., "Electrospun functional polymeric nanofibers for active food packaging: A review", *Food Chemistry*, 391: 133239 (2022).
"https://doi.org/10.1016/j.foodchem.2022.133239"
- Gulzar, S., Tagrida, M., Prodpran, T., and Benjakul, S., "Antimicrobial film based on polylactic acid coated with gelatin/chitosan nanofibers containing nisin extends the shelf life of Asian seabass slices", *Food Packaging And Shelf Life*, 34: 100941 (2022).
"https://doi.org/10.1016/j.fpsl.2022.100941"
- Amjadi, S., Emaminia, S., Davudian, S. H., Pourmohammad, S., Hamishehkar, H., and Roufegarinejad, L., "Preparation and characterization of gelatin-based nanocomposite containing chitosan nanofiber and ZnO nanoparticles", *Carbohydrate Polymers*, 216: 376–384 (2019).
"https://doi.org/10.1016/j.carbpol.2019.03.062"
- Wu, F., Misra, M., and Mohanty, A. K., "Challenges and new opportunities on barrier performance of biodegradable polymers for sustainable packaging", *Progress In Polymer Science*, 117: 101395 (2021).
"https://doi.org/10.1016/j.progpolymsci.2021.101395"
- Arkoun, M., Daigle, F., Heuzey, M.-C., and Ajji, A., "Mechanism of action of electrospun chitosan-based nanofibers against meat spoilage and pathogenic bacteria", *Molecules*, 22 (4): 585 (2017).
"https://doi.org/10.3390/molecules22040585"
- Balasubramaniam, S. L., Patel, A. S., and Nayak, B., "Surface modification of cellulose nanofiber film with fatty acids for developing renewable hydrophobic food packaging", *Food Packaging And Shelf Life*, 26: 100587 (2020).
"https://doi.org/10.1016/j.fpsl.2020.100587"
- Fonseca, L. M., dos Santos Cruxen, C. E., Bruni, G. P., Fiorentini, Á. M., da Rosa Zavareze, E., Lim, L.-T., and Dias, A. R. G., "Development of antimicrobial and antioxidant electrospun soluble potato starch nanofibers loaded with carvacrol", *International Journal Of Biological Macromolecules*, 139: 1182–1190 (2019).
"https://doi.org/10.1016/j.ijbiomac.2019.08.096"
- Doğan, N., Doğan, C., Eticha, A. K., Gungor, M., and Akgul, Y., "Centrifugally spun micro-nanofibers based on lemon peel oil/gelatin as novel edible active food packaging: Fabrication, characterization, and application to prevent foodborne pathogens E. coli and S. aureus in cheese", *Food Control*, 139: 109081 (2022).
"https://doi.org/10.1016/j.foodcont.2022.109081"
- Flórez, M., Guerra-Rodríguez, E., Cazón, P., and Vázquez, M., "Chitosan for food packaging: Recent advances in active and intelligent films", *Food Hydrocolloids*, 124: 107328 (2022).
"https://doi.org/10.1016/j.foodhyd.2021.107328"
- Eticha, A. K. and Akgul, Y., "Optimization of gelatin nanofibrous webs fabricated via electrically assisted solution blow spinning for air filtration applications", *International Journal Of Environmental Science And Technology*, 1–18 (2024).
"https://doi.org/10.1007/s13762-024-05482-2"
- Lu, Y., Luo, Q., Chu, Y., Tao, N., Deng, S., Wang, L., and Li, L., "Application of gelatin in food packaging: A review", *Polymers*, 14 (3): 436 (2022).
"https://doi.org/10.3390/polym14030436"
- Zhang, X., Do, M. D., Casey, P., Sulistio, A., Qiao, G. G., Lundin, L., Lillford, P., and Kosaraju, S., "Chemical Modification of Gelatin by a Natural Phenolic Cross-linker, Tannic Acid", *Journal Of Agricultural And Food Chemistry*, 58 (11): 6809–6815 (2010).
"https://doi.org/10.1021/jf1004226"
- Gulzar, S., Tagrida, M., Nilsuwan, K., Prodpran, T., and Benjakul, S., "Electrospinning of gelatin/chitosan nanofibers incorporated with tannic acid and chitoooligosaccharides on polylactic acid film: Characteristics and bioactivities", *Food Hydrocolloids*, 133: 107916 (2022).
"https://doi.org/10.1016/j.foodhyd.2022.107916"
- Akhrouy, G., Eticha, A. K., Dogan, C., Dogan, N., Calisir, M. D., Toptas, A., Aziz, F., and Akgul, Y., "Electro-blown micro-nanofibrous mats with *Origanum elongatum* essential oil for enhancing the shelf life of tomato (*Solanum lycopersicum*)", *International Journal Of Food Science & Technology*, ijfs.17600 (2024).
"https://doi.org/10.1111/ijfs.17600"

15. Noorbakhsh-Soltani, S. M., Zerafat, M. M., and Sabbaghi, S., "A comparative study of gelatin and starch-based nano-composite films modified by nano-cellulose and chitosan for food packaging applications", *Carbohydrate Polymers*, 189: 48–55 (2018).
"https://doi.org/10.1016/j.carbpol.2018.02.012"
16. Bombin, A. D. J., Dunne, N. J., and McCarthy, H. O., "Electrospinning of natural polymers for the production of nanofibres for wound healing applications", *Materials Science And Engineering: C*, 114: 110994 (2020).
"https://doi.org/10.1016/j.msec.2020.110994"
17. Kargarzadeh, H., Mariano, M., Huang, J., Lin, N., Ahmad, I., Dufresne, A., and Thomas, S., "Recent developments on nanocellulose reinforced polymer nanocomposites: A review", *Polymer*, 132: 368–393 (2017).
"https://doi.org/10.1016/j.polymer.2017.09.043"
18. Zhou, C., Chu, R., Wu, R., and Wu, Q., "Electrospun Polyethylene Oxide/Cellulose Nanocrystal Composite Nanofibrous Mats with Homogeneous and Heterogeneous Microstructures", *Biomacromolecules*, 12 (7): 2617–2625 (2011).
"https://doi.org/10.1021/bm200401p"
19. Wei, Z., "Research process of polymer nanofibers prepared by melt spinning", (2018).
"doi:10.1088/1757-899X/452/2/022002"
20. ABI, J., Ahmed, S. B., Dogan, C., Dogan, N., and Akgul, Y., "Production and Characterization of Electro-Blown Nanofibers Incorporated with Pine Pollen for Fast-Dissolving Tablet Applications", *Available At SSRN 4768545*,.
"https://doi.org/10.1016/j.jddst.2024.106222"
21. Ahmed, S. B., Doğan, N., Doğan, C., and Akgul, Y., "A Novel Approach to Crosslink Gelatin Nanofibers Through Neutralization-Induced Maillard Reaction", *Food And Bioprocess Technology*, 1–15 (2023).
"https://doi.org/10.1007/s11947-023-03146-6"
22. ETİCHA, A. K., TOPTAŞ, A., AKGÜL, Y., and KILIÇ, A., "Electrically assisted solution blow spinning of PVDF/TPU nanofibrous mats for air filtration applications", *Turkish Journal Of Chemistry*, 47 (1): 47–53 (2023).
"https://doi.org/10.55730/1300-0527.3515"
23. Akhouy, G., Aziz, K., Gebrati, L., El Achaby, M., Akgul, Y., Yap, P.-S., Agustiono Kurniawan, T., and Aziz, F., "Recent applications on biopolymers electrospinning: strategies, challenges and way forwards", *Polymer-Plastics Technology And Materials*, 1–22 (2023).
"https://doi.org/10.1080/25740881.2023.2234459"
24. Dadol, G. C., Kilic, A., Tijing, L. D., Lim, K. J. A., Cabatingan, L. K., Tan, N. P. B., Stojanovska, E., and Polat, Y., "Solution blow spinning (SBS) and SBS-spun nanofibers: Materials, methods, and applications", *Materials Today Communications*, 25: 101656 (2020).
"https://doi.org/10.1016/j.mtcomm.2020.101656"
25. Singh, H. K., Patil, T., Vineeth, S. K., Das, S., Pramanik, A., and Mhaske, S. T., "Isolation of microcrystalline cellulose from corn stover with emphasis on its constituents: corn cover and corn cob", *Materials Today: Proceedings*, 27: 589–594 (2020).
"https://doi.org/10.1016/j.matpr.2019.12.065"
26. Thomas, M. G., Abraham, E., Jyotishkumar, P., Maria, H. J., Pothan, L. A., and Thomas, S., "Nanocelluloses from jute fibers and their nanocomposites with natural rubber: Preparation and characterization", *International Journal Of Biological Macromolecules*, 81: 768–777 (2015).
"https://doi.org/10.1016/j.ijbiomac.2015.08.053"
27. Naduparambath, S., Jinita, T. V., Shaniba, V., Sreejith, M. P., Balan, A. K., and Purushothaman, E., "Isolation and characterisation of cellulose nanocrystals from sago seed shells", *Carbohydrate Polymers*, 180: 13–20 (2018).
"https://doi.org/10.1016/j.carbpol.2017.09.088"
28. Moriana, R., Vilaplana, F., and Ek, M., "Cellulose nanocrystals from forest residues as reinforcing agents for composites: a study from macro-to nano-dimensions", *Carbohydrate Polymers*, 139: 139–149 (2016).
"https://doi.org/10.1016/j.carbpol.2015.12.020"
29. Morsi, M., Oraby, A., Elshahawy, A., and Abd El-Hady, R., "Preparation, structural analysis, morphological investigation and electrical properties of gold nanoparticles filled polyvinyl alcohol/carboxymethyl cellulose blend", *Journal Of Materials Research And Technology*, 8 (6): 5996–6010 (2019).
"https://doi.org/10.1016/j.jmrt.2019.09.074"
30. Li, Z., Mei, S., Dong, Y., She, F., and Kong, L., "High efficiency fabrication of chitosan composite nanofibers with uniform morphology via centrifugal spinning", *Polymers*, 11 (10):

- 1550 (2019).
"https://doi.org/10.3390/polym11101550"
31. Abdollahi, A., Roghani-Mamaqani, H., Salami-Kalajahi, M., Razavi, B., and Sahandi-Zangabad, K., "Encryption and optical authentication of confidential cellulosic papers by ecofriendly multi-color photoluminescent inks", *Carbohydrate Polymers*, 245: 116507 (2020).
"https://doi.org/10.1016/j.carbpol.2020.116507"
32. Sameen, D. E., Ahmed, S., Lu, R., Li, R., Dai, J., Qin, W., Zhang, Q., Li, S., and Liu, Y., "Electrospun nanofibers food packaging: trends and applications in food systems", *Critical Reviews In Food Science And Nutrition*, 62 (22): 6238–6251 (2022).
"https://doi.org/10.1080/10408398.2021.1899128"
33. Gong, X., Kalantari, M., Aslanzadeh, S., and Boluk, Y., "Interfacial interactions and electrospinning of cellulose nanocrystals dispersions in polymer solutions: a review", *Journal Of Dispersion Science And Technology*, 43 (7): 945–977 (2022).
"https://doi.org/10.1080/01932691.2020.1847137"
34. Kargarzadeh, H., Sheltami, R. M., Ahmad, I., Abdullah, I., and Dufresne, A., "Cellulose nanocrystal: A promising toughening agent for unsaturated polyester nanocomposite", *Polymer*, 56: 346–357 (2015).
"https://doi.org/10.1016/j.polymer.2014.11.054"
35. Habibi, S. and Hajinasrollah, K., "Electrospinning of nanofibers based on chitosan/gelatin blend for antibacterial uses", *Russian Journal Of Applied Chemistry*, 91 (5): 877–881 (2018).
"https://doi.org/10.1134/S1070427218050191"
36. Hivechi, A., Bahrami, S. H., and Siegel, R. A., "Drug release and biodegradability of electrospun cellulose nanocrystal reinforced polycaprolactone", *Materials Science And Engineering: C*, 94: 929–937 (2019).
"https://doi.org/10.1016/j.msec.2018.10.037"
37. Jalaja, K., Naskar, D., Kundu, S. C., and James, N. R., "Potential of electrospun core-shell structured gelatin-chitosan nanofibers for biomedical applications", *Carbohydrate Polymers*, 136: 1098–1107 (2016).
"https://doi.org/10.1016/j.carbpol.2015.10.014"
38. Kumar, S., Mudai, A., Roy, B., Basumatary, I. B., Mukherjee, A., and Dutta, J., "Biodegradable hybrid nanocomposite of chitosan/gelatin and green synthesized zinc oxide nanoparticles for food packaging", *Foods*, 9 (9): 1143 (2020).
"https://doi.org/10.3390/foods9091143"
39. Duan, M., Sun, J., Huang, Y., Jiang, H., Hu, Y., Pang, J., and Wu, C., "Electrospun gelatin/chitosan nanofibers containing curcumin for multifunctional food packaging", *Food Science And Human Wellness*, 12 (2): 614–621 (2023).
"https://doi.org/10.1016/j.fshw.2022.07.064"
40. Rojas, A., Velasquez, E., Pina, C., Galotto, M. J., and de Dicastillo, C. L., "Designing active mats based on cellulose acetate/polycaprolactone core/shell structures with different release kinetics", *Carbohydrate Polymers*, 261: 117849 (2021).
"https://doi.org/10.1016/j.carbpol.2021.117849"
41. Liu, Y., Qin, Y., Bai, R., Zhang, X., Yuan, L., and Liu, J., "Preparation of pH-sensitive and antioxidant packaging films based on κ-carrageenan and mulberry polyphenolic extract", *International Journal Of Biological Macromolecules*, 134: 993–1001 (2019).
"https://doi.org/10.1016/j.ijbiomac.2019.05.175"
42. Ribeiro, A. S., Costa, S. M., Ferreira, D. P., Abidi, H., and Fanguero, R., "Development of chitosan-gelatin nanofibers with cellulose nanocrystals for skin protection applications", *Key Engineering Materials*, 893: 45–55 (2021).
"https://doi.org/10.4028/www.scientific.net/KE M.893.45"
43. Qiao, C., Ma, X., Zhang, J., and Yao, J., "Molecular interactions in gelatin/chitosan composite films", *Food Chemistry*, 235: 45–50 (2017).
"https://doi.org/10.1016/j.foodchem.2017.05.045"
44. Li, J., Shi, X., Yang, K., Guo, L., Yang, J., Lan, Z., Guo, Y., Xiao, L., and Wang, X., "Fabrication and characterization of carvacrol encapsulated gelatin/chitosan composite nanofiber membrane as active packaging material", *International Journal Of Biological Macromolecules*, 282: 137114 (2024).
"https://doi.org/10.1016/j.ijbiomac.2024.137114"
45. Cheah, Y. J., Yunus, M. H. M., Fauzi, M. B., Tabata, Y., Hiraoka, Y., Phang, S. J., Chia, M. R., Buyong, M. R., and Yazid, M. D., "Gelatin-chitosan-cellulose nanocrystals as an acellular scaffold for wound healing application: fabrication, characterisation and cytocompatibility towards primary human skin

cells", *Cellulose*, 30 (8): 5071–5092
(2023). "<https://doi.org/10.1007/s10570-023-05212-w>"

46. "ANTIBACTERIAL COMPOSITE FILM
PREPARED FROM MICROCRYSTALLINE
CELLULOSE-CHITOSAN FROM LIBR
SOLUTION WITH GARLIC EXTRACTION",
*International Journal Of Biology, Pharmacy
And Allied Sciences*, 12 (1): (2023).
"<https://doi.org/10.31032/IJBPAS/2023/12.1.6714>"



16 ULUSLARARASI
LİF VE POLİMER
ARAŞTIRMALARI
SEMPOZYUMU

16th INTERNATIONAL FIBER AND POLYMER RESEARCH SYMPOSIUM

Sürdürülebilir ve İşlevsel Lif ve Polimerler
Sustainable and Functional Fibers & Polymers



9-10 Mayıs
May 2025

İstanbul Teknik Üniversitesi
Gümüşsuyu Prof. Dr. Necmettin Erbakan Yerleşkesi
İstanbul Technical University
Gumussuyu Prof. Dr. Necmettin Erbakan Campus

Curing properties of covalently bonded polyoxazoline-imidazole thermal latent curing agents for one-component epoxy resins

Ceren Özsaltık^{a,b}, Asu Ece Ateşpare^{a,b}, Cuma Ali Uçar^{a,b}, Bekir Dizman^{a,b}

^aIntegrated Manufacturing Technologies Research and Application Center & Composite Technologies Center of Excellence, Sabanci University, Istanbul, Turkey, 34906

^bFaculty of Engineering and Natural Sciences, Materials Science and Nano Engineering, Sabanci University, Istanbul, Turkey, 34956

*Corresponding author: Bekir Dizman, bekirdizman@sabanciuniv.edu

ABSTRACT

Epoxy resins are the most commonly utilized resins for the fabrication of polymer matrix composites. One-component epoxy resins (OCERs) are commonly utilized since they are easier to process, have a longer shelf life, produce higher-end products, and use less energy than two-component epoxy resins. Increasing the shelf life and modifying the curing temperature are crucial for OCERs. To address stability issues in OCERs, latent curing agents are employed. In this study, polyoxazoline-imidazole (POZ-Im) thermal latent curing agents (TLCs) were prepared by synthesizing different types of POZs and terminating them with imidazole. Diglycidyl ether bisphenol A (DGEBA) resin was mixed with POZ-Im TLCs to produce OCERs, and the curing behavior of the resulting OCERs was examined with DSC. The stability, uniformity, and thermal latency behavior of the OCERs were examined in relation to the hydrophilicity of the POZ.

Keywords: One-component epoxy resins; Imidazole; Polyoxazoline; Thermal latent curing agents;

I. INTRODUCTION

Epoxy resins are widely used as matrix materials in polymer matrix composites (PMCs) in aerospace, automotive and defense industry applications. These resins can be prepared as either single or two-component systems. Commonly used two-component resins contain a resin and a curing agent separately. Since these components react rapidly with each other, the shelf life of the mixtures is very short, which makes the process inefficient and costly [1,2]. Unlike two-component resins, one-component epoxy resins

(OCERs) are available as a combination of resin and a latent curing agent. OCERs are stable at room temperature and can be cured at high temperatures. These resins are highly preferred because they have a longer shelf life compared to two-component resins and initiate curing at high temperatures with a longer curing time [2]. In addition, OCERs save energy and money by eliminating the need for cooling during storage and transportation [3]. Thanks to the benefits they provide, they provide longer shelf life, precisely tuned curing performance, ease of processing, increased energy efficiency, and reduced costs.

Thermal latent curing agents (TLCs) are widely used due to their ease of use. Examples of TLCs include complexes or conjugates formed by different imidazole derivatives with polyethylene glycol (PEG) and polymer-curing agent systems in matrix or core-shell structures obtained by encapsulating the curing agent with different polymers [4]. In studies where PEG and imidazole were used to form complexes and conjugates, it was determined that the shelf life of epoxy formulations was extended, and curing temperatures increased. Since the copolymers used in these systems were synthesized by the free radical polymerization method, the polymer structure and therefore the polymer properties could not be controlled well. Complexes of polyoxazoline (POZ) polymers with imidazole have been shown in recent research to thermally hinder epoxy curing. [5-7].

POZs are obtained by polymerizing oxazoline monomers using the cationic ring-opening polymerization method. Controlled polymerization allows the synthesis of well-defined polymers, which in turn results in better control of chemical and physical properties of the polymers. Properties such as hydrophilicity, amphiphilicity, composition, shape and molecular weight of POZs can be controlled very easily [8-13]. In this study, POZ-based polymers were synthesized and terminated with imidazole to obtain TLCs.

II. EXPERIMENTAL METHOD

2.1 Materials and Preparation Techniques

2-Ethyl-2-oxazoline (EOZ) and 2-phenyl-2-oxazoline (PhOZ) monomers were commercially available. 2-Propyl-2-oxazoline (PrOZ) was synthesized using the nitrile route reported in literature [14]. POZs of all monomers were synthesized following the procedures reported by our group except for the termination step [5]. Polymerizations were conducted in round-bottom flasks dried at 120 °C and cooled under nitrogen. 4M concentration of monomers in chlorobenzene was used

for the polymerizations considering the total concentration of monomers in each reaction. Triflic acid (TfOH) was used as the initiator and termination was performed with imidazole dissolved in DCM overnight.

The prepared POZ-Im conjugates were cooled to subzero temperature and ground with a mortar and pestle. The ground powder was mixed with DGEBA resin at 5% molar ratio (imidazole to epoxy) using a homogenizer in a glass vial at 1500 rpm for 20 min to prepare the OCERs.

2.1.1. Characterization of materials

To analyze the curing properties of OCERs, a Mettler Toledo HP DSC 2+ instrument was used. The dynamic DSC thermograms were obtained from the first heating run in the range of 25 to 250 °C with a heating rate of 10 °C/min under a nitrogen atmosphere.

III. RESULTS AND DISCUSSIONS

Thermal latency of the OCERs were analyzed using a dynamic DSC analysis. Three different monomers were used to prepare the POZ-Im thermal latent curing agents. The impact of their compatibility with DGEBA on the curing temperature was examined because of the differences in their hydrophilicity: PEOZ is the most hydrophilic and PPhOZ is the most hydrophobic. **Figures 1-3** display the dynamic DSC thermograms of the OCERs. The thermograms of all of the samples had a shoulder, suggesting a two-step curing process. The OCERs containing PEOZ-Im, PPrOZ-Im, and PPhOZ-Im had corresponding left limit values of 91.75 °C, 103.28 °C, and 94.22 °C, respectively. Furthermore, the measured curing enthalpy values were 89.11 J/g, 86.12 J/g, and 151.26 J/g, respectively. The highest latency was obtained with PPrOZ-Im, which has a moderate level of hydrophobicity among the three of them.

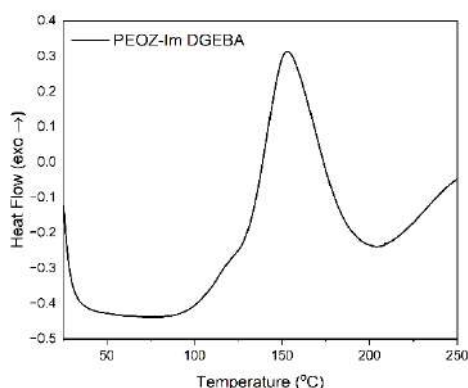


Figure 1. DSC thermogram of the OCER with PEOZ-Im TLC

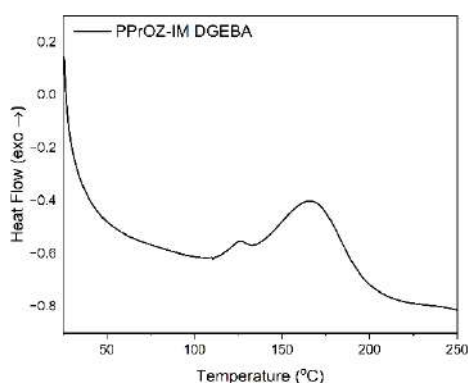


Figure 2. DSC thermogram of the OCER with PPrOZ-Im TLC

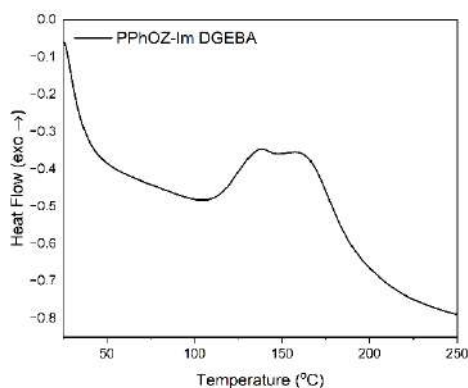


Figure 3. DSC thermogram of the OCER with PPhOZ-Im TLC

IV. CONCLUSIONS

These findings show that POZ-Im TLCs have the potential to be efficient TLCs by improving thermal latency to the DGEBA curing process. Furthermore, the POZ-Im TLCs' overall latency performance

differences were not substantially different, indicating that the three polymers offer similar thermal latency during epoxy curing. The TLCs' and OCERs' controlled and simple syntheses make them incredibly effective. They could be useful tools for improving energy efficiency and regulating the quality of the finished product in the composite industry.

ACKNOWLEDGMENT

This work has been carried out in the Sabanci University Integrated Manufacturing Technologies Research and Application Center (SUIMC). This work was supported by the Scientific and Technological Research Council of Turkey (TUBITAK) with project code 121Z597.

REFERENCES

- [1] Frick K. (2009). Two Component Adhesive of Epoxy resins and Amine Compound. US Patent 7,511,097
- [2] Antelmann B. (2007). Use of Urea Derivatives as Accelerators for Epoxy Resins. US Patent 0,027,274
- [3] Lal G. (2017). One Component Epoxy Curing Agents Comprising Hydroxyalkylamino Cycloalkanes. EP 3,199,564
- [4] Chen, K. L., Shen, Y. H., Yeh, M. Y., & Wong, F. F. (2012). Complexes of imidazole with poly (ethylene glycol) s as the thermal latency catalysts for epoxy–phenolic resins. *Journal of the Taiwan Institute of Chemical Engineers*, 43(2), 306-312.
- [5] Atespare, A. E., Behrooz Kohlan, T., Salamatgharamaleki, S., Yildiz, M., Menciloglu, Y. Z., Unal, S., & Dizman, B. (2024). Poly (2-alkyl/aryl-2-oxazoline)-imidazole complexes as thermal latent curing agents for epoxy resins. *ACS omega*, 9(34), 36398-36410.
- [6] Behrooz Kohlan, T., Atespare, A. E., Yildiz, M., Menciloglu, Y. Z., Unal, S., & Dizman, B. (2023). Amphiphilic Polyoxazoline Copolymer–Imidazole

Complexes as Tailorable Thermal Latent Curing Agents for One-Component Epoxy Resins. *ACS omega*, 8(49), 47173-47186.

Substituted-2-Oxazolines. *J. Comb. Chem.* **2009**, 11 (2), 274– 280, DOI: 10.1021/cc800174d

[7] Salamatgharamaleki, S., Atespare, A. E., Behroozi Kohlan, T., Yildiz, M., Menciloglu, Y. Z., Unal, S., & Dizman, B. (2025). Partially Hydrolyzed Poly (2-alkyl/aryl-2-oxazoline) s as Thermal Latent Curing Agents: Effect of Composition and Pendant Groups on Curing Behavior. *ACS Omega*.

[8] Zalipsky, S., Hansen, C. B., Oaks, J. M., & Allen, T. M. 1996. "Evaluation of blood clearance rates and biodistribution of poly (2-oxazoline)-grafted liposomes." *Journal of pharmaceutical sciences*, 85(2), 133-137.

[9] Gaertner, F. C., Luxenhofer, R., Blechert, B., Jordan, R., & Essler, M. 2007. "Synthesis, biodistribution and excretion of radiolabeled poly (2-alkyl-2-oxazoline) s". *Journal of Controlled Release*, 119(3), 291-300.

[10] Adams, N., & Schubert, U. S. 2007. "Poly (2-oxazolines) in biological and biomedical application contexts." *Advanced drug delivery reviews*, 59(15), 1504-1520.

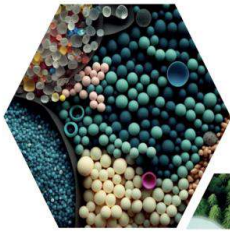
[11] Kempe, K., Lobert, M., Hoogenboom, R. & Schubert, U. S. 2009. "Screening the synthesis of 2-substituted-2-oxazolines." *J. Comb. Chem.* 11, 274– 280

[12] Viegas, T. X., Bentley, M. D., Harris, J. M., Fang, Z., Yoon, K., Dizman, B., ... & Veronese, F. M. (2011). Polyoxazoline: chemistry, properties, and applications in drug delivery. *Bioconjugate chemistry*, 22(5), 976-986.

[13] Moreadith, R. W. 2017. "Clinical development of a poly(2-oxazoline) (POZ) polymer therapeutic for the treatment of Parkinson's disease – Proof of concept of POZ as a versatile polymer platform for drug development in multiple therapeutic indications." *Eur. Polym. J.* 88, 524–552

[14] Kempe, K.; Lobert, M.; Hoogenboom, R.; Schubert, U. S. Screening the Synthesis of 2-

16. Uluslararası Lif ve Polimer Araştırmaları Sempozyumu (16. ULPAS)
9-10 Mayıs 2025, İstanbul Teknik Üniversitesi (İTÜ), İstanbul, Türkiye



16 ULUSLARARASI
LİF VE POLİMER
ARAŞTIRMALARI
SEMPOZYUMU

16th INTERNATIONAL FIBER AND POLYMER RESEARCH SYMPOSIUM

Sürdürülebilir ve İşlevsel Lif ve Polimerler
Sustainable and Functional Fibers & Polymers



9-10 Mayıs
May 2025

İstanbul Teknik Üniversitesi
Gümüşsuyu Prof. Dr. Necmettin Erbakan Yerleşkesi
İstanbul Technical University
Gumussuyu Prof. Dr. Necmettin Erbakan Campus

Microecocell ve Micromodal İpliklerin Karşılaştırmalı Analizi: Ring ve Vortex Eğirme Sistemlerinin İplik ve Kumaş Özelliklerine Etkisi

Seyma Satil^{1*}, Tulin Kaya Nacarkahya¹, Gonca Balci Kılıç², Musa Kılıç², Asaf Özmen¹, Burak Ayyıldız¹, Servet Öztürk¹

¹Karafiber Tekstil San. ve Tic. A.Ş. R&D Center, Gaziantep, TÜRKİYE

²Dokuz Eylül Üniversitesi Tekstil Mühendisliği Bölümü, İzmir, TÜRKİYE

*Sorumlu Yazar: arge@karaholding.com

ÖZET

Tekstil endüstrisinde sürdürülebilirlik ve yüksek performans kriterlerinin ön plana çıkmasıyla birlikte, mikro incelekte selülozik lifler artan bir ilgiyle karşılanmaktadır. Bu kapsamda, doğal kaynaklı hammaddelerden üretilen MMCF- rejenere selülozik liflerin mikro lif özelliklerinde üretilmesi nihai kullanımdaki ürüne katacağı farklı fiziksel özellik bakımından dikkat çekmektedir. Mikro lifler; ince yapısı ve yumuşak tutum gibi niteliklerinin yanı sıra, özellikle iplik üretiminde sundukları avantajlar ile ön plana çıkmaktadır. Bu çalışmada, %100 Mikrolyosel ve %100 Mikromodal liflerinden Ne 40/1 iplik numarasında, ring ve vortex eğirme sistemleri kullanılarak üretilen ipliklerin performans özellikleri karşılaştırmalı olarak değerlendirilmiştir. Mikrolyosel lifi olarak Ecocell marka lif ile çalışmalar gerçekleştirilmiştir. USTER düzgünlük, IPI, mukavemet ve uzama testleri başta olmak üzere çeşitli iplik testleri gerçekleştirilmiş, farklı lif tiplerinin ve eğirme teknolojilerinin iplik kalitesi üzerindeki etkileri analiz edilmiştir.

Anahtar Kelimeler: Microecocell, Micromodal, Ring Eğirme, MVS Eğirme, İplik Performansı

Comparative Analysis of Microecocell and Micromodal Yarns: Influence of Ring and Vortex Spinning on Yarn and Fabric Properties

ABSTRACT

With the rise of sustainability and high-performance criteria in the textile industry, micro-fine cellulosic fibers are receiving increasing interest. In this context, the production of MMCF-regenerated cellulosic fibers produced from natural raw materials with microfiber properties draws attention in terms of the different physical properties they will add to the final product. Microfibers: in addition to their qualities such as fine structure and soft handle, they stand out with the advantages they offer especially in yarn production. In this study, the performance properties of yarns produced from 100% Microlyocell and 100% Micromodal fibers in Ne 40/1 yarn count using ring and vortex spinning systems were comparatively evaluated. Studies were carried out with Ecocell brand fiber as microlyocell fiber. Various yarn tests, primarily USTER unevenness, IPI, tenacity and elongation tests, were performed, and the effects of different fiber types and spinning technologies on yarn quality were analyzed.

Keywords: Microecocell, Micromodal, Ring Spinning, MVS Spinning, Yarn Performance

I. GİRİŞ

Tekstil endüstrisinde sürdürülebilirlik hedefleri doğrultusunda, yenilenebilir kaynaklardan elde edilen ve çevresel etkisi düşük olan liflere yönelik ilgi giderek artmaktadır. Bu bağlamda, selülozik esaslı rejenere lifler; doğada biyolojik olarak parçalanabilir olmaları, doğal kaynakların verimli kullanımıyla üretilmeleri ve tekstil ürünlerinde sağladıkları yüksek performans özellikleri sayesinde önemli bir alternatif olarak öne çıkmaktadır. Modal, liyosel ve benzeri rejenere selülozik lif türleri bu sınıfın önde gelen örnekleri arasında yer almakta, gelişen üretim teknikleri ile mikro yapıli formlarının elde edilmesi sayesinde kullanım alanları daha da genişlemektedir. Son yıllarda hem sürdürülebilirlik kavramının önem kazanması hem de değişen tüketici ve pazar beklentileri nedeniyle rejenere selülozik mikrolif üretiminin yaygınlaştığı görülmektedir.

0,1-1,0 dtex arasında doğrusal yoğunluğa sahip ve konvansiyonel liflerden daha ince olan mikrolifler, enine kesit alanında daha fazla lif bulunması nedeniyle ürün özelliklerini olumlu yönde etkilemektedir. Mikrolifler, iplik enine kesitinde daha sıkı bir paketlenmeye olanak sağladığı için yüksek rüzgar bariyeri, doğal ıslanma direnci ve daha iyi hava geçirgenliği sunmaktadır. Bu doğal avantajları nedeniyle mikrolifler, kimyasal bir işleme ihtiyaç duymadan çok çeşitli ürünlerde kullanılabilir [1,2].

Modal lifi; kayın ağacından üretilen selülozik esaslı yapısıyla yüksek yumuşaklık, nem emicilik ve parlaklık gibi tekstil kullanım konforunu artıran özellikleriyle tanınmaktadır [3]. Bu lifin daha ince lif çapına sahip mikro formu olan Mikromodal ise, iplik yapısında daha fazla lif içeriği, yüksek yüzey alanı ve dolayısıyla daha pürüzsüz, ipeksi bir yüzey tuşesi sunarak kullanıcı deneyimini üst seviyeye

taşımaktadır. Ayrıca, Mikromodal liflerin yüksek polimerizasyon derecesi, yaş ve kuru halde dayanıklılığını korumasına olanak tanımakta, bu da iplik üretiminde istikrarlı bir yapı sağlamaktadır [4].

Bir liyosel lif markası olan Ecocell™, odun kökenli selülüzün çevre dostu bir çözücü olan N-metilmorfolin-N-oksit (NMMO) ile çözülerek elde edildiği, üçüncü nesil rejenere selülozik elyaflardan biridir. Kapalı devre üretim sistemi sayesinde kimyasal geri kazanımı %99,6 oranına ulaşan Ecocell™ prosesi, düşük çevresel etkisiyle öne çıkmakta ve bu yönüyle sürdürülebilir tekstil üretiminin önemli bir temsilcisi olarak kabul edilmektedir. Lif yapısı oldukça düzenli ve kristalin olduğu için yüksek kuru ve ıslak mukavemete, iyi nem yönetimine ve pürüzsüz yüzey yapısına sahiptir [5].

Literatürde mikroliflerden üretilen kumaşların özelliklerini inceleyen çeşitli çalışmalar bulunmaktadır. Bu çalışmalar incelendiğinde, genel olarak mikroliflerden üretilen kumaşların termal konfor, nem yönetimi ve geçirgenlik özelliklerinin incelendiği görülmektedir [6-10].

Bu çalışmada ise, Ne 40/1 iplik numarasına sahip, ring ve vortex eğirme teknolojileri ile üretilen Mikroecocell ve Mikromodal ipliklerinin yapısal, fiziksel ve mekanik özelliklerinin karşılaştırılması amaçlanmıştır.

II. MATERYAL VE METOT

2.1 Materyal

Çalışma kapsamında, Ecocell (1.3 dtex, 38 mm), Micromodal (1.0 dtex 38 mm) ve Mikroecocell (1.0 dtex, 38 mm) liflerinden geleneksel ring ve MVS eğirme teknolojilerinde Ne 40/1 numaralı iplikler üretilmiştir. Tüm tiplerin üretimi aynı hammadde hazırlık ve eğirme hazırlık makinalarında

gerçekleştirilmiştir. Tarak bantları Trützschler TC7, cer bantları ise Trützschler TD 02 ve TD 03 makinalarında üretilmiştir. MVS ipliklerinin üretiminde 3 pasaj cer işlemi uygulanmıştır. Geleneksel ring ipliklerin üretimi sırasında Zinser 668 fitil, Zinser 351 ring ve Autoconer 5 bobinleme makinalarında, MVS ipliklerin üretimi ise Muratech 870 EX makinasında gerçekleştirilmiştir.

2.2 Metot

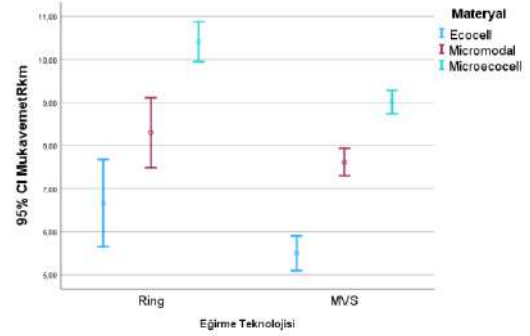
Çalışma kapsamında üretilen ipliklerin mekanik ve fiziksel özelliklerinin belirlenmesi amacıyla iplik kopma mukavemeti ve uzaması, düzgünsüzlük, tüylülük ve sürtünme testleri yapılmıştır. Mukavemet testleri Uster Tensorapid 5 cihazında, düzgünsüzlük, sık rastlanan hatalar ve tüylülük testleri Uster Tester 6 S800'de ve iplik-metal sürtünme testleri de Lawson-Hemphill CTT cihazında gerçekleştirilmiştir.

Hammadde ve eğirme teknolojisinin çalışma kapsamında üretilen ipliklerin mekanik ve fiziksel özellikleri üzerindeki etkilerinin incelenmesi amacıyla SPSS paket programında $\alpha=0.05$ önem seviyesi için ANOVA testleri yapılmış ve sonuçlar %95 güven aralığı grafikleri yardımıyla görselleştirilmiştir.

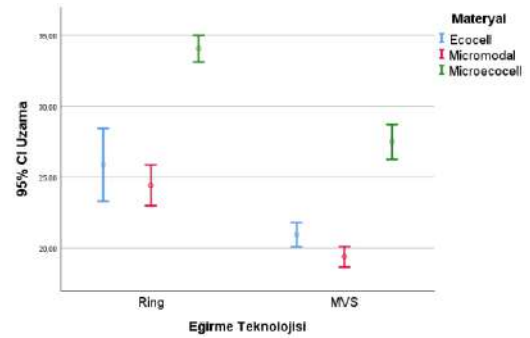
III. BULGULAR VE TARTIŞMA

3.1. İplik Mekanik Özellikleri

Çalışma kapsamında üretilen ipliklerin kopma mukavemeti (R_{km}) ve kopma uzamasına (%) ait %95 güven aralığı grafikleri Şekil 1 ve Şekil 2'de yer almaktadır.



Şekil 1. Mukavemet (R_{km}) değerleri için %95 GA grafikleri

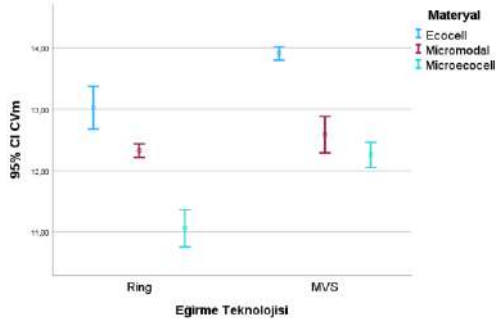


Şekil 2. Kopma uzaması (%) değerleri için %95 GA grafikleri

ANOVA sonuçları ve güven aralığı grafiklerinden görüldüğü üzere hammaddenin ve eğirme teknolojisinin iplik mukavemeti ve uzaması üzerindeki etkileri istatistiksel olarak anlamlıdır ($p<0.05$). Şekil 1 incelendiğinde, literatüre paralel olarak mikro liflerden üretilen ipliklerin kopma mukavemeti değerlerinin daha yüksek olduğu görülmektedir. Bununla birlikte, Micromodal ve Microecocell lifleri arasındaki fark istatistiksel açıdan önemlidir ($p<0.05$). Şekil 2'de Microecocell liflerinden üretilen ipliklerin kopma uzaması değerlerinin diğer tiplere göre daha yüksek olduğu görülmektedir.

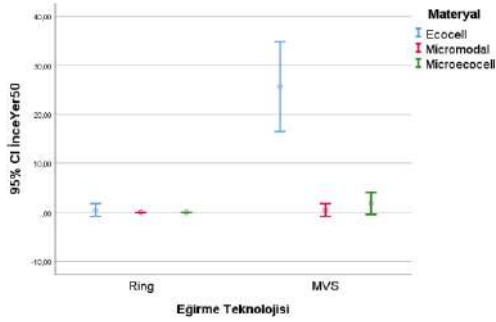
3.2. Düzgünsüzlük ve Sık Rastlanan Hatalar

Çalışma kapsamında üretilen ipliklerin düzgünsüzlük ($\%CV_m$) ve sık rastlanan hata (km^{-1}) değerlerine ait %95 güven aralığı grafikleri Şekil 3-6'da yer almaktadır.

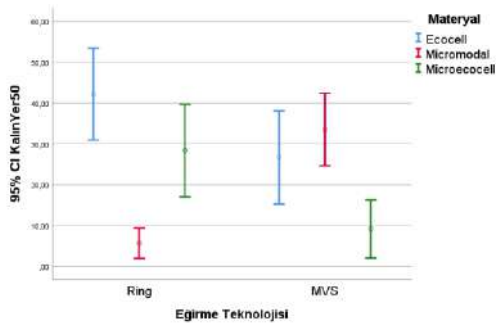


Şekil 3. Düzgünsüzlük (%CVm) değerleri için %95 GA grafikleri

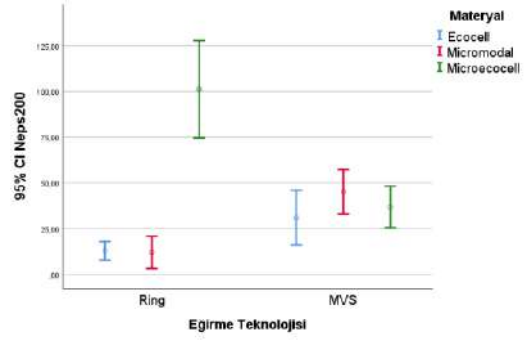
Şekil 3'ten görüldüğü üzere mikro liflerden üretilen ipliklerin düzgünsüzlük değerleri geleneksel liflerden üretilenlere göre daha düşüktür. Bununla birlikte, hem ring hem de MVS teknolojisi için Micrococell liflerinden üretilen ipliklerin düzgünsüzlükleri Micromodal liflerinden üretilenlere göre daha düşüktür ve aradaki farklar istatistiksel açıdan anlamlıdır ($p < 0.05$).



Şekil 4. İnce yer -%50 (km^{-1}) değerleri için %95 GA grafikleri



Şekil 5. Kalın yer +%50 (km^{-1}) değerleri için %95 GA grafikleri

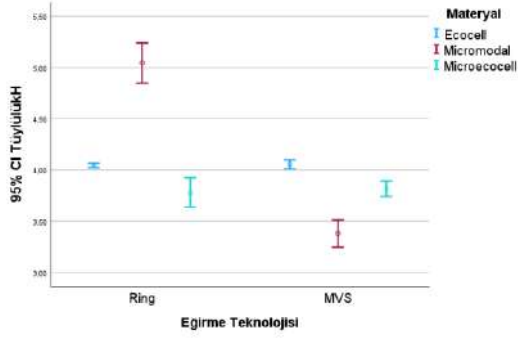


Şekil 6. Neps +%200 (km^{-1}) değerleri için %95 GA grafikleri

Şekil 4 incelendiğinde mikroliflerden üretilen ipliklerin ince yer değerleri arasındaki farkın istatistiksel olarak anlamlı olmadığı görülmektedir. Bununla birlikte, literatüre paralel olarak mikro liflerden üretilen ipliklerin ince yer değerlerinin geleneksel liflerden üretilenlere göre daha düşük olduğu söylenebilir [11,12]. Kalın yer açısından bir değerlendirme yapıldığında gerek eğirme sistemi gerekse de hammadde açısından sistematik bir değişim gözlenmemektedir. Geleneksel ring iplik teknolojisinde üretilen ipliklerde Micromodal iplikleri daha düşük değerlere sahipken MVS teknolojisinde üretilen ipliklerde Micrococell lifleri daha düşük değerlere sahiptir (Şekil 5). Neps değerleri üzerinde genel olarak hammadde hazırlık işlemlerinin önemli etkisi bulunmaktadır. Şekil 6 incelendiğinde MVS eğirme teknolojisi için hammaddenin neps değerleri üzerinde istatistiksel olarak anlamlı bir etkisi bulunmazken ring eğirme teknolojisinde üretilen Micrococell liflerinin değerleri dikkat çekmektedir.

3.3. Tüylülük

Çalışma kapsamında üretilen ipliklerin tüylülük (H) değerlerine ait %95 güven aralığı grafikleri Şekil 7'de yer almaktadır.

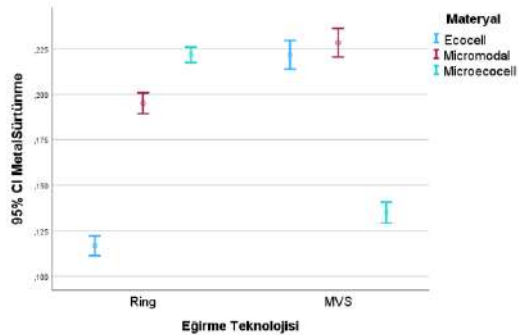


Şekil 7. Tüylülük (H) değerleri için %95 GA grafikleri

ANOVA sonuçları ve güven aralığı grafikleri (Şekil 7) incelendiğinde gerek hammadde gerekse eğirme teknolojisi, mikro liflerden üretilmiş ipliklerin tüylülük değerleri üzerinde istatistiksel olarak anlamlı farklar yaratmaktadır. Ancak, geleneksel ring iplik teknolojisinde Microecocell'den üretilmiş iplikler daha az tüylü iken MVS teknolojisinde Micromodal'den üretilmiş ipliklerin daha az tüylü olduğu görülmektedir. Bu etkilerin, eğirme teknolojileri özelinde iplik oluşum mekanizmaları ve özellikle liflerin eğilme rijitliği değerleriyle birlikte açıklanabileceği düşünülmektedir.

3.4. Yüzey Özellikleri

Çalışma kapsamında üretilen ipliklerin iplik-metal sürtünme katsayısı değerlerine ait %95 güven aralığı grafikleri Şekil 8'de yer almaktadır.



Şekil 8. İplik-metal sürtünme katsayısı değerleri için %95 GA grafikleri

Şekil 8 incelendiğinde genel olarak MVS iplik eğirme teknolojisinde üretilen ipliklerin sürtünme katsayısı değerlerinin geleneksel ring eğirme teknolojisinde

üretilenlerden daha yüksek olduğu görülmektedir. Bu durum, MVS ipliklerindeki kuşak liflerinin etkisiyle artan stick-slip hareketinin beklenen bir sonucudur. Bununla birlikte, Microecocell'den üretilen MVS ipliklerinin iplik-metal sürtünme katsayıları oldukça düşük çıkmaktadır.

IV. SONUÇLAR

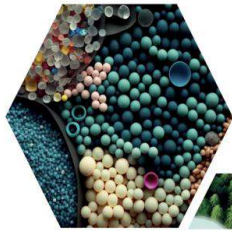
Çalışmada elde edilen bulgular, mikro liflerin iplik üretiminde geleneksel liflere kıyasla önemli avantajlar sunduğunu göstermektedir. Mikro liflerden üretilen iplikler, daha yüksek kopma mukavemeti ve daha düşük düzgünsüzlük değerleri sergileyerek, tekstil ürünlerinde kalite ve performansın artırılmasına olanak tanımaktadır.

Bunun yanı sıra, eğirme teknolojisinin de iplik özellikleri üzerinde belirleyici bir rolü olduğu görülmüştür. Ring ve MVS eğirme sistemleri arasında iplik özellikleri açısından farklılıklar bulunmakla birlikte, mikro liflerin her iki sistemde de olumlu sonuçlar verdiği belirlenmiştir. İplik-metal sürtünme katsayısı gibi yüzey özellikleri de hammadde ve eğirme teknolojisine bağlı olarak değişiklik göstermekte, bu da nihai ürünün kullanım özelliklerini etkileyebilmektedir.

Sonuç olarak, rejenere selülozik mikro lifler tekstil endüstrisinde sürdürülebilirlik ve yüksek performans hedeflerine ulaşmada önemli bir rol oynamaktadır. Özellikle Microecocell liflerinin yüksek mukavemet, düşük düzgünsüzlük ve yüksek uzama özellikleri, bu lifi teknik tekstillerden moda ürünlerine kadar geniş bir yelpazede ticari açıdan cazip kılmaktadır. Çevre dostu üretim süreçleri ve yenilikçi özellikleriyle Microecocell, tekstil sektöründe katma değeri yüksek, rekabetçi ürünlerin geliştirilmesine öncülük ederek, pazar payını artırma potansiyeline sahiptir.

KAYNAKLAR

- [1] American Fiber Manufacturers Association Inc., (2016), <http://www.fibersource.com/fiber-products/microfiber/#2>. Erişim 24 Aralık 2017
- [2] Mukhopadhyay, S. (2002). Microfibres – An Overview. Indian Journal of Fibre & Textile Research. 27(3): 307-314.
- [3] Lenzing (2025) . <https://www.lenzingindustrial.com/TechnologyAndFiber/FiberTypes>. Erişim 18 Nisan 2025
- [4] Kıvrak NM (2017) Yeni Nesil Liflerden ve Bunların Pamuk Karışımlarından Üretilen İpliklerin Performans Özelliklerinin Araştırılması, Ege Üniversitesi
- [5] Ecocell (2025), <https://ecocell.tr/>. Erişim 18 Nisan 2025
- [6] Demiroz Gun, A. (2011). Dimensional, Physical and Thermal Comfort Properties of Plain Knitted Fabrics Made from Modal Viscose Yarns Having Microfibers and Conventional Fibers. Fibers and Polymers, 12(2): 258-267.
- [7] Kandhavadvu, P., Ranthinamoorthy, R. and Surjit, R. (2015). Moisture and Thermal Management Properties of Woven and Knitted Tri-Layer Fabrics. Indian Journal of Fibre & Textile Research. 40 (3): 243-249.
- [7] Sampath, M.B. and Senthilkumar, M. (2009). Effect of Moisture Management Finish on Comfort Characteristics of Microdenier Polyester Knitted Fabrics. Journal of Industrial Textiles, 39(2): 163-173.
- [8] Srinivasan, J., Ramakrishnan, G., Mukhopadhyay, S and Manoharan, S. (2007). A Study of Knitted Fabrics from Polyester Microdenier Fibres. The Journal of The Textile Institute, 98(1): 31-35.
- [9] Suganthi, T. and Senthilkumar, P. (2018). Moisture-Management Properties of Bi-Layer Knitted Fabrics for Sportswear. Journal of Industrial Textiles, 47(7), 1447-1463
- [10] Demiroz Gun, A. and Bodur, A. (2017). Thermo-Physiological Comfort Properties of Double-Face Knitted Fabrics Made from Different Types of Polyester Yarns and Cotton Yarn. The Journal of The Textile Institute, 108(9): 1518-1527.
- [11] Kıvrak N.M, Ozdil, M., Süpüren Mengüç, G. (2018). Characteristics of the Yarns Spun from Regenerated Cellulosic Fibers, Textile and Apparel, 28(2): 107-117.
- [12] Skenderi, Z., Kopitar, D., Vrljicak, Z., Ivekovic, G. (2018). Unevenness of air-jet spun yarn in comparison with ring and rotor spun yarn made from micro modal fibers. Tekstil, 67(1-2):14-26.



16 ULUSLARARASI
LİF VE POLİMER
ARAŞTIRMALARI
SEMPOZYUMU

16th INTERNATIONAL FIBER AND POLYMER RESEARCH SYMPOSIUM

Sürdürülebilir ve İşlevsel Lif ve Polimerler
Sustainable and Functional Fibers & Polymers



9-10 Mayıs
May 2025

İstanbul Teknik Üniversitesi
Gümüşsuyu Prof. Dr. Necmettin Erbakan Yerleşkesi
Istanbul Technical University
Gumussuyu Prof. Dr. Necmettin Erbakan Campus



Application of biopolymeric nanocomposites in bone tissue engineering

Cem GÖK*, Gülşah SUNAL

Department of Biomedical Engineering, Faculty of Engineering and Architecture, Izmir Bakırçay University, Izmir, Türkiye

** Corresponding author: cem.gok@bakircay.edu.tr*

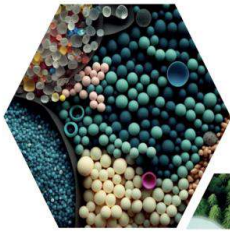
ABSTRACT

Bone tissue engineering (BTE) focuses on the repair of critical-sized bone defects through the integration of cells, biomolecules, and biomaterials. In this study, we developed alginate–chitosan–nanomaterial-based bionanocomposite scaffolds using the solvent casting and electrospinning methods. The scaffolds were designed to achieve high porosity and interconnected pore structures, which are critical for osteoconduction.

Characterization of the fabricated scaffolds was performed using scanning electron microscopy (SEM) for morphological analysis, Fourier-transform infrared spectroscopy (FTIR) for chemical structure confirmation, and mechanical testing for compressive strength evaluation. Preliminary results demonstrated that the scaffolds exhibited a porosity of approximately 90%, with an average pore size suitable for bone tissue ingrowth. The compressive strength was found to be in the range compatible with cancellous bone.

The combination of alginate's ionic crosslinking ability, chitosan's antibacterial properties, and the surface area enhancement provided by nanomaterials significantly improved osteoblast attachment and proliferation in initial in vitro assays. These findings suggest that alginate–chitosan–nano scaffolds are promising candidates for the development of bioactive and eco-friendly bone graft substitutes.

Keywords: Tissue Engineering; Bone Scaffolds; Biopolymers; Nanocomposite



16 ULUSLARARASI
LİF VE POLİMER
ARAŞTIRMALARI
SEMPOZYUMU

16th INTERNATIONAL FIBER AND POLYMER RESEARCH SYMPOSIUM

Sürdürülebilir ve İşlevsel Lif ve Polimerler
Sustainable and Functional Fibers & Polymers



9-10 Mayıs
May 2025

İstanbul Teknik Üniversitesi
Gümüşsuyu Prof. Dr. Necmettin Erbakan Yerleşkesi
İstanbul Technical University
Gumussuyu Prof. Dr. Necmettin Erbakan Campus

Effect of Surface-Active Agents on Liquid Transfer Properties of Hydroentangled Nonwoven Fabrics

Ebru Celikten^{a,*}, Mehmet Dasedmir^{a,b}, Tülin Kaya Nacarkahya^c, Seyma Satil^c, Mehmet Topalbekiroglu^a

^a Gaziantep University, Textile Engineering Department, Turkey.

^b North Carolina State University, Nonwovens Institute, United States.

^c Karafiber Tekstil Ind. Trade Inc. R&D Center, Gaziantep, Turkey.

*Corresponding author: ebruucelikten@hotmail.com

ABSTRACT

Nonwoven surfaces are widely used in various fields, including medical, hygiene, and automotive applications. Different chemical processes are applied to enhance the performance of these surfaces and provide specific functional properties. Surface-active agents or surfactants are crucial additives that improve the absorption, distribution, and interaction of liquids with nonwoven surfaces. These chemicals directly influence product performance by optimizing the hydrophilic or hydrophobic balance of nonwoven materials. In this study, different concentrations of surfactants were applied to hydroentangled nonwoven fabric samples with the same (plain) patterns and 100% polyester fiber content at different weights (30 g/m², 45 g/m², 60 g/m²) under laboratory conditions. The samples obtained after the process were subjected to liquid strike-through times and rewet (wetback) tests. The results indicated that the surfactants significantly reduced the initial liquid strike-through time. On the other hand, the liquid strike-through times increased as the basis weight increased due to the amount of fiber per unit area. Furthermore, there was a decrease in the wetback values.

Keywords: Hydroentangled nonwoven, surfactants, liquid strike-through time, wetback

I. INTRODUCTION

Nonwoven surfaces are widely used in various industries such as textiles, hygiene, medical, automotive, and filtration. Nonwoven fabrics have been produced from various natural and synthetic fibers [1, 2]. The finishing process of nonwoven fabrics is important for adding value to the final product through different finishing methods. Several finishing processes are applied to enhance the properties of these surfaces. Finishing can be classified

as either wet finishing (chemical) or dry finishing (mechanical) [1]. Wet finishing includes washing (scouring), dyeing, coating, and chemical applications such as antistatic agents, antimicrobial treatment, flame-retardant, and hydrophobic or hydrophilic finishes [2].

Surface-active agents or surfactants are important additives that enable nonwoven materials to absorb better, spread, and become compatible with the surface of water or other liquids. The surface-wetting

chemicals are used especially to increase hydrophilicity [3]. Nonwoven surfaces can sometimes have a water-repellent (hydrophobic) structure, depending on the raw material used (synthetic fiber). Hydrophilic surface-active agents allow water to spread better on the surface. These substances consist of water-loving (hydrophilic) polar and water-hating (hydrophobic) apolar groups. According to their chemical structures, these are classified as anionic, cationic, nonionic, and amphoteric [3, 4, 5].

Shepherd and Xiao (1999) reported in a study that surfactants used as rewetting agents can reduce the water absorption time of paper products. Among the different surfactants, cationic surfactants showed better performance [6]. Cai et al. (2003) investigated the adsorption mechanism of surfactants on nonwoven fabrics made from polypropylene and polyethylene terephthalate. The study examines how different types of surfactants (anionic, cationic, and nonionic) adsorb onto these materials [4]. Zhu et al. (2006) reported the wetting behavior of thermally bonded polyester nonwoven fabrics and the importance of porosity in this process. Samples of nonwoven fabrics with different weights consisting of 85% polyethylene terephthalate and 15% polybutylene terephthalate fibers were evaluated. According to the study, the porosity of the fabric is a critical factor in its wetting behavior [7]. Zhou and Zhang (2012) compared the absorbency rate, water-vapor transmission rate, and diffusion area in a solution of three different polyester/viscose spunlaced nonwoven fabrics [8]. This experimental study aims to investigate the effects of the surfactants applied at different rates on the liquid transfer properties of hydroentangled nonwovens with different basis weights and 100% polyester fiber content.

II. EXPERIMENTAL METHOD / THEORETICAL METHOD

The hydroentangled nonwoven samples were produced on the ANDRITZ neXline spunlace line at Karafiber Tekstil San ve Tic AŞ (Gaziantep/Turkey). The samples were produced at different basis weights (30 g/m², 45 g/m², 60 g/m²) with the same (plain) pattern and 100% polyester fibers. In the study, a surface-active agent (surfactant) with surface wetting properties was used. Firstly, a 10% concentration of a non-ionic surfactant was prepared. The prepared chemical was applied to the nonwoven surface at concentrations of 0.5% and 1% using a laboratory pad-dry machine. It was then dried in an oven at 120 °C for approximately 2 minutes. The chemically treated samples and the control samples (untreated) were subjected to liquid strike-through time and wetback tests. The sample properties are given in Table 1.

Table 1. Properties of hydroentangled nonwovens

| Sample No | Basis Weight (g/m ²) | Fiber Composition (PET wt%) | Surfactant (%) |
|-----------|----------------------------------|-----------------------------|----------------|
| SPL1 | 30 | 100 | 0 (Control) |
| SPL2 | 30 | 100 | 0.5 |
| SPL3 | 30 | 100 | 1 |
| SPL4 | 45 | 100 | 0 (Control) |
| SPL5 | 45 | 100 | 0.5 |
| SPL6 | 45 | 100 | 1 |
| SPL7 | 60 | 100 | 0 (Control) |
| SPL8 | 60 | 100 | 0.5 |
| SPL9 | 60 | 100 | 1 |

*SPL: Spunlaced (Hydroentangled)

All samples were conditioned in the laboratory at 20 ± 2°C and 60% relative humidity for 24 hours. Each nonwoven sample was tested 3 times and averaged. Mass per unit area was measured with an accuracy of 0.001 g using a precision balance, following NWSP 130.1. R0 (20)- Mass per unit area standards. Measured using a digital thickness tester according to NWSP 120.1.R0 20-Thickness of nonwoven fabrics standards. The liquid strike-through time (Repeated) tests were measured using a Lister tester, following

NWSP 070.7.R2 (20)- (Repeated liquid strike-through time (simulated urine)) standards. Wetback or rewetting tests were measured using a wetback tester according to NWSP 070.8.R1 (19)- (Wetback after repeated strike-through time (simulated urine)). In addition to the standards, a colouring dyestuff was added to the prepared simulated urine liquid to detect the spread of the liquid and its migration to the filter paper on wetback.

III. RESULTS AND DISCUSSIONS

The basis weight and thickness values of the hydroentangled nonwovens are given in Table 2.

Table 2. The basis weight and thickness test results of hydroentangled nonwovens

| Sample No | Basis Weight (g/m ²) | Thickness (mm) |
|-----------|----------------------------------|----------------|
| SPL1 | 32 | 0.98 |
| SPL2 | 31 | 0.95 |
| SPL3 | 31 | 0.95 |
| SPL4 | 46 | 1.05 |
| SPL5 | 45 | 1.04 |
| SPL6 | 47 | 1.05 |
| SPL7 | 60 | 1.45 |
| SPL8 | 61 | 1.44 |
| SPL9 | 60 | 1.47 |

In order to investigate the liquid transfer properties of nonwoven surfaces used in hygiene products, liquid strike-through times and wetback tests were carried out. The results are shown in Figure 1 and Figure 2, respectively.

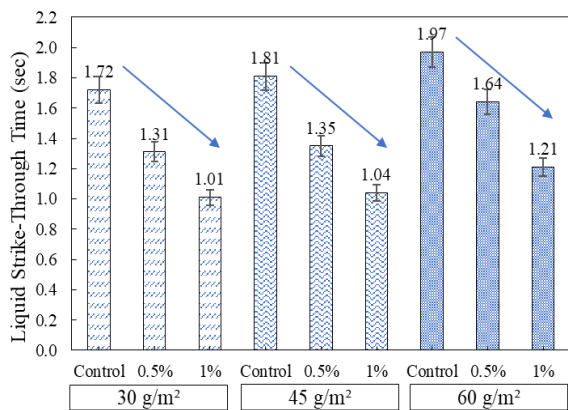


Figure 1. Liquid strike-through times test results

To investigate the effect of the surfactants, the liquid strike-through times and wetback tests were initially applied to control nonwoven samples. The results showed that the control samples exhibited higher liquid strike-through times compared to those treated with 0.5% and 1% surfactants. On the other hand, as expected, a decrease in liquid strike-through time was observed with the addition of surfactants. This indicates that the application of surfactants enhanced the hydrophilicity of the nonwoven structure, allowing the liquid to penetrate more quickly into the lower layers. The surface-active agents facilitate the passage of the liquid between the fibers by increasing the wettability of the surface [4]. This effect was observed consistently across all basis weight groups. Furthermore, samples with higher basis weights demonstrated longer strike-through times due to increased fiber density and nonwoven thickness with increasing basis weight.

Low wetback values are particularly important for nonwoven surfaces used in hygiene products, as they ensure a sensation of dryness during use [13]. The results of the wetback tests were obtained quite low (Figure 2). These results show that the liquid passes through the filter paper at a very low rate.

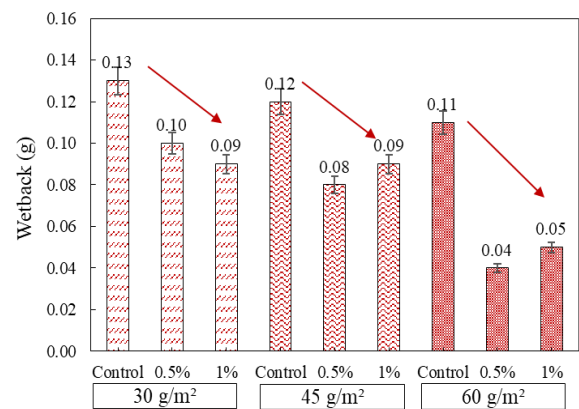


Figure 2. Wetback test results

Although the differences among the samples were relatively small, the control samples exhibited slightly higher wetback values. It was observed that the application of 0.5% and 1% surfactant had a reducing

effect on rewetting. This can be explained by the fact that surfactants provide rapid and homogeneous transfer of liquid to the lower layers without accumulating on the surface.

The samples were photographed after the liquid strike-through time test and after the wetback test. The images are shown in Figures 3 to 11. Analyzing the figures, it can be seen that there are traces (circled areas) on the filter paper after wetback in the control samples. This result shows that the use of surfactant plays an important role even in the wetback tests.

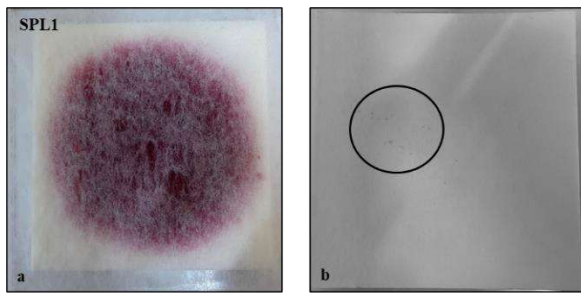


Figure 3. (SPL1) 30 g/m² control nonwoven (a) SPL1 sample after liquid strike-through times test, (b) filter paper after wetback test

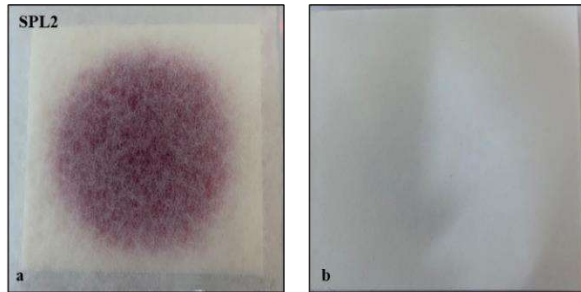


Figure 4. (SPL2) 0.5% surfactant application on 30 g/m² nonwoven surface, (a) SPL2 sample after liquid strike-through times test, (b) filter paper after wetback test

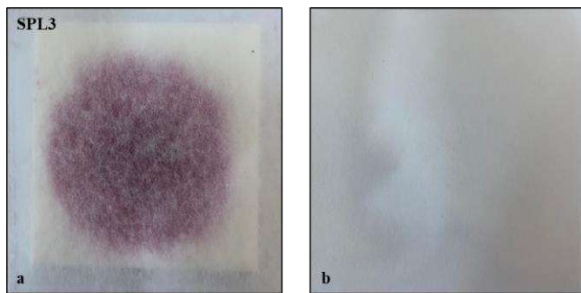


Figure 5. (SPL3) 1% surfactant application on 30 g/m² nonwoven surface, (a) SPL3 sample after liquid strike-through times test, (b) filter paper after wetback test

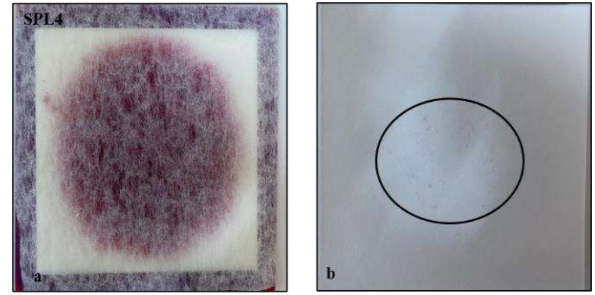


Figure 6. (SPL4) 45 g/m²-control nonwoven (a) SPL4 sample after liquid strike-through times test, (b) filter paper after wetback test

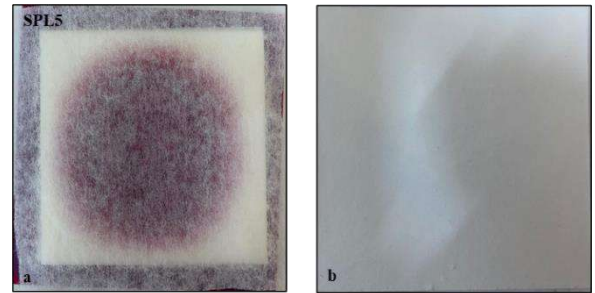


Figure 7. (SPL5) 0.5% surfactant application on 45 g/m² nonwoven surface, (a) SPL5 sample after liquid strike-through times test, (b) filter paper after wetback test

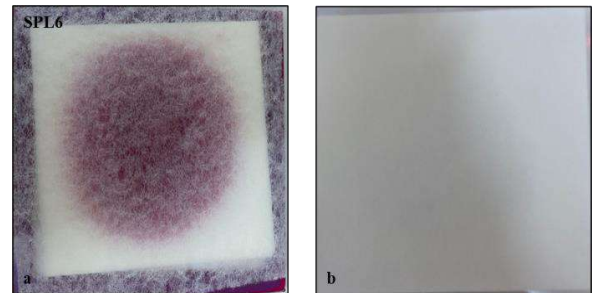


Figure 8. (SPL6) 1% surfactant application on 45 g/m² nonwoven surface, (a) SPL6 sample after liquid strike-through times test, (b) filter paper after wetback test

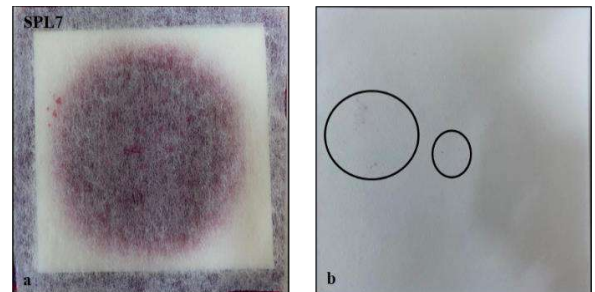


Figure 9. (SPL7) 60 g/m² control nonwoven (a) SPL7 sample after liquid strike-through times test, (b) filter paper after wetback test

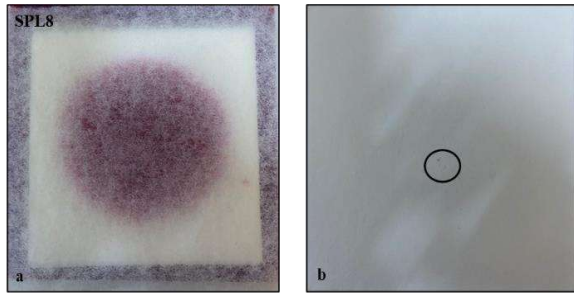


Figure 10. (SPL8) 0.5% surfactant application on 60 g/m² nonwoven surface, (a) SPL8 sample after liquid strike-through times test, (b) filter paper after wetback test

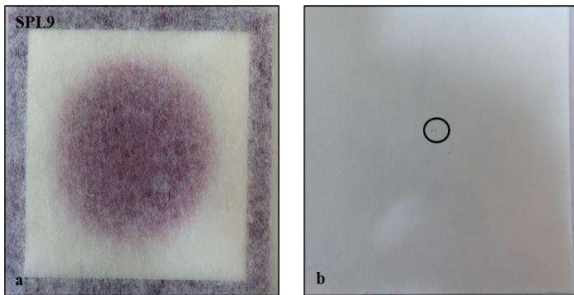


Figure 11. (SPL9) 1% surfactant application on 60 g/m² nonwoven surface, (a) SPL9 sample after liquid strike-through times test, (b) filter paper after wetback test

IV. CONCLUSIONS

This study demonstrates the significant influence of surface-active agents on the liquid transfer properties of polyester-based nonwoven fabrics, particularly in hygiene applications where liquid management is essential. Due to the hydrophobic nature of polyester, liquid transfer occurs more slowly. However, the incorporation of surface-active agents enhances hydrophilicity and facilitates faster liquid penetration. Additionally, higher basis weights result in longer liquid strike-through times due to increased fiber density and reduced pore size, which slow down liquid movement through the nonwoven fabric structure.

In addition, the surfactants not only make the surface hydrophilic, but they also allow the liquid to spread more evenly and to be absorbed into the fibers more quickly. This means that the liquid goes directly to the substrate without pooling on the surface. In this way, no liquid remains on the surface. The results show that

the wetting agent also affects the rewetting (wetback) properties. This is a critical parameter in hygiene applications where leakage prevention is important.

The results also emphasize that the impact of the basis weight on liquid strike-through time should be carefully considered when designing nonwoven fabrics for hygiene applications to ensure optimal liquid transfer properties. Future studies can assess the long-term performance of surface-active treatments under real-use conditions. In addition, different types of surfactants (anionic, cationic, nonionic, and amphoteric) can be used to study their effects on liquid transfer properties.

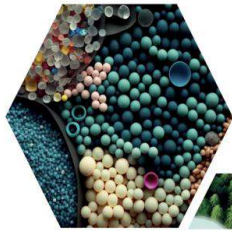
ACKNOWLEDGMENT

This study was financially supported by the Scientific and Technological Research Council of Turkey (TUBITAK) under Project No. 3180941. The hydroentangled nonwoven sample production was carried out in Karafiber Tekstil San ve Tic AS nonwoven production facilities.

REFERENCES

- [1] Karthik, T., Rathinamoorthy, R., Karan, C. P. (2016). Nonwovens: Process, structure, properties and applications. Woodhead Publishing India Pvt. Ltd.
- [2] Pourmohammadi, A. (2013). Nonwoven materials and joining techniques. Woodhead Publishing Limited.
- [3] Ciftci, M. F. (2015). Tekstil endüstrisinde yüzey aktif maddelerin kullanımı. TMMOB Kimya Mühendisleri Odası.
- [4] Cai, B., Zheng, Q. K., Li, R. X., Wu, D. C. (2003). Adsorption mechanism of surfactants on nonwoven fabrics. Journal of Applied Polymer Science, 89 (12), 3210-3215. <https://doi.org/10.1002/app.12478>.

- [5] Gündüz Isık, S., Okur, S., Kalkan, E. B., Çevik, A., Güleç Ünlü, S., Özkan, M. H., Yılmaz, M., Kırbıyık, M. (2018). Yüzey aktif organik maddelerin tayini. Gümrük Ticaret Dergisi.
- [6] Shepherd, I., Xiao, H. (1999). The role of surfactants as rewetting agents in enhancing paper absorbency. *Colloids and Surfaces A: Physicochemical and Engineering Aspects*, 157 (1-3), 235-244.
- [7] Zhu, L., Perwuelz, A., Lewandowski, M., Campagne, C. (2006). Wetting behavior of thermally bonded polyester nonwoven fabrics: The importance of porosity. *Journal of Applied Polymer Science*, 102(1), 387-394. <https://doi.org/10.1002/app.24108>.
- [8] Zhou, Z., Zhang, R. (2012). Effect of polyester and viscose content on the performance of spunlaced nonwoven dressings. *Advanced Materials Research*, 627, 293-297. <https://doi.org/10.4028/www.scientific.net/AMR.627.293>.
- [9] NWSP 130.1.R0-15. (2015). Mass per unit area. European Nonwovens Production and Deliveries. Brussels: EDANA.
- [10] NWSP 120.1.R0-15. (2015). Thickness of nonwoven fabrics. European Nonwovens Production and Deliveries. Brussels: EDANA.
- [11] NWSP 070.7.R1-20. (2020). Repeated Liquid Strike-Through Time (Simulated Urine). European Nonwovens Production and Deliveries. Brussels: EDANA.
- [12] NWSP 070.8.R1-20. (2020). Wetback after repeated strike-through time (simulated urine). European Nonwovens Production and Deliveries. Brussels: EDANA.
- [13] Culfa, G., Sarioglu, E., Dasdemir, M., Celikten, E., Nacarkahya, T. K. (2022). Investigation of Fluid Distribution and Rewet Performance with the Use of Different Inner Layer Design and Top Sheets in Sanitary Napkins, *Tekstil ve Mühendis*, 29:128, 301-307. <https://doi.org/10.7216/teksmuh.1222535>.



16 ULUSLARARASI
LİF VE POLİMER
ARAŞTIRMALARI
SEMPOZYUMU

16th INTERNATIONAL FIBER AND POLYMER RESEARCH SYMPOSIUM

Sürdürülebilir ve İşlevsel Lif ve Polimerler
Sustainable and Functional Fibers & Polymers



9-10 Mayıs
May 2025

İstanbul Teknik Üniversitesi
Gümüşsuyu Prof. Dr. Necmettin Erbakan Yerleşkesi
İstanbul Technical University
Gümüşsuyu Prof. Dr. Necmettin Erbakan Campus

Advances and outlook in capacitive pressure sensors: the role of nanofibrous architecture

Özge Alişan^a, Mehmet Durmuş Çalışır^{a,*}

^aRecep Tayyip Erdogan University, Rize, 53100, Türkiye.

*Corresponding author: mehmetdurmus.calisir@erdogan.edu.tr

ABSTRACT

Capacitive pressure sensors (CPSs) are attracting increasing interest in wearable and flexible electronics applications due to their high sensitivity, fast response time, low energy consumption and compact structure. Intensive research has been focused on the potential of nanofibrous structures to improve sensor performance and flexibility. This work reviews the current developments in nanofibrous CPSs and highlights the effect of nanofibers integration in the dielectric and electrode layers. The role of different polymeric materials such as polyimide (PI), polydimethylsiloxane (PDMS) and polyvinylidene fluoride (PVDF) as well as advanced conductive materials such as graphene, MXene and carbon nanotubes in enhancing sensitivity, reducing hysteresis and extending the measurement range are discussed. Furthermore, innovations in ionic double layer (EDL) mechanisms enable ultra-sensitive and multifunctional sensor designs. However, significant challenges remain to be overcome, such as achieving sensitivity-flexibility trade-off, minimizing hysteresis while resisting external interference, and maintaining structural uniformity while reducing manufacturing costs. Solving these problems is critical for future applications in wearable health monitoring and robotic touch systems.

Keywords: capacitive pressure sensors; nanofibrous structures; polymeric material; dielectric layer

I. INTRODUCTION

In daily life, pressure sensors are used in many fields such as sound detection, robotics, medical diagnostics, body motion monitoring and weight measurement [1], [2]. Although conventional MEMS-based pressure sensors offer low measurement errors, their flexibility is limited because they are made of rigid materials. This situation increases the need for the development of bendable sensors for use in wearable and flexible systems.

Pressure sensors are divided into four main groups: capacitive [3], piezoresistive [4], piezoelectric [5] and

triboelectric [6]. Figure 1 schematizes the working mechanisms of the most studied sensors [7].

Piezoresistive sensors offer the advantages of low cost and simple manufacturing, but are sensitive to temperature, humidity effects and hysteresis problems [8]. CPSs, on the other hand, are characterized by high sensitivity, low energy consumption, fast response times and compact structures [9], [10]. Piezoelectric and triboelectric sensors, although they can generate their own energy, are limited in sensing static pressures [8].

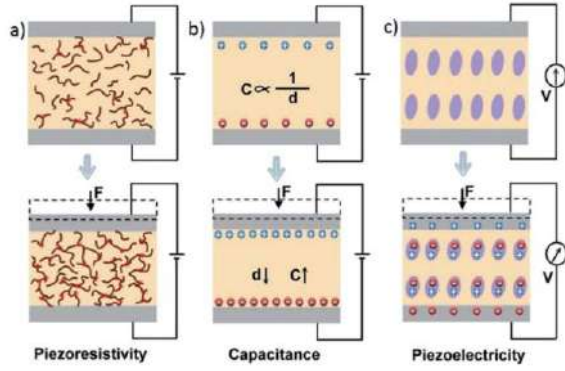


Figure 1. Schematic visualizations of transduction methods: (a) piezoresistivity, (b) capacitance, (c) piezoelectric effect [7]

CPSs are based on the creation of an electric field between two conductive plates. With the dielectric material between these plates, the capacitance is directly proportional to the area (A) and dielectric permittivity (ϵ) of the plates and inversely proportional to the distance (d) between the plates. Physical effects such as pressure or strain affect the capacitance of the sensor by changing the distance between the plates. However, due to small capacitance changes, these sensors usually show low sensitivity [7].

The performance of capacitive sensors is evaluated by parameters such as sensitivity, response time, accuracy, detection limit, resolution and reliability. Accuracy defines the difference between the measured and ideal capacitance. The detection limit specifies the lowest measurable pressure value. Sensitivity refers to the consistency of repeated measurements, while resolution defines the smallest pressure change corresponds to the perceptible capacitance change. Sensitivity refers to the ratio of the change in input to the change in capacity at the output. Response time is the time it takes for the signal to stabilize after pressure is applied. In addition, factors such as nonlinearity, hysteresis and stability are also important parameters affecting sensor performance. [11].

Current research focuses on material innovation, sensor design optimization and signal processing techniques to improve the sensitivity and response

speed of these sensors. In the last 10 years, the number of research has increased about 10 times (Figure 2).

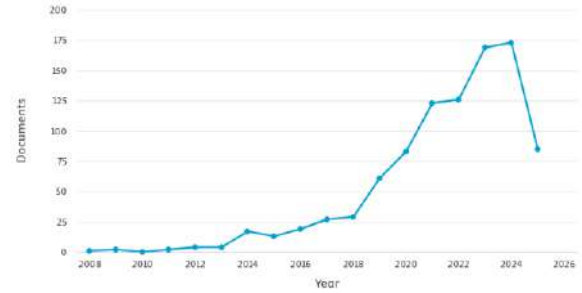


Figure 2. Distribution of research articles with the keywords 'nanofiber', 'capacitive', and 'pressure' by year in Scopus

In this paper, current research on CPSs particularly focusing polymeric nanofibrous structures, will be discussed; the technical approaches used will be classified and future development directions will be discussed.

II. EXPERIMENTAL METHOD

2.1 Polymer Based Functional Materials Used in CPSs

The basic components of CPSs can be divided into three main groups: substrate materials, electrodes and dielectric layers.

2.1.1 Base materials

The substrate materials are the materials on which the sensor is built and provide mechanical strength to the sensor. Among the base materials, polymers such as polyimide (PI), polyurethane (PU), polydimethylsiloxane (PDMS) and polyethylene terephthalate (PET) are commonly used [7]. PU is characterized by its wide temperature range (-100 to 300 °C) and high tensile strength [12], while PET is the most widely used base material due to its low cost and long life [13]. PDMS is ideal for flexible sensors due to its flexibility and high dielectric properties [14].

2.1.2 Electrodes and dielectric layers

Electrodes are critical components that affect the flexibility and sensitivity of pressure sensors.

Although metal electrodes (gold, silver, copper) offer high conductivity, their flexibility is limited. Therefore, materials such as carbon nanotubes, graphene and silver nanowires (AgNW) coated/composited with materials such as carbon nanotubes, graphene and silver nanowires (AgNW) are preferred as they offer both flexibility and conductivity advantages [15]. Conductive polymers such as PEDOT:PSS can also be used as electrodes, but their low flexibility and low conductivity may limit device performance [16].

The dielectric layer senses capacitance changes and polymer-based materials are widely used due to their low cost and processability. PDMS is suitable for microstructure fabrication with its formability and low elastic modulus, but it has a low dielectric constant and high hysteresis [17]. Ecoflex offers biocompatibility and high elongation ability, but has low durability [18]. Polyurethane is chemically resistant but shows viscoelastic losses [19]. PVDF and P(VDF-TrFE) are used in sensitive applications with high dielectric constant, but their flexibility is limited and expensive [20].

2.2 Microstructuring and Its Effects on Performance

Microstructured dielectric layers have been developed to improve the performance of pressure sensitive sensors. Figure 3 schematizes the general process of microstructural design of electrode and dielectric layers in capacitive sensors [21]. Micropyramid, microdom, microneedle/column and microporous structures increase the sensitivity of sensors. These structures reduce the elastic modulus, provide a wider deformation range and offer fast response with low hysteresis [10]. For example, Mannsfeld et al [17] used regular patterned structures to improve the performance of microstructured PDMS dielectric layers. Micro-patterned PDMS shows about 30 times higher pressure sensitivity compared to flat PDMS films.

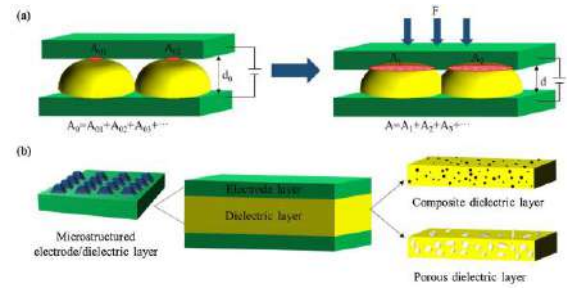


Figure 3. Microstructural designs of electrode and dielectric layers in CPSs: (a) changes in distance or area of electrodes, (b) three methods to improve capacitive sensor sensitivity [20]

III. RESULTS AND DISCUSSIONS

Nanofibrous structures are widely used in CPSs as two basic components: dielectric layer and electrode materials. In this section, current studies and future perspectives in CPSs will be discussed.

3.1 Dielectric Layers

Nanofibrous dielectric layers increase pressure sensitivity and enhance the response of sensors to low pressures. Wu et al [22] compared CPSs containing different dielectric layers (PDMS, PI tape and PI nanofiber membranes). In Figure 4, the relationship between the capacitance change and the applied pressure obtained using PDMS, PI and PI nanofiber membranes is compared. The PI nanofiber membrane was found to have the highest performance, having fibers with a diameter of 200-250 nm. The 138 μm thick PI nanofiber membrane provided high sensitivity (0.0235 kPa^{-1}) in the range 0-37.04 kPa and very sensitive measurements at low pressures (0-6.17 kPa). In addition, this structure showed flexibility and could be bent up to 90° .

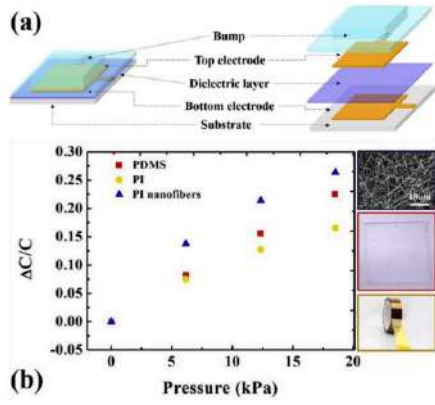


Figure 4. (a) Structural diagram of capacitive pressure sensor; (b) Relationship between capacitance variation and pressure using PI nanofiber membrane, PDMS and PI tape dielectric layers [22]

In another study, a flexible capacitive sensor was developed using PDMS coating and PI/GO nanofiber membrane [23]. Figure 5(a) shows the layered structure of a flexible capacitive force sensor that can detect vertical and horizontal forces using PI/GO nanofiber membrane as the dielectric layer. This sensor showed high sensitivity (3 MPa^{-1}) between 0-242 kPa in the normal direction and high accuracy in the horizontal direction. It was observed that GO doping improves the performance of the sensor by decreasing the compression modulus of the nanofiber membrane and increasing the dielectric constant. As shown in Figure 5(b), the dielectric constant provided the highest value in the whole force range when the amount of GO was 0.088 wt%.

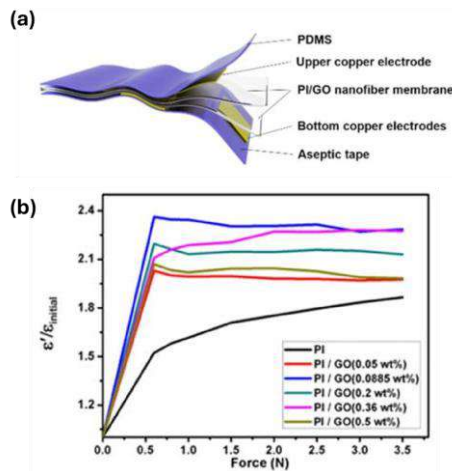


Figure 5. (a) Schematic diagram of flexible capacitive force sensor using PI/GO nanofiber as dielectric membrane. (b) Effect of GO amount on dielectric constant [23]

Qing et al [24] studied the effect of CNT doping on PVDF nanofiber membranes and found that surface roughness and fiber diameter decreased at low CNT ratios, while CNT deposition increased at high ratios. The highest sensitivity was obtained in the sensor containing 0.05% CNT (Figure 6).

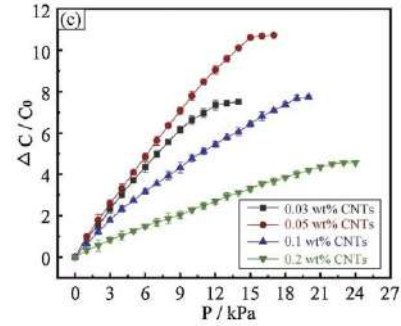


Figure 6. Initial capacitance values of sensors produced at different carbon nanotube (CNT) doping ratios [24]

In CPSs, ionic and hybrid layers based on electrical double layer (EDL) formation are also used in addition to the aforementioned approach. These layers increase the sensitivity of the sensor by using ion conductive gels or liquid electrolytes instead of conventional solid dielectric materials. Yue et al. [25] developed a high sensitivity sensor by optimizing EDL formation with oriented TPU nanofibers and a polyelectrolyte membrane. In Figure 7(a-f), the fabrication process of the capacitive sensor containing TPU nanofibers and polyelectrolyte membrane is shown step by step. As pressure is applied, the reorganization of ions and charge distribution changes, increasing capacitance. This structure enables the detection of low pressures, fast response time and wide measurement range. Figure 7(j) shows the change in contact and ion mobility with pressure, while Figure 7(k) schematically shows the EDL structure formed in the fiber voids. Iontronic layers can be combined with different sensing principles to obtain multifunctional sensors. As shown in Figure 7(m) in the range of 0-100 kPa, the sensitivity comparisons before and after 2000 cycles show that the sensor works extremely stable.

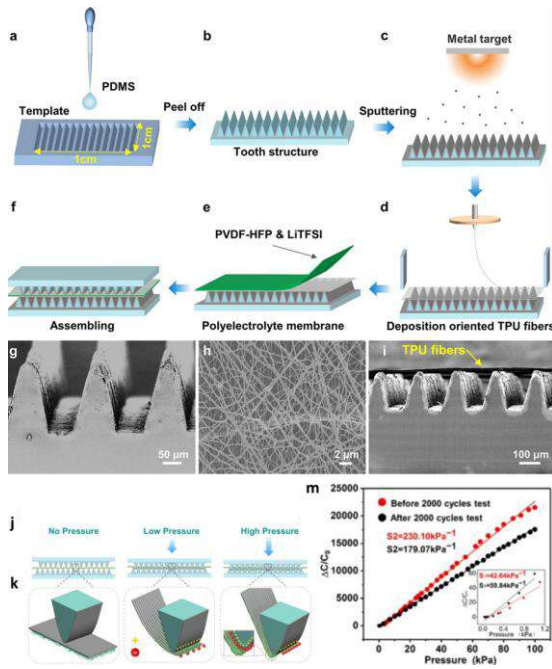


Figure 7. (a-f) Fabrication steps of CPSs; microstructure images of (g) tooth-structured Au-coated PDMS electrode, (h) polyelectrolyte membrane, (i) TPU nanofibers on PDMS; (j, k) schematic of EDL structure formed by electrode-electrolyte contact; (m) sensor sensitivity curve (0-100 kPa) [24]

Sharma et al. [26] developed a high-sensitivity capacitive pressure sensor containing MXene and lithium salts. Thanks to its sensing mechanism based on hydrogen bonds, it can detect pressures as low as 2 Pa, reaching a sensitivity of 230.10 kPa^{-1} and a response time of 70.4 ms. Figure 8 shows the ionic nanofiber membrane structure produced with MXene-LS-PVA blend. The oriented TPU fibers are stretched by pressure, resulting in EDL formation, which leads to an increase in capacitance. The sensor is sensitive to both low and high pressures, offering a wide sensing range.

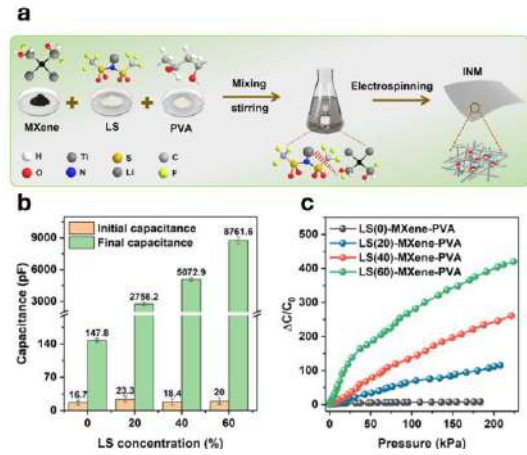


Figure 8. (a) Fabrication process of ionic nanofiber membranes. (b) Initial and final capacitance values. (c) $\Delta C/C_0$ variation under static pressure at different LS concentrations [26].

3.2 Electrode

Electrospun conductive nanofibers offer excellent interfacial contact and flexibility by combining with materials such as MXene, AgNWs, CNTs or PEDOT:PSS. Zhang et al [2] developed iontronic piezocapacitive sensors composed entirely of nanofibers. In Figure 9(a), the fabrication process of the ionic pressure sensor (IPS) is shown with the steps of electrospinning, vacuum filtration, and assembly of layers. TPU nanofiber membranes were fabricated by electrospinning method and electrodes were formed by depositing graphene (GR) and CNF-containing ink on TPU NFDs by vacuum filtration. In Figure 9(b), when pressure is applied, ion mobility increases and the ion distribution between the electrodes changes, thus activating the pressure sensing mechanism of the IPS. The best performance was obtained in the sensor with 80% IL content, which showed a sensitivity of 217.5 kPa^{-1} in the range 0-5 kPa. IPS(80) detects small pressure changes quickly (30-60 ms) and showed only 5.5% performance loss in 4000 cycles.

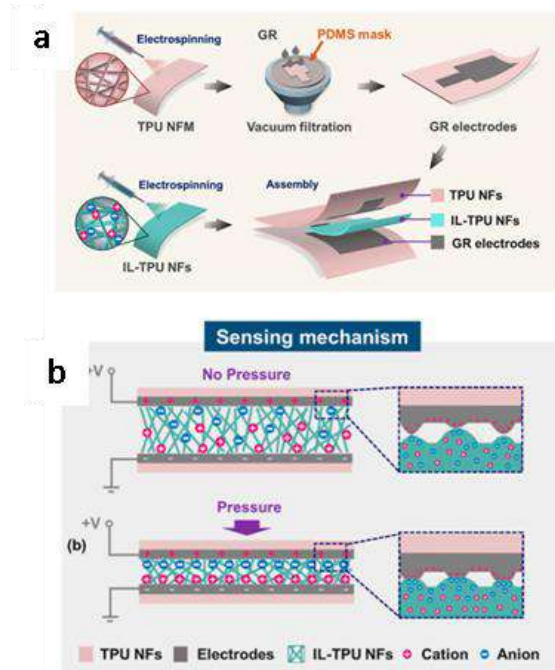


Figure 9. a) Production scheme of IPS b) Pressure sensing mechanism of IPS [2]

3.3. Challenges and Outlook

There is a conflict between sensitivity and flexibility in CPSs. Microstructures that provide low hysteresis and high sensitivity often cannot withstand large strains [27], whereas sensitivity decreases in sensors with a wide strain range while maintaining structural integrity [28]. The design of microstructures that combine these two properties remains a major technical challenge.

Another challenge is the trade-off between hysteresis reduction and resistance to external interference. While the air phase integrated into the structure reduces hysteresis, the initial capacitance and signal-to-noise ratio decrease due to the low dielectric constant. This reduces accuracy, especially in applications requiring high integration [20]. The balance between hysteresis and anti-interference is a fundamental problem to be solved in sensor design.

There is also a trade-off between manufacturing cost and structural uniformity. Although precision techniques such as photolithography provide high uniformity, they are expensive and time consuming

[29]. In contrast, the use of natural structures is inexpensive, but inconsistency between products occurs due to random pore distribution [30]. This is an obstacle for mass production.

IV. CONCLUSIONS

CPSs offer significant advantages such as high sensitivity, flexibility and low energy consumption thanks to the advancing material technologies and micro/nano structural designs. In this study, the effects of nanofibrous architectures on sensor performance have been discussed in detail.

The dielectric and electrode layers formed by orientated nanofibrous structures increased the sensitivity and flexibility of the sensors for low pressure sensing. Microstructured forms of polymers such as PI, PDMS and PVDF have attracted attention with low hysteresis and wide measurement ranges. Moreover, electrodes enriched with nanomaterials such as graphene, AgNW and MXene provided fast response time and high cycling resistance.

Structures based on the EDL effect offer much higher sensitivity than conventional systems and enable the development of multi-stimulus sensitive sensors by combining with hybrid architectures. In this respect, sensors have a wide application potential in areas such as wearable electronics and medical diagnostic systems.

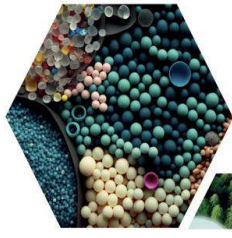
However, engineering challenges such as sensitivity-flexibility balance, hysteresis-to-noise ratio, and cost-uniformity relationship still await solutions. By overcoming these obstacles, more advanced, multifunctional and widely applicable versions of CPSs can be developed.

REFERENCES

- [1] Chen S, Lou Z, Chen D, Jiang K, Shen G (2018) Noncontact Heartbeat and Respiration Monitoring Based on a Hollow Microstructured Self-Powered

- Pressure Sensor. ACS Appl Mater Interfaces 10:3660–3667. <https://doi.org/10.1021/acsami.7b17723>
- [2] Lin X, Xue H, Li F, Mei H, Zhao H, Zhang T (2022) All-Nanofibrous Ionic Capacitive Pressure Sensor for Wearable Applications. ACS Appl Mater Interfaces 14:31385–31395. <https://doi.org/10.1021/acsami.2c01806>
- [3] Wang J, Wu Z, Pan L, Xu M, Zhang Z, Shi Y, Zhi C (2015) A highly sensitive and flexible pressure sensor with electrodes and elastomeric interlayer containing silver nanowires. Nanoscale 7:2926–2932. <https://doi.org/10.1039/C4NR06494A>
- [4] Kim SW, Lee H, Kim J, Oh Y, Kim DH, Lim Y, Park I (2024) Mechanically Robust and Linearly Sensitive Soft Piezoresistive Pressure Sensor for a Wearable Human–Robot Interaction System. ACS Nano 18:3151–3160. <https://doi.org/10.1021/acs.nano.3c09016>
- [5] Nassar H, Zhang J, Chibli H, Chanda D (2023) Fully 3D printed piezoelectric pressure sensor for dynamic tactile sensing. Addit Manuf 71:103601. <https://doi.org/10.1016/j.addma.2023.103601>
- [6] Lee HJ, Chun KY, Oh JH, Han CS (2021) Wearable Triboelectric Strain-Insensitive Pressure Sensors Based on Hierarchical Superposition Patterns. ACS Sens 6:2411–2418. <https://doi.org/10.1021/acssensors.1c00640>
- [7] Bijender, Kumar A (2022) Recent progress in the fabrication and applications of flexible capacitive and resistive pressure sensors. Sens Actuators A Phys 344:113770. <https://doi.org/10.1016/j.sna.2022.113770>
- [8] Qin J, Wu L, Wu X, Zhao X, Huang L, Yang W (2021) Flexible and Stretchable Capacitive Sensors with Different Microstructures. Adv Mater 33:2008267. <https://doi.org/10.1002/adma.202008267>
- [9] Sakthivelpathi V, Li T, Qian Z, Lee C, Taylor Z, Chung JH (2024) Advancements and applications of micro and nanostructured capacitive sensors: A review. Sens Actuators A Phys 377:115701. <https://doi.org/10.1016/j.sna.2024.115701>
- [10] Yuan H, Zhang X, Liu J, Wang Y, Feng Y, Wang Z (2024) Progress and challenges in flexible capacitive pressure sensors: Microstructure designs and applications. Chem Eng J 485:149926. <https://doi.org/10.1016/j.cej.2024.149926>
- [11] Mishra RB, El-Atab N, Hussain AM, Hussain MM (2021) Recent Progress on Flexible Capacitive Pressure Sensors: From Design and Materials to Applications. Adv Mater Technol 6:2001023. <https://doi.org/10.1002/admt.202001023>
- [12] Sekitani T, Zschieschang U, Klauk H, Someya T (2010) Flexible organic transistors and circuits with extreme bending stability. Nat Mater 9:1015–1022. <https://doi.org/10.1038/nmat2896>
- [13] Kaltenbrunner M, White MS, Głowacki ED, Sekitani T, Someya T, Sariciftci NS, Bauer S (2013) An ultra-lightweight design for imperceptible plastic electronics. Nature 499:458–463. <https://doi.org/10.1038/nature12314>
- [14] Quan Y, Liang X, Guo L, Yang Z, Zhang Y, Zhang Q (2017) Highly sensitive and stable flexible pressure sensors with micro-structured electrodes. J Alloys Compd 699:824–831. <https://doi.org/10.1016/j.jallcom.2016.12.414>
- [15] Basarir F, Madani Z, Vapaavuori J (2022) Recent Advances in Silver Nanowire Based Flexible Capacitive Pressure Sensors: From Structure, Fabrication to Emerging Applications. Adv Mater Interfaces 9:2200866. <https://doi.org/10.1002/admi.202200866>
- [16] Xu B, Chen L, Wang W, Yang W, Zhang W, Chen L (2017) Functional solid additive modified PEDOT:PSS as an anode buffer layer for enhanced photovoltaic performance and stability in polymer solar cells. Sci Rep 7:45079. <https://doi.org/10.1038/srep45079>
- [17] Mannsfeld SCB, Tee BCK, Stoltenberg RM, Chen CH, Barman S, Muir BV, Sokolov AN, Reese C,

- Bao Z (2010) Highly sensitive flexible pressure sensors with microstructured rubber dielectric layers. *Nat Mater* 9:859–864. <https://doi.org/10.1038/nmat2834>
- [18] Choi J, Kwon D, Kim K, Lee J, Eom J, Lee S, Jeong Y, Choi M, Kim J (2020) Synergetic Effect of Porous Elastomer and Percolation of Carbon Nanotube Filler toward High Performance Capacitive Pressure Sensors. *ACS Appl Mater Interfaces* 12:1698–1706. <https://doi.org/10.1021/acsami.9b20097>
- [19] Chen K, Li Z, Guo J, Yang X, Guo B, Shen H (2024) A Flexible Capacitive Pressure Sensor Based on Thermoplastic Polyurethane Porous Films by Non-Solvent Induced Phase Separation. *IEEE Sens J* 24:12217–12224. <https://doi.org/10.1109/JSEN.2024.3372587>
- [20] Guo Y, Gao S, Yue W, Zhang C, Li Y (2019) Anodized Aluminum Oxide-Assisted Low-Cost Flexible Capacitive Pressure Sensors Based on Double-Sided Nanopillars by a Facile Fabrication Method. *ACS Appl Mater Interfaces* 11:48594–48603. <https://doi.org/10.1021/acsami.9b17966>
- [21] Li R, Li Y, Deng J, Yang J, Li H, Wei Y, Liu L (2021) Research progress of flexible capacitive pressure sensor for sensitivity enhancement approaches. *Sens Actuators A Phys* 321:112425. <https://doi.org/10.1016/j.sna.2020.112425>
- [22] Zhu Y, Huang J, Li X, Pei S, Zhang X, Zhang H (2020) A flexible capacitive pressure sensor based on an electrospun polyimide nanofiber membrane. *Org Electron* 84:105759. <https://doi.org/10.1016/j.orgel.2020.105759>
- [23] Wu D, Ma C, Liu W, Zhang M, Xie X, Wang Y (2022) A flexible tactile sensor that uses polyimide/graphene oxide nanofiber as dielectric membrane for vertical and lateral force detection. *Nanotechnology* 33:405205. <https://doi.org/10.1088/1361-6528/ac73a4>
- [24] Yang X, Wang Y, Qing X (2019) A flexible capacitive sensor based on the electrospun PVDF nanofiber membrane with carbon nanotubes. *Sens Actuators A Phys* 299:111579. <https://doi.org/10.1016/j.sna.2019.111579>
- [25] Yue Q, Deng C, Shao Y, Xie Y, Xu T, Xiao X, Zeng Z (2022) Ultra-sensitive pressure sensors based on large alveolar deep tooth electrode structures with greatly stretchable oriented fiber membrane. *Chem Eng J* 443:136370. <https://doi.org/10.1016/j.cej.2022.136370>
- [26] Sharma S, Chhetry A, Sharifuzzaman M, Yoon H, Park JY (2021) Hydrogen-Bond-Triggered Hybrid Nanofibrous Membrane-Based Wearable Pressure Sensor with Ultrahigh Sensitivity over a Broad Pressure Range. *ACS Nano* 15:4380–4393. <https://doi.org/10.1021/acsnano.0c07847>
- [27] Cheng W, Wang J, Ma B, Li W, Zhao S, He X (2018) Flexible Pressure Sensor With High Sensitivity and Low Hysteresis Based on a Hierarchically Microstructured Electrode. *IEEE Electron Device Lett* 39:288–291. <https://doi.org/10.1109/LED.2017.2784538>
- [28] Yang T, Xie D, Li Z, Zhu H (2017) Recent advances in wearable tactile sensors: Materials, sensing mechanisms, and device performance. *Mater Sci Eng R Rep* 115:1–37. <https://doi.org/10.1016/j.mser.2017.02.001>
- [29] He B, Yan Z, Zhou Y, Zhou J, Wang Q, Wang Z (2018) FEM and experimental studies of flexible pressure sensors with micro-structured dielectric layers. *J Micromech Microeng* 28:105001. <https://doi.org/10.1088/1361-6439/aaca5d>
- [30] Yang J, Li X, Wen Y, Wang Y, Yuan X, Wu S, Wei Z (2019) Flexible, Tunable, and Ultrasensitive Capacitive Pressure Sensor with Microconformal Graphene Electrodes. *ACS Appl Mater Interfaces* 11:14997–15006. <https://doi.org/10.1021/acsami.9b02049>



16

ULUSLARARASI LİF VE POLİMER ARAŞTIRMALARI SEMPOZYUMU

16th INTERNATIONAL FIBER AND POLYMER RESEARCH SYMPOSIUM

Sürdürülebilir ve İşlevsel Lif ve Polimerler
Sustainable and Functional Fibers & Polymers



9-10 Mayıs
May 2025

İstanbul Teknik Üniversitesi
Gümüşsuyu Prof. Dr. Necmettin Erbakan Yerleşkesi
İstanbul Technical University
Gumussuyu Prof. Dr. Necmettin Erbakan Campus

Farklı modakrilik elyaf karışım oranına sahip kumaşların performans özelliklerinin incelenmesi

Gülşah Karakaya^{a*}, Dilek Toprakkaya Kut^b

^{a,b}Tekstil Mühendisliği, Uludağ Üniversitesi, 16059 Bursa, Türkiye.

^aAKSA Akrilik Kimya Sanayii A.Ş., Müşteri Hizmetleri ve Kalite İzleme Departmanı, 77600 Yalova, Türkiye.

*Sorumlu Yazar: gulsah.karakaya@aksa.com

ÖZET

Teknik tekstiller arasında yer alan koruyucu tekstiller, (Protech) son yıllarda artan iş sağlığı ve güvenliği kuralları ile önemini arttırmıştır. İşyerlerinde kişisel koruyucu donanım kullanımı'nın zorunlu hale getirilmesi de bu pazarın büyümesini teşvik etmiştir. Bu çalışmada, koruyucu kıyafetlerde sıklıkla kullanılan elyaf türleri, elyaf halinde harman yapılarak ring İplik eğirme sistemi ile 9 farklı iplik halini almıştır. Bu iplikler ayrı ayrı örülerek örme kumaş haline dönüştürülmüştür. İpliklerin mukavemet ve uzama değerleri ölçülmüş olup, kumaş formunda ise hava geçirgenliği testi yapılmıştır. Sonuçlar incelendiğinde, modakrilik-aramid karışımları diğer elyaf karışımlarına oranla daha iyi sonuç vermiştir.

Anahtar Kelimeler Modakrilik elyaf ; Aramid elyaf ; Pamuk elyaf ; İplik parametresi ; Hava geçirgenliği ; Güç tutuşur elyaf

Investigation of the performance properties of fabrics with different modacrylic fiber blends

ABSTRACT

Protective textiles (Protech), which are an important subgroup of technical textiles, have gained increased significance in recent years due to the rising standards of occupational health and safety. In particular, the mandatory use of personal protective equipment in workplaces has stimulated both product diversity and the growth of this market segment. In this study, fiber types commonly used in protective clothing were blended and processed into nine different yarn compositions using the ring spinning system. These yarns were separately knitted to produce fabric samples, which were then subjected to various physical tests. The tensile strength and elongation properties of the yarns were measured, while the air permeability of the fabrics was also tested. The results indicate that blends containing modacrylic and aramid fibers exhibited superior performance compared to other fiber combinations. These blends demonstrated optimal properties for protective textile applications.

Keywords: Modacrylic fiber; Aramid fiber; Cotton fiber ; Yarn parameter ; Air-permeability ; Flame resistance fiber

I. GİRİŞ

Estetik ve görsel özelliklerinden ziyade teknik ve performans özellikleri ile bilinen teknik tekstiller, son dönemde tekstil sektöründeki pazar payı artmıştır.

Paketleme, spor, ev tekstili, askeri, balistik, otomotiv, inşaat, denizcilik, havacılık gibi endüstrilerde kullanım alanına sahiptir. Genel olarak öne çıkan özellikleri arasında ise, iyi bir dayanım, esneklik, iyi aşınma direnci, iyi kimyasal dayanım ve boyutsal stabilite vb. olmaktadır.

Koruyucu tekstiller (ProTech), tehlikeli durumlardan çalışan ve KKD ekipmanları kullanan çalışanların güvenliğini sağlamaya yöneliktir. Çalışma koşulları nedeni ile darbe, kesilme, patlama, alev, elektrik voltajı, kimyasal gibi sağlık için tehlike oluşturacak kaynaklardan korunmayı sağlamaktadır. Bu alanda genellikle yüksek performans sınıfına giren tekstil elyafı kullanılmaktadır (aramid, modakrilik, FR viskon, PBI, PBO vb.).



Şekil 1. Koruyucu tekstiller kullanım alanları

KKD, insan vücudunu bahsedildiği gibi çevresel koşullardan korumak için palto, eldiven, t-shirt, ceket, pantolon, ayakkabı, yelek gibi özel koruyucu giysilerden oluşmaktadır. Bu alandaki giysilerde dayanım özelliği olduğu kadar konfor özelliği de olması önem taşımaktadır [1].

Bu çalışmada ise, koruyucu tekstillerde kullanılan modakrilik elyafını, farklı elyaf ve karışım oranına sahip iplik ve kumaş formuna dönüştürerek performansını incelemektir.

Aleve karşı dayanım veya güç tutuşurluk özelliği, tekstil elyafına bitim işlemi ile veya polimerik yapısı sebebi ile kazandırılabilir. Çalışmada odaklanılan modakrilik elyafı ise, polimerik yapısı gereği güç tutuşur özelliği olan bir elyaftır.

Bu çalışmada; farklı karışım oranına sahip 9 adet elyaf harmanı, ring eğirme sisteminde iplik haline getirilerek mekanik özellikleri incelenmiştir.

II. DENEYSEL METOT / TEORİK METOD

2.1 Materyal

Bu çalışmada temel materyal olarak; 7 adet farklı elyaf 9 farklı harman oranı ile ring iplik eğirme sisteminde NM 47/2 numarasında çift kat ipliğe dönüşmüştür. Kullanılan 7 farklı elyaf tipi detay bilgilerine Tablo 1'de yer verilmiştir.

Tablo 1. Çalışmada kullanılan elyaf bilgileri

| Kullanılan Elyaf Tipi | Elyaf Numara Bilgisi (dtex) | Kesim Boyu (mm) |
|-----------------------|-----------------------------|-----------------|
| Modakrilik | 1.7 | 38 |
| Pamuk | 1.3 | 30 |
| Lyocell | 1.4 | 38 |
| Viskon | 1.3 | 38 |
| Viskon FR | 1.7 | 51 |
| Para-aramid | 1.7 | 51 |
| Meta-aramid | 1.67 | 50 |

2.2 Metot

Bu çalışmada üretilen 9 adet iplik, düz örme makinasında, 150-180 gsm aralığında örme kumaş halini almıştır. Kumaşların karışım oran ve gramaj bilgileri Tablo 2'de yer almaktadır.

Tablo 2. Çalışmada kullanılan kumaş kompozisyon ve gramaj bilgisi

| Numune Kodu | Kumaş Kompozisyon Bilgisi (%) | Gramaj (gr/m ²) |
|-------------|-------------------------------|-----------------------------|
| R1 | %55 Modakrilik %45 Pamuk | 150.8 |
| R2 | %55 Modakrilik %45 Lyocell | 162 |

16. Uluslararası Lif ve Polimer Araştırmaları Sempozyumu (16. ULPAS)
9-10 Mayıs 2025, İstanbul teknik Üniversitesi (İTÜ), Türkiye

| | | |
|-----|------------------------------------------------------|-------|
| R5 | %55 Modakrilik %45 Viskon FR | 170.2 |
| R6 | %55 Modakrilik %45 Viskon | 151.3 |
| R8 | %54 Meta-aramid %40 Modakrilik %6 Para- aramid | 151 |
| R9 | %69 Modakrilik %25 Meta-aramid %6 Para- aramid | 151 |
| R10 | %60 Meta-aramid %34 Modakrilik %6 Para- aramid | 177.3 |
| R11 | %50 Meta-aramid %50 Viskon FR | 150.1 |
| R12 | %65 Viskon FR %35 Meta-aramid | 152.2 |

İpliklerin tek katına yapılan mukavemet/uzama testi sonuçlarına Tablo 3'te yer verilmiştir.

Tablo 3. Tek kat iplik mukavemet/uzama sonuçları

| İplik Kodu | İplik Mukavemet Sonuçları | | İplik Uzama Sonuçları | |
|------------|---------------------------|----------|-----------------------|----------|
| | Ortalama (rkm) | s (σ) | Ortalama (%) | s (σ) |
| R1 | 8.42 | 1.63 | 5.33 | 0.97 |
| R2 | 11.91 | 1.45 | 5.74 | 0.98 |
| R5 | 10.03 | 0.61 | 7.45 | 0.93 |
| R6 | 12.41 | 1.03 | 11.83 | 1.42 |
| R8 | 22.75 | 1.87 | 15.74 | 1.37 |
| R9 | 19.48 | 2.28 | 17.74 | 2.51 |
| R10 | 21.32 | 2.52 | 13.81 | 2.49 |
| R11 | 15.84 | 2.13 | 7.02 | 0.89 |
| R12 | 15.42 | 2.44 | 6.70 | 1.03 |

Çalışmada karışım elyaf harmanından yapıldığı için, iplik ve kumaş kodları aynı olmakla beraber, karışım oranı da aynıdır.

Kumaşların performans özelliğini değerlendirebilmek adına, hava geçirgenliği testi yapılmıştır. Her kumaş numunesine 5 adet tekrar yapılmış olup, ortalaması alınmıştır.

Tablo 4. Kumaş hava geçirgenliği sonuçları

| Kumaş Kodu | Hava Geçirgenliği Sonuçları | |
|------------|-----------------------------|--|
| | l/m ² /s | |
| R1 | 3630 | |
| R2 | 4432 | |
| R5 | 3568 | |
| R6 | 3306 | |
| R8 | 4158 | |
| R9 | 4550 | |
| R10 | 4588 | |
| R11 | 3872 | |
| R12 | 3864 | |

2.3 Test ve analiz yöntemleri

Ring iplik eğirme sistemi ile üretilen 9 adet ipliğin, AKSA Akrilik Kimya Sanayi A.Ş.'ye ait pilot tesiste, iplik numarası, mukavemet ve uzama değerleri ölçülmüştür.

2.3.1. İplik mukavemeti ve uzaması

Şekil 2'te verilen Uster Tensorapid 4 cihazına 10 adet farklı kopstan iplik sarılır. İplik, cihazda bulunan alt ve üst çeneye yerleştirilerek kuvvet uygulanır. Çeneler arası mesafe 500mm olup, alt çene hızı 5000mm/dk'dır. İpliğin koptuğu noktada ölçüm biter.

Şekil 2. USTER Tensorapid 4 cihazı

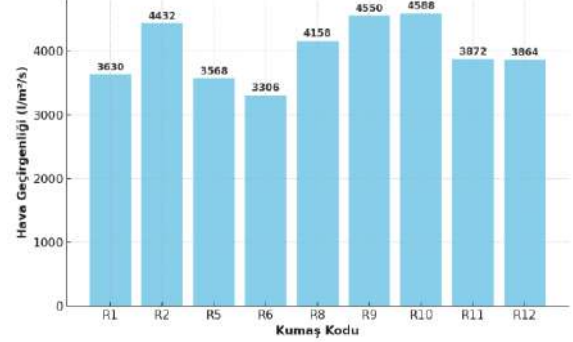


Şekil 3. SDL Atlas hava geçirgenliği test cihazı



Sonuçlar incelendiğinde en yüksek değerler mukavemet değerinde olduğu gibi belirgin fark ile sırasıyla R9, R8 ve R10 olmuştur. Modakrilik oranı arttıkça, uzama değeri de artmıştır.

Şekil 6. Kumaş hava geçirgenliği ölçüm sonuçları



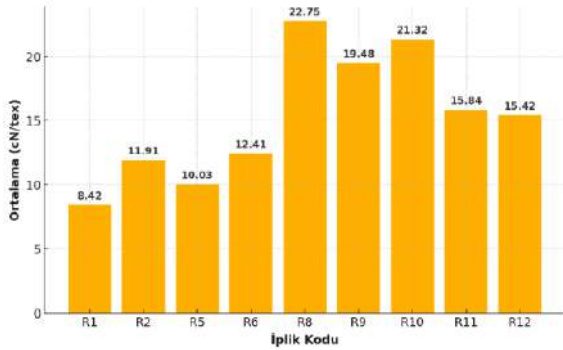
Kumaş sonuçları incelendiğinde sırasıyla R10, R9 ve R2 olmuştur. Lyocell elyafı pamuk ve viskona göre daha iyi nefes alabilirlik özelliği göstermiştir.

III. BULGULAR VE TARTIŞMA

İplik mukavemet ölçüm sonuçları incelendiğinde;

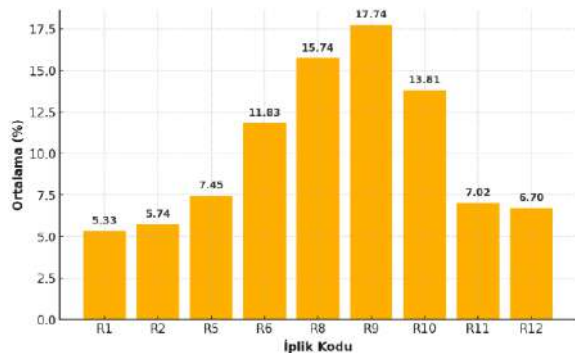
Çalışma için hazırlanan ipliklere ait mukavemet ölçüm sonuçlarına Şekil 4'te yer verilmiştir.

Şekil 4. İplik mukavemet ölçüm sonuçları



Grafik incelendiğinde sırasıyla, R8, R10, R9 iplikleri diğer ipliklere göre yüksektir. Aramid içeriği olması sebebi ile bu sonuç beklenirken, karışım meta-aramid eklendiğinde mukavemetin görülür bir fark yarattığı ortaya çıkıyor.

Şekil 5. İplik uzama ölçüm sonuçları



IV. SONUÇLAR

Bu tez çalışması kapsamında, koruyucu kıyafetlerde sıklıkla kullanılan elyaf ve harman oranları ile iplik ve kumaş testleri yapılmış olup, modakrilik elyafın performans özelliği incelenmiştir.

İplik mukavemet ve uzama analizinde selülozik elyaf ile modakrilik elyafı karışımı yapıldığında en iyi sonuç, viskon elyafı ile görülmüştür. Sonuçlarda genellikle mukavemet ve uzama değerinin doğru orantılı bir ilişkisi olduğu söylenebilir. Özellikle para-aramid elyaf oranı sabit tutulup, meta-aramid oranı arttığında mukavemet ve uzama değeri artış göstermiştir.

Kumaş hava geçirgenliği sonuçları incelendiğinde ise, birbirine yakın değerler bulunmuştur. Viskon elyafı ile yapılan karışım, mukavemet/uzama değeri olarak diğer selülozik elyaf karışım kumaşlarına göre daha iyi iken, hava geçirgenliği değeri bu kumaşlara göre daha kötü bir sonuç göstermiştir.

Bu üç parametre birlikte değerlendirildiğinde en optimum sonucu gösteren R9 isimli kumaş olmuştur.

Kumaşlara ISO 15025 testi yapılmıştır.



In-process vertical reinforcement of 3D printed concrete structures

Seyedmansour Bidoki^{1,*}, Mahsa Bidoki², Hasan Haroglu³, Adil Kahwash Al-Tamimi⁴, Oguzhan Sahin⁵, Ali Demir⁶

1- Faculty of Textile Technologies and Design, Istanbul Technical Uni., Istanbul, Türkiye bidoki@itu.edu.tr & Textile Engineering Department, Yazd Uni., Yazd, Iran, smbidoki@yazd.ac

2- Faculty of Dentistry, Istanbul Kent University, Istanbul, Turkey, bidokimahsa@gmail.com

3- Department of Construction Engineering, Engineering Faculty, University of Doha for Science and Technology, Doha, Qatar, hasan.haroglu@udst.edu.qa

4- College of Engineering, American University of Sharjah, Sharjah, U.A.E, atamimi@aus.edu

5- Civil Engineering Department, Ankara University, Ankara, Türkiye, ohsahin@ankara.edu.tr

6- Faculty of Textile Technologies and Design, Istanbul Technical Uni., Istanbul, Türkiye, ademir@itu.edu.tr

*Corresponding author: bidoki@itu.edu.tr

ABSTRACT

Additive manufacturing, particularly in the context of 3D concrete printing (3DCP), has gained significant interest due to its material efficiency and ability to achieve geometries with high complexity. One of the various challenges within 3DCP is the low interlayer bonding, leading to anisotropic mechanical properties. The present study summarizes some of the in-process vertical mechanical reinforcing techniques to address this issue, including mechanical insertions, wire embedding, and sophisticated integration of reinforcements. The article covers recent progress, patents, and experimental studies, highlighting their benefits and limitations. The patented technique recently filed for in-process weaving or knitting the reinforcing mesh inside the printed layers called Bidoki method is also introduced for the first time which upon development in industrial scale has the potential to revolutionize 3DCP building industry. Through its incorporation of automation, material adaptability, and structural optimization, this new method offers a scalable template to 3D printing of concrete and polymeric composite, thus unlocking the prospects for resource-efficient, high-strength, and geometrically advanced constructions.

Keywords: 3D Concrete Printing, Carbon Fibers, Vertical Reinforcement, In-situ Mesh Formation, Embedded Reinforcement

I. INTRODUCTION

The rapid development of 3D concrete printing (3DCP) has transformed the construction industry by reducing material waste and enabling shorter construction times. However, interlayer adhesion remains a critical issue, leading to structural defects under tensile and shear loads. Traditional reinforcement methods, such as post-printing steel reinforcement and fiber-reinforced concrete, possess their own limitations in addressing interlayer bond strength comprehensively. To mitigate this, various reinforcement strategies have been proposed, which are categorized under thermal bonding, chemical adhesion, ultrasonic/vibrational enhancement, and mechanical reinforcement [1]. The current study addresses mechanical reinforcement techniques, in particular, in-process vertical reinforcement.

II. MECHANICAL REINFORCEMENT IN 3DCP

Mechanical reinforcement methods can be categorized into pre-printing, in-process, and post-printing techniques. Pre-printing reinforcement comprises the addition of high-tensile fibers to the cement-based material for improved tensile performance with cracking reduction. Extrusion challenges and non-uniform fiber content are still limitations [2]. Post-printing reinforcement shown in figure 1, typically consists of the installation of rebar or mesh into the printed structure to obtain traditional construction strength at the expense of additional labor and materials [3].

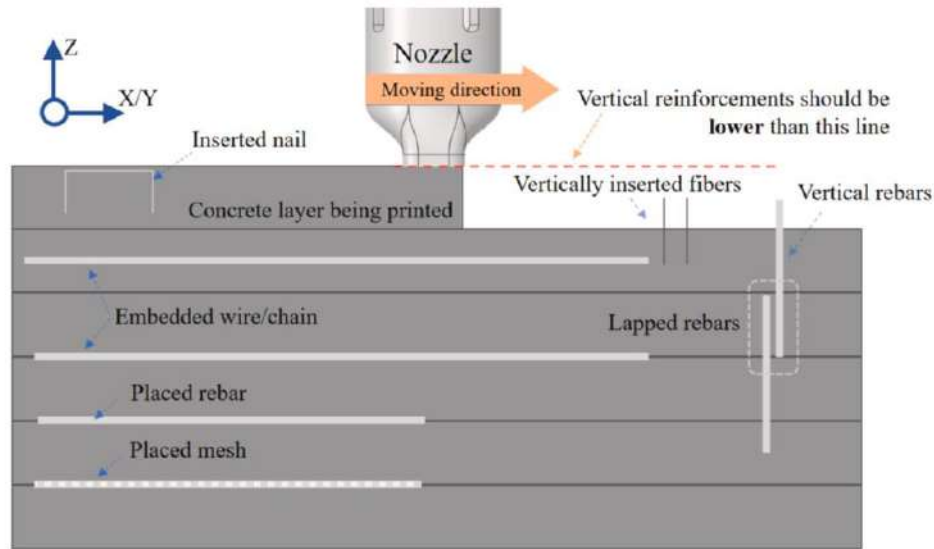


Figure 1- Current Post process and In-process Reinforcement Techniques which lacks vertical continuity [3]

III. IN-PROCESS VERTICAL REINFORCEMENT TECHNIQUES

To overcome the limitations of pre- and post-printing reinforcement, various methods of in-process reinforcement have been established. Tamimi et al. designed and produced 3D concrete bridge element that achieved approximately 65% of the load-bearing capacity of traditional reinforced concrete segments is seen as a promising result, highlighting the viability of 3DCP in structural applications. It suggests a path forward in enhancing the technology to match or surpass conventional construction methods. The implications of this research are significant, suggesting that with further development in reinforcement strategies, 3DCP could revolutionize the construction industry by combining environmental sustainability with structural integrity [4]

One of the first designs proposed for multi-dimensional reinforcement of 3D-printed structures was proposed by Khoshnevis in 2004 [5]. Khoshnevis developed a new reinforcement method to include reinforcement in the Contour Crafting printing process. Steel reinforcement used here consists of many small steel elements (Figure 2), which can be shaped into different shapes (strip and mesh). The printing procedure is run under the control of a gantry system which consists of a nozzle for shell printing, a steel component assembly robot, and a concrete formwork filling feeder. The complexity of this expensive and highly detailed printing system makes it challenging to apply in real construction procedures.

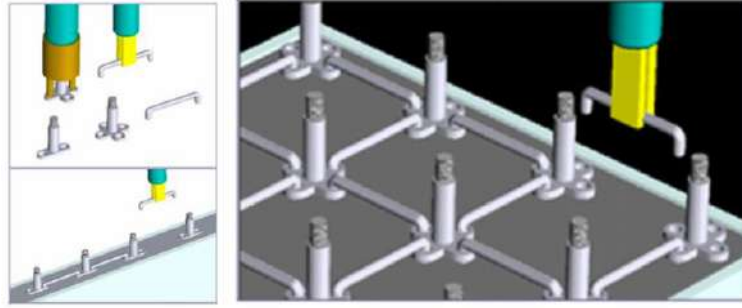


Figure 2- Assembling steel elements inside a shell printed by a 3D printer and subsequent burying of the steel elements by pouring in concrete into the shell developed by Khoshnevis [5]

Other in-process and post process methods invented and proposed for vertical reinforcement are summarized in the following section.

3.1. Robotic Steel Bar Insertion

In this method, steel reinforcement bars are inserted while printing, specifically targeting poor interlayer interfaces. This method effectively prevents cold joints and enhances structural performance. Classen et al. introduced an Additive Manufacturing of Reinforced Concrete (AMoRC) process combining intermittent stud welding and continuous concrete extrusion to generate a 3D mesh structure embedded within printed concrete [6].

Wire Arc Additive Manufacturing (WAAM), a metal 3D printing technique, allows the fabrication of reinforcement elements drop-wise with geometric flexibility. But high heat generated during printing steel can ruin adjacent concrete layers, and hence the process becomes costly and complicated as shown in figure 2 [7, 11]. Figure 3 depicts a gas-metal arc welding system (a) and printed steel reinforcement (b), highlighting heat-related challenges.

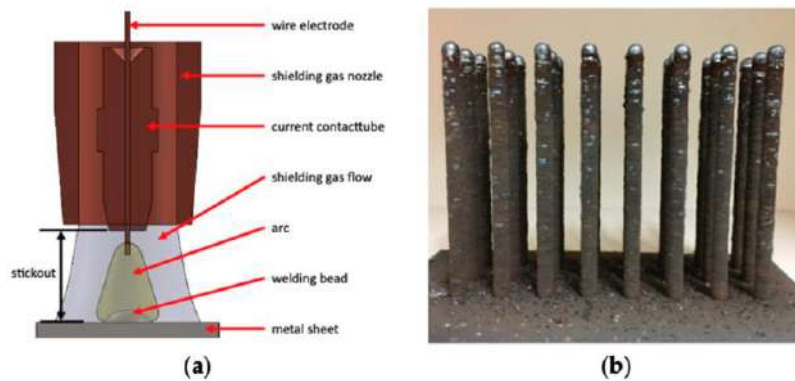


Figure 3- Steel printing concept of generating steel bars automatically while printing the concrete: (a) gas-metal arc welding system and (b) printed steel bars [6]

3.2. Metallic and Polymeric Filaments

Introduction of continuous metallic or polymeric filaments during the extrusion improves interlayer adhesion in the printed layers. US 10,173,410 B2 patent suggests using long fiber reinforcement integrated into the process of extrusion to enhance interlayer adhesion as shown in figure 4 [8, 9].

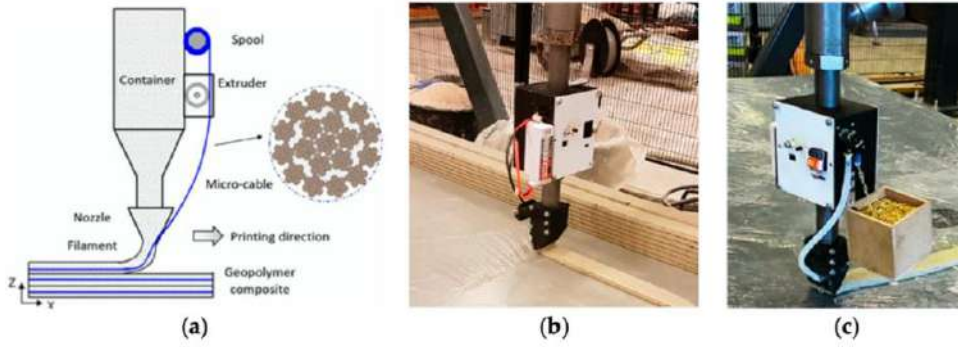


Figure 4- Different type of horizontal reinforcement used in concrete 3d printing (a)continuous steel cable, (b) wire rope, (c) steel chain [9]

3.3. Textile-Based Reinforcement

2.5D textile reinforcement, suggested by Mechtcherine et al., utilizes mesh insertion in continuous manner to improve interlayer adhesion. The process interconnects the adjacent layers non-continuously, improving shear strength without complete vertical integration as shown in figure 5 [10]. Figure 5 shows vertical steel mesh placement (a), nozzle cross-sections (b), and layer overlaps (c).

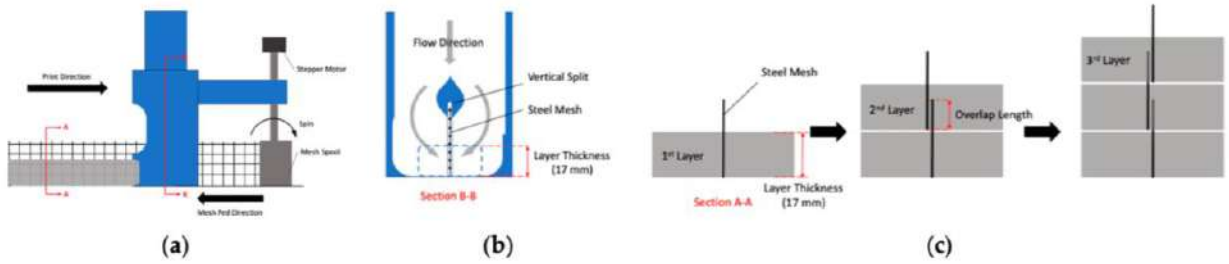


Figure 5- Vertically placed wire mesh for non-continuous reinforcement and inter layer bonding: (a) placement of vertical steel mesh reinforcement, (b) cross section of nozzle head, and (c) overlapping of steel mesh between printed layers [10]

3.4. Sewing Method for Reinforcement

Jacquet et al. proposed a novel method using a sewing machine-type system to sew together neighboring layers with reinforcing cables shown in figure 6. While this technique supports horizontal and vertical reinforcement, its effectiveness is limited by the bond between the cable surface and printed material [11].

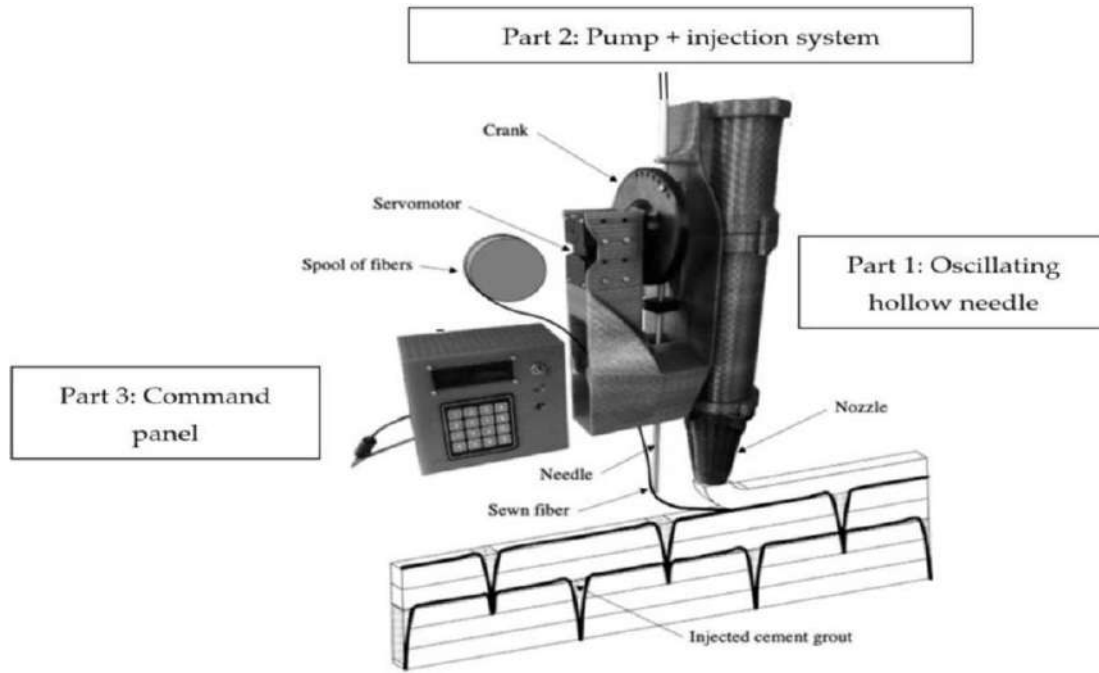


Figure 6- Sewing technique for vertical reinforcement of 3D printed concrete layers [11]

3.5. Post Process In-situ Mesh fabrication technique

X. Cao et. al. reported a method of digging holes in different directions inside the printed structure and filling the holes with special epoxy resin to form a continuous reinforcing structure in vertical and horizontal direction as shown in figure 7. Although the technique provides all direction adhesion between the layers, it is a kind of post reinforcement process and needs additional equipment's and cannot be done simultaneously as the 3D printing process. Limited strength of the epoxy resins for level of tensile strength needed for the concrete structures is another limiting criterion [12].

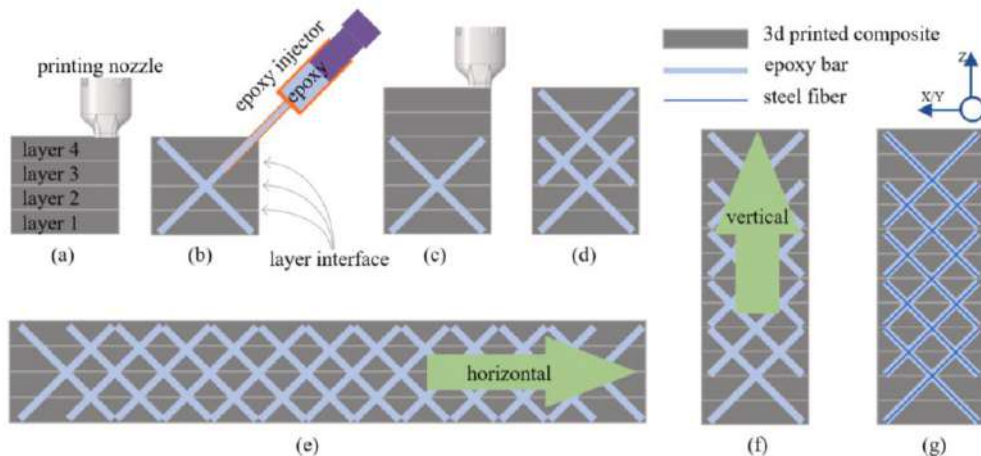


Figure 7- In-situ mesh formation with epoxy resins. (a) 3DPC layers stacked, (b) two crossing epoxy bars are injected at the interfaces of the layers using a common injector, (c) additional stacking of composite layers, (d) two other epoxy bars are added to the previous ones in order to create a mesh—produced horizontally in (e) and vertically in (f), and (g) steel reinforcement is inserted within the epoxy bars [12]

3.6. Wrapping the Printed Layers

WO 2021/233905 A1, discloses a reinforcement method for 3D printed structures by incorporating continuous filaments during the printing process to enhance mechanical properties. This method bonds the printed layers in the vertical direction from the outside while embedding the reinforcement filament between the layers in only the horizontal direction perpendicular to the printing direction as shown in figure 8 [13].

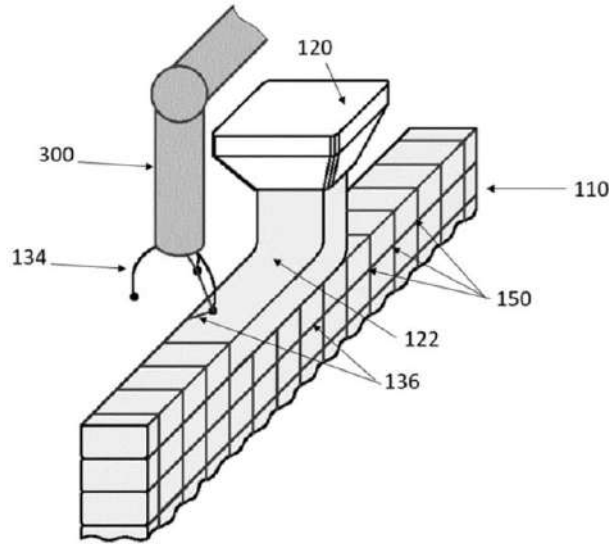


Figure 8-Reinforcement method and device in which the constructing material (122) is extruding out of the nozzle (120) and a robotic arm (300) leading 3 needles (134) to move and connect the reinforcement yarn (136) from the top layer to the lower layer reinforcement strand or weave [13]

The reinforcements serve as mechanical anchors that bridge adjacent layers and distribute stresses more effectively throughout the structure which protect the layers in vertical direction from outside of the structure. It involves inter-weaving or knitting embodiments which weave or knit a texture around each layer whilst connecting them to the previously 3D printed layer. While this reinforcement strategy improves the structural integrity of the printed material, it may introduce risks during tensile loading. Perhaps, the orientation of the reinforcement would have caused the longitudinal forces to act horizontally, causing crack formation in that direction as seen in most concrete and mortar structures subjected to stress. This may complicate the printing process by relying on external reinforcement materials and limit the compatibility of the process with specific materials or geometries. Connecting the top layers reinforcing yarns and weave them to the previously woven texture around the previous layer is another challenge in the above-mentioned embodiment as it needs very sophisticated technological needles and robotic arms to manage the knotting and inter weaving process and also the speed of interweaving and knotting may affect the total 3D printing speed in an adverse manner.

3.7. Recent Patent on In-Process Reinforcement

The most recent invention relates to novel products and methods addressing the challenges associated with in-process, three-dimensional reinforcement of additively manufactured (3D printed) structures filed by Bidoki et al. titled “Continuous and In-Situ Buried Vertical and Horizontal Reinforcement for Additive Manufacturing Structures” [14]. Specifically, the invention introduces innovative techniques to reinforce

printed layers by interconnecting them in the X, Y, and Z directions using flexible metallic or nonmetallic wires, cables, rods, or in a continuous and integrated manner as shown in figure 9.

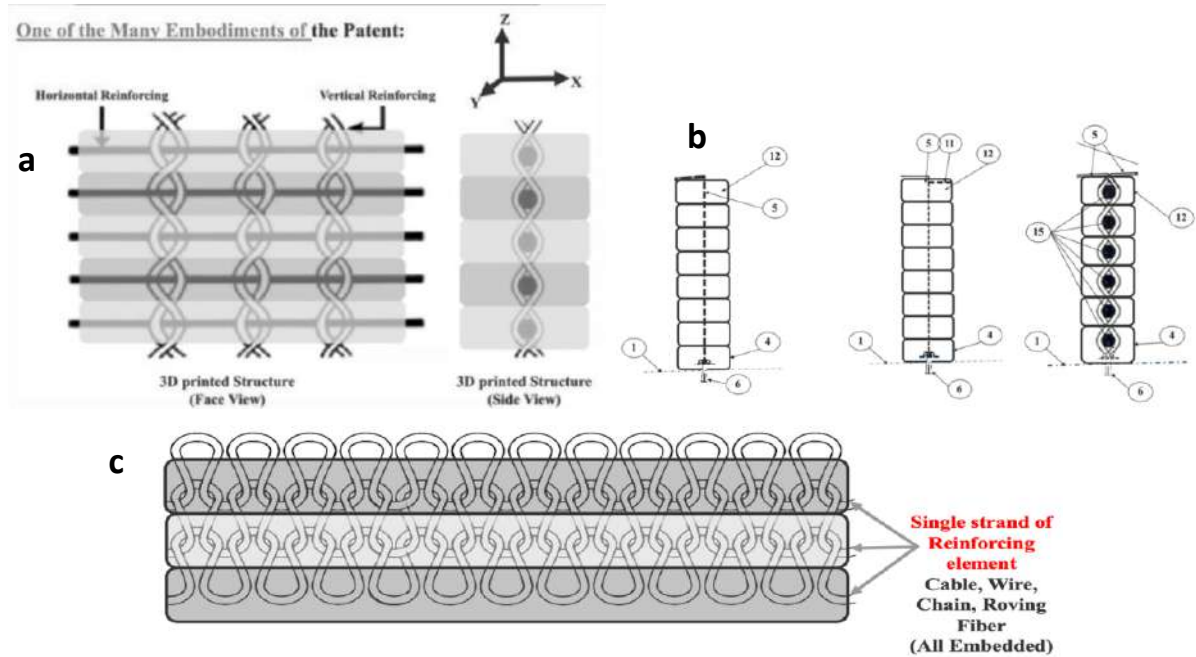


Figure 9-Recent patented method for In-process reinforcement in horizontal and vertical directions. In-situ inter-weaving of a mesh fabric layer by layer (a), Vertical positioning of reinforcing flexible elements inside the printed layers during the printing process (b), In-situ inter-knitting of a connected mesh inside the printed structures layer by layer (c) [14]

In another embodiment of Bidoki method a 1.5 layers vertical mesh or reinforcing structure can be connected to the previously placed elements by in-process sewing, welding or gluing procedures guarantying continuity of the reinforcing structure in the vertical direction which was not previously reported. The concept is shown in figure 10 for two examples of vertical reinforcement.

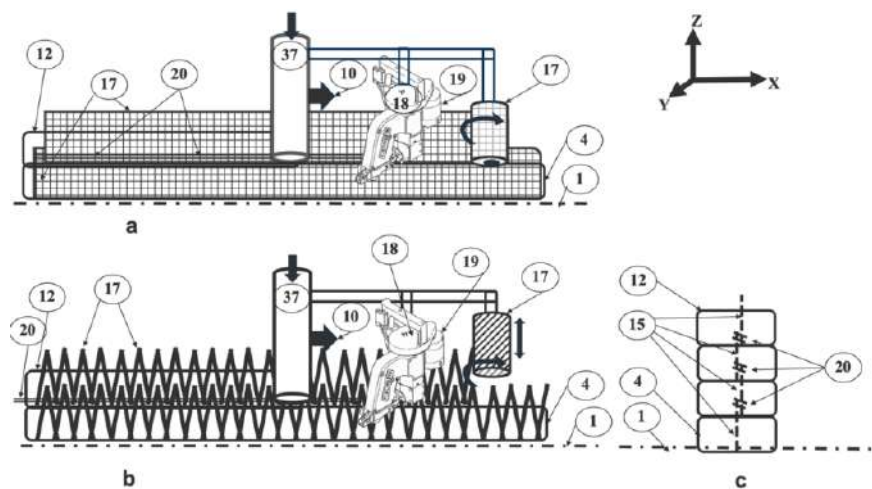


Figure 10- Connecting 1.5 layers reinforcing elements with sewing (a), welding (b) which connects the separately positioned vertical reinforcement together with connection lines (c) [14]

Assembling Solo Reinforcing Elements (SRE) in single or multi directional style and their placement by a robotic hand and connection to the previously placed elements along with a special conveying system is the other reinforcement method brought forward in Bidoki patent shown in figure 11.

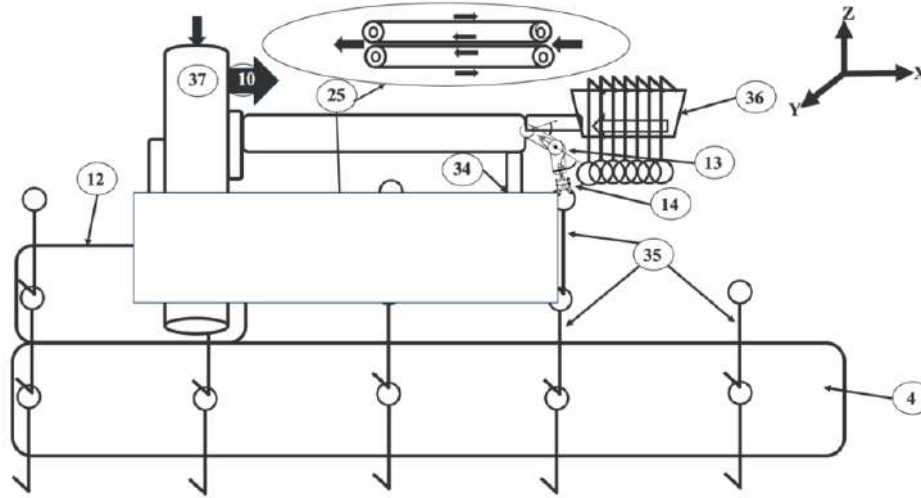


Figure 11- Vertical reinforcement using Solo Reinforcing elements which is taken from a cartridge (36) and connected to the previously positioned solo elements in previous layer by a suitable mechanism or robotic hand [14].

Bidoki method proposes a system capable of delivering reinforcement elements in the form of continuous strands or woven/knitted fabric structures at a speed synchronized with the 3D printing process. The method achieves simultaneous reinforcement in the X, Y, and critically, the Z directions. Unlike previously reported techniques, which typically focus on two-dimensional reinforcement or post-process integration, this invention embeds inter-knitted or inter-woven reinforcement textures directly within the layers during the additive manufacturing process, thereby ensuring consistent mechanical integrity across all three dimensions.

The reinforcement level can be tailored to meet specific mechanical or structural requirements, with options for one-, two-, or three-dimensional reinforcement. The reinforcement elements, which may be composed of flexible and bendable materials of any origin with any surface structure and longitudinal form and curvature with different surface coatings are designed to be used in this system.

This recent invention unlocks the full potential of integrating textured reinforcing elements into 3D printing procedures, extending beyond the limitations of knitted or woven textures. The invention encompasses all currently known methods, as well as any future-developed techniques, for preparing textured or single or multi-dimensional reinforcing elements that can be seamlessly embedded into additively manufactured layers.

This approach enables the creation of complex, reinforced structures by incorporating a wide variety of reinforcement configurations, including but not limited to woven, braided, interlocked, or other textured elements, alongside single-dimensional strands, ribbons, meshes, cables, or wires. The invention ensures flexibility in design and adaptability to diverse reinforcement needs, paving the way for innovations that enhance the mechanical properties and structural integrity of 3D-printed objects.

IV. CHALLENGES AND FUTURE DIRECTIONS

Despite the remarkable advances, there are challenges to fully integrating vertical reinforcement in 3DCP. These are:

- Optimization of reinforcement placement to achieve a uniform stress distribution.
- Economical automation for reinforcement integration.
- Compatibility of reinforcement material and cementitious matrix. Material compatibility issues arise with hydrophobic coatings on reinforcement elements, necessitating chemical adhesion studies.
- Current robotic systems for reinforcement integration face speed limitations; future work could explore AI-driven mechanisms.

V. CONCLUSION

The development of in-process vertical reinforcement techniques for 3D concrete printing (3DCP) addresses the critical problem of anisotropic mechanical behavior caused by inadequate interlayer bonding. Various mechanical reinforcement strategies, including robotic steel bar embedding, metallic/polymeric filaments, textile-based mesh integration, sewing methods, and in-situ epoxy mesh printing, are reviewed in this paper. While these methods enhance interlayer adhesion and structural integrity, they are hindered by material compatibility issues, process complexity, and reliance on post-processing procedures.

The development of Bidoki method as in-process reinforcement technique that adds inter-knitted or woven textures in printed layers during production is a breakthrough. The technology offers three-dimensional (X, Y, Z) reinforcement with mechanical anchoring and stress distribution that is superior to two-dimensional or after-printing conventional techniques. Its ability to synchronize reinforcement placement with print speed and adapt to diverse material setups is what gives it a potential for groundbreaking development in the 3DCP industry. Unlike prior 2D methods, the technique enables 3D reinforcement via interwoven textures, synchronized with printing speed.

However, there remain challenges in the optimization of reinforcement placement for even stress distribution, cost-saving automation, and the compatibility of reinforcement materials with the cementitious matrix. Future research has to cover the refinement of robotic systems for imperceptible integration, the creation of scalable and sustainable reinforcement materials, and the confirmation of long-term performance under real loading conditions. The resolution of these challenges will unlock the full potential of 3DCP, enabling the production of structurally viable, geometrically complex, and resource-efficient concrete structures.

Other than cementitious materials, Bidoki patented technology holds high potential for polymer composite 3D printing, where reinforcement integration has the tendency of being troublesome in offering equal fiber distribution and interfacial bonding. With the incorporation of flexible, high-strength fibers like carbon, glass, or aramid as in-situ woven/knitted meshes through extrusion, this technology would be able to offer unbroken, multidirectional reinforcement suitable to the anisotropic demands of polymer composites. This would enhance mechanical performance (e.g., tensile strength, impact resistance) without sacrificing design freedom and process efficiency. The future work can explore synergies between the method's synchronized delivery of reinforcement and thermoplastic/thermoset matrices, with new prospects in lightweight aerospace components, automotive parts, and multifunctional smart structures.

REFERENCES:

- [1] J.F. Caron et al., "Reinvent Reinforced Concrete with Robotics and 3D Printing," 41st International Symposium on Automation and Robotics in Construction (ISARC 2024).
- [2] M. Classen et al., "Additive Manufacturing of Reinforced Concrete," Applied Sciences, 10(11), 2020. DOI:10.3390/app10113791.
- [3] V. Mechtcherine et al., "Integration der Bewehrung beim 3D-Druck mit Beton," Beton- und Stahlbetonbau, Vol. 113, No. 7, pp. 496–504, 2018. DOI:10.1002/best.201800003.

- [4] A. Khaldoune, A. Tamimi, H. Hassan, W. Abouetia, T. Kablan and Y. Kaied,, “ Structural performance of bridge segments by 3D concrete printing under static cycling loading” Journal of Engineering Science and Technology, Special Issue on AIEC2024 Vol. 20, No. 1 (2025) 37 – 48.
- [5] Khoshnevis, B., Automated construction by contour crafting—Related robotics and information technologies. *Autom. Constr.* **2004**, *13*, 5–19
- [6] T. Marchment et al., "Mesh Reinforcing Method for 3D Concrete Printing," Automation in Construction, vol. 109, 2020. DOI:10.1016/j.autcon.2019.102992.
- [7] Mechtcherine, V.; Grafe, J.; Nerella, V.N.; Spaniol, E.; Hertel, M.; Füssel, U. 3D-printed steel reinforcement for digital concrete construction—Manufacture, mechanical properties and bond behaviour. *Constr. Build. Mater.* **2018**, *179*, 125–137
- [8] US Patent 10,173,410 B2, "Device and Methods for 3D Printing with Long Fiber Reinforcement."
- [9] Z. Wu, A.M. Memari, J.P. Duarte, State of the Art Review of Reinforcement Strategies and Technologies for 3D Printing of Concrete,
- [10] V. Mechtcherine et al., "Integrating Reinforcement in Digital Fabrication with Concrete," Journal of Cement and Concrete Composites, 2021. DOI:10.1016/j.cemconcomp.2021.103964.
- [11] Y. Jacquet, "Sewing Concrete Device—Combining In-Line Rheology Control and Reinforcement System for 3D Concrete Printing," Materials (Basel), 2023. DOI:10.3390/ma16145110.
- [12] X. Cao, S. Wu, H. Cui, “Experimental study on in-situ mesh fabrication for reinforcing 3D-printed concrete”, Automation in Construction, Volume 170, February 2025, 105923
- [13] Danmarks Tekniske Universitet, World Patent, Apparatus and Method for Manufacuring Reinforced 3D Printed Structures, WO/2021/233905, 2021
- [14] SM. Bidoki, M. Bidoki, patent pending titled “Katmanlı Üretim Yapıları İçin Sürekli ve Yerinde Gömülü Dikey ve Yatay Takviye” (English Translation: “Continuous and In-Situ Buried Vertical and Horizontal Reinforcement for Additive Manufacturing Structures”), Turkish Patent pending Application No: 2025/001794, 14.02.2025.



Superhydrophobic PVDF nanofiber piezoelectric sensor reinforced with core–shell ZnO@ZIF-8 structure

Milad Atighi ^{a,b}, Mahdi Hasanzadeh ^{a,*}, Roohollah Bagherzadeh ^b

^a Department of Textile Engineering, Yazd University, Yazd 89195-741, Iran.

^b Advanced Fibrous Materials Laboratory (AFM-LAB), Institute for Advanced Textile Materials and Technologies (ATMT), Textile Engineering Department, Amirkabir University of Technology, 159163-4311, Tehran, Iran.

*Corresponding author: m.hasanzadeh@yazd.ac.ir

ABSTRACT

We report the development of flexible piezoelectric nanogenerators based on electrospun PVDF fibers incorporating core–shell ZnO@ZIF-8 composites. Core–shell ZnO@ZIF-8 particles were prepared via a self-templating route and dispersed into 25 wt % PVDF solutions at loadings of 1–10 wt %. Electrospinning yielded uniform, bead-free nanofibers whose average diameter decreased from ~253 nm (pure PVDF) to ~153 nm (1 wt % composite). X-ray diffraction revealed that β -phase content increased with filler loading up to 5 wt %, while excessive 10 wt % loading caused filler aggregation and a decline in β -phase fraction. Water contact angle measurements showed enhanced hydrophobicity, rising from 111.6° for neat PVDF to 125.9° for the highest composite content. Under cyclic mechanical stimulation (2.5 N, 1 Hz), the PVDF/(ZnO@ZIF-8)-5% nanofiber mat produced a peak voltage exceeding 5 V more than double that of the pristine PVDF. The PVDF/(ZnO@ZIF-8)-5% nanofibrous composite demonstrated optimal balance between fiber uniformity, β -phase nucleation, and mechanical robustness, making it a promising candidate for superhydrophobic self-powered sensing in wearable and flexible electronics.

Keywords: E-Textiles; Metal-organic framework; Nanofiber; Piezoelectric; Zinc Oxide

I. INTRODUCTION

Zeolitic imidazolate framework-8 (ZIF-8) is a prototypical metal–organic framework (MOF) composed of Zn²⁺ ions bridged by 2-methylimidazolate linkers, renowned for its exceptional chemical and thermal stability as well as high porosity and tunable pore size, making it suitable for applications in gas storage, separation, and sensing [1]. Core–shell ZnO@ZIF-8 composites, wherein ZIF-

8 grows in situ on ZnO templates, combine the semiconducting properties of ZnO with the molecular sieving and high surface area of ZIF-8, yielding materials advantageous for photocatalysis and electrocatalysis [2,3].

Poly(vinylidene fluoride) (PVDF) is a semicrystalline fluoropolymer exhibiting piezoelectricity when crystallized in its electroactive β -phase, which can be induced via mechanical stretching or high electric

fields [4,5] Electrospinning of PVDF solutions not only fabricates nanofibers with diameters in the submicron range but also promotes β -phase formation in situ due to the high electric field and mechanical stretching experienced by the polymer jet, eliminating the need for post-poling [6,7].

Incorporation of fillers such as ZnO nanoparticles or MOFs into PVDF during electrospinning has been demonstrated to further enhance β -phase nucleation by providing heterogeneous nucleation sites and interfacial interactions, thereby improving piezoelectric response [7–10]. Recent reports of PVDF/MOF nanofibrous composites used as nanogenerators have shown output voltages on the order of several volts under cyclic loading, highlighting the potential of these hybrid materials for self-powered sensing [11–13]. However, excessive filler loading can lead to particle aggregation, fiber defects, and diminished piezoelectric performance, necessitating optimization of composite content [14].

This study synthesises core-shell ZnO@ZIF-8 composites via a self-template method and produces PVDF/(ZnO@ZIF-8) nanofibers using electrospinning. We systematically investigate the effects of different composite loadings (1–10 wt %) on fiber morphology, crystal phase composition, surface wettability, and piezoelectric output to identify the optimal formulation for flexible sensor applications.

II. EXPERIMENTAL METHOD

2.1 Materials

Zinc oxide (ZnO, 99.0%), 2-methylimidazole (2-MIM), and zinc nitrate hexahydrate ($\text{Zn}(\text{NO}_3)_2 \cdot 6\text{H}_2\text{O}$ 98%) were sourced from Merck Co. (Germany). Poly(vinylidene fluoride) (PVDF) with a molecular weight of 350,000 g/mol was acquired from Kynar Co. (USA), while N,N-dimethylformamide (DMF, $M_w=73.09$ g/mol, 99.0%) was obtained from Neutron

Pharmaceutical Co. (Iran) and used without additional purification.

2.2 Synthesis of ZnO@ZIF-8 and Electrospinning of PVDF Nanofibers Containing ZnO@ZIF-8

Here, a Core-shell ZnO@ZIF-8 composite was synthesized following a modified procedure based on Previous research (Ref). Initially, 0.164 g of 2-methylimidazole (2-MIM) was dissolved in 15 mL of N,N-dimethylformamide (DMF) and preheated to 70 °C. In a separate container, 0.140 g of ZnO powder was stirred for 15 minutes and then added to the preheated 2-MIM solution. Three drops of an anionic surfactant were subsequently incorporated, and the resulting suspension was continuously stirred at 70 °C for 5 hours, ensuring the uniform formation of the ZnO@ZIF-8 composite.

Following the composite synthesis, the fabrication of PVDF-(ZnO@ZIF-8) nanofibers was carried out via electrospinning. First, PVDF powder was dissolved in DMF (25 wt %) at 50 °C under gentle stirring for 12 hours. Thereafter, predetermined amounts of the ZnO@ZIF-8 composite (ranging from 1 to 10 wt %) were added, and the mixture was stirred for an additional 12 hours. To enhance dispersion, the solution was sonicated in an ultrasound bath for 20 minutes. The well-dispersed polymer solution was then loaded into 5 mL plastic syringes equipped with a 22-gauge needle. The electrospinning process was performed using a horizontal apparatus (Nano-Azma, Iran) with a controlled flow rate of 0.2 mL/h set by a syringe pump. A DC high-voltage power supply set at 25 kV was applied, establishing a 12 cm gap between the needle tip and the grounded collector. Nanofibers were collected on a rotating drum operating at 2000 RPM in traverse mode for 4 hours under conditions of 27 °C and 28% relative humidity, with these settings optimized based on preliminary experiments.

Table 1. Electrospinning conditions of PVDF/ZnO@ZIF-8 nanofibrous

| Composite amount (wt%) | Applied voltage (kV) | Spinning distance (cm) | Volume flow rate (mL/h) | Drum speed (rpm) |
|------------------------|----------------------|------------------------|-------------------------|------------------|
| 0 | 30 | 14 | 0.2 | 3000 |
| 1 | 30 | 14 | 0.2 | 3000 |
| 3 | 30 | 14 | 0.2 | 3000 |
| 5 | 30 | 14 | 0.2 | 3000 |
| 10 | 30 | 14 | 0.2 | 3000 |

2.3 Piezoelectric Nanogenerator Fabrication

The piezoelectric behavior of the PVDF/ZnO@ZIF-8 nanofibrous composites was assessed using a customized experimental setup. Nanofibrous specimens ($2 \times 2 \text{ cm}^2$) were positioned between two aluminum foils, after which two exposed copper wires were affixed to the lower and upper electrodes with conductive copper paste. In order to eliminate the triboelectric effect, residual air between the PVDF/ZnO@ZIF-8 nanofibrous mat and the aluminum foil was expelled by applying low pressure and compressing the assembly. Subsequently, the piezoelectric sensor was encapsulated with commercial adhesive tape to safeguard it against mechanical damage. A cyclic force of 2.5 N at a frequency of 1 Hz was applied to the samples, and the resulting output voltage waveform was captured using a digital oscilloscope (OWON, DS7072E, China). The piezoelectric setup picture shown in figure 1.

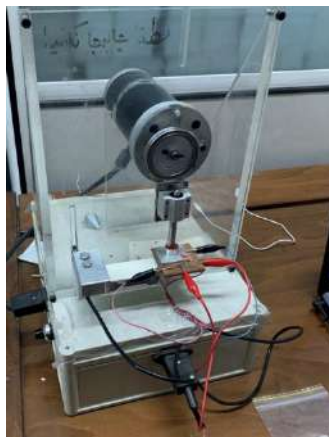


Figure 1. Image of piezoelectric setup.

2.4 Characterizations

The morphology of the created composite and nanofibers was analysed using FESEM. Digimizer software assessed the diameter distribution by measuring the diameter of 50 randomly selected fibers from the FESEM images. The crystalline properties of the synthesized composite and nanofibers were examined through XRD technique. Contact angle measured to study the surface wettability of the nanofibrous mat.

III. RESULTS AND DISCUSSIONS

3.1 Characteristics of Composite Powder

Creating a flawless ZIF-8 shell layer around the core is crucial for developing a core-shell ZIF-8-based structure. Typically, the core needs modification with organic groups or ZIF-8 seeds to promote ZIF-8 layer formation. As illustrated in Fig 2, the surface of the ZnO core was densely coated with hexahedron ZIF-8 nanocrystals, indicating successful growth of the ZIF-8 shell layer core.

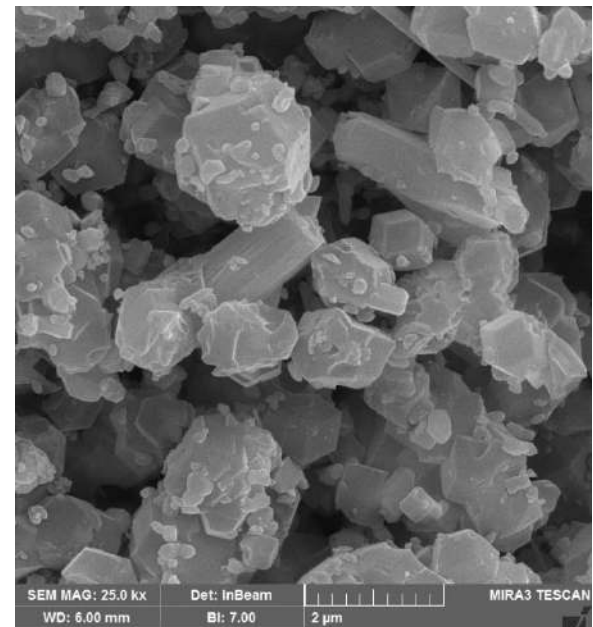


Figure 2. FESEM image of (ZnO@ZIF-8) composite.

Figure 3 displays the XRD patterns for ZnO, ZIF-8, and their (ZnO@ZIF-8) composites. The ZnO XRD

pattern reveals a crystalline structure with prominent peaks at 2θ values of 31.8° , 34.5° , 36.42° , 47.5° , 56.6° , 62.8° , and 69.1° , corresponding to the (100), (002), (101), (102), (110), (103), (200), (112), and (201) planes. For the MOF crystals, key peaks are observed at 2θ values of 7.3° , 10.3° , 12.8° , 16.5° , 18.1° , 19.7° , 22.2° , 24.6° , 25.7° , 26.8° , 28.9° , and 29.8° , linked to the (011), (002), (112), (013), (222), (123), (114), (233), (224), (134), (125), and (044) planes, respectively. These results align well with previous reports [15,16]. The XRD pattern of the (ZnO@ZIF-8) composite reveals peaks corresponding to both ZnO and ZIF-8. Similar findings have been documented in related studies [2].

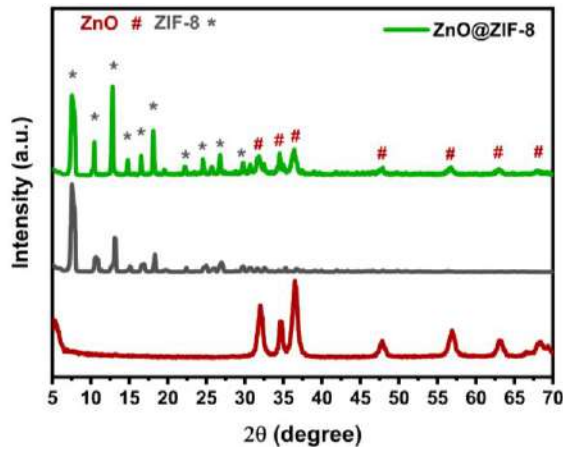


Figure 3. X-ray diffraction pattern of ZnO, ZIF-8 and (ZnO@ZIF-8) powders.

3.2 Size and Morphology of Nanofibers

Figure 4 shows the morphology and fiber diameter distribution of PVDF and PVDF/(ZnO@ZIF-8)-10% electrospun nanofibers. Both of the nanofibers displayed an interconnected network of random fibers with smooth surfaces and uniform diameter distribution. The PVDF nanofibers exhibited a bead-free uniform morphology with an average diameter of 253 nm. As a result of the introduction of composite particles to the PVDF nanofibers, the smooth surface of the PVDF nanofibers is found to be wrapped with a layer of composite crystals. Also the average diameter

of nanofibers was reduced to ~ 153 nm by adding 1 wt% of composite to PVDF solution.

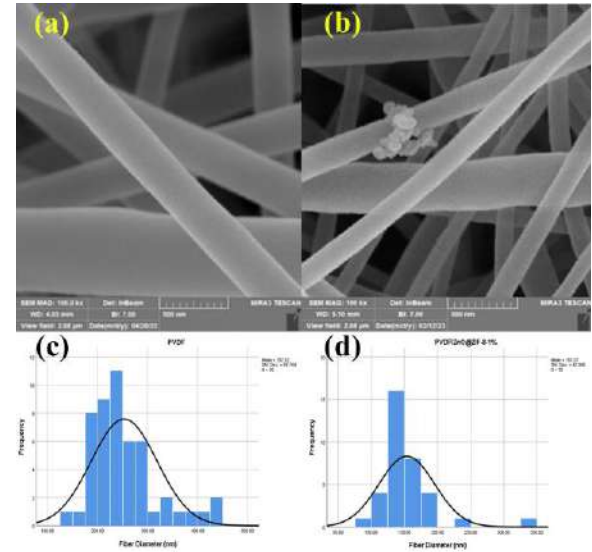


Figure 4. FESEM image and diameter distribution histogram of (a,c) PVDF and (b,d) PVDF/(ZnO@ZIF-8)-1% nanofibers, Respectively.

3.3 Phase Analysis

As shown in Figure 5, the characteristic diffraction peaks of PVDF appear at $2\theta = 18.8^\circ$ and 20.5° , corresponding to the α - and β -crystalline phases, respectively. Peaks at $2\theta = 12.8^\circ$ and 7.3° , marked with *, are assigned to the (112) and (011) planes of ZIF-8. Additionally, the reflections of ZnO indexed to the (100), (002), (101), (102), (110), (103), (200), (112), and (201) planes are indicated by # in the same pattern.

Quantitative analysis of the PVDF/(ZnO@ZIF-8) nanofiber composites reveals that the β -phase peak intensity increases steadily with composite loading up to 5 wt %. The incorporation of ZnO@ZIF-8 promotes greater chain alignment during electrospinning, facilitating the $\alpha \rightarrow \beta$ phase transformation. Moreover, both ZnO and ZIF-8 serve as effective nucleating agents thanks to their Zn^{2+} centers, further enhancing β -phase formation. These findings corroborate

previous XRD, which likewise report elevated β -phase content in MOF-reinforced PVDF relative to the neat polymer [10,12].

However, at 10 wt % composite loading, the XRD patterns exhibit pronounced ZIF-8 and ZnO reflections, indicating excessive filler aggregation. This high content also disrupts the electrospinning process and leads to a marked decrease in β -phase content, underscoring the need to balance filler incorporation for optimized piezoelectric performance [17].

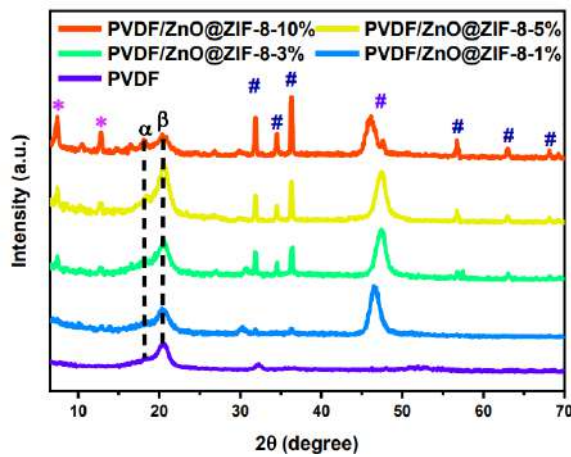


Figure 5. X-ray diffraction of PVDF and PVDF/(ZnO@ZIF-8) nanofibers.

3.4 Surface Wettability

Contact angle measurements reveal that adding ZnO@ZIF-8 composite increases the hydrophobicity of the PVDF nanofibrous mat, with values of 111.6 for PVDF and 125.9 for PVDF/(ZnO@ZIF-8)-10%.

The differing wettability of the composite results from the hydrophilic properties of ZnO and the hydrophobic nature of ZIF-8. While these factors somewhat counterbalance each other, the dominant presence of ZIF-8 on the composite's surface governs its overall behavior: the static water contact angles for all PVDF/ZnO@ZIF-8 nanofiber mats exceed that of pure PVDF. This increased hydrophobicity in the piezoelectric nanofiber layer affirms its practical

suitability for sensor applications. The slight decrease in contact angle due to ZnO can be explained by its inherent hydrophilicity [18].

3.5 Piezoelectric Response

As illustrated in Figure 6, the pristine PVDF nanofiber mat exhibits a piezoelectric output of approximately 2 V. Upon incorporation of ZnO@ZIF-8, the output steadily increases with composite loading, reaching over 5 V for the 5 wt % sample. At 10 wt % loading, however, a pronounced drop in output is observed, which we attribute to reduced fiber uniformity at high filler content. Despite this, the combined nucleating effects of ZnO and ZIF-8 together with the high specific surface area contributed by the ZIF-8 shell and the resulting decrease in fiber diameter enhance both the mechanical integrity and structural homogeneity of the mat, leading to higher peak-to-peak voltages. Taken together, the PVDF/(ZnO@ZIF-8)-5% nanofiber composite stands out as the best-performing sensor, delivering the highest piezoelectric output, enhanced superhydrophobicity.

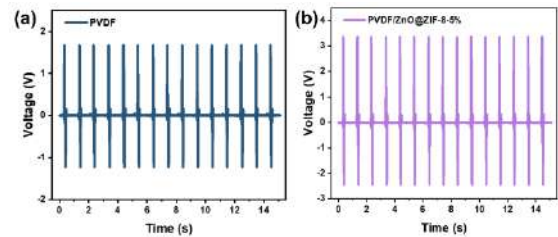


Figure 6. Piezoelectric output voltage of (a) PVDF and (b) PVDF/(ZnO@ZIF-8)-5%.

IV. CONCLUSIONS

The integration of core-shell ZnO@ZIF-8 composites into electrospun PVDF nanofibers successfully enhanced piezoelectric performance and hydrophobicity. Optimal filler content at 5 wt % yielded uniform, bead-free fibers with significantly increased β -phase content, confirmed by XRD. Contact angle measurements demonstrated augmented surface hydrophobicity, beneficial for sensor

durability in humid environments. Under cyclic mechanical excitation (2.5 N, 1 Hz), the PVDF/5 wt % ZnO@ZIF-8 nanofibrous mat delivered the highest output voltage (>5 V) and current across a wide resistance range, outperforming both the neat PVDF and higher filler loadings. Excessive composite addition (10 wt %) led to fiber nonuniformity and reduced piezoelectric output, underscoring the importance of balancing nucleation effects with fiber integrity. Overall, the PVDF/ZnO@ZIF-8-5 % composite stands out as the most promising candidate for self-powered piezoelectric sensors, combining high electrical output, and favorable surface properties.

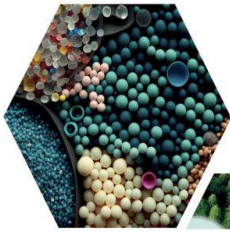
ACKNOWLEDGMENT

We acknowledge the Iran National Elite Foundation, the Research Laboratory of Yazd University for their support.

REFERENCES

- [1] M. Atighi, M. Hasanzadeh, A. Asghar Sadatalhosseini, H. Reza Azimzadeh, Metal–Organic Framework@Graphene Oxide Composite-Incorporated Polyacrylonitrile Nanofibrous Filters for Highly Efficient Particulate Matter Removal and Breath Monitoring, *Industrial & Engineering Chemistry Research* 0 (2022). <https://doi.org/10.1021/acs.iecr.2c03825>.
- [2] G. Ren, Z. Li, W. Yang, M. Faheem, J. Xing, X. Zou, Q. Pan, G. Zhu, Y. Du, ZnO@ZIF-8 core-shell microspheres for improved ethanol gas sensing, *Sens Actuators B Chem* 284 (2019) 421–427. <https://doi.org/10.1016/j.snb.2018.12.145>.
- [3] B. Yu, F. Wang, W. Dong, J. Hou, P. Lu, J. Gong, Self-template synthesis of core–shell ZnO@ZIF-8 nanospheres and the photocatalysis under UV irradiation, *Mater Lett* 156 (2015) 50–53. <https://doi.org/10.1016/j.matlet.2015.04.142>.
- [4] R. Bagherzadeh, S. Abrishami, A. Shirali, A.R. Rajabzadeh, Wearable and flexible electrodes in nanogenerators for energy harvesting, tactile sensors, and electronic textiles: novel materials, recent advances, and future perspectives, *Materials Today Sustainability* 20 (2022) 100233. <https://doi.org/10.1016/j.mtsust.2022.100233>.
- [5] P. Martins, A.C. Lopes, S. Lanceros-Mendez, Electroactive phases of poly(vinylidene fluoride): Determination, processing and applications, *Prog Polym Sci* 39 (2014) 683–706. <https://doi.org/10.1016/J.PROGPOLYMSCI.2013.07.006>.
- [6] D. Lolla, J. Gorse, C. Kisielowski, J. Miao, P.L. Taylor, G.G. Chase, D.H. Reneker, Polyvinylidene fluoride molecules in nanofibers, imaged at atomic scale by aberration corrected electron microscopy, *Nanoscale* 8 (2016) 120–128. <https://doi.org/10.1039/C5NR01619C>.
- [7] G. Kalimuldina, N. Turdakyn, I. Abay, A. Medeubayev, A. Nurpeissova, D. Adair, Z. Bakenov, A Review of Piezoelectric PVDF Film by Electrospinning and Its Applications, *Sensors* 2020, Vol. 20, Page 5214 20 (2020) 5214. <https://doi.org/10.3390/S20185214>.
- [8] M.S. Sorayani Bafqi, R. Bagherzadeh, M. Latifi, Fabrication of composite PVDF-ZnO nanofiber mats by electrospinning for energy scavenging application with enhanced efficiency, *Journal of Polymer Research* 22 (2015). <https://doi.org/10.1007/s10965-015-0765-8>.
- [9] P. Fakhri, B. Amini, R. Bagherzadeh, M. Kashfi, M. Latifi, N. Yavari, S. Asadi Kani, L. Kong, Flexible hybrid structure piezoelectric nanogenerator based on ZnO nanorod/PVDF nanofibers with improved output, *RSC Adv* 9 (2019) 10117–10123. <https://doi.org/10.1039/C8RA10315A>.
- [10] M. Atighi, M. Hasanzadeh, Highly sensitive self-powered piezoelectric poly(vinylidene fluoride)-based nanofibrous mat containing microporous metal–organic framework nanostructures for energy harvesting applications, *Applied Physics A* 129 (2023) 801. <https://doi.org/10.1007/s00339-023-07080-4>.

- [11] M. Atighi, M. Jalali, M. Hasanzadeh, S.M. Bidoki, PVDF nanofibers composite containing core-shell (ZnO@ZIF-8) for use in smart textile applications, *Journal of Innovative Engineering and Natural Science* 2 (2023) 37–44.
<https://doi.org/10.29228/JIENS.70341>.
- [12] B.H. Moghadam, M. Hasanzadeh, A. Simchi, Self-Powered Wearable Piezoelectric Sensors Based on Polymer Nanofiber-Metal-Organic Framework Nanoparticle Composites for Arterial Pulse Monitoring, *ACS Appl Nano Mater* 3 (2020) 8742–8752.
<https://doi.org/10.1021/acsanm.0c01551>.
- [13] M. Atighi, M. Hasanzadeh, Design and Characterization of Electrospun PVDF Nanofibers Containing Graphene Oxide/Metal-Organic Framework Composites for Potential Piezoelectric Applications, in: *International Seminar on Polymer Science and Technology (ISPST)*, 2022.
- [14] L. Ruan, X. Yao, Y. Chang, L. Zhou, G. Qin, X. Zhang, Properties and Applications of the β Phase Poly(vinylidene fluoride), *Polymers (Basel)* 10 (2018) 228.
<https://doi.org/10.3390/POLYM10030228>.
- [15] W. Muhammad, N. Ullah, M. Haroon, B.H. Abbasi, Optical, morphological and biological analysis of zinc oxide nanoparticles (ZnO NPs) using *Papaver somniferum* L., *RSC Adv* 9 (2019) 29541–29548.
<https://doi.org/10.1039/C9RA04424H>.
- [16] N.M. Mahmoodi, M. Oveisi, A. Taghizadeh, M. Taghizadeh, Synthesis of pearl necklace-like ZIF-8@chitosan/PVA nanofiber with synergistic effect for recycling aqueous dye removal, *Carbohydr Polym* 227 (2020) 115364.
<https://doi.org/10.1016/j.carbpol.2019.115364>.
- [17] M.S. Sorayani Bafqi, A.-H. Sadeghi, M. Latifi, R. Bagherzadeh, Design and fabrication of a piezoelectric out-put evaluation system for sensitivity measurements of fibrous sensors and actuators, *Journal of Industrial Textiles* 50 (2021) 1643–1659.
<https://doi.org/10.1177/1528083719867443>.
- [18] A. Popa, D. Toloman, M. Stan, M. Stefan, T. Radu, G. Vlad, S. Ulinici, G. Baisan, S. Macavei, L. Barbu-Tudoran, O. Pana, Tailoring the RhB removal rate by modifying the PVDF membrane surface through ZnO particles deposition, *J Inorg Organomet Polym Mater* 31 (2021) 1642–1652.
<https://doi.org/10.1007/s10904-020-01795-0>.



16

ULUSLARARASI
LİF VE POLİMER
ARAŞTIRMALARI
SEMPOZYUMU

16th INTERNATIONAL FIBER AND POLYMER RESEARCH SYMPOSIUM

Sürdürülebilir ve İşlevsel Lif ve Polimerler
Sustainable and Functional Fibers & Polymers



9-10 Mayıs
May 2025

İstanbul Teknik Üniversitesi
Gümüşsuyu Prof. Dr. Necmettin Erbakan Yerleşkesi
İstanbul Technical University
Gumussuyu Prof. Dr. Necmettin Erbakan Campus

Biyo-organik malzeme tabanlı biyosensörün farklı derişimlerdeki tarım ilaçlı su çözeltisine tepkisinin elektriksel karakterizasyon yöntemiyle incelenmesi

Burak Taş^{a,*}, Hüseyin Muzaffer ŞAĞBAN^b, Ümit Hüseyin Kaynar^c, Özge Tüzün Özmen^c

^aElektrik Elektronik Mühendisliği Bölümü ABD, Lisansüstü Eğitim Enstitüsü, İzmir Bakırçay Üniversitesi, 35665 İzmir, Türkiye.

^bOptisyenlik Bölümü, İstanbul Beykent Üniversitesi, 34398 İstanbul, Türkiye.

^cTemel Bilimler Bölümü, İzmir Bakırçay Üniversitesi, 35665 İzmir, Türkiye.

*Sorumlu Yazar: burak.tas@bakircay.edu.tr

ÖZET

Sağlık teknolojileri insanın yaşam kalitesinin standartlarını artırmada büyük öneme sahiptir. Bunun yanısıra, kovid-19 pandemisi sürecinde küresel çapta yaşanan kriz sürecinde ve sonrasında ölümlerin yoğun bir şekilde artışı, hastalığın olmasa bile ölümlerin önüne geçmede erken teşhisin gerekliliğini bir kez daha ispatlamıştır. Erken teşhisin bu kritik önemine istinaden, bunu gerçekleştirmeye imkan tanıyan alanlardan birisi de biyosensör teknolojisidir. Biyosensör teknolojisi, hem biyoyumluluk hem de biyobozunurluk özelliklerine sahip olabildiğinde çevresel ve tıbbi atık oluşturmama yönüyle de daha çok tercih sebebi olacaktır. Malzeme teknolojisinin gelişimine paralel olarak, biyosensörler üzerine yapılan bilimsel çalışmalar arasında elektrokimyasal biyosensörler en çok talep gören türdür. Bu çalışmada, organik malzeme olarak P3HT ve biyomalzeme olarak da PLA kullanıldı. P3HT ve PLA'nın ortak çözücüsü kloroformdur. Kloroformda çözünmüş P3HT ve PLA kullanılarak kaplanan ve üretilen bir biyosensörün, sulu çözeltide bulunan tarım ilacına tepkisi elektriksel karakterizasyon yöntemi kullanılarak incelendi. Daha sonra çözeltinin derişimi değiştirilerek aynı şekilde biyosensör tepkisi karakterize edildi. Böylece bu yeni biyosensörün doğruluğu ve hassasiyeti elde edilen veriler analiz edilerek gözlemlendi. Sonuç olarak, bu yeni biyosensör üzerine damlatılan çözeltideki tarım ilacı miktarı arttıkça biyosensör yapısındaki malzemenin direnci daha çok zayıfladı ve önceki derişimlere göre daha fazla akım geçirdi. Bu akım değerleri kaydedildikten sonra grafik üzerinde karşılaştırıldı ve biyosensörün çözeltideki tarım ilacına verdiği tepkinin doğruluğu kanıtlandı.

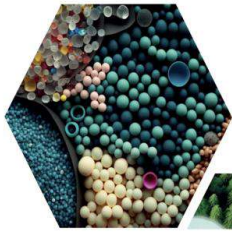
Anahtar Kelimeler: Biyosensör; Biyo-organik malzeme; Tarım ilacı tespiti; Sağlık teknolojileri

Investigation of the response of bio-organic material based biosensor to pesticide water solution at different concentrations by electrical characterization method

ABSTRACT

Health technologies are of great importance in increasing the standards of human quality of life. In addition, the intense increase in deaths during and after the global crisis during the Covid-19 pandemic has once again proven the necessity of early diagnosis in preventing deaths, even if not the disease. Based on the critical importance of early diagnosis, one of the areas that allows this to be achieved is biosensor technology. Biosensor technology will be more preferred when it has both biocompatibility and biodegradability features and does not create environmental and medical waste. In parallel with the development of material technology, electrochemical biosensors are the most demanded type among scientific studies on biosensors. In this study, P3HT was used as an organic material and PLA as a biomaterial. The common solvent of P3HT and PLA is chloroform. The response of a biosensor coated and produced using P3HT and PLA dissolved in chloroform to pesticides in aqueous solution was investigated using the electrical characterization method. Then, the biosensor response was characterized in the same way by changing the concentration of the solution. Thus, the accuracy and sensitivity of this new biosensor were observed by analyzing the obtained data. As a result, as the amount of pesticide in the solution dropped onto this new biosensor increased, the resistance of the material in the biosensor structure weakened and it passed more current compared to the previous concentrations. After these current values were recorded, they were compared on the graph and the accuracy of the biosensor's response to the pesticide in the solution was proven.

Keywords: Biosensor; Bio-organic material; Pesticide detection; Health technologies



16 ULUSLARARASI
LİF VE POLİMER
ARAŞTIRMALARI
SEMPOZYUMU

16th INTERNATIONAL FIBER AND POLYMER RESEARCH SYMPOSIUM

Sürdürülebilir ve İşlevsel Lif ve Polimerler
Sustainable and Functional Fibers & Polymers



9-10 Mayıs
May 2025

İstanbul Teknik Üniversitesi
Gümüşsuyu Prof. Dr. Necmettin Erbakan Yerleşkesi
Istanbul Technical University
Gumussuyu Prof. Dr. Necmettin Erbakan Campus

Recovery of textile waste: The effect of recycled cotton fibers obtained from different fabric structures on yarn quality

Kübra BAYKAN ÖZDEN^{a*}, İbrahim Erkan EVRAN^b, Prof. Dr. Züleyha DEĞİRMENCİ^c

^{a,b}Sanko Textile, R&D Centeri, 3. Organize Sanayi Bölgesi 83209 nolu cad.no:4 27127 Başpınar Gaziantep, Türkiye.

^cGaziantep University, Faculty of Engineering, Department Of Textile Engineering,, 15 Temmuz, Üniversite Blv., 27410 Şahinbey Gaziantep, Türkiye.

*Corresponding author: kubra.baykan@sanko.com.tr

ABSTRACT

The textile industry exerts significant pressure on natural resources due to the rapidly increasing global population and evolving consumption habits. In particular, the production of natural fibers such as cotton raises serious sustainability concerns because of high water consumption and negative environmental impacts. In this context, recycling and reusing both natural and synthetic fibers in textile production plays a critical role in reducing environmental footprints and controlling resource consumption.

This study compares the properties of recycled cotton fibers obtained from woven and knitted fabrics using mechanical recycling techniques. The effects of fabric production methods (woven and knitted) on the quality of the recycled fibers were examined, and the suitability of these fibers for reuse in production was evaluated. Additionally, the quality parameters of ring-spun yarns produced by blending recycled cotton fibers with polyester and recycled polyester fibers were analyzed. The study aims to contribute to the existing literature on ring-spun yarns produced from blends of recycled cotton and polyester/recycled polyester fibers. The data obtained were analyzed using statistical software to ensure objective and reliable results.

Keywords: Recycled cotton fiber; Sustainability; Woven and knitted fabrics; Polyester; Cotton

I. INTRODUCTION

The depletion of natural resources has driven many sectors, including the textile industry, to seek alternative or renewable resources. In this context, the replacement of natural fibers with synthetic alternatives, as well as the recycling and reuse of both natural and synthetic fibers, has emerged as a growing global trend and a promising field within textile production. Sustainable and environmentally friendly production approaches in textiles have gained

prominence not only worldwide but also in Turkey. The use of recycled fibers is increasingly seen as one of the key eco-conscious methods in textile manufacturing, attracting significant market interest. Products made using recycled fibers are expected to demonstrate performance levels comparable to those produced with virgin fibers, thereby ensuring customer satisfaction.

The consumption of textile products continues to rise steadily. This increase can be attributed to several factors, including the growth of the global population, the rise in individual consumption, the expanding use of textile materials in technical applications, the increase in purchasing power and living standards, and the diversification of disposable textile products. Along with the increasing demand for fibers, environmental problems associated with textile fiber production have also intensified. The growing use of recycling techniques that convert textile products back into fiber form contributes to mitigating these environmental impacts.

Today, recycling has gained significance as a means to eliminate or reduce the environmental burden caused by new production processes. Textile manufacturing not only consumes natural resources but also contributes to environmental pollution due to the use of harmful chemicals during production. Additionally, the consumption of heat and electricity in production results in a substantial carbon and water footprint. The increasing popularity of textile recycling has led many well-known brands to promote their recycled product lines [1].

Globally, only approximately 2.5% of total water resources are safely accessible for domestic, agricultural, and industrial use [2]. Water scarcity is becoming increasingly evident. In Turkey, the annual per capita availability of water is 1,519 m³ [3], and this amount is expected to decrease further in the coming years if necessary measures are not taken. The production of a single cotton T-shirt requires approximately 2,700 liters of water [4], while producing 1 kg of cotton requires about 20,000 liters of water [3]. This level of water consumption highlights the importance of recycling in textiles, as the continuous use of virgin cotton leads to significant water resource depletion.

Textile waste used in recycling processes is categorized into two main types: pre-consumer and post-consumer waste. Recycled cotton production also utilizes waste textiles from both pre- and post-consumer sources.

Pre-consumer waste refers to textile materials that are discarded during manufacturing, before reaching the consumer. These generally include waste by-products from fiber, yarn, textile, and garment production processes [5].

Post-consumer waste consists of textiles that are discarded by individuals due to wear, damage, or obsolescence. These include used or worn garments, bed linens, towels, and other household textiles [5].

Textile products are subjected to repeated sorting processes based on similar fiber properties and fabric structures until they are reduced to fiber form. The fabrics are initially cut into small clippings using a guillotine machine. These small clippings are then fed into opening machines equipped with saw-toothed and needle-covered rollers, which tear and open the fabrics, converting them into fiber form.

Woven fabric is a textile surface formed by interlacing warp and weft yarns at right angles in a specific, repetitive pattern. During the weaving process, the yarns are subjected to high tension. Therefore, warp yarns are treated with sizing agents to improve their resistance to friction and tension before weaving, while weft yarns undergo a heat-setting process to stabilize the twist prior to weaving [1].

Knitted fabrics are formed by interlooping yarns, which gives them elasticity. In contrast, woven fabrics are produced by interlacing warp and weft yarns at right angles. Because knitted fabrics are made from a single continuous yarn, they are stretchable in multiple directions. Knitting yarns are generally soft, have low twist levels, and are resistant to abrasion.

In woven fabric production, a wide variety of yarn types can be used with different types of weaving machines. Compared to knitting, warp yarns used in weaving are typically more tightly twisted to withstand high tension, while weft yarns have properties similar to those used in knitting.

In warp knitting, preliminary processes include warp and weft preparation, warp tying, and drawing-in. In weft knitting, pre-processes such as bobbin winding and waxing are performed. In weaving, preparatory steps include warp and weft yarn preparation, sizing, drawing-in, and warp tying.

Woven fabrics generally possess a more rigid and durable structure. In knitted fabric production, a single yarn or a group of warp yarns is converted into loop structures using knitting elements. These loops are interconnected to form the knitted fabric. Woven fabric is produced through the interlacing of warp and weft yarns in a predetermined pattern.

Due to their structural nature, knitted fabrics exhibit multidirectional stretch and flexibility. The durability of knitted fabrics depends on the type and quality of fiber used, yarn strength, knitting pattern, and loop density. The durability of woven fabrics, on the other hand, is influenced by the type and quality of the fiber, yarn strength, twist level and structure, fabric weave pattern, and yarn density. Generally, woven fabrics are more durable than knitted fabrics.

Knitted fabrics typically have a looser and more porous structure compared to woven fabrics. As a result, they offer better thermal and air permeability. In contrast, the compact and stable structure of woven fabrics results in lower thermal and air conductivity compared to knits.

It is well known that the most significant products traded in the global fiber and yarn industry include synthetic and artificial filament yarns, synthetic and artificial filament tows and staple fibers, cotton yarns,

and raw cotton. Regenerated yarn production is carried out extensively in many Far Eastern countries, particularly China. However, in these countries, there is still limited progress in terms of systematization and quality standards; the primary focus has been on producing low-cost products through traditional methods. In the coming years, with advancements in technology, competitive environments will emerge, and as a result, greater emphasis will be placed on quality standards and research and development efforts.

As is known, China and other Far Eastern countries have posed a competitive threat to Turkey's textile industry since the late 1990s. Given the relatively low labor, energy, and raw material costs in these countries, it is an undeniable fact that Turkish textile manufacturers can only remain competitive by focusing on the production of high-quality goods. Accordingly, in the regenerated yarn sector, it is also clear that prioritizing quality is essential for maintaining competitiveness. When higher-quality yarns are produced in greater quantities, producers can better position themselves in the global market and ensure their sustainability.

In Turkey, there is currently a lack of institutionalized approaches among producers in terms of both production optimization and yarn quality parameters in the regenerated yarn sector. Therefore, it is necessary to conduct studies on how yarn quality should be standardized and how production efficiency can be improved studies which should also be supported by the industry. Such efforts would help establish quality benchmarks and standardization within the regenerated yarn sector across Turkey, eventually setting standards that could be adopted internationally.

As a result of rapid population growth, economic expansion, and industrial development, the overall consumption of materials has increased, which has

also led to a corresponding rise in waste generation. The need to eliminate waste without harming the environment and to recover its economic value has made recycling inevitable. The primary advantage of recycling is its contribution to the conservation of natural resources. Materials such as used metals, plastics, paper, textile waste, and other materials can persist in the environment for many years and reduce soil productivity. Recycling not only protects the environment but also lowers raw material costs in production and improves energy efficiency.

In Turkey, the recycling rate of textile waste is gradually increasing thanks to the efforts of both private enterprises and scientific institutions. In this context, processing textile waste and reintegrating it into the economy as regenerated fiber creates significant value for Turkey from both economic and environmental perspectives. The more optimally we use our natural resources today, the greater the chance future generations will have to benefit from them. In a world where natural resources are rapidly depleting, it is critically important for companies, research centers, and universities to place greater emphasis on and raise awareness about the regenerated fiber and recycling sector. Doing so will contribute to a more livable world for future generations, both economically and environmentally.

For Turkey to become a key player in the global regenerated yarn sector, it must prioritize quality and standardization [6].

One of the key sub-sectors of the textile and apparel industry is the denim sector. Approximately 53% of the environmental impact of denim fabric originates from its raw material, namely cotton fiber [8]. Cotton is the most widely used natural fiber in denim production. Currently, the annual amount of cotton-based textile waste has reached approximately 3 million tons [9].

Cotton fiber has significant environmental impacts due to high water consumption, land use, energy requirements, and the use of fertilizers and pesticides, all of which may pose risks to both environmental and human health [8], [10]. One potential solution to reduce the resources used in cotton cultivation and its associated environmental impacts is the use of recycled cotton fiber [10].

Compared to conventional cotton, recycled cotton requires significantly fewer resources. Recycled cotton fiber is mechanically obtained from cotton waste products through cutting and shredding processes [7].

Due to its widespread use and excellent performance, polyethylene terephthalate (PET) fibers are in high demand across the global textile industry. PET fibers account for nearly 40% of all fiber types produced worldwide each year. The use of PET waste in the production of regenerated PET offers advantages such as lower pollution and reduced production costs [11]. Compared to virgin fibers, the quality of recycled fibers has historically been a major limiting factor for their market adoption [12].

On the other hand, blended fabrics are widely used in the textile sector due to the various advantages they offer. Blends refer to the combinations of different fiber polymers, which can vary in their physical or chemical properties, creating numerous possible fiber populations [13]. Blending has become a key strategy to meet the growing consumer demand by optimizing wear comfort and introducing new trends into the fashion industry. Polyester fibers are commonly blended with cotton or viscose, and these blends are produced in large volumes. Polyester fibers rank first among all synthetic fibers due to their superior mechanical properties, such as high strength, easy washability, good durability, resistance to abrasion, and wrinkle resistance [14]. However, polyester fabrics have low moisture affinity, are oleophilic, and

are prone to pilling [15]. The primary purpose of blending polyester with cellulosic fibers is to improve moisture absorbency and enhance garment comfort.

There is a substantial body of literature on the use of recycled fibers [16], [17]. However, studies specifically focusing on the use of recycled cotton and polyester fibers in the production of PES/CO (polyester/cotton) blended fabrics are relatively abundant. Comparing the performance properties of recycled fabrics with those of virgin fabrics is useful for evaluating the potential of using recycled fibers as substitutes for virgin ones. Therefore, this study is expected to contribute meaningfully to the existing body of literature.

Mechanical recycling is a sustainable method that aims to reprocess textile waste into fiber, yarn, or fabric through physical means. This process typically begins with the collection of textile waste such as post-consumer garments, surplus production fabrics, or cutting scraps. The waste materials are first sorted based on quality and then cleaned by removing foreign objects such as metal buttons and zippers. After cleaning, the textile waste is mechanically shredded using specialized opening machines, reducing the material back to fiber form. The recycled fibers obtained are often blended with recycled polyester or virgin fibers to reduce strength loss and achieve the desired quality standards in yarn production. This blend is processed through conventional spinning stages such as blending, carding, drawing, and roving, and is subsequently spun into ring-spun yarn. The resulting yarns can then be transformed into final textile products using surface production techniques such as weaving or knitting.

The mechanical recycling process is environmentally advantageous due to the absence of chemical usage; however, the reduction in fiber length may limit the physical performance of recycled products compared to their original counterparts. This situation

necessitates the optimization of process parameters and the use of appropriate fiber blends [18],[19].

Woven fabrics are constructed by tightly interlacing warp and weft yarns at right angles. This tight structure provides the fabric with high stability and durability, but it also increases resistance to disintegration during mechanical recycling. As a result, the opening process of woven fabrics is more challenging, leading to greater fiber breakage and the production of shorter, low-length, and more irregular fibers. As fiber length decreases, problems that may arise during yarn production such as reduced strength, increased pilling, and a higher risk of breakage tend to increase [19].

This study aims to address the question of which type of fabric, when mechanically recycled, yields fibers with properties closest to those of virgin cotton and can therefore be effectively reused in production. The higher twist level of yarns in woven fabrics compared to knitted fabrics, as well as differences in yarn count and fabric weight per unit area, influence the quality of the recycled fibers obtained. Moreover, the finishing processes applied to fabrics vary depending on the fabric type, which also affects the resulting fiber characteristics.

Since fiber parameters cannot be directly controlled in the recycling process, the most adjustable factor for improving yarn properties is the fiber blend composition.

II. MATERIAL AND METHOD

The use of different fibers in blended form within the textile industry enables yarns and the fabrics produced from these yarns to acquire diverse properties. Blended fabrics are widely preferred due to the various advantages they offer. In particular, blending polyester fibers with cotton fibers provides significant benefits such as high tensile strength, ease of washing, and enhanced durability, which are inherent characteristics of polyester. Conversely, cotton fibers are often

selected in blend fabric production due to their advantageous properties, including breathability, high moisture absorbency, and natural origin. However, polyester is a synthetic, non-breathable fiber, which comes with certain drawbacks such as low moisture absorbency, a tendency to pill, and limited air permeability. As a result, fabrics produced from 100% polyester yarns may negatively affect wearer comfort.

In this study, the %U, Thin -50%, Thick +50%, and Neps +200% values of Ne 26/1 conventional ring-spun yarns—produced with three different fiber blends—were analyzed using the Uster Tester 6 device. The first blend included recycled cotton obtained from knitted fabric waste, the second blend included recycled cotton from woven fabric waste, and the third blend utilized conventional virgin cotton. All fiber types were blended with recycled polyester fibers. Abbreviations for the fiber types are presented in Table 1, while abbreviations for the blend ratios are provided in Table 2. The recycled knitted fabric fiber, recycled woven fabric fiber, and conventional cotton fiber used in the study were tested using the Uster AFIS Pro 2 device, and the values of total neps, L(n) (mean fiber length based on number), and SFC(n) (percentage of fibers shorter than 12.7 mm, based on number) were evaluated. The relationship between the quality of the input fibers and the resulting yarn quality was statistically analyzed.

Table 1. Abbreviations used for fibers

| FIBER | ABBREVIATION |
|-------------------------|--------------|
| Recycled knitted fabric | RK |
| Recycled woven fabric | RW |
| Conventional cotton | C |
| Recycled polyester | RP |

Table 2. Blend abbreviation

| BLEND | ABBREVIATION |
|--------------------------------------------------------------------------------|--------------|
| 30% Conventional cotton – 30% Recycled knitted fabric – 40% Recycled polyester | C30RK30RP40 |
| 30% Conventional cotton – 30% Recycled woven fabric – 40% Recycled polyester | C30RW30RP40 |
| 60% Conventional cotton – 40% Recycled polyester | C60RP40 |

III. RESULTS AND DISCUSSIONS

When the AFIS fiber values presented in Table 3 are examined, it is observed that the total neps, fiber length (L(n)), and the percentage of short fibers below 12.7 mm (SFC(n)) deteriorate in recycled cotton fibers compared to conventional cotton fibers. The higher neps values, along with shorter fiber lengths and an increased proportion of short fibers in recycled cotton, lead to yarn irregularities in the form of unevenness, thin and thick places, and neps, as compared to yarns made from conventional cotton.

Table 3. Fiber afis values

| AFIS | RK | RW | C | RP |
|--------------------|------|------|------|------|
| Total neps (Cnt/g) | 1163 | 509 | 374 | 108 |
| L(n) (mm) | 10,7 | 10,3 | 17,8 | 30,7 |
| SFC(n) (%<12.7 mm) | 62,2 | 65,2 | 35,2 | 0,7 |

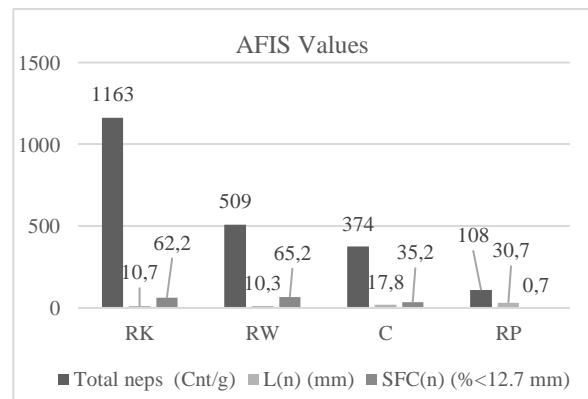


Figure 1. Fiber afis values

When the Ne 26/1 conventional ring-spun yarns listed in Table 4 are examined based on their blend ratios, it is observed that the blend C60RP40 exhibits the best quality values, while the blend C30RK30RP40 shows the poorest performance.

Table 4. Quality parameters of ne 26/1 yarns

| USTER Parameters | C30RK30RP40 | C30RW30RP40 | C60RP40 |
|------------------|-------------|-------------|---------|
| %U | 14,8 | 14,34 | 11,48 |
| Thin -50% | 27 | 31 | 3 |
| Thick 50% | 1057 | 821 | 164 |
| Neps 200% | 1167 | 789 | 139 |

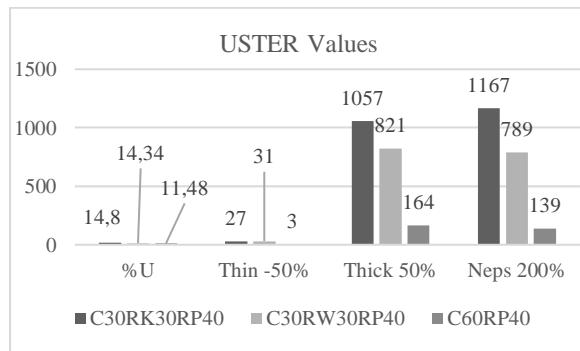


Figure 2. Yarns uster values

IV. STATISTICAL ANALYSIS

The statistical analyses of the study were conducted using the SPSS 26.0 software package. Homogeneity tests and one-way ANOVA were performed to evaluate the differences within the fiber groups and to determine the effects of blend types on yarn quality parameters.

One-way ANOVA test results, which assess whether the total neps, L(n), and SFC(n) properties of fibers obtained from the opening of woven fabrics, knitted fabrics, and recycled polyester fibers differ significantly from each other at a 95% confidence level, are presented in Table 5.

Table 5. One way anova for fiber afis values

| | Sum of Squares | df | Mean Square | F | Sig. |
|-------------------|----------------|----|-------------|----------|------|
| Total neps | 1810973,333 | 3 | 603657,778 | 324,083 | 0 |
| | 14901,333 | 8 | 1862,667 | | |
| | 1825874,667 | 11 | | | |
| L(n) | 823,643 | 3 | 274,548 | 2241,204 | 0 |
| | 0,98 | 8 | 0,122 | | |
| | 824,623 | 11 | | | |
| SFC(n) | 8075,447 | 3 | 2691,816 | 1576,466 | 0 |
| | 13,66 | 8 | 1,708 | | |
| | 8089,107 | 11 | | | |

According to the table, the total neps, L(n), and SFC(n) values of the fibers examined in the study differ significantly from each other ($p < 0.001$). Based on this finding, different blends were created using these fibers, and yarns of the same count were produced using the ring spinning method. Subsequently, the quality parameters of these yarns (%U, Thin -50%, Thick +50%, Neps +200%) were analyzed using a one-way ANOVA test to determine whether the differences among them were statistically significant. The results are presented in Table 6.

Table 6. One way anova for yarns quality values

| | Sum of Squares | df | Mean Square | F | Sig. |
|------------------|----------------|----|-------------|---------|-------|
| %U | 32,308 | 2 | 16,154 | 114,238 | 0 |
| | 1,697 | 12 | 0,141 | | |
| | 34,005 | 14 | | | |
| Thin -50% | 2320,533 | 2 | 1160,267 | 12,209 | 0,001 |
| | 1140,4 | 12 | 95,033 | | |
| | 3460,933 | 14 | | | |
| Thick 50% | 2145458,8 | 2 | 1072729,4 | 93,714 | 0 |
| | 137361,6 | 12 | 11446,8 | | |
| | 2282820,4 | 14 | | | |
| Neps 200% | 2701195,6 | 2 | 1350597,8 | 81,189 | 0 |
| | 199624 | 12 | 16635,333 | | |
| | 2900819,6 | 14 | | | |

According to the table, the fibers examined in the study show statistically significant differences ($p < 0.005$) in U%, Thin -50%, Thick +50%, and Neps

+200% values. While changes in the blend composition had a significant effect on thick places and neps values of the yarns, it was observed that the blends containing recycled knitted fabric and recycled woven fabric exhibited similar behavior in terms of thin places and unevenness.

Tukey post-hoc test results for the analyzed parameters are provided in Tables 7 through 10. These results were used to determine which specific group differences contributed to the overall significance observed in the ANOVA tests.

Table 7. Tukey test results for %u values

| %U | | | | |
|-------------------------|---|--------|--------|--|
| Tukey HSD ^a | | | | |
| Subset for alpha = 0.05 | | | | |
| Blend | N | 1 | 2 | |
| C40RP60 | 5 | 11,482 | | |
| C30RW30RP40 | 5 | | 14,336 | |
| C30RK30RP40 | 5 | | 14,802 | |
| Sig. | | 1 | 0,165 | |

Table 8. Tukey test results for thin -50% values

| Thin -50% | | | | |
|-------------------------|---|-----|-------|--|
| Tukey HSD ^a | | | | |
| Subset for alpha = 0.05 | | | | |
| Blend | N | 1 | 2 | |
| C40RP60 | 5 | 2,6 | | |
| C30RK30RP40 | 5 | | 27 | |
| C30RW30RP40 | 5 | | 30,6 | |
| Sig. | | 1 | 0,831 | |

Table 9. Tukey test results for thick 50% values

| Thick 50% | | | | |
|-------------------------|---|-------|-------|--------|
| Tukey HSD ^a | | | | |
| Subset for alpha = 0.05 | | | | |
| Blend | N | 1 | 2 | 3 |
| C40RP60 | 5 | 163,6 | | |
| C30RW30RP40 | 5 | | 821,4 | |
| C30RK30RP40 | 5 | | | 1057,4 |
| Sig. | | 1 | 1 | 1 |

Table 10. Tukey test results for neps 200% values

| Neps 200% | | | | |
|-------------------------|---|-------|-------|------|
| Tukey HSD ^a | | | | |
| Subset for alpha = 0.05 | | | | |
| Blend | N | 1 | 2 | 3 |
| C40RP60 | 5 | 139,4 | | |
| C30RW30RP40 | 5 | | 788,8 | |
| C30RK30RP40 | 5 | | | 1167 |
| Sig. | | 1 | 1 | 1 |

Pearson correlation analysis was conducted to examine the effects of fiber and blend variations on fiber and yarn quality parameters. According to the results of the analysis, a very strong correlation was found at the 0.01 significance level between the raw material and the fiber properties, specifically neps, L(n), and SFC(n). Furthermore, these fiber characteristics were found to moderately influence yarn parameters such as U%, Thin -50%, Thick +50%, and Neps +200%. As the neps content in the fibers increased, the thick places and neps values in the yarns also increased. It was observed that changes in the fiber blend had a significant effect on yarn unevenness, thin places, thick places, and neps. A strong positive correlation was also identified between the number of thin places and the number of neps in the yarns.

In conclusion, it was determined that changes in raw material had a significant impact on fiber quality properties, while changes in blend composition significantly affected yarn quality parameters.

V. CONCLUSIONS

The quality of the recycled fiber used has a direct impact on the quality of the resulting yarn. In the mechanical recycling process, the fabric structure of the textile waste—whether woven or knitted—significantly affects the quality, length, and strength of the recycled fiber obtained. These differences arise from the structural characteristics of each fabric type.

In addition to fabric structure, the yarn count (thickness) of the yarns used in these fabrics also directly influences the physical properties of the resulting fibers during the mechanical recycling process. As the yarn count increases (i.e., as the yarn becomes finer), changes occur in twist level, fiber cohesion, and tensile strength. This, in turn, affects the tendency of fibers to break, curl, or entangle during the opening process, ultimately influencing neps formation.

When examining the AFIS values of RK fiber, the neps count was found to be significantly high. Considering the L(n) and SFC(n) values, the C30RK30RP40 blend resulted in the highest neps values among all yarn samples. It also showed relatively high thin and thick place values.

For RW fiber, the AFIS data indicated that the neps value was lower than that of RK fiber but higher than that of conventional cotton (C). Taking into account the L(n) and SFC(n) values, the C30RW30RP40 blend exhibited higher neps, thin, and thick place values compared to the C60RP40 blend.

The reuse of fibers obtained through mechanical recycling in yarn and fabric production is not merely a technical recycling practice but also a strategic approach that supports environmental and economic sustainability. This method reduces the volume of textile waste sent to landfills, limits the consumption of natural resources, and lowers energy usage and carbon emissions associated with the production of virgin fibers. As a result, the textile manufacturing process is restructured with a lower environmental footprint and re-evaluated in line with the principles of the circular economy.

Therefore, mechanical recycling should not be viewed solely as a waste management method, but rather as a powerful tool for green transformation, carbon-neutral production, and responsible production-consumption systems. Efforts aimed at improving the quality of

recycled fibers and optimizing the recycling process will play a leading role in guiding the sustainable transformation of the textile industry.

ACKNOWLEDGMENT

This study was carried out as an outcome of the projects conducted by the Sanko Textile R&D Center: 23-BSP-003 (Development of Recycled Products on 100% Cotton and Cotton-Polyester Knitted Fabrics) and 23-BSP-004 (Sustainable Product Development through the Reuse of Denim Fabric Waste).

REFERENCES

- [1] Şengün N (2024) Influence Of Mechanical Raising Process On The Fabric Properties Of Recycled Cotton Woven Fabrics, Pamukkale University Institute Of Science Textile Engineering
- [2] Chin, D. A. (2000) Water-Resources Engineering, New Jersey: Prentice Hall.
- [3] Pamukta Sürdürülebilir Tarımın Yaygınlaştırılması İçin Öneriler İyi Pamuk İncelemesi (2024) <https://www.wwf.org.tr/?13800/iyi-pamuk-incelemesi> (17 Nisan 2024).
- [4] Kadem, F. D., Özdemir, Ş., (2020) A Study on Selected Comfort Properties of Post-Consumer Recycled Denim Fabrics Çukurova University Journal of the Faculty of Engineering and Architecture, 35(2), pp. 379-388, June 2020
- [5] Öner, E. (2023). Investigation of Consumer Attitudes towards the Recycling of Post-Consumer Textile Waste . Investigation of Consumer Attitudes towards the Recycling of Post-Consumer Textile Waste,,6(3),2009-2022.
<https://doi.org/10.47495/okufbed.1158689>
- [6] Ersoy, Y., Zıraplı M. (2014) Importance of Recycling Spinning and Yarn Production Methods Düzce University Science and Technology Journal pp 425-432
- [7] Alp G., Yıldırım N., Kertmen M., Türksoy H.G.

Investigation of Performance Properties of Denim Fabrics Produced from Recycled Cotton Blended Yarns DEUFMD 25(74), 275-285.

[8] Fidan Ş., Aydoğan E.K., Uzal N., 2021. An Integrated Life Cycle Assessment Approach for Denim Fabric Production Using Recycled Cotton Fibers and Combined Heat and Power Plant, *Journal of Cleaner Production*, Volume 287, 125439, DOI: 10.1016/j.jclepro.2020.125439.

[9] Haule L.V., Carr C.M., Rigout M., 2016, Investigation into The Supramolecular Properties of Fibres Regenerated From Cotton Based Waste Garments, *Carbohydrate Polymers*, 144,131-139.

[10] Moazzem S., Crossin E., Daver F., Wang L., 2021. Assessing Environmental Impact Reduction Opportunities Through Life Cycle Assessment of Apparel Products, *Sustainable Production and Consumption*, Volume 28, , 663-674

[11] Atav R., Soysal S., Yıldız F., Effect of Using Recycled PES versus Virgin PES in PES/CO Fabrics

Çorlu Faculty of Engineering, Tekirdağ Namık Kemal University *European J. Eng. App. Sci.* 6(2), 120-123, 2023

[12] S.S. He, M.Y. Wei, M.H. Liu, W.L. Xue Characterization of virgin and recycled poly(ethylene terephthalate) (PET) fibers, *J. Text. Inst.*, 106 (8) (2015), pp. 800-806

[13] Anış, P., & Eren, H.A. (2003). Poliester/Pamuk Karışımlarının Boyanması: Uygulamalar ve Yeni Yaklaşımlar. *Uludağ Üniversitesi Mühendislik-Mimarlık Fakültesi Dergisi*, 8(1): 131-139

[14] Almetwally, A.A. (2022). Alkaline Hydrolysis of Polyester Woven Fabrics and Its Influence on Thermal Comfort Properties, *Egyptian Journal of Chemistry*, 65(12): 259-274.

[15] Zeronian, S.H., Collins, M.J. (1989). Surface Modification of Polyester By Alkaline Treatments, *Textile Progress*, 20(2): 1-26.

[16] Inoue, M., & Yamamoto, S. (2004). Performance and Durability of Woven Fabrics Including Recycled Polyester Fibers, *Journal of Textile Engineering*, 50

[17] Liu, Y., Huang, H., Zhu, L., Zhang, C., Ren, F., & Liu, Z. (2020). Could the recycled yarns substitute for the virgin cotton yarns: a comparative LCA. *The International Journal of Life Cycle Assessment*, 25(10), 2050-2062.

[18] Yousef S., 2019 A new strategy for using textile waste as a sustainable source of recovered cotton 359-369

[19] Ütebay B., Çelik P., Çay A., 2019 Effects of cotton textile waste properties on recycled fibre quality 29-35.



Fabrication of nanofibrous proton exchange membranes with significantly enhanced proton conductivity based on sulfonated polyether ether ketone/polydopamine-coated multi-walled carbon nanotubes

Zahra Esmaeilzadeh^{a,*}, Mohamad karimi^a, Ahmad Mousavi Shoushtari^a, Mehran Javanbakht^b

^aSchool of Materials and Advanced Process Engineering, Department of Textile Engineering, Amirkabir University of Technology, Tehran, Iran

^bDepartment of Chemistry, Amirkabir University of Technology, Tehran, Iran

*Corresponding author: zahraesmaeilzade@aut.ac.ir

ABSTRACT

Proton exchange membranes (PEMs) are critical components of proton exchange membrane fuel cells (PEMFCs), which are promising candidates for clean energy generation. Among various PEM materials, sulfonated polyether ether ketone (SPEEK) is known for its thermal and mechanical stability but suffers from relatively low proton conductivity. In this study, a novel nanofibrous PEM was fabricated by electrospinning SPEEK, followed by a densification process to convert the porous web into a dense structure suitable for PEM applications. The densification was optimized through multiple methods involving thermal pressing, vacuum treatment, and impregnation with dilute SPEEK solution. To further enhance proton transport, polydopamine-coated multi-walled carbon nanotubes (P@MWCNTs) were incorporated into the nanofiber matrix. Scanning electron microscopy (SEM) confirmed uniform fiber morphology and effective filler dispersion. The effect of different P@MWCNT concentrations on the membrane's proton conductivity was investigated. The optimized membrane containing 1 wt% P@MWCNT showed a tenfold increase in proton conductivity compared to neat SPEEK membranes. This study presents a novel approach for fabricating nanostructured composite PEMs with significantly enhanced conductivity, offering a promising alternative to conventional techniques.

Keywords: Nanofibers; Proton_exchange_membrane; MWCNT; Polydopamine; Proton_conductivity

I. INTRODUCTION

The rising global demand for energy, along with environmental concerns, has led to significant investigations into the development of alternative and eco-friendly energy sources, including fuel cells [1]. In recent years, proton exchange membrane fuel cells (PEMFCs) have attracted considerable attention. The proton exchange membrane (PEM), serving as the key

component of this system, effectively separates the anode and cathode while allowing proton conduction [2]. Nafion[®] has been widely used as the benchmark PEM material; however, its high cost and poor performance at elevated temperatures have led to extensive research into alternative polymers. Sulfonated polyether ether ketone (SPEEK) has received considerable attention due to its excellent

mechanical properties and lower cost. However, the relatively low proton conductivity of SPEEK membranes remains a critical challenge [2]. Various strategies have been explored to improve SPEEK's proton conductivity, including incorporation of inorganic fillers, polymer blending, and structural modifications. Among these, the use of carbon nanotubes (CNTs) has shown potential owing to their high aspect ratio, mechanical strength, and ability to form continuous proton transport pathways [3][4].

CNTs can enhance proton transport when aligned within electrospun nanofibers, offering a pathway to create nanostructured membranes with improved conductivity. Recently, achieving separated nanophase morphology within membrane structures has emerged as a crucial approach for enhancing the overall properties of PEMs. Electrospinning serves as a commonly used method for attaining this objective, leading to a "nano-phase separation" morphology with long-range proton transport channels. By selecting appropriate electrospinning materials, fiber volume fractions, and experimental conditions, this morphology allows for modifications in material organization, diffusion network dispersion, and the hydrophilic/hydrophobic properties of the ionomers throughout a wide spectrum [5]. Despite this, one major issue with this approach is that the produced electrospun webs are porous, whereas proton exchange membranes must be dense. Consequently, another component is necessary for the process of densification. This densifying agent may consist of a neutral polymer that lacks proton conductivity or an alternative polymer that facilitates proton conduction.

In this study, we aim to fabricate a nanofibrous composite PEM by electrospinning SPEEK with incorporated polydopamine-coated multi-walled carbon nanotubes (P@MWCNTs), followed by a densification process to overcome the inherent porosity of electrospun mats, systematically

investigating the effects of filler concentration and membrane morphology on proton conductivity.

II. EXPERIMENTAL METHOD

Polyether ether ketone (PEEK) polymer and dopamine hydrochloride were obtained from Sigma-Aldrich, and dimethylacetamide (DMAc) solvent was acquired from Merck. Carboxyl-functionalized multi-walled carbon nanotubes (MWCNTs) were obtained from US Research Nanomaterials. The sulfonation degree of SPEEK achieved 65%, and the polydopamine coating process of MWCNTs was conducted according to the procedure described in reference [6].

2.1 Modification of MWCNTs with Polydopamine (P@MWCNT)

To prepare polydopamine-coated MWCNTs, carboxyl-functionalized MWCNTs were dispersed in 10 mM Tris-HCl buffer (pH 8.5, 1 mg/ml) using ultrasonication for 30 min in an ice bath. Dopamine hydrochloride was added at a weight ratio of 1.11:1 (dopamine:MWCNT), and the mixture was stirred for 14.8 h. The polydopamine coated MWCNTs were washed by centrifugation and dried overnight at 80°C [6].

2.2 Electrospinning of Nanofibers

Nanofibrous webs were fabricated by electrospinning a 23 wt% SPEEK solution in DMAc. Electrospinning was performed at 15 kV with a 15 cm collector distance. The resulting webs were dried at room temperature for 24 h and then heat-treated at 120 °C for 16 h in an oven.

To manufacture the SPEEK nanofibers incorporated MWCNTs, a particular amount of nanotubes (0.5, 1, 1.5, and 2 wt.% respect to polymer mass) was distributed into the DMAc solution using an ultrasonic process, then SPEEK was added to it, followed by the

electrospinning procedure as same as the pristine SPEEK nanofiber.

2.3 Membrane Characterization

The morphology of the nanofibers and nanofiber based membranes was analyzed using SEM (SERON, South Korea). Proton conductivity was measured using an Autolab potentiostat/galvanostat. Prior to measurement, samples were pretreated in 1 M H₂SO₄ at 60 °C for 2 h and then immersed in deionized water for 48 h. Measurements were conducted under full hydration using a two-probe setup with Pt electrodes. Conductivity (σ , S/cm) was calculated using the following equation:

$$\sigma = \frac{l}{RA} \quad (1)$$

Where l is membrane thickness (cm), R is resistance (Ω , the membrane resistance was derived from the low-frequency), and A is electrode area (cm²).

The mechanical property testing was performed using INSTRON 5566 (Instron, USA) with an extension rate of 10 mm/min at room temperature. The samples were prepared in 5 mm width and 60 mm length and were tested.

Porosity of the nanofiber web (P) was calculated based on thickness (measured by digital micrometer), weight, and polymer density using the following equation:

$$p(\%) = 1 - \frac{(M_n / \rho)}{(A_n \times l_n)} \quad (2)$$

Where M_n is mass (g), L_n is thickness (cm), A_n is surface area (cm²), and ρ is polymer density (g/cm³).

2.4 Densification Process

To densify the nanofibrous structure, diluted SPEEK polymer (4 wt% solution in deionized water at 80°C) was utilized as a pore filler. The densification process was carried out based on four different methods, as outlined in Table 1. All samples underwent immersion in an aqueous SPEEK solution. Prior to immersion, some samples were subjected to a heat press (160°C, 5 bar, 5 minutes) to reduce web voids. Additionally, some samples were processed with a vacuum system (using a Büchner funnel) after immersion to remove excess SPEEK solution from the nanofiber web surface. In a distinct case, other samples received both heat pressing and vacuum processing. The weight of all densified membranes was increased compared to the pristine nanofiber web due to impregnation process; which was measured and reported in table 1.

Table 1. Different applied methods to fabricate a dense nanofiber membrane (“-”: done; “+”: not done) and the average added weight to the final membrane obtained from three measurements.

| Sample | heat press before immersion | Vacuum after immersion | the average added weight (%) |
|---------|-----------------------------------|------------------------------|------------------------------------|
| SP-N40 | - | - | 40 |
| SP-V20 | - | + | 20 |
| SP-PV10 | + | + | 10 |
| SP-P20 | + | - | 20 |

III. RESULTS AND DISCUSSIONS

3.1 Morphology of nanofibers

Figure 1(a) illustrates that the SPEEK nanofibers exhibited a smooth and uniform surface without of bead-like imperfections, with an average fiber diameter of 150 nm.

To study how nanostructured additives affect the material, 0.5 wt% of MWCNT-COOH and P@MWCNT were added to the electrospinning solution, and nanocomposite nanofibers called SPEEK/MWCNT-COOH-0.5% and SPEEK/P@MWCNT-0.5% were produced; SEM images of these nanofibers are presented in Figure 1(b) and 1(c), respectively. These images confirm that the

addition of nanotubes did not disrupt the nanofiber morphology or induce defects such as bead-like structures. Notably, the average fiber diameter decreased to 128 nm for SPEEK/P@MWCNT and 120 nm for SPEEK/MWCNT-COOH nanocomposite nanofibers, compared to the pristine SPEEK nanofibers. This reduction in diameter is consistent with previous reports, which attributes the phenomenon to the enhanced electrical conductivity and altered solution viscosity imparted by carbon nanotubes during electrospinning [7][6].

Further, nanocomposite nanofibers containing 1, 1.5, and 2 wt% P@MWCNT were prepared, with their SEM images shown in Figure 1(d), (e), and (f), respectively. The average diameters of these composite nanofibers remained lower than that of pristine SPEEK nanofibers; however, they were slightly larger than the 0.5 wt% P@MWCNT sample. This marginal increase in diameter at higher nanotube loadings may be attributed to the increased likelihood of nanotube aggregation within the nanofibrous structure.

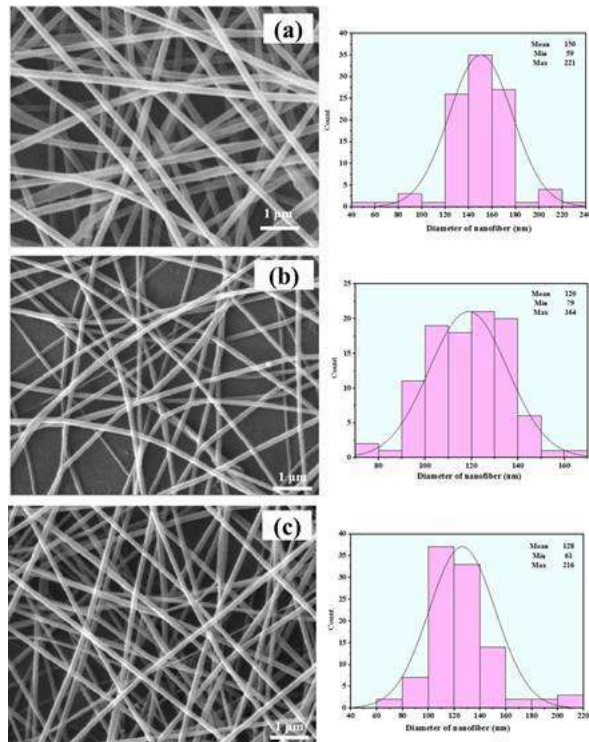


Figure 1: SEM images and diameter distribution of (a) SPEEK nanofibers, (b) SPEEK/MWCNT-COOH-0.5%, (c) SPEEK/P@MWCNT-0.5%, (Figure continued on the next column)

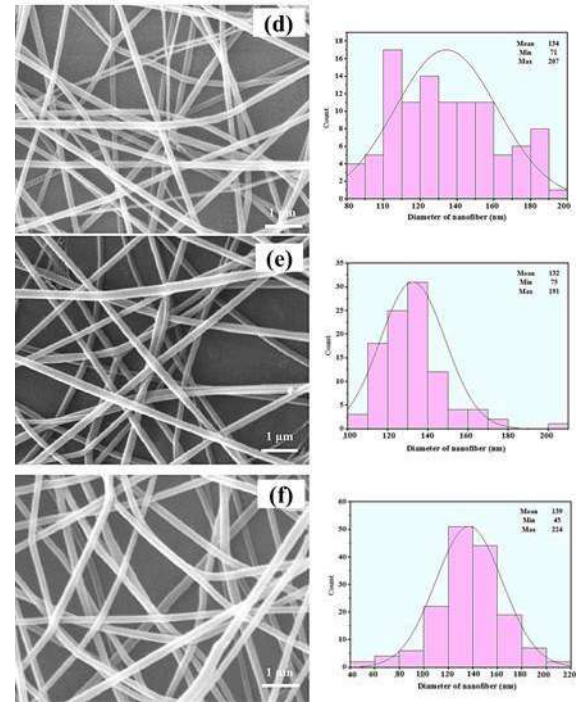


Figure 1: continued: (d) SPEEK/P@MWCNT-1%, (e) SPEEK/P@MWCNT-1.5%, and (f) SPEEK/P@MWCNT-2%.

3.2 Mechanical Properties of Nanofiber Webs

In proton exchange membrane fuel cells (PEMFCs), cyclic swelling and contraction of the membrane induce stresses that can cause delamination or pinhole formation [8]. To evaluate the mechanical properties of the electrospun nanofiber webs prior to densification, tensile strength tests were conducted on SPEEK and SPEEK/P@MWCNT nanocomposite nanofibers, with results presented in Table 2.

Tensile tests, with results shown in Table 2, indicate that adding P@MWCNT increases the modulus of composite nanofibers compared to pristine SPEEK nanofibers, but the stress at break decreases in all samples, and elongation at break increases. This result may confirm the lack of proper adhesion between the filler and the polymer matrix [6].

Table 2. Tensile Properties of SPEEK and SPEEK/P@MWCNT Nanofiber Webs.

| Sample | Modulus (MPa) | Tensile strength (MPa) | Elongation at break (%) |
|-------------------|---------------|------------------------|-------------------------|
| SPEEK | 6.7 | 7.7 | 41.7 |
| SPEEK/P@MWCNT-0.5 | 7.2 | 6.1 | 27.5 |
| SPEEK/P@MWCNT-1 | 17.1 | 7.2 | 17.1 |
| SPEEK/P@MWCNT-1 | 13.9 | 5.1 | 13.9 |
| SPEEK/P@MWCNT-1.5 | 19.6 | 4.9 | 19.6 |

3.3 Optimizing the densification process of nanofibers

To prepare dense nanofibrous membranes suitable for proton exchange membrane fuel cells (PEMFCs), the inherent porosity of electrospun nanofibrous webs posed a significant challenge. While porosity is advantageous in many applications, PEMs require gas-impermeable structures to prevent crossover of gases like hydrogen and oxygen. To address this, the polymer immersion method was employed, where nanofibrous webs were soaked in a dilute polymer solution to fill voids with it, creating a compact membrane. Due to SPEEK's solubility in solvents like DMF and DMAc, and its swelling in acetone, the choice of polymer solution was limited to water-soluble options. PVA and chitosan as water soluble polymers have been used as pore filling polymer but because of the lower intrinsic proton conductivity of these polymers the final membrane performance would be impacted negatively [9][10].

To ensure compatibility between nanofiber/matrix interface and minimize the damaging effect of the solvent on the nanofiber structure, SPEEK was selected as filler polymer. SPEEK was dissolved in water at 80°C at 4 wt. %, its dilution facilitates the

preparation process into the nanofibrous web's pores because of the lower chain entanglement.

Four distinct methods were developed to control the filler content and its impact on membrane properties, as summarized in Table 1. The initial porosity of the SPEEK nanofibrous web was approximately 70%, which reduced to 45% after hot-pressing, limiting the space available for filler polymer and thus reducing the filler uptake in pressed samples. SE7.2M images (Figure 2) confirmed that the pristine SPEEK web contained numerous voids which makes it unsuitable for PEM applications. In SP-N40, these voids were fully filled with SPEEK, creating a dense structure but the contribution of matrix in resultant nanofibrous membrane is relatively high (40% added weight). In SP-V20, partial void filling is occurred due to vacuum-induced polymer removal, leading to an uneven filler distribution. SP-PV10 exhibited the least filler content, the SEM images also indicating insufficient densification, potentially allowing fuel crossover. SP-P20, which was hot-pressed, had a well-balanced structure with enough filling of gaps and a consistent thickness (70–100 µm), providing better control over the membrane's morphology than the samples that weren't pressed. Therefore, SP-P20 densification method was selected as a proper one for following study.

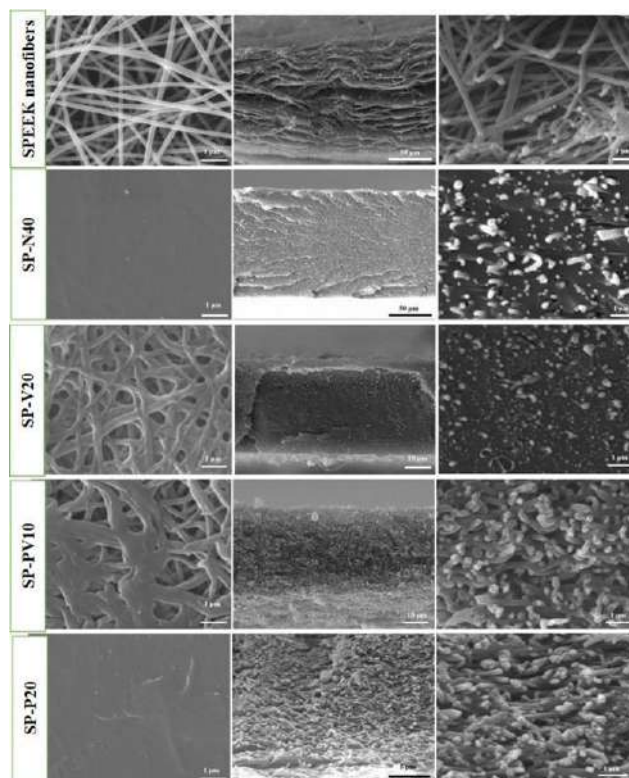


Figure 2: SEM images of membranes (1) surface web (left column), (2) cross-section (middle column), and (3) magnified cross-section (right column). Rows 1 to 5, respectively, show SPEEK nanofibers, SP-N40, SP-V20, SP-PV10, and SP-P20.

3.4 Proton conductivity of nanofibrous membranes

Proton conductivity tests (Table 3) revealed significant variations among the membranes. The SP-N40 membrane exhibited the lowest conductivity (2.7 mS cm^{-1}), likely due to disrupted ionic channel formation caused by excessive filler polymer, hindering proton transport. SP-V20 and SP-P20 membranes, with reduced filler content, showed improved conductivities of 4.0 mS cm^{-1} and 4.3 mS cm^{-1} , respectively, reflecting better preservation of nanofiber-driven proton pathways. The SP-PV10 membrane achieved a remarkably high conductivity of 19.8 mS cm^{-1} , attributed to the higher nanofiber proportion, which enhanced ionic channel continuity along the fiber axis. However, SEM analysis indicated that the structure of SP-PV10 was insufficiently dense, posing risks for fuel crossover, making it unsuitable for PEM applications.

To balance proton conductivity and structural integrity, SP-P20 was selected for further optimization. The hot-pressing step in SP-P20 not only reduced thickness variability but also enhanced nanofiber interconnectivity, facilitating proton transport. This aligns with the hypothesis that proton conduction is more efficient along the nanofiber axis, potentially due to ionic channels formed centrally within the fibers, as supported by prior studies [11].

Table 3. Proton conductivity densified nanofibrous membrane based on various method.

| Sample | The average proton conductivity (mS cm^{-1}) |
|---------|---------------------------------------------------------|
| SP-N40 | 2.7 |
| SP-V20 | 4.0 |
| SP-PV10 | 19.8 |
| SP-P20 | 4.3 |

To further enhance performance, nanocomposite membranes were prepared by incorporating P@MWCNTs into the SP-P20 structure at 0.5, 1, 1.5, and 2 wt% relative to the polymer mass. Proton conductivity results (Figure 3 (a)) demonstrated a significant improvement with 0.5 wt% P@MWCNTs, increasing conductivity from 4.3 mS cm^{-1} to 24.5 mS cm^{-1} . At 1 wt%, conductivity peaked at 45 mS cm^{-1} , a tenfold increase over the pristine SP-P20 nanofibrous membrane, likely due to the alignment of modified nanotubes along the nanofiber axis, enhancing ionic channel efficiency (Figure 3 (b)). Beyond 1 wt%, conductivity declined, possibly due to nanotube aggregation obstructing proton pathways, consistent with literature reports [12][13]. In contrast, cast SPEEK/P@MWCNT films showed only a threefold conductivity increase at 3.5 wt% [6], underscoring the superior efficacy of nanofibrous structures in leveraging nanotube alignment for proton transport.

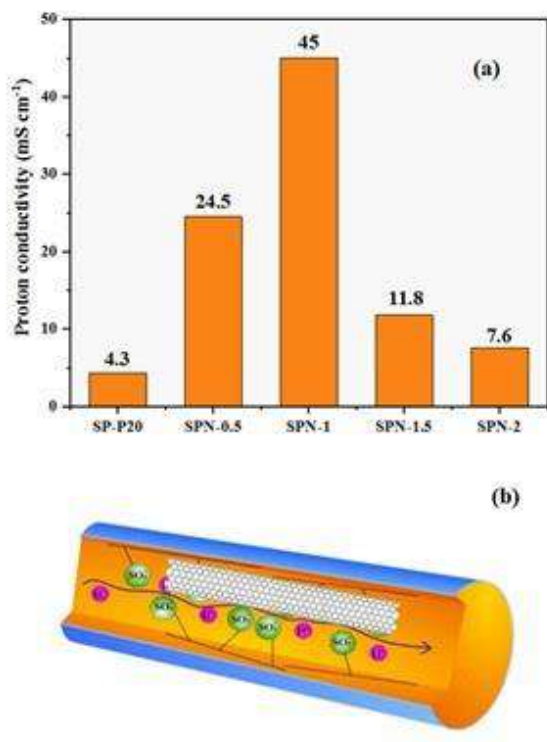


Figure 3: Proton conductivity of selected dense structure containing P@MWCNT at 0.5, 1, 1.5, and 2 wt% (a) and schematic of proposed proton conduction mechanism through SPEEK-P@MWCNT nanofiber (b).

IV. CONCLUSIONS

This study developed SPEEK and SPEEK/P@MWCNT nanocomposite nanofibrous membranes for PEMFCs, optimized through electrospinning, hot-pressing, and immersion in dilute SPEEK solutions to create fully densified, gas-impermeable structures. By employing SPEEK as both the nanofiber material and the filler polymer, the membranes achieved exceptional interfacial compatibility between the nanofibers and the void-filling matrix, preserving proton conductivity unlike less conductive fillers.

The incorporation of 1 wt% P@MWCNT dramatically boosted proton conductivity to 45 mS cm⁻¹, a tenfold enhancement over SP-P20, driven by the alignment of nanotubes with ionic channels along the nanofiber axis. This strategic use of identical polymers for nanofibers and filler, combined with nanotube

reinforcement, enabled these nanocomposite membranes to surpass traditional SPEEK films in performance. The fully densified structure, achieved through hot-pressing and polymer filling, positioning these nanofibrous membranes as highly promising candidates for advancing proton exchange membrane fuel cell technology.

ACKNOWLEDGMENT

REFERENCES

- [1] S. Sharma and B. G. Pollet, "Support materials for PEMFC and DMFC electrocatalysts - A review," *J. Power Sources*, vol. 208, pp. 96–119, 2012, doi: 10.1016/j.jpowsour.2012.02.011.
- [2] D. J. Kim, M. J. Jo, and S. Y. Nam, "A review of polymer-nanocomposite electrolyte membranes for fuel cell application," *J. Ind. Eng. Chem.*, vol. 21, pp. 36–52, 2015, doi: 10.1016/j.jiec.2014.04.030.
- [3] K. D. Kreuer, "On the development of proton conducting polymer membranes for hydrogen and methanol fuel cells," *J. Memb. Sci.*, vol. 185, no. 1, pp. 29–39, 2001, doi: 10.1016/S0376-7388(00)00632-3.
- [4] C. Gong *et al.*, "A new strategy for designing high-performance sulfonated poly(ether ether ketone) polymer electrolyte membranes using inorganic proton conductor-functionalized carbon nanotubes," *J. Power Sources*, vol. 325, pp. 453–464, 2016, doi: 10.1016/j.jpowsour.2016.06.061.
- [5] R. Sood, S. Cavaliere, D. J. Jones, and J. Rozière, "Electrospun nanofibre composite polymer electrolyte fuel cell and electrolysis

- membranes,” *Nano Energy*, vol. 26, pp. 729–745, 2016, doi: 10.1016/j.nanoen.2016.06.027.
- [6] Z. Esmailzadeh, M. Karimi, A. M. Shoushtari, and M. Javanbakht, “Linking interfacial energies with proton conductivity in sulfonated poly (ether ether ketone) nanocomposite,” *Polymer (Guildf)*., vol. 230, p. 124067, Jul. 2021, doi: 10.1016/j.polymer.2021.124067.
- [7] H. Chen, Z. Liu, and P. Cebe, “Chain confinement in electrospun nanofibers of PET with carbon nanotubes,” *Polymer (Guildf)*., vol. 50, no. 3, pp. 872–880, 2009, doi: 10.1016/j.polymer.2008.12.030.
- [8] J. B. Ballengee and P. N. Pintauro, “Preparation of nanofiber composite proton-exchange membranes from dual fiber electrospun mats,” *J. Memb. Sci.*, vol. 442, pp. 187–195, 2013, doi: 10.1016/j.memsci.2013.04.023.
- [9] H. Zhang, Y. He, J. Zhang, L. Ma, Y. Li, and J. Wang, “Constructing dual-interfacial proton-conducting pathways in nanofibrous composite membrane for efficient proton transfer,” *J. Memb. Sci.*, vol. 505, pp. 108–118, 2016, doi: 10.1016/j.memsci.2016.01.013.
- [10] Y. He *et al.*, “Synergistic proton transfer through nanofibrous composite membranes by suitably combining proton carriers from the nanofiber mat and pore-filling matrix,” *J. Mater. Chem. A*, vol. 3, no. 43, pp. 21832–21841, 2015, doi: 10.1039/c5ta03601a.
- [11] T. Tamura and H. Kawakami, “Aligned electrospun nanofiber composite membranes for fuel cell electrolytes,” *Nano Lett.*, vol. 10, no. 4, pp. 1324–1328, 2010, doi: 10.1021/nl1007079.
- [12] M. N. Feng, Z. J. Pu, P. L. Zheng, K. Jia, and X. B. Liu, “Sulfonated carbon nanotubes synergistically enhanced the proton conductivity of sulfonated polyarylene ether nitriles,” *RSC Adv.*, vol. 5, no. 43, pp. 34372–34376, 2015, doi: 10.1039/c5ra03973h.
- [13] G. He *et al.*, “Functionalized carbon nanotube via distillation precipitation polymerization and its application in Nafion-based composite membranes,” *ACS Appl. Mater. Interfaces*, vol. 6, no. 17, pp. 15291–15301, 2014, doi: 10.1021/am503760u.



Tailoring PET/PLA Film Properties Through Transesterification During Melt Processing

Maryam Kheirandish^{a*}, Mohammad Reza Mohaddes Mojtahedi ^a, Hossein Nazockdast^b

^a Department of Textile Engineering, Amirkabir University of Technology, Tehran, Iran

^b Department of Polymer Engineering, Amirkabir University of Technology, Tehran, Iran

*Corresponding author: m.kheirandish@aut.ac.ir

ABSTRACT

Due to the growing demand for various functional materials, the production of biodegradable plastic products has rapidly increased in recent years. These materials can be used in different applications, most notably in the packaging industry. In this research, a polymer film was prepared by blending polylactic acid (PLA), a biodegradable polyester, with polyethylene terephthalate (PET). Surface tension measurements were used to estimate the surface energy values between the two components, and the results indicated good adhesion between them. The microstructure was examined using scanning electron microscopy (SEM), and the findings showed that PET and PLA were immiscible, but compatible with each other. FTIR studies were conducted to investigate the structure. Interactions were analyzed using ¹H NMR, and the transesterification reaction was confirmed. DSC results indicated shifts in glass transition temperature (T_g), which suggests interactions between these materials. Due to the formation of copolymers via transesterification, the crystallization process in the film became more difficult as PLA was added to the PET matrix. The presence of PET crystals in the blended film was confirmed by X-ray scattering patterns.

Keywords: polylactic acid; polyethylene terephthalate; transesterification; polymer film; PET/PLA copolymer

I. INTRODUCTION

Today, awareness regarding the use of fossil resources is increasing. These resources have such a significant impact on the climate that they could potentially drive human life into crisis. Therefore, fossil-based resources need to be gradually phased out and replaced with renewable alternatives. Along with this shift in energy sources, a transformation in material production is also necessary. In the realm of plastics, which are conventionally derived from fossil sources,

bio-based polymers with significant potential to improve carbon dioxide balance can play a crucial role [1].

Polyethylene terephthalate (PET) is a commercially important thermoplastic polymer that is widely used around the world due to its favorable thermal and mechanical properties, low permeability, and chemical resistance [2]. PET plastics are strong, inexpensive, durable, and easy to process. Initially introduced as a substitute for glass soda bottles, PET has since found

expanded use in packaging, textile fibers, engineering plastics, automotive, electronics, and vascular tissue engineering [3]. Its primary application lies in single-use packaging for beverages and food. While not inherently hazardous, PET is derived from petroleum sources and can take thousands of years to degrade. Nevertheless, it is lightweight, transparent, and recyclable, and recycling PET back into plastic is widely practiced [4].

However, the production of PET and other synthetic polyesters increases fossil fuel consumption, contributes to landfill waste, and lacks biodegradability. As a result, the volume of PET waste has increased significantly. Many efforts have been made to enhance its degradability and address environmental concerns, one of which involves blending it with biodegradable polymers [5].

One of the biodegradable polymers that can be produced from renewable sources such as starch and sugar is polylactic acid (PLA). In natural environments, PLA can be fully converted into water and carbon dioxide [6]. This linear aliphatic thermoplastic polyester has attracted much attention due to its environmental friendliness, suitable mechanical properties, thermoplastic processability, and biodegradability. It can be synthesized not only through ring-opening polymerization of lactide but also via the polycondensation of lactic acid [1].

Among its notable features are renewability, biodegradability, and biocompatibility. The price of PLA is slightly higher compared to common commercial polymers [7]. Thanks to its transparency and good mechanical strength, PLA has applications across various industries. However, at room temperature, it tends to be brittle and exhibits low crystallization rate and thermal resistance [8].

Due to the chiral carbon atom in lactic acid, PLA exists in two isomeric forms: L-lactide (PLLA) and D-lactide (PDLA). Many important properties of PLA are

controlled by the ratio and sequence of these enantiomers in the polymer chain [9]. PLLA is approximately 37% crystalline, with a glass transition temperature (T_g) between 50°C and 80°C and a melting temperature between 173°C and 178°C [10]. PLA containing more than 90% PLLA tends to crystallize more readily. As the PLLA content decreases, the melting point, glass transition temperature, and crystallization rate also decrease.

Properties such as thermal stability and impact resistance of PLA are lower than conventional thermoplastic polymers, making PLA less than ideal for competing with them in its pure form. To improve its properties and broaden its potential applications, lactic acid copolymers with other monomers, such as styrene and acrylates, have been developed. Modifications like copolymerization and composite formation have been used to enhance its toughness, permeability, crystallization behavior, and thermal stability [11].

The rapid advancement of technology has increasingly created new applications for polymeric materials with diverse properties. This often necessitates modifying existing polymers to meet specific needs. Among the various polymer modification methods, polymer alloying holds a prominent position due to its flexibility in material selection—especially from an economic standpoint. One major area of focus in polymer alloy studies is controlling the compatibility of constituent components and their microstructure, which significantly affects rheological behavior, processability, and the final product's physical and mechanical properties.

Blending PLA with various polymers has been a topic of significant interest in recent years, with a variety of approaches explored to enhance its properties. For example, In 2011, Yeom and colleagues developed a new bicomponent spunbond structure to achieve large surface area fibers [12]. The fibers used in this

spunbond process included a sacrificial sheath polymer and a core-forming polymer. After mechanical entanglement using high-energy water jets, the sheath polymer was dissolved in a 6% NaOH solution at 90°C, revealing the final structure of the fibers. They used various polymer combinations, including PET as the core and PLA as the sheath. SEM analysis showed fiber diameters of up to 21 microns, and it is noteworthy that the fibers were produced at a speed of 2000 m/min.

In 2014, a comparative study was conducted on the miscibility and biodegradability of PLA/PET and PLA/chitosan blends [13]. The degradation of the samples was measured over six months in real soil, accelerated by pressurized air. In this study, chitosan's miscibility within the PET matrix was reported to be lower compared to PLA. The results revealed weak interactions between components, likely through secondary hydrogen bonding or electrostatic forces. Saturation of PLA in the polymer matrix was observed up to 10 wt%, while chitosan above 5 wt% became brittle. The best miscibility and biodegradability performance for the PET/chitosan system was achieved with 5 wt% chitosan.

Another group of researchers produced PET/PLA composite films via extrusion[14]. Their results indicated that the addition of a small amount of PLA increased the crystallinity of PET during injection molding, but the degradation temperature and tensile/flexural strength of the blends decreased with increasing PLA content. Meanwhile, the degradation rate increased.

Considering that polymer films are typically produced at high temperatures, which increases the possibility of transesterification and copolymer formation, some researchers attempted to avoid high temperatures by preparing PLA/PET electrospun fibers at room temperature using solvents [4]. Nanofibrous layers were analyzed both as-spun and after cold

crystallization treatment. In amorphous as-spun fibers, the addition of PLA prevented the formation of beads. In some blend ratios, two distinct glass transition temperatures were observed, indicating phase separation in the fiber-forming solution. Crystallinity of both polymers decreased in the presence of the other, and overall crystallinity in the blended electrospun fibers was lower than in homopolymer nanofibers [4].

Researchers in Mexico studied the dependence of microstructure and mechanical properties on the PLA content in the PET matrix[3]. They added various PLA concentrations (1, 2.5, 5, and 7.5 wt%) to the PET matrix using a single-screw extruder on a small laboratory scale. Thermal analysis results showed a shift in glass transition temperature with different amounts of PLA. SEM and AFM images revealed two types of microstructures: miscible and partially miscible. Fourier Transform Infrared Spectroscopy (FTIR) confirmed the presence of physical interactions and hydrogen bonding in the polymer blends. Impact resistance and tensile strength decreased with the addition of PLA.

In another study, nanofiber mats were produced using solutions of PET and three types of PLA (one commercial and two branched) to support trypsin enzyme collection during whey protein hydrolysis [15]. The PET/PLA nanofiber mats with immobilized trypsin could be stored in water at 4°C for at least 30 days and reused up to eight times without enzyme washing.

In 2020, Wang and colleagues fabricated PET/PLA foams using in-situ nanofibrillar composites and investigated the foamability and thermal insulation of the final product [16]. They observed that the presence of PET nanofibrils significantly improved PLA's crystallinity, viscoelasticity, and melt strength, thereby enhancing its foamability.

In another investigation, various PET/PLA blend samples—with and without graphene oxide and layered graphite nanoparticles—were prepared using a twin-screw extruder [5]. The study evaluated thermal and hydrolytic degradation behaviours. It was observed that, unlike layered graphite, the addition of graphene oxide reduced the thermal stability of the samples but, due to better dispersion, improved oxygen barrier properties.

Recent advances have also highlighted the role of nanoclay additives in enhancing the morphological and thermal properties of recycled PET/PLA blends, providing improved stability and structural integrity under mechanical stress [17].

Moreover, a 2023 investigation confirmed the biodegradability potential of PET/PLA blends under composting conditions, showing considerable disintegration rates during degradation [18]

As mentioned, PLA, due to its renewable origin, is widely used in various applications and, because of its biodegradability, is often preferred over synthetic fibers in fields such as medicine. However, PLA suffers from some inherent limitations, such as brittleness, which restricts its usage in certain applications.

Therefore, blending PLA with synthetic polymers not only helps mitigate its drawbacks but also enhances the biodegradability of PET. In this study, an alloy of these two polymers was prepared, and the properties of the final product, in film form, were evaluated. It is worth mentioning that since the transesterification phenomenon significantly impacts the final product's properties, and no prior research has thoroughly examined this reaction during melt processing in film form, this study aimed to investigate this phenomenon and evaluate the resulting properties.

II. EXPERIMENTAL METHOD / TEORETICAL METHOD

2.1 Materials and Preparation Techniques

The materials used in this study include polylactic acid (PLA) grade 4043 obtained from NatureWorks (USA), with a weight-average molecular weight of 110,000 g/mol and containing 4–4.5 wt% D-lactide isomer. Polyethylene terephthalate (PET) with a melting temperature of 260°C and intrinsic viscosity of 0.65 dl/g was supplied by Tondgouyan Petrochemical Company. Dichloromethane solvent was purchased from Merck.

2.2. Preparation of Polymer Film

To prepare the polymer film, the PLA and PET polymers were first dried to prevent hydrolysis. Drying was performed in an oven at 80°C for PLA and 120°C for PET, each for 24 hours. Then, both polymers—individually and as blends with 20 wt% PLA—were melted and mixed using an internal mixer (manufactured in Iran) at 60 RPM for 10 minutes at 270°C. The molten blends were then molded into rectangular films with a thickness of 1 mm by hot pressing under 50 bar pressure at 270°C for 5 minutes.

2.3. Characterization of the Films

2.3.1. Surface energy and interfacial tension analysis

To analyze the microstructure of the PLA/PET blend, it is necessary to determine the surface energy of both polymers. Therefore, contact angle measurements were carried out using the static sessile drop method. Film samples with dimensions of 2 × 4 cm were placed on a fixed base, and 10 µL droplets of various liquids were deposited at three distinct points on each sample surface using a microsyringe. The droplets were photographed with a Sony SSCDC318P camera (Japan), and the contact angles were measured using Digimizer software. The test liquids used were water, benzyl alcohol, ethylene glycol, and toluene.

The surface tension (γ), polar component (γ^p), and dispersive component (γ^d) of the test liquids are provided in Table 1. These values were used to calculate the surface energies of the PLA and PET films at processing temperature using the Owens-Wendt-Rabel-Kaelble (OWRK) method [19,20].

Table 1. Surface tension (γ) and its components for reference liquids [21].

| Liquid | γ (mN/m) | γ^d (mN/m) | γ^p (mN/m) |
|-----------------|-----------------|-------------------|-------------------|
| Water | 72.8 | 26.4 | 46.4 |
| Benzyl alcohol | 39.0 | 30.3 | 8.7 |
| Ethylene glycol | 47.7 | 26.4 | 21.3 |
| Toluene | 28.4 | 26.1 | 2.3 |

2.3.2. Investigation of surface microstructure by scanning electron microscopy (SEM)

Morphological images were obtained using a scanning electron microscope (SEM) model XL30 (Philips, Netherlands). Film samples were coated with a thin layer of gold and examined from their cross-sectional surfaces. To further study the phase distribution, the samples were immersed in dichloromethane solvent for 1 hour at room temperature to selectively dissolve the PLA phase from the blend.

2.3.3. Fourier transform infrared spectroscopy (FTIR)

To analyze the chemical structure of the polymer films, FTIR spectra were recorded using a Nicolet Nexus 670 spectrometer in the range of 400–4000 cm^{-1} . This technique was applied to both pure and blended samples to observe the presence of functional groups and potential interactions.

2.3.4. ^1H Nuclear magnetic resonance (^1H NMR)

^1H NMR analysis was performed using a Bruker 400 MHz Ultrashield NMR spectrometer. Both neat and blended polymer films were dissolved in a solvent mixture of deuterated trifluoroacetic acid (TFA) and chloroform-d (CDCl_3) in a 70/30 weight ratio. Tetramethylsilane (TMS) was used as the internal standard, and all spectra were recorded at room temperature with reference to CDCl_3 .

2.3.5. Differential scanning calorimetry (DSC)

Thermal properties of the polymer blends were evaluated using a Q500 TGA (DSC) instrument from the USA. The analysis was performed under a nitrogen atmosphere from room temperature up to 300°C, with a heating rate of 10°C/min for the first heating cycle and 5°C/min for the cooling cycle. Samples were held at 300°C for 2 minutes before cooling. Melting

temperature (T_m) and crystallization temperature (T_c) were recorded from the DSC thermograms.

The degree of crystallinity (ϕ_c) was calculated using the Eq.1 below, assuming 140 J/g as the enthalpy of fusion for 100% crystalline PET:

$$\phi_c = \frac{\Delta H(m) - \Delta H(c)}{\Delta H(m^\circ)w} \quad (1)$$

Where:

- ΔH_m = enthalpy of melting
- ΔH_c = enthalpy of cold crystallization
- ΔH_m° = enthalpy of melting for 100% crystalline PET
- w = weight fraction of the polymer in the blend

2.3.6. X-ray diffraction (XRD)

XRD patterns of the produced films were recorded using an Inel Equinox 3000 diffractometer. Crystallinity of the samples was examined in the 2 θ range of 5–40°. The data were analyzed using X'Pert HighScore Plus software (PANalytical).

III. RESULTS AND DISCUSSIONS

3. 1. Contact Angle Evaluation

The contact angles of the prepared films in different liquids were measured and the results are presented in Table 2.

Table 2. Contact angles (in degrees) of PLA and PET films

| Polymer | Water | Benzyl Alcohol | Ethylene Glycol | Toluene |
|----------|-------|----------------|-----------------|---------|
| PET Film | 86° | 53° | 67° | 37° |
| PLA Film | 82° | 56° | 61° | 34° |

As observed, PLA shows a lower contact angle than PET in water, indicating that PLA is more hydrophilic. Using the contact angle data and the OWRK method, surface energy values were calculated at the processing temperature (270°C), as shown in Table 3.

Note: Since the interfacial energy equations require the contact angle data of the pure components only, the alloy film values were not calculated.

Table 3. Surface energy values of pure polymers at 270°C

| Polymer | Total γ (mN/m) | Dispersive γ^d | Polar γ^p |
|---------|-----------------------|-----------------------|------------------|
| PET | 9.305 | 7.036 | 2.269 |
| PLA | 11.290 | 7.210 | 4.080 |

Then, using the surface energy data, the interfacial energy between the two polymers was calculated.[22–24] . The results can be seen in Table 4.Using these surface energy values, the interfacial tension (γ_{12}) between PLA and PET was calculated using both and geometric and harmonic mean equations, shown below in Eq2. and Eq3. respectively:

- Geometric Mean:

$$\gamma_{12} = \gamma_1 + \gamma_2 - 2(\sqrt{\gamma_1^d \gamma_2^d} + \sqrt{\gamma_1^p \gamma_2^p}) \quad (2)$$

- Harmonic Mean:

$$\gamma_{12} = \gamma_1 + \gamma_2 - 4\left(\frac{\gamma_1^d \gamma_2^d}{\gamma_1^d + \gamma_2^d} + \frac{\gamma_1^p \gamma_2^p}{\gamma_1^p + \gamma_2^p}\right) \quad (3)$$

Where γ_1 , γ_2 , are the surface tensions of polymers 1 and 2, γ_1^d , γ_2^d , γ_1^p , and γ_2^p are the dispersive and polar fractions of the surface tensions of polymers 1 and 2, respectively. The harmonic equation is generally well-suited to low-energy materials [25]. For low-energy surfaces, the geometric-mean equation is inadequate [24], but it is recommended for both high and low-energy surfaces [23].

Table 4. Interfacial tension (γ_{12}) between PET and PLA

| Polymer Pair | Harmonic Mean (mN/m) | Geometric Mean (mN/m) |
|--------------|----------------------|-----------------------|
| PET-PLA | 0.519 | 0.338 |

The low interfacial tension values suggest good compatibility and interfacial adhesion between the two components [19], which was confirmed by SEM results in Figure 1. This also supports the thermodynamic argument that good interfacial interaction facilitates blending and potentially improves the final properties of the film [26].

3.2. Scanning electron microscopy (SEM)

Microscopic images of the fractured surface of PET and PLA films and their blends are shown in Figure 1. The fractured surface in Figure 1(b) clearly shows that the PLA film has a brittle structure. In part (c) of Figure 1, the presence of spherical PLA droplets inside the PET matrix and the immiscibility of the two components can be seen. In part (d) of Figure 1, the PLA phase has been selectively separated from the matrix by dichloromethane.

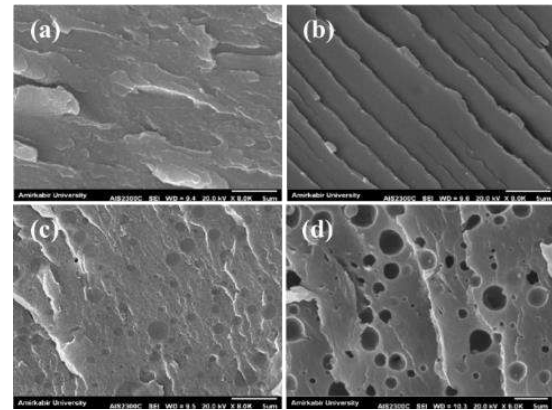


Figure 1. Microstructure of the films: (a) pure PET, (b) pure PLA, (c) PET/PLA blend film containing wt20% PLA and (d) PET/PLA blend film containing wt20% PLA after the dispersion component was removed

As can be seen, the dispersed PLA phase in the PET matrix is located in the dark empty cavities visible on the fractured surface. In part (c) of the figure, it can be seen that the connection of all the dispersed phase particles with the matrix is not spaced and no phase separation is seen at the common surface, and in fact, the dispersed component and the polymer matrix have good uniformity due to sufficient compatibility with each other [27]. In other words, the interface region between the phases indicates low surface tension between the components, which results in the connection of PLA particles to the matrix and the adhesion between the two phases seems good. This finding is consistent with the calculated interfacial energy between PET and PLA, which was observed in Table 4.

Based on thermodynamic principles, comparing the solubility quantities of two or more polymers can

predict their miscibility [2], Hansen's solubility value for PET and PLA predicts that they should be miscible [28,29]. Andrew et al. believe that the molar volume and the size of the repeating unit are important factors that cause immiscibility in the blend of PET and PLA. PET has a structure with large benzene rings and as evident from its higher molar volume than PLA, this could explain the immiscibility of the two phases of these polymers in the molten state [30]. Our results seem to be closer to their findings and the different molar volumes of the two phases caused the immiscibility between PET and PLA.

3.4. FTIR Spectroscopy

FTIR analysis was performed to investigate the chemical structure of the samples in pure and blended state. Figure 2 shows the FTIR spectra of PET, PLA films and their blends.

The PET spectrum shows characteristic peaks related to O-H stretching at 3432 cm^{-1} which is related to the ethylene glycol end group of the PET molecule chain, aromatic C-H stretching at 3060 cm^{-1} and aliphatic C-H stretching at $2964\text{--}2910\text{ cm}^{-1}$. 1719 cm^{-1} represents C=O stretching and $11577\text{--}1504\text{ cm}^{-1}$ indicates the aromatic structure stretching band, $11454\text{--}1340\text{ cm}^{-1}$ peak related to CH₂, 11407 cm^{-1} para substitution in the benzene ring and $11248\text{--}1097\text{ cm}^{-1}$ O-C stretching of the ester group.

The aromatic 1,4 substitution is observed at 11018 cm^{-1} and the O-CH₂ stretching of the ethylene glycol moiety is observed at 971 cm^{-1} and the C-H corresponding to the two adjacent paired hydrogens on the benzene ring is observed at 1873 cm^{-1} [13,31].

The main absorption peaks of PLA are as follows: 3505 represents the O-H stretching vibration 2998 and 2946 cm^{-1} are the CH₃ stretching vibration in the asymmetric and symmetric states. The peak at 1760 cm^{-1} is related to the C=O stretching of the aliphatic units, the peak at 1454 represents the unsymmetrical CH₃ bending vibration and the peaks at 1384 cm^{-1} and

1361 are related to the C-H group, 1189 and $\text{cm}^{-1}1093$ are related to the O-C cm^{-1} stretching vibration of the aliphatic ester. and 869 cm^{-1} shows C-C-O absorption [32].

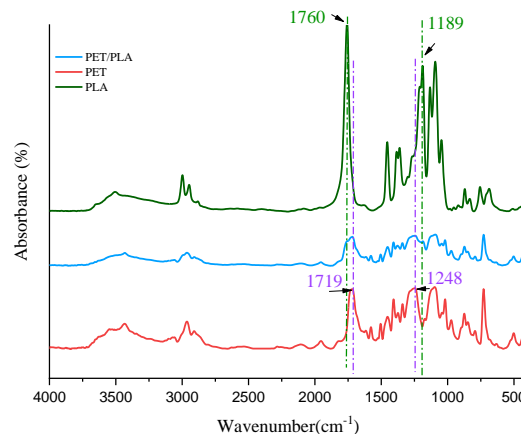


Figure 2. FTIR diagram of the produced films.

As shown in Figure 2, in the composite film, characteristic peaks attributed to the carbonyl ester and the ester group for the PET polymer present in the structure are visible. However, the peaks related to PLA (peak $\text{cm}^{-1}1760$ which is related to the carbonyl ester of PLA) in the composite film are slightly transformed into a comb and the peak at $\text{cm}^{-1}1189$ is only partially visible. The lack of visibility of PLA peaks in the composite may be due to the low percentage of PLA compared to the main matrix, PET.

3.5. ¹H NMR Results

¹H NMR evaluation was performed to determine the molecular structure of the PET/PLA composite film and the resulting graphs are shown in Figure 3.

In the case of PET, the characteristic peaks in this analysis are as follows: hydrogens attached to the aromatic ring and ethylene groups between two terephthalate units in the repeating chain of this polymer are seen at 13.8 ppm and 85.4 ppm . The signals at 20.4 ppm and 66.4 ppm are related to the ethylene oxide hydrogens of the end group [33,34]. In the diagram for PLA film, the characteristic peaks of

this polymer structure are observed at 60.1 ppm and 26.5 ppm, which are related to the CH₃ and CH groups in the main chain of this polymer, respectively [33].

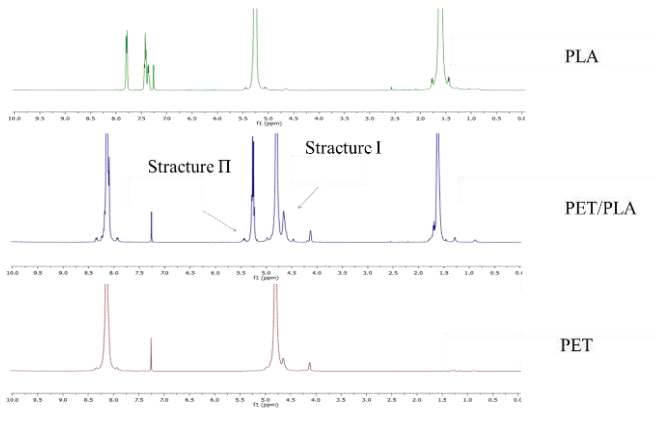


Figure 3. ¹H NMR spectra of polyethylene terephthalate, polylactic acid and polyethylene terephthalate/polylactic acid films

As a result of the ester exchange phenomenon and the placement of the PLA chain between the PET chains, two possible structures can be formed (Figure 4). In the first structure, this polymer is attached to the ethylene groups in ethylene terephthalate, and in the second structure, the PLA chains are directly attached to the benzene ring in the PET chain. The placement of PLA in each of these positions causes peaks to appear in the ¹H NMR spectrum. In structure I, the ethylene oxide hydrogens located in this position show the corresponding signal in a lower field, which can overlap with the peaks related to the end groups of PET. In calculations and measurements, the area under the diagram related to each of the hydrogens must be subtracted from the area under the diagram of the end groups. In case II, the hydrogen related to the CH group shows itself in a higher field due to its attachment to the electron-withdrawing group of terephthalates, and in other words, the appearance of this peak confirms the formation of the second structure. In the blending of polyesters, when the blending process occurs at temperatures close to or above the melting temperature, the possibility of transesterification is very likely [35]. The observation of peaks corresponding to each of the possible

structures seen in the ¹H NMR diagram (Figure 3) confirms the occurrence of transesterification between the two polyesters forming the blend.

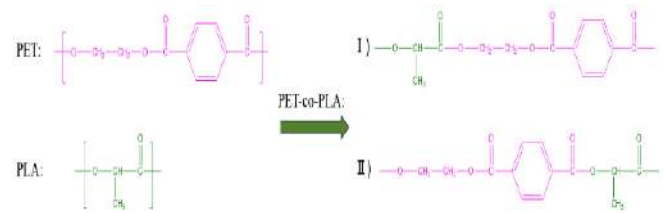


Figure 4. Possible structures formed by ester exchange.

3.6. Thermal Analysis

The DSC diagrams of pure films and semi-crystalline PET/PLA composite films during heating and cooling are shown in Figure 5, respectively.

Table 5 shows the results of PET crystallization during heating and cooling of the films in non-isothermal crystallization. In Figure 5, pure PET film is seen with a crystallization temperature of 125 °C, a melting temperature of 257 °C, and a degree of crystallinity of 0.192. The peak near 80 °C is attributed to the glass transition of PET. In the pure PLA sample, a degree of crystallinity of 0.36 and a melting temperature of 150 °C are observed. In the PET/PLA composite film, two glass transition temperatures at temperatures of 63 and 78 °C are clearly seen, which are related to the T_g of PLA and PET polymers, respectively, and indicate the immiscibility of the two polymers [36], which was also clearly seen in the microscopic images (Figure 1). The decrease in T_g in PET and its closer approximation to the T_g of polylactic acid can be a confirmation of the interactions between these two polymers [37]. In this film diagram of the combination of the two polymers, the peak corresponding to the melting temperature of PLA is not seen. With the addition of PLA, the melting temperature of PET and its enthalpy of melt have decreased, and the crystallization rate of PET after the addition of PLA reaches 0.139.

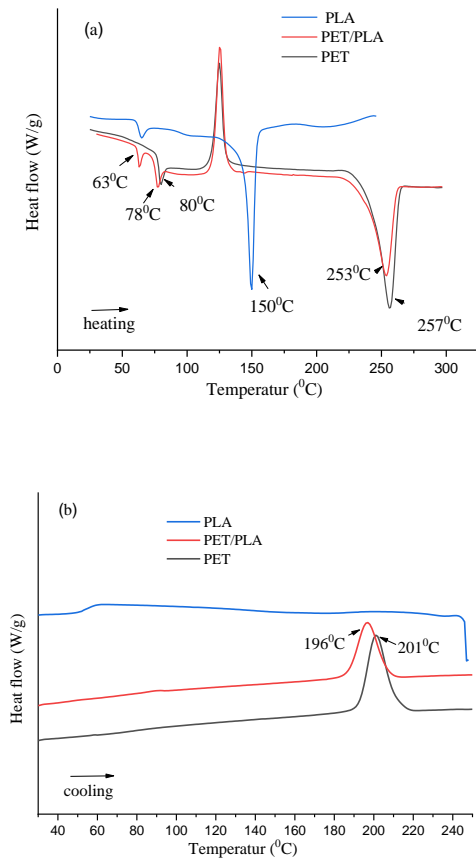


Figure 5. DSC diagram of pure PET, PLA and PLA blended film
(a) first heating (b) cooling from the melt.

When semi-crystalline polymers are blended with other polymers, the decrease in T_m indicates a degree of miscibility between the blend components due to favorable thermodynamic interactions between PET and PLA, indicating that the PLA repeating units often interrupt the linear crystallographic sequences of PET chains [20,40–42]. Furthermore, the crystallinity of PET becomes difficult with the addition of PLA. This conclusion is consistent with the X-ray results shown in Figure. 6. On the other hand, the PET-PLA structure resulting from ester exchange is difficult to incorporate into the PET crystal, causing the PET crystallinity to decrease in the blends. The ^1H NMR results confirm these findings. In the graph of Fig. 6(b) which is related to the cooling of the samples, the crystallinity of PET in the blend is observed, but this does not happen for the PLA chains. In other words,

the PET chains affect and hinder the crystallization of PLA. The addition of PLA caused the crystallization of PET melt to decrease from 201 °C to 196 °C and the melt crystallinity to increase from 0.319 to 0.299.

It has been reported that this effect could be due to the formation of PET-PLA copolymers resulting from the transesterification reaction at the melt processing temperature of polyesters. The copolymer is primarily found at the interface and its role in reducing interfacial tension and increasing miscibility is widely known in reactive processes [38]. On the other hand, PLA units are incorporated into the crystal lattice as a result of transesterification interactions between PET and PLA units, resulting in the production of a block copolymer [39].

On the other hand, PLA units are the soft parts in the copolymer structure. Due to the low T_g of PLA, these PLA blocks should have higher mobility than PET blocks at the crystallization temperature. Therefore, the lower crystallization onset and lower crystallinity in the polymer blend is due to the increased mobility of the soft segments of PLA [39].

Table 5. Data related to DSC

| PET/PLA Ratio | ΔH_c (J/g) (Heating) | T_m (°C) (PET) | ΔH_m (J/g) PET | Φ_c PET (Heating) | ΔH_c (J/g) PET (Cooling) | Φ_c PET (Cooling) |
|------------------|------------------------------------|------------------------|------------------------------|---------------------------|----------------------------------------|---------------------------|
| 0/100 | 63.19 | 257 | 50.46 | 0.192 | 65.44 | 0.319 |
| 20/80 | 83.21 | 253 | 44.37 | 0.139 | 45.33 | 0.299 |

3.7. X-ray diffraction

The presence of one component can affect the crystallinity of another component, so to investigate this effect, X-ray diffraction tests were performed on the samples and the results are shown in Figure 6. As can be seen, the main peaks related to PET are seen at angles of 16.33, 17.50, 21.45, 22.63 and 26.19 degrees, which are related to the crystal planes (01 $\bar{1}$), (010), (11 $\bar{1}$), (1 $\bar{1}$ 0) (100). As can be seen, this semi-

crystalline polymer has a broad amorphous peak and crystallization peaks at the mentioned angles [13]. As a result, this polymer has a triclinic structure [13,40].

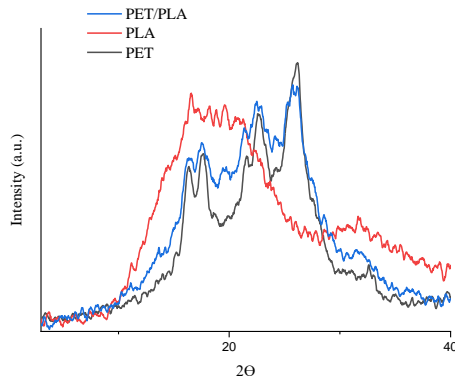


Figure 6. X-ray diffraction pattern of PET, PLA, and PET/PLA films

The diffraction pattern of PLA film is visible with a peak at $2\theta=16.81$ with Miller index corresponding to the (200/110) plane, which is broader and appears almost asymmetric compared to the PET peak [41,42]. Such asymmetric peaks may actually be interpreted as a combination of the symmetric amorphous structure and several scattered peaks from incomplete or very small crystallites.

The crystal structure in the composite film has the triclinic structure of PET, since the five mentioned Bragg angles correspond only to the PET crystal planes. This result indicates that PET crystals are formed separately in PET-rich blends, rather than forming PET/PLA crystallites. It may not be clear whether the peaks of PLA overlap slightly with those of PET, but according to the DSC result (Fig. 5), PLA cannot crystallize in the blend film and the PLA peak corresponding to the (200/1100) planes is absent in the film. Therefore, the crystal structure of PET does not change with the addition of PLA and no additional peaks are observed for the blend film.

In addition, the interpenetration and entanglement of the two types of polymer chains during the crystallization process of the PET/PLA blend reduces the segmental mobility and prevents the formation of crystals of PET and PLA polymer chains [43].

Another factor that may limit the development of the crystal structure in the blends is the formation of block copolymers as a result of ester exchange [34]. Evidence of this reaction is shown in the ^1H NMR of the molten PET/PLA blend in Fig. 3. Transesterification is likely in this study because the extrusion temperature was chosen to be 270°C and the polymer remained in the molten state for more than 5 min.

IV. CONCLUSIONS

PET is a petroleum-based polymer whose hydraulic degradation can take decades. The increasing interest in biodegradable polymers has led to the use of materials such as PLA in various industries in recent years. PET/PLA blend film was prepared using a melt process. PLA particles and PET matrix had good surface adhesion in the PET/PLA blend. This combination had a significant effect on the structure and properties of the blend film in the studied ranges. The experimental results showed that transesterification occurred during the melt compounding process and PET/PLA copolymers were formed. Transesterification reduced the melting point, crystallization temperature and crystallinity of the samples. XRD and DSC results on the film samples showed individual PET crystals instead of co-crystallization and it was found that a small amount of PLA had an inhibitory effect on the crystallinity of PET in the melt process.

REFERENCES

- [1] G. Reiter, J. Xu, S. Körber, K. Moser, J. Diemert (2022) Development of High Temperature Resistant Stereocomplex PLA for Injection Moulding, Mdpi.Com.

- <https://doi.org/10.3390/polym14030384>.
- [2] M. Aldas, C. Pavon, H. De La Rosa-Ramírez, J.M. Ferri, D. Bertomeu, M.D. Samper, J. López-Martínez (2021) The Impact of Biodegradable Plastics in the Properties of Recycled Polyethylene Terephthalate, *J. Polym. Environ.* 2686–2700. <https://doi.org/10.1007/S10924-021-02073-X>.
- [3] A.M. Torres-Huerta, D. Del Angel-López, M.A. Domínguez-Crespo, D. Palma-Ramírez, M.E. Perales-Castro, A. Flores-Vela (2016) Morphological and mechanical properties dependence of PLA amount in PET matrix processed by single-screw extrusion, *Polym. - Plast. Technol. Eng.* 672–683. <https://doi.org/10.1080/03602559.2015.1132433>.
- [4] K. Li, B. Mao, P. Cebe (2014) Electrospun fibers of poly(ethylene terephthalate) blended with poly(lactic acid), *J. Therm. Anal. Calorim.* 1351–1359. <https://doi.org/10.1007/s10973-013-3583-4>.
- [5] S.M.A. Jafari, R. Khajavi, V. Goodarzi, M.R. Kalaei, H.A. Khonakdar, Development of degradable poly(ethylene terephthalate)-based nanocomposites with the aid of polylactic acid and graphenic materials: Thermal, thermo-oxidative and hydrolytic degradation characteristics, *J. Appl. Polym. Sci.* 137 (2020). <https://doi.org/10.1002/app.48466>.
- [6] G. Wang, J. Zhao, G. Wang, H. Zhao, J. Lin (2022), Strong and super thermally insulating in-situ nanofibrillar PLA/PET composite foam fabricated by high-pressure microcellular injection molding, Elsevier. <https://www.sciencedirect.com/science/article/pii/S1385894720305118>
- [7] M. Boruvka, C. Cermak, L. Behalek, P. Brdlik (2021) Effect of in-mold annealing on the properties of asymmetric poly(L-lactide)/poly(D-lactide) blends incorporated with nanohydroxyapatite, *Polymers (Basel)*. 13. <https://doi.org/10.3390/polym13162835>.
- [8] S.W. Lin, Y.Y. Cheng (2010) Miscibility, thermal and mechanical properties of melt-mixed poly(lactic acid)/poly(trimethylene terephthalate) blends, *Polym. - Plast. Technol. Eng.* 1001–1009. <https://doi.org/10.1080/03602559.2010.482078>.
- [9] A.J.R. Lasprilla, G.A.R. Martinez, B.H. Lunelli, A.L. Jardini, R.M. Filho (2012) Poly-lactic acid synthesis for application in biomedical devices - A review, *Biotechnol. Adv.* 321–328. <https://doi.org/10.1016/j.biotechadv.2011.06.019>.
- [10] K. Madhavan Nampoothiri, N.R. Nair, R.P. John (2010) An overview of the recent developments in polylactide (PLA) research, *Bioresour. Technol.* 8493–8501. <https://doi.org/10.1016/j.biortech.2010.05.092>.
- [11] R. Auras, L. Lim, S. Selke, H. Tsuji, (2018) Poly (lactic acid): synthesis, structures, properties, processing, and applications.
- [12] B.Y. Yeom, B. Pourdeyhimi (2011) Web fabrication and characterization of unique winged shaped, area-enhanced fibers via a bicomponent spunbond process, *J. Mater. Sci.* 3252–3257. <https://doi.org/10.1007/s10853-010-5212-y>.
- [13] A.M. Torres-Huerta, D. Palma-Ramírez, M.A. Domínguez-Crespo, D. Del Angel-López, D. De La Fuente (2014) Comparative assessment of miscibility and degradability on PET/PLA and PET/chitosan blends, *Eur. Polym. J.* 285–299.

- <https://doi.org/10.1016/j.eurpolymj.2014.10.016>.
- [14] X.L. Xia, W.T. Liu, X.Y. Tang, X.Y. Shi, L.N. Wang, S.Q. He, C.S. Zhu (2014) Degradation behaviors, thermostability and mechanical properties of poly (ethylene terephthalate)/polylactic acid blends, *J. Cent. South Univ.* 1725–1732. <https://doi.org/10.1007/s11771-014-2116-z>.
- [15] T. Silva, D. Rodrigues, J. Rocha, ... M.G.-B., undefined (2015), Immobilization of trypsin onto poly (ethylene terephthalate)/poly (lactic acid) nonwoven nanofiber. <https://www.sciencedirect.com/science/article/pii/S1369703X15001680> (accessed May 6, 2018).
- [16] G. Wang, J. Zhao, G. Wang, H. Zhao, J. Lin, G. Zhao, C.B. Park (2020) Strong and super thermally insulating in-situ nanofibrillar PLA/PET composite foam fabricated by high-pressure microcellular injection molding, *Chem. Eng. J.* 390. <https://doi.org/10.1016/j.cej.2020.124520>.
- [17] M.P. Belioka, G. Markozanne, K. Chrissopoulou, D.S. Achilias (2023) Advanced Plastic Waste Recycling—The Effect of Clay on the Morphological and Thermal Behavior of Recycled PET/PLA Sustainable Blends, *Polym.* 2023, Vol. 15, Page 3145.3145. <https://doi.org/10.3390/POLYM15143145>.
- [18] M. Kheirandish, M.R. Mohaddes Mojtahedi, H. Nazockdast (2023) Assessing compatibility, transesterification, and disintegration of PET/PLA fiber blend in composting conditions, *Front. Mater.* 1225200. <https://doi.org/10.3389/FMATS.2023.1225200/BIBTEX>.
- [19] A. Anstey, A. Codou, M. Misra, A.K. Mohanty (2018) Novel Compatibilized Nylon-Based Ternary Blends with Polypropylene and Poly(lactic acid): Fractionated Crystallization Phenomena and Mechanical Performance, *ACS Omega*. 2845–2854. <https://doi.org/10.1021/acsomega.7b01569>.
- [20] C. Chandavas, M. Xanthos, K.K. Sirkar, C.G. Gogos (2001) Polypropylene blends with potential as materials for microporous membranes formed by melt processing, *Polymer (Guildf)*. 781–795. [https://doi.org/10.1016/S0032-3861\(01\)00654-1](https://doi.org/10.1016/S0032-3861(01)00654-1).
- [21] C. Rulison (2000) Two-component surface energy characterization as a predictor of wettability and dispersability.
- [22] Polymer Interface and Adhesion by Wu (Author) (2017).
- [23] R. Cardinaud, T. McNally (2013) Localization of MWCNTs in PET/LDPE blends, *Eur. Polym. J.* 1287–1297. <https://doi.org/10.1016/j.eurpolymj.2013.01.007>.
- [24] M. Nofar, R. Salehiyan, U. Ciftci, A. Jalali, A. Durmuş (2020) Ductility improvements of PLA-based binary and ternary blends with controlled morphology using PBAT, PBSA, and nanoclay, *Compos. Part B Eng.* 182 <https://doi.org/10.1016/j.compositesb.2019.107661>.
- [25] S. Wu, *Polymer interface and adhesion*, CRC Press, (2017). <https://doi.org/10.1201/9780203742860>.
- [26] M.R. Snowden, A.K. Mohanty, M. Misra (2017) (Miscibility and Performance Evaluation of Biocomposites Made from Polypropylene/Poly(lactic acid)/Poly(hydroxybutyrate-cohydroxyvalerate) with a Sustainable

- Biocarbon Filler, ACS Omega. 6446–6454.
<https://doi.org/10.1021/acsomega.7b00983>.
- [27] M. Mehrabi Mazidi, M.K. Razavi Aghjeh (2015) Effects of blend composition and compatibilization on the melt rheology and phase morphology of binary and ternary PP/PA6/EPDM blends, Polym. Bull. 1975–2000. <https://doi.org/10.1007/s00289-015-1384-6>.
- [28] M. Serhan, M. Sprowls, D. Jackemeyer, M. Long, I.D. Perez, W. Maret, N. Tao, E. Forzani (2019) Total iron measurement in human serum with a smartphone, AIChE Annu. Meet. Conf. Proc. <https://doi.org/10.1039/x0xx00000x>.
- [29] R. Auras, B. Harte, S. Selke (2006) Sorption of ethyl acetate and d-limonene in poly(lactide) polymers, J. Sci. Food Agric. 648–656. <https://doi.org/10.1002/jsfa.2391>.
- [30] A.R. McLauchlin, O.R. Ghita (2016) Studies on the thermal and mechanical behavior of PLA-PET blends, J. Appl. Polym. Sci. <https://doi.org/10.1002/app.44147>.
- [31] M. Djebara, J.P. Stoquert, M. Abdesselam, D. Muller, A.C. Chami (2012) FTIR analysis of polyethylene terephthalate irradiated by MeV He +, Nucl. Instruments Methods Phys. Res. Sect. B Beam Interact. with Mater. Atoms. 70–77. <https://doi.org/10.1016/j.nimb.2011.11.022>.
- [32] Y.X. Weng, Y.J. Jin, Q.Y. Meng, L. Wang, M. Zhang, Y.Z. Wang (2013) Biodegradation behavior of poly(butylene adipate-co-terephthalate) (PBAT), poly(lactic acid) (PLA), and their blend under soil conditions, Polym. Test. 32 918–926. <https://doi.org/10.1016/j.polymertesting.2013.05.001>.
- [33] A.M. Kenwright, S.K. Peace, R.W. Richards, A. Bunn, W.A. MacDonald (1999) End group modification in poly(ethylene terephthalate). [https://doi.org/10.1016/S0032-3861\(98\)00433-9](https://doi.org/10.1016/S0032-3861(98)00433-9).
- [34] G. Wu, J.A. Cuculo (1999) Structure and property studies of poly(ethylene terephthalate)/poly(ethylene-2,6-naphthalate) melt-blended fibres. [https://doi.org/10.1016/s0032-3861\(98\)00317-6](https://doi.org/10.1016/s0032-3861(98)00317-6).
- [35] R.S. Porter, L.H. Wang (1992) Compatibility and transesterification in binary polymer blends, Polymer (Guildf). 2019–2030. [https://doi.org/10.1016/0032-3861\(92\)90866-U](https://doi.org/10.1016/0032-3861(92)90866-U).
- [36] S.W. Lin, Y.Y. Cheng (2010) Miscibility, thermal and mechanical properties of melt-mixed poly(lactic acid)/poly(trimethylene terephthalate) blends, Polym. - Plast. Technol. Eng. 1001–1009. <https://doi.org/10.1080/03602559.2010.482078>.
- [37] B.M. Lekube, C. Burgstaller (2022) Study of mechanical and rheological properties, morphology, and miscibility in polylactid acid blends with thermoplastic polymers, J. Appl. Polym. Sci. <https://doi.org/10.1002/app.51662>.
- [38] X.L. Xia, W.T. Liu, X.Y. Tang, X.Y. Shi, L.N. Wang, S.Q. He, C.S. Zhu (2014) Degradation behaviors, thermostability and mechanical properties of poly(ethylene terephthalate)/polylactic acid blends, J. Cent. South Univ. 1725–1732. <https://doi.org/10.1007/s11771-014-2116-z>.
- [39] I. Acar, A. Durmuş, S. Özgümüş (2007) Nonisothermal crystallization kinetics and morphology of polyethylene terephthalate modified with polydactic acid, J. Appl. Polym. Sci. 4180–4191. <https://doi.org/10.1002/app.26982>.

- [40] L.A. Baldenegro-Perez, D. Navarro-Rodriguez, F.J. Medellin-Rodriguez, B. Hsiao, C.A. Avila-Orta, I. Sics (2014) Molecular weight and crystallization temperature effects on poly(ethylene terephthalate) (PET) homopolymers, an isothermal crystallization analysis, *Polymers* (Basel). 583–600.
<https://doi.org/10.3390/polym6020583>.
- [41] M.A. Abdelwahab, A. Flynn, B. Sen Chiou, S. Imam, W. Orts, E. Chiellini (2012) Thermal, mechanical and morphological characterization of plasticized PLA-PHB blends, *Polym. Degrad. Stab.* 1822–1828.
<https://doi.org/10.1016/j.polymdegradstab.2012.05.036>.
- [42] Y. Wang, H. Zhang, M. Li, W. Cao, C. Liu, C. Shen (2015) Orientation and structural development of semicrystalline poly(lactic acid) under uniaxial drawing assessed by infrared spectroscopy and X-ray diffraction, *Polym. Test.* 163–171.
<https://doi.org/10.1016/j.polymertesting.2014.11.010>.
- [43] H. Liang, F. Xie, F. Guo, B. Chen, F. Luo, Z. (2008) Jin, Non-isothermal crystallization behavior of poly(ethylene terephthalate)/poly(trimethylene terephthalate) blends, *Polym. Bull.* 115–127.
<https://doi.org/10.1007/s00289-007-0832-3>.



Recycled fiber composites enabling the circular textiles economy loop

Hasabo Abdelbagi Mohamed Ahmed^{a,b,*}, Nevin Çiğdem Gursoy, Pelin Altay^c

^a Sudan University of science and Technology, Khartoum Sudan.

^c Istanbul Technical University, Textile Technology and Design, Istanbul, Türkiye.

*Corresponding author: profhasabo@gmail.com

ABSTRACT

Textile and fashion waste has become a global issue. There are two types of such waste: waste produced during the production and processing of textiles and fashion, such as production waste and excess industrial or pre-consumption waste. The other type occurs at the end-of-life stage of products and is referred to as post-consumer waste. Pre-consumer textile waste is more easily recyclable since it is of known composition and origin, whereas post-consumer textile and fashion waste consists of various mixed materials that need to be sorted for further regeneration. Valuable resources held within this mixed waste stream are often lost. Considering that approximately 50% of reclaimed clothing is suitable for re-wear, the remaining portion could be recycled. The recyclable fraction can enter a new industrial process, initiating a new manufacturing cycle and, consequently, a new product life cycle. In general, textile and clothing recycling reduces environmental impact when compared to incineration and landfilling. This study examines various approaches to identify appropriate technologies that could guide product manufacturing towards the development of valuable products, while considering recyclable materials as a viable and effective alternative. Composite materials are among the technologies used for waste recovery, transforming textile waste into secondary raw materials, thus promoting circularity and reducing environmental impact. Studies have demonstrated that various types of textile and clothing waste can be utilized in composite solutions. The use of such reinforcements has emerged as a significant research focus in recent years. This study aims to investigate composite solutions that incorporate recycled textile waste, thereby contributing to the circular textile and fashion economy.

Keywords: Composites; Textiles; circular economy; Recycled fiber; environment

I. INTRODUCTION

Globally, more than 2 billion tons of municipal solid waste (MSW) are generated each year. It is projected that by 2025, approximately 3.5 billion tons of global waste will be produced [1-3]. The global direct cost of waste management is estimated at USD 252 billion. When accounting for the hidden costs of

pollution, poor health, and climate change resulting from inadequate waste disposal practices, the total cost increases to USD 361 billion. Approximately 16 million tons of textile waste are discarded annually, most of which ends up in landfills, while only a small fraction is recycled. The textile recycling market was valued at USD 6.9 billion in 2022 and is expected to reach USD 9.4 billion by 2027, growing at a

compound annual growth rate (CAGR) of 6.4%. Istanbul as a mega city generates over 19,000 tonnes of municipal waste daily. The textiles and plastic waste in Istanbul amounts to 17%. Waste recycling and reuse, composting, incineration, landfilling, and biogas production technologies have been explored by the Istanbul Metropolitan Municipality. Almost all types of plastic, glass, paper, and metals from MSW can be recycled profitably in Istanbul, particularly in industrial zones due to the large volumes and high economic value of materials in these areas. There is an strategy in Turkey towards transition of textile and fashion industry from linear economy to circular economy, see Fig. 1 [4, 5].

Textiles represent the fourth highest pressure category in terms of primary raw material consumption, with the cost of input materials reaching up to 66% of the product value. Every year, more than 100–150 billion pieces of garments are produced, consuming 93 billion cubic meters of water, yielding 1.2 billion tons of CO₂ as atmospheric emission, and 500 thousand tons of micro-plastic fibers dumped into oceans [6]. If we consider critical situation of the water footprint in denim manufacturing, the global average is approximately 1,500 liters for a single pair of jeans. The textile and fashion industry ranks fifth in terms of global greenhouse gas (GHG) emissions, following the food, housing, and transport sectors [7]. It is estimated that less than 1% of all textiles globally are recycled into new textile products. To align the textile and fashion industries with the principles of the circular economy and to reduce their environmental footprint, several strategic measures must be adopted. These include: developing eco-design strategies to ensure textile products are suitable for circularity; promoting the use of secondary raw materials; addressing the issue of hazardous chemicals; and empowering businesses and consumers to make sustainable choices and access reuse and repair services more easily.

Moreover, efforts should be directed toward enhancing textile sorting, reuse, and recycling through technological innovation and supportive policy instruments, such as extended producer responsibility (EPR) schemes [8].

A critical social consideration in this context is the role of poverty alleviation, particularly for vulnerable communities involved in recycling activities. It is estimated that 20 to 35 jobs can be created for every 1,000 tonnes of textiles collected for reuse, making the textile sector the most labor-intensive recycling industry [9].

II. TEXTILE & FASHION SECTOR IN TURKIYE

The Turkish textile and fashion sector accounts for approximately 4.8% of the country's Gross Domestic Product (GDP) and provides employment to around one million people. As previously mentioned, the sector is characterized by a high level of raw material consumption, which highlights the urgent need to generate added value—a challenge for which the circular textile economy offers a promising solution [10].

Major strengths of Turkish textile and fashion Sector, which are critical for circular textile transformation, can be summarized as below:

Industrial Experience and Geographical Advantage:

- Türkiye ranks as the seventh-largest textile exporter globally, with exports valued at USD 9.8 billion, representing a 3% share of the global market. In the clothing sector, Turkey is recognized as one of the leading manufacturing countries. Both the textile and fashion industries make significant positive contributions to the national foreign trade balance.

- Türkiye's strategic geographical location places it within a 3,000-kilometer radius of major European markets, offering a logistical advantage for international trade and export activities.

Diverse and Flexible Manufacturing:

- Türkiye possesses a robust manufacturing capability, supported by a well-developed infrastructure, reliable energy supply, technologically advanced machinery, a highly skilled labor force, and established intermediate goods industries.
- Vertical integration at the national level allows for end-to-end production from fiber to fabric to finished garments within three major production clusters, which is particularly advantageous for the implementation of a circular textile economy.
- Close collaborations with major European brands and manufacturers have fostered a strong fashion orientation in Türkiye, aligned with European Union market demands and quality expectations.
- The country's existing R&D and production capacity, although currently oriented towards fast fashion, demonstrates sufficient flexibility to enable on-demand and sustainable production models.
- Türkiye also has established recycling expertise, with operational recycling facilities for fiber production, alongside demonstrated socio-economic contributions and adherence to fair labor practices.
- From a social perspective, the Turkish textile and fashion sector plays a significant role in national employment, representing the highest employment share within the manufacturing industry. The sector employs approximately one million individuals, accounting for 7% of all registered employees in the national social security system and 65% of registered

employment in manufacturing, with 41% of the workforce comprising women compared to the national female employment rate of 31%. Efforts to expand textile and fashion trade are positively influencing social development indicators, thereby contributing to responsible consumption and production patterns.

- The presence of social welfare standards and strict compliance mechanisms further strengthens the positioning of Türkiye's textile and fashion sector, particularly in terms of ethical labor and sustainability practices.

Entrepreneurial Leadership

- Turkish textile and fashion sector is characterized by a strong entrepreneurial spirit,, which is critical for such an investment-intense industry. For circular textile transitioning, this leadership and commitment can be very influential; bringing in the speed and flexibility needed for the success.
- These leaders also have strong ties within Europe and with Turkish Government, which is important when setting up new structures and market definitions around circular textile [5].

Given these strengths, the transition of Türkiye's textile and fashion sector from a linear to a circular economy model has increasingly attracted the attention of researchers, particularly in the area of innovative waste utilization see Fig. 1. This includes the valorization of both industrial and municipal garment and textile waste. The present study focuses on the conversion of various types of textile waste into fiber form through mechanical processes such as tearing and garneting, enabling their use as reinforcement materials in composite applications [5–7]. Furthermore, recycled textiles have been hybridized with different types of plastic waste to

improve specific properties, or used in the form of laminates [8].



Figure 1.a Linear Economy

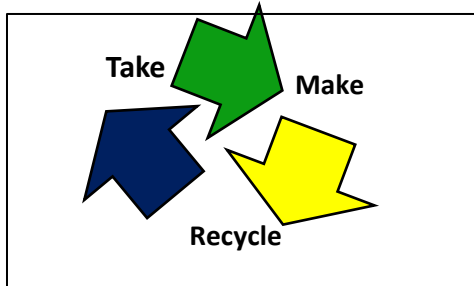


Figure 1.b- circular economy

III. Recycled fiber composite

3.1 Composite definition

The word “composite” refers to a material consisting of two or more distinct components. Thus, a material composed of two or more clearly identifiable constituent materials or phases may be considered a composite material. The reinforcement and the matrix represent the two primary phases of a composite material. However, we recognize materials as composites only when the constituent phases do not dissolve into one another and possess significantly different physical properties, resulting in composite properties that are distinctly different from those of the individual constituents see Fig. 2.

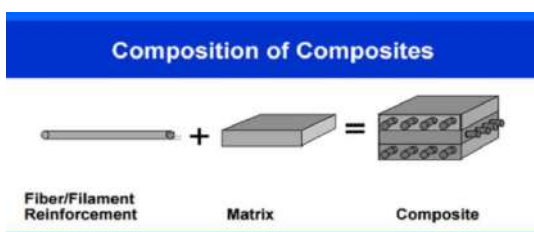


Fig.2. Composite composition [11]

A material is considered as the composite material when:

- The combination of materials should result in significant changes in properties.

- The content of the constituents is generally greater than 10%.

- In general, the property of one constituent is much greater (≥ 5 times) than that of the other constituent.

- One constituent is called the reinforcing phase, and the other, in which it is embedded, is called the matrix. The reinforcing phase material may be in the form of fibers, particles, or flakes, while the matrix phase is generally continuous.

- Reinforcement can be in the form of fibers, fabric particles, or whiskers. These reinforcements are primarily used to enhance the mechanical properties of a composite.

The main purpose of the reinforcement is to: Provide superior levels of strength and stiffness to the composite [12, 13]. See Figures 2, 3 and 4.

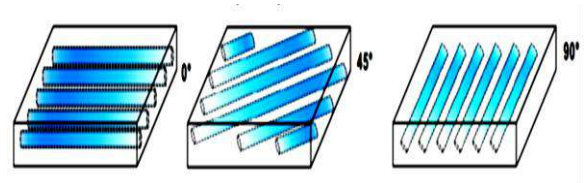


Fig. 3 Continuous fiber composite plies with different orientation, a zero , 45°, and 90°[14]

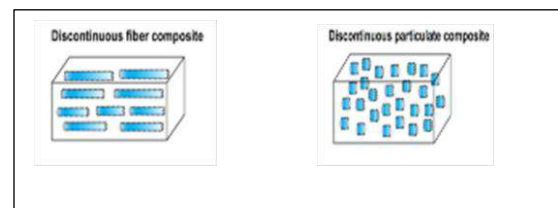


Figure 4. Discontinuous fibers and particles [15]

3.2 Reinforcing Materials

Composites can be classified according to their matrices. The most widely used form of reinforcement in high-performance composites is fiber tows, which are untwisted bundles of continuous filaments.

Fiber monofilaments are used in polymer matrix composites (PMCs), metal matrix

composites (MMCs), and ceramic matrix composites (CMCs); they consist of a single fiber with a diameter greater than or equal to 100 μm .

In MMCs, particulates and chopped fibers are the most commonly used reinforcement morphology, and these are also applied in PMCs.

Whiskers and platelets are used to a lesser degree in both PMCs and MMCs.

3.3 The matrix material

The matrix material is the homogeneous and monolithic material in which a reinforcement system of a composite is embedded and is completely continuous.

The main purpose of the matrix is to bind the reinforcements together by virtue of its cohesive and adhesive characteristics [16-19].

3.4 Recycled denim fiber composite

Denim fabric, characterized by its woven structure and high tensile strength, has been effectively utilized in composites. Its reinforcement capabilities stem from its cotton-based composition, which provides strong interlocking with polymer matrices. Studies have demonstrated that denim-reinforced composites exhibit enhanced stiffness, tensile strength, and impact resistance. For instance, Hassani et al. examined phenolic resin-bonded recycled denim as an alternative sound absorber. Nonwoven composites with varying bulk

densities (61–102 kg/m^3) and resin contents (10%–35%) were produced and tested using the impedance tube method. Results showed that sound absorption increases with bulk density and resin content, performing well at high frequencies. Compared to commercial glass wool, the composites demonstrated competitive noise control properties, making them an eco-friendly and cost-effective alternative [20-22].

Lee et al.[23] investigated denim fabric as reinforcement for PLA composites using a hand layup method. The authors noted that increasing denim layers enhanced impact strength, tensile strength, and thermal properties, with the best results observed in three-layer composites (82 J/m impact strength, 75.76 MPa tensile strength, and 4.65 GPa tensile modulus). Numerical modeling confirmed the elastic modulus improvements. PLA/denim composites demonstrated potential as eco-friendly alternatives to glass or carbon fiber composites.

Wei et al. [24] investigated discarded denim fabric as reinforcement for polypropylene (PP) composites. Using hand layup and hot pressing, composites with varying fiber weight fractions were fabricated. The 84 wt% denim-reinforced composite showed superior tensile (57 MPa) and impact

strength (5.1 J/mm) compared to ramie/PP and flax/PP composites. Flame-retardant modifications improved the limiting oxygen index to 28.7%. These composites demonstrated excellent mechanical and fire-resistant properties, making them suitable for automotive, packaging, and engineering applications.

Furthermore, using denim fibers reduces the reliance on virgin materials while leveraging the mechanical integrity of post-consumer textiles. Research on natural fiber-reinforced composites has consistently highlighted the value of woven fabrics for structural applications due to their ability to evenly distribute loads across the matrix. Todor et al.[25] explored recycling textile waste into composite materials to reduce environmental impact and production costs. While pre-consumer waste was easier to recycle, post-consumer textiles required separation and regeneration. Recycling textiles reduced landfill waste and enabled circular material use. The authors noted that recycled textile waste can serve as effective reinforcement in composite solutions, making it a growing area of interest.

The integration of recycled HDPE and denim fibers into composite materials addresses two critical environmental issues: plastic and textile waste management. Additionally, incorporating MAPP as a

coupling agent enhances fiber–matrix bonding, improving the mechanical performance of the composite [26]. However, the challenge lies in understanding how the addition of natural fibers, such as denim, affects both the mechanical and thermal properties of the composite.

The motivation behind this research stems from the need to develop sustainable materials that offer both environmental and mechanical benefits. By combining recycled HDPE with denim fibers, the goal is to create a composite material with enhanced strength, stiffness, and durability. The use of MAPP as a coupling agent is intended to address the compatibility issues between the hydrophobic HDPE matrix and the hydrophilic denim fibers, ensuring effective fiber–matrix interaction. The successful development of such a composite could provide a model for other recycled materials, offering a pathway towards a circular economy. The use of recycled materials in composites has gained increasing attention over the past decade. Studies have demonstrated the potential of recycled HDPE in composite applications, [27] particularly when reinforced with natural fibers. For instance, research by Lei et al [28], shows that recycled HDPE composites reinforced with natural fibers, such as wood and bagasse fillers, exhibit

improved mechanical properties such as impact strength.

Despite these advancements, the specific use of recycled denim fibers in HDPE composites has not been explored. Most studies on natural fiber reinforcement focus on agricultural fibers like hemp, flax, jute, wood, and bagasse. Denim, being a textile fiber with a different structural composition, presents unique challenges and opportunities. Research indicates that textile fibers, including those from waste garments, can contribute to enhanced tensile properties and thermal insulation in composite materials [29]. However, there is limited understanding of how denim fibers, in particular, interact with polymer matrices like HDPE and how they affect the overall mechanical and thermal properties.

3.5 Recycled Reinforcing Fibers (FRC)

Many studies have focused on using recycled reinforcing fibers from recycled plastics, end-of-life-tires and construction waste. Recycling the waste to produce new materials, like concrete or mortar, has been raised as one of the best solutions, due to economic and ecological advantages as well as energy saving in their disposal. Therefore, the interest of using recycled fibers (mainly steel and polymeric fibers) in FRC is

increasing, as shown in recent reviews [30-33].

IV. CONCLUSIONS

The increasing urgency of addressing textile and fashion waste on a global scale has propelled the development of innovative strategies aligned with circular economy principles. This study has examined the potential of recycled textile waste particularly post-consumer and pre-consumer materials as valuable raw inputs in the production of composite materials. The Turkish textile and fashion sector, with its strong industrial foundation, geographical advantage, and entrepreneurial leadership, presents a unique opportunity to lead this transformation. Türkiye's integrated supply chains, established recycling infrastructure, and significant employment contributions position it as a promising case for sustainable textile circularity.

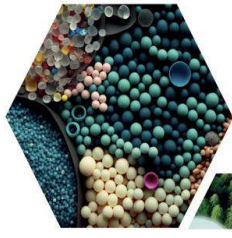
In conclusion, this study underscores the viability of recycled textile waste particularly denim as a reinforcement material in composite applications. It advocates for the continued advancement of textile recycling technologies, the adoption of eco-design strategies, and stronger policy support. The pursuit of circularity in textiles not only mitigates environmental impact but also unlocks socio-economic opportunities, positioning the composite sector as a

catalyst for sustainable transformation in the textile and fashion industries.

REFERENCES

- [1] A. Yattoo, B. Hamid, T. Sheikh, S. Ali, S. Bhat, S. Ramola, M. Ali, Z. Baba, and S. Kumar, "Global perspective of municipal solid waste and landfill leachate: generation, composition, eco-toxicity, and sustainable management strategies," *Environmental Science and Pollution Research*, vol. 31, pp. 1-30, 2024.
- [2] A. UNEP, "Global Waste Management Outlook 2024" 28 February 2024 28 February 2024
- [3] W. Bank., "Trends in Solid Waste Management," USA2024.
- [4] M. DENİZER, "TURKISH TEXTILE INDUSTRY, CIRCULAR ECONOMY AND DEDICATION TO SUSTAINABILITY," Brussels, MUSTAFA DENİZER BOARD MEMBER OF ITHIBMay 2022.
- [5] R. Netherlands Enterprise Agency, "DEFINING CIRCULARITY OF TEXTILE INDUSTRY IN TURKEY," Turkey, AnkaraApril 2021.
- [6] M. Shamsuzzaman, M. Islam, M. A. A. Mamun, R. Rayyaan, K. Sowrov, S. Islam, and A. S. M. Sayem, "Fashion and textile waste management in the circular economy: A systematic review," *Cleaner Waste Systems*, vol. 11, p. 100268, 2025/06/01/ 2025.
- [7] A. K. Das, M. F. Hossain, B. U. Khan, M. M. Rahman, M. A. Z. Asad, and M. Akter, "Circular economy: A sustainable model for waste reduction and wealth creation in the textile supply chain," *SPE Polymers*, vol. 6, p. e10171, 2025.
- [8] Ellen MacArthur Foundation, "Pushing the boundaries of EPR policy for textiles," (2024).
- [9] J. Gutberlet, "Waste, poverty and recycling," *Waste management (New York, N.Y.)*, vol. 30, pp. 171-3, 2010.
- [10] I. N. Ruja, " Programs, Opportunities, and Challenges in Poverty Reduction:," *A Systematic Review. SAGE Open.*, (2024).
- [11] O. Ahmed, A. Aabid, J. s. Ali, M. Hrairi, and N. Yatim, "Progresses and Challenges of Composite Laminates in Thin-Walled Structures: A Systematic Review," *ACS Omega*, vol. 8, p. 14, 2023.
- [12] M. BİNGÖL and K. Cavdar, "Effects of Different Reinforcements for Improving Mechanical Properties of Composite Materials," *Uludağ University Journal of The Faculty of Engineering*, vol. 21, p. 123, 2016.
- [13] D. Rajak, D. Pagar, R. Kumar, and C. Pruncu, "Recent progress of reinforcement materials: A comprehensive overview of composite materials," *Journal of Materials Research and Technology*, vol. 8, 2019.
- [14] K. S. Ravi Chandran, "Review: Fatigue of Fiber-Reinforced Composites, Damage and Failure," *Journal of the Indian Institute of Science*, vol. 102, pp. 439-460, 2022/01/01 2022.
- [15] D. K. Rajak, D. D. Pagar, R. Kumar, and C. I. Pruncu, "Recent progress of reinforcement materials: a comprehensive overview of composite materials," *Journal of Materials Research and Technology*, vol. 8, pp. 6354-6374, 2019/11/01/ 2019.
- [16] M. Such, C. Ward, and K. Potter, "Aligned discontinuous fibre composites: a short history," *J. Multifunct. Compos*, vol. 2, pp. 155-168, 2014.
- [17] N. van de Werken, M. S. Reese, M. R. Taha, and M. Tehrani, "Investigating the effects of fiber surface treatment and alignment on mechanical properties of recycled carbon fiber composites," *Composites Part A: Applied Science and Manufacturing*, vol. 119, pp. 38-47, 2019/04/01/ 2019.
- [18] T. Adam, R. Dickson, C. Jones, H. Reiter, and B. Harris, "A power law fatigue damage model for fibre-reinforced plastic laminates," *Proceedings of the Institution of Mechanical Engineers, Part C: Journal of Mechanical Engineering Science*, vol. 200, pp. 155-166, 1986.
- [19] P. Curtis, "The fatigue behaviour of fibrous composite materials," *The Journal of Strain Analysis for Engineering Design*, vol. 24, pp. 235-244, 1989.

- [20] P. Hassani, P. Soltani, M. Ghane, and M. Zarrebini, "Porous resin-bonded recycled denim composite as an efficient sound-absorbing material," *Applied Acoustics*, vol. 173, p. 107710, 2021.
- [21] G. Fernando, R. Dickson, T. Adam, H. Reiter, and B. Harris, "Fatigue behaviour of hybrid composites: Part 1 Carbon/Kevlar hybrids," *Journal of Materials Science*, vol. 23, pp. 3732-3743, 1988.
- [22] E. Akca and A. Gursel, "A review on the matrix toughness of thermoplastic materials," *Periodicals of engineering and natural sciences*, vol. 3, pp. 1-8, 2015.
- [23] J. T. Lee, M. W. Kim, Y. S. Song, T. J. Kang, and J. R. Youn, "Mechanical properties of denim fabric reinforced poly (lactic acid)," *Fibers and Polymers*, vol. 11, pp. 60-66, 2010.
- [24] B. Wei, F. Xu, S. W. Azhar, W. Li, L. Lou, W. Liu, and Y. Qiu, "Fabrication and property of discarded denim fabric/polypropylene composites," *Journal of Industrial Textiles*, vol. 44, pp. 798-812, 2015.
- [25] M. Todor, M. Rackov, I. Kiss, and V. Cioata, "Composite solutions with recycled textile wastes," in *Journal of Physics: Conference Series*, 2022, p. 012030.
- [26] M. Suffo, M. Brey, J. Orellana, and J. García-Morales, "Feasibility of utilization of recycled HDPE in manhole covers for urban traffic areas and industrial zones," *Journal of Cleaner Production*, vol. 425, p. 138818, 2023.
- [27] A. Ghasemkhani, G. Pircheraghi, and M. Shojaei, "An innovative polymer composite prepared through the recycling of spent lead-acid battery separators," *SUSTAINABLE MATERIALS AND TECHNOLOGIES*, vol. 38, DEC 2023.
- [28] Y. Lei, Q. Wu, F. Yao, and Y. Xu, "Preparation and properties of recycled HDPE/natural fiber composites," *Composites Part A: Applied Science and Manufacturing*, vol. 38, pp. 1664-1674, 2007.
- [29] P. Vera, E. Canellas, and C. Nerín, "Designing safe recycled high-density polyethylene (HDPE) for child toys," *J Hazard Mater*, vol. 478, p. 10, 2024.
- [30] S. Marinković, J. Dragaš, I. Ignjatović, and N. Tošić, "Environmental assessment of green concretes for structural use," *Journal of Cleaner Production*, vol. 154, pp. 633-649, 2017.
- [31] D. R. Vieira, J. L. Calmon, and F. Z. Coelho, "Life cycle assessment (LCA) applied to the manufacturing of common and ecological concrete: A review," *Construction and Building Materials*, vol. 124, pp. 656-666, 2016.
- [32] A. Caggiano, P. Folino, C. Lima, E. Martinelli, and M. Pepe, "On the mechanical response of hybrid fiber reinforced concrete with recycled and industrial steel fibers," *Construction and Building Materials*, vol. 147, pp. 286-295, 2017.
- [33] P. Asokan, M. Osmani, and A. D. Price, "Improvement of the mechanical properties of glass fibre reinforced plastic waste powder filled concrete," *Construction and Building Materials*, vol. 24, pp. 448-460, 2010.



16 ULUSLARARASI
LİF VE POLİMER
ARAŞTIRMALARI
SEMPOZYUMU

16th INTERNATIONAL FIBER AND POLYMER RESEARCH SYMPOSIUM

Sürdürülebilir ve İşlevsel Lif ve Polimerler
Sustainable and Functional Fibers & Polymers



9-10 Mayıs
May 2025

İstanbul Teknik Üniversitesi
Gümüşsuyu Prof. Dr. Necmettin Erbakan Yerleşkesi
İstanbul Technical University
Gumussuyu Prof. Dr. Necmettin Erbakan Campus



LOI Prediction of Flame-Retardant Polypropylene Composites Using XGBoost

Uğur Özveren*, Dicle Eren

Department of Chemical Engineering, Marmara University, Istanbul, Turkey.

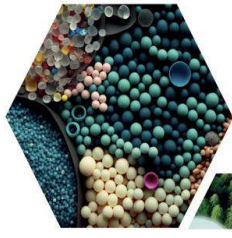
**Corresponding author: ugur.ozveren@marmara.edu.tr*

ABSTRACT

In order to optimize the formulation of flame-retardant polypropylene (PP) composites, the LOI (Limiting Oxygen Index) value must be estimated accurately and interpretably. However, the LOI value is quite difficult to predict using conventional methods due to the complex and non-linear interactions between the additives used. This difficulty is particularly evident in systems where halogenated, phosphorus-nitrogen and metal hydroxide additives are used together. Therefore, a modelling approach is needed that can provide meaningful results in terms of both accuracy and interpretability.

In this study, the Extreme Gradient Boosting (XGBoost) algorithm was used for LOI estimation from an experimental dataset where only six common additives (wt% ratios: AO 1010, DBDPE, Sb₂O₃, ZHS/ZS, Mg(OH)₂ and DOPO) were used. Machine learning was preferred because it offers higher predictive power compared to traditional regression methods in such multivariate, non-linear systems. XGBoost stands out because it offers both high accuracy and allows the interpretation of the effects of variables thanks to its decision tree-based structure. The ideal XGBoost model (300 trees, $\eta = 0.05$, maximum depth = 8) obtained because of Bayesian hyperparameter optimization achieved high prediction accuracy with 10-fold shuffle-split cross-validation.

Keywords: Limiting Oxygen Index (LOI); Flame-Retardant Composites; Machine Learning; XGBoost



16 ULUSLARARASI
LİF VE POLİMER
ARAŞTIRMALARI
SEMPOZYUMU

16th INTERNATIONAL FIBER AND POLYMER RESEARCH SYMPOSIUM

Sürdürülebilir ve İşlevsel Lif ve Polimerler
Sustainable and Functional Fibers & Polymers



9-10 Mayıs
May 2025

İstanbul Teknik Üniversitesi
Gümüşsuyu Prof. Dr. Necmettin Erbakan Yerleşkesi
İstanbul Technical University
Gumussuyu Prof. Dr. Necmettin Erbakan Campus

Polymeric Superplasticizer Driven Concrete Strength Forecasting Using Ensemble Random Forests

Uğur Özveren*, Dicle Eren

Department of Chemical Engineering, Marmara University, Istanbul, Turkey.

**Corresponding author: ugur.ozveren@marmara.edu.tr*

ABSTRACT

This study investigated the prediction of compressive strength of concrete using a machine learning approach using a dataset of 1030 high-performance concrete mixtures compiled from different experimental studies reported in the literature. Eight input variables (cement, fly ash, blast furnace slag, water, polymeric superplasticizer, coarse aggregate and fine aggregate amounts and concrete age) were used to predict compressive strength of concrete. The polymeric material in the concrete is an anionic polyelectrolyte consisting of sulfonated naphthalene-formaldehyde and fatty acid copolymer; the high surface charge density and bulky side chains of this polymer create electrostatic repulsion and steric hindrance between cement grains, maintaining fluidity even at very low water/binder ratios and thus increasing compressive strength.

In this study, the Random Forest algorithm was preferred as a machine learning approach, which is low sensitivity to the noise content of the input parameters, successful in capturing multivariate nonlinear relationships and able to quantitatively present the importance of variables. The correlation constant R^2 value was calculated as high as 0.95 and the obtained results surpassed the complex and advanced modelling techniques developed with this data set in the literature. In addition, the variable importance analysis revealed the significant effect of polymeric admixture on the strength of concrete. The results show that it allows the quantitative and explanatory evaluation of the contribution of polymeric chemical admixtures to structural performance.

Keywords: Polymeric Superplasticizer; Random Forest; High-performance Concrete; Machine Learning

16th International Fiber and Polymer Research Symposium (16th ULPAS)
9-10 May, 2025, Istanbul technical University (ITU), Istanbul, Türkiye



The Impact of Pigment Dyeing and Pigment Washing on the Mechanical Properties of 3D Knitted Fabrics

Arda DEVECİ¹

^aArGe Merkezi, Almaxtex Tekstil Sanayi ve Ticaret A.Ş.(Yeşim Grup), 16300 Bursa, Türkiye.

*Sorumlu Yazar: arda.deveci@yesim.com

ABSTRACT

Recent technological advancements and evolving consumer expectations have led to significant innovations in the textile industry, particularly in the development of three-dimensional (3D) fabrics. Among these, waffle knit fabrics stand out for their bulkiness, elasticity, comfort, and aesthetic appeal. While such structures can be produced by both weaving and knitting, circular knitting offers additional advantages, including better flexibility and a luxurious hand feel. However, finishing processes such as dyeing and washing may negatively affect key properties of these fabrics, including surface appearance, elasticity, and bursting strength.

This study investigates the impact of pigment dyeing and washing processes on the mechanical properties of waffle knit fabrics. The fabric's flexibility, recovery ability, and dimensional stability (shrinkage in width, length, and skewing) were evaluated before and after processing. Furthermore, the unique loop piling effect created by the tuck cam mechanism in circular knitting machines, which gives the fabric its 3D form, was analyzed for its structural contribution. The findings aim to support the potential of waffle fabrics in advanced textile applications and suggest alternative finishing methods that preserve their advantageous properties.

Keywords: Three-Dimensional Structure, Mechanical Properties, Pigment Dyeing, Waffle Knit Fabric, Pigment Wash

ÖZET

Gelişen teknoloji ve değişen tüketici beklentileri, tekstil sektöründe özellikle üç boyutlu (3D) kumaşların geliştirilmesiyle önemli yenilikleri beraberinde getirmiştir. Bu yapılar arasında yer alan waffle örme kumaşlar, kabarıklığı, esnekliği, konforu ve estetik görünümüyle dikkat çeker. Dokuma ve örme yöntemleriyle üretilen bu kumaşlar, yuvarlak örme makinelerinde esneklik ve yumuşak tutum açısından avantaj sağlar. Ancak, boya ve yıkama gibi bitim işlemleri, kumaşın yüzey görünümü, esneklik ve patlama mukavemeti gibi önemli özelliklerini olumsuz etkileyebilir.

Bu çalışmada, waffle örme kumaşın pigment boyama ve yıkama işlemleri sonrası mekanik özellikleri incelenmiştir. İşlem öncesi ve sonrası esneklik, geri toplama yeteneği ve en-boy çekme gibi boyutsal stabilite değerleri karşılaştırılmıştır. Ayrıca, yuvarlak örme makinelerinde askı çeliği mekanizmasıyla oluşturulan ilmek yığılmalarının 3D yapıya katkısı değerlendirilmiştir. Elde edilen bulgular, waffle kumaşların ileri tekstil uygulamalarındaki potansiyelini desteklemekte ve avantajlı özelliklerini koruyacak alternatif bitim yöntemleri önermektedir.

Keywords: 3 - boyutlu yapı, mekanik özellikler, pigment boyama, waffle örme kumaş, pigment yıkama

I. INTRODUCTION

Advancements in technology, the growing awareness of consumers, and the steady increase in global consumption have prompted industries across the world to develop an inherent reflex to continuously renew and improve themselves. As in many other industries, the textile sector is expected to respond rapidly to ongoing advancements and technological developments have significantly facilitated this process. One of the most valuable contributions of emerging technologies to the textile industry is the development of fabrics with three-dimensional structures [1]. Although such fabrics can also be produced using weaving techniques, their adaptation to circular knitting machines is driven by specific advantages [2]. These include the visually appealing nature of bulky fabrics, elasticity and comfort compared to woven fabrics, and a soft hand feel that enhances the desirability.

Fabrics knitted on circular knitting machines have a self-acquired recovery feature. Since visibility is at the forefront in 3D fabrics, these advantages may be lost after a standard dyeing and finish treatments. In this study, the bulky surface, flexibility and bursting strength that may lose their effect will be tested and alternative pigment dyeing and washing processes were carried out. The reason for this is to prove that the tensile values, surface, flexibility and bursting strength of the waffle fabric to be tested can be preserved after the processes due to waffle fabrics structure [3].

Waffle structures, one of the fabrics developed in recent years, can be produced with knitting and weaving techniques. Waffle knit is an improved version of the basic rib knit pattern. At the same time, the domination varies in the literature according to the three-dimensional structure it forms on the surface. The reasons why waffle fabrics are preferred are due to their flexibility, comfort, air permeability and bulkiness, as well as being a report that can be easily worked with cotton, polyester and other fibers [4].

The movements of the loops in circular knitting machines are decided by a system called cam mechanism. The adjustment of these systems varies according to the knitted quality, which increases the diversity [5]. The type of steel used for waffle quality is tuck steel. While in a stitch system the loop in the needle bed is dropped from the plate of the needles to make room for a new one, in the tuck system there is a structure that does not allow the loop to fall. In this way, the loop waiting in the needle bed is piled

up during knitting [6]. These piled ups are the most important parameters that form the 3D structure.

One of the major drawbacks of cotton fabrics is their tendency to wrinkle easily after washing, primarily due to the swelling of cellulosic fibers. This phenomenon occurs when mechanical stress and moisture cause polymer chains in the amorphous regions to shift and form new hydrogen bonds, resulting in permanent creases. Traditionally, to enhance wrinkle resistance, cotton fabrics are first dyed and then treated with crosslinking agents and catalysts in a separate durable press finishing step. An alternative approach, known as one-bath dyeing and durable press finishing, integrates dyeing and finishing into a single process. This technique offers significant advantages, including reduced energy consumption, shorter production time, and lower use of chemicals and water, making it a more economical and sustainable method [7].

Normal washing is a widely used and cost-effective garment finishing process, primarily aimed at removing surface impurities such as dirt, dust, and starch without causing fabric shrinkage. The visual and tactile effects of normal washing can be adjusted by modifying parameters such as temperature, duration, and detergent concentration. Pigment washing follows a similar process, but its main purpose is to create a faded or worn look on the fabric surface and around the seams [8].

II. MATERIAL

In this study, Ne 28/1 %100 cotton yarn was used for waffle fabric. Machine diameter was 34 inch, gauge was 20, stitch length was 4. For one step pad-dry-cure process; water, binder, anti migration agent, dyestuff was used. For pigment wash; caustic soda, sodium carbonate, soap was used. In dryer machine we used polyethylene.

III. METHOD

Pigment dyeing process was carried out with pad dry cure technique. In this technique, the parameters of the stenter machine are prepared as follows; pick up: %90, fan setting: %60, temperature: 150 °C, fabric feed rate: 10 m/dk, padding pressure: 4 bar. The machine used for the washing process is the Texcolour NG 6 DM model. The fabric, washed at 50°C for 40 minutes, was subsequently subjected to a neutralization process at 40°C for 20 minutes following rinsing. Last step was in fabric dryer machine at 80 °C for 20 minutes.

3.1 TEST METHODS

Waffle fabric was tested according to ASTM D4964-96 (2016) standard for elasticity and recovery tests. Bursting strength were tested according to ASTM D6797-15 standard. For fabric surface comparison Vizoo Fabric Scanning device was used.

IV. RESULT & DISCUSSION

The waffle fabric was compared before and after washing in terms of elasticity and recovery, bursting strength, fabric surface appearance and dimensional properties including shrinkage and spirality. The results showed significant differences and met the required criteria.

Shrinkage in knitted fabrics can be categorized into construction, processing, and drying shrinkage. Construction shrinkage results from the inherent design and loop configuration of the fabric, while processing shrinkage arises from dimensional changes caused by dyeing and finishing steps. Drying shrinkage occurs as fibers, yarns, and loops return to a lower energy state during moisture loss, leading to loop rounding and fabric relaxation [8].

Fabric elasticity and recovery test results were shown in Table 1, and dimensional properties and fabric weight test results were shown in Table 2. The increase in elasticity in the course direction is attributed to the looped and suspended (hanging) structure of the fabric, which allows greater lateral movement. Additionally, fabrics washed and dried in a relaxed state—freely immersed in liquid and agitated—undergo expected dimensional changes due to fiber swelling, fluid interaction, and inter-fabric friction [8].

Table 1. Comparison of elasticity and recovery before and after washing

| Condition | Elasticity and Recovery (LBS) | |
|----------------|-------------------------------|------------|
| | Width (%) | Length (%) |
| Before Washing | 12.26 | 25.36 |
| After Washing | 24.61 | 12.28 |

Table 2. Comparison of shrinkage, spirality and fabric GSM before and after washing

| Condition | Shrinkage | | Spirality | Fabric GSM (g/cm ²) |
|----------------|-----------|--------|-----------|---------------------------------|
| | Width | Length | | |
| Before washing | -7 | -7 | 0 | 270 |
| After washing | -1 | -3 | 2 | 290 |

The test results for bursting strength of fabrics were given in Table 3. It is known that an increase in the tuck stitch in knitted fabrics tends to reduce bursting strength. Based on the after wash results, it was observed that the fabric became compacted due to exposure to heat and friction with other fabrics during the washing process, leading to a decrease in bursting strength [6].

Table 3. Comparison of bursting strength before and after washing

| Condition | Bursting strength (lbf) |
|----------------|-------------------------|
| Before Washing | 47.89 |
| After Washing | 32.86 |

Technical face of fabrics were visualized by fabric scanning device and shown in Figure 1. As expected, the bulges that form the three-dimensional structure of the fabric were noticeably reduced when comparing the images taken in raw, before washing, and after washing stages. This outcome is consistent with our evaluation criteria.

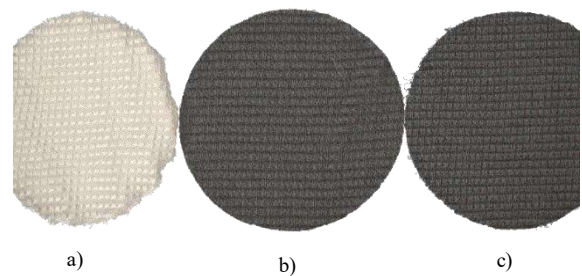


Figure 1. a) Technical face of the raw waffle fabric b) Before washing c) After washing

VI. CONCLUSIONS

This study demonstrated that the applied pigment dyeing and washing processes significantly affected the mechanical properties of waffle knit fabrics. Notably, elasticity and recovery values showed considerable variation before and after washing, while the visual and dimensional stability of the 3D fabric structure was preserved. The findings suggest that waffle fabrics can maintain their functional and aesthetic performance under appropriate post-treatment processes. The successful application of these techniques may also provide a foundation for future developments in finishing processes for other three-dimensional knitted fabrics.

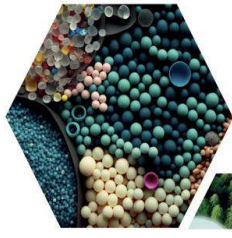
ACKNOWLEDGMENTS

This study was carried out by the Almaxtex Textile R&D Center, supported by the Ministry of Industry

and Technology of Turkey, with the AGM-S1-P24 project code.

REFERENCES

- [1] FOSTER, Karis R. (2017) Factors influencing the adoption of 3D Knitting technologies by US companies: A case-study analysis. North Carolina State University, pp 16-17
- [2] Akter, R., Sarker, T. R., Murad, S., & Shaikh, E. (2023). Investigating the effect of fabric design on properties of different weft knit fabrics. <https://doi.org/10.53430/ijeru.2023.4.2.0019>
- [3] Chowdhury, M. R., & Tipu, A. H. (2021). Effects of various fabric structures and GSM on bursting strength of single jersey weft knit derivatives fabric. Southeast University Journal of Textile Engineering, 1(1), pp 73-80.
- [4] MARMARALI Arzu (2008) Yuvarlak Örme Makineleri (Atkı Örmeciliği Ders Notu), E.Ü. Mühendislik Fakültesi Tekstil Müh. Bölümü, pp 58-59
- [5] CHOWDHURY, M.R. (2018) Effect Of Change In Yarn Count & Cylinder Stitch Length On Waffle Knit Fabric Gsm / Faculty, Department of Textile Engineering, Southeast University, Tejgaon I/A, Dhaka, Bangladesh. ISSN-1997-2571 (Online)
- [6] Uyanik, S., Degirmenci, Z., Topalbekiroglu, M., & Geyik, F. (2016). Examining the relation between the number and location of tuck stitches and bursting strength in circular knitted fabrics. *Fibres & Textiles in Eastern Europe*, (1 (115), 114-119. DOI: 10.5604/12303666.1170266
- [7] Özdemir, P. S., & Şaşmaz, S. (2018). Economical one step process for simultaneous application of pigment dyeing and wrinkle recovery finishing of cotton fabrics. *El-Cezeri*, 5(2), 425-436.
- [8] Hossain, M., Rony, M. S. H., Hasan, K. F., Hossain, M. K., Hossain, M. A., & Zhou, Y. (2017). Effective mechanical and chemical washing process in garment industries. *American Journal of Applied Physics*, 2(1), 1-25 , 2.1: 1-25.



16 ULUSLARARASI
LİF VE POLİMER
ARAŞTIRMALARI
SEMPOZYUMU

16th INTERNATIONAL FIBER AND POLYMER RESEARCH SYMPOSIUM

Sürdürülebilir ve İşlevsel Lif ve Polimerler
Sustainable and Functional Fibers & Polymers



9-10 Mayıs
May 2025

İstanbul Teknik Üniversitesi
Gümüşsuyu Prof. Dr. Necmettin Erbakan Yerleşkesi
Istanbul Technical University
Gumussuyu Prof. Dr. Necmettin Erbakan Campus

Design of glitter-effect denim and non-denim surfaces with a novel coating material

Gökhan GÜNEŞ^{a,*}, Osman BABAARSLAN^b

^aCalik Denim Textile A.Ş. R&D Department, 44900 Malatya, Türkiye.

^bCukurova University, Engineering Faculty, Department of Textile Engineering, 01250 Adana, Türkiye.

*Corresponding author: gokhan.gunes@calikdenim.com

ABSTRACT

This study aims to enhance the aesthetic and mechanical properties of denim and non-denim fabrics through glitter coating. Within the project, metallic glitters were applied to the fabric surface using the stencil printing method, and post-coating fabrics underwent weight, crocking, stiffness, elasticity, tear resistance, and shrinkage tests. Results indicated a significant increase in fabric weight (from 384 g/m² to 449 g/m²) without compromising functionality. Wet crocking tests revealed acceptable colour loss levels, while stiffness increased by 400% (from 1.16 kg to 6.53 kg), and tear resistance improved. Although a slight reduction in elasticity was observed (from 38% to 25-27%), it did not adversely affect performance due to denim's inherent rigidity. The produced garments emerged as innovative and visually striking products in fashion design. The coating process preserved dimensional stability within expected limits for denim, with shrinkage values aligning with industry standards. Glitter-coated fabrics demonstrated enhanced durability and a glossy surface, offering designers flexibility in creating unique styles. Findings prove that glitter coating enriches denim fabrics both visually and mechanically, making it viable for industrial applications. The project successfully bridges traditional denim aesthetics with modern design demands, highlighting the potential of surface treatments in textile innovation.

Keywords: Denim, Glitter Coating; Stencil Printing; Surface Modification; Crocking; Tear Resistance.

I. INTRODUCTION

The textile industry is undergoing continuous transformation, driven by evolving consumer demands and technological advancements. Denim fabrics, in particular, have transcended traditional uses to become prominent in fashion and functional designs. However, innovative approaches to enhance their aesthetic and mechanical properties remain critical for industrial competitiveness. In this context, surface

modification techniques are widely employed to add value to textile products. Decorative applications such as glitter coating not only impart shine and visual appeal to fabrics but also offer functional benefits like durability. This study systematically investigates the effects of glitter coating, applied via stencil printing, on the aesthetic and mechanical performance of denim and non-denim fabrics.

Existing literature highlights various techniques (flock printing, transfer printing, digital printing) for achieving metallic effects on textile surfaces. However, most of these methods face limitations such as high costs, complex production processes, or limited pattern control. Stencil printing, chosen for this study, stands out due to its cost-effectiveness, flexibility, and precision in pattern application. Furthermore, comprehensive analyses of glitter coating's impact on fabric physical properties are scarce, forming the core motivation for this research.

In this study, metallic glitters were applied to 100% cotton denim fabrics using a water-based adhesive, followed by weight, crocking, stiffness, elasticity, tear resistance, and shrinkage tests. Results revealed a significant increase in fabric weight (from 384 g/m² to 449 g/m²) without compromising functionality. While wet crocking tests indicated minor colour loss (1-2%), stiffness increased by 400% (from 1.16 kg to 6.53 kg), and tear resistance improved. The reduction in elasticity (from 38% to 25-27%) did not adversely affect performance due to denim's inherent rigidity.

These findings demonstrate that glitter coating serves as a dual-purpose solution in the textile industry, offering both aesthetic richness and mechanical durability. Additionally, the garments produced through this method encourage creativity in fashion design, underscoring its industrial applicability. The study aims to bridge traditional denim manufacturing with modern design requirements, emphasizing the role of surface modification techniques in textile innovation. By integrating empirical data with practical applications, this research contributes to advancing sustainable and innovative textile practices.

II. EXPERIMENTAL METHOD / TEORETICAL METHOD

In this study, a new coating material was developed for the design of denim and non-denim surfaces with glitter effects. Within the scope of the research, eight different recipes (R1-R8) were created using X1 and X2 chemical pastes at different concentrations.

2.1 Materials and Preparation Techniques

2.1. Chemical Composition

The coating pastes used in the study consist of X1 and X2 pastes certified as ZDHC (Zero Discharge of Hazardous Chemicals) Compliance Level 3. X1 paste was used in recipes R1, R3, R5, and R7; X2 paste was used in recipes R2, R4, R6, and R8. The concentration of each paste was adjusted at two different dosages: low (150 grams) and high (300 grams).

Table 1. Composition of Coating Formulations

| Recipe Code | X1 Paste (g) | X2 Paste (g) | Colorant |
|-------------|--------------|--------------|----------|
| R1 | 150 | - | - |
| R2 | - | 150 | - |
| R3 | 300 | - | - |
| R4 | - | 300 | - |
| R5 | 150 | - | X |
| R6 | - | 150 | X |
| R7 | 300 | - | X |
| R8 | - | 300 | X |

2.2 Application Procedure

The coating process was carried out on textile surfaces under controlled pressure and temperature conditions. Following application, drying and heat treatment steps were followed for optimal fixation of the coating on the textile surface. After the coating process, the glitter effect on the surfaces was visually evaluated.

III. RESULTS AND DISCUSSIONS

Physical performance properties of denim and non-denim surfaces with glitter effects were comprehensively examined. Stiffness, elasticity, tensile strength, tear resistance, and hydrophility properties of fabrics coated with different recipes were evaluated.

Tablo 2. Test Results

| | STIFFNESS (kg) | ELASTICITY (%) 1,36 kg | ELASTICITY GROWTH (%) 1,36kg | | TENSİLE (kgf) | | TEAR (grf) | |
|------------------------------|------------------|-----------------------------|--------------------------------------|----|--------------------|------|-----------------|------|
| | | | 30" | 2° | WARP | WEFT | WARP | WEFT |
| R1 (X1 Paste 150 G) | 3,06 | 26 | 9 | 6 | 79 | 44 | 6459 | 4567 |
| R2 (X2 Paste 150 G) | 5,45 | 26 | 9 | 5 | 90 | 44 | 6393 | 5154 |
| R3 (X1 Paste 300 G) | 5,15 | 25 | 9 | 5 | 92 | 45 | 6393 | 4502 |
| R4 (X2 Paste 300 G) | 6,53 | 27 | 9 | 5 | 95 | 43 | 6393 | 4110 |
| R5 (X1 Paste 150 G + Colour) | 4,05 | 25 | 8 | 4 | 91 | 43 | 6524 | 4567 |
| R6 (X2 Paste 150 G + Colour) | 4,88 | 26 | 9 | 5 | 93 | 45 | 6524 | 4502 |
| R7 (X1 Paste 300 G + Colour) | 5,06 | 25 | 7 | 3 | 93 | 44 | 6393 | 4632 |
| R8 (X2 Paste 300 G + Colour) | 6,11 | 26 | 11 | 6 | 91 | 43 | 6328 | 4306 |

The glitter effect coating process caused significant changes in the physical performance properties of the fabric. After the coating process, the stiffness of the fabric increased while its elasticity decreased. This is due to the coating pastes filling the fabric structure and restricting the mobility between fibres.

X2 paste provided higher stiffness values compared to X1 paste. Additionally, increasing the paste amount (from 150 g to 300 g) caused an increase in stiffness values. The addition of colorant generally decreased stiffness values. This may be due to the colorant agents modifying the paste structure, making the coating more flexible.

According to tensile strength test results, the coating process decreased strength in the warp direction while causing a slight increase in the weft direction. This can be explained by the coating paste particularly restricting the mobility of warp yarns.

No significant change was observed in tear resistance values after the coating process. However, the increase in tear resistance in the warp direction in recipes with added colorant (R5 and R6) is noteworthy.

Hydrophilicity test results showed that the R3 recipe (X1 Paste 300 G) had the lowest hydrophilicity time. This indicates that when X1 paste is used in high

concentration, it increases the water absorption property of the fabric.

According to spray test results, recipes containing X2 paste (R4 and R6) exhibited higher water repellency properties. This result suggests that X2 paste contains components with water-repellent properties in its structure.

IV. CONCLUSIONS

In this study, the effects of coating material developed for the design of glitter effect denim and non-denim surfaces on physical performance properties were investigated. The results obtained can be summarized as follows:

- The coating process caused a significant increase in the stiffness of the fabric while leading to a decrease in elasticity.
- X2 paste provided higher stiffness values compared to X1 paste.
- Increasing the paste amount (from 150 g to 300 g) caused an increase in stiffness values.
- The addition of colorant generally caused a decrease in stiffness values.
- In the tensile strength test, the coating process decreased strength in the warp direction while causing a slight increase in the weft direction.
- No significant change was observed in tear resistance values after the coating process.
- R3 recipe containing X1 paste had the lowest hydrophilicity time, while R4 and R6 recipes containing X2 paste exhibited the highest water repellency properties.
- R8 recipe containing X2 Paste 300 G + Color showed the highest value in the elasticity growth test.

In light of these results, it has been determined that the type and amount of paste used in the glitter effect coating process have a significant impact on the

physical performance properties of the fabric. Selecting the appropriate recipe according to the desired performance properties is critical in the product development process.

ACKNOWLEDGMENT

We extend our heartfelt gratitude to Calık Denim Textile A.Ş for their support in conducting this research.

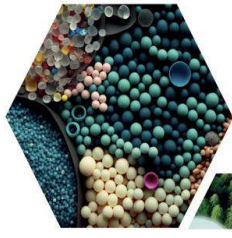
REFERENCES

Hsieh, P., Xu, Q., & Yu, H. (2023). A new technique for the removal of red fungal stains on traditional Chinese painting on silk. *International Biodeterioration & Biodegradation*, 181, 105622.

Ahmadian, M., Derakhshankhah, H., & Jaymand, M. (2023). Biosorptive removal of organic dyes using natural gums-based materials: A comprehensive review. *Journal of Industrial and Engineering Chemistry*, 124, 102-131.

Sekhar, V. C., Dasore, A., Yalamasetti, B., Madhuri, K. S., & Narendar, G. (2023). Flexural behavior of natural fiber epoxy composites. *Materials Today: Proceedings*.

Bellmann, C., Caspari, A., Albrecht, V., Doan, T. L., Mäder, E., Luxbacher, T., & Kohl, R. (2005). Electrokinetic properties of natural fibres. *Colloids and surfaces A: Physicochemical and engineering aspects*, 267(1-3), 19-23.



16 ULUSLARARASI
LİF VE POLİMER
ARAŞTIRMALARI
SEMPOZYUMU

16th INTERNATIONAL FIBER AND POLYMER RESEARCH SYMPOSIUM

Sürdürülebilir ve İşlevsel Lif ve Polimerler
Sustainable and Functional Fibers & Polymers



9-10 Mayıs
May 2025

İstanbul Teknik Üniversitesi

Gümüşsuyu Prof. Dr. Necmettin Erbakan Yerleşkesi
Istanbul Technical University
Gumussuyu Prof. Dr. Necmettin Erbakan Campus

The Effect of Ecocell™ Fiber on Some Performance Properties of Apparel Fabrics

Yasemin Dülek^{a,*}, İpek Yıldırım^a, Buğçe Sevinç^a, Hatice Salar^a, Tülin Kaya Nacarkahya^b, Şeyma Satıl^b, Cem Güneşoğlu^c

^aS.Y.K. Textile Industry and Trade Inc., R&D Center, DOSAB Çiğdem 1 Street No:5 Osmangazi 16369 Bursa, Türkiye.

^bKarafiber Tekstil Ind. Trade Inc. R&D Center, 2. OSB, 83221 Street. No:6 Şehitkamil 27600 Gaziantep, Türkiye.

^cTextile Engineering, Gaziantep University, Şehitkamil 27410 Gaziantep, Türkiye.

*Corresponding author: yasemindulek@sykteks.com

ABSTRACT

Nowadays, environmental sustainability is becoming increasingly important in the textile industry. In this context, the use of biodegradable, eco-friendly, and renewable fiber sources is gaining prominence. Regenerated cellulosic fibers have gained importance in sustainable textile production due to their natural origin and lower environmental impact during manufacturing processes. Among the technologies used in the production of regenerated fibers, the lyocell process has recently attracted attention thanks to its low environmental footprint, use of closed-loop solvent systems, and high fiber strength. In this study, it was aimed to evaluate various performance properties of two different local and imported regenerated cellulosic fiber woven fabrics produced with lyocell fiber production technology. Color values, color fastness, tensile strength, seam slippage, pilling resistance, abrasion resistance, air permeability, hydrophilicity, stiffness and thermal properties of the fabric samples were measured. The findings of the study are expected to contribute to the development of new alternatives that offer both environmental and economic advantages through the use of domestic raw materials.

Keywords: Lyocell; Ecocell™; twist coefficient; woven fabric

I. INTRODUCTION

In today's world, environmental sustainability is becoming increasingly important in the textile industry. In this context, the use of biodegradable, eco-friendly, and renewable fiber sources is gaining prominence. While cotton remains a widely used natural fiber, various chemical fibers have been developed as alternatives. Among these, viscose is one of the most commonly used regenerated cellulosic

fibers. However, due to its low wet strength, it has been further developed into modal fiber. Subsequently, lyocell fiber, produced through more environmentally friendly methods, has emerged. In our country, lyocell fibers and yarns are largely imported and used.

Regenerated cellulosic fibers have gained importance in sustainable textile production due to their natural origin and lower environmental impact during

manufacturing processes. Among the technologies used in the production of regenerated fibers, the lyocell process has recently attracted attention thanks to its low environmental footprint, use of closed-loop solvent systems, and high fiber strength.

1.1 Lyocell Fiber

Despite its widespread use, viscose fiber raises environmental concerns due to the chemicals used in its production and high energy consumption. In contrast, lyocell fiber stands out as a next-generation cellulosic fiber produced with an eco-friendly solvent system. Unlike traditional cellulosic fibers, lyocell is produced through a simple, closed-loop, and sustainable method [1].

The first stage of the lyocell production process is the selection of raw materials. Wood pulp, typically sourced from sustainable forests (especially from tree species such as eucalyptus, beech, or pine), is used. This wood pulp is dissolved in N-methylmorpholine-N-oxide (NMMO), a non-toxic and recyclable solvent, to convert the cellulose into a viscous form. During the production of fibers and yarns from the resulting solution, approximately 99.5% of the used NMMO is recovered and reused [2-3]. Thanks to this eco-friendly production method, lyocell offers a more efficient alternative in terms of water and energy consumption compared to other cellulosic fibers.

1.2 Ecocell™ Fiber

Ecocell™ fibers are a product produced by the textile industry in Türkiye to meet the demand for sustainable fibers, offering an environmentally friendly alternative to imported lyocell fibers. This local initiative in Türkiye aims to reduce dependence on imported materials and provide an eco-friendly alternative, while also increasing the sustainability of the industry and minimizing the carbon footprint related to transportation and production [4].

Ecocell™ fibers are produced from trees sourced from sustainable forests and are manufactured in an environmentally friendly manner using a closed-loop system that conserves resources. The production process utilizes a non-toxic organic solvent that can be 99.5% recovered, minimizing waste and environmental impact. Ecocell™ fibers stand out due to their physical properties such as high strength, excellent moisture absorption, softness on the skin, and breathability. These fibers provide comfort by maintaining coolness and dryness even in hot and humid environments. As a member of the lyocell class, these fibers differentiate themselves from other cellulose fibers in terms of sustainability and performance [5].

In the literature, Rana et al. discussed the production technologies, properties, market shares, environmental impacts, and potential applications of regenerated cellulose fibers (such as viscose, modal, lyocell, and bamboo viscose). Lyocell fiber is fully biodegradable, with high moisture absorption and excellent strength in both dry and wet conditions. It can easily blend with flax, cotton, and wool. The surface fibrils that form when wet provide an aesthetic appearance. Lyocell fabrics offer advantages such as wrinkle resistance, wash stability, the ability to be dyed in vibrant and various color tones, and good coverability [1-6-7-8-9].

The most characteristic feature of lyocell fiber is its tendency to fibrillate due to its high crystallinity, which makes it susceptible to mechanical effects [10]. Jeyaraj et al. developed a hybrid fabric made from a blend of polyester (weft) and silk fibers, utilizing the moisture-absorbing and fibrillation properties of lyocell fiber. Compared to 100% silk fabric, the hybrid fabric exhibited higher moisture absorption, water vapor permeability, and air permeability values, thanks to the presence of lyocell fiber [9].

Toprak et al. investigated sustainable dyeing methods for knitted fabrics containing different ratios of Tencel/Lyocell and cotton by applying three different dyeing processes. It was found that for blends containing 50% or more cotton, the dyeing method performed in a bleaching bath was effective and emerged as an environmentally friendly alternative. On the other hand, for fabrics with 75% or more Tencel content, only alkaline washing was sufficient, resulting in energy and chemical savings [11].

Zhang et al. conducted a comparative analysis of the production process, environmental impact, and structural and mechanical properties of lyocell - a regenerated, eco-friendly cellulose fiber - against viscose fibers. Lyocell, produced via a dry-jet wet spinning process using the NMMO solvent, stands out for its high crystallinity, uniform fiber structure, and solvent recovery system, making it a sustainable alternative. Owing to its superior mechanical and thermal properties, the study concluded that lyocell is a strong candidate for both textile and technical applications [12].

Şardağ examined the mechanical performance properties of woven fabrics produced from 100% lyocell, combed cotton, and various lyocell/cotton blend yarns. The study observed improvements in tensile strength, tear resistance, and drapability with increasing lyocell content [13].

Güler et al. investigated the performance properties of three-thread fabrics produced with different blend ratios using Ecocell™ fiber, a domestically developed lyocell alternative in Türkiye. In fabrics combined with cotton, hemp, and recycled polyester yarns, it was observed that increasing the Ecocell™ content led to a decrease in wet rubbing fastness and bursting strength. However, the overall physical properties remained within customer specifications [14].

Ke et al. examined the effects of tannic acid pretreatment on the dyeing behavior of lyocell fabrics using natural dyes. The results indicated that tannic acid pretreatment significantly improved color intensity and fastness properties, while preserving the chemical integrity of the lyocell fibers [15].

Polat et al. investigated the performance and dyeing properties of domestically produced Ecocell™ fibers in woven fabrics. The study revealed certain disadvantages, such as lower tensile and tear strength, limited recovery ability, and reduced shrinkage resistance. In particular, pilling resistance was found to be below expectations in dark-colored and elastane-containing fabrics. Nevertheless, the domestic production of Ecocell™ yarns was emphasized as a significant step toward promoting environmental sustainability in the textile industry [16].

Ghazal et al. examined the dyeability of lyocell fabrics with both synthetic and natural dyes, and also evaluated the dyeing performance of blend fabrics composed of different fibers such as cotton, silk, and polyamide. The study found that the highest K/S values were achieved with vat dyes (e.g. indigo), indicating that these dyes provided the most effective color yield on lyocell fabrics [10].

Elibüyük et al. investigated the single-bath reactive dyeability of woven fabrics made from 100% cotton, cotton/acrylic, and Ecocell™/acrylic blends. No adverse effects were observed in fastness properties after dyeing; blend fabrics exhibited higher hydrophilicity. K/S values were lower, with a slightly speckled and matte surface appearance. The study demonstrated that single-bath reactive dyeing is applicable for blended fabrics [17].

The aim of this research is to assess the comparability of Ecocell™, a locally produced lyocell fiber, to its international counterparts in terms of textile performance and to evaluate its applicability in

sustainable textile production. For this purpose the performance properties of apparel fabrics produced using two different yarns - one imported and one locally produced - based on lyocell fiber technology were comparatively analyzed. The local manufactured Ecocell™ fiber, with four different twist levels, was evaluated as an alternative to imported lyocell fibers. The fabrics were characterized in terms of color coordinates, color fastness, tensile strength, seam slippage, pilling resistance, abrasion resistance air permeability, hydrophilicity, stiffness and thermal properties.

The findings of the study are expected to contribute to the development of new alternatives that offer both environmental and economic advantages through the use of domestic raw materials.

II. EXPERIMENTAL METHOD

2.1 Materials

In the study, 5 different woven fabrics, the properties of which are given in Table 1, were produced using plain weave using 20 denier polyester recycle yarn in the warp, Ecocell™ yarns with 4 different twist values and imported lyocell yarns in the weft.

Table 1. Woven fabrics properties.

| | Fabric Sample Name | | | | |
|-----------------------------|------------------------------------------|----------------------------|----------------------------|----------------------------|----------------------------|
| | Lyocell | Ecocell™ a=3,6 | Ecocell™ a=3,8 | Ecocell™ a=4,0 | Ecocell™ a=4,2 |
| Composition (%) | %85 Lyocell %15 Polyester Recycle | | | | |
| Warp Yarn | 20 Denier Polyester Monofilament Recycle | | | | |
| Weft Yarn | Ne 30 Lyocell | Ne 30 Ecocell™ a=3,6 | Ne 30 Ecocell™ a=3,8 | Ne 30 Ecocell™ a=4,0 | Ne 30 Ecocell™ a=4,2 |
| Warp/Weft Density (yarn/cm) | 48/30 | | | | |
| Weave | Plain Weave | | | | |
| Weight (g/m²) | 86 | 88 | 92 | 91 | 91 |

2.2 Method

After the same pretreatment processes, the woven fabrics were dyed using reactive dyes and disperse dyes at 3% concentration according to black color recipe in a 10:1 liquor ratio using Fong's brand HT dyeing machine. The dyed fabrics were made ready for

use by applying a same finishing process. The fabric samples were then characterized by color coordinates, color fastness, tensile strength, seam slippage, pilling and abrasion resistance, air permeability, hydrophilicity, stiffness and thermal properties measurements.

Tensile properties of yarns were measured by Uster® Tensojet in accordance with TS EN ISO 2062 test method at a gauge length of 500 mm and an extension speed of 5000 mm/min. Uster® Tester 5 was used to determine CVM%, total imperfections (thin places, thick places and neps) and hairiness at a speed of 400 m/min according to ISO 16549 test method.

Color coordinates of the samples were measured with a spectrophotometer (Datacolor SF600 / USA). The measurements were run according to the CIELab color space under D65 daylight using a 10° standard observer with a 6.6 mm aperture. Color fastness tests were run after laundry of the samples by Gyrowash (James H. Heal / UK). Then color fastness to washing according to TS EN ISO 105-C06 A1S, to water according to TS EN ISO 105-E01, to acid and alkaline perspiration according to TS EN ISO 105 E04, to dry and wet rubbing according to TS EN ISO 105 X12 were completed. Tensile strength tests were completed by universal strength tester (James H.Heal Titan 3 / UK) according to TS EN ISO 13934-2. Seam Slippage tests were completed by universal strength tester (James H.Heal Titan 3 / UK) according to TS EN ISO 13936-2. Pilling resistance tests after 2000 cycles were carried out on a Martindale (James H. Heal Midi-Martindale / UK) according to TS EN ISO 12945-2. Abrasion resistance tests were completed by a Martindale (James H. Heal Midi-Martindale / UK) according to TS EN ISO 12947-3 and the percent weight loss was calculated after 2000, 4000, 6000, 8000, 10000 and 12000 cycles.

Air Permeability tests were completed by Prowhite-II Airtest device according to TS 391 EN ISO 9237.

Hydrophilicity tests were completed according to DIN 53 924:1997 vertical wetting test standart. For the vertical wicking test, five samples of 200x25 mm in size were prepared in the weft direction. A clip weighting 1.45 g was attached to one end of the prepared samples and immersed 10 mm into distilled water. The amount of water rising on the fabric was recorded in centimeters by taking measurements once in 2-5-10-15-20-25-30 minutes. Circular bending stiffness tests were completed by SDL Atlas Digital Pneumatic Stiffness Tester according to ASTM D4032-08(2016). Thermal properties measurements were made accordance with in-house Alambeta device standard derived from ISO 11092. The measurements were repeated 5 times and average values were recorded.

III. RESULT AND DISCUSSION

The Uster tester results are given in Table 2. Table 2 showed that Ecocell™ yarns showed better performance in terms of unevenness, hairiness, thick / thin places and neps counts, especially in higher twist level. Also Ecocell™ yarns exhibited better strength and breaking force as a certain result of even yarn structure and increased twist coefficient also enhanced strength as expected.

Table 2. Yarn strenght and unevenness test results.

| | Lyocel l | Ecocell ™ α=3,6 | Ecocell™ α=3,8 | Ecocell™ α=4,0 | Ecocell™ α=4,2 |
|------------------------------|-------------|-----------------------|-------------------|-------------------|-------------------|
| U% | 9,50 | 8,76 | 8,73 | 8,64 | 8,68 |
| CVm% | 11,98 | 11,07 | 11,03 | 10,90 | 10,95 |
| Thin Places -50% | 0 | 0 | 0 | 0 | 1 |
| Thick Places +50% | 12,0 | 6,0 | 5,1 | 3,3 | 4,1 |
| Neps +200% | 45,00 | 35,40 | 21,20 | 19,00 | 25,70 |
| H Hairiness | 6,20 | 5,92 | 5,66 | 6,60 | 5,44 |
| Neps +140%/km | 152 | 202,90 | 113,30 | 105,66 | 143,40 |
| Thin Places -40%/km | 30 | 5,9 | 11,6 | 9,3 | 8,7 |
| Thick Places +35%/km | 119 | 78 | 57 | 60 | 60 |
| Yarn Elongation % | 8,89 | 8,66 | 8,38 | 8,61 | 9,13 |
| B-Force (cN) | 500,6 | 562,13 | 561,70 | 577,92 | 554,89 |
| Tensile Strenght (Rkm) | 25,93 | 29,12 | 29,10 | 29,60 | 28,75 |

Color measurement results are given in Table 3. When lyocell fabric was taken as the reference color, the color difference of Ecocell™ based fabrics was obtained within an acceptable range ($\Delta E_{CMC} \leq 1$). The variaton in ΔL values were contributed to selected black color; however Ecocell™ samples exhibited lower chroma values.

Table 3. CIELab test results.

| Sample Name | ΔL^* | Δa^* | Δb^* | ΔC^* | Δh^* | ΔE_{CMC} |
|----------------|--------------|--------------|--------------|--------------|--------------|------------------|
| Lyocell | Standard | | | | | |
| Ecocell™ α=3,6 | 0,07 | 0,14 | 0,79 | -0,79 | 4,83 | 0,81 |
| Ecocell™ α=3,8 | 0,74 | 0,13 | 0,59 | -0,59 | 4,15 | 0,96 |
| Ecocell™ α=4,0 | -0,19 | 0,09 | 0,37 | -0,37 | 2,34 | 0,43 |
| Ecocell™ α=4,2 | 0,47 | 0,13 | 0,8 | -0,80 | 4,31 | 0,94 |

The results of the dyed fabrics for washing, water, acidic and alkaline perspiration and rubbing color fastness are given in Table 4-8. According to all fastness test results, the results of all fabrics were obtained in the acceptable range (4-5) and there was no difference between Lyocell fabric and Ecocell™ samples in terms of fastness. The increase in the yarn twist coefficient in fabrics containing Ecocell™ did not negatively affect the color fastness results.

Table 4. Washing fastness test results.

| Sample Name | Washing Fastness | | | | | | Color Change |
|-----------------------|------------------|--------|----------|-----------|---------|------|-----------------|
| | Staining | | | | | | |
| | Acetate | Cotton | Polyamid | Polyester | Acrylic | Wool | |
| Lyocell | 4-5 | 4-5 | 4-5 | 4-5 | 4-5 | 4-5 | 4-5 |
| Ecocell™ $\alpha=3,6$ | 4-5 | 4-5 | 4-5 | 4-5 | 4-5 | 4-5 | 4-5 |
| Ecocell™ $\alpha=3,8$ | 4-5 | 4-5 | 4-5 | 4-5 | 4-5 | 4-5 | 4-5 |
| Ecocell™ $\alpha=4,0$ | 4-5 | 4-5 | 4-5 | 4-5 | 4-5 | 4-5 | 4-5 |
| Ecocell™ $\alpha=4,2$ | 4-5 | 4-5 | 4-5 | 4-5 | 4-5 | 4-5 | 4-5 |

Table 5. Water fastness test results.

| Sample Name | Water Fastness | | | | | | Color Change |
|----------------|----------------|--------|----------|-----------|---------|------|--------------|
| | Staining | | | | | | |
| | Acetate | Cotton | Polyamid | Polyester | Acrylic | Wool | |
| Lyocell | 4-5 | 4-5 | 4-5 | 4-5 | 4-5 | 4-5 | 4-5 |
| Ecocell™ α=3,6 | 4-5 | 4-5 | 4-5 | 4-5 | 4-5 | 4-5 | 4-5 |
| Ecocell™ α=3,8 | 4-5 | 4-5 | 4-5 | 4-5 | 4-5 | 4-5 | 4-5 |
| Ecocell™ α=4,0 | 4-5 | 4-5 | 4-5 | 4-5 | 4-5 | 4-5 | 4-5 |
| Ecocell™ α=4,2 | 4-5 | 4-5 | 4-5 | 4-5 | 4-5 | 4-5 | 4-5 |

Table 6. Acidic perspiration fastness test results

| Sample Name | Acidic Perspiration Fastness | | | | | | Color Change |
|-----------------------|------------------------------|--------|----------|-----------|---------|------|--------------|
| | Staining | | | | | | |
| | Acetate | Cotton | Polyamid | Polyester | Acrylic | Wool | |
| Lyocell | 4-5 | 4-5 | 4-5 | 4-5 | 4-5 | 4-5 | 4-5 |
| Ecocell™ $\alpha=3,6$ | 4-5 | 4-5 | 4-5 | 4-5 | 4-5 | 4-5 | 4-5 |
| Ecocell™ $\alpha=3,8$ | 4-5 | 4-5 | 4-5 | 4-5 | 4-5 | 4-5 | 4-5 |
| Ecocell™ $\alpha=4,0$ | 4-5 | 4-5 | 4-5 | 4-5 | 4-5 | 4-5 | 4-5 |
| Ecocell™ $\alpha=4,2$ | 4-5 | 4-5 | 4-5 | 4-5 | 4-5 | 4-5 | 4-5 |

Table 7. Alkaline perspiration fastness test results

| Sample Name | Alkaline Perspiration Fastness | | | | | | Color Change |
|-----------------------|--------------------------------|--------|----------|-----------|---------|------|--------------|
| | Staining | | | | | | |
| | Acetate | Cotton | Polyamid | Polyester | Acrylic | Wool | |
| Lyocell | 4-5 | 4-5 | 4-5 | 4-5 | 4-5 | 4-5 | 4-5 |
| Ecocell™ $\alpha=3,6$ | 4-5 | 4-5 | 4-5 | 4-5 | 4-5 | 4-5 | 4-5 |
| Ecocell™ $\alpha=3,8$ | 4-5 | 4-5 | 4-5 | 4-5 | 4-5 | 4-5 | 4-5 |
| Ecocell™ $\alpha=4,0$ | 4-5 | 4-5 | 4-5 | 4-5 | 4-5 | 4-5 | 4-5 |
| Ecocell™ $\alpha=4,2$ | 4-5 | 4-5 | 4-5 | 4-5 | 4-5 | 4-5 | 4-5 |

Table 8. Wet and dry rubbing fastness test results.

| Sample Name | Rubbing Fastness | | | |
|-----------------------|------------------|------|------|------|
| | Dry | | Wet | |
| | Weft | Warp | Weft | Warp |
| Lyocell | 4 | 4 | 3 | 3 |
| Ecocell™ $\alpha=3,6$ | 4 | 4 | 3 | 3 |
| Ecocell™ $\alpha=3,8$ | 4 | 4 | 3 | 3 |
| Ecocell™ $\alpha=4,0$ | 4 | 4 | 3 | 3 |
| Ecocell™ $\alpha=4,2$ | 4 | 4 | 3 | 3 |

The tensile strength and seam slippage test results of the fabric samples are given in Table 9. The fabric samples in which Ecocell™ yarns of higher strength were used also exhibited higher fabric breaking strength values than that of Lyocell sample. Also, Ecocell™ samples gave lower seam slippage values which is contributed to even yarn structure. Higher twist coefficient also supported seam slippage of Ecocell™ samples.

Table 9. Tensile strength and seam slippage test results.

| Sample Name | Tensile Strength (N) | | Seam Slippage (mm) | |
|-----------------------|----------------------|--------|--------------------|------|
| | Weft | Warp | Weft | Warp |
| Lyocell | 98,37 | 178,91 | 5,03 | 3,91 |
| Ecocell™ $\alpha=3,6$ | 157,83 | 179,87 | 4,83 | 3,65 |
| Ecocell™ $\alpha=3,8$ | 159,41 | 172,50 | 4,53 | 3,69 |
| Ecocell™ $\alpha=4,0$ | 169,45 | 174,27 | 4,15 | 3,34 |
| Ecocell™ $\alpha=4,2$ | 194,74 | 189,45 | 4,10 | 3,45 |

The pilling test results given in Table 10 showed that Lyocell and Ecocell™ yarns utilization did not show any difference on pilling performance of woven fabrics; on the other hand Ecocell™ samples clearly exhibited better abrasion resistance (Table 11) which is also another outcome of difference in yarn properties. Twist coefficient also had significant effect on abrasion resistance of Ecocell™ samples.

Table 10. Pilling resistance test results.

| Sample Name | Pilling Resistance | |
|-----------------------|--------------------|------|
| | Face | Back |
| Lyocell | 4-5 | 4-5 |
| Ecocell™ $\alpha=3,6$ | 4-5 | 4-5 |
| Ecocell™ $\alpha=3,8$ | 4-5 | 4-5 |
| Ecocell™ $\alpha=4,0$ | 4-5 | 4-5 |
| Ecocell™ $\alpha=4,2$ | 4-5 | 4-5 |

Table 11. Abrasion resistance test results.

| Sample Name | Lyocell | Ecocell™ $\alpha=3,6$ | Ecocell™ $\alpha=3,8$ | Ecocell™ $\alpha=4,0$ | Ecocell™ $\alpha=4,2$ |
|-----------------------|---------|-----------------------|-----------------------|-----------------------|-----------------------|
| Before Abrasion (g) | 0,105 | 0,105 | 0,105 | 0,110 | 0,110 |
| After 2000 cycle (g) | 0,095 | 0,095 | 0,095 | 0,105 | 0,105 |
| After 4000 cycle (g) | 0,090 | 0,095 | 0,095 | 0,100 | 0,105 |
| After 6000 cycle (g) | 0,085 | 0,085 | 0,090 | 0,095 | 0,100 |
| After 8000 cycle (g) | 0,080 | 0,075 | 0,080 | 0,085 | 0,095 |
| After 10000 cycle (g) | 0,060 | 0,065 | 0,060 | 0,080 | 0,090 |
| After 12000 cycle (g) | 0,050 | 0,060 | 0,055 | 0,065 | 0,080 |
| Total Weight Loss (%) | 52% | 43% | 48% | 41% | 36% |

The vertical wicking tests (Figure 1) showed that samples with Ecocell™ yarn of the lowest twist coefficient had similar hydrophilicity to Lyocell sample. The increase in twist coefficient reduced

capillarity and resulted loss in wicking behavior of the fabrics.

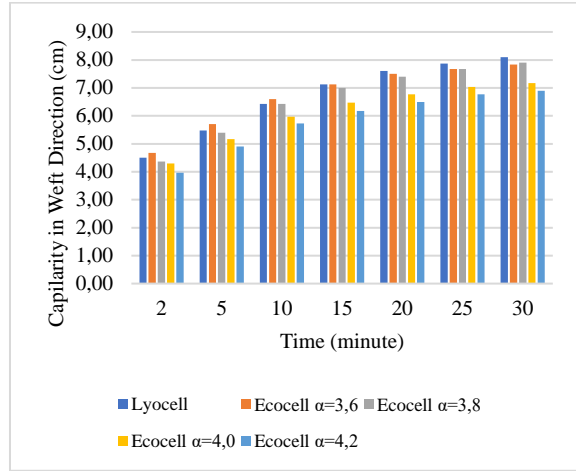


Figure 1. Hydrophilicity test results.

Table 12 shows air permeability and bending stiffness test results together. Lyocell fabrics had better air permeability but higher rigidity than Ecocell™ samples. Ecocell™ yarn usage clearly affected fabric softness in positive manner.

Table 12. Air permeability and stiffness test results.

| Sample Name | Fabric Density (g/cm ³) | Air Permeability (mm/s) | Stiffness (GF) |
|----------------|-------------------------------------|-------------------------|----------------|
| Lyocell | 0,450 | 789,2 | 0,065 |
| Ecocell™ α=3,6 | 0,403 | 689,3 | 0,063 |
| Ecocell™ α=3,8 | 0,422 | 690,8 | 0,062 |
| Ecocell™ α=4,0 | 0,448 | 754,7 | 0,060 |
| Ecocell™ α=4,2 | 0,445 | 848,4 | 0,062 |

Thermal properties were summarized in Table 13. Since the fabrics had similar construction and density values, they showed similar thermal resistance however Ecocell™ samples showed higher heat flow and thermal conductivity, which shows higher heat loss from body. On the other hand, thermal diffusivity is also an important parameter in decision of thermal comfort assessment. The usage of Ecocell™ yarn with twist coefficient of 4.0 gave higher heat flow and thermal conductivity with lower diffusivity which makes it better choice for summer clothing.

Table 13. Thermal properties test results.

| Sample Name | Thermal Conductivity (W/m K) x 10 ⁻³ | Thermal Diffusivity (m ² /s) x 10 ⁻⁶ | Thermal Absorptivity (W.s ^{1/2} /m ² K) | Thermal Resistance (Km ² /W) x 10 ⁻³ | Maximum Heat Flow (W/m ²) |
|----------------|-------------------------------------------------|------------------------------------------------------------|-------------------------------------------------------------|------------------------------------------------------------|---------------------------------------|
| Lyocell | 17,70 | 0,0055 | 236,50 | 11,80 | 450,58 |
| Ecocell™ α=3,6 | 18,35 | 0,0063 | 232,45 | 12,28 | 451,90 |
| Ecocell™ α=3,8 | 18,38 | 0,0068 | 224,80 | 11,85 | 462,85 |
| Ecocell™ α=4,0 | 17,95 | 0,0048 | 252,70 | 11,70 | 458,28 |
| Ecocell™ α=4,2 | 17,80 | 0,0073 | 212,78 | 11,73 | 450,15 |

IV. CONCLUSIONS

This study compares various properties of identical apparel dyed woven fabrics which are separated in using Lyocell or Ecocell™ yarns as weft. First of all, Ecocell™ yarns exhibited better yarn evenness and tensile properties which also resulted with better fabric mechanical properties. After dyeing, there was no difference in terms of color fastness of samples and acceptable color difference were obtained between Lyocell and Ecocell™ samples. However, Lyocell yarns showed better performance in wicking and air permeability in general but Ecocell™ samples exhibited better heat transfer performance and better handle. So it was concluded that Ecocell™ which is produced in Türkiye using regenerated cellulose spinning technology, very similar to Lyocell system, may be used in apparel fabric production.

ACKNOWLEDGMENT

This study was carried out within the scope of project number PR-01-24-SYK-00 in cooperation with S.Y.K. Textile R&D Center and Karafiber Textile R&D Center supported by the Ministry of Industry and Technology of the Republic of Türkiye.

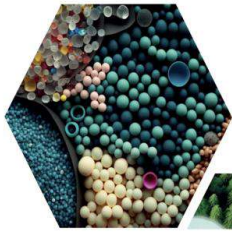
REFERENCES

- [1] Rana S, Pichandi S, Parveen S, Figueiro R (2014) Regenerated Cellulosic Fibers and Their Implications on Sustainability. Road to Sustainable Textiles and Clothing 239-276. DOI: 10.1007/978-981-287-065-0_8.

- [2] Ardiç Y (2007) Selülozik Liflerin Farklı Şartlarda Fibrilleşme ve Yorulma Davranışlarının İncelenmesi. Dissertation, Republic of Turkey Bursa Uludag University Institute of Science
- [3] Jiang X, Bai Y, Chen X, Liu W (2020) A review on raw materials, commercial production and properties of lyocell fiber. *Journal of Bioresources and Bioproducts* Vol.5 (1):16-25. <https://doi.org/10.1016/j.jobab.2020.03.002>
- [4] What is Ecocell™? <https://ecocell.com.tr/what-is-ecocell/>. Erişim 24 Mart 2024.
- [5] Uyanık S, Kaya Nacarkahya T (2025) Examination of the properties of sustainable yarns with Ecocell™ fiber and bast fibers in comparison with conventional cotton yarn and organic cotton yarn. *International Journal of Clothing Science and Technology*. <https://doi.org/10.1108/IJCST-01-2024-0021>.
- [6] White P, Hayhurst M, Taylor J, Slater A (2005) Lyocell Fibers. In: Blackburn, R.S., Ed., *Biodegradable and Sustainable Fibers*, Woodhead Publishing Ltd., Cambridge, 158-188. <https://doi.org/10.1533/9781845690991.157>.
- [7] Singha K (2012) Importance of the Phase Diagram in Lyocell Fiber Spinning. *International Journal of Materials Engineering* 2(3): 10-16. DOI: 10.5923/j.ijme.20120203.01.
- [8] Borbely E (2008) Lyocell, The New Generation of Regenerated Cellulose. *Acta Polytechnica Hungarica* Vol. 5(3): 11-18.
- [9] Jeyaraj JM, Arumugam M, Kulandaiappan V (2015) A study on the functional properties of silk and polyester/lyocell mixed fabric. *Matéria (Rio J.)* 20 (4): 924-935. <https://doi.org/10.1590/S1517-707620150004.0097>.
- [10] Ghazal H, Khaleed N, Shaker S, Hassabo AG (2024) An Overview of the Dyeing Process of Lyocell Fabric and its Blends. *J. Text. Color. Polym. Sci.* Vol. 21 (1): 49-62. DOI:10.21608/JTCPS.2023.221105.1211.
- [11] Toprak T, Şardağ S, Anis P (2018) A New Environmentally-Friendly Method of Dyeing Lyocell/Cotton Blended Fabrics. *AATCC Journal of Research* Vol. 5(5): 23-30. <https://doi.org/10.14504/ajr.5.5.4>.
- [12] Zhang S, Chen C, Duan C, Hu H, Li H, Li J, Liu Y, Ma X, Stavik J, and Ni Y (2018) Regenerated cellulose by the Lyocell process, a brief review of the process and properties. *BioRes.* 13(2). 4577-4592. DOI: 10.15376/biores.13.2.Zhang.
- [13] Bilir TB, Şardağ S (2019) Investigation of Mechanical Properties of Fabrics Woven with Lyocell/Cotton Blend Yarns. *Textile and Apparel* Vol.29 (2):162-170. DOI: 10.32710/tekstilvekonfeksiyon.503392.
- [14] Güler B, Kaya A, Gürel R, Satıl Ş, Kaya Nacarkahya T (2023) Sportswear Collection Developed From Pulp Based Biodegradable Regenerated Cellulose Fibers. *XVIth International Izmir Textile and Apparel Symposium*, October 25-27.
- [15] Ke G, Mulla MS, Peng F, Chen S (2023) Dyeing properties of natural Gardenia on the lyocell fabric pretreated with tannic acid. *Cellulose* Vol.30:611–624. <https://doi.org/10.1007/s10570-022-04896-w>.
- [16] Polat E, Md.Tanzir H, Adnan MA, Muhammet U (2023) Evaluation of weaving and dyeing properties of local regenerated yarns. *TEKSTİLNA INDUSTRIJA* Vol.71 (4): 14-22. DOI: 10.5937/tekstind2304014P.
- [17] Aras Elibuyuk S, Çörekcioglu M, Koptur Tasan P, Demir Güneç Ö, Satıl Ş, Gökpınar B, Kaya Nacarkahya T (2024). Evaluation of the Performance of Fabrics Produced with Oncedye Acrylic™, Ecocell™, and Cotton Fiber Blends Contributing to

16th International Fiber and Polymer Research Symposium (16th ULPAS)
9-10 May, 2025, Istanbul technical University (ITU), Istanbul, Türkiye

Sustainability Goals. The European Journal of
Research and Development Vol.4 (4), 178–187.
<https://doi.org/10.56038/ejrnd.v4i4.537>.



16

ULUSLARARASI
LİF VE POLİMER
ARAŞTIRMALARI
SEMPOZYUMU

16th INTERNATIONAL FIBER AND POLYMER RESEARCH SYMPOSIUM

Sürdürülebilir ve İşlevsel Lif ve Polimerler
Sustainable and Functional Fibers & Polymers



9-10 Mayıs
May 2025

İstanbul Teknik Üniversitesi
Gümüşsuyu Prof. Dr. Necmettin Erbakan Yerleşkesi
Istanbul Technical University
Gumussuyu Prof. Dr. Necmettin Erbakan Campus



The Effect of Fiber Cross-section of Polyester Yarn on Dyeing Behavior of Microwave Assisted and Conventional Dyeing

Yasemin Dülek^{a,*}, İpek Yıldırım^a, Buğçe Sevinç^a, Esra Mert^a, Yasemin Özdemir^a, Cem Güneşoğlu^b

^aS.Y.K. Textile Industry and Trade Inc., R&D Center, DOSAB Çiğdem 1 Street No:5 Osmangazi 16369 Bursa, Türkiye.

^bTextile Engineering, Gaziantep University, Şehitkamil 27410 Gaziantep, Türkiye.

*Corresponding author: yasemindulek@syteks.com

ABSTRACT

Microwave (MW) technology is investigated on utilization for wet textile treatments including dyeing through advantages in energy consumption and process performance. There are various papers studying MW assisted dyeing of various textile fibers and advantages in duration, colour strength, fastness, number of rinsing have been reported. This paper combines the effect of MW dyeing on colour strength and fiber cross-section of 100% Polyester woven fabrics and compares the results with that of conventional high temperature dyeing (HT). Polyester is a synthetic fiber widely preferred in the textile industry due to its properties such as high strength, abrasion resistance and dimensional stability. However, its structural hydrophobic character limits the dye uptake capacity and reduces the efficiency of traditional dyeing methods. In this context, new dyeing methods using alternative energy sources are gaining importance. For the study, 100% Polyester yarns with three different cross-sections have been used as weft yarns and dyeing has been completed by disperse dyes with different colours in accordance with HT and MW dyeing recipes. All samples were subjected to same pre-treatment and post-dyeing process; and after dyeing reflectance spectrophotometer and colour fastness measurements have been conducted. The study showed that dyeing performance can be enhanced by MW process and different levels can be achieved at different cross-sections.

Keywords: Polyester; disperse dye; fiber cross-section; microwave

I. INTRODUCTION

Sustainability approaches and innovative production methods are becoming increasingly important in the textile industry. In particular, intensive studies are being carried out on alternative dyeing techniques in order to increase energy efficiency, reduce environmental impacts and optimize performance properties in the dyeing of synthetic fibers such as

polyester. In this context, microwave (MW) assisted dyeing technology stands out with its advantages such as high color acquisition capacity in a short time and low energy consumption. The fact that microwaves accelerate diffusion mechanisms by creating heat directly and homogeneously within the fiber makes the dyeing process efficient in terms of both time and resource use.

Nowadays, microwave (MW) energy is widely used in many sectors such as food, chemistry, textile, metallurgy, ceramics and furniture. It has been stated that MW energy is effectively used in processes such as heating, drying, condensation, dyeing, printing and finishing, as well as in surface modifications of textile materials in the textile industry [1]. In recent years, microwave (MW) assisted dyeing methods have emerged as a promising alternative in the application of disperse dyes on polyester. The main difference between conventional heating and microwave heating is related to the mechanism of heat generation and transmission [2]. Microwave energy directly penetrates the inner structure of the fabric and produces heat at the molecular level with the dielectric heating mechanism, allowing the dye to diffuse into the fiber more quickly and effectively. In the study conducted by Farooq et al. [3], it was shown that polyester fabrics dyed with microwaves exhibited higher color density (K/S) and better color fastness values in a shorter time. Similarly, Arain et al. [4] showed that natural dyes such as henna can be effectively fixed onto polyester fabrics by microwave-assisted dyeing method; microwave heat shortens the dyeing time by 60–65% and increases the dye uptake by approximately three times compared to conventional heating. It was also emphasized that this method offers significant advantages in terms of both environmental sustainability and economic efficiency.

In the study conducted by Elshemy et al. [5], it was revealed that microwave energy significantly increased both the speed and efficiency of the dyeing process. In the study of Adeel et al. [6], the sustainability of polyester fabric dyeing with microwave radiation was investigated and it was found that microwave treatment shortened the dyeing time and increased the color strength, providing an environmentally friendly and efficient process. As a result, the color depth of the dyed fabrics increased and better fastness values were obtained.

One of the most important morphological properties of textile fibers is their cross-sectional shape [7]. The cross-sectional shape of textile fibers is one of the basic morphological parameters that directly affect the physical, mechanical and aesthetic properties of the fiber. The structure of the fiber depends not only on its raw material but also on the geometric form it gains during the production process. Especially synthetic fibers can be designed in different cross-sectional shapes (e.g. round, trilobal, channel, hollow, etc.) during production. These cross-sectional shapes significantly change the surface area of the fiber, light reflection and refraction properties, dye intake capacity and general behavior of the fabric. In the study conducted by Becerir, Karaca and Ömeroğlu [8], eight different disperse dyed fabrics produced from round, hollow round, trilobal and hollow trilobal cross-sectional fibers were subjected to four different abrasion cycles and then the color and strength values were evaluated. As a result of the research, it was determined that there were significant differences between the abrasion behaviors of fabrics produced from solid and hollow fibers, especially in terms of color values. It was determined that fabrics produced from hollow fibers were more sensitive to increasing abrasion cycles. Toydemir and Vatansever Bayramol [9] evaluated the basic parameters such as tensile strength, elongation at break, breaking load, irregularity and shrinkage in boiling water of trilobal, flat and hollow section filaments. In particular, it was determined that trilobal section yarns had higher tensile strength, elongation at break and breaking load values compared to flat and hollow section yarns. In contrast, flat section yarns showed the highest irregularity and shrinkage rates in boiling water. Babaarslan [10], who examined the effects of section shape on durability, elongation at break, curl and shrinkage, found that round and octolobal section shapes provided high strength and elongation at break, while trilobal and hexa sections provided lower values.

This study comparatively investigates the dyeing performances of 100% polyester fabrics with different fiber cross-sections (round, trilobal and channel cross-section) using microwave-assisted (MW) and conventional high temperature (HT) methods. Considering the effect of fiber cross-section structure on dye diffusion, fiber orientation and fabric performance, the behavior of each structure in microwave environment was analyzed in detail. The dyeability of each fiber cross-section in microwave environment was evaluated based on performance criteria such as color density (K/S), color fastness, tear strength and pilling obtained with the disperse dyes used. The effect of fiber orientation and morphology on dye absorption and final fabric properties during microwave dyeing process was investigated.

This comparative analysis aims to provide a new perspective for the development of sustainable and high-performance dyeing processes. Since studies on the interaction of microwave dyeing with fiber cross-sectional structure are limited in the literature, this study aims to fill an important gap and provide original contributions in both academic and industrial terms.

II. EXPERIMENTAL METHOD

2.1 Materials

In this study, round, trilobal and channel cross-section polyester yarns were supplied and the fabrics shown in Table 1 were produced. 3 different disperse dyes (yellow, red and blue) were supplied for the dyeing of woven polyester fabrics. The cross-section of the polyester fiber used in the weft is given in Figure 1, and the surface images (Olimpos brand microscope at X12 magnification) of the yellow-dyed woven fabric are given in Figure 2.

Table 1. Woven fabrics properties.

| Fabric Name | Round | Trilobal | Channel |
|-----------------------------|---------------------------|------------------------------|-----------------------------|
| Fabric Composition (%) | 100% Polyester | | |
| Warp Yarn | 70den/72f Polyester | | |
| Weft Yarn | 75den/48f Polyester Round | 75den/48f Polyester Trilobal | 75den/48f Polyester Channel |
| Warp/Weft Density (yarn/cm) | 60/45 | | |
| Weave | Twill | | |
| Weight (g/m ²) | 110 | | |

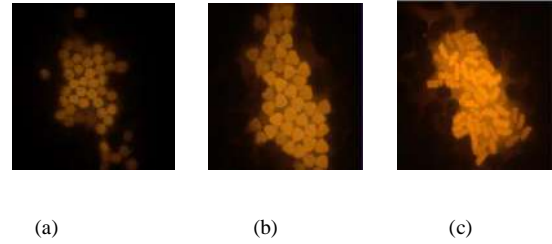


Figure 1. Polyester yarn sections (a) Round, (b) Trilobal, (c) Channel

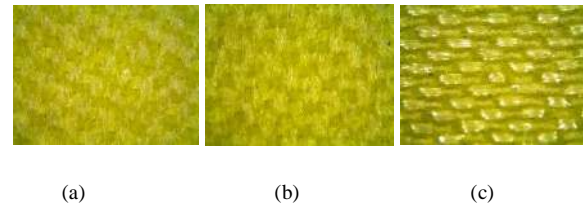


Figure 2. Microscope x12 magnification images of different cross-section fabrics (a) Round, (b) Trilobal, (c) Channel

2.2 Method

Conventional dyeing of polyester fabrics is carried out according to the traditional high temperature dyeing method (HT) as shown in Figure 3. In the study, the traditional dyeing process (HT) was carried out under pressure at 130°C for 40 minutes with 3 different disperse dyes at 0.3% concentration in 10:1 liquor and pH 5.5 using Ahiba sample dyeing machine.

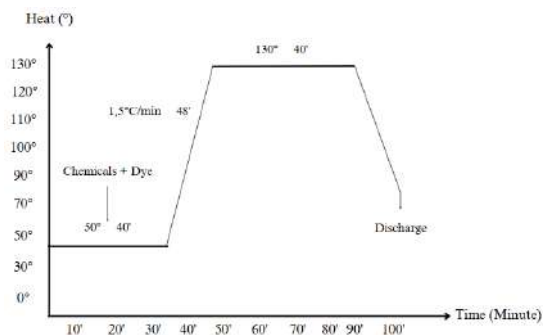


Figure 3. Conventional (HT) disperse dyeing diagram.

Microwave dielectric heating is achieved by direct conversion of wave energy into thermal energy. Substances with high dielectric constants such as water, salt and alcohol can be heated rapidly by dipole motion under microwave radiation. This feature allows microwave heat to be used effectively as a heat source in dyeing processes. While traditional heating methods cause problems such as dye migration, microwave heating increases dyeing speed and efficiency by providing homogeneous heat distribution [11].

In MW irradiation dyeing, the dye molecules absorb the radiation energy directly and diffuse faster into the fiber, while conventional heating provides slower heat transfer by conduction.

In the literature, Xu and Yang [12] reported that they achieved higher dye uptake rates in the dyeing process they carried out by exposing polyester fabric to microwave radiation at 400 W power compared to traditional methods.

In this study, microwave assisted dyeing processes (Arçelik MD 820 model, maximum power 1200 W, 2450 MHz frequency) were carried out according to the time-temperature diagram given in Figure 4. The process conditions of the microwave dyeing method were determined according to the optimum values obtained from the literature [12] and the AG-02-22-SYK project previously carried out within the company. The fabrics prepared as 5 grams each in a 50:1 bath ratio in a balloon glass beaker for microwave dyeing were first dyed at 480 Watt for 7.5 minutes and then at 160 Watt for 12.5 minutes.

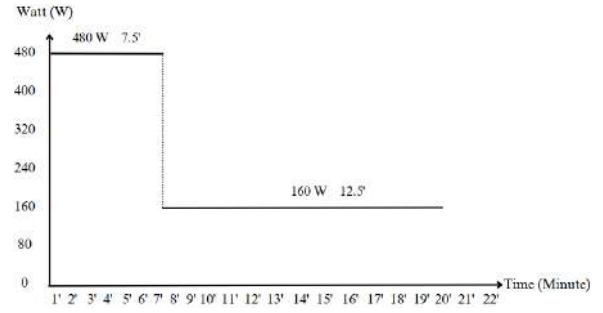


Figure 4. Microwave (MW) assisted disperse dyeing diagram.

Color coordinates of the samples were measured with a spectrophotometer (Datacolor SF600 / USA). The measurements were run according to the CIELab color space under D65 daylight using a 10° standard observer with a 6.6 mm aperture. Color fastness tests were run after laundry of the samples by Gyrowash (James H. Heal / UK). Then color fastness to washing according to TS EN ISO 105-C06 A1S, to water according to TS EN ISO 105-E01, to acid and alkaline perspiration according to TS EN ISO 105 E04, to dry and wet rubbing according to TS EN ISO 105 X12 were completed. Tear strength tests were completed by universal strength tester (James H.Heal Titan 3 / UK) according to TS EN ISO 13937-2. Pilling resistance tests after 2000 cycles were carried out on a Martindale (James H. Heal Midi-Martindale / UK) according to TS EN ISO 12945-2.

III. RESULT AND DISCUSSION

Color measurement parameters and color strength (K/S) values for microwave dyed fabrics and conventionally dyed fabrics are given in Table 2. Fabric images are given in Figures 5-7. K/S measurement results show that the MW method tends to give higher K/S values (color intensity) after disperse dyeing. This finding shows that microwave energy increases the diffusion of the dye into the fiber, thus providing a high potential for deeper and darker colors. According to the fiber cross-section, the highest color intensity was obtained in fabrics woven from circular, trilobal and channel cross-section yarns, respectively. It is known that MW modifies the

internal structure of the fibers; fibers with circular (round) cross-section have higher and channel-shaped have lower specific surface area, which affects MW assisted modification and dye uptake as final result. The polyesters yarns used in this study were not staple and had similar count, so the contribution of fiber length and fineness on MW assisted modification were eliminated. According to the spectrophotometric analysis results, it is predicted that the reference colors can be obtained with lower dye concentrations by optimizing the dye ratios in the recipe. In addition, microscopic examinations (Figure 2) performed on yellow fabrics with an Olimpos brand microscope at X12 magnification were found to support these results.

Table 2. CIELab test results.

| Sample Name | L* | a* | b* | C* | h° | K/S | ΔEcmc |
|--------------------|------|-------|-------|------|-------|------|-------|
| Round-Yellow-HT | 83,3 | -3,5 | 77,2 | 77,3 | 92,6 | 0,04 | |
| Round-Yellow-MW | 83,7 | -3,9 | 73,2 | 73,3 | 93,0 | 0,03 | 3,98 |
| Trilobal-Yellow-HT | 85,2 | -4,4 | 73,8 | 73,9 | 93,4 | 0,03 | |
| Trilobal-Yellow-MW | 84,5 | -3,3 | 75,6 | 75,6 | 92,5 | 0,03 | 2,22 |
| Channel-Yellow-HT | 85,6 | -4,5 | 71,4 | 71,6 | 93,6 | 0,03 | |
| Channel-Yellow-MW | 84,3 | -2,2 | 83,2 | 83,2 | 91,5 | 0,02 | 12,10 |
| Round-Red-HT | 52,2 | 48,7 | 1,1 | 48,7 | 1,3 | 0,03 | |
| Round-Red-MW | 48,5 | 49,3 | 3,6 | 49,5 | 4,2 | 0,03 | 4,46 |
| Trilobal-Red-HT | 55,3 | 47,5 | -0,7 | 47,5 | 359,2 | 0,03 | |
| Trilobal-Red-MW | 50,4 | 49,3 | 2,2 | 49,4 | 2,5 | 0,03 | 5,94 |
| Channel-Red-HT | 56,7 | 45,8 | -1,3 | 45,8 | 358,4 | 0,02 | |
| Channel-Red-MW | 52,8 | 47,2 | 1,6 | 47,2 | 1,9 | 0,03 | 4,99 |
| Round-Blue-HT | 54,6 | -1,6 | -35,1 | 35,2 | 267,4 | 0,07 | |
| Round-Blue-MW | 51,1 | -0,04 | -36,3 | 36,3 | 269,9 | 0,10 | 4,03 |
| Trilobal-Blue-HT | 56,2 | -2,3 | -34,7 | 34,8 | 266,2 | 0,07 | |
| Trilobal-Blue-MW | 54,4 | -0,9 | -34,4 | 34,4 | 268,6 | 0,08 | 2,37 |
| Channel-Blue-HT | 54,8 | -1,3 | -35,9 | 36,0 | 267,9 | 0,06 | |
| Channel-Blue-MW | 54,2 | -0,8 | -34,8 | 34,8 | 268,8 | 0,08 | 1,41 |

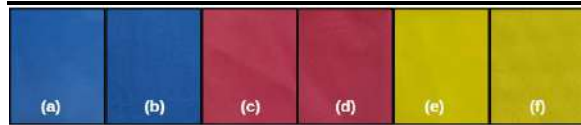


Figure 5. Microwave and HT dyed fabrics (a) Round-Blue-HT, (b) Round-Blue-MW, (c) Round-Red-HT, (d) Round-Red-MW, (e) Round-Yellow-HT, (f) Round-Yellow-MW



Figure 6. Microwave and HT dyed fabrics (a) Trilobal-Blue-HT, (b) Trilobal-Blue-MW, (c) Trilobal-Red-HT, (d) Trilobal-Red-MW, (e) Trilobal-Yellow-HT, (f) Trilobal-Yellow-MW

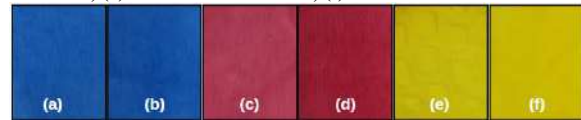


Figure 7. Microwave and HT dyed fabrics (a) Channel-Blue-HT, (b) Channel-Blue-MW, (c) Channel-Red-HT, (d) Channel-Red-MW, (e) Channel-Yellow-HT, (f) Channel-Yellow-MW

Color fastness test results for microwave dyed fabrics and conventionally dyed fabrics are given in Table 3-7. According to all color fastness test results (washing, water, acidic/alkaline perspiration, dry/wet rubbing), the results of fabrics dyed with both HT and MW methods were high (4-5); it was concluded that microwave dyeing did not adversely affect the fastness results.

Table 3. Washing fastness test results.

| Sample Name | Washing Fastness | | | | | |
|--------------------|------------------|--------|----------|-----------|---------|------|
| | Staining | | | | | |
| | Acetate | Cotton | Polyamid | Polyester | Acrylic | Wool |
| Round-Yellow-HT | 4-5 | 4-5 | 4-5 | 4-5 | 4-5 | 4-5 |
| Round-Yellow-MW | 4-5 | 4-5 | 4-5 | 4-5 | 4-5 | 4-5 |
| Trilobal-Yellow-HT | 4-5 | 4-5 | 4-5 | 4-5 | 4-5 | 4-5 |
| Trilobal-Yellow-MW | 4-5 | 4-5 | 4-5 | 4-5 | 4-5 | 4-5 |
| Channel-Yellow-HT | 4-5 | 4-5 | 4-5 | 4-5 | 4-5 | 4-5 |
| Channel-Yellow-MW | 4-5 | 4-5 | 4-5 | 4-5 | 4-5 | 4-5 |
| Round-Red-HT | 4-5 | 4-5 | 4-5 | 4-5 | 4-5 | 4-5 |
| Round-Red-MW | 4-5 | 4-5 | 4-5 | 4-5 | 4-5 | 4-5 |
| Trilobal-Red-HT | 4-5 | 4-5 | 4-5 | 4-5 | 4-5 | 4-5 |
| Trilobal-Red-MW | 4-5 | 4-5 | 4-5 | 4-5 | 4-5 | 4-5 |
| Channel-Red-HT | 4-5 | 4-5 | 4-5 | 4-5 | 4-5 | 4-5 |
| Channel-Red-MW | 4-5 | 4-5 | 4-5 | 4-5 | 4-5 | 4-5 |
| Round-Blue-HT | 4-5 | 4-5 | 4-5 | 4-5 | 4-5 | 4-5 |
| Round-Blue-MW | 4-5 | 4-5 | 4-5 | 4-5 | 4-5 | 4-5 |
| Trilobal-Blue-HT | 4-5 | 4-5 | 4-5 | 4-5 | 4-5 | 4-5 |
| Trilobal-Blue-MW | 4-5 | 4-5 | 4-5 | 4-5 | 4-5 | 4-5 |
| Channel-Blue-HT | 4-5 | 4-5 | 4-5 | 4-5 | 4-5 | 4-5 |
| Channel-Blue-MW | 4-5 | 4-5 | 4-5 | 4-5 | 4-5 | 4-5 |

Table 4. Water fastness test results.

| Sample Name | Water Fastness | | | | | |
|--------------------|----------------|--------|----------|-----------|---------|------|
| | Staining | | | | | |
| | Acetate | Cotton | Polyamid | Polyester | Acrylic | Wool |
| Round-Yellow-HT | 4-5 | 4-5 | 4-5 | 4-5 | 4-5 | 4-5 |
| Round-Yellow-MW | 4-5 | 4-5 | 4-5 | 4-5 | 4-5 | 4-5 |
| Trilobal-Yellow-HT | 4-5 | 4-5 | 4-5 | 4-5 | 4-5 | 4-5 |
| Trilobal-Yellow-MW | 4-5 | 4-5 | 4-5 | 4-5 | 4-5 | 4-5 |
| Channel-Yellow-HT | 4-5 | 4-5 | 4-5 | 4-5 | 4-5 | 4-5 |
| Channel-Yellow-MW | 4-5 | 4-5 | 4-5 | 4-5 | 4-5 | 4-5 |
| Round-Red-HT | 4-5 | 4-5 | 4-5 | 4-5 | 4-5 | 4-5 |
| Round-Red-MW | 4-5 | 4-5 | 4-5 | 4-5 | 4-5 | 4-5 |
| Trilobal-Red-HT | 4-5 | 4-5 | 4-5 | 4-5 | 4-5 | 4-5 |
| Trilobal-Red-MW | 4-5 | 4-5 | 4-5 | 4-5 | 4-5 | 4-5 |
| Channel-Red-HT | 4-5 | 4-5 | 4-5 | 4-5 | 4-5 | 4-5 |
| Channel-Red-MW | 4-5 | 4-5 | 4-5 | 4-5 | 4-5 | 4-5 |
| Round-Blue-HT | 4-5 | 4-5 | 4-5 | 4-5 | 4-5 | 4-5 |
| Round-Blue-MW | 4-5 | 4-5 | 4-5 | 4-5 | 4-5 | 4-5 |
| Trilobal-Blue-HT | 4-5 | 4-5 | 4-5 | 4-5 | 4-5 | 4-5 |
| Trilobal-Blue-MW | 4-5 | 4-5 | 4-5 | 4-5 | 4-5 | 4-5 |
| Channel-Blue-HT | 4-5 | 4-5 | 4-5 | 4-5 | 4-5 | 4-5 |
| Channel-Blue-MW | 4-5 | 4-5 | 4-5 | 4-5 | 4-5 | 4-5 |

Table 5. Acidic perspiration fastness test results

| Sample Name | Acidic Perspiration Fastness | | | | | |
|--------------------|------------------------------|--------|----------|-----------|---------|------|
| | Staining | | | | | |
| | Acetate | Cotton | Polyamid | Polyester | Acrylic | Wool |
| Round-Yellow-HT | 4-5 | 4-5 | 4-5 | 4-5 | 4-5 | 4-5 |
| Round-Yellow-MW | 4-5 | 4-5 | 4-5 | 4-5 | 4-5 | 4-5 |
| Trilobal-Yellow-HT | 4-5 | 4-5 | 4-5 | 4-5 | 4-5 | 4-5 |
| Trilobal-Yellow-MW | 4-5 | 4-5 | 4-5 | 4-5 | 4-5 | 4-5 |
| Channel-Yellow-HT | 4-5 | 4-5 | 4-5 | 4-5 | 4-5 | 4-5 |
| Channel-Yellow-MW | 4-5 | 4-5 | 4-5 | 4-5 | 4-5 | 4-5 |
| Round-Red-HT | 4-5 | 4-5 | 4-5 | 4-5 | 4-5 | 4-5 |
| Round-Red-MW | 4-5 | 4-5 | 4-5 | 4-5 | 4-5 | 4-5 |
| Trilobal-Red-HT | 4-5 | 4-5 | 4-5 | 4-5 | 4-5 | 4-5 |
| Trilobal-Red-MW | 4-5 | 4-5 | 4-5 | 4-5 | 4-5 | 4-5 |
| Channel-Red-HT | 4-5 | 4-5 | 4-5 | 4-5 | 4-5 | 4-5 |
| Channel-Red-MW | 4-5 | 4-5 | 4-5 | 4-5 | 4-5 | 4-5 |
| Round-Blue-HT | 4-5 | 4-5 | 4-5 | 4-5 | 4-5 | 4-5 |
| Round-Blue-MW | 4-5 | 4-5 | 4-5 | 4-5 | 4-5 | 4-5 |
| Trilobal-Blue-HT | 4-5 | 4-5 | 4-5 | 4-5 | 4-5 | 4-5 |
| Trilobal-Blue-MW | 4-5 | 4-5 | 4-5 | 4-5 | 4-5 | 4-5 |
| Channel-Blue-HT | 4-5 | 4-5 | 4-5 | 4-5 | 4-5 | 4-5 |
| Channel-Blue-MW | 4-5 | 4-5 | 4-5 | 4-5 | 4-5 | 4-5 |

Table 6. Alkaline perspiration fastness test results

| Sample Name | Alkaline Perspiration Fastness | | | | | |
|--------------------|--------------------------------|--------|----------|-----------|---------|------|
| | Staining | | | | | |
| | Acetate | Cotton | Polyamid | Polyester | Acrylic | Wool |
| Round-Yellow-HT | 4-5 | 4-5 | 4-5 | 4-5 | 4-5 | 4-5 |
| Round-Yellow-MW | 4-5 | 4-5 | 4-5 | 4-5 | 4-5 | 4-5 |
| Trilobal-Yellow-HT | 4-5 | 4-5 | 4-5 | 4-5 | 4-5 | 4-5 |
| Trilobal-Yellow-MW | 4-5 | 4-5 | 4-5 | 4-5 | 4-5 | 4-5 |
| Channel-Yellow-HT | 4-5 | 4-5 | 4-5 | 4-5 | 4-5 | 4-5 |
| Channel-Yellow-MW | 4-5 | 4-5 | 4-5 | 4-5 | 4-5 | 4-5 |
| Round-Red-HT | 4-5 | 4-5 | 4-5 | 4-5 | 4-5 | 4-5 |
| Round-Red-MW | 4-5 | 4-5 | 4-5 | 4-5 | 4-5 | 4-5 |
| Trilobal-Red-HT | 4-5 | 4-5 | 4-5 | 4-5 | 4-5 | 4-5 |
| Trilobal-Red-MW | 4-5 | 4-5 | 4-5 | 4-5 | 4-5 | 4-5 |
| Channel-Red-HT | 4-5 | 4-5 | 4-5 | 4-5 | 4-5 | 4-5 |
| Channel-Red-MW | 4-5 | 4-5 | 4-5 | 4-5 | 4-5 | 4-5 |
| Round-Blue-HT | 4-5 | 4-5 | 4-5 | 4-5 | 4-5 | 4-5 |
| Round-Blue-MW | 4-5 | 4-5 | 4-5 | 4-5 | 4-5 | 4-5 |
| Trilobal-Blue-HT | 4-5 | 4-5 | 4-5 | 4-5 | 4-5 | 4-5 |
| Trilobal-Blue-MW | 4-5 | 4-5 | 4-5 | 4-5 | 4-5 | 4-5 |
| Channel-Blue-HT | 4-5 | 4-5 | 4-5 | 4-5 | 4-5 | 4-5 |
| Channel-Blue-MW | 4-5 | 4-5 | 4-5 | 4-5 | 4-5 | 4-5 |

Table 7. Wet and dry rubbing fastness test results.

| Sample Name | Rubbing Fastness | | | |
|--------------------|------------------|------|------|------|
| | Dry | | Wet | |
| | Weft | Warp | Weft | Warp |
| Round-Yellow-HT | 4-5 | 4-5 | 4-5 | 4-5 |
| Round-Yellow-MW | 4-5 | 4-5 | 4-5 | 4-5 |
| Trilobal-Yellow-HT | 4-5 | 4-5 | 4-5 | 4-5 |
| Trilobal-Yellow-MW | 4-5 | 4-5 | 4-5 | 4-5 |
| Channel-Yellow-HT | 4-5 | 4-5 | 4-5 | 4-5 |
| Channel-Yellow-MW | 4-5 | 4-5 | 4-5 | 4-5 |
| Round-Red-HT | 4-5 | 4-5 | 4-5 | 4-5 |
| Round-Red-MW | 4-5 | 4-5 | 4-5 | 4-5 |
| Trilobal-Red-HT | 4-5 | 4-5 | 4-5 | 4-5 |
| Trilobal-Red-MW | 4-5 | 4-5 | 4-5 | 4-5 |
| Channel-Red-HT | 4-5 | 4-5 | 4-5 | 4-5 |
| Channel-Red-MW | 4-5 | 4-5 | 4-5 | 4-5 |
| Round-Blue-HT | 4-5 | 4-5 | 4-5 | 4-5 |
| Round-Blue-MW | 4-5 | 4-5 | 4-5 | 4-5 |
| Trilobal-Blue-HT | 4-5 | 4-5 | 4-5 | 4-5 |
| Trilobal-Blue-MW | 4-5 | 4-5 | 4-5 | 4-5 |
| Channel-Blue-HT | 4-5 | 4-5 | 4-5 | 4-5 |
| Channel-Blue-MW | 4-5 | 4-5 | 4-5 | 4-5 |

The tear strength test results of fabrics dyed yellow with MW and HT methods are given in Table 8. According to the tear strength results, a significant increase was observed especially in the weft strength of the fabrics dyed with the microwave method. This is an indication that the fibers received less catalytic damage in the dyeing process under MW energy.

Table 8. Tear strength (single tear method) test results.

| Sample Name | Tear Strenght (N) | |
|--------------------|-------------------|-------|
| | Weft | Warp |
| Round-Yellow-HT | 22,01 | 25,27 |
| Round-Yellow-MW | 33,22 | 24,68 |
| Trilobal-Yellow-HT | 24,00 | 24,73 |
| Trilobal-Yellow-MW | 31,71 | 25,74 |
| Channel-Yellow-HT | 18,82 | 23,13 |
| Channel -Yellow-MW | 21,61 | 24,13 |

The pilling resistance test results of fabrics dyed yellow with the MW and HT methods are given in Table 9. According to the pilling test results, it was concluded that the dyeing method did not create a significant difference in fabrics woven in trilobal and channel croos-sections, and the pilling values of the fabric with round croos-section dyed with the microwave method were better.

Table 9. Pilling resistance test results.

| Sample Name | Pilling Resistance | |
|--------------------|--------------------|------|
| | Face | Back |
| Round-Yellow-HT | 3-4 | 3-4 |
| Round-Yellow-MW | 4-5 | 4-5 |
| Trilobal-Yellow-HT | 4 | 4 |
| Trilobal-Yellow-MW | 3 | 3 |
| Channel-Yellow-HT | 3 | 3 |
| Channel-Yellow-MW | 3 | 3 |

IV. CONCLUSIONS

As a result of the microwave assisted dyeing applications carried out within the scope of this study, good color properties and acceptable color fastness were obtained in polyester fabrics, and no negative change was observed in the tear strength of the fabrics. Spectrophotometric analyses showed that the samples dyed with the microwave method reached darker tones; this revealed that the same color tone could be obtained with lower dye concentrations. The short heating of the dye bath in the microwave environment saved both time and energy compared to the traditional high temperature (HT) method.

In the applications carried out with disperse dyes used within the company, it was determined that the microwave dyeing method provided industrial acceptance ranges in terms of color fastness. The findings obtained show that microwave technology offers significant advantages in textile dyeing processes in terms of economy, environment and time. It was concluded that dyeing processes carried out with microwave energy allow efficient results to be obtained in a shorter time with lower energy consumption and thus increase cost effectiveness.

Considering the potential use of microwave technology in textile dyeing and finishing applications in Türkiye, it has been concluded that this method constitutes a promising alternative in terms of energy efficiency, process performance and sustainable production targets.

ACKNOWLEDGMENT

This study was carried out within the scope of project number AG-01-23-SYK-00 within the S.Y.K. Textile R&D Center supported by the Ministry of Industry and Technology, The Republic of Türkiye.

REFERENCES

- [1] Buyukakinci BY (2012) Usage of Microwave Energy in Turkish Textile Production Sector. *Energy Procedia* 14 (2012) 424 – 431. <https://doi.org/10.1016/j.egypro.2011.12.953>
- [2] El-Molla MM, Haggag K, Ahmed KA (2013) Dyeing of Polyester Fabrics Using Microwave Irradiation Technique. *International Journal of Science and Research (IJSR)* Vol.4 (2):2274 – 2279.
- [3] Farooq A, Shahzadi I, Ashraf MA, Irshad F, Khan N (2024) Effect of Microwave Irradiation on Coloring and Mechanical Properties of Direct Dyed Fabric. *AATCC Journal of Research* Vol. 11(2):101–108. <https://doi.org/10.1177/24723444231215446>
- [4] Arain RA, Ahmad F, Khatri Z, Peerzada MH (2021) Microwave assisted henna organic dyeing of polyester fabric: a green, economical and energy proficient substitute. *Natural Product Research* Vol. 35(2):327-330. <https://doi.org/10.1080/14786419.2019.1619721>
- [5] Elshemy NS, Elshakankery MH, Shahien SM, Haggag K, El-Sayed H (2017) Kinetic Investigations on Dyeing of Different Polyester Fabrics Using Microwave Irradiation. *Egypt. J. Chem* Vol. 60. The 8th. Int. Conf. Text. Res. Div., pp.79- 88. DOI: 10.21608/ejchem.2017.1604.1131
- [6] Adeel S, Khan SG, Shahid S, Saeed M, Kiran S, Suleman M, Akhtar N (2018) Sustainable Dyeing of

Microwave Treated Polyester Fabric using Disperse
Yellow 211 Dye. J. Mex. Chem. Soc. Vol. 62(1):1-9.
DOI: <http://dx.doi.org/10.29356/jmcs.v62i1.580>

[7] Badrul Hasan MM, Dutschk V, Brunig H, Mader E, Haussler L, Hassler R, Cherif Ch, Heinrich G (2008) Comparison of Tensile, Thermal, and Thermo-Mechanical Properties of Polyester Filaments Having Different Cross-Sectional Shape. Journal of Applied Polymer Science Vol. 111(2):805-812.
<https://doi.org/10.1002/app.29097>

[8] Becerir B, Karaca E, Omeroglu S (2007) Assessing colour values of polyester fabrics produced from fibres having different cross-sectional shapes after abrasion. Coloration Technology 123(4):252-259.
<https://doi.org/10.1111/j.1478-4408.2007.00092.x>

[9] Toydemir Y, Vatansever Bayramol D (2021) Properties investigation of polyester yarns with different cross-sections. BEU Journal of Science 10(1):170-176.
<https://doi.org/10.17798/bitlisfen.793752>

[10] Ozkan Hacıogulları S, Babaarslan O (2018) An investigation on the properties of polyester textured yarns produced with different fiber cross-sectional shapes. Industria Textila 69(4):270-276.
<http://doi.org/10.35530/IT.069.04.1281>

[11] Kim SS, Leem SG, Ghim HD, Kim HJ, Lyoo WS (2003) Microwave Heat Dyeing of Polyester Fabric. Fibers and Polymers 4(4): 204-209.
<https://doi.org/10.1007/BF02908280>

[12] Xu W, Yang C (2002) Hydrolysis and dyeing of polyester fabric using microwave irradiation. Coloration and Technology 118(5): 211-214.
<https://doi.org/10.1111/j.1478-4408.2002.tb00101.x>



16

ULUSLARARASI
LİF VE POLİMER
ARAŞTIRMALARI
SEMPOZYUMU

16th INTERNATIONAL FIBER AND POLYMER RESEARCH SYMPOSIUM

Sürdürülebilir ve İşlevsel Lif ve Polimerler
Sustainable and Functional Fibers & Polymers



9-10 Mayıs
May 2025

İstanbul Teknik Üniversitesi
Gümüşsuyu Prof. Dr. Necmettin Erbakan Yerleşkesi
İstanbul Technical University
Gumussuyu Prof. Dr. Necmettin Erbakan Campus

Spunbond dokusuz kumaş üretiminde bitim işlemi için yenilikçi bir prototip sisteminin geliştirilmesi

Halil İbrahim Çelik^a, Gülistan Canlı^b

^aTekstil Mühendisliği, Gaziantep Üniversitesi, 27310 Gaziantep, Türkiye.

^bLidersan Sağlık ve Gıda Ürünleri A.Ş., 27600 Gaziantep, Türkiye.

*Sorumlu Yazar: hcelik@gaziantep.edu.tr

ÖZET

Spunbond nonwoven kumaş üretiminde 3-5 metre enlerinde üretimler gerçekleştirilmektedir. Nonwoven kumaş kullanım alanına göre hidrofilik (suyu tutan) veya hidrofobik (su geçirmez) özellikte olabilmektedir. Spunbond kumaşlara hidrofilik veya hidrofobik özelliği, üretim esnasında gerçekleştirilen bitim işlemleri ile kazandırılmaktadır. Hidrofilik (su emici) ürün üretilirken, doğal olarak tüm kumaş eninde kiss-roll ile temas edilerek hidrofilik özellik kazandıracak kimyasal solüsyon kumaşa aktarılmaktadır. Ancak bazı müşteri taleplerinde farklı enlerden hidrofilik kumaşa ihtiyaç duyulmaktadır. Bu durumda hem hidrofilik hem de hidrofobik üretimi aynı anda yapılması gerekmektedir. Mevcut durumda farklı enlerde farklı özelliklerde (hidrofilik veya hidrofobik) üretim yapılması gerektiğinde çok fazla fire kumaş oluşmaktadır. Sunulan çalışma kapsamında Spunbond kumaşların farklı enlerde ve farklı özelliklerde üretilebilmesi amacı ile sistem tasarımları yapılmıştır. Geliştirilen sistem ile kısmi hidrofilik uygulaması için yenilikçi bir tasarım oluşturulmuştur. Mevcut kiss-roll makinelerine doğrudan adapte edilebilecek farklı tasarım örnekleri geliştirilmiştir. Daha sonra, tasarım alternatifleri için karar matrisi hazırlanarak en uygun tasarıma belirlenmiştir.

Anahtar Kelimeler: Spunbond kumaş; Hidrofilik; Hidrofobik; Sistem tasarımı; Kiss-roll

Development of an innovative prototype system for finishing in spunbond nonwoven fabric production

ABSTRACT

In Spunbond nonwoven fabric production, 3-5 metre widths are produced. Nonwoven fabric can be hydrophilic (water retaining) or hydrophobic (waterproof) according to the area of use. Spunbond fabrics are given hydrophilic or hydrophobic properties by finishing processes performed during production. When producing hydrophilic (water absorbent) products, the chemical solution that will provide hydrophilic properties is transferred to the fabric by contacting the kiss-roll in the entire fabric width. However, in some customer demands, hydrophilic fabrics of different widths are required. In this case, both hydrophilic and hydrophobic production should be done at the same time. In the current situation, when it is necessary to produce different properties (hydrophilic or hydrophobic) in different widths, a lot of waste fabric is formed. Within the scope of the presented study, system designs have been made in order to produce Spunbond fabrics in different widths and with different properties. With the developed system, an innovative

design has been created for partial hydrophilic application. Different design examples that can be directly adapted to existing kiss-roll machines have been developed. Then, a decision matrix was prepared for the design alternatives and the most suitable design was determined.

Keywords: Spunbond fabric; Hydrophilic; Hydrophobic; System design; Kiss-roll

I. GİRİŞ

Nonwoven sektöründe ve özellikle bebek bezi sektöründe yenilikçi ve katma değerli ürünler üretilmekte ve araştırmalar yapılmaktadır. Küresel olarak karşılaşılan sorunlar veya eksiklikler, Ar-ge alanında çalışan bilim insanlarını bu alanlarda yeni sistemler geliştirmeye teşvik etmektedir. Nonwoven sektörü son 10-15 yıldır hızla büyümektedir ve bu gelişmelere ciddi şekilde ihtiyaç duymaktadır.

Tek kullanımlık bebek bezi, tüm toplumlarda bebek ve çocuk sağlığı açısından önemli bir üründür. Günümüzde bebek bezleri eski bezlere göre çok daha ince ve emici olup cilt tahrişini ve bulaşıcı hastalıkları önlemede oldukça etkilidir. Nonwoven kumaşlar, çeşitli işlevlere sahip malzeme ve katmanların bir araya getirilmesiyle elde edilen bebek bezleri ve pedlerde geniş kullanım alanına sahiptir. İşlem adımlarını sürekli olarak gerçekleştiren modern bebek bezi makineleri 25 ila 45 metre uzunluğundadır. Tek kullanımlık bebek bezlerinin hijyenik ürünler pazarındaki payı %50'ye yakındır. Pazar otoritesi açısından dünyada ABD ve Çin firmaları öne çıkmıştır. Türkiye'de özellikle İstanbul bölgesi ve Gaziantep'te bebek bezi üretimi yoğun olarak yapılmaktadır. Bebek bezi ihracatı giderek artan ülkemizde Irak'a ihracat büyük oranda yapılmaktadır [1].

Bebek bezi üretiminde birçok katman bulunmaktadır. Bu katmanlar yukarıdan aşağıya şu şekilde sıralanabilir; topsheet, adl, corecover (üst doku), core (sap-palp karışımı), dustinglayer (alt doku), backsheet, cuff, frontear, backear, frontal tape, fastening tape. Bu katmanların bir kısmı gereksinimlerine göre hidrofilik

(su emici) bir kısmı ise hidrofobik (su itici) kumaşlardır. Ayrıca bu katmanlar ultrasonik bağlama veya laminasyon gibi bazı yöntemlerle birbirine nüfuz ettirilir. Bu nüfuz etme sırasında kumaşlar bazı işlem özellikleri nedeniyle birbirlerini olumsuz etkileyebilir. Spunbond kumaş hidrofilik veya hidrofobik özelliği, üretim esnasında gerçekleştirilen bitim işlemleri ile kazandırılmaktadır. Spunbond kumaş üreticileri, mevcut üretim kapasiteleri ve ürün siparişi durumuna göre hem hidrofilik hem de hidrofobik kumaşın eş zamanlı olarak üretilmesine yönelik çalışmalar yapmaktadır. Eş zamanlı olarak farklı özelliklerde ve farklı enlerde Spunbond kumaş üretimi yapılamadığı için üretimde çok fazla fire oluşmaktadır. Önceki çalışmalarda daha düşük fire ile daha kısa sürede farklı enlerde hidrofilik ve hidrofobik Spunbond kumaş üretimi için yaklaşımlar sunulmuştur.

Xavier ve arkadaşlarının (2007) yayınladığı [2] patent çalışmasında, Nonwoven kumaşların kısmi hidrofilik yapma işlemi plazma yöntemiyle ve enjeksiyon yapılarak denenmiştir.

Jankevics ve Roberts, tarafından sunulan patentte [3] emici bir maddenin tek bir bileşeninde üst tabaka ve bacak manşetinin ayrı işlevlerini birleştiren bölgesel hidrofilik bir SMS (Spunbond-Meltblown-Spunbond) üretilmiştir. Hidrofilik bir bölge oluşturmak için yüzey aktif madde ile muamele edilmiştir. Böylece SMS kumaşın yüzey aktif maddeyle kaplanmamış alanları hidrofobik özellik kazanırken bariyer kısmı işlevini yerine getirmektedir.

Kimyasal aplikasyon işlemi ile spunbond kumaşlara farklı fonksiyonel özellikler kazandırılması konusunda yapılmış çalışmalar bulunmaktadır [4-12].

Ancak, mevcut kiss-roll makinelerine adapte edilecek, kısmı olarak farklı enlerde hidrofilik ve hidrofobik özelliklerde kumaş üretimine imkân sağlayan sistem tasarımı konusunda yapılmış çalışmaya rastlanmamıştır. Fonksiyonel özellikler içerisinde en çok ihtiyaç duyulan ise hidrofilik özelliktir. Mevcut teknolojide Spunbond kumaşlara kimyasal aplikasyon tam en olarak uygulanmaktadır. Ancak, farklı enlerde kimyasal aplikasyon uygulanmak istediğinde manuel olarak kiss-roll adı verilen makine üzerinde modifikasyonlar yapılarak belirlenen ende kimyasal aktarımı engellenmektedir. Ancak, bu yöntem uzun zaman alan, maliyetli ve verimliliği düşük bir yöntemdir.

Sunulan çalışmada Spunbond üretim makinelerinde ve hatlarında kullanılabilecek yenilikçi bir çözüm geliştirilmiştir. Spunbond kumaş üretim hattının mevcut hidrofilik uygulama kısmına (kiss-roll ünitesine) aynı anda hem hidrofilik hem de hidrofobik üretim yapabilmek için yeni bir sistem tasarlanarak eş zamanlı ve verimli üretim mümkün kılınmıştır. Bu amaçla, farklı sistem tasarımları geliştirilerek bu sistemler karşılaştırılmıştır. Sonuç olarak, endüstriyel olarak uygulanabilecek en uygun sistem tasarımı belirlenmiştir.

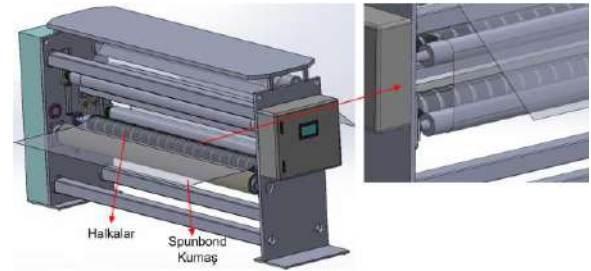
II. DENEYSEL METOT

Yapılan araştırmalarda neticesince bölgesel kimyasal uygulama için 3 farklı prototip tasarımı gerçekleştirilmiştir. Prototip sistem tasarımları Solidworks programı kullanılarak 3 boyutlu görsel haline getirilmiş ve detaylandırılarak gerçeğe çok yakın çizimler hazırlanmıştır. Bölgesel hidrofilik yapı oluşturmak amacı ile geliştirilen 3 farklı tasarım arasında karşılaştırma yapılarak tasarımların avantaj ve dezavantajları belirlenmiştir.

2.1 Tasarım-1: Halka Sistemi

İlk prototip, kiss-roll rulosu olarak kullanılmak üzere tasarlanmış tek bir silindir içermektedir. Ancak bu merdane standart kiss-roll merdanesine kıyasla daha düşük bir kalınlık sergilemektedir. Rulonun içinde hareketli halkaların bulunması kalınlığın azalmasına katkıda bulunmaktadır. Bu halkalar hidrofilik alanın ayarlanmasını kolaylaştırır. Halka boyutu 100 mm olarak seçilmiştir ve her ürünün boyutlarına göre ayarlanmasına izin vermektedir (Şekil 1).

Prototip tasarımı, Spunbond kumaş bir halkalı diğeri boş olmak üzere iki silindir arasından geçirilerek sarılmaktadır. Beslenen kumaş numunesi üzerinde hidrofilik ve hidrofobik olarak ayarlanmak istenilen enler belirlenerek sadece hidrofilik olarak hedeflenen bölgelerde halkaların yerleştirilmesi böylece sadece bu kısımlarda kimyasal aktarımının gerçekleştirilmesi sağlanacaktır.



Şekil 1. Halkalardan oluşan tasarım (patent başvurusu yapılmıştır)

Sistemin Avantajları:

- Ürün hidrofilik ve hidrofobik olarak istenilen ölçülerde makineden otomatik olarak üretililebilecektir.
- Hidrofilik kimyasalların transferi mevcut kiss-roll mantığında ve aynı teknikle olacağından herhangi bir proses değişikliğine gerek kalmayacaktır.
- Halka genişlikleri küçük olduğu için istenilen ürün uzunluğuna ve hedeflenen yola göre düzenleme yapmak mümkün olmaktadır.

Sistemin Dezavantajları:

- Kiss-roll benzeri bir silindir üzerindeki bu modifikasyon yüksek maliyet gerektirmektedir.
- Silindir üzerindeki halkaların istenilen ürüne göre ayarlanması çok zor bir işlemdir ve hem işçilik maliyetini artıracaktır hem de uzun zaman alacaktır.
- Tasarım, aktivasyon ve deaktivasyonun kolaylıkla sağlanamayacağı bir tasarımıdır.
- Devreye alma ve devre dışı bırakma işlemlerinin önemli zaman kaybına sebep olacağı öngörülmektedir.

2.2 Tasarım-2: Sıyırıcı Sistem

Sunulan tasarım, istenmeyen bölgelerde kimyasal maddelerin kiss-roll yüzeyinden uzaklaştırılmasını kolaylaştıran sıyırıcı aparatlar içermektedir (Şekil 2). Bu aparatların uygulanması ile, kimyasalın kumaşa geçmemesini sağlar ve böylece hidrofobik ve hidrofilik bölgelerden oluşan çift fazlı bir sistem oluşturulabilmektedir. Sistemin aktivasyon ve deaktivasyon süreci basit ve verimlidir. Otomatik kontrol sistemi ile sadece hedeflenen bölgelerdeki sıyırıcıların kiss-roll ile temas etmesi sağlanacaktır.

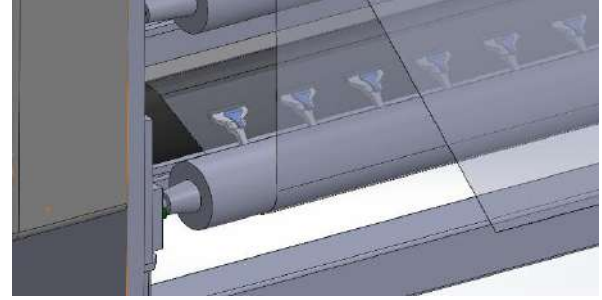
Sıyırıcıların sayısı ve konumu otomatik olarak ayarlanabilmektedir. Sunulan konfigürasyon, kullanıcının ihtiyacına bağlı olarak sıyırıcıların kiss-roll' e yakınlıklarını ayarlayarak geçici olarak etkinleştirilmesine veya devre dışı bırakılmasına olanak tanımaktadır.

Sistemin Avantajları:

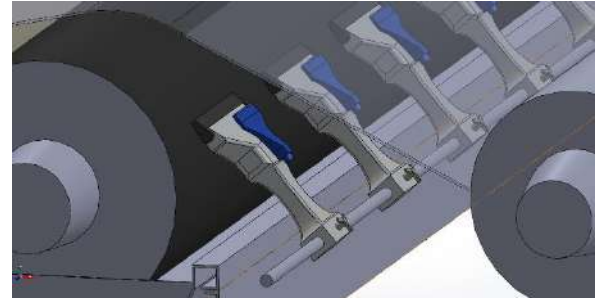
- Devreye alınması ve devre dışı bırakılması nispeten kolaydır.
- Otomasyon sistemine bağlanarak daha da kolaylaştırılabilir.
- İşçilik maliyeti yoktur.
- Üretime göre küçük genişliklerde sıyırıcılar kullanılacağından, istenen sayıda sıyırıcı kullanılarak ürünün istenen genişliği ayarlanabilir.

Sistemin Dezavantajları:

Sistemin sıyırıcı performansı çok önemlidir. Optimum sıyırma performansını sağlamak için uygun malzemelerin seçimi çok önemlidir. Yanlış malzeme seçimleri, sıyırıcının veya kiss-roll' un bütünlüğünü tehlikeye atma potansiyeline sahiptir ve sonuç olarak sürecin etkinliğini etkiler. Dahası, kiss-roll' un hasar görmesi önemli mali sonuçlara yol açabilir.



(a) Kiss-roll üzerinde sıyırıcılar



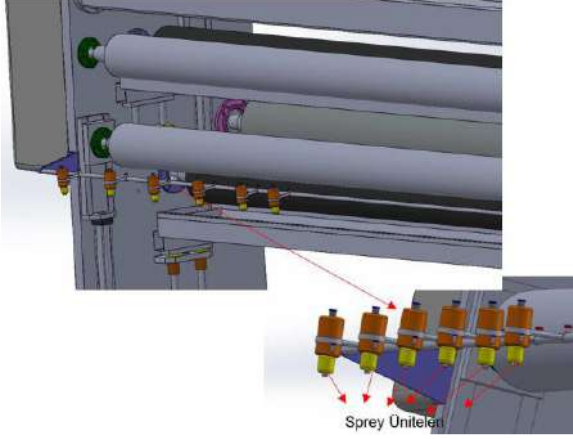
(b) Sıyıcı ünite detaylı

Şekil 2. Sıyırıcı Sistem (patent başvurusu yapılmıştır)

2.3 Tasarım-3: Sprey Sistemi

Tasarımda, püskürtme için özel nozullar ve valfler kullanılarak bölgesel hidrofilik işlem uygulanacaktır vermektedir (Şekil 3). Püskürtme başlıkları olarak kullanılan nozullar kiss-roll' den bağımsız olarak çalıştırılacaktır ve kimyasal hazneden çıkarılan solüsyon kumaş yüzeyine belirli bir hızda dağıtılacaktır. Kimyasalın dağılımı, kumaş yüzeyindeki erişimine göre hassas şekilde kalibre edilebilecektir. Bu amaçla, püskürtme valfleri tüm genişliği kapsayacak şekilde analiz edilerek konumlandırılacaktır. Sprey nozulu püskürme genişliğine göre nozulların sıklığı ve birbirine göre

mesafesi ayarlanacaktır. PLC otomasyon yazılımı ile pnömatik sistem kontrol edilecek ve hedeflenen bölgelerde kimyasal uygulaması için sadece ilgili valfler aktif hale getirilerek istenilen alana göre püskürme işlemi gerçekleştirilecektir.



Şekil 3. Sprey Sistemi (patent başvurusu yapılmıştır)

Sistemin Avantajları:

- Sistem, tüm genişliği boyunca düzenli aralıklarla püskürtme valfleri içerir.
- Bu valflerin etkinleştirilmesi ve devre dışı bırakılması kimyasalın bağlantısı kesilerek gerçekleştirilebilir.
- Sistem ek işçilik maliyetlerine neden olmaz.

Sistemin Dezavantajları:

- Sistemde damlama sorunu yaşanabilir.
- Püskürtme açısının ayarlanması zordur.
- Püskürtme dozaj miktarının belirlenmesi ve kontrol edilmesi de önemli bir sorundur.

III. BULGULAR VE TARTIŞMA

Geliştirilen tasarımlar avantaj ve dezavantajlarına göre karşılaştırma yapılarak değerlendirilmiştir. Tasarım karşılaştırması Tablo 1’de sunulmaktadır. İlk tasarım olan halka sistemi tasarımı önemli maliyetlere neden olduğu görülmektedir. Sistemin kurulumu devreye alınması ve devre dışı bırakılmasıyla ilgili süreçlerin diğer tasarımlara göre daha zor ve zaman alan süreçler

olduğu değerlendirilmiştir. Diğer taraftan, halka tasarımı yine yüksek işçilik maliyeti gerektirmektedir. Her bir çalışma eni için halkaların işçiler tarafından sisteme yerleştirilmesi gerekmektedir. Bu yüzden zaman alan ve işçilik maliyeti yüksek bir sistem olarak değerlendirilmiştir.

Üçüncü tasarım olan sprey sistemi halka sistemine göre nispeten bazı kolaylıklar ve daha düşük maliyetlere sahip olacağı öngörülmektedir. Sprey sistem kurulumunun orta düzeyde bir maliyete sebep olacağı, halka sisteminden daha düşük bir maliyet ile kurulabileceği düşünülmektedir. Sistemin kurulumunun daha kolay şekilde yapılabileceği ancak sistemin aktive edilmesi veya belirli bölgeler için devre dışı bırakılmasının orta düzeyde zorluk içereceği düşünülmektedir. Pnömatik sistem kontrolünün orta düzeyde zorluk içereceği düşünülmektedir. Ancak, uygulama sırasında uygulama açısını ve valfler aracılığı ile solüsyon dozajının ayarlanmasının zor olduğu da görülmüştür.

İkinci tasarım olan sıyrıcı sistem tasarımının düşük maliyetli ve kolay kurulumu sahip olacağı düşünülmektedir. Pnömatik sistemlerde çok daha fazla sayıda ekipmana ihtiyaç duyulduğu için sprey sistemine göre daha kolay kurulacağı düşünülmektedir. Sıyrıcı sistemde hedeflenen bölgede sıyrıcıların aktive edilmesi veya devre dışı bırakılması daha kolay şekilde kontrol edilebilecektir. Bu yüzden, sıyrıcı sistemin daha düşük maliyet ile daha kısa amortisman süresine sahip olacağı düşünülmektedir. Sıyrıcı sistemin iş gücü gereksinimi de diğer sistemlere göre çok daha düşüktür sadece bir operatör ile kontrol edilebilecektir. Bu tasarımların kapsamlı bir değerlendirmesi yapıldığında, sonuç olarak ikinci tasarım olan sıyrıcı sistem tasarımını diğer tasarımlara göre daha avantajlı olduğuna karar verilmiştir.

Tablo 1. Tasarım sistemlerin karşılaştırması

| Tasarım | Halka Sistemi | Sıyrıcı Sistem | Sprey Sistem |
|----------------------------|---------------|----------------|--------------|
| Maliyet | Yüksek | Düşük | Orta |
| Kurulum | Zor | Kolay | Kolay |
| Aktivasyon ve Deaktivasyon | Zor | Kolay | Orta |
| Amortisman | Uzun Süre | Kısa Süre | Kısa Süre |
| Ticarileşme | Zor | Kolay | Kolay |
| Üretilebilirlik | Zor | Kolay | Orta |
| İşçilik | Yüksek | Düşük | Orta |
| Kontrol Edilebilirlik | Zor | Kolay | Orta |

IV. SONUÇLAR

Sunulan çalışmada, Spunbond kumaş üretiminde farklı enlerde ve farklı özelliklerde ürünlerin aynı anda üretilmesine imkân sağlayacak sistem tasarımları gerçekleştirilmiştir. Mevcut kiss-roll ünitelerine adapte edilebilecek, istenilen enlerde hidrofilik ve hidrofobik kumaşların aynı anda üretilmesi amaçlanmıştır. Çalışma kapsamında üç farklı sistem tasarımı sunulmuştur. Geliştirilen sistemler; Halka Sistemi, Sıyrıcı Sistem ve Sprey Sistem olarak adlandırılmıştır. Sistem özellikleri açıklanarak, maliyet, kurulum, aktivasyon ve deaktivasyon, amortisman, ticarileşme, üretilebilirlik, işçilik ve kontrol edilebilirlik kriterlerine göre karşılaştırılmıştır. Sonuç olarak en uygun sistemin sıyrıcı sistem olduğuna karar verilmiştir. Endüstriyel sisteme adapte edildiğinde firelerin azaltılması, üretim maliyetlerinin düşürülmesi ve daha esnek üretim planlaması yapılabilmesi hedeflenmektedir.

TEŞEKKÜR

Bu çalışma 5230087 numaralı Tübitak 1505 projesi kapsamında Gaziantep Üniversitesi ile Üniversite-Sanayi projesi olarak desteklenmiştir.

KAYNAKLAR

[1]. Uyanık, S., & Baykal, P. D. (2016). Bebek bezi üretimi. Çukurova Üniversitesi Mühendislik-Mimarlık Fakültesi Dergisi, 31(2), 327-342. <https://doi.org/10.21605/cukurovaummfd.31030>

[2]. Trillas, X., Pano, R. G., & Riera, R. G. (2007). *U.S. Patent Application No. 11/296,926*.

[3]. Jankevics, J., & Roberts, G. (2000). U.S. Patent No. 6,139,941. Washington, DC: U.S. Patent and Trademark Office.

[4]. Ahmed, E. M. (2015). Hydrogel: Preparation, characterization, and applications: A review. *Journal of advanced research*, <https://doi.org/10.1016/j.jare.2013.07.006>

[5]. Dönmez, U., et al. (2019). A study on hydrophilic efficiency in disposable spunbond fabrics. *Journal of Industrial Textiles*, 49(8), 1020-1035. <https://doi.org/10.21923/jesd.445212>

[6]. Indi, Y. M., et al. (2014). Finishing of nonwovens: Effects of mechanical and chemical treatments. *Textile Finishing Journal*, 18(3), 215-230. <https://doi.org/10.1016/B978-0-12-818912-2.00011-2>

[7]. Onan, M. (2010). Disposable hydrophilic antimicrobial nonwoven laminated sheet. *Journal of Medical Textiles*, 22(4), 300-312. <https://doi.org/10.1108/09556221111136485>

[8]. Wang, C., et al. (2011). Enhancing the hydrophilic and antifouling properties of polypropylene nonwoven fabric membranes by the grafting of poly(N-vinyl-2-pyrrolidone) via the ATRP method. *Journal of Membrane Science*, 379(1-2), 191-200. <https://doi.org/10.1016/j.jcis.2011.01.094>

[9]. Wang, Z. (2019). Effect of polyethylene film lamination on the water absorbency of hydrophilic-finished polypropylene non-woven fabric. *Polymer Engineering & Science*, 59(7), 1452-1463. <https://doi.org/10.1007/s12221-019-8802-6>

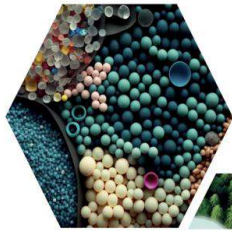
[10]. Zhou, X., et al. (2016). Fabrication of hydrophilic and hydrophobic sites on polypropylene nonwoven for oil spill cleanup: Two dilemmas affecting oil sorption. *Journal of*

*16. Uluslararası Lif ve Polimer Arařtırmaları Sempozyumu (16. ULPAS)
9-10 Mayıs 2025, İstanbul teknik Üniversitesi (İTÜ), Türkiye*

Environmental Management, 182, 295-302.

<https://doi.org/10.1021/acs.est.5b06007>

- [11]. Zhou, X., et al. (2016). Adsorption of phthalic acid esters (PAEs) by amphiphilic polypropylene nonwoven from aqueous solution: The study of hydrophilic and hydrophobic microdomain. Chemical Engineering Journal, 287, 185-195.
<https://doi.org/10.1016/j.jhazmat.2014.03.029>



16 ULUSLARARASI
LİF VE POLİMER
ARAŞTIRMALARI
SEMPOZYUMU

16th INTERNATIONAL FIBER AND POLYMER RESEARCH SYMPOSIUM

Sürdürülebilir ve İşlevsel Lif ve Polimerler
Sustainable and Functional Fibers & Polymers



9-10 Mayıs
May 2025

İstanbul Teknik Üniversitesi

Gümüşsuyu Prof. Dr. Necmettin Erbakan Yerleşkesi
İstanbul Technical University
Gumussuyu Prof. Dr. Necmettin Erbakan Campus

Effects of Hemp fiber content on yarn quality for Ring and Vortex yarns

Kübra Özşahin^a, Emel Çinçik^b, Hatice Kübra Kaynak^{*c}

^aMEM Textile R&D Department, Kahramanmaraş, Türkiye.

^bTextile Engineering Department, Erciyes University, Kayseri, Türkiye.

^cTextile Engineering Department, Gaziantep University, Türkiye.

*Corresponding author: tuluce@gantep.edu.tr

ABSTRACT

Hemp fiber is an important environmentally friendly fiber type due to its biobased and biodegradable character. It is important to determine the convenient fiber types, blend ratio and spinning technology for a good level of hemp yarn quality. In this study, in order to investigate the effects of hemp fiber content on yarn quality, polyester/cotton/hemp blended yarns were produced via Vortex and Ring spinning technology. As a result of this study, it is observed that the increase in hemp fiber content cause increase in yarn irregularity and thick place. Also, higher hairiness values are observed for hemp blended Ring yarn samples in this study. Strength values of Ring yarns are higher than Vortex yarns, but not consistent regarding yarn number or hemp fiber content.

Keywords: Hemp Fiber; Yarn Quality; Vortex Yarn; Ring Yarn

I. INTRODUCTION

Hemp is a very important industrial plant used in many different areas. While the seed part of hemp is evaluated as food material or flour by breaking the shell, oil is obtained from the seed by pressing. The obtained oil is widely used in food, biofuel, paint and cosmetics. Its pulp is used as food material such as animal feed, beer or protein powder. The stalk part is peeled and the fiber part is separated. Depending on the quality of the fiber part, it is used as raw material in products such as fabric, textile products, panel production, cellulose, paper. The remaining part after the fiber is separated from the hemp stalk is evaluated

in many areas such as animal feed, compost, animal bedding or mortar material in the construction sector. The flower part is mostly used in the pharmaceutical and cosmetic industries, while the pulp can be used as fish feed, fertilizer and animal bedding. The strong and hard fiber structure of hemp fibers has a hardness similar to glass fibers, and therefore hemp fibers can also be used as reinforcement material in composite structures [1-8].

In the literature, there are studies examining the properties of yarns produced from blends of hemp fiber with different fiber types. In the production of microporous polyester and hemp fiber blended yarn, it

has been reported that the strength decreases as the hemp fiber ratio increases in the yarn structure. It was also observed that the yarn has a more regular structure and the elongation at break increases with the increase in the polyester ratio in the structure. It was stated that the yarn irregularity depends on the hemp length distribution [9]. For 100% cotton and 70%/30% cotton hemp blended ring yarns and dual-core yarns with T400 and elastane in the core, it was found that hemp blended yarns had higher irregularity, imperfection and hairiness values, lower breaking strength and higher elongation at break [10]. It was observed that thin place, thick place and nep defects increased with the increase in hemp fiber ratio in hemp blended core yarns. On the other hand, it was determined that strength decreased with the increase in hemp fiber ratio in the yarn and that filament cores in the center contributed positively to yarns strength [11]. For single core and double core ring yarns with hemp fiber blend, it was observed that the addition of core component to yarn structure have no effect on yarn irregularity. On the other hand, thick place, thin place and nep faults were higher in double core yarns than single core yarns. Also, the faults increased even more with the addition of lycra and lycra+T400 as the core component. Yarn samples containing hemp had higher yarn faults. Regarding the yarn hairiness, it was observed that the addition of lycra and lycra+T400 as the core component in double core yarns have no effect on yarn hairiness [12]. In a study, 20%/80% hemp/cotton blended open-end and ring yarns produced with different yarn counts which contain hemp fibers that have treated to bleaching, cottonizing and degumming processes were compared with 20%/80% linen/cotton blended yarns. It was determined that open-end yarns produced with hemp fibers that were treated to bleaching, cottonizing, degumming processes exhibited superior properties in terms of yarn irregularity and yarn defects compared to linen blended yarns, and exhibited similar properties

in terms of hairiness and strength. When linen and hemp blended ring yarns were compared, it was stated that the yarns showed similar properties in terms of strength and elongation, irregularity, thin places, thick places, hairiness [13]. In ring yarns produced with different blend ratios of hemp fiber and cotton, viscose, lyocell fibers, it was observed that yarn strength and elongation decreased with the increase in the hemp ratio in the blends, and yarn irregularity, defects, and hairiness increased [14]. In the study examining the liquid absorption, drying, strength, and electrical conductivity properties of yarns produced from hemp and flax fibers, it was stated that linen and hemp yarns produced in wet condition from fibers treated to boiling and bleaching processes had higher liquid absorption capacity. It was determined that wet strength values for linen and hemp yarns were higher than dry strength values [15].

Hemp fiber textile products are gaining importance gradually due to its environmentally friendly properties. So, it is important to determine the convenient fiber types, blend ratio and spinning technology for a good level of yarn quality and production efficiency. It will be possible to produce high quality textile products by optimizing the process parameters in hemp yarn production.

II. EXPERIMENTAL METHOD

In this study, in order to investigate the effects of hemp fiber content on yarn quality, polyester/cotton/hemp blended yarns were produced via Vortex and Ring spinning technology. Polyester, cotton and hemp fiber properties used in the study are given in Tables 1, 2 and 3, respectively.

Table 1. Polyester fiber properties used in the study

| Property | Value |
|---------------------------|-------|
| Fiber fineness (denier) | 1,21 |
| Fiber length (mm) | 39,2 |
| Fiber strength (g/denier) | 6,96 |
| Elongation (%) | 18,68 |

Table 2. Cotton fiber properties used in the study

| Property | Value |
|--------------------------------------|-------|
| Fiber fineness (<i>micronaire</i>) | 5,02 |
| Fiber length (<i>mm</i>) | 29,17 |
| Fiber strength (<i>g/tex</i>) | 32,8 |
| Elongation (%) | 7,1 |

Table 3. Hemp fiber properties used in the study

| Property | Value |
|-----------------------------------|-------|
| Fiber fineness (<i>tex</i>) | 4,1 |
| Fiber length (<i>mm</i>) | 70 |
| Fiber strength (<i>cN/dtex</i>) | 4,7 |
| Elongation (%) | 3 |

In this study, Ne 10/1, Ne 20/1 Ring and Vortex spun yarns were produced with blends of 50/50% Cotton/Polyester, 48/47/5% Cotton/Polyester/Hemp, 45/45/10% Cotton/Polyester/Hemp, 40/40/20% Cotton/Polyester/Hemp. In addition, Ne 30/1 Ring and Vortex spun yarns were produced with blends of 50/50% Cotton/Polyester, 48/47/5% Cotton/Polyester/Hemp, 45/45/10% Cotton/Polyester/Hemp. By this way, a total of 22 yarn samples were obtained. In order to determine the yarn quality levels; yarn unevenness, number of thin place and number of thick places, neps and hairiness values were determined by Uster Tester device. Yarn breaking strength and breaking elongation were measured by the Uster Tensojet device.

III. RESULTS AND DISCUSSIONS

In the study, for yarn quality CVm, number of thin places (-50%), number of thick places (+50%) and hairiness test results were investigated and test results are given in Figures 1-4, respectively.

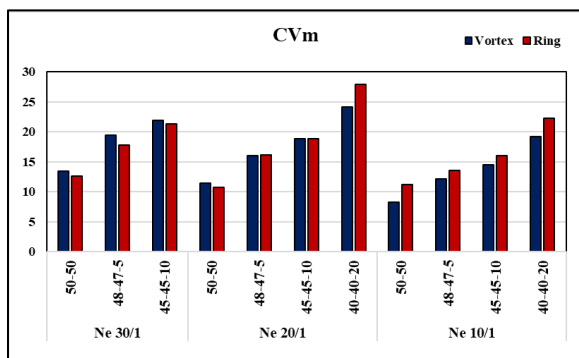


Figure 1. CVm values for yarn samples

As it can be seen in Figure 1, irregularity values increase with the increase in hemp content for all

samples. Also, the irregularity values are increased as the yarns get finer. Regarding the yarn spinning technology, there is no consistent trend in yarn irregularity.

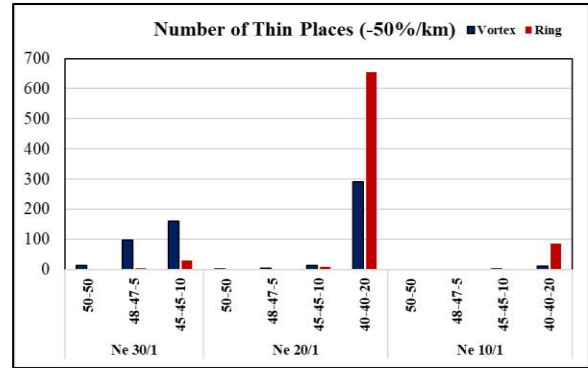


Figure 2. Number of thin places for yarn samples

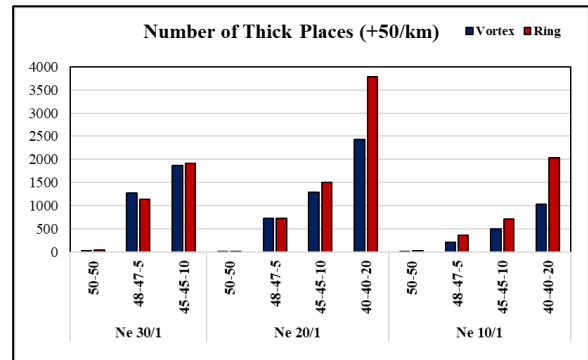


Figure 3. Number of thick places for yarn samples

If Figures 2 and 3 are considered for number of thin and thick places, the values of thin places do not exhibit a tendency according to hemp content, yarn number or yarn spinning technology. On the other hand, number of thick places continuously increase as the hemp fiber content increase and yarns get finer. Also, in general yarns produced with ring spinning technology have higher number of thick places.

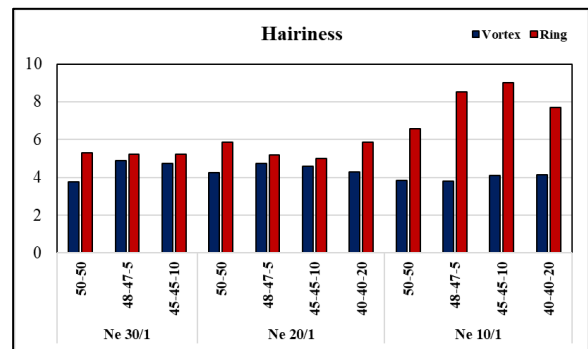


Figure 4. Hairiness of yarn samples

In Figure 4, hairiness values of sample yarns are seen. It can be seen that the most considerable effect on yarn hairiness is yarn spinning technology that ring yarn samples have higher yarn hairiness values. The effect of yarn spinning technology on hairiness is especially obvious for Ne 10/1 yarn samples. The lower hairiness values of Vorteks yarns can be attributed to presence of wrapping fibers around yarn body.

In the study, yarn strength and elongation values were investigated and the test results are given in Figures 5 and 6, respectively.

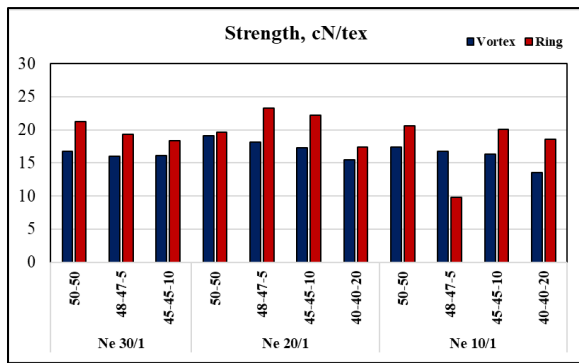


Figure 5. Strength of yarn samples

As it can be seen from Figure 5, there is a consistent decrease in yarn strength as the hemp fiber content increase for only Vortex yarn samples. On the other hand, Ring yarn samples generally have higher yarn strength values but there is no consistent effect of yarn number or hemp fiber content on yarn strength for Ring yarn samples.

For yarn breaking elongation values which are seen in Figure 6, Ring yarn samples have higher breaking elongation than Vorteks yarn samples. On the other hand, there is no consistent effect of yarn number or hemp fiber content on yarn elongation.

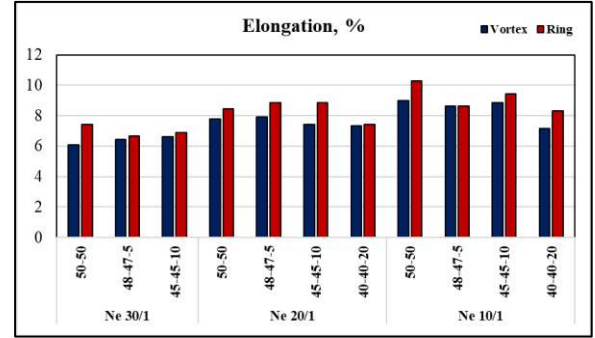


Figure 6. Breaking elongation of yarn samples

IV. CONCLUSIONS

This study aims to investigate the effects of hemp fiber content, yarn spinning technology and yarn number on yarn quality and strength for hemp blended yarns. As stated in the previous studies, the increase in hemp fiber content caused increase in yarn irregularity and thick place. Also, higher hairiness values for Ring yarn samples are observed in this study. This result was later contradicted by Satil et. al. [14]. Strength values of Ring yarns are higher than Vortex yarns but not consistent regarding yarn number or hemp fiber content. Consequently, considering mostly desired yarn quality parameters increasing the hemp fiber content negatively affects yarn quality. Also, similar yarn quality levels can be achieved with Vortex spinning technology instead of Ring spinning technology with lower cost by eliminating production steps.

ACKNOWLEDGMENT

This study was supported by TUBİTAK-TEYDEB with the project number of 5220147.

REFERENCES

- [1] Thomsen, A. B., Thygesen, A., Bohn, V., Nielsen, K.V., Pallesen, B., & Jorgensen, M.S. (2006). Effects of chemical-physical pre-treatment processes on hemp fibres for reinforcement of composites and for textiles, *Industrial Crops and Products*, 24(2):113-118. <https://doi.org/10.1016/j.indcrop.2005.10.003>
- [2] Chen, Y., Sun, L., Negulescu, I., Wu, Q., & Henderson, G. (2007). Comparative Study of Hemp Fiber for Nonwoven Composites, *Journal*

- of Industrial Hemp, 12(1):27–45.
https://doi.org/10.1300/J237v12n01_04.
- [3] Shahzad A. (2012). Hemp fiber and its composites – a review, *Journal of Composite Materials*, 46(8): 973-986. doi:10.1177/0021998311413623
- [4] Liu, M. (2016). Pretreatment of hemp fibers for utilization in strong biocomposite materials. PhD thesis. Technical University of Denmark, Denmark.
- [5] Oran, (2019). Kenevir Yetiştiriciliği. ORAN Kalkınma Ajansı. https://www.oran.org.tr/images/dosyalar/20190318134910_0.pdf
- [6] Manaia, J.P., Manaia, A.T., & Rodrigues, L. (2019). Industrial Hemp Fibers: An Overview. *Fibers*, 7(12), 106:1-16. <https://doi.org/10.3390/fib7120106>
- [7] Başer, U., & Bozoğlu, M. (2020). Türkiye'nin Kenevir Politikası ve Piyasasına Bir Bakış. *Tarım Ekonomisi Araştırmaları Dergisi*, 6(2):127-135.
- [8] Demirek, D., & Oktav Bulut, M. (2021). Kenevir Liflerinin Eldesi, Özellikleri ve Kompozit Uygulama Alanları. *Bartın University International Journal of Natural and Applied Sciences*, 4(2):176-191.
- [9] Zhang, H., Zhang J., & Gao, Y. (2014). Study on the Relationship Between Blending Ratio and Performance of Hemp/Polyester Yarn, *Journal of Natural Fibers*, 11(2):136-143. <https://doi.org/10.1080/15440478.2013.861780>
- [10] Avcı Ertek, M., Yıldırım, N., & Türksöy, H. G., (2019, Eylül). %70/%30 Pamuk Kenevir Karışımı Ring ve Dual-Core İpliklerin Fiziksel Özelliklerinin Karşılaştırılması Olarak İncelenmesi. *Ulusal Çukurova Tekstil Kongresi*, 481-486.
- [11] Avcı Ertek, M., & Demiryürek O. (2022). Development of sustainable and ecological hybrid yarns. *Hemp Fiber in Denim Fabric Production, Cellulose Chemistry and Technology*, 56 (9-10):1089-1100. 10.35812/cellulosechemtechnol.2022.56.97
- [12] Okyay, G., Demiryürek, O., Avcı, M., & Bilgiç, H., (2023). Development and characterization of hemp-containing hybrid yarns for clothing, *Cellulose Chemistry and Technology*, 57(1-2):193-206. 10.35812/cellulosechemtechnol.2023.57.19
- [13] İbrakçı, A., Oruç, A., & Tarakçı A. (2020, Kasım). Sürdürülebilir Tekstil için Kenevir Elyafından Farklı İplik Yapılarının Geliştirilmesi. *İTÜ Ulusal Tekstil Kongresi ve II. Ar-Ge Günü, Akademi Sanayi Buluşması*, 67-69.
- [14] Satıl, Ş., Çelikten E., Özden, K., & Nacarkahya T. (2020, Kasım). Optimization of yarn Quality parameters of hemp fiber blended yarn produced by ring spinning system. *The International Conference of Materials and Engineering Technology TICMET*, 402-415
- [15] Mustata, A., & Mustata F.C. (2013). Moisture Absorption and Desorption in Flax and Hemp Fibres and Yarns, *Fibres & Textile in Eastern Europe*, 21, 3 (99): 26-30.



Amphiphilic Functional Polymers as Polypropylene Nonwoven Surface Treatment

Mehmet Sinan Tübcil^{a,b}, Saeed Salamatgharamaleki^{a,c}, Şebnem Kemaloğlu Doğan^d, Bekir Dızman^{a,c,*}

^a Integrated Manufacturing Technologies Research and Application Center & Composite Technologies Center of Excellence, Sabanci University, Istanbul, Turkey

^b Molecular Biology, Genetics and Bioengineering Program, Faculty of Engineering and Natural Sciences, Sabanci University, Istanbul, Turkey

^c Materials Science and Nano Engineering Program, Faculty of Engineering and Natural Sciences, Sabanci University, Istanbul, Turkey

^d Hayat Kimya R&D Center, Kocaeli, Turkey

*Corresponding author: bekir.dizman@sabanciuniv.edu

ABSTRACT

Polypropylene nonwovens (PP NWs) are utilized commonly in baby diapers, adult incontinence products, feminine hygiene items, and wet wipes. Due to the inherent hydrophobic character of these NWs, their properties are significantly influenced by hydrophilic surface treatments to enhance both their performance and the user experience. Although polymer-based formulations offer great versatility, small molecule applications are more prominent in industry. This study proposes an amphiphilic functional polymer-based surface treatment for NW disposable hygiene products. Such polymer offers odor control, enzymatic inhibition, pH control, controlled release of active agents, and antimicrobial activity. This article discusses the synthesis of the as-utilized polymer, succinylated Poly(2-propyl-2-oxazoline-co-ethyleneimine) (S-PPrOZ-PEI), and its characterization by both Fourier-Transform Infrared Spectroscopy (FTIR) and Nuclear magnetic resonance (NMR). Additionally, the preparation of a dilute polymer-based aqueous formulation, and its utilization as a surface treatment to PP NWs are described here. S-PPrOZ-PEI modifies the PP NW surface through its hydrophobic interactions with PP and makes the surface more hydrophilic due to the presence of acid functional groups in its structure. The performance of the applied formulation is evaluated through contact angle measurements, and then they are compared to commercial small-molecule-based surface treatment formulations, which are found to be similar.

Keywords: Nonwoven Surface Treatments, Amphiphilic Polymers, Hydrophilicity, Contact Angle

I. INTRODUCTION

Poly(2-alkyl-2-oxazoline)s (POZ) have garnered significant attention in recent years due to their tunable physicochemical properties, biocompatibility, and potential for post-polymerization modifications. Among them, poly(2-propyl-2-oxazoline) (PPrOZ) is of particular interest owing to its slightly hydrophobic nature, and capability to be modified to obtain amphiphilic structures, which makes it a promising candidate for surface modification as well as biomedical applications. However, its inherently limited hydrophilicity poses a challenge for

applications where enhanced wettability, and aqueous compatibility are desired.

Surface hydrophilization of polymeric substrates, especially NW materials composed of PP, is critical in various fields, including filtration, medical textiles, and personal care products. These materials are naturally hydrophobic, which limits their ability to interact with the aqueous media. As a result, considerable research efforts have focused on developing effective surface functionalization strategies to modulate their wettability [1].

In this study, a multi-step chemical approach to enhance the hydrophilic properties of PP NW substrates through tailored polymer coatings is reported. Initially, a PPrOZ homopolymer was synthesized through a cationic ring-opening polymerization (CROP), and then it was subsequently hydrolyzed to obtain a copolymer with poly(ethyleneimine) (PEI) segments. The as-hydrolyzed copolymer was then subjected to succinylation, which introduced pendant carboxylic acid groups, and yielded the S-PPrOZ-PEI derivative. The as-modified polymers were characterized by both ^1H NMR and FTIR spectroscopy to confirm successful structural transformations at each stage.

To assess the surface performance of these polymers, contact angle measurements were conducted on PP NW substrates treated with PPrOZ, S-PPrOZ-PEI, and two different commercial benchmark formulations. By analyzing the dynamic behavior of water droplets on the as-treated surfaces, the influence of each formulation on the NW materials' surface was evaluated.

This work aims to contribute to the development of next-generation surface functionalization methods by using tailored polyoxazoline-based polymers, offering a sustainable and efficient alternative to conventional hydrophilic coatings for polymeric substrates.

II. EXPERIMENTAL METHOD

2.1 Synthesis of PPrOZ Homopolymer

The synthesis of PPrOZ homopolymer was carried out following the previously established methodologies by the current research group [2,3]. Briefly, the monomer (2-propyl-2-oxazoline) and chlorobenzene were added into a N_2 -purged, oven-dried round-bottom flask. The monomer concentration of the monomer was adjusted to 4M. Here, trifluoromethanesulfonic acid (TfOH) was employed as the initiator, and a monomer-to-initiator ratio

($[\text{M}]/[\text{I}]$) of 50 was maintained to achieve a targeted molecular weight of approximately 5,000 g/mol. The polymerization was quenched by the addition of a methanolic potassium hydroxide (KOH) solution. After the termination of the polymerization, solvents were removed under reduced pressure. The residual solids were dissolved in dichloromethane (DCM) and then filtered. The organic phase was dried by using sodium sulfate (Na_2SO_4) and filtered. Following the DCM's evaporation, the polymer was redissolved in methanol, and then it subsequently precipitated in cold diethyl ether ($(\text{C}_2\text{H}_5)_2\text{O}$).

2.2 Hydrolysis of PPrOZ Homopolymer

Hydrolysis of the PPrOZ homopolymer was performed in accordance with current group's earlier kinetic studies, and protocols¹. The homopolymer was weighed and dissolved in 4 M HCl solution in a two-neck flask. The reaction was proceeded at 100 °C for 52 minutes to reach approximately 25% hydrolysis level. Following the reaction, the aqueous phase was washed once with diethyl ether, and then, neutralized with sodium hydroxide (NaOH) until the pH exceeded 10. Water was removed via evaporation, and the remaining material was first dissolved in ethanol, and then filtered, and subjected to further solvent removal under reduced pressure. The residual solids were redispersed in acetonitrile and maintained at 50 °C. The resulting mixture was filtered by using a Büchner funnel, and the organic layer was collected. After evaporating the solvent under vacuum, the PPrOZ-PEI copolymer was successfully isolated.

2.3 Succinylation of PPrOZ-PEI Copolymer

Succinylation of the PPrOZ-PEI copolymer was conducted in acetonitrile as the reaction medium. Initially, 4.16 g (0.9 mmol, 1 equivalent) of the copolymer was placed into a dry round-bottom flask,

followed by the addition of 44 mL acetonitrile. The residual moisture was removed through azeotropic distillation, and 25 mL of the solvent was evaporated under vacuum. Succinic anhydride (1.17 g, 10 mmol, 12.60 equivalents) and triethylamine (3.25 g, 30 mmol, 36 equivalents) were then introduced. The mixture was refluxed under N₂ atmosphere at 80 °C for 24 h. Upon reaction completion, excess triethylamine and the solvent were removed under reduced pressure. The resulting solids were dissolved in 15 mL methanol, and then they precipitated into 250 mL of cold diethyl ether. After filtration, the polymer was redissolved in 40 mL of alkaline water (pH > 10) and extracted with 150 mL of diethyl ether. The aqueous layer was collected, acidified down to pH 2, and the remaining water was removed under vacuum. The final product was dissolved in 45 mL ethanol, filtered to remove NaCl, and the ethanol was evaporated to yield 4.8 g of S-PPrOZ-PEI as a light brown solid (Yield: 89%).

2.4 Characterization of Polymers

To verify the structures of the as-synthesized PPrOZ, PPrOZ-PEI, and S-PPrOZ-PEI polymers, proton nuclear magnetic resonance (¹H NMR) spectroscopy was carried out on 500 MHz Varian spectrometer by using CDCl₃ and CD₃OD as solvents. Also, the FTIR spectra were collected on a ThermoScientific Nicolet iS50 instrument equipped with an attenuated total reflectance (ATR) accessory.

2.5 Contact Angle Measurements

The performance of the formulations was assessed by contact angle measurements. In this method, a water droplet is placed on as-prepared PP NW samples, and its behavior is monitored over time. The droplet's movement is recorded by using a high-resolution camera, and the contact angle values at specific time

intervals are determined through a dedicated image analysis software.

III. RESULTS AND DISCUSSIONS

The synthesis of PPrOZ homopolymer via CROP yielded a sample with well-defined spectral characteristics that are consistent with the previous reports about POZ systems.

In the ¹H NMR spectrum of the PPrOZ homopolymer, the signal appeared in the range of $\delta_a = 3.80\text{--}3.28$ ppm (4H), corresponds to the methylene protons of the $-\text{CH}_2\text{--CH}_2\text{--N}-$ segments in the polymer backbone. Additionally, the propyl side chain protons were identified at $\delta_c = 2.22\text{--}2.47$ ppm (2H, $-\text{CH}_2$), $\delta_d = 1.50\text{--}1.71$ ppm (2H, $-\text{CH}_2$), and $\delta_e = 0.85\text{--}1.05$ ppm (3H, $-\text{CH}_3$), as respectively shown in **Figure 1**.

Following the hydrolysis process, a new signal in the range of $\delta_b = 3.00\text{--}2.65$ ppm (4H) was observed and was assigned to the $-\text{NH--CH}_2\text{--CH}_2-$ polymer backbone protons of the resulting ethyleneimine units. The hydrolysis degree was calculated in accordance with a previous study¹, by using the PPrOZ-PEI sample showing a hydrolysis rate of 23% after 52 minutes of reaction. Upon subsequent modification with succinyl anhydride, the peak attributed to the ethyleneimine units disappeared, and it had replaced by a new peak at $\delta = 2.35\text{--}2.60$ ppm, corresponding to the methylene protons on the carboxylic acid side chains, confirming the successful succinylation.

Complementary FTIR analyses of PPrOZ 5K, PPrOZ-PEI, and S-PPrOZ-PEI are presented in **Figure 2**. All polymers exhibited characteristic CH₃ and CH₂ stretching vibrations at 2873–2961 cm⁻¹ region, along with polyamide carbonyl (C=O) bands at 1626 cm⁻¹. In the FTIR spectrum of PPrOZ-PEI, a peak appeared at 3296 cm⁻¹, corresponding to the $-\text{NH}$ stretching vibration of the ethyleneimine units, which was absent

in the PPrOZ 5K homopolymer. Additionally, the band at 1135 cm^{-1} , attributed to C–N stretching of secondary amines, further supported the presence of hydrolyzed units. As for S-PPrOZ-PEI, a distinct C=O stretching vibration was observed at 1728 cm^{-1} , confirming the presence of carboxylic acid groups. The complete disappearance of the –NH stretch in the modified polymer further indicated the successful and complete conversion during the succinylation step.

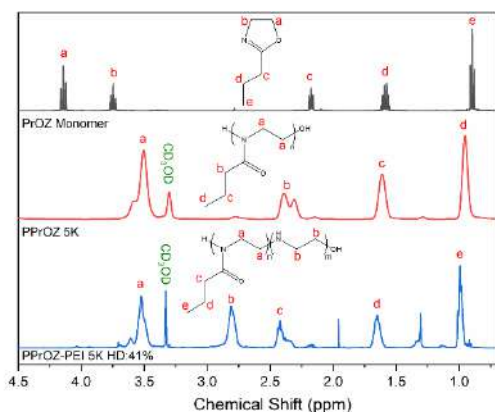


Figure 1. ^1H NMR spectra of PPrOZ, PPrOZ-PEI, and S-PPrOZ-PEI polymers.

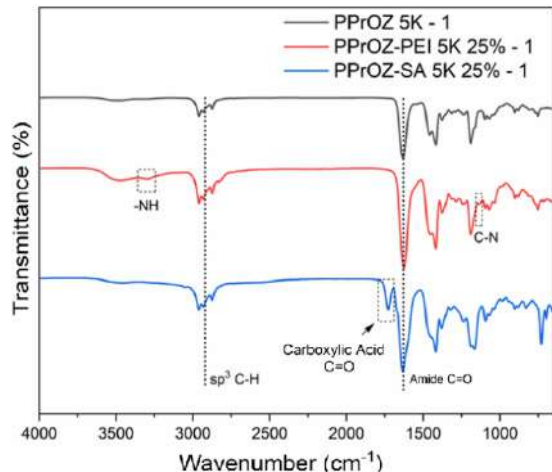


Figure 2. FTIR spectra of PPrOZ, PPrOZ-PEI, and S-PPrOZ-PEI polymers.

Here, the contact angle measurements revealed that the untreated NW samples exhibited a highly hydrophobic character, as expected (**Table 1**). The application of the PPrOz-based formulation resulted in a moderate decrease in contact angle values; however, it did not reach the level of hydrophilicity observed in commercial formulations. In contrast, the S-PPrOZ-PEI formulation demonstrated a notable enhancement

in surface hydrophilicity. The comparative analysis of both initial ($t = 0\text{ s}$) and later ($t = 3\text{ s}$) time points further emphasized the superior wetting performance of the commercial formulations. Water droplets applied to the as-treated surfaces spread rapidly, their indicating improved surface wettability.

Table 1. Contact angle degrees of both treated and untreated PP NW samples

| Sample | t=0s (left) | t=3s (right) | t=0s (left) | t=3s (right) |
|-------------------------------------|----------------|-----------------|----------------|-----------------|
| Washed untreated NW | 140,36 | 139,53 | 139,03 | 138,73 |
| Commercial formulation-1 treated NW | 115,90 | 117,50 | 65,86 | 64,99 |
| Commercial formulation-2 treated NW | 107,59 | 109,15 | 19,57 | 21,97 |
| PPrOz Treated NW | 137,78 | 138,24 | 137,72 | 137,26 |
| 1% S-PPrOZ-PEI treated NW | 122,05 | 118,57 | 117,98 | 115,73 |

The contact angle measurements provided quantitative insights into the wettability performance of the formulations applied on PP NW substrates. Here, the untreated and simply washed PP NWs exhibited contact angles greater than 139° , affirming their inherent hydrophobicity. Additionally, the treatment with the PPrOZ homopolymer slightly reduced the contact angle to $\sim 137^\circ$, suggesting limited surface interactions due to the polymer's amphiphilic but mostly hydrophobic character. In contrast, the S-PPrOZ-PEI-coated surfaces demonstrated a substantial reduction in contact angle (122.05° at $t = 0\text{ s}$, 115.73° at $t = 3\text{ s}$), revealing their enhanced surface hydrophilicity.

When compared with two commercial hydrophilic coatings, S-PPrOZ-PEI showed competitive yet moderate performance. The commercial formulation-2 resulted in the lowest contact angle of 19.57° , indicating rapid water spreading likely due to the presence of high-density hydrophilic or surfactant groups. However, it is worth noting that such formulations may exhibit lower durability or

biocompatibility compared to polyoxazoline-based coatings, which offer both a balance in functionality and the environmental compatibility.

The results demonstrate that the introduction of carboxylic acid groups onto the PPrOZ backbone via succinylation significantly improves surface wettability, positioning S-PPrOZ-PEI as a promising eco-friendly alternative for polymeric surface's modification. The controlled tunability of hydrophilicity through partial hydrolysis and further functionalization possibility underscores the potential of poly(oxazoline) chemistry for advanced surface engineering applications.

IV. CONCLUSIONS

In this study, a new PPrOZ homopolymer was successfully synthesized, and then post-functionalized through both partial hydrolysis and subsequent succinylation to obtain carboxylated polyethylenimine-based derivatives. Her the as-prepared sample's structural characterization by ¹H NMR and FTIR confirmed the efficiency of each modification step. The final product, S-PPrOZ-PEI, demonstrated significantly improved wettability performance on PP NW surfaces compared to the unmodified polymer.

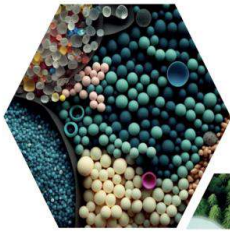
The contact angle results revealed that the carboxylic acid functionalization effectively enhanced the surface hydrophilicity, though not to the extent of commercial hydrophilic coatings. However, the poly(oxazoline)-based formulation offers advantages in terms of chemical tunability, potential biocompatibility, as well as the environmental safety. These findings support the potential of S-PPrOZ-PEI as a promising candidate for hydrophilic surface modification of polymeric materials.

ACKNOWLEDGMENTS

This study was supported by Türkiye Bilimsel ve Teknolojik Araştırma Kurumu; Scientific and Technological Research Council of Turkey (TÜBİTAK), Grant Numbers: 5220091, 118C047

REFERENCES

- [1] Tubcil, MS, Kemaloglu Dogan, S, & Dizman, B (2025). Nonwoven surface treatments for disposable hygiene products. *Polymer Engineering & Science*, 65(3), 950–969. doi:10.1002/pen.27099
- [2] Salamatgharamaleki, S, Atespare, AE, Behrooz Kohlan, T, Yildiz, M, Menciloglu, YZ, Unal, S, & Dizman, B (2025). Partially Hydrolyzed Poly(2-alkyl/aryl-2-oxazoline)s as Thermal Latent Curing Agents: Effect of Composition and Pendant Groups on Curing Behavior. *ACS Omega* 10,6753–6767. <https://doi.org/10.1021/acsomega.4c08659>
- [3] Atespare, AE, Behrooz Kohlan, T, Salamatgharamaleki, S, Yildiz, M, Menciloglu, YZ, Unal, S, & Dizman, B (2024) Poly(2-alkyl/aryl-2-oxazoline)-Imidazole Complexes as Thermal Latent Curing Agents for Epoxy Resins. *ACS Omega* <https://doi.org/10.1021/acsomega.4c03904>.



16

ULUSLARARASI
LİF VE POLİMER
ARAŞTIRMALARI
SEMPOZYUMU

16th INTERNATIONAL FIBER AND POLYMER RESEARCH SYMPOSIUM

Sürdürülebilir ve İşlevsel Lif ve Polimerler
Sustainable and Functional Fibers & Polymers



9-10 Mayıs
May 2025

İstanbul Teknik Üniversitesi
Gümüşsuyu Prof. Dr. Necmettin Erbakan Yerleşkesi
İstanbul Technical University
Gumussuyu Prof. Dr. Necmettin Erbakan Campus

Blown Üretim Teknolojisi ile Hafızalı ve İşlevsel Elastik Film Üretimi

İlker TÜRKMEN, Akif DİK

Lidersan Sağlık ve Gıda Ürünleri A.Ş. Arge Merkezi, 27500, Gaziantep, Türkiye.

*İlker TÜRKMEN: ilker.turkmen@altunkaya.com

Akif DİK: akif.dik@altunkaya.com

ÖZET

Elastik filmler; esnek, gerilebilir ve hafızalı bir yapıya sahip ince malzeme tabakalarına (film) verilen isimdir. Bu tür filmler, elastomer bazlı polimerlerden yapılır ve yüksek oranda hafızası olması nedeniyle eski formuna dönebilme özelliğine sahiptir. Bu özellikleri onları çok çeşitli uygulamalarda kullanışlı hale getirir. Bebek bezleri, bir çok farklı komponentin bir araya gelmesiyle oluşan kompleks bir yapıdır ve bu komponentlerden bir tanesi de esnek kulakçıklardır. Esnek kulakçıklar, iki nonwoven kumaş arasına ultrasonik olarak lamine edilen elastik bir film sayesinde kullanıcın bezi bedene sabitleyebilmesini sağlar. Bu çalışma; global anlamda blown film üretim prosesine uygun olmayan ve cast film prosesiyle üretilen SEBS (Stiren-Etilen-Bütillen-Stiren) bazlı elastik filmlerin, blown film üretim tekniği ile standart elastik film performansına yaklaşmak için yapılan deneme çalışmalarına ve bebek bezi esnek kulakçık komponentindeki uygulamalarına yöneliktir.

Anahtar Kelimeler: Elastik Film; SEBS, Bebek Bezi; Blown Film, Polimer

Production of Memory and Functional Elastic Film with Blown Production Technology

ABSTRACT

Elastic films are the name given to thin material layers (films) that are flexible, stretchable and have a memory structure. Such films are made of elastomer-based polymers and have the ability to return to their original form due to their high memory. These features make them useful in a wide variety of applications. Diapers are a complex structure formed by the combination of many different components and one of these components is flexible earflaps. Flexible earflaps allow the user to fix the diaper to the body thanks to an elastic film that is ultrasonically laminated between two nw (nonwoven) fabrics. This study; is aimed at the trial studies conducted to approach the standard elastic film performance with the blown film production technique of SEBS (Styrene-Ethylene-Butylene-Styrene) based elastic films, which are not suitable for the blown film production process in the global sense and are produced with the cast film process, and their applications in the flexible earflap component of the baby diaper.

Keywords: Elastic Film; SEBS; Diaper; Blown Film; Polymer

I. GİRİŞ

1.1. Elastik Filmler

Elastik film, esnek ve gerilebilir bir yapıya sahip ince malzeme tabakalarına verilen isimdir. Bu tür filmler, genellikle elastomer bazlı polimerlerden yapılır ve yüksek derecede esneklik, esneme ve geri dönüş özellikleri sunar. Elastomerler; viskoelastisiteye (yani hem viskozite hem de elastikiyet), zayıf moleküller arası kuvvetlere, genellikle düşük Young modülüne ve diğer malzemelere kıyasla yüksek kırılma gerilimine sahip olup son olarak ise camsı geçiş sıcaklıklarının üzerinde olan amorf polimerlerdir. Bu sayede kovalent bağlar kırılmadan önemli ölçüde moleküler yeniden yapılandırma (reorganizasyon) mümkündür.

Elastik filmler, gerildiğinde orijinal şekillerine dönebilme yetenekleri nedeniyle "elastik" olarak tanımlanır. Bu özellikleri onları çok çeşitli uygulamalarda kullanışlı hale getirir.

1.2. Elastik Film Türleri

1.2.1. Polimer Bazlı Elastik Filmler

a.) SEBS (Stiren-Etilen-Bütilen-Stiren)

Termoplastik elastomerler arasında yer alır ve elastik filmler için sıkça kullanılır.

b.) SBS (Stiren-Butadien-Stiren)

Elastik özellikleri ile bilinen bir diğer termoplastik elastomerdir.

c.) TPU (Termoplastik Poliüretan)

Elastik özellikleri ve dayanıklılığı ile yaygın kullanılan bir malzemedir.

1.2.2. Silikon Bazlı Elastik Filmler

Silikon elastomerleri; geniş sıcaklık aralıklarında esneklik gösteren, biyouyumlu ve kimyasal dirençli elastik filmlerdir.

1.2.3. Lateks Bazlı Elastik Filmler

Genellikle esnek ve esnek yapısı ile lateks, tıbbi malzemeler ve koruyucu eldivenlerde elastik film olarak kullanılır.

1.3. Elastik Filmlerin Kullanım Alanları

1.3.1. Medikal Ürünler

a.) Bebek bezleri

Arka kulak (back ear) bölgesi gibi elastik bölümlerde kullanılır. Elastik back ear panellerin birkaç üretim tekniği vardır. Bunlardan ilki bizim de işletmemizde kullandığımız teknoloji olan ultrasonik kaynak yöntemidir. Bir diğeri de akıtma yöntemiyle hotmelt tutkal uygulamasıdır. Son olarak ise elastik NW kullanılarak mono yapıda esneyen elastik panellerdir.

b.) Yara örtüleri

Elastik filmler, yara örtüsü üretiminde kullanılarak yaraların hava almasını ve iyileşme sürecini destekler.

c.) Tıbbi bantlar ve elastik bandajlar

Yaraların sarılması veya desteklenmesi için elastik filmler kullanılır.

1.3.2. Ambalaj Endüstrisi

a.) Esnek ambalajlar

Elastik filmler, gıda ve diğer ürünlerin ambalajlanmasında esnek, dayanıklı ve sızdırmaz bir bariyer olarak kullanılabilir.

b.) Tekstil ve Moda Endüstrisi

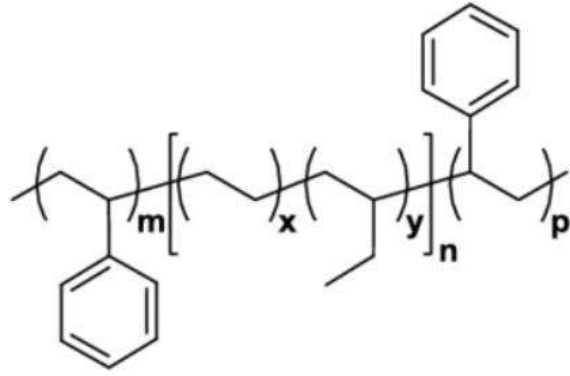
Elastik filmler, giyim ürünlerinde esneklik ve rahatlık sağlamak için kullanılır. Özellikle iç çamaşırı ve spor giyim gibi ürünlerde tercih edilir.

c.) Otomotiv ve Endüstriyel Uygulamalar

Yalıtım, conta ve sızdırmazlık malzemeleri olarak elastik filmler kullanılır.

1.4. SEBS

SEBS(Styrene-Ethylene-Butylene-Styrene), termoplastik elastomer (TPE) ailesine ait, stiren ve olefin bloklarından oluşan bir kopolimerdir. Hem plastiklerin işlenebilirliğine hem de elastomerlerin esnekliğine sahiptir.



Şekil 1. SEBS'in kimyasal yapısı

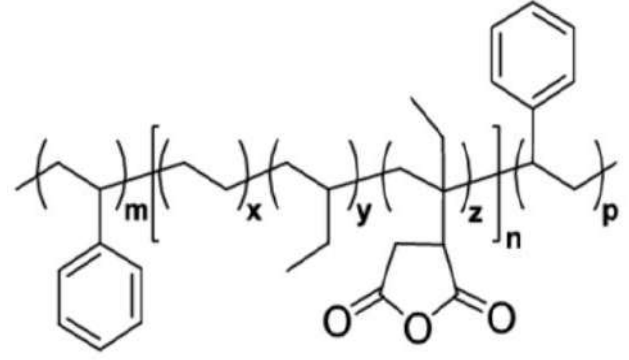
Blok kopolimer yapısında;

Stiren blokları (S) sertlik ve mekanik dayanım sağlar. Sert ve amorf yapıdadır. Bu bloklar polimerin mekanik dayanımını ve şekil bellek özelliklerini sağlar. Stiren, aromatik bir bileşik olup, yüksek sıcaklıklara ve UV ışınlarına dayanıklıdır. Etilen-Bütlen blokları (EB) ise elastikiyeti ve yumuşaklığı sağlar. Elastik özellikler sağlayan esnek ve amorf bloklardır. Etilen ve Bütlen, doymuş hidrokarbonlardır ve bu da SEBS'e kimyasal direnç kazandırır. [1]

SEBS, apolar bir malzemedir ve polar katmanlara yapışması zayıftır. SEBS'in yüzey enerjisi MAH sayesinde yükselir ve polar yapılarla kimyasal uyum sağlar. SEBS-g-MAH, farklı polimerleri bir arada karıştırmak için bağlayıcı olarak kullanılır.

SEBS elastik filmlere maleik anhidrit (MAH) aşılması, özellikle uyumluluk, yapışma ve reaktif modifikasyon gibi özel işlevler için yapılan bir kimyasal işlemidir. Maleik anhidrit aşılması, SEBS zincirlerine MAH (Maleik Anhidrit) fonksiyonel gruplarının kimyasal olarak bağlanmasıdır.

SEBS, doymamış bir polimer değildir, bu nedenle reaktifliği düşüktür. Genellikle dicumyl peroxide (DCP) gibi bir başlatıcı kullanılarak ısı etkisi altında başlatıcı radikaller oluşturulur SEBS zincirinde aktif yer açılır. MAH bu aktif noktaya bağlanarak, SEBS zincirine polar fonksiyonel grup kazandırılır. [2]



Şekil 2. SEBS-g-MAH kimyasal yapısı

1.4.1 SEBS'in Özellikleri

1.4.1.1. Mekanik Özellikler

Tablo 1. SEBS'in mekanik özellikleri

| Özellik | Açıklama |
|--------------------------|-----------------------------------------------------------------------------|
| Yüksek Gerilme Dayanımı | SEBS, yüksek elastikiyetinin yanı sıra iyi bir gerilme dayanımına sahiptir. |
| Yüksek Yırtılma Dayanımı | Dayanıklı bir yapıya sahiptir ve yırtılma dayanımı yüksektir. |

1.4.1.2. Fiziksel Özellikler

Tablo 2. SEBS'in fiziksel özellikleri

| Özellik | Açıklama |
|-------------------------|-----------------------------------------------------------------------------------------------------|
| Elastiklik | Yüksek elastikiyete sahiptir, uzun süreli gerilim altında şeklini korur. |
| Düşük Sıcaklık Dayanımı | -30°C'ye kadar dayanıklıdır. |
| Termal Dayanım | 150°C'ye kadar özelliklerini korur. |
| Termoplastiklik | Isı ile şekil alabilirler bu da onları şekillendirme ve işleme süreçlerinde kullanışlı hale getirir |

1.4.1.3. Kimyasal Özellikler

Tablo 3. SEBS'in kimyasal özellikleri

| Özellik | Açıklama |
|--------------------|------------------------------------------------------------------------------|
| Kimyasal Direnç | Asitlere, bazlara, deterjanlara ve çözücülere karşı dirençlidir |
| UV ve Ozon Direnci | Özellikle dış mekan uygulamalarında UV ışınları ve ozona karşı dayanıklıdır. |
| Su ve Nem Direnci | Düşük su emilimi ve iyi hidrokarbon dayanımı vardır |

1.4.2 SEBS Bazlı Elastik Film Üretim Yöntemi

Elastik filmler Cast (dökme) teknolojisi ile üretilirler.

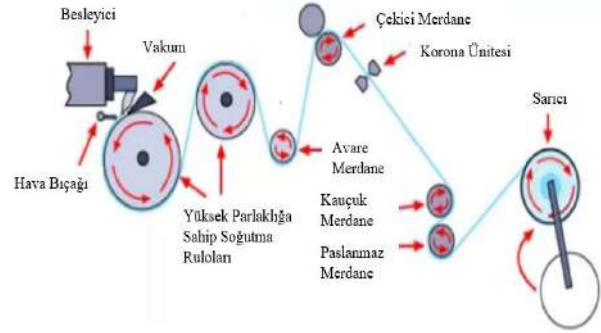
1.4.2.1. Cast Film Üretim Teknolojisi

Cast film teknolojisi, termoplastik polimerlerin eritilip düz bir kalıptan (die) geçirilerek düz bir yüzey üzerinde (genellikle soğutma silindiri) inceltilip katılaştırılması işlemidir. Bu yöntemde film, döner bir silindir üzerine dökülerek hızla soğutulur ve katlaşır. [3]

Elastik film üretiminde genellikle cast film teknolojisinin tercih edilmesinin arkasında, bu teknolojinin sağladığı işlem hassasiyeti, yüzey kalitesi ve katman yapısı kontrolü gibi avantajlar yatar.

Tablo 4. Elastik film üretiminde cast film teknolojisinin tercih edilme nedenleri

| Özellik | Açıklama |
|------------------------------------|-----------------------------------------------------------------------------------------------------------------------------------------------------------------------------------------------------------------------------------------------------------------------|
| Yüksek Kalınlık ve Katman Kontrolü | Elastik filmler çok hassas kalınlık dağılımı gerektirir. Cast teknolojisinde chill roll ile bu dağılım çok daha homojen sağlanır. |
| Gelişmiş Çok Katmanlı Yapı | Elastik filmler genellikle 3-5-7 katlı yapıya sahiptir. Her katmana farklı bir fonksiyon (örneğin; elastomerik merkez, yumuşak dış yüzey) verilebilir. Cast hatlarda layer dizaynı çok esnekler. |
| Elastomerik Polimerlerle Uyum | Elastik film üretiminde SEBS, SBC, POE, EVA gibi elastomerler kullanılır. Bu polimerler, cast hatlarda daha stabil işlenir, çünkü blown filmde balon stabilitesi bozulabilir. Bunun sebebi performans gösterecek hammaddelerin yüksek mfi değerine sahip olmalarıdır. |
| Oryantasyon Yönünün Kontrolü | Cast filmde oryantasyon sadece makine yönündedir (Machine Direction). Bu, elastik filmin tek yönlü esneme (örneğin bel bandı) istenen uygulamalarında çok avantajlıdır. Blown film çift yönlü Oryante olur, bu durum mekanik özellikleri etkiler. |
| Soğutma Hızının Avantajı | Cast filmde soğutma daha hızlı ve kontrollü olduğu için elastomerik yapı daha düzenli kristalize olur veya amorf halde stabilize edilebilir. |
| Üretim Hızı ve Fire Oranı | Elastik filmler hassas ürünlerdir, blown hatlarda balon homojenliği sağlanmaz ise stabil hale gelmediği için kopuşlar yaşanır. Film bölgesel farklılık gösterebilir. Cast hatlarda daha stabil ve fire oranı düşük üretim yapılabilir. |
| Rulo Kalitesi ve Sarım | Elastik filmler hassas sarım ister. Cast hatlarda sarım sistemi daha hassas çalışır (gerilim ayarı, kenar kontrolü, sarım hızı). |



Şekil 3. Cast film üretim metodu

1.4.2.2. Blown Film Üretim Teknolojisi

Blown film üretim yöntemi; plastik filmlerin üretiminde yaygın olarak kullanılan bir prosestir. Bu yöntem, özellikle ambalaj endüstrisinde, tek ve çok katmanlı plastik filmlerin üretiminde kullanılır. Blown film üretim süreci, plastik granüllerinin eritilerek ince filmler halinde çıkarılması prensibine dayanır.

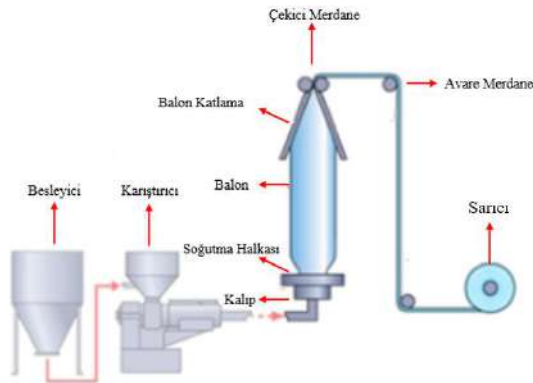
Polimer granüller, ekstrüzyon makinesinin extruderine belirli oranlarda gravimetrik tartımlar yapılarak beslenir. Ekstruderler, polimer granülleri yüksek sıcaklıkta eritir ve aynı zamanda içindeki sonsuz vida dönerek eriyiği karıştırır. Sıcaklık, kullanılan polimere bağlı olarak yaklaşık 200-250°C arasında değişir. Eriyik, ekstruderin uç kısmındaki bir nozul (delik) aracılığıyla çıkar ve içine basınçlı hava üflenerek bir alan içine alınır. Hava üflendikçe tüp şişer ve film şekli almaya başlar. Bu şişirme işlemi, "balon" şeklinde bir yapının ortaya çıkmasına neden olur. Bu yapı, filmin düzgün, homojen ve ince olmasını sağlar. Şişirme oranı, tüpün genişliğinin, nozulun çapına oranıdır. Örneğin, şişirme oranı 1:2 ise, tüp ilk başta nozul çapının 2 katı genişliğine kadar şişirilir. Balon, yukarıya doğru şişerken etrafında yer alan soğutma sistemleri ile soğutulur. Bu soğutma, genellikle soğutma halkaları ya da havalandırma sistemi ile sağlanır. Soğutma, filmin düzgün bir şekilde amorf yapıya geçişini sağlar. Havanın hızla soğutması, filmdeki

polimer moleküllerinin düzenli bir yapıda katılaşmasına yardımcı olur. [4]

Blown film teknolojisi, pek çok film türü için avantajlı olsa da elastik film üretiminde genellikle tercih edilmez. Bunun arkasında hem malzeme işleme zorlukları hem de film performansı ve proses stabilitesiyle ilgili teknik sınırlamalar vardır.

Tablo 5. Elastik film üretiminde blown film teknolojisinin tercih edilmeme nedenleri

| Problem | Açıklama |
|--------------------------------------|---------------------------------------------------------------------------------------------------------------------------------------------------------------------------------------------------------------------------------------------------------|
| Balon Stabilesi Sorunu | Blown film prosesi bir balonun dikey olarak şişirilmesine dayanır. SEBS gibi elastomerler yüksek mfi değerine sahiptir, yani eriyik halindeyken çok yumuşaktırlar. Bu da balonun stabil durmasını engeller, sık sık yırtılmalara, kopuşlara neden olur. |
| Kontrol Edilemeyen Kalınlık Dağılımı | Balon geometrisi, hem makine yönünde (Machine Direction) hem enine yönde (Transverse Direction) Oryante olur. Ancak elastik filmlerde genellikle tek yönlü oryante (Machine Direction) istenir. Blown filmde bu mümkün değildir. |
| Düşük Proses Hızı | Elastomerlerin işlenmesi zordur; yüksek mfi ve soğuma hızı yavaş olduğundan blown film hattında bu daha da yavaştır. Genellikle düşük çıkış hızlarında çalışmak gerekir. |
| Yetersiz Soğutma / Şekil Koruma | Blown filmde soğutma hava akışıyla olur, bu ise elastomerik yapı için %100 yeterli olmadığında film tam olarak soğumadığı için şekil bozulmaları, yapışmalar ve boyutsal kararsızlıklar yaşanabilir. |
| Yüksek Fire Oranı | Balon kopması ve balon oynamalarından dolayı oluşan kırıklık gibi nedenlerle fire oranı yüksektir. |
| Katman Kontrolünün Sınırlı Olması | Elastik filmler genellikle multilayer (3-5-7 kat) yapılarla üretilir. Blown filmde bu yapı karmaşıktır ve her katmanın kalınlığını hassas kontrol etmek zordur. Oysa cast filmde bu kolaylıkla yapılabilir. |



Şekil 4. Blown film üretim metodu

1.5. SEBS Bazlı Elastik Filmlerin Reolojisi

Reolojik özellikler, bir malzemenin akış ve deformasyon davranışlarını tanımlar. Elastik filmlerin reolojisi, malzemenin elastik modül, viskozite, akış özellikleri ve bu özelliklerin sıcaklık, zaman ve gerilme gibi faktörlerle nasıl değiştiğini inceleyen bir analiz içerir.

Elastik filmler, polimerik yapılar olup, elastik özellikleri nedeniyle gerildiklerinde eski şekillerine geri dönebilirler. Reolojik açıdan elastik filmler, viskoelastik özellikler gösterirler yani hem viskoz (sıvı gibi akışkan) hem de elastik (katı gibi şekil değiştirebilen) özellikler sergilerler.

1.5.1. Elastik Modül (Young Modülü)

Elastik modül; bir malzemenin elastik özelliklerini, yani şekil değiştirildikten sonra eski haline dönme yeteneğini belirler. Elastik filmlerde Young modülü genellikle çok düşüktür. Bu, elastik filmin esnek ve gerilmeye karşı dayanıklı olmasını sağlar.

Yüksek elastik module sahip elastik filmler daha sert ve şekil değiştirmeye karşı daha dirençli olup düşük elastik module sahip elastik filmler daha esnek ve yumuşak özelliktedirler ve kolayca deforme olabilir.

1.5.2. Viskozite ve Akışkanlık

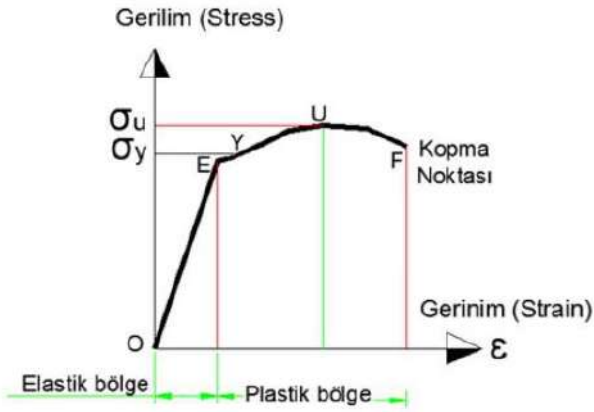
Viskozite, bir sıvının akışkanlık direncini belirler. Elastik filmler genellikle viskoelastik malzemeler oldukları için, hem elastik (sert) hem de viskoz (akışkan) özellikler gösterirler.

Elastik filmler için düşük viskozite, daha hızlı akış özellikleri sağlar. Viskozite, ısınan veya gerilen filmlerle birlikte değişebilir, çünkü polimerler sıcaklıkla daha fazla akışkanlık gösterir. Ayrıca elastik filmler genellikle non-Newtonian akış davranışı sergiler. Yani akış hızı, uygulanan gerilme oranına bağlı olarak değişebilir. Bu, filmin moleküler yapısının akışa karşı nasıl tepki verdiğini gösterir.

1.5.3. Gerilme (Stress) ve Deformasyon (Strain)

Elastik filmlerin deformasyonu, uygulanan gerilme ile ilişkilidir. Gerilme (stress) ve deformasyon (strain), genellikle gerilme-deformasyon eğrisi (stress-strain curve) üzerinden incelenir.

Elastik filmler, belirli bir gerilme seviyesine kadar elastik (geri dönüşümlü) deformasyona uğrarlar. Bu bölge, filmin orijinal formuna geri dönebildiği kısımdır. Ancak gerilme arttıkça, filmin elastik özellikleri zayıflar ve film plastik deformasyon yaşar. ve deformasyon sonrasında, film eski haline geri dönemez.



Şekil 5. Gerilme-Deformasyon grafiği

Şekil.5 incelendiğinde;

Elastik bölge (OE) genellikle doğrusaldır ve gerilme ile deformasyon arasındaki ilişki doğrudan orantılıdır. Malzeme bu bölgede esnektir ve kuvvet kaldırıldığında eski haline döner.

Akma noktasında (EY) gerilme artarken malzeme artık esneklik özelliklerini kaybeder ve plastik deformasyon başlar.

Plastik bölgede (YF) malzeme şekil değiştirmeye devam eder ancak geri dönüşümsüzdür. Gerilme arttıkça, deformasyon daha da büyür.

Kırılma/Kopma Noktası (F) filmin dayanabileceği en yüksek gerilme noktasıdır. Bu noktada, malzeme kopar ve yapısal bütünlüğü kaybolur.

1.5.4. Akma ve Yumuşama

Elastik filmler, belirli bir gerilme sınırını aşarsa, akma (yielding) meydana gelir. Bu noktada film, elastik özelliklerini kaybeder ve plastikleşir. Bu genellikle filmde kalıcı deformasyonların olduğu noktadır.

Elastik filmlerin sıcaklıkla viskozitesi değişir ve daha yumuşak hale gelir. Yüksek sıcaklıklarda, filmler daha az elastik, daha akışkan hale gelir ve daha kolay şekil değiştirilebilir.

1.5.5. Sıcaklık ve Zaman

Reolojik özellikler, sıcaklıkla doğrudan ilişkilidir. Elastik filmlerin viskoelastik özellikleri, sıcaklık arttıkça değişir. Sıcaklık artışı ile elastik filmlerin elastik modülü genellikle düşer. Bu da daha yumuşak ve daha esnek film özelliklerine yol açar. Bununla beraber elastik filmlerin reolojisi, zamanla da değişir. Uzun süreli gerilme veya ısınma, filmin deformasyonunu ve geri dönüşünü etkiler.

II. DENEYSEL METOT / TEORİK METOD

Bu çalışmada elastomerik (SEBS, plastomer) yapıda cast teknolojisiyle üretilen bu elastik filmlerin blown teknolojisi ile üretilebilmesi ve teknik açıdan mevcut test değerlerine yaklaşılabilesi amaçlanmıştır. Mevcut bünyemizde cast hattının olmayışından dolayı yurtdışından ithal ettiğimiz bu özel filmi, 9 extruderli ve teknik özelliklerinin bu filme teknolojik anlamda yeterli olacağını öngördüğümüz yüksek teknolojiyi hattımızda özel polimer hammaddeler ile formülasyon çalışmaları ile geliştirmeler yapılmıştır.

2.1. Polimer Hammadde Çalışmaları

Çalışmanın blown film üretim hattında yapılmasından dolayı özellikle bu teknolojiye uygun performans polimerler tercih edilmiş olup, hammaddelerin yoğunluk, mfi, modulus değerleri, mekanik ve optik tüm özellikleri incelenmiş, bu hammaddeler pilot blown film üretim hattına %100 oranında beslenerek 50 mikron kalınlığında filmler elde edilmiştir. Üretilen filmler testlere tabi tutularak hammaddelerin TDS verileri ile

karşılaştırılmalar yapılmıştır. Böylece, hammadde seçimi için karakterizasyon çalışmaları yapılmıştır.

2.2. Formülasyon Çalışmaları

Bu çalışmada standart cast elastik filme muadil ürün eldesi için dört farklı formül denenmiş olup formülasyon içeriğine ait detaylar Tablo.6'da verilmiştir.

Tablo 6. Blown film üretim hattında yapılan denemelere ait formülasyon içerikleri

| Deneme No | Kalınlık (μ) | SEBS İçeriği (%) | Performans Polimer (%) | Poliölefin Polimer (%) |
|-----------|--------------------|------------------|------------------------|------------------------|
| D1 | 55 | 20,8 | 35,5 | 43,7 |
| D2 | 55 | 22,8 | 41,7 | 35,5 |
| D3 | 50 | 25,6 | 40,8 | 33,6 |
| D4 | 50 | 40,3 | 40,3 | 19,4 |

III. BULGULAR VE TARTIŞMA



Resim 1. Blown Film denemelerine ait elastik film örneği

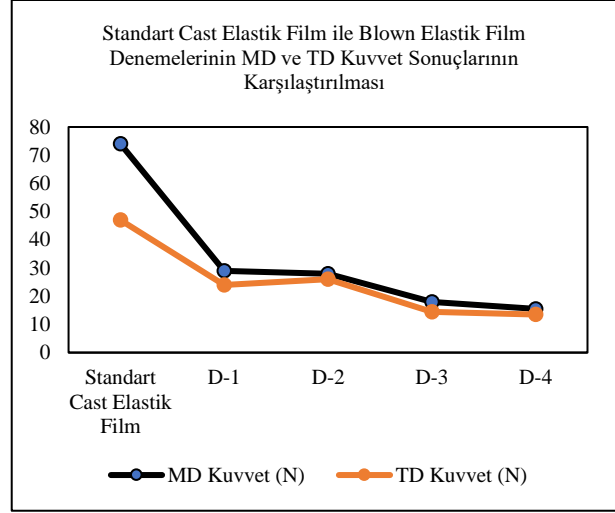
Deneme-1'de üretilen filmin stifness özelliğinin yüksek, kırılğan ve uzamaya elverşi olmadığı tespit edildi ve dolayısıyla deformasyon yüzdesi yüksek ölçüldü. Filmin sert-kırılğan olduğu görüldü. Ayrıca filmin geri toplama performansı da istenilen seviyede olmamıştır.

Deneme-2'de SEBS oranı artırılarak modülüs düşürüldü yani stifness özelliği azaltıldı kırılğanlık düştü fakat istediğimiz deformasyon ve proses sürekliliği performansına ulaşılammıştır.

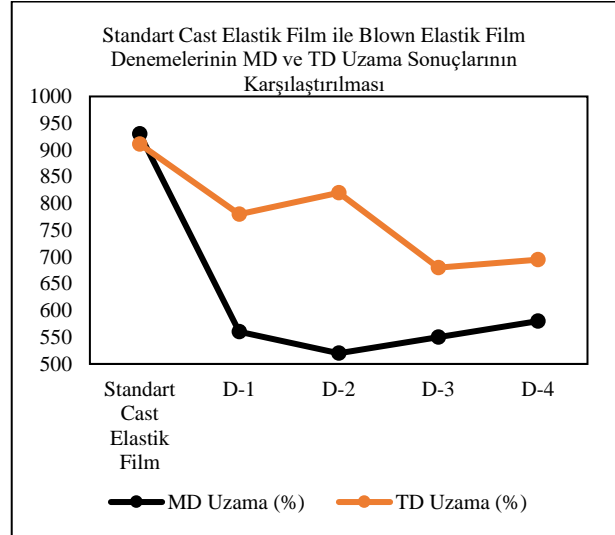
Deneme-3'te mevcut SEBS yerine MAH oranı daha düşük farklı bir SEBS kullanılıp ve kalınlık %10 azaltılmıştır. Modülüs'ün daha da düştüğü ve filmin yumuşadığı ancak hala elastik deformasyonun fazla ve geri toplama oranının düşük olduğu tespit edilmiştir. Proses edilebilirlikte olumlu yönde bir gelişim sağlanamamıştır.

Deneme-4'te MAH oranı düşük olan SEBS'in oranı iç ve dış katlarda artırıldı. Modülüs değerinin daha da düştüğü ve film yumuşaklığının daha iyi olduğu görülmüştür. Elastik deformasyonda ve filmin geri toplamasında iyileşmeler olmuştur. Film üretim prosesi ve balon stabilitesi sağlanarak deneme üretimi tamamlanmıştır.

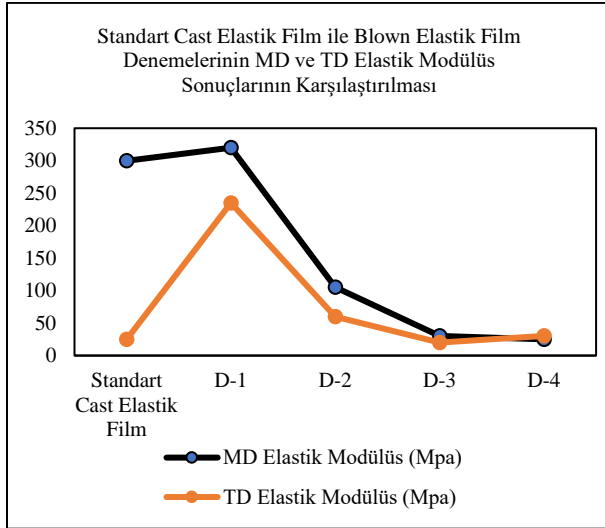
IV. SONUÇLAR



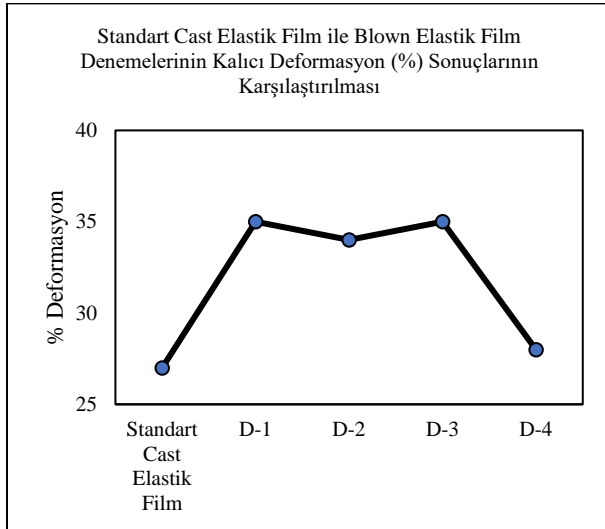
Şekil 6. Standart cast elastik film ile blown elastik film denemelerinin MD (Machine Direction) ve TD (Transverse Direction) kuvvet sonuçlarının karşılaştırılması



Şekil 7. Standart cast elastik film ile blown elastik film denemelerinin MD (Machine Direction) ve TD (Transverse Direction) uzama sonuçlarının karşılaştırılması



Şekil 8. Standart cast elastik film ile blown elastik film denemelerinin MD (Machine Direction) ve TD (Transverse Direction) elastik modülüs sonuçlarının karşılaştırılması



Şekil 9. Standart cast elastik film ile blown elastik film denemelerinin kalıcı deformasyon (%) sonuçlarının karşılaştırılması

Sonuç olarak; bu çalışmadaki amacımız cast teknolojiyle üretilen ve yurtdışından ithal ettiğimiz bu özel elastik filmi, 9 extruderli makinemizle blown film üretim teknolojisi kullanarak olarak üretebilmektir. Bu süreçte de filmin teknik özelliklerini, özel polimer hammaddeler ve formülasyon çalışmaları yaparak geliştirmek ve bunu yaparken de ithal edilen ürün yerine yerli üretim yaparak hem mevcut teknik yeterlilikleri sağlamak hem de ülkemiz için katma değerli ürün üretimine katkı sağlamaktır.

Bu çalışmadaki en büyük yenilik; cast üretim teknolojisi yerine, çocuk bezi kalite standartlarını değiştirilmeden ve blown üretim teknolojisi ile birlikte formülasyon çalışmaları yapılarak sürdürülebilir üretim proses değerlerine ulaşarak üretilen elastik filmin, back ear (elastik esnek kulak) olarak son üründe görev yapmasını sağlamaktır.

Bu amaç doğrultusunda yapılan denemeler ve grafiklerde bahsedilen sonuçlar değerlendirildiğinde;

Farklı yüzdelerde kullanılan SEBS ve özel polimerler oranına bağlı olarak, proses şartlarının da optimize edilmesi göz önünde tutularak elastik filmlerin testleri yapılmıştır.

Mekanik olarak standart elastik filmlere göre geride kalan noktalarda iyileştirmelerin yapılması gerektiği görülmüş olup elastik modülüs değerlerinde ise filmin işlevini yerine getirmesi için istenen TD değeri elde edilmiştir.

% Deformasyon değerinin, D-4 denemesinde diğer denemelere göre standart elastik film performansına daha yakınlaşmış olması bu noktada çok önemlidir.

D-4 ile üretilen elastik film back ear (elastik arka kulak) hatında denemesi yapılmış olup, çocuk bezi üretim prosesinde denemesi tamamlanmıştır. Çocuk bezi üretim prosesinde olumsuz bir durum ile karşılaşılmamıştır.

Çalışmamız bu doğrultuda son kullanıcı olan bebek bezi üreticisi tarafından ilk onayını almıştır. Geliştirmeler, endüstriyel deneme onayı sürecinde de formülasyon ve proses iyileştirme çalışmalarıyla devam edecektir.

KAYNAKLAR

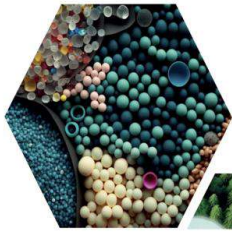
- [1] Pei Dai, Zhao-Hua Mo, Ri-Wei Xu, Shu Zhang, and Yi-Xian Wu. Cross-Linked Quaternized Poly(styrene-b-(ethylene-co-butylene)-b-styrene) for Anion Exchange Membrane: Synthesis, Characterization and Properties. *ACS Applied Materials & Interfaces* 2016, 8 (31), 20329-20341. <https://doi.org/10.1021/acsami.6b04590>

*16. Uluslararası Lif ve Polimer Arařtırmaları Sempozyumu (16. ULPAS)
9-10 Mayıs 2025, İstanbul teknik Üniversitesi (İTÜ), Türkiye*

[2] Tjong, S.C., Xu, S.A. & Mai, Y.W. (2003) Tensile deformation mechanism of polyamide 6,6/SEBS-g-MA blend and its hybrid composites reinforced with short glass fibers. <https://doi.org/10.1023/A:1021132725370>

[3] Damian Dziadowiec, Danuta Matykiewicz, Marek Szostak, Jacek Andrzejewski (2023), Overview of the Cast Polyolefin Film Extrusion Technology for Multi-Layer Packaging Applications
<https://doi.org/10.3390/ma16031071>

[4] Joseph Dooley, Jeff Robacki, Steve Jenkins, Robert Wrisley, Patrick C. Lee (2016), Development of microlayer blown film technology by combining film die and layer multiplication concepts.
<https://doi.org/10.1002/pen.24285>



16 ULUSLARARASI
LİF VE POLİMER
ARAŞTIRMALARI
SEMPOZYUMU

16th INTERNATIONAL FIBER AND POLYMER RESEARCH SYMPOSIUM

Sürdürülebilir ve İşlevsel Lif ve Polimerler
Sustainable and Functional Fibers & Polymers



9-10 Mayıs
May 2025

İstanbul Teknik Üniversitesi
Gümüşsuyu Prof. Dr. Necmettin Erbakan Yerleşkesi
Istanbul Technical University
Gumussuyu Prof. Dr. Necmettin Erbakan Campus

Towards Sustainable and Green Synthesis of Metal-Organic Frameworks (MOFs): A Pathway to Industrial Viability

Seif El Islam Lebouachera^{a,b,*}, Mahdi Hasanazadeh^{c,*}

^a UMR IPREM (Institut des Sciences Analytiques et de Physico-Chimie Pour l'Environnement et les Matériaux), Université de Pau et des Pays de l'Adour, CNRS, Technopôle Hélioparc, 2 Avenue du Président Pierre Angot, 64053 Pau, France.

^b SCT Société des Céramiques Techniques, ZI Ouest Route d'Oursbelille, BP 9, 65460, Bazet, France.

^c Department of Textile Engineering, Yazd University, Yazd 89195-741, Iran.

*Corresponding authors: s.lebouachera@univ-pau.fr; m.hasanazadeh@yazd.ac.ir

ABSTRACT

Metal organic frameworks (MOFs) have emerged as promising materials for diverse applications ranging from gas storage and catalysis to environmental remediation and drug delivery. However, the industrial translation of MOFs remains hindered by challenges related to their environmental impact, synthesis cost, and lifecycle stability. This review explores recent advancements in the sustainable design and green synthesis of MOFs, highlighting alternative strategies that align with the principles of the circular economy and green chemistry. A growing body of research demonstrates the feasibility of using recycled feedstocks such as PET plastic waste and industrial effluents as low-cost sources of organic linkers and metal precursors. Additionally, solvent-free mechanochemical methods, water- and ethanol-based solvothermal synthesis, and vapor-phase approaches offer promising routes to minimize toxic solvent usage, reduce energy demands, and enhance scalability. The implementation of the "safe and sustainable by design" (SSbD) framework provides a structured pathway to design MOFs that are not only high-performing but also degradable, recyclable, and environmentally benign. We also discuss life cycle assessments (LCAs) of MOF production, identifying reactive extrusion and microwave-assisted synthesis as particularly low-impact technologies. By integrating recent findings across synthesis methods, material reuse, and environmental safety, this review outlines a roadmap for the green industrialization of MOFs and proposes critical directions for future research.

Keywords: Metal-Organic Frameworks; Green Synthesis; Sustainability



Surface Modification of Wool Fabrics with Metal-Organic Framework for Eco-Friendly Sustainable Natural Dyeing

Maryam Pishehvar^a, Motahareh Moradi^a, Aminoddin Haji^a, Mahdi Hasanazadeh^{a,*}

^a Department of Textile Engineering, Yazd University, Yazd 89195-741, Iran.

*Corresponding author: m.hasanazadeh@yazd.ac.ir

ABSTRACT

Metal-organic frameworks (MOFs), as novel crystalline porous materials, have received considerable attention in recent years. In this study, Zn-based MOF (ZIF-8) was synthesized into the wool fabric through the single-step in-situ growth of ZIF-8 crystals. The morphological features and elemental analysis of wool-MOF fabric was evaluated by field emission scanning electron microscopy (FESEM) and energy-dispersive X-ray spectroscopy (EDS), respectively. The FESEM images showed that the MOF crystals were completely deposited on the wool surface, and the wool fibrils were densely enveloped with MOFs. Moreover, EDS analysis displayed the presence of Zn element (12.52 wt.%) besides carbon, oxygen, nitrogen, and sulphur elements of the wool structure. The obtained results confirmed the successful formation of the MOF crystal within the wool fabric structure. The pristine wool and wool-MOF samples were dyed with weld (*Reseda luteola*) without any auxiliary such as metal mordant. The colour strength of the wool-MOF fabric (19.97) was significantly higher than that of the pristine wool fabric (14.99). The wash fastness of the wool fabric was also improved upon modification with ZIF-8. This confirmed the ability of the proposed process to improve the dyeability and fastness properties of wool fibre with natural dyes.

Keywords: Metal-organic framework; Wool fabric; Natural dyeing

I. INTRODUCTION

Metal-organic frameworks (MOFs) are a type of crystalline porous material composed through the coordination of inorganic metal ions or clusters and organic ligands. The exceptional structure of MOFs leads to a wide variety of properties, such as high surface area, adjustable pore size and functionality, and outstanding adsorption behaviour. Such properties render MOFs extremely versatile for numerous

applications, such as gas storage, catalysis, and environmental remediation [1]. There has been considerable interest in the recent past in integrating MOFs into textile substrates to promote functionalities [2]. The application of metal-organic frameworks (MOFs) to wool fabrics represents one avenue for the alteration of textile functionality. Several reports have demonstrated that the deposition of different MOFs onto wool achieves many desirable outcomes. More

specifically, the application of zeolitic imidazolate frameworks (ZIFs), including ZIF-67 and ZIF-8, in wool composite systems has proven highly effective not only at removing pollutants from wastewater, but also at biomedical applications.

The research demonstrates the potential of ZIF@wool composites to adsorb pharmaceutical intermediates and reactive dyes efficiently, thereby illustrating their application in water purification processes [1, 3]. Further, the application of (Co & Ni)-BTC MOFs in wool fabrics has been demonstrated for the effective removal of sulfa drugs from aqueous media, illustrating recyclability and efficiency of the method [4]. Apart from application in water purification, MOFs have also been researched for their ability to improve the flame retardancy of wool. In-situ growth of iron-loaded metal-organic frameworks (Fe-MOFs) on the surface of wool has exhibited great enhancement in flame retardancy along with suppression of smoke generation at the same time. This takes advantage of the creation of a metal oxide layer upon thermal decomposition that works as a physical barrier inhibiting further burning and entrapping gases and smoke. The findings indicate that the quantity of assembly layers of the Fe-MOF directly dictates the flame retardant capacity of the wool fabric [5]. In addition, ZIF-8 has been assessed for its ability to stabilize natural dyes, such as curcumin, for better wool dyeing processes. The strategy shows the potential for MOFs to provide better colorfastness and quality to naturally dyed textiles [6]. $\text{NH}_2\text{-UiO-66 (Zr)}$ modification of waste wool fibers has also shown promise towards improving dye adsorption from water [7].

This study aims to investigate the potential of surface-modification of wool fabrics through single-step in-situ synthesis of highly porous MOF as a eco-friendly sustainable natural dyeing approach.

II. EXPERIMENTAL METHOD

2.1 Materials

Zinc nitrate hexahydrate ($(\text{Zn}(\text{NO}_3)_2) \cdot 6\text{H}_2\text{O}$), 2-methyl imidazole (2-MIM), and methanol were purchased from Merck Co. (Germany) and used without further purification. Wool fabric with plain weave (250 g/m^2) was obtained from Iran-Merinos Co., Tehran, Iran. Weld (*Reseda luteola*) was obtained from a local market in Ardakan, Iran.

2.2 Modification of wool with MOF

Wool-MOF fabric was prepared by single-step in-situ growth of ZIFs within wool fabrics. Briefly, 2-MIM (4 g) and zinc nitrate (2 g) were added in methanol, separately and stirred vigorously for 30 min. Wool fabric specimens were submerged in zinc nitrate solution and stirred for 30 min. Then, 2-MIM solution was added slowly to the above solution followed by stirring at 50°C . Then, it was left to stand 60 min for crystallization at room temperature. After that, the modified wool fabrics were removed, washed with methanol and then oven-dried at 60°C .

2.3 Dyeing

Each sample was dyed using 50% owf (on weight of fabric) weld powder. The dyeing process began at 40°C , with the temperature gradually increased at a rate of 2°C/min until reaching boiling point. Dyeing was maintained for one hour. Afterward, the dyebath was cooled back down to 40°C , and the samples were rinsed and dried.

2.4 Characterization

In this study, the size and morphologies of MOF nanoparticles and wool-MOF fabric were assessed using field-emission scanning electron microscopy (FESEM, MIRA III, TESCAN, Czech Republic). Employing energy dispersive X-ray spectroscopy (EDS), the elemental composition of the wool-MOF fabric was investigated. The color strength (K/S) of the

dyed wool fabrics was calculated using the Kubelka-Munk equation, following the measurement of reflectance with a Color-eye 7000A spectrophotometer (X-rite, USA). Wash fastness of the dyed samples was evaluated according to ISO-105 C06 A1M standard.

III. RESULTS AND DISCUSSIONS

The FESEM micrograph of the wool-MOF fabrics is shown in Figure 1. It can be seen that the MOF crystals were completely deposited on the wool surface, and the wool fibrils were densely enveloped with MOFs. Moreover, EDS analysis (Figure 2) displayed the presence of Zn element (12.52 wt.%) besides carbon, oxygen, nitrogen, and sulfur elements of the wool structure.

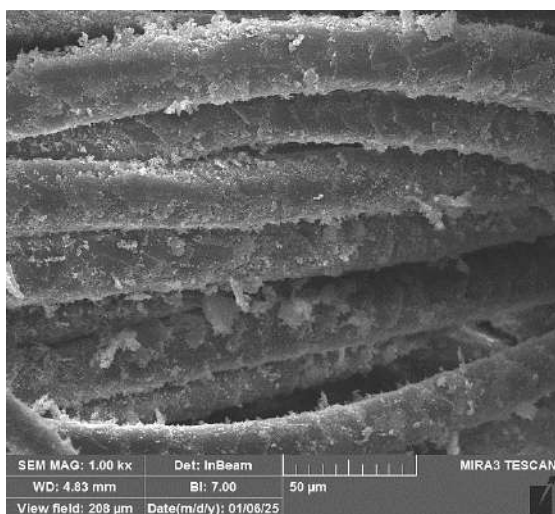


Figure 1. FESEM micrograph of wool-MOF fabric.

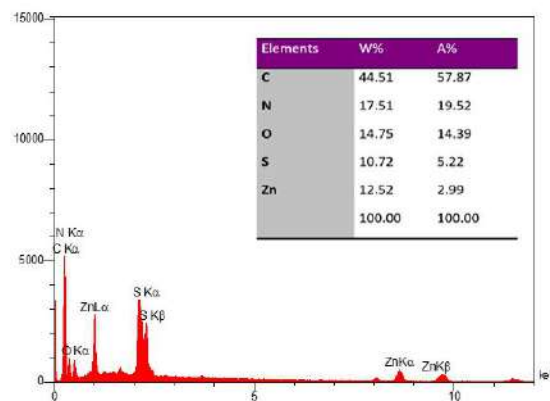


Figure 2. EDS spectra micrograph of wool-MOF fabric.

Table 1 shows the color coordinates of the raw and wool-MOF samples after dyeing with weld. The MOF-treated sample exhibited lower L value compared to the Raw sample, indicating that the MOF treated sample is darker. The wool-MOF fabric showed a positive a^* value, suggesting a reddish hue, while the raw wool fabric had a negative a^* value, indicating a greenish hue. The wool-MOF fabric had a higher b^* value compared to the raw sample indicating a more yellowish tone in the wool-MOF samples.

The K/S values shown in Figure 3 indicate that the color strength is higher for the wool-MOF fabric compared to the raw wool fabric, suggesting that the synthesis of MOF on wool fabric has increased the dye adsorption and bonding on wool fibers. Investigating the wash fastness of modified samples also revealed the significant contribution of MOFs on enhancing the wash fastness properties of wool fabrics. Wash fastness results showed that modification of wool with ZIF-8 increased the wash fastness grade from 2 to 4.

Table 1. Color coordinates of the dyed samples.

| Samples | L* | a* | b* |
|----------|-------|-------|-------|
| Raw wool | 70.03 | -3.07 | 38.53 |
| Wool-MOF | 61.21 | 1.30 | 45.36 |

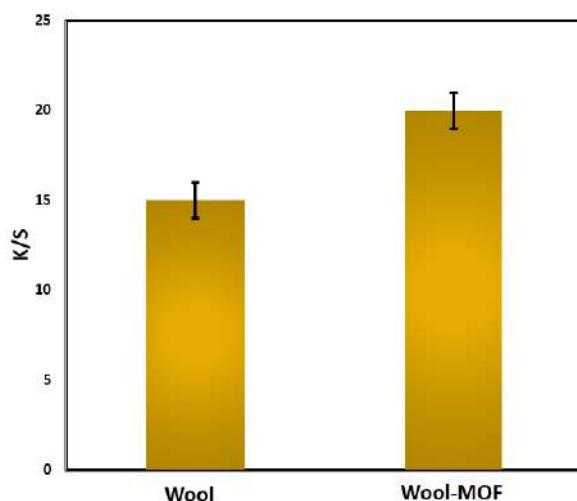


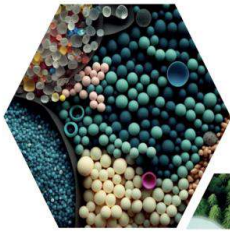
Figure 3. Color strength of the dyed samples.

IV. CONCLUSIONS

The surface modification of wool fabric with metal-organic frameworks (MOFs) was successfully carried out using direct in-situ growth of MOF on wool fabric. FESEM and EDS analyses confirmed the formation of MOF with uniform and dense distribution within wool fibers. The results showed that the wool-MOF fabric has higher color strength than the raw wool fabric. In conclusion, the modification of wool fabric with MOF heralds a novel approach for enhancing the dyeability and fastness properties of wool fibre with natural dyes without any auxiliary such as metal mordant.

REFERENCES

- [1] Abdelhameed, R.M. and H.E. Emam, Design of ZIF(Co & Zn)@wool composite for efficient removal of pharmaceutical intermediate from wastewater. *Journal of Colloid and Interface Science*, 2019. 552: p. 494-505.
- [2] Lis, M.J., et al., In-Situ Direct Synthesis of HKUST-1 in Wool Fabric for the Improvement of Antibacterial Properties. *Polymers*, 2019. 11(4): p. 713.
- [3] Qiao, X., et al., Preparation of zeolitic imidazolate framework-67/wool fabric and its adsorption capacity for reactive dyes. *Journal of Environmental Management*, 2022. 321: p. 115972.
- [4] Alzahrani, S.O., et al., Remarkable remove of sulfa drugs from water by one-pot synthesized recyclable composite based on wool and (Co & Ni)-BTC. *Inorganic Chemistry Communications*, 2023. 158: p. 111695.
- [5] Long, S.-J., et al., In situ construction of iron-rich metal-organic frameworks on wool surface for enhanced flame retardancy and low smoke generation. *Colloids and Surfaces A: Physicochemical and Engineering Aspects*, 2024. 692: p. 134034.
- [6] Wang, X., et al., Optimization of wool fabric dyeing process by natural curcumin stabilized pigment based on ZIF-8 adsorption encapsulation. *Pigment & Resin Technology*, 2025. ahead-of-print(ahead-of-print).
- [7] Yin, H., et al., NH₂-UiO-66 (Zr) modified waste wool fibers for efficient adsorption of dye from water. *Desalination and Water Treatment*, 2024. 318: p. 100305.



16 ULUSLARARASI
LİF VE POLİMER
ARAŞTIRMALARI
SEMPOZYUMU

16th INTERNATIONAL FIBER AND POLYMER RESEARCH SYMPOSIUM

Sürdürülebilir ve İşlevsel Lif ve Polimerler
Sustainable and Functional Fibers & Polymers



9-10 Mayıs
May 2025

İstanbul Teknik Üniversitesi
Gümüşsuyu Prof. Dr. Necmettin Erbakan Yerleşkesi
İstanbul Technical University
Gumussuyu Prof. Dr. Necmettin Erbakan Campus

A STUDY ABOUT WATER REPELLENT AND SOIL RESISTANCE BEHAVIOR OF AUTOMOTIVE SEAT FABRICS

Selenay Elif İşler^{a,*}, Benamir Fidancı^{a,*}, Emir Baltacıoğlu^a

^aMartur Fompak International, NOSAB 302. Sok. No.1 Nilüfer 16145 Bursa / TÜRKİYE

*Corresponding author: Benamir.Caylakoglu@marturfompak.com

ABSTRACT

In the automotive industry, fabrics are expected to be soil-resistant and easily cleanable, which makes waterproof applications a preferred solution. PFAS-based chemicals are widely used in waterproofing processes due to their superior performance in repelling water. However, the environmental and health-related concerns associated with PFAS have led to a growing demand for PFAS-free alternatives, driven by automotive original equipment manufacturers (OEMs). This study evaluates the performance of PFAS-free waterproofing treatments compared to their PFAS-based counterparts on a single fabric. The investigation focuses on assessing water repellency and stain resistance behaviours in accordance with automotive standards. The findings aim to provide insights into the feasibility of PFAS-free solutions in meeting industry expectations, contributing to the transition towards safer and more sustainable chemical applications.

Keywords: Automotive Seat Fabrics, PFAS's, PFAS's-free, Water Repellent, Soil Resistancy

I. INTRODUCTION

Automotive textiles constitute a significant field within technical textiles. Globally, automotive textiles account for approximately 20% of all technical textiles produced. In a standard passenger vehicle, around 20 kg of textile materials are used, with approximately 3.5 kg of this being seat upholstery fabrics [1,2]. Technical textiles used in the transportation sector rank first in terms of monetary value among all technical textiles, and second in production volume after packaging textiles. Various textile products with different structures and functions are utilized in automobiles. These products are typically found in seat upholstery, headliners, carpets, sun visors, door panels, dashboards, seat belts, and airbags [3].

Traditionally produced automotive seat upholstery fabrics generally consist of a three-layered structure. These layers include a woven, circular knitted, or warp-knitted fabric on the top surface, a laminated foam layer in the middle, and a circular knitted or warp-knitted backing fabric on the underside, which are combined using lamination techniques. The fabrics used for the top surface are usually made of polyester (PET), the foam layer in the middle is based on polyurethane (PU), and the backing fabrics are made from either PET or polyamide (PA) materials [4].

During the lamination process, the top surface fabric, the foam layer, and the backing fabric are bonded together to form a three-layer composite structure. This process is typically carried out using

flame lamination, which offers a fast and cost-effective solution. Flame lamination is a continuous lamination method that utilizes the adhesive properties of the foam [5].

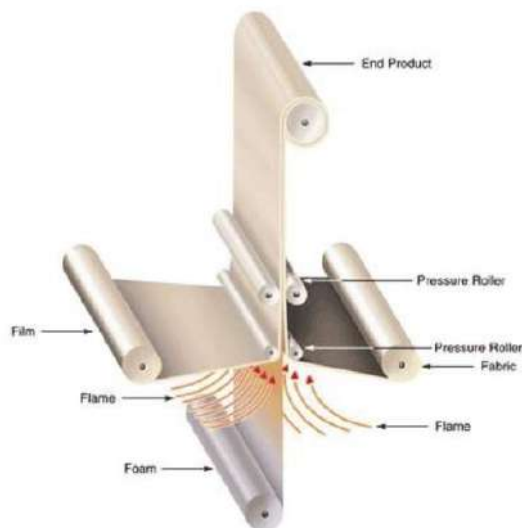


Figure 1. Flame Lamination Technique [3]

Waterproofing and stain resistance are important properties that protect textile surfaces from liquids and contaminants. In automotive seat covers, waterproofing prevents liquids from penetrating the fabric in case of spills or leaks, while stain resistance prevents dirt and stains from being absorbed by the fabric. As a result, the seats remain clean and look new for a longer time, and maintenance becomes easier. The waterproofing process creates a hydrophobic layer around the fabric using fluorocarbons, enhancing both durability and aesthetics. Additionally, such fabrics offer high durability, compatibility, and easy cleaning, making them especially suitable for applications like car seat covers. There is many commercially available water- and oil-repellent chemicals that can be classified into two categories: fluorocarbon based, or non-fluorocarbon based. [6,7].

Perfluoroalkyl and polyfluoroalkyl substances (PFASs) are a diverse group of synthetic chemicals known for their unique physicochemical properties, such as high thermal stability, hydrophobicity, and low surface energy [8]. These attributes have made PFASs

indispensable across a variety of industries, particularly in producing water-, oil-, and stain-resistant materials used in textiles, firefighting foams, lubricants, food packaging, and building products [9]. Moreover, PFASs play a crucial role in high-performance applications, including aerospace components, semiconductors, and medical devices, highlighting their extensive utility [10].

A key mechanism underlying PFAS applications is their ability to reduce surface tension. Surface tension is governed by cohesion forces among molecules within a liquid and adhesion forces between the liquid and a surface. By disrupting these forces, PFASs create surfaces where water and oils form beads rather than spreading, resulting in exceptional water and oil repellency. This property, combined with PFASs' durability, has been widely exploited in water-resistant coatings [8,11].

In the automotive industry, seat cover fabrics represent one of the primary uses of PFASs due to their ability to repel stains, dirt, and water [12]. Automotive seat covers are subjected to constant exposure to various contaminants, including liquids, oils, and dirt, which can compromise both aesthetics and functionality [13]. PFAS-treated fabrics provide a protective barrier, maintaining the cleanliness and durability of seat covers over time.

However, the extensive use of PFASs comes with significant environmental and health costs. The carbon-fluorine bonds that confer PFASs' chemical stability are among the strongest in organic chemistry, rendering these compounds highly resistant to degradation. This resistancy to the degradation, PFASs persist in ecosystems, bioaccumulate in living organisms, and have been detected in remote environments such as polar ice caps and deep ocean sediments. PFAS can enter the human body through drinking water, inhalation, food, dust, and skin contact, and they remain in the body for a long time.

The available data suggest that perfluoroalkyls are not metabolized nor do they undergo chemical reactions in the body. PFAS compounds can bind to a protein in the body called PPAR α , which activates certain genes as well as other intracellular proteins. This protein plays a key role in regulating important body functions such as fat metabolism, energy balance, and inflammation. PFAS substances are not easily excreted by the kidneys because specific transporter proteins reabsorb them back into the body, leading to accumulation over time. Epidemiological studies have shown that PFAS exposure is associated with kidney and testicular cancers, endocrine disruption, and immunotoxicity. In addition, it has been found to negatively affect the liver and the immune system. [11,13,14,15].

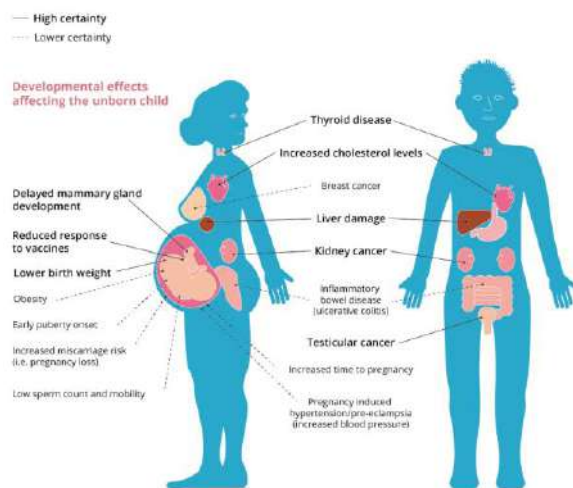


Figure 2. Effects of PFAS on Human Health

Growing regulatory and consumer pressure has led industries to seek PFAS-free alternatives, particularly in non-essential applications like automotive textiles [12]. Alternative treatments, such as silicone-based coatings, biodegradable polyesters, and cellulose-based finishes, are being explored to achieve similar levels of stain and water resistance without the environmental and health risks associated with PFAS [10]. Transitioning to these alternatives not only aligns with global sustainability goals but also provides an opportunity for innovation in developing safer and greener products for the automotive sector.

In the scope of this study, the effect of flourocarbon based and PFAS free chemical treatments on automotive fabrics are investigated for the liquid and soil repellency properties regarding the specifitations defined by main automobile manufacturers.

II. EXPERIMENTAL METHOD

In this study, a fabric with a twill structure was produced. After the production, finishing process was applied. Then, a waterproof chemical treatment was carried out on the treated fabric. Following this step, flame lamination was performed. During the lamination process, PU foam, scrim, and the treated fabric were combined to obtain the final product.

2.1 Materials and Preparation Techniques

2.1.1. Fabric Production

As a beginning of the study, fabric selection was made. Twill structure is chosen due to large usage of this design on the automotive seat covers. Fabric is produced with dobby weave technique. Warp and weft count, structure and weight of the twill fabric is shown on below table.

Table 1. Fabric Details

| Fabric Name | Warp | Weft | Weight (g/m ²) | | | Structure |
|-------------|------|------|----------------------------|------|-------|-----------|
| | | | Fabric | Foam | Scrim | |
| Twill | 28 | 20 | 261 | 147 | 28 | |

2.1.2. Finishing Process

Finishing process is contained three different processes. Those processes can be listed as; open width washing, tumbler and stentering. Finishing process steps are carried out as continue system from beginning to end. Fabric was washed at 70°C as an open-width and then tumbler process is initiated. Tumbler process is preferred for increasing the handle (touche) of the fabric during drying. In order to ensure the dimensional stability of the fabric, the stentering

process is applied. Stentering degree is 150°C and settled as the final width.

2.1.3. Waterproof Chemical Application

Chemical application is applied by after the finishing process is completed. Two different finishing process is applied to the fabric separately. One of the applications is done by using PFAS contained chemical, and the other is done by using PFAS-free chemical.

This treatment is applied when waterproof feature is requested to the fabrics. Impregnation technique was being used. First fulard batch have been prepared for the PFAS contained trial with 6 Carbon chemical and ratio is 40gr/L. Second fulard have been prepared for PFAS-free chemical trial with 20 g/L of water based aliphatic PU and 20 g/L of polysiloxane derivative water-based dispersion. Water-based aliphatic PU and polysiloxane derivative water-based dispersion were used in equal proportions to impart oil and water repellency to automotive textiles. The polyurethane component enhances flexibility and durability on the fabric surface, while the polysiloxane-based dispersion reduces surface energy to prevent liquid adhesion. This synergistic combination provides long-lasting stain resistance and easy cleanability on textile surfaces.

Both fulard is 165°C. Add-on ratio is 60-70%. Fulard cylinders pressure was 1,5 P and speed is 10 m/dk.

2.1.4. Lamination Process

Treated fabric need to be a composite material with foam and scrim to create automotive seating fabric. Flame lamination method is being used to get this three-layered composite material. Face fabric will be a treated fabric. Foam will be the used on the middle layer to get the resilience feature and gives a feeling of comfort. Scrim layer is minimizing the frictions between lamination foam and the seat foam and thanks to that minimization trimming process will be easier.

2.2. Characterization of Materials

2.2.1 Liquid Repellency Test

This procedure is used to assess the presence of liquid repellent coatings on interior seating fabric materials. This test has been performed as Ford's testing specifications. Test specimen has been prepared as 100x100 mm dimensions. The specimen should not contain any stitching and should be lay flat. Test specimen is placed on the flat surface with grid board or ruler for reference and when once is placed it should not be moved. The deionized water is slowly poured with using syringe. Water amount is 5 ml and syringe placement should be height of approximately 10 mm. Picture is taken of specimen with the reference ruler or grid board after the water is poured immediately. Picture will take in the same condition with the first picture after waiting 30 minutes. Test results evaluation is started after taking two pictures of the specimen. Two picture is compared between them, and size of water pool will check. Ruler or grid board is used as a reference doing this comparison. Water pool dimensions needs to stay same after the 30 minutes of waiting. If the water pool dimensions are got smaller after the 30 minute, test results are not acceptable according to automotive testing standard.

2.2.2. Staining Determination Test

This test is performed to determined the staining performance of the automotive seat cover fabrics. This test have been performed as Toyota's testing specifications. Test specimen has been prepared as 220x20 mm dimensions. White cotton cloths are used during the testing. 30 pieces of cotton cloths are prepared as 50x50 mm. Cotton cloth has to be to cover up the test specimens all surfaces. Test specimens L, a, b color values is taken by using spectrophotometer. This measurement values are reference values. Staining powder is prepared by using mixture of three different ingredients. These three ingredients are 20(±0,2) g soil with particle diameter 27-31 µm,

80($\pm 0,8$) g concrete dust with particle diameter 13-17 μm and 0,1($\pm 0,001$) g carbon black. The average particle diameter of prepared staining powder is 10-30 μm . 5 grams of staining powder is placed into 1 L of metal jar box. 10 pieces of cotton cloth is placed to the metal jar with staining powder. Metal jar's cap closed tightly and shaken to spread the staining powder to the cotton cloths. This procedure is repeated until all cotton cloths are done.

2.2.3 Liquid and Oil Repellency Test

This test is performed to evaluate the oil and water repellency performance of automotive seat cover fabrics in both the initial state and after abrasion. This test have been performed as Renault's testing specifications. Abrasion is performed using the Martindale method. In this method, only abrasion fabric is used (without Velcro band), and the test is conducted for 5000 cycles. After abrasion, the following test steps are carried out. Fabric specimens are prepared by cutting them into 100x100 mm pieces. Each sample is placed face-up on a flat surface. Oil repellency is tested using the chemicals listed in below tables.

Table 2. Chemicals to be used in oil repellency test

| Chemical | Test Liquid Number | Surface Tension (N/m at 25°C)*10 |
|------------------------------------------------------|--------------------|----------------------------------|
| complete penetration of paraffin oil into the fabric | 0 | |
| Paraffin Oil | 1 | 31,5 |
| Paraffin Oil / n-hekzadekan blend (65:35) | 2 | 29,6 |
| n-hekzadekan | 3 | 27,3 |
| n-tetradekan | 4 | 26,4 |
| n-dodekan | 5 | 24,7 |
| n-dekan | 6 | 23,5 |
| n-oktan | 7 | 21,4 |
| n-heptan | 8 | |
| n-hekzan | 9 | |

Table 3. Chemicals to be used in water repellency test

| Solutions | Test Liquid Number |
|----------------------------------|--------------------|
| Distilled Water (100%) | 0 |
| Water and Alcohol Solution (2%) | 1 |
| Water and Alcohol Solution (5%) | 2 |
| Water and Alcohol Solution (10%) | 3 |
| Water and Alcohol Solution (20%) | 4 |
| Water and Alcohol Solution (30%) | 5 |
| Water and Alcohol Solution (40%) | 6 |
| Water and Alcohol Solution (50%) | 7 |
| Water and Alcohol Solution (60%) | 8 |
| Water and Alcohol Solution (70%) | 9 |
| Water and Alcohol Solution (80%) | 10 |
| Water and Alcohol Solution (90%) | 11 |
| Alcohol (100%) | 12 |

Starting with the lowest-numbered liquid, three drops (approx. 8 mm in diameter) are applied to the fabric surface with a 4 cm gap between each. The dropper should be held no more than 10 mm above the fabric without touching it. The drops are observed for 30 (± 2) seconds from a 45° angle to check for absorption. Evaluation is made visually according to the following criteria:

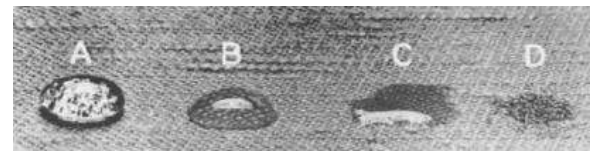


Figure 3. Visual evaluation references

- A: Pass – round, intact droplet
- B: Partial pass – slight darkening with round droplet
- C: Fail – visible absorption and wetting
- D: Fail – complete wetting

If there is no wetting or absorption, the next higher-numbered chemical is tested on a new specimen. A separate fabric specimen is used for each test liquid.

Testing continues until visible wetting is observed. When wetting occurs, the back side of the fabric is also checked for penetration. The repellency rating is determined as the highest-numbered liquid that shows no wetting or absorption within 30 (± 2) seconds. A score of "0" indicates full penetration of paraffin oil (for oil test) or pure water (for water test). Darkening or shadowing at the fabric-liquid interface indicates wetting. On dark-colored fabrics, wetting is detected by the loss of droplet gloss.

The test is repeated on a second sample. Out of the total six drops (three per sample):

- If 4 or more show result C or D, the sample fails.
- If 4 or more show result A, the sample passes.
- If 4 or more show result B, the test is considered partially successful, and the rating is reduced by 0.5 points.

For both initial and post-abrasion conditions, the back side of the fabric is checked for any fluid traces, and final results are recorded by comparing measured values with the required limits.

2.2.4 Flammability Test

The method described is designed to assess the flammability properties of textile surfaces, in accordance with the guidelines established by ISO 3795 and FMVSS-302 standards. This procedure involves positioning the specimen horizontally on a flat surface, after which a controlled flame is introduced at one edge of the fabric. The duration of the flame exposure is strictly regulated according to the specifications provided in the standard. Once the flame is extinguished, the rate at which the flame propagates across the material is carefully measured between two predetermined points marked on the specimen. This testing procedure plays a vital role in evaluating the material's resistance to ignition, as well as its ability to control and slow the spread of fire. The results are of critical importance in a variety of

industries where textiles are used, particularly in safety-critical applications such as automotive interiors, upholstered furniture, and apparel. By determining how a fabric behaves when exposed to flame, manufacturers can ensure that the materials used meet the necessary safety standards, thereby minimizing the risk of fire hazards in everyday environments.

III. RESULTS AND DISCUSSION

Test results of the samples are shown below.

Table 4. Samples Test Results

| Treatment Type | Liquid Repellency | | Staining Determination |
|-----------------------------------|-----------------------------|-------|------------------------|
| Sample A (PFAS's Based) | PASS (No Soak In) | | 3/4 |
| Sample B (PFAS's Free) | PASS (No Soak In) | | 2/3 |
| Treatment Type | Liquid /Oil Repellency Test | | Flammability |
| | Oil | Water | |
| Sample A (PFAS's Based) | 5 | 4 | Self Extinguish |
| Sample B (PFAS's Free) | 0 | 1 | Self Extinguish |

Both Sample A (PFAS's-based) and Sample B (PFAS's-free) passed the liquid repellency test, indicating that neither sample allowed water to soak in or change the size of the water pool after the 30-minute observation period. This shows that both treatments provide sufficient water repellency for static liquid exposure. However, visual inspection alone may not fully capture long-term performance, thus further testing under dynamic conditions could be beneficial.

When the staining determination test is evaluated, Sample A showed a staining rating of 3/4, whereas Sample B scored 2/3. This indicates that the PFAS's-contained treatment is more effective in resisting particulate staining compared to the PFAS's-free alternative. The slightly higher score of Sample A suggests a better ability to prevent discoloration and

maintain surface cleanliness after exposure to common automotive contaminants.

Significant differences were observed in liquid and oil repellency test. Sample A demonstrated superior repellency, with scores of 5 for oil and 4 for water. In contrast, Sample B showed poor resistance, with a score of 0 for oil and 1 for water. This highlights a key limitation of the PFAS-free treatment in terms of protection against oily and aqueous substances. The performance gap indicates that PFA-based chemicals still offer considerable advantages in terms of dynamic repellency, which is critical in automotive interiors where various liquids may contact the fabric.

Both samples were rated as “Self-Extinguish,” meaning neither fabric continued to burn after the ignition source was removed. This result confirms that the absence of PFAS in Sample B did not compromise the flammability resistance required by automotive safety standards. It is a promising outcome, suggesting that alternative chemistries can be used without negatively affecting flame resistance.

IV. CONCLUSION

This study examined the performance of two different treatments—one containing PFAS and one that is PFAS-free—applied to automotive seat fabrics. The main goal was to evaluate how well these treatments could protect the fabric from water and dirt. Results showed that both types met the essential safety and durability standards required for car interiors.

However, the PFAS-based treatment showed better results, especially in terms of oil repellency and resistance to dirt and stains, even under conditions that reflect daily use. This points to the ongoing difficulty of making PFAS-free alternatives that can match the performance of traditional PFAS treatments in real-world situations.

The PFAS-free option did show some positive features. It provided good water repellency and

maintained its flame resistance, which are both important in the automotive field. Still, its lower resistance to oil and particulate stains shows that further improvements are needed. The gap in performance suggests that existing PFAS-free chemistries require further optimization to match the durability and protective qualities provided by traditional PFAS solutions. Looking ahead, developing advanced PFAS-free formulations—potentially through hybrid chemical systems or nanotechnology-based coatings—could improve performance while also meeting growing environmental and regulatory demands.

In conclusion, this study offers helpful insights for the automotive textile industry. By identifying both the benefits and the current limitations of PFAS-free solutions, it supports the shift toward more sustainable, safe, and high-performance materials for automotive seats.

REFERENCES

- [1] Fung, W., Hardcastle, M. (2001). Textiles in Automotive Engineering. Woodhead Publishing Limited, Cambridge, England.
- [2] Akkuş, İ. (2019). Otomotiv döşemelik kumaş tasarımı ve tasarımı belirleyen faktörlerin incelenmesi (Yüksek lisans tezi). Eskişehir Teknik Üniversitesi, Endüstriyel Sanatlar Anabilim Dalı, Eskişehir.
- [3] Powell, N.B. (2006). Design management for performance and style in automotive interior textiles, *Journal of the Textile Institute*, 97:1, 25-37. doi:10.1533/joti.2005.0166
- [4] Horrocks, A.R. (2016). Technical textiles in transport (land, sea, and air), Editors: Horrocks, A.R. Anand, S.C., *Handbook of Technical Textiles (Second Edition)*, Woodhead Publishing, pp:325-356.
- [5] Ömeroğulları Başyigit, Z. (2019). Improvement of multifunctional automotive textile. *Textile and Apparel*, 29 (2), 113-120. doi:10.32710/tekstilvekonfeksiyon.475490
- [6] Joshi, M., & Adak, B. (2019). 6. Nanotechnology-based Textiles: A Solution for the Emerging Automotive Sector. *Rubber Nanocomposites and Nanotextiles*, 179–230. doi:10.1515/9783110643879-006
- [7] Nazari, A., Jalili, Y. S., & Derakhshan, S. J. (2017). Design and Waterproof of Car Coatings Using Art Simulation Techniques and Flora Polyacrylamide. *International Journal of Applied Arts Studies (IJAPAS)*, 1(1). Retrieved from <http://www.ijapas.ir/index.php/ijapas/article/view/41>
- [8] Kissa, E. (2001). *Fluorinated Surfactants and Repellents* (2nd ed.). CRC Press.
- [9] Dias, D., Bons, J., Kumar, A., Kabir, M. H., & Liang, H. (2024). Forever Chemicals, Per- and Polyfluoroalkyl Substances (PFAS), in *Lubrication. Lubricants*, 12(4), 114.
- [10] Wang, Z., Cousins, I. T., Scheringer, M., & Hungerbühler, K. (2013). Fluorinated alternatives to long-chain perfluoroalkyl carboxylic acids (PFCAs), perfluoroalkane sulfonic acids (PFASs) and their potential precursors. *Environment International*, 60, 242–248.
- [11] Lau, C., Anitole, K., Hodes, C., Lai, D., Pfahles-Hutchens, A., & Seed, J. (2007). Perfluoroalkyl Acids: A Review of Monitoring and Toxicological Findings. *Toxicological Sciences*, 99(2), 366–394.
- [12] Bălan, S. A., Bruton, T. A., & Hazard, K. G. (Eds.). (2023). *Toward a PFAS-free Future: Safer Alternatives to Forever Chemicals* (No. 81). Royal Society of Chemistry.
- [13] Blum, A., Balan, S. A., Scheringer, M., Trier, X., Goldenman, G., Cousins, I. T., ... & Fletcher, T. (2015). The Madrid Statement on Poly- and Perfluoroalkyl Substances (PFASs). *Environmental Health Perspectives*, 123(5), A107–A111.
- [14] Agency for Toxic Substances and Disease Registry (ATSDR). 2020. Toxicological Profile for Perfluoroalkyls. Atlanta, GA: U.S. Department of Health and Human Services, Public Health Service. [ATSDR Perfluoroalkyls \(PFAS\) ToxGuide](#)
- [15] Spyraakis, F.; Dragani, T.A. The EU's Per- and Polyfluoroalkyl Substances (PFAS) Ban: A Case of Policy over Science. *Toxics* 2023, 11,721. <https://doi.org/10.3390/toxics11090721>



16 ULUSLARARASI
LİF VE POLİMER
ARAŞTIRMALARI
SEMPZYUMU

16th INTERNATIONAL FIBER AND POLYMER RESEARCH SYMPOSIUM

Sürdürülebilir ve İşlevsel Lif ve Polimerler
Sustainable and Functional Fibers & Polymers



9-10 Mayıs
May 2025

İstanbul Teknik Üniversitesi
Gümüşsuyu Prof. Dr. Necmettin Erbakan Yerleşkesi
Istanbul Technical University
Gumussuyu Prof. Dr. Necmettin Erbakan Campus



An investigation study about LMF Co-PET fiber utilization on flat knitted automotive fabric structure

Osman AYDIN^{a*}, Semih OYLAR^b, Nur Ceyda UYANIKTIR^c

^aMartur Fompak International, NOSAB 302. Sok. No.1 Nilüfer 16145 Bursa / TÜRKİYE

*Corresponding author: osman.aydin@martur.com

ABSTRACT

Technical textile products provide the fulfillment of many needs with textile surfaces today. Agriculture textiles, construction textiles, medical textiles are some important sub-branches of technical textile groups. Automotive textiles, as another sub-group of technical textiles, must meet the technical requirements determined by car manufacturers as well as providing comfort features to the vehicle user. These technical requirements are basically tests performed with methods determined by automotive manufacturers such as abrasion resistance, resistance to climatic conditions, color fastness, UV resistance, and flame retardancy. Apart from technical requirements, regulations on sustainability enable automobile manufacturers to set new targets for their products and production, requiring the production methods used and the selected raw materials to be reconsidered. In this context, Flat Knit knitting technology has gained importance in recent years in the production of automotive textiles with its advantages such as fast preparation time and waste-free production. The use of fabrics produced with this technology has already been included in some concept vehicles. Within the scope of this study, it was investigated whether the fabrics produced with Flat Knitting technology to be used on automobile textile surfaces, supported by co-polyester yarn structures, had an improvement effect on the tests determined by automotive manufacturers.

Keywords: Automotive Textiles; Flat Knit Technology Sustainability in Textiles; Technical Performance Tests; Co-Polyester Yarns

I. INTRODUCTION

Technical textiles are an important and rapidly developing area of the global textile industry. These textiles are produced mainly for their functional properties rather than their appearance. They are widely used in fields such as medical, geotextile, protective, and especially automotive sectors. In the automotive industry, the need for advanced materials has grown. As a result, technical textiles have become more valuable for improving both the performance and comfort of vehicle interiors [1].

Automotive textiles comprise around 50 square meters of fabric per vehicle, depending on the model, and are employed in applications such as seat covers, roof and door liners, carpets, insulation, and safety belts [2].

These fabrics are expected to demonstrate high abrasion resistance, UV stability, flame retardancy, dimensional stability, and resistance to pilling, while also meeting the design expectations of Original Equipment Manufacturers (OEMs) [3].

In addition to technical requirements, interest in sustainability and environmentally friendly production methods has increased in the automotive sector. In this context, demand for production technologies that lead to less waste production and lower energy consumption has significantly grown [4]. One of the promising approaches that aligns with these sustainability goals is the V-bed flat knitting technique. Unlike traditional fabric production methods such as weaving, circular knitting, or warp knitting, flat knitting eliminates production waste

generating fabrics exactly in the shape and dimensions of the programmed pattern. This method results in zero fabric offcuts, as the material is knitted only where needed, effectively reducing raw material usage and industrial textile waste. Furthermore, since the knitted fabric does not require subsequent cutting or sewing, the energy consumption associated with these additional processes is completely avoided, which not only streamlines production but also enhances overall energy efficiency. This makes flat knitting not only a technically efficient option but also a more environmentally responsible alternative in the production of automotive interiors, where sustainability is becoming an ever more critical criterion [5,6].

To successfully integrate such sustainable methods into the automotive upholstery sector, it is essential to determine design and production techniques that can satisfy both environmental concerns and the quality standards set by automotive manufacturers. In this regard, the appropriate use of flat knitting technologies, combined with suitable material selection, can contribute to meeting OEM requirements. Design strategies tailored to the specific demands of the automotive industry play a crucial role in achieving performance, durability, and aesthetic goals while also supporting environmentally conscious manufacturing [7].

Traditionally, woven and warp-knitted fabrics have dominated automotive interior applications due to their well-established mechanical strength and dimensional stability. However, advancements in V-bed flat knitting technology have opened new possibilities by enabling the creation of three-dimensional, double-layered, and form-fitting textile structures. These capabilities not only enhance the functional performance of textile components but also provide greater freedom in aesthetic and ergonomic design—allowing for seamless integration into complex interior geometries. Therefore, when strategically employed, V-bed flat knitting emerges as a forward-looking production method that aligns with both the technical and sustainability expectations of the modern automotive sector [8].

Moreover, V-bed flat knitting offers designers capabilities that rival, and in certain aspects, surpass those of traditional weaving. This technology allows a diverse range of yarns, including chenille, flock, and fine bouclé, allowing for intricate surface textures and jacquard patterns that rival color weaving techniques. Additionally, the knit geometry allows for greater

stretch and flexibility, which can be advantageous when shaping the fabric to complex panel forms [9].

Although V-bed flat knitting technology offers significant advantages in terms of sustainability and design flexibility, it faces some technical challenges that prevent its widespread use in automotive textile applications. In particular, the insufficient structural stability of flat knitted fabrics makes them more elastic and less dimensionally stable than traditional woven materials. This can lead to performance problems in applications where form retention and durability are critical, such as seat covers and molded interior panels. In addition, the production speed of flat knitting machines is relatively lower than that of looms, which can affect large-scale production efficiency [10]. To overcome these limitations, the integration of low melt fibers in flat knitted structures is emerging as a promising solution.

LMF is a bi-component fiber produced especially with the composition of Co-PET/PET (copolyester/polyethylene terephthalate). This fiber contains a low melting point Co-PET on the outside and a high melting point PET core on the inside. Thanks to this structure, LMF fibers can melt between 60–180°C and be bonded with other polyester fibers through heat [11,12]. This structure improves the mechanical properties and processability of the material. LMF Co-PET offers better flexibility and thermal forming ability while maintaining the hardness and durability of PET. The use of LMF co-PET in the production of fabrics that require improvement in dimensional stability and strength properties, such as flat knitted fabrics, contributes to the fibers melting and acting as a binder and obtaining a more stable structure when the fabric production is completed and subjected to the steaming process. Thus, LMF co-PET plays a key role in meeting the technical standards set by Original Equipment Manufacturers (OEMs) [13].

In this study, two fabric samples containing LMF co-PET fiber and one without LMF co-PET fiber were produced in the v-bed flat knit machine. Then, they were tested according to automotive specifications and the effect of co-PET was investigated.

Since flat knitted fabrics are produced directly in the shape and dimensions of the final product, conventional roll-to-roll lamination processes cannot be applied. Therefore, the appropriate lamination method for flat knitted fabrics is piece lamination. In this study, the tests were conducted on non-laminated fabric samples. However, since the test specifications

were determined for laminated fabrics, this may have influenced the test results and is considered a potential factor affecting the outcomes.

II. EXPERIMENTAL METHOD

Double-layered knitting structure that can meet automotive standards created on V-bed flat knitting machines. In this context, one sample was produced with PET and another sample was PET/Co-PET yarns combinations. These two samples were tested and compared between each other according to automotive specifications.

2.1 Materials and Preparation Techniques

PET based yarns are traditionally used in automotive industry, which are the most suitable for Oem's requirements. Durability, light and heat resistance, abrasion and pilling resistance behaviors of PET yarns are spotting between other fiber types. According to automotive seat cover fabrics requirements, production method and machine gauge 600 denier total thickness PET yarns were used on sampling. However, for raising surface covering of sample 300 den 96f DTY yarns were fed in yarn carrier 2 times for each layer on sample1. In this way of use, it makes the sample surface area more closed due to its voluminous structure and naturally supports the creation of tighter loops. On the other hand, since knitted structures have weaker behaviors such as abrasion and stitching compared to woven structures. Therefore, different materials are needed that will support the structure of the weave and will not be visible in the pattern. To meet this demand, LMF co-PET yarns were selected to support the structure, acting as a binder after heat treatment. In order to investigate the effects of co-pet yarn, sample 2 was fed with 2 layers of 300den 96f yarn and 75/14f LMF yarn to the same yarn carrier.

Table 1. Used Materials of the Knitted Fabrics

| Samples | Yarn Type | Yarn Feeding |
|---------|-----------------------------------------|--------------|
| Sample1 | PET 300 den 96f DTY | 2 |
| Sample2 | PET 300 den 96f DTY /75den 14f coPET | 2+1 |

The CMS530 Ki BcW model of Stoll, one of the well-known manufacturers of V-bed flat knitting machines, was used for sample production along with the determination of yarns.



Figure 1. Stoll CMS530 Ki BcW Multigauge

As mentioned before, in order to meet the requirements of automotive technical tests, it is important that the loop structure in knitted fabrics is tight. In this context, the loop lengths for front loops (NP5), back loops (NP6) and connections (NP7) were defined separately as below in the table.

Table 2. Loop Length Values

| Samples | NP5 | NP6 | NP7 |
|----------|------|------|-----|
| Sample 1 | 10,8 | 10,8 | 8,5 |
| Sample 2 | 10,8 | 10,8 | 8,5 |

After definition of all the parameters such as; yarn type, production method and loop lengths, design was created and checked with Stoll M1+ design program as figure2.

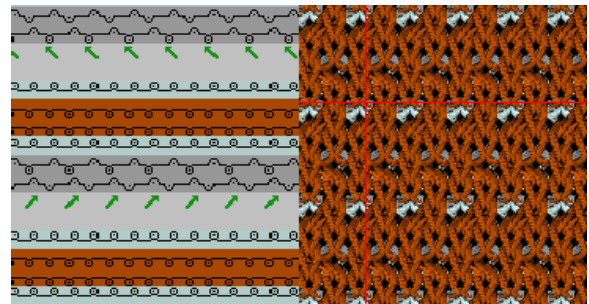


Figure2. Needle Notation and Simulation of Design

4 pieces for each were produced. As a final step all the samples were subjected to the finishing process as below.

Tumbler washing 30°C → Drying at room temperature → Hot steaming between 120°C to 150°C → Conditioning at laboratory norms

2.2. Characterization of materials

2.2.1. Thickness and Weight Measurement

Thicknesses have been measured of the produced fabric samples in accordance with VOLKSWAGEN DIN EN ISO 5084. The thickness (mm) was determined using thickness gauge for textile structures. Weight have been measured of samples according to the DIN EN 12127. The produced fabrics are cut into round shapes with an area of one square meter. Then, they are weighed on a precision scale.

2.2.2. Martindale Abrasion Test

The Martindale abrasion resistance of the laminated fabrics was tested in accordance with the VOLKSWAGEN DIN EN ISO 12947-1 standard. Prior to testing, fabric samples were conditioned for at least 24 hours under standard atmospheric conditions of 23 (± 2) °C temperature and 50 (± 5) % relative humidity. Circular test specimens with a diameter of 38 mm were then prepared from each fabric.

The abrasion test was conducted using a Martindale abrasion tester. A Martindale standard abrasion fabric, with a diameter of at least 140 mm or dimensions of 140x140 mm, was placed on the lower holder of the device. The number of abrasion cycles was determined based on the intended application area of the fabric in automotive interior trim. Tests were carried out at 10,000, 35,000, 50,000 and 70,000 cycles.

At the end of the test, samples were evaluated using the ISO grey scale to assess the degree of abrasion. Additional signs such as yarn breakage and pilling were also observed and reported. Surface wear was rated on a scale from 1-5. According to VOLKSWAGEN DIN EN ISO 12947-1 and DIN EN 20105-A02 standards, a minimum grade of 3 on the greyscale is required, and no yarn breakage should be visible on the fabric surface.



Figure 3. Martindale test device

2.2.3. Velcro Hook Fastener Test

The samples were tested to evaluate their abrasion durability according to the VOLKSWAGEN PV 3961 standard. 3 circular samples with a diameter of 150 mm are cut from the fabric to be tested and prepared. The samples to be tested are conditioned by



waiting for at least 24 hours in a laboratory environment with a temperature of 23 (± 2) °C and a relative humidity of 50 (± 6) %. If the fabric to be tested is laminated, the total thickness should be 5 mm at most. If a non-laminated fabric is being tested or if the total thickness is less than 3 mm, felt in accordance with the DIN EN ISO12947-1 method should be placed under the sample. The fabric to be tested is fixed to the lower table of the device. A 100% PA velcro tape, 38 mm in diameter, is cut and placed on the moving upper head of the device and a foam in accordance with the DIN EN 12947-1 standard is added under the velcro tape. An additional weight of 12 kPa is placed on the test sample. The cycle number is set to 50 turns and the test is started. At the end of the test, any defects in appearance, such as pilling, pilling, etc. on the fabric surface are evaluated and graded in a light cabin under D65 daylight with the help of evaluation scales.



Figure 4. Velcro Test Device

2.2.4. Schopper Abrasion Test

The schopper abrasion resistance of the laminated fabrics was tested in accordance with the VOLKSWAGEN PV 3908 standard. The samples to be tested are conditioned by waiting for at least 24 hours in a laboratory environment with a temperature of 23 (± 2) °C and a relative humidity of 50 (± 5)%. A circular sample of 100 cm² in diameter is cut from the fabric to be tested. The prepared test sample is attached to the Schopper abrasion device and a weight of 10 N

(980 g) is placed on the device. Abrasive sandpaper is attached to the device. The device is set for a total of 500 cycles to the right and 500 cycles to the left, 100 cycles to the right and 100 cycles to the left. The total number of cycles should be 1000 cycles. The change on the fabric surface is evaluated by checking with the ISO gray scale. It should be checked whether there is any yarn breakage, pilling, etc. on the fabric surface.

Figure 5. Schopper test device

2.2.5. Static Elongation Test

The samples were tested to evaluate their static elongation properties under load according to the VOLKSWAGEN PV 3909 standard. For the test, three specimens each were prepared in the transverse and longitudinal directions. All samples were conditioned for at least 24 hours at 23 (±2) °C and 50 (±6) % relative humidity prior to testing.

A 100 mm gauge length was marked at the center of each sample. The specimens were then mounted in the upper and lower grips of the testing device along these marks without applying any pre-tension. A load of 25 N was applied to the lower end of each sample, and the samples were left under this load for 30 minutes. After the specified duration, the elongated length (L1) was measured. The static elongation percentage was calculated using the formula:

$$\text{STATIC ELONGATION \%} = [(L1 - L0) / L0] * 100$$

2.2.6. Flammability Test

The flammability behavior of the fabric samples was tested in accordance with the VOLKSWAGEN TL1010 standard. Before the test, the samples were conditioned by waiting for 24 hours at 23 (±2) °C temperature and 50% (±6) relative humidity conditions. Each sample was prepared in 356 x 100 mm dimensions and a maximum thickness of 13 mm. The test sample was placed on a U-shaped holder and positioned at 19 mm distance from the burner. The lower end of the sample was in contact with the flame for 15 seconds and the combustion was monitored by starting the chronometer when the flame reached the reference line (38 mm). The chronometer was stopped when the flame was extinguished or when it reached the 2nd reference line (254 mm) and the elapsed time (T) was recorded. The burning distance (S) was

measured, and the burning rate (Vc) was calculated in mm/min.

$$Vc = 60 \times (S / T)$$

If the sample is self-extinguishing, the burning rate is stated as "0". In completely burnt samples, the burning rate is recorded as "BR (burn rate)"; for self-extinguishing ones, "SE/BR" and for burning times shorter than 60 seconds, "SE/NBR" are used. The maximum burning rate value obtained after each test is recorded as the test result. According to the related standard, the maximum acceptance value is 100 mm/min.

2.2.7. Seam Fatigue Test

The seam fatigue behavior of the fabric samples was tested in accordance with the VW 50105 standard. The prepared test samples are fixed by attaching them to the jaws of the tensile device. The tensile direction should be perpendicular to the stitch. The stitch is adjusted in the middle of the jaws, so that there is equal distance at the bottom and top. The distance between the jaws is set to 100 (±1) mm. The test speed is set to 100 (±10) mm/min and the test is started. The maximum breaking force is recorded in Newton. The way the breakage occurs is reported. It is specified in detail as fabric tearing, fabric tearing from the jaws, fabric tearing from the seam, sewing thread breakage, thread coming out, etc. In tests resulting in fabric tearing from the seam, sewing thread breakage, thread coming out, etc., the average of the maximum forces is taken in Newton and the values found for each direction are rounded to the nearest value in the figure below.

III. RESULTS AND DISCUSSIONS

Table 3. Thickness and weight measurements

| Samples | Thickness (mm) | Weight (g/m ²) |
|----------|----------------|----------------------------|
| Sample 1 | 2,23 | 927 |
| Sample 2 | 2,26 | 937 |

Comparison of sample1 and sample2 thicknesses shows usage of co-PET not effecting thickness. But weight was raised.

Table 4. Martindale test results

| Samples | 10k | 35k | 50k | 70k |
|----------|-----|-----|-----|-----|
| Sample 1 | 4 | 4 | 3 | 2/3 |
| Sample 2 | 4/5 | 4/5 | 4 | 3 |

Sample1 failed under 70k there are yarn breakage and whitening on tested specimen Sample2 passed all the 10K, 35K, 50K and 70K martindale tests

Table 5. Velcro and schopper test results

| Samples | Velcro result | Schopper result |
|----------|---------------|-----------------|
| Sample 1 | 1 | 2/3 |
| Sample 2 | 2 | 3 |

Evaluation of velcro results sample1 is hairier according to sample2.

On the other hand, on schopper tested sample2 specimen is exceptable according to OEM's requirements.

Table 6. Static elongation and flammability test results

| Samples | Static elong | | Flammability | |
|----------|--------------|-------|--------------|-------|
| | Length | Width | Length | Width |
| Sample 1 | 7,29 | 7,21 | SE | SE |
| Sample 2 | 1,91 | 3,18 | SE | SE |

Regarding elongation test results, when sample1 and sample2 were compared, sample2 (LMF co-PET used fabric) worked as more supportive on the permanent elongation testing. As observed, it brought the elongation values in both width and length directions to the level of values specified in the specifications.

According to flammability test results, both samples produced are self-extinguishing. coPET yarn had no positive or negative effect on flammability results.

IV. CONCLUSIONS

In this study, the utilization of Low Melt Fiber (LMF) Co-PET in flat knitted automotive fabrics was investigated in terms of mechanical performance and structural efficiency. The results demonstrated that LMF Co-PET fiber reinforcement enhanced the overall tensile strength and dimensional stability of the fabric without compromising flexibility. These findings suggest that incorporating LMF Co-PET into knitted structures offers a promising developing sustainable, high-performance textile components in the automotive sector. Beyond its technical contributions, this study also supports the industry's shift toward more eco-friendly materials and processing techniques. Further research is recommended to explore long-term durability, recyclability, and cost analysis in real-life automotive interior applications.

REFERENCES

- [1] Horrocks, A. R., & Anand, S. C. (Eds.). (2000). *Handbook of technical textiles*. Elsevier.
- [2] Shishoo, R. (Ed.). (2008). *Textile advances in the automotive industry*. Elsevier.
- [3] Parmar, S., & Malik, T. (2018). Application of textiles in automobile application.
- [4] Şengel, A. (2024). Otomotiv Sektöründe Sürdürülebilirlik ve Otomotiv Üretici Firmalarının Sürdürülebilirlik Stratejileri. *Çevre İklim Ve Sürdürülebilirlik*, 25(2), 87-96.
- [5] Liu S, Mao S, Zhang P. Toward on integrally-formed knitted fabrics used for automotive seat cover. *Journal of Engineered Fibers and Fabrics*. 2021;16. doi:[10.1177/15589250211006544](https://doi.org/10.1177/15589250211006544)
- [6] Underwood, J., & Islam, S. (2024). Garment machinery for regenerative manufacturing. In *Sustainable Innovations in the Textile Industry* (pp. 405–426). The Textile Institute Book Series. <https://doi.org/10.1016/B978-0-323-90392-9.00017-3>
- [7] Powell, N. B. (2006). Design management for performance and style in automotive interior textiles. *Journal of the Textile Institute*, 97(1), 25-37.
- [8] Abounaim, M., & Cherif, C. (2012). Flat-knitted innovative three-dimensional spacer fabrics: A

competitive solution for lightweight composite applications. *Textile Research Journal*, 82(9), 897–904. <https://doi.org/10.1177/0040517511426609>

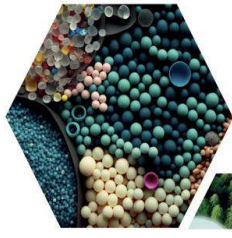
[9] Shima Seiki (2025) WHOLEGARMENT® knitting technology. <https://www.shimaseiki.com/product/knit/feature/>. Accessed 6 April 2025

[10] Choi, W., & Powell, N. B. (2005). Three dimensional seamless garment knitting on V-bed flat knitting machines. *Journal of Textile and Apparel, Technology and Management*, 4(3), 1-33.

[11] Fiberpartner (2025) Recycled Low Melt BiCo. <https://fiberpartner.com/products/recycled-low-melt-bico/>. Accessed 9 April 2025

[12] Intraros (2025) Staple fiber for non-wovens – LMF. <https://intraros-fibers.com/en/product/staple-fiber-for-non-wovens/lm/lmf/>. Accessed 10 April 2025

[13] Çelikel, D. C., & Babaarslan, O. (2017). Effect of Bicomponent Fibers on Sound Absorption Properties of Multilayer Nonwovens. *Journal of Engineered Fibers and Fabrics*, 12(4), 155892501701200. doi:10.1177/15589250170120040



16 ULUSLARARASI
LİF VE POLİMER
ARAŞTIRMALARI
SEMPOZYUMU

16th INTERNATIONAL FIBER AND POLYMER RESEARCH SYMPOSIUM

Sürdürülebilir ve İşlevsel Lif ve Polimerler
Sustainable and Functional Fibers & Polymers



9-10 Mayıs
May 2025

İstanbul Teknik Üniversitesi
Gümüşsuyu Prof. Dr. Necmettin Erbakan Yerleşkesi
İstanbul Technical University
Gumussuyu Prof. Dr. Necmettin Erbakan Campus

Identification of bisphenol A (BPA) sources in textile products and its contamination of wastewater

Hülya Kıcık^{a*}, Ayşe Ceren Şen^a

^aElyaf Tekstil, Ar-GeMerkezi, 16450 Bursa, Türkiye.

*Corresponding author: hulya.kicik@elyaf.com

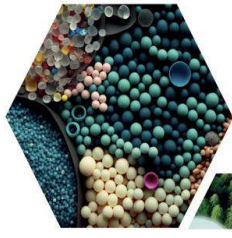
ABSTRACT

According to the US EPA, bisphenol A (BPA) are one of the most widely produced chemicals worldwide. BPA is used as a monomer in the production of polycarbonate plastics, epoxy resins, acrylic resins and polysulfones. Bisphenol A is a synthetic endocrine disrupting chemical and endocrine disrupting chemicals cause adverse health consequences. This chemical compound has been observed to trigger genotoxic and epigenetic responses.

Several studies have been conducted on bisphenol A in daily clothes. Bisphenol A was found in end products made from different compositions, mostly recycled products. However, no detailed study was carried out on whether the main source of this problem was the production processes, the yarns, or the chemicals. The purpose of the present work was to identify the origin of bisphenol A in textile products.

In the scope of the study, the presence of BPA was analysed in 24 yarns, 20 fabrics, 25 dyes, 30 chemicals and 28 different pre-treatment, dyeing or washing baths by using LC-MS/MS. Test results show that the main source of BPA is recycled yarns. BPA levels of recycled yarns are between 35 - 2500 ppb. The level of BPA in fabric gradually decreases after the production processes. However, this also increases the presence of BPA in the process wastewater. The study also shows that BPA levels in products significantly increase when left in sunlight.

Keywords: Bisphenol A (BPA); Recycled Polymers; Health Risks; Textile Wastewater



16 ULUSLARARASI
LİF VE POLİMER
ARAŞTIRMALARI
SEMPOZYUMU

16th INTERNATIONAL FIBER AND POLYMER RESEARCH SYMPOSIUM

Sürdürülebilir ve İşlevsel Lif ve Polimerler
Sustainable and Functional Fibers & Polymers



9-10 Mayıs
May 2025

İstanbul Teknik Üniversitesi
Gümüşsuyu Prof. Dr. Necmettin Erbakan Yerleşkesi
İstanbul Technical University
Gumussuyu Prof. Dr. Necmettin Erbakan Campus



Production of facial sheet masks by adding green synthesized Ag nanoparticles with plant extracts and collagen to PCL composite nanofibers: Use in acne and wrinkle removal.

Cansu Güneş^a, Fatma Ahsen Öktemer^b, Edanur Korkmaz^c, Ahmet Avcı^{d,*}

^a İzmir Vocational School, Biomedical Device Technology Program, Dokuz Eylül University, 35210, İzmir, Türkiye

^b Biomedical Engineering Department, Necmettin Erbakan University, Konya, 42090, Türkiye

^c Biomedical Engineering Department, Necmettin Erbakan University, Konya, 42090, Türkiye

^d Mechatronics Engineering Department, KTO Karatay University, Konya, Postal Code, Türkiye

*Corresponding author: ahmet.avci@karatay.edu.tr

ABSTRACT

Acne, which occurs when the skin's pores become clogged with oil, dead skin or bacteria, is the 8th most common disease in the world and experienced by 80% of teenagers. Wrinkles occur on the face due to reasons such as slowing down collagen production with age, using excessive facial expressions, dry skin, pores blocked by dead skin cells, etc.

This study consists of two parts. In the first part, encapsulated Ag nanoparticles were produced with green synthesis using chamomile extract, aloe vera and collagen, which are effective against acne-causing bacteria. In the second part, different Ag nanoparticles were produced using wrinkle-preventing yoghurt herb, aloe vera that keeps the skin moist and collagen that nourishes the tissues.

Biodegradable PCL nanofibers containing Ag nanoparticles encapsulated with plant extracts were prepared with electrospinning technique for anti-acne and anti-wrinkle facial masks. The active ingredients in plant extracts can be transported to the skin in a controlled manner by means of biodegradable PCL nanofibers. Ag nanoparticles with antibacterial properties also eliminate bacteria on the skin.

The morphologies of Ag nanoparticles encapsulated with plant extracts and PCL composite nanofibers were analysed by scanning electron microscopy (FE-SEM) and transmission electron microscopy (TEM) images. The composite nanofibers were characterized by structural analysis technique using Fourier transform infrared spectroscopy (FT-IR). In addition, the strength of nanofibers with tensile tests and antibacterial activities with antibacterial tests were examined.

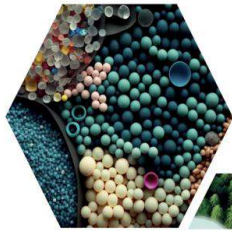
Keywords: Facial mask; PCL nanofibers; Green synthesis; Acne; Facial wrinkle

ORCID: Cansu güneş: 0000-0002-8870-0962

Fatma Ahsen Öktemler: 0000-0002-1838-0633

Edanur Korkmaz: 0000-0002-6694-6371

Ahmet Avcı: 0000-0002-1946-6260



16 ULUSLARARASI
LİF VE POLİMER
ARAŞTIRMALARI
SEMPOZYUMU

16th INTERNATIONAL FIBER AND POLYMER RESEARCH SYMPOSIUM

Sürdürülebilir ve İşlevsel Lif ve Polimerler
Sustainable and Functional Fibers & Polymers



9-10 Mayıs
May 2025

İstanbul Teknik Üniversitesi
Gümüşsuyu Prof. Dr. Necmettin Erbakan Yerleşkesi
İstanbul Technical University
Gumussuyu Prof. Dr. Necmettin Erbakan Campus

Development of Air Pre-Filter Materials from Chicken Feather Fibers by Dry Laid Method

Emirhan Bay, Jan Sena Altınay, Mediha Demet Aysin, Sümeyye Üstüntağ*

Textile Engineering, Erciyes University, 38030 Kayseri, Türkiye.

**Corresponding author: sumeyyeustuntag@erciyes.edu.tr*

ABSTRACT

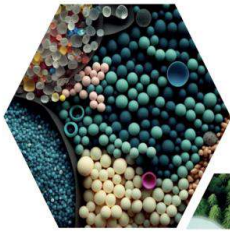
Nonwoven fabrics are widely used in various air filtration applications, such as industrial air purifiers, automotive filters, air conditioning units, and surgical masks. Owing to their porous structure, nonwoven materials provide high filtration efficiency by effectively capturing airborne particles and pollutants. In addition, they offer low air resistance, which enhances energy efficiency and optimizes airflow. The filtration performance of these materials varies depending on the type of raw material, web-forming method, and production technique.

Chicken feathers are a naturally hard-to-degrade by-product. Much of this material is considered waste and unsuitable for direct use in its raw form. A feather has four main components: rachis, barbs, barbules, and hooklets. The barbs can be separated from the rachis and used to produce nonwoven fabrics.

In this study, nonwoven fabrics were produced by the dry-laid method from a blend of chicken feather fibers (barbs) and recycled polyethylene terephthalate (rPET) for pre-air filtration applications. The blend ratios of chicken feather fibers to rPET were 60/40, 50/50, and 40/60 by weight. The total fiber weights were adjusted to 40 g, 30 g, and 20 g. The filtration efficiency of the produced nonwoven fabrics was evaluated. The highest filtration efficiency was observed in the sample produced with a total weight of 40 g, consisting of a 50/50 blend of chicken feather fibers and rPET.

Keywords: Chicken feather fiber; Nonwoven; Filtration efficiency; Pressure drop

Acknowledgments: This study was supported by TÜBİTAK 1001-Scientific and Technological Research Projects Support Program with the project code 122M485. We want to thank Erciyes University Research Deanship for providing the necessary infrastructure and laboratory facilities in the ArGePark research building for the conduct of our study.



16

ULUSLARARASI
LİF VE POLİMER
ARAŞTIRMALARI
SEMPOZYUMU

16th INTERNATIONAL FIBER AND POLYMER RESEARCH SYMPOSIUM

Sürdürülebilir ve İşlevsel Lif ve Polimerler
Sustainable and Functional Fibers & Polymers



9-10 Mayıs
May 2025

İstanbul Teknik Üniversitesi
Gümüşsuyu Prof. Dr. Necmettin Erbakan Yerleşkesi
İstanbul Technical University
Gumussuyu Prof. Dr. Necmettin Erbakan Campus

Pamuk iplikçiliğinde farklı işlem uygulanmış bobin yapılarının iplik ve çözgü hazırlık performansına etkileri

Gökhan Tandoğan^{a, c, *}, Yasemin Korkmaz^b, Kıymet Kübra Denge^{b, c}, Uğur Gündoğan^c, Sami Gizir^c

^aBursa Uludağ University, Engineering Faculty, Department of Textile Engineering, 16059 Bursa, Türkiye.

^bSütçü İmam University, Engineering Faculty, Department of Textile Engineering, Kahramanmaraş, 46100, Türkiye.

^cKipaş Mensucat İşletmeleri A.Ş. Ar-Ge Merkezi, 46100, Kahramanmaraş, Türkiye.

*Sorumlu Yazar: gtandogan@kipas.com.tr

ÖZET

Pamuk iplik üretiminde uygulanan her işlem lifte ve iplikte farklı gerilime neden olur. Bu iplikler büküm yönünün tersine dönme ve kendi üzerine kıvrılma eğilimindedirler. Bu özellik iplik canlılığı olarak tanımlanmaktadır. İplik büküm canlılığı bobinleme, çözgü çekme, dokuma ve örme gibi eğirme sonrası süreçlerde pek çok soruna neden olmakta ve verimliliği düşürmektedir. Günümüzde, bu problemleri engelleyebilmek için iplikler, vakumlu ortamda, farklı sıcaklıklarda fikse işlemine tabi tutulsa da ipliğin tüylülüğü, inceliği, bobin sarım yoğunluğu, büküm yapısı kıvrılma etkisini önemli ölçüde etkilemektedir.

Bu çalışmada pamuk iplikçiliğinde, ipliğin fikse sonrası davranışlarını incelemek, dokuma kumaş çözgü hazırlık süreçlerinde ipliğin performansını geliştirmek amacıyla aynı Ne ve bükümde konvansiyonel ve kompakt yapıda ipliklerden farklı bobin sarım yoğunluğunda farklı fikse ısılarında prosesler uygulanarak çözgü hazırlık süreçlerinde iyileştirme adımları incelenmiştir.

Bu amaçla 30/1 Ne inceliğinde ve 4.3 sabit bükümde, bobin sarım yoğunlukları farklı hazırlanan konvansiyonel ve kompakt pamuk ipliklere 60°C de ve 80°C de iki farklı fikse işlemleri uygulanmıştır. İşlem sonrası iplik uster test sonuçları ve çözgü hazırlık süreçlerinde ki iplik kopuşları açısından değerlendirilmiştir.

Çalışma sonunda aynı Ne’de hazırlanan kompakt ve konvansiyonel iplik performansları incelendiğinde fikse işleminin ve fikse ısısının artmasının ve bobin sarım yoğunluğunun azalmasının mukavemeti ve elastikiyet değerlerini %2-8 oranında arttırdığı görülmüştür. Çözgü hazırlık aşamasında konvansiyonel iplik denemelerinde bobin yoğunluğu ve sertliği arttıkça fiksenin özellikle iplik üzerine etkisinin azalmasına, çözgü hazırlık aşamasında çözgü kopuş oranının artmasına, bobin sarım yoğunluğu az olan kompakt ipliklerde ise mukavemet ve elastikiyet değerlerinin yüksek olması, fikse sonrası tüylülüğün az olması çözgü kopuş oranına olumlu katkı sağlamıştır.

Sonuç olarak çözgü hazırlık performansında 10⁶ çözgü kopuşu değerleri incelendiğinde en iyi değerler kompakt boya bobin yapısı ve sarım yoğunluğu düşük olan bobinlerde görülmüştür.

Anahtar Kelimeler: Kompak tiplik; Bobin sarım yoğunluğu; İplik fikse prosesi.

Effects of different processed bobbin structures on yarn and warp preparation performance in cotton spinning

ABSTRACT

Each process applied in cotton yarn production causes different tension in the fiber and yarn. These yarns tend to turn against the twist direction and curl on themselves. This feature is defined as yarn liveliness. Yarn twist liveliness causes many problems in post-spinning processes such as winding, warp drawing, weaving and knitting and reduces efficiency. Today, in order to prevent these problems, yarns are subjected to fixation in vacuum environments at different temperatures, but the hairiness, fineness, bobbin winding density and twist structure of the yarn significantly affect the curling effect.

In this study, in order to examine the behavior of the yarn after fixation in cotton spinning and to improve the performance of the yarn in woven fabric warp preparation processes, processes were applied at different fixation temperatures with different bobbin winding densities from conventional and compact yarns at the same Ne and twist, and improvement steps were examined in warp preparation processes.

For this purpose, two different fixation processes were applied to conventional and compact cotton yarns prepared with different package winding densities at 60°C and 80°C with 30/1 Ne fineness and 4.3 constant twist. After the process, the yarn was evaluated in terms of uster test results and yarn breaks in warp preparation processes.

At the end of the study, when the performances of compact and conventional yarns prepared at the same Ne were examined, it was seen that the fixation process and the increase in the fixation temperature and the decrease in the package winding density increased the strength and elasticity values by 2-8%. In conventional yarn tests at the warp preparation stage, as the package density and hardness increased, the effect of the fixation, especially on the yarn, decreased the warp breakage rate at the warp preparation stage, and in compact yarns with low package winding density, the high strength and elasticity values and the low hairiness after fixation contributed positively to the warp breakage rate.

As a result, when the 10⁶ warp break values in the warp preparation performance were examined, the best values were seen in bobbins with compact dye package structure and low winding density.

Keywords: Compact yarn; Bobbin winding density; Yarn fixing process.

I. GİRİŞ

Tekstil liflerinin yüksek sıcaklıklarda bozulduğu genel olarak bilinse de, ısı ve nemin birleşik etkileri çok az incelenmiştir. Bu nedenle, Amerika Birleşik Devletleri Tekstil Araştırma Enstitüsü ve Ulusal Standartlar Bürosu tarafından yürütülen tekstil kurutma çalışmaları sırasında bu konuya özel bir ilgi gösterilmiştir. Çamaşırhaneler ve kuru temizleme tesisleri dahil olmak üzere tekstil endüstrisinin çeşitli dallarında kurutulan malzemeler ve kullanılan prosedürler o kadar çeşitlidir ki, hiçbir malzeme ve koşul kümesinin geriye kalanını temsil ettiği düşünülemez [1].

Gözeneklilik, tekstil yapısının en önemli özelliklerinden biridir. Bir giysinin nefes alabilirliğini ve ısı iletkenliğini etkileyerek konforunu etkileyebilir. Boyama işlemi sırasında, boyama çözeltisi alt tabaka ile temas eder; boyama çözeltisinin alt tabakaya emilimi

gözenekliliğine bağlı olacaktır. Kumaş iplikleri arasındaki gözeneklilik kavramı yaygın bir olgudur; ancak, iplikteki lifler arasındaki gözeneklilik, kumaşın boyama davranışını da etkileyebilir. Rotor iplikler, ring ipliklere kıyasla daha yüksek gözenekliliğe ve boya fiksasyonuna ve sahiptir. Boyama ve fikse davranışı ayrıca iplik sayısına da bağlıdır. Özellikle, 30/s iplikler, 25/s ipliklere kıyasla daha yüksek boya fiksasyonuna sahiptir [2].

Elyaftan iplik üretim sürecinin önemli bir yönü, elde edilen ipliğin kalitesidir. İplik, optimum ürün özelliklerine (ve minimum hataya) sahip olmalıdır. Teoride, bu amaç bir optimizasyon algoritması kullanılarak gerçekleştirilebilir. Bununla birlikte, elyaftan ipliğe üretim sürecinin karmaşıklığı çok yüksektir ve tüm süreci temsil eden bilinen bir matematiksel fonksiyon yoktur [3].

Yeni eğrilmiş, bükülmüş iplikler, üretim sırasında, çeşitli mekanik zorlanmalara maruz kaldıklarından, iç gerilime sahip olmaktadır ve serbest kalıncada kendi üstlerine sarılmaya, katlanmaya, karmakarışık olmaya meyillerler. Bu duruma, özellikle ipliklerin bobinlerden sağlanması durumunda rastlanır. Eğer bu durum engellenmezse, mamulün kalitesi bozuk çıkar. Bu yüzden rahat bir kullanım için fikse işlemiyle, iplikteki aşırı ve uygunsuz iç gerilmelerinin dengelenmesi, ipliklerin dinlendirilip, kolay işlenir hale getirilmesi gerekir [4].

Günümüzde tekstil makinalarında üretim hızları devamlı artmaktadır. Dolayısıyla yüksek hızlı makinalarda çalışılacak ipliklerin kalitesinin de yüksek olması istenmektedir. Diğer taraftan da yüksek hız, ipliğin rutubet değerini sık sık minimum değere düşürmektedir. Rutubetdeki bu düşüş de ipliğin mukavemet özelliklerini olumsuz yönde etkilemektedir. Daha iyi nem düzeyi, ipliğin mukavemet özelliklerini arttırdığı için, iplik dokuma ve örmede daha verimli çalışmaktadır. Diğer taraftan tekstil işletmelerinde her işlem lifte ve iplikte gerilime neden olmaktadır. İplikler gerilimlerden kurtulmak için kıvrımlanma, bükümlenme eğilimindedirler. Gerginlik ve kıvrımlanma takip eden proseslerde problemlere yol açmakta ve verimliliği düşürmektedir. Bu gibi sebeplerden dolayı ipliklerin üzerindeki nem miktarı artırılmalı ve gerilimleri yok edilmelidir [5].

Dış faktörler, lifler ve bu liflerden yapılan iplikler üzerinde büyük bir etkiye sahiptir. Bu faktörlerin başında ortamın rutubet miktarı gelmektedir. İplikteki doğru bir yöntemle verilmiş uygun rutubet ipliğin fiziksel özelliklerini iyileştirdiği gibi ipliğin satışında üreticiye ticari bir kazanç da sağlamaktadır. Dolayısıyla ideal olan, arzu edilen nemin iplik üretiminden sonra çok kısa bir sürede ipliğe kazandırılması ve ipliğin kalitesinin kalıcı olarak yükseltilmesidir [6].

Özellikle pamuk iplik işletmelerinde yüksek hızlarda çalışan iplik makinelerinin ve çevre şartlarının da etkisiyle iplik üzerindeki rutubet miktarı % 5'lere kadar düşmektedir [7]. Bu değer ise gerek ticari açıdan gerekse ipliğin sahip olması gereken mukavemet özellikleri açısından yeterli değildir. Dolayısıyla ipliğin sahip olduğu rutubet değeri artırılmalıdır. Pamuk lifi higroskopik bir materyaldir ve buhardan su absorblama yeteneğine sahip olduğu için ortamın izafi rutubet miktarı arttıkça lif tarafından absorbe edilen nem miktarı artacaktır. Bu artış lifin enine kesitinde bir şişmeye neden olacak ve bükülmüş iplik yapısı içinde

lif-lif sürtünmesini arttıracaktır. Bu değişiklik ise ipliğin mukavemet özelliklerinde iyileşme meydana getirecektir [8].

Düzgün bir şekilde uygulanan buharlama işlemi ipliğin sadece nem düzeyini arttırmakla kalmaz, ipliğin mukavemet özelliklerini artırır, kıvrılma bükümleşme gibi problemleri ortadan kaldırır, işlemler esnasında oluşan toz, çepel miktarlarını düşürür ve aynı zamanda buharlama işleminin, süresine, sıcaklığına, basıncına bağlı olarak daha sonraki proseslerde (dokuma, örme, v.b) daha az problem çıkararak verimliliği artırır, boyama esnasında daha düzgün boya alımı sağlar ve çizgilerin oluşmasını engeller, standart rutubet değerine ulaştığı için ticaret de kayıplara neden olmaz. İpliklere uygulanan vakumlu buharlama işlemi tekstil prosesler içinde önemli bir yere sahiptir ve bu işlemin daha düzgün ve hatasız bir şekilde yapılması gerekmektedir [9].

II. DENEYSEL METOT

Bu çalışmada pamuk iplikçiliğinde, ipliğin fikse sonrası davranışlarını incelemek, dokuma kumaş çözgü hazırlık süreçlerinde ipliğin performansını geliştirmek amacıyla aynı Ne, büküm değerleri ile konvansiyonel ve kompakt yapıda ipliklerden farklı bobin sarım yoğunluğunda farklı fikse ısılarında prosesler uygulanarak çözgü hazırlık süreçlerinde iyileştirme adımları incelenmiştir.

2.1. Malzemeler ve Hazırlama Teknikleri

Çalışma kapsamında hazırlanan deney planına göre projede yöre pamuğu kullanılmıştır. Ring eğirme yöntemi ile 30/1 Ne lineer yoğunluğunda konvansiyonel ve kompakt iplik üretimi için farklı bobin yapılarında ve sarım yoğunluğunda iplik üretimleri gerçekleştirilmiştir. İplik fikse işlemleri Xorella fikse makinesinde gerçekleştirilmiştir.

2.1.1. Malzemelerin karakterizasyonu

Deneme üretimler için yöre pamuklarından harman yapılarak farklı sarım yoğunluğunda, Şekil 1.de belirtilen delikli boya bobini ve konik bobin yapısında 30/1 Ne'de ring eğirme sistemi kullanılarak iplik üretimleri gerçekleştirilmiştir. Kullanılan hammadde

16. Uluslararası Lif ve Polimer Araştırmaları Sempozyumu (16. ULPAS)
9-10 Mayıs 2025, İstanbul teknik Üniversitesi (İTÜ), Türkiye

ve malzeme özellikleri Tablo 1. Ve Tablo 2. De belirtilmiştir.

2.2. Tablolar ve Şekiller

Tablo 1. Kullanılan yöre pamuğun HVI test sonuçları

| SCI | Unf | Mic | Uzunluk (mm) | Elastikiyet (%) | Str (g/hex) | SFI (%) |
|-----|------|-----|-----------------|--------------------|----------------|------------|
| 141 | 83.2 | 4,9 | 30,9 | 4.5 | 32,4 | 8,1 |

Tablo 2. Bobin form özellikleri

| Bobin formu | Ebatları | Yapısı |
|--------------|-----------------|---------------------|
| Kağıt (SS) | 4.4*6.4*172 | Konik |
| Plastik (BB) | Flex, 170*59*54 | Delikli boya Bobini |



Şekil 1. Konik bobin (a) Boya bobini (b)

Proje bünyesinde üretilen 30/1 Ne kompakt ve konvansiyonel penye ipliklerde 4.3 sabit büküm faktörü uygulanmıştır. İplik üretimi sonrası bobin ağırlığı, sarım yoğunluğu, fikse bekleme süreleri ve fikse ısıları için deney planı ve hazırlama teknikleri Tablo 3. De verilmiştir.

Tablo 3. Ring İplik Üretim sonrası fikse şartları ve bobin yapısı

| Deneme | Eğirme | Sarım Yoğunluğu (g/cm ³) | Bobin Patron Yapısı | Bobin Ağırlığı (g) | Fikse Isısı (°C) | Fikse Bekleme Süresi (dk) |
|--------|---------------|-----------------------------------------|---------------------|-----------------------|---------------------|------------------------------|
| 1 | Penye Kompakt | 0,424 | SS | 2350 | 0 | 0 |
| 2 | | 0,424 | SS | 2350 | 60 | 5+30 |
| 3 | | 0,424 | SS | 2350 | 80 | 20+20 |
| 4 | | 0,387 | BB | 1030 | 0 | 0 |
| 5 | | 0,387 | BB | 1030 | 60 | 5+30 |
| 6 | | 0,387 | BB | 1030 | 80 | 20+20 |
| 7 | Penye | 0,424 | SS | 2350 | 0 | 0 |
| 8 | | 0,424 | SS | 2350 | 60 | 5+30 |
| 9 | | 0,424 | SS | 2350 | 80 | 20+20 |
| 10 | | 0,387 | BB | 1030 | 0 | 0 |
| 11 | | 0,387 | BB | 1030 | 60 | 5+30 |
| 12 | | 0,387 | BB | 1030 | 80 | 20+20 |

Fikse işlemleri tamamlanan bobinler Tablo 4.de belirlenen dokuma kumaş üretimi için çözgü ipliği olarak hazırlanmıştır.

Tablo 4. Dokuma kumaş konstrüksiyon bilgisi

| Kumaş Örgüsü | Tarak Eni cm | Mekanik atkı sıklığı | Tarak No | Toplam Tel Sayısı |
|--------------|-----------------|-------------------------|----------|-------------------|
| Bezayağı | 169 | 21 | 240/2 | 8112 |

III. BULGULAR VE TARTIŞMA

Özellikle pamuklu iplik üretimi sonrası çevre şartlarının da etkisiyle iplik üzerindeki rutubet miktarı ciddi oranda düşmektedir. Bu durum gerek dokumada gerekse de örme aşamalarında kopuş problemine neden olurken beraberinde ise hatalı üretime ve verimsizliğe neden olmaktadır.

Çalışma kapsamında ring eğirme sisteminde kompakt ve konvansiyonel hatlarda aynı büküm faktörü ile üretilmiş ipliklere uygulanan farklı fikse şartlarının ve bobin denemelerinin iplik kalitesine ve çözgü hazırlık süreçlerine etkileri incelenmiştir. İplik kalitesine etkileri ve uster test sonuçları Tablo 5.de verilmiştir.

Üretilen ipliklerden 1, 4, 7,10 nolu deneme bobinlere fikse işleminin ipliğe etkilerini görmek ve referans oluşturmak adına fikse işlemi yapılmamıştır.

Tablo 5. Üretilen ipliklerin uster test sonuçları

| Deneme | CVm | Neps +140 | Neps +200 | H | B-Force | Elg. | Rkm |
|--------|-------|-----------|-----------|-----|---------|------|-------|
| 1 | 11,21 | 45 | 4 | 4,2 | 391 | 5,47 | 19,88 |
| 2 | 11,43 | 85 | 8 | 3,9 | 400 | 6,08 | 20,31 |
| 3 | 12,30 | 145 | 23 | 4,3 | 425 | 6,51 | 21,61 |
| 4 | 11,36 | 51 | 11 | 4,1 | 383 | 5,35 | 19,48 |
| 5 | 11,54 | 70 | 10 | 4,1 | 414 | 6,07 | 21,02 |
| 6 | 11,95 | 105 | 9 | 4,1 | 404 | 6,16 | 20,54 |
| 7 | 11,89 | 113 | 11 | 5,5 | 339 | 5,33 | 17,20 |
| 8 | 12,07 | 165 | 13 | 5,9 | 362 | 5,67 | 18,38 |
| 9 | 12,65 | 270 | 27 | 5,8 | 357 | 4,63 | 18,14 |
| 10 | 11,56 | 66 | 10 | 6,1 | 331 | 5,54 | 16,80 |
| 11 | 11,69 | 118 | 20 | 6,5 | 308 | 5,83 | 15,65 |
| 12 | 12,57 | 236 | 13 | 6,1 | 341 | 6,34 | 17,33 |

İplik uster değerleri incelendiğinde fikse ısısında ve bekleme süresinde ki artış hem kompakt hem de konvansiyonel iplik yapısında mukavemet ve elastikiyet değerlerini %2 ila %10 oranlarında arttırırken neps değerlerini de yapısına aldığı nem nedeni ile geriye götürmektedir. Fikse işlemi boya bobinlerinde sarım yoğunluğu azaldıkça daha etkin olmakla birlikte neps değerlerini özellikle konvansiyonel ring sisteminde geriye götürdüğü gözlemlenmiştir.

Literatürde de bahsedildiği gibi iplik üretiminde uygulanan her işlem lifte ve iplikte gerilime neden olmaktadır. Gerginlik ve kıvrımlanma takip eden proseslerde problemlere yol açmakta ve verimliliği düşürmektedir [5]. İplik üretimleri sonrası yapılan fikse işlemlerinin kıvrılma canlılığına etkisi ve çözgü hazırlık performansında 10⁶ çözgü kopuşu değerleri Tablo 6.da verilmiştir.

Tablo 6. İplik kıvrılma canlılığı ve çözgü kopuş değerleri

| Deneme | İplik Kıvrılma Canlılığı (Kr) | 10 ⁶ çözgü kopuşu |
|--------|-------------------------------|------------------------------|
| 1 | - | 0,7 |
| 2 | 47 | 0,6 |
| 3 | 30 | 0,5 |
| 4 | - | 0,7 |
| 5 | 38 | 0,5 |
| 6 | 32 | 0,5 |
| 7 | - | 0,8 |
| 8 | 46 | 0,6 |
| 9 | 22 | 0,6 |
| 10 | - | 0,9 |
| 11 | 36 | 0,8 |
| 12 | 33 | 0,7 |

İplik kıvrılma canlılığı değerlerinde fikse ısısı ve fikse bekleme süresi arttıkça kıvrılma canlılığının azaldığı kompakt ipliklerde ise aynı işlemlerde kıvrılma canlılığının daha yüksek olduğu gözlemlenmiştir.

Çözgü kopuşunu etkileyen en önemli etkenler iplik kalitesi, 10⁶ çözgü kopuş değerleri incelendiğinde en

iyi değerler fikse ısısı yüksek 3, 5 ve 6 nolu kompakt iplik denemelerinde görüldürken, 10 nolu konvansiyonel fiksiz iplik denemesinde ise kopuş değerleri diğer denemelere oranla oldukça yüksek çıkmıştır.

IV. SONUÇLAR

Bu çalışmada aynı harman ve aynı lineer yoğunluk kullanılarak üretilen konvansiyonel ve kompakt %100 pamuk ring iplik üretim farkının, bobin yapılarının ve iplik fikse işlemlerinin iplik kalitesine ve dokumada çözgü hazırlık performansına katkıları incelenmiştir. Bu sonuçlara göre;

- İplik fikse işleminde ısı ve bekleme süresi arttıkça uzama ve mukavemet (rkm) değerlerinin iyileştiği, özellikle kompakt iplik üretiminde kalite parametrelerinde iyileşmenin daha olumlu olduğu,
- İplik üretimi sonrası yapılan fikse işleminin ipliğin iç gerilimini azaltarak kıvrılma eğilimini ve kıvrılma canlılığını (kr) azalttığı görülmüştür. Bu durum özellikle yüksek hızda çalışan dokuma makinelerinde çözgü kopuşlarının azaltılması açısından oldukça kritiktir.
- 30/1 Ne %100 Pamuk karışımı deneme ipliklerden üretilen 1/1 bezayağı dokuma kumaşların 10⁶ çözgü kopuş değerlerinde ise kompakt ve fiksli denemelerin daha başarılı olduğu görülmüştür.
- Bununla birlikte fikseleme sonrası ipliğin nem kaybını önlemek amacıyla uygulanan streçleme işlemi ve bobinlerin uygun ortam koşullarında bekletilmesi de sürecin başarısını doğrudan etkileyen faktörlerdendir. Streçleme sayesinde ipliğin boyutsal stabilitesi korunurken, kontrollü bekletme koşulları ile nem dengesi sağlanarak ipliğin performans özellikleri muhafaza edilebilir.

TEŞEKKÜR

Bu çalışmada Kipaş Tekstil Ring İşletmeleri üretim ve Ar-ge Merkezi laboratuvar alt yapısı kullanılmıştır. Sonuçlar Prof. Dr. Yasemin Korkmaz hocamız ile birlikte değerlendirilmiş olup katkılarından dolayı kendisine ve proje ekibine teşekkür ederiz.

KAYNAKLAR

[1] Wiegerink JG. Effects of drying conditions on properties of textile yarns. Textile Research. 1940;10(12):493-509. doi:10.1177/004051754001001202.

[2] [Yousfani, S.H.S.H.](#), [Farooq, S.](#), [Mohtashim, Q.](#) and [Gong, H.](#) (2023), "Yarn porosity and its relationship with the dyeing behavior", [Pigment & Resin Technology](#), Vol. 52 No. 6, pp. 747-754. <https://doi.org/10.1108/PRT-12-2021-0138>

[3] Sette S, Boullart L, Van Langenhove L, Kiekens P. Optimizing the fiber-to-yarn production process with a combined neural network/genetic algorithm approach. Textile Research Journal. 1997;67(2):84-92. doi:10.1177/004051759706700203

[4] Gülrodop G. (2005), Yün ipliklerinde büküm fikse şartlarının iplik özelliklerine etkisi üzerine bir araştırma, Uludağ Üniversitesi.

[5] Özdemir, Ö., & Şardağ, S., (2005). İpliklerde vakumlu buharlama işlemleri uygulama alanları ve gelişmeler. Pamukkale Üniversitesi Mühendislik Bilimleri Dergisi, 11(2), 239-248.

[6] Toggweiler P, Gleich S., Wanger F., Steiner, F. 1995 "Improved quality with contextxor conditioned cotton yarn" Melliand English 9/1995.

[7] Anonymous, 2003. Xorella Contexxor, 2003 Katolog.

[8] Dayik, M., Özdemir, Ö. 2000. "Vakumlu ortamda doymuş buharla kondisyonlama şartlarının iplik özellikleri üzerine etkisi" Tekstil Maraton Dergisi Sayı 5, Kasım-Aralık 6/2000, s: 41-57.

[9] Özdemir, Ö., & Şardağ, S., (2005). İpliklerde vakumlu buharlama işlemleri uygulama alanları ve gelişmeler. Pamukkale Üniversitesi Mühendislik Bilimleri Dergisi, 11(2), 239-248.



From hydrophobic nanofibers to antimicrobial slippery liquid infused surfaces: A two-step surface strategy

Sena Kardelen Dinc^{a,b}, Oznur Akbal Vural^c, Nalan Oya San Keskin^{a,*}

^aNanosan Laboratory, Department of Biology, Polatlı Science and Literature Faculty, Ankara Hacı Bayram Veli University, 06900, Ankara, Türkiye

^bInstitute of Graduate Programs and Department of Biology, Polatlı Science and Literature Faculty, Ankara Hacı Bayram Veli University, Ankara 06900, Türkiye

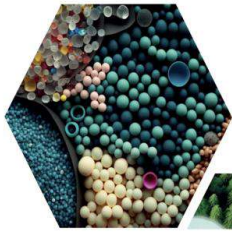
^cAdvanced Technologies Application and Research Center, Hacettepe University, Ankara 06800, Türkiye

*Corresponding author: nalan.san@hbyv.edu.tr

ABSTRACT

The ongoing challenge of microbial attachment on surfaces poses significant health and economic consequences across various applications. Slippery Liquid-Infused Surfaces (SLIPS) have recently attracted interest as a bioinspired approach for preventing microbial colonization. This research presents the preparation of a beaded polysulfone nanofiber (bPSU_Nf)-based SLIPS design incorporating *Eucalyptus globulus* oil (EGO), offering a two-step surface design. bPSU_Nfs were fabricated and coated onto glass substrates to enhance hydrophobicity and surface roughness. Bead density was optimized based on slippery behavior. The bPSU_Nf coated surfaces (bPSU_NfCS) were then infused with EGO, a natural lubricant with antimicrobial properties. The substrate showed a 47.5° water contact angle (WCA), indicating hydrophilicity. bPSU_NfCS showed hydrophobicity with a WCA of 127°, which decreased to 59.6° after EGO infusion, confirming SLIPS formation. SLIPS had 100% antibacterial efficacy against both *Escherichia coli* and *Staphylococcus aureus* according to the ISO 22196 test method, but the bPSU_NfCS did not inhibit bacterial attachment. Also, the fungal attachment assay with *Candida albicans* revealed $105 \pm 4.5 \times 10^4$ CFU/mL for the control group, $100.5 \pm 1.5 \times 10^4$ for the substrate, and $113 \pm 3.6 \times 10^4$ for the bPSU_NfCS. However, SLIPS showed no fungal growth, demonstrating 100% fungal attachment inhibition. Furthermore, the substrate and bPSU_NfCS showed 0.19 ± 0.03 optical density (OD₅₉₅) values, while the SLIPS surface showed a significantly reduced OD₅₉₅ of 0.03 ± 0.002 , indicating an 84% inhibition in biofilm formation. These findings highlight the potential of a simplified two-step SLIPS design as a sustainable and highly effective antimicrobial surface strategy.

Keywords: Electrospinning; Biofilm Inhibition; Liquid-repellent Surfaces; Anti-adhesion; Electrospun Polymeric Surfaces



16 ULUSLARARASI
LİF VE POLİMER
ARAŞTIRMALARI
SEMPZYUMU

16th INTERNATIONAL FIBER AND POLYMER RESEARCH SYMPOSIUM

Sürdürülebilir ve İşlevsel Lif ve Polimerler
Sustainable and Functional Fibers & Polymers



9-10 Mayıs
May 2025

İstanbul Teknik Üniversitesi
Gümüşsuyu Prof. Dr. Necmettin Erbakan Yerleşkesi
Istanbul Technical University
Gumussuyu Prof. Dr. Necmettin Erbakan Campus



Photocatalytic Activity of Ag-ZnO Structures Deposited onto Glass Fibers

M. Damla YAGMUR^a, Halil I. AKYILDIZ^{a*}

^aTextile Engineering, Bursa Uludag University, 16095 Bursa, Türkiye.

*Corresponding author: halilakyildiz@uludag.edu.tr

ABSTRACT

Water pollution and depletion of water resources constitute a critical problem today. Although photocatalysis has emerged as an effective method for water pollution treatment, the efficiency of the materials used has not yet reached sufficient levels. In this study, an approach to increase photocatalytic efficiency on glass fabrics was developed. Glass fabrics were modified by a combination of two different methods to form thin films on them. In the first step, plain woven glass fabrics were conformally coated with ZnO in the desired thickness by atomic layer deposition (ALD). Then, silver nanoparticles were deposited onto the ZnO-coated fabrics using the photodeposition method under UV light. The photocatalytic activities of the samples were compared in terms of different Ag salt solutions, Ag salt solution concentrations, and photodeposition times. Photodeposition was carried out using AgNO₃ and AgC₂H₃O₂ salts at 0.01 M and 0.05 M concentrations. Three different photodeposition times were determined as 1, 2, and 5 minutes. The photocatalytic activity of the obtained samples was evaluated by the degradation rate in methylene blue (MB) solution. The structural and chemical properties of the samples were investigated by Raman and XPS characterization methods. This study shows that the Ag salt used in the photodeposition method on the textile surface, its concentration and the photodeposition time have significant effects on the photocatalytic activity. These findings suggest that it is important to optimize different parameters to increase the application potential of photocatalytic processes on textile surfaces.

Keywords: Nanoparticle; ALD; Photocatalysis; Photodeposition; ZnO

16th International Fiber and Polymer Research Symposium (16th ULPAS)
9-10 May, 2025, Istanbul technical University (ITU), Istanbul, Türkiye



Fused Deposition Modeling (FDM) – methods, materials and applications for flexible fabric structures

A. Sapkota, S. K. Ghimire and S. Adanur

Department of Mechanical Engineering, Auburn University, Auburn, Alabama, USA

Corresponding author: adanusa@auburn.edu

ABSTRACT

Fused Deposition Modeling (FDM), an extrusion-based additive manufacturing (AM) technique, has emerged as a transformative technology for fabricating complex structures. The current state of FDM, its challenges, and its application in flexible fibrous materials is explored. FDM works by extruding molten polymer layer by layer, offering versatility in processing various polymers. However, FDM-produced parts often face issues such as compromised mechanical properties and surface quality, which are critical for fabric applications.

To address these challenges, researchers have focused on two primary strategies: optimizing process parameters and enhancing material quality. Key parameters like extrusion temperature, layer height, and print speed significantly influence part quality. Additionally, advanced materials, such as reinforced filaments and polymer blends, have expanded FDM's capabilities. Blending PLA with TPU enhances flexibility, while incorporating fibers like carbon or glass improves strength. Recent studies have explored FDM for creating woven, knitted, and braided fabric structures, as well as hybrid materials by depositing polymers onto textile substrates. Despite progress, challenges like weak interlayer bonding, roughness, and limited comfort in wearable applications persist.

The future of FDM for fabric structures lies in further optimizing process parameters and developing specialized materials. Potential applications include smart textiles, biomedical scaffolds, and customized wearables, which could revolutionize industries like healthcare and fashion.

FDM holds significant potential for fabricating flexible fabric structures, but realizing this potential requires addressing key challenges through process optimization and material innovation.

Keywords: fused deposition modeling (FDM), process parameters, flexible fabric structures, mechanical properties, additive manufacturing



Effect of porosity distribution in FRP laminate on interfacial shear stresses in cracked beams strengthened with variable fiber spacing

Khamis Hadjazi^{a,*}, Mohamed Larbi Bennagadi^a, Nawel Bentata^a, lahouaria Errouane, Zouaoui Sereir^a

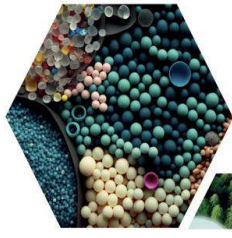
^aFaculty of Mechanic Engineering, University of Science and Technology of Oran (USTO), Composite Structures and Innovative Materials Laboratory (LSCMI), Oran, Algeria

*Corresponding author: khamishadji@yahoo.fr

ABSTRACT

The repair of cracked structures using FRP plates with variable volume fraction is a promising process, as it helps recover the lost stiffness of beams due to crack formation. However, an important issue related to flexural strengthening of structures is the debonding of the reinforcement plate, caused either by poor adhesion or by non-compliance with the proportionality between the reinforcement elements due to the presence of porosities in the FRP plate. These porosities generally occur in the structures during the manufacturing process. In the present study, an improved analytical model has been proposed to describe the shear stresses along the interface using a bilinear cohesive law model to analyze a cracked beam repaired with a porous FRP plate. The results obtained for interfacial shear stress distribution near the crack are compared to the analytical model from the literature. The effect of porosity on the stiffness of the FRP plate has been modeled in the form of a power polynomial along the direction of the plate's thickness. The study highlights that porosity and material gradient indices significantly affect the load-carrying capacity, softening and debonding behavior, and the durability of the repaired structure.

Keywords: Analytical model; Strengthened beam; Flexural crack; Imperfect FRP plate; Interfacial stresses.



16 ULUSLARARASI
LİF VE POLİMER
ARAŞTIRMALARI
SEMPOZYUMU

16th INTERNATIONAL FIBER AND POLYMER RESEARCH SYMPOSIUM

Sürdürülebilir ve İşlevsel Lif ve Polimerler
Sustainable and Functional Fibers & Polymers



9-10 Mayıs
May 2025

İstanbul Teknik Üniversitesi
Gümüşsuyu Prof. Dr. Necmettin Erbakan Yerleşkesi
İstanbul Technical University
Gumussuyu Prof. Dr. Necmettin Erbakan Campus

Sound Absorption Performance of Three-dimensional Flexible Spacer Fabric Enhanced by Polyurethane Foam

Milad Atighi ^{a,b}, Mohammad Davoudabadi Farahani ^{a,b}, Mahdi Hasanazadeh ^{a,*}

^a Department of Textile Engineering, Yazd University, Yazd 89195-741, Iran.

^b Department of Textile Engineering, Amirkabir University of Technology, 159163-4311 Tehran, Iran.

*Corresponding author: m.hasanzadeh@yazd.ac.ir

ABSTRACT

Noise pollution is an escalating concern in modern environments, necessitating the development of effective and adaptable sound-absorbing materials. Here, the structural and sound absorption performance of the 3D spacer fabric-reinforced PU foam (3D-F/PUF) composite has been investigated through the field emission-scanning electron microscope (FESEM), energy-dispersive X-ray (EDX) spectroscopy, and impedance tube tests. The developed 3D-F/PUF composite exhibits superior sound absorption coefficient (SAC) values across a wide frequency range compared to the individual PUF and spacer fabric. This study highlights the rational design of hybrid sound-absorbent systems based on PU foam and 3D spacer fabrics for promising applications as construction materials that are flexible, lightweight, and with high SAC values.

Keywords: PU foam; Spacer fabric; Sound absorption coefficient; Open cell

I. INTRODUCTION

Noise pollution has emerged as a significant issue in contemporary settings, affecting human health, productivity, and overall comfort. The increasing presence of industrial machinery, transportation systems, and residential areas has led to a heightened demand for effective sound-absorbing materials. While traditional acoustic solutions like dense foams, perforated panels, and fibrous textiles have been commonly employed to mitigate noise, these materials often present challenges such as bulkiness, limited flexibility, and poor adaptability to complex surfaces [1–4].

In contrast, textile-based sound absorbers have attracted greater interest for their lightweight, flexible properties that suit various applications [2,5]. Unlike conventional rigid absorbers, textile designs such as knitted, woven, non-woven, and spacer fabrics, provide high porosity, enabling sound waves to enter the material and dissipate energy through viscous friction and thermal conduction mechanism. Spacer fabrics offer a standout advantage with their 3D structure that enhances sound absorption over a wider frequency range. Their customizable features, including fiber type, thickness, and pore size, facilitate tailored acoustic performance, fitting for use in

automotive interiors, building acoustics, and wearable noise control systems [1,2,6]. By integrating specialized treatments like coating, lamination, or forming composites with foam, textile-based absorbers can further enhance noise reduction while ensuring breathability and mechanical strength.

Polyurethane foam (PUF) is widely regarded for its effectiveness as a sound-absorbing material, known for its high porosity, low density, and viscoelastic characteristics. As a soft, open-cell foam, PU efficiently mitigates noise via various mechanisms, including porous absorption, vibration damping, and resonance attenuation [7–9]. Its cellular composition captures incoming sound waves, directing them through interconnected pores where friction and heat conversion facilitate energy dissipation. The material's flexibility and adaptability make it suitable for numerous acoustic applications such as wall panels, vehicle insulation, and industrial noise control [1,10].

This study investigates the sound absorption performance of 3D spacer fabric reinforced PU foam (3D-F/PUF) copmposite as a hybrid system that leverages the efficient sound absorption of foam as well as the tunability and breathability features of textile materials.

II. EXPERIMENTAL METHOD

2.1 Materials

3D warp-knitted spacer fabric (3D-F) is created using double needle bar Raschel machines, featuring a gauge of 22 with 6 guide bars. The fabrics are designed with a simple knit structure for the back surface and an open-hole structure for the front surface. The front and back surface layers utilize multifilament yarns, while the middle layer consists of monofilament yarn. Table 1 shows the specification of prepared spacer fabric. The POLYMOK HR-335 (polyol) and ISOMOK-8054

(isocyanate) were obtained from Mokarrar Engineering Materials. Co, Iran.

Tablo 1. The spacer fabric parameters.

| wale per centimeter | course per centimeter | Fabric Thickness | Material |
|---------------------|-----------------------|------------------|----------|
| 6 | 4 | 10 | 100% PET |

2.2 Synthesis of PUF

To synthesize polyurethane foam, first sufficient amount of polyol was poured into a mold, followed by the addition of 1–2 droplets of water. Then the above mixture thoroughly stirred for 30 s to achieve uniform solution. Then, the isocyanate was introduced to the above mixture at a weight ratio of 55/100 (w/w) based on the initial polyol amount, excluding the powders and water. Finally, to complete the curing process, the sample was placed in an oven at 60°C for 6 h to ensure complete reaction and proper foam formation.

2.3 Fabrication of 3D-F/PUF composite

A similar method was employed to develop a new 3D-F/PUF structure, with a slight modification to the mold setup. The mold was designed to ensure that the fabric entirely covered the lid, enabling the foam to penetrate through the fabric due to the pressure created during the foam forming reaction. Subsequently, both sides of the fabric were meticulously trimmed with a sharp blade to remove any residuals. Notably, the top side of the fabric was placed inward in the container, ensuring that the foam was evenly distributed across the fabric as it was dispensed.

2.4 Characterization

Field emission-scanning electron microscope (FE-SEM) was utilized to study the surface morphology and macrostructure of the 3D-F, PUF, and 3D-F/PUF. Energy-dispersive X-ray (EDX) analysis was also conducted to reveal the elemental composition of the PUF by identifying characteristic X-ray emissions from the elements N, O, and C.

The sound absorption coefficient (SAC) was assessed using the two-microphone impedance tube method, as shown in Figure 1. This approach involves sound waves directly impacting the test sample, with the absorption coefficient calculated according to ASTM 1050 standards. The microphone closest to the sound source captures the incident waves, while a second microphone records the reflected waves from the sample. These measurements are analyzed at various frequencies with VA-Lab IMP software to compute the SAC. For accurate evaluations, samples were sized to fit the impedance tube diameter (100 mm for the 63-1600 Hz range and 30 mm for the 800-6300 Hz range) ensuring the front surface of each sample aligned with the sound source, as illustrated in Figure 1. Each SAC value is the average of three measurements to guarantee accuracy.

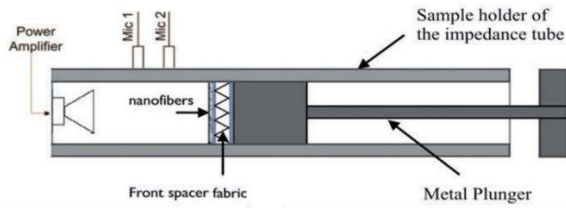


Figure 1. Two-microphone impedance tube setup.

III. RESULTS AND DISCUSSIONS

The FE-SEM micrograph of the PUF (Figure 2) shows a porous, open-cell structure with interconnected pores, allowing sound waves to penetrate instead of reflecting off the surface. As sound moves through these open cells, it experiences friction and thermal exchanges along the cell walls, which dissipate acoustic energy [11]. This morphology is vital for efficient noise reduction, especially when paired with the spacer fabric, as its fibrous network offers additional pathways for wave attenuation. Figure 3 shows the EDX spectrum, which indicates that the PUF primarily contains carbon (C), nitrogen (N), and oxygen (O), aligning with the expected chemical

makeup of polyurethane. It also shows there are no impurities in the foam structure. Although hydrogen is also present in polyurethane chains, it cannot be detected by EDX, making its absence in the elemental analysis typical.

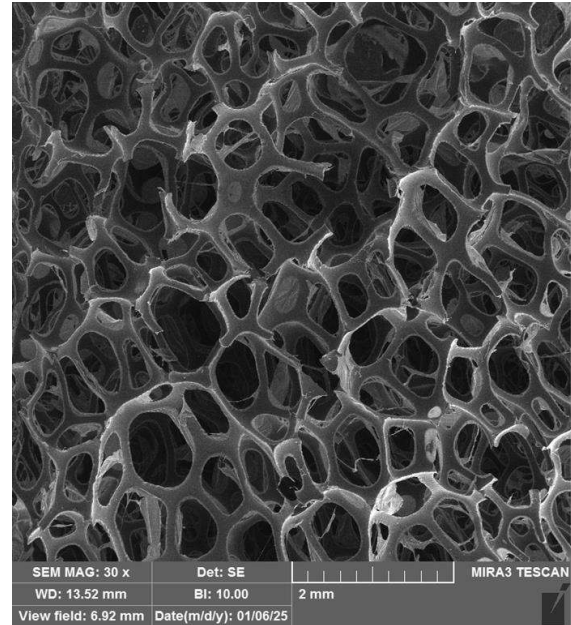


Figure 2. FE-SEM micrograph of synthesized PUF.

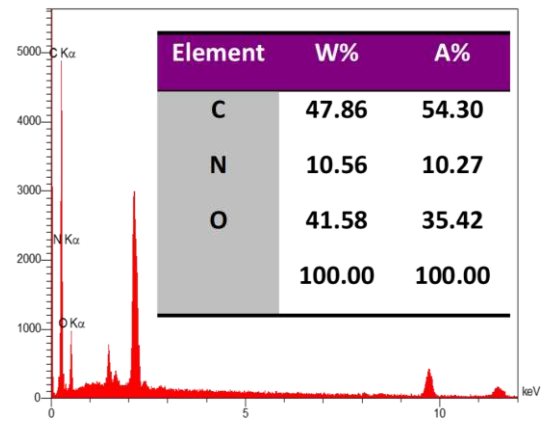


Figure 3. EDX spectra of synthesized PUF.

The SAC values of 3D-F, PUF, and 3D-F/PUF composite are shown in Figure 4. The 3D-F/PUF composite displays the highest SAC values across a wide frequency range, demonstrating that the combination of the open-cell foam and the 3D fabric structure significantly improves acoustic damping. In

contrast, pristine PUF (red line) exhibits moderate-to-high absorption at high frequencies, primarily because the fact that the open-cell network permits sound waves to enter and dissipate through friction. However, the 3D-F (black line) shows comparatively lower SAC values at lower frequencies. This is because the spacer fabrics relying on their internal pores and fiber arrangement to dissipate sound, which may not provide enough thickness or complexity for optimal absorption. Once the open-cell foam is integrated with the 3D fabric, the resulting composite benefits from multiple absorption mechanisms: (i) the interconnected pores of foam could trap the sound waves and convert acoustic energy into heat through viscous and thermal losses; (ii) the layered architecture of the spacer fabric creates extra pathways for sound scattering, reflection, and resonance. This dual-structure design significantly improves sound absorption performance, especially at higher frequencies, as indicated by the 3D-F/PUF composite (blue line), exceeding both individual components.

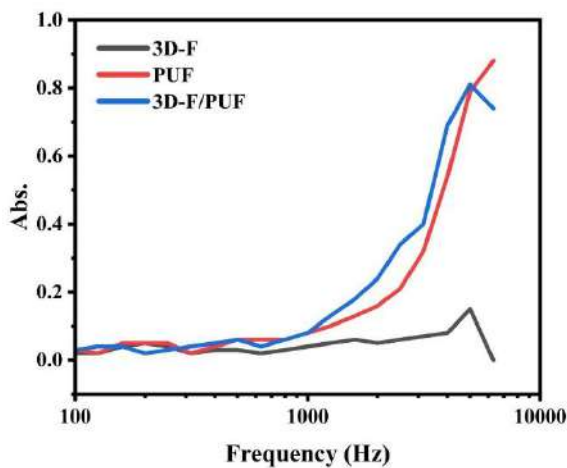


Figure 4. The sound absorption coefficient of 3D-F, PUF and 3D-F/PUF layers.

The sound absorption characteristics of these materials are primarily influenced by (i) viscous energy losses, where the air movement in narrow pores transforms sound energy into heat; and (ii) thermal losses, where temperature differences within the pores dissipate energy. The 3D-F enhances these mechanisms by

adding a layer with its own network of pores and fibers, which increases the sound wave's path length and facilitates further energy dissipation. When PUF is incorporated into the 3D-F, its open cells occupied the gaps within the fabric, creating a composite system where air must navigate multiple interfaces to pass through. As a result, the 3D-F/PUF composite demonstrates exceptional absorption over a broader frequency spectrum. Each layer (fabric and foam) provides additional chances for sound to be scattered, dampened, and finally converted into heat. This synergy accounts for the consistently superior SAC values of the 3D-F/PUF composite in comparison to either the PUF or 3D-F individually, highlighting the significance of combining open-cell foams with spacer fabrics for enhanced acoustic performance.

IV. CONCLUSIONS

The integration of warp-knitted 3D-F with PUF produces a robust composite that significantly enhances SAC values compared to its components. FE-SEM and EDX analyses confirmed the formation of ideal open-cell structure and chemical composition of PUF. The spacer fabric not only contributes its intrinsic porosity and scattering capabilities, but also complements the viscous and thermal dissipation mechanisms of foam. As a result, the 3D-F/PUF composite exhibits superior SAC values across a wide frequency range, making it a promising candidate for advanced noise control applications in automotive, architectural, and industrial settings.

REFERENCES

- [1] P. Paul, R. Mishra, B.K. Behera, Acoustic behaviour of textile structures, *Textile Progress* 53 (2021) 1–64.
<https://doi.org/10.1080/00405167.2021.1986325>.
- [2] X. Liu, H. Sheng, Z. Du, H.P. Lee, Y. Zhong, Enhanced broadband sound absorption of multi-layer

composite material based on three-dimensional warp-knitted spacer fabric, (2024).

<https://doi.org/10.1177/00405175241260064>.

[3] M. Davoudabadi Farahani, A.A. Asgharian Jeddi, M. Jamshidi, Investigation of sound absorption of Warp Knitted Spacer Fabric with nanofiber coating, *Journal of Textile Science and Technology* 10 (2021) 18–25.

https://www.jtst.ir/article_151143.html.

[4] M.D. Farahani, A.A.A. Jeddi, M. Hasanzadeh, Predicting the Sound Absorption Performance of Warp-Knitted Spacer Fabrics via an Artificial Neural Network System, *Fibers and Polymers* 24 (2023) 1491–1501.

<https://doi.org/10.1007/S12221-023-00151-6/METRICS>.

[5] M. Zhu, Y. Huang, W.S. Ng, J. Liu, Z. Wang, Z. Wang, H. Hu, C. Zhi, 3D spacer fabric based multifunctional triboelectric nanogenerator with great feasibility for mechanized large-scale production, *Nano Energy* 27 (2016) 439–446.

<https://doi.org/10.1016/j.nanoen.2016.07.016>.

[6] H.S. Seddeq, N.M. Aly, A. Marwa A, M. Elshakankery, Investigation on sound absorption properties for recycled fibrous materials, *Journal of Industrial Textiles* 43 (2013) 56–73.

<https://doi.org/10.1177/1528083712446956>.

[7] A.E. Tiuc, H. Vermeşan, T. Gabor, O. Vasile, Improved Sound Absorption Properties of Polyurethane Foam Mixed with Textile Waste, *Energy Procedia* 85 (2016) 559–565.

<https://doi.org/10.1016/J.EGYPRO.2015.12.245>.

[8] L. Zhang, E.D. Yilmaz, J. Schjødt-Thomsen, J.C. Rauhe, R. Pyrz, MWNT reinforced polyurethane foam: Processing, characterization and modelling of mechanical properties, *Compos Sci Technol* 71 (2011) 877–884.

<https://doi.org/10.1016/J.COMPSCITECH.2011.02.002>.

[9] J.G. Gwon, S.K. Kim, J.H. Kim, Sound absorption behavior of flexible polyurethane foams with distinct cellular structures, *Mater Des* 89 (2016) 448–454.

<https://doi.org/10.1016/J.MATDES.2015.10.017>.

[10] M. Toyoda, R.L. Mu, D. Takahashi, Relationship between Helmholtz-resonance absorption and panel-type absorption in finite flexible microperforated-panel absorbers, *Applied Acoustics* 71 (2010) 315–320.

<https://doi.org/10.1016/j.apacoust.2009.10.007>.

[11] S. Singh, Z. Kamble, G. Neje, Compressive performance of three-dimensional multilevel

sandwich composite structures, (2024).

<https://doi.org/10.1177/10996362241298156>.



Converting waste leather into photothermal oil absorbing fibers for efficient crude oil spill cleanup

Yaping Wang^{a,b,c}, Mohammed Mahmoud Nasef^{a,c*}

^aDepartment of Chemical and Environmental Engineering, Universiti Teknologi Malaysia, Jalan Sultan Yahya Petra, 54100 Kuala Lumpur, Malaysia.

^bSchool of Materials and Textile Engineering, Jiaxing University, Guangqiong Road, Jiaxing City, Zhejiang Province 314001, China.

^cCenter of Hydrogen Energy, Universiti Teknologi Malaysia, Jalan Sultan Yahya Petra, 54100 Kuala Lumpur, Malaysia.

*Corresponding author: mahmoudeithar@cheme.utm.my; mohdmahmoud@utm.my

ABSTRACT

Oil spills, particularly those involving highly viscous crude oil, pose significant environmental and economic challenges. Traditional oil-absorbing materials often fail to address these spills effectively due to their limited adsorption capacity and inability to reduce oil viscosity. This study presents a novel approach to fabricate a high-performance, photothermal oil absorbing fibres using waste leather as a raw material. The waste leather, primarily composed of collagen fibres, was mechanically disintegrated and modified with carbon nanoparticles (CNPs) followed by treatment with polydimethylsiloxane (PDMS). The resulting absorbent exhibited excellent photothermal conversion efficiency, capable of reaching temperatures up to 81.8°C under simulated solar irradiation (1.0 kW/m²) with a CNP content of 5%, significantly reducing the viscosity of crude oil and facilitating its rapid absorption within 60 seconds. The absorbent demonstrated high oil absorption capacity (up to 11.9 g/g for crude oil), multiple reusability (consistent performance over 20 cycles), and excellent stability under varying pHs (pH 5–14) and temperatures (0–120°C). This study not only provides a sustainable solution for oil spill remediation but also offers a valuable approach for the recycling of leather waste, contributing to environmental preservation and resource utilization.

Keywords: Photothermal oil absorbent; Collagen fibers; Crude oil removal; Waste leather; Environmental remediation



Investigation of the usability of kaolin/agar biocomposite in the removal of U(VI) ions from aqueous solutions

Pinar Aykin^{a,b,*}, Sabriye Yusan^a

^aEge University, İnstitute of Nuclear Sciences, 35100 Bornova, İzmir, TURKEY

^bRepublic of Turkey Ministry of Trade, 35220 Alsancak, İzmir, TURKEY

*Corresponding author: pinaraykin@gmail.com

ABSTRACT

This study explores the feasibility of utilizing a composite material, created by modifying the widely available and economical kaolin mineral through acid and base treatments (1) and integrating it with agar biopolymer (2), for the removal of uranium (VI) ions from aqueous solutions. The treated and untreated kaolin samples were mixed with agar-agar to form composites. The kaolin sample (1%) synthesized using raw kaolin and agar was named RK-Agar, acid-modified kaolin and agar was named AK-Agar, and base-modified kaolin and agar was named BK-Agar. The impact of the modifications on the structure of the synthesized kaolin/agar biocomposite was analyzed using Scanning Electron Microscope (SEM), X-Ray Diffraction (XRD), and Fourier Transform Infrared (FT-IR) techniques. The effects of various parameters such as pH, initial U(VI) ion concentration, temperature and contact time on adsorption efficiency were investigated using the batch operation technique. The amount of U(VI) remaining in the aqueous solution after adsorption was determined using Inductively Coupled Plasma Optical Emission (ICP-OES) spectrometry. Maximum removal efficiency and capacity of uranium (VI) on AK-Agar were 96% and 21.57 mg/g (pH = 5, m/V = 1.0 g/L, T = 25 °C, Time = 90 min), and on BK-Agar were 97% and 21.55 mg/g (pH = 5, m/V = 1.0 g/L, T = 25 °C, Time = 60 min), respectively. These values were higher than those of RK-Agar, which showed 90% removal efficiency and 18.37 mg/g capacity (pH = 6, m/V = 1.0 g/L, T = 30 °C, Time = 180 min). The adsorption efficiency was analyzed using Langmuir, Freundlich, and Dubinin-Radushkevich isotherms, and the relevant parameters were calculated. Characterization results demonstrated that uranium (VI) was successfully immobilized on AK-Agar and BK-Agar. As a result, the AK-Agar and BK-Agar biocomposites we produced may serve as alternative, novel, eco-friendly, and highly effective adsorbents compared to previously known ones.

Keywords: Kaolin, Agar, Biocomposite, Uranium, Adsorption.

References:

1. Nwosu, F.O., Ajala, O.J., Owoyemi, R.M. and Raheem, B.G. 2018, Preparation and characterization of adsorbents derived from bentonite and kaolin clays, *Applied Water Science*, 8:195.
2. Bezerra de Araujo CM, Wernke G, Ghislandi MG, Diório A, Vieira MF, Bergamasco R, et al. Continuous removal of pharmaceutical drug chloroquine and Safranin-O dye from water using agar-graphene oxide hydrogel: Selective adsorption in batch and fixed-bed experiments. *Environ Res.* 2023 Jan 1; 216:114425.

Acknowledgements: This study was financially supported by Ege University Scientific Research Project Unit Project No. FM-YLT-2024-32076.



Tailoring PET/PLA Film Properties Through Transesterification During Melt Processing

Maryam Kheirandish^{a*}, Mohammad Reza Mohaddes Mojtahedi ^a, Hossein Nazockdast^b

^a Department of Textile Engineering, Amirkabir University of Technology, Tehran, Iran

^b Department of Polymer Engineering, Amirkabir University of Technology, Tehran, Iran

*Corresponding author: m.kheirandish@aut.ac.ir

ABSTRACT

Due to the growing demand for various functional materials, the production of biodegradable plastic products has rapidly increased in recent years. These materials can be used in different applications, most notably in the packaging industry. In this research, a polymer film was prepared by blending polylactic acid (PLA), a biodegradable polyester, with polyethylene terephthalate (PET). Surface tension measurements were used to estimate the surface energy values between the two components, and the results indicated good adhesion between them. The microstructure was examined using scanning electron microscopy (SEM), and the findings showed that PET and PLA were immiscible, but compatible with each other. FTIR studies were conducted to investigate the structure. Interactions were analyzed using ¹H NMR, and the transesterification reaction was confirmed. DSC results indicated shifts in glass transition temperature (T_g), which suggests interactions between these materials. Due to the formation of copolymers via transesterification, the crystallization process in the film became more difficult as PLA was added to the PET matrix. The presence of PET crystals in the blended film was confirmed by X-ray scattering patterns.

Keywords: polylactic acid; polyethylene terephthalate; transesterification; polymer film; PET/PLA copolymer

I. INTRODUCTION

Today, awareness regarding the use of fossil resources is increasing. These resources have such a significant impact on the climate that they could potentially drive human life into crisis. Therefore, fossil-based resources need to be gradually phased out and replaced with renewable alternatives. Along with this shift in energy sources, a transformation in material production is also necessary. In the realm of plastics, which are conventionally derived from fossil sources,

bio-based polymers with significant potential to improve carbon dioxide balance can play a crucial role [1].

Polyethylene terephthalate (PET) is a commercially important thermoplastic polymer that is widely used around the world due to its favorable thermal and mechanical properties, low permeability, and chemical resistance [2]. PET plastics are strong, inexpensive, durable, and easy to process. Initially introduced as a substitute for glass soda bottles, PET has since found

expanded use in packaging, textile fibers, engineering plastics, automotive, electronics, and vascular tissue engineering [3]. Its primary application lies in single-use packaging for beverages and food. While not inherently hazardous, PET is derived from petroleum sources and can take thousands of years to degrade. Nevertheless, it is lightweight, transparent, and recyclable, and recycling PET back into plastic is widely practiced [4].

However, the production of PET and other synthetic polyesters increases fossil fuel consumption, contributes to landfill waste, and lacks biodegradability. As a result, the volume of PET waste has increased significantly. Many efforts have been made to enhance its degradability and address environmental concerns, one of which involves blending it with biodegradable polymers [5].

One of the biodegradable polymers that can be produced from renewable sources such as starch and sugar is polylactic acid (PLA). In natural environments, PLA can be fully converted into water and carbon dioxide [6]. This linear aliphatic thermoplastic polyester has attracted much attention due to its environmental friendliness, suitable mechanical properties, thermoplastic processability, and biodegradability. It can be synthesized not only through ring-opening polymerization of lactide but also via the polycondensation of lactic acid [1].

Among its notable features are renewability, biodegradability, and biocompatibility. The price of PLA is slightly higher compared to common commercial polymers [7]. Thanks to its transparency and good mechanical strength, PLA has applications across various industries. However, at room temperature, it tends to be brittle and exhibits low crystallization rate and thermal resistance [8].

Due to the chiral carbon atom in lactic acid, PLA exists in two isomeric forms: L-lactide (PLLA) and D-lactide (PDLA). Many important properties of PLA are

controlled by the ratio and sequence of these enantiomers in the polymer chain [9]. PLLA is approximately 37% crystalline, with a glass transition temperature (T_g) between 50°C and 80°C and a melting temperature between 173°C and 178°C [10]. PLA containing more than 90% PLLA tends to crystallize more readily. As the PLLA content decreases, the melting point, glass transition temperature, and crystallization rate also decrease.

Properties such as thermal stability and impact resistance of PLA are lower than conventional thermoplastic polymers, making PLA less than ideal for competing with them in its pure form. To improve its properties and broaden its potential applications, lactic acid copolymers with other monomers, such as styrene and acrylates, have been developed. Modifications like copolymerization and composite formation have been used to enhance its toughness, permeability, crystallization behavior, and thermal stability [11].

The rapid advancement of technology has increasingly created new applications for polymeric materials with diverse properties. This often necessitates modifying existing polymers to meet specific needs. Among the various polymer modification methods, polymer alloying holds a prominent position due to its flexibility in material selection—especially from an economic standpoint. One major area of focus in polymer alloy studies is controlling the compatibility of constituent components and their microstructure, which significantly affects rheological behavior, processability, and the final product's physical and mechanical properties.

Blending PLA with various polymers has been a topic of significant interest in recent years, with a variety of approaches explored to enhance its properties. For example, In 2011, Yeom and colleagues developed a new bicomponent spunbond structure to achieve large surface area fibers [12]. The fibers used in this

spunbond process included a sacrificial sheath polymer and a core-forming polymer. After mechanical entanglement using high-energy water jets, the sheath polymer was dissolved in a 6% NaOH solution at 90°C, revealing the final structure of the fibers. They used various polymer combinations, including PET as the core and PLA as the sheath. SEM analysis showed fiber diameters of up to 21 microns, and it is noteworthy that the fibers were produced at a speed of 2000 m/min.

In 2014, a comparative study was conducted on the miscibility and biodegradability of PLA/PET and PLA/chitosan blends [13]. The degradation of the samples was measured over six months in real soil, accelerated by pressurized air. In this study, chitosan's miscibility within the PET matrix was reported to be lower compared to PLA. The results revealed weak interactions between components, likely through secondary hydrogen bonding or electrostatic forces. Saturation of PLA in the polymer matrix was observed up to 10 wt%, while chitosan above 5 wt% became brittle. The best miscibility and biodegradability performance for the PET/chitosan system was achieved with 5 wt% chitosan.

Another group of researchers produced PET/PLA composite films via extrusion[14]. Their results indicated that the addition of a small amount of PLA increased the crystallinity of PET during injection molding, but the degradation temperature and tensile/flexural strength of the blends decreased with increasing PLA content. Meanwhile, the degradation rate increased.

Considering that polymer films are typically produced at high temperatures, which increases the possibility of transesterification and copolymer formation, some researchers attempted to avoid high temperatures by preparing PLA/PET electrospun fibers at room temperature using solvents [4]. Nanofibrous layers were analyzed both as-spun and after cold

crystallization treatment. In amorphous as-spun fibers, the addition of PLA prevented the formation of beads. In some blend ratios, two distinct glass transition temperatures were observed, indicating phase separation in the fiber-forming solution. Crystallinity of both polymers decreased in the presence of the other, and overall crystallinity in the blended electrospun fibers was lower than in homopolymer nanofibers [4].

Researchers in Mexico studied the dependence of microstructure and mechanical properties on the PLA content in the PET matrix[3]. They added various PLA concentrations (1, 2.5, 5, and 7.5 wt%) to the PET matrix using a single-screw extruder on a small laboratory scale. Thermal analysis results showed a shift in glass transition temperature with different amounts of PLA. SEM and AFM images revealed two types of microstructures: miscible and partially miscible. Fourier Transform Infrared Spectroscopy (FTIR) confirmed the presence of physical interactions and hydrogen bonding in the polymer blends. Impact resistance and tensile strength decreased with the addition of PLA.

In another study, nanofiber mats were produced using solutions of PET and three types of PLA (one commercial and two branched) to support trypsin enzyme collection during whey protein hydrolysis [15]. The PET/PLA nanofiber mats with immobilized trypsin could be stored in water at 4°C for at least 30 days and reused up to eight times without enzyme washing.

In 2020, Wang and colleagues fabricated PET/PLA foams using in-situ nanofibrillar composites and investigated the foamability and thermal insulation of the final product [16]. They observed that the presence of PET nanofibrils significantly improved PLA's crystallinity, viscoelasticity, and melt strength, thereby enhancing its foamability.

In another investigation, various PET/PLA blend samples—with and without graphene oxide and layered graphite nanoparticles—were prepared using a twin-screw extruder [5]. The study evaluated thermal and hydrolytic degradation behaviours. It was observed that, unlike layered graphite, the addition of graphene oxide reduced the thermal stability of the samples but, due to better dispersion, improved oxygen barrier properties.

Recent advances have also highlighted the role of nanoclay additives in enhancing the morphological and thermal properties of recycled PET/PLA blends, providing improved stability and structural integrity under mechanical stress [17].

Moreover, a 2023 investigation confirmed the biodegradability potential of PET/PLA blends under composting conditions, showing considerable disintegration rates during degradation [18]

As mentioned, PLA, due to its renewable origin, is widely used in various applications and, because of its biodegradability, is often preferred over synthetic fibers in fields such as medicine. However, PLA suffers from some inherent limitations, such as brittleness, which restricts its usage in certain applications.

Therefore, blending PLA with synthetic polymers not only helps mitigate its drawbacks but also enhances the biodegradability of PET. In this study, an alloy of these two polymers was prepared, and the properties of the final product, in film form, were evaluated. It is worth mentioning that since the transesterification phenomenon significantly impacts the final product's properties, and no prior research has thoroughly examined this reaction during melt processing in film form, this study aimed to investigate this phenomenon and evaluate the resulting properties.

II. EXPERIMENTAL METHOD / TEORETICAL METHOD

2.1 Materials and Preparation Techniques

The materials used in this study include polylactic acid (PLA) grade 4043 obtained from NatureWorks (USA), with a weight-average molecular weight of 110,000 g/mol and containing 4–4.5 wt% D-lactide isomer. Polyethylene terephthalate (PET) with a melting temperature of 260°C and intrinsic viscosity of 0.65 dl/g was supplied by Tondgouyan Petrochemical Company. Dichloromethane solvent was purchased from Merck.

2.2. Preparation of Polymer Film

To prepare the polymer film, the PLA and PET polymers were first dried to prevent hydrolysis. Drying was performed in an oven at 80°C for PLA and 120°C for PET, each for 24 hours. Then, both polymers—individually and as blends with 20 wt% PLA—were melted and mixed using an internal mixer (manufactured in Iran) at 60 RPM for 10 minutes at 270°C. The molten blends were then molded into rectangular films with a thickness of 1 mm by hot pressing under 50 bar pressure at 270°C for 5 minutes.

2.3. Characterization of the Films

2.3.1. Surface energy and interfacial tension analysis

To analyze the microstructure of the PLA/PET blend, it is necessary to determine the surface energy of both polymers. Therefore, contact angle measurements were carried out using the static sessile drop method. Film samples with dimensions of 2 × 4 cm were placed on a fixed base, and 10 µL droplets of various liquids were deposited at three distinct points on each sample surface using a microsyringe. The droplets were photographed with a Sony SSCDC318P camera (Japan), and the contact angles were measured using Digimizer software. The test liquids used were water, benzyl alcohol, ethylene glycol, and toluene.

The surface tension (γ), polar component (γ^p), and dispersive component (γ^d) of the test liquids are provided in Table 1. These values were used to calculate the surface energies of the PLA and PET films at processing temperature using the Owens-Wendt-Rabel-Kaelble (OWRK) method [19,20].

Table 1. Surface tension (γ) and its components for reference liquids [21].

| Liquid | γ (mN/m) | γ^d (mN/m) | γ^p (mN/m) |
|-----------------|-----------------|-------------------|-------------------|
| Water | 72.8 | 26.4 | 46.4 |
| Benzyl alcohol | 39.0 | 30.3 | 8.7 |
| Ethylene glycol | 47.7 | 26.4 | 21.3 |
| Toluene | 28.4 | 26.1 | 2.3 |

2.3.2. Investigation of surface microstructure by scanning electron microscopy (SEM)

Morphological images were obtained using a scanning electron microscope (SEM) model XL30 (Philips, Netherlands). Film samples were coated with a thin layer of gold and examined from their cross-sectional surfaces. To further study the phase distribution, the samples were immersed in dichloromethane solvent for 1 hour at room temperature to selectively dissolve the PLA phase from the blend.

2.3.3. Fourier transform infrared spectroscopy (FTIR)

To analyze the chemical structure of the polymer films, FTIR spectra were recorded using a Nicolet Nexus 670 spectrometer in the range of 400–4000 cm^{-1} . This technique was applied to both pure and blended samples to observe the presence of functional groups and potential interactions.

2.3.4. ^1H Nuclear magnetic resonance (^1H NMR)

^1H NMR analysis was performed using a Bruker 400 MHz Ultrashield NMR spectrometer. Both neat and blended polymer films were dissolved in a solvent mixture of deuterated trifluoroacetic acid (TFA) and chloroform-d (CDCl_3) in a 70/30 weight ratio. Tetramethylsilane (TMS) was used as the internal standard, and all spectra were recorded at room temperature with reference to CDCl_3 .

2.3.5. Differential scanning calorimetry (DSC)

Thermal properties of the polymer blends were evaluated using a Q500 TGA (DSC) instrument from the USA. The analysis was performed under a nitrogen atmosphere from room temperature up to 300°C, with a heating rate of 10°C/min for the first heating cycle and 5°C/min for the cooling cycle. Samples were held at 300°C for 2 minutes before cooling. Melting

temperature (T_m) and crystallization temperature (T_c) were recorded from the DSC thermograms.

The degree of crystallinity (ϕ_c) was calculated using the Eq.1 below, assuming 140 J/g as the enthalpy of fusion for 100% crystalline PET:

$$\phi_c = \frac{\Delta H(m) - \Delta H(c)}{\Delta H(m^\circ)w} \quad (1)$$

Where:

- ΔH_m = enthalpy of melting
- ΔH_c = enthalpy of cold crystallization
- ΔH_m° = enthalpy of melting for 100% crystalline PET
- w = weight fraction of the polymer in the blend

2.3.6. X-ray diffraction (XRD)

XRD patterns of the produced films were recorded using an Inel Equinox 3000 diffractometer. Crystallinity of the samples was examined in the 2 θ range of 5–40°. The data were analyzed using X'Pert HighScore Plus software (PANalytical).

III. RESULTS AND DISCUSSIONS

3. 1. Contact Angle Evaluation

The contact angles of the prepared films in different liquids were measured and the results are presented in Table 2.

Table 2. Contact angles (in degrees) of PLA and PET films

| Polymer | Water | Benzyl Alcohol | Ethylene Glycol | Toluene |
|----------|-------|----------------|-----------------|---------|
| PET Film | 86° | 53° | 67° | 37° |
| PLA Film | 82° | 56° | 61° | 34° |

As observed, PLA shows a lower contact angle than PET in water, indicating that PLA is more hydrophilic. Using the contact angle data and the OWRK method, surface energy values were calculated at the processing temperature (270°C), as shown in Table 3.

Note: Since the interfacial energy equations require the contact angle data of the pure components only, the alloy film values were not calculated.

Table 3. Surface energy values of pure polymers at 270°C

| Polymer | Total γ (mN/m) | Dispersive γ^d | Polar γ^p |
|---------|-----------------------|-----------------------|------------------|
| PET | 9.305 | 7.036 | 2.269 |
| PLA | 11.290 | 7.210 | 4.080 |

Then, using the surface energy data, the interfacial energy between the two polymers was calculated.[22–24] . The results can be seen in Table 4.Using these surface energy values, the interfacial tension (γ_{12}) between PLA and PET was calculated using both and geometric and harmonic mean equations, shown below in Eq2. and Eq3. respectively:

- Geometric Mean:

$$\gamma_{12} = \gamma_1 + \gamma_2 - 2(\sqrt{\gamma_1^d \gamma_2^d} + \sqrt{\gamma_1^p \gamma_2^p}) \quad (2)$$

- Harmonic Mean:

$$\gamma_{12} = \gamma_1 + \gamma_2 - 4\left(\frac{\gamma_1^d \gamma_2^d}{\gamma_1^d + \gamma_2^d} + \frac{\gamma_1^p \gamma_2^p}{\gamma_1^p + \gamma_2^p}\right) \quad (3)$$

Where γ_1 , γ_2 , are the surface tensions of polymers 1 and 2, γ_1^d , γ_2^d , γ_1^p , and γ_2^p are the dispersive and polar fractions of the surface tensions of polymers 1 and 2, respectively. The harmonic equation is generally well-suited to low-energy materials [25]. For low-energy surfaces, the geometric-mean equation is inadequate [24], but it is recommended for both high and low-energy surfaces [23].

Table 4. Interfacial tension (γ_{12}) between PET and PLA

| Polymer Pair | Harmonic Mean (mN/m) | Geometric Mean (mN/m) |
|--------------|----------------------|-----------------------|
| PET-PLA | 0.519 | 0.338 |

The low interfacial tension values suggest good compatibility and interfacial adhesion between the two components [19], which was confirmed by SEM results in Figure 1. This also supports the thermodynamic argument that good interfacial interaction facilitates blending and potentially improves the final properties of the film [26].

3.2. Scanning electron microscopy (SEM)

Microscopic images of the fractured surface of PET and PLA films and their blends are shown in Figure 1. The fractured surface in Figure 1(b) clearly shows that the PLA film has a brittle structure. In part (c) of Figure 1, the presence of spherical PLA droplets inside the PET matrix and the immiscibility of the two components can be seen. In part (d) of Figure 1, the PLA phase has been selectively separated from the matrix by dichloromethane.

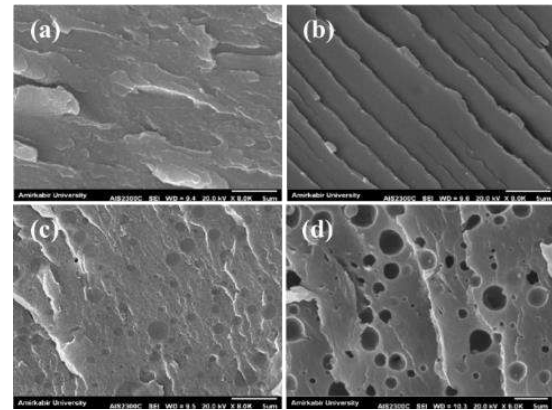


Figure 1. Microstructure of the films: (a) pure PET, (b) pure PLA, (c) PET/PLA blend film containing wt20% PLA and (d) PET/PLA blend film containing wt20% PLA after the dispersion component was removed

As can be seen, the dispersed PLA phase in the PET matrix is located in the dark empty cavities visible on the fractured surface. In part (c) of the figure, it can be seen that the connection of all the dispersed phase particles with the matrix is not spaced and no phase separation is seen at the common surface, and in fact, the dispersed component and the polymer matrix have good uniformity due to sufficient compatibility with each other [27]. In other words, the interface region between the phases indicates low surface tension between the components, which results in the connection of PLA particles to the matrix and the adhesion between the two phases seems good. This finding is consistent with the calculated interfacial energy between PET and PLA, which was observed in Table 4.

Based on thermodynamic principles, comparing the solubility quantities of two or more polymers can

predict their miscibility [2], Hansen's solubility value for PET and PLA predicts that they should be miscible [28,29]. Andrew et al. believe that the molar volume and the size of the repeating unit are important factors that cause immiscibility in the blend of PET and PLA. PET has a structure with large benzene rings and as evident from its higher molar volume than PLA, this could explain the immiscibility of the two phases of these polymers in the molten state [30]. Our results seem to be closer to their findings and the different molar volumes of the two phases caused the immiscibility between PET and PLA.

3.4. FTIR Spectroscopy

FTIR analysis was performed to investigate the chemical structure of the samples in pure and blended state. Figure 2 shows the FTIR spectra of PET, PLA films and their blends.

The PET spectrum shows characteristic peaks related to O-H stretching at 3432 cm^{-1} which is related to the ethylene glycol end group of the PET molecule chain, aromatic C-H stretching at 3060 cm^{-1} and aliphatic C-H stretching at $2964\text{--}2910\text{ cm}^{-1}$. 1719 cm^{-1} represents C=O stretching and $11577\text{--}1504\text{ cm}^{-1}$ indicates the aromatic structure stretching band, $11454\text{--}1340\text{ cm}^{-1}$ peak related to CH₂, 11407 cm^{-1} para substitution in the benzene ring and $11248\text{--}1097\text{ cm}^{-1}$ O-C stretching of the ester group.

The aromatic 1,4 substitution is observed at 11018 cm^{-1} and the O-CH₂ stretching of the ethylene glycol moiety is observed at 971 cm^{-1} and the C-H corresponding to the two adjacent paired hydrogens on the benzene ring is observed at 1873 cm^{-1} [13,31].

The main absorption peaks of PLA are as follows: 3505 represents the O-H stretching vibration 2998 and 2946 cm^{-1} are the CH₃ stretching vibration in the asymmetric and symmetric states. The peak at 1760 cm^{-1} is related to the C=O stretching of the aliphatic units, the peak at 1454 represents the unsymmetrical CH₃ bending vibration and the peaks at 1384 cm^{-1} and

1361 are related to the C-H group, 1189 and $\text{cm}^{-1}1093$ are related to the O-C cm^{-1} stretching vibration of the aliphatic ester. and 869 cm^{-1} shows C-C-O absorption [32].

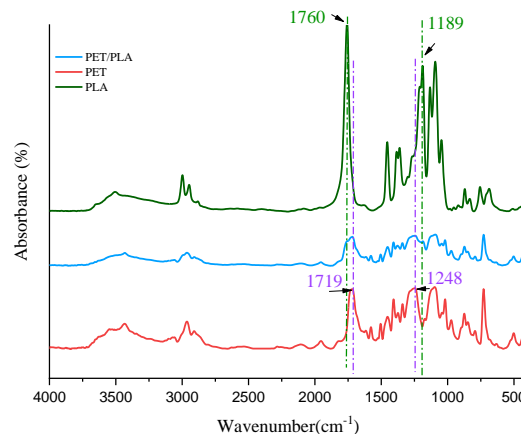


Figure 2. FTIR diagram of the produced films.

As shown in Figure 2, in the composite film, characteristic peaks attributed to the carbonyl ester and the ester group for the PET polymer present in the structure are visible. However, the peaks related to PLA (peak $\text{cm}^{-1} 1760$ which is related to the carbonyl ester of PLA) in the composite film are slightly transformed into a comb and the peak at $\text{cm}^{-1}1189$ is only partially visible. The lack of visibility of PLA peaks in the composite may be due to the low percentage of PLA compared to the main matrix, PET.

3.5. ¹H NMR Results

¹H NMR evaluation was performed to determine the molecular structure of the PET/PLA composite film and the resulting graphs are shown in Figure 3.

In the case of PET, the characteristic peaks in this analysis are as follows: hydrogens attached to the aromatic ring and ethylene groups between two terephthalate units in the repeating chain of this polymer are seen at 13.8 ppm and 85.4 ppm . The signals at 20.4 ppm and 66.4 ppm are related to the ethylene oxide hydrogens of the end group [33,34]. In the diagram for PLA film, the characteristic peaks of

this polymer structure are observed at 60.1 ppm and 26.5 ppm, which are related to the CH₃ and CH groups in the main chain of this polymer, respectively [33].

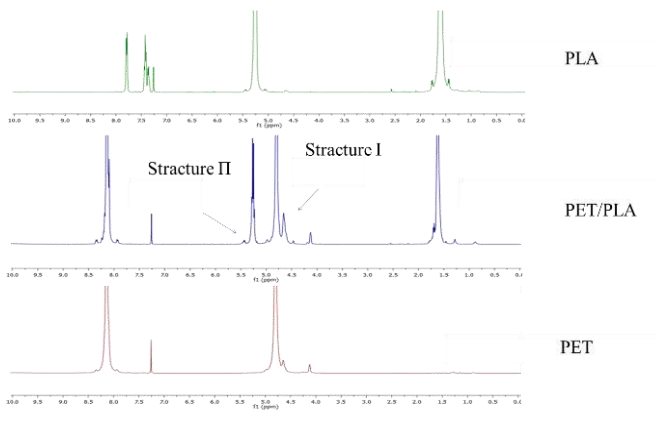


Figure 3. ¹H NMR spectra of polyethylene terephthalate, polylactic acid and polyethylene terephthalate/polylactic acid films

As a result of the ester exchange phenomenon and the placement of the PLA chain between the PET chains, two possible structures can be formed (Figure 4). In the first structure, this polymer is attached to the ethylene groups in ethylene terephthalate, and in the second structure, the PLA chains are directly attached to the benzene ring in the PET chain. The placement of PLA in each of these positions causes peaks to appear in the ¹H NMR spectrum. In structure I, the ethylene oxide hydrogens located in this position show the corresponding signal in a lower field, which can overlap with the peaks related to the end groups of PET. In calculations and measurements, the area under the diagram related to each of the hydrogens must be subtracted from the area under the diagram of the end groups. In case II, the hydrogen related to the CH group shows itself in a higher field due to its attachment to the electron-withdrawing group of terephthalates, and in other words, the appearance of this peak confirms the formation of the second structure. In the blending of polyesters, when the blending process occurs at temperatures close to or above the melting temperature, the possibility of transesterification is very likely [35]. The observation of peaks corresponding to each of the possible

structures seen in the ¹H NMR diagram (Figure 3) confirms the occurrence of transesterification between the two polyesters forming the blend.

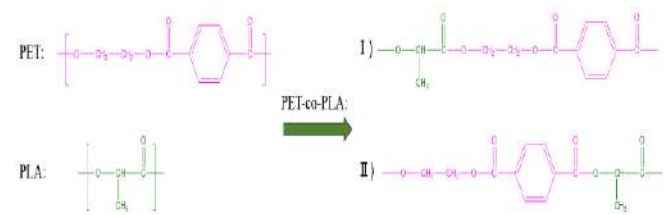


Figure 4. Possible structures formed by ester exchange.

3.6. Thermal Analysis

The DSC diagrams of pure films and semi-crystalline PET/PLA composite films during heating and cooling are shown in Figure 5, respectively.

Table 5 shows the results of PET crystallization during heating and cooling of the films in non-isothermal crystallization. In Figure 5, pure PET film is seen with a crystallization temperature of 125 °C, a melting temperature of 257 °C, and a degree of crystallinity of 0.192. The peak near 80 °C is attributed to the glass transition of PET. In the pure PLA sample, a degree of crystallinity of 0.36 and a melting temperature of 150 °C are observed. In the PET/PLA composite film, two glass transition temperatures at temperatures of 63 and 78 °C are clearly seen, which are related to the T_g of PLA and PET polymers, respectively, and indicate the immiscibility of the two polymers [36], which was also clearly seen in the microscopic images (Figure 1). The decrease in T_g in PET and its closer approximation to the T_g of polylactic acid can be a confirmation of the interactions between these two polymers [37]. In this film diagram of the combination of the two polymers, the peak corresponding to the melting temperature of PLA is not seen. With the addition of PLA, the melting temperature of PET and its enthalpy of melt have decreased, and the crystallization rate of PET after the addition of PLA reaches 0.139.

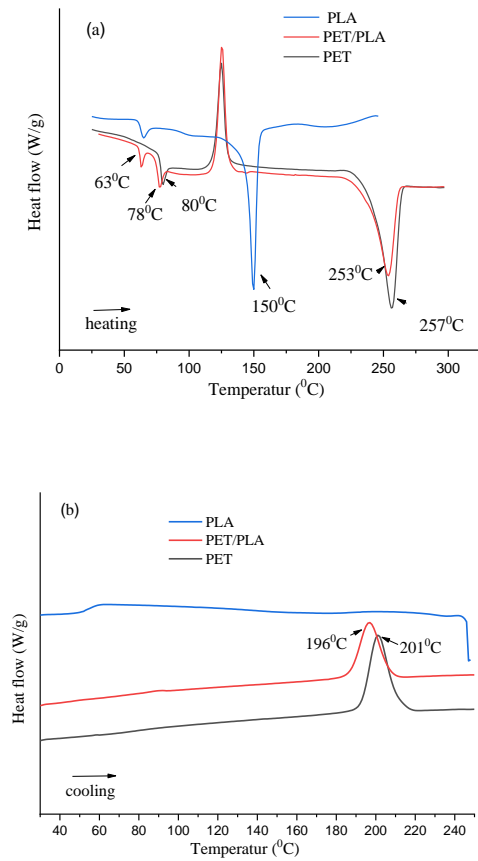


Figure 5. DSC diagram of pure PET, PLA and PLA blended film
(a) first heating (b) cooling from the melt.

When semi-crystalline polymers are blended with other polymers, the decrease in T_m indicates a degree of miscibility between the blend components due to favorable thermodynamic interactions between PET and PLA, indicating that the PLA repeating units often interrupt the linear crystallographic sequences of PET chains [20,40–42]. Furthermore, the crystallinity of PET becomes difficult with the addition of PLA. This conclusion is consistent with the X-ray results shown in Figure. 6. On the other hand, the PET-PLA structure resulting from ester exchange is difficult to incorporate into the PET crystal, causing the PET crystallinity to decrease in the blends. The ^1H NMR results confirm these findings. In the graph of Fig. 6(b) which is related to the cooling of the samples, the crystallinity of PET in the blend is observed, but this does not happen for the PLA chains. In other words,

the PET chains affect and hinder the crystallization of PLA. The addition of PLA caused the crystallization of PET melt to decrease from 201 °C to 196 °C and the melt crystallinity to increase from 0.319 to 0.299.

It has been reported that this effect could be due to the formation of PET-PLA copolymers resulting from the transesterification reaction at the melt processing temperature of polyesters. The copolymer is primarily found at the interface and its role in reducing interfacial tension and increasing miscibility is widely known in reactive processes [38]. On the other hand, PLA units are incorporated into the crystal lattice as a result of transesterification interactions between PET and PLA units, resulting in the production of a block copolymer [39].

On the other hand, PLA units are the soft parts in the copolymer structure. Due to the low T_g of PLA, these PLA blocks should have higher mobility than PET blocks at the crystallization temperature. Therefore, the lower crystallization onset and lower crystallinity in the polymer blend is due to the increased mobility of the soft segments of PLA [39].

Table 5. Data related to DSC

| PET/PLA Ratio | ΔH_c (J/g) (Heating) | T_m (°C) (PET) | ΔH_m (J/g) PET | Φ_c PET (Heating) | ΔH_c (J/g) PET (Cooling) | Φ_c PET (Cooling) |
|------------------|------------------------------------|------------------------|------------------------------|---------------------------|----------------------------------------|---------------------------|
| 0/100 | 63.19 | 257 | 50.46 | 0.192 | 65.44 | 0.319 |
| 20/80 | 83.21 | 253 | 44.37 | 0.139 | 45.33 | 0.299 |

3.7. X-ray diffraction

The presence of one component can affect the crystallinity of another component, so to investigate this effect, X-ray diffraction tests were performed on the samples and the results are shown in Figure 6. As can be seen, the main peaks related to PET are seen at angles of 16.33, 17.50, 21.45, 22.63 and 26.19 degrees, which are related to the crystal planes (01 $\bar{1}$), (010), (11 $\bar{1}$), (1 $\bar{1}$ 0) (100). As can be seen, this semi-

crystalline polymer has a broad amorphous peak and crystallization peaks at the mentioned angles [13]. As a result, this polymer has a triclinic structure [13,40].

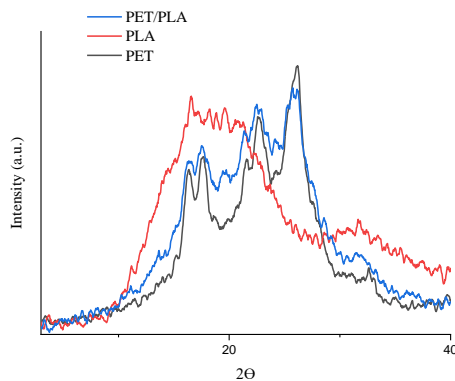


Figure 6. X-ray diffraction pattern of PET, PLA, and PET/PLA films

The diffraction pattern of PLA film is visible with a peak at $2\theta=16.81$ with Miller index corresponding to the (200/110) plane, which is broader and appears almost asymmetric compared to the PET peak [41,42]. Such asymmetric peaks may actually be interpreted as a combination of the symmetric amorphous structure and several scattered peaks from incomplete or very small crystallites.

The crystal structure in the composite film has the triclinic structure of PET, since the five mentioned Bragg angles correspond only to the PET crystal planes. This result indicates that PET crystals are formed separately in PET-rich blends, rather than forming PET/PLA crystallites. It may not be clear whether the peaks of PLA overlap slightly with those of PET, but according to the DSC result (Fig. 5), PLA cannot crystallize in the blend film and the PLA peak corresponding to the (200/1100) planes is absent in the film. Therefore, the crystal structure of PET does not change with the addition of PLA and no additional peaks are observed for the blend film.

In addition, the interpenetration and entanglement of the two types of polymer chains during the crystallization process of the PET/PLA blend reduces the segmental mobility and prevents the formation of crystals of PET and PLA polymer chains [43].

Another factor that may limit the development of the crystal structure in the blends is the formation of block copolymers as a result of ester exchange [34]. Evidence of this reaction is shown in the ^1H NMR of the molten PET/PLA blend in Fig. 3. Transesterification is likely in this study because the extrusion temperature was chosen to be 270°C and the polymer remained in the molten state for more than 5 min.

IV. CONCLUSIONS

PET is a petroleum-based polymer whose hydraulic degradation can take decades. The increasing interest in biodegradable polymers has led to the use of materials such as PLA in various industries in recent years. PET/PLA blend film was prepared using a melt process. PLA particles and PET matrix had good surface adhesion in the PET/PLA blend. This combination had a significant effect on the structure and properties of the blend film in the studied ranges. The experimental results showed that transesterification occurred during the melt compounding process and PET/PLA copolymers were formed. Transesterification reduced the melting point, crystallization temperature and crystallinity of the samples. XRD and DSC results on the film samples showed individual PET crystals instead of co-crystallization and it was found that a small amount of PLA had an inhibitory effect on the crystallinity of PET in the melt process.

REFERENCES

- [1] G. Reiter, J. Xu, S. Körber, K. Moser, J. Diemert (2022) Development of High Temperature Resistant Stereocomplex PLA for Injection Moulding, Mdpi.Com.

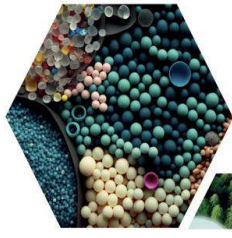
- <https://doi.org/10.3390/polym14030384>.
- [2] M. Aldas, C. Pavon, H. De La Rosa-Ramírez, J.M. Ferri, D. Bertomeu, M.D. Samper, J. López-Martínez (2021) The Impact of Biodegradable Plastics in the Properties of Recycled Polyethylene Terephthalate, *J. Polym. Environ.* 2686–2700. <https://doi.org/10.1007/S10924-021-02073-X>.
- [3] A.M. Torres-Huerta, D. Del Angel-López, M.A. Domínguez-Crespo, D. Palma-Ramírez, M.E. Perales-Castro, A. Flores-Vela (2016) Morphological and mechanical properties dependence of PLA amount in PET matrix processed by single-screw extrusion, *Polym. - Plast. Technol. Eng.* 672–683. <https://doi.org/10.1080/03602559.2015.1132433>.
- [4] K. Li, B. Mao, P. Cebe (2014) Electrospun fibers of poly(ethylene terephthalate) blended with poly(lactic acid), *J. Therm. Anal. Calorim.* 1351–1359. <https://doi.org/10.1007/s10973-013-3583-4>.
- [5] S.M.A. Jafari, R. Khajavi, V. Goodarzi, M.R. Kalaei, H.A. Khonakdar, Development of degradable poly(ethylene terephthalate)-based nanocomposites with the aid of polylactic acid and graphenic materials: Thermal, thermo-oxidative and hydrolytic degradation characteristics, *J. Appl. Polym. Sci.* 137 (2020). <https://doi.org/10.1002/app.48466>.
- [6] G. Wang, J. Zhao, G. Wang, H. Zhao, J. Lin (2022), Strong and super thermally insulating in-situ nanofibrillar PLA/PET composite foam fabricated by high-pressure microcellular injection molding, Elsevier. <https://www.sciencedirect.com/science/article/pii/S1385894720305118>
- [7] M. Boruvka, C. Cermak, L. Behalek, P. Brdlik (2021) Effect of in-mold annealing on the properties of asymmetric poly(L-lactide)/poly(D-lactide) blends incorporated with nanohydroxyapatite, *Polymers (Basel)*. 13. <https://doi.org/10.3390/polym13162835>.
- [8] S.W. Lin, Y.Y. Cheng (2010) Miscibility, thermal and mechanical properties of melt-mixed poly(lactic acid)/poly(trimethylene terephthalate) blends, *Polym. - Plast. Technol. Eng.* 1001–1009. <https://doi.org/10.1080/03602559.2010.482078>.
- [9] A.J.R. Lasprilla, G.A.R. Martinez, B.H. Lunelli, A.L. Jardini, R.M. Filho (2012) Poly-lactic acid synthesis for application in biomedical devices - A review, *Biotechnol. Adv.* 321–328. <https://doi.org/10.1016/j.biotechadv.2011.06.019>.
- [10] K. Madhavan Nampoothiri, N.R. Nair, R.P. John (2010) An overview of the recent developments in polylactide (PLA) research, *Bioresour. Technol.* 8493–8501. <https://doi.org/10.1016/j.biortech.2010.05.092>.
- [11] R. Auras, L. Lim, S. Selke, H. Tsuji, (2018) Poly (lactic acid): synthesis, structures, properties, processing, and applications.
- [12] B.Y. Yeom, B. Pourdeyhimi (2011) Web fabrication and characterization of unique winged shaped, area-enhanced fibers via a bicomponent spunbond process, *J. Mater. Sci.* 3252–3257. <https://doi.org/10.1007/s10853-010-5212-y>.
- [13] A.M. Torres-Huerta, D. Palma-Ramírez, M.A. Domínguez-Crespo, D. Del Angel-López, D. De La Fuente (2014) Comparative assessment of miscibility and degradability on PET/PLA and PET/chitosan blends, *Eur. Polym. J.* 285–299.

- <https://doi.org/10.1016/j.eurpolymj.2014.10.016>.
- [14] X.L. Xia, W.T. Liu, X.Y. Tang, X.Y. Shi, L.N. Wang, S.Q. He, C.S. Zhu (2014) Degradation behaviors, thermostability and mechanical properties of poly (ethylene terephthalate)/polylactic acid blends, *J. Cent. South Univ.* 1725–1732. <https://doi.org/10.1007/s11771-014-2116-z>.
- [15] T. Silva, D. Rodrigues, J. Rocha, ... M.G.-B., undefined (2015), Immobilization of trypsin onto poly (ethylene terephthalate)/poly (lactic acid) nonwoven nanofiber. <https://www.sciencedirect.com/science/article/pii/S1369703X15001680> (accessed May 6, 2018).
- [16] G. Wang, J. Zhao, G. Wang, H. Zhao, J. Lin, G. Zhao, C.B. Park (2020) Strong and super thermally insulating in-situ nanofibrillar PLA/PET composite foam fabricated by high-pressure microcellular injection molding, *Chem. Eng. J.* 390. <https://doi.org/10.1016/j.cej.2020.124520>.
- [17] M.P. Belioka, G. Markozanne, K. Chrissopoulou, D.S. Achilias (2023) Advanced Plastic Waste Recycling—The Effect of Clay on the Morphological and Thermal Behavior of Recycled PET/PLA Sustainable Blends, *Polym.* 2023, Vol. 15, Page 3145.3145. <https://doi.org/10.3390/POLYM15143145>.
- [18] M. Kheirandish, M.R. Mohaddes Mojtahedi, H. Nazockdast (2023) Assessing compatibility, transesterification, and disintegration of PET/PLA fiber blend in composting conditions, *Front. Mater.* 1225200. <https://doi.org/10.3389/FMATS.2023.1225200/BIBTEX>.
- [19] A. Anstey, A. Codou, M. Misra, A.K. Mohanty (2018) Novel Compatibilized Nylon-Based Ternary Blends with Polypropylene and Poly(lactic acid): Fractionated Crystallization Phenomena and Mechanical Performance, *ACS Omega*. 2845–2854. <https://doi.org/10.1021/acsomega.7b01569>.
- [20] C. Chandavas, M. Xanthos, K.K. Sirkar, C.G. Gogos (2001) Polypropylene blends with potential as materials for microporous membranes formed by melt processing, *Polymer (Guildf)*. 781–795. [https://doi.org/10.1016/S0032-3861\(01\)00654-1](https://doi.org/10.1016/S0032-3861(01)00654-1).
- [21] C. Rulison (2000) Two-component surface energy characterization as a predictor of wettability and dispersability.
- [22] Polymer Interface and Adhesion by Wu (Author) (2017).
- [23] R. Cardinaud, T. McNally (2013) Localization of MWCNTs in PET/LDPE blends, *Eur. Polym. J.* 1287–1297. <https://doi.org/10.1016/j.eurpolymj.2013.01.007>.
- [24] M. Nofar, R. Salehiyan, U. Ciftci, A. Jalali, A. Durmuş (2020) Ductility improvements of PLA-based binary and ternary blends with controlled morphology using PBAT, PBSA, and nanoclay, *Compos. Part B Eng.* 182 <https://doi.org/10.1016/j.compositesb.2019.107661>.
- [25] S. Wu, *Polymer interface and adhesion*, CRC Press, (2017). <https://doi.org/10.1201/9780203742860>.
- [26] M.R. Snowden, A.K. Mohanty, M. Misra (2017) (Miscibility and Performance Evaluation of Biocomposites Made from Polypropylene/Poly(lactic acid)/Poly(hydroxybutyrate-cohydroxyvalerate) with a Sustainable

- Biocarbon Filler, ACS Omega. 6446–6454.
<https://doi.org/10.1021/acsomega.7b00983>.
- [27] M. Mehrabi Mazidi, M.K. Razavi Aghjeh (2015) Effects of blend composition and compatibilization on the melt rheology and phase morphology of binary and ternary PP/PA6/EPDM blends, Polym. Bull. 1975–2000. <https://doi.org/10.1007/s00289-015-1384-6>.
- [28] M. Serhan, M. Sprowls, D. Jackemeyer, M. Long, I.D. Perez, W. Maret, N. Tao, E. Forzani (2019) Total iron measurement in human serum with a smartphone, AIChE Annu. Meet. Conf. Proc. <https://doi.org/10.1039/x0xx00000x>.
- [29] R. Auras, B. Harte, S. Selke (2006) Sorption of ethyl acetate and d-limonene in poly(lactide) polymers, J. Sci. Food Agric. 648–656. <https://doi.org/10.1002/jsfa.2391>.
- [30] A.R. McLauchlin, O.R. Ghita (2016) Studies on the thermal and mechanical behavior of PLA-PET blends, J. Appl. Polym. Sci. <https://doi.org/10.1002/app.44147>.
- [31] M. Djebara, J.P. Stoquert, M. Abdesselam, D. Muller, A.C. Chami (2012) FTIR analysis of polyethylene terephthalate irradiated by MeV He +, Nucl. Instruments Methods Phys. Res. Sect. B Beam Interact. with Mater. Atoms. 70–77. <https://doi.org/10.1016/j.nimb.2011.11.022>.
- [32] Y.X. Weng, Y.J. Jin, Q.Y. Meng, L. Wang, M. Zhang, Y.Z. Wang (2013) Biodegradation behavior of poly(butylene adipate-co-terephthalate) (PBAT), poly(lactic acid) (PLA), and their blend under soil conditions, Polym. Test. 32 918–926. <https://doi.org/10.1016/j.polymertesting.2013.05.001>.
- [33] A.M. Kenwright, S.K. Peace, R.W. Richards, A. Bunn, W.A. MacDonald (1999) End group modification in poly(ethylene terephthalate). [https://doi.org/10.1016/S0032-3861\(98\)00433-9](https://doi.org/10.1016/S0032-3861(98)00433-9).
- [34] G. Wu, J.A. Cuculo (1999) Structure and property studies of poly(ethylene terephthalate)/poly(ethylene-2,6-naphthalate) melt-blended fibres. [https://doi.org/10.1016/s0032-3861\(98\)00317-6](https://doi.org/10.1016/s0032-3861(98)00317-6).
- [35] R.S. Porter, L.H. Wang (1992) Compatibility and transesterification in binary polymer blends, Polymer (Guildf). 2019–2030. [https://doi.org/10.1016/0032-3861\(92\)90866-U](https://doi.org/10.1016/0032-3861(92)90866-U).
- [36] S.W. Lin, Y.Y. Cheng (2010) Miscibility, thermal and mechanical properties of melt-mixed poly(lactic acid)/poly(trimethylene terephthalate) blends, Polym. - Plast. Technol. Eng. 1001–1009. <https://doi.org/10.1080/03602559.2010.482078>.
- [37] B.M. Lekube, C. Burgstaller (2022) Study of mechanical and rheological properties, morphology, and miscibility in polylactid acid blends with thermoplastic polymers, J. Appl. Polym. Sci. <https://doi.org/10.1002/app.51662>.
- [38] X.L. Xia, W.T. Liu, X.Y. Tang, X.Y. Shi, L.N. Wang, S.Q. He, C.S. Zhu (2014) Degradation behaviors, thermostability and mechanical properties of poly(ethylene terephthalate)/polylactic acid blends, J. Cent. South Univ. 1725–1732. <https://doi.org/10.1007/s11771-014-2116-z>.
- [39] I. Acar, A. Durmuş, S. Özgümüş (2007) Nonisothermal crystallization kinetics and morphology of polyethylene terephthalate modified with polydactic acid, J. Appl. Polym. Sci. 4180–4191. <https://doi.org/10.1002/app.26982>.

- [40] L.A. Baldenegro-Perez, D. Navarro-Rodriguez, F.J. Medellin-Rodriguez, B. Hsiao, C.A. Avila-Orta, I. Sics (2014) Molecular weight and crystallization temperature effects on poly(ethylene terephthalate) (PET) homopolymers, an isothermal crystallization analysis, *Polymers* (Basel). 583–600.
<https://doi.org/10.3390/polym6020583>.
- [41] M.A. Abdelwahab, A. Flynn, B. Sen Chiou, S. Imam, W. Orts, E. Chiellini (2012) Thermal, mechanical and morphological characterization of plasticized PLA-PHB blends, *Polym. Degrad. Stab.* 1822–1828.
<https://doi.org/10.1016/j.polymdegradstab.2012.05.036>.
- [42] Y. Wang, H. Zhang, M. Li, W. Cao, C. Liu, C. Shen (2015) Orientation and structural development of semicrystalline poly(lactic acid) under uniaxial drawing assessed by infrared spectroscopy and X-ray diffraction, *Polym. Test.* 163–171.
<https://doi.org/10.1016/j.polymertesting.2014.11.010>.
- [43] H. Liang, F. Xie, F. Guo, B. Chen, F. Luo, Z. (2008) Jin, Non-isothermal crystallization behavior of poly(ethylene terephthalate)/poly(trimethylene terephthalate) blends, *Polym. Bull.* 115–127.
<https://doi.org/10.1007/s00289-007-0832-3>.

16. Uluslararası Lif ve Polimer Araştırmaları Sempozyumu (16. ULPAS)
9-10 Mayıs 2025, İstanbul Teknik Üniversitesi (İTÜ), İstanbul, Türkiye



16 ULUSLARARASI
LİF VE POLİMER
ARAŞTIRMALARI
SEMPOZYUMU

16th INTERNATIONAL FIBER AND POLYMER RESEARCH SYMPOSIUM

Sürdürülebilir ve İşlevsel Lif ve Polimerler
Sustainable and Functional Fibers & Polymers



9-10 Mayıs
May 2025

İstanbul Teknik Üniversitesi
Gümüşsuyu Prof. Dr. Necmettin Erbakan Yerleşkesi
İstanbul Technical University
Gumussuyu Prof. Dr. Necmettin Erbakan Campus

Dikişsiz örgü ve delikli vücut haritalama tasarımıyla iç giyimde konfor ve performans artışı

Sultan Aras Elibüyük^a, Mustafa Çörekcioğlu^a, Perinur Koptur Tasan^a, Özlem Demir Günenç^a

^aOzanteks Tekstil San. ve Tic. A.Ş., 20020 Denizli, Türkiye.

*Sultan ARAS ELİBÜYÜK: saras@ozanteks.com.tr

ÖZET

Sağlık için oldukça önemli olan iç çamaşırları vücuda direkt temas eden ürünlerdir. Söz konusu tene direkt temastan dolayı bu giysi türünün hangi materyallerden üretildiği oldukça önemli bir noktadır. Genellikle bilinen bu iç çamaşırları kişisel konfor da göz önüne alındığında rahat, koku yapmayan, nefes alabilir, ince ve sıvı transferi kolay olacak bir özellik sağlamalıdır. Ayrıca iç çamaşırı seçimi, hem sağlık hem de rahatlık açısından oldukça önemlidir. İç çamaşırı, gün boyunca cilt ile sürekli temas halinde olduğu için yanlış bir seçim, kaşıntı, alerji, enfeksiyon veya rahatsızlık gibi problemlerine yol açabilmektedir. Özellikle spor veya egzersiz yaparken doğru iç çamaşırı seçimi, rahatlık ve performans için oldukça önemlidir. İç çamaşırı seçimi stil ve görünümünü de etkileyebilmektedir. Bu nedenle genellikle selülozik içerikli iç çamaşırları tercih edilmektedir. Bu çalışma elde edilen altı farklı içeriğe sahip ürünlerin diğer iç çamaşırlarından farkı, ürünlerin farklı bölgelerinde farklı boyutlarda delikli yapıya sahip olması sayesinde ilgili bölgelerin hava almasıdır. Yapılan fiziksel testler ve haslık testleri değerlendirilmiştir. Seamless teknolojisinin avantajı ile ürünlerde ter bölgelerinde delikli örgü yapılıncı terleme azalmış, tenin hava almasını sağlanmış ve kötü kokuların oluşması engellenmiştir. İplik içeriği selülozik ve sentetik olacak şekilde su emici iplikler kullanılması sayesinde daha emici ve daha hızlı kuruma özelliği olan bir iç çamaşırı ortaya koyulmuştur. Doğal iplikler kullanılması sayesinde sağlığa daha yararlı bir çamaşır giyim konforu sunmuştur.

Anahtar Kelimeler: Dikişsiz Örgü Teknolojisi; Vücut haritalama, Delikli Örgü, Karışım İplik, İç giyim.

Performance and comfort enhancement in underwear through seamless knitting and perforated body mapping design

ABSTRACT

Underwear, which plays a crucial role in health, is a type of garment that comes into direct contact with the body. Due to this direct contact with the skin, the materials used in its production are of significant importance. Underwear must provide comfort, odor resistance, breathability, thinness, and effective moisture transfer. Inappropriate fabric choices

can lead to skin irritation, allergies, infections, or general discomfort due to the garment's prolonged contact with the body throughout the day. Therefore, both comfort and health aspects must be considered when selecting underwear. This is particularly critical during physical activities, where the right choice contributes to improved comfort and performance. Additionally, underwear selection can also influence style and appearance. As a result, cellulosic-based fabrics are commonly preferred.

This study focuses on evaluating the performance of six underwear samples with different fiber contents. The innovative design feature that distinguishes these seamless garments is the use of perforated knit structures in various regions of the product, enabling improved air circulation to targeted body zones. Physical and colorfastness tests were conducted to evaluate product performance. The integration of perforated knit structures, particularly in high-sweat areas through seamless technology, has resulted in reduced perspiration, enhanced breathability, and odor prevention. Moreover, the use of cellulosic and synthetic moisture-absorbing yarns has produced underwear with high absorbency and faster drying capabilities. The incorporation of natural fibers has contributed to enhanced skin compatibility and overall wearing comfort.

Keywords: Seamless knitting technology; body mapping; perforated structure; blended yarn; underwear

16th International Fiber and Polymer Research Symposium (16th ULPAS)

9-10 May, 2025, Istanbul technical University (ITU), Istanbul, Türkiye

BURSALI

DEVELOPMENT AND APPLICATION OF REACTIVE DYE MICROCAPSULES FOR COTTON FABRIC DYEING

Sevil GÜNÇ, Saliha Büşra KARAKELLE, Eyüphan YENER

Abstract

Different methods and environmentally friendly processes

- The textile industry renews itself day by day and begins to expand its presence in the sector with different production methods and environmentally friendly processes. Although textile industries do not want to give up conventional methods, responding to user demands and increasing market share is important in today's technology.

Sustainability

- The demand for textiles that encourage "well-being" will persist due to people's desire for a more fruitful and healthy way of living. With active delivery from microcapsules, textiles can "interact" with the user to promote comfort, relaxation, and a reduction in stress.

Reactive colorant

- A substitute for traditional cellulosic fiber dyeing, and they are now the most popular for cotton fibers. Their basic idea is based on addition and substitution processes involving the fiber's hydroxyl groups.

Conventional Dyeing Problems;

- Different exhaustion profiles
- Consumption of energy, water and time
- Faulty dyeing



Experimental

| MATERIAL | METHOD |
|-------------------------------------------------------------------------------------------------------------------------------------------------------------------------------------------------------------------------------------------------------------------------------------------------------------------------|------------------------------------------------------------------------------------------------------------------------------------------------------------------------------------------------------------------------------------------------------------------------------------------------------------------------------------------------------------------------------------------------------------|
| <ul style="list-style-type: none">Lint: 20/1 Cotton RingWeft: 16/1 Cotton O.EWarp: 20/2 Cotton RingEthyl Cellulose - UFSaltReactive DyeCitric Acid and Acetic AcidSoda Solution and Tween 80Ethyl Acetate - Tween 20 - Chloroform | First the water, ethyl cellulose and formaldehyde mixed to make the outer shell of the microcapsule. After that Na2SO4 added to make the intermediate material. Reactive trichromatic recipe added as a dye mixture. To adjust the alkalinity and pH we added soda and Tween 80 mixture. All of the application has been made at 45 degrees while mixing for 10 min after each ingredient have been added. |

Table 1: Material & Method

Color Change;

Most of the results are in the reasonable area while being under 1. Mauve, purple and power blue results show us that they are well below 1 and nearly identical. All of the colors are acceptable as a microcapsule.

| Color | Production Process | Explanation |
|------------|---------------------|-------------|
| Light Grey | Conventional Dyeing | 0.87 |
| Light Grey | Microcapsule | |
| Dark Brown | Conventional Dyeing | 0.71 |
| Dark Brown | Microcapsule | |
| Mauve | Conventional Dyeing | 0.49 |
| Mauve | Microcapsule | |
| Purple | Conventional Dyeing | 0.53 |
| Purple | Microcapsule | |
| Power Blue | Conventional Dyeing | 0.49 |
| Power Blue | Microcapsule | |
| Mustard | Conventional Dyeing | 0.72 |
| Mustard | Microcapsule | |

Table 2: Color Change



Picture 1: Microcapsüle Machine

Results

Table 3: Washing Fastness

| Color | Production Process | Washing Fastness | | | | | |
|------------|---------------------|------------------|---------|-----------|-----------|--------|---------|
| | | Wool | Acrylic | Polyester | Polyamide | Cotton | Acetate |
| Light Grey | Conventional Dyeing | 4/5 | 4/5 | 4/5 | 4/5 | 4 | 4/5 |
| Light Grey | Microcapsule | 4/5 | 4/5 | 4/5 | 4/5 | 3/4 | 4/5 |
| Dark Brown | Conventional Dyeing | 4/5 | 4/5 | 4/5 | 4/5 | 4 | 4/5 |
| Dark Brown | Microcapsule | 4/5 | 4/5 | 4/5 | 4/5 | 3/4 | 4/5 |
| Mauve | Conventional Dyeing | 4/5 | 4/5 | 4/5 | 4/5 | 4 | 4/5 |
| Mauve | Microcapsule | 4/5 | 4/5 | 4/5 | 4/5 | 3/4 | 4/5 |

WASHING FASTNESS;

Washing fastness results shows us that there is a slight decrease in staining performance with cotton, other than that the results are identical and well in the acceptable area. Color change for all dyeings resulted as 4/5.

Table 4: Washing Fastness

| Color | Production Process | Washing Fastness | | | | | |
|------------|---------------------|------------------|---------|-----------|-----------|--------|---------|
| | | Wool | Acrylic | Polyester | Polyamide | Cotton | Acetate |
| Purple | Conventional Dyeing | 4/5 | 4/5 | 4/5 | 4/5 | 3/4 | 4/5 |
| Purple | Microcapsule | 4/5 | 4/5 | 4/5 | 4/5 | 3/4 | 4/5 |
| Power Blue | Conventional Dyeing | 4/5 | 4/5 | 4/5 | 4/5 | 3/4 | 4/5 |
| Power Blue | Microcapsule | 4/5 | 4/5 | 4/5 | 4/5 | 3/4 | 4/5 |
| Mustard | Conventional Dyeing | 4/5 | 4/5 | 4/5 | 4/5 | 4 | 4/5 |
| Mustard | Microcapsule | 4/5 | 4/5 | 4/5 | 4/5 | 3/4 | 4/5 |

WASHING FASTNESS;

Washing fastness results shows us that there is a slight decrease in staining performance with cotton, other than that the results are identical and well in the acceptable area. Color change for all dyeings resulted as 4/5.

Table 5: Color Fastness to Rubbing

| Color | Production Process | Rubbing Fastness | | Color | Production Process | Rubbing Fastness | |
|------------|---------------------|------------------|-----|------------|---------------------|------------------|-----|
| | | Dry | Wet | | | Dry | Wet |
| Light Grey | Conventional Dyeing | 4/5 | 4/5 | Purple | Conventional Dyeing | 4/5 | 4/5 |
| Light Grey | Microcapsule | 4/5 | 4/5 | Purple | Microcapsule | 4/5 | 4/5 |
| Dark Brown | Conventional Dyeing | 4/5 | 4/5 | Power Blue | Conventional Dyeing | 4/5 | 4/5 |
| Dark Brown | Microcapsule | 4/5 | 4/5 | Power Blue | Microcapsule | 4/5 | 4/5 |
| Mauve | Conventional Dyeing | 4/5 | 4/5 | Mustard | Conventional Dyeing | 4/5 | 4/5 |
| Mauve | Microcapsule | 4/5 | 4/5 | Mustard | Microcapsule | 4/5 | 4/5 |

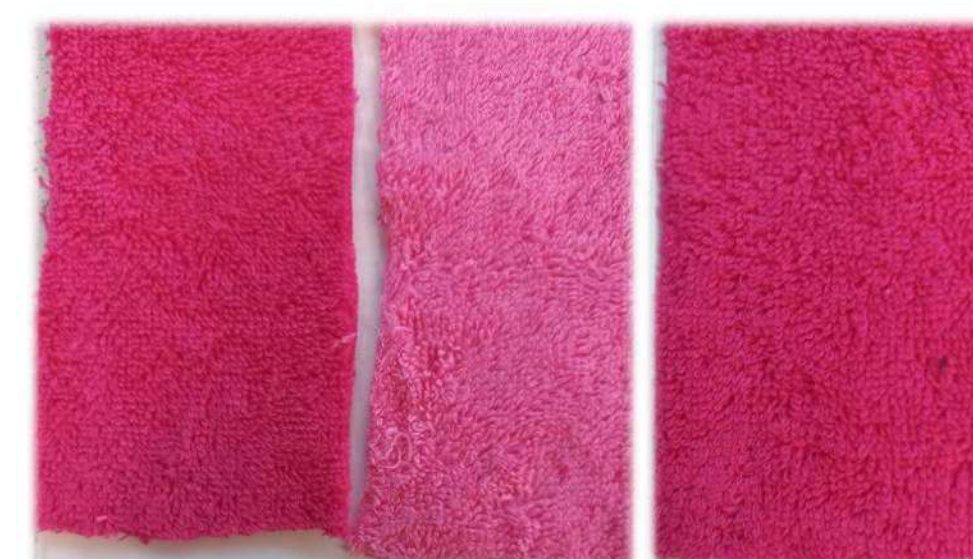
COLOR FASTNESS TO RUBBING;

Results show us nearly perfect scores. All of the colors that undergo the test for both conventional and microcapsule is identical. This shows us that the microcapsules are very well exhausted into the fiber.

Discussion

- The samples have been tested according to washing fastness, color fastness to rubbing and their color change (DE) by a spectrophotometer. According to the results for color change with micro capsules we have all the results under 1, which is acceptable and for mauve, purple and power blue below 0.5 value which is nearly identical with the original sample. For washing fastness, the results are identical only showing a slight reduction in cotton for microcapsules which stays in a reasonable area for washing fastness. Lastly for color fastness to rubbing it shows us identical and nearly perfect results.
- The results show us that there is a potential for work and more colors and recipes could be tried. But the potential shows us that the microcapsules could give us a more sustainable method for dyeing and there could be more growing potential.
- At the same time; an oral presentation was made together with Istanbul Technical University at the RDCONF23 International Research-Development and Design Conference 2023 Orclver Research and Science Group's annual conference.
- The project output has been protected by Patent Application and Patent registration is pending by the Turkish Patent and Trademark Office. Patent Application Number: 2023/008268.

Photos of Samples;





Investigation of Mechanical Properties of Polycarbonate/ASA/Walnut Shell Composites

Aysu ÇAVUŞOĞLU^{a,*}, Tuana ORHUN^a, Yasemin BALÇIK TAMER^b, Harun SEPETÇİOĞLU^c, İdris KARAGÖZ^b

^aPolymer Materials Engineering, Institute of Graduate Studies, Yalova University, 77200 Yalova, Türkiye.

^bPolymer Materials Engineering, Faculty of Engineering, Yalova University, 77200 Yalova, Türkiye.

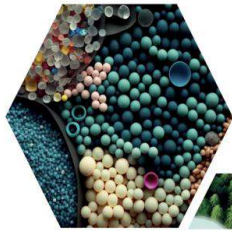
^cMetallurgy and Materials Engineering, Faculty of Engineering, Selcuk University, 422250, Türkiye

*Corresponding author: aysucvsoglu@gmail.com

ABSTRACT

In this study, different polymer composites were prepared by incorporating acrylonitrile-styrene-acrylate (ASA) and walnut shell (WS) fillers into a polycarbonate (PC) matrix. The PC content was kept constant at 80 wt% across all formulations, while ASA and WS ratios were varied (20%, 15-5%, 10-10%, and 5-15%, respectively). The samples prepared were subjected to tensile and flexural tests to evaluate their mechanical performances. The neat PC sample exhibited a tensile strength of 58.7 MPa and a flexural strength of 495.7 MPa, while the neat ASA sample showed 42.2 MPa and 353.9 MPa, respectively. The PC80ASA20 composite achieved a tensile strength of 57.7 MPa and a flexural strength of 501.1 MPa, showing mechanical properties close to neat PC. As the walnut shell content increased, an enhancement in elastic modulus was observed, whereas tensile strength and elongation at break decreased significantly. Particularly, in the PC80ASA05WS15 sample containing 15% WS, the elastic modulus increased to 1313.53 MPa; however, the tensile strength dropped to 23.6 MPa, and elongation at break decreased to 1.98%. The results demonstrate that walnut shell reinforcement can effectively improve the stiffness properties of PC/ASA composites, but at the expense of ductility and strength. Therefore, these biocomposites show potential for applications where high stiffness and dimensional stability are prioritized.

Keywords: Polycarbonate; ASA; Walnut Shell; Biocomposite; Mechanical Properties



16 ULUSLARARASI
LİF VE POLİMER
ARAŞTIRMALARI
SEMPOZYUMU

16th INTERNATIONAL FIBER AND POLYMER RESEARCH SYMPOSIUM

Sürdürülebilir ve İşlevsel Lif ve Polimerler
Sustainable and Functional Fibers & Polymers



9-10 Mayıs
May 2025

İstanbul Teknik Üniversitesi
Gümüşsuyu Prof. Dr. Necmettin Erbakan Yerleşkesi
İstanbul Technical University
Gumussuyu Prof. Dr. Necmettin Erbakan Campus

Eco-Friendly ASA Composites Reinforced with Walnut Shell as a Sustainable Filler

Aysu ÇAVUŞOĞLU^a, Tuana ORHUN^a, Harun SEPETÇİOĞLU^b, İdris KARAGÖZ^c Yasemin BALÇIK TAMER^c

^aPolymer Materials Engineering, Institute of Graduate Studies, Yalova University, 77200 Yalova, Türkiye

^bMetallurgy and Materials Engineering, Selcuk University, 422250, Türkiye

^cPolymer Materials Engineering, Yalova University, 77200 Yalova, Türkiye.

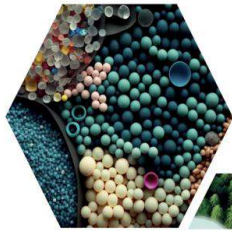
*Corresponding author: yasemin.tamer@yalova.edu.tr

ABSTRACT

Acrylonitrile styrene acrylate (ASA) is an engineering thermoplastic that draws attention with its high UV resistance, superior resistance to atmospheric conditions and mechanical performance. While maintaining ABS-like impact resistance and processability properties, ASA offers long-term resistance to outdoor environmental effects, making it an ideal material especially for automotive, construction, and outdoor applications. However, the petrochemical origin of ASA poses significant challenges to environmental sustainability. Reinforcing the ASA matrix with natural materials emerges as a promising strategy to enhance its mechanical, thermal, and physical properties, and also reduce the production costs and promote eco-friendly sustainability. In this study, it was aimed to develop environmentally friendly composites by adding walnut shell (WS) powder, an agricultural and food industry waste, to the ASA matrix as a natural filler material. Walnut shell is well compatible with polymer matrices and has the potential to increase mechanical performance, due to its high lignocellulosic structure.

In this study, walnut shell containing ASA composites were prepared by using melt blending technique. WS powder was added to ASA at different ratios (5%, 10%, 15% and 20%) and the mechanical, thermal and morphological properties of the resulting composites were characterized, and the effect of WS ratio on the properties of ASA composites was determined. In addition, the effect of filler addition on the physical properties of ASA such as time-dependent water absorption, density and color change was investigated to comprehensively evaluate the potential of walnut shell-filled ASA composites as sustainable material alternatives

Keywords: Acrylonitrile styrene acrylate; walnut shell powder; sustainable composites; natural fillers



16 ULUSLARARASI
LİF VE POLİMER
ARAŞTIRMALARI
SEMPOZYUMU

16th INTERNATIONAL FIBER AND POLYMER RESEARCH SYMPOSIUM

Sürdürülebilir ve İşlevsel Lif ve Polimerler
Sustainable and Functional Fibers & Polymers



9-10 Mayıs
May 2025

İstanbul Teknik Üniversitesi
Gümüşsuyu Prof. Dr. Necmettin Erbakan Yerleşkesi
İstanbul Technical University
Gumussuyu Prof. Dr. Necmettin Erbakan Campus



Self-Adaptive Outlier Pruning and Monte-Carlo Validation in Hydrogel Swelling Prediction

Ugur Ozveren*, Burçe Peker, Dicle Eren, İdil Sena Bayrak

Department of Chemical Engineering, Marmara University, Istanbul, Turkey.

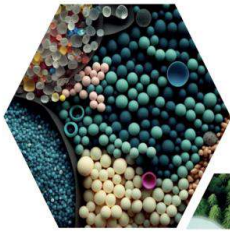
**Corresponding author: ugur.ozveren@marmara.edu.tr*

ABSTRACT

A Monte-Carlo cross-validated artificial neural network (ANN) was developed to predict the swelling ratio of SA/κ-carrageenan@Fe₃O₄ magnetic hydrogel beads. The data matrix with 802 entries was fed into the modelling pipeline without prior statistical cleaning. Instead, a self-cleaning routine removed observations with a high residual value only when the global coefficient of determination (R^2) increased. Monte Carlo validation regenerated an 80 : 20 hold-out split for 5 000 independent random seeds. Each split trained a 6–48–64–96–32–1 ANN for 50 epochs using the Levenberg–Marquardt optimizer and generated paired train/test R^2 values whose empirical distribution characterised the model variance under sampling uncertainty. Kernel density estimation of these 5 000 R^2 pairs yielded a tight bivariate mode at (0.88, 0.90) and a 95% confidence ellipse spanning ± 0.01 R^2 , demonstrating dramatic suppression of volatility caused by partitioning. After convergence of the residual splitting loop, the representative model achieved a test $R^2 = 0.912$ together with a train $R^2 = 0.904$.

Correlation heat maps indicated that the correlations between attributes in the training and test groupings remained constant. The study demonstrates that Monte Carlo cross-validation is a useful method for quantifying and reducing hold-out uncertainty in small to medium-sized experimental material data. Combined with residual-based self-cleaning, the protocol provides reproducible AI models with high fidelity suitable for the rational design of stimuli-responsive hydrogels and similar complex soft matter systems.

Keywords: Monte-Carlo cross-validation; artificial neural network; swelling prediction; magnetic hydrogel



16

ULUSLARARASI LİF VE POLİMER ARAŞTIRMALARI SEMPOZYUMU

16th INTERNATIONAL FIBER AND POLYMER RESEARCH SYMPOSIUM

Sürdürülebilir ve İşlevsel Lif ve Polimerler
Sustainable and Functional Fibers & Polymers



9-10 Mayıs
May 2025

İstanbul Teknik Üniversitesi
Gümüşsuyu Prof. Dr. Necmettin Erbakan Yerleşkesi
İstanbul Technical University
Gumussuyu Prof. Dr. Necmettin Erbakan Campus

Kablo Uygulamaları İçin Huntit-Hidromanyezit İçeren Kompozitlerin Alev Geciktirici ve Mekanik Performanslarının İncelenmesi

Tuğba YILMAZ^{a,b,*}, Erdinç DOĞANCI^{b,c}

^aVatan Kablo Ar-Ge Merkezi, 59870 Tekirdağ, Türkiye

^bFen Bilimleri Enstitüsü, Polimer Bilimi ve Teknolojisi, Kocaeli Üniversitesi, 41001 Kocaeli, Türkiye

^cKimya ve Kimyasal İşleme Teknolojileri Bölümü, Kocaeli Üniversitesi, 41001 Kocaeli, Türkiye

*Sorumlu Yazar: tugba.yilmaz@vatan.com.tr

ÖZET

Elektrik kabloları, enerji iletimi ve iletişim sistemlerinin güvenli ve verimli çalışabilmesi için kritik bir rol oynar. Bu kabloların dış kılıf malzemeleri, mekanik dayanım sağlamanın yanı sıra yangın güvenliği açısından belirli standartları karşılamak zorundadır. Yangın dayanımı, CPR (Construction Products Regulation) gibi global güvenlik standartları tarafından zorunlu kılınan bir gerekliliktir. Yangın sırasında kabloların alev yayılımını engellemesi, ısı açığa çıkışını azaltması ve toksik gaz üretimini sınırlaması, hem bireysel güvenliği hem de altyapıların işlevselliğini korumak açısından büyük önem taşır. Bu sebeple, çevre dostu ve sürdürülebilir malzemelerin kullanımı, elektrik kablolarının dış kılıf malzemeleri için kritik bir özellik haline gelmiştir. Bu çalışma, halojen içermeyen mineral bazlı alev geciktirici bileşenlerin (alüminyum hidroksit, magnezyum hidroksit, huntit, hidromanyezit) polimer kompozitlere entegrasyonunu inceleyerek, bu kompozitlerin elektrik kablolarının dış kılıf malzemesi olarak potansiyel kullanımını değerlendirmektedir. Mineral bileşenler, belirli oranlarda polimerlerle karıştırılarak granül formda hazırlanmış ve ekstrüzyon işlemi ile kablo dış kılıfına dönüştürülmüştür. Bu işlem, malzemenin homojen bir şekilde karışmasını ve kablo kılıfının gerekli mekanik ve alev geciktirici özelliklere sahip olmasını sağlamaktadır. Kompozitlerin alev geciktirici özellikleri, termogravimetrik analiz (TGA), diferansiyel taramalı kalorimetri (DSC) ve limit oksijen indeksi (LOI) testleri ile değerlendirilmiştir. Ayrıca, CPR standardı (EN 50399) çerçevesinde, alev yayılması, ısı açığa çıkışı ve duman üretimi gibi yangın anındaki davranışlar da test edilmiştir. Sonuçlar, mineral bazlı bileşenlerin entegrasyonu ile kompozitlerin yangına karşı dayanıklılığının arttığını ve mekanik özelliklerinin kabul edilebilir sınırlar içinde kaldığını göstermektedir. Bu bulgular, çevre dostu ve sürdürülebilir kablo dış kılıf malzemeleri geliştirilmesi açısından yüksek potansiyel taşımaktadır.

Anahtar Kelimeler: LOI; alev geciktiricilik; mineral bazlı katkıları; huntit-hidromanyezit; elektrik kabloları

Investigation of Flame Retardant and Mechanical Properties of Huntite-Hydromagnesite Containing Composites for Cable Applications

ABSTRACT

Electric cables play a critical role in ensuring the safe and efficient operation of energy transmission and communication systems. The outer sheath materials of these cables must not only provide mechanical strength but also meet specific standards for fire safety. Fire resistance, as mandated by global safety standards such as the Construction Products Regulation (CPR), is a crucial requirement. During a fire, it is essential that cables prevent flame spread, reduce heat release, and limit the production of toxic gases to safeguard both individual safety and the functional sustainability of infrastructures. Therefore, the use of environmentally friendly and sustainable materials has become a key feature for cable sheath applications. This study investigates the integration of halogen-free, mineral-based flame retardant components (aluminum hydroxide, magnesium hydroxide, huntite, hydromagnesite) into polymer composites, evaluating their potential use as outer sheath materials for electric cables. The mineral components are blended with polymers in specific ratios to form granules, which are then transformed into the cable sheath through an extrusion process. This procedure ensures the homogeneous mixing of the material and the achievement of the required mechanical and flame retardant properties for the cable sheath. The flame-retardant properties of the composites were evaluated using thermogravimetric analysis (TGA), differential scanning calorimetry (DSC), and the limit oxygen index (LOI) tests. Additionally, fire performance behaviors such as flame spread, heat release, and smoke production were tested according to the CPR standard (EN 50399). The results show that the integration of mineral-based flame retardant components significantly improves the fire resistance of the composites, while their mechanical properties remain within acceptable limits. These findings demonstrate the high potential of halogen-free mineral components for developing environmentally friendly and sustainable cable sheath materials.

Keywords: flame retardancy; mineral-based additives; huntite-hydromagnesite; electric cables

16th International Fiber and Polymer Research Symposium (16th ULPAS) 9-10 May, 2025,

Istanbul technical University (ITU), Istanbul, Türkiye

İç Mekan Havasını Arındıran Fonksiyonel Döşemelik Kumaş Geliştirmesi

Hakan Altuncu , Berrin Ünür

Kadifeteks Mensucat San. A.Ş.

hakan.altuncu@kadifeteks.com



KADİFETEK

Mensucat Sanayi A.Ş.

Proje Özeti

Her yıl, antropojenik hava kirliliği, çeşitli solunum yolu hastalıkları nedeniyle 7 milyon insanın ölmesine neden oluyor ve iç mekan hava kalite insanların sağlığı üzerinde önemli bir etkiye sahiptir. COVID-19 salgınının ortaya çıkmasıyla birlikte temiz hava ve iyi iç mekan hava kalitesi en önemli hale geldi.

Endüstrileşmiş ülkelerde, insanlar zamanlarının %70-90'ını kapalı alanlarda (ev, ofis, okul, otomobil, uçak, fabrika vb.) geçirmektedir, bu süreç içerisinde kapalı ortamın doğası kişilerin sağlığını, hayat kalitesini ve üretkenliğini önemli ölçüde etkilemektedir. İç hava kirliliği, gaz veya parçacık formundaki kirlenmelerin iç hava atmosferini değiştirerek insan sağlığı ve konforunu olumsuz yönde etkilemesi olarak tanımlanabilir. İç hava kalitesi (İHK) ise genel anlamda; iç ortamda solunan havanın ne kadar 'iyi' ya da ne kadar 'kötü' olduğunu gösteren bir ölçüttür. İç ortamda bulunan kirlenmeler birçok sağlık problemlerine ve ölümlere neden olabilmektedir. Her kirlenme tipinin kendine özgü yapısından kaynaklanan farklı zararları olmakla birlikte en yaygın görülen sağlık etkileri; konjunktival tahriş, burun ve boğazda tahriş; baş ağrısı, deride alerjik reaksiyonlar, nefes darlığı, koordinasyon kaybı, bulantı; burun kanaması, yorgunluk, halsizlik, akciğer, böbrek ve merkezi sinir sisteminde hasardır. Bazı organik maddeler hayvanlarda, bazı maddeler de insanlarda kansere neden olabilmektedir.

İç hava kalitesi termal konfor, havalandırma, iç mekândaki kirlenmeler ve malzeme emisyonlarıyla yakından ilişkilidir. Isıtma/havalandırma sistemlerinin tasarımı, bina malzemeleri ve mobilyaların seçimi de İHK üzerinde önemli etkilere sahiptir.

İç hava kalitesini bozan ve kirlilik oluşturan zararlı maddeleri ancak çeşitli gruplar altında toplayarak tanımlamak mümkündür. İç hava kalitesinin bozan kirlenme grupları şöyle sıralanabilir.

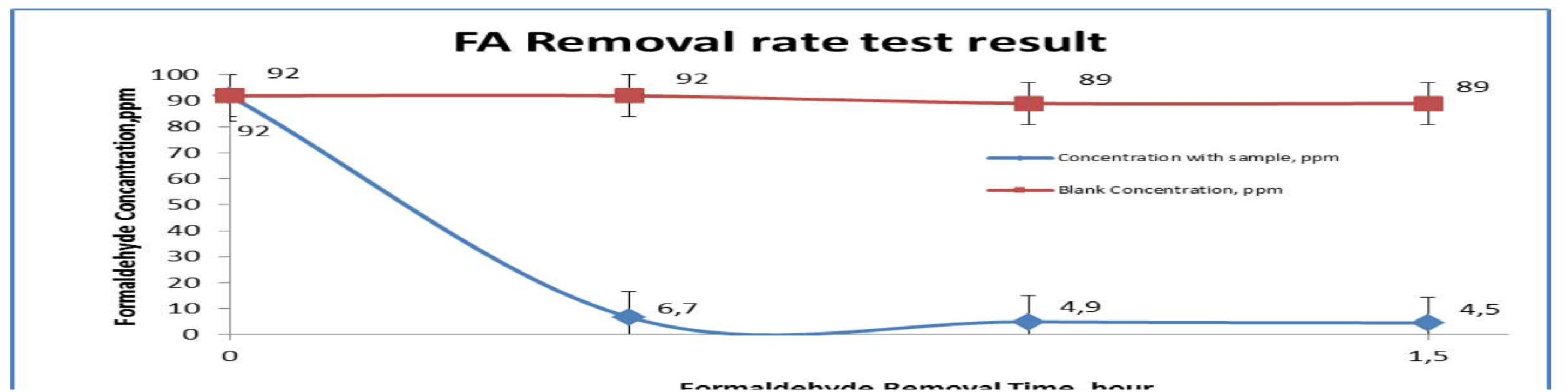
1. Solunan havadaki karbondioksit oranı (İnsanların ve canlıların solunumları ve yanma kaynaklıdır.)
2. Koku (İnsan kaynaklıdır.)
3. Mikroorganizmalar (çevre ve insan kaynaklıdır.)
4. Nem (Çevre ve pişirme gibi insan kaynaklıdır.)
5. Radon Gazı (Toprak kaynaklıdır.)
6. Organik buharlar (Kullanılan eşya ve bina elemanları kaynaklıdır.)
7. Toz (Çevre ve kullanılan eşya kaynaklıdır.)
8. Alerjin maddeler ve canlılar (Çevre kaynaklıdır.)
9. Sigara dumanı (İnsan kaynaklıdır.)
10. Diğer kaynaklar (Yukarıda sayılanların dışında hava kalitesine etki eden daha pek çok faktör vardır. Bunlar içinde elektronik kirlenmeden, radyasyona kadar pek çok faktör sayılabilir.

Sonuçlar

Kaplama denemelerinde herhangi bir problemle karşılaşılması. Testler ve yeterlilikler standartları karşıladı. Testleri başarılı geldi. Diğer teknolojilerle birlikte çalıştığımızda, diğer teknolojilerin etkinliğini azalttığı anlaşıldı. 3m² muamele edilmiş dokuma kumaşın 30m³ 'lük odadaki uçucu organik bileşiklerin uzaklaştırılması;

Kumaş numunesi 200g/m², özel hazırlanmış kimyasal ile muamele edilir.

3m² dokuma kumaş 30m³ 'lük bir kapalı iç ortam havasını 1,2s içinde uçucu organik bileşiklerden temizler. Test şartları: Gaz geçirmez 30 L cam kavanoz kullanılmıştır. Bir enjeksiyon bloğunda 160°C'ye ısıtılan 10 µl %37 (1009,9 g/L) formaldehit solüsyonu buharlaştırıldı. Cam-kavanoz içine enjekte edilmiştir.



| Removal Time, hours | 0 | 0,5 | 1 | 1,5 |
|------------------------------------------------------|--------|-----|-----|-----|
| Concentration with sample, ppm | 92 | 6,7 | 4,9 | 4,5 |
| Blank Concentration, ppm | 92 | 92 | 89 | 89 |
| Initial concentration, ppm | 92 | | | |
| Sample area, m ² | 0,04 | | | |
| Removal rate, FA (ppm) / m ² fabric /hour | 1458,3 | | | |

| AMONYAK GAZI | | |
|--------------------------|------------------------------------------------------------------------------------------------------------------------------------------------------------|---------------------------------------------------------------------------------------|
| Konsantrasyon Seviyeleri | İnsan Üzerindeki Etkileri | Süreler ve Sonuçları |
| 25 ppm | Birçok insan tarafından kokusu alınabilir. | 8 saatten fazla sürede bir maruziyet olmamalıdır. |
| 100 ppm | Gözlerde yanma, kaşıntı oluşabilir. Göz nezlesi olabilir. Göz kapaklarında şişlik oluşabilir. Gözlerde sulanma olabilir. Dudaklar kuruyabilir. | Kısa süreli maruziyet limitinin üzerinde bir seviyedir, uzun süre maruz kalmamalıdır. |
| 400-700 ppm | Ağız içinde ve boğazda yanma oluşabilir. Gözlerde ve solunum yolları tahriş olabilir. | 1 saate kadar maruz kalınması durumunda ciddi problemler oluşur. |
| 1.700 ppm | Öksürük ve solunum yolu problemleri oluşabilir. | Yarım saat ve üzerindeki bir süre maruz kalınması durumunda ölüme sonuçlanabilir. |
| 2.000-3.000 ppm | - | 15 dakikadan fazla maruz kalındığında ölüme sonuçlanabilir. |
| 5.000-10.000 ppm | - | Birkaç dakika içinde ölüme sonuçlanabilir. |

Deneyisel

Yapılan çalışmada yün , dokuma polyester numune kumaşına , 40gr/l özel hazırlanmış kimyasal uygulandı. Numune kumaşları teste verildi.

Test Numunesi: yün , dokuma polyester numune kumaş

Hava temizleme uygulamalarının Formaldehit içeriğine karşı test sonuçları:

Yapılan testlerin hesaplanması ve yorumlanması:

3m² muamele edilmiş dokuma kumaşın 30m³ 'lük odadaki uçucu organik bileşiklerin uzaklaştırılması;

Kumaş numunesi 200g/m², 40gr/l özel hazırlanmış kimyasal ile muamele edilir.

1m² muamele edilmiş dokuma kumaşın 1 saat içinde uzaklaştırdığı uçucu organik bileşik miktarı: 121,21 mg/(m³*h)

3 m² [3.6 yd²] muamele edilmiş dokuma kumaş 220kg plywood malzemeli 30m³ oda için elverişlidir.

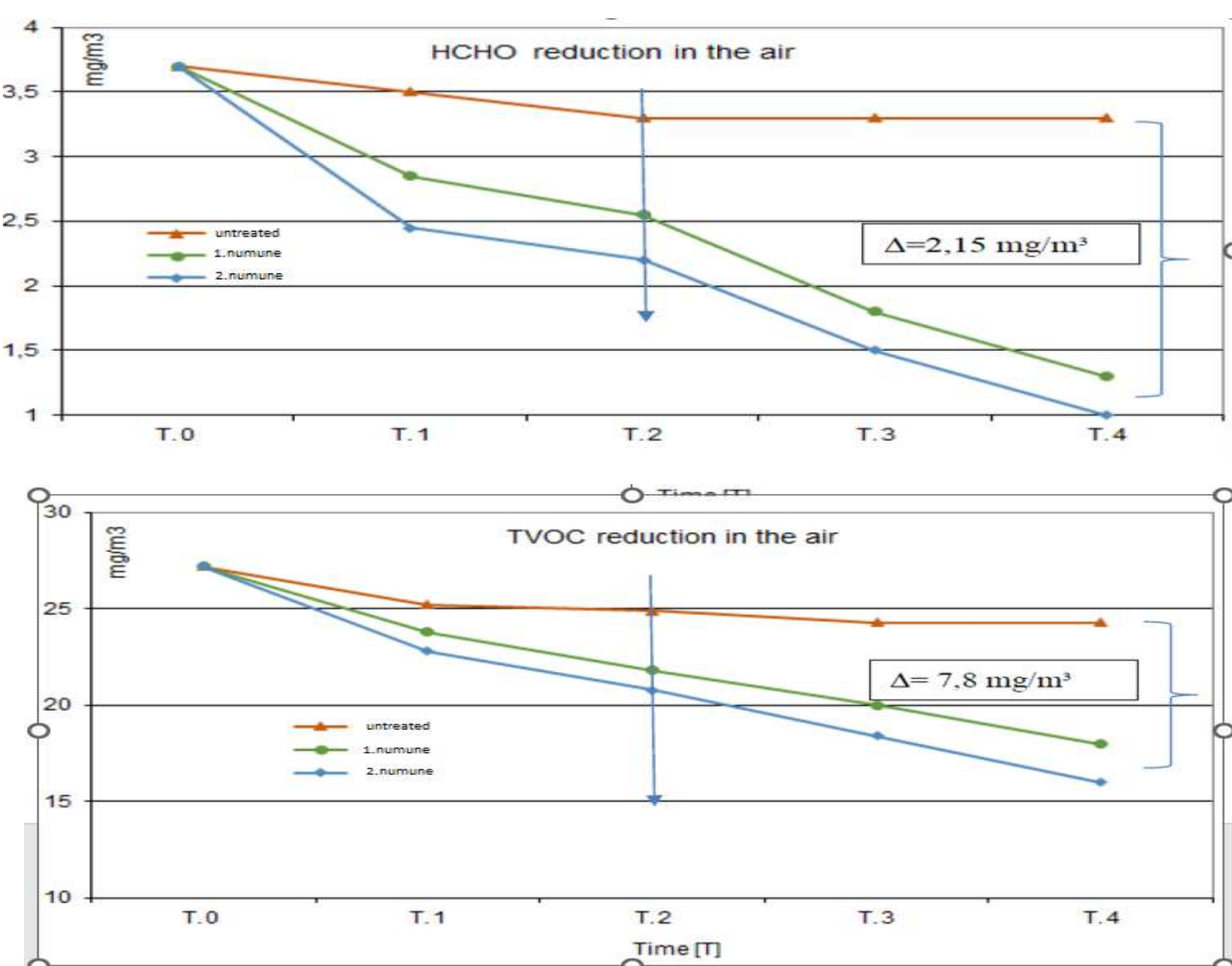
30m³ oda için kullanılan plywood malzemesi = 220kg

Tahmini toplam bir oda için uçucu organik bileşik miktarı:

= 220 kg x 0.002 mg/gr = 440 mg

=440 mg / 121,21 mg/m³/h / 3 m²= 1,2 h

3m² dokuma kumaş 30m³ 'lük bir kapalı iç ortam havasını 1,2s içinde uçucu organik bileşiklerden temizler.



Tartışma

Kapalı bir bina içi atmosferine ait solunan havanın kalitesini, birden fazla ve çok değişik tipte kirlenme bozabilmektedir. Durağan havanın bu kirlenmeleri biriktirdiği ve ortam atmosferini yoğunlaştırdığı bir gerçektir. Temiz hava döngüsü bu nedenle önem kazanmaktadır. Son yıllarda, genelde iç ortamda yaşayan kişilerin sağlıkları ile ilgili bir takım yakınmalar söz konusu olmuştur. Bu yakınmalar, enerjinin korunması amacıyla ısı yalıtımının gerçekleştirildiği ve buna bağlı olarak iç ortam hava sirkülasyonunun en az düzeye indiği, yetersiz havalandırmanın yapıldığı, duvardan duvara halı, duvar kaplamasında kullanılan kumaşlar gibi tekstil ürünü materyallerin fazlası ile kullanıldığı, dış ortama açılmayan pencerelerin bulunduğu ve klima cihazlarının kullanıldığı iç ortamlarda çeşitli reaksiyonlar şeklinde kendisini göstermektedir. İç havada bulunan kirlenmelerin sağlık üzerine etkisi, insanlarla karşılaştıktan hemen sonra veya yıllar sonra ortaya çıkabilmektedir. Eğer etken belirlenmişse, bunun yok edilmesiyle ve tedaviyle bu rahatsızlıklar giderilebilir. Hava kirliliğinin büyüme çağındaki çocukların büyüme oranları ile doğduktan sonra yaşadıkları yerdeki kirlilik düzeyi arasında bir bağlantı olduğu sonucuna varılmıştır. Uzun yıllar etkiye maruz kalındıktan sonra veya etkinin tekrarlanan periyotlarından sonra ise bazı solunum sistemi ve kalp rahatsızlıkları, organ kanserleri ortaya çıkabilmekte, ileri derecede zayıflık, hatta ölümlere bile rastlanmaktadır.

Hava kirliliğine karşı alınacak önlemlerin olmaz ise olmazı; hava kirliliğinin bağımsız/özerk bir kuruluş tarafından izlenmesidir. Sonuçlar, günlük olarak tıpkı meteoroloji raporları gibi kitle iletişim araçları tarafından, toplumun bilgisine sunulmalıdır. Başka bir söylemle, toplumun bilgilendirilmesi yalnızca bilgilendirme eşiği aşılmıyca değil sürekli olarak yapılmalıdır. Böylece bir yandan toplumda farkındalık yaratılırken öte yandan da toplum bilinçlendirilmelidir.

Referanslar

1. <https://dergipark.org.tr/tr/download/article-file/265901>
2. <https://dergipark.org.tr/tr/download/article-file/3548696>
3. https://acikbilim.yok.gov.tr/bitstream/handle/20.500.12812/676050/yokAcikBilim_9014079.pdf?sequence=-1&isAllowed=y
4. <https://www.sciencedirect.com/science/article/abs/pii/S2213343723017852>



16 ULUSLARARASI
LİF VE POLİMER
ARAŞTIRMALARI
SEMPOZYUMU
16th INTERNATIONAL FIBER AND POLYMER RESEARCH SYMPOSIUM
Sürdürülebilir ve İşlevsel Lif ve Polimerler
Sustainable and Functional Fibers & Polymers

9-10 Mayıs
May 2025
İstanbul Teknik Üniversitesi
Gümüşsuyu Prof. Dr. Necmettin Erbakan Yerleşkesi
Istanbul Technical University
Gumussuyu Prof. Dr. Necmettin Erbakan Campus



16th International Fiber and Polymer Research Symposium (16th ULPAS) 9-10 May, 2025,

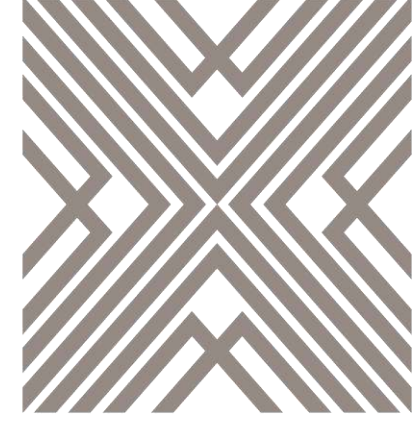
Istanbul Technical University (ITU), Istanbul, Türkiye

YENİ TRENDLERE UYGUN ANTİVİRAL, ANTİBAKTERİYEL ETKİ SAĞLAYAN OTOMOTİV DÖŞEMELİK KUMAŞ GELİŞTİRİLMESİ

Osman TÜRKMEN, Sümeyra OĞUZ

Kadifeteks Mensucat San. A.Ş.

osman.turkmen@kadifeteks.com



KADİFETEK S
Mensucat Sanayi A.Ş.

Proje Özeti

Bu proje, otomotiv sektöründe kullanılacak döşemelik kumaşların hem estetik hem de fonksiyonel açıdan yenilikçi bir yaklaşımla geliştirilmesini hedeflemiştir. Projenin ana amacı, uluslararası standartlara uygun, antiviral özellikli, sıvı geçirmez ve nefes alabilir kumaşların, güncel moda ve renk trendleriyle uyumlu şekilde tasarlanması ve üretilmesidir. Covid-19 pandemisiyle birlikte artan hijyen ihtiyacı, otomotiv iç mekanlarında kullanılan tekstil ürünlerinde antiviral özelliklerin önemini artırmıştır. Proje kapsamında, moda ve renk trendleri analiz edilmiş, antiviral tekstil teknolojileri araştırılmış, farklı iplik ve örgü teknikleriyle çeşitli kumaş varyantları tasarlanmış ve üretilmiştir. Ayrıca, geliştirilen kumaşların performans ve dayanıklılık testleri yapılmış, antiviral kimyasal uygulamalarının etkileri değerlendirilmiştir. Sonuç olarak, hem kullanıcı sağlığını koruyan hem de estetik açıdan yenilikçi kumaşlar sektöre kazandırılmıştır.

Proje Konusunu Belirleyen İhtiyaçlar

- Otomotiv kumaşlarının uluslararası standartlara ve yanmazlık şartlarına uygun olması
- Müşteriler, moda ve yeni renklere uygun, estetik kumaşlar istemesi
- Sıvı geçirmez, nefes alabilen ve konforlu kumaşlar tercih edilmesi
- Farklı renk ve desen seçenekleriyle müşteri memnuniyeti sağlanması

Proje Hedefleri:

- Moda ve trendlere uygun, estetik ve yenilikçi kumaşlar tasarlamak.
- Müşteri isteklerine göre renk ve desen seçeneklerini artırmak
- Çevreye duyarlı ve yenilikçi üretim yöntemleri kullanmak

Deneyisel

Kimyasal Temini ve Uygulaması

Tekstilde kullanılan antiviral ürünler kimyasal yapıları, etkileri, dayanıklılıkları ve fiyatları gibi özelliklerine göre çeşitlilik göstermektedir. Son yıllarda tekstil alanında kullanılabilecek pek çok antiviral ürün geliştirilmiştir.

Projede, antiviral ve antibakteriyel özellik kazandırmak amacıyla uygun kimyasal firmalardan temin edilen kimyasallar laboratuvarda test edilerek etkin olanlar seçilmiş ve üretimde kullanılmıştır. Ayrıca, kumaşlara sıvı geçirmezlik ve nefes alabilirlik kazandırmak için poliüretan, PTFE, polyester ve poliamid gibi malzemelerden üretilen membranlar laminasyon yöntemiyle uygulanmış, en iyi performans gösterenler tercih edilmiştir. Böylece, hem koruyucu hem de konforlu, yenilikçi kumaşlar geliştirilmiştir. Bazı sentetik lif esaslı antiviral liflerin ticari isimleri ve üreticileri Tablo 1'de verilmiştir. Sektörde en çok tercih edilen bazı antiviral maddeler tablo 2'de sunulmuştur.

| Lif Cinsi | Üretici Firma | Ticari İsmi |
|------------------|---------------|-----------------------|
| Poliester | Trevira | Trevira Bioactive |
| | Montefibre | Terital sanewear |
| | Brilen | Bacterbril |
| Poliakrilonitril | Dupont | Coolmax Fresh FX |
| | Accordis | Amicor |
| | Sterling | Biofresh |
| Poliamid | Kaneba | Livefresh |
| | R-stat | R-stat |
| | Nylstar | Meryl Skinlife |
| Polipropilen | Asota | Asota AM Sanitary |
| Polivinilklorid | Rhovyl | Rhovyls Antibacterial |
| Rejenere Selüloz | Zimmer AG | Sea Cell Activated |
| Asetat | Novaceta | Silfresh |

Tablo1 : Sentetik Antiviral Lifler

Deneme Üretimlerinin Yapılması

Otomotiv sektörü için yeni döşemelik kumaş tasarımlarında, en çok tercih edilen renk ve desenler seçildikten sonra farklı kumaş türleri ve ipliklerle çeşitli numuneler üretilirdi. Bu numunelere, araç içi hijyen ve güvenliği artırmak amacıyla, bitim işlemlerinde iki farklı kimyasal firmasından temin edilen antiviral ve antibakteriyel ürünler kullanılarak uygulamalar yapıldı. Saten, kadife ve çözümlü örme otomotiv döşemelik kumaşlarının her biri, uygun kimyasallar ile kaplanarak veya emdirilerek işlendi. Kimyasal uygulama sonrası kumaşlar kurutulup fikse edildi ve böylece koruyucu özelliklerin kalıcı olması sağlandı. Üretilen otomotiv döşemelik kumaşlarının kalite, hijyen ve güvenliğini değerlendirmek için dayanıklılık, renk haslığı, antiviral etki, sıvı geçirmezlik, nefes alabilirlik, yanmazlık ve yıkama sonrası etkinlik gibi çeşitli testler uygulanarak en uygun ürünler seçildi.

Saten, kadife ve çözümlü örme kumaşların her biri laboratuvarda test edildi. Her kumaş türü için gramaj, en, aşınma (abrazyon), tüyleşme (pilling), sürtme ve ışık haslığı, dikiş açma, yırtılma ve kopma mukavemeti gibi temel performans değerleri ölçüldü. Test sonuçları, kumaşların kalite ve dayanıklılığını gösterdi.

Sonuçlar

Saten, kadife ve çözümlü örme (yuvarlak örme) kumaşların her biri, laboratuvar ortamında kapsamlı performans testlerine tabi tutuldu. Her kumaş türü için gramaj, en, aşınma (abrazyon), tüyleşme (pilling), sürtme ve ışık haslığı, dikiş açma, yırtılma ve kopma mukavemeti gibi temel kalite ve dayanıklılık kriterleri ölçüldü.

Saten kumaşlarda 600 g/m² gramaj, 142 cm en, 100.000 devir aşınma dayanımı, 4/5 pilling ve sürtme haslığı, 1689-1165 N kopma mukavemeti gibi yüksek performans değerleri elde edildi. Kadife kumaşlarda ise 515 g/m² gramaj, 150 cm en, 100.000 devir aşınma dayanımı, 4/5 pilling ve sürtme haslığı, 1565-924 N kopma mukavemeti ile hem estetik hem de sağlamlık ön plana çıktı. Çözümlü örme kumaşlarda ise 470 g/m² gramaj, 140 cm en, 60.000 devir aşınma dayanımı, 4/5 pilling ve sürtme haslığı, 500-750 N kopma mukavemeti gibi dengeli ve güvenilir sonuçlar elde edildi.

Tablo1 : Saten kumaşların performans değerleri

| Test Adı | Standart | Sonuç | Değer | Yatay |
|----------------------------------|------------------------------|-------|---------|-------|
| Kumaş En | ISO 3932 | | 142 | |
| Kumaş Gramaj | EN 12127 | | 600 | |
| Hartindale | EN ISO 12947-2 | = | 100,000 | |
| Hartindale 3.000 Devir | EN ISO 20105-A02 | | | |
| Hartindale | IWS TH 112 | = | | |
| Hartindale - Pilling 2.000 Devir | EN ISO 12945-2 | | | |
| Hartindale - Pilling 1.000 Devir | IWS TH 196 | | | |
| Dikiş Açma Testi | EN ISO 13936-2 | 1.8 | 1.8 | |
| Dikiş Açma Testi | IWS TH 117 | | | |
| Yırtılma Mukavemeti | EN ISO 13937-3 | 80 | 50 | |
| Kopma Mukavemeti | EN ISO 13934-1 | 1689 | 1163 | |
| Elongation | % | | | |
| Laminasyon Açılması | EN ISO 13937-2 | | | |
| Sürtme Haslığı | EN ISO 105-X12 (Kuru/Yas) | 4/5 | 4/5 | |
| Yık Haslığı Testi - Avrupa | EN ISO 105-B02 (Grade 6 / 8) | 5 | | |

Tablo2 : Kadife kumaşların performans değerleri

| Test Adı | Standart | Sonuç | Değer | Yatay |
|----------------------------------|------------------------------|-------|---------|-------|
| Kumaş En | ISO 3932 | | 150 | |
| Kumaş Gramaj | EN 12127 | | 515 | |
| Hartindale | EN ISO 12947-2 | = | 100,000 | |
| Hartindale 3.000 Devir | EN ISO 20105-A02 | | 4/5 | |
| Hartindale | IWS TH 112 | = | | |
| Hartindale - Pilling 2.000 Devir | EN ISO 12945-2 | | 4/5 | |
| Hartindale - Pilling 1.000 Devir | IWS TH 196 | | | |
| Dikiş Açma Testi | EN ISO 13936-2 | 1.5 | 1.6 | |
| Dikiş Açma Testi | IWS TH 117 | | | |
| Yırtılma Mukavemeti | EN ISO 13937-3 | 95 | 56 | |
| Kopma Mukavemeti | EN ISO 13934-1 | 1565 | 924 | |
| Elongation | % | | | |
| Laminasyon Açılması | EN ISO 13937-2 | | | |
| Sürtme Haslığı | EN ISO 105-X12 (Kuru/Yas) | 4/5 | 4/5 | |
| Yık Haslığı Testi - Avrupa | EN ISO 105-B02 (Grade 6 / 8) | 5-6 | | |

Tablo3 : Çözümlü Örme performans değerleri

| Test Adı | Standart | Sonuç | Değer | Yatay |
|----------------------------------|---------------------------|-------|--------|-------|
| Kumaş En | ISO 3932 | | 140 | |
| Kumaş Gramaj | EN 12127 | | 470 | |
| Hartindale | EN ISO 12947-2 | = | 60,000 | |
| Hartindale 3.000 Devir | EN ISO 20105-A02 | | 4 | |
| Wyzenbeek | ASTM D4157 | = | | |
| Hartindale - Pilling 2.000 Devir | EN ISO 12945-2 | | 4/5 | |
| Snash Pilling | D3511-99A | | | |
| Farça Testi | Öncesi | | | |
| Farça Testi | D3511-99A | | | |
| Dikiş Açma Testi | EN ISO 13936-2 | 2.5 | 2.2 | |
| Yırtılma Mukavemeti | EN ISO 13937-3 | 45 | 65 | |
| Kopma Mukavemeti | EN ISO 13934-1 | 500 | 750 | |
| Elongation | % | | | |
| Laminasyon Açılması | EN ISO 13937-2 | | | |
| Sürtme Haslığı | EN ISO 105-X12 (Kuru/Yas) | 4/5 | 4/5 | |

Bu testler sayesinde, geliştirilen tüm kumaşların hem kalite hem de dayanıklılık açısından otomotiv sektörünün gereksinimlerini başarıyla karşıladığı kanıtlanmış oldu. Her bir kumaş türü, hem uzun ömürlü kullanım hem de estetik beklentiler açısından güvenle tercih edilebilecek düzeyde performans sergiledi.

Tartışma

- Otomotiv döşemelik kumaşlarda güç tutuşurluk (yanmazlık) özelliklerinin ECE R 118 gibi uluslararası standartlara uygun şekilde kazandırılması, ürünün pazara girişinde önemli bir avantaj sağlamaktadır. Ancak, bu tür kimyasal uygulamaların kumaşın konfor, nefes alabilirlik ve çevre dostu olma gibi diğer kritik özellikleri üzerindeki etkileri dikkatle değerlendirilmelidir.
- Moda ve renk trendlerinin entegrasyonu, müşteri memnuniyetini ve marka değerini artırmakla birlikte, tekstil sektöründe trendlerin hızla değişmesi, üretim süreçlerinde esneklik ve hızlı adaptasyon gerektirmektedir. Bu nedenle, üretim teknolojilerinin ve tedarik zincirinin, değişen taleplere hızlı yanıt verebilecek şekilde yapılandırılması gerekmektedir.
- Yanmazlık sağlayan kimyasalların ve fonksiyonel katkıların, kumaşın dokusuna, yumuşaklığına ve nefes alabilirliğine etkisi, kullanıcı konforu açısından detaylı olarak değerlendirilmelidir. Özellikle otomotiv sektöründe, hem güvenlik hem de konforun bir arada sunulması beklenmektedir.
- Antiviral ve antibakteriyel kimyasalların yıkama dayanımı, uzun ömürlü ve fonksiyonel kumaş üretimi için kritik bir parametredir. Test sonuçları olumlu olsa da, farklı deterjanlar ve yıkama koşulları altında etkinliğin korunup korunmadığı uzun vadeli çalışmalarla desteklenmelidir. Ayrıca, bu kimyasalların insan sağlığı ve çevre üzerindeki potansiyel etkileri de dikkate alınmalıdır.
- Sürdürülebilirlik ve çevre dostu üretim, otomotiv tekstilinde günümüzde önemli bir beklenti haline gelmiştir. Kullanılan kimyasalların çevreye ve insan sağlığına etkileri, geri dönüştürülebilirlik ve karbon ayak izi gibi konular, gelecekteki Ar-Ge çalışmalarında öncelikli olarak ele alınmalıdır.
- Sektördeki hızlı teknolojik gelişmeler, akıllı tekstil uygulamalarının (örneğin sensörlü veya kendini temizleyen kumaşlar) otomotiv döşemeliklerinde de yaygınlaşmasını gündeme getirmektedir. Bu tür yeniliklerin entegrasyonu, hem maliyet hem de üretim süreçleri açısından yeni fırsatlar ve zorluklar yaratmaktadır.
- Müşteri beklentilerinin ve pazar taleplerinin sürekli değişmesi, ürün geliştirme süreçlerinde esnekliği ve inovasyonu zorunlu kılmaktadır. Bu nedenle, müşteri geri bildirimlerinin düzenli olarak toplanması ve ürün tasarımına entegre edilmesi önem taşımaktadır.

Referanslar

- Shahidi, F., & Wiener, K. (2012). Antiviral ve antimikrobiyal tekstil uygulamaları
- Akaydın, B., & Kalkancı, A. (2014). Tekstil sektöründe antiviral maddeler.
- Altınok, S. (2008). Antiviral tekstil ürünlerinde kullanılan maddeler.
- Enhancing the Antimicrobial Activity of a Vinyl-Coated Fabric Product (2024)
- Pilling Resistance of Automotive Upholstery Fabrics (Textile Research Journal, 2021)
- Color Fastness of Automotive Textiles (Coloration Technology, 2020)
- Mechanical Properties of Automotive Upholstery Fabrics (Fibres & Textiles in Eastern Europe, 2022)

16th International Fiber and Polymer Research Symposium (16th ULPAS) 9-10 May, 2025,

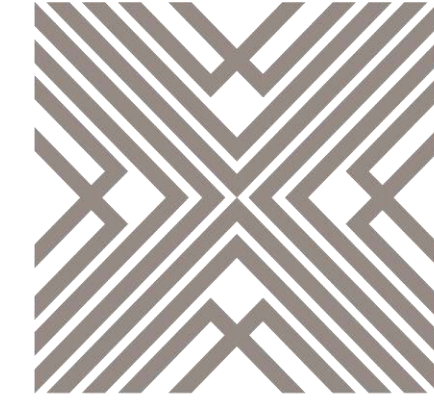
Istanbul technical University (ITU), Istanbul, Türkiye

Sürdürülebilirlik Odaklı Halı ve Döşemelik Kumaş Geliştirme

Osman TÜRKMEN¹, Elif KOYUNCU²

Kadifeteks Mensucat San. A.Ş.

osman.turkmen@kadifeteks.com



KADİFETEKs

Mensucat Sanayi A.Ş.

Proje Özeti

Döşemelik kumaş sektöründe, müşteri ihtiyaçlarına ve çevreye duyarlı üretim anlayışına paralel olarak, yeni ve sürdürülebilir üretim sistemlerinin geliştirilmesi büyük önem kazanmıştır. Geleneksel transfer baskılı ürünlerin üretiminde genellikle iki veya üç ayrı proses adımı gerekmekte, bu da hem enerji ve kaynak israfına hem de üretim maliyetlerinin artmasına yol açmaktadır. Özellikle, kumaşların ram makinesinde temizlenmesi ve ardından transfer baskı ile laminasyon işlemlerinin ayrı ayrı yapılması, süreçte zaman kaybı ve gereksiz atık oluşumuna neden olmaktadır.

Bu proje ile, tüm bu adımların tek bir transfer baskı sistemi içerisinde birleştirilmesi ve çok fonksiyonlu, çevreye duyarlı bir üretim hattı oluşturulması hedeflenmektedir. Proje kapsamında, transfer baskı makinesinin önüne entegre edilecek fırçalı ve vakumlu bir temizleme sistemi sayesinde, kumaşlar proses sırasında gereksiz enerji ve su tüketimi olmadan doğrudan transfer baskı sistemine iletilecektir.

Ayrıca, bazı kumaşlar için gerekli olan laminasyonlu astar kaplama işlemi de sisteme entegre edilerek, tüm işlemler tek adımda ve verimli bir şekilde gerçekleştirilecektir.

Proje Konusunu Belirleyen İhtiyaçlar

- Yüksek üretim maliyetleri ve fazla enerji/işçilik kullanımı
- Çevreye zarar veren, su ve kimyasal tüketimi yüksek geleneksel yöntemler
- Fazla proses adımı nedeniyle kaynak ve zaman kaybı
- Yüksek iş gücü ihtiyacı ve insan hatası riski
- Teslimatlarda gecikme, müşteri taleplerine yavaş yanıt

Proje Hedefleri:

- Üretimde kalite ve verimliliği artırmak
- Zaman, enerji ve iş gücü tasarrufu sağlamak
- Kaynak kullanımı ve atık miktarını azaltmak
- Transfer baskı ile üretim sürecini optimize etmek
- Ekonomik ve çevreci üretim hedeflerine ulaşmak

DeneySEL

Materyal ve Metod

Bu süreçte, transfer baskıya uygun kağıt seçimi, desen belirleme, baskı işlemleri, renk uyumu ve mukavemet testleri gibi temel parametreler değerlendirilmiştir. Özellikle, baskının kağıda düzgün aktarılabilmesi için yüksek mukavemetli ve süblimasyona uygun kağıtlar tercih edilmiştir. Seçilen kağıtlar, kullanım alanına uygun ölçülerde hazırlanmış ve desenler pres boyutuna göre uygulanmıştır. Ayrıca, farklı renk denemeleriyle desenlerin kumaşa uygunluğu test edilerek, baskı işlemlerinin doğruluğu ve kalitesi sağlanmıştır.

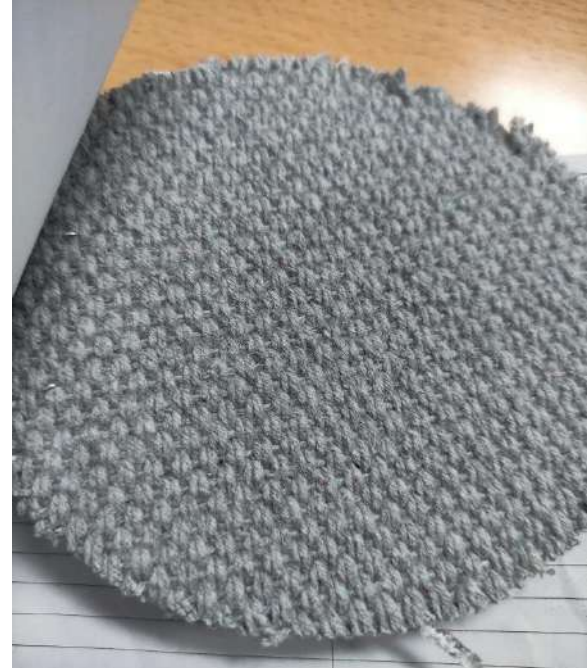
Akrilik ve viskon kumaşlarda sürtme haslığı sorunları yaşandığı için, transfer baskıda polyester kompozisyonlu kumaşlar tercih edilmektedir. Bu doğrultuda, firmamızda tabanı pamuk, yüzeyi tamamen polyester olan kaliteler üretilmeye başlanmıştır.

Süblimasyon baskıda ise yüksek baskı kalitesi elde edebilmek için sıcaklık, hız, kağıt ve boya seçiminin doğru yapılması gerekmektedir. Yapılan çalışmalar sonucunda, en iyi sonuçlar için 225°C sıcaklık ve 4.5 m/dk hız değerleri belirlenmiştir. Kaliteli süblimasyon kağıdı ve inkjet (dispers) boya kullanılmış, baskı odası sıcaklığı ise 25±2°C olarak ayarlanmıştır. Bu parametreler sayesinde, renk canlılığı ve kontrastı yüksek, kaliteli baskılar elde edilmiştir.

Ayrıca, koyu renkli desenlerde yaşanan gölgelenme problemi, firmamızın yaptığı kapsamlı testlerle çözülmüştür. Farklı kağıt türleri, boyutları, boya miktarları ve makine ayarları denenerek en iyi baskı kalitesi, renk tonu ve dayanıklılık sağlanmıştır. Bu çalışmalar sonucunda ürün kalitesi artmış, gölgelenme sorunu giderilmiş ve müşteri memnuniyeti yükselmiştir. Elde edilen optimum ayarlar ise gelecekteki üretimler için referans olmuştur.

Aşağıda tabloda yapılan çalışmalara ait görseller verilmiştir.

Tablo 1 : PES tabanlı Numune



Tablo 2: Baskılı Çalışma 1



Tablo 3: Baskılı Çalışma



Tablo 4 : Baskılı Çalışma



Sonuçlar

Bu projede geliştirilen entegre transfer baskı ve laminasyon sistemi, sürdürülebilirlik hedeflerine uygun ve yenilikçi bir üretim modeli sunmaktadır. Proseslerin birleştirilmesi ve otomasyon sayesinde enerji kullanımı %20, atık miktarı %40 ve üretim maliyetleri %15 oranında azalmıştır. Ayrıca, transfer baskı yönteminde su hiç kullanılmadığı için su tüketimi sıfıra inmiş ve atık su oluşmamıştır. Atık yönetimi ve geri dönüşüm süreçlerinin geliştirilmesiyle çevreye olan olumsuz etkiler en aza indirilmiştir.

Otomasyon ve süreç iyileştirmeleriyle iş gücü verimliliği artmış, iş güvenliği ve ergonomi iyileştirilmiş, çalışan memnuniyeti yükselmiştir. Tüm bu gelişmeler, projenin çevresel, ekonomik ve sosyal sürdürülebilirlik hedeflerine başarıyla ulaştığını göstermektedir. Kadifeteks, bu proje ile sürdürülebilir üretim alanında sektörde önemli bir adım atmıştır.

Tablo 1: Proje Değerlendirmesi

| Gösterge | Proje Öncesi (1m ²) | Proje Sonrası (1m ²) | Değişim (%) | Açıklama |
|--------------------------|---------------------------------|----------------------------------|-------------|-----------------------------------------|
| Enerji Tüketimi (kWh) | 0.10 | 0.08 | -20 | Proses entegrasyonu ve optimizasyon |
| Su (m ³) | 0.20 | 0 | -20 | Su tüketimin ortadan kalkması |
| Atık Miktarı (kg) | 10 | 6 | -40 | Fire ve proses atıklarında azalma |
| Karbon Ayak izi (kg CO2) | 25 | 18.75 | -25 | Enerji ve atık azaltımı |
| Üretim Maliyeti (\$) | 1 | 0.85 | -15 | Otomasyon ve kaynak tasarrufu |
| Fire Oranı (%) | 0.5 | 0.3 | -40 | Hatalı üretim ve fire miktarında azalma |

Tablo 2: Proje Kıyaslaması

| Kaynak | Geleneksel Yöntem | Proje Sonrası Durum | Sürdürülebilirlik Katkısı |
|--------------|-------------------------------------------|----------------------------------------------------|-------------------------------------------------|
| Enerji | Fazla proses, çoklu makine, yüksek enerji | Prosesler birleştirildi, otomasyon, daha az makine | Enerji verimliliği, karbon ayak izinin azalması |
| Su | Yüksek tüketim (yaş prosesler, yıkama) | Sıfıra yakın (transfer baskıda su kullanılmıyor) | Su tasarrufu, atık su oluşumunun önlenmesi |
| Hammadde | Yüksek fire ve atık, çoklu işlem | Fire ve atık azaldı, optimize hammadde kullanımı | Atık azaltımı, kaynak verimliliği |
| İş Gücü | Çok adimli, fazla operatör ihtiyacı | Otomasyon, entegre sistem, daha az iş gücü | İş güvenliği, verimlilik, insan hatası azalması |
| Zaman | Uzun üretim süresi, çoklu adım | Kısa üretim süresi, tek adımda çoklu işlem | Hızlı üretim, termin avantajı, esneklik |
| Atık/Emisyon | Yüksek atık ve emisyon | Atık ve emisyonlar minimize edildi | Çevreye duyarlılık, sürdürülebilir üretim |

Tartışma

Transfer baskılı ve laminasyonlu döşemelik kumaşların üretimi, Kadifeteks'in mevcut ürün portföyünde bulunmayan, yenilikçi ve yüksek katma değerli bir ürün grubunu sektöre kazandırmıştır. Bu yeni üretim modeli, su ve enerji tüketimini minimuma indirerek, atık ve emisyonları azaltmakta ve çevre dostu bir üretim altyapısı oluşturmaktadır. Özellikle transfer baskı yönteminde suyun hiç kullanılmaması, su tüketiminin sıfıra indirilmesini ve atık su oluşumunun tamamen önlenmesini sağlamaktadır.

Otomasyon ve proses entegrasyonu sayesinde, farklı desen ve kumaş tiplerinde hızlı ve esnek üretim yapılabilmekte, müşteri taleplerine daha hızlı ve etkin yanıt verilebilmektedir. Bu esneklik, özel siparişler ve küçük parti üretimlerinde rekabet gücünü artırırken, üretim süreçlerinde verimlilik ve kaliteyi de yükseltmektedir. Proseslerin birleştirilmesi ve enerji verimliliğiyle, üretim maliyetleri ve atık oranları önemli ölçüde düşürülmekte, böylece kârlılık artırılmaktadır.

Atık yönetimi ve geri dönüşüm oranlarının artırılması, döngüsel ekonomi prensiplerine katkı sağlamakta ve firmanın çevresel sorumluluklarını güçlendirmektedir. Enerji ve kaynak tasarrufu ile karbon ayak izi azaltılırken, sürdürülebilirlik odaklı üretim yaklaşımı sayesinde Kadifeteks, sektörde çevreye duyarlı ve yenilikçi bir firma imajı oluşturmaktadır.

Yasal çevre standartları ve uluslararası sertifikasyon gereklilikleri karşılanmakta, çevre dostu ürün etiketleriyle uluslararası pazarlarda yeni müşteri segmentlerine ulaşılmaktadır. Maliyet avantajı sayesinde, fiyat rekabetinde öne çıkılarak pazar payı artırılmakta; sürdürülebilirlik odaklı üretimle de kurumsal sosyal sorumluluk projelerine katkı sağlanmaktadır. Üretim süreçlerinde enerji ve su tüketimi sürekli izlenmekte, bu sayede sürekli iyileştirme ve optimizasyon sağlanmaktadır.

Sonuç olarak, Kadifeteks bu proje ile hem çevresel hem de ekonomik ve sosyal sürdürülebilirlik hedeflerine ulaşmakta, sektörde öncü bir konuma yükselmektedir.

Referanslar

- Textile Printing – Leslie W.C. Miles, Society of Dyers and Colourists, 2003
- Digital Textile Printing – Susan Carden, Bloomsbury Publishing, 2015
- Textile Inkjet Printing – Warren S. Perkins, CRC Press, 2015
- TSI - Brushes for Printing Machines
- Chemical Technology in the Pre-Treatment Processes of Textiles by S.R. Karmakar
- Handbook of Textile and Industrial Dyeing, Volume 1: Principles, Processes and Types of Dyes Edited by M. Clark



Influence of formulation parameters on film morphology and fabric performance in waterborne polyurethane textile coatings

Canberk Yüksel^{a*}, Canan Öztürk^b,

^a*Silicone and Organic Technology Platform R&D Department, Akkim Kimya San. ve Tic. A.Ş., 77602 Yalova, Türkiye*

*Corresponding author: Canberk.Yuksel@Akkim.com.tr

ABSTRACT

Waterborne polyurethane (WPU) dispersions have emerged as versatile agents for imparting tailored functional properties to textile coatings. In this study, five aliphatic WPU dispersions were synthesized via systematic variation of key formulation parameters: the NCO/OH ratio, chain extender type, and polyol composition. Each dispersion was characterized for its physicochemical attributes, including pH, solid content, ionic character, particle size distribution, and zeta potential. Film samples cast from the dispersions were subjected to tensile and elongation testing to evaluate their mechanical performance. Subsequently, the dispersions were knife-coated onto polyester fabric substrates, and the coated fabrics were assessed for hydrostatic resistance (water column test) and breaking strength. Results indicate that increasing the NCO/OH ratio enhanced both film tensile strength and hydrostatic resistance, while variations in chain extender chemistry influenced elongation at break and ionicity. Polyol selection was found to critically affect particle size and zeta potential, thereby modulating dispersion stability and coating uniformity. Correlations between polymer chain structure and both film and fabric performance metrics were established, demonstrating that targeted molecular design can optimize coating functionality. These findings provide valuable insights for the development of high-performance WPU-based textile coatings with customizable mechanical and barrier properties.

Keywords: Polyurethane; Textile; Application ; Waterborne; Coating

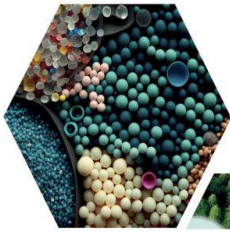
EXPERIMENTAL METHOD

In this study, five different waterborne polyurethane dispersions were synthesized. The formulations varied in terms of the NCO/OH ratio as well as the composition of soft and hard segments.

| Sample | Polyol | Isocyanate | NCO/OH | Chain Extender |
|--------|---------------------------------|------------|--------|----------------|
| PUD-1 | Polyether | IPDI | 2,4 | Polyamine |
| PUD-2 | Polyether | IPDI | 2,4 | Diamine |
| PUD-3 | Polyether | IPDI | 2,0 | Polyamine |
| PUD-4 | Polyether | IPDI | 2,4 | Polyamine |
| PUD-5 | /Polycarbonate Polyether/TMP | IPDI | 2,4 | Polyamine |

RESULTS

| Sample | Particle Size (nm) | Zeta Potential (mV) | pH | Fmax (N) | Elongation (%) |
|--------|--------------------|---------------------|------|----------|----------------|
| PUD-1 | 80 | -33 | 9,27 | 36 | 900 |
| PUD-2 | 117 | -29 | 9,41 | 33 | 670 |
| PUD-3 | 110 | -36 | 8,73 | 7 | 1100 |
| PUD-4 | 102 | -29 | 9,74 | 42 | 800 |
| PUD-5 | 87 | -34 | 8,12 | 44 | 600 |



16 ULUSLARARASI
LİF VE POLİMER
ARAŞTIRMALARI
SEMPOZYUMU

16th INTERNATIONAL FIBER AND POLYMER RESEARCH SYMPOSIUM

Sürdürülebilir ve İşlevsel Lif ve Polimerler
Sustainable and Functional Fibers & Polymers



9-10 Mayıs
May 2025

İstanbul Teknik Üniversitesi
Gümüşsuyu Prof. Dr. Necmettin Erbakan Yerleşkesi
İstanbul Technical University
Gumussuyu Prof. Dr. Necmettin Erbakan Campus

Investigation of the suitability of some piezoelectric materials with nanofiber structure for the field of health technology

Muratcan Çam^{a,*}, Burak Taş^a, Ümit Hüseyin Kaynar^b, Özge Tüzün Özmen^b

^aPostgraduate education institute, Izmir Bakircay University, 35665 Izmir, Türkiye.

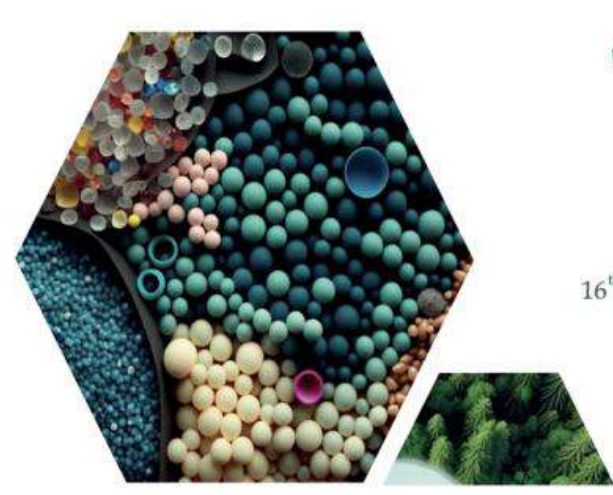
^bDepartment of basic sciences, Izmir Bakircay University, 35665 Izmir, Türkiye.

*Corresponding author: muratcancam@gmail.com.tr

ABSTRACT

The interaction of different branches of science enables the emergence of new technologies in the field of health. Piezoelectricity, one of these innovations, attracts great interest in various fields from sensor technologies to energy production with its ability to convert mechanical energy into electrical energy. The piezoelectric effect is based on the principle of electric potential formation by charge polarization as a result of applied mechanical force, and with this feature, piezoelectricity is used in applications such as energy generation and pressure sensitive sensors. In particular, the health sector makes extensive use of the many advantages offered by piezoelectric technology, from sensitive diagnostic tools to treatment methods, from wearable health devices to biomedical implants. Therefore, nanofiber-based piezoelectric materials, which attract attention with their flexible, lightweight and adaptable structures, have recently come to the fore. Nanofibers are very effective in piezoelectric applications due to their high surface area/volume ratio, flexibility and ease of surface functionalization. In this study, piezoelectric capacity of composite nanofiber materials (ZnO₂+PVDF, BaZrO₂, CuZrO₂, CuZrO₂+PVDF, GdZrO₂+PVDF, ZnO+PVDF) were investigated and the output values were measured. Among these measured nanofiber structured materials, BaZrO₂ material showed the highest performance and provided power generation at the level of 0.2 nW. Considering the studies and developments made on nanoscale sensors in recent years, it is predicted that the energy requirement at nW and pW levels will gain critical importance. As a result, the values obtained as a result of the study offer an alternative solution for use in these sensors.

Keywords: Piezoelectric; Nanotechnology; Nanofiber



16 ULUSLARARASI
LİF VE POLİMER
ARAŞTIRMALARI
SEMPZYUMU
16th INTERNATIONAL FIBER AND POLYMER RESEARCH SYMPOSIUM
Sürdürülebilir ve İşlevsel Lİf ve Polimerler
Sustainable and Functional Fibers & Polymers

9-10 Mayıs
May 2025
İstanbul Teknik Üniversitesi
Gümüşsuyu Prof. Dr. Necmettin Erbakan Yerleşkesi
Istanbul Technical University
Gumussuyu Prof. Dr. Necmettin Erbakan Campus



**BURSA TEKNİK
ÜNİVERSİTESİ**

16th International Fiber and Polymer Research Symposium (16th ULPAS)

9-10 May, 2025, Istanbul technical University (ITU), Istanbul, Türkiye

EFFECT OF CHAIN BRANCHING ON THE MECHANICAL AND CREEP BEHAVIOR OF UHMWPE FIBERS PRODUCED BY GEL SPINNING

Oğuz Kağan Ünlü¹, Aslı Ertan¹

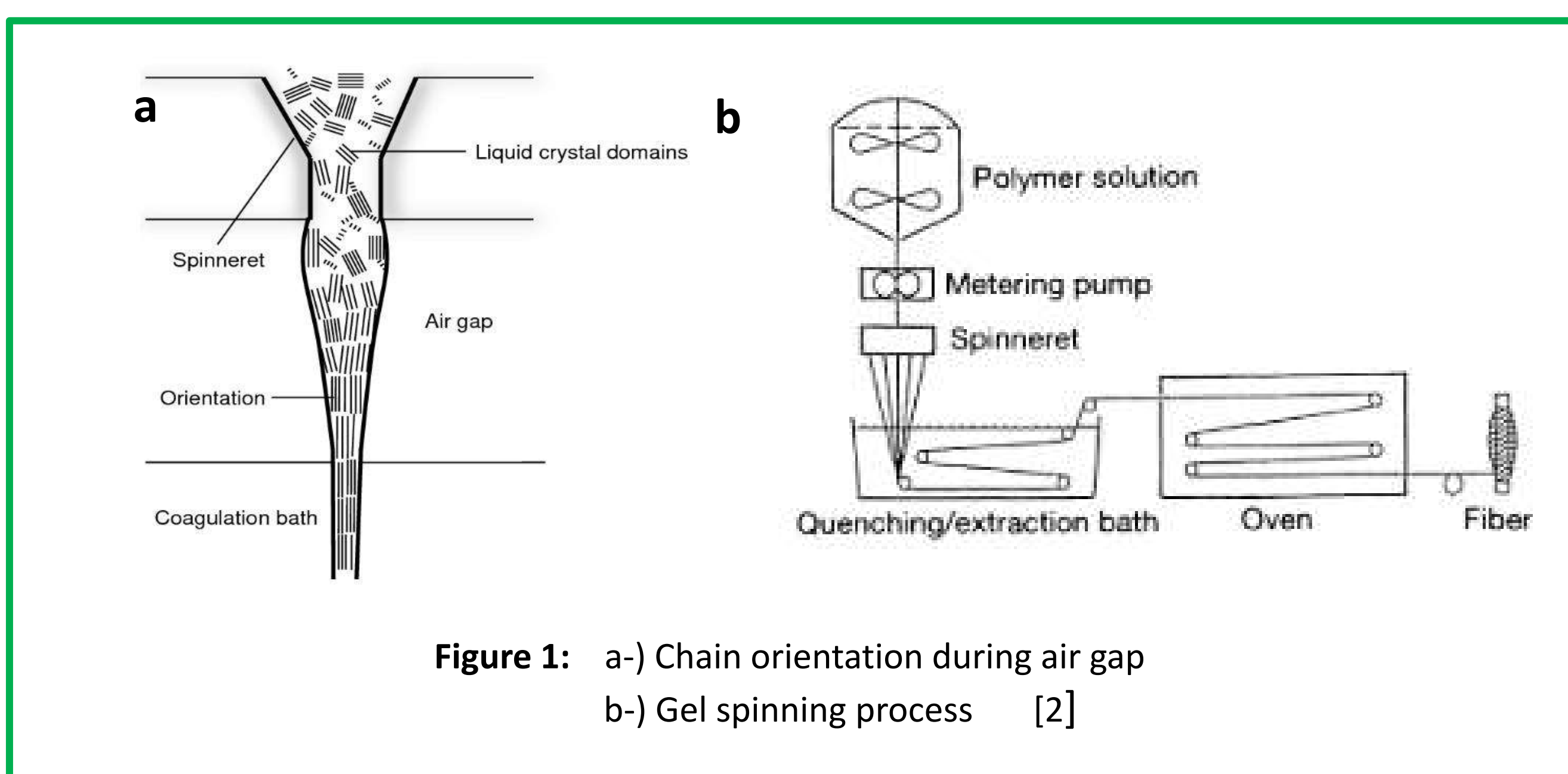
Oguz.unlu@aksa.com

¹AKSA Akrilik Kimya Sanayii A.Ş., R&D Department, 77602 Yalova, Türkiye.



Abstract

Fibers are characterized by their high length-to-diameter ratios and can be engineered to have specific fineness and mechanical properties. High-performance fibers are known for their exceptional characteristics such as high tensile strength, high modulus, excellent abrasion resistance and low density. One of the key techniques for producing these fibers is gel spinning. [1], [2].



This study aims to comparatively investigate the processability and final product properties of two different Ultra High Molecular Weight Polyethylenes (UHMWPEs) fiber with varying degrees of branching structures using the gel spinning method.;

- Evaluating the impact of structural differences on performance by measuring the mechanical properties (tensile strength, elongation) of the obtained filaments.
- Determining the time-dependent deformation behavior through creep tests and to explain this behavior in relation to branching.
- Compare the solution behavior of the molecular structures by conducting Intrinsic Viscosity (IV) measurements for viscosity analysis.

Experimental

In this study, two different UHMWPE raw materials with the same molecular weight (5 million g/mol) but different chain architectures were used to evaluate the mechanical, structural, and rheological properties of filaments produced via the gel spinning method. The two polymers were designated as UHM-1 and UHM-2. The raw materials were dissolved in a suitable solvent to prepare gel spinning solutions.

Intrinsic Viscosity (IV)

To evaluate the behavior of the molecular structure in solution, intrinsic viscosity (IV) measurements were performed to UHMWPEs. The IV measurements were conducted according to the ISO 1628-3 standard. To assess the behavior of the polymer chains in solution, intrinsic viscosity (IV) measurements were carried out, providing insight into the hydrodynamic volume and conformation of the molecular structures. These measurements serve as an indirect method to evaluate the degree of branching within the polymer chains.

Tenacity

To evaluate the influence of polymer chain architecture on the mechanical performance of the filaments, key mechanical properties such as tensile strength and elongation at break were measured. These properties provide critical insight into how variations in chain branching affect the load-bearing capacity and ductility of the material. Measurements were conducted according to ASTM D2256 standard.

Creep Measurements

Creep resistance test is the time-dependent permanent deformation of a material under a constant load (stress) as 20% of the tensile strength. In fiber materials, creep is a critical property in terms of performance, especially in applications exposed to long-term mechanical loading (ropes, armor systems, medical implants, textile structures, etc.).



Figure 2: Final product called mithra



Figure 3: Instron universal tensile tester

Results

Dissolution of UHMWPE, extrusion, spinning as in form of mono- or multiflament, drying and obtaining the final product are the main steps of the gel spinning method. High intrinsic viscosity (IV) values indicate that these polymers possess a more linear chain structure [4].

Linear chains tend to extend more freely in solution, resulting in a larger hydrodynamic volume. This increased volume leads to higher solution viscosity and, consequently, higher IV values. Therefore, IV measurements serve as an effective indirect method for evaluating the conformational structure and degree of branching of polymer chains. Linear UHMWPE chains, characterized by the absence or minimal presence of short- or long-chain branching, enable efficient chain packing during the fiber formation process. This structural regularity facilitates the development of highly crystalline regions and promotes extended chain alignment along the fiber axis during drawing.

Table 1: Summary of Experimental Characterization Results for Various Polymer Samples

| Material | UHM-1 | UHM-2 |
|--------------------|--------------|------------|
| IV Value | ~22.25 | ~19.67 |
| Tenacity (cN/dtex) | 44,16 ± 1,45 | 36 ± 1,38 |
| Elongation (%) | 2,39 ± 0,44 | 3,5 ± 0,27 |
| Creep Measurements | ~ 1 month | ~ 6 months |

The strong intermolecular Van der Waals forces between closely packed, extended chains result in increased resistance to tensile deformation, thereby enhancing the fiber's tenacity. According to table UHM-2 shows better creep performance. According to the table, UHM-2 shows better creep performance. The more linear polymer exhibited earlier failure under constant load. The more linear polymer exhibited earlier failure under constant load Branching hinders the slippage of polymer chains under load by introducing steric obstacles and increasing molecular complexity. As a result, it restricts chain mobility and improves resistance to creep deformation [5].

Discussion

- A high intrinsic viscosity (IV) value indicates that UHMWPE chains possess a more linear structure and occupy more volume in solution, leading to higher viscosity.
- Linear UHMWPE chains, due to the absence of short and long branches, allow for more efficient chain packing and the formation of crystalline regions during drawing.

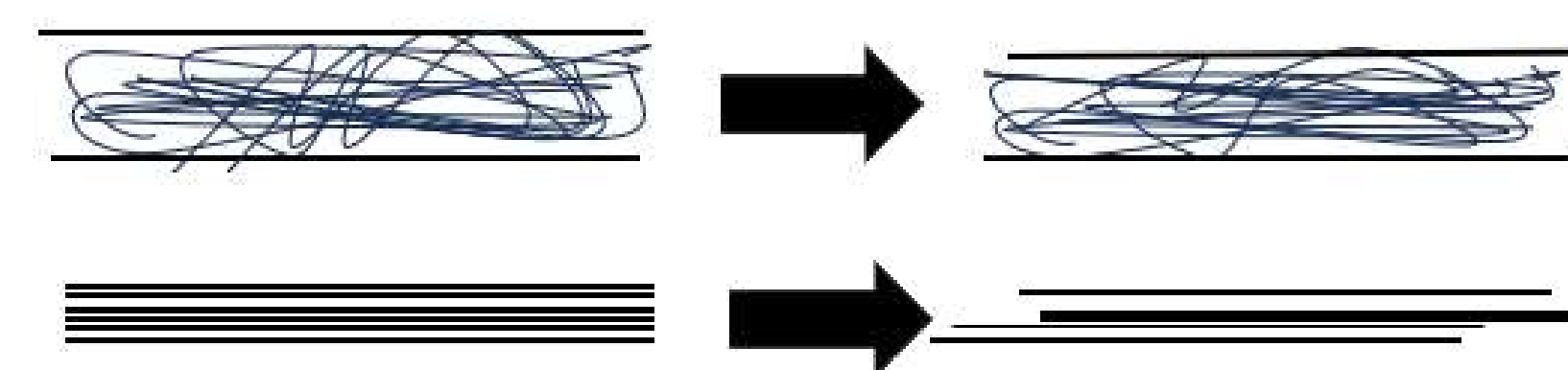


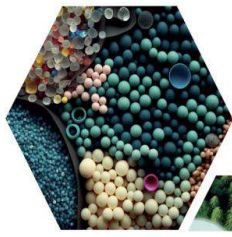
Figure 4: Schematic representation of the effect of chain branching on slippage under load

- Branching restricts chain slippage, thereby increasing resistance to creep deformation; however, it can limit tensile strength.
- This branching enhances long-term load-bearing capacity under constant stress.

Kaynakça

- Enhancement Of Interfacial Properties For High Performance Polyethylene Fibers Produced Via Gel Spinning – Oğuz Kağan Ünlü/2023
- High-performance ballistic protection using polymer nanocomposites D.K.Y. Tam S. Ruan P. Gao T. Yu <https://doi.org/10.1533/9780857095572.2.213>
- www.uckantest.com.tr
- Yao, J., Bastiaansen, C., & Peijs, T. (2014). High Strength and High Modulus Electrospun Nanofibers, Fibers, 2(2), 158–186.
- Short branch effects on the creep properties of the ultra-high strength polyethylene fibers Yasuo Ohta, Hiroshige Sugiyama, Hiroshi Yasuda <https://doi.org/10.1002/polb.1994.090320207>

16th International Fiber and Polymer Research Symposium (16th ULPAS)
9-10 May, 2025, Istanbul technical University (ITU), Istanbul, Türkiye



16 ULUSLARARASI
 LİF VE POLİMER
 ARAŞTIRMALARI
 SEMPOZYUMU

16th INTERNATIONAL FIBER AND POLYMER RESEARCH SYMPOSIUM

Sürdürülebilir ve İşlevsel Lif ve Polimerler
 Sustainable and Functional Fibers & Polymers



9-10 Mayıs
 May **2025**

İstanbul Teknik Üniversitesi
 Gümüşsuyu Prof. Dr. Necmettin Erbakan Yerleşkesi
 Istanbul Technical University
 Gumussuyu Prof. Dr. Necmettin Erbakan Campus



Water Exposure Effects on the Mechanical Properties of Glass Fiber-Reinforced HDPE Unidirectional Tapes

Melisa Yeke^a, Gülnur Başer^{a,*}, Serkan İlker Bengü^a

^a*Metiyx Composites-Telateks A.Ş., Manisa, 45030, Turkey.*

^{*}*Corresponding author: gulnur.baser@telateks.com*

ABSTRACT

This study investigates the development of glass fiber reinforced HDPE (high-density polyethylene) based unidirectional (UD) tape products and the effect of water absorption of the developed UD tape on mechanical performance. These tapes, which contain HDPE matrix and glass fiber reinforcement, provide superior tensile strength and increase performance. In the tensile tests conducted on the developed thermoplastic UD tape samples, the tensile strength of the samples impregnated with water for 150, 300, 450 and 600 hours was investigated. The results show that there is a significant decrease in the strength of the tapes as the water exposure time increases. That water has a significant effect on the mechanical properties of the material. These findings provide an important indicator when evaluating the performance of UD tapes under the influence of water.

Keywords: Unidirectional (UD) Tape; HDPE (High-Density Polyethylene); Glass Fiber Reinforcement; Thermoplastic Composite; Mechanical Strength

I. INTRODUCTION

Composite materials are preferred in many industries such as aerospace, automotive, maritime, and construction due to their lightweight and high mechanical performance. Polymer matrix composites are primarily divided into two categories based on the matrix: thermoplastic and thermoset [1]. Today, thermoplastic composites have become a focus of research due to their advantages, such as re-shapeability, short cycle times, and recyclability. In this field, unidirectional (UD) tape products, especially those in tape form, stand out due to their ability to directly respond to directional strength requirements [2-3].

The environmental resistance of polymer matrix composites, particularly their resistance to moisture and water, directly affects their long-term performance. Literature has shown that water absorption leads to significant losses in mechanical properties [4]. However, studies on the performance of thermoplastic matrix UD tape products, particularly those based on HDPE, when exposed to water, are quite limited. This situation points to a significant knowledge gap, especially in structural applications that may be exposed to outdoor environmental conditions.

This study aims to develop HDPE-based UD tapes reinforced with glass fibers and investigate the effect of water absorption on their mechanical performance. The developed UD tape samples were exposed to water for 150, 300, 450 and 600 hours, and then subjected to tensile tests. The results showed a noticeable decrease in tensile strength as the exposure time to water increased. These findings provide important data for evaluating the environmental resistance of thermoplastic composites and highlight the need for careful material selection in applications where UD tapes may be exposed to water.

II. EXPERIMENTAL METHOD

2.1 Materials

In this study, HDPE (high-density polyethylene) with a density of 0.955 g/cm^3 , a melting point of 128°C , and a yield tensile strength of 250 kg/cm^2 was used, reinforced with glass fiber. The glass fiber has a unit area weight of $450\text{-}480 \text{ g/m}^2$ and a minimum content of 62% by weight.

2.2 Preparation Techniques

In this method, the HDPE polymer is homogeneously integrated onto the glass fiber strands using the hotmelt coating technique, where the fibers are coated with molten resin (Fig 1). Then, This production method also brings the advantages of using thermoplastic materials, as HDPE is a material that can be reheated and shaped, offering a suitable option for recycling. These features provide a sustainable solution both economically and environmentally.

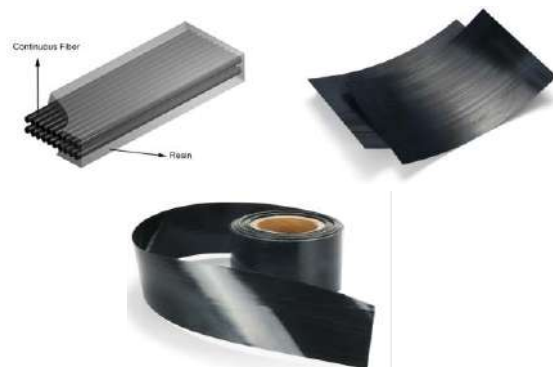


Figure 1. Structural representation and final product forms of UD tape.

III. RESULTS AND DISCUSSIONS

Samples from two different rolls were tested, and a noticeable decrease in tensile strength was observed as the exposure time to water increased. The results for Roll 1 are presented in Table 1, and for Roll 2 in Table 2. The tensile strength of Roll 1 in the dry condition was $1072.16 \pm 77.95 \text{ N/mm}^2$, which decreased to $940.63 \pm 56.42 \text{ N/mm}^2$ after 150 hours of water exposure, $874.07 \pm 47.69 \text{ N/mm}^2$ after 300 hours, and $780.12 \pm 36.51 \text{ N/mm}^2$ after 450 hours. For Roll 2, the dry tensile strength was $1052.10 \pm 43.47 \text{ N/mm}^2$, which decreased to $847.60 \pm 83.19 \text{ N/mm}^2$ after 150 hours, $807.99 \pm 35.03 \text{ N/mm}^2$ after 300 hours, and $709.00 \pm 30.04 \text{ N/mm}^2$ after 450 hours. After 600 hours of water exposure, the tensile strength of Roll 2 further decreased to $632.04 \pm 34.10 \text{ N/mm}^2$. For Roll 3, the tensile strength after 600 hours of water exposure was measured as $687.38 \pm 28.04 \text{ N/mm}^2$. The tensile strength results show a decrease in parallel with the increase in water exposure time, and these data are summarized in Figure 2 as a line graph.

Table 1. Tensile strength results of roll_2

| Samples | Tensile Strength (N/mm ²) 0 hour-dry | Tensile Strength (N/mm ²) 150 hour-wet | Tensile Strength (N/mm ²) 300 hour-wet | Tensile Strength (N/mm ²) 450 hour-wet | Tensile Strength (N/mm ²) 600 hour-wet |
|-----------|-----------------------------------------------------|-------------------------------------------------------|-------------------------------------------------------|-------------------------------------------------------|-------------------------------------------------------|
| Mean | 1052,10 | 847,60 | 807,99 | 709,00 | 632,04 |
| Std. Dev. | 43,47 | 83,19 | 35,03 | 30,04 | 34,10 |
| CoV | 4% | 10% | 4% | 4% | 5% |

Table 2. Tensile strength results of roll_3

| Samples | Tensile Strength (N/mm ²) 0 hour-dry | Tensile Strength (N/mm ²) 150 hour-wet | Tensile Strength (N/mm ²) 300 hour-wet | Tensile Strength (N/mm ²) 450 hour-wet | Tensile Strength (N/mm ²) 600 hour-wet |
|-----------|-----------------------------------------------------|-------------------------------------------------------|-------------------------------------------------------|-------------------------------------------------------|-------------------------------------------------------|
| Mean | 1072,16 | 940,63 | 874,07 | 780,12 | 687,38 |
| Std. Dev. | 77,95 | 56,42 | 47,69 | 36,51 | 28,04 |
| CoV | 7% | 6% | 5% | 5% | 4% |

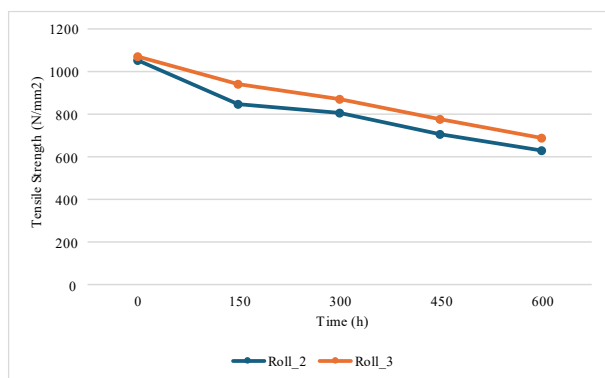


Figure 2. Graphical summary of tensile strength results

IV. CONCLUSIONS

In conclusion, the results of this study indicate that the tensile strength of both Roll 1 and Roll 2 samples decreases significantly as the exposure time to water increases. The dry tensile strength was considerably higher compared to the wet conditions, with both rolls showing a gradual reduction in strength over time. These findings highlight the impact of environmental factors, such as water exposure, on the mechanical properties of HDPE-based UD tapes reinforced with glass fibers. The observations emphasize the importance of considering environmental conditions in real-world applications of such materials. The reduction in tensile strength due to water absorption may be attributed to the poor hydrolytic stability of the matrix resin or the coupling agent applied on the glass fibers, which is responsible for the fiber-matrix interfacial bonding. Future works will focus on investigating and improving the hydrolytic resistance of both the matrix resin and the coupling agent.

REFERENCES

- [1] Hsissou R, Seghiri R, Benzekri Z, Hilali M, Rafik M, Elharfi A (2021) Polymer composite materials: A comprehensive review. *Composite Structures* 262:113640. <https://doi.org/10.1016/j.compstruct.2020.113640>
- [2] Vaidya, U. K., & Chawla, K. K. (2008). Processing of fibre reinforced thermoplastic composites.

International Materials Reviews, 53(4), 185–218. doi:10.1179/174328008x325223

[3] Kropka M, Muehlbacher M, Neumeyer T, Altstaedt V (2017) From UD-tape to final part – A comprehensive approach towards thermoplastic composites. *Procedia CIRP* 66:96–100. <https://doi.org/10.1016/j.procir.2017.03.312>

[4] Krzyżak A, Gąska J, Duleba B (2013) Water absorption of thermoplastic matrix composites with polyamide 6. *Sci J Marit Univ Szczecin* 33(105):62–68. ISSN 1733-8670.

16th International Fiber and Polymer Research Symposium (16th ULPAS)

9-10 May, 2025, Istanbul technical University (ITU), Istanbul, Türkiye

COMPARATIVE ANALYSIS OF PIEZOELECTRIC OUTPUT PERFORMANCES OF Gd AND Al DOPED ZnO PRODUCED IN NANOFIBER STRUCTURE WITH RESPECT TO THEIR NON-DOPED (PURE) FORM

Burak TAŞ, Ahmet Batuhan TOĞRUL, Ümit Hüseyin KAYNAR, Özge Tüzün ÖZMEN

Abstract

Project Motivation

In the last quarter, technological developments have gained great momentum, and the tendency from macro-scale structures to micro and even nanotechnological structures has increased. This new situation has increased the need for energy and has led to energy demands at mW and μ W levels. At this point, it was discovered that as the size of the material decreases, its physical properties as well as its chemical properties change. For example, some substances that do not exhibit any electrical properties in their normal size, when reduced to nano size and pressure or vibration is applied to them, they begin to produce electricity at various levels. Materials that produce energy when subjected to pressure or vibration are called piezoelectric materials. In this study, the piezoelectric properties of ZnO material produced by adding Gadolinium (Gd) and Aluminum (Al) at different rates in a fibrous structure using the electrospinning method at İzmir Bakırçay University Basic Sciences Laboratory were investigated.

Project goals:

- Since the required energy levels vary, it is necessary to determine at what levels energy can be produced by nanofibrous materials.
- Investigation of the effect of fibrous structure of nanomaterials on piezoelectricity.
- Comparative investigation of piezoelectric performances of various materials produced by electrospinning method at İzmir Bakırçay University Fundamental Sciences Laboratory.

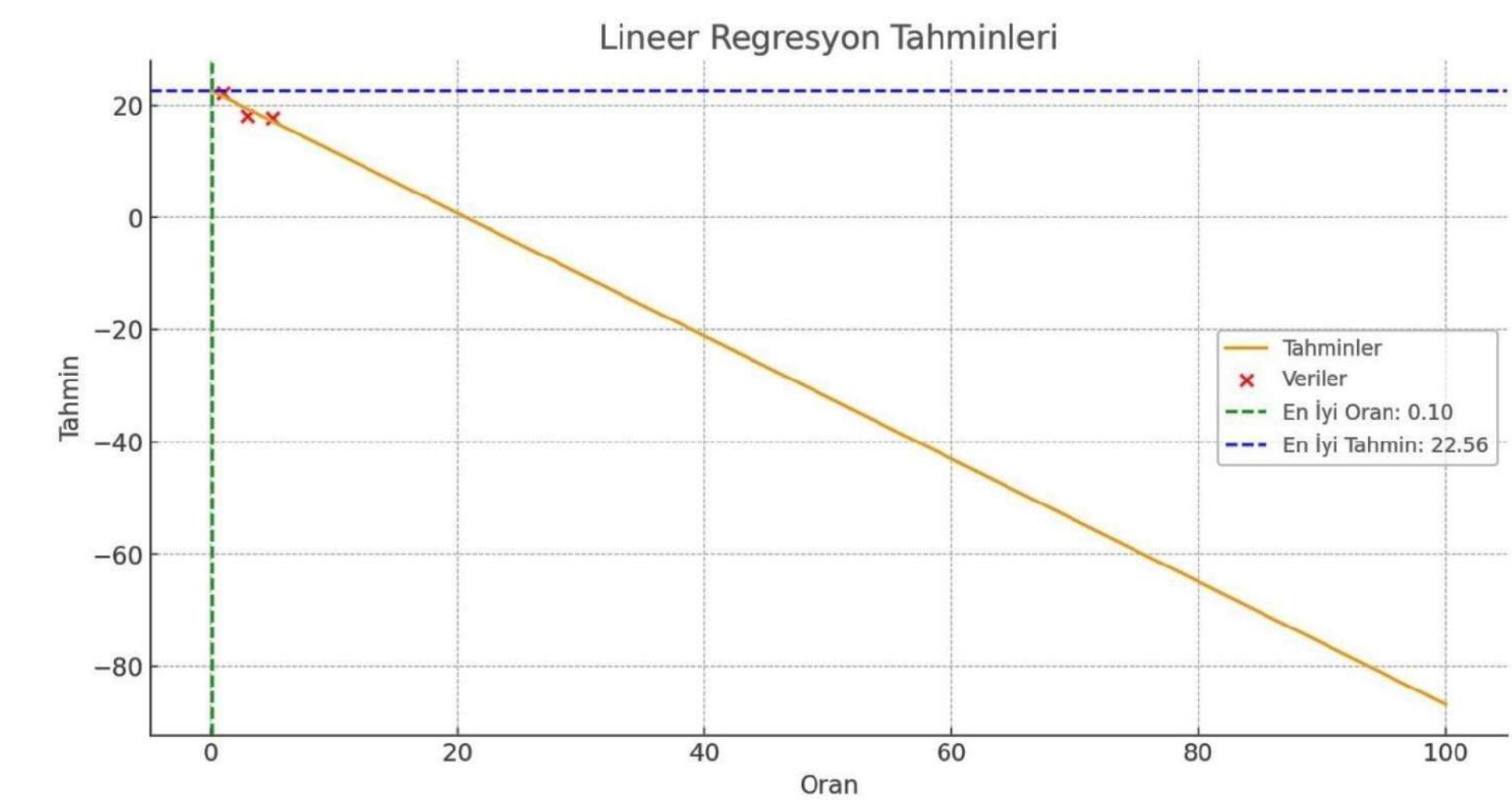
Results

| Added material | Contribution rate (%) | Generated voltage (mV) |
|----------------|-----------------------|------------------------|
|----------------|-----------------------|------------------------|

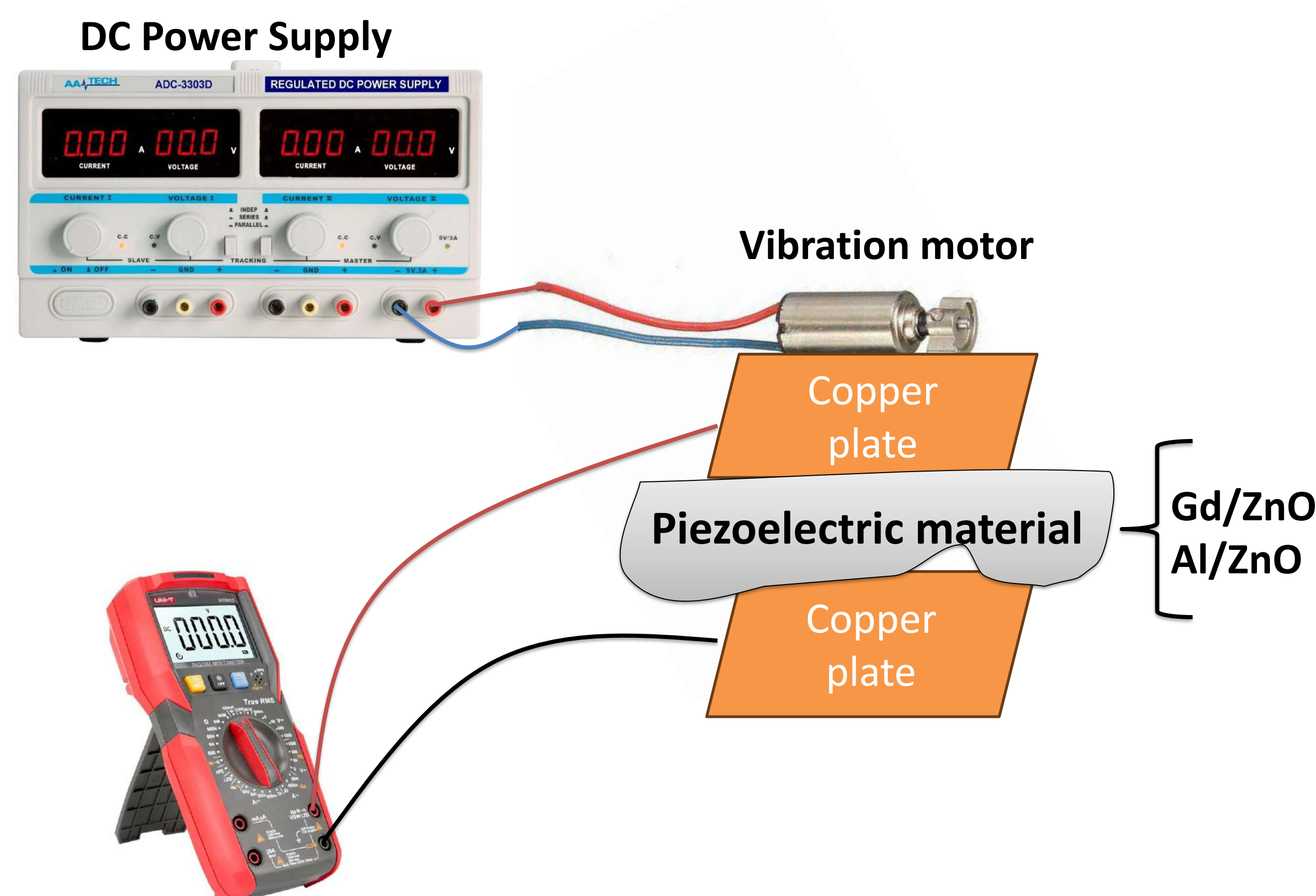
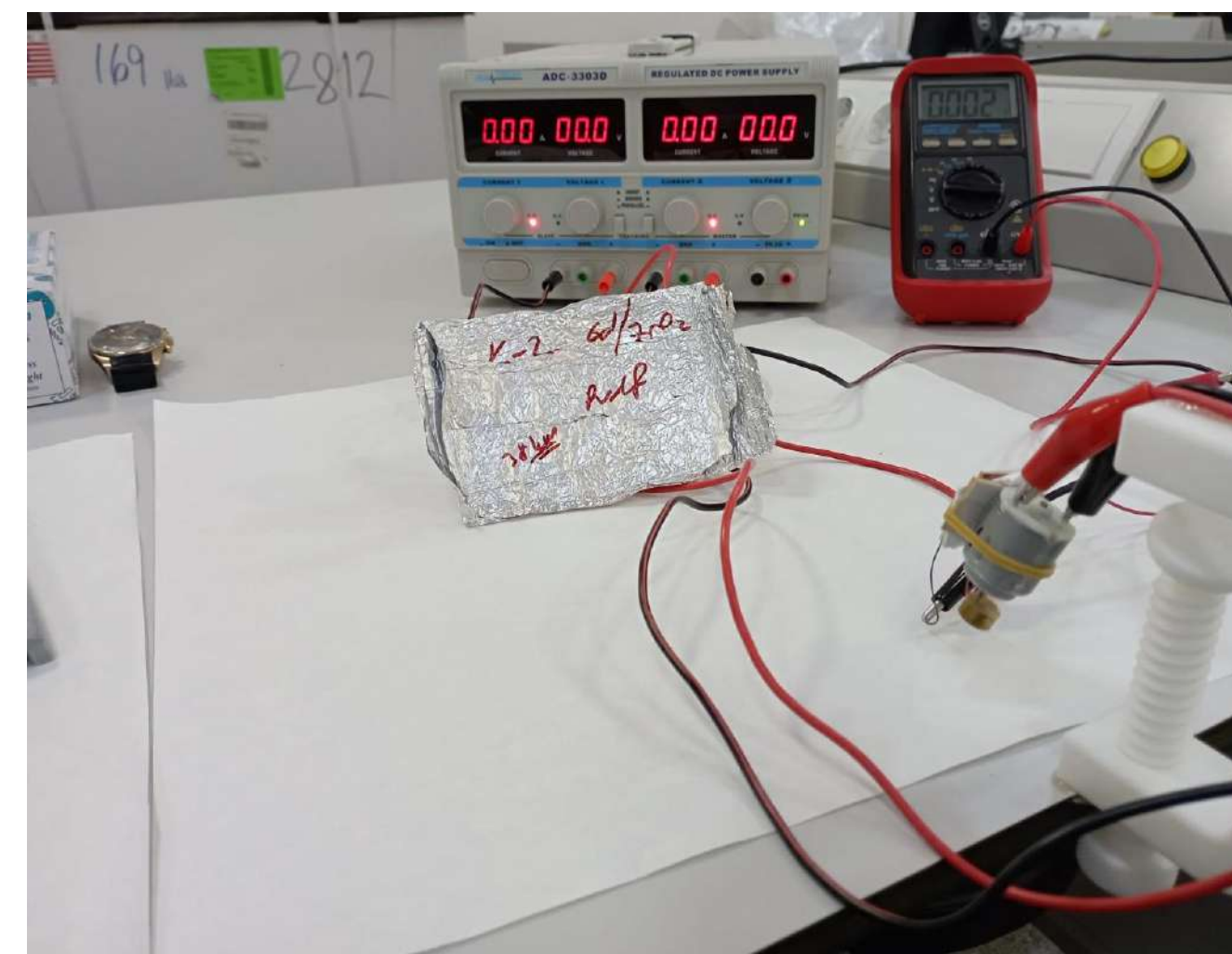
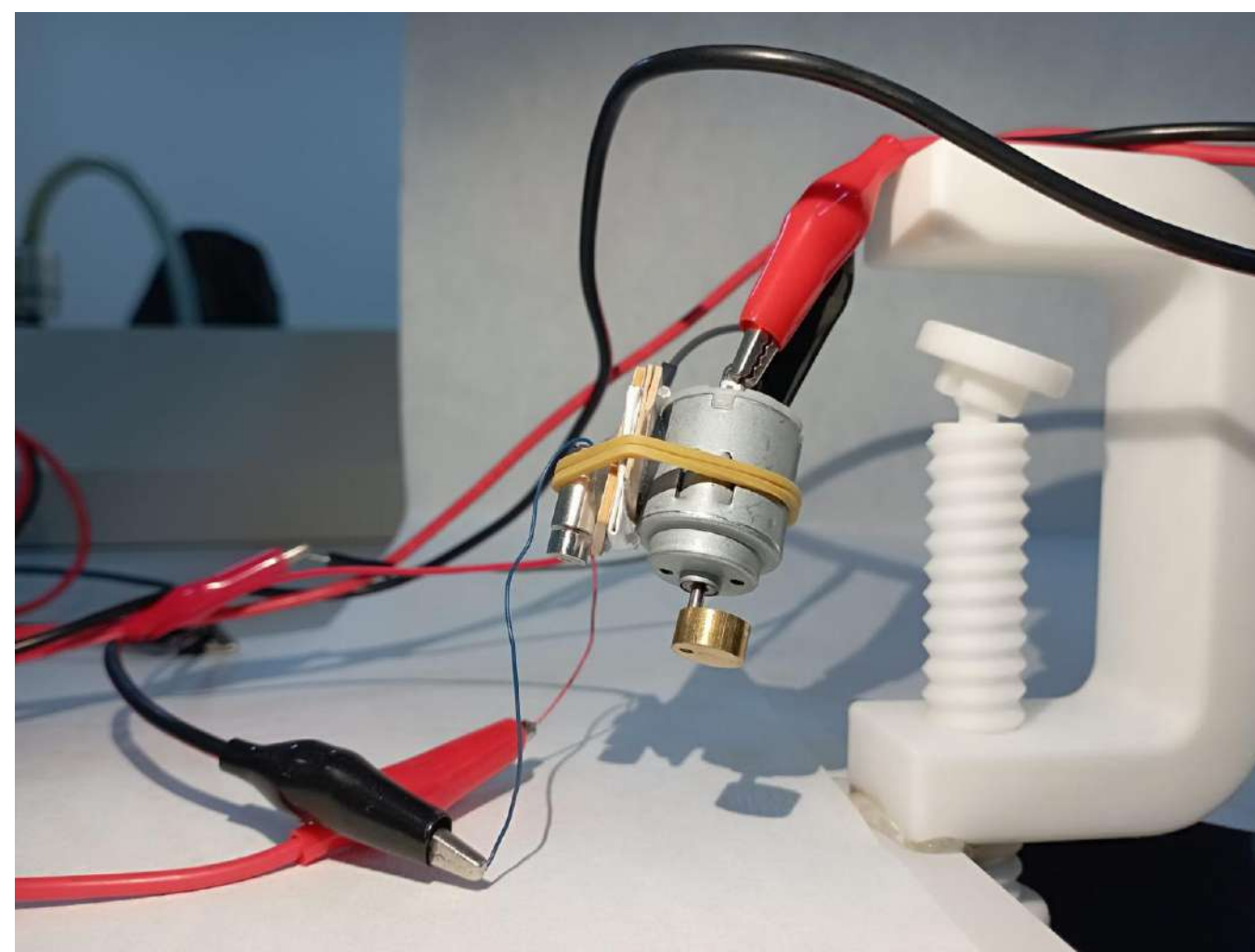
| | | |
|----|---|-------|
| Gd | 1 | 22,16 |
| Gd | 3 | 18,22 |
| Gd | 5 | 17,78 |
| Gd | 7 | 5,49 |

| Added material | Contribution rate (%) | Generated voltage (mV) |
|----------------|-----------------------|------------------------|
|----------------|-----------------------|------------------------|

| | | |
|----|---|------|
| Al | 1 | 1,35 |
| Al | 3 | 1,92 |
| Al | 5 | 2,48 |
| Al | 7 | 2,24 |



Experimental



Discussion

When the studies in the literature were examined, it was observed that when the ZnO in the nanowire structure was exposed to mechanical pressure, the piezoelectric energy production performance varied between 100 mV and 5 V. In the study we carried out in the laboratory environment, Gd or Al was doped into ZnO at different rates and the electricity production capacity was compared according to the pure state. The obtained results were examined and analyzed comparatively. According to the results of this analysis, ZnO nanowires have higher production power when they are pure without Gd and Al additives, but when they are separately doped with the mentioned materials, the piezoelectric performance decreases. Another point that stands out in the study is that as Gd doping increases, the piezoelectric performance of ZnO decreases almost linearly; as the Al doping ratio changes, the piezoelectric performance of ZnO exhibits a complex feature. Although a conclusion has been reached regarding the additive materials discussed in this study, it is aimed to test new materials and increase the output performance of pure ZnO in future studies.

16th International Fiber and Polymer Research Symposium (16th ULPAS)

9-10 May, 2025, Istanbul technical University (ITU), Istanbul, Türkiye

RECYCLING OF THE FUTURE: SMART AND SUSTAINABLE SEPARATION METHODS FOR TEXTILE WASTE

Aliye Akarsu ÖZENÇ*¹, Zaide Saka DİNÇ*, Semiha EREN*, Hüseyin Aksel EREN*

*Bursa Uludağ University, Department of Textile Engineering, Bursa, Türkiye

¹- aakarsu@uludag.edu.tr



Abstract

Effective sorting of textile wastes is a critical step for the transition to a circular economy; however, the inadequacy of traditional methods in sorting textile wastes necessitates new approaches. In this study, artificial intelligence-supported visual systems offering high accuracy and speed; NIR spectroscopy enabling non-destructive and rapid analysis; environmentally friendly enzymatic sorting; robotic systems increasing efficiency through automation; magnetic/density-based pre-sorting methods based on metal and weight differences; and smart label technologies providing traceability throughout the product life cycle are discussed. By discussing the advantages of each method and their challenges in scale implementation, the necessity of an integrated sorting strategy in textile waste management is emphasized.

Discussion

The textile industry is one of the most polluting industries in the world [1]. In 2014, 16.22 million tons of textile waste was generated in the US, of which only 16% was recycled [2]. In the EU, most of the 16 million tons of annual waste is incinerated [3]. The low recycling rates necessitate a transition to a circular economy model. This system reduces resource use, lowers carbon emissions and creates new jobs [4-5]. Effective separation of textile waste is critical for this transformation [6]. Traditional textile waste separation methods cannot effectively separate complex fiber blends as they involve manual, time-consuming and error-prone processes [7]. These methods are inadequate in the face of the increasing amount of textile waste, which makes it difficult to achieve sustainability goals. Innovative methods such as artificial intelligence, sensor-based systems and biotechnological approaches are needed for faster, accurate and efficient separation [8].

Each of these innovative methods offers significant advantages in sorting textile waste. AI-based visual systems offer an effective solution for sorting mixed material waste by identifying fiber types and colors with high accuracy and speed. Thanks to AI-based vision systems, it significantly improves efficiency by increasing sorting speed while reducing manual labor [9].

NIR (Near Infrared) spectroscopy makes a great contribution to recycling processes thanks to its ability to quickly analyze the material composition without destroying it. This method allows for the rapid identification and accurate classification of textile waste, as well as the efficient separation of recyclable materials [10].

Biochemical separation methods offer an environmentally friendly alternative, especially with the use of enzymes that selectively degrade natural fibers (e.g. cotton). This method provides a precise separation of natural and synthetic fibers, while reducing the use of chemicals. In the use of this method, certain conditions must be met for the enzymes to work efficiently [11].

Robotic sorting systems enable the automatic sorting of waste using robots equipped with sensors. This technology significantly reduces labor and makes sorting processes faster. However, the initial costs of such systems are high and require a large investment in this technology [12].

Magnetic and intensity-based separation is particularly useful for the pre-separation of fabrics containing metals or fabrics of different weight classes. This method allows for coarse separation of materials prior to detailed sorting, thereby increasing the efficiency of finer sorting methods [13].

Finally, smart labels and digital tracking technologies enable tags such as RFID or QR codes to be attached to textiles during production. Thanks to these tags, it is possible to trace the products until the end use and helps to accurately identify textile waste in the recycling process. These systems allow the circular economy model to operate more transparently and efficiently [14]. Innovative methods such as these allow significant progress to be made in the sorting of textile waste. Each method presents its own challenges, so factors such as the feasibility, cost-effectiveness and large-scale integration of these technologies should be considered [15-16].

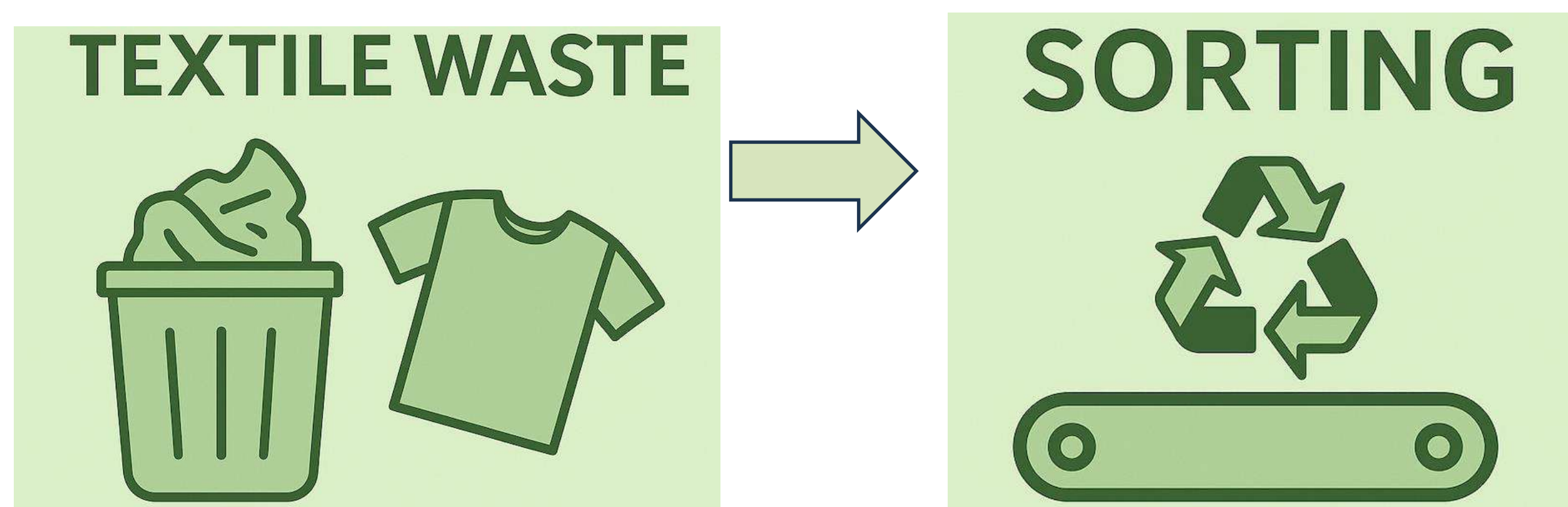
Results

Innovative textile waste sorting and recycling methods offer promising solutions to the growing global waste problem. While traditional systems fall short in terms of speed, accuracy and sustainability, technologies such as artificial intelligence, NIR spectroscopy, robotic sorting and smart labels increase efficiency, traceability and material recovery rates. These developments support circular economy goals and reduce environmental impacts by transforming waste into valuable resources. Continued research and investment is essential to make these methods widespread and increase their economic viability.

References

- Garvert, U. (2017). A comparative study of recycling in the European and Brazilian textile industry (Doctoral dissertation).
- Epa, U. (2015). Advancing sustainable materials management: 2014 fact sheet. United States Environmental Protection Agency, Office of Land and Emergency: Washington, DC, USA.
- European Commission. (2017). Circular Economy in Practice—Reducing Textile Waste.
- Agenda, I. (2016, January). The new plastics economy rethinking the future of plastics. In World Economic Forum (Vol. 36).
- Sustainability, M. (2015). Europe's circular-economy opportunity.
- Leal Filho, W., Ellams, D., Han, S., Tyler, D., Boiten, V. J., Paço, A., ... & Balogun, A. L. (2019). A review of the socio-economic advantages of textile recycling. Journal of cleaner production, 218, 10-20.
- Chaturvedi, D. K., & Chanana, B. (2024, November). Eco-conscious Design: Innovating Post Textile Waste into Sustainable Solutions. In International Conference on Sustainable Fashion and Technical Textiles (pp. 112-128). Singapore: Springer Nature Singapore.
- Ozek, A., Seckin, M., Demircioglu, P., & Bogreki, I. (2025). Artificial Intelligence Driving Innovation in Textile Defect Detection. Textiles, 5(2), 12.
- H. (2025). CIRCULAR ECONOMY IN TEXTILE MANUFACTURING: AI-DRIVEN APPROACHES TO WASTE REDUCTION. AMERICAN JOURNAL OF EDUCATION AND LEARNING, 3(4), 454-460.
- Du, W., Zheng, J., Li, W., Liu, Z., Wang, H., & Han, X. (2022). Efficient recognition and automatic sorting technology of waste textiles based on online near infrared spectroscopy and convolutional neural network. Resources, Conservation and Recycling, 180, 106157.
- Navone, L., Moffitt, K., Hansen, K. A., Billico, J., Payne, A., & Speight, R. (2020). Closing the textile loop: Enzymatic fibre separation and recycling of wool/polyester fabric blends. Waste Management, 102, 149-160.
- Zhou, J., Zou, X., & Wong, W. K. (2022). Computer vision-based color sorting for waste textile recycling. International Journal of Clothing Science and Technology, 34(1), 29-40.
- Manjiri P, Ashok A. Textile Waste Management-Innovative Separation Techniques. Curr Trends Fashion Technol Textile Eng 2024; 9(2): 555757.
- Heim, H. (2021, June). Label conscious: communicating verifiable sustainable impact by labelling garments with smart technology. In International Conference on Fashion communication: between tradition and future digital developments (pp. 173-186). Cham: Springer International Publishing.
- Tang, K. H. D. (2023). State of the art in textile waste management: A review. Textiles, 3(4), 454-467.
- Lanz, I. E., Laborda, E., Chaine, C., & Blecua, M. (2024). A Mapping of Textile Waste Recycling Technologies in Europe and Spain. Textiles, 4(3), 359-390.

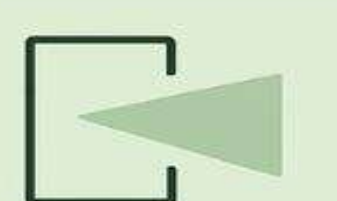
Experimental



Innovative Methods for Textile Waste Sorting



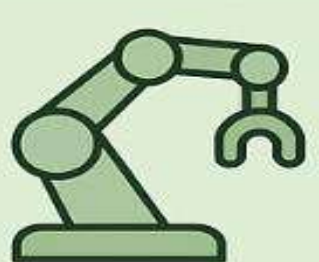
AI-Based Vision Systems



NIR (Near-Infrared) Spectroscopy



Biochemical Sorting



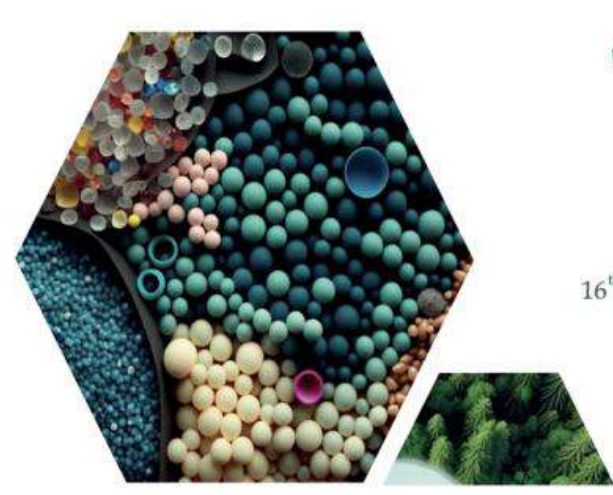
Robotic Sorting Systems



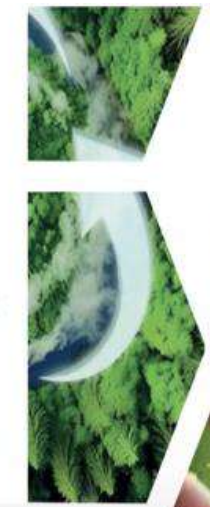
Magnetic & Density-Based Separation



Smart Tags & Digital Tracing



16 ULUSLARARASI
LİF VE POLİMER
ARAŞTIRMALARI
SEMPOZYUMU
16th INTERNATIONAL FIBER AND POLYMER RESEARCH SYMPOSIUM
Sürdürülebilir ve İşlevsel Lİf ve Polimerler
Sustainable and Functional Fibers & Polymers



9-10 Mayıs **2025**
İstanbul Teknik Üniversitesi
Gümüşsuyu Prof. Dr. Necmettin Erbakan Yerleşkesi
İstanbul Technical University
Gumussuyu Prof. Dr. Necmettin Erbakan Campus



16th International Fiber and Polymer Research Symposium (16th ULPAS)

9-10 May, 2025, Istanbul technical University (ITU), Istanbul, Türkiye

RECYCLING TECHNIQUES FOR FIBER REINFORCED POLYMER COMPOSITES

Zaide SAKA DİNÇ^{*1}, Aliye AKARSU ÖZENÇ^{*}, Semiha EREN^{*}, Hüseyin Aksel EREN^{*}

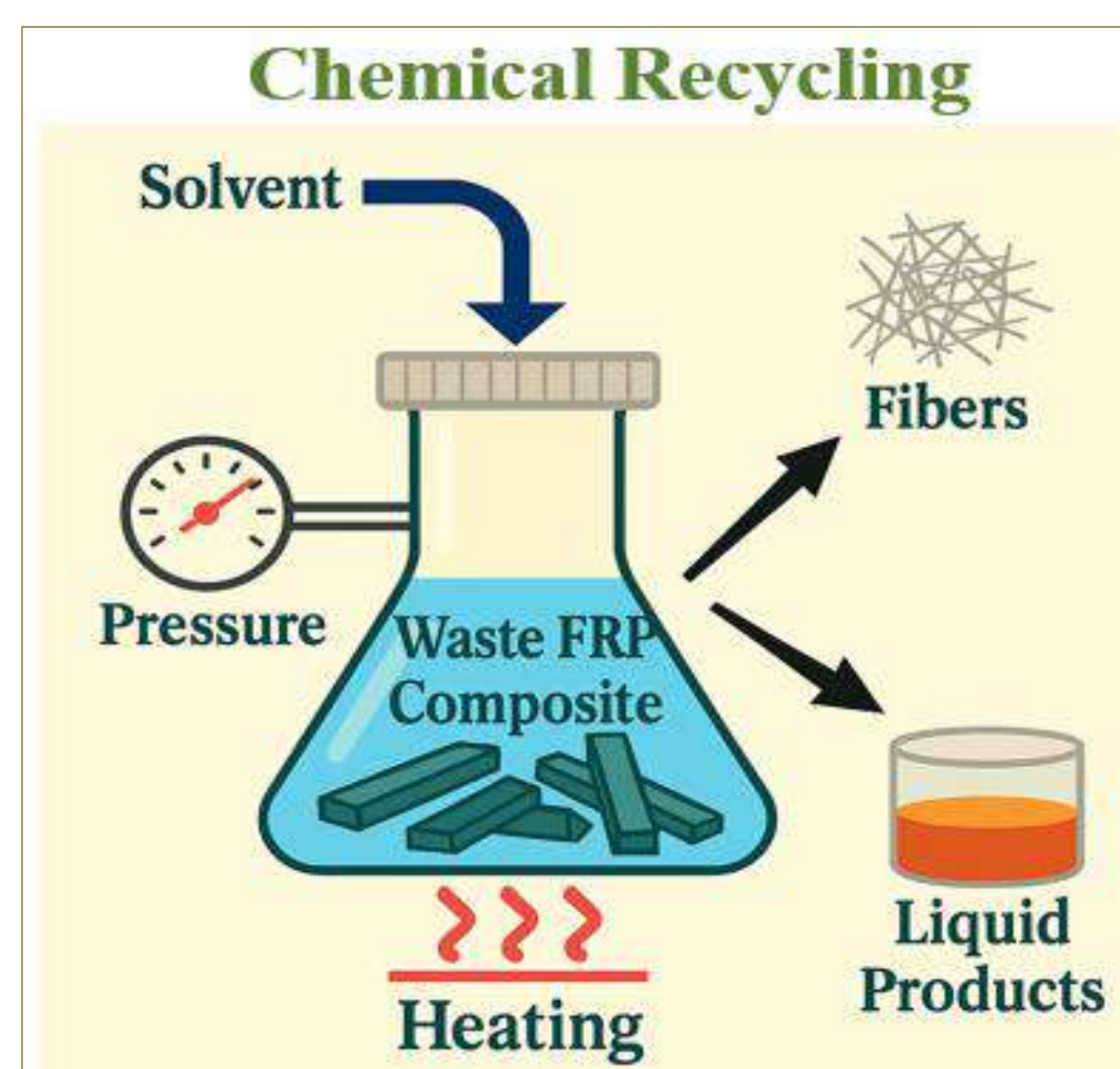
^{*}Bursa Uludag University, Department of Textile Engineering, Bursa, Türkiye

¹- zaidesaka@uludag.edu.tr



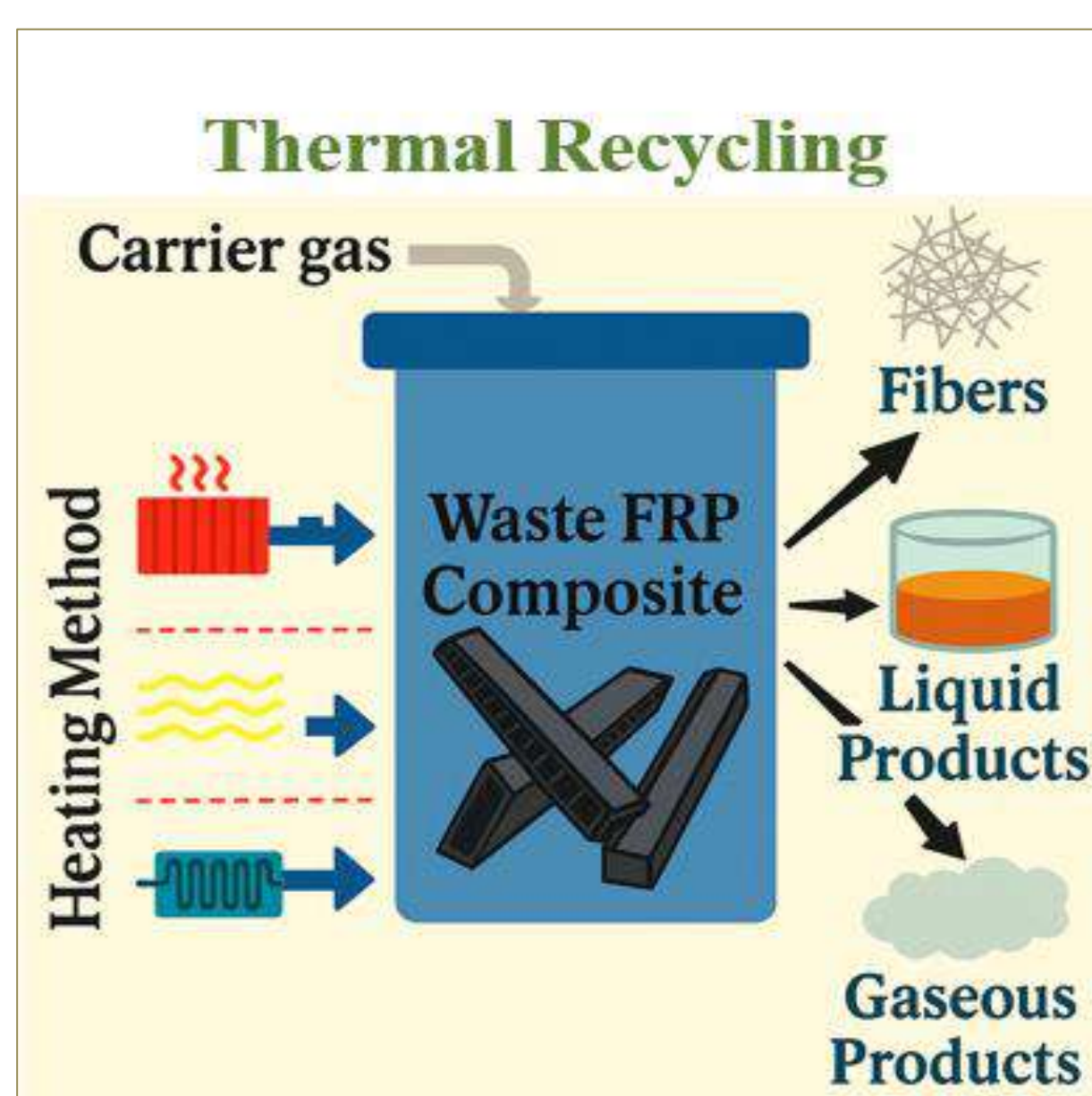
ABSTRACT

This review outlines the three main recycling methods for fiber-reinforced polymer (FRP) waste: chemical, mechanical, and thermal recycling, highlighting their principles, advantages, and limitations. Chemical recycling involves matrix degradation using solvents under elevated temperature and pressure, enabling high-quality fiber recovery but is limited by high operational costs and environmental concerns. Mechanical recycling reduces FRP waste to powders or fillers, mainly for use in the construction industry; although cost-effective and environmentally favorable, it does not allow for the recovery of structurally viable fibers. Thermal recycling, particularly pyrolysis, thermally decomposes the matrix to retrieve fibers, with temperature and duration being critical to fiber quality. While advanced pyrolysis techniques improve outcomes, challenges such as fiber degradation and char formation persist. Overall, despite progress, each method faces scalability and performance limitations that hinder widespread industrial adoption.



Chemical recycling involves the degradation and subsequent removal of the matrix phase through the use of organic solvents, water, or acidic solutions under elevated temperature and pressure conditions. Based on the solvent system employed, chemical recycling is categorized into solvolysis, hydrolysis, and acid-catalyzed degradation under relatively mild conditions. Solvolysis typically utilizes organic solvents such as propanol, ethanol, or acetic acid under subcritical, supercritical, or atmospheric pressure environments, while hydrolysis employs water under similar pressure regimes [1-5]. Among acid-based methods, nitric acid has been the most commonly used reagent [6]. These chemical approaches enable the recovery of fibers with superior mechanical properties and ensure the complete elimination of the polymer matrix. At ambient temperatures, chemical recycling generally requires extended processing times ranging from 4 to 12 hours—to achieve full resin degradation [1,7]. However, under more severe conditions (300–450°C and 50–300 bar), the decomposition process can be significantly accelerated, often requiring less than 2 hours [3-5]. Despite this advantage, the high operational costs associated with subcritical and supercritical processing remain a significant drawback. In addition, the toxicity and environmental impact of solvents used in solvolysis present major obstacles for industrial-scale application. Consequently, chemical recycling continues to face challenges in scalability due to the absence of economically viable and environmentally sustainable processes.

Mechanical recycling primarily involves reducing FRP waste materials into small particles or powder. These materials are mostly used as fillers or aggregate in the construction industry, and to a lesser extent, in the composites sector [12-17]. Various studies have reported improvements in the mechanical properties of plain polymer concrete through the addition of aggregate-like materials such as glass fibers, carbon fibers, and recycled polyethylene terephthalate (PET) bottles [18,19]. Despite the demonstrated benefits of using ground FRP waste in terms of cost efficiency, material performance, and environmental sustainability, this approach does not enable fiber recovery suitable for high-performance structural applications.

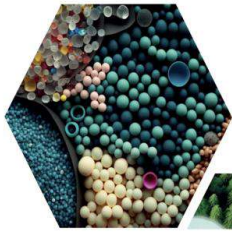


Thermal recycling primarily involves pyrolysis, a process in which the matrix phase adhered to the fibers is thermally decomposed at elevated temperatures, typically ranging from 500 to 800 °C, to recover the reinforcing fibers [20,21]. The key parameters affecting the mechanical performance of the recovered fibers are the pyrolysis temperature and duration. Advanced techniques such as microwave-assisted pyrolysis and catalyst-assisted pyrolysis have been shown to reduce processing time and enhance the mechanical properties of the recovered fibers relative to conventional pyrolysis methods [22-24]. In addition to fiber recovery, the pyrolysis process also generates gaseous and liquid by-products that may serve as valuable chemical feedstocks. Nonetheless, significant challenges remain, including char deposition on the surface of recovered fibers and a decline in mechanical performance at higher operating temperatures. To obtain fibers with properties comparable to those of virgin fibers, it is essential to conduct thorough experimental studies aimed at optimizing the pyrolysis conditions, particularly temperature and duration.

Mechanical recycling involves the cutting and grinding of end-of-life composite materials, followed by a sieving process that yields both powder and fibrous fractions. However, this method often results in the degradation of fiber properties, thereby limiting their applicability in high-performance structural applications. In contrast, thermal recycling technologies employ elevated temperatures under inert or oxygen-rich atmospheres to recover fibers and decompose the resin matrix. The potential for reusing the recovered fibers is primarily determined by their morphological and mechanical characteristics, which are influenced by factors such as the presence of carbonaceous residues on the fiber surface and the specific operating temperatures used. Chemical recycling, which utilizes solvents or supercritical/subcritical fluids, enables the recovery of high-quality fibers. Nevertheless, challenges such as the disposal of spent solvents and the requirement for high operational parameters hinder its large-scale industrial implementation, although ongoing research seeks to enhance its economic and environmental viability.

References

- [1] Yang P, Zhou Q, Li X-Y, et al. Chemical recycling of fiber reinforced epoxy resin using a polyethylene glycol/NaOH system. *J Reinforc Plast Compos* 2014; 33: 2106–2114.
- [2] Okajima I, Hiramatsu M, Shimamura Y, et al. Chemical recycling of carbon fiber reinforced plastic using supercritical methanol. *J Supercrit Fluids* 2014; 91: 68–76.
- [3] Jiang G, Pickering SJ, Lester EH, et al. Characterisation of carbon fibres recycled from carbon fibre/epoxy resin composites using supercritical n-propanol. *Compos Sci Technol* 2009; 69: 192–198.
- [4] Kim YN, Kim Y-O, Kim SY, et al. Application of supercritical water for green recycling of epoxy-based carbon fiber reinforced plastic. *Compos Sci Technol* 2019; 173: 66–72.
- [5] Yuyan L, Guohua S and Linghui M. Recycling of carbon fibre reinforced composites using water in subcritical conditions. *Mater Sci Eng, A* 2009; 520: 179–183.
- [6] Hanaoka T, Ikematsu H, Takahashi S, et al. Recovery of carbon fiber from prepreg using nitric acid and evaluation of recycled CFRP. *Compos B Eng* 2022; 231: 109560.
- [7] Ma C, Sanchez-Rodríguez D and Kamo T. Influence of thermal treatment on the properties of carbon fiber reinforced plastics under various conditions. *Polym Degrad Stab* 2020; 178: 109199.
- [8] Krauklis AE, Karl CW, Gagani AI, et al. Composite material recycling technology—state-of-the-art and sustainable development for the 2020s. *Journal of Composites Science* 2021; 5(1).
- [9] Khalil YF. Sustainability assessment of solvolysis using supercritical fluids for carbon fiber reinforced polymers waste management. *Sustain Prod Consum* 2019; 17: 74–84.
- [10] Koçak G, Yapıcı E, Özkan A, et al. Recycling of composite waste by sequential application of multi-criteria decisionmaking, pyrolysis, and reproduction. *J Reinforc Plast Compos* 2021; 41: 245–256.
- [11] Wang Y, Cui X, Yang Q, et al. Chemical recycling of unsaturated polyester resin and its composites via selective cleavage of the ester bond. *Green Chem* 2015; 17: 4527–4532.
- [12] Meira Castro AC, Carvalho JP, Ribeiro MCS, et al. An integrated recycling approach for GFRP pultrusion wastes: recycling and reuse assessment into new composite materials using Fuzzy Boolean Nets. *J Clean Prod* 2014; 66: 420–430.
- [13] Rangelov M, Nassiri S, Haselbach L, et al. Using carbon fiber composites for reinforcing pervious concrete. *Construct Build Mater* 2016; 126: 875–885.
- [14] Hossain MZ and Awal ASMA. Flexural response of hybrid carbon fiber thin cement composites. *Construct Build Mater* 2011; 25: 670–677.
- [15] Yazdanbakhsh A, Bank LC and Chen C. Use of recycled FRP reinforcing bar in concrete as coarse aggregate and its impact on the mechanical properties of concrete. *Construct Build Mater* 2016; 121: 278–284.
- [16] de Souza Abreu F, Ribeiro CC, da Silva Pinto JD, et al. Influence of adding discontinuous and dispersed carbon fiber waste on concrete performance. *J Clean Prod* 2020; 273: 122920.
- [17] Thomas C, Borges PHR, Panzera TH, et al. Epoxy composites containing CFRP powder wastes. *Compos B Eng* 2014; 59: 260–268.
- [18] Asdollah-Tabar M, Heidari-Rarani M and Aliha MRM. The effect of recycled PET bottles on the fracture toughness of polymer concrete. *Compos Commun*. 2021; 25: 100684.
- [19] Sett K and Vipulanandan C. Properties of polyester polymer concrete with glass and carbon fibers. *ACI Materials Journal* 2004; 101: 30–41.
- [20] López FA, Rodríguez O, Alguacil FJ, et al. Recovery of carbon fibres by the thermolysis and gasification of waste prepreg. *J Anal Appl Pyrol* 2013; 104: 675–683.
- [21] Jeong J-S, Kim K-W, An K-H, et al. Fast recovery process of carbon fibers from waste carbon fibers-reinforced thermoset plastics. *J Environ Manag* 2019; 247: 816–821.
- [22] Deng J, Xu L, Zhang L, et al. Recycling of carbon fibers from CFRP waste by microwave thermolysis. *Processes* 2019; 7(4).
- [23] Ren Y, Xu L, Shang X, et al. Evaluation of mechanical properties and pyrolysis products of carbon fibers recycled by microwave pyrolysis. *ACS Omega* 2022; 7: 13529–13537.
- [24] Pender K and Yang L. Investigation of the potential for catalyzed thermal recycling in glass fibre reinforced polymer composites by using metal oxides. *Compos Appl Sci Manuf* 2017; 100: 285–293.



16

ULUSLARARASI LİF VE POLİMER ARAŞTIRMALARI SEMPOZYUMU

16th INTERNATIONAL FIBER AND POLYMER RESEARCH SYMPOSIUM

Sürdürülebilir ve İşlevsel Lif ve Polimerler
Sustainable and Functional Fibers & Polymers



9-10 Mayıs
May 2025

İstanbul Teknik Üniversitesi
Gümüşsuyu Prof. Dr. Necmettin Erbakan Yerleşkesi
İstanbul Technical University
Gumussuyu Prof. Dr. Necmettin Erbakan Campus

Bebek bezlerinde nefes alabilirlik özelliğinin ölçümü için metot geliştirme

Melcenur KILIÇ^{a,*}, Eda DOĞU^a, Nimet UZUN KALENDER^a

^aEvyap Ar-Ge Merkezi, Hijyen Bölümü, İstanbul Deri Organize Sanayi Bölgesi, 34957, İstanbul, Türkiye.

*Sorumlu Yazar: mekilic@evyap.com.tr

ÖZET

Tek kullanımlık bebek bezleri, bebek hijyeninin sağlamlasında kullanılan önemli bir hızlı tüketim ürünüdür. Bebek bezleri, farklı işlevleri olan birkaç katmandan oluşur. Temel katmanlar; iç yüzey, emici tabaka ve dış yüzeydir. Bezi oluşturan tüm katmanlar gözenekli ve tek başlarına değerlendirildiğinde nefes alabilir katmanlar olsa da ürün tasarımında ürüne nefes alma özelliğini kazandıran ve bu özellik açısından belirleyici olan katman dış yüzey ve hatta bu yüzeyi oluşturan polietilen filmidir. Dış yüzey katmanının nefes alabilirlik özelliği, sektörde yerleşik olarak kullanılan metotlarla, bu katmanın su buharı geçirgenlik hızı ölçülerek belirlenir ancak bu malzemeyi içeren bitmiş ürünün nefes alabilirlik özelliğinin ölçümü için yaygın olarak kullanılan yerleşik bir metot bulunmamaktadır. Bu çalışmada, bebek bezlerinin nefes alabilirlik özelliğinin belirlenmesi için toplam su buharı geçirgenliğini ölçmek üzere bir metot geliştirilmiştir. Bebek bezi numunelerinin hazırlanmasında nefes alabilen ve alamayan dış yüzey katmanları kullanılmıştır. Bez kullanmama durumunu test etmek amacıyla bebek giyiminde kullanılan pamuklu kumaşların da geliştirilen metotla toplam su buharı geçirgenlikleri özelliği ölçülmüş ve bebek bezi ölçümleriyle karşılaştırılmıştır. Analizlerden elde edilen sonuçlara göre nefes alabilen polietilen film numuneleri, nefes alamayanlara göre 37 kat daha yüksek toplam su buharı geçirgenliğine sahiptir. Nefes alabilen dış yüzeyle üretilen bebek bezlerinin, nefes alamayan dış yüzeyle üretilen bebek bezlerine kıyasla 2 kat daha fazla toplam su buharı geçirgenliğine sahip olduğu görülmüştür. Pamuklu kumaşlar ise nefes alabilen bebek bezine göre 2 kat, nefes alamayan bebek bezine göre ise 5 kat daha yüksek toplam su buharı geçirgenliğine sahiptir.

Anahtar Kelimeler: Bebek bezi, Su buharı geçirgenliği, Dış yüzey, Nefes alabilir, Nefes alamayan, Polietilen film, Pamuklu kumaş

Developing a method for measuring breathability of baby diapers

ABSTRACT

Disposable diapers are important fast-moving consumer products used to provide baby hygiene. Diapers consist of several layers with different functions. The basic layers are topsheet, absorbent core and backsheet. Although all layers forming diaper are porous and breathable layers when evaluated individually, the layer that gives the product the

breathability feature is the backsheet and even polyethylene film that used in the backsheet structure. Breathability of backsheet is determined by measuring water vapor transmission rate of this layer with well-known methods widely used in hygiene industry, but there is no standard method used for measuring breathability of baby diaper. In this study, a method was developed to measure total water vapor permeability in order to determine breathability of baby diaper. Breathable and non-breathable backsheet layers were used for preparation of diaper samples. In order to test the situation of no diaper use, total water vapor permeability of cotton fabrics used in baby clothing was measured and compared with the diaper measurements. According to test results, breathable polyethylene film samples have 37 times higher total water vapor permeability than non-breathable ones. It was observed that diapers produced with breathable backsheet have 2 times higher total water vapor permeability than their non-breathable counterparts. Cotton fabrics have 2 and 5 times higher total water vapor permeability than breathable and non-breathable diapers, respectively.

Keywords: Baby diaper, Water vapor permeability, Backsheet, Breathable, Non-breathable, Polyethylene film, Cotton fabric

I. GİRİŞ

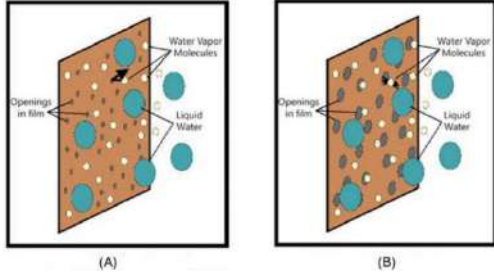
Sentetik materyallerden yapılan tek kullanımlık bebek bezlerine alternatif olarak tekrar kullanılabilir kumaş bebek bezleri pamuk veya bambu gibi emici doğal liflerden oluşur ve yıkanarak yeniden kullanılabilir. Tek kullanımlık bebek bezlerine kıyasla daha az atık üretse de kumaş bezlerin gerçekten daha sürdürülebilir olup olmadığı konusunda bir tartışma vardır, çünkü üretim aşamalarında çeşitli kaynaklar tüketilir ve ürünlerin sık sık sıcak suyla yıkanmaları çevre dostu değildir. Tek kullanımlık bezlere kıyasla, kullanılan emici kumaş katmanlarının sayısına bağlı olarak idrar ve dışkı sızıntı riski daha yüksek olacağından bunu önlemek için bezin daha sık değiştirilmesi gerekebilir. Bakteriyel kontaminasyonu önlemek ve kötü kokuyu azaltmak için bezlerin iyice temizlenmesi ve dezenfekte edilmesi gereklidir, bu da ebeveynlerin iş yükünü artırabilir [1].

Tek kullanımlık bebek bezleri her ne kadar PE film, nonwoven (PP), sap (sodyum poliakrilat) gibi sentetik malzemelerden oluşsa da içerdiği katmanların sağladığı emme kapasitesi ve bezdeki sıvıyı dışarı vermeyi önleyen dış yüzeyi (backsheet) sayesinde daha uzun süreli kullanım sağlar. Dış yüzey katmanı

tercihe göre nefes alabilen (Breathable-BR) ve nefes alamayan (Nonbreathable-NBR) özellikte olabilir. BR bebek bezinin ilk kez piyasaya sürüldüğü 1990 yılının ortalarından bu yana, birçok bebek bezi markası nefes alabilen özelliğe sahip dış yüzey kullanmaktadır. Dış yüzeyin bu özelliğinin bebek cildinin nefes almasını sağlarken aynı zamanda cilt bariyerini koruyarak pişik oluşumunu azalttığı da gözlemlenmiştir [2, 3].

Bu özelliğe sahip dış yüzey katmanı, fiber yapılı nonwoven (dokumasız kumaş) ve polietilen (PE) filmin birbirine yapıştırılmasıyla (laminasyon işlemi) elde edilir. BR bir laminat üretmek için talk gibi çok ince bir mineral olan kalsiyum karbonat (kalsit) PE filme eklenir. CaCO_3 tozu, PE pelletlerine eklenerek karışım bir eritme vidasına beslenmeden önce homojen bir şekilde karıştırılır. Film ekstrüde edildikten sonra, bir grup kalender tarafından gerdirilir.

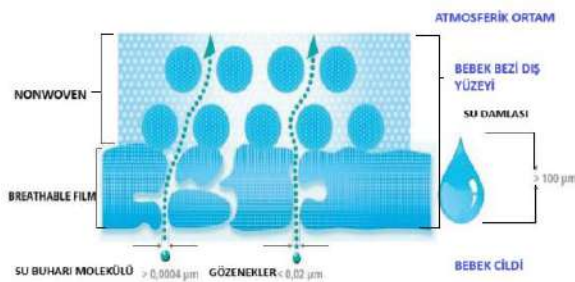
Germe işlemi sonucunda PE film üzerinde milyonlarca mikro delik oluşur ve bu sayede film nefes alabilir özellik kazanır [2, 3]. Şekil 1'de BR ve NBR PE film yapısı daha anlaşılır bir biçimde şematize edilmiştir [4].



Şekil 1: PE film yapısı (A) NBR PE film (B) Nefes alabilir PE film.

NBR filmlerde, PE pelletlerine eklenen kalsit oranı düşüktür. Bu nedenle, film gerdirildiğinde oluşan mikroskopik çatlakların boyutu, su buharı moleküllerinden daha küçüktür. Böylece, bu tip filmlerden su ve su buharı geçişi mümkün olmaz. BR filmlerde ise polimerik katkıya (masterbatch) eklenen kalsit oranı daha yüksektir. Bu durum, film çekme işlemi sırasında daha yoğun ve daha büyük çaplı mikro gözeneklerin oluşmasına neden olur. Oluşan bu gözenekli yapı sayesinde film, su buharını geçirebilir hale gelir [2, 3].

Şekil 2' de şematize edildiği gibi 100 μm 'den büyük boyuttaki su damlaları, BR film yüzeyinden geçemez. Ancak idrardan buharlaşan ve yaklaşık 0,0004 μm 'den büyük boyutlardaki su buharı, filmde bulunan 0,02 μm 'den küçük gözeneklerden geçerek bebeğin cildinin nefes almasını ve böylelikle kuru kalmasını sağlar [2].



Şekil 2: BR film yüzeyi geçirgenlik şeması.

Çeşitli araştırma raporları, NBR dış yüzey kullanılarak bebek cildinin idrarla daha yoğun temas etmesinden, BR dış yüzey kullanılarak idrarın bezden dışarı buharlaşması ve ciltle temas eden idrar miktarının azaltılması durumunda bebek cildinde oluşabilecek

pişik ihtimalini azalttığını doğrulamıştır. Çocuk doktorları bebeklerde cilt tahrişi ile karşılaştıklarında ebeveynlere bebek bezini değiştirmeden önce birkaç dakikalığına bebeğin cildinin nefes almasına izin vermelerini önermektedirler. Bu durum, bebek bezinde BR film kullanımının önemini vurgulamaktadır [2, 3].

BR dış yüzey içeren bir bebek bezi kullanıldığında, bezin emici tabakası sürekli ıslansa dahi idrarın buharlaşmasıyla oluşan su buharı, bezin dış yüzeyinden atmosferik ortama çıkabilir, ilgili görsel Şekil 3'te şematize edilmiştir [5].



Şekil 3: Bebek bezi katmanlarının geçirgenlik şeması.

Lamine dış yüzeyin film kısmındaki gözeneklerin yoğunluğu; filme eklenen kalsit oranı, kalsitin özellikleri, film kalınlığı ve prosesteki gerdirme oranı gibi faktörlere bağlı olarak değişkenlik gösterir. Buhar geçişini ölçmenin en yaygın yolu, bir gün içerisindeki su buharı iletim hızını (WVTR) hesaplamaktır. Standart laboratuvar koşullarında, dış yüzeyden geçen su buharı miktarını belirlemek için kullanılan basit bir yöntem ise beher içinde yapılan ağırlık kaybı ölçümüdür.

Bu test sonucunda elde edilen değer, $\text{g/m}^2/\text{day}$ cinsinden ifade edilir [3]. Tablo 1'de dünya çapındaki çeşitli tek kullanımlık bebek bezlerinde hesaplanan WVTR aralıkları gösterilmiştir [2, 3].

Tablo 1: Dünya çapında bebek bezinde WVTR aralıkları.

| WVTR (g/m ² /day) | Koku Algısı |
|------------------------------|-------------|
| <1000 | Düşük |
| 3000 | Orta |
| 6000 | Yüksek |
| 9000 | Çok Yüksek |
| >12,000 | Yoğunlaşma |

WVTR değeri ne kadar yüksekse, bezin dış yüzeyinden atmosferik ortama buharlaşan idrar miktarı fazla olur ve çevreye o kadar fazla koku yayılır. Tüketiciler genellikle BR bir dış yüzey ile NBR bir dış yüzey arasındaki farkı ürünün görünüşünden tespit edemez. Tüketicileri BR bir bezin faydaları konusunda bilinçlendirmek kolay olsa da su buharı geçişi sonucu ortaya çıkan koku da ebeveynler için rahatsız edici bir durumdur. Tüketicilerin bezden salınan kokuyu ne kadar kabul ettiğini belirleyen birkaç faktör vardır. Muhtemelen en önemli faktörler bebek bezinin tüketildiği coğrafi konum, bölgedeki kültür ve bez değişim sıklığı alışkanlıklarıdır. Dünyanın en yüksek bez değiştirme oranına sahip Güney Kore ve Japonya gibi ülkelerde, tüketiciler yalnızca yüksek WVTR değerine sahip BR dış yüzey içeren ürünleri tercih etmekle kalmaz, bunu üreticiden talep eder ve NBR dış yüzey içeren bir bez satın almayı tercih etmezler. Aynı zamanda bebeğin cildinin mümkün olduğunca kuru olduğundan emin olmak isterler. Koku alma duyularını bez değiştirme konusunda ek bir gösterge olarak kullanırlar ve su buharı geçişi sonucunda oluşan kokuyu alarak daha sık bez değiştirir ve böylelikle pişik riskini azaltmış olurlar [3].

Su buharı geçirgenliğinin ölçüldüğü literatür çalışmaları incelendiğinde; standart koşullarda, desikatör koşulunda ve etüv içerisinde belli sıcaklıklarda 0-24 saat arasında bekletilerek ölçüm alınacak şekilde farklı metotlar geliştirilmiştir. S. Memiş'in yaptığı çalışmada, filmlerin su buharı geçirgenliğini hesaplamak için cam tüplerin iç kısmına %0 nem koşulu sağlamak amacıyla silika jel yerleştirilmiş ve üzerine PE film gerdirilmiştir. Ardından PE film numunesi, lastik ve parafilm

yardımlarıyla sabitlenmiştir. Test tüpleri, saf su içeren desikatöre yerleştirilip 25°C'de 24 saat bekletilmiştir. Cam tüplerin ağırlıkları her üç saatte bir kaydedilmiş ve zamana bağlı su buharı geçirgenliği hesaplanmıştır [6].

S. Aslan'ın gerçekleştirdiği çalışmada, kumaşlar 24 saat boyunca atmosferik koşullarda şartlandırıldıktan sonra kaplara saf su eklenmiş ve su seviyesi ile kumaş arasındaki mesafe 10 mm olacak şekilde ayarlanmıştır. Ardından kumaş numunesi kabın üzerine gerilerek sabitlenmiştir. 24 saat boyunca belirli zaman aralıklarında kaptaki, kumaş ve su gramajı ölçümleri kaydedilerek gramaj farkları hesaplanmıştır. Test sistemindeki gramaj farkları, 1 m² yüzey alanı başına 24 saat içinde buharlaşan su miktarına oranlanarak su buharı geçirgenliği hesaplanmıştır [7].

SCA Hygiene Products AB firması tarafından geliştirilen patent (WO2018038656A1) çalışmasında ise farklı birim ağırlıklara (g/m²) sahip BR ve NBR PE film materyalleri üzerinde WVTR değerleri EDANA/INDA NWSP 070.4.R.0 metoduna göre MOCON PERMATRAN-W Model 101 K cihazı kullanılarak ölçülmüştür. Bu çalışmada blown filmde cast filmlere kıyasla daha yüksek WVTR değeri hesaplanmıştır, NBR filmin WVTR değeri 0 g/m²/day olarak ölçülmüştür [8].

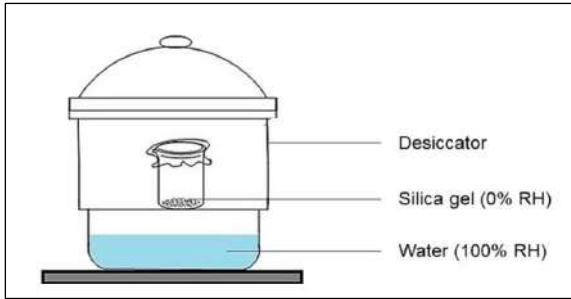
Literatürde bahsedilen test metotları PE film materyalinin nefes alabilirlik özelliğinin ölçümü içindir. Bu çalışmada ise bitmiş ürün olan bebek bezinin nefes alabilirlik özelliğini ölçmek üzere bir metot geliştirilmiştir.

Yapılan çalışmada bebek bezinde kullanılan dış yüzey malzemesinin nefes alabilir özellikte olmasının bebeğin cildinin nefes almasını sağlayarak pişik ve diğer dermatolojik problemlerin önlenmesine sağladığı katkıyı vurgulamak, aynı zamanda NBR dış yüzey kullanıldığında ise bezden su buharı geçişi engellendiğinden dolayı artan yoğun idrar temasının

pişiğe zemin hazırladığı sonucunu göstermek amaçlanmaktadır.

II. DENEYSEL METOT / TEORİK METOD

Bu çalışmada, BR ve NBR PE filmler içeren dış yüzey materyallerinin, bu dış yüzey materyallerinin kullanılması ile üretilen bebek bezi numunelerinin ve pamuklu kumaşın, tek ve çift katlı olacak şekilde, geliştirilen WVTR test metoduyla nefes alma özellikleri ölçülmüştür. S. Memiş'in yaptığı çalışmadaki test metodu referans alınarak geliştirilen metot Şekil 4' te şematize edilmiştir [6, 9].



Şekil 4: Geliştirilen test metodunun şematize edilmiş görseli.

İlk olarak, yapısında yer alabilecek olası nemin uzaklaştırılması için içerisinde 5'er g silika jel içeren beherler ve desikatör 24 saat boyunca etüv içerisinde 105 °C'de şartlandırılmıştır. Ardından beherlerin ağzına test edilecek numuneler gerdirilerek lastik ve parafilm yardımıyla sıkıca kapatma işlemi yapılır ve numuneler sabitlenir (Şekil 5). Tartılan silika jel ve PE film gramajları, deney sonrasında filminden geçen su buharı miktarının hesaplanmasında kullanılmak üzere kaydedilir.



Şekil 5: Nefes alabilirlik testi uygulanacak PE film numunesinin teste hazırlanması.

Ayrı bir yerde nefes alma testinde kullanılacak çözelti hazırlanır. Bu çalışmada, bebeğin idrarını simüle edebilmek için 1 L saf suya %0,9'luk konsantrasyonda olacak şekilde NaCl eklenmesiyle elde edilen tuzlu su çözeltisi kullanılmıştır. Hazırlanan çözelti ısıtıcı manyetik karıştırıcıda kaynayana kadar ısıtılır. Kaynayan çözelti Şekil 4'te gösterildiği gibi desikatör içerisine döküldükten sonra desikatörün tabanına, uygun boyutta ve ısı transferini sağlayan delikli yapıdaki porselen disk yerleştirilir. Ardından Şekil 5'te gösterildiği gibi hazırlanan numuneler desikatör içerisine yerleştirilir ve ortamdaki bağıl nemi %100 civarında tutmak için, su sıcaklığı ortam koşullarına gelene kadar numuneler yaklaşık 8 saat boyunca Şekil 6'da gösterilen kapalı desikatör içerisinde tutulur.



Şekil 6: Nefes alabilirlik testi uygulanan PE film numunelerinin test sırasındaki görünümü.

Test bitiminde PE film ve silika jel gramajları tekrar tartılır. Silika jelin ölçülen son ağırlığı ile analiz başlangıcındaki ağırlığı arasındaki fark hesaplanarak PE filmlerin su buharı geçirgenlik değerleri belirlenir.

PE film numunelerine ek olarak, çalışmanın ikinci aşamasında PE filmler kullanılarak üretilen bebek bezi numunelerinin de su buharı geçirgenlikleri ölçülmüştür. BR ve NBR filmlerin, nefes alabilirlik özelliği açısından, bitmiş ürün üzerindeki etkisi gözlenmiştir. Bebek bezleri için numune hazırlık süreci PE film numuneleri için tarif edildiği şekildedir ancak bu aşamada bezin bebek cildiyle temas eden iç yüzeyinin beherin dışında kalacak şekilde

yerleştirilmesi önemlidir. Bunun temel sebebi, su buharının geçiş yönünü bebek bezi ürününün gerçek kullanımı sırasında olduğu gibi sağlamak yani bebek beze idrarını yaptıktan sonra bez içerisinde oluşan su buharının bezden dış ortama geçişini simüle etmektir. Desikatör içerisine yerleştirilen örnek bebek bezi numuneleri Şekil 7’de gösterilmektedir.



Şekil 7: Nefes alabilirlik testi uygulanacak bebek bezi numunelerinin teste hazırlanması.

Testlerde kanallı ve kanalsız olmak üzere 2 farklı türde bebek bezi numunesi kullanılmıştır. Kanallı bezlerde, kanal olarak adlandırılan bölge, emici tabaka malzemelerinin yer almadığı, malzeme yoğunluğunun bezin diğer bölgelerine göre düşük olduğu ve bundan dolayı da su buharı geçişini hızlandırabilecek bölgelerdir. Kullanılan bebek bezi numunelerinin özellikleri Tablo 2’de özetlenmiştir.

Tablo 2: Nefes alabilirlik testinde kullanılan bez numunelerinin özellikleri.

| Bebek Bezi | BR/NBR | Kanallı /Kanalsız |
|------------|--------|-------------------|
| A | BR | Kanalsız |
| B | NBR | Kanalsız |
| C | BR | Kanallı |
| D | NBR | Kanallı |

Çalışmanın üçüncü ve son aşamasında, bebeğin bebek bezi kullanmadan yalnızca iç çamaşırı giydiği durumu simüle etmek amacıyla pamuklu kumaş numunesi kullanılmıştır. Bu durumda nefes alabilirlik özelliği maksimum olacaktır ve bebek bezlerinin cildin nefes almasını ne ölçüde kısıtladığını anlamak amacıyla bu numunelerle test yapılması amaçlanmıştır. Test yöntemi, önceki ölçümlerde uygulanan prosedürle aynıdır. Sadece, giyim alışkanlıkları düşünülerek tek

katlı pamuklu kumaş ve çift katlı pamuklu kumaş olacak şekilde test numuneleri hazırlanmıştır. Hazırlanan numunelere ait görseller Şekil 8’de verilmiştir.



Şekil 8: Nefes alabilirlik testi uygulanacak pamuklu kumaş numunelerinin teste hazırlanması.

Literatürde karşılaşılan metotlarda, su buharı geçirgenliği hesaplanırken 2 farklı formül kullanıldığı görülmüştür:

$$WVTR = \frac{w}{t} \times \frac{x}{\Delta P \times A} \quad (1)$$

$$WVTR = \frac{24 \times M}{A \times t} \quad (2)$$

Formül 1’de yer alan w / t ifadesi, kararlı durumda sistem tarafından emilen su miktarının doğrusal regresyonla ($R^2 > 0.99$) hesaplanan eğimini temsil eder. Burada A, nem transferine maruz kalan film alanını ($1.539 \times 10^{-4} \text{ m}^2$), x ortalama numune kalınlığını ve ΔP ise 25 °C’deki filmin kısmi basınç farkını (kPa) ifade etmektedir [6].

Formül 2’de ise su buharı miktarı $\text{g/m}^2/\text{day}$ birim ölçüsünde hesaplanır. Burada M, zamana bağlı olarak beherdeki kütle değişimini (g); t, tartım alınana kadar sistemde bekletilen süreyi (h); A numunenin su buharı geçirgenliği ölçülen yüzey alanını (m^2) ifade etmektedir [2].

Bu çalışmada, literatürde sıklıkla karşılaşılan zamana bağlı su buharı geçirgenlik ölçüm yöntemlerinden farklı olarak, ürün performansına odaklanan ve zamana bağlı bir parametre kullanılmadan, ilgili özellikle ilgili olarak, belli bir süre sonunda

gerçekleşen toplam performansı ölçmek üzere geliştirilen alternatif bir metot sunulmuştur. Literatürde yer alan birçok çalışmada, genellikle saf su 25°C sıcaklığında bir desikatör ya da hareketli bir sistem içerisine yerleştirilmekte ve numunelerin kütle değişimleri belirli zaman aralıklarında (3, 6, 9, 12, 18 ve 24 saat) ölçülmektedir.

Literatürdeki çalışmalarda zamana bağlı bir buhar geçiş profili oluşturulmuş olsa da bu çalışmada kullanılacak metodolojide, 25 °C'deki su buharı geçiş hızının sınırlı olması nedeniyle, ürün performans değerlendirmesi etkin olarak yapılamamaktadır. Bu yüzden, çalışma kapsamında zamana bağlı bir buhar geçiş eğrisi yerine, zorlanmış koşullar altında gerçekleştirilen tek seferlik ölçümlerle numunelerin su buharı geçirgenlik performansları test edilmiştir.

Uygulanan yöntemde, her numune bir beherin ağzına gerdirilerek sabitlenmiştir. Beherin bulunduğu ortama kaynar su eklenmiş ve sistem, suyun ortam sıcaklığı olan 25 °C'ye kadar soğuması süresince gözlemlenmiştir. Bu süreçte yalnızca ilk ve son ölçüm değerleri arasındaki kütle farkı dikkate alınmıştır.

Bu fark, ilgili numunenin su buharı geçirgenliğine dair performans göstergesi olarak değerlendirilmiştir. Ölçülen kütle farkı, test esnasında buhar geçişi sağlanan numune yüzey alanına oranlanarak Formül 3'te ifade edilmiştir.

$$WVT = \frac{M}{A} \quad (3)$$

Elde edilen sonuçlarda, su buharı geçirgenliği literatürde belirtilen ve (g/m²·h) birimiyle su buharı geçirgenlik hızı yerine, toplam su buharı geçirgenliği (g/m²) olarak tanımlanmakta olup; bu değer, numunenin belli bir süre boyunca zorlanmış koşullarda buhar geçirgenliğine yönelik kabiliyetini göstermektedir.

III. BULGULAR VE TARTIŞMA

Çalışmanın ilk aşamasında, film örneklerinin nefes alabilirlik özellikleri, BR ve NBR olmak üzere iki gruba ayrılarak test edilmiştir. Test sonuçları Tablo 3'te verilmiştir.

Tablo 3: BR ve NBR PE Film numunelerinin toplam su buharı geçirgenlikleri.

| Numune | Silika jelin çektiği su miktarı, Toplam su buharı geçirgenliği (g/m ²) |
|-------------|------------------------------------------------------------------------------------------|
| BR PE Film | 2,22 |
| NBR PE Film | 0,06 |

Tablo 3'te görüldüğü üzere, NBR film numunelerinde tespit edilen su buharı geçiş miktarı oldukça düşüktür ve BR filminden 37 kat daha azdır. Test sonucunda, toplam buhar geçirgenliği NBR film için sıfır olarak kaydedilmese ve 0,06 g/m² bir veri tespit edilse de BR film ile NBR film arasındaki dramatik fark NBR filmin su buharı geçişine karşı neredeyse hiç geçirgen olmadığını ortaya koymaktadır. NBR film kullanılarak üretilen bir bebek bezinde üründe biriken sıvı, PE film kalınlığı boyunca dış ortama doğru buharlaşamaz ve bebeğin cildini BR filme göre çok daha nemli bırakarak kuru tutmakta yetersiz kalır. Bu da bebeğin cildinde pişik oluşum riskinin önemli ölçüde artması anlamına gelmektedir.

Buna karşın, BR filmler ise test süresince silika jelde anlamlı miktarda su buharı birikimine neden olmuştur. Ölçülen 2,22 g/m² değeri, bu filmlerin yüksek düzeyde buhar geçirgenliğine sahip olduğunu göstermektedir. Bu özellikteki ürün tarafından emilen ve ürün bünyesinde tutulan nem miktarı, NBR filme göre, çok daha az olduğu için bebek cildini kuru tutmakta daha başarılı olabileceğini söylemek mümkündür. Böylelikle, ciltteki ıslaklık miktarı azaltılarak pişik oluşumuna karşı daha koruyucu bir etki ve bu etkiye sahip bir ürün tasarlamaya olanak sağlanmış olur.

Tablo 4'te nefes alabilirlik özellikleri Tablo 3'te paylaşılmış olan PE filmler kullanılarak üretilmiş

bebek bezi ürünlerinin toplam su buharı geçirgenlikleri verilmiştir.

Tablo 4: Bebek bezi numunelerinin toplam su buharı geçirgenlikleri.

| Numune | Kanallı/ Kanalsız | BR/NBR | Toplam su buharı geçirgenliği (g/m ²) |
|------------|----------------------|--------|------------------------------------------------------------|
| Bebek bezi | Kanalsız | BR | 1,21 |
| Bebek bezi | Kanalsız | NBR | 0,18 |
| Bebek bezi | Kanallı | BR | 1,48 |
| Bebek bezi | Kanallı | NBR | 0,22 |

BR filmle üretilen bebek bezlerinin NBR filme üretilenlere göre 2 kat daha fazla nefes alabilir özellikte olduğu görülmektedir. Sadece PE filmle yapılan testlerde (ürüne dönüşmeden önceki durum, hammadde testi) BR filmin NBR filme göre 37 kat daha fazla nefes alabilir olduğu tespit edilmişti. Bu filmler kullanılarak elde edilen ürünlerle yapılan testlerde sonucunda elde edilen bu dramatik fark dış yüzey katmanının üzerinde konumlandırılan diğer bebek bezi bileşenlerinin su buharı geçişini büyük ölçüde kısıtladığını ortaya koymaktadır. Ancak yine de BR film kullanılarak elde edilen ürünün daha nefes alabilir özellikte olması ürünün cildi sağlıklı koşullarda tutması açısından kayda değer ve önemlidir.

Buhar geçişinin kısıtlanmadığı ve maksimum seviyede olduğu durum pamuklu kumaşlar kullanılarak test edilmiştir ve test sonuçları Tablo 5'te verilmiştir.

Tablo 5: Pamuklu kumaş numunelerinin toplam su buharı geçirgenlikleri.

| Ürün | Toplam su buharı geçirgenliği (g/m ²) |
|------------------------|------------------------------------------------------|
| Tek Kat Pamuklu Kumaş | 3,14 |
| Çift Kat Pamuklu Kumaş | 3,2 |

Tablo 5'te görüleceği üzere pamuklu kumaşın çift kat olarak kullanılması su buharı geçirgenliğini kısıtlamamakta ve her iki durumda da benzer sonuçlar elde edilmektedir.

Her ne kadar cildin nefes alabilirliği açısından pamuklu kumaşlar sentetik dokulara göre daha avantajlı görünse de cilt sağlığı ve pişik unsuru dikkate alındığında, bebek bezi kullanımının pişik riskini azalttığı görülmektedir.

Tüm numuneler için beherin ağız kısmındaki yüzey alanı 0,25 m² olarak hesaplanmıştır. Formül 3 kullanılarak tüm numunelerin su buharı geçirgenlikleri hesaplanmış ve aşağıdaki Tablo 6'da gösterilmiştir.

Tablo 6: Tüm numunelerin su buharı geçirgenlikleri.

| Numune No | Ürün | Kanallı/ Kanalsız | BR/NBR | Tek/ çift kat | Toplam su buharı geçirgenliği (g/m ²) |
|-----------|---------------|----------------------|--------|------------------|------------------------------------------------------------|
| 1 | PE film | - | BR | - | 2,22 |
| 2 | PE film | - | NBR | - | 0,06 |
| 3 | Bebek bezi | Kanalsız | BR | - | 1,21 |
| 4 | Bebek bezi | Kanalsız | NBR | - | 0,18 |
| 5 | Bebek bezi | Kanallı | BR | - | 1,48 |
| 6 | Bebek bezi | Kanallı | NBR | - | 0,22 |
| 7 | Pamuklu kumaş | - | - | Tek | 3,14 |
| 8 | Pamuklu kumaş | - | - | Çift | 3,2 |

Pamuklu kumaşa ait sonuçlar bebek bezi numuneleriyle karşılaştırıldığında pamuklu kumaşlarda (bebek bezi kullanmama durumu) su buharı geçirgenliğinin bebek bezine göre 2 kat azaldığı görülmüştür. Bu sonuçlara dayanarak, bebek bezi kullanıldığında kullanmama durumuna göre nefes alabilirlik özelliğinin 2 kat kısıtlandığı yorumunu yapmak mümkündür.

IV. SONUÇLAR

Bu çalışmada, bebek bezlerinin nefes alabilirliği su buharı geçirgenliği değerleri üzerinden 3 farklı aşamada incelenmiştir. İlk aşamada gerçekleştirilen analizlerde, BR film numunelerinin, NBR film numunelerine göre yaklaşık 37 kat daha fazla su buharı geçirgenliğine sahip olduğu tespit edilmiştir.

Çalışmanın ikinci aşamasında, ilgili hammaddeler kullanılarak elde edilen ürün formlarının sonuçları değerlendirilmiştir. BR film ürüne dönüştürüldüğünde elde edilen bebek bezlerinin toplam su buharı geçirgenliklerinde tek başına filme göre anlamlı bir değişim gözlenmemiştir.

Bu durum bezde kullanılan diğer katmanların fiber yapılı ve gözenekli katmanlar olması sebebiyle su buharı geçirgenliklerinin film kadar kısıtlayıcı olmamasıyla açıklanabilir. NBR bebek bezi, NBR filme kıyasla yaklaşık 3 kat daha yüksek nefes alabilirliğe sahiptir. BR film ile elde bezlerden farklı eğilimde olan bu sonuç film üretim prosesindeki farklılıklardan kaynaklanabilir. BR film üretim prosesinde filme nefes alabilir özellik kazandırmak amacıyla proses esnasında makine akış yönünde film gerdirilir. Bu gerdirme oranına paralel olarak da filmde gözenekler oluşur. NBR filmler daha düşük gerdirme oranlarında üretilirler. Dolayısıyla, filmin hala bir gerdirme payı mevcuttur. Bebek bezi üretimi esnasında makine konfigürasyonu ve PE filmin besleme noktasından makineye girene kadarki yolun uzunluğuna bağlı olarak maruz kaldığı çekme kuvveti değişkenlik gösterebilir. PE filmi makinede yürütmek üzere uygulanan bu çekme kuvveti hala bir gerdirme/uzama payı olan filmin nefes alabilirliğinin artmasına sebep olabilir. BR bebek bezi NBR bebek bezi ile karşılaştırıldığında 2 kat daha fazla nefes alabilir yapıda olduğu görülmektedir.

Çalışmanın üçüncü aşamasında pamuklu kumaşlar değerlendirildiğinde BR bebek bezine göre 2 kat daha fazla, NBR bebek bezine göre ise 5 kat daha fazla nefes alabilir olduğu gözlemlenmiştir. Pamuklu kumaş ve NBR bez arasındaki farkın fazla olması cildin nefes alması ve pişik oluşum riskinin azaltılması açısından BR bez kullanımının önemini ortaya koymaktadır.

TEŞEKKÜR

Bu çalışma, Evyap Sabun Yağ Gliserin Sanayi ve Ticaret Anonim Şirketi Ar-Ge Merkezi tarafından Ar-Ge projesi kapsamında desteklenmiştir.

KAYNAKLAR

[1] Uber M, Imoto R. R, Carvalho O. V, Cloth versus disposable diapers: an exploratory study on family habits, 2025, *Jornal de Pediatria*, Volume 101, Issue 2, 276-281, ISSN 0021-7557

<https://doi.org/10.1016/j.jpmed.2024.10.008>.

[2] Uyanık S, Kaynak K. H, 2018, A comparative study on the performance properties of breathable and non-breathable baby diaper back sheet. *Technical Journal*, 12, 74-78. <https://doi.org/10.31803/tg-20180125164806>

[3] Richer C, The Paradigm of Diaper Smell: How much WVTR is good enough in a baby diaper? 2014, *Nonwovens Industry*, https://www.nonwovens-industry.com/issues/2014-01-01/view_features/the-paradigm-of-diaper-smell/

[4] Perma-Chink Systems INC, 2025, What is a Breathable Film, USA, <https://www.permachink.com/resources/what-is-a-breathable-film>, Erişim tarihi: 13.04.25.

[5] I Stock by Getty Images, <https://www.istockphoto.com/tr/ill%C3%BCstrasyon/mattress-close-up>, Canada, Erişim Tarihi: 13.04.25.

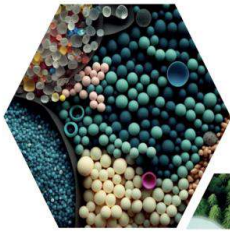
[6] Memiş S, Çemen Tohumu Bazlı Nanokil Katkılı Biyobozunur Nanokompozit Film Üretimi ve Karakterizasyonu, 2017, Yıldız Teknik Üniversitesi, Yüksek Lisans Tezi, Gıda Mühendisliği Anabilim Dalı.

[7] Aslan S, Şekil Hafızalı Polimer Esaslı Fonksiyonel Tekstil Yapılarının Geliştirilmesi, 2017, Süleyman Demirel Üniversitesi Fen Bilimleri Enstitüsü, Doktora Tezi, Tekstil Mühendisliği Anabilim Dalı.

*16. Uluslararası Lif ve Polimer Arařtırmaları Sempozyumu (16. ULPAS)
9-10 Mayıs 2025, İstanbul teknik Üniversitesi (İTÜ), Türkiye*

[8] SCA Hygiene Products AB, 2018, Göteborg, Sweden, WO2018038656A1.

[9] Hanry, E. L., & Surugau, N, 2024, Optimization of biomass-to-water ratio and glycerol content to develop antioxidant- enriched bioplastics from whole seaweed biomass of Kappaphycus sp. Journal of Applied Phycology, 36(2), 917–934, <https://doi.org/10.1007/s10811-024-03197-y>.



16

ULUSLARARASI
LİF VE POLİMER
ARAŞTIRMALARI
SEMPOZYUMU

16th INTERNATIONAL FIBER AND POLYMER RESEARCH SYMPOSIUM

Sürdürülebilir ve İşlevsel Lif ve Polimerler
Sustainable and Functional Fibers & Polymers



9-10 Mayıs
May 2025

İstanbul Teknik Üniversitesi
Gümüşsuyu Prof. Dr. Necmettin Erbakan Yerleşkesi
İstanbul Technical University
Gumussuyu Prof. Dr. Necmettin Erbakan Campus



Pad-batch boyamada üre kullanımını azaltmaya yönelik süreç iyileştirmesi

Perinur Koptur Tasan^a, Mustafa Çörekcioglu^a, Sultan Aras Elibüyük^a, Özlem Demir Günenç^a

^aOzanteks Tekstil San. ve Tic. A.Ş., 20020 Denizli, Türkiye.

*Perinur Koptur Tasan: perinur.koptur@ozanteks.com.tr

ÖZET

Pad-batch yöntemi, reaktif boyar maddelerle yapılan boyamalarda enerji tasarrufu sağlayan ve düşük tuz tüketimiyle çevre dostu bir proses olarak öne çıkmaktadır. Ancak bu yöntemde kumaşın nem dengesinin korunması ve boyar madde çözünürlüğünün sağlanması amacıyla genellikle yardımcı kimyasal olarak üre kullanılmaktadır. Üre kullanımı, özellikle yüksek sıcaklıkların hâkim olduğu yaz aylarında boyama kalitesi üzerinde kritik bir rol oynamakta, ancak aynı zamanda maliyet ve çevresel yük açısından dezavantaj oluşturmaktadır.

Bu çalışmada, işletme koşullarında üre kullanımını azaltmaya yönelik bir süreç iyileştirmesi gerçekleştirilmiş; sıcaklık değişimlerinin boyama sonuçları üzerindeki etkisi dikkate alınarak alternatif bir yaklaşım geliştirilmiştir. Yaz ve kış mevsimlerinde yapılan karşılaştırmalı denemeler ile sıcaklık kaynaklı farklılıklar analiz edilmiş, nem yönetiminin optimize edilmesiyle birlikte üre ihtiyacının azaltılabileceği gösterilmiştir. Çalışma sonucunda, yaz aylarında dahi istenen renk derinliği ve boyama haslıklarının üresiz veya düşük üreli reçetelerle sağlanabildiği görülmüş ve böylece hem kimyasal tüketimi hem de çevresel etki azaltılmıştır.

Elde edilen bulgular, pad-batch boyama prosesinin daha sürdürülebilir hâle getirilmesi yönünde önemli bir katkı sağlamaktadır ve tekstil işletmeleri için uygulanabilir bir dönüşüm modeli ortaya koymaktadır.

Anahtar Kelimeler: Pad-batch boyama; üre azaltımı; sürdürülebilir tekstil; reaktif boyama.

Process optimization aimed at reducing urea consumption in pad-batch dyeing

ABSTRACT

The pad-batch method is a dyeing process that stands out for providing energy savings and being environmentally friendly with low salt consumption, especially when reactive dyes are used. However, in this process, urea is commonly used as an auxiliary chemical to maintain the fabric's moisture balance and ensure the solubility of the dye. Urea usage

plays a critical role in dyeing quality, particularly during the summer months when high temperatures dominate, but it also presents disadvantages in terms of cost and environmental impact.

In this study, a process improvement aimed at reducing urea usage under operational conditions was carried out; an alternative approach was developed considering the effects of temperature fluctuations on dyeing results. Comparative experiments conducted in both summer and winter analyzed temperature-induced differences, and it was demonstrated that optimizing moisture management could reduce the need for urea. As a result, it was found that even in summer, desired color depth and dyeing fastness could be achieved with urea-free or low-urea formulations, thereby reducing both chemical consumption and environmental impact.

The findings provide a significant contribution to making the pad-batch dyeing process more sustainable and offer a practical transformation model for textile businesses.

Keywords: Pad-batch dyeing; urea reduction; sustainable textiles; reactive dyeing.

I. GİRİŞ

Tekstil endüstrisinde sürdürülebilir üretim yaklaşımlarına olan ilgi, artan çevresel kaygılar ve ekonomik baskılar nedeniyle her geçen gün önem kazanmaktadır. Özellikle boyama proseslerinde su, enerji ve kimyasal tüketimini azaltmaya yönelik teknikler, çevresel etkilerin minimize edilmesi açısından kritik rol oynamaktadır. Bu bağlamda, reaktif boyar maddelerle yapılan pad-batch yöntemi, düşük enerji tüketimi ve az tuz kullanımı gibi avantajlarıyla çevre dostu bir alternatif olarak öne çıkmaktadır [1].

Ancak bu yöntemin etkinliğini koruyabilmek için kumaşın nem seviyesinin dengelenmesi ve boyar maddelerin çözünürlüğünün sağlanması gerekmektedir. Bu amaçla, uygulamada genellikle yardımcı kimyasal olarak üre kullanılmakta, ancak bu kullanım hem maliyet hem de atık yükü açısından olumsuz sonuçlar doğurabilmektedir [2].

Literatürde, ürenin reaktif boyama sürecindeki işlevi ve performans etkisi üzerine çeşitli çalışmalar bulunmaktadır. Üre, özellikle düşük sıcaklıklarda boyar madde çözünürlüğünü artırarak renk verimliliğini iyileştirdiği bilinmektedir [1]. Bununla birlikte, özellikle yaz aylarında, sıcaklıkların arttığı

dönemde üre kullanımı daha yaygın hale gelir, çünkü yüksek sıcaklıklar boyama sürecinde kullanılan flotte sıcaklığını artırabilir, bu da boyar maddelerin etkinliğini yükseltir. Yaz sıcaklıkları, üreye olan ihtiyacı artırarak boyama sırasında çözünürlük ve renk derinliğini iyileştirebilir. Kış aylarında ise düşük sıcaklıklar nedeniyle çözünürlük ve etkinlik azalabilir [3].

Bu bilgiler ışığında, mevsimsel sıcaklık değişimlerinin pad-batch boyama üzerindeki etkilerinin değerlendirilmesi ve üre kullanımını azaltmaya yönelik sürdürülebilir yaklaşımların geliştirilmesi güncel ve uygulamaya dönük bir araştırma alanı olarak öne çıkmaktadır.

Bu çalışma, pad-batch yönteminde üre kullanımını azaltmaya yönelik alternatif bir yaklaşım geliştirmeyi ve farklı sıcaklık koşullarında proses parametrelerinin optimize edilmesini hedeflemektedir. Bu amaçla, üretim sürecinde sıcaklık değişimlerinin ve nem yönetiminin boyama performansı üzerindeki etkileri değerlendirilmiş, üre kullanımının en aza indirilmesine yönelik uygulanabilir bir iyileştirme önerisi sunulmuştur. Böylece hem kimyasal tüketimi hem de çevresel etkiler azaltılarak daha sürdürülebilir bir üretim yaklaşımı ortaya konmuştur.

II. DENEYSEL METOT / TEORİK METOD

Boyama işlemlerinde, %100 pamuklu kumaşlar kullanılmıştır. Kumaşlar, ön işleminden geçirilmiş ve tüm deney boyunca aynı parti kumaşlarla çalışılarak deneysel tutarlılık sağlanmıştır. Farklı renklerin boya etkinliğinin değerlendirilmesi amacıyla, çeşitli tonlarda boyama denemeleri yapılmıştır. Bu sayede, farklı renk gruplarının proses parametrelerine verdiği tepkiler ve üre kullanımına karşı duyarlılıkları analiz edilebilmiştir.

Pad-batch yöntemiyle gerçekleştirilen boyama işlemlerinde, sabit oranlarda boya, alkali ve ıslatıcı içeren üç farklı reçete hazırlanmıştır:

- %0 üre içeren (kontrol grubu)
- Azaltılmış üre içeren reçete
- Standart üre oranlı reçete (referans grup)

Boyama işlemini takiben, tüm numuneler sabunlama ve durulama adımlarından geçirilmiş ve ardından kurutulmuştur. Kurutulan kumaş numuneleri üzerinde renk ölçümleri spektrofotometre ile değerlendirilmiştir. Ek olarak, TS EN ISO 105-C06 standardına uygun olarak yıkama haslığı testleri gerçekleştirilmiş, boyaların kumaş üzerindeki kalıcılığı ve performansı karşılaştırmalı olarak analiz edilmiştir.

Ortam sıcaklıkları yüksek olduğunda kumaşların nemlendirilmesi için püskürtücü başlıklar kullanılmıştır.

III. BULGULAR VE TARTIŞMA

Çalışma kapsamında, pad-batch yönteminde farklı oranlarda üre kullanılarak gerçekleştirilen boyama işlemleri sonucunda elde edilen renk ölçümleri ve yıkama haslığı değerleri Tablo 1 ve 2’de sunulmuştur.

Denemelerde kullanılan düşük ve sıfır üre içeren reçetelerle yapılan boyamalarda, özellikle sıcaklık ve nem koşullarına bağlı olarak renk performansında anlamlı farklılıklar gözlemlenmiştir.

Tablo 1. Farklı Üre Oranlarında Ks ve ΔE Değerleri

| Numune | ΔE | Ks Değeri |
|---------------------|-----|-----------|
| R1 (kontrol) | 1,8 | 12,5 |
| R2 (azaltılmış üre) | 1,5 | 12,7 |
| R3 (referans) | 0 | 12,9 |

Tablo 2. Numunelerin evsel ve ticari yıkamaya karşı yıkama haslığı sonuçları

| | Kirlenme | | | | | |
|----------------------------|----------|-----|-----|----|-----|----|
| | WO | PAN | PES | PA | CO | CA |
| R1 (kontrol) | 5 | 5 | 5 | 5 | 4-5 | 5 |
| R2 (azaltılmış üre) | 5 | 5 | 5 | 5 | 4-5 | 5 |
| R3 (referans) | 5 | 5 | 5 | 5 | 5 | 5 |

Tablo verilerine göre, azaltılmış üre içeren reçetelerle elde edilen K/S ve ΔE değerleri, standart üre içeren reçetelerle benzer seviyelerde gerçekleşmiş ve bu durum bazı renk gruplarında boyar maddenin kumaşa etkin şekilde nüfuz ettiğini göstermiştir.

Evsel ve ticari yıkamaya karşı gerçekleştirilen yıkama haslığı testlerinde, tüm numuneler yüksek düzeyde performans sergilemiştir. Kirlenme değerleri incelendiğinde, üre içermeyen ve üre oranı azaltılmış reçetelerle boyanan kumaşların, sentetik (WO, PAN, PES, PA) ve selülozik (CA) elyaf türlerinde tam haslık (5) düzeyine ulaştığı görülmüştür. Pamuklu (CO) kumaşa ise çok iyi düzeyde (4/5) haslık değerleri elde edilmiştir.

Bu bulgular, üre miktarındaki azaltımın yıkama haslığı üzerinde belirgin bir olumsuzluk yaratmadığını; tüm reçetelerin kirlenme transferine karşı yüksek direnç gösterdiğini ve renk kalitesini koruduğunu ortaya koymaktadır.

Numunelerin sürtünme haslığı sonuçları Tablo 3’de verilmiştir.

Tablo 3. Numunelerin sürtünme haslığı sonuçları

| | Sürtme Haslığı | |
|----------------------------|----------------|------------|
| | Kuru Sürtme | Yaş Sürtme |
| R1 (kontrol) | 4-5 | 4-5 |
| R2 (azaltılmış üre) | 5 | 4-5 |
| R3 (referans) | 5 | 4-5 |

Tablo 3 incelendiğinde; üre miktarının azaltıldığı numunede, yaş sürtme haslığı kontrol ve referans gruplarına benzer şekilde yüksek düzeyde korunmuştur. Ancak kuru sürtme haslığı, standart üre oranı içeren reçetede en yüksek seviyede (5) gözlenmiş; üre azaltımı durumunda ise bu değerde hafif bir düşüş yaşanmıştır. Bu durum, ürenin boyarmaddenin lif yüzeyine bağlanma düzeyini artırıcı etkisine bağlı olarak yorumlanabilir. Genel olarak değerlendirildiğinde, üre azaltımı sürtünme haslığı üzerinde belirgin bir olumsuzluk yaratmazken, kuru sürtme açısından sınırlı bir etki gözlenmiştir.

Çalışma süresince ortam sıcaklığının yüksek olduğu koşullarda ürenin sistemden tamamen çıkarılması durumunda, özellikle koyu tonlarda renk nüfuzunun yetersiz kaldığı ve istenen renk derinliğinin elde edilemediği gözlemlenmiştir. Bu durum, boyarmaddenin kumaş yüzeyine eşit dağılmaması ve selüloz lifine sınırlı difüzyonuyla ilişkilendirilmiştir. Ancak üre kullanımını azaltırken sisteme entegre edilen yeni nesil püskürtme nodüllerinin etkisiyle, proses sırasında flotenin sıcaklığının kontrollü biçimde artırılması sayesinde bu olumsuzlukların büyük ölçüde önüne geçilmiştir. Elde edilen bulgular, nodül destekli püskürtme yöntemiyle sağlanan termal katkının, ürenin çözünürlük ve difüzyon üzerindeki işlevini kısmen yerine getirebildiğini göstermektedir. Böylece, üre kullanımında ciddi oranda azalma sağlanırken, renk sapmaları minimize edilmiş ve boyama kalitesi büyük oranda korunmuştur.

Çalışma kapsamında açık, orta ve koyu tonlarda farklı renk gruplarında boyama denemeleri gerçekleştirilmiş ve elde edilen veriler karşılaştırmalı olarak analiz edilmiştir. Ancak, temsili bir değerlendirme sunmak amacıyla yalnızca bir renk grubuna ait sonuçlar paylaşılmıştır. Diğer renk gruplarında da benzer eğilimler gözlemlenmiştir.

IV. SONUÇLAR

Bu çalışmada, pad-batch boyama prosesi kapsamında çevresel etkilerin azaltılması amacıyla üre kullanımının minimize edilmesi hedeflenmiştir. Organize sanayi bölgesi dışında yer alan işletmemizde, atık suyun arıtılması sorumluluğu tamamen firmamıza ait olduğundan, üre gibi azotlu kimyasalların kullanımı atık yükünü ve arıtma maliyetlerini artırmaktadır. Bu nedenle, boyama reçetelerinde üre kullanımı kademeli olarak azaltılmış ve belirli koşullarda tamamen elimine edilmiştir. Özellikle yaz aylarında ortam sıcaklığının yüksek olduğu dönemlerde, “çiller” olarak adlandırılan püskürtme sistemleri yardımıyla flotte sıcaklığı kontrol altında tutulmuş ve ürenin difüzyon ve çözünürlük üzerindeki işlevi fiziksel yöntemlerle karşılanmaya çalışılmıştır. Yapılan uygulamalar sonucunda, boyanan ürünlerin renk bütünlüğü, sürtünme haslığı ve genel kalite parametrelerinde herhangi bir olumsuzluk gözlenmemiştir. Elde edilen bulgular, uygun proses koşulları sağlandığında, üre kullanımının azaltılmasının hem çevresel sürdürülebilirlik hem de ürün kalitesi açısından mümkün olduğunu göstermektedir.

TEŞEKKÜR

Bu çalışma Ozanteks Tekstil Ar-Ge Merkezi tarafından Özkaynak projesi 24S01 numarası ile desteklenmiştir. Ayrıca bu çalışma TÜBİTAK 2244 Sanayi Doktora Programı kapsamında sürdürülebilir ürünlerin geliştirilmesine katkı sağlamaktadır.

KAYNAKLAR

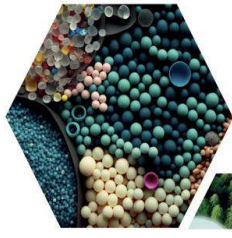
- [1] Textile Learner (2023) Reactive Dyes – Classification, Dyeing Mechanism and Factors. Textilelearner.net. <https://textilelearner.net/reactive-dyes-classification-dyeing-mechanism>.
- [2] Alay, E., Duran, K, Korlu, A. (2016) Sample work on green manufacturing in textile industry. Sustainable Chemistry and Pharmacy, 3, 39-46.

*16. Uluslararası Lif ve Polimer Arařtırmaları Sempozyumu (16. ULPAS)
9-10 Mayıs 2025, İstanbul teknik Üniversitesi (İTÜ), Türkiye*

[3] Broadbent AD (2001) Basic Principles of Textile Coloration. Society of Dyers and Colourists, Bradford

[4] Bechtold T, Turcanu A (2010) Application of reactive dyes in pad-batch dyeing processes. Text Chem Color 42(2):33–38

[5] Güngör Z, Demir A, Yılmaz T (2021) The effect of temperature and humidity in pad-batch dyeing of cotton fabrics. Tekstil ve Konfeksiyon 31(4):287–293



16 ULUSLARARASI
LİF VE POLİMER
ARAŞTIRMALARI
SEMPOZYUMU

16th INTERNATIONAL FIBER AND POLYMER RESEARCH SYMPOSIUM

Sürdürülebilir ve İşlevsel Lif ve Polimerler
Sustainable and Functional Fibers & Polymers



9-10 Mayıs
May 2025

İstanbul Teknik Üniversitesi
Gümüşsuyu Prof. Dr. Necmettin Erbakan Yerleşkesi
İstanbul Technical University
Gumussuyu Prof. Dr. Necmettin Erbakan Campus

The effect of stacking sequence on mechanical performance of hybrid natural fiber reinforced composites

Hülya Karaçeper^{a,b,*}, Ayşe Bedeloğlu^{a,*}

^aPolymer Materials Engineering, Bursa Technical University, 16310 Bursa, Türkiye.

^bMaterial Research & Validation Department, Sazcılar Automotive, 16140 Bursa, Türkiye.

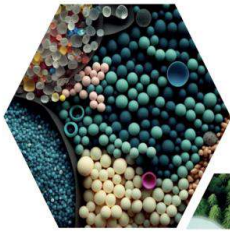
*Corresponding author: hulya.arslan@sazcilar.com.tr, ayse.bedeloglu@btu.edu.tr

ABSTRACT

Today, hybrid composite materials are attracting more and more attention due to their potential to combine superior mechanical and physical properties. The main objective of these materials is to design structures with optimum performance by utilizing the synergy of different reinforcement types. In this direction, hybrid composite systems that incorporate more than one reinforcement group have become an attractive research area.

In this study, four different groups of hybrid composites were produced using basalt, glass, and hemp reinforcements combined with polyester resin through the vacuum infusion method. Although the number of fiber layers was consistent across all samples, the stacking sequence of the fibers varied. The results showed that the highest compression strength was achieved when basalt fibers were positioned in the middle of the structure. In contrast, the highest tensile strength was obtained when hemp natural fiber was used as the outer skin layer. The samples that featured both basalt and glass fibers in the outer skin layer demonstrated the highest bending and inter-laminar shear strength. However, the stacking sequence of the fibers did not influence the impact and shear strength. This study not only enhances our understanding of fiber performance but also offers valuable guidance on how to strategically design fiber sequences tailored to meet the mechanical demands of composite parts in various applications.

Keywords: Hybrid composites; Natural Reinforced Composites; thermoset; composites; Vacuum infusion



16

ULUSLARARASI LİF VE POLİMER ARAŞTIRMALARI SEMPOZYUMU

16th INTERNATIONAL FIBER AND POLYMER RESEARCH SYMPOSIUM

Sürdürülebilir ve İşlevsel Lif ve Polimerler
Sustainable and Functional Fibers & Polymers



9-10 Mayıs
May 2025

İstanbul Teknik Üniversitesi
Gümüşsuyu Prof. Dr. Necmettin Erbakan Yerleşkesi
İstanbul Technical University
Gumussuyu Prof. Dr. Necmettin Erbakan Campus

Boyama proseslerinde proses entegrasyonu ve ekolojik kazanımlar: akrilik – ecocell karışımli seamless üretimde tek banyo uygulaması

Sultan Aras Elibüyük^a, Mustafa Çörekcioğlu^a, Perinur Koptur Tasan^a, Özlem Demir Günenç^a, Tülin Kaya Nacarkahya^b

^aOzanteks Tekstil San. ve Tic. A.Ş., Ar-Ge Merkezi, 20020 Denizli, Türkiye.

^bKarafiber Tekstil San. ve Tic. A.Ş., Ar-Ge Merkezi, Gaziantep, Turkey

*Sultan ARAS ELİBÜYÜK: saras@ozanteks.com.tr

ÖZET

Çevre ile ilgili artan bilinç ve iklim değişikliği sürdürülebilir üretimi artık gerekli kılmaktadır. Bu nedenle firmalar su tüketimi çok yüksek olan tekstil sektöründe insanlara ve çevreye zararlı yöntemler yerine alternatif teknolojiler ve maddeler aramaktadır. Boyahanelerde su tüketimini azaltmak için süreç değişikliklerine gidilmektedir. Sürdürülebilir ve çevreye zarar vermeyen farklı içeriklere sahip ipliklerle örülmüş kumaşların tek banyoda boyamalar ile ilgili literatürde çok çeşitli çalışmalar bulunmaktadır.

Bu çalışmada, dikişsiz örme yöntemi ile farklı akrilik iplikli içeren karışımlarda kumaşlara standart poliamid boyama prosesi uygulanmıştır. Tek seferde yapılan boyama yönteminde kumaşlarda melanj efekti olmaksızın parlak nüanslı renkler elde etmek amaçlanmıştır. Poliamid- Pamuk- Elastan (CO-PA-EA), Akrilik-Pamuk-Elastan (Akrilik-Co-EA) ve Ecocell-Akrilik-Poliamid-Elastan karışımli kumaşlar önce % 0,5 ve % 2 olacak şekilde RED DB ile çektirme yöntemi boyama yapılmıştır. Kumaşlara; Evsel ve ticari yıkamaya karşı renk haslığı – (ISO 105-C06), Sürtünmeye karşı renk haslığı tayini – (TS EN ISO 105-E04), Hidrofilite (AATCC 79 (sn)) testleri standartlarına uygun yapılmıştır. CIE LAB Değerleri spektrofotometre ile ölçülmüştür, Boncuklanma Dayanımı, Quick Dry Test ve Water Absorption Capacity testlerine tabi tutulmuştur. Poliamid denemelerinde test sonuçlarına bakıldığında pamuk karışımlarının daha parlak renk verdiğini gözlemlerken ecocell ve akrilik karışımli numunelerin daha mat renkler sergilemiştir. Fakat melanj efekti vermemiştir. Son deneme olarak daha parlak nüanslarda ve pastel tonlardan olan Yellow HF 4GL% 0,3gr boyama denemesi yapılmıştır. K/S değerlerinde başarı sağlanmış parlak ve melanj efekti olmayan kumaşlar elde edilmiştir. Sonuç olarak baktığımızda ise, tek seferde poliamid boyama prosesi ile akrilik içerikli kumaşlara boyamanın yapılabilirliği görülmüştür. Akrilik boyama proses adımı azaltılmış sudan kimyasaldan ve maliyetten tasarruf sağlanmıştır.

Anahtar Kelimeler: Dikişsiz giyim; sürdürülebilir üretim; Ecocell-Akrilik, Poliamid Karışımli Kumaş; K/S değeri, Tek Banyoda Akrilik Karışım Boyama

Process integration and ecological benefits in dyeing operations: single-bath application in seamless production of acrylic–ecocell blends

ABSTRACT

With the growing awareness of environmental challenges and the urgency of climate change, sustainable production methods have become essential, particularly in the water-intensive textile industry. This study investigates the feasibility and environmental benefits of single-bath dyeing processes applied to seamless fabrics composed of various acrylic-based yarn blends. The objective was to achieve bright and uniform color shades without melange effects using a standard polyamide dyeing procedure.

Seamless knitted fabrics consisting of PA-CO-EA (Polyamide-Cotton-Elastane), Acrylic-CO-EA (Acrylic-Cotton-Elastane), and Ecocell-Acrylic-PA-EA (Ecocell-Acrylic-Polyamide-Elastane) blends were dyed using the exhaustion method with RED DB at concentrations of 0.5% and 2%. A range of tests was conducted to evaluate dyeing performance and functional properties, including ISO 105-C06 (color fastness to washing), ISO 105-E04 (rubbing fastness), AATCC 79 (wettability), CIE LAB (spectrophotometric color analysis), pilling resistance, quick dry, and water absorption capacity. The results revealed that cotton-containing blends exhibited brighter colors, while Ecocell and acrylic blends showed more matte finishes, without creating a melange effect. In a final trial using Yellow HF 4GL at 0.3%, vivid pastel tones with high K/S values and no melange appearance were successfully achieved. In conclusion, the study demonstrates that acrylic-containing seamless fabrics can be effectively dyed using a single-bath polyamide dyeing process, eliminating the need for a separate acrylic dyeing step. This approach contributes to water, chemical, and cost savings, supporting the textile industry's shift toward more sustainable production practices

Keywords: Ecocell-Acrylic -Polyamide blended fabric; K/S value; seamless apparel; single-bath dyeing of acrylic blends; sustainable production

I. Giriş

Pamuk iplikleri, yüksek lif sayısı, yumuşak dokusu ve nefes alabilirliği ile tanınan tekstil endüstrisinin temel malzemelerinden biridir. Özellikle kumaş üretiminde geniş bir kullanım alanına sahip olan pamuk, kullanıcı konforu açısından birçok avantaj sunar. Hava dolaşımına izin vererek cildin nefes almasını sağlar ve terlemeyi azaltır. Bu nedenle yazlık giysilerden iç çamaşırlarına kadar birçok üründe kullanılır. Doğal bir lif olması sayesinde pamuk, çevre dostu bir seçenek olarak da öne çıkar. Sürdürülebilirliği ve geri dönüştürülebilirliği sayesinde küresel ısınmaya olan olumsuz etkisi daha düşüktür. Pamuk, farklı dokuma teknikleri ve iplik türleriyle harmanlanarak çeşitli dokular ve özellikler kazandırılabilir.

Akrilik iplikler ise sentetik lifler olup, tekstil sektöründe yumuşaklıkları, dayanıklılıkları ve renk

özellikleri ile bilinirler. İlk olarak 1940'lı yıllarda tescillenen akrilik lif, yün benzeri yapısı nedeniyle kışlık giyim ve ev tekstilinde yaygın olarak kullanılır [1]. Literatürde, akrilik ipliklerin yüksek ısı yalıtım özelliklerine sahip olduğu ve sıcaklığı etkili bir şekilde koruduğu belirtilmektedir. Akrilik ipliklerin bir diğer önemli özelliği ise renk tutma kapasiteleridir. Akrilik lifler boyayı iyi emdiği için kalıcı renklerin oluşmasını sağlar ve ürünlerde uzun süreli renk canlılığı sunar [2]. Bu özellik, özellikle moda ve dekorasyon alanlarında akrilik ipliklerin cazibesini artırır. Ayrıca, akrilik iplikler doğal liflere göre daha hafiftir, bu da kullanımda konfor sağlar ve giysilerin ağırlığını azaltır [3]. Akrilik ipliklerin dayanıklılığı ve elastikiyeti de önemli avantajlar sunar. Yüksek kopma direnci ve esnekliği ile uzun ömürlü tekstil ürünleri için uygundurlar. Aynı zamanda yıkama ve kurutma işlemlerine karşı dayanıklı olmaları ve bakım

kolaylığı, onları tercih sebebi yapar [4]. Bu özellikler sayesinde yüksek kaliteli akrilik iplikler hem performans hem estetik açıdan birçok avantaj sunar.

Lyocell lifleri ise çevre dostu üretim bileşenleri ve sürdürülebilir özellikleriyle öne çıkan ürünlerdir. Doğal kaynaklardan elde edilen biyopolimerlerin özel bir işlemle lifi dönüştürülmesiyle üretilen bu lifler, endüstride ekolojik alternatifler arayan tüketiciler tarafından özellikle tercih edilir [5]. Lyocell liflerinin en önemli özelliklerinden biri biyolojik olarak doğada çözünebilir olmasıdır [6]. Doğal kaynaklı bir malzeme olduğundan cilt dostu bir yapıya sahiptir ve alerjik hassasiyetleri olan bireyler için uygun bir seçenektir [7]. Doğal selüloz bazlı yapısı ve üstün nem yönetimi yeteneği ile Ecocell markalı lyocell lifi öne çıkar. Yüksek nem emme kapasitesi sayesinde vücut ısını düzenlemeye katkıda bulunur, konforu artırır ve yapısal rahatlık sağlar. Bu özellikler, spor giyim gibi yüksek performans ve konfor gerektiren uygulamalar için bu lifi ideal bir seçenek haline getirir. Lyocell lifleri ürünlerin ömrünü uzatır ve yıpranmalarını geciktirir. Bu dayanıklılık, sürdürülebilir bir ekonomi açısından önemlidir çünkü uzun ömürlü tekstil ürünleri sürekli değişim ihtiyacını azaltır ve büyüme kaynaklı etkileri minimize eder [8]. Ecocell, üretim sırasında düşük enerji ve su tüketimiyle çevre dostu bir alternatif sunar ve bu da onu sürdürülebilir tekstil üretimi için önemli bir çözüm haline getirir. Bu özellikler, çevresel etkileri azaltmaya yönelik büyümeyi destekler ve tekstil ekonomisinde sürdürülebilirliğe odaklanan üretim yaklaşımını güçlendirir.

Bu çalışmada seamless teknolojisi ile üretilmiş poliamid karışımı akrilik pamuk ve ecocell numunelerin tek banyoda boyanabilirlik özelliklerini çıkan test sonuçları ve proses adımının azalması ile gerçekleşen tasarruf miktarı incelenmiştir.

II. Deneysel Metot / Teorik Metot

Bu çalışmada, Aksa Akrilik tarafından geliştirilen reaktif boyanabilir akrilik lif, Karafiber Tekstil tarafından geliştirilen Ecocell lyocell lifi ve pamuk lifi, iplik üretim harmanında kullanılmıştır. İplikler Karafiber Tekstil tarafından üretilmiş, kumaş üretimi ve boyama işlemleri ise Ozanteks tarafından gerçekleştirilmiştir. Bu bağlamda, ring iplik eğirme sistemi kullanılarak Ne 40/1 numaralarında, %50 akrilik / %50 pamuk ve %50 akrilik / %50 Ecocell oranlarında harmanlanmış iplikler üretilmiştir. Üretilen bu iplikler, Ozanteks Tekstil'in Seamless örme biriminde Poliamid-Pamuk-Elastan (CO-PA-EA), Akrilik-Pamuk-Poliamid-Elastan (PAN-Co-EA) ve Ecocell-Akrilik-Poliamid-Elastan (Ecocell- PAN-PA-EA) karışımı kumaşlar tüp formunda üretilmiştir. Kumaşlar, numune parça boyama makinesinde tek banyoda RED RED DBR % 0,5 ve % 2 ile boya boyanmıştır. Boyama işleminin ardından kumaşlara Kumaşlara; Evsel ve ticari yıkamaya karşı renk haslığı – (ISO 105-C06), Sürtünmeye karşı renk haslığı tayini – (TS EN ISO 105-E04), Hidrofilite (AATCC 79 (sn)) testleri standartlarına uygun yapılmıştır. CIE LAB Değerleri spektrofotometre ile ölçülmüştür, Boncuklanma Dayanımı, Quick Dry Test ve Water Absorption Capacity testlerine tabi tutulmuştur.

III. Bulgular ve tartışma

Co/PA/EA, PAN/Co/PA/EA ve ecocell/PAN/PA/EA iplik karışımlarından üretilen kumaşların tek banyoda boyanabilirliğinin incelenmesi aşamasında yapılan test ve analizler alt başlıklar altında incelenmiştir.

Evsel ve ticari yıkamaya karşı renk haslığı – (ISO 105-C06) ve Sürtünmeye karşı renk haslığı – (TS EN ISO 105-E04)

Numunelerin yıkamaya karşı renk haslığı Tablo 1 ve sürtünme haslığı ölçümleri test sonuçları Tablo 2' de sunulmuştur. Haslık değerlendirmeleri, paslanmaz çelik kaplara eklenen 4 g/L ECE formüllü fosfatsız referans deterjan içeren 150 mL su çözeltisi kullanılarak gerçekleştirilmiştir. Boyalı numune, 25

çelik bilye ile birlikte kaba yerleştirilmiştir. Yıkama, 40°C'de 30 dk boyunca gerçekleştirilmiştir. Durulama ve kurutmadan sonra, numunenin ve miltifiber kumaşının rengindeki değişim, gri skala kullanılarak değerlendirilmiştir. Kuru ve ıslak sürtünme haslığı testleri, bir crockmeter cihazı kullanılarak gerçekleştirilmiştir.

Tablo 1. Numunelerin evsel ve ticari yıkamaya karşı yıkama haslığı sonuçları

| | Kirlenme | | | | | |
|-----------------------|----------|-----|-----|-----|-----|----|
| | WO | PAN | PES | PA | CO | CA |
| CO PA EA 0,5 | 5 | 5 | 5 | 5 | 5 | 5 |
| PAN CO PA EA 0,5 | 5 | 5 | 5 | 5 | 4/5 | 5 |
| Ecocell PAN PA EA 0,5 | 5 | 5 | 5 | 4-5 | 4-5 | 5 |
| CO PA EA 2,0 | 5 | 5 | 5 | 5 | 5 | 5 |
| PAN CO PA EA 2,0 | 5 | 5 | 5 | 5 | 5 | 5 |
| Ecocell PAN PA EA 2,0 | 5 | 5 | 5 | 5 | 4-5 | 5 |

Tablo 2. Numunelerin sürtünme haslığı sonuçları

| | Sürtme Haslığı | |
|-----------------------|----------------|------------|
| | Kuru Sürtme | Yaş Sürtme |
| CO PA EA 0,5 | 4-5 | 4-5 |
| PAN CO PA EA 0,5 | 5 | 4 |
| Ecocell PAN PA EA 0,5 | 5 | 4-5 |
| CO PA EA 2,0 | 5 | 4-5 |
| PAN CO PA EA 2,0 | 5 | 4-5 |
| Ecocell PAN PA EA 2,0 | 5 | 4-5 |

Hidrofilite testi (EN ISO 14697)

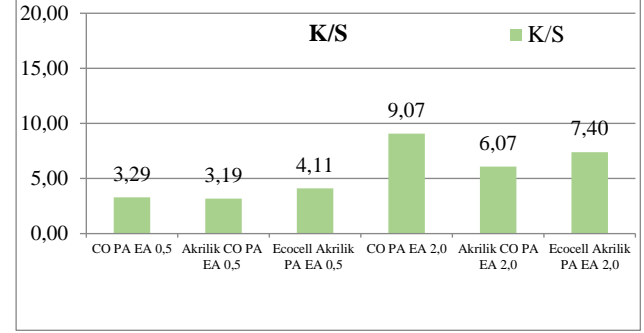
Kumaşlar 10x10 cm'lik parçalara kesilerek, ön yüzleri suya bakacak şekilde damıtılmış su dolu bir beherin yüzeyine düz bir şekilde bırakıldı. Kronometre ile numunenin tamamen ıslanması için gereken süre kaydedildi. Testlerden önce kumaşlar kondisyonlandı. Deney 5 kez daha tekrarlandı ve sonuçların aritmetik ortalaması hesaplanarak kumaşların ıslanma süreleri belirlendi. Ortalama süre ne kadar kısa ise kumaş o kadar emici olarak değerlendirildi. Hidrofilite testinin sonuçları Tablo 3'de sunulmaktadır.

Tablo 3. Hidrofilite test değerleri

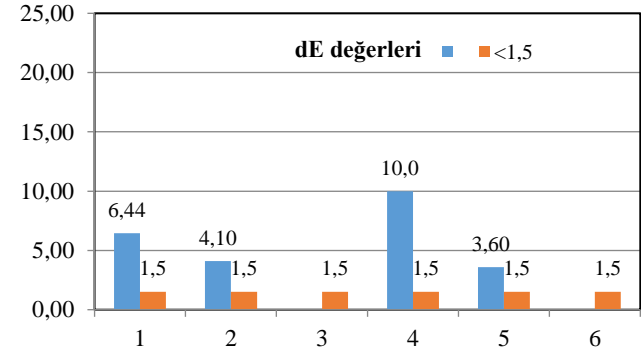
| | Hidrofilite (AATCC 79) |
|-----------------------|------------------------|
| CO PA EA 0,5 | 1,22 |
| PAN CO PA EA 0,5 | 1,04 |
| Ecocell PAN PA EA 0,5 | 1,15 |
| CO PA EA 2,0 | 1,35 |
| PAN CO PA EA 2,0 | 1,24 |
| Ecocell PAN PA EA 2,0 | 1,40 |

Spektrofotometre ile K/S değerlendirme testi

Kumaş renk değerlerinin ölçümleri D65 gün ışığında, 10° gözlem açısıyla yapıldı. K/S değerleri (Şekil 2) ve CIE Lab* dE değerleri (Şekil 3) spektrofotometre tarafından üretilen beş ölçümün ortalaması alınarak hesaplandı.



Şekil 2. Numunelerin K/S değerleri



Şekil 3. Numunelerin dE değerleri

Boncuklanma Dayanımı (TS EN ISO 12945-3)

Bu çalışmada, TS EN ISO 12945-3 Tekstil - Kumaşlarda yüzey tüylenmesi ve boncuklanma yatkınlığının tayini - Bölüm 2: Geliştirilmiş Martindale metodu ile 2000 tur sayısı için ölçüm yapılmıştır. Sonuçlar Tablo 4 de verilmektedir.

Tablo 4. Boncuklanma dayanımı test değerleri

| | Boncuklanma Dayanımı |
|-----------------------|----------------------|
| CO PA EA 0,5 | 4 |
| PAN CO PA EA 0,5 | 3 |
| Ecocell PAN PA EA 0,5 | 3 |
| CO PA EA 2,0 | 4 |
| PAN CO PA EA 2,0 | 3 |
| Ecocell PAN PA EA 2,0 | 3 |

Kolay kuruma testi ve su tutma kapasitesi testi

Tekstilde "kolay kuruma" testi, genellikle kumaşın ıslatıldıktan sonra belirli koşullar altında ne kadar sürede kurduğunu ölçmek için yapılan standartlaştırılmış bir laboratuvar testidir. Su tutma

kapasitesi testi ise; kumaşın kendi kuru ağırlığına göre ne kadar su tutabildiğini gösterir. Sonuçlar tablo 5 de verilmiştir.

Tablo 5. Kolay kuruma testi ve su tutma kapasitesi testi sonuçları

| | Kolay kuruma testi | Su tutma kapasitesi |
|-----------------------|--------------------|---------------------|
| CO PA EA 0,5 | 1,24 | 0,13 |
| PAN CO PA EA 0,5 | 1,66 | 0,15 |
| Ecocell PAN PA EA 0,5 | 1,36 | 0,16 |
| CO PA EA 2,0 | 1,28 | 0,13 |
| PAN CO PA EA 2,0 | 1,99 | 0,14 |
| Ecocell PAN PA EA 2,0 | 1,42 | 0,19 |

Çalışmada kullanılan seamless kumaşlar yukarıda belirtilen testlere tabi tutulmuştur. Yıkama haslığı çok iyi sonuçlar verirken, sürtünme haslığı değerlerinin beklentilerin bir puan altında kaldığı görülmüştür. Islak sürtünme haslığı için iyileştirme alternatifleri düşünülmelidir. Boyalı numunelerin renk verimi (K/S) ve CIE Lab* dE değerleri bir spektrofotometre kullanılarak ölçülmüştür.

%100 pamuklu poliamid elastan karışımı kırmızı boyalı kumaş olan kontrol kumaşının renk verimi (K/S değerleri) incelendiğinde değerlerin birbirlerine yakın olduğu görülmüştür. Kontrol numunelerine renk değerleri bakımından en yakın olan kumaşlar Akrilik-pamuk-poliamid-elastan karışımı kumaşlardır.

IV. Sonuçlar

Bu çalışmada, akrilik-pamuk-poliamid-elastan ve akrilik-ekosell-poliamid-elastan karışımı kumaşların tek bir banyoda tek seferde boyanması araştırılmaktadır. Kumaşların renk haslığı, yıkama haslığı, sürtünme haslığı, hidrofilisite ve K/S değerleri karşılaştırılmış ve kumaş üzerindeki etkileri incelenmiştir. Karışım kumaşların ve %100 pamuklu kumaşın haslık değerleri karşılaştırıldığında, yıkama ve sürtünme haslığı değerlerinin ticari olarak kabul edilebilir olduğu ve benzer sonuçlar gösterdiği bulunmuştur. Hidrofilisite testi, karışım kumaşların kontrol kumaşlarından daha hidrofilik olduğunu gösterdi. Karışım kumaşların K/S değerleri, kontrol

kumaşlarına kıyasla daha açıktı, hafif melanj ve mat bir renk gösteriyordu.

Poliamid denemelerinde test sonuçlarına bakıldığında pamuk karışımlarının daha parlak renk verdiğini gözlemlerken ecocell ve akrilik karışımı numunelerin daha mat renkler sergilemiştir. Fakat melanj efekti vermemiştir. Son deneme olarak daha parlak nüanslarda ve pastel tonlardan olan Yellow HF 4GL% 0,3gr boyama denemesi yapılmıştır. K/S değerlerinde başarı sağlanmış parlak ve melanj efekti olmayan kumaşlar elde edilmiştir. Sonuç olarak baktığımızda ise, tek seferde poliamid boyama prosesi ile akrilik içerikli kumaşlara boyamanın yapılabilirliği görülmüştür. Akrilik boyama proses adımı azaltılmış sudan kimyasaldan ve maliyetten tasarruf sağlanmıştır.

Teşekkür

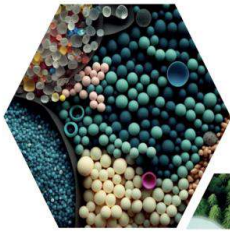
Bu çalışma Ozanteks Tekstil Ar-Ge Merkezi tarafından Özkaynak projesi 24SU01 numarası ile desteklenmekte olup Karafiber Tekstil Ar-Ge Merkezi ile ortak bir projedir. Ayrıca bu çalışma TÜBİTAK 2244 Endüstriyel Doktora Programı Projesi 119C070 numarası kapsamında sürdürülebilir ürünlerin geliştirilmesine katkı sağlamaktadır.

Kaynaklar:

- [1] Kirk-Othmer. (2000). Acrylic fibers. In Kirk-Othmer Encyclopedia of Chemical Technology (pp. 1- 10). John Wiley & Sons.
- [2] Karahan, M. (2013). Fiber and Textile Engineering. Ap
- [3] Wong, A. S., & Li, Y. (2005). Thermal comfort in clothing. In Improving Comfort in Clothing,
- [4] Kadolph, S. J. (2007). Textiles (10th ed., pp. 34
- [5] Borbély, E. (2008). Lyocell, the new generated cellulose. Acta Polytechnica Hungarica, 5(3)
- [6] Zhao, C., & Koo, K. (2020). Biodegradable fibers in the textile industry. Journal of Sustainable Textiles, 15(3), 210-224.
- [7] Lee, M., Kim, H., & Park, S. (2019). Environmentally friendly fibers and their applications in clothing. International Journal of Textile Research, 12(2), 8

*16. Uluslararası Lif ve Polimer Arařtırmaları Sempozyumu (16. ULPAS)
9-10 Mayıs 2025, İstanbul teknik Üniversitesi (İTÜ), Türkiye*

- [8] Taylor, R. (2018). Durability and environmental impact of sustainable fibers. Environmental Textile Journal, 22(4),



16

ULUSLARARASI LİF VE POLİMER ARAŞTIRMALARI SEMPOZYUMU

16th INTERNATIONAL FIBER AND POLYMER RESEARCH SYMPOSIUM

Sürdürülebilir ve İşlevsel Lif ve Polimerler
Sustainable and Functional Fibers & Polymers



9-10 Mayıs
May 2025

İstanbul Teknik Üniversitesi
Gümüşsuyu Prof. Dr. Necmettin Erbakan Yerleşkesi
İstanbul Technical University
Gumussuyu Prof. Dr. Necmettin Erbakan Campus

Sentetik İpliklerde Kullanılan Spin Finish Yağının Geliştirilmesi: Performans ve Verimlilik Açısından OPU Değerlerinin İncelenmesi

Naciye GÜL^a, Merve KANDEMİR^{b,*}

^a Petro Yağ ve Kimyasallar San. ve Tic. A.Ş., Petro Yağ Araştırma ve Geliştirme Merkezi, Gebze, Kocaeli, Türkiye

^b Petro Yağ ve Kimyasallar San. ve Tic. A.Ş., Petro Yağ Araştırma ve Geliştirme Merkezi, Gebze, Kocaeli, Türkiye

*Naciye GÜL: naciye.gul@petroyag.com

ÖZET

Tekstil sektörü, dünya genelinde birçok ülkenin ekonomisinde önemli bir rol oynamakta ve sektördeki teknolojik gelişmeler ve ürün yenilikleri, küresel pazarlarda büyük etkiler yaratmaktadır. Tekstil sanayisinde, iplik, kumaş ve elyaf üretim süreçlerinde çeşitli yağlayıcılar kullanılmaktadır. Bu yağlayıcı gruplarından biri olan spin finish yağı, çok yönlü fonksiyonel özellikleriyle dikkat çekmektedir. Sentetik iplik üretiminde statik elektrik yüklerinin birikimi engellemek için tasarlanmış özel yağlayıcılardır. Spin finish yağları işlem sırasında ipliklerin aşınmasını önlerken, metal-metal ve lif-lif arasındaki dengeli yapışmayı sağlayarak, statik yük oluşumunu azaltır. Yüksek termal stabiliteye sahip olup dumanlanma oluşturmaz. Antibakteriyel etkisi ve emülsiyon edilebilir olmaları sayesinde sulu sistemlerde kullanım kolaylığı sağlar.

Bu çalışma kapsamında, sentetik iplik üretiminde kullanılmak üzere, ipliğe antistatik özellik kazandırarak sarım işlemini kolaylaştıran yeni bir spin finish yağı formülasyonu geliştirilmiştir. Formülasyon, baz yağ ve çeşitli performans katkı maddelerini içermektedir. Geliştirilen formülasyon, endüstriyel ölçekli sentetik iplik üretimi sırasında uygulanmış ve iplik numunelerinde manuel yöntemle yapılan yağ alma miktarı (Oil Pick-Up -OPU) analizleri, formülasyonun etkinliğini ortaya koymuştur. Çalışma sonunda, geliştirilen spin finish formülasyonu, sentetik iplik üretiminde statik yük miktarını başarılı bir şekilde azalttığı, aynı zamanda yağlayıcı özellikleri ile ipliğin sarım performansını kolaylaştırdığı belirlenmiştir. Ayrıca, sistemin yüksek sıcaklıklara karşı termal stabilitesinin güçlü olduğu, üretim sürecinde dumanlanma ve bozunma göstermediği belirlenmiştir. Bu bulgular, formülasyonun hem işlevsel verimlilik hem de proses uyumluluğu açısından sentetik iplik üretiminde etkin bir katkı maddesi olarak kullanılabileceğini ortaya koymaktadır.

Anahtar Kelimeler: Spin Finish; Antistatik; Sentetik iplik; Yağ miktarı; Tekstil

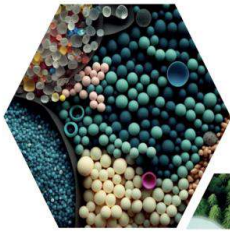
Development of Spin Finish Oil Used in Synthetic Yarns: Examination of OPU Values in Terms of Performance and Efficiency

ABSTRACT

The textile sector plays a significant role in the economy of many countries worldwide, and technological advancements and product innovations within the industry have substantial impacts on global markets. In the textile industry, various lubricants are used during yarn, fabric, and fiber production processes. One such group of lubricants is spin finish oil, which is notable for its multifunctional properties. These are specially designed lubricants used in synthetic yarn production to prevent the accumulation of static electric charges. Spin finish oils prevent yarn abrasion during processing and reduce static charge formation by ensuring balanced adhesion between metal-metal and fiber-fiber interfaces. They possess high thermal stability and do not produce fumes. Thanks to their antibacterial effect and emulsifiability, they are easy to use in aqueous systems.

In this study, a new spin finish oil formulation was developed for use in synthetic yarn production, aimed at imparting antistatic properties to the yarn and facilitating the winding process. The formulation consists of a base oil and various performance additives. The developed formulation was applied during industrial-scale synthetic yarn production, and the oil pick-up (OPU) analyses carried out manually on the yarn samples demonstrated the formulation's effectiveness. At the conclusion of the study, it was determined that the developed spin finish formulation successfully reduced the amount of static charge in synthetic yarn production and, through its lubricating properties, facilitated the winding performance of the yarn. Additionally, it was observed that the system exhibited strong thermal stability against high temperatures and did not produce fumes or degradation during the production process. These findings demonstrate that the formulation can be effectively used as a functional and process-compatible additive in synthetic yarn production.

Keywords: Spin Finish; Antistatic; Synthetic yarn; Oil content; Textile



16

ULUSLARARASI LİF VE POLİMER ARAŞTIRMALARI SEMPOZYUMU

16th INTERNATIONAL FIBER AND POLYMER RESEARCH SYMPOSIUM

Sürdürülebilir ve İşlevsel Lif ve Polimerler
Sustainable and Functional Fibers & Polymers



9-10 Mayıs
May 2025

İstanbul Teknik Üniversitesi
Gümüşsuyu Prof. Dr. Necmettin Erbakan Yerleşkesi
İstanbul Technical University
Gumussuyu Prof. Dr. Necmettin Erbakan Campus

Ortopedik biyomedikal uygulamalar için kolajen ile modifiye edilmiş polilaktik asit esaslı hammadde geliştirilmesi

Ayşegül Uzuner-Demir^a, Zehra Betül Ahi^{b,*}, Beyza Çay^b

^aKocaeli Üniversitesi, Polimer Bilimi ve Teknolojisi Bölümü, Kocaeli, 41380, Türkiye

^bKazlıçeşme Ar&Ge Merkezi, İstanbul, 34956, Türkiye

*Sorumlu Yazar: zehraahi@kazlicesme.com.tr

ÖZET

Bu çalışmada, ortopedik biyomedikal uygulamalar için kolajen ile modifiye edilmiş polilaktik asit (PLA) esaslı biyokompozit bir hammadde geliştirilmiştir. PLA, halka açılma polimerizasyonu ile L- ve D-laktit dimerlerinden sentezlenmiş, molekül ağırlığı heksametilen diizosiyanat (HDI) zincir uzatıcı kullanılarak artırılmıştır. Optimum koşullarda sentezlenen PLAÖB10 örneği, 159.844 Da ağırlıkça molekül ağırlığına ulaşarak hedeflenen yapısal özellikleri sağlamıştır. Elde edilen PLA, kolajen, hidroksiapatit (HA), polietilen glikol (PEG) ve 1,4-fenilen diizosiyanat (PDI) ile harmanlanarak ekstrüzyon ve enjeksiyon yöntemleriyle kalıplanmıştır.

Geliştirilen biyokompozitler FTIR, DSC, TGA, GPC ve SEM analizleri ile karakterize edilmiş; ayrıca mekanik dayanım, kristalizasyon davranışı, hidrofiliklik, yüzey morfolojisi ve MTT biyoyumluluk testleri gerçekleştirilmiştir. Sert kemik doku uygulamaları için %70 PLA, %10 kolajen, %20 HA içeren formülasyon (PLAÖB10-1), yumuşak doku içinse %70 PLA, %20 kolajen, %10 HA, %10 PEG içeren yapı (PLAÖB10-2) optimum olarak belirlenmiştir. Test sonuçları, geliştirilen ürünün ≥ 40 MPa çekme dayanımı, >300 °C termal stabilitesi, %90'ın üzerinde hücre canlılığı ve düşük yüzey temas açısı ile hedeflenen performans düzeylerini karşıladığını göstermektedir. Elde edilen bulgular, biyopolimer temelli kompozitlerin, fonksiyonel modifikasyonlarla doku mühendisliği ve rejeneratif tıp alanlarında güçlü bir alternatif oluşturabileceğini ortaya koymaktadır.

Anahtar Kelimeler: Polilaktik asit; Kolajen; Hidroksiapatit; Biyomedikal kompozitler; Halka açılma polimerizasyonu

Development of collagen-modified polylactic acid based raw material for orthopedic biomedical applications

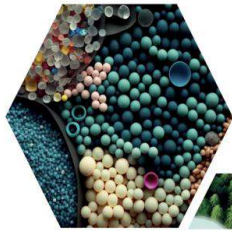
ABSTRACT

In this study, a collagen-modified polylactic acid (PLA)-based biocomposite raw material was developed for orthopedic biomedical applications. PLA was synthesized via ring-opening polymerization of L- and D-lactide dimers, and its molecular weight was increased using hexamethylene diisocyanate (HDI) as a chain extender. The optimized PLA

sample (PLAÖB10) achieved a weight-average molecular weight of 159,844 Da, meeting the structural property requirements for biomedical use. The synthesized PLA was compounded collagen, hydroxyapatite (HA), polyethylene glycol (PEG), and 1,3-propanediisocyanate (PDI) through extrusion and injection molding techniques.

The resulting PLA-based biocomposites were characterized by FTIR, DSC, TGA, GPC, and SEM analyses. Additionally, mechanical strength, crystallization behavior, hydrophilicity, surface morphology, and MTT-based biocompatibility assays were conducted. The formulation consisting of 70% PLA, 10% collagen, and 20% HA (PLAÖB10-1) was found optimal for hard bone tissue applications, while the formulation with 70% PLA, 20% collagen, 10% HA, and 10% PEG (PLAÖB10-2) was identified as suitable for soft tissue. The developed materials exhibited a tensile strength above 40 MPa, thermal stability exceeding 300 °C, surface contact angles indicating improved wettability, and cell viability rates over 90%, confirming their performance targets. These findings demonstrate that PLA-based composites, modified with natural biopolymers, can be tailored into high-performance, biocompatible materials, offering a promising alternative for orthopedic applications in tissue engineering and regenerative medicine.

Keywords: Polylactic acid; Collagen; Hydroxyapatite; Biomedical composites; Ring-opening polymerization



16 ULUSLARARASI
LİF VE POLİMER
ARAŞTIRMALARI
SEMPOZYUMU

16th INTERNATIONAL FIBER AND POLYMER RESEARCH SYMPOSIUM

Sürdürülebilir ve İşlevsel Lif ve Polimerler
Sustainable and Functional Fibers & Polymers



9-10 Mayıs
May 2025

İstanbul Teknik Üniversitesi
Gümüşsuyu Prof. Dr. Necmettin Erbakan Yerleşkesi
İstanbul Technical University
Gumussuyu Prof. Dr. Necmettin Erbakan Campus

Design of bone powder-enhanced cage structures for kyphoplasty application in vertebral compression fractures

Zeynep Turna^{a,*}, Serkan Yıldız^b, Şebnem Düzyer Gebizli^c, Çağatay Öztürk^d, Aslı Hockenberger^e, Şehime Gülsün Temel^f

^aBiomaterials, Bursa Uludag University, 16110 Bursa, Türkiye.

^{b,c}Textile Engineering, Bursa Uludag University, 16110 Bursa, Türkiye.

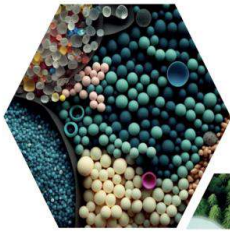
^d, Medicine, Istinye University, 34340 İstanbul, Türkiye.

*Corresponding author: biyomuhendis.zeynepturna@gmail.com

ABSTRACT

Vertebral compression fractures resulting from osteoporosis or trauma compromise spinal integrity and often require surgical intervention. Kyphoplasty is a minimally invasive technique aimed at restoring vertebral height by inserting and inflating a balloon within the fractured vertebra, followed by the injection of bone cement into the created cavity. In this study, electrospun cage systems composed of biocompatible and biodegradable poly(butylene succinate) (PBS) reinforced with bone powder were developed to enhance mechanical support and prevent cement leakage. A 10% (w/v) PBS solution was prepared using a chloroform and dimethylformamide (DMF) mixture, with the addition of 5% bone powder to achieve optimal viscosity for the electrospinning process. Electrospinning was performed under the following parameters: a feed rate of 1.0 mL/h, a tip-to-collector distance of 15 cm, and an applied voltage of 20 kV. The resulting nanofibrous surfaces were morphologically evaluated under a light microscope and exhibited visually homogeneous and defect-free fiber formation under selected conditions. The incorporation of bone powder into biocompatible PBS improved the mechanical stability of the structure and is considered promising for enhancing compatibility with bone tissue. The nanofibrous layers are designed to act as an internal mold that may assist in guiding cement placement while reducing leakage risk. Preliminary observations suggest potential for bone powder-reinforced PBS nanofiber scaffolds in kyphoplasty applications; however, further quantitative and in vivo evaluations are needed to confirm their efficacy.

Keywords: Kyphoplasty; Vertebral Compression Fracture; Electrospinning; Poly(butylene succinate) (PBS); Bone Powder; Nanofiber Scaffold; Cement Leakage Prevention; Biocompatibility; Mechanical Reinforcement; Spinal Augmentation



16

ULUSLARARASI
LİF VE POLİMER
ARAŞTIRMALARI
SEMPOZYUMU

16th INTERNATIONAL FIBER AND POLYMER RESEARCH SYMPOSIUM

Sürdürülebilir ve İşlevsel Lif ve Polimerler
Sustainable and Functional Fibers & Polymers



9-10 Mayıs
May 2025

İstanbul Teknik Üniversitesi
Gümüşsuyu Prof. Dr. Necmettin Erbakan Yerleşkesi
İstanbul Technical University
Gumussuyu Prof. Dr. Necmettin Erbakan Campus

Farklı orijinli pamuk liflerinin iplik kalite özellikleri üzerine etkilerinin incelenmesi

Yusuf Şenel^a, Ekin Ünlü^a, Mustafa Şıhlı Der^a

^aBiska Tekstil San. Tic. ve A.Ş., 27090, Gaziantep, Türkiye.

*Sorumlu Yazar: yusufsenel632@gmail.com

ÖZET

Tekstil endüstrisi, gelişen üretim teknolojileri ve artan üretim kapasitesi ile birlikte önemli bir dönüşüm geçirmiştir. Küresel rekabetin giderek yoğunlaşması ve tüketici beklentilerinin yükselmesi, tekstil ürünlerinden beklenen performans kriterlerini de daha ileri seviyelere taşımıştır. Günümüzde tekstil ürünlerinde kalite, yalnızca estetik ve konforla sınırlı kalmayıp, mukavemet, aşınma direnci, esneklik, renk haslığı ve genel dayanıklılık gibi çok boyutlu performans göstergeleri ile değerlendirilmekte; bu durum üretim süreçlerinde hata toleranslarını minimum seviyeye indirme zorunluluğunu doğurmaktadır. Tekstil ürünlerinin mekanik ve fiziksel özellikleri, kullanılan hammaddenin niteliklerine ve üretim süreçlerine doğrudan bağlıdır. İplik üretiminde özellikle pamuk gibi doğal liflerin morfolojik, fiziksel ve kimyasal özellikleri, nihai ürünün performansını belirleyen en kritik değişkenler arasında yer almaktadır. Pamuk liflerinin uzunluğu, inceliği (mikroner değeri), olgunluğu, mukavemeti, esnekliği ve içerdiği yabancı madde oranı gibi parametreler, üretilen ipliğin mukavemet, düzgünlük, tüylülük, esneklik ve boyama davranışları gibi özelliklerini doğrudan etkilemektedir. Bu nedenle, farklı kullanım alanları için optimum iplik özelliklerinin elde edilebilmesi, uygun hammadde seçimi veya karışımı ve üretim parametrelerinin hassas şekilde kontrol edilmesini gerektirmektedir.

Bu çalışmada, farklı orijinli (farklı yörelere ait) pamuk lifleri ile farklı karışım oranlarında iplik numuneleri üretilmiştir. Kullanılan pamuk numunelerinden tip-1; ortalama 29 mm uzunluk, 5.19 mic kalınlık, %8 kısa lif oranı, 29,9 g/tex mukavemet ve %7 uzama değerlerine sahipken, tip-2; ortalama 31 mm uzunluk, 4,94 mic kalınlık, %7,4 kısa lif oranı, 32,33 g/tex mukavemet ve 8,3% uzama değerlerine sahiptir. Yapılan farklı karışım oranları iplik dayanım özelliklerini yanı sıra kalite değerlerinin iyileştirilmesi hedeflenmiştir. İplik numarası ve eğirme yöntemi sabit tutularak pamuk lif özelliklerinin iplik mukavemet ve kalite değerleri üzerindeki etkileri incelenmiştir. Sunulan çalışmada iki farklı orijinli pamuk lifi, üç farklı karışım oranlarında iplik numunelerinin üretilmesinde kullanılmıştır. Sonuç olarak, pamuk lif özelliklerinin iplik mukavemet ve kalite değerleri üzerine etkileri ortaya konulmuştur. Elde edilen sonuçlara göre iplik yapısı içerisinde tip-2 pamuk oranı artırıldığında kalite parametresi olan IPI (imperfections) değerlerinde yaklaşık %45 iyileşme sağlanırken, mukavemet değerlerinde %6'lık bir artış elde edilmiştir. Yapılan literatür araştırmasında; Gordon ve Fakirov (2020), pamuk lif uzunluğu parametrelerinin (UHML, UI, SF) iplik kalitesiyle ilişkisini istatistiksel modellerle incelemiştir. Çalışmada, ortalama lif uzunluğu (UHML-Upper Half Mean Length)'in iplik mukavemetiyle en güçlü korelasyona sahip olduğu, kısa lif oranının (Short Fiber Index) >%20 olmasının ise iplik düzensizliğini artırdığı belirlenmiştir. Özellikle ince iplik üretiminde düzgünsüzlük (UI-Uniformity Index)'in kritik öneme sahip olduğu vurgulanmıştır. Zhang ve Wang (2021), organik ve konvansiyonel pamuk yetiştirme sistemlerinin lif kalite indeksi (Fiber Quality Index) ve SCI (Spinning

Consistency Index) üzerindeki etkilerini karşılaştırmıştır. Organik pamuğun daha tutarlı bir eğirme performansı (yüksek SCI) sergilediği, buna karşın konvansiyonel pamuğun pestisit kullanımı nedeniyle daha yüksek lif mukavemetine ulaştığı tespit edilmiştir. Bennett ve Myers (2019), pamuk genotipi, yaprak döküm zamanı ve mevsimsel koşulların lif kesitsel özelliklerine etkisini incelemiştir. Erken yaprak dökümünün lif olgunluğunu azaltarak iplik kalitesini düşürdüğü, uzun lifli genotiplerin (ör. Pima) ise iplik mukavemetini %15 artırdığı tespit edilmiştir. Sonuç olarak elde edilen bulguların literatürden elde edilen çıktılar ile örtüştüğü, pamuk lif karışımında ortalama lif uzunluğu ve lif mukavemeti artışının iplik mukavemet ve kalite değerlerini iyileştirdiği belirlenmiştir.

Anahtar Kelimeler: Ring eğirme; Pamuk ipliği; Pamuk lif özellikleri; İplik kalite özellikleri; İplik mukavemeti

Investigation of the effects of cotton fibres from different origin on yarn quality properties

ABSTRACT

The textile industry has undergone a significant transformation, driven by the development of production technologies and the expansion of production capacity. The intensification of global competition and the escalating expectations of consumers have elevated the performance criteria expected from textile products to unprecedented levels. The quality of textile products is now evaluated not only by aesthetic and ergonomic criteria, but also by a range of performance indicators, including strength, abrasion resistance, flexibility, colour fastness and general durability. This has led to a need to minimise fault tolerances in production processes. The mechanical and physical properties of textile products are directly dependent on the qualities of the raw material used and the production processes. In yarn production, the morphological, physical and chemical properties of natural fibres such as cotton are among the most critical variables that determine the performance of the final product. Parameters such as length, fineness (micronaire value), maturity, strength, elasticity and foreign matter content of cotton fibres directly affect the properties of the yarn, including strength, evenness, hairiness, elasticity and dyeing behaviour. Consequently, the achievement of optimal yarn properties for diverse applications necessitates the selection or combination of appropriate raw materials and the meticulous regulation of production parameters.

In this study, yarn samples were produced with cotton fibres of different origin (from different regions) at different blend ratios. Among the cotton samples used, type-1 has an average length of 29 mm, 5.19 mic thickness, 8% short fibre ratio, 29.9 g/tex strength and 7% elongation, while type-2 has an average length of 31 mm, 4.94 mic thickness, 7.4% short fibre ratio, 32.33 g/tex strength and 8.3% elongation. It was aimed to improve the yarn strength properties as well as quality values with different blend ratios. The effects of cotton fibre properties on yarn strength and quality values were investigated by keeping the yarn count and spinning method constant. In the present study, cotton fibres of two different origins were used to produce yarn samples at three different blend ratios. As a result, the effects of cotton fibre properties on yarn strength and quality values were revealed. According to the results obtained, when the ratio of type-2 cotton in the yarn structure is increased, an improvement of approximately 45% is achieved in IPI (imperfections) values, which is a quality parameter, while an increase of 6% is obtained in strength values. In the literature research; Gordon and Fakirov (2020) examined the relationship between cotton fibre length parameters (UHML, UI, SF) and yarn quality with statistical models. In the study, it was determined that the average fibre length (UHML-Upper Half Mean Length) has the strongest correlation with the yarn strength, while the short fibre ratio (Short Fibre Index) >20% increases the yarn irregularity. It is emphasised that the unevenness (UI-Uniformity Index) is of critical importance

especially in fine yarn production. Zhang and Wang (2021) compared the effects of organic and conventional cotton growing systems on Fibre Quality Index (FQI) and Spinning Consistency Index (SCI). It was found that organic cotton exhibited a more consistent spinning performance (higher SCI), whereas conventional cotton achieved higher fibre strength due to the use of pesticides. Bennett and Myers (2019) examined the effect of cotton genotype, defoliation time and seasonal conditions on fibre cross-sectional properties. It was found that early defoliation decreased yarn quality by reducing fibre maturity, while long-fibre genotypes (e.g. Pima) increased yarn strength by 15%. As a result, it was determined that the findings obtained agreed with the outputs obtained from the literature and that the increase in average fibre length and fibre strength in cotton fibre blend improved yarn strength and quality values.

Keywords: Ring spinning; Cotton yarn; Cotton fibre properties; Yarn quality properties; Yarn strength



Green synthesized selenium nanoparticles attached electrospun polycaprolactone nanofiber mats for fast photo degradation of dyes

Sezin Demirci^{a,b}, Nalan Oya San Keskin^{b,*}

^aNanosan Laboratory, Department of Biology, Polatlı Science and Literature Faculty, Ankara Hacı Bayram Veli University, 06900 Ankara, Türkiye

^bInstitute of Graduate Programs and Department of Biology, Polatlı Science and Literature Faculty, Ankara Hacı Bayram Veli University, 06900 Ankara, Türkiye

*Corresponding author: nalan.san@hbv.edu.tr

ABSTRACT

In recent years, nanofibers have emerged as one of the sustainable routes that can be applied in wastewater treatment. Herein, we reported the preparation of electrospun Polycaprolactone nanofibers (PCL-Nfs) attached with Selenium nanoparticles (SeNPs) synthesized via bacteria supernatant and their application in the photocatalytic degradation of Methylene Blue (MB) and Reactive Blue (RB). TEM observations revealed the spherical shape of biogenic selenium (Se) particles with ~ 130 nm diameters. Also, PCL-Nfs and SeNP attached PCL-Nfs was examined by SEM. In addition, EDX analysis confirmed the presence of Se elements in the nanofiber structure. Initially, 10 ppm MB dye was photodegraded in the presence of SeNPs with up to 80% degradation efficiency under UV irradiation after 1 hours. Furthermore, SeNPs attached onto the PCL-Nfs with by a dipping method for 1 hour, 24 hour and 4 day and used for the dye removal. The degradation percentage reached up to 90% after 1h using SeNPs attached PCL-Nfs. The photocatalytic performance of the biogenic SeNPs revealed that the RB degradation was also 12.40 ± 0.09%. However, SeNPs exhibited rapid adsorption of RB, removal reaching up to 95.65 ± 0% at pH 2. According to the removal rates, 4 days attachment was more effective at removal compared to another of attachment times. Moreover, the as-prepared mats have also tested for the reusability after four cycles and ~ 37% of the MB decolorization capacity was obtained. These results underline the use of effective, low-cost and easily available mats for the degradation of dyes from wastewater.

Keywords: Biogenic Nanoparticles; Degradation; Nanofiber, Photocatalyst; Wastewater treatment



Development of yarn tension sensor for winding machines

Ibrahim GEZGIN^a, Recep EREN^{b,*}

^aTextile Engineering department, Bursa Uludag University, Bursa, 16059, Türkiye.

^bTextile Engineering department, Bursa Uludag University, Bursa, 16059, Türkiye

*Corresponding author: 502317019@ogr.uludag.edu.tr

ABSTRACT

Control of yarn tension is an important parameter in high quality bobbin winding machines to keep winding homogeneity constant from empty to full bobbin. Measurement of tension is essential for each winding unit to control and monitor the tension of individual bobbins in high precision in winding machines. Available tension sensors in the market are costly to use and limits the competitiveness for especially local winding machine manufacturers. This presentation makes an attempt to develop a strain gauge based cheaper tension measurement sensor for winding machines. A small size thin metal plate (aluminium and steel) was used in 25mmx15mm size and 4 strain gauges were fixed on the upper and lower surfaces and wheatstone bridge circuit was formed. The yarn tension was converted to voltage and then signal was amplified and filtered. A commercial tension sensor and developed one were used together on a test stand with a winding unit. Yarn tension from both sensors were read and recorded with short time intervals and evaluated. It was shown that the developed sensor and the commercial sensor recorded very similar tension traces. Changing filtering frequency also changed the yarn tension traces. It was concluded that using the same filtering frequency can give very close yarn tension trace to commercial sensor. As a final conclusion the developed sensor could be used with industrial winding machines if it is supported with proper filtering and amplifier circuits, developed for this sensor.

Keywords: Yarn Tension; Tension Sensor; Winding; Strain Gauges

16th International Fiber and Polymer Research Symposium (16th ULPAS)
9-10 May, 2025, Istanbul technical University (ITU), Istanbul, Türkiye

BURSALI

INVESTIGATION OF THE DYEABILITY OF CELLULOSIC PRODUCTS WITH PRETREATMENT AND REACTANT DYESTUFFS IN ONE BATH

Sevil GÜNÇ, Saliha Büşra KARAKELLE, Eyüphan YENER

Abstract

The dyeing process of cellulosic products consists of four stages: pre-treatment, dyeing, washing and finishing. These processes take an average of 8 hours and the chemical waste load is high. Different studies are needed to minimise the environmental impacts of this situation. The project created in this context is a dyeing process initiated for the dyeing of raw cotton products in a single bath without pre-treatment. In this process, dyeing process is carried out without using pre-treatment process and bleaching chemicals applied to the fabric. With the chemical and dyeing processes developed in this context, the raw (hydrophilic and untreated fabric structure) fabric was dyed with reactive dyestuff.



Results

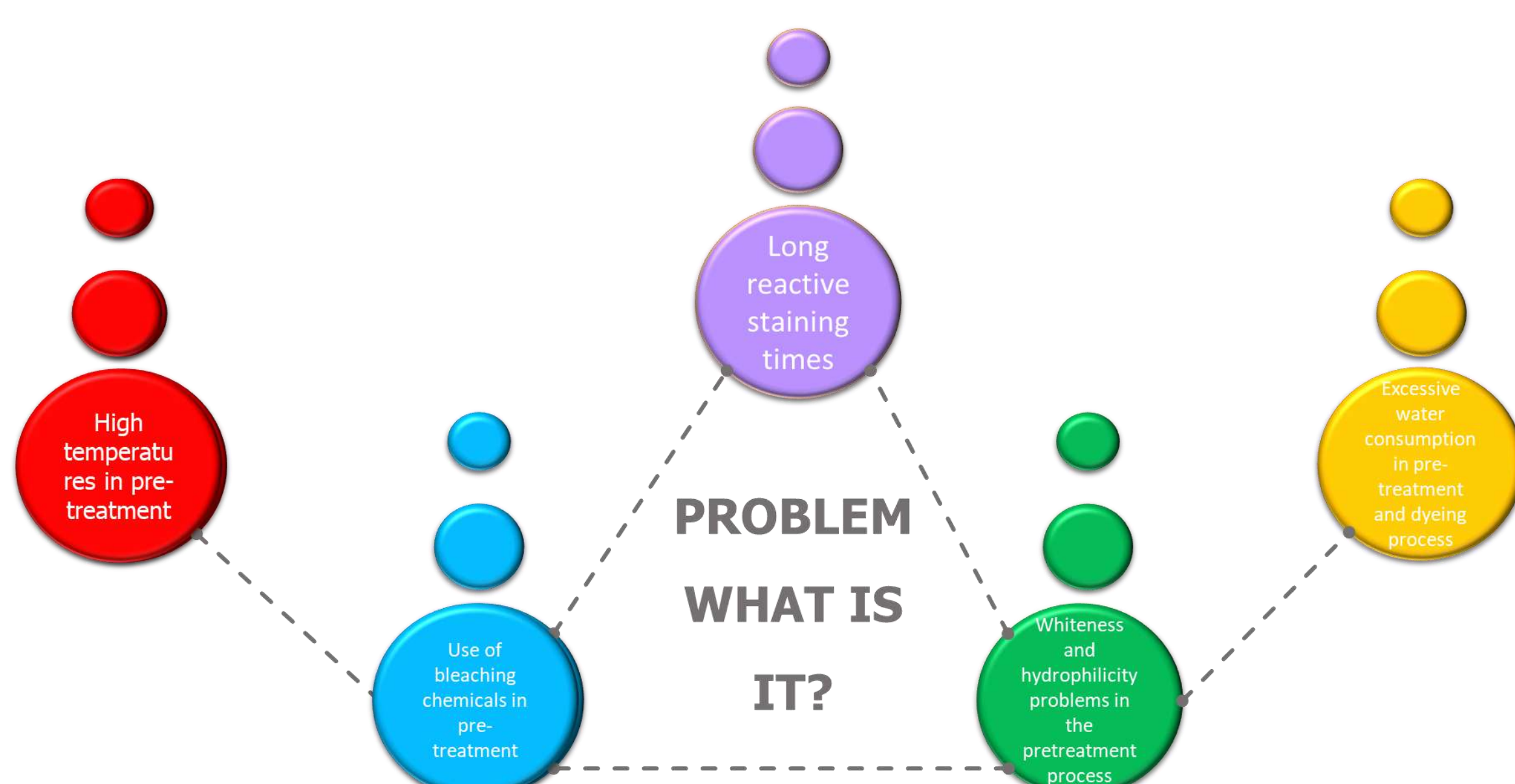
In the literature study, single bath dyeing processes using enzymes were generally found. When these processes were examined, it was observed that the dyeing process was generally carried out after a pre-treatment. Within the scope of the project; chemicals that can provide hydrophilicity and can be used in the same bath with the dyestuff instead of the chemicals used in the traditional pretreatment process have been determined and supplied. Prescriptions were created in the determined ratios and the process of raw yarns and fabrics with reactive dyestuffs in a single bath was started. Optimisation studies were carried out on time, temperatures and chemical ratios for both yarn and fabric in dyeing recipes. After the dyeing, the fabric surfaces were compared with the original dyed fabrics and the colour differences (ΔE) values were compared on the DataColor device. In addition, washing and rubbing fastness tests were applied to the samples obtained. When the results of all physical and chemical tests performed within the scope of the project were analysed; the values obtained in the conventional dyeing process were reached. In the first stage, the process was extended to medium and dark tone dye recipes.

| | |
|------------|------------|
| COLOR CODE | 152734 |
| COLOR NAME | Purple |
| DATE | 27.03.2023 |

| | Dry | Wet | Acetate | Cotton | Nylon | Pes | Acrylic | Wool | ΔE | Hydrophilicity |
|------------|-----|-----|---------|--------|-------|-----|---------|------|------------|----------------|
| pH Reglast | 4/5 | 3/4 | 4/5 | 4 | 4/5 | 4/5 | 4 | 4/5 | 1.44 | 3.51 |
| pH Reglast | 4/5 | 3/4 | 4/5 | 3/4 | 4/5 | 4/5 | 4/5 | 4/5 | 0.68 | 3.55 |
| pH Reglast | 4/5 | 3/4 | 4/5 | 3/4 | 4/5 | 4/5 | 4/5 | 4/5 | 1.17 | 5.08 |
| pH Reglast | 4/5 | 3/4 | 4/5 | 3/4 | 4/5 | 4/5 | 4/5 | 4/5 | 0.79 | 5.10 |
| pH Reglast | 4/5 | 3/4 | 4/5 | 3/4 | 4/5 | 4/5 | 4/5 | 4/5 | 0.76 | 7.51 |
| pH Reglast | 4/5 | 3/4 | 4/5 | 3/4 | 4/5 | 4/5 | 4/5 | 4/5 | 0.41 | 7.15 |
| pH Reglast | 4/5 | 3/4 | 4/5 | 3/4 | 4/5 | 4/5 | 4 | 4/5 | 0.42 | 6.02 |
| pH Reglast | 4/5 | 3/4 | 4/5 | 3/4 | 4/5 | 4/5 | 4/5 | 4/5 | 0.64 | 5.15 |

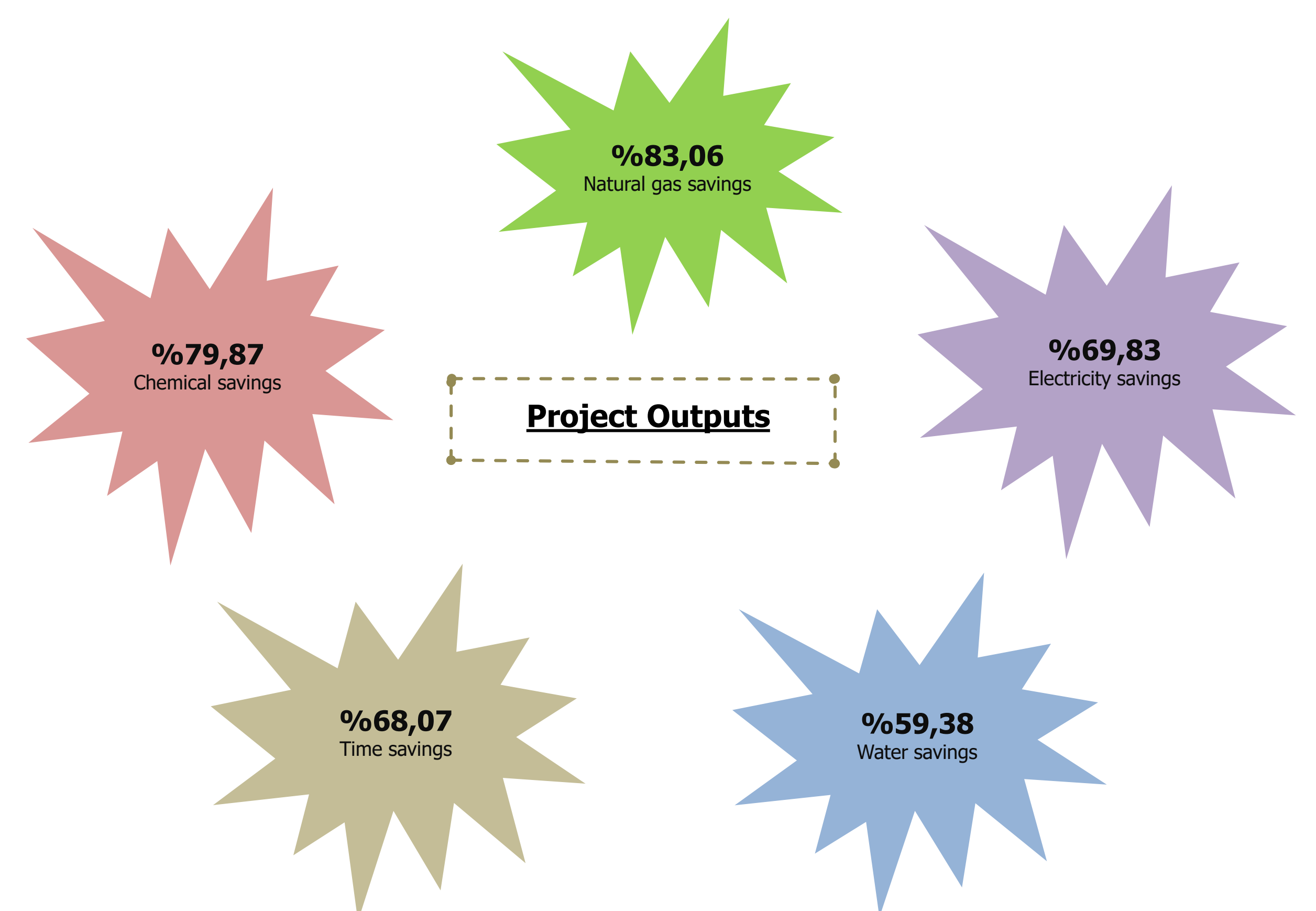
Experimental

- In production, the pre-treatment process is carried out at 98°C - 45 minutes.
- During this process, auxiliary and bleaching chemicals are used and the pollution load of the pretreatment bath increases (Hydrogen peroxide: 4g/L, caustic: 3 g/L, wetting and stabiliser: 1g/L).
- Together with the loading and preparation of the fabric, this step takes approximately 4-5 hours.
- Then, the fabric surface is dyed in the desired colours after whiteness and hydrophilicity are achieved.
- At this stage, dyeing auxiliary chemicals are used as well as dyestuffs. Then, it is transferred to drying and garment.
- Within the scope of the project developed; it is aimed to create a final product by proceeding to the dyeing step without pre-treatment of cotton fabrics woven in raw form.
- With this project, dyeing was carried out in a single bath without the need for any pre-treatment.



Discussion

- With the developed process, an environmentally friendly dyeing process has been introduced to the textile industry by using less energy, water and chemicals in reactive dyeing.
- The project output has been protected with a Patent Application and Patent registration is pending by the Turkish Patent and Trademark Office. Patent Application Number: 2022/016800.



16th International Fiber and Polymer Research Symposium (16th ULPAS)

9-10 May, 2025, Istanbul technical University (ITU), Istanbul, Türkiye

BURSALI

DEVELOPMENT OF ECOLOGICAL NON-SLIP MATS WITH INCREASED CONTACT SURFACE

Sümeyye REÇEL ASLAN, Sevil GÜNÇ, Saliha Büşra KARAKELLE

Abstract

In order to provide non-slip effect in existing bath mat products, some coating methods are applied with silicone. However, after some time after the product is used, the silicone breaks, cracks, mold formation and lack of washing resistance, as well as the harmful chemical structures contained in silicone by some customers and the test standards they apply, we have pushed us to search for new sources. In our new product, it was preferred to use a technical yarn with PVC coated around it. In this way, the desired effects will be given to the product directly during production and there will be no need for extra processes and costs.



Experimental

PVC coated yarn was procured as a result of the researches carried out to ensure non-slip and stable stance effect with yarn. Many weave shapes were tried with this yarn and the mat weaving with the weave in the last image was realized by making the necessary adjustments in the machine.

The yarn does not contain any substances that are harmful to human health, as well as the functional properties it provides itself:

- Anti-Bacterial,
- Anti-Fungal,
- High Strength,Washable,
- It does not disintegrate easily,
- Stable fabric structureDirt, mold, oil,
- salt, chemicals and UV resistance,
- Resistant up to 160°C,
- Flame retardant due to its structure,
- Non-carcinogenic PVC component.



is one of the advantages of the yarn to the existing product. [3]

In order to prove the non-slip effect of the woven mat, it was tested at **UZGE (National Floor Safety Institute)** according to TS EN 14231 standard and as a result, it was proved that it has a lower slip potential compared to standard mats.

| Classification | Pendulum value | Cof | Slip potential |
|----------------|----------------|-----------|-----------------|
| Z | < 24 | < 0.25 | Very high → (5) |
| Y | 25-34 | 0.25-0.34 | High → (4) |
| X | 35-44 | 0.36-0.46 | Middle → (3) |
| W | 45-54 | 0.47-0.59 | Low → (2) |
| V | > 54 | > 59 | Very low → (1) |

Table 1. Interpretation of slip resistance according to slip potential [2]

While the Slip Potential of the standard mats is **3**, the Slip Potential of the PVC Floor Mat is evaluated as **2**.

Results

Project outcome,

The PVC yarn used in the mat product, which is the output of the project, has not shown any deformation in the final product even after 30 washes, and there is no shrinkage in the dimensional stability of the product,

- Compared to a standard 100% cotton mat, the PVC yarn used in the structure of the product is observed to dry faster than the current situation,
- The fact that the PVC-coated yarn used in our developed mat product has not been used in towel weaving looms before adds richness to the project in terms of its innovative and R&D quality.
- After the literature research, a Utility Model application numbered **2020/04339** was made for the mat product produced with PVC yarn.

The result is an innovative product that complies with European and US test standards and is harmless to the environment and human health.



References

- [1] "Investigation of the Process Parameters Affecting the Single Face Coating Process Using the Roller Top Knife Method," Textiles and Engineering, vol. 18, no. 84, pp. 15-22, 2011.
- [2]G. Çoşkun and G. Sarıışık, "Slip Safety Risk Analysis of Surface Properties by Determining the Coefficients of Friction (COF) of Natural Stones," Cumhuri. Univ. Fac. Sci. Sci. J., vol. 38, no. 2, pp. 219-233, 2017.
- [3]F. Retardant, www.tepar.com.
- [4]D. Eyl and D. Yavuzkasap, "An investigation on the mechanical properties of upholstery fabrics," 2011.

16th International Fiber and Polymer Research Symposium (16th ULPAS)

9-10 May, 2025, Istanbul technical University (ITU), Istanbul, Türkiye

BURSALI

APPLICATION OF INTERMINGLING TO NATURAL YARNS TO IMPROVE THE COMFORT PROPERTIES OF PRODUCTS

Sümeyye REÇEL ASLAN, Eyüphan YENER, Saliha Büşra KARAKELLE

Abstract

Products with pile structures have an important place in the home textile sector. Especially low twist yarns are desired to be used in the formation of these pile structures. However, since low-twist yarns alone do not meet the tensions to be exposed to weaving, they are woven by folding with synthetic structured PVA. The fact that the PVA yarn used cannot be completely removed in the finishing stages, is harmful to the environment and causes extra costs has led to the search for different solutions in the sector to increase the strength of low twist yarns. This study is the first time that the intermingling process, which was previously used to improve the handle of synthetic yarns, has been applied to a natural yarn.

Experimental

Intermingling process is mixed with the separation of the filaments forming the yarn by entering the effect of the turbulent and cold air-jet impinging the yarn in the vertical direction and the separation of the filaments that form the yarn and the winding of the separated filaments back to each other in the regions where the air flow is partially reduced. The result is a complex collective structure. Since the center jet fails to open this part when the previously mixed part comes in front of it, the opened and mixed sections follow each other. In this way, the filaments in the yarn are brought together.

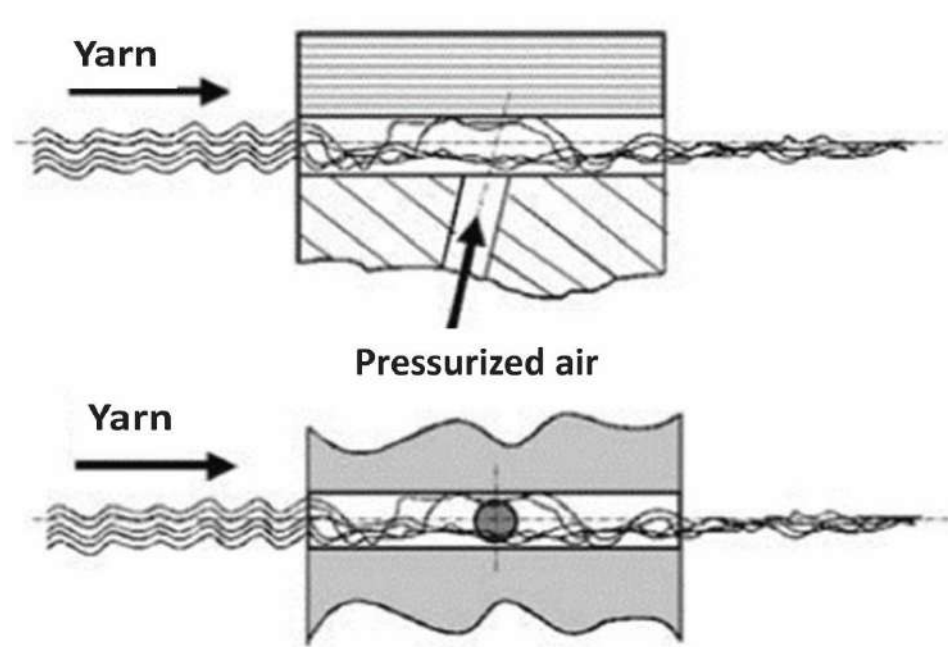


Figure 1. As compressed air flows, the filaments are mixed by random vibration [1]

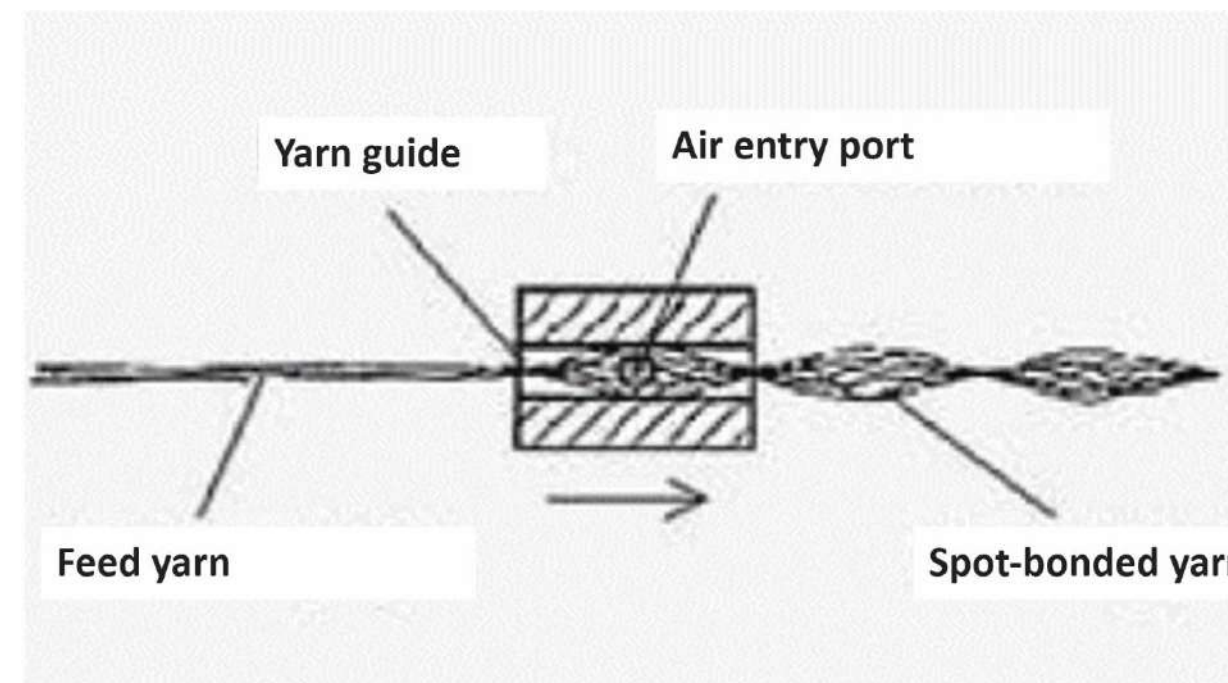


Figure 2. A tailstock is formed before and after the continuously flowing compressed air inlet hole [1]

Intermingling process was applied to Ne12/1 cotton yarns with the method shown in Figure 1 and Figure 2. As a result of the process, it is aimed to increase the existing hairiness of the yarn. The strength comparison of the results of the centering process with the centerless yarn, the sizing breaking strengths of the centered and main yarn were tested with the TITAN 5 device in accordance with TS EN ISO 2062 standard and the graphs are as follows:

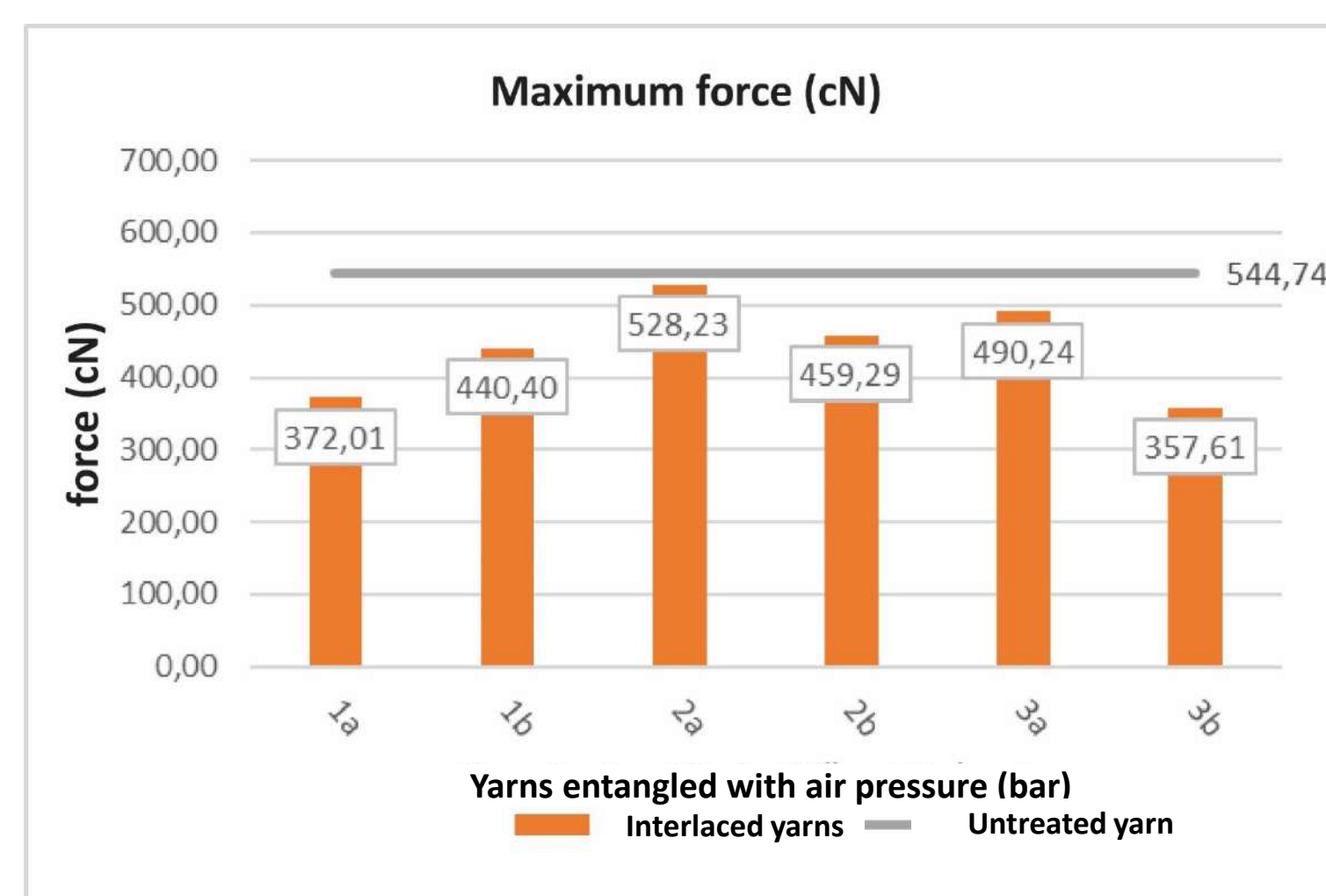


Figure 3. Strength results of Ne 12/1 yarn at different bar pressures (*a and b symbolize different level headings.)

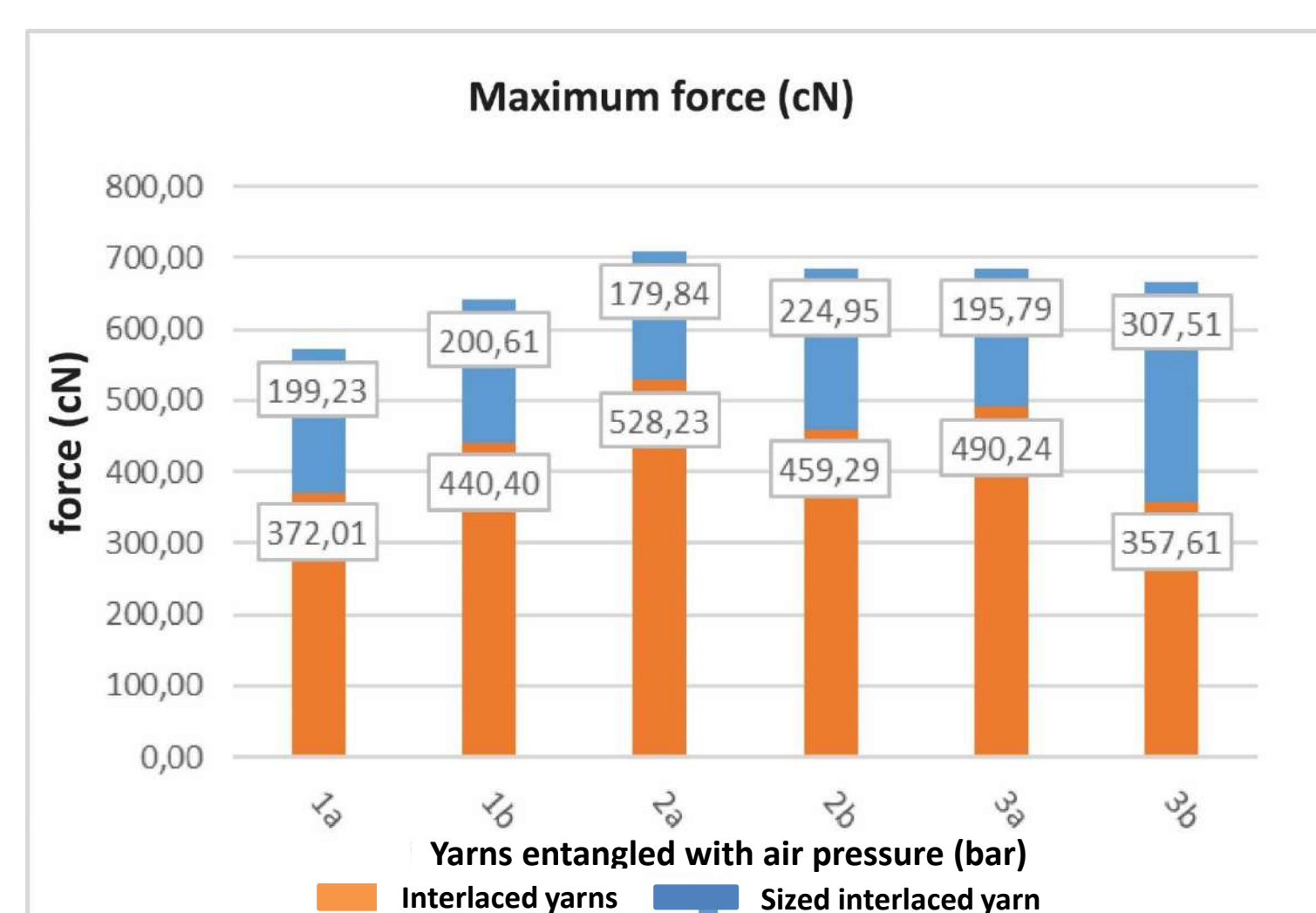


Figure 4. Strength results of Ne12/1 intermingled yarn after sizing (*a and b symbolize different level headings.)

The comparison of centerless yarn and centerless yarn strength, center yarn and main yarn breaking strength tested with TITAN 5 device in accordance with TS EN ISO 2062 standard are given in Figure 3 and Figure 4.

Results



Figure 2. A tailstock is formed before and after the continuously flowing compressed air inlet hole. [5]

As a result of the intermingling process performed with certain pressure and speed, the strength of the low twist cotton yarn increased and the hairiness increased visibly.

The main yarn and the center-treated yarns were carried out using the Zweigle G567 hairiness measuring device and the values are shown in the adjacent graph:

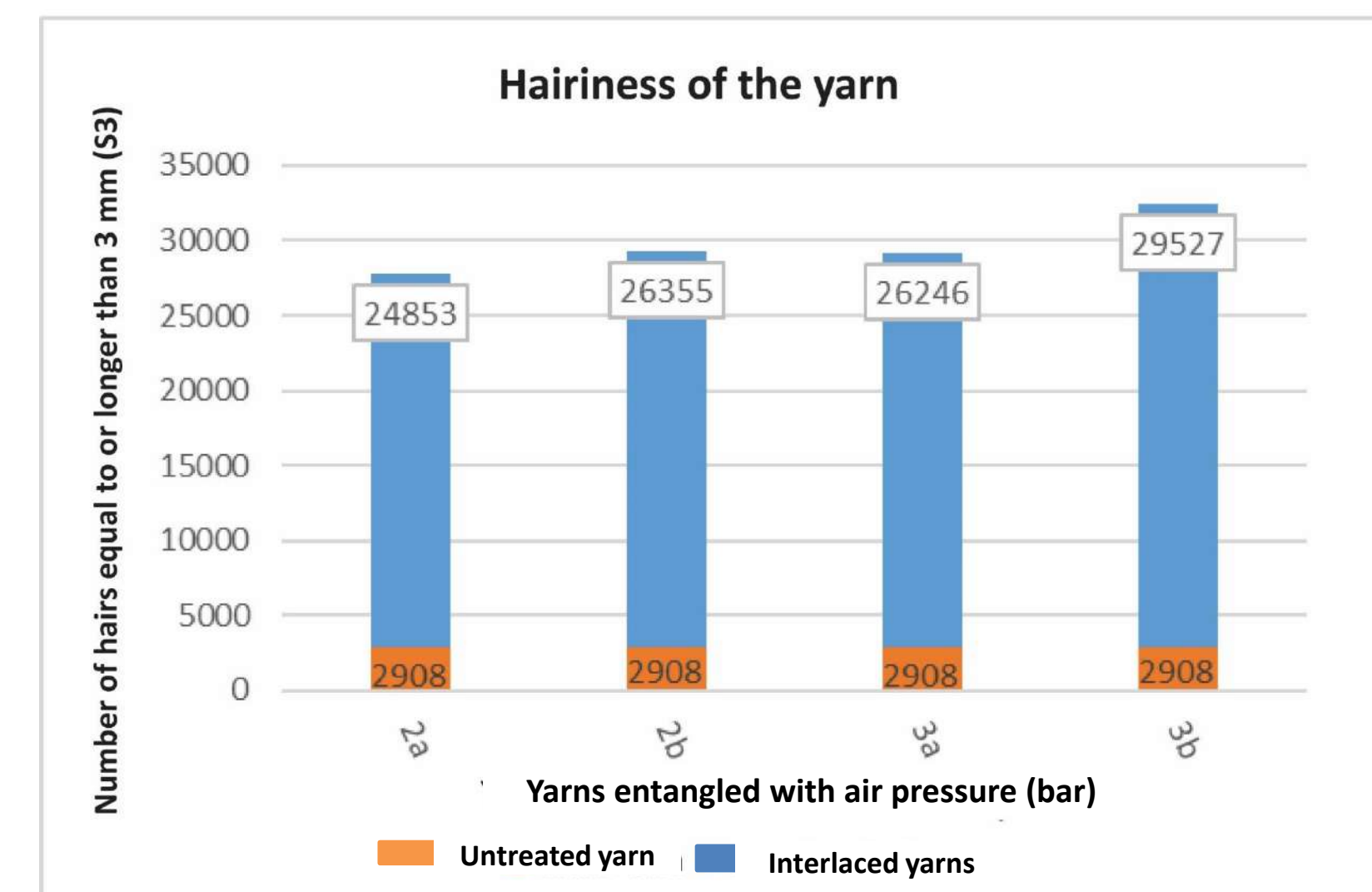


Figure 5. Hairy measurement results of Ne 12/1 yarn after interlaced



Figure 6. Interlaced cotton yarns and woven terry products [5]

Instead of using PVA, a physical effect on the yarn was achieved, resulting in strength gain, an environmentally friendly production and a cost advantage. As a result of the centering process performed with certain pressure and nozzle, the strength and hairiness of the low-twisted cotton yarn increased. In line with the results obtained, the weaving process of the low-twist yarn, which was knotted, was performed directly in the mill without being folded with PVA.

A patent application numbered **2019/13864** has been filed for this process, which is not applied to natural fiber yarns together with the literature search.

References

- [1] DEMİR, A., Synthetic Filament Yarn Production and Texturing Technologies, Istanbul, March 2006. ISBN 975-97055-2-4.
- [2]I. Ozkan and P. D. Baykal, "The effect of manufacturing parameters and filament properties on tailstock quality in the spotting process," Textiles and Engineering, vol. 19, no. 87, pp. 1-6, 2012, doi: 10.7216/130075992012198701.
- [3] S. Alay, F. Göktepe, Suleyman Demirel University Faculty of Engineering, Department of Textile Engineering, "Comparison of Test Results of the Different Yarn Hairiness Testers," vol. 3, pp. 422–427, 2006.
- [4] Turkish Patent Application(2019/13864)
- [5] Bursa R&D and Design Center Laboratory

16th International Fiber and Polymer Research Symposium (16th ULPAS)

9-10 May, 2025, Istanbul technical University (ITU), Istanbul, Türkiye

DEVELOPING ENVIRONMENTAL BURDEN AND COST-REDUCING PROCESSES TO ELIMINATE SALT USE IN REACTIVE DYEING

Eyüphan YENER, Sevil GÜNÇ, Saliha Büşra KARAKELLE

Abstract

Today, reactive dyestuffs are generally used in the dyeing of cotton fabrics. Cotton; It is a fiber type that consumes a high amount of water and energy in pretreatment and dyeing processes. After dyeing, a high amount of colored wastewater is formed, wastewater is discharged to receiving environments and increases the existing pollution load. In recent years, processes that increase the dye affinity of the fiber by ionic modification of cotton fiber have been widely used. Thanks to these processes (plasma technology, ionic modification, nano technology, etc.), the fiber's affinity for dye is increased or new functional properties are added to the fiber. The most important of these is the cationization process. With the cationization process, it turns the slightly anionic ionicity of the cotton fibers in the aqueous medium to cationic; By increasing its affinity against anionic dyestuffs, it provides less dyestuff usage in dyeing in the same color tone. Within the scope of this project, it is aimed to create an environmentally friendly dyeing process by cationizing cotton fiber. In this way, the amount of dyestuff used, salt and environmental load will be reduced. By reducing the dyestuff used, the amount of color and pollution in the waste water is reduced. The most important dyestuff group used in dyeing cotton fiber is reactive dyestuffs. These dyestuffs require a large amount of salt in the dyebath to adhere to the fiber. Salt; It eliminates the negative charge between the dyestuff and the cotton fiber and ensures that the dyestuff is attracted by the fibers. The addition of salt to the dyebath is related to the substantivity and diffusion ability of the dyestuff to the fibers. Since the substantivities of reactive dyestuffs are generally low in dyeings made according to the shrinkage method, a large amount of salt is added to the liquor. It is aimed to ensure that the cotton fiber, which is cationized after the cationization process, increases its affinity for the solution in the dyebath and is dyed using less or no salt. In this way, salt consumption was reduced, the cost item paid for salt was eliminated and the stock area used for salt was saved. In addition, cationic cotton fiber provided more dyestuff affinity than dye solution compared to normal cotton fiber. In this way, the rate of dyestuff mixed with waste water was reduced, minimizing the environmental damage caused by colored waste water, which is difficult to dispose of and harms the environment.

Keywords: Salt-free Dyeing Process, Reactive Dye, Cotton

Experimental

Cotton products; It can be dyed with direct, substantive, sulfur, cube, indigo, pigment and reactive dyestuffs. Especially among these dyestuffs, the most preferred dyestuff group is reactive dyestuffs. Reactive dyestuffs, unlike all other dyestuffs, are anionic dyestuffs that react with fiber macromolecules, bind to fibers with real covalent bonds, and are highly water-soluble like direct dyestuffs. In addition, they are preferred because they provide sufficient fastness after dyeing of cotton products, have a wide color palette and the dyeing method is simple. However, reactive dyestuffs have disadvantages due to low chlorine fastness, hydrolysis of the reactive group in a basic environment, increased water, energy consumption and time spent in post-dyeing washing processes. Especially in this context, studies are being carried out on new dyestuffs, dyeing methods and dyeing machines for dyeing cotton products.

In the project, it was aimed to increase the affinity of the fiber to the dyestuff and to achieve more effective dyeing by using the ionic modification method in the dyeing of cotton products. When cellulose fibers come into contact with water, they form a negatively charged surface due to ionization in the hydroxyl groups. However, most of the dyestuffs used in dyeing cotton (especially reactive and direct dyestuffs) show anionic characteristics in water. Negative charges on the fiber cause repulsion of anionic dyestuffs, limiting the affinity of the dyestuff in the dye bath onto the fiber. For this reason, high amounts of electrolyte (especially sodium sulfate salt or sodium chlorite) substance is used in dyeing cotton products with anionic dyes. Electrolytes help minimize the repulsive force between the negatively charged cotton fibers and the dyestuff. Despite the use of electrolyte, not all of the dyestuff in the dye bath can be consumed and colored wastewater containing high amounts of salt is discharged into the receiving environment. Within the scope of the project, studies were carried out on cationization of cotton fiber and dyeing of cationic cotton without or using little salt.

Material and Method

Current literature searches were conducted regarding reactive dyestuffs in cotton dyeing. In this context, innovations in fiber, dyestuffs, dyeing processes and dyeing machines were examined. Particularly the modification methods applied to fibers have attracted attention. Compared to the traditional reactive cotton dyeing process, studies on increasing the dyeing efficiency by changing the structure of the cotton fiber have come to the fore. In this context, four different cationic chemicals used in the cationization of cotton products were provided. Trial recipes were created for cationic substances at different concentrations (0.5-5%), temperature (30-80°C) and duration (10-45 min). The cotton fiber has been subjected to pre-treatment to remove impurities and gain hydrophilic properties. The specified cationization process was performed on the cotton fiber, where the desired whiteness and hydrophilicity was achieved, and a reactive dyeing process was applied to the cationic cotton fiber at 60°C for 60 minutes. In the light-medium-dark tone dyeings used within the company, the process was continued with two different cationic chemicals. The obtained samples were compared with the samples dyed according to the original reactive dyeing process. In this context, the DataColor spectrophotometer device was used and the L, a, b, c, h and ΔE values of the scanned samples were examined. Then, washing and rubbing fastnesses were applied to the samples and the results were compared with the original fabrics.

Then, as another stage of the study, it was evaluated whether the amount of dyestuff adhering to the surface could be removed from the surface in case of possible errors. In this context, the existing hydrosulphide fading process for the removal of dye from the cationic cotton fiber surface was studied. It was observed that the dismantlings obtained were not sufficient. In addition, since the hydrosulphide chemical used in the current process threatens the environment and human health in terms of odor and consumption, a search for new chemicals has emerged. Considering the literature review, it was seen that the chemical containing thiourea, called ecological hydrosulfide, was used. Recipe trials were conducted with the thiourea chemical provided within the scope of the study at different concentrations (1-15 g/L), duration (15- 45 min) and temperatures (30-80°C). It was observed that the fabric suffered less strength loss as a result of disassembly performed at lower temperatures and times compared to the current disassembly process. Fabric and pile strength tests also support this result. The dyeing process was applied again to the dismantled surface, and the resulting sample was compared with the original dyed fabric. It has been observed that there is no painting unevenness and the surface provides homogeneous paint uptake.

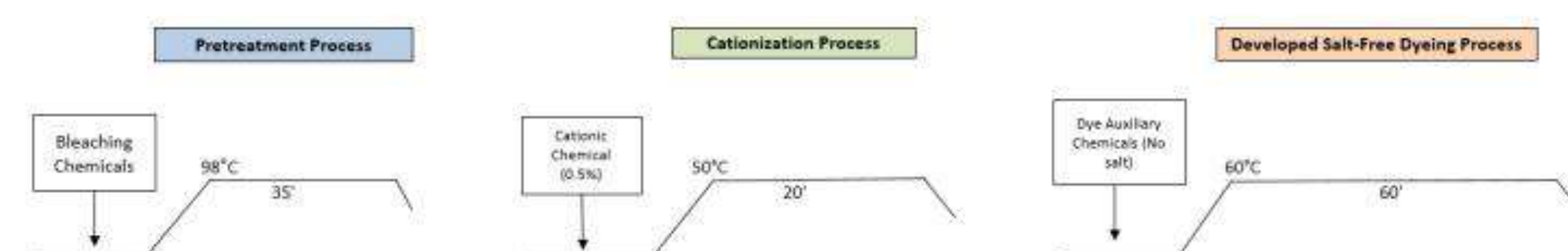


Figure 1. Process



- Salt has been completely eliminated in the developed dyeing process.
- In order to dissolve approximately 360 tons of salt per month in the current dyehouse salt usage, 1092 tons of water is consumed, 576 kW of energy is consumed and 192 hours are spent on labor.
- In the salt-free dyeing process, a 53.8% saving was achieved on the chemical cost per 100 kg of product for mid-tone dyeing (1.5 - 2%).

| | | | | | |
|------------|------------|------------|------------|------------|-----------------------|
| Std. CIE L | Std. CIE a | Std. CIE b | Std. CIE c | Std. CIE h | Std. K/S ₂ |
| 0.08 | 0.53 | 0.12 | 0.55 | 12.78 | 49598.0001 |

| | | | | | | | | | | | |
|--------------------------|--------|--------|--------|--------|--------|--------|--------|-----------------------|--------------------|--------------------|--------------------|
| Batch Name | CIE DL | CIE Da | CIE Db | CIE Dc | CIE Dh | CIE Ds | CMC DE | CMC P/F Determination | CIE Dy Description | CIE Ds Description | CIE DL Description |
| 173351Green 90.52m Turus | 0.07 | 0.55 | 0.13 | 0.56 | 0.00 | 0.00 | 0.04 | 0.04 | delta a | delta b | delta c |

$\Delta E < 1$

$\Delta E < 1$

Conclusions

The project output has been protected by a Patent Application and patent registration is awaited by the Turkish Patent and Trademark Office. Patent Application Numbers: 2021/012824, 2022/014831. A more environmentally friendly dyeing process has been achieved with the developed post-cationization dyeing process. The amount of dyestuffs and auxiliary chemicals used has been reduced. Space savings are achieved especially in areas where salt storage areas and salt solution tanks are located. It was determined that there was half a point improvement in the washing - rubbing fastness of the samples obtained. By reducing the use of dyestuffs and chemicals used, dyeing samples with less color and lower waste load were obtained. In addition, the amount of water consumed in the afterwashing processes to remove the dyestuff that has no affinity to the fiber surface or is hydrolyzed after dyeing has also been reduced.

REFERENCES

- [1] Asaye D and Nalankilli G. A Salt-Free Reactive Dyeing Approach for Cotton by Cationization with Amino Acid Derived from Soya Bean Hull. Adv Res Text Eng. 2018; 3(3):1032
- [2] N. Arivithamani, V.R. Giri Dev / Journal of Cleaner Production 183 (2018) 579-589.
- [3] Richard S. Blackburn, Stephen M. Burkinshaw., Journal of Applied Polymer Science, Vol.89, 1026 – 1031 (2003)© 2003 Wiley Periodicals, Inc

16th International Fiber and Polymer Research Symposium (16th ULPAS)

9-10 May, 2025, Istanbul technical University (ITU), Istanbul, Türkiye

BURSALI

DEVELOPMENT OF COLOR CHANGING TEXTILE SURFACES AGAINST BACTERIA

Sevil GÜNÇ, Saliha Büşra KARAKELLE, Eyüphan YENER, Sümeyye REÇEL ASLAN

Abstract

This research project is to produce innovative surfaces based on cotton and polyester with biosensor properties for use mainly in medical purposes, with multiple disciplined participations involved the fields of textile, chemistry, and medical. First, project partners will select two widely used dyestuff molecules (sulfonphthaleine and anthocyanin) with halochromic (which can change color with pH) properties to avoid having to develop a completely new dyestuff/s, and then apply to cotton and polyester surfaces by dyeing and digital printing methods. Secondly, considering the chemical structures of the existing dyestuffs, new halochromic dyestuff/s will be chemically modified and synthesized and then applied to cotton and polyester surfaces by dyeing and digital printing methods. For quality checking, performance tests of surfaces will be performed after the dyeing and printing experiments on the laboratory and pilot scale. All experimental results will be used for developing the designs of processes, machines, and dyestuffs. Project objectives are summarized as follows: - Modification, synthesis, and characterization of halochromic dyestuff/s. -Production of new surfaces with halochromic properties. -Development of dyeing and printing processes for each surface, using less energy, chemical, and water in line with the social responsibility policies of the project partners, considering the environmental impacts and the sustainability of production. In recent years, many epidemic and pandemic diseases such as COVID-19, Influenza, and Salmonella, have negatively affect both individual and public health, and caused great damage to the economies. During the Covid 19 pandemic, the number of deaths is estimated to be over 20 million, when the coronavirus cases are almost 450 million. For this reason, people have focused on protective textile products such as masks, gloves, and aprons to protect themselves from diseases. Demands, the medical textile market reached from USD 25 billion in 2020 to USD 29 billion in 2021 and is expected to grow at a CAGR of 4.5% by 2030. One of the most critical steps in the fight against diseases is to quickly observe the growth of microorganisms. However, new and practical tools and materials are needed for detecting them. Development and use of chromic textiles have a great potential, and they can also be used to visualize any change in environmental conditions. This property may facilitate the recognition/detection, and they can become a powerful tool for monitoring/observation. The textile surface treated with dyestuff with chromic property, can react quickly and visible.

Results

The first experimental results are described with the data below, and studies to improve the functional properties of the product continue. pH changes and washing results of anthocyanin and halochromic dyes are given in the images below;

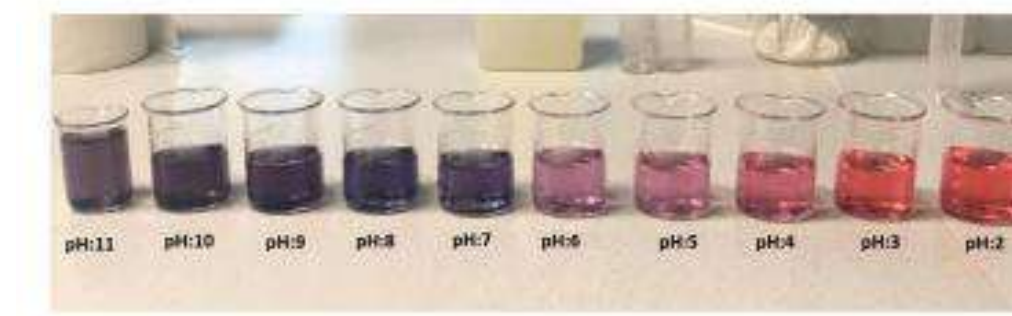


Figure 3. Black Carrot The color change of the anthocyanin supplied in powder form between pH 2-11 is as in the figure.

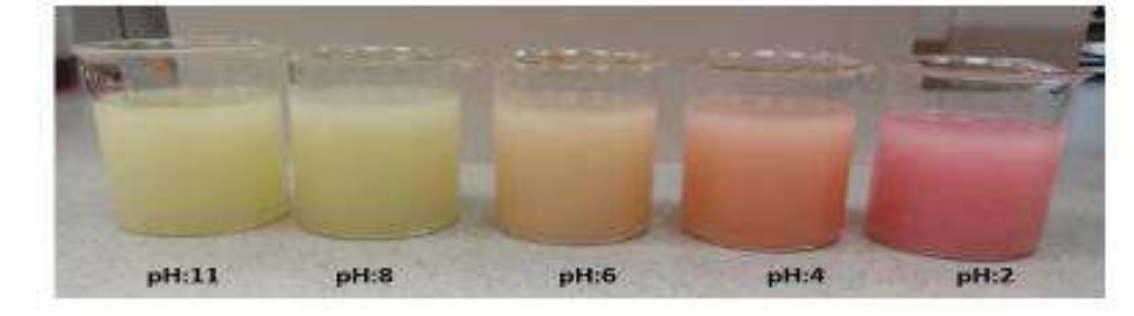


Figure 4. Halochromic dyes the color change of the anthocyanin supplied in powder form between pH 2-11 is as in the figure..

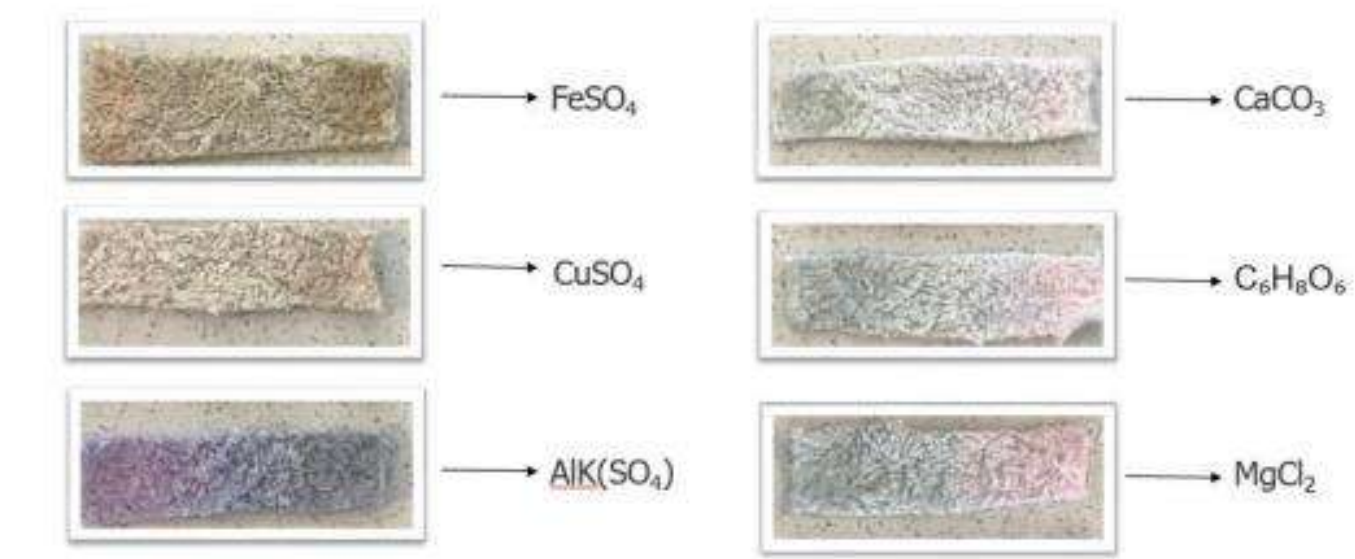


Figure 5. Colors obtained as a result of Anthocyanin dyeing by using different mordants



Figure 6. Colors obtained as a result of Anthocyanin dyeing by using different mordants

Experimental

Cotton and polyester surfaces will be dyed and digitally printed with three different chromic dyestuffs (anthocyanin, pH indicator), and the most suitable process conditions will be determined. After dyeing, color changes of the surfaces will be examined due to both solutions with different pH (2-10) and the growth of Escherichia coli (ATCC 25922) and Staphylococcus aureus (ATCC 6538). Finally, surface characterization analyses (SEM, SEM-EDX, FTIR), and physical and chemical tests (ISO 13934-2, ISO 105-C06, ISO 105-X12, ISO 105-E03, and ISO 105-E04) will be performed.



Figure 1. Black Carrot



Figure 2. Halochromic dyes

Anthocyanin;

- It is the most important group of flavonoids among plant pigments.
- Since it is a signal for microorganisms, its use as a biological indicator is available in the food sector.
- Black Carrot is a natural colorant containing a high percentage of anthocyanin groups.
- It has red, purple and blue colors.
- It dissolves well in water.

Halochromic dyes used in the study;

- It is used by encapsulation of pH indicators or as a direct pH indicator.
- The dyestuffs used are completely soluble in water.
- Since these dyestuffs are liquid, they are suitable for automation system.

Discussion

As a result of the first experimental results, color change was observed in different pH ranges on the fabric surfaces dyed with anthocyanin and halochromic dyes. Although fabrics may fade after washing, color change continues in different pH ranges. Process optimization studies continue.



Figure 7. Colors obtained as a result of Anthocyanin dyeing by using different mordants

REFERENCES

- [1] Ezenarro, J.J., et al., Advances in bacterial concentration methods and their integration in portable detection platforms: a review. Analytica Chimica Acta, 2021: p. 339079.
- [2] Yoo, S.M. and S.Y. Lee, Optical biosensors for the detection of pathogenic microorganisms. Trends in Biotechnology, 2016. 34(1): p. 7-25.
- [3] Xu, J., D. Suarez, and D.S. Gottfried, Detection of avian influenza virus using an interferometric biosensor. Analytical and Bioanalytical Chemistry, 2007. 389(4): p. 1193-1199.

16th International Fiber and Polymer Research Symposium (16th ULPAS)

9-10 May, 2025, Istanbul technical University (ITU), Istanbul, Türkiye

BURSALI

IMPROVEMENT OF PERFORMANCE PROPERTIES OF CELLULOSIC BASED FIBRES

Sevil GÜNÇ, Saliha Büşra KARAKELLE, Eyüphan YENER, Sümeyye REÇEL ASLAN

Abstract

It is known that cotton plant is mostly used as natural fibre in the textile sector. The rapidly growing world population causes an increase in demand in the textile sector. However, the natural fibres that are currently known and produced by conventional methods will not be sufficient to meet this demand after a while. The increase in textile consumption day by day has led to the investigation of the usability of different cellulosic natural fibres in textiles. As a result of the literature reviews, it has been observed that cellulosic based fibres such as hemp, bamboo, soy, kapok, nettle and pineapple have different performance properties in addition to cotton fibre. The blending of these fibres with 100% cotton in different ratios or with each other in different ratios was decided by considering the yarn production methods. The yarns supplied were integrated into the production with the conventional method. In addition, the behaviour of the properties of the fibres after their production in pile structure was examined and different improvements were made on the basis of the existing final product.

With the rapidly increasing world population, the number of consumers is also increasing. Cotton fibre is the most common fibre in the use of cellulosic based fibres in the textile sector. However, the cotton plant consumes a lot of water during the production phase. Researches have shown that approximately 9788-9958 litres of water is consumed for the production of 1 kilo of cotton. Considering the principle of sustainability within the scope of the project we have carried out, the effects of the different performance and comfort properties of cellulosic-based fibres such as hemp, bamboo, soy, kapok, nettle and pineapple, which we can use instead of cotton fibre or in a mixture with cotton fibre, will provide us with a qualified product range. In addition, testing the usability of different cellulosic structures that can be processed by conventional method in the sector is an important output of the project.

Experimental

In line with the researches carried out, the first studies have focused on hemp fibre, which we will hear more and more in the coming days, and the first studies have been on the mixture of this fibre and cotton. The amount of water consumed in hemp plant production is approximately 1/3 of the amount of water used for the production of cotton plants. In addition to the fact that hemp fibre is biodegradable, the fact that no chemicals are needed during the cultivation of the hemp plant will increase the preferability of the use of hemp fibre in the textile sector in the coming years. In addition, hemp fibre has high absorbency, breathability, high strength and anti-microbial properties. The fact that hemp fibre does not cause pilling and static electrification increases its preferability. Towel production was carried out by supplying 100% Hemp, 50% Hemp-50% Cotton and 30% Hemp-70% cotton blended yarns from different companies. With the new use of hemp fibre in the sector, it has been studied to optimise the suitability of blended yarns for towel weaving looms.



Figure 1. Towel Produced with 50% Hemp and 50% Cotton Blended Yarn



Figure 2. Towel Produced with 30% Hemp and 70% Cotton Blended Yarn

Results

Yarn count, twist and fibre blend ratio were determined by considering yarn spectra, hemp fibre structure and pile formation mechanisms in the weaving machine. While it was not possible to produce a suitable sample with 100% hemp yarn, two different samples were produced with 50% and 30% hemp-cotton blended yarns supplied from different companies with the same production techniques. These samples were subjected to certain tests to examine their performance properties. The tests performed and measured values and sample information are given in Table 1.

| Sample | Description | Hydrophilicity (sn) | Air Permeability (mm/s) | Tensile Strength (N) | | Pilling (1000 rpm) |
|--------|---------------------|---------------------|-------------------------|----------------------|-----------|--------------------|
| | | | | Ort. Weft | Ort. Warp | |
| 1 | %100 Cotton | 1,56 | 248,6 | 184,32 | 211,4 | 3-4 |
| 2 | %50 Hemp-%50 Cotton | 0,88 | 250,6 | 209,3 | 197,38 | 3-4 |
| 3 | %30 Hemp-%70 Cotton | 0,57 | 386 | 264,8 | 247,6 | 4 |

Table 1. Test Results of Towel Samples Produced with 100% Cotton, 50% Hemp, 50% Cotton, 30% Hemp, 70% Cotton Blended Yarn

Hydrophilicity test TS 866, Air Permeability test EN ISO 9237 Special, Tensile Strength test TS EN ISO 13934-2 and finally Pilling test were measured in accordance with TS EN ISO 12945-2 standards.

Discussion

Among the cellulosic fibres investigated as an alternative to cotton fibre, hemp fibre was studied due to its cultivation advantage, sustainability and fibre properties. Physical tests were carried out to see the performance properties of the samples obtained with Hemp-Cotton blend ratios that form the appropriate yarn form. When the values in Table 1 are examined, it is determined that especially the yarn containing 30% Hemp-70% Cotton fibre provides a homogeneous blend and the unevenness of the yarn produced is better than the yarn containing 50% Hemp. This homogenous distribution is clearly seen in the breaking strength test results. When the other test results are examined, it is concluded that the performance properties are improved compared to cotton products thanks to the distinctive properties of hemp fibre.

REFERENCES

1. Dündar, E. 2008. Comparison of the Performance of Knitted Fabrics Produced from Various Cellulosic Yarns. Istanbul Technical University, Department of Engineering, Master Thesis, Istanbul, 1-96.
2. Cimilli, S., Nergis, B. U., Candan, C., Özdemir, M. 2010. A Comparative Study of Some Comfort-related Properties of Socks of Different Fibre Types. Textile Research Journal, 80(10):, 948-957.
3. Horne, M. R. L. 2012. Bast fibres: hemp cultivation and production, Woodhead Publishing Limited. <https://doi.org/10.1533/9780857095503.1.114>
4. Sabir, E. C., Zervent Ünal, B. 2017. The Using of Nettle Fibre in Towel Production and Investigation of the Performance Properties. Journal of Natural Fibres, 14(6):, 781-787.
5. Yılmaz Şahinbaşkan, B. 2019. The Effect of Enzymatic Pretreatments on Hemp Woven Fabric. International Journal of Advances in Engineering and Pure Sciences, 208-213.

16th International Fiber and Polymer Research Symposium (16th ULPAS)

9-10 May, 2025, Istanbul technical University (ITU), Istanbul, Türkiye

Utilization of Conductive Yarns in Cotton Fabric Structure and Investigation of Performance Properties

Eyüphan YENER, Sevil GÜNÇ, Saliha Büşra KARAKELLE

BURSALI

Abstract

The cooperation of textile science with the ever-growing electronics industry has started to play a role in many fields such as textile products, industry, military, space, medicine, which can be used for protection, defense, health, communication, automation. This study tries to explain the methods of obtaining conductive textile materials (fiber, yarn, fabric, etc.) and the usage areas of these materials within the framework of the studies on this subject. Conductive textiles will continue to be used in many interesting applications in the future with their advanced properties and diversity of production methods. The textile industry is making great progress in the fields of smart and multifunctional textiles, including high performance materials (fibers, yarns and technical textiles). In this respect, textile products that fulfill various functions using smart materials are becoming more and more important both in industry and in daily life. Within the scope of the project, the production methods, performance and quality values of conductive yarns in pile fabric construction will be investigated.

In the study to be carried out within the scope of the project; it is aimed to improve the functional properties of mop fabrics by weaving with conductive yarns with different constructions. With these functional properties; mop fabric will be developed with features such as fast drying, moisture absorption, prevention of odor formation, negative energy absorption, etc. By heating the products with the circuit system to be developed, a new market will be sought in order to create a new product range, appeal to more masses and increase the export share.

Keywords: Conductive yarn, Sensor, Smart textiles, Towel textile,

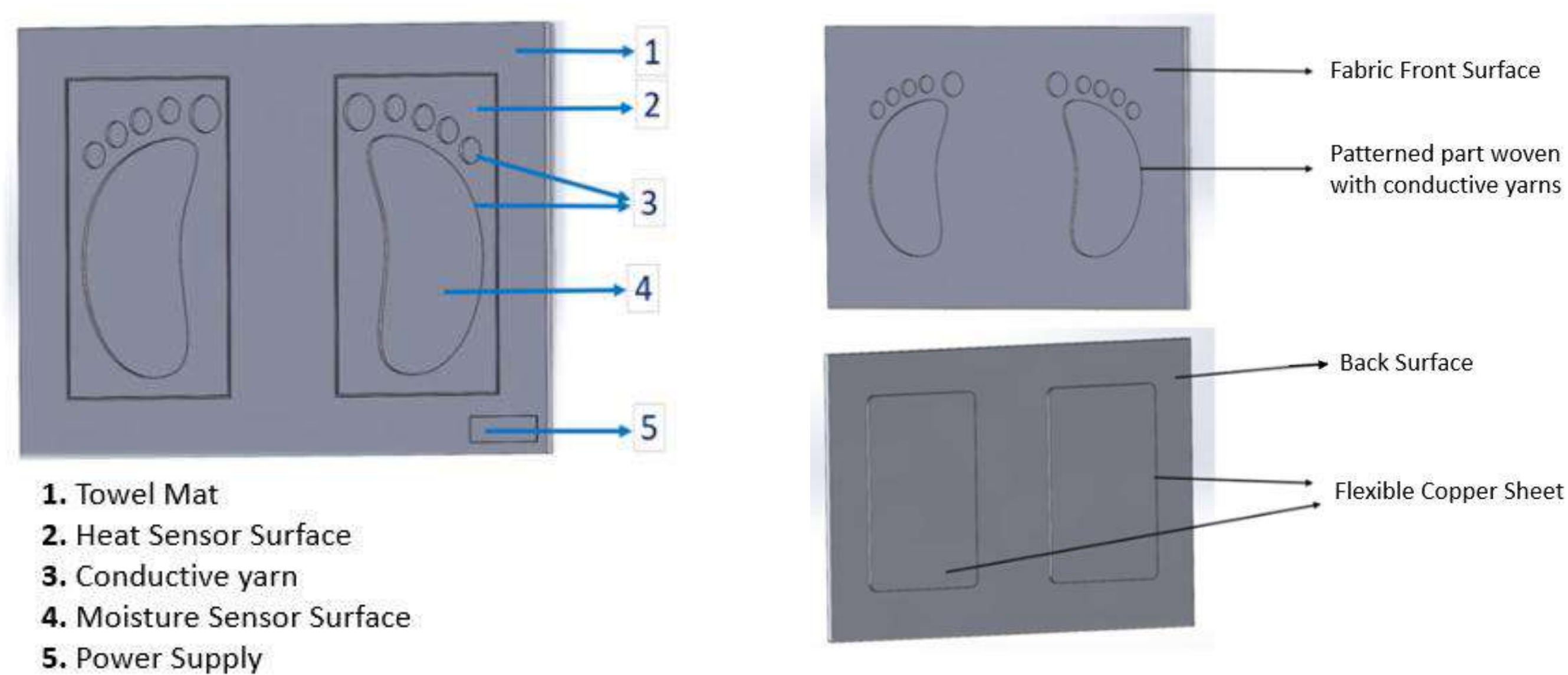


Experimental

Towel and bathrobe fabrics, which are produced as final products in our company, are generally given standard features such as softness and water absorbency as a finishing process. In order to adapt to the rapidly developing technology and to develop more comfortable products for our customers, it is aimed to make weavings by integrating conductive yarns with different properties into towel fabric constructions. In the work to be carried out within the scope of the project; it is aimed to improve the functional properties of mop fabrics by weaving with conductive yarns with different constructions. With these functional properties; fast drying, moisture absorption, prevention of odor formation, negative energy absorption, etc. mop fabric will be developed with features such as. By heating the products with the circuit system to be developed, it is aimed to create a new product range and appeal to more masses.

Humidity and temperature sensors were integrated into the Arduino system used in this study. As a result of this integration, the heat and humidity level of the product was kept within the desired range by utilizing the conductivity of the yarn together with the values received from the sensors. In the trials carried out on the products, the 5V output of the Arduino was taken and the temperature to eliminate the moisture on the yarn was provided. In addition to this integrated system, a 5V relay card was also added. With the relay used, healthier energy transfer and homogeneous temperature distribution were provided with intermittent energy.

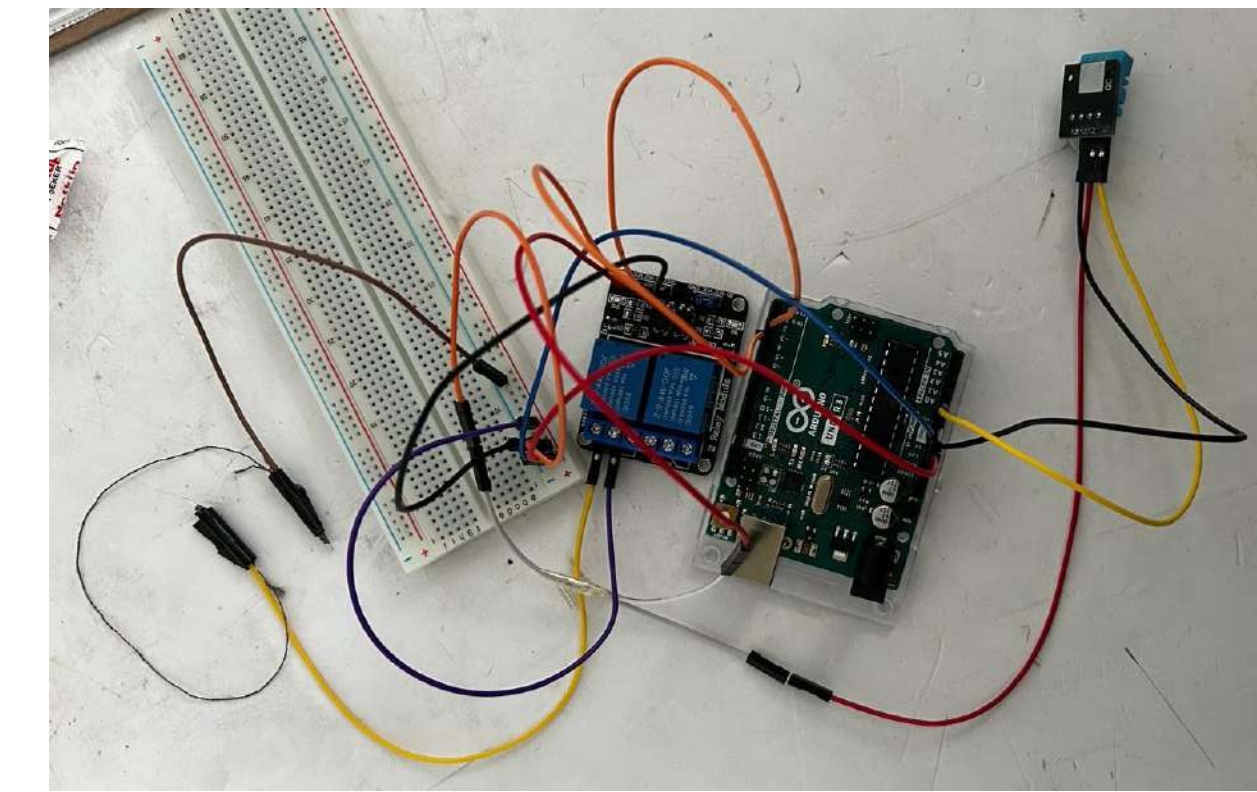
In the experimental studies; Conductive yarns in the range of 35-110 Ω/m and conductive yarns with a thickness of 235/36 dtex were used. Fabric constructions in the range of 800-1000 g/m² for mats and 300-500 g/m² for towels were preferred. Conductive yarns were incorporated into the towel construction by weaving and embroidery method.



Results

Bursa R&D center has adopted the mission of being a pioneer in the textile industry and contributing to the national economy by developing value-added products. Thanks to the products to be developed with conductive yarns within the scope of the project, innovative functional product groups will be obtained in the home textile mop and bathrobe group with high added value. The project output has been protected with a Patent Application and is awaiting Patent registration by the Turkish Patent and Trademark Office. Patent Application Numbers: 2023/018319 and 2023/018313.

As a result of the experimental studies, the surfaces created on terry cloth with conductive yarns were proven to be workable with arduino system and thermal cameras. Since conductive yarns suitable for washing resistance were selected, their conductivity continues after 20 washes.



Arduino System



Before Processing



After Processing



Embroidery Process



Weaving Process

Discussion

The technical data obtained within the scope of the project will be a guide to produce the best option to meet the right product with the desired quality in one go. In the study; the fact that conductive yarns have not been used in pile fabric structures before reveals the innovative aspect and quality of the project. With this innovative aspect, developments will be made in the field of integrating electronic textiles into cotton textile production in the mats to be developed. Thanks to the products to be developed with conductive yarns, innovative functional product groups will be obtained in the home textile mop and bathrobe group with high added value.



16 ULUSLARARASI
LİF VE POLİMER
ARAŞTIRMALARI
SEMPZYUMU
16th INTERNATIONAL FIBER AND POLYMER RESEARCH SYMPOSIUM
Sürdürülebilir ve İşlevsel Lif ve Polimerler
Sustainable and Functional Fibers & Polymers

9-10 Mayıs 2025
İstanbul Teknik Üniversitesi
Gümüşsuyu Prof. Dr. Necmettin Erbakan Yerleşkesi
İstanbul Technical University
Gumussuyu Prof. Dr. Necmettin Erbakan Campus



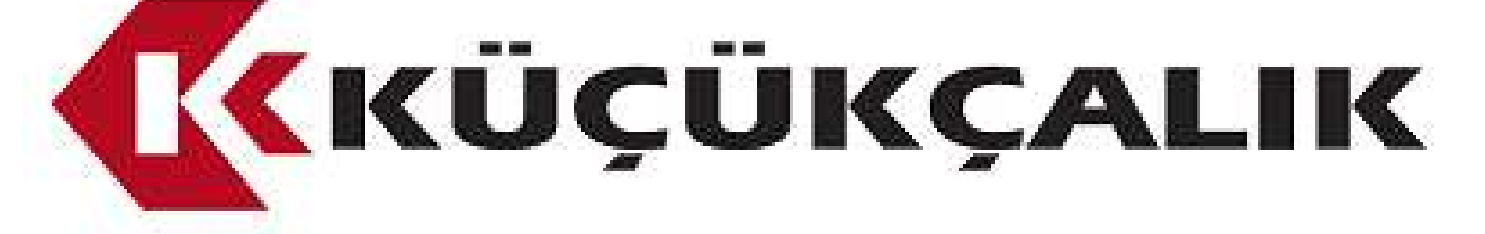
16th International Fiber and Polymer Research Symposium (16th ULPAS)

9-10 May, 2025, Istanbul technical University (ITU), Istanbul, Türkiye

PERDELEME UYGULAMALARINA YÖNELİK TEKSTİL ÜRÜNÜ

Zeynep BATUR, Hale GÜRLER, Muzaffer KARS

zeynep.batur@kcalik.com

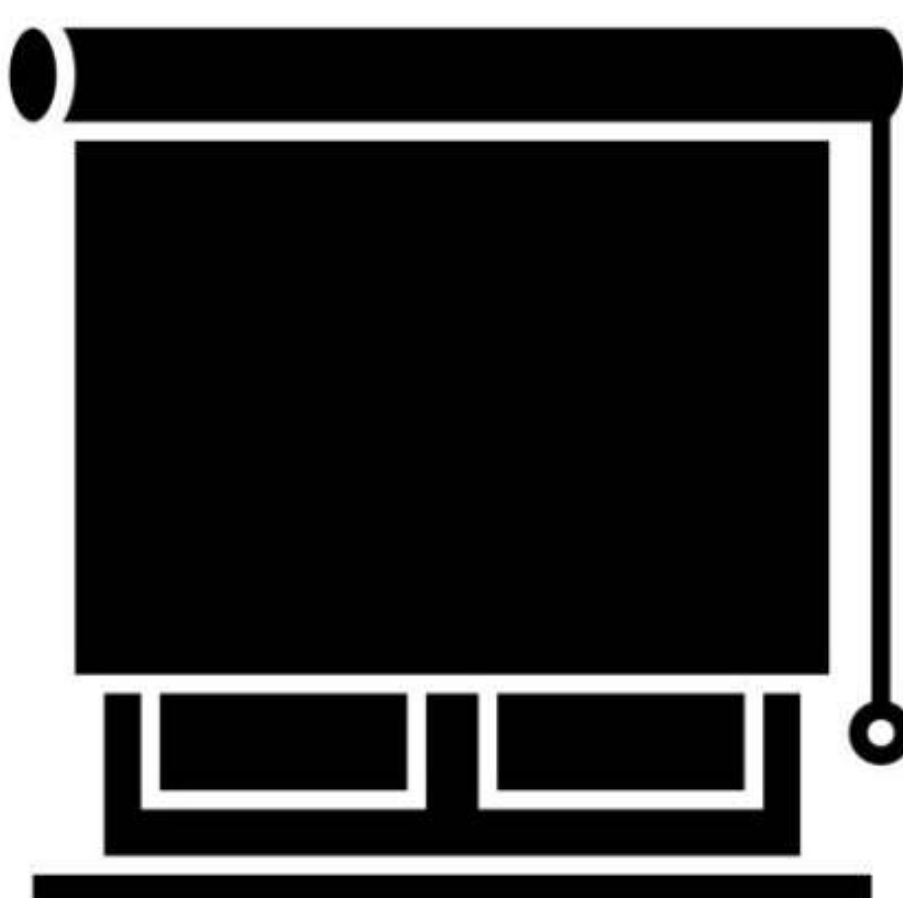


Proje Özeti

Proje gerekçe

Tekstil sektöründe sürdürülebilirlik ve ekolojik yaklaşım kavramlarının ön plana çıkması sonucunda geri dönüşüme/geri dönüştürülmüş ve çevre dostu ürünlere olan talep hızla artmıştır. Özellikle iç-dış mekanlarda kullanılan perdelerin, kullanımı oldukça yaygın ve sağlam bir yapıya yani tüm çevresel şartlara dayanıklı olması talep edilmektedir. İç-dış mekanlarda perdelemede koruma ve gölgelendirme yapılırken aydınlanmanın da sağlanması istenmektedir. Mevcut teknikte, iç ve dış mekan perdelerinde kullanılan iplikler, insan sağlığı açısından zararlı olan ve geri dönüştürülemeyen polivinil klorür (PVC) malzemesi ile kaplıdır. PVC'nin zaman içinde biçim ve boyut değiştirmesi, kötü koku oluşturmaya, geri dönüşüme imkan tanımaması ve yapay bir görünüm ile tuşe oluşturmaya en büyük dezavantajları arasında yer almaktadır. Ayrıca iç iplik olarak cam elyaf kullanımı da mevcut teknikte yaygındır. Bu tip bir iç ipliğe sahip olacak şekilde elde edilen kumaşın perdenin yapımı aşamasında kesilirken cam elyafın tozuması da insan sağlığı açısından risk taşımaktadır.

Proje hedefleri



Şekil 1: Perdeleme uygulamasına yönelik şematik bir örnek

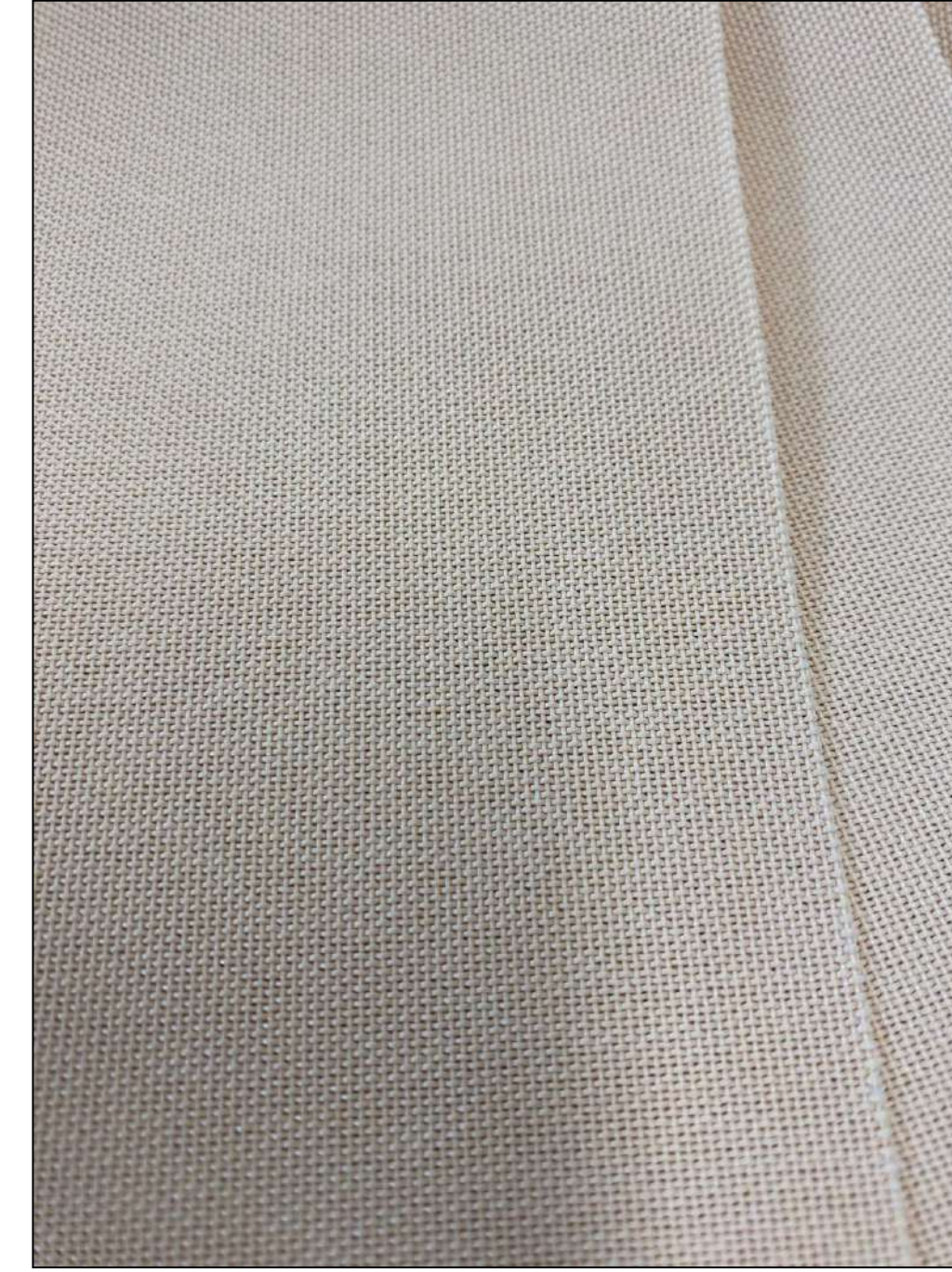
PVC içermeyen, uzun ömürlü, çevre dostu ve geri dönüştürülebilir bir ürün elde etmektir. Perdeleme uygulamasına yönelik şematik bir örnek Şekil 1'de mevcuttur.

- Zorlu hava koşullarına uyum sağlayabilecek iç ve dış ortam uygulamaları için yüksek performans gösterecek ve istenen UV dayanımına sahip bir kompozit iplik ile bu iplikten elde edilen bir kumaş sağlamaktır.

Deneyisel

Bu çalışmada kullanılan iplik kaliteleri iki bileşenden oluşmaktadır. İç iplik; poliester (PES) polimerden üretilen 200 tur bükümlü kesik elyaf olup iç iplik üzerine sarılan dış iplik olarak da düşük sıcaklıkta eriyebilen 75 denye 24 filaman iç-içe bikomponent FDY PET lif kullanılmıştır. Büküm prosesi ile birleştirilerek oluşturulan kompozit iplik; bezayağı konstrüksiyonda ve 18 çözgü/tel ile 13 atkı/tel sıklığında dokunmuştur. Dokunan ham kumaşa, bir ard proses olan termal tekstil terbiye işlemi uygulanarak kompozit iplik yapısındaki eriyen iplik, bu işlem sırasında uygulanan ısı ile erimekte, kumaşı sertleştirmekte, stabilize etmekte ve şekil kazandırmaktadır.

Sonuçlar



Şekil 2: Perdeleme uygulamasına yönelik üretilen tekstil yüzeyi

Tüketiciler için önemli kullanım özelliklerinden biri olan ışık haslığı testi, tekstil ürünlerinin kullanımı sırasında güneş ışığına maruz kaldığı zaman gerçekleşen renk değişimini ifade etmektedir. Yapılan testin standardı ISO 105 B02 olup, üretilen kumaş numunesi Şekil 2'de mevcuttur. Tablo 1'de mamul kumaşın ışığa maruz kalmadan-orijinal hali- ile ilgili test sonuçları mevcuttur. Tablo 2'de ise 1000 saatlik ışık haslığı sonrasında elde edilen

sonuçlar mevcuttur. Laboratuvar alt yapımızda bulunan Titan 1 test cihazımızda loadcell (yük hücresi) 600 N kapasitesine sahip olup, sonuçlar bu doğrultuda verilmiştir.

Tablo 1: Kopma mukavemeti ve ışık haslığı test sonuçları

| Kopma Mukavemeti ISO 13934-1 | Atkı (N) | Çözgü (N) |
|---------------------------------|----------|-----------|
| | 592.23 | >600 |
| Işık Haslığı ISO 105 B02 | 6 | |

Tablo 2: 1000 saat ışık haslığı sonrası kopma mukavemeti ve ışık haslığı test sonuçları

| Kopma Mukavemeti ISO 13934-1 | Atkı (N) | Çözgü (N) |
|---------------------------------|----------|-----------|
| | >600 | >600 |
| Işık Haslığı ISO 105 B02 | 6 | |

Tüm numuneler ve veriler incelendiğinde, haslık değerlerinin ticari değer gören bir aralıkta yer aldığı ve kabul gördüğü belirlenmiştir.

Tartışma

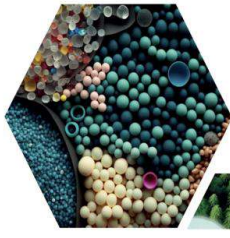
Bu çalışma sonucunda elde edilen ürünün, dayanıklılık ve uzun ömür ile renk haslığı ve yüzey kalitesi açısından klasik perde performansı ile benzer performans sergilediği görülmektedir. Bu bulgular, çevre dostu perdeleme sistemlerinin hem çevresel etkilerin azaltılmasına hem de kullanıcıların taleplerine uygun ürünlerin sunulmasına katkı sağladığını göstermektedir. Çevre dostu perdelerin bölgesel pazar trendlerine uygun olarak geliştirilebilmesi, sektördeki yenilikçi ve sürdürülebilir yaklaşımların önemini vurgulamaktadır.

Referanslar

*Faure, B., Salazar-Alvarez, G., Ahnizay, A., Villaluenga, I., Berriozabal, G., De Miguel, Y. R., & Bergström, L. (2013). Dispersion and surface functionalization of oxide nanoparticles for transparent photocatalytic and UV-protecting coatings and sunscreens. *Science and technology of advanced materials*, 14(2), 023001.

*Aydemir, H., & Demiryürek, O. (2014). Stor perdeler kumaşlarının kopma mukavemeti, hava geçirgenliği ve su geçirmezlik özelliklerinin incelenmesi. *Erciyes Üniversitesi Fen Bilimleri Enstitüsü Fen Bilimleri Dergisi*, 30(4), 240-247.

16th International Fiber and Polymer Research Symposium (16th ULPAS)
9-10 May, 2025, Istanbul technical University (ITU), Istanbul, Türkiye



16 ULUSLARARASI
LİF VE POLİMER
ARAŞTIRMALARI
SEMPOZYUMU

16th INTERNATIONAL FIBER AND POLYMER RESEARCH SYMPOSIUM

Sürdürülebilir ve İşlevsel Lif ve Polimerler
Sustainable and Functional Fibers & Polymers



9-10 Mayıs
May 2025

İstanbul Teknik Üniversitesi
Gümüşsuyu Prof. Dr. Necmettin Erbakan Yerleşkesi
Istanbul Technical University
Gumussuyu Prof. Dr. Necmettin Erbakan Campus

PBT-Based Hard Tissue Implant

Songül ÖZAY^a, Ebru ERDAL^b, Barış BATUR^c, Gülben AKCAN^d, Merve BAKICI^e, Hasret Tolga ŞİRİN^f, Caner BAKICI^g, Lokman UZUN^h, Murat DEMİRBILEK^{a,*}

^{a,f}Ankara Hacı Bayram Veli University, Biology Department, 06900, Ankara, Turkey.

^bYıldırım Beyazıt University, Advanced Technologies Application and Research Center, 06010, Ankara, Turkey

^{c,g}Ankara University, Faculty of Veterinary Medicine, 06110, Ankara, Turkey.

^dKto Karatay University, Faculty of Medicine, Department of Basic Medical Sciences, 42290, Konya, Turkey.

^eKırıkkale University, Faculty of Veterinary Medicine, 71450, Kırıkkale, Turkey.

^hHacettepe University, Chemistry Department, 06800, Ankara Turkey.

*Corresponding author: muratscaffold@gmail.com

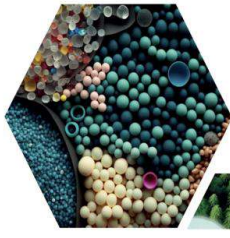
ABSTRACT

The study aims to fabricate cellulose acetate butyrate-polybutylene terephthalate (CAB-PBT) conjugates to promote bone regeneration.

Autografts and allografts are commonly used for the regeneration of bone defects; however, they come with certain disadvantages. Consequently, the development of a matrix capable of replacing both autografts and allografts is fundamental to the field of bone tissue engineering. The composition and structure of this matrix significantly influence cellular activities, making it essential to create an appropriate scaffold.

In this context, PBT has been conjugated with CAB to produce spongy scaffolds. The mechanical properties of these scaffolds will be evaluated. Additionally, MC 3T3 cells will be cultured on the scaffold, and cellular activity will be assessed through the expression of alkaline phosphatase, osteocalcin, and collagen type 1. Concurrently, the in vivo biocompatibility of the scaffold will be investigated through implantation tests. This study was supported by Ankara Hacı Bayram Veli University Scientific Research Projects Coordination Unit, TYL-2025-111.

Keywords: Tissue engineering; osteoblast activity; bone tissue; PBT-CAB conjugation



16

ULUSLARARASI
LİF VE POLİMER
ARAŞTIRMALARI
SEMPOZYUMU

16th INTERNATIONAL FIBER AND POLYMER RESEARCH SYMPOSIUM

Sürdürülebilir ve İşlevsel Lif ve Polimerler
Sustainable and Functional Fibers & Polymers



9-10 Mayıs
May 2025

İstanbul Teknik Üniversitesi
Gümüşsuyu Prof. Dr. Necmettin Erbakan Yerleşkesi
Istanbul Technical University
Gumussuyu Prof. Dr. Necmettin Erbakan Campus

Development of high-efficiency polysulfone nanofiber filters for the removal of *Candida auris*: Comparison of aligned and random morphology

Merve Açıksoz^{a,b}, Ayse Kalkanci^c, Ozlem Guzel Tunccan^c, Nalan Oya San Keskin^{b,*}

^aNanosan Laboratory, Department of Biology, Polatlı Science and Literature Faculty, Ankara Hacı Bayram Veli University, 06900 Ankara, Türkiye

^bInstitute of Graduate Programs and Department of Biology, Polatlı Science and Literature Faculty, Ankara Hacı Bayram Veli University, 06900 Ankara, Türkiye

^cDepartment of Medical Microbiology, Faculty of Medicine, Gazi University, 06100, Ankara, Türkiye,

*Corresponding author: nalan.san@hbv.edu.tr

ABSTRACT

In recent years, nanofiber filters are promising materials for the treatment of wastewater containing microorganisms. In this study, a nanomaterial-based microorganism treatment approach using polysulfone nanofiber (PSU-Nf) filters is presented. The targeted yeast, *Candida auris*, has gained thermotolerance with global warming and developed multidrug resistance. Using electrospinning technique, PSU-Nf filters were produced in random and aligned morphology. In order to mimic hospital wastewater, *Candida auris* culture was adjusted to McFarland 0.5 and live colony counts were performed from samples taken from the liquid passing through the filter for 1 min, 10 min and 60 min by providing continuous flow at a flow rate of 0.5 mL/min from the produced PSU Random-Nf and aligned-Nf filters. Wastewater containing $4.8 \pm 9 \times 10^5$ CFU/mL yeasts was filtered with PSU_Random-Nf filter for 1 min, 10 min and 60 min and as a result, 127 ± 1 CFU/mL, 7 CFU/mL and 0 colonies were determined respectively. In PSU aligned-Nf filter, yeast removal with 100% efficiency after 1 min filtration. Compared to conventional polymeric filters, which typically show limited microorganism retention without additional biocidal agents, PSU-Nf filters provide superior passive removal performance. Furthermore, electrospinning is a scalable technique already adapted for industrial Nf production, making these PSU-Nf filters feasible for real-world applications. These results highlight the availability of innovative, accessible materials with high filtration efficiency for the removal of pathogens from aquatic environments. This study is supported by the Research Universities Support Program (ADEP) (Gazi University) under the project ID: 9116.

Keywords: Electrospinning; Nanofiber; Pathogen; Filter



Evaluation of the microbial corrosion protection performance of essential oil-loaded nanofiber coatings on stainless steel

Ayça Gül Özdağ^{a,b}, Nalan Oya San Keskin^{b,*}

^aNanosan Laboratory, Department of Biology, Polatlı Science and Literature Faculty, Ankara Hacı Bayram Veli University, 06900 Ankara, Türkiye

^bInstitute of Graduate Programs and Department of Biology, Polatlı Science and Literature Faculty, Ankara Hacı Bayram Veli University, 06900 Ankara, Türkiye

*Corresponding author: nalan.san@hby.edu.tr

ABSTRACT

Corrosion and microbial corrosion are important problems for metals and alloys that are widely used in many fields. Microorganisms cause accelerated corrosion due to the metabolites they produce as a result of their metabolic activities. In recent years, nanofiber coatings produced by electrospinning method have gained importance in metal/alloy corrosion protection studies due to their large surface area, porous structure, light weight and functionalizable properties. In this study, nanofibers containing natural and highly antimicrobial Tea Tree Oil (TTO) were fabricated as anti-corrosion coatings and their potential to protect 304L stainless steel (SS) alloy, which is widely used in aquatic environments, from microbial corrosion was evaluated. 304L SS disks were coated with Polycaprolactone (PCL) nanofibers carrying TTO and incubated in Nutrient Broth containing 3.5% NaCl under abiotic and biotic conditions containing *Pseudomonas aeruginosa* bacteria for 10 days. As a result of electrochemical corrosion analysis, it was determined that Nf coatings significantly reduced the corrosion intensity, thus effectively protecting 304L SS from corrosion in abiotic and biotic environments. The Scientific and Technological Research Council of Turkey (TÜBİTAK, project 2209A 1919B012205896) is acknowledged for funding the research.

Keywords: Electrospinning; Essential Oil; Corrosion; Microbial Corrosion; Nanofiber Coatings



Nanofiber-Halloysite Systems for Sustained Microbial Support in Industrial Wastewater Treatment

Yigitcan Algul^{a,b}, Nalan Oya San Keskin^{a,*}

^aNanosan Laboratory, Department of Biology, Polatlı Science and Literature Faculty, Ankara Hacı Bayram Veli University, 06900 Ankara, Türkiye
^bInstitute of Graduate Programs and Department of Biology, Polatlı Science and Literature Faculty, Ankara Hacı Bayram Veli University, 06900 Ankara, Türkiye

*Corresponding author: nalan.san@hbv.edu.tr

ABSTRACT

Biological treatment of industrial wastewater depends on the metabolic activity of microorganisms. However, lack of nutrients, rapid depletion or toxicity of the environment can limit the efficiency of these processes. Therefore, suitable carrier systems are needed to ensure long-term stability of microorganisms and increase their treatment efficiency. In this study, bacteria were attached to halloysite nanotube (HNT) integrated polysulfone nanofibers (PSU-Nf) carrying yeast extract necessary for the growth of microorganisms and used for Nickel (Ni) treatment. The Nfs showed maximum release on day 4. The Ni removal efficiency of Nf mat containing only bacteria attached to PSU-Nf was 17.6%, while the removal efficiency of PSU-Nf integrated with halloysite nanotube (HNT) carrying yeast extract was 31%. These results indicate that nutrient-carrying HNT/PSU nanofiber systems can significantly improve the efficiency of biological treatment processes for heavy metal removal by supporting the activity of microorganisms.

Keywords: Halloysite; Electrospun Nanofiber; Wastewater treatment



Investigation of the effect of bio-based finishing chemical on knitted fabric

Filiz Emiroğlu^{a,b,*}, Ayşe Çelik Bedeloğlu^{a,*}

^a Polimer Malzeme Mühendisliği, Bursa Teknik Üniversitesi, 16310 Bursa, Türkiye

^b Almaxtex Ar-Ge Merkezi, Almaxtex Tekstil San.ve Tic. A.Ş., 16300 Bursa, Türkiye

*Corresponding author : filiz.emiroglu@yesim.com, ayse.bedeloglu@btu.edu.tr

ABSTRACT

The primary objective of this study is to develop a biomaterial-based textile coating that reduces the cleaning requirements of textile products, thereby minimizing water and energy consumption and contributing to sustainable and circular textile strategies. In order to reduce the need for frequent cleaning, extend product lifespan, and achieve significant water and energy savings, the most sought-after functional and comfort properties in the textile industry include UV protection, water repellency, stain resistance, and odor control. However, the chemical agents commonly used to impart or enhance these properties often pose environmental and human health risks. Additionally, no single textile coating or finishing chemical currently available on the market is capable of simultaneously providing all these functionalities. The primary aim of this study is to investigate and conduct experimental research on enhancing the durability and performance of a bio-based finishing chemical that imparts UV protection, water repellency, stain resistance, and odor control to textile surfaces.

Keywords: Durability of Bio-Based Textile Coating; Stain-Resistant; Water-Repellent; UV-Protective; Odor-Control; Knitted Fabric.

ACKNOWLEDGEMENT

This study was financially supported by The Scientific and Technological Research Council Of Turkey (No. 9230053).

REFERENCES

- [1] Köhler, A., Watson, D., Trzepacz, S., Löw, C., Liu, R., Danneck, J., Konstantas, A., Donatello, S. and Faraca, G., (2021), Circular Economy Perspectives in the EU Textile sector, EUR 30734 EN, Publications Office of the European Union, Luxembourg, ISBN 978-92-76-38646-9, doi:10.2760/858144, JRC125110.
- [2] European Commission. (2022). EU Strategy for Sustainable and Circular Textiles. COM(2022) 141 final. Retrieved from [\[https://environment.ec.europa.eu/document/download/74126c90-5cbf-46d0-ab6b-60878644b395_en?filename=COM_2022_141_1_EN_ACT_part1_v8.pdf\]](https://environment.ec.europa.eu/document/download/74126c90-5cbf-46d0-ab6b-60878644b395_en?filename=COM_2022_141_1_EN_ACT_part1_v8.pdf)
- [3] Sedaghifar H., Ragauskas A.(2020). Lignin as a UV Light Blocker-A Review. MDPI Journer, Polymers.
- [4] Moghaddam S., Biazar E., Esmaeili J., Kheilnezhad B., Goleij F., Heidari S.(2023) Tannic acid as a Green Cross-linker for Biomaterial Applications. Mini-Reviews in Medicinal Chemistry, 2023, 23, 1320-1340.

16th International Fiber and Polymer Research Symposium (16th ULPAS)
9-10 May, 2025, Istanbul technical University (ITU), Istanbul, Türkiye



16 ULUSLARARASI
LİF VE POLİMER
ARAŞTIRMALARI
SEMPOZYUMU

16th INTERNATIONAL FIBER AND POLYMER RESEARCH SYMPOSIUM

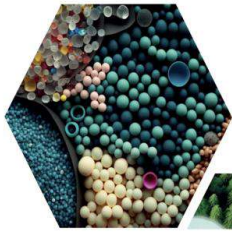
Sürdürülebilir ve İşlevsel Lif ve Polimerler
Sustainable and Functional Fibers & Polymers



9-10 Mayıs
May **2025**

İstanbul Teknik Üniversitesi
Gümüşsuyu Prof. Dr. Necmettin Erbakan Yerleşkesi
Istanbul Technical University
Gumussuyu Prof. Dr. Necmettin Erbakan Campus





16 ULUSLARARASI
LİF VE POLİMER
ARAŞTIRMALARI
SEMPZYUMU

16th INTERNATIONAL FIBER AND POLYMER RESEARCH SYMPOSIUM

Sürdürülebilir ve İşlevsel Lif ve Polimerler
Sustainable and Functional Fibers & Polymers



9-10 Mayıs
May 2025

İstanbul Teknik Üniversitesi
Gümüşsuyu Prof. Dr. Necmettin Erbakan Yerleşkesi
Istanbul Technical University
Gumussuyu Prof. Dr. Necmettin Erbakan Campus



Advanced emulsion fabrication of alkyd resins: effect of phase inversion and processing conditions

Pelin Aksoy ^{a*}, Abdulvahap Selim Çifçi ^a

^aALFA KİMYA A.Ş., Istanbul 34953, Türkiye.

<https://orcid.org/0009-0007-5472-4054>

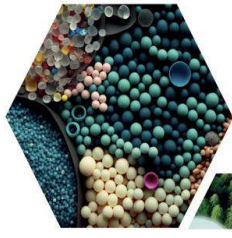
*Corresponding author: peлин.aksoy@alfakimyaas.com

ABSTRACT

In this study, the usability of an alkyd resin synthesized from vegetable oil-derived fatty acids as a binder in emulsion paint formulations was investigated. The resin was synthesized through a two-stage process involving alcoholysis and esterification, using glycerol, pentaerythritol, phthalic anhydride, and maleic anhydride. The reaction was carried out in the presence of xylene as an azeotropic solvent, and the progress was monitored by acid value titration. Upon reaching the desired acid number, the resin was diluted with white spirit to obtain the target solid content and viscosity. The synthesized long-oil alkyd resin was then emulsified into water using a high-speed mechanical stirrer and non-ionic surfactants. The resulting water-reducible alkyd emulsion was used in a standard emulsion paint formulation. Characterization of the resin and the emulsion was performed by FTIR spectroscopy, gel permeation chromatography (GPC), particle size analysis, and standard paint performance tests. FTIR results confirmed the presence of characteristic functional groups.

The emulsion-based paint was evaluated for gloss, hardness, flexibility, drying time, water resistance, and chemical resistance. The results demonstrated that the alkyd resin synthesized from renewable fatty acids can be effectively emulsified and incorporated into water-based paint formulations, offering desirable performance properties. This study supports the feasibility of producing environmentally friendly, solvent-reduced coating systems using alkyd chemistry adapted to emulsion technologies.

Keywords: Emulsion formation; Alkyd resins; Emulsion paint; Water-based alkyd; Solvent-reduced coatings



16 ULUSLARARASI
LİF VE POLİMER
ARAŞTIRMALARI
SEMPOZYUMU

16th INTERNATIONAL FIBER AND POLYMER RESEARCH SYMPOSIUM

Sürdürülebilir ve İşlevsel Lif ve Polimerler
Sustainable and Functional Fibers & Polymers



9-10 Mayıs
May 2025

İstanbul Teknik Üniversitesi
Gümüşsuyu Prof. Dr. Necmettin Erbakan Yerleşkesi
Istanbul Technical University
Gumussuyu Prof. Dr. Necmettin Erbakan Campus

Fabrication and antioxidant activities of polyethylene oxide/sodium alginate/zinc oxide electrospun nanofibers

Azra Huner^{a,b}

^a Science and Technology Application and Research Center, Yıldız Technical University, Esenler, 34200 Istanbul, Turkey

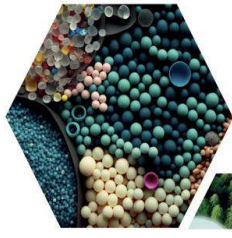
^b Department of Chemistry, Istanbul Technical University, Maslak, 34469 Istanbul, Turkey

*Corresponding author: azra.huner@yildiz.edu.tr

ABSTRACT

Nanofibers produced by the electrospinning method have various properties such as a high surface area/volume ratio and a void ratio, which allows these nanofibers to be used in many biomedical applications. Polymers such as polyethylene oxide and sodium alginate are widely used in the production of nanofibers by electrospinning. In this study, polyethylene oxide/sodium alginate/zinc oxide nanofibers in which zinc oxide was incorporated at different ratios were produced by electrospinning. These nanofibers were characterized by FT-IR and XRD. Their surface morphologies were examined by SEM. It was observed that zinc oxide increased the crystallinity of the nanofibers and caused slightly beaded structures in the surface morphology. According to ABTS analysis, it was observed that the produced nanofibers had antioxidant activity, and the highest antioxidant activity was obtained from the nanofiber containing 9% zinc oxide with 160 µg TE/mg values.

Keywords: Antioxidant; Nanofiber; Zinc oxide



16 ULUSLARARASI
LİF VE POLİMER
ARAŞTIRMALARI
SEMPOZYUMU

16th INTERNATIONAL FIBER AND POLYMER RESEARCH SYMPOSIUM

Sürdürülebilir ve İşlevsel Lif ve Polimerler
Sustainable and Functional Fibers & Polymers



9-10 Mayıs
May 2025

İstanbul Teknik Üniversitesi
Gümüşsuyu Prof. Dr. Necmettin Erbakan Yerleşkesi
İstanbul Technical University
Gumussuyu Prof. Dr. Necmettin Erbakan Campus



Electrospun gelatin/sodium alginate nanofibers for cephalexin delivery

Azra Huner^{a,b}

^a Science and Technology Application and Research Center, Yıldız Technical University, Esenler, 34200 Istanbul, Turkey

^b Department of Chemistry, Istanbul Technical University, Maslak, 34469 Istanbul, Turkey

*Corresponding author: azra.huner@yildiz.edu.tr

ABSTRACT

Electrospinning has been gaining increasing attention in the last decade due to its potential use in many areas such as filtration, biomedical materials, optoelectronics, catalysis, and drug delivery systems. Among these, drug delivery is one of the most promising applications. Gelatin and sodium alginate are non-toxic natural polymers with excellent biocompatibility, and their electrospun nanofibers are widely used in medical applications, especially wound healing and drug delivery. This study focused on the potential of a gelatin/sodium alginate biopolymer-based nanofiber matrix in the delivery of cephalexin, which is used as a model drug. Electrospun nanofibers were produced from solutions prepared using sodium alginate at different ratios compared to gelatin. In addition, gelatin/sodium alginate nanofibers loaded with cephalexin were produced. These nanofibers were characterized using scanning electron microscopy (SEM) and X-ray diffractometry (XRD). The release mechanism of cephalexin was measured by an ultraviolet absorption spectrophotometer. The results showed that cephalexin-loaded gelatin/sodium alginate nanofibers have the potential of a controlled release system.

Keywords: Gelatin; Sodium alginate; Nanofiber



Effect of porosity distribution in FRP laminate on interfacial shear stresses in cracked beams strengthened with variable fiber spacing

Khamis Hadjazi^{a,*}, Mohamed Larbi Bennegadi^a, Nawel Bentata^a, Lahouaria Errouane, Zouaoui Sereir^a

^aFaculty of Mechanic Engineering, University of Science and Technology of Oran (USTO), Composite Structures and Innovative Materials Laboratory (LSCMI), Oran, 31000, Algeria

*Corresponding author: khamishadj@yahoo.fr

ABSTRACT

The repair of cracked structures using FRP plates with variable volume fraction is a promising process, as it helps recover the lost stiffness of beams due to crack formation. However, an important issue related to flexural strengthening of structures is the debonding of the reinforcement plate, caused either by poor adhesion or by non-compliance with the proportionality between the reinforcement elements due to the presence of porosities in the FRP plate. These porosities generally occur in the structures during the manufacturing process. In the present study, an improved analytical model has been proposed to describe the shear stresses along the interface using a bilinear cohesive law model to analyze a cracked beam repaired with a porous FRP plate. The results obtained for interfacial shear stress distribution near the crack are compared to the analytical model from the literature. The effect of porosity on the stiffness of the FRP plate has been modeled in the form of a power polynomial along the direction of the plate's thickness. The study highlights that porosity and material gradient indices significantly affect the load-carrying capacity, softening and debonding behavior, and the durability of the repaired structure.

Keywords: Analytical model; Strengthened beam; Flexural crack; Imperfect FRP plate; Interfacial stresses

I. INTRODUCTION

Concrete structures, essential to many modern infrastructures, are frequently subjected to various forms of degradation over time, such as steel rebars corrosion, cracking, and the effects of environmental conditions. These deteriorations reduce the load-bearing capacity of concrete, which can lead to structural weakening and increased risk of failure [1-2]. To restore this load-bearing capacity, innovative repair and reinforcement techniques are needed,

among which the use of FRP (Fibre Reinforced Polymer) plates has become prominent [3-4].

FRP plates, due to their high strength and lightweight properties, offer an effective solution for reinforcing damaged concrete. However, the presence of manufacturing defects, such as porosity, can significantly impact their mechanical properties, particularly their stiffness and shear strength. The porosities usually occur in the structures during the manufacturing process. Excessive porosity can decrease the stiffness of the plate, altering the shear

stresses that develop at the interface between the FRP plate and the concrete beam. This may lead to activate the debonding process in long term of the plate, compromising the reinforcement's effectiveness.

Various studies, such as those by [5] and [6], have shown that porosity in BFG plates reduces their rigidity, resulting in increased deflections of the porous plates. These analytical methods demonstrated that porosity affects the distribution of shear stress in a more pronounced way compared to the distribution of normal stress. Other research, including that by [7], explores the hygro-thermal vibration behavior of functionally graded porous curved beams using the generalized finite element method.

The study of buckling by [8] and post-buckling by [9] of porous FG plates has drawn significant attention from researchers. Vaghefi [9] investigated the elastoplastic post-buckling behavior of porous functionally graded (FG) plates with various porosity distributions, supported by Winkler/Pasternak foundations under both uniaxial and biaxial in-plane loading. Meanwhile, Sobhy and Zenkour, [8] analyzed the buckling behavior of porous FG nanoplates resting on an elastic foundation.

An additional approach in FRP plate design involves using plates having variable fiber volume fraction. This technique allows for precise control over the distribution of fibers within the polymer, optimizing the mechanical properties of the plate. FRP plates having variable fiber spacing can create stronger areas where shear stresses are highest and lighter, more porous areas where increased strength is unnecessary. This variation in the fiber volume fraction can help compensate for the negative effects of porosity while providing better control over the distribution of interfacial shear stresses induced by intermediate flexural crack.

In literature, several studies have investigated the effect of variable fibers spacing on vibration and

buckling problems of composites plates. The influence of the fiber redistribution in the bonded plates on the lateral deflections of reinforced concrete coupled shear walls under three different earthquakes, using the mixed finite element method, is presented by [10]. The study shows that the composite plates with variable fiber spacing significantly influence the lateral deflections of RC coupled shear walls and demonstrate the feasibility of mitigating the seismic response of RC coupled shear walls building structures. To control or customize thermal deformations [11], developed a functionally graded material (FGM) by varying the fiber volume fraction in a symmetrical laminated beam. They investigated how different fiber volume fraction distributions affect the in-plane expansion coefficient and the axial stiffness. Nourmohammadi et al. [12-13] determined the effective bending modulus of a thin composite lamina with both uniform and non-uniform fiber spacing using the Euler-Bernoulli beam model. Their findings indicate that the effective bending modulus is influenced by factors such as the geometry ratio, fiber volume fraction ratio, fiber shift ratio, and the number of fibers through the thickness. Haoren et al. [14], presented an innovative approach for manufacturing Continuous Fiber Reinforced Composites, featuring an adjustable nozzle that allows control over the variable volume fraction of continuous fibers. This method was validated through advanced simulations, demonstrating its effectiveness in enhancing the mechanical properties of composites plate with a central hole. Experimental validation showed a 61.04% increase in tensile strength, without any increase in fiber content. The study demonstrates the potential of this strategy to advance composite material technology with improved mechanical performance.

In all the models proposed by [15-16-17-18-19-20] the effects of porosity and variable volumetric fraction along the thickness direction of the FRP plate are

ignored in the determination of interfacial peel and shear stresses.

This paper presents an analytical model based on the cohesive zone model to investigate the effects of porosity and variable volumetric fraction on the evolution of shear stresses at the concrete-FRP interface. The cohesive zone model, commonly used to predict the distribution of interfacial shear stresses in concrete beams strengthened with FRP plates and crack evolution, is particularly suited to understanding how manufacturing defects (such as porosity) and the non-uniform distribution of volumetric fraction affect the mechanical response of the system. By accounting for variations in FRP composition, this model will facilitate the analysis of the impact of porosity and variable volumetric fraction on the adhesion between the concrete and the plate, as well as crack propagation and interfacial shear stress near the intermediate crack. The proposed analytical model aims to enhance the understanding of the interaction between concrete and FRP plates, providing recommendations for optimizing plate design to maximize the load-bearing capacity of structures repaired with porous FRP plates.

II. COHESIVE ZONE MODEL OF A MID-SPAN CRACKED BEAM

Consider a simply-supported reinforced concrete beam, as presented in figure 1, reinforced with an imperfect FRP plate due to the effect of porosities in its material properties distribution, and subjected to a three-point bending load with a flexural crack at mid-span.

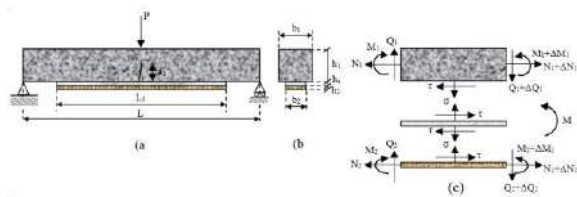


Figure 1. The FRP-repaired beam and cross section of plate beam analysed.

This study examines two types of porosity distribution in the modeling of the FRP laminates plate having variable fibers spacing as shown in Figure 2.

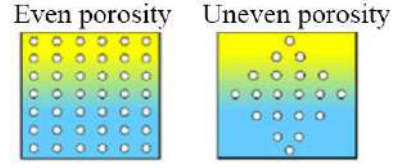


Figure 2. Two types of porosity distribution.

The concrete beam and FRP plate are modeled as linear elastic simple beams. For this reason, the axial forces N_i and bending moments M_i for these two beams ($i = 1, 2$) read:

$$\begin{Bmatrix} N_i \\ M_i \end{Bmatrix} = \begin{bmatrix} C_i & B_i \\ B_i & D_i \end{bmatrix} \begin{Bmatrix} u_i' \\ w_i' \end{Bmatrix} \quad (1)$$

Where u_i and w_i are respectively the axial and vertical displacements of beam i ($i=1,2$). C_i , B_i , and D_i are the extensional, coupling, and bending stiffness matrices, respectively. Based on Eq. (2), C_i , B_i , and D_i can be expressed as [21]:

$$[C_i, B_i, D_i] = b_i \int_{-h_i/2}^{h_i/2} E_i(y) (1, y, y^2) dy \quad (2)$$

Where E_i , b_i and h_i are the Young's modulus, the width and the thickness of beam i ($i = 1, 2$)

2-1 Rigidity of FRP plate having variable spacing and porosity

Porosity can significantly reduce the material properties of the FRP plate, meaning that as the porosity coefficient increases, the Young's modulus of the FRP plate decreases [5]. By applying the law of mixtures, the rigidity of the FRP plate can be expressed in terms of the properties of the fiber and matrix materials [22].

In this study, two porosity distribution models are considered: the even and uneven porosity models. The expression for the rigidity of the FRP plate, which accounts for the effects of variable fiber spacing and porosity factors, can be written as [5]:

- ✓ For even porosity, the effective Young's modulus of FRP plate is given as follows:

$$E_2(y) = E_m + (E_f - E_m)V_f - \frac{\zeta}{2}(E_f + E_m) \quad (3)$$

- ✓ For uneven porosity, the effective Young's modulus of FRP plate is given as follows:

$$E_2(y) = E_m + (E_f - E_m)V_f - \left(1 - \frac{2|y|}{h_2}\right) \frac{\zeta}{2}(E_f + E_m) \quad (4)$$

In the Eq. 3 and 4 f , m and ζ denotes properties of the fiber, matrix and the porosity volume fraction index ($\zeta \ll 1$ and is a non-negative constant) respectively. The volume fractions of the fibers in the FRP plate are given as:

$$V_f(y) = \left(\frac{2y}{h_2}\right)^\alpha \quad (5)$$

Where α denotes the power-law index.

Figure 3 shows the variation of the elastic modulus in the y-direction, across the FRP plate, which is composed of fiber and matrix with properties outlined in Table 2, for power-law index $\alpha=1$ and 2. It is evident that porosity decreases the effective Young's modulus of the FRP plate by creating voids within the material. In the case of uniform porosity, its effect on the reduction of Young's modulus is consistent throughout the thickness of the plate. However, for uneven porosity, the reduction in Young's modulus is more pronounced at the mid-plane, where voids are concentrated, while porosity has minimal effect on the effective Young's modulus at both the top and bottom surfaces of the FRP plate.

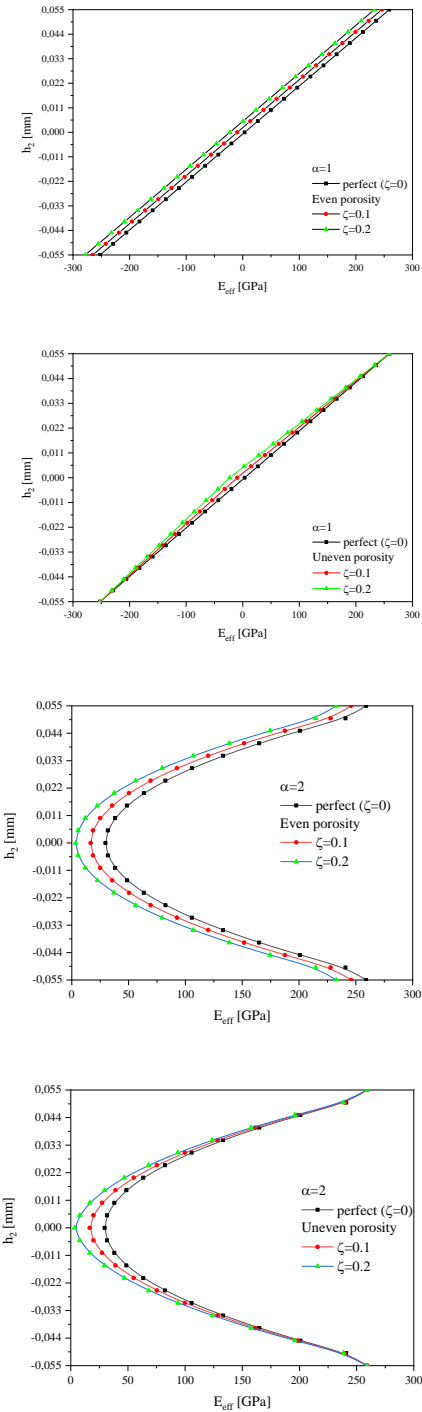


Figure 3. The variation of the rigidity of the FRP porous plates.

2-2 Effect of the power-law index

Figure 4 illustrates the variations in the volume fractions of fiber and matrix with respect to the y-direction. A plot of the fiber volume fraction (V_f) through the thickness for $n=2, 4$ and 6 is shown in the same Figure. In this study, the fiber volume fraction varies parabolically, as described by Eq. (5),

depending on n , through the thickness. With the above variation in fiber spacing, the material at the plate edges ($V_f = 1$) consists of pure fibers, while at the center of the plate, the material is composed entirely of matrix.

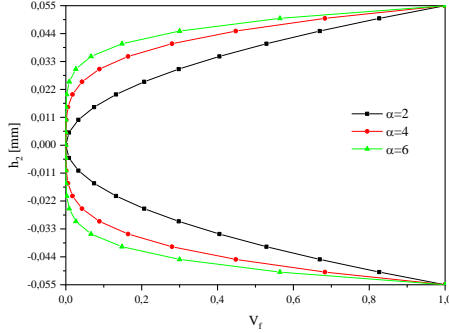


Figure 4. Fiber volume fraction distribution through the thickness of the FRP plate.

Displacement discontinuities in the axial direction at the crack location (Fig. 1a), caused by flexural cracks, can conventionally be modeled as a rotational spring with negligible thickness at the crack location. According to [23], the stiffness can be calculated by considering the material properties of the beam and the geometry of the crack.

$$K_r = c(a_1, h_1) D_1 \quad (6)$$

Where a_1 is the depth of the crack and $c(a, h_1)$ is determined by the crack geometry. For $a/h_1 < 0.6$, $c(a, h_1)$ is already given by [23]. As shown in Fig. 1,c the coupled global equilibrium condition of typical infinitesimal isolated body of the plated concrete beam are given as:

$$\begin{cases} \frac{dN_1}{dx} = b_2 \tau \\ \frac{dN_2}{dx} = -b_2 \tau \\ M = M_1 + M_2 + N_2 \left(\frac{h_1 + h_2}{2} \right) \end{cases} \quad (7)$$

Where τ is the interface shear stress and M is the total applied moment.

In this study, a triangular-type cohesive law (bi-linear bond-slip) is used, as shown in Fig. 3. The triangular

traction-separation curve exhibits two distinct slopes. The initial slope represents the initial elastic stiffness of the FRP-concrete interface ($K_b = \tau_f / \delta_1$), where τ_f is the maximum interfacial traction and δ_1 is the corresponding relative displacement. The descending portion of the cohesive law represents the linear stress-softening stage. The bond-slip model shown in Fig. 3 is used to relate the shear stress to the relative displacement (slip) between the FRP plate and the concrete beam. An analytical model based on the cohesive zone approach was developed to predict the distribution of interfacial shear stresses in concrete beams strengthened by porous composite plates. This model successfully simulates the elastic, softening, and debonding stages.

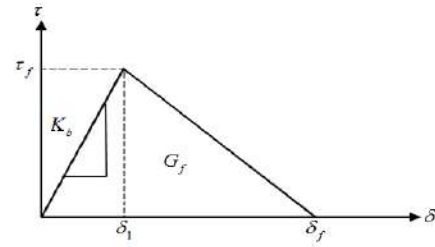


Figure 5. Triangular traction-separation laws.

The area under the traction-relative displacement curve (fig. 3) is fracture toughness, also known as fracture energy, which can be calculated by

$$G_f = \int_0^{\delta_f} \tau d\delta = \frac{1}{2} \delta_f \tau_f \quad (8)$$

Where δ_f is the separation slip which corresponds to the interface shear stress approaching zero.

The behavior of concrete beams reinforced by FRP plate using the cohesive zone model for these three stages can be described by the following equation:

$$\tau = \begin{cases} \frac{\tau_f}{\delta_1} \delta & 0 \leq \delta \leq \delta_1 \\ \frac{\delta_f - \delta}{\delta_f - \delta_1} \tau_f & \delta_1 \leq \delta \leq \delta_f \\ 0 & \delta > \delta_f \end{cases} \quad (9)$$

Where δ is the slip along the interface induced by the transverse displacement (axial) of the top of the FRP plate and the bottom of the concrete beam is given by:

$$\delta = u_1 - \frac{h_1}{2} w_1' - u_2 - \frac{h_2}{2} w_2' \quad (10)$$

Stage I : elastic stage:

At small loads, the governing equation of the bond-slip relation in this stage can be obtained by substituting Eq. (10) into the first equation of Eq. (9). Differentiating both sides of this Equation gives us:

$$\tau' = \frac{\tau_f}{\delta_1} (u_1' - Y_1 w_1'' - u_2' - Y_2 w_2'') \quad (11)$$

Using Eq. (1), the longitudinal strains induced by the longitudinal forces can be expressed as [16]:

$$\begin{aligned} u_1' &= \frac{N_1}{C_1} \\ u_2' &= \frac{N_2}{b_2} (C_2^* - Y_2 B_2^*) \end{aligned} \quad (12)$$

Where C_2^* and B_2^* are the inverse extension and coupling matrices, respectively.

Substituting Eqs. (12) into Eqs. (11) we have:

$$\tau' = \frac{\tau_f}{\delta_1} \left(\frac{N_1}{C_1} - Y_1 w_1'' - \frac{N_2}{b_2} (C_2^* - Y_2 B_2^*) - Y_2 w_2'' \right) \quad (13)$$

According to the literature [24-25] the FRP plate and the concrete beam have the same curvature, i.e.:

$$w_1'' = w_2'' \quad (14)$$

Substituting Eq. (14) and Eq. (1) into Eq. (7) we have:

$$w_1'' = -\frac{M}{D_1 + \frac{b_2}{D_2^*}} + \frac{\frac{B_2^*}{D_2^*} + Y_1 + Y_2}{D_1 + \frac{b_2}{D_2^*}} N_2 \quad (15)$$

Substituting Eq. (14) and Eq. (15) into Eq. (13) we obtain:

$$\tau' = \frac{\tau_f}{\delta_1} \left(\frac{N_1}{C_1} - N_2 \left(\frac{(C_2^* - Y_2 B_2^*)}{b_2} + \left(\frac{B_2^*}{D_2^*} + Y_1 + Y_2 \right) \left(\frac{1}{D_1 + \frac{b_2}{D_2^*}} \right) \right) + \frac{(Y_1 + Y_2)}{D_1 + \frac{b_2}{D_2^*}} M \right) \quad (16)$$

The second derivative of the Eq. (16) with respect to x and considering Eq. (7), is as follows:

$$\tau'' = \frac{\tau_f}{\delta_1} \left(\frac{1}{C_1} + \frac{(C_2^* - Y_2 B_2^*)}{b_2} + \left(\frac{B_2^*}{D_2^*} + Y_1 + Y_2 \right) \left(\frac{1}{D_1 + \frac{b_2}{D_2^*}} \right) \right) b_2 \tau + \frac{\tau_f (Y_1 + Y_2)}{\delta_1 \left(D_1 + \frac{b_2}{D_2^*} \right)} M' \quad (17)$$

The solution of the differential equation of the second order (17) takes the form:

$$\tau = A e^{-\lambda_1 x} + B e^{\lambda_1 x} + \tau_c \quad (18)$$

Where:

$$\begin{cases} \lambda_1 = C_\lambda \sqrt{\frac{\tau_f}{\delta_1}} \\ C_\lambda = \sqrt{b_2 \left(\frac{1}{C_1} + \frac{(C_2^* - Y_2 B_2^*)}{b_2} + \left(\frac{B_2^*}{D_2^*} + Y_1 + Y_2 \right) \left(\frac{1}{D_1 + \frac{b_2}{D_2^*}} \right) \right) (Y_1 + Y_2)} \\ \tau_c = C_\tau M' \\ C_\tau = \frac{Y_1 + Y_2}{\left(D_1 + \frac{b_2}{D_2^*} \right) C_\lambda^2} \end{cases} \quad (19)$$

When x is sufficiently large, shear stress is limited and converges to its particular solution τ_c , so $B = 0$, [26]. A is coefficients to be determined by the displacement boundary conditions at $x = 0$ and Eq. (20). Substituting the value of constant A in the shear stress Eq. (18), the maximum value of load P_E applied to the beam without causing softening in the FRP-concrete interface can then be obtained.

Displacement continuity conditions at the flexural-crack location can be written as [15]:

$$\delta|_{x=0} = \frac{Y_1}{2Kr} M_1|_{x=0} \quad (20)$$

From equations (9) and (18), the corresponding slip δ along the interface evolves as a function of the shear stress in the elastic stage, which can be expressed by the following relation:

$$\delta = \frac{\delta_1}{\tau_f} (A e^{-\lambda_1 x} + \tau_c) \quad (21)$$

Stage II : Elastic softening stage

When the load exceeds the elastic limit ($P > P_e$), part of the interface begins to soften as slip occurs, resulting in the formation of two distinct regions along the interface:

a) **Elastic region**, In this region, the solution for shear stress takes the same form as in Eq. (18), where the shear stress is given by:

$$\tau = A_1 e^{-\lambda_1(x-a)} + \tau_c \quad (22)$$

And the slip δ at the interface is expressed as:

$$\delta = \frac{\delta_1}{\tau_f} \left(A e^{-\lambda_1(x-a)} + \tau_c \right) \quad (23)$$

Where a is the microcrack length. The constant A_1 is determined based on the following boundary condition:

$$\tau|_{x=a} = \tau_f \quad (24)$$

b) **Softening region**, if the load P is increased after reaching the elastic limit, a microcrack zone forms between the elastic region and the central flexural crack. By substituting Eq. (7) in the second expression of bond-slip law, and then we differentiating both sides with respect to x , Eq. (17) becomes :

$$\tau' = \frac{-\tau_f}{\delta_f - \delta_1} \left(\frac{1}{C_1} + \frac{(C_2^* - Y_2 B_2^*)}{b_2} + \left(\frac{B_2^* + Y_1 + Y_2}{D_2^*} \right) \left(\frac{Y_1 + Y_2}{D_1 + \frac{b_2^*}{D_2^*}} \right) \right) b_2 \tau - \frac{\tau_f}{\delta_f - \delta_1} \left(\frac{Y_1 + Y_2}{D_1 + \frac{b_2^*}{D_2^*}} \right) M' \quad (25)$$

The solution of the second-order differential equation (25) can be expressed as:

$$\tau = C \cos(\lambda_2(x-a)) + D \sin(\lambda_2(x-a)) + \tau_c \quad (26)$$

By combining Eqs. (9) and (26), the slip δ along the interface in this region can be written as:

$$\delta = \delta_f - \frac{\delta_f - \delta_1}{\tau_f} (C \cos(\lambda_2(x-a)) + D \sin(\lambda_2(x-a)) + \tau_c) \quad (27)$$

Where:

$$\lambda_2 = \lambda_1 \sqrt{\frac{\delta_1}{\delta_f - \delta_1}} \quad (28)$$

Constants C and D are two constant determined by the continuity conditions at $x = a$:

$$\tau|_{x=a^-} = \tau_f, \quad \tau'|_{x=a^-} = -\frac{\delta_1}{\delta_f - \delta_1} \tau'|_{x=a^+} \quad (29)$$

The microcrack length, a , can be determined by substituting Eqs. (23) and (26) into Eq. (29).

Stage III: Elastic-softening- debonding stage

When the external load increases to or exceeds the ultimate load ($P \geq P_u$), the maximum slip (δ) at the

location of the flexural crack ($x = 0$) reaches δ_f . An initial unbonded portion (crack) of length d is considered, and this crack develops along the interface. As a result, the interface transitions through three stages: elastic (E), softening (S), and debonding (D). In the debonded zone, the interfacial shear stress becomes zero, indicating full separation between the FRP plate and the concrete beam. Using a similar procedure described in the previous section, the interfacial shear stress along the interface can be determined by the following relationship:

$$\bullet \text{ Elastic region : } \tau = A_1 e^{-\lambda_1(x-d-a_u)} + \tau_c \quad (30)$$

\bullet Softening region

$$\tau = C \cos(\lambda_2(x-d-a_u)) + D \sin(\lambda_2(x-d-a_u)) + \tau_c \quad (31)$$

$$\bullet \text{ Debonding region : } \tau = 0 \quad (32)$$

These shear stress profiles are derived from the material properties and the loading conditions, taking into account the transition from elastic to softening and eventually debonding as the external load increases. The corresponding load, referred to as the ultimate load P_u , can be determined by combining equations (29), (31), and the following conditions:

$$\tau|_{x=0} = 0 \quad (33)$$

The maximum size of the softening zone a_u and the ultimate load P_u leading to a separation d can be determined in the same way as in the previous step (elastic-softening). a_u is reached when, [27]:

$$\frac{dP_u}{da_u} = 0 \quad (34)$$

III. RESULTS AND DISCUSSIONS

In this section, a validation followed by a parametric study will be presented to highlight the effectiveness and sensitivity of our model. For all our applications, the mechanical and geometrical characteristics provided in Tables 1, 2, and 3 are identical to those used in [15, 16].

Table 1. Geometrical properties of FRP-concrete.

| L mm | L ₁ mm | h ₁ mm | b ₁ mm | b ₂ mm | h ₂ mm | b _a mm |
|---------|----------------------|----------------------|----------------------|----------------------|----------------------|----------------------|
| 750 | 700 | 150 | 100 | 100 | 0.11 | 100 |

Table 2: Parameters of CZM used in this study.

| τ_f [Mpa] | K_b [MPa/mm] | G_f [N/mm] |
|----------------|----------------|--------------|
| 1.8 | 160 | 0.5 |

Table 3: Mechanical properties of FRP-concrete.

| E_f [Gpa] | E_c [Gpa] | E_m [Gpa] |
|-------------|-------------|-------------|
| 25 | 259 | 3.4 |

3.1 Validation des résultats

Figure 3 illustrates the variation of shear stress along the interface of a cracked beam repaired with a non-porous plate ($\xi=0$). From this figure, it is clear that the general shape of the shear stress in the present analytical model is identical to those of the other models found in the literature [15-24], which validates the solution of this study. Each curve is subdivided into two zones: the elastic zone and the softening zone of length a_1 . This figure also examines the effects of porosity on the distribution of interfacial stresses, for the power-law index $n=2$. The variation in the type of porosity (even or uneven) has a notable impact on the distribution of interfacial shear stresses. These variations can influence the shear stress evolution, particularly in the softening and debonding phases, where stress concentrations may accelerate the initiation of debonding. This highlights the critical role of porosity, both uniform and uneven, in the mechanical performance of the interface between the FRP plate and the concrete beam.

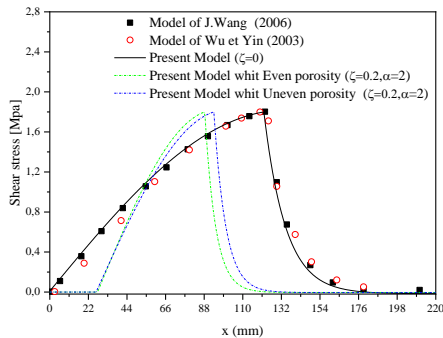


Figure 6. Shear stress distribution along the interface.

3.2 Effect of porosity on the evolution of the interface shear stress

Figure 7 illustrates the effect of porosity ($\xi = 10\%$, 20% , and 30%) on the evolution of interface shear stress along the FRP-concrete interface, considering

two types of porosity distributions: Even and Uneven, with a power-law index of $\alpha = 2$. It is observed that the extent of the softening zone is significantly influenced by the variation in the porosity coefficient ξ and the type of porosity distribution. In both Even and Uneven porosity cases, an increase in the porosity coefficient ξ results in a decrease in the rigidity of the FRP plates, leading to a reduction in the shear stress at the location of the flexural crack. As ξ increases, the maximum size of the softening zone (a_u) decreases. Therefore, an increase in the porosity coefficient accelerates the debonding process along the adhesive layer, especially with Even porosity. The effects of Even porosity on the evolution of interface shear stress are more pronounced than those of Uneven porosity.

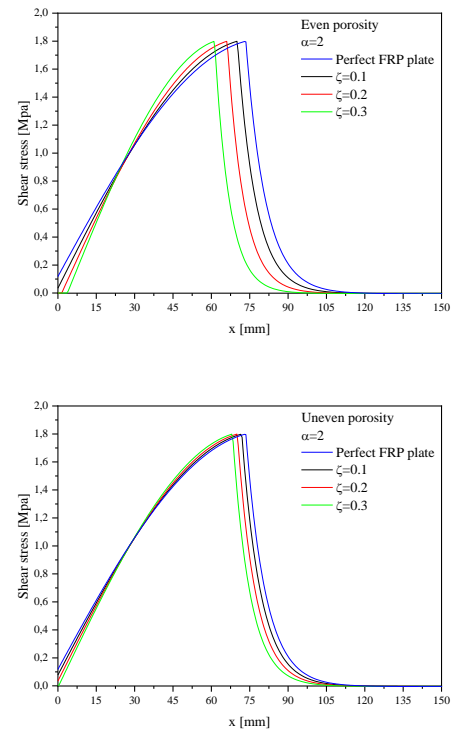


Figure 7. Effect of the porosity on the shear stress distributions.

3.3 Effect of the power-law index (α) on the evolution of the interface shear stress:

The distribution of shear stress along the FRP-concrete interface is presented for three values of the power-law index ($\alpha = 2, 4$, and 6) with $\xi = 0.1$, and two types of porosity distributions (Even and Uneven), as shown in Fig. 7. It is notable that the evolution of interface shear

stress along the FRP-concrete interface depends not only on the type of porosity distribution but also on the material's gradient index. The increase in the power-law index significantly influences the shear stress distribution, particularly in the softening and debonding stages. In general, the maximum size of the softening zone along the FRP-concrete interface is larger for the Uneven porosity distribution compared to the Even porosity distribution. However, the size of the debonding zone is smaller for the Uneven porosity. To extend the durability of the retrofitted beam, it is necessary to use materials with a power-law index of $\alpha = 2$, as this offers the best balance between durability and performance.

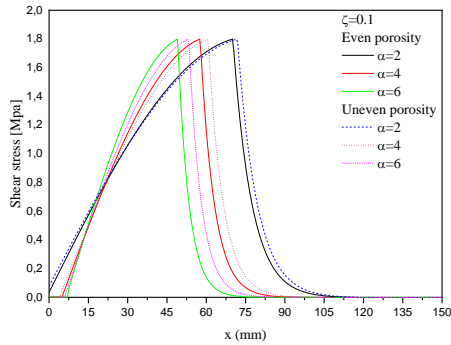


Figure 8. Effect of material gradient index whit Even and Uneven porosity.

3.4 Effect of Even and Uneven Porosity on the Capacity of the FRP-Concrete Interface

Fig. 11 examines the effect of different types of porosity distributions on the evolution of externally applied load versus bond slip at the FRP-concrete interface. In this figure, two types of porosity (Even and Uneven) are considered to analyze the load capacities of the FRP-concrete interface. For both types of porosity, three stages are identified: elastic (OA), softening (AB), and debonding (C). It is observed that as the porosity coefficient (ξ) increases, the capacity of the FRP-concrete interface decreases for both Even and Uneven porosities. Notably, the limit of the elastic stage is smaller compared to the softening stage. The softening limit is reduced from

9.93 kN for Uneven porosity to 9.12 kN for Even porosity. It is important to note that the presence of porosity reduces the stiffness of the FRP plates. Consequently, the capacity of concrete beams reinforced with porous FRP plates is lower than those reinforced with perfect FRP plates. In general, the capacity of the concrete beam reinforced with FRP plates having Uneven porosity is higher than that of FRP plates with Even porosity. This indicates that Uneven porosity may provide a more favorable load transfer mechanism, despite the overall reduction in capacity compared to non-porous FRP plates.

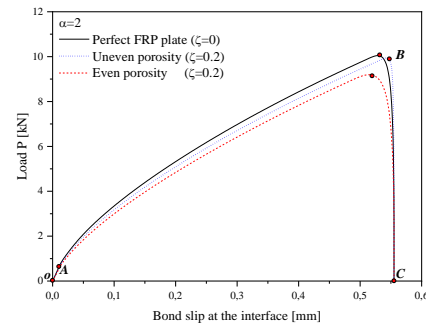


Figure 9. Load-slip curves for both type Even and Uneven of porosity distributions.

3.5 Effect of Porosity on the Externally Applied Load Evolution against the Bond Slip

Figure 8 presents the load-slip curves for the concrete beam bonded with an FRP plate, demonstrating the effect of the plate material properties on the capacity of the FRP-concrete interface. The behavior of the retrofitted beam is shown as a function of the porosity coefficient ξ ($\xi = 10\%$, 20% , and 30%) and two types of porosity distribution (Even and Uneven). The results indicate that a higher load capacity of the concrete beam bonded with a perfect FRP plate corresponds to a stronger or more efficient bond between the concrete and the FRP plate. As the stiffness of the FRP plate decreases due to the presence of porosity, the softening limit becomes smaller in both the Even and Uneven porosity cases. A higher porosity value (e.g., $\xi = 30\%$) weakens the bond and reduces the overall capacity of the FRP-concrete

interface. Furthermore, Even porosity has a more significant impact on the structural performance of the retrofitted beam and the interface quality in FRP strengthening applications compared to Uneven porosity.

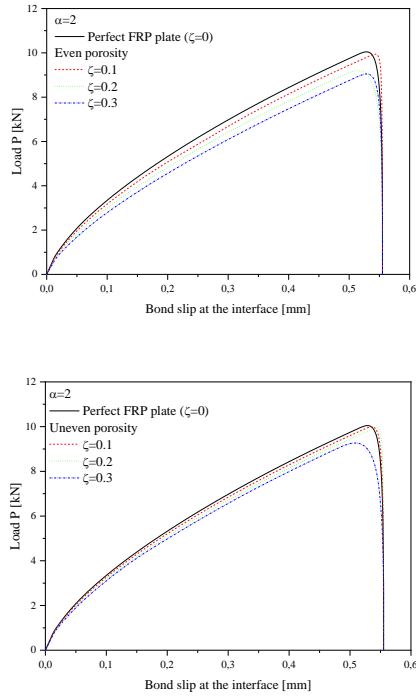


Figure 10. The variation of Load-slip curves as functions of the porosity coefficient

3.6 Effect of power-law index on the externally applied load evolution against the bond slip

The bond-slip relationship in retrofitted concrete beams is a crucial factor in determining the overall performance and structural integrity of the system. Figure 13 illustrates the bond-slip behavior at the interface ($x = 0$) under varying external loads for three different power-law indices, considering both Even Porosity and Uneven Porosity. From the figure, it is clear that the power-law index significantly influences the interaction between the FRP plate and the concrete beam, especially when accounting for porosity effects. As the power-law index increases, the material stiffness of the FRP plate near the bond improves, thereby enhancing the load-carrying capacity for both Even and Uneven Porosity. In particular, for Uneven Porosity, the increase in the power-law index results in

a more pronounced improvement in bond strength compared to Even Porosity, where localized weaknesses due to regular porosity may lead to premature failure. For both Even and Uneven Porosity, a higher power-law index helps maintain a balance between stiffness and ductility, preventing premature failure in weaker regions (such as near cracks). Ultimately, the power-law index, in conjunction with the type of porosity, plays a vital role in determining the structural behavior of the repaired concrete beam.

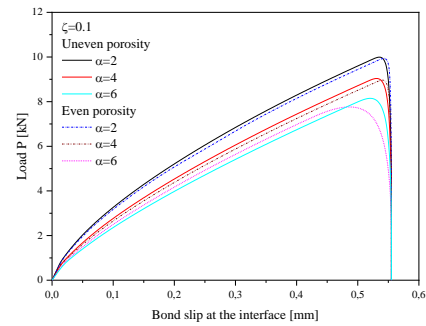


Figure 11. Impact of the Power-Law Index and porosity on the overall capacity of the repaired beam.

The effects of the power-law index α and porosity ξ on the variation of shear stresses at the location of the crack (at $x=0$) for even and Uneven porosity are presented in Fig. 5. It is obvious that the power-law index α affects strongly on the variation of the shear stresses at the location of the crack. When the porosity coefficient ξ increases, the shear stresses for both Even and Uneven porosities decrease. The zero shear stress at the location of the flexural crack, indicated a full softening zone is created

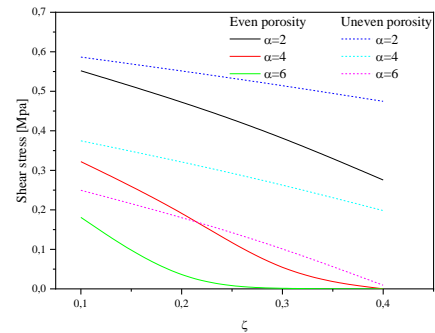


Figure 12. Shear stress at the location of the crack.

3.7 Behavior of Concrete Beams Strengthened with FRP Plates: Effects of Porosity and Power-Law Index

Table 3 presents the effect of the porosity coefficient on the elastic and ultimate loads, as well as the size of the softening and debonding zones, for different power-law index values of the FRP plate. It is clearly observed that an increase in both the porosity coefficient (for Even and Uneven porosity distributions) and the power-law index leads to a reduction in the elastic and ultimate loads, indicating a reduction in the overall strength of the retrofitted system. In addition, the size of the softening zone decreases with both porosity and the power-law index, suggesting that the material's ability to resist further deformation weakens more rapidly in these regions. On the other hand, the debonding zone is the area where the FRP plate starts to separate from the concrete beam.

Table 3. Behavior of concrete beams repaired with FRP Plate.

| Porosity | ζ | α | $P_e [N]$ | $P_u [N]$ | $a_u [mm]$ | $d [mm]$ |
|----------|---------|----------|-----------|-----------|------------|----------|
| Perfect | 0 | 2 | 685.4 | 10425 | 76.5 | 0 |
| | | 4 | 568.2 | 9575.4 | 60.5 | 5.50 |
| | | 6 | 506.0 | 9130.8 | 51.5 | 7.50 |
| Even | 0.1 | 2 | 643.8 | 10120.1 | 71 | 2.00 |
| | | 4 | 512.8 | 9178 | 52.5 | 7.50 |
| | | 6 | 438.9 | 8650.5 | 42.5 | 8.50 |
| | 0.2 | 2 | 598.1 | 9791 | 64.5 | 4.50 |
| | | 4 | 447.3 | 8710.3 | 43.5 | 8.50 |
| | | 6 | 351.5 | 8030.7 | 30.0 | 9.50 |
| Uneven | 0.1 | 2 | 665.1 | 10275.9 | 74 | 1.00 |
| | | 4 | 541.5 | 9382 | 56.5 | 6.50 |
| | | 6 | 474.2 | 8903 | 47 | 8.00 |
| | 0.2 | 2 | 643.8 | 10122.1 | 71 | 2.00 |
| | | 4 | 512.8 | 9177.1 | 52.5 | 7.50 |
| | | 6 | 338.9 | 8652.4 | 42.5 | 8.50 |

Therefore, as both porosity and the power-law index increase, the debonding zone becomes larger, suggesting that higher porosity and a higher power-

law index contribute to an earlier initiation of failure at the interface between the FRP and the concrete.

IV. CONCLUSIONS

This study presents an analytical model to predict the evolution of shear stresses along the interface of a cracked concrete structure repaired with FRP porous plates under bending stresses. The model is based on a bilinear cohesive zone law and incorporates the effect of porosity in the FRP plate through variations in the power law index. The results showed good convergence and accuracy of the proposed model.

The analysis indicates that porosity and the power-law index significantly impact the load-carrying capacity, softening and debonding behavior, and the longevity of the repaired structure. Therefore, these factors should be carefully considered in the design of repaired concrete beams to ensure optimal performance.

Acknowledgments

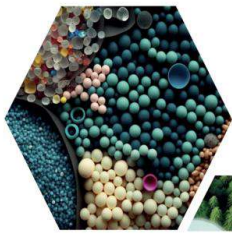
The authors would like to thank the director of the Laboratory for Structures of Composites and Innovative Materials as well as all members of the laboratory, for their contributions.

REFERENCES

- [1] Bennegadi, M., Hadjazi, K., Sereir, Z., Amziane, S., & El Mahi, B. (2016). General cohesive zone model for prediction of interfacial stresses induced by intermediate flexural crack of FRP-plated RC beams. *Engineering Structures*, 126, 147–157. <https://doi.org/10.1016/j.engstruct.2016.07.030>
- [2] Soliman, E., Kandil, U.F., Taha, M.R., (2012) Limiting shear creep of epoxy adhesive at the FRP–concrete interface using multi-walled carbon nanotubes. *Int. J. Adhes. Adhes* 33, 36-44. DOI:10.1016/j.ijadhadh.2011.09.006
- [3] Errouane, H., Deghoul, N., Sereir, Z. and Chateaneuf, A. (2017). Probability analysis of optimal design for fatigue crack of aluminium plate repaired with bonded composite patch. *Structural*

- Engineering and Mechanics, Vol. 61, No. 3, P.325-334. <https://doi.org/10.12989/sem.2017.61.3.325>
- [4] Houachine, H. R. E., Sereir, Z., & Amziane, S. (2022). Creep model for the long-term behaviour of combined cohesive-bridging model of FRP-concrete interface debonding under axial loading. *Euro. J of Envir. and Civ. Eng.*, 26(12), 5594–5616. <https://doi.org/10.1080/19648189.2021.1910864>
- [5] Pham, V. V., Le Quang, H., (2022). Finite element analysis of functionally graded sandwich plates with porosity via a new hyperbolic shear deformation theory. *Defence Technology*. Vol. 18, P. 490-508. <https://doi.org/10.1016/j.dt.2021.03.006>
- [6] Zenkour, A.M., (2020). Quasi-3D refined theory for functionally graded porous plates: displacements and stresses. *Physical Mesomechanics*. vol. 23, P. 39-53. <https://doi.org/10.1134/S1029959920010051>
- [7] Quoc-Hoa Pham, Van Ke Tran, Phu-Cuong Nguyen, (2022) Hygro-thermal vibration of bidirectional functionally graded porous curved beams on variable elastic foundation using generalized finite element method, *Case Studies in Thermal Engineering* Volume 40, December 2022, 102478. <https://doi.org/10.1016/j.csite.2022.102478>
- [8] Sobhy, M., Zenkour, A.M., (2019). Porosity and inhomogeneity effects on the buckling and vibration of double-FGM nanoplates via a quasi-3D refined theory, *Composite Struct.* 220, P. 289-303. <https://doi.org/10.1016/j.compstruct.2019.03.096>
- [9] Vaghefi, R., (2024). Three-dimensional elastoplastic post-buckling analysis of porous FG plates resting on Winkler/Pasternak foundation using meshless RRKPM. *Thin-Walled Struct.* Vol. 200, 111915. <https://doi.org/10.1016/j.tws.2024.111915>
- [10] S.A. Meftah, R. Yeghnem, A. Tounsi, E.A. Adda bedia, (2007) Seismic behavior of RC coupled shear walls repaired with CFRP laminates having variable fibers spacing. *Construction and Building Materials* 21, 1661–1671.
- [11] M. Bouremana, A. Tounsi, A. Kaci, I. Mechab (2009) Controlling thermal deformation by using composite materials having variable fiber volume fraction. *Materials and Design* 30 , 2532–2537
- [12] Nourmohammadi N, O'Dowd NP, Weaver PM. (2020) Effective bending modulus of thin ply fibre composites with uniform fibre spacing. *Int J Solids Struct* ;196–197:26–40.
- [13] Nourmohammadi N, O'Dowd N. P., Weaver P. M. (2021) Effective bending modulus of thin-ply composites with non-uniform fibre spacing. *Composite Structures* 278 (2021) 114660
- [14] Haoren Wang, Yafeng Han, Jiping Lu, Shuiyuan Tang, Hongli Fan, Yuhan Xia, Zezhi Xiang, Chenglong Gong, Run Wang, Shiye Chen, Le Tang, (2024), Additive manufacturing of continuous fiber reinforced composites with variable volume fractions. *Composites: Part A* 187 (2024) 108504
- [15] Wang, J. (2006) cohesive zone model of intermediate crack-induced debonding of FRP-plated concrete beam. *Int. J. of Solids and Structures*, Vol. 43 (21), P. 6630-6648.
- [16] Hadjazi, K., Sereir, Z., & Amziane, S. (2012). Cohesive zone model for the prediction of interfacial shear stresses in a composite-plate RC beam with an intermediate flexural crack. *Comp. Struct.* 94(12), 3574-3582. <https://doi.org/10.1016/j.compstruct.2012.05.027>
- [17] Houachine, H.R.E., Sereir, Z., Kerboua, B., Hadjazi, K., (2013). Combined cohesive- bridging zone model for prediction of the debonding between the FRP and concrete beam interface with effect of adherend shear deformations. *Comp.: Part B* 45 871–80. <http://dx.doi.org/10.1016/j.compositesb.2012.08.009>
- [18] Deghoul, N., Errouane, H., Sereir, Z., Chateaneuf, A., Amziane, S., (2019). Effect of temperature on the probability and cost analysis of mixed-mode fatigue crack propagation in patched aluminium plate. *International J. of Adhesion and*

- Adhesives. Vol. 94, 53–63. bonded steel/composite laminates, structural Eng. Vol. 18, No. 1, 27s-39s
<https://doi.org/10.1016/j.ijadhadh.2019.05.004>
- [19] Zhang, X., Wu, J., Fan, Z., Yang, S., Huang, F., Wang, A., (2019). Cohesive shear stress and strength prediction of composite patch bonded to metal reinforcement. *International J. of Adhesion and Adhesives*. Vol. 90, P.144–153.
<https://doi.org/10.1016/j.ijadhadh.2019.02.008>
- [20] Harshdeep, S., Akhilendra, S., (2024). Numerical implementation of a modified cohesive zone model for HCF behavior of adhesively bonded composite laminates under mixed mode loading. *International J. of Fatigue*. Vol. 181, 108128.
<https://doi.org/10.1016/j.ijfatigue.2023.108128>
- [21] Chen, D., Yang, J., Kitipornchai, S., (2016). Free and forced vibrations of shear deformable functionally graded porous beams. *International J. of Mechanical Sciences*. 108-109, P.14-22.
<http://dx.doi.org/10.1016/j.ijmecsci.2016.01.025>
- [22] S.A. Meftah, R. Yeghnem, A. Tounsi, E.A. Adda Bedia (2008) Lateral stiffness and vibration characteristics of composite plated RC shear walls with variable fibres spacing. *Materials and Design* 29 (2008) 1955–1964
- [23] Paipetis, S. A., Dimarogonas, A. D. (1986) *Analytical Methods in Rotor Dynamics*. Elsevier Applied Science, London.
- [24] Rasheed H. A., Pervaiz S. (2002) Bond slip analysis of fiber-reinforced polymer-strengthened beams. *J. of Engineering Mechanics* Vol. 128, P. 78-86.
- [25] Wu, Z., Yin, J. (2003) Fracture behaviors of FRP-strengthened concrete structures. *Eng. Fracture Mech.* Vol. 70, P. 1339-1355.
- [26] Wang, J., Qiao, P., (2004). Interface crack between two shear deformable elastic layers. *J. of the Mechanics and Physics of Solids*. Vol. 52, P. 891-905.
[http://dx.doi.org/10.1016/S0022-5096\(03\)00121-2](http://dx.doi.org/10.1016/S0022-5096(03)00121-2)
- [27] Hong Y., Zhishen, Hiroyuki Y. (2001) theoretical solutions on interfacial stress transfer of externally



16 ULUSLARARASI
LİF VE POLİMER
ARAŞTIRMALARI
SEMPOZYUMU

16th INTERNATIONAL FIBER AND POLYMER RESEARCH SYMPOSIUM

Sürdürülebilir ve İşlevsel Lif ve Polimerler
Sustainable and Functional Fibers & Polymers



9-10 Mayıs
May 2025

İstanbul Teknik Üniversitesi
Gümüşsuyu Prof. Dr. Necmettin Erbakan Yerleşkesi
Istanbul Technical University
Gumussuyu Prof. Dr. Necmettin Erbakan Campus

Mechano-reliability model of a bio-sourced plate based on Alfa/Greenpoxy 56

Aboubakr AMRANE^a, Lahouaria ERROUANE^{*a}, Mohammed El Larbi BENNEGADI^a, Zouaoui SEREIR^a,
Christophe POILANE^b Alexandre VIVET^b

^aLaboratory of Composite Structures and Innovative Materials University of Science and Technology MB. Oran, Algeria.

^b Normandie Univ., ENSICAEN, UNICAEN, CEA, CNRS, CIMAP, 14000 Caen, France.

*Corresponding author: herrouane@yahoo.fr

ABSTRACT

A mechanical reliability model is developed on the ANSYS APDL software in order to evaluate the sensitivity of a Bio-Based Composites (BBC) with random arrangement of short Alfa fibers. For that, we developed a program which transfers the geometry from the real image to the numerical model. Next, a program developed in Ansys APDL software was combined with the Matlab program to reproduce geometrically a plate with limited zone containing almost 300 short Alfa fibers impregnated in epoxy matrix. After that, we simulated the tensile test to compute the stress distribution; specially at the fiber/matrix interfaces. To examine the sensitivity of the maximum interfacial stress, the Monte-Carlo method was used to compute the cumulative distribution function of the failure probability according to the design variables (DV). In the reliability analysis, the dispersion of the design variables causes great variability of output parameters; where the geometric design variables (length, orientation and diameter) have a considerable effect on the sensitivity of the maximal stress.

Keywords: mechanical behaviour_1; Alfa fiber_2; bio-composite_3; A mechanical reliability model _4; sandwich panel_5

I. INTRODUCTION

Currently, biosourced materials used as reinforcements for composites - mainly natural fibers, are arousing keen interest for their degradable nature in the ecosystem and respect for the environment [1]. The advantages of biosourced materials are numerous, such as their low density, often their low cost, their recyclability, as well as, as regards the fibres, the existence of less polluting treatments than for artificial glass and carbon fibres [2]. The use of these materials in composite structures has disadvantages, such as low thermal resistance and high moisture absorption [3,4,5]. It is with this in mind that bio-sourced composites have been developed. It follows that many works and innovations have been patented over the last two decades [6] and [9]. In Algeria, natural fibers such as Alfa and the date palm occupy a large area. They are also represented in abundance in the regions of North

Africa. One of the product interests of Alfa fiber composites is that they can be used as skins for bio-based sandwich panels. Due to their specific characteristics, sandwich panels are widely used in marine applications and are used in construction and automobiles. For their design, sandwiches must have rigid and bending-resistant skins resting on a shear-resistant core [10].

In the present, a mechanical-probabilistic study to test the sensitivity of the composite fracture stress to the geometric and mechanical parameters of the elementary components was proposed. The random short fiber distribution was considered by the 3D Finite Element (FE) mesh technique to evaluate the tensile strength, damage growth, and interface fiber/matrix debonding. To examine the sensitivity of the maximum interfacial stress, the Monte-Carlo method was used to predict the cumulative distribution function of the failure probability according to the design variables (DV).

These andom DV were the Young modulus and Poisson ratio of fibers and the matrix as well as the geometric characteristics of the selected fibers (Misalignment, Diameter irregularity, Arrangement, Angle orientation and Length).

II. MECHANICAL CHARACTERISTICS OF THE COMPONENT ELEMENTS OF THE COMPOSITE PLATE

It is necessary to know the properties of the elementary components of the composite plate. For the Greenpoxy 56 resin, a tensile was made to predict the Young's modulus ($2,65 \pm 0,14\text{GPa}$), the ultimate stress ($82,2 \pm 6,3\text{MPa}$) and the break strain ($5,64 \pm 1,7\%$). a few dispersion was observed for all mechanical properties.

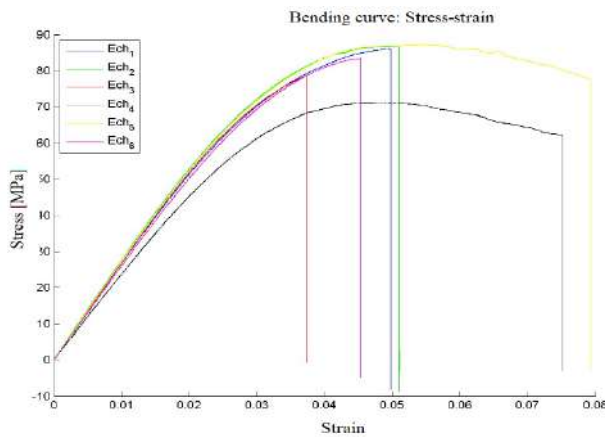


Figure.1 Greenpoxy 56 resin Stress-strain curve.

Fig. 2 illustrates the stress-strain curves in tension of the batch of 25 Alfa fibers. In this figure we notice at the beginning of loading that the stress-strain curve presents a non-linear phase explained by the initial tensioning of the fiber. The Young's modulus obtained for this fiber is 7.37 GPa , the ultimate stress and strain (140.6 MPa , $\epsilon = 3.45\%$). its evident an important dispersion was observed for the tensile test.

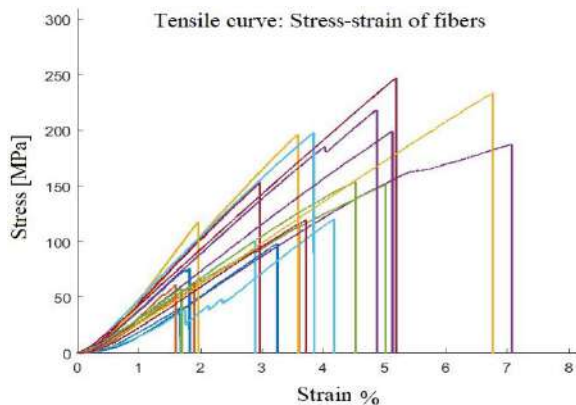


Figure 2. Stress-strain curves of Alfa fibers.

Table 1 presents the average tensile mechanical properties retained for the 25 Alfa fibers. For some specimens, a quasi-linear stress-strain relationship is obtained until rupture, while for others, rupture occurs after significant softening. This reveals a high sensitivity of this material to the presence of internal defects and also because of the geometric variation of the fibers. Therefore, we observe a significant variability (table 1) represented by a significant standard deviation (SD). Hence the need to the mechano-reliability analysis

Table 1. Mechanical properties of Alfa fibers.

| | <i>Pr</i> (N) | <i>E</i> (GPa) | σ_r (MPa) | ϵ_r (%) | <i>S</i> (mm ²) | <i>D</i> (mm) |
|--------------|------------------|----------------|---------------------|---------------------|-----------------------------|------------------|
| Value | 4,57 | 6,77 | 140,6 | 3,45 | 0,03 | 0,20 |
| SD | 1,80 | 1,51 | 60,3 | 1,33 | 0,01 | 0,03 |

Table 2. Mechanical properties of Alfa fibers available in the literature.

| | <i>E</i> (GPa) | σ_r (MPa) | ϵ_r (%) | <i>Fibres</i> |
|------------------|-----------------|------------------|------------------|---------------|
| Reference | $6,77 \pm 1,51$ | 141 ± 60 | $3,45 \pm 1,33$ | Non treated |
| [11] | $28,4 \pm 4,1$ | 474 ± 103 | $2,43 \pm 0,58$ | |
| [12] | 22 | 565 | $5,8 \pm 2$ | treated |
| [13] | 21,5 | 247 | 1,9 | treated |
| [14] | $5 \pm 3,2$ | 78 ± 46 | $1,5 \pm 0,23$ | Non treated |

The table 3 shows the mechanical properties of the resin obtained from tensile tests.

Table 3. Mechanical properties of the resin.

| | <i>E</i> (GPa) | σ_r (MPa) | ϵ_r (%) |
|---------------|----------------|------------------|------------------|
| Résine | 2,74 | 51,1 | 2,4 |

III. MODELING OF THE COMPOSITE PLATE

Fig. 3 represents an Alfa fiber/Greenpoxy Square composite plate ($L=B=25\text{mm}$ and $e=0.3\text{mm}$) with $V_m=5\%$, i.e. 298 fibers with lengths, diameters and orientations distributed randomly over the entire volume of the plate. The diameter, length and orientation of each fiber was measured optically using an automated profile projector.

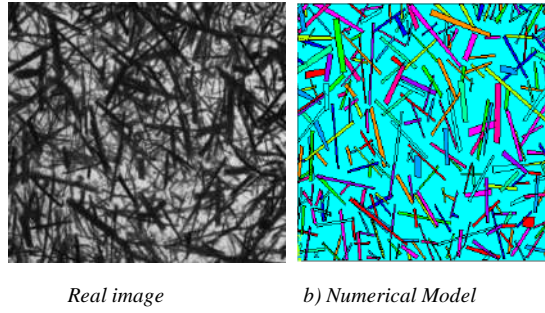


Figure 3. SFRP composite plate with 5% fiber content

This Fig. illustrates the geometry of the real image of the plate (Fig.3.a) and that of the geometrically reproduced numerical model (Fig.3.b) containing 298 short Alfa fibers impregnated with greenpoxy matrix. For the geometry meshing, the BEAM188 elements is used to mesh the fibers and SHELL63 elements for the matrix. The plate is simply supported on the 4 sides and loaded uniaxially in tension as shown in Fig.4. The pressure applied on the surface of the model is equivalent to the experimental force divided by the surface of the sample.

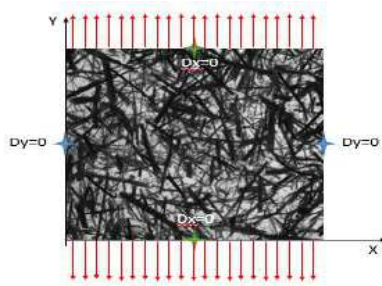


Figure 4. Composite plate with boundaries and loading conditions.

The distribution of equivalent stress in the composite plate and in the fibers is illustrated in Fig.5.

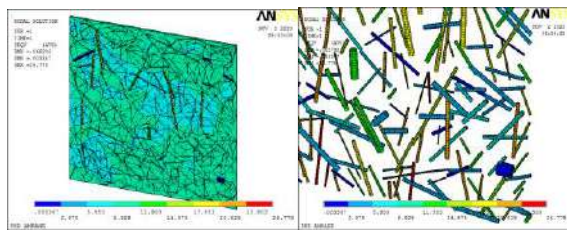


Figure 5. Distribution de la contrainte équivalente dans la plaque en composite.

IV. MECHANO-RELIABILITY MODEL

Table 4 groups the input parameters of a composite plate reinforced with Alfa fibers (298 fibers constituting the plate proposed in the probabilistic mechanical model). The input parameters include for the fibers the geometric characteristics (length, diameter and orientation), the mechanical properties

(Young's modulus and Poisson's ratio), as well as the elastic properties of the polymer matrix, considering a log-normal distribution for all these input variables with an initial coefficient of variation COV of 5%. For 20 000 iterations, the calculation requires from one week to 10 days of computer time. Each case studied in this work required this computation time.

Table 4. Input variables of an Alfa/Greenpoxy 56 fiber plate model.

| Parameters | Meane | COV % | Ecart-type | Distribution |
|--------------------------------------------|--------|-------|------------|--------------|
| $L_i(\text{mm})$ | 3,5875 | 5% | 0,1793 | Log-normale |
| $R_i(\text{mm})$ | 0,0880 | 5% | 0,0044 | Log-normale |
| $\theta_i(^{\circ})$ | 85,97 | 5% | 4,3 | Log-normale |
| $L_{50}(\text{mm})$ | 1,9091 | 5% | 0,095 | Log-normale |
| $R_{50}(\text{mm})$ | 0,0641 | 5% | 0,0032 | Log-normale |
| $\theta_{50}(^{\circ})$ | 135,05 | 5% | 6,75 | Log-normale |
| $L_{200}(\text{mm})$ | 1,9907 | 5% | 0,099 | Log-normale |
| $R_{200}(\text{mm})$ | 0,0595 | 5% | 0,003 | Log-normale |
| $\theta_{200}(^{\circ})$ | 67,47 | 5% | 3,37 | Log-normale |
| Module d'Young des fibres E (MPa) | 6,77 | 5% | 0,34 | Log-normale |
| Coefficient de Poisson des fibres ν | 0,34 | 5% | 0,017 | Log-normale |
| Module d'Young de la matrice E (GPa) | 2,74 | 5% | 0,137 | Log-normale |
| Coefficient de Poisson de la matrice ν | 0,25 | 5% | 0,0125 | Log-normale |

L_i = length, R_i = radius, and θ_i = orientation of fiber i

The histogram of the equivalent stress distribution function is shown in Fig.5. It is noted that the stress varies widely in the range 24.2– 48.98 MPa, the mean value and standard deviation are 27.13 MPa and 1.62 MPa, respectively. The statistical characteristics of this stress distribution are provided in table 2 with a confidence level of 0.95.

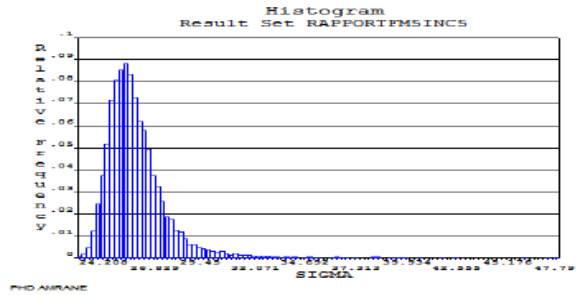


Figure 6. Histogram of the σ_{equi} distribution function

As shown in Fig. 6, the dispersion of the input parameters results in a significant variability of the output parameters, with the coefficient of variation (CV) of the constraint reaching 5.99%. Finally, the cumulative distribution curve of the equivalent stress is presented in Fig. 7."

The failure probability of the composite plate stressed in tension with an applied pressure of 20 N.mm² is given by the probability that the stress σ_{equi} is less than the breaking stress σ_r (value of 27.13MPa).

The failure probability of our composite plate is therefore about 69%, which indicates that the failure of the composite plate is statistically unlikely.

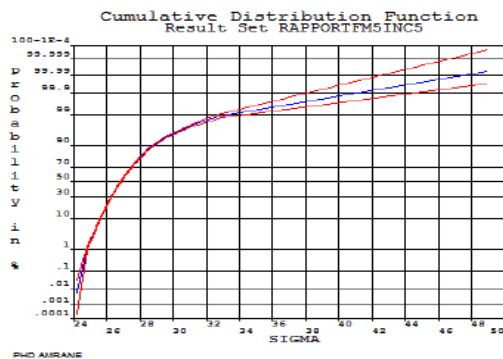


Figure 7. Cumulative distribution curve of the σ_{equi} distribution

IV.1 Sensitivity analysis of output variables

According to Figure 8, it can be observed that three parameters considered in the simulation have an impact on the sensitivity of the equivalent stress. These three parameters account for more than 31% of this sensitivity. They are the orientation of fiber No. 102, which contributes approximately 13% to the sensitivity, the diameter of fiber No. 102, which accounts for 10%, and the orientation of fiber No. 295, which contributes 8%.

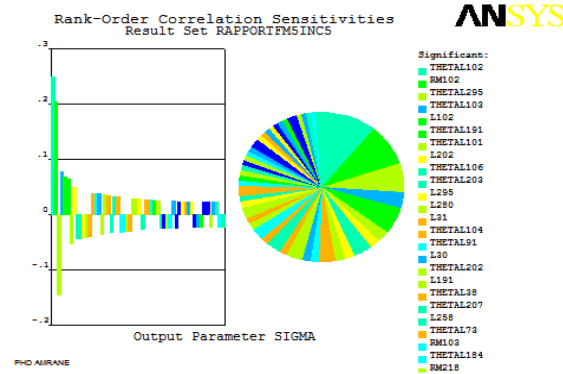


Figure 8. Influence of input parameters on the stress level

V. CONCLUSION

In this paper, a reliability model for composite plates made from Alfa fibers and the natural resin 'Greenpoxy 56' is proposed. The model is based on FEM simulation of an SFRP composite plate under uniaxial tensile loading, coupled with the Monte Carlo method. This approach accounts for the uncertainties related to the geometric parameters and the mechanical properties of both the fibers and the matrix that make up the plate. The mechanical properties of the bio-based composite were determined through tensile tests, which revealed that increasing the fiber content significantly enhanced the stiffness of the composites.

In conclusion, understanding the impact of each parameter that constitutes the bio-based composite plate, which directly affects the sensitivity of the stress, allows for a better identification of the key factors. This knowledge can be used to optimize the development process during the manufacturing of the plate.

REFERENCES

- [1] Shanmugam V. *et al.*, « Circular economy in biocomposite development: State-of-the-art, challenges and emerging trends », *Composites Part C: Open Access*, vol. 5, p. 100138, juill. 2021.
- [2] Arrakhiz F. Z., Elachaby M., Bouhfid R., Vaudreuil S., Essassi M., et Quass A., « Mechanical and thermal properties of polypropylene reinforced with Alfa fiber under different chemical treatment », *Materials & Design*, vol. 35, p. 318-322, mars 2012.
- [3] A. Bessadok, S. Roudesli, S. Marais, N. Follain, et L. Lebrun, « Alfa fibres for unsaturated polyester composites reinforcement: Effects of chemical treatments on mechanical and permeation properties », *Composites Part A: Applied Science and Manufacturing*, vol. 40, no 2, p. 184-195, févr. 2009.

- [4] Sundarakannan R., Arumugaprabu V., Manikandan V., and Vigneshwaran S., « Mechanical property analysis of biochar derived from cashew nut shell waste reinforced polymer matrix », *Mater. Res. Express*, vol. 6, no 12, p. 125349, janv. 2020.
- [5] Da O. s and al., « The need for fully bio-based facemasks to counter coronavirus outbreaks: A perspective », *Science of The Total Environment*, vol. 736, p. 139611, sept. 2020, doi: 10.1016/j.scitotenv.2020.139611.
- [6] Pizzi A. and Mittal K. L., Éd., *Handbook of adhesive technology*, 2nd ed., rev. Expanded. New York: M. Dekker, 2003.
- [7] Moubarik A., Pizzi A., Allal A., Charrier F., and Charrier B., « Cornstarch and tannin in phenol-formaldehyde resins for plywood production », *Industrial Crops and Products*, vol. 30, no 2, p. 188-193, sept. 2009.
- [8] Vázquez G., Antorrena G., Francisco J. L., and González J., « Properties of phenolic- tannin adhesives from pinus pinaster bark extracts as related to bond quality in eucalyptus plywoods », *Holz als Roh- und Werkstoff*, vol. 50, no 6, p. 253-256, juin 1992.
- [9] von Leyser E. and Pizzi A., « The formulation and commercialization of glulam pine tannin adhesives in Chile », *Holz als Roh- und Werkstoff*, vol. 48, no 1, p. 25-29, janv. 1990.
- [10] Li Z., Wang Z., Wang X., et Zhou W., « Bending behavior of sandwich beam with tailored hierarchical honeycomb cores », *Thin-Walled Structures*, vol. 157, p. 107001, déc. 2020.
- [11] Khaldi M. and al., « Etude en rupture d'un composite à fibres végétales d'Alfa », *Conférence Matériaux, colloque 01 Ecomatériaux*, p. 10, nov. 2014.
- [12] Bessadok A. and al., « Effect of chemical treatments of Alfa (*Stipatenacissima*) fibres on water-sorption properties », *Composites Science and Technology*, vol. 67, n° 3, p. 685-697, mars 2007.
- [13] El-Abbassi F. E., Assarar M., Ayad R., Bourmaud A., et Baley C., « A review on alfafibre (*Stipatenacissima* L.): From the plant architecture to the reinforcement of polymer composites », *Composites Part A: Applied Science and Manufacturing*, vol. 128, p. 105677, 2020.
- [14] Hanana S., Elloumi A., Placet V., Tounsi H., Belghith H., et Bradai C., « An efficient enzymatic-based process for the extraction of high-mechanical properties alfafibres », *Industrial Crops and Products*, vol. 70, p. 190-200, août 2015.



Open access

Keynote speech

presentation files

The Role of Artificial Intelligence in Advancing Fiber Science

Prof. Dr. Melih Günay

Akdeniz University

Computer Engineering



Abstract

AI is transforming fiber science by accelerating material discovery, improving manufacturing efficiency, and enhancing quality control.

It enables predictive modeling of fiber properties, real-time defect detection, and automation in production.

Talk will navigate through the key developments and techniques that relates to AI and Textiles

Traditional Textiles

Standardized Production

- Manufacturing processes were optimized using **fixed rules and mechanical adjustments**
- Customization and responsiveness to changes were minimal

Manual Quality Control

- Inspection of prototypes was **visual and human-dependent**, often subjective and prone to error

Long Development Cycles

- Discovery and commercialization of new fibers took **years**, due to slower testing and validation

Traditional Textiles R & D

Separate Disciplines

- Research in chemistry, physics, and engineering was conducted in **silos**
- Less collaboration across disciplines slowed innovation

Experimental and Trial-Based Approach

Relied heavily on **manual experimentation** and **trial-and-error** to develop new fibers and fabrics

Material properties were tested through **physical prototypes** and lab experiments

Basic Data Analysis

- Data is collected manually and analyzed using **basic statistical methods**
- Limited ability to detect complex patterns or predict long-term behavior

Emergence of AI in Scientific Research

From automating experiments to simulating complex systems, AI **enhances** both the **speed and depth of scientific inquiry**.

Ability to **process massive datasets**, identify complex patterns, and make accurate predictions

Its integration is reshaping how research is conducted, making it more efficient, data-driven, and innovative.

Artificial Intelligence has become a **transformative tool across scientific disciplines**.



NOBELPRISET I FYSIK 2024 THE NOBEL PRIZE IN PHYSICS 2024



KUNGL.
VETENSKAPS-
AKADEMIEN

THE ROYAL SWEDISH ACADEMY OF SCIENCES



Photo: Mary Whitham

John J. Hopfield

Princeton University, NJ, USA



Photo: University of Toronto

Geoffrey E. Hinton

University of Toronto, Canada

"för grundläggande upptäckter och uppfinningar som möjliggör maskininlärning med artificiella neuronnätverk"

"for foundational discoveries and inventions that enable machine learning with artificial neural networks"

THE
NOBEL
PRIZE



NOBELPRISET I KEMI 2024 THE NOBEL PRIZE IN CHEMISTRY 2024



KUNGL.
VETENSKAPS-
AKADEMIEN

THE ROYAL SWEDISH ACADEMY OF SCIENCES



Photo: University of Washington

David Baker
University of Washington
USA

"för datorbaserad proteindesign"

"for computational protein design"



Photo: The Royal Society

Demis Hassabis
Google DeepMind
United Kingdom

"för proteinstrukturprediktion"

"for protein structure prediction"

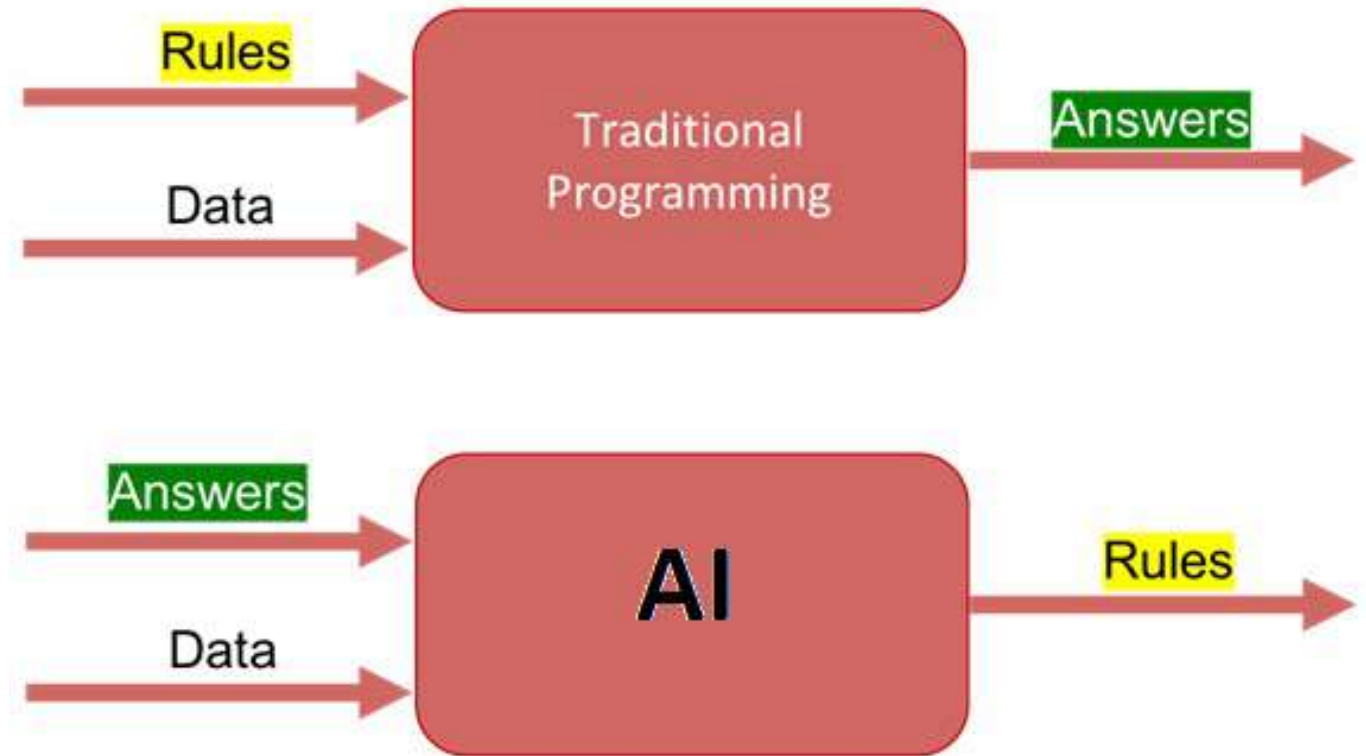


Photo: BBVA Foundation

John M. Jumper
Google DeepMind
United Kingdom

What is Artificial Intelligence?

AI is the field of computer science focused on creating systems that can **simulate human intelligence**.



Key Capabilities of AI

Learning: Acquiring knowledge from data (machine learning)

Perception: Interpreting input like images, sounds, or text

Reasoning: Making decisions or solving problems

Interaction: Communicating via speech, text, or gestures

Autonomy: Acting independently to achieve goals

Branches of AI: ML, DL, NLP

Machine Learning (ML) – Neural Networks

- Enables computers to **learn from data** and improve over time without being explicitly programmed
- Used in tasks like pattern recognition, prediction, and classification

Example: Predicting fabric strength based on fiber composition

Deep Learning - Deep Neural Networks DNN

- A subset of ML that uses ****neural networks with many layers****
- Excellent for processing ****complex data**** like images, video, or sound

Example: Identifying textile defects using images

Key Concepts: ML, DL, Generative - NLP

Recurrent Neural Networks - Transformers – Generative Networks

- Allows machines **to understand, interpret, and generate text/image**
- Used for text analysis, language translation, and image generation

Example: Analyzing product reviews to improve textile design, ChatBots

Reinforcement Learning – RL

- Allows machines **to learn by acting. Award/Penalty**
- Used for ****self-driving****, learn to walk
- Example: Robots in Textile Factories

Many Others are popping up like Graph Neural Networks

How to integrate AI into fiber science

Traditional Approach

Manual trial-and-error experimentation

Visual, human-based defect detection

Basic statistical analysis

Disconnected scientific disciplines

Fixed, rule-based production

Long development timelines

Limited customization

AI-Driven Approach

Predictive modeling for material behavior

Real-time computer vision quality control

Machine learning on large, complex datasets

Interdisciplinary, data-integrated research

Adaptive, AI-optimized manufacturing

Accelerated discovery through simulation & automation

Personalized design via generative algorithms

Historic Perspective of Material Discovery

Ancient Concept – Four Elements Theory (Soil, Air, Water, Fire)

This model was qualitative, not quantitative, and lacked experimental evidence. It remained dominant until the Scientific Revolution.

Realization: Air Is Not One Substance

"Phlogisticated Air": Part of the Phlogiston Theory (~17th–18th century), which suggested combustible materials released "phlogiston" during burning.

Key Discovery: **Scientists began noticing different "airs":**

- Carbon dioxide (then called "fixed air") by Joseph Black.
- Hydrogen ("inflammable air") by Henry Cavendish.
- Oxygen (initially "dephlogisticated air") by Joseph Priestley, later fully described by Lavoisier.

Rise of Modern Chemistry–Lavoisier, Cavendish, Dalton

Antoine Lavoisier (1770s):

Disproved phlogiston theory.

Named Oxygen (O_2) and Hydrogen (H_2) - Nomenclature

Established the Law of Conservation of Mass.

Wrote the first modern list of elements (~33 items)

Henry Cavendish (1780s):

Discovered Hydrogen, described it as “inflammable air”.

H_2 with Oxygen to form water — an experimental cornerstone.

Dalton's Atomic Theory (1803)

Matter is made of indivisible atoms and each element is made of identical atoms.

Atoms combine in fixed ratios to form compounds. This quantified chemistry and led to: Modern atomic weights. **Concept of chemical formulas** (e.g., H_2O , CO_2).

Atomic Structure

Mendeleev's Periodic Table (1869)

- Arranged known elements (63 at that time) in order of increasing atomic mass, **observing repeating patterns**.
- Left **gaps for undiscovered elements** (like Gallium, Germanium), which were later found.
- **Predicted properties of unknown elements** with surprising accuracy.

Evolved into the modern Periodic Table, based on **atomic number instead of mass** by Henry Moseley

Discovery of Subatomic Structure

Electron (-) discovered by J.J. Thomson (1897).

Nucleus proposed by Ernest Rutherford after gold foil experiment (1911).

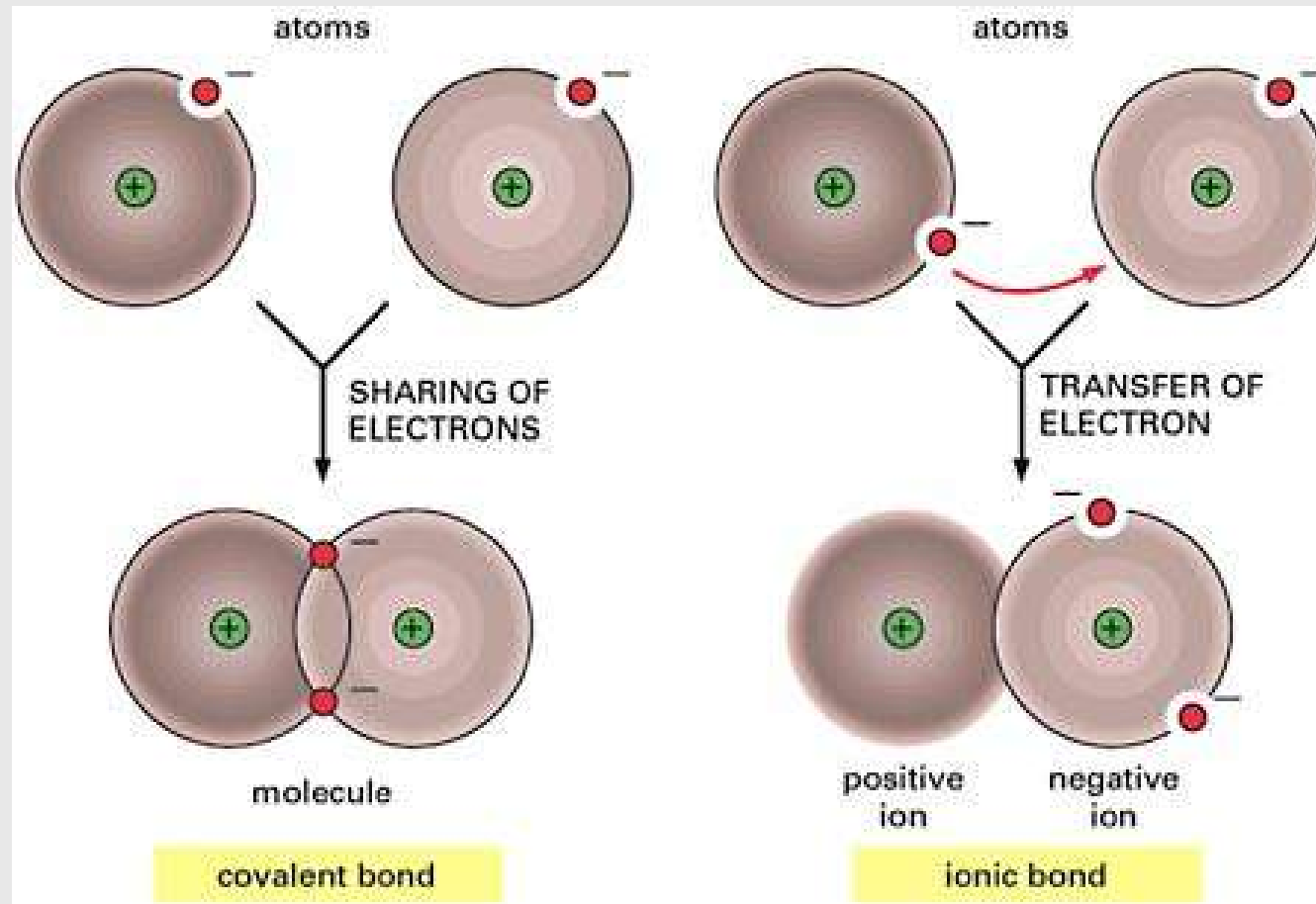
Proton (+) identified as a positively charged particle in nucleus (by Rutherford).

Neutron discovered later by James Chadwick (1932).

Discovered that atoms are **divisible and composed of smaller parts**.

Chemical Bonds - What keeps atoms together

Chemical bonds through the sharing of atom (Covalent) or Transfer of Electron



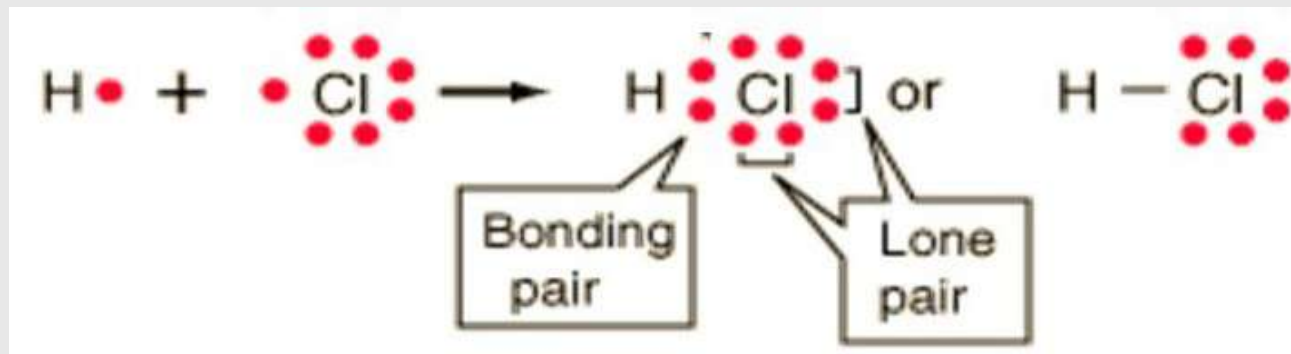
Chemical Bonds – Electric Forces

In Covalent Bonds Equal Sharing of Atoms cause No Polarity (Non-Polar) vs Unequal Sharing of them cause Polarity. (Polar)

Non-Polar:

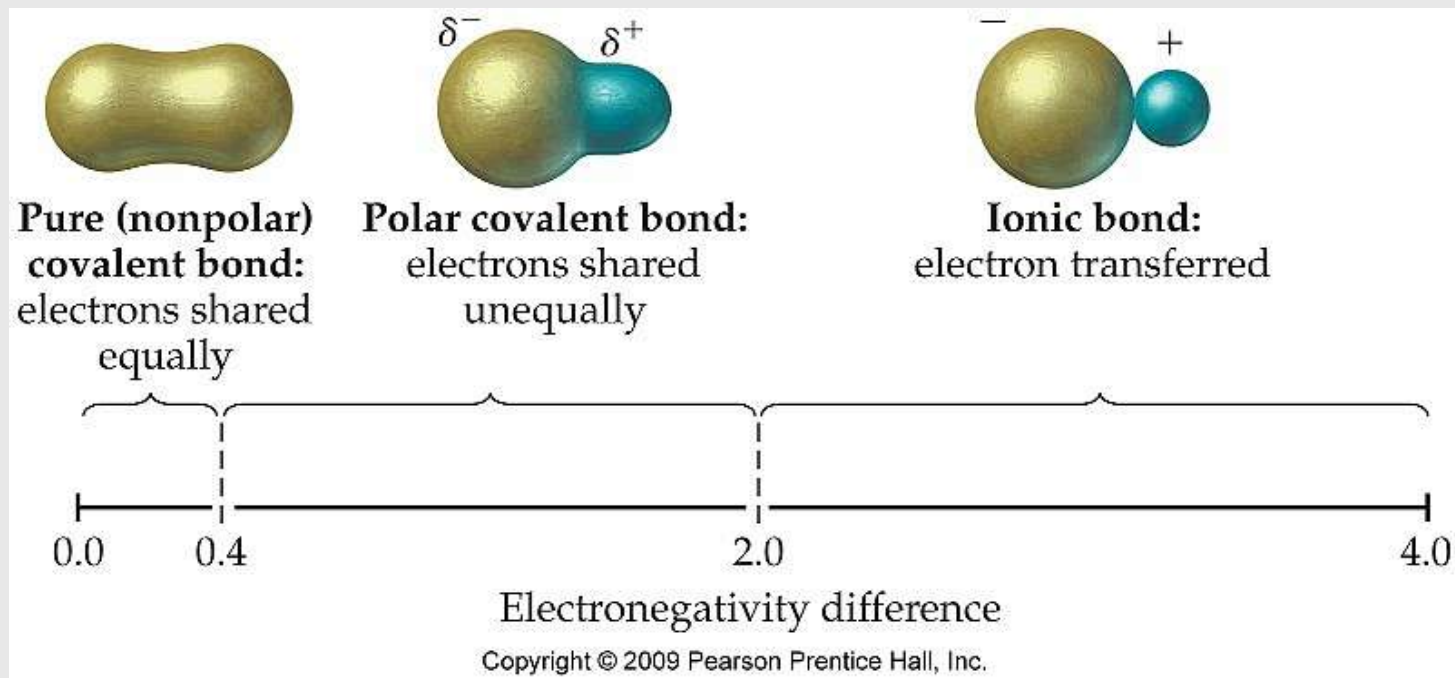
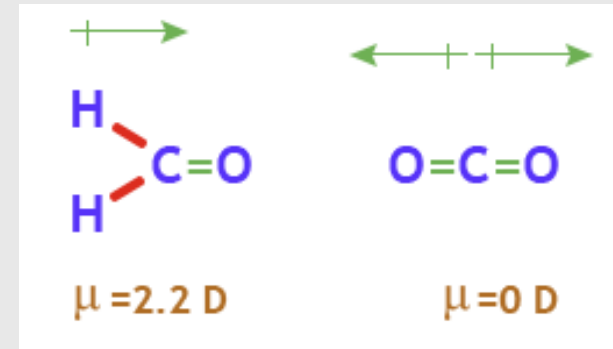


Polar:



Dipole Moment

A large difference in electronegativity between two bonded atoms will cause a dipole.



Polymer Folding Governed By

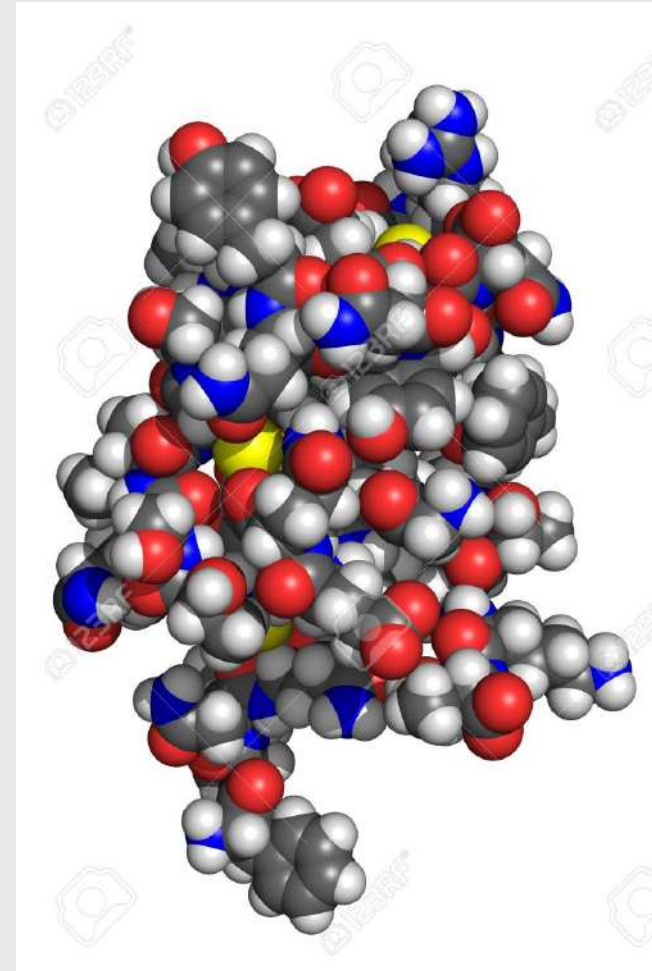
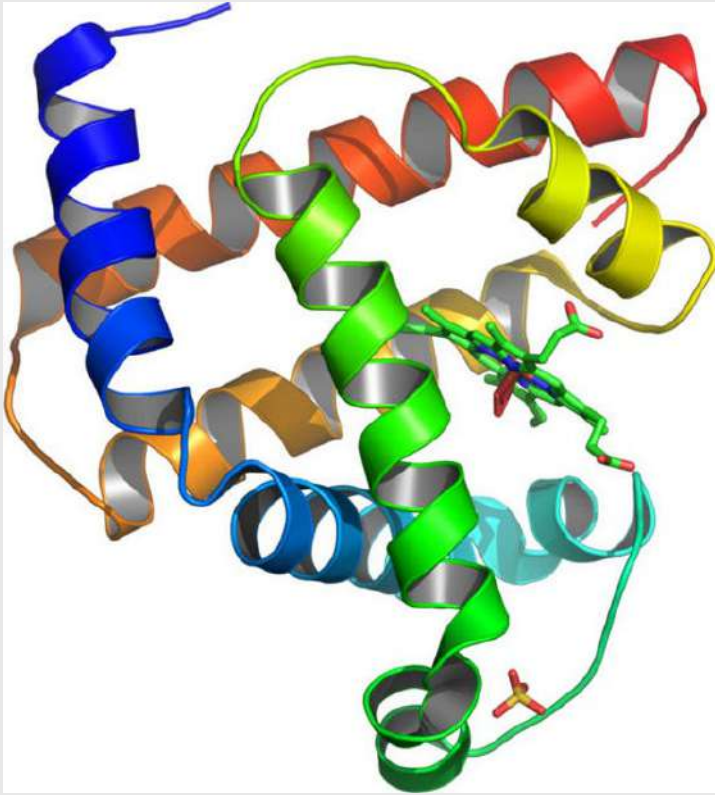
- **Intermolecular-Electrical forces** (hydrogen bonding, van der Waals, ionic)
- **Solvent effects** (e.g., hydrophobic collapse)
- **Mechanical effects with Temperature, pH, and pressure**
- **Chain length and side-group interactions**

Due to the immense **combinatorial possibilities** of atomic arrangements, it is difficult to model polymer folding from first principles.

AI is here to help ! Computers can try many things very fast... & can learn

Polymer (Protein) Folding Problem

This is how we design vaccines and drugs...



AI is here to predict how it may fold

| Model/Tool | Focus Area | Description |
|-------------------------------------|---------------------|------------------------------------------------------------------------------------------------------------|
| AlphaFold (DeepMind) | Protein Folding | Predicts 3D protein structures from amino acid sequences with high accuracy. |
| Graph Neural Networks (GNNs) | Polymer Topology | Model how molecular graphs (atoms as nodes) fold in 3D space. |
| Molecular Dynamics + ML | Dynamics Prediction | ML models reduce computational cost of simulating folding over time. |
| Inverse Design with AI | Polymer Engineering | AI generates polymer sequences expected to fold into desired properties (e.g., self-assembling materials). |

Predict Material Properties

Traditionally trial-and-error experiments in the lab. Testing one material combination at a time -**slow and expensive**

Computational Methods

Description

1. **Physics-based simulations**

Quantum mechanical methods like DFT, molecular dynamics (MD), finite element methods (FEM).

2. **Machine learning models**

Train AI on known materials to predict properties of new, unseen materials.

3. **Empirical and semi-empirical models**

Use fitting formulas and heuristic models based on experimental trends.

Predict Material Properties

ML trained on existing material data can:

- Predict how new fiber compositions will behave without needing physical samples
- Identify optimal combinations of polymers, additives, or treatments
- Simulate fiber behavior under different conditions (e.g., temperature, pressure, wear)

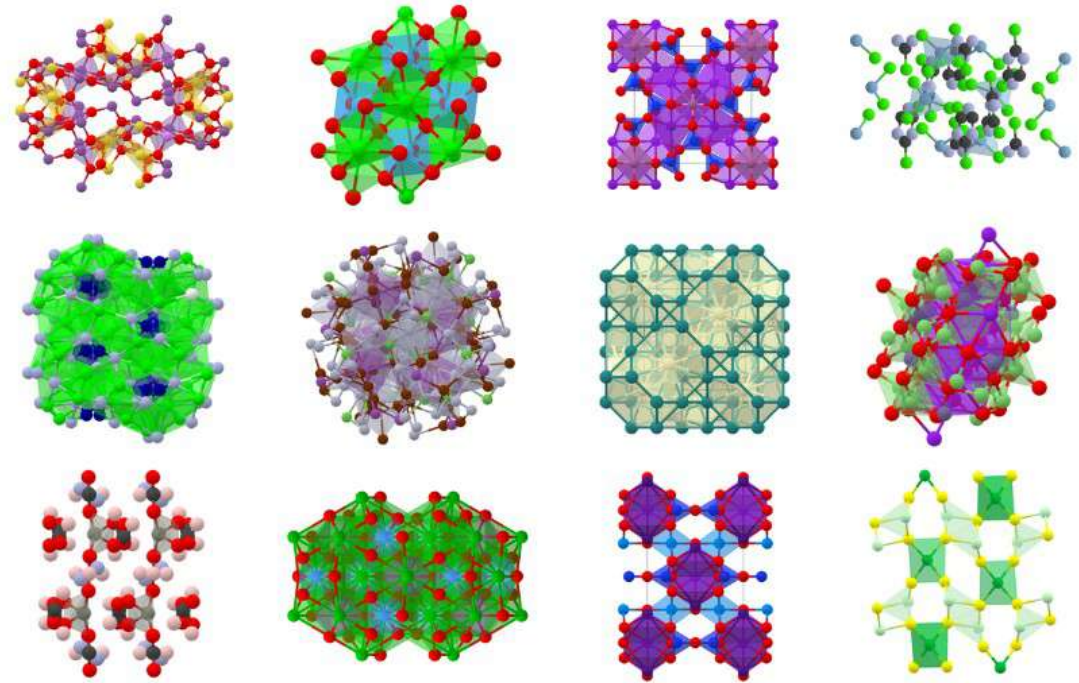
| Model | Target Property | Source |
|--------|--------------------------------------|------------------------------------------|
| CGCNN | Bandgap, formation energy | Xie & Grossman, 2018 |
| SchNet | Quantum chemistry (energies, forces) | Schütt et al., 2018 |
| MEGNet | Multi-property materials prediction | Chen et al., 2019 |

Materials Databases

Materials discovered computationally are registered to databases for other researchers use.

Materials created virtually revolutionized the invention of new materials

Simulating their properties, Researchers can focus on the most promising ones.



Others: AFLOWLIB NOMAD Open Quantum Materials DB (OQMD)

The Materials Project

Harnessing the power of supercomputing and state-of-the-art methods, the Materials Project provides open web-based access to computed information on known and predicted materials as well as powerful analysis tools to inspire and design novel materials.

[Login or Register](#)[See a Random Material](#)[Browse Apps](#)

The Materials Project by the numbers

MATERIALS

200,487

REGISTERED USERS

560,000+

INTERCALATION ELECTRODES

5,602

CITATIONS

32,000+

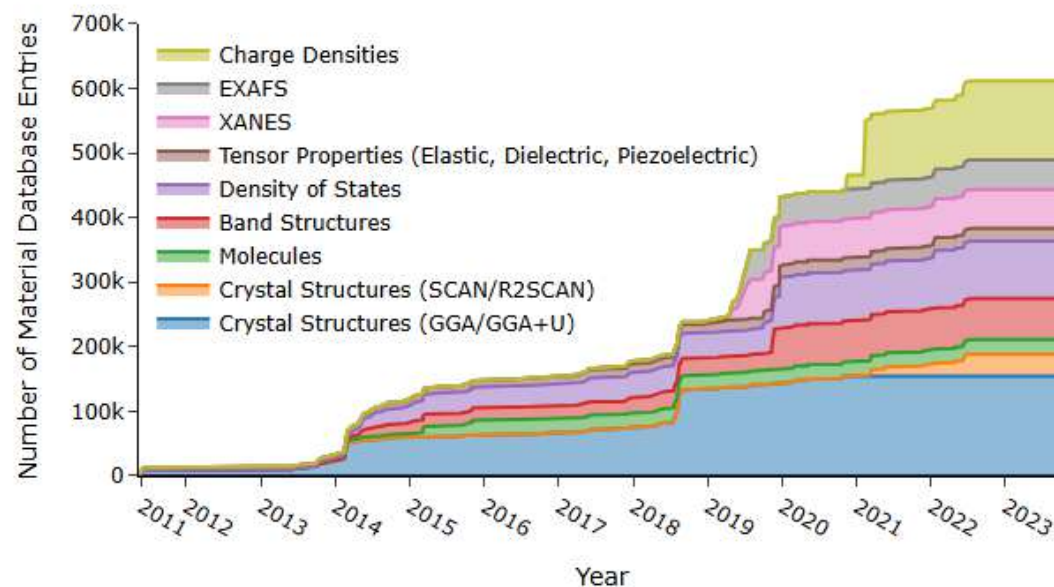
MOLECULES

577,813

CPU HOURS/YEAR

100 million



DATABASE ENTRIES



[nature](#) > [articles](#) > article

Article | [Open access](#) | Published: 29 November 2023

Scaling deep learning for materials discovery

[Amil Merchant](#) , [Simon Batzner](#), [Samuel S. Schoenholz](#), [Muratahan Aykol](#), [Gowoon Cheon](#) & [Ekin Dogus Cubuk](#) 

[Nature](#) **624**, 80–85 (2023) | [Cite this article](#)

274k Accesses | **420** Citations | **1005** Altmetric | [Metric](#)

Article | [Open access](#) | Published: 29 November 2023

An autonomous laboratory for the accelerated synthesis of novel materials

[Nathan J. Szymanski](#), [Bernardus Rendy](#), [Yuxing Fei](#), [Rishi E. Kumar](#), [Tanjin He](#), [David Milsted](#), [Matthew J. McDermott](#), [Max Gallant](#), [Ekin Dogus Cubuk](#), [Amil Merchant](#), [Haegyeom Kim](#), [Anubhav Jain](#), [Christopher J. Bartel](#), [Kristin Persson](#), [Yan Zeng](#)  & [Gerbrand Ceder](#) 

[Nature](#) **624**, 86–91 (2023) | [Cite this article](#)

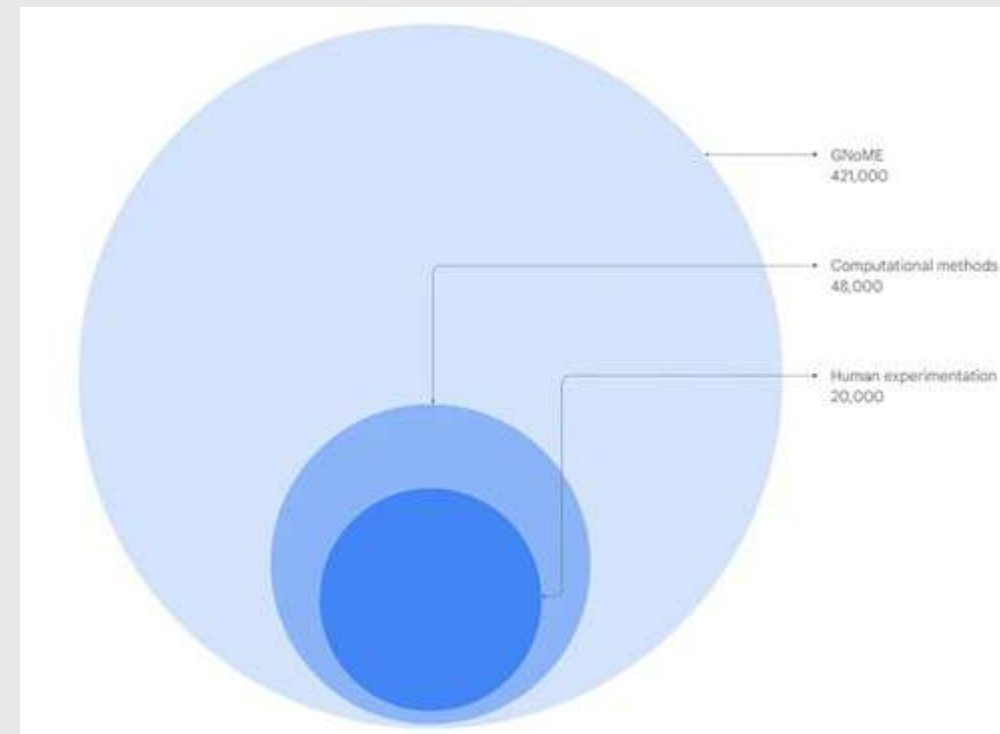
Key Approaches used in Materials Discovery

GNoME (Graph Networks for Materials Exploration)

- Predicts thermodynamically stable crystal structures from millions of hypothetical candidates.
- Uses **Active Reinforcement Learning** to iteratively refine model predictions with new data.

Has predicted over **2.2 million new stable materials**, of which 421,000 are experimentally viable. 736 have already been independently experimentally realized.

Equivalent to nearly 800 years' worth of knowledge

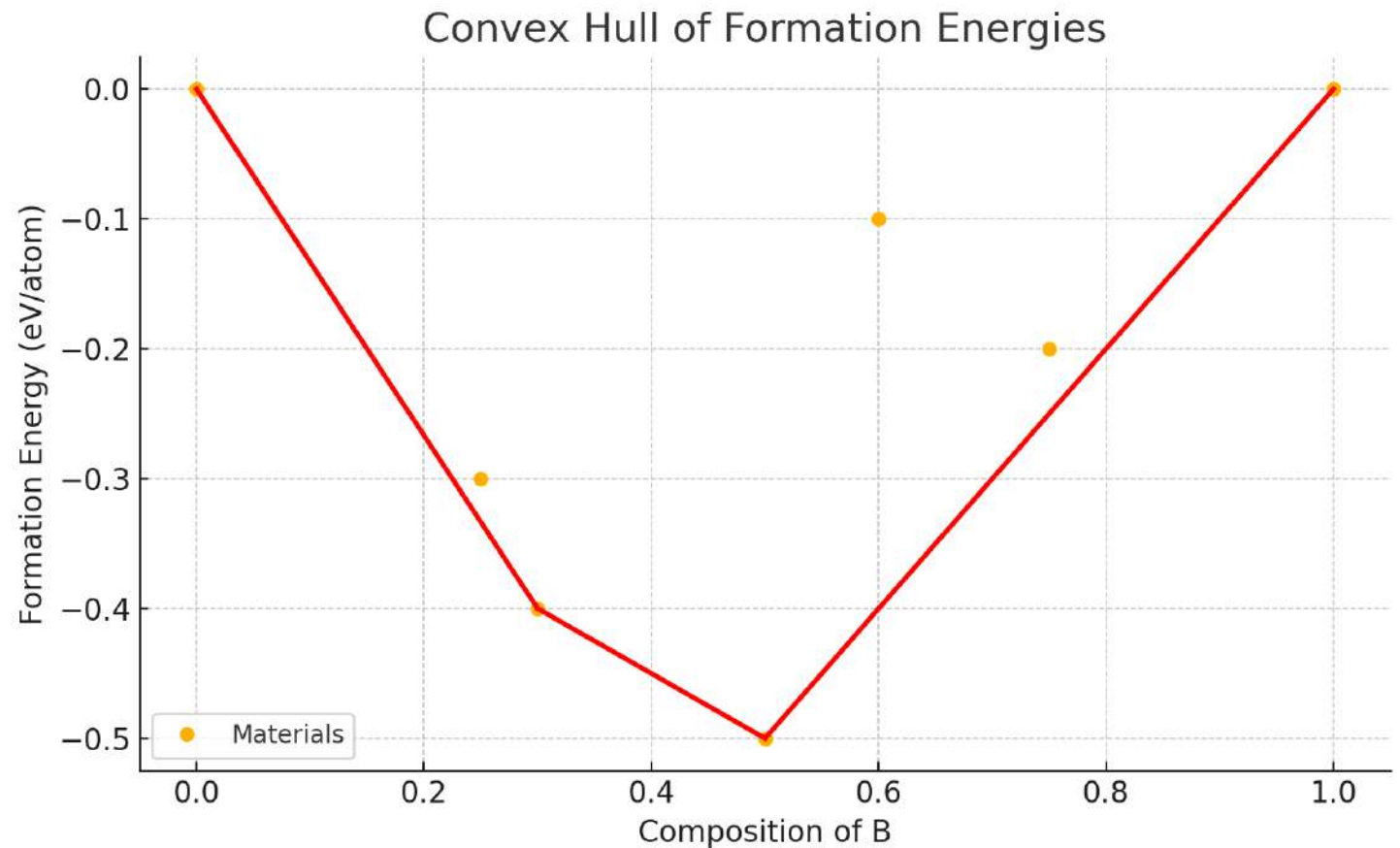


Convex Hull

For a material to be considered stable, it must not decompose into similar compositions with lower energy.

Mathematically, these materials lie on the **convex hull**.

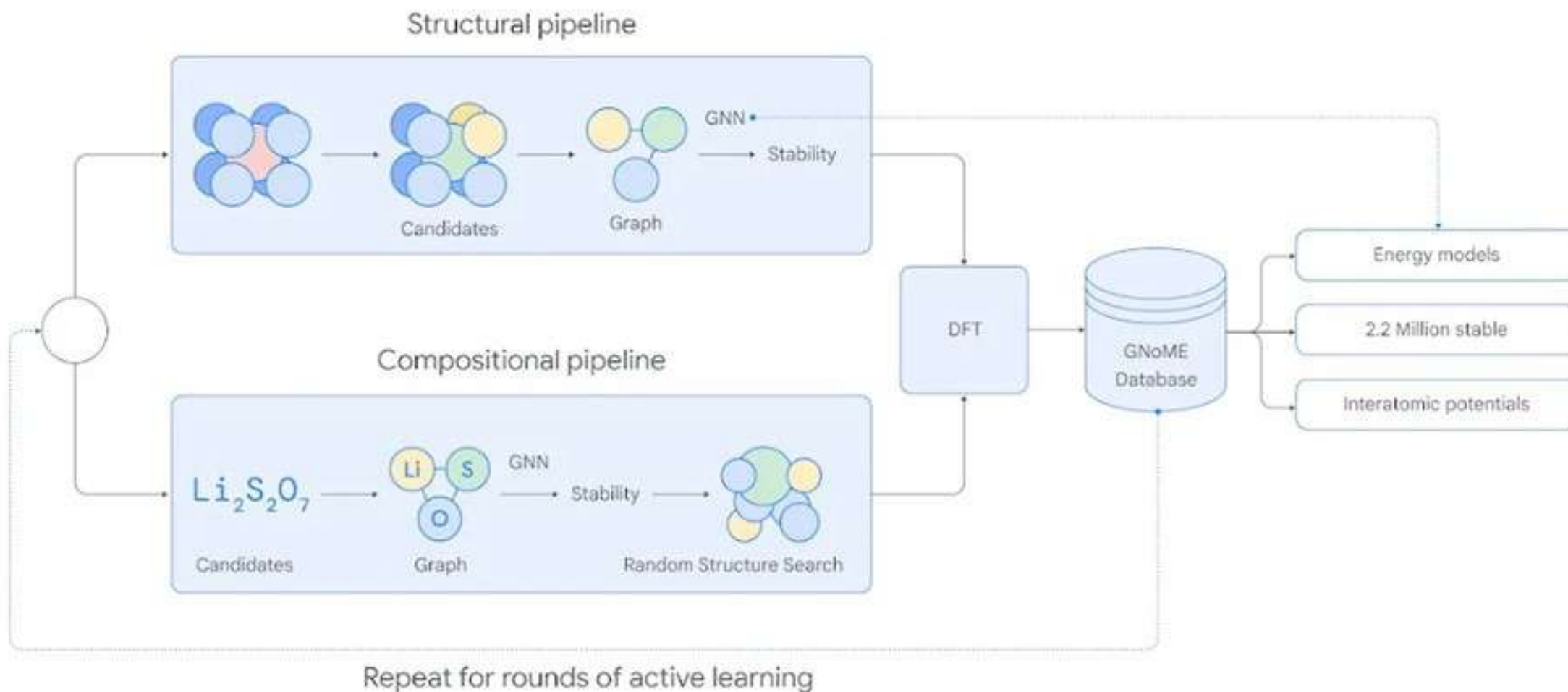
For example, carbon in a graphene-like structure is stable compared to carbon in diamonds.



GNoME - Active Learning

Uses two pipelines. The **structural pipeline** creates candidates with structures similar to known crystals, while the **compositional pipeline** follows a more randomized approach based on chemical formulas.

The outputs of both pipelines are evaluated using established **Density Functional Theory** calculations and those results are added to the GNoME database, informing the next round of active learning.



Autonomous LAB

At Berkeley Lab

Using materials from the Materials Project, the autonomous lab **created new recipes for crystal structures and successfully synthesized** more than 41 new materials of GnoME.



How to use Materials Database

The Materials Project API allows anyone to have direct access to current, up-to-date information from the Materials Project database in a structured way.

This allows for analysis, development of automated tools, and downloading personal copies of the Materials Project database.

How to use Materials Database

ML can be trained to predict material properties using

- Crystal structure,
- Chemical composition,
- Electronic band structures as inputs

generate novel ideas for solid-state synthesis and crystal structure determination with physical insights.

The API is offered free-of-charge and have several tools to help you get started.

Pymatgen – Python Library

Case Study for ML in Materials Prediction

The main purpose of machine learning here is the prediction of properties of a given material. This property can either be a class (the classification problem) or a quantity (the regression problem).

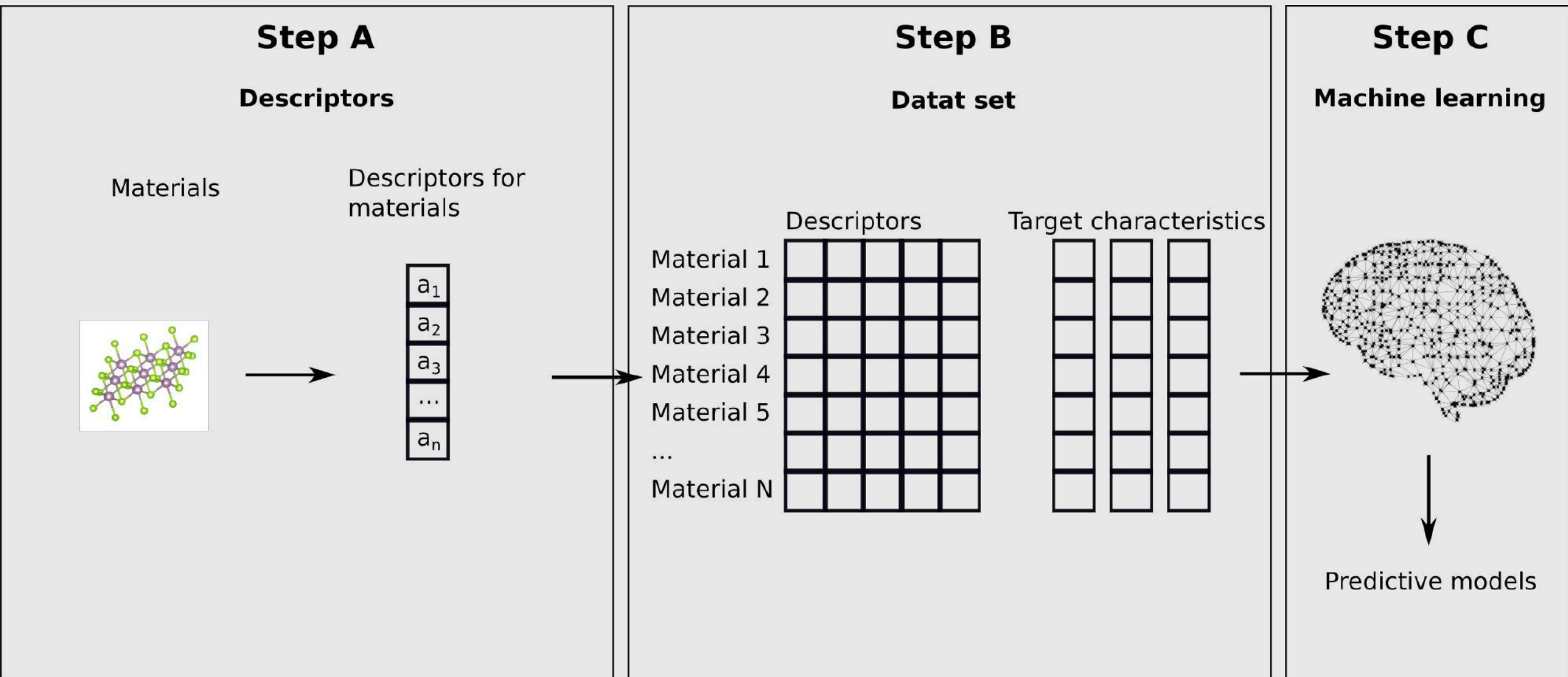
For Example:

- Is a given material metallic or semiconducting? <https://doi.org/10.1038/ncomms15679>
- What is the specific heat capacity of a material? <https://doi.org/10.1002/adts.201900208>

The machine learning workflow in 3 steps:

- First, find numerical/categorical **descriptors** that can describe your material. That is: every material in your dataset should be uniquely represented by an array of numbers/categories.
- Then, apply your procedure to your entire dataset of structures to form a sheet of material descriptors vs. **target properties**.
- Use machine learning to predict the target properties based on the descriptors.

Steps



Predicting Mechanical Properties of Textile Fibers

ML models are trained on datasets of textile fiber compositions and test results **to predict **tensile strength**, **elasticity**, and **abrasion resistance****.

- Saves physical testing by forecasting fabric performance during early design.
- Cotton-polyester blends optimized for softness and stretch using AI regression models.

Nanofiber Discovery via AI Optimization

Bayesian optimization has been used to discover optimal combinations of nanomaterials for fabrics with UV protection or antibacterial properties.

AI-Driven Textiles&Engineering

Yarn and Fabric Engineering

AI is used to evaluate yarn characteristics during spinning.

Combines ****sensor data**** and ML to predict yarn breakage points and recommend blend ratios or twist angles for different applications (denim, sportswear, etc.)

Reduced material waste and higher-quality fabrics.

Deep learning models are used to ****design textile structures backward given desired properties**

e.g., moisture wicking or thermal insulation), the AI predicts what weave or knit pattern should be used.

Garment Design

Functional Smart Textiles Design (e.g., Sensors, Heating)

- AI algorithms are used to design the placement and composition of conductive fibers in **smart garments**.
- MIT's "**Fabrics that Compute**" project uses AI to generate textile sensor patterns that maintain flexibility and data fidelity.

Generative AI tools (e.g., DALL·E, Midjourney) can auto-generate textile patterns and garment designs.

Digital Fabric Twins for Property Simulation

- Digital twins of fabrics are created using AI to simulate stretch, drape, and wear in real time.
- Platforms like CLO and Browzwear integrate ML for virtual textile prototyping.

AI in dyeing

Color Matching & Recipe Prediction

- AI algorithms **predict the exact dye combination to achieve target shades.**
- Reduces trial-and-error and dye waste.

Process Optimization

- Reinforcement learning and predictive modeling are used to **adjust dyeing temperature, time, and pH for consistent** output.
- Energy and water savings through smart process control

Quality Control

- Machine vision + AI detects **color uniformity** issues, bleeding, or **defects in real time during production.**
- Reduces labor and subjective inspection

Sustainable Dyeing

- AI helps optimize **eco-friendly dye formulations and minimize chemical usage.**
- Predicts environmental impact scores of different recipes.

Digital Twin Modeling

- Simulates dyeing processes digitally using real-time sensor data + historical data to predict outcomes without physical trials

Optimization in Planning & Manufacturing

AI-Driven Production Scheduling

- › **Machine Learning** forecasts demand, allocates machines, and sequences jobs optimally using Genetic algorithms, ant colony optimization, and reinforcement learning.
 - **Minimized idle time**, better delivery adherence.

Inventory & Supply Chain Optimization

- AI predicts stock levels, raw material needs, and lead times.
- **Just-in-Time (JIT)** systems reduce holding costs and waste.

Optimization in Planning & Manufacturing

Cutting & Material Utilization

- › **Nesting algorithms** and CAD/CAM systems optimize fabric layout to reduce waste.
- › Real-time sensors ensure precise fabric measurement and cut accuracy.

Workforce Allocation

- › AI dynamically assigns human resources based on skill, fatigue, and task complexity.
- › Results in better worker satisfaction and productivity.

Sensor data and process control

Sensor Data and Process Control represent the backbone of **smart manufacturing**, enabling real-time decisions, precision, and automation.

Data Collection Platforms

- **SCADA Systems (Supervisory Control and Data Acquisition)** for centralized control.
- **IoT (Internet of Things)** platforms aggregate sensor data across factory units.
- **Edge computing** enables local processing near machines for faster feedback.

Process Control Technologies

Real-Time Monitoring and Dashboards

Live visualization of sensor feeds alerts for threshold breaches (e.g., overheating, pH drift).

Automated Process Control (APC)

Uses feedback and feedforward loops to stabilize variables like temperature, tension, and speed.

Model Predictive Control (MPC)

Advanced control system that anticipates future events using process models.

Predictive maintenance

Using sensor data (vibration, temperature) AI predicts and prevents breakdowns. Reduces downtime and maintenance cost, extending asset life, and optimizing maintenance schedules.

The integration of real-time IoT sensor data with AI models has become a key driver in transitioning from reactive to proactive maintenance strategies.

Real-time adjustments

Automated Weaving Machines

- Adjusts tension, yarn feed rate, and warp stop motions based on real-time sensor feedback.
- Reduces yarn breakage and improves fabric uniformity.

Smart Yarn Tension Control

- Monitors and adjusts yarn tension while knitting or winding.
- Prevents defects like uneven fabric structure or curling edges.

Defect Detection in Fabric Inspection

- Uses AI-based cameras to spot defects and alert/adjust the process instantly.
- Reduces post-production inspection costs and fabric waste.

Real-time adjustments

Thermal Setting of Synthetic Fibers

- Adjusts roller speed and temperature in response to fiber thermal behavior during heat setting.
- Maintains desired elasticity and texture in technical textiles.

Smart Sewing Machines

- Adjusts stitch length, speed, and thread tension in real-time based on fabric thickness and pattern complexity.
- Ensures precision in automated garment assembly.

Real-time adjustments

Moisture Management in Finishing

- Real-time moisture sensors modulate drying temperature and speed.
- Prevents over-drying and fiber degradation.

Digital Textile Printing

- Adjusts inkjet nozzles, ink density, and alignment during print runs.
- Maintains print precision, especially on stretchy or variable-thickness fabrics.

Color Matching Systems

- Real-time spectrophotometric feedback adjusts dye injection in dyeing machines.
- Ensures color consistency across batches without stopping production.

Quality Control and Defect Detection

- Computer vision for defect detection
- Reducing human judgement errors
- Consistent quality

Market trends and innovations

Trend Forecasting via **Social media**, (Instagram, Pinterest, TikTok), **fashion blogs for sales data and consumer feedback**

- › AI predict upcoming colors, textures, and styles.
- › Tools like Heuritech and Google Trends AI help brands stay ahead of fashion cycles.

Competitive analysis identifies white space in the market and pricing strategies. NLP algorithms can scan:

- Competitor websites
- Product catalogs
- Market reports

Sustainability and Waste Reduction

Sustainability Innovation

AI models help **optimize energy and material**.

- **Dye recipes** to use less water or chemicals.
- Eco-friendly material prediction
- Support Recycling

- **Predicts environmental impact** of materials across the lifecycle.
- Drives green innovations and compliance with eco-regulations.

Customization and Personalization

AI helps create hyper-personalized experiences:

- › Recommending styles based on body type and preferences
- › Virtual try-ons using AR + AI vision models

Improves conversion rates and customer satisfaction.

Challenges and Limitations

- Data availability and quality
- Interpretability of AI models
- Integration with existing systems
- Ethical considerations

Future Outlook

- **Autonomous production using AI-controlled robotics (weaving, dyeing, quality checks)**
- **Environment/Emotion-aware textiles** (changing color/heat/texture with mood, biometrics, weather)
- Integration of **blockchain + AI** for transparent, traceable supply chains
- Personalized experiences will become the norm in online and physical retail.
 - › **Adaptive Recommendation** followed by on demand garment manufacturing integrated with body scan at store.

Acknowledgments and References

The organizing committee for inviting me.

Prof. Dr. Ali Demir for his advise during my career development.

Q&A

Piezoelectric Nanofibers: Challenges and Future Aspects

Prof Nader Shehata

Alexandria University (Egypt)

& Kuwait College of Science and Technology (KCST)

16th International Fiber and Polymer Research Symposium (ULPAS)

Istanbul, Turkey, 2025

Brief Bio

- Professor, Department of Engineering Mathematics and Physics, Faculty of Engineering, Alexandria University (on-leave)
- Associate Director, Center of Smart Materials, Nanotechnology and Photonics (CSMNP), Smart CI Research Center of Excellence, Alexandria University.

Director, Office of Research, Innovation, and Sustainability (ORIS),
Kuwait College of Science and Technology (KCST), Kuwait

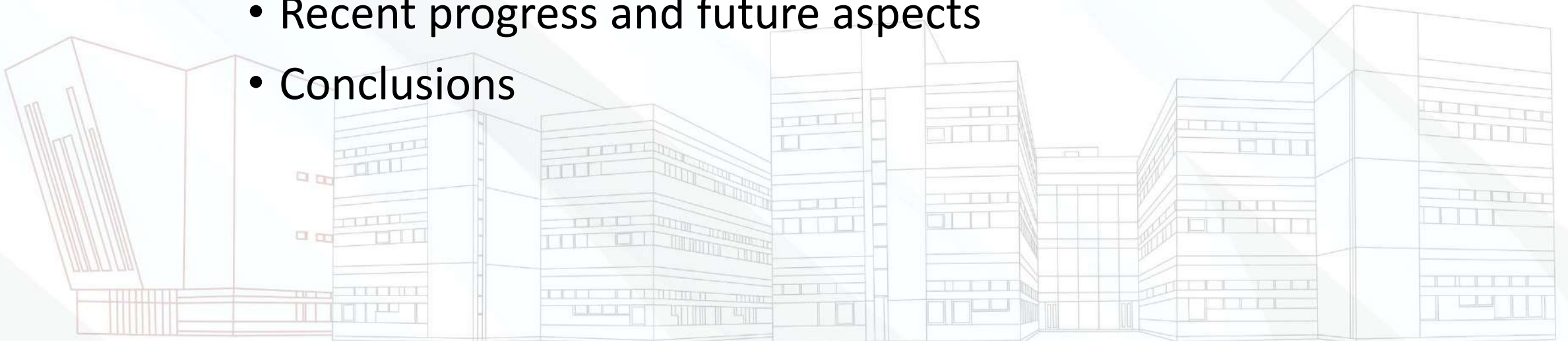
Associate Professor, Department of Physics, KCST, Kuwait



- Adjunct Associate Professor, Faculty of Science, Utah State University.
- Former Lecturer of Electronic Engineering in (Ulster University, Belfast, Northern Ireland, UK & Virginia Tech, Blacksburg, VA, US).
- Research Interests: Energy harvesting nanostructures, solar cells, and optical fluorescence sensors.
- Grants: +2M \$, +75 journal publications< +30 conference appearance
- Editor in Chief (Integrated Nano, Science Park Publisher) and Editor (Alexandria Engineering Journal, Elsevier)

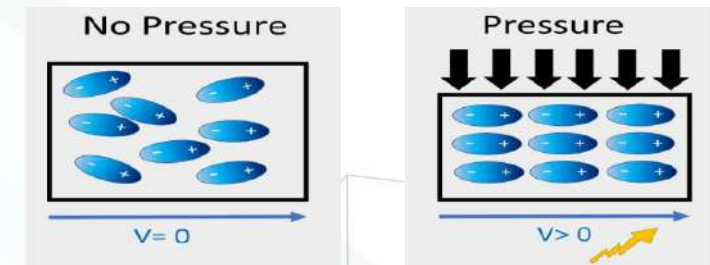
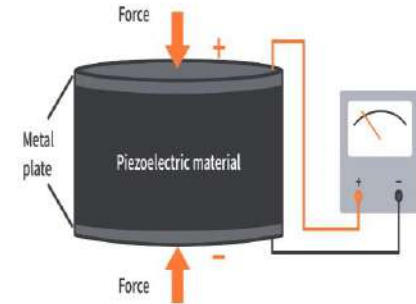
Contents

- **Introduction to piezoelectric nanofibers**
- Different Applications
- Experimental Procedures
- Challenges facing piezoelectric polymers
- Recent progress and future aspects
- Conclusions



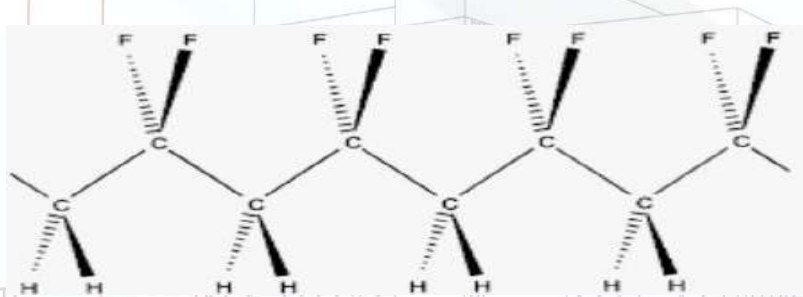
Introduction

- Piezoelectric transducing mechanism is the mechano-electric transducing where the mechanical energy including vibrations, pressures, bending, and tensions stresses can be converted into electrical energy.
- Usage in wide variety of energy harvesting applications/actuators such as biomedical sensors, wearable electronics, and smart textile.
- Detection/harvesting of sound acoustic wave has been recently investigated in many fields including energy harvesting, industrial manufacturing, health care.
- Materials:
 - Ceramics: Lead Zirconate Titanate (PZT).
 - Polymers: poly (vinylidene fluoride) PVDF.
 - Pros/Cons:
 - Ceramics have much larger piezoresponse.
 - Ceramics are less bio-friendly materials.
 - Polymeric mats may have more bending/stretching flexibility.
 - NFs have higher surface-to-volume ratio compared to cast polymers.



Theoretical Background

- Among different organic materials, poly (vinylidene fluoride) (PVDF) has unique piezoelectric properties due to internal polar crystalline nature, without the need for stretching or poling treatments.
- Features: Lightweight, flexibility, high purity, resistance to solvents, and stability under high electric field.
- Outcome: Relatively large voltages with low applied forces makes it much favorable to use in piezoelectricity.
- Piezoelectricity of PVDF nanofibers (NFs) prepared through electrospinning has been strongly introduced in the recent research.
- The molecular structure of PVDF consists of repeated monomer units such as $(-\text{CH}_2\text{-CF}_2-)_n$.
- PVDF exists in different crystalline forms such as alpha (non-polar), beta, and gamma (last two are polar) phases. Piezoelectricity of PVDF nanofibers (NFs) via electrospinning are higher response.
- The crystallinity can reach up to 50%, at lower melting point of 177 degree Celsius.
- However, most of the processed piezoelectric polymers have some drawbacks involving mechanical stretching.

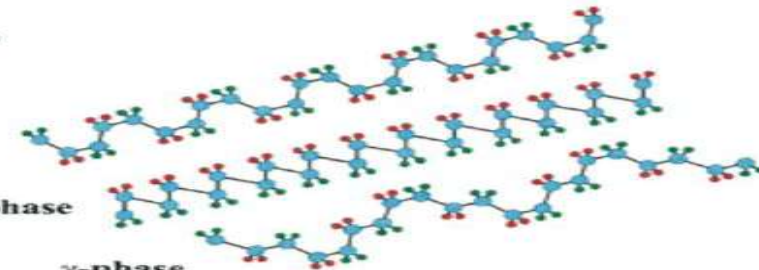


• Hydrogen
• Fluorine
• Carbon

α -phase

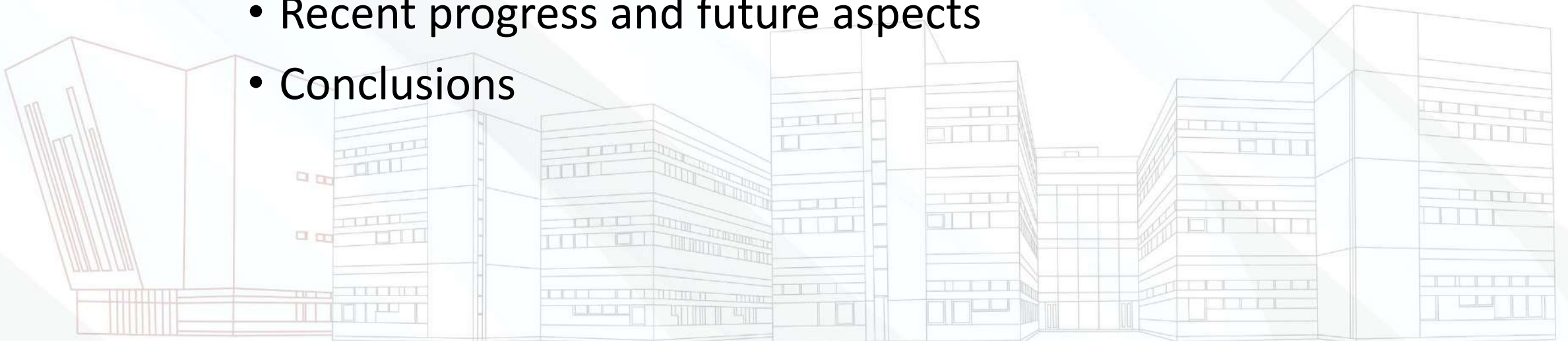
β -phase

γ -phase



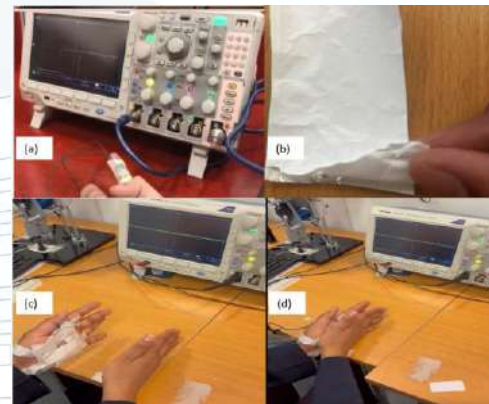
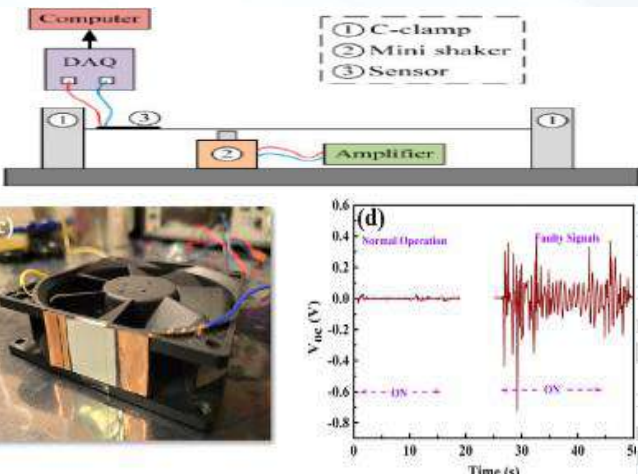
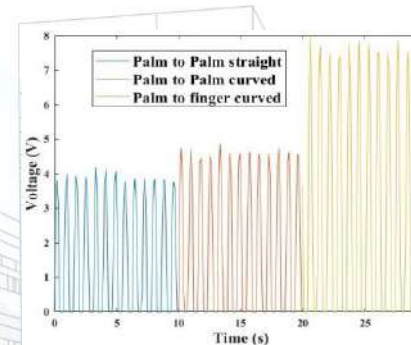
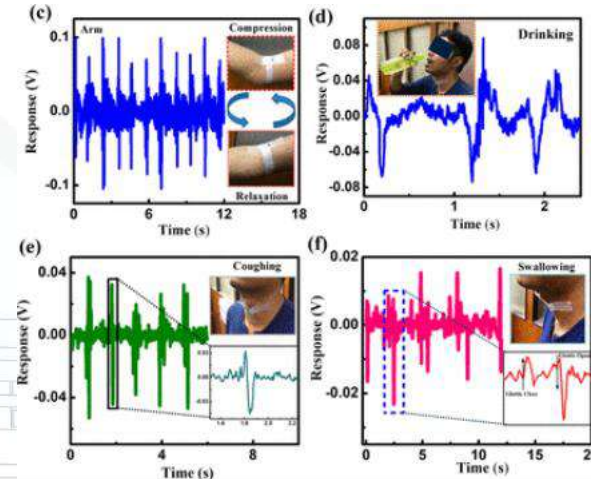
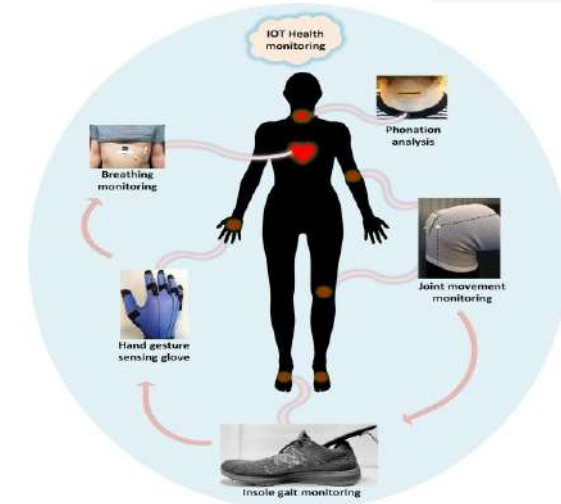
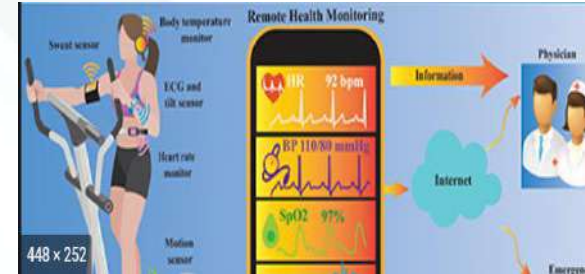
Contents

- Introduction to piezoelectric nanofibers
- **Different Applications**
- Experimental Procedures
- Challenges facing piezoelectric polymers
- Recent progress and future aspects
- Conclusions



Mechanical Energy Harvesting

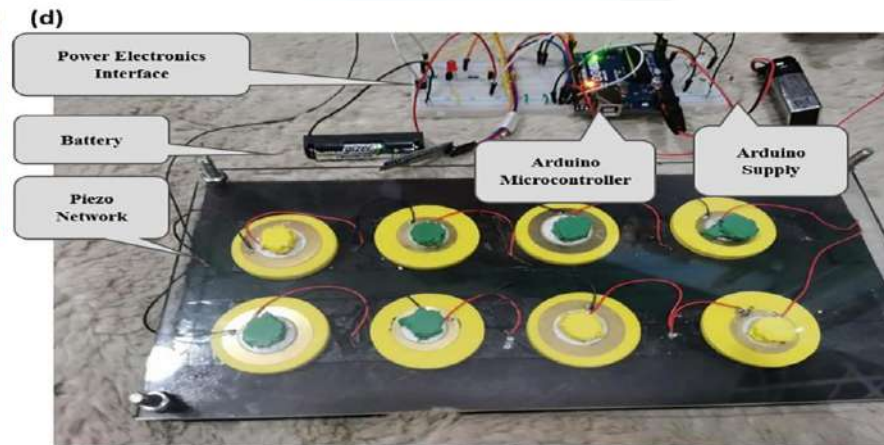
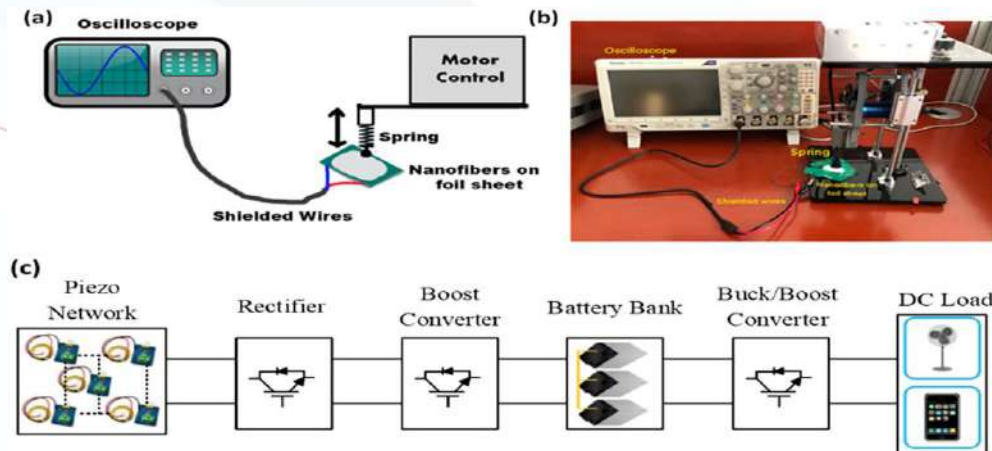
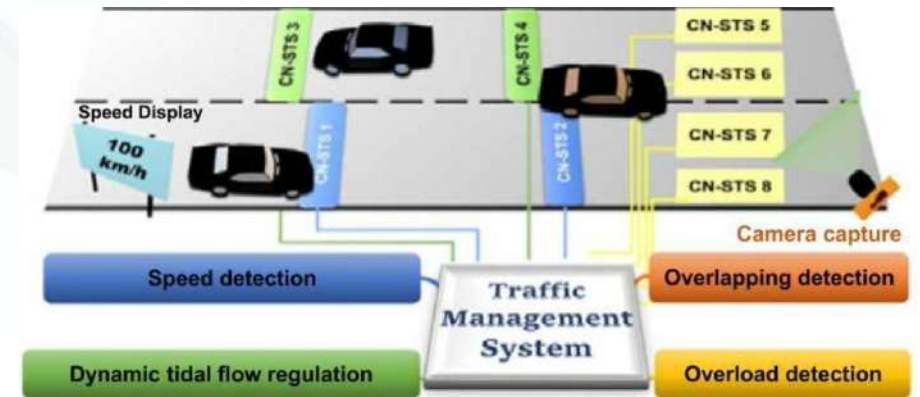
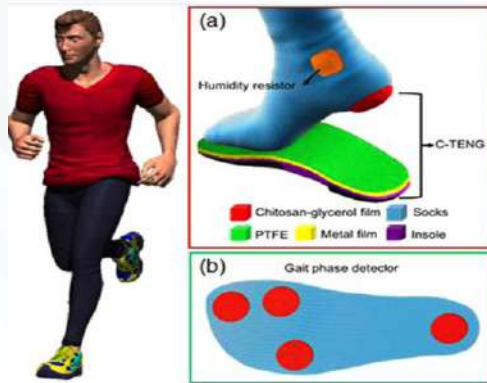
- Wearable Electronics:
 - Motion harvesting.
 - Health Monitoring.
 - Breathing/pulses sensor.
 - Cough monitoring.
 - Assistive Technology-based support.
 - Can be integrated with IoT!
- Detection of low-frequency vibrations: Industrial Applications.



- Kuntal Maity, Samiran Garain, Karsten Henkel, Dieter Schmeißer, and Dipankar Mandal, Self-Powered Human-Health Monitoring through Aligned PVDF Nanofibers Interfaced Skin-Interactive Piezoelectric Sensor, *ACS Applied Polymer Materials* 2020 2 (2), 862-878
 - Sengupta, D., Romano, J. & Kottapalli, A.G.P. Electrospun bundled carbon nanofibers for skin-inspired tactile sensing, proprioception and gesture tracking applications. *npj Flex Electron* 5,
 - Singh, R.K.; Lye, S.W.; Miao, J. PVDF Nanofiber Sensor for Vibration Measurement in a String. *Sensors* 2019, 19, 3739. <https://doi.org/10.3390/s19173739>
 - B. S. Athira, Ashitha George, K. Vaishna Priya, U. S. Hareesh, E. Bhoje Gowd, Kuzhichalil Peethambharan Surendran, and Achu Chandran, High-Performance Flexible Piezoelectric Nanogenerator Based on Electrospun PVDF-BaTiO₃ Nanofibers for Self-Powered Vibration Sensing Applications, *ACS Applied Materials & Interfaces* 2022 14 (39), 44239-44250 29 (2021).

Mechanical Energy Harvesting

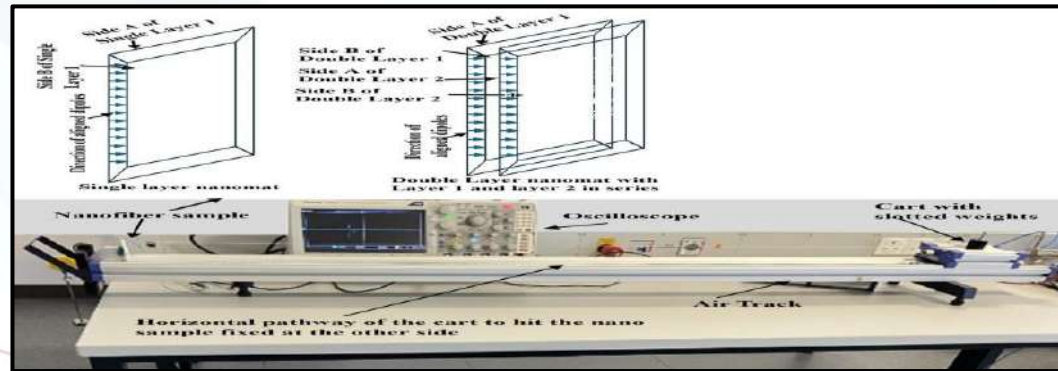
- Foot-step Generation: Energy Harvesting, cheap lightening, smart traffic.



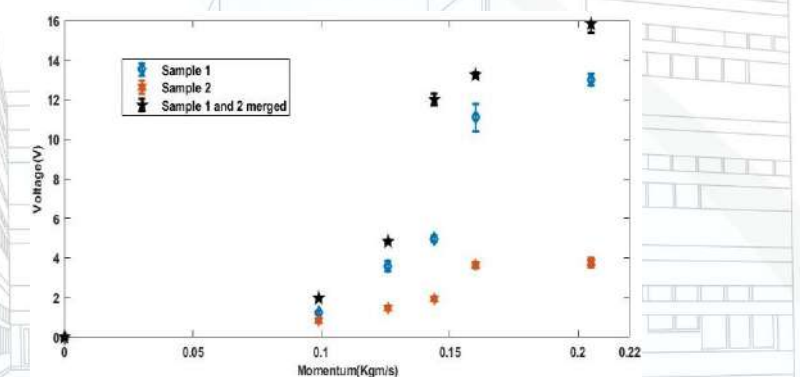
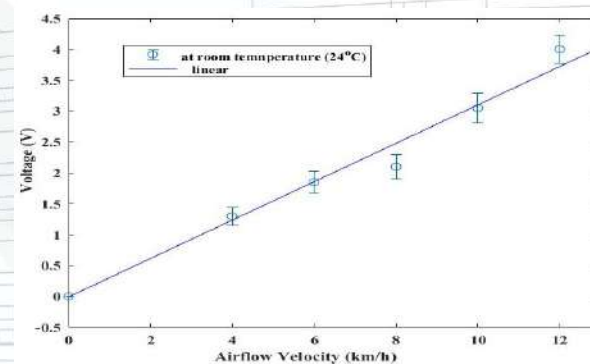
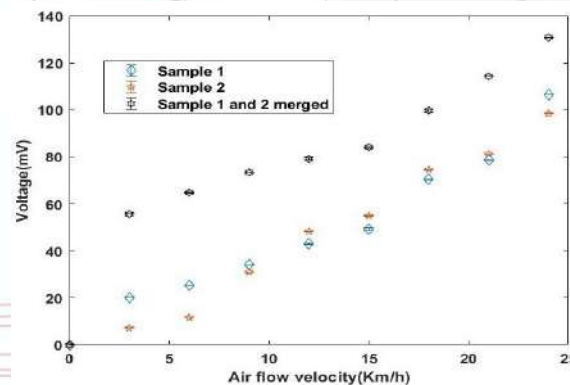
Xiya Yang, Guangqing Liu, Qiyao Guo, Haiyang Wen, Ruiyuan Huang, Xianghe Meng, Jialong Duan, Qunwei Tang, Triboelectric sensor array for internet of things based smart traffic monitoring and management system, Nano Energy, 2022, 92, 106757.

Mechanical shocks/Airflow/Vibrations sensing

- By altering the object's momentum and the speed at which it strikes the sample, the produced electrospun nanomat's reaction to mechanical shocks is examined.
- The discovery of a favorable reaction to mechanical shocks demonstrated the potential of these nanomats for energy harvesting applications involving mechanical shocks.

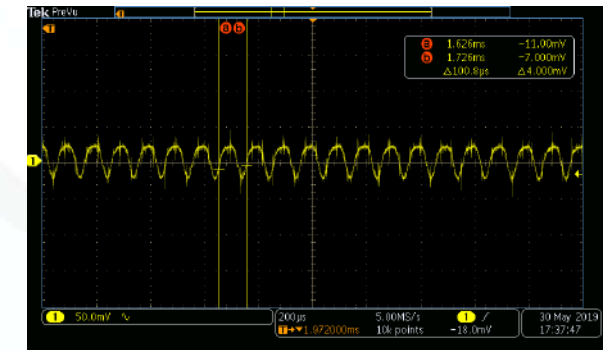
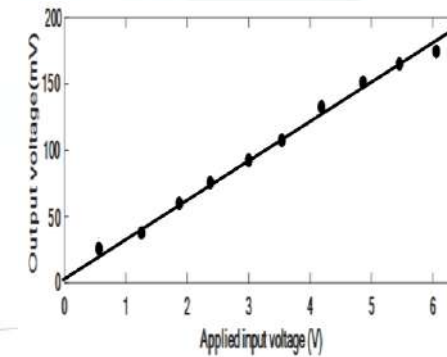
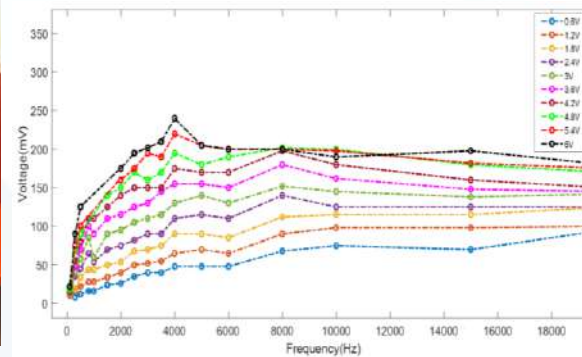


| Applied Frequency (Hz) | Pure PVDF | | | PVDF TPU 15 wt% | | |
|------------------------|----------------------------|-------------------------|-------------------|-------------------------|----------------------|-------------------|
| | Output Voltage(V) at 0.5 N | Output Voltage(V) at 2N | Sensitivity (V/N) | Output Voltage at 0.5 N | Output Voltage at 2N | Sensitivity (V/N) |
| 10 | 1.51±0.04 | 5.30 ± 0.22 | 2.37 | 3.43±0.23 | 8.53±0.29 | 3.29 |
| 12.5 | 3.56±0.29 | 11.4±0.23 | 4.96 | 4.3±0.11 | 12.8±0.61 | 5.48 |
| 15 | 5.58±0.20 | 12.97±0.08 | 6.97 | 5±0.26 | 17.3±0.40 | 7.92 |
| 17.5 | 7.43±0.12 | 14±0.11 | 5.2 | 6±0.17 | 20.23±0.4 | 9.16 |
| 20 | 8.98±0.31 | 15.06±0.17 | 4.74 | 6.62±0.14 | 21.97±0.26 | 9.53 |
| 22.5 | 9.92±0.19 | 15.86±0.12 | 3.93 | 8.5±0.15 | 24.7±0.74 | 10.06 |
| 25 | 10.9±0.28 | 16.4±0.23 | 3.62 | 9.95±0.35 | 30±0.29 | 13.63 |
| 27.5 | 13.9±0.14 | 18.16±0.44 | 2.84 | 14±0.66 | 35±0.58 | 14.6 |
| 30 | 16.6±0.30 | 20.2±0.44 | 2.28 | 16.73±0.1 | 38±0.58 | 15.13 |

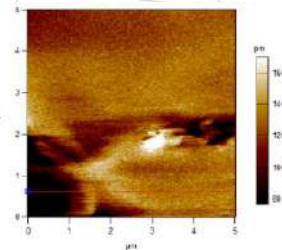
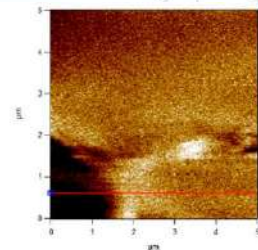
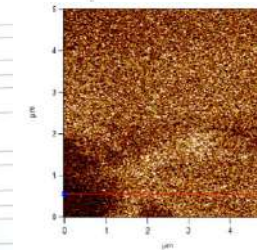


More applications...

- Acoustic Detector:
 - To detect and harvest acoustic signals.
 - Signal Retracing: An example of the retraced voltage signal by PVDF nanofibers mat, according to input acoustic signal of 6 kHz with a retraced frequency approximately equals to the input frequency (<1% error!).



- Self-cleaning filters and anti-bacterial mats:
 - Mechanically-vibrated surface under DC applied voltage.
 - Self-cleaning surface/filter.
 - Oil removal and permeability of the membranes.
 - Smart Facemasks, static charges for anti-bacterial (less count).

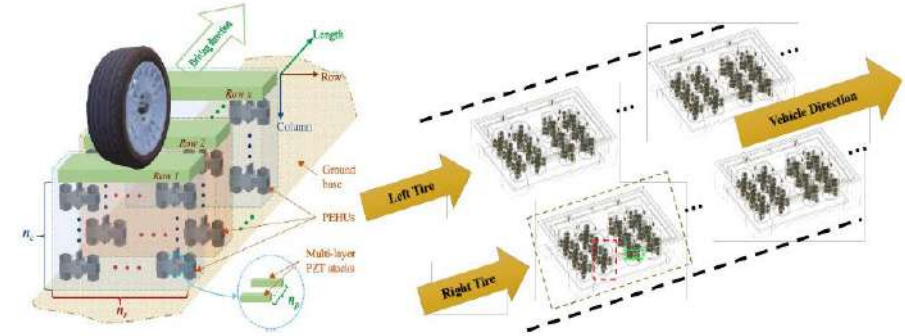


M. El-kaliouby, A. Khalil, A. El-Khatib, N. Omran, M. Gamal, A. Hassanin, I. Kandas, I. Shyha, and N. Shehata, Antimicrobial Impact of Locally Generated Piezoelectric Fields from Solution-Blown PVDF/PVDF-TPU Nanofiber Mats, Scientific Reports, 2024, In press.

N. Shehata, A.H. Hassanin, E. Elnabawy, R. Nair, S. Bhat, I. Kandas, Acoustic Energy Harvesting and Sensing via Electrospun PVDF Nanofiber Membrane, Sensors 2020, 20, 3111.

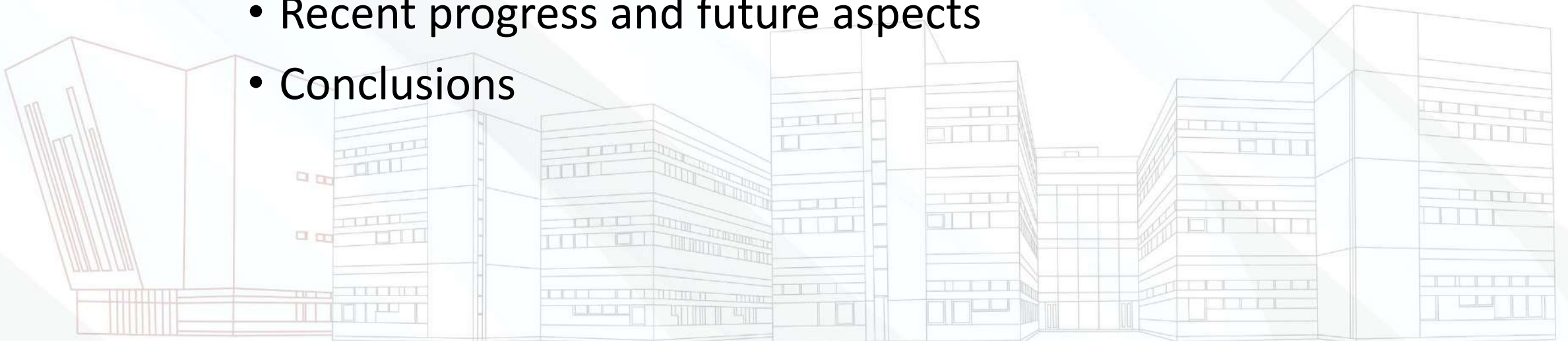
Mechanical Energy Harvesting (Case studies)

- PYRO-E (San Jose, CA, United States, 2017-2023)
 - Harvesting an electrical power from traffic, using arrays of piezoelectric units (piezo towers)
 - One-mile-long roadway has the potential to generate 72,800 kilowatt-hours of energy per year, that could power up to 5,000 homes from just a half-mile of highway
 - For heavy trucks, the annual electric energy over one mile of a one-lane highway can be as high as 907,873 kilowatt-hours, which is equivalent to a reduction of 300 metric tons of carbon dioxide
 - Higher possibility of using the roads for data collection, recording traffic conditions and aiding navigation for self-driving cars
- PaveGen (UK)
 - It depends on piezoelectric ceramics with mechanism optimization
 - Up to 4 Joule per step
 - Multiple projects: UK, UAE, India
- More R&D at nanofibers level for wearable electronics.



Contents

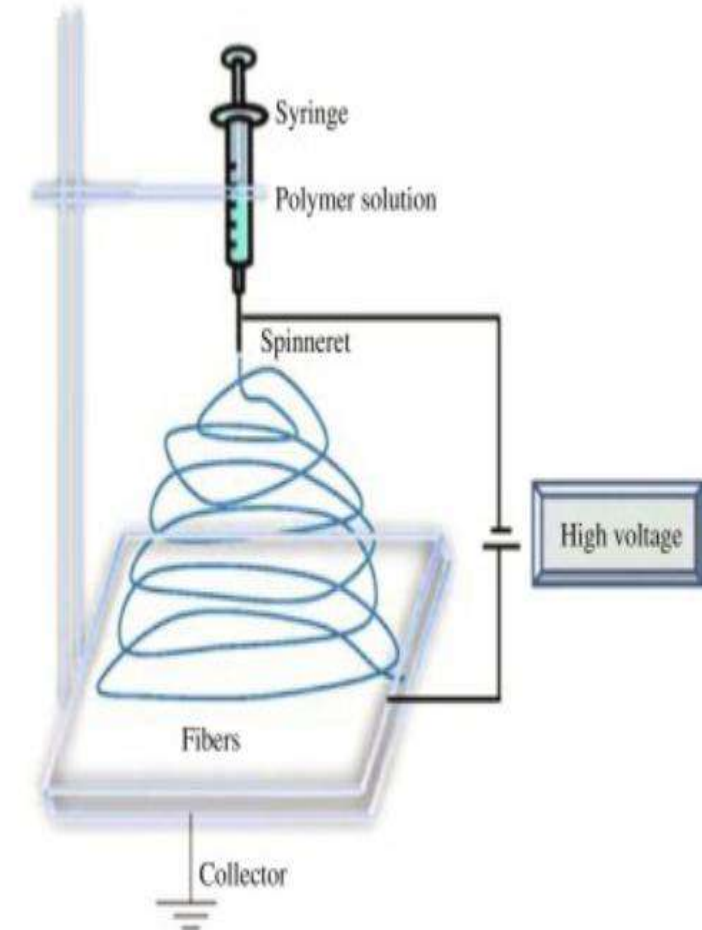
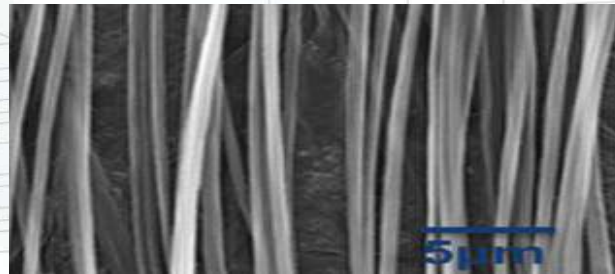
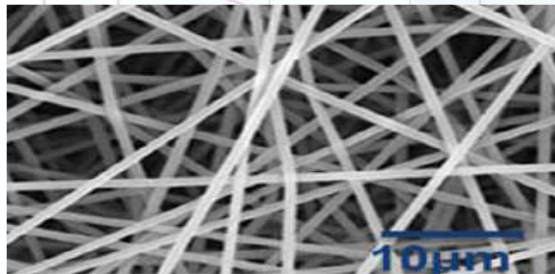
- Introduction to piezoelectric nanofibers
- Different Applications
- **Experimental Procedures**
- Challenges facing piezoelectric polymers
- Recent progress and future aspects
- Conclusions



Experimental Procedures- NFs Fabrication

- Electrospinning:

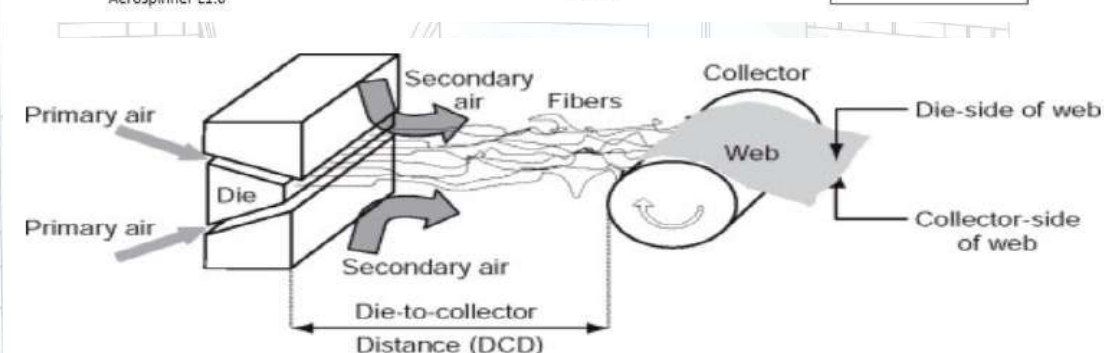
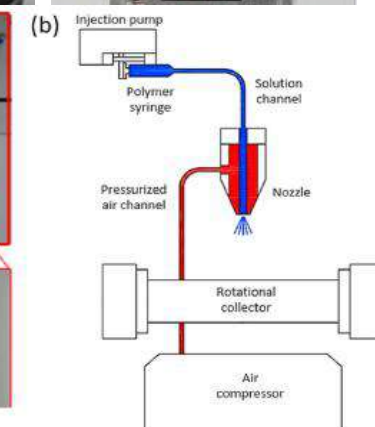
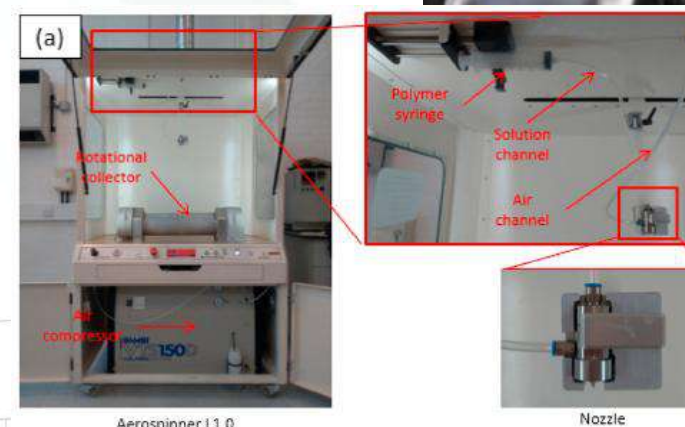
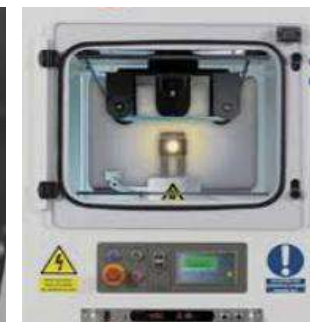
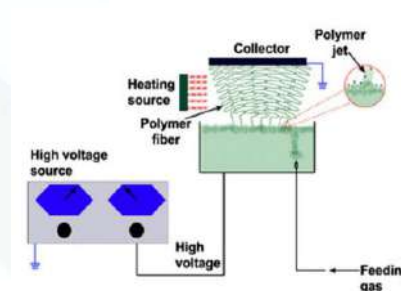
- Principle: uniaxial stretching of a polymer solution which is viscoelastic by applying electrostatic forces.
- A continuous set of nanofibers can be generated without any disruption given an enough solution to feed.
- Here, a high DC voltage is applied to the needle of a syringe where the solution is fed using a precision pump.
- Random/aligned nanofibers can be generated depending on the collector side (stationary or high-speed rotatory drum, respectively) and other parameters.
- Mean diameter > 70 nm.



<https://www.sciencedirect.com/topics/materials-science/electrospinning>
<https://www.nanofiberlabs.com/solutions/introductory-tutorial-for-electrospinning.html>

Experimental Procedures-Fabrication

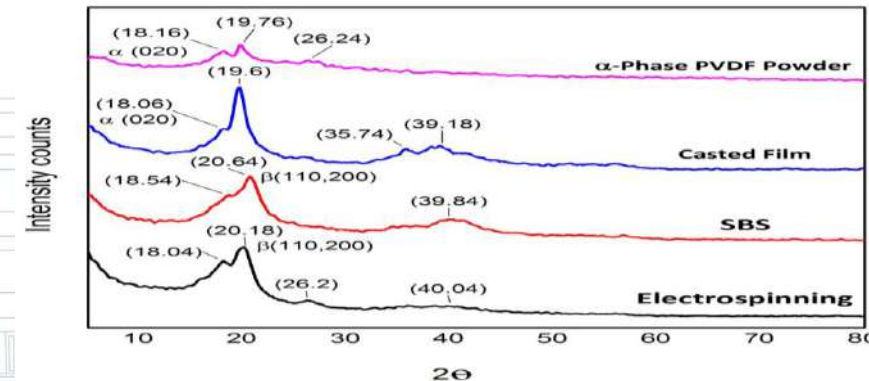
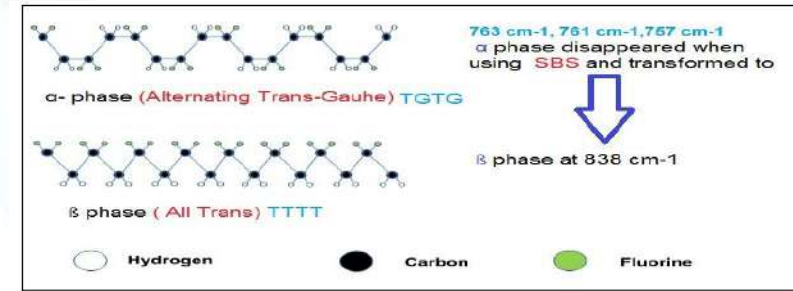
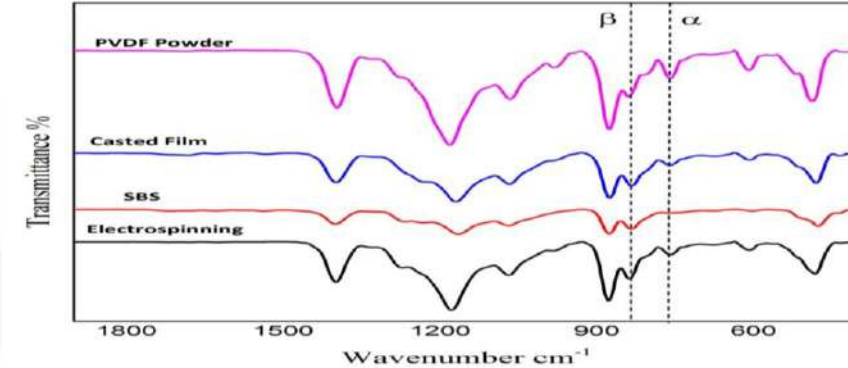
- Needleless Electrospinning
 - This mechanism depends on a matrix of small holes in a metallic drum immersed in the polymeric solution to form a multi-jet emitter.
 - No needle/nozzle, reduced repulsive impact.
 - Capability of scaling-up.
 - Commercial Examples: Nanospider.
- Solution-blown spinning
 - Air blowing instead of electric field.
 - Special nozzle design.
 - Higher scaling-up opportunity.
 - Mechanical vs Electric poling!
- Melt-blown spinning
 - Best scaling-up (Facemasks).
 - Micro to nanofibers internal stage.
 - Heating challenge.



Characterizations-FTIR/XRD

- In FTIR, Peaks at 757 cm^{-1} and 761 cm^{-1} for both PVDF powder and cast film, which is indicative of the α phase (TGTG).
- The spectra for NFs case shows a raised peak 838 cm^{-1} to represent the formation of polarized β -PVDF (TTTT).
- β -PVDF can be calculated from intensity fraction, where all-trans (TTTT) zigzag chain conformation.
- Dipole moment alignment which is parallel to the force resulted from the applied electric field/air pressure that stretched PVDF.
- Similar aspect in XRD, depending on angles of both α and β phases (planes 110 and 200).

$$\beta(\%) = \left(\frac{A(\beta)}{A(\alpha) + A(\beta)} \right) \times 100 \%$$



Characterizations-piezoelectric coefficient (d_{ij})

- The piezoelectric charge coefficient relates the electric charge generated per unit area with an applied mechanical force and is expressed in the unit of Coulomb/Newton (C/N).
- This constant is most frequently used to evaluate the performance of a piezoelectric material.

$d = \text{Charge density open circuit} / \text{Applied stress}$

- The d constant is associated with three important materials properties through the following the equation (d_{33} and d_{31}), where force is applied at parallel or perpendicular to the polarization axis (C/N or m/V):

$$d_{31} = k_{31} \sqrt{\epsilon_0 k_3^T s_{11}^E}$$

$$d_{33} = k_{33} \sqrt{\epsilon_0 k_3^T s_{33}^E}$$

where k is the electromechanical coupling coefficient, k^T denotes the relative dielectric constant at constant stress, and s^E is elastic compliance at a constant electrical field.

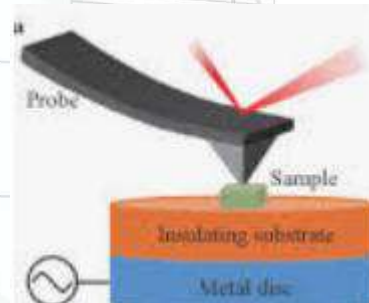
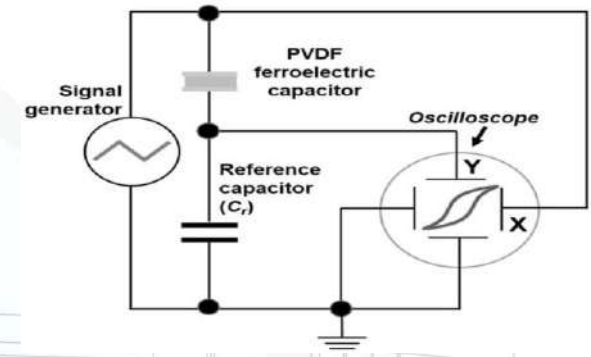
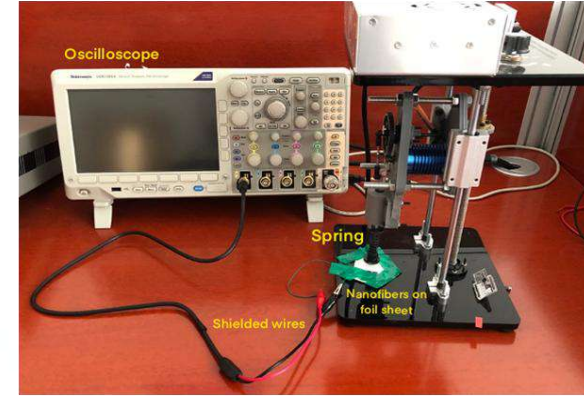
- It can be calculated or experimentally measured.
- The piezoelectric voltage coefficient is also called voltage output constant, which is defined as the ratio of the electric field produced to the mechanical stress applied.

$$g = \text{Field developed} / \text{Applied mechanical stress} = d/\epsilon$$

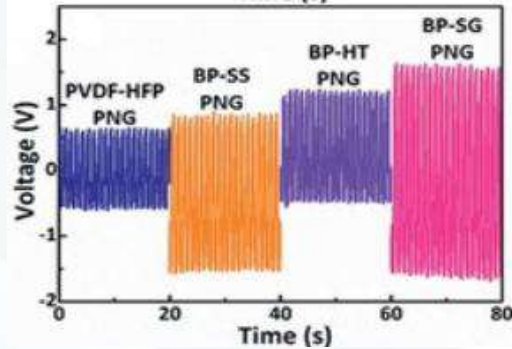


Characterizations-Piezo analysis

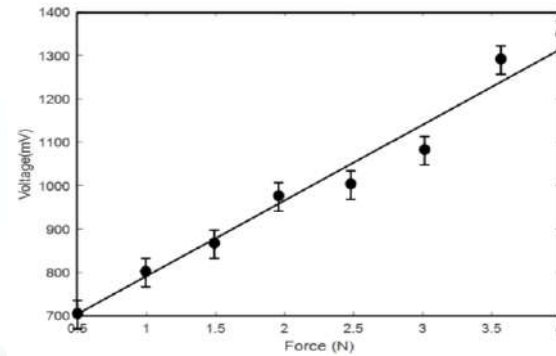
- Generated voltage versus time at different applied mechanical excitations such as force/pressure, bending, and tension. (Factors: Amplitude, frequency, or impulse!).
- The nanofiber mat is tested under a cyclic loads. The sample is sandwiched between two sheets of foil that are connected through shielded wires to a high impedance oscilloscope to record the output voltage when being underneath the plunger.
- Sensitivity: The ratio of charge or voltage developed to the applied force that is responsible for generation of the voltage (Volt/Newton)
- Current and power-density calculations.
- Polarization-field hysteresis: using Sawyer-Tower circuit.
- Piezo Force Microscope:
 - Detection of generated voltage under applied mechanical vibrations.
 - In opposite, PFM can detect surface roughness under applied DC voltage.



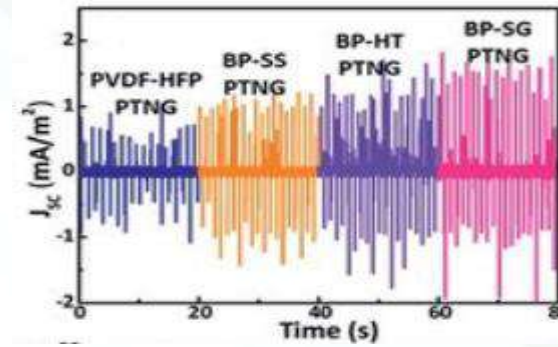
Examples of piezoelectric analysis



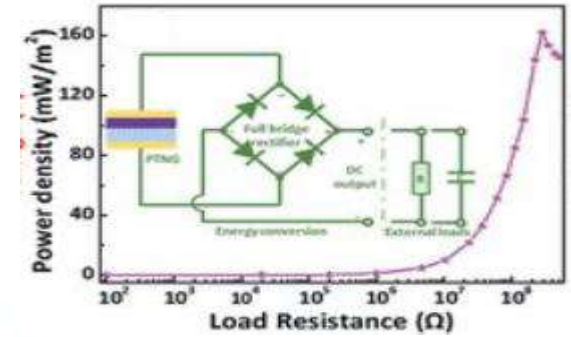
Voltage per cyclic applied force/pressure



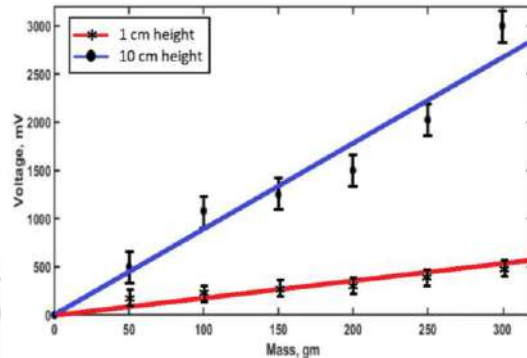
Voltage per force at constant frequency



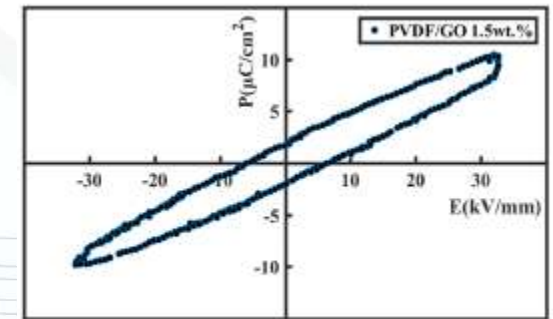
Current density per cyclic force/pressure



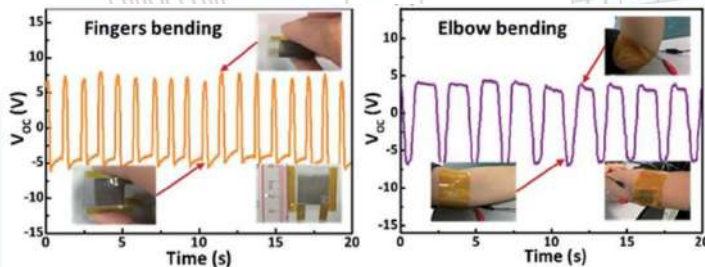
Power density



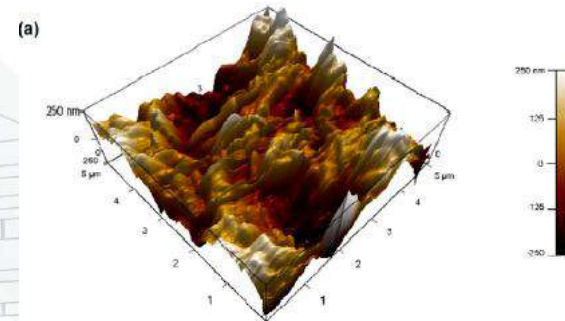
Voltage per falling masses



Polarization-Electric field analysis



Generated voltage per bending

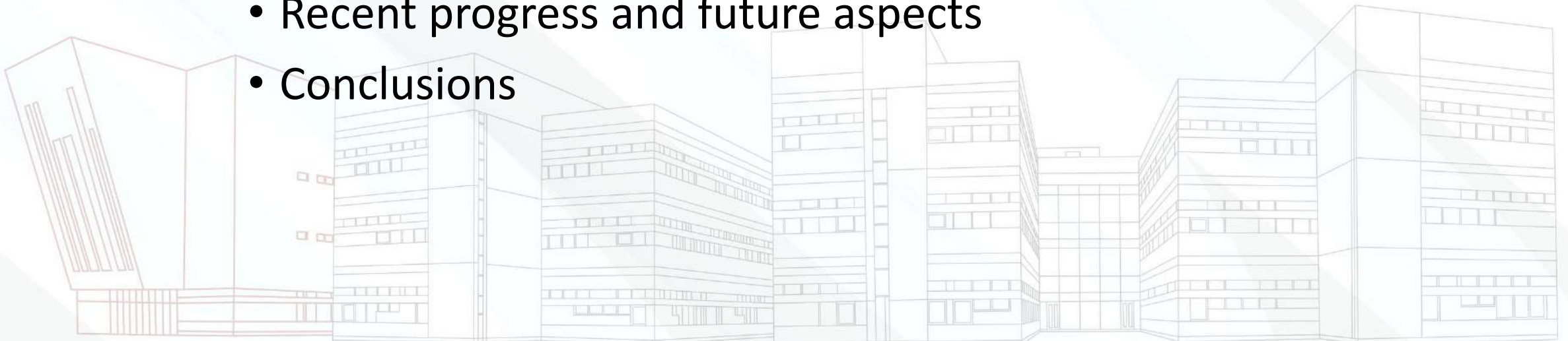


PFM analysis

Yinghong Wu, Jingkui Qu, Walid A. Daoud, Lingyun Wang and Tao Qi, Flexible composite-nanofiber based piezo-triboelectric nanogenerators for wearable electronics, J. Mater. Chem. A, 2019, 7, 13347-13355

Contents

- Introduction to piezoelectric nanofibers
- Different Applications
- Experimental Procedures
- **Challenges facing piezoelectric polymers**
- Recent progress and future aspects
- Conclusions



Technical Challenges

- Still away from piezoelectric ceramics
 - d_{33} of less than 50 pC/N \ll ceramic ranges of around +600 pC/N
 - Lower density of dipoles, less crystallinity degree.
- Optimization of Electrospinning Parameters:
 - β -phase content, and crystallinity depends on precise control of electrospinning parameters (voltage, flow rate,..etc).
- Material and Structural Design:
 - Additives: Complexity in fabrication and consistency concerns (uniform dispersion of fillers).
 - Still brittle, not stretchable.
 - Used solvents are not biocompatible such as Dimethylformamide (DMF) and chloroform.
- Durability and Electrode Compatibility:
 - For wearable and flexible devices, maintaining long-term durability is a concern (cyclic mechanical effect and number of washing times).
 - Reliable electrode integration is challenging. Electrodes must be compatible with the nanofiber mats and withstand repeated mechanical stress without degrading performance.

Fabrication Challenges

•Scaling-up:

- It is hard to be compatible with the mass production and commercialization need (the productivity rate of the nanofibers from electrospinning is extremely low, of range 0.01 to 2 g/h, compared to other processes).
- Mechanically-based spinning processes may not generate higher piezosensitivity of nanofibers, compared to electrospun piezoelectric nanofibers, due to the absence of electric field that may be more effective in alignment of dipoles and forming higher concentration of beta sheets, compared to mechanical impact.
- In addition, the melt-blown spinning (extruding) negatively effect on the properties of the polymers along with possible phase changes with reduced piezosensitivity.
- Also, the melt-blown spinning can generate microfibers scale, larger than 10 microns, which is less effective in piezo generation compared to nanofibers.
- Thermal degradation of some piezoelectric nanofibers is a concern!

Application-related Challenges

- Scalability and Textile Integration:
 - Integrating nanofibers into real textile-level devices with consistent biocompatibility, wearability, and multifunctionality is still a major hurdle.
 - System integration for large-area, mass-produced devices is not yet fully realized.
- Measurement and Standardization:
 - There is a lack of standardized methods for measuring and comparing piezoelectric properties.
- Biofouling and Environmental Stability:
 - In filtration and biomedical applications: Fouling and environmental degradation (limited lifespan).
- Clinical Translation:
 - For tissue regeneration and biomedical uses, challenges include safety/robust performance in biological environments and ensuring noninvasive operation.

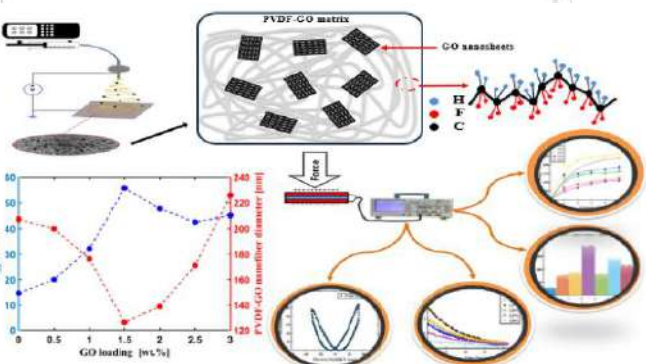
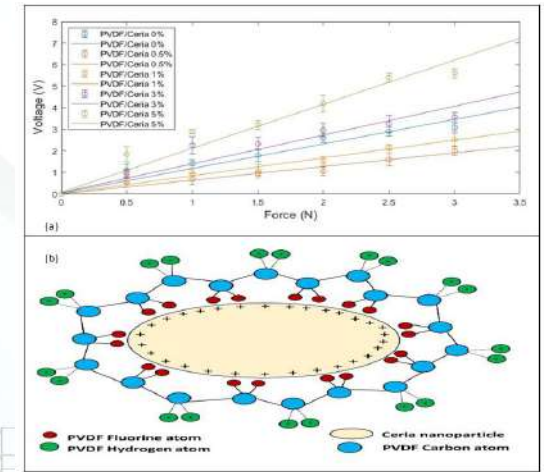
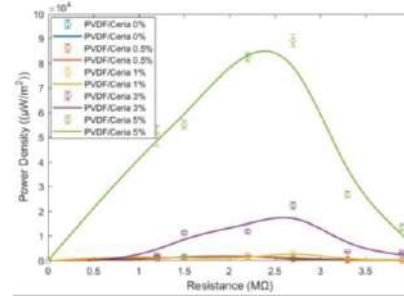
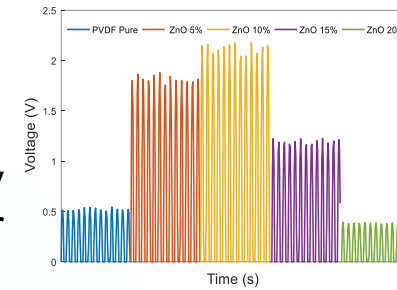
Contents

- Introduction to piezoelectric nanofibers
- Different Applications
- Experimental Procedures
- Challenges facing piezoelectric polymers
- **Recent progress and future aspects**
- Conclusions



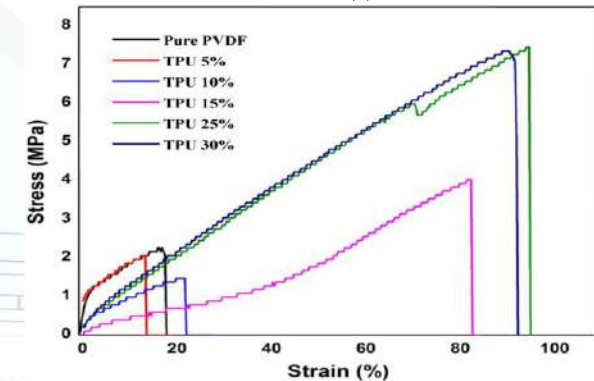
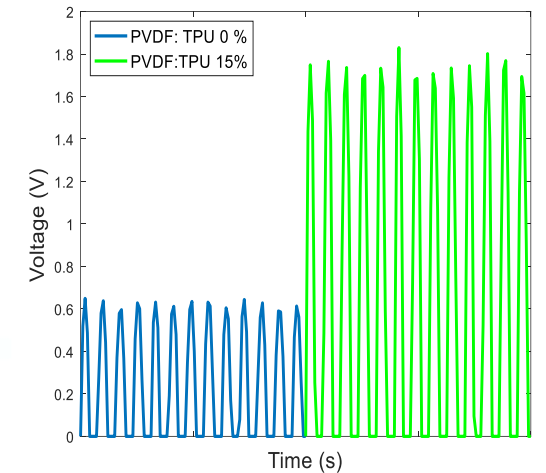
Additives-based piezoelectric nanocomposites

- Functionalized additives/Nucleating agent:
 - Heterogeneous nucleation sites for the β -phase, and consequently considered as attraction centres where PVDF chains are adsorbed over the outer surface of the nanoparticle
 - Nanofiller is positioned in between isolated polymer backbones, that can develop micro-capacitor structures with a better charge accumulation inside the nanofibers
 - Examples:
 - ZnO: has significant spontaneous polarization as a common piezoelectric material including an asymmetric crystalline structure
 - CeO_{2-x}: Multi-functional nanocomposite (fluorescent!)
 - GO: Up to d_{33} of 55 pC/N with output power density of 150 $\mu\text{W}/\text{cm}^2$.
 - Carbon nanofibers (CNFs)/Carbon nanotubes (CNTs):
 - Synergistic interaction between CNFs and additional electrical polarization processes (5.80 V, 1.2 ± 0.1 mA).
 - When CNTs are added to PVDF, the polymer's electrical conductivity is improved, which improves the mobility of electrons inside the polymer matrix (Trade off!)



Additives-based piezoelectric nanocomposites

- Mixed polymers
 - Elastomers (Mechanical stretchability enhancement)
 - Adding Thermoplastic Polyurethane (TPU)
 - Innovative Outcome (reducing cost, enhanced piezoresponse, improved stretchability)
 - TPU additive of 10-15 wt.%, enhances the piezoresponse of PVDF along with improving the mechanical stretchability (maximum allowed strain)
 - Proved for electrospinning and solution-blown spinning
 - Mxene and Potassium Sodium Niobate (KNN) have some potential contribution
- More Examples (current highest d_{33}):
 - Ba(Ti_{0.80}Zr_{0.20})O₃-0.5(Ba_{0.70}Ca_{0.30})TiO₃ (BTZ-0.5BCT) nanofibers with 180 pm/V
 - Cellulose pulp nanofibers of 145 pC/N
 - Electrospun BaTiO₃ and (Na,K)NbO₃ (NKN) nanofibers have demonstrated d_{33} values up to 76 pm/V for individual crystallites within the fibers
 - DET-BTO/PVDF composite nanofibers have reached a d_{33} of ~40 pC/N, which is the highest among reported BTO/PVDF composites



scientific reports

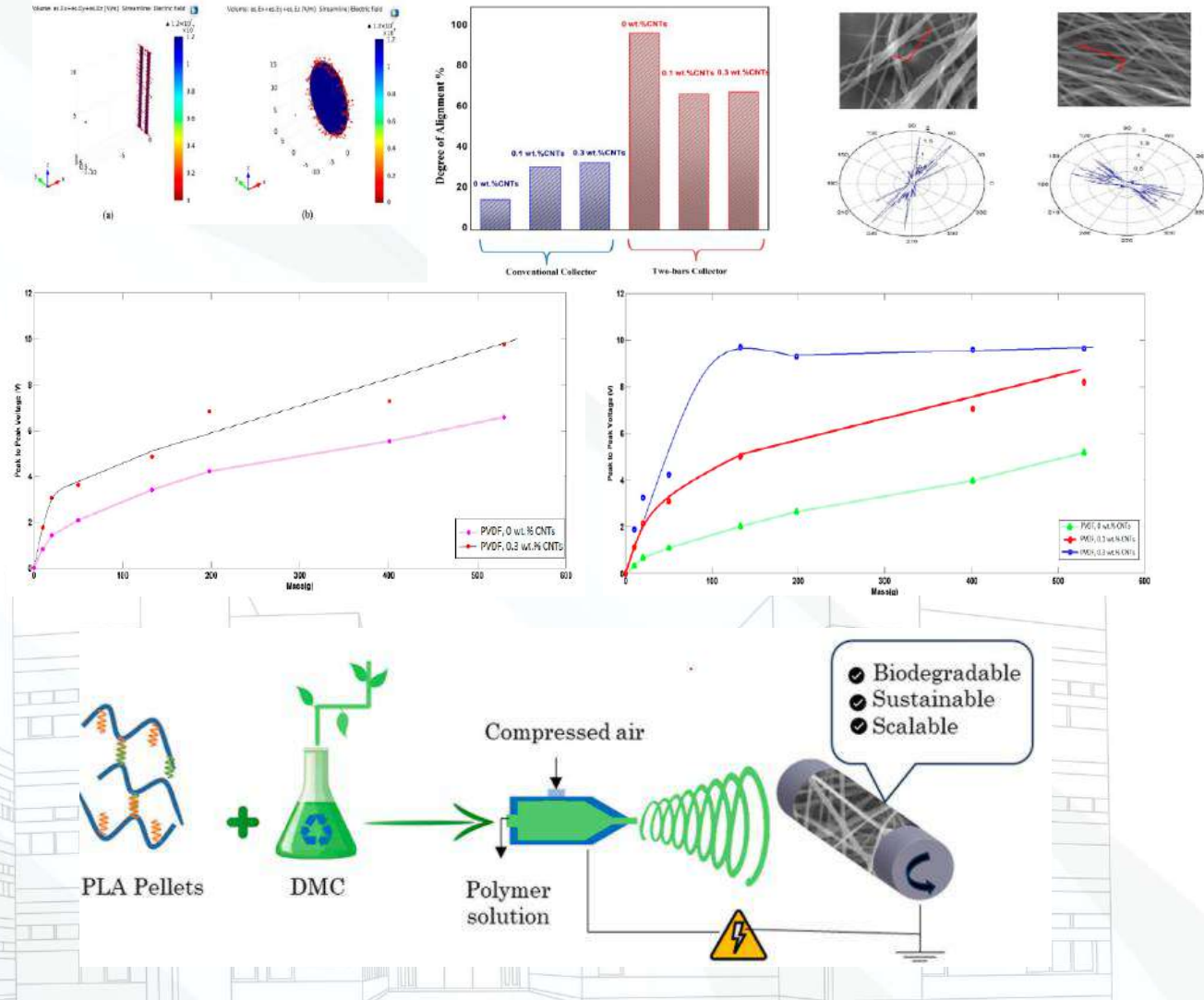
OPEN

Stretchable nanofibers of polyvinylidene fluoride (PVDF)/thermoplastic polyurethane (TPU) nanocomposite to support piezoelectric response via mechanical elasticity

Nader Shehata^{1,2,*}, Remya Nair¹, Rehab Boulayen^{1,3}, Isahac Kandas^{1,3,4}, Abdulrazak Mesran^{1,5}, Eman Elnebewy², Nada Omran¹, Mohammed Gamal² & Ahmed H. Hassanin^{6,7,8}

Processing

- Electrospinning:
 - Focusing electric field (dipoles alignment)
 - High speed rotating drum (fibers alignment)
 - 3D Fibers (in scaffolds, trade off between thickness and electromechanical coupling)
- Electro-mechanical spinning:
 - Integrating electrospinning and solution-blown spinning.
 - Both effects of electric field and airflow merged driving forces showed a remarkable improvement in the produced structure as well as solution jet stability.
 - Nanofiber mats with higher scaling up with minimum beads and uniform mean diameter.



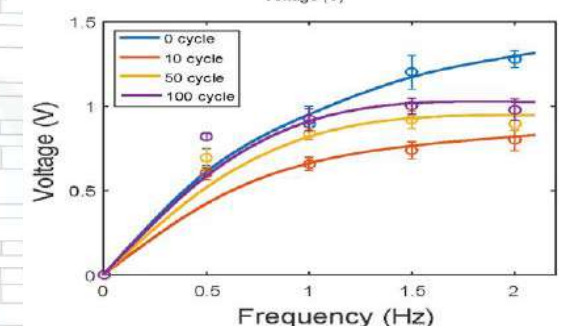
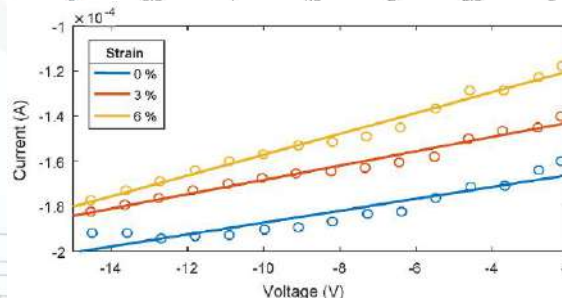
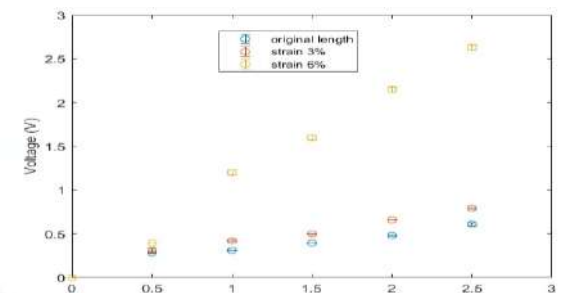
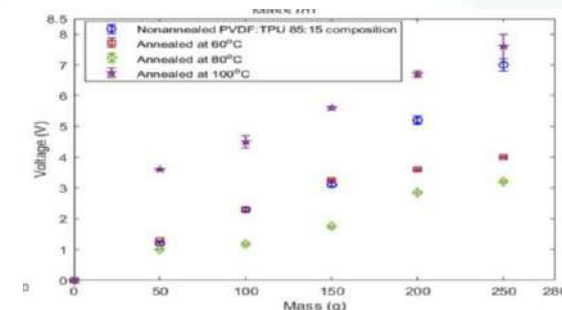
N. Shehata, E. Elnabawy, M. Abdelkader, A. Hassanin, M. Salah, R. Nair, S. Bhat, Static-Aligned Piezoelectric Poly (Vinylidene Fluoride) Electrospun Nanofibers/MWCNT Composite Membrane: Facile Method, Polymers 2018, 10 (9), 965.

Eman Elnabawy, Dongyang Sun, Neil Shearer, Islam Shyha, The effect of electro blow spinning parameters on the characteristics of polylactic acid nanofibers: Towards green development of high-performance biodegradable membrane, Polymer, 311, 2024, 127553

Eman Elnabawy, Dongyang Sun, Neil Shearer, Islam Shyha, Electro-blown spinning: New insight into the effect of electric field and airflow hybridized forces on the production yield and characteristics of nanofiber membranes, Journal of Science: Advanced Materials and Devices, 8, 2, 2023, 100552

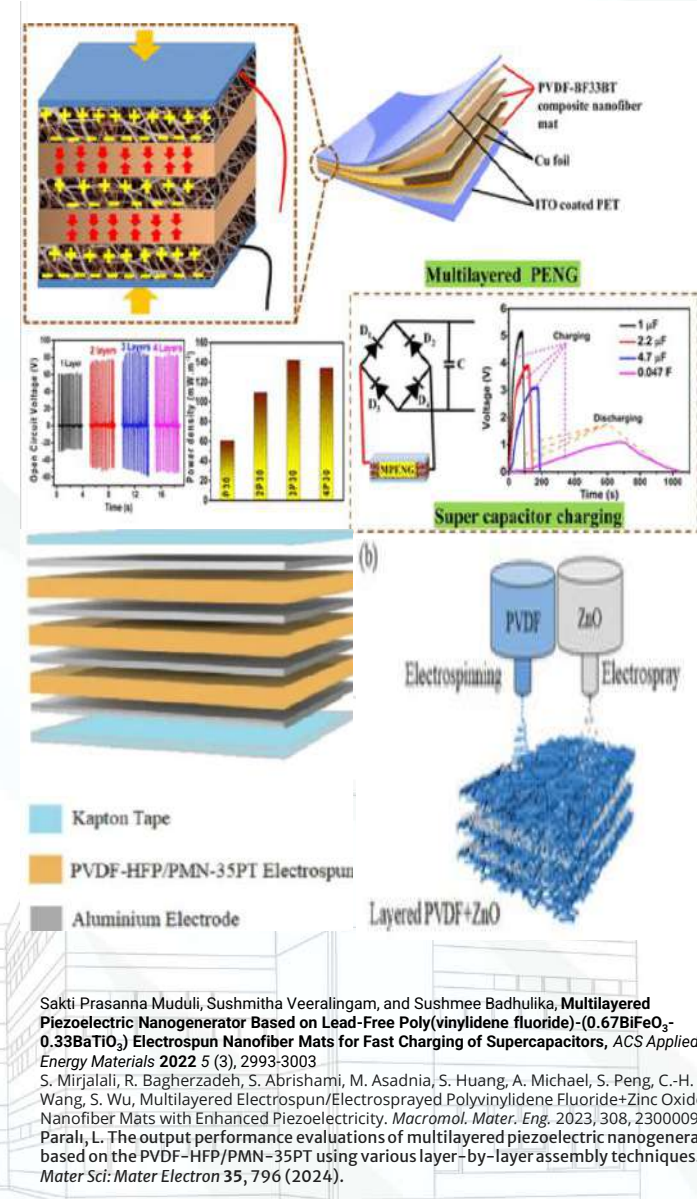
Post-treatment

- Heating:
 - Increased thermal heating leads to slight improvement of beta-sheets alignment.
 - Examples:
 - Commercial graded PVDF electrospun nanofibers showed an increased piezoresponse at heating up to 100°C for 4 hours exposure.
 - PVDF/ poly(trifluoroethylene) (TrFe) nanofibers has an increased piezoelectric constant up to 48.5 pm/V when annealed for 2 hours at 135 °C in vacuum environment, compared to 29.1 pm/V at non-heated nanofibers case.
- Mechanical Impact (Stretching):
 - Mechanical stretching can lead to enhanced piezoresponse.
 - Valuable in wearable electronics applications (multi-functionalized as strain sensor).
- Electric Poling:
 - Following step to either electrospinning or mechanical spinning.
 - DC High voltage for relatively short distance (1 kV/ 1 cm for 15 minutes).
 - More alignment of internal electric dipoles.



Device Design

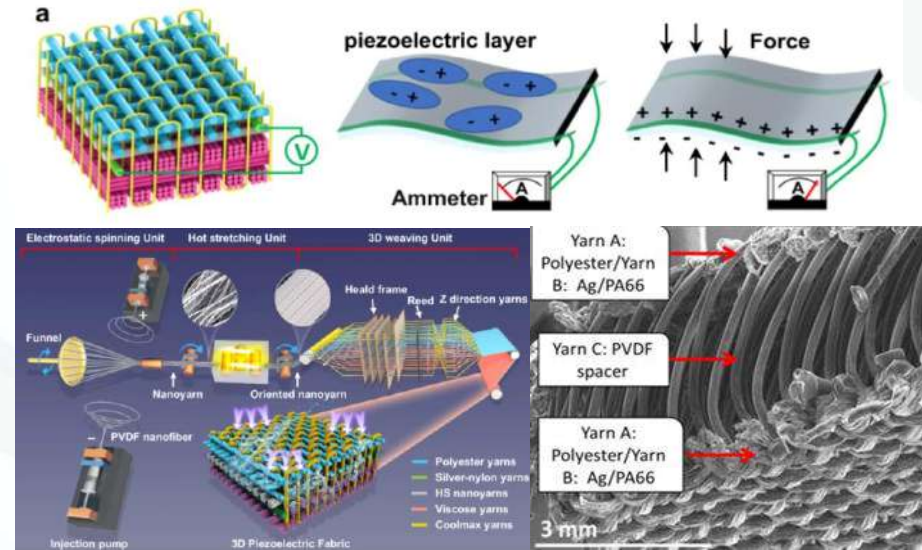
- Multiple layers (Piezo-Tower)
 - Static charges accumulation between different layers.
 - Incremented voltage and power density.
 - Examples:
 - Poly(vinylidene fluoride) (PVDF) with 30 wt.% of $[0.67(\text{BiFeO}_3)-0.33(\text{BaTiO}_3)]$ (BF33BT) electrospun nanofiber mats.
 - With three layers (Optimized), it shows an open-circuit voltage, short-circuit current, and instantaneous power density of 83 V, $1.62 \mu\text{A}$, and 142 mW m^{-2} , respectively, at 0.1 kgf at 3 Hz frequency.
 - 65 times better than single PVDF layer!
 - Charging a supercapacitor (0.047 F) up to 1.5 V in 11 min.
- Integrating electrospinning/electrospraying technique:
 - PVDF nanofiber mats by electrospaying zinc oxide (ZnO) nanoparticles between layers of PVDF nanofibers (Current is an issue!)
- Parallel stacked layers, separated by metallic layers:
 - PVDF layers separated by Aluminum electrodes (parallel in compact)
 - For four parallel connections, the unit output has an open-circuit voltage of 0.4 V (V_{RMS}) and a maximum electrical power of $0.3 \mu\text{W}$ (P_{RMS}) by drawing a current (I_{RMS}) of $1.46 \mu\text{A}$ under a resistive load of $140.2 \text{ K}\Omega$.



Device Design

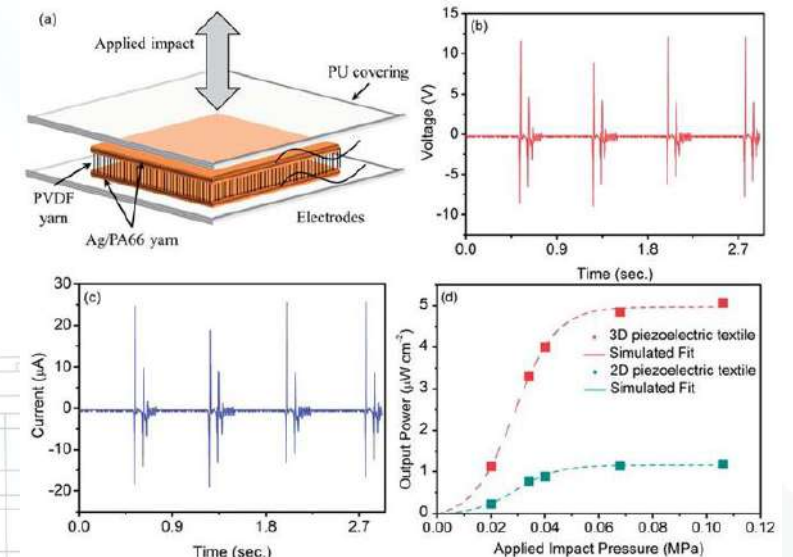
• 3D device/Spacer

- Piezoelectric yarn can be between different conductive and insulating layers.
- Example: The conductive yarn was Ag coated PA66 yarn denoted by 'A', the insulating yarn was PET yarn denoted by 'B' and the piezoelectric yarn was PVDF monofilament denoted by 'C'.
- The PVDF monofilament was used as a spacer yarn in this knitted structure.
- The output voltage and current generated by the fabric-based piezoelectric nanogenerator were 14 V and 29.8 μA , respectively under 0.1 MPa for 6s.
- Power density is up to 5.1 μWcm^{-2}



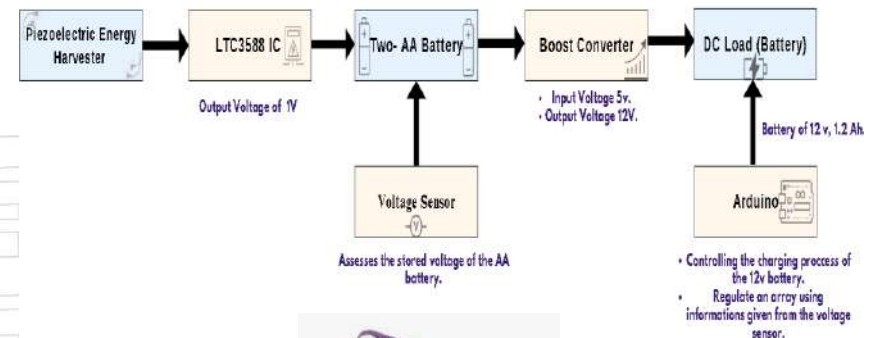
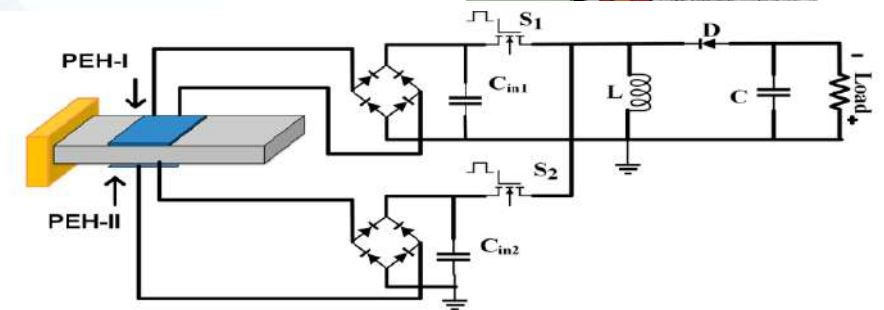
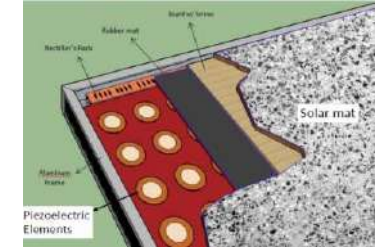
• Variable capacitor build-up

- Adding PVDF layer between other movable layers.
- Example: self-charging piezo-supercapacitor (SCPC) device shows capacitance (111 F/g at 5 mV/s scan rate)) with ~95 % of cyclic stability upto ~2000 CV cycles
- dielectric constant of ~31 at 10 wt% incorporation of the LCuMO nanoparticles



External support (Circuits)

- Matrix of series/parallel nodes can increment voltage/current
 - limited applications, possibly hybrid ceramic/fibers.
 - Mechanical design/springs are important.
 - It can be integrated with vertical cascaded piezo-stages.
 - Part of Solar-piezo mat!
- Voltage amplifiers/rectifiers
 - Buck-boost converter.
 - Example: with 2000 footsteps on 6x6 hybrid ceramic/fiber series/parallel strands. Open circuit voltage can reach up to 13.2V.
 - It can be connected to super capacitor (for example: 1F) (charging time: minutes?)
 - Converter can reduce up to 20% of charging time.
 - Current is trade-off/parallel connections to compensate!
- Piezo harvester chips
 - Compensation for full-wave rectifier loss (LTC 3588)
- Current amplifier: Challenging from nA to mA



Contents

- Introduction to piezoelectric nanofibers
- Different Applications
- Experimental Procedures
- Challenges facing piezoelectric polymers
- Recent progress and future aspects

- **Conclusions**



Conclusions

- Piezoelectric nanofibers are promising in wide variety of applications based on flexibility, cost, more bio-friendly.
- Challenges:
 - Lower piezoresponse.
 - Durability.
 - Processing limits.
- Solutions:
 - Material additives.
 - Processes-development.
 - Post-treatment.
 - Design of matrix (cascaded in 2D/3D)/Circuits contribution
- Should we collaborate with other engineering disciplines? **Ultimately Needed!**

Collaboration

Team (Egypt & Kuwait)



+10
PhD/MSc/undergraduate
students



- Thanks to funders and Academic/Industrial partners

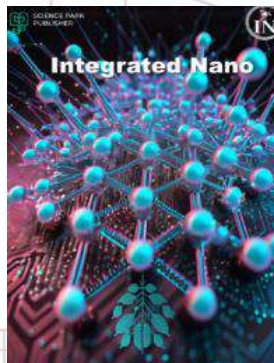


Collaboration

- Joint research proposals (KCST and Alexandria University)
 - AI/IoT/ML-embedded polymer industry, energy harvesting with embedded-electronics, and biomedical analysis
 - KFAS, TUBITAK, Erasmus, HORIZON, UKRI
- Conferences at KCST (Examples: S4IoT, ASTN, CERC), may host ULPAS in Kuwait in 2027?



- Integrated Nano (IN), Alexandria Engineering Journal (AEJ)

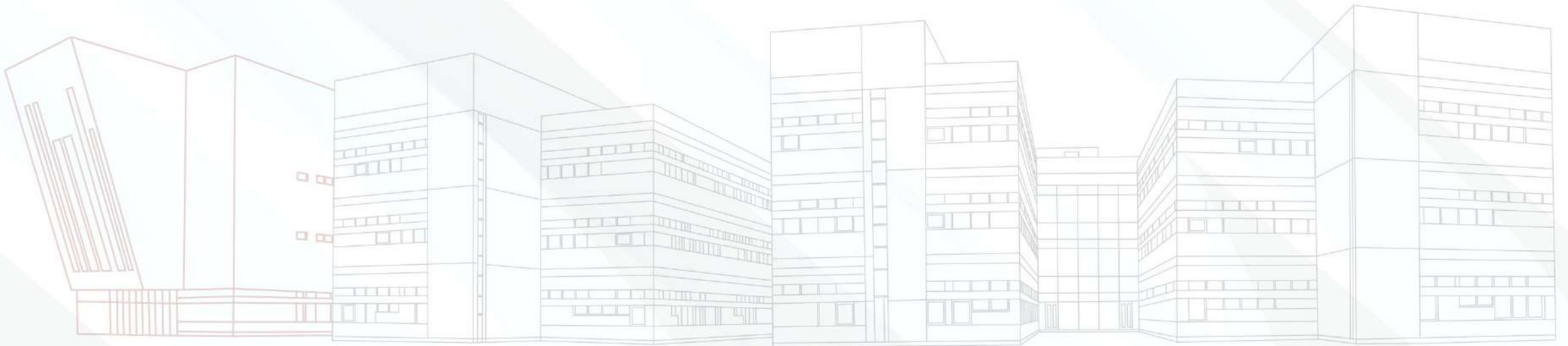


SDG alignment



Thank you!

Questions?





Effect of modified Hydrothermal Nanotitania on the viability of Streptococcus Pneumoniae.

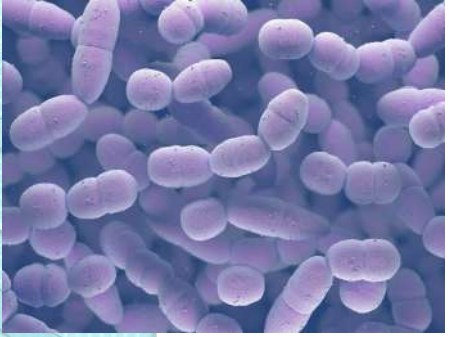
Ahmad Mukifza Harun (UMS)

Nor Farid Mohd Noor (UniSZA)

Mohamad Ezany Yusoff (USM)

Dalilah Nur Affendi (UITM)

Motivation



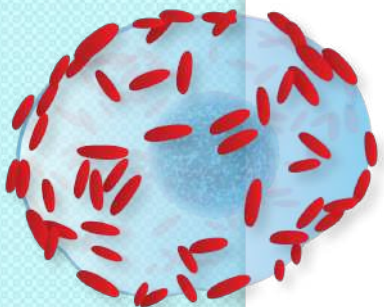
Bacteria and viruses increasingly threaten immunity through antibiotic resistance, rapid mutation but globally spread.

Streptococcus Pneumoniae is one of the world significant infectious disease, commonly found in the human lung and other human body areas such as vertebra, kidneys, and brain.

It is spread via tiny droplets released into the air via coughs and sneezes. The bacteria will settle in the host's lungs and multiply itself leading to active disease or dormant condition

Nanomaterials have shown its potential antimicrobial activity.

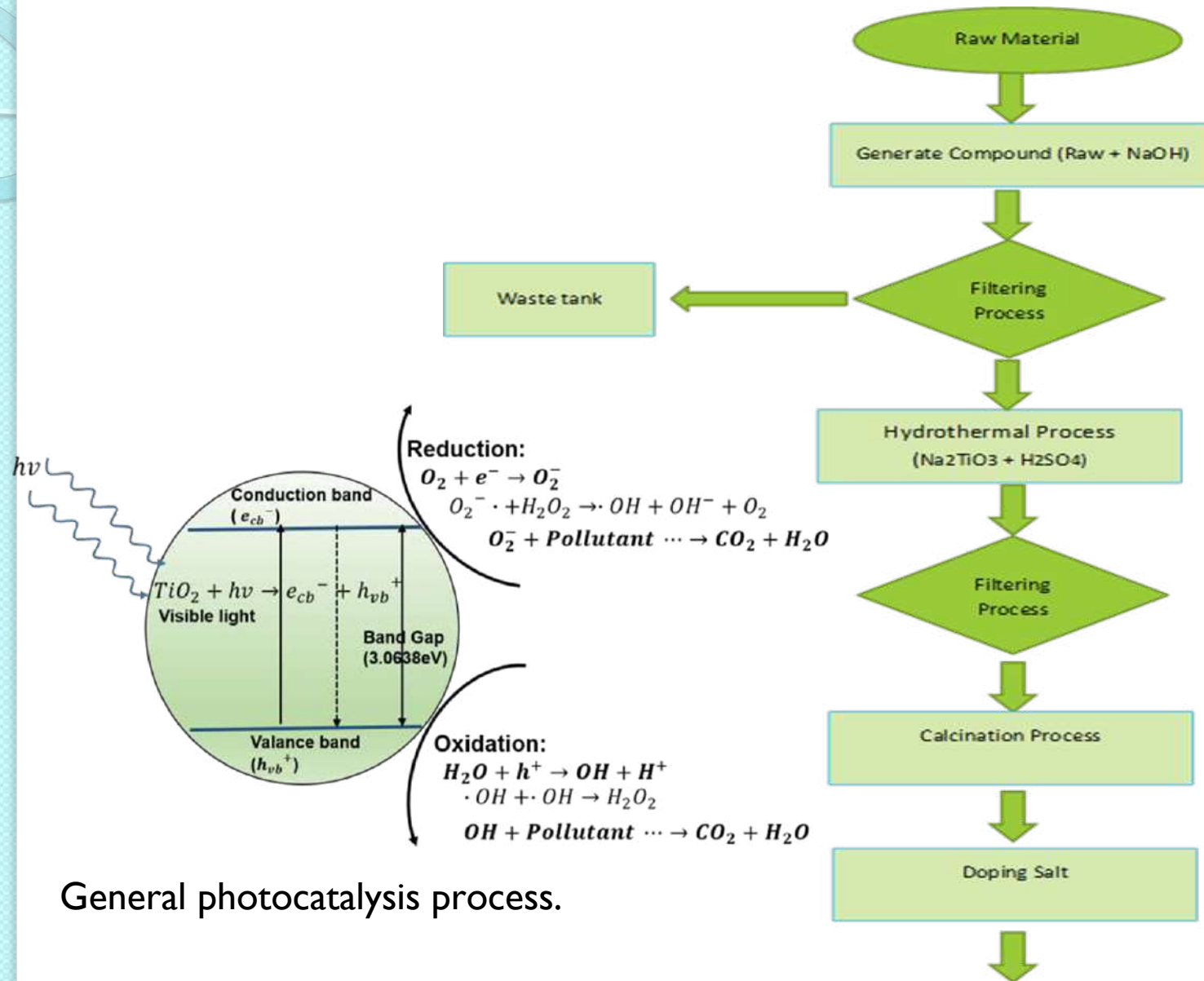
In this research, we focus our effort on nanotitania, as a potential substance in inhibiting the *Streptococcus Pneumoniae* growth.



Objectives

- In this study, *Streptococcus Pneumoniae* was tested with the modified hydrothermal nanotitania to test whether this substance able to inhibit the bacterial growth.
- Here, the modified hydrothermal nanotitania extract was mixed with *Streptococcus Pneumoniae* in the culture media preparation to determine whether it can resist the growth of the bacteria.

Past Studies



General photocatalysis process.



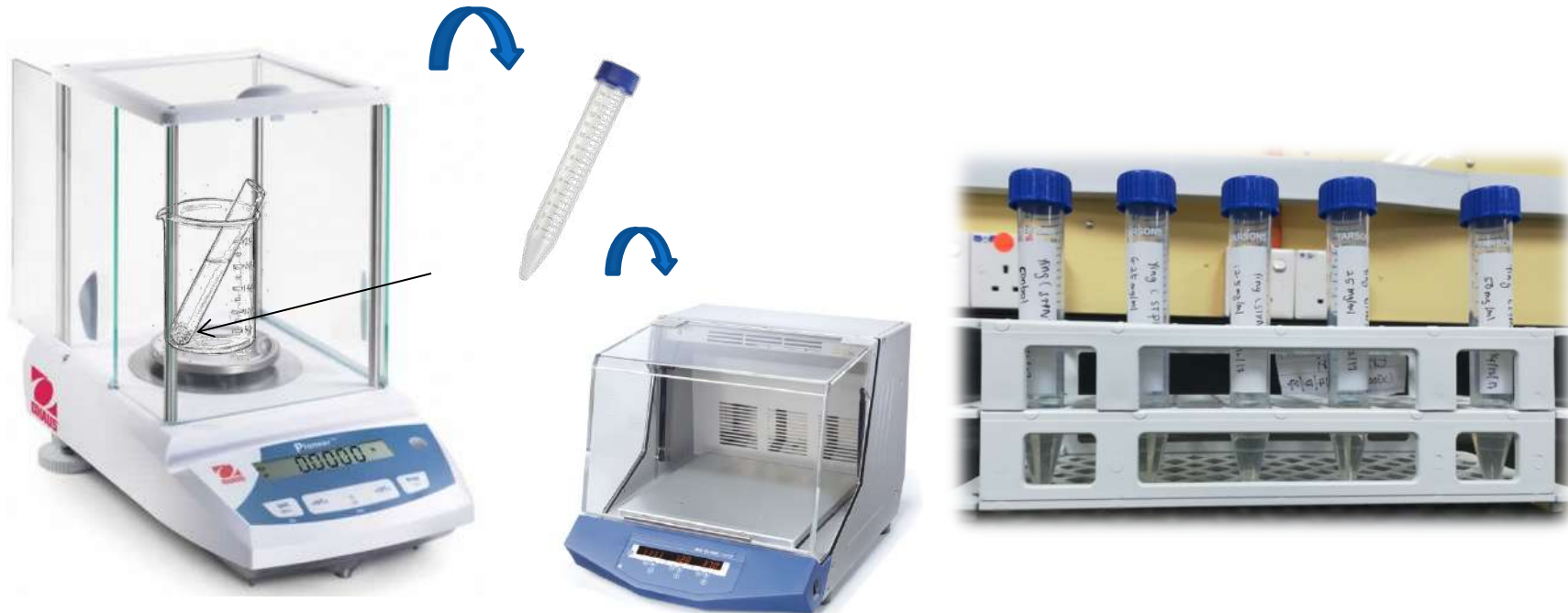
Methodology

1. **Bacteria and material preparation**

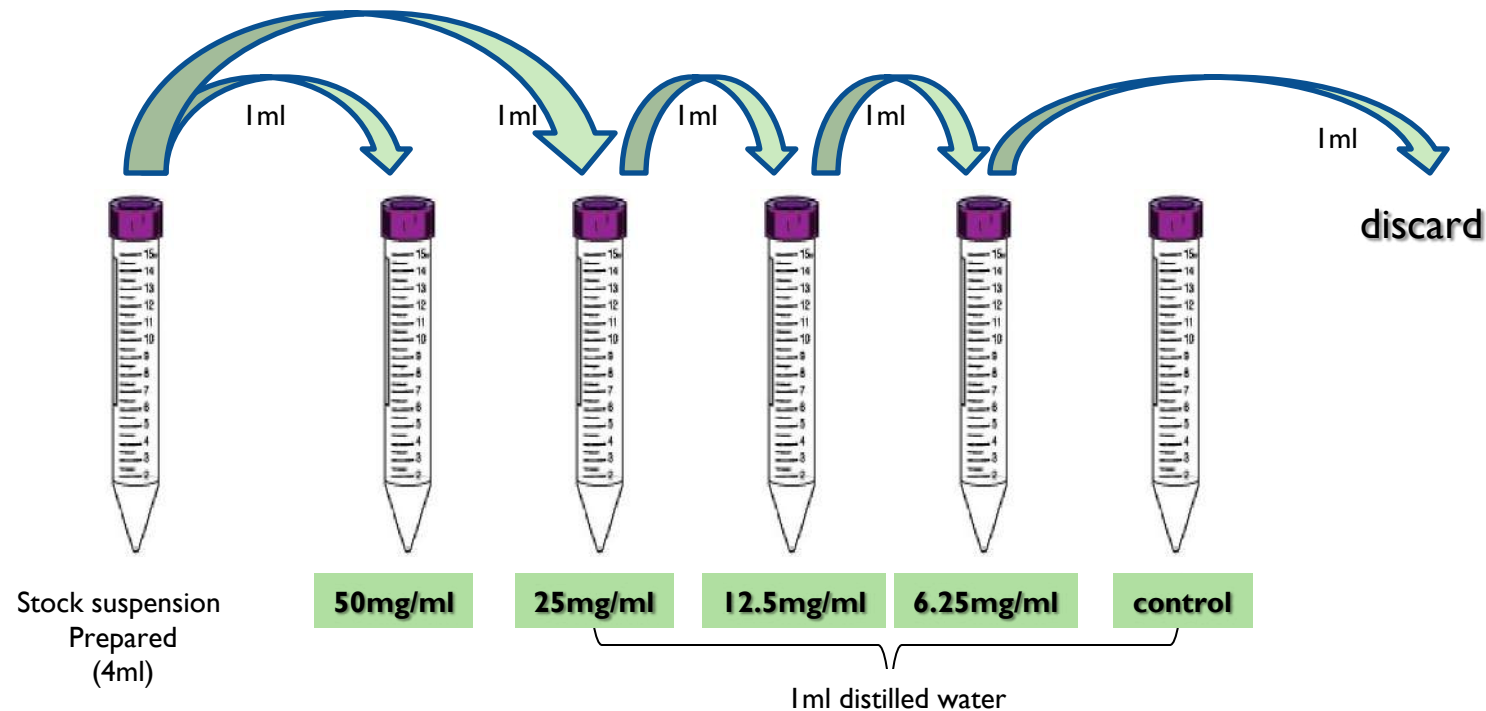
2. The bacteria were obtained from a stock culture from Hospital Universiti Sains Malaysia.
 - Nanotitania extract was obtained from University of Sabah Malaysia, which was prepared via modified hydrothermal method using abundance ilmenite from tin mining waste.

2. Evaluation of antibacterial activity

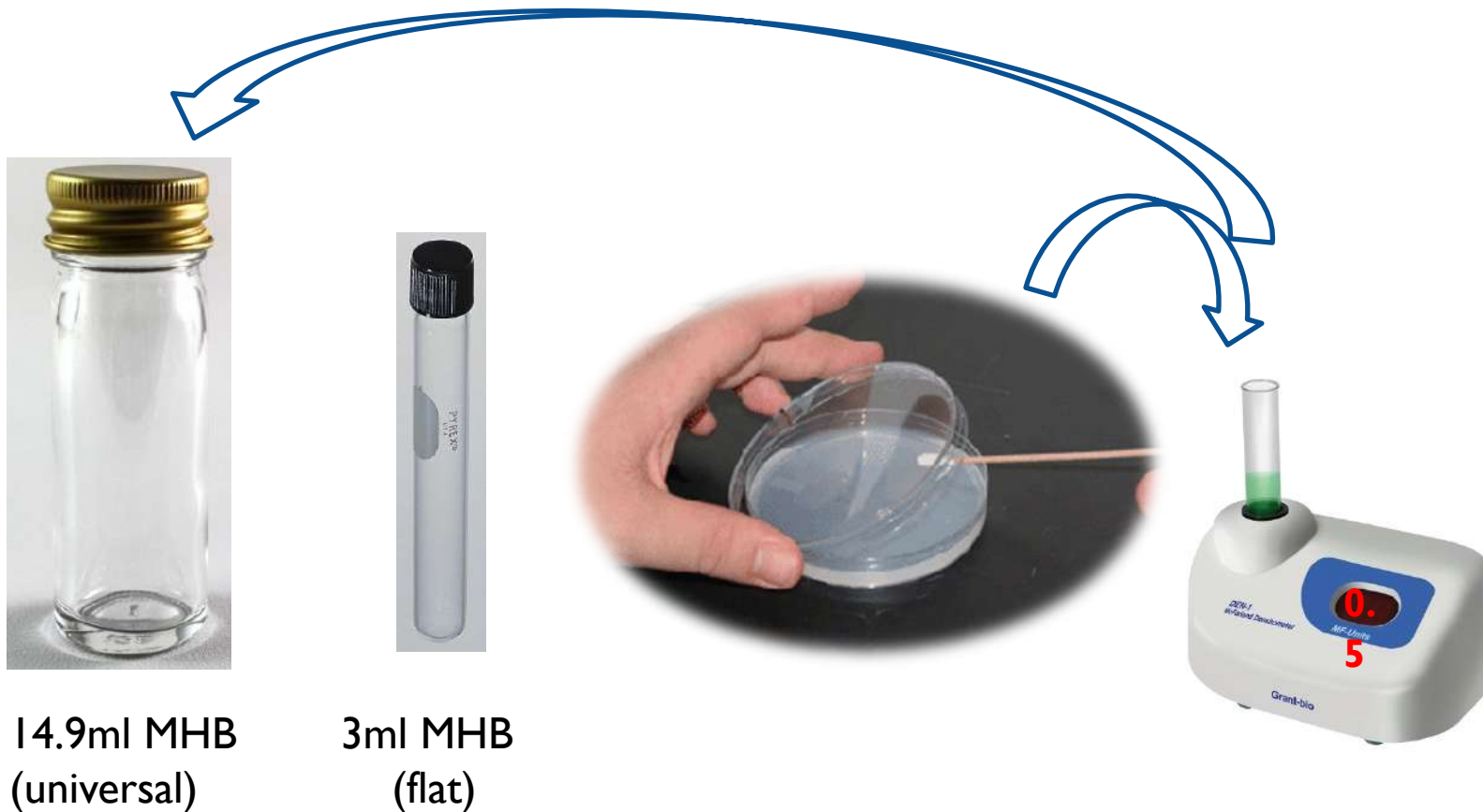
- Suspensions of 50mg/ml nanotitania extract with 1%, 3% and 5% silver were prepared by suspending 200mg of TiO_2 nanoparticles powder in 4ml distilled water and the solution was put in incubator shaker overnight to get the homogenous suspension.
- The stock suspension and five 15ml conical tubes were exposed to ultraviolet (UV) light for 30 minutes for sterilization. Another four conical tubes with 1ml of distilled water were prepared.



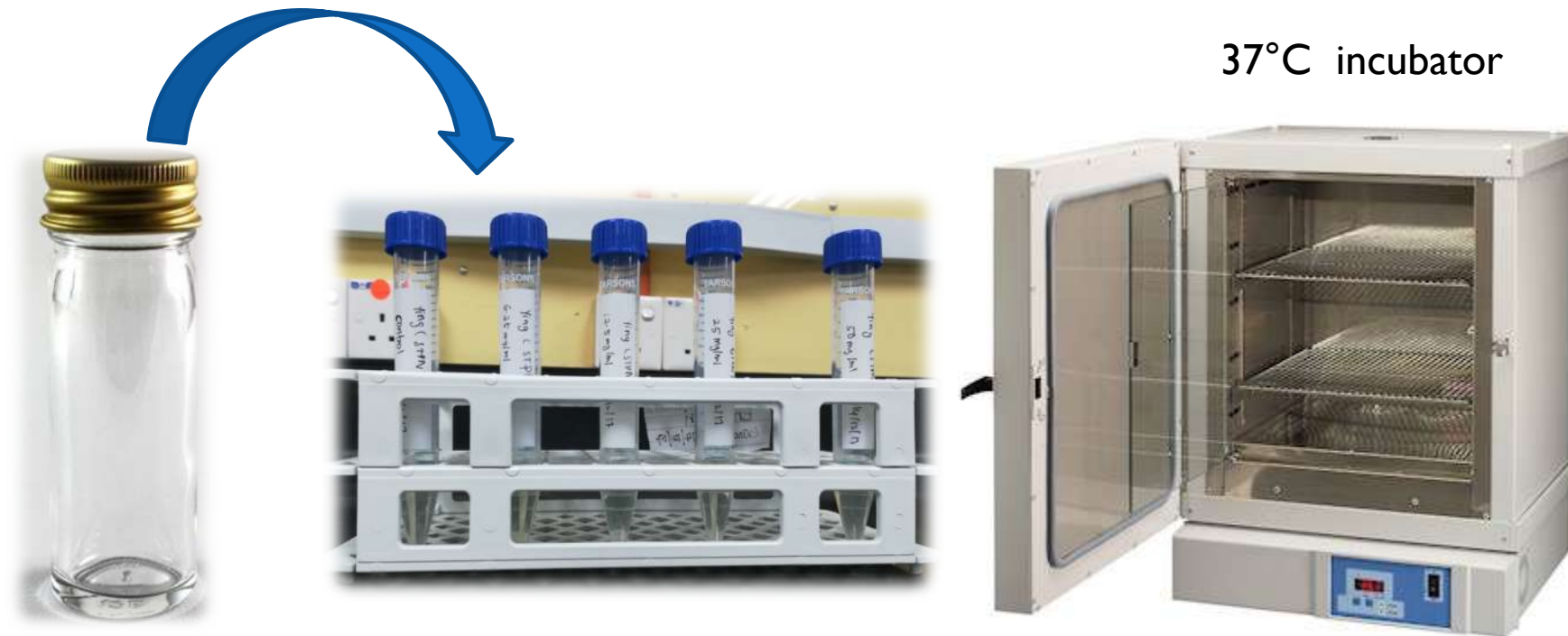
- In order to prepare other concentrations of suspension, 1ml of 50mg/ml suspension was then transferred into a prepared conical tube, then 1ml of the mixture was transferred into the subsequent conical tubes. By doing this macrodilutional method, 25mg/ml, 12.5mg/ml and 6.25mg/ml concentrations of the samples were produced.



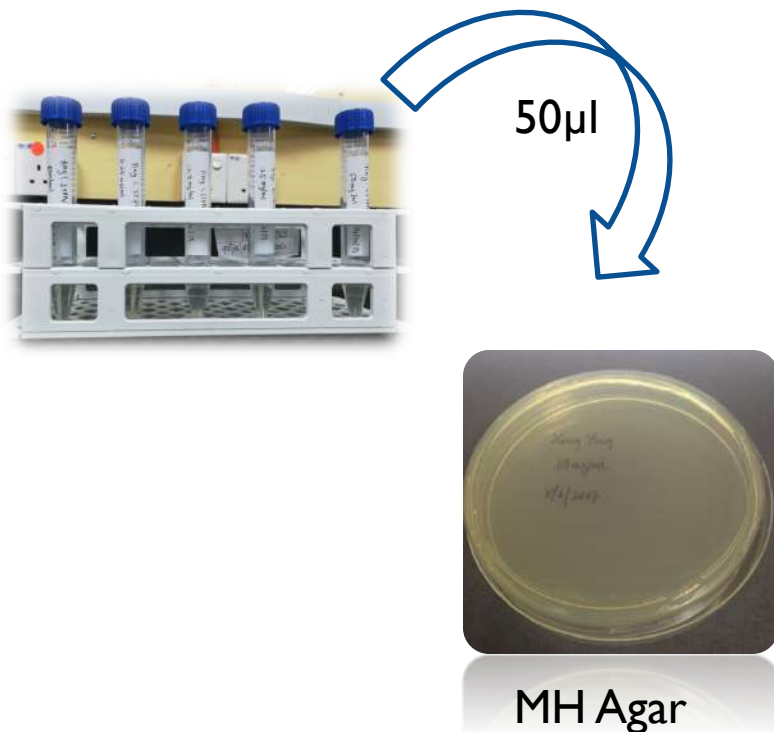
- 14.9ml Mueller Hinton Broth (MHB) was prepared in an universal bottle and another 3ml of MHB was prepared in a flat bottle. Bacteria were added into the flat bottle using cotton swab, which was equivalent to 0.5 MacFaland (1×10^8 bacteria). 0.1 ml of MHB was then transferred from flat bottle into universal bottle.



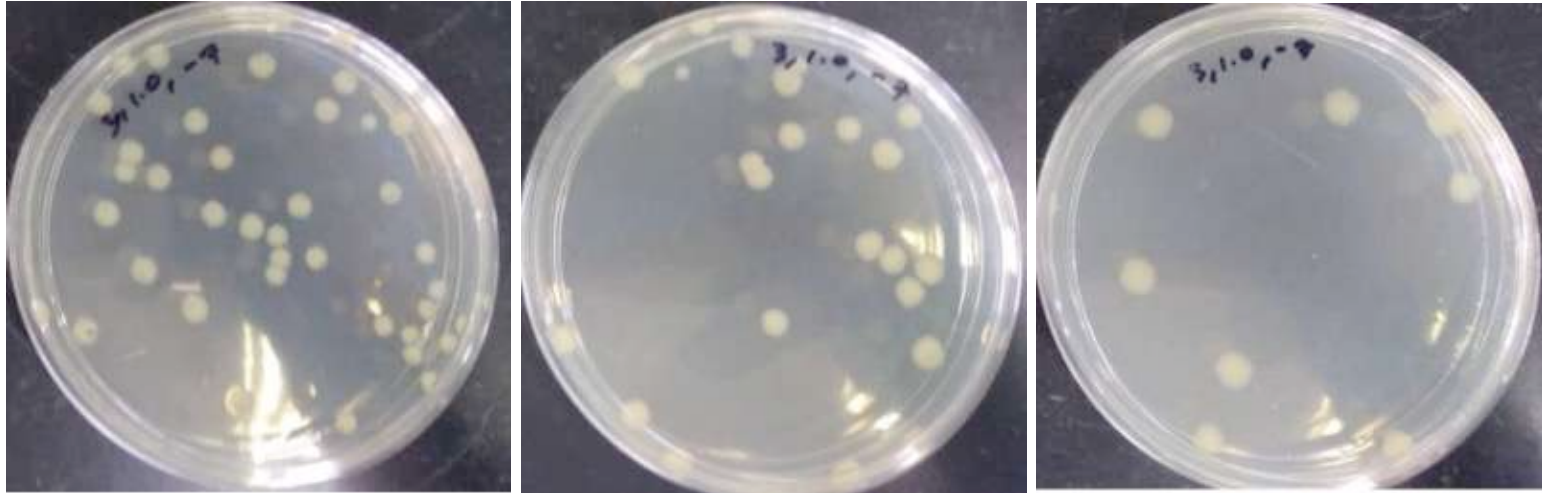
- 30μl of the Mueller Hinton Broth (MHB) from universal bottle was added into all five conical tubes. For control, the broth containing only bacteria without TiO_2 was used as a negative control.
- All these suspensions were placed in an incubator for 24 hours in temperature of 37°C.



- 50µl of suspension were spread on MH agar by using hockey stick and incubated in respective incubators at 37 °C for another 24 hours.
- The growth of bacteria was observed after 24 hours, 36 hours and 72 hours.



Results



PVA (in polymer solution) with nanotitania at 0 minutes and 60minuts.
Percentage of bacteria's count as in the table below

| Incubation time (min) | PVA (CFU%) | TiO ₂ (CFU%) | Nano anatase TiO ₂ (CFU%) |
|-----------------------|---------------|----------------------------|-----------------------------------------|
| 0 | 100 | 100 | 100 |
| 60 | 82.97 | 22.37 | 0.0018 |

The Growth of bacteria visualization (SEM)

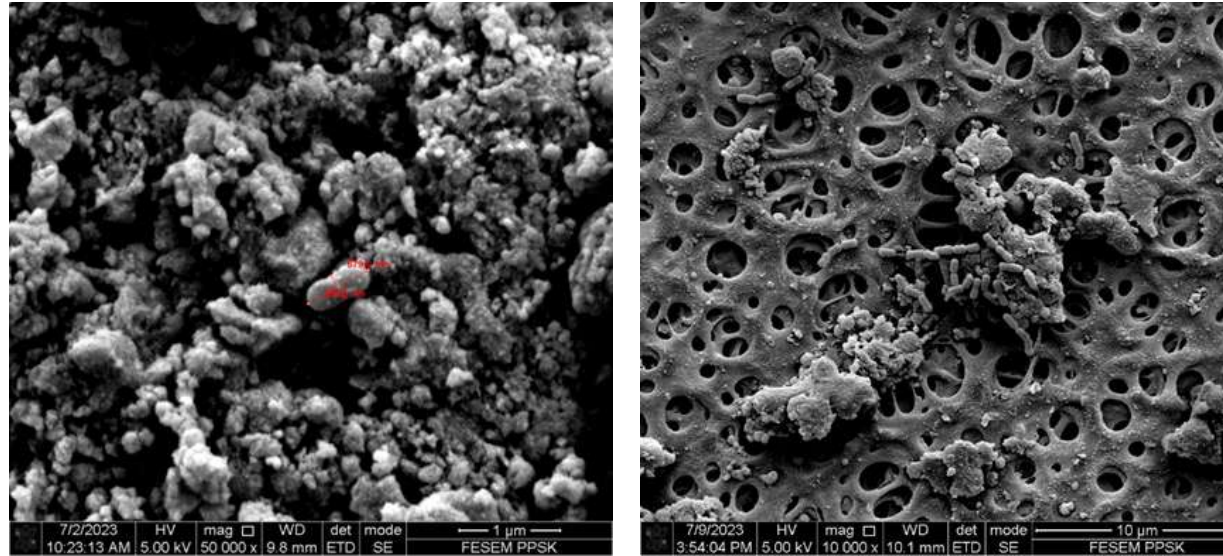


Figure above show SEM images of hydrothermal nanotitania extract after 24 hours of being exposed to *S. mutans* bacteria obtained from individuals with dental caries. The images were taken at a magnification of 10,000X. Figure illustrates the adhesion of a minimal number of *S. mutans* on the hydrothermal nanotitania extract with a magnification of 50,000X. In contrast, Figure F demonstrates the adherence of *S. mutans* on the cellulose as a positive control.

Discussions

- The capability of the nanotitania extract with or without silver has at least partly restored our confidence in the potential of antibacterial medications
- This material has been proven that it can be used as an antibacterial agent to control the infection especially in clinics or hospitals.

Scientific Finding

- The results showed the modified hydrothermal nanotitania extract was capable to be mentioned as having antibacterial properties up to 72 hours of post addition in the agar containing nanotitania extract. These results explain the potential of the modified hydrothermal nanotitania extract to be used for as antibacterial.

Conclusion

- The modified hydrothermal nanotitania extract inhibits the growth of *Streptococcus Pneumoniae*.
- The previous testing results on 6 types of respiratory bacteria and fungus (Candida Albicans) have shown inhibition the bacteria growth.
- The previous testing also includes cytotoxic and toxicology studies.



Way Forward

- Embedding nanotitania into nonwoven material



Fused Deposition Modeling (FDM) – methods, materials and applications for flexible fabric structures

Sabit Adanur

Professor, Department of Mechanical Engineering, Auburn University
Auburn, Alabama, USA

Ashok Sapkota

Graduate student, Auburn University

Shree Kaji Ghimire

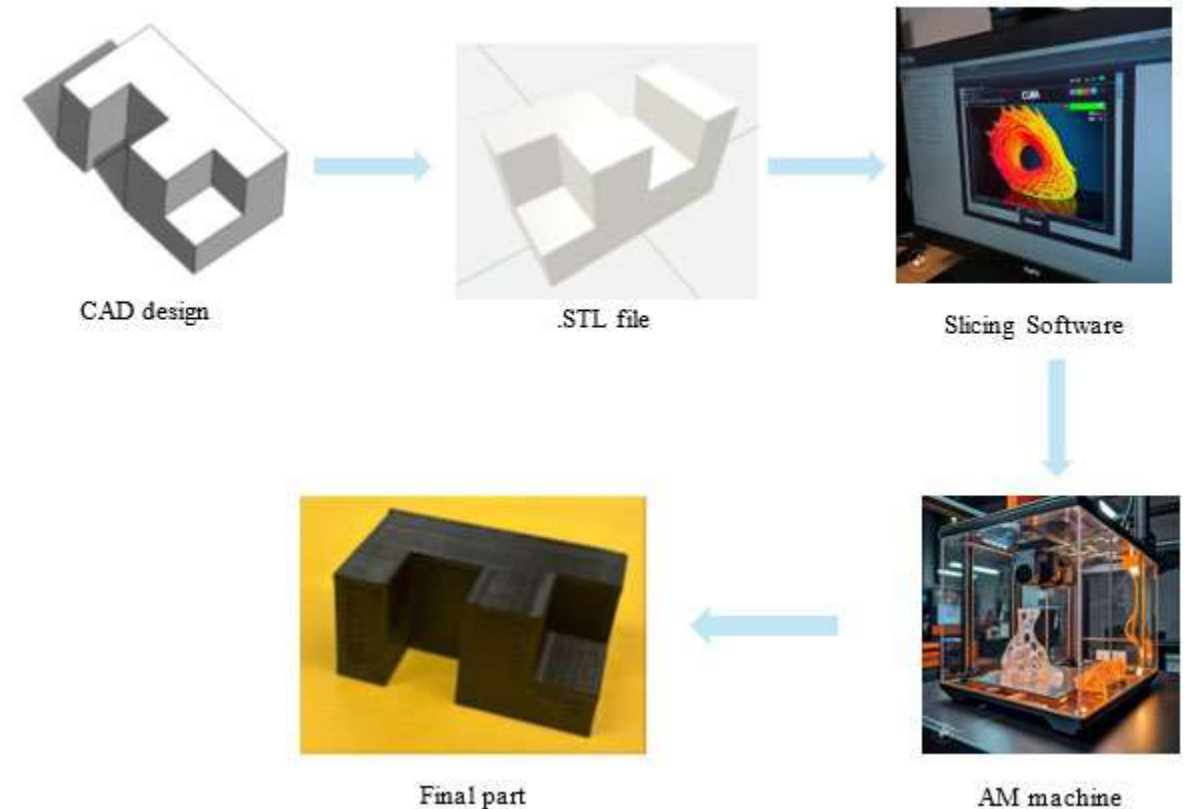
Graduate student, Auburn University



What is additive manufacturing?

How does it work?

- Additive manufacturing (AM) is layer-by-layer fabrication technology
- A CAD file is generated and .stl file is used to generate G-code (contains tool path)
- AM takes the G code and deposited material layer by layer based on G-code
- Simply a digital to physical conversion



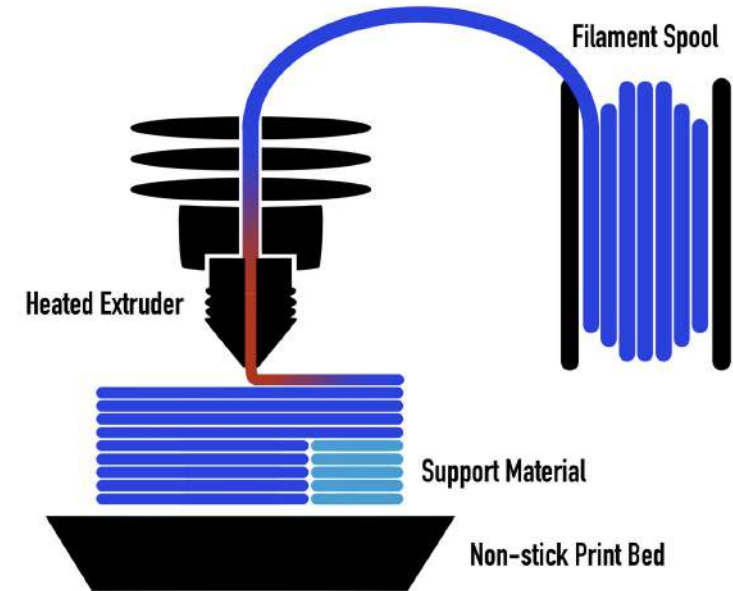
Fundamental additive manufacturing methods (for polymers)

Material extrusion method

Type of material processed – Thermoplastic polymer

Key characteristics

- Selective deposition of molten material through nozzle
- Economic and easy to process
- Higher surface roughness
- Low speed and accuracy
- Material anisotropy
- Suitable for multi-material processing



Source:

https://dozuki.umd.edu/Wiki/Introduction_to_Fused_Deposition_Modeling_%28FDM%29

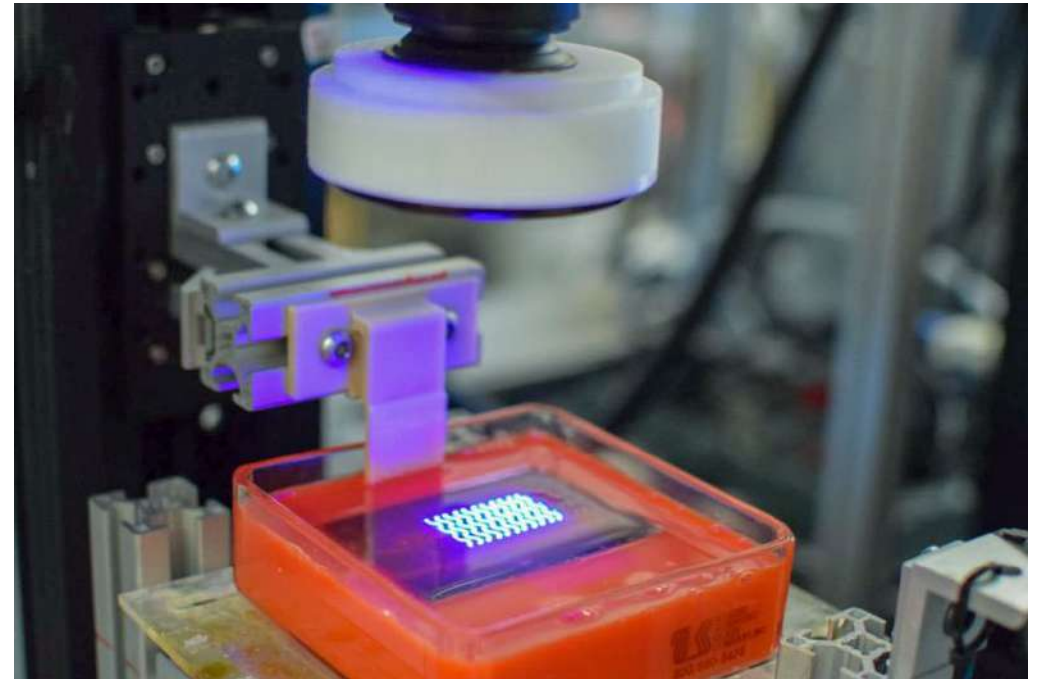
Fundamental additive manufacturing methods (for polymers)

Vat Photopolymerization

Type of material processed – Polymer

Key characteristics

- Liquid monomer or oligomer selectively cured using light source
- Has tendency to shrinkage after curing
- Degree of shrinkage depends on nature of the material processed
- Transfer agents can be mixed to reduce brittleness



Source: <https://dreams.mii.vt.edu/research/novel-additive-manufacturing-processes/vat-photopolymerization.html>

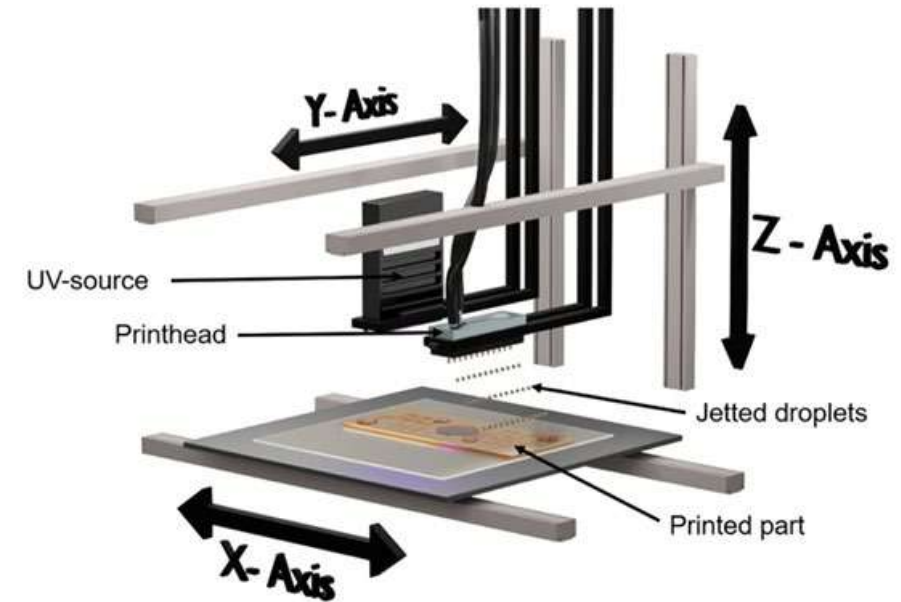
Fundamental additive manufacturing methods (for polymers)

Material jetting

Type of material processed – Polymer

Key characteristics

- Combination of photopolymerization and 3D printing
- Selectively deposited liquid material through nozzle is cured using UV light
- Very thin layer thickness which results excellent surface finish
- No post processing and curing needed



Fundamental additive manufacturing methods (for polymers)

Sheet lamination

Type of material processed – Polymer and metals

Key characteristics

- In this process, sheets of materials are bonded together to form a 3-dimensional object
- It is a solid based AM method where a final product is achieved with solid geometries
- Sheet joining is done by either bonding, ultrasonic welding or brazing method
- Each sheet, which acts like individual layer, are cut in desired shape to give final 3D shape
- Post processing is required for better surface and mechanical quality

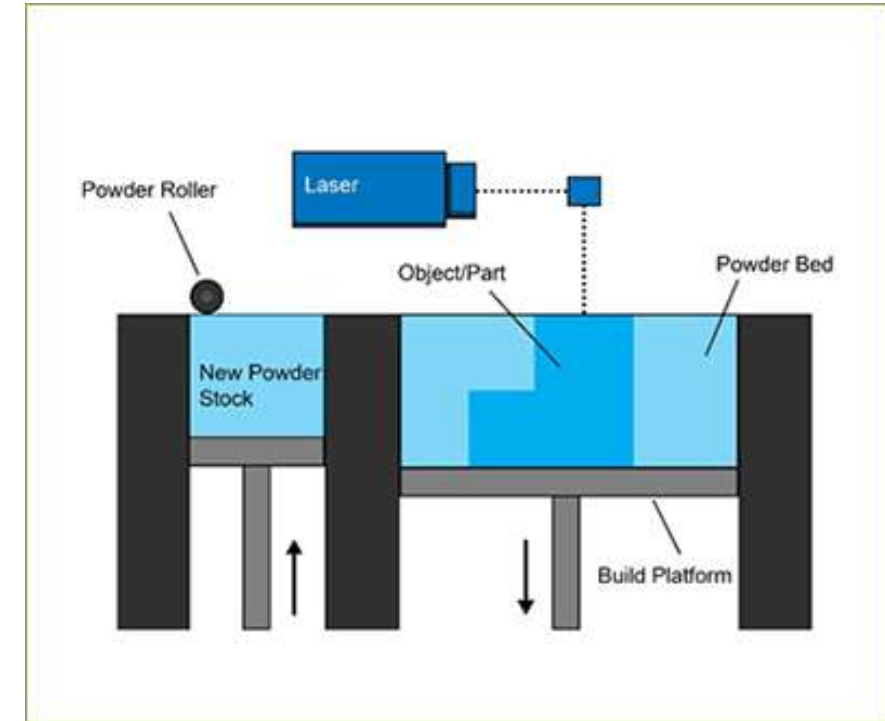
Fundamental additive manufacturing methods (for polymers)

Powder bed fusion

Type of material processed – Polymer, ceramics and metals

Key characteristics

- Fine particles of materials in layer-by-layer arrangement are fused together with heat source
- Heat source may be selected from electron beam gun or laser beam or UV light source
- Suitable for processing complex geometries
- Process parameters influence the properties of the final product



Source:

<https://www.lboro.ac.uk/research/amrg/about/the7categoriesofadditivemanufacturing/powderbedfusion/>

Fused deposition modeling (FDM)

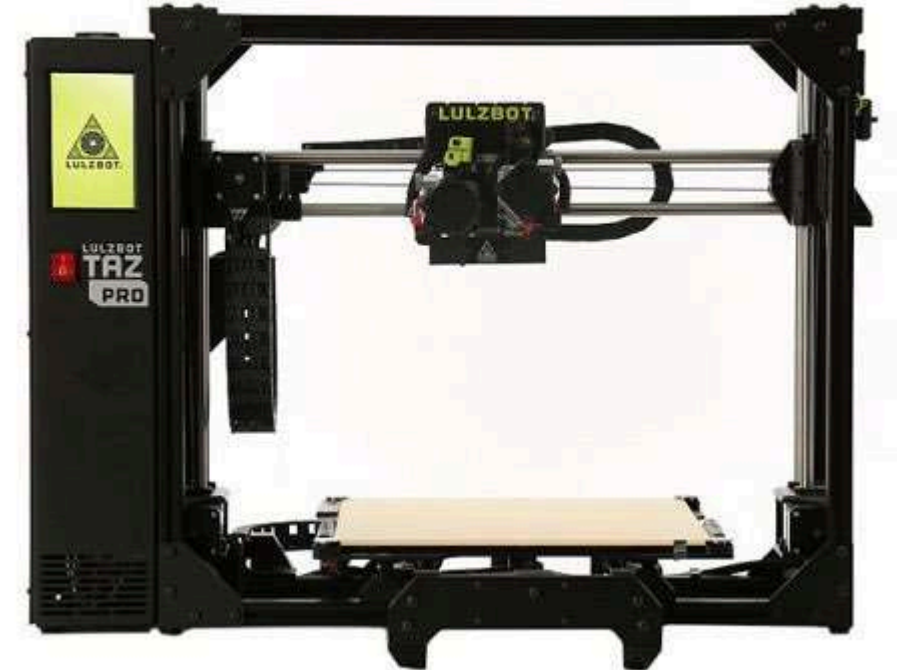
Definition:

FDM, also known as Fused Filament Fabrication (FFF), is a hot-melt extrusion process for additive manufacturing.

Working Principle: Layer-by-layer deposition of molten polymer filament that solidifies into a solid object.

Common materials:

- PLA
- ABS
- PEEK
- TPE
- PC
- PETG



Dual extruder FDM machine

Fused deposition modeling (FDM)

Key consideration:

- Common filament diameters acceptable to machine is either 1.75 mm or 2.85 mm
- Diameter does not affect part properties but may impact feed quality and production time
- Polymer's molecular weight, crystallinity, and intermolecular forces affect printed part properties
- Not all polymers are FDM-compatible



MakerBot MP06572 PLA Filament Spool

Fused deposition modeling (FDM) – Advantages

| Advantage | Description |
|-------------------------------------------------|---------------------------------------------------------------------------|
| Ease of Operation | Simple setup and user-friendly interface; minimal training required |
| Low Cost | Economical hardware and filament materials |
| Low Material Waste | Efficient material usage with minimal scrap or excess |
| Lower Process Toxicity | Safer to operate, especially with biopolymers like PLA |
| Flexible Design Capabilities | Can fabricate complex geometries and customized internal structures |
| Mass Customization & Personalization | Ideal for producing one-off, tailor-made items like prosthetics and shoes |
| Wide Material Compatibility | Supports many thermoplastics (PLA, ABS, PETG, etc.) |
| Functional Applications | Increasing use in final-use parts due to improved mechanical performance |

Fused deposition modeling (FDM) – Limitations

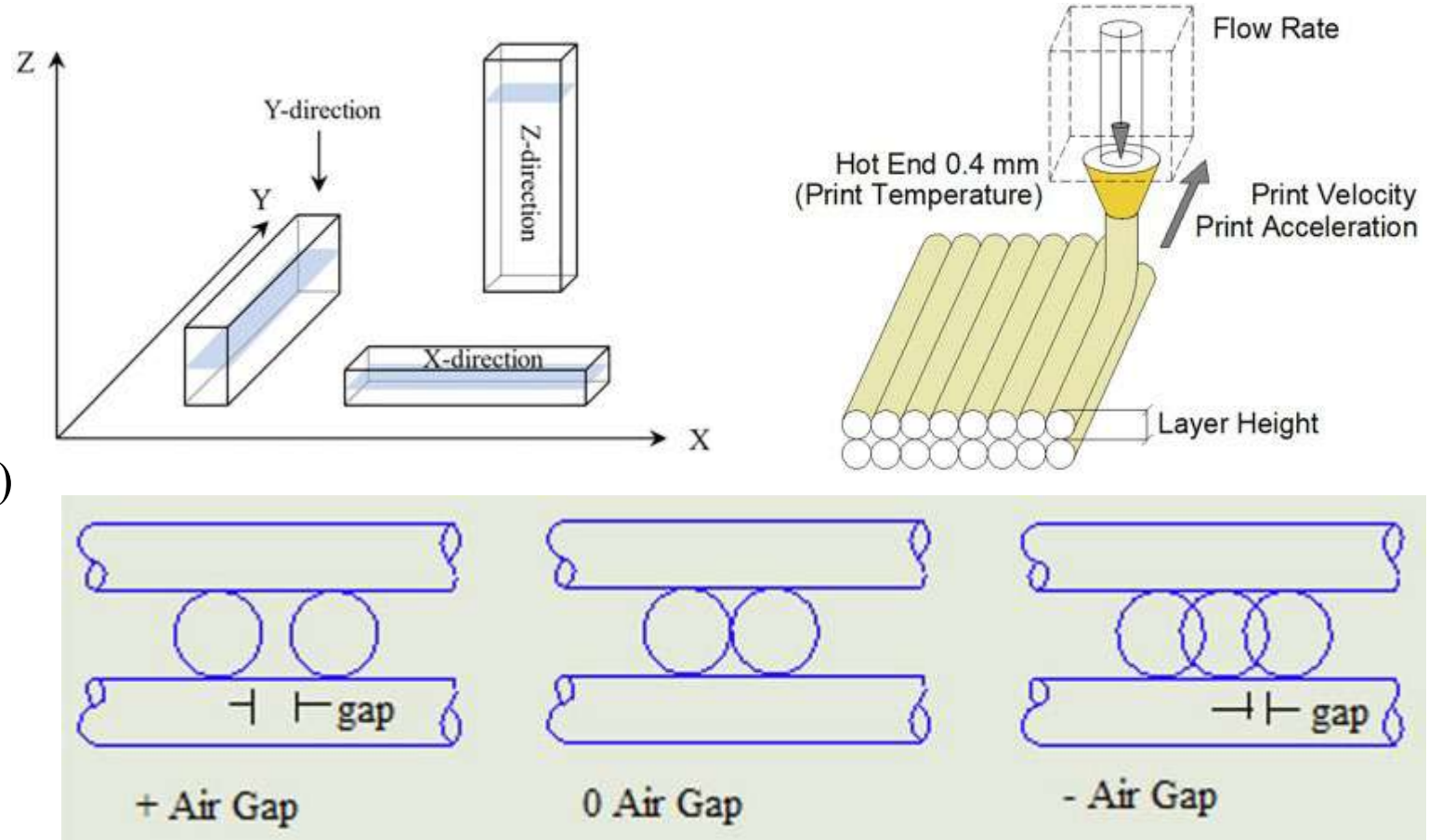
| Limitation | Description |
|---------------------------------|------------------------------------------------------------------------------------|
| Low Printing Speed | FDM is generally slower compared to other AM technologies. |
| Limited Surface Quality | Produces visible layer lines and requires post-processing for smooth finish. |
| Compromised Mechanical Strength | Interlayer bonding is weak, reducing tensile strength and durability. |
| Anisotropic Properties | Mechanical properties vary depending on the print orientation. |
| Limited Material Compatibility | Not all polymers can be processed with FDM due to thermal or chemical limitations. |
| Dimensional Accuracy Issues | Part shrinkage and warping can affect accuracy, especially with large parts. |
| Small Build Volume | Standard machines are limited in the size of parts they can produce. |
| Void Formation | Layer-by-layer deposition can leave gaps, affecting strength and density. |

FDM Vs. Injection molding

| Polymer type | Injection molding | | Fused deposition modeling | |
|----------------|------------------------|-----------------------|---------------------------|-----------------------|
| | Tensile strength (MPa) | Elastic modulus (GPa) | Tensile strength (MPa) | Elastic modulus (GPa) |
| ABS | 40 | 2.3 | 27-30 | 1.7-1.8 |
| PLA | 44-59 | 3.7-4.2 | 52-54 | 3.3 |
| Polypropylene | 40 | 1.9 | 28-32 | 1-1.05 |
| Polyamide 12 | 40 | 1.3 | 35 | 1.5 |
| Polyamide 6 | 70 | 1.8 | 36 | 2.4 |
| PEEK | 100 | 4 | 32-57 | 1.2 |
| Polyetherimide | 130 | 8.7 | 75-110 | 2.6-2.9 |
| Polycarbonate | 70 | 2.6 | 36-54.7 | 2.1-2.4 |
| HIPS | 24.1 | 1.65 | 22 | 1.55 |
| TPU | 17-65 | 0.15-2.3 | 26.7 | very small |
| PMMA | 78 | 3.3 | 2.91 | 0.223 |
| PHA | 10-39 | 0.32-3.8 | 17 | 0.35 |

Major FDM process parameters

- Layer thickness
- Extrusion temperature
- Built orientation
- Print speed
- Infill density (Infill percentage)
- Print orientation
- Infill geometry
- Air gap
- Nozzle diameter



Effect of FDM process parameters on part properties – Surface quality

Layer thickness

- Smaller layer thickness improves surface finish by allowing uniform polymer flow, better interlayer bonding, and fewer micro-voids.
- Larger layer thickness increases surface roughness due to visible layer lines, weaker bonding, and potential delamination or shrinkage.
- Thicker layers cause residual stress from temperature variation, leading to surface distortion.
- Fewer layers at higher thickness reduce detail resolution, especially on curves and angled surfaces, making the finish rougher

Effect of FDM process parameters on part properties – Surface quality

Infill density

- Higher infill density (near 100%) → Smoother surface (less internal voids, better support).
- Lower infill density (e.g., 20-50%) → Rougher surface (potential sagging/warping).
- 100% infill → Best finish (no pattern influence, fully solid structure).
- Beyond 100% density (negative air gap) → Risk of over-extrusion & roughness.

Infill pattern

- Grid/Honeycomb patterns → Better support, smoother surfaces at lower densities.
- Rectilinear/Gyroid patterns → May cause visible infill lines/textures.
- Pattern impact diminishes at high infill densities ($\geq 80\%$).
- Optimal balance: 60-80% density + supportive pattern (e.g., honeycomb) for strength & smoothness.



Effect of FDM process parameters on part properties – Surface quality

Extrusion temperature

- At higher temperature, material gets deposited in elliptical shape instead of circular cross section due to reduced viscosity
- The elliptical shaped deposition reduces the depth of the gap formed between the adjacent layers. This results better surface properties



Raster Gap

Negative raster gap (some degree of overlapping between adjacent layers) also enhances surface quality



Effect of FDM process parameters on part strength

Layer thickness

- Thinner layer results better material distribution, reduces internal voids and enhances interlayer bonding
- For shear loading, thick layer reduces interlayer sliding
- Selection of layer height depends on application and load scenario

Thinner Layers (0.1-0.2mm)

- ✓ Higher tensile strength
- ✓ Better surface finish
- ✗ Longer print time

Thicker Layers (0.3mm+)

- ✓ Faster print time
- ✓ Higher compressive strength
- ✗ Weaker impact resistance



Effect of FDM process parameters on part strength

Infill density

- 100 % density is recommended for best strength
- Lower density will have internal gaps and voids

Print speed

Medium print speed is recommended for best quality

At high speed, the layers will not get deposited accurately at desired location

However, extremely low speed is also not recommended. In this case previous layer already cools down. Hence, next layer can not form strong interlayer bonding

Process parameter optimization for FDM

Key Observations:

- Process parameters significantly affect mechanical properties of FDM parts.
- Optimized parameters are material-specific. The outcome varies material to material

Examples:

- Polypropylene (PP):
 - Layer thickness: 0.2 mm → Tensile strength: 20 MPa
- ABS:
 - Layer thickness: 0.1 mm → Tensile strength: 28.1 Mpa
 - Layer thickness: 0.075 mm → Tensile strength: 27.5 MPa

Inconsistencies may arise due to:

- Different FDM machines
- Influence of unreported parameters

Source: 49 76 112

Reference: Carnerio et al. 2015, Nidagundi et al. 2015, Shubham et al. 2016



Process parameter optimization for FDM

Challenges:

- Inconsistent optimum parameters across studies
- Limited research on extrusion temperature, raster width, infill density, air gap
- Rarely studied interactive effects of parameters

Research Gaps:

- Need for multi-parameter studies
- Evaluate machine-specific influence
- Important for new FDM-based structures (e.g., textiles)

Conclusion:

Optimized process parameters are crucial but must be tailored to both material and machine. Broader, more integrated studies are essential.

Filament materials for FDM

| Material | Source | Advantage | Disadvantage |
|----------|-------------------------|-----------------------------------------------------------------------------|-------------------------------------------------------------------------|
| ABS | Petroleum | Impact resistant, tough, and inexpensive | Possibility of warping, chance of unpleasant gas byproduct |
| PLA | Plant starch | Warp resistant, biodegradable, inexpensive | Compromised mechanical properties, brittle, high roughness |
| PC | Bisphenol | Strong, flexible | High print temperature, moisture absorption |
| PEEK | Bisphenolate | Rigid, strong, light weight, heat, and chemical resistant | High print temperature, expensive and prone to warp |
| PEI | Bisphenol-A dianhydride | Heat resistant, rigid, and strong | High print temperature and difficult to print, expensive, prone to warp |
| Nylon | Crude oil | Enhanced mechanical properties, inexpensive, wear resistant, heat resistant | Prone to warp, high printing temperature |
| HIPS | Petroleum | Dissolvability, impact resistant, biodegradable | Prone to warp, heated build platform needed |

Filament materials for FDM – Price and properties

| Filament type | Price range (USD per Kg) (As of 2024) | Melt temperature- T_m (°C) | Glass transition temperature- T_g (°C) | Mechanical properties |
|---------------------------------------------|------------------------------------------|---------------------------------|---------------------------------------------|----------------------------------------------------------------------------------------------------------------------------------------|
| Acrylonitrile Butadiene Styrene (ABS) | 16-30 | 230-270 | 105-110 | σ =36-72 MPa ε =3-20 % E =0.1-2.4 GPa ρ =1.01-1.2 g/cm ³ Flexural Strength = 2.25 GPa |
| Polylactic Acid (PLA) | 12-55 | 146.4-180 | 45-63.4 | σ =21-60 MPa ε =2 - 9.3 % E =3.4 – 7.0 GPa ρ =1.21-1.25 g/cm ³ |
| Thermoplastic Polyurethane (TPU) | 23.75-180 | 210-215 | -33 | σ =40-50 MPa ε =400-550 % ρ =1.10-1.3 g/cm ³ |

Filament materials for FDM – Price and properties

| Filament type | Price range (USD per Kg) (As of 2024) | Melt temperature- T_m (°C) | Glass transition temperature- T_g (°C) | Mechanical properties |
|------------------------------------------------|------------------------------------------|---------------------------------|---------------------------------------------|----------------------------------------------------------------------------------------------------------------------------------------------------------------------------------|
| Polycarbonate (PC) | 23-73.42 | 280-300 | 147 | σ =50-54 MPa ϵ =20% E=1.9-2.6 GPa |
| Polyether Ether Ketone (PEEK) | 595-740 | 306-350 | 153.1-165 | σ =32.4-100 MPa E=380-600 MPa ϵ =8-15 % Elastic limit=72 MPa Compressive modulus=3.8 GPa Bending Modulus = 4 GPa ρ =1.3 g/cm ³ |
| Polyethylene Terephthalate Glycol (PETG) | 11.04-57 | 200-230 | 76-79 | σ =26 MPa E=2150 MPa ϵ =70 % ρ =1.27 g/cm ³ |

Composite filaments for enhanced properties

- Natural fibers (e.g., jute, flax, hemp) and synthetic (e.g., carbon, glass, Kevlar) fibers enhance strength, stiffness, and durability when mixed with pure polymer
- Metal particles (iron, titanium, etc.) improve mechanical performance but may affect processability
- Polymer blends (e.g., PLA/TPU, ABS/PC) offer balanced properties: strength, flexibility, surface finish
- Critical factors: particle size, fiber shape, orientation, and volume fraction affect printability
- Challenges include nozzle clogging and filament breakage, especially with particulates



Nylon Carbon fiber filament by MatterHackers
(<https://www.matterhackers.com/>)

Composite filaments for enhanced properties

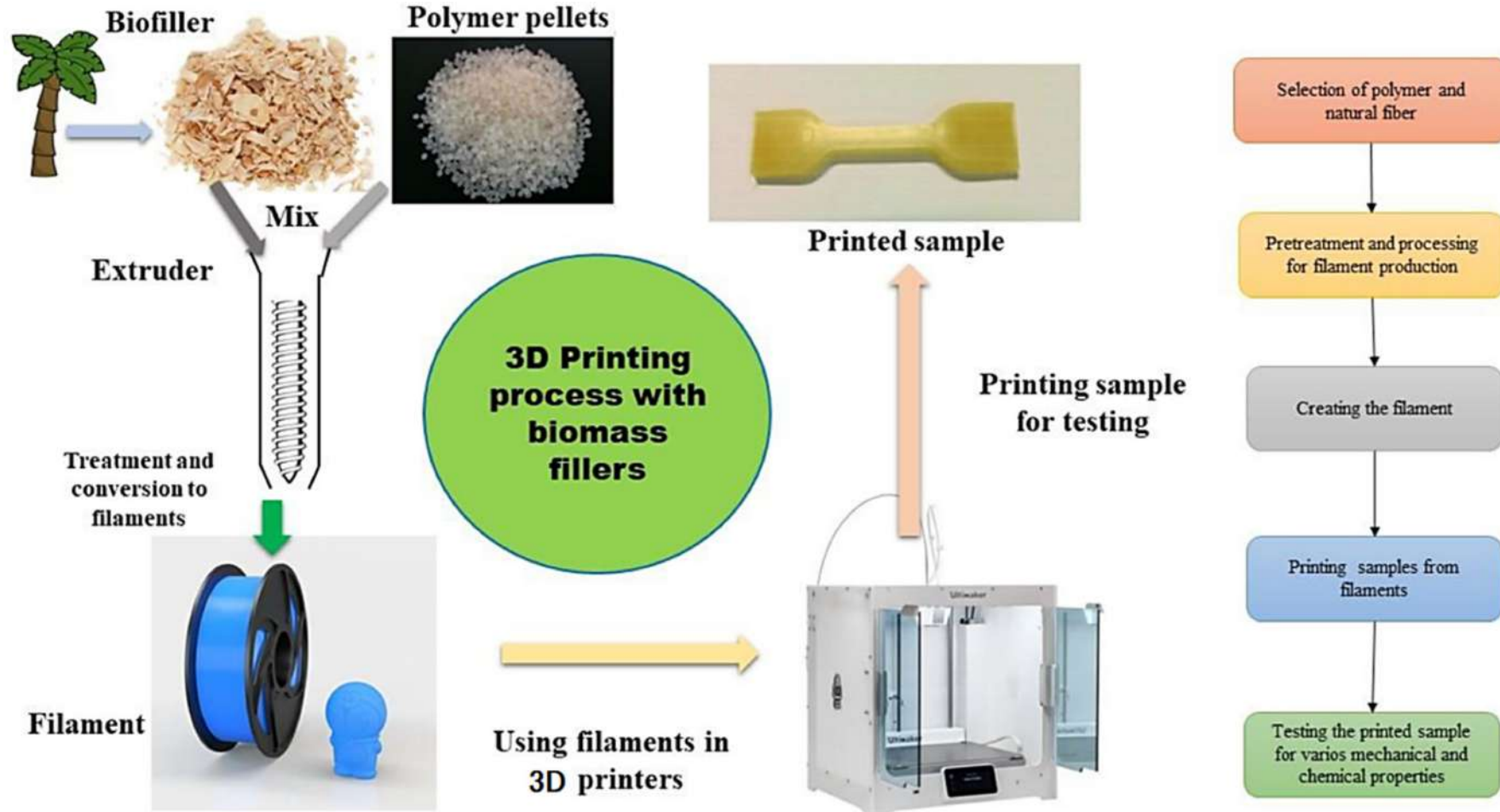
Three main additives

- particulates (rigidity), fibers (tensile strength), blends (balanced properties)

Few examples

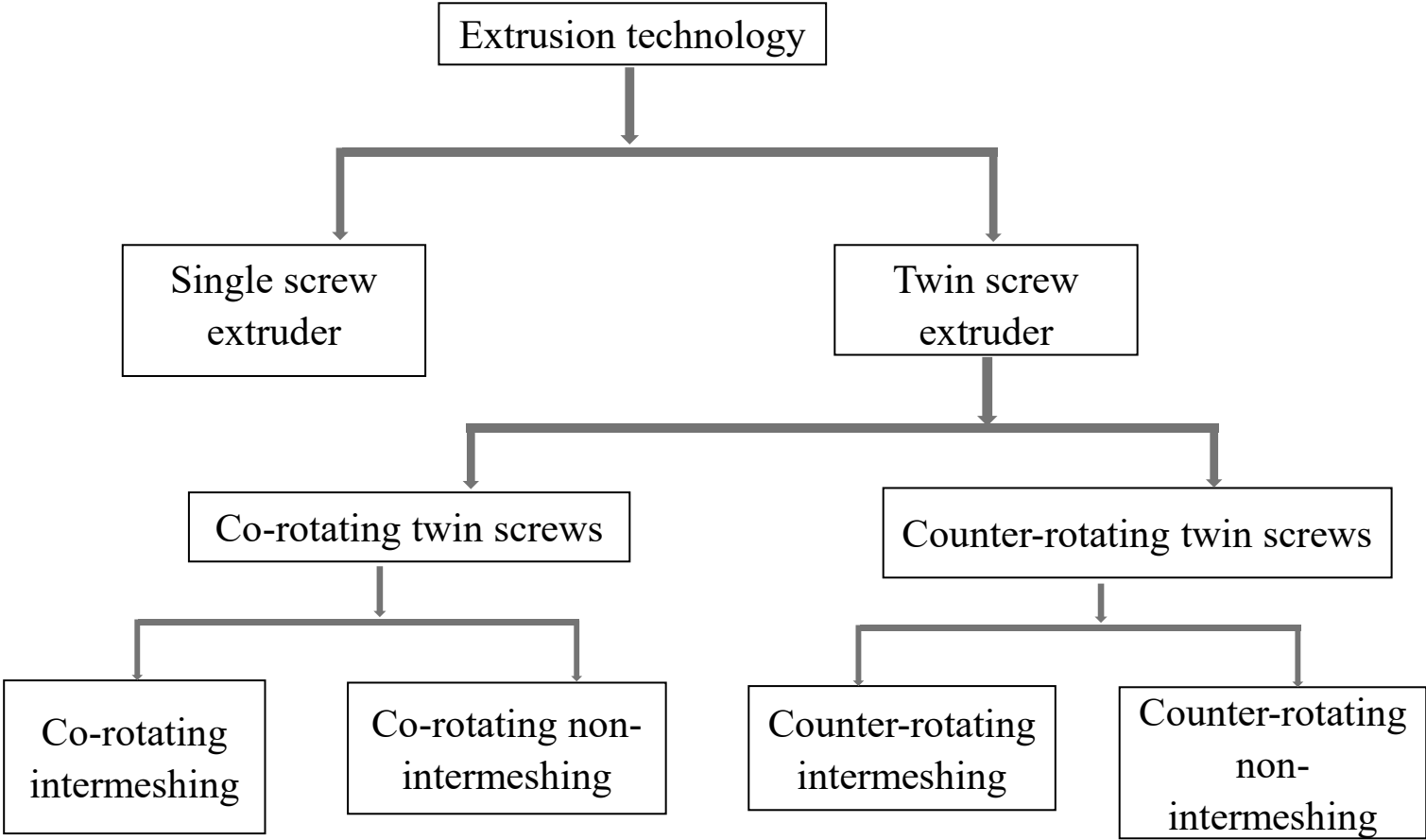
- PLA + cocoa shell: Modulus increased (19 → 27 MPa), but elongation dropped
- PLA/TPU blends: Elongation rose dramatically with higher TPU content (up to 729%)
- PC/ABS blends: Strength improved (39 → 46 MPa with higher PC content)
- PLA/TPU blends are promising for flexible, fabric-like FDM applications

Composite filaments for enhanced properties



Source Ahmed et al. 2020, <https://doi.org/10.3390/ma13184065>

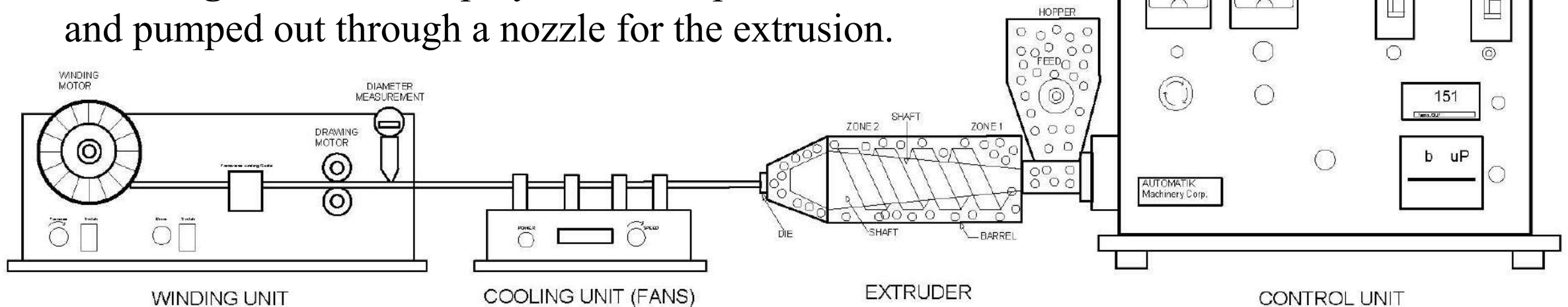
Classification of extrusion techniques to produce filaments for FDM method.



Single Screw Extrusion

- Three major sections in the screw:
Feed section, Transition section and Metering section.
- Feed section:** closest to the hopper & responsible for providing a controlled amount of feedstock into the screw.
- Transition/ mixing section:** an intermediate section where the feedstock material is mixed, melted and pumped forward.
- Metering zone:** Molten polymer is compressed and pumped out through a nozzle for the extrusion.

Note: Scale of different units and extruder unit in the figure are not in exact ratio



Single Screw Extrusion

Dimensions of screw for single screw extruder in terms of screw diameter (D)

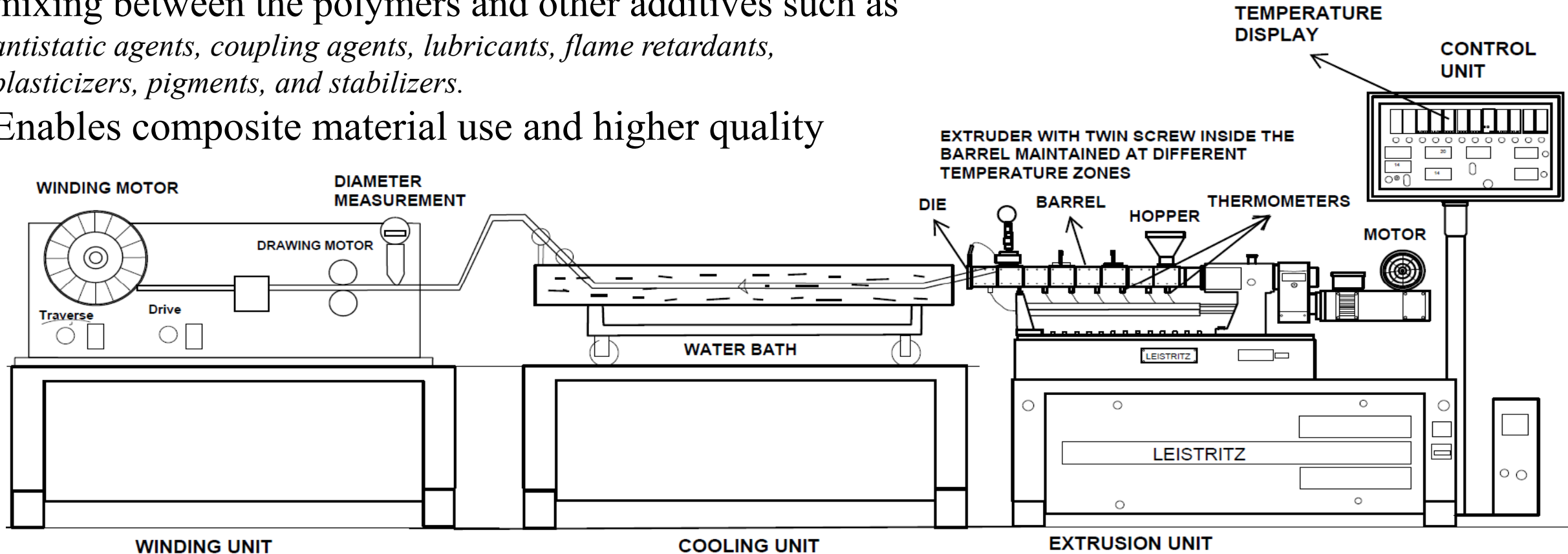
| Screw element | Dimensions |
|-------------------------|-------------|
| Total length | 20-30 D |
| Length of metering zone | 4-8 D |
| Screw pitch | 1 D |
| Flight width | 0.1 D |
| Depth of feed zone | 0.1-0.015 D |
| Barrel-flight clearance | 0.0025 D |

Diameter of the screw varies depends on:

- **Type of polymer,**
- **Quantity of the polymer to process,**
- **Mass feed rate, etc.**

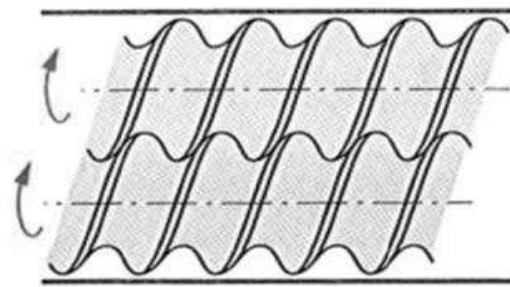
Twin Screw Extrusion

- Used to prepare polymer blend of different materials
- Intermeshing screws interferes the flow to provide better mixing between the polymers and other additives such as *antistatic agents, coupling agents, lubricants, flame retardants, plasticizers, pigments, and stabilizers.*
- Enables composite material use and higher quality

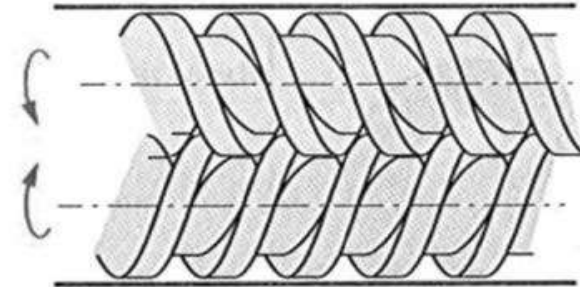


Twin Screw Extrusion

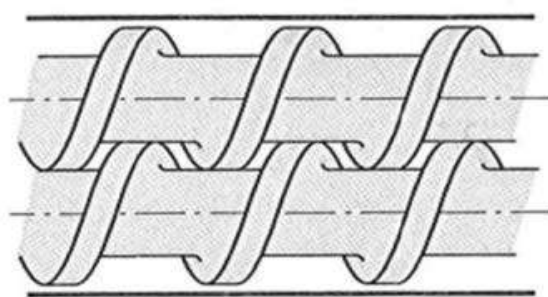
Types of screws



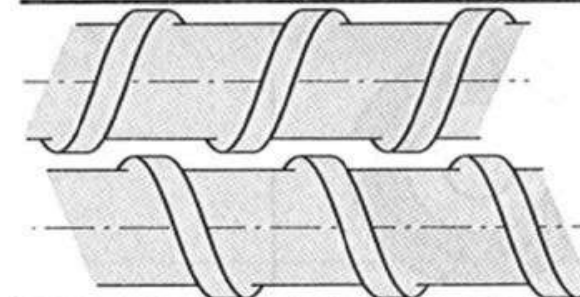
Co-rotating screws



Counter-rotating screws



Interpenetrated screws



Non-Interpenetrated screws

Single Screw vs Twin Screw Extrusion

| Single Screw | Twin Screw |
|--------------------------|---------------------------|
| Low Cost | High Cost |
| Poor Mixing Quality | Excellent Mixing Quality |
| Limited Material Variety | Wide (composites, blends) |
| Simple design | Complex design |

Application of FDM in flexible fabric structures

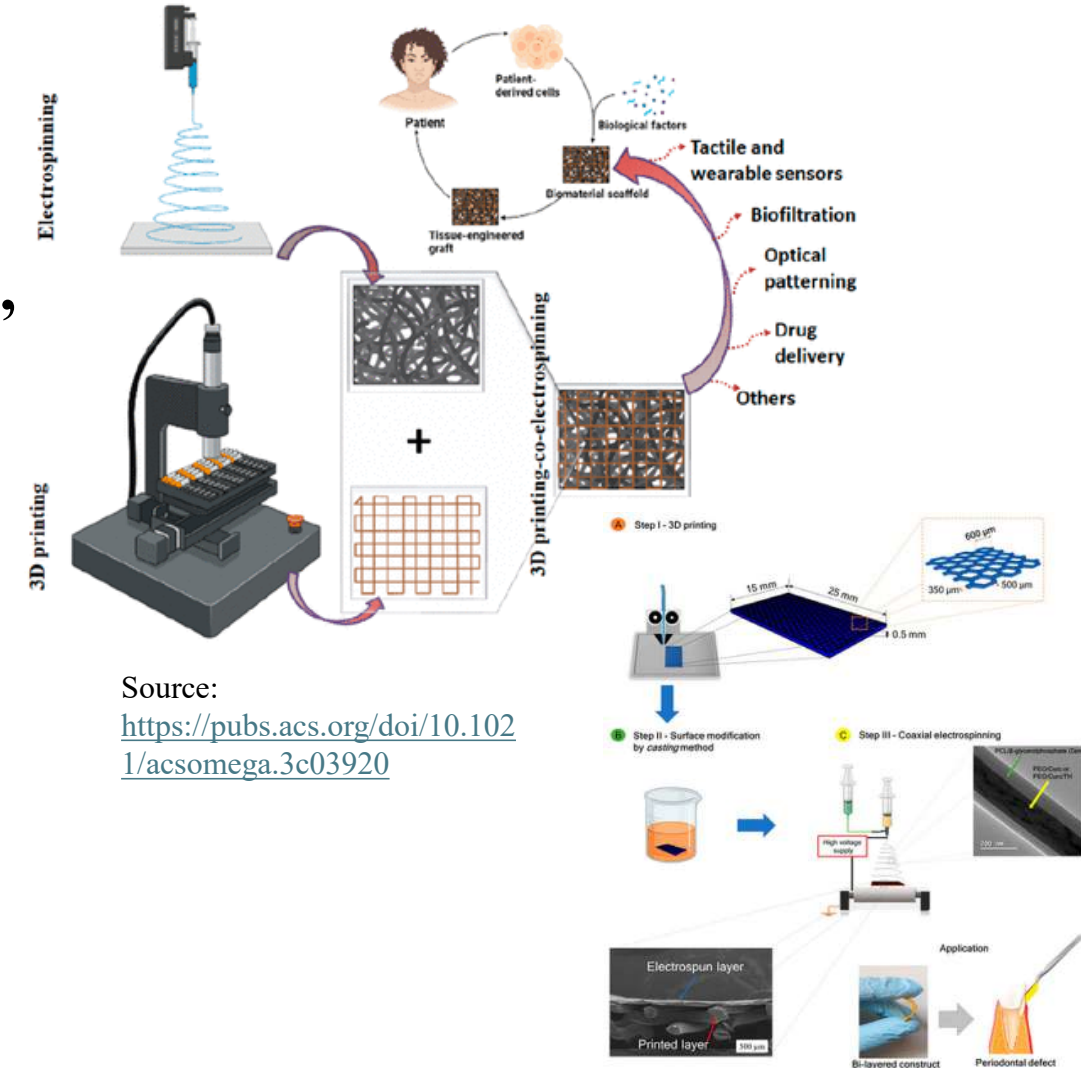
- Fabric structures have evolved far beyond clothing and footwear.
- Now used in **biomedical, aerospace, sports, infrastructure.**
- Enabled by:

Additive manufacturing (AM)

Nanotechnology

Novel material developments

- **FDM (Fused Deposition Modeling)** offers direct-from-polymer textile fabrication.

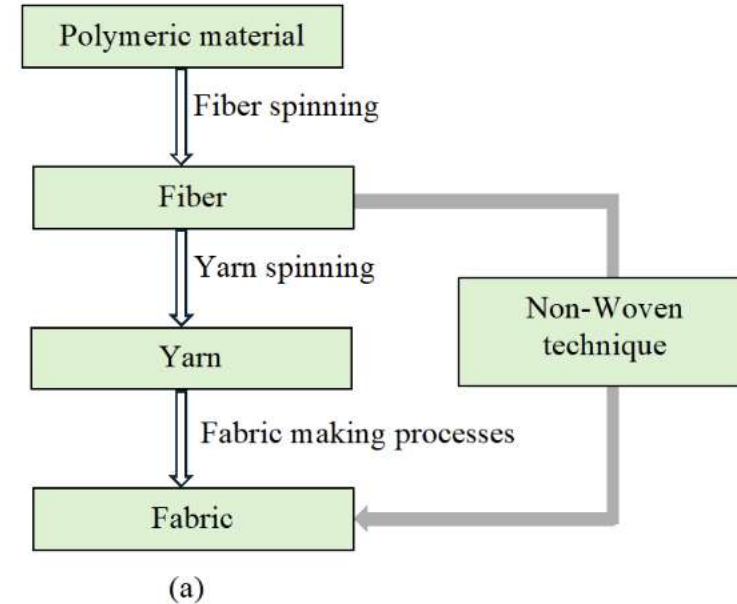




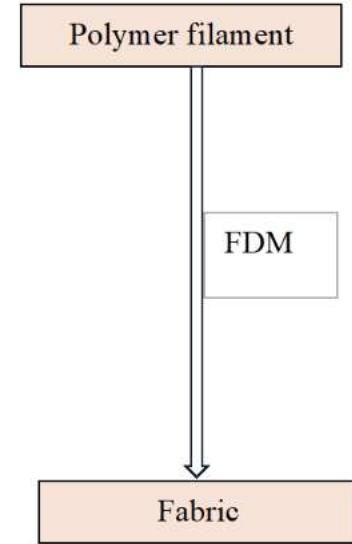
Application of FDM in flexible fabric structures

Why FDM for Textiles?

- Traditional textile manufacturing is **multi-step, cost-intensive, and wasteful**.
- Polymer → Fiber spinning → Yarn → Fabric
- FDM eliminates intermediate steps:
Saves time, cost, and reduces waste.
Enables design flexibility and on-demand production.



(a)



(b)

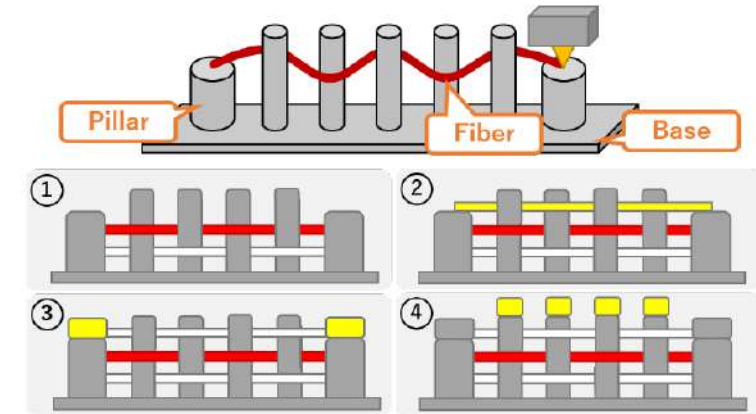
(a) Traditional fabric manufacturing process flow and (b), fabric manufacturing flow with FDM

Application of FDM in flexible fabric structures

Recent Scientific study and findings

Programmable Textiles – Takahashi & Kim

- Developed **woven structures** using PLA on Creality CR-10S.
- Design elements:
 - Base, support, weaving fiber.
- Properties:
 - Foldable in weft, breakable in warp.
 - Load capacity: up to **4 kg**.
- Introduced **programmable textile concept**.



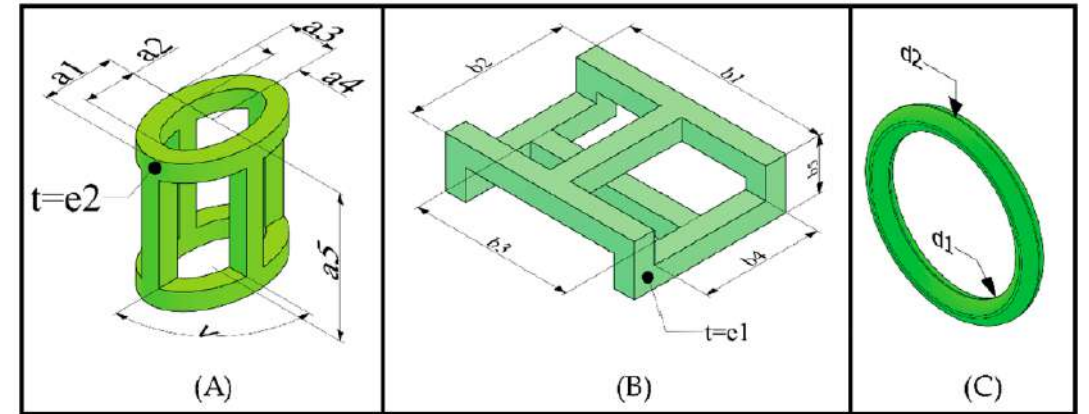
Source: Takahashi H and Kim J, 2019, [10.1145/3332165.3347896](https://doi.org/10.1145/3332165.3347896).

Application of FDM in flexible fabric structures

Recent Scientific study and findings

Structured Fabric Designs – Fajardo et al.

- Compared **FDM** vs **SLA** printed fabrics.
- Types:
 - Cylindrical, prismatic, annular.
- Key findings:
 - **Prismatic elements** had highest tensile strength.
 - Element **linking & spacing** impact flexibility.
 - **Geometry design** critical for comfort and stress handling.



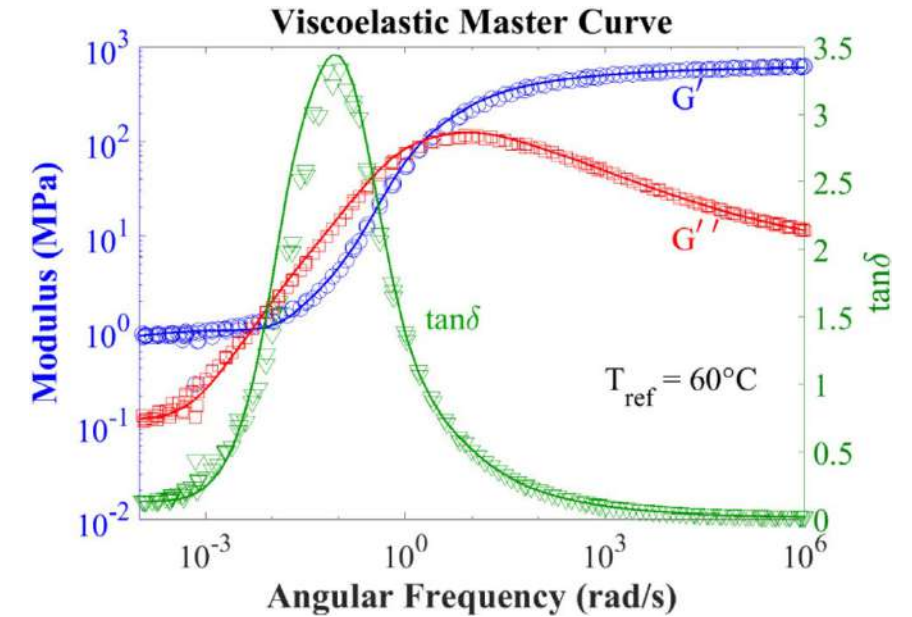
Designs of the elements that are composed of the different textile structures. (A) Cylindric element; (B) prismatic element; (C) annular element.

Application of FDM in flexible fabric structures

Recent Scientific study and findings

Viscoelastic Properties – Jayswal et al.

- Created interlaced weaved fabric; studied viscoelastic behavior.
- Used DMA (Dynamic Mechanical Analysis).
- Key insights:
 - **Hysteresis loop** widened near glass transition ($T_g \sim 60^\circ\text{C}$).
 - Fabric's dynamic behavior matched that of standard PLA.



Viscoelastic master curve of FDM woven fabric

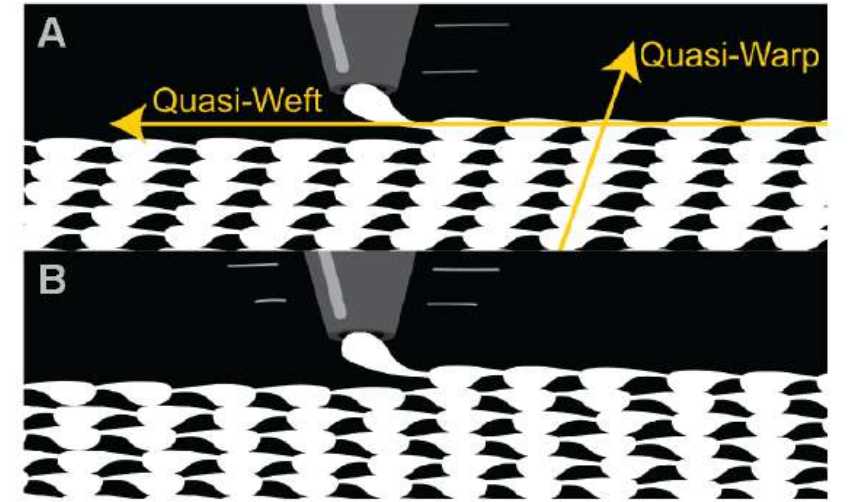
Source: Jayswal et al. 2023 [10.1002/pen.26319](https://doi.org/10.1002/pen.26319).

Application of FDM in flexible fabric structures

Recent Scientific study and findings

Quasi-Woven Fabrics – Forman et al.

- Introduced **DefeXtiles** using under-extrusion technique.
- Features:
 - **Micro- to macro-scale** control.
 - Print perpendicularly for pleats, curves, etc.
 - **Breathability, stretchability, aesthetics.**
- Applications: **Smart textiles, toys, fashion.**



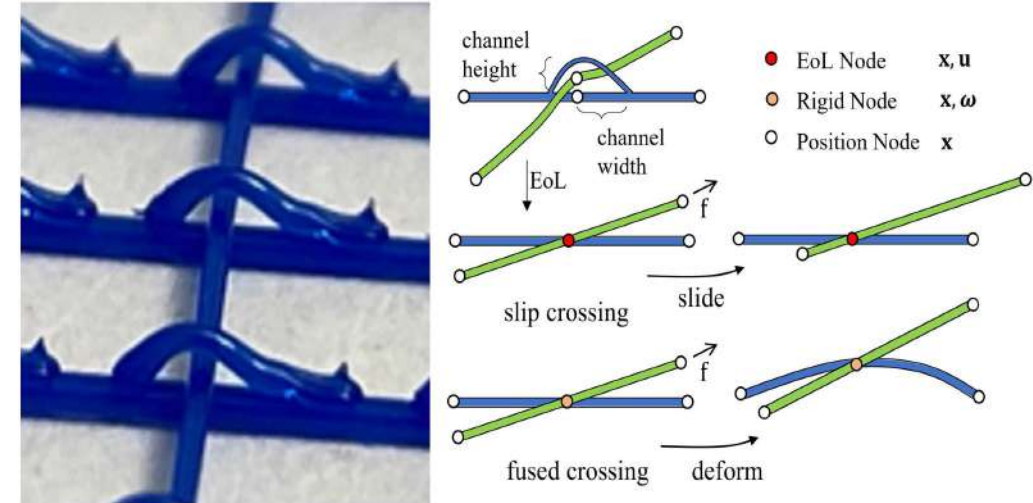
A) shows gap-stretch behavior which generates a “quasi-warp” and “quasi-weft”. For A) the nozzle prints from right to left causing the pillars to lean right. For B) the quasi-warp is straight as the nozzle alternates direction each layer.

Application of FDM in flexible fabric structures

Recent Scientific study and findings

Sliding Connections – Li et al.

- Created **3D printable sliding yarn connections**.
- Results:
 - Programmable, **non-linear & direction-dependent** properties.
 - Flexible for **flat-to-curved transformations**.
 - Fused vs sliding: **Stiff vs flexible**.



Close-up of 3D-printed channels at sliding connetions (*left*) and schematic view of the corresponding simulation model (*middle*).

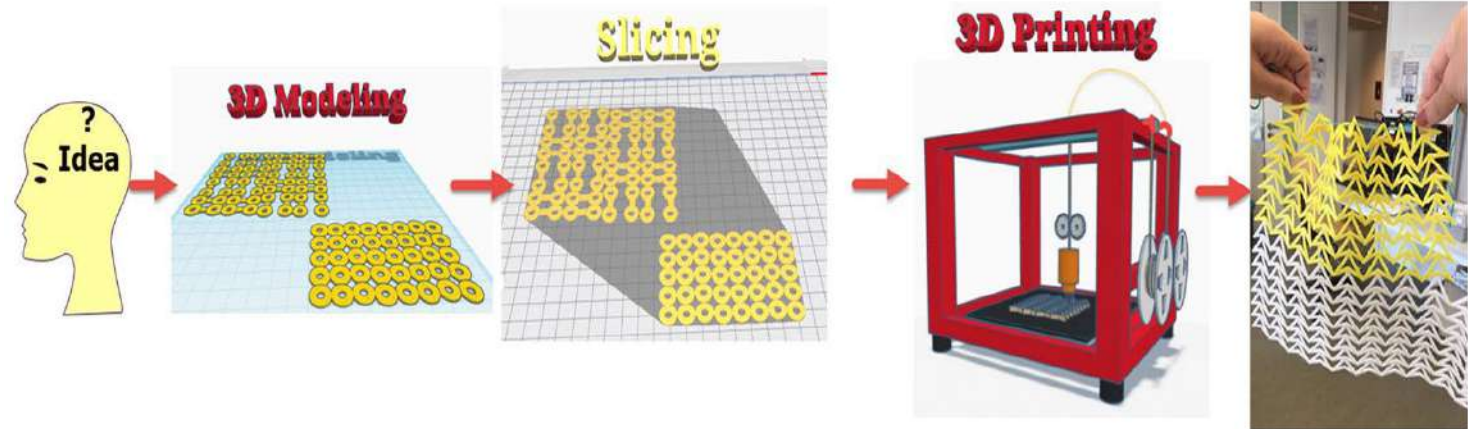
Source: Li et al. 2022 [10.1109/LRA.2022.3145948](https://doi.org/10.1109/LRA.2022.3145948).

Application of FDM in flexible fabric structures

Recent Scientific study and findings

Fashion Applications – Spahiu et al.

- Created **wearable dress** using 33 printed parts.
- Materials tested: PLA, TPU, nylon.
- Public perception:
 - **Positive and optimistic** about 3D-printed garments.
- Highlight: **FilaFlex dress** – flexible, comfortable, aesthetic.



Workflow of the main steps followed in this work.

Source: Spahiu et al. 2020 [10.1177/1558925020948216](https://doi.org/10.1177/1558925020948216).

Application of FDM in flexible fabric structures

Recent Scientific study and findings

Multi-Material Textiles – Uysal & Stubbs

- Printed garments using PLA + LAY-FOMM 40 elastomer.
- Software: Blender + Netfabb.
- Findings:
 - **Pattern size affects rigidity and strength.**
 - Created **sensor gloves** and **custom logos** on fabric.



3D printed glove: A) sewing pattern printed from two materials, B) surface design of glove, C) flexible sewing pattern with inner lining, D) pattern pieces sewn together to form three-dimensional garment

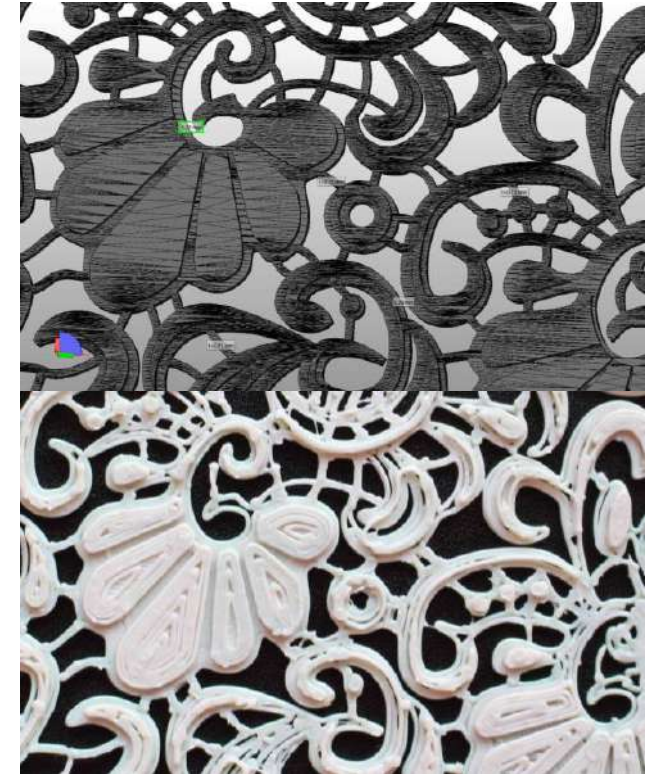
Source: Uysal et al. 2019 [10.14502/Tekstilec2019.62.248-257](https://doi.org/10.14502/Tekstilec2019.62.248-257).

Application of FDM in flexible fabric structures

Recent Scientific study and findings

Material Exploration – Melnikova et al.

- Compared **FDM** vs **SLS**.
- Developed lace, knitted patterns using PLA and Lay Tekkks.
- Challenges:
 - Some materials failed (e.g. ABS).
 - **Soft PLA** performed best with no supports needed.
- Demonstrated feasibility of intricate **multi-material prints**.



Multi-layer lace pattern, depicted in “netfabb” (Upper), and the resulting 3D print (Lower)

Application of FDM in flexible fabric structures

Recent Scientific study and findings

PLA Composites on Jute Fabrics: Franco-Urquiza et al.

- Created **PLA composites** using **woven jute fabrics** as filler.
- Mechanical testing showed **no improvement** over pure PLA.
- Despite fabric modifications, **adhesion remained inadequate**.



Photographs and schematic representations of: (a) jute fabrics, (b) 3D printing on jute fabric

Source: Franco et al. 2021 [10.3390/polym13193202](https://doi.org/10.3390/polym13193202).

Application of FDM in flexible fabric structures

Recent Scientific study and findings

Printed Patterns and Fabric Drape: Spahiu et al.

- Printed **geometric patterns** (squares, triangles, circles) on skirt fabrics.
- Materials used: **White polyester** and **grey polyamide**.
- **PLA filament** chosen for its excellent textile adhesion.
- Pattern design impacted:
 - **Drape coefficient**
 - **Number of nodes**
 - **Garment flow and aesthetics**



The skirt with imprinted 3D patterns on front and back.

Source: Spahiu et al. 2017 [10.1088/1757-899X/254/17/172023](https://doi.org/10.1088/1757-899X/254/17/172023).



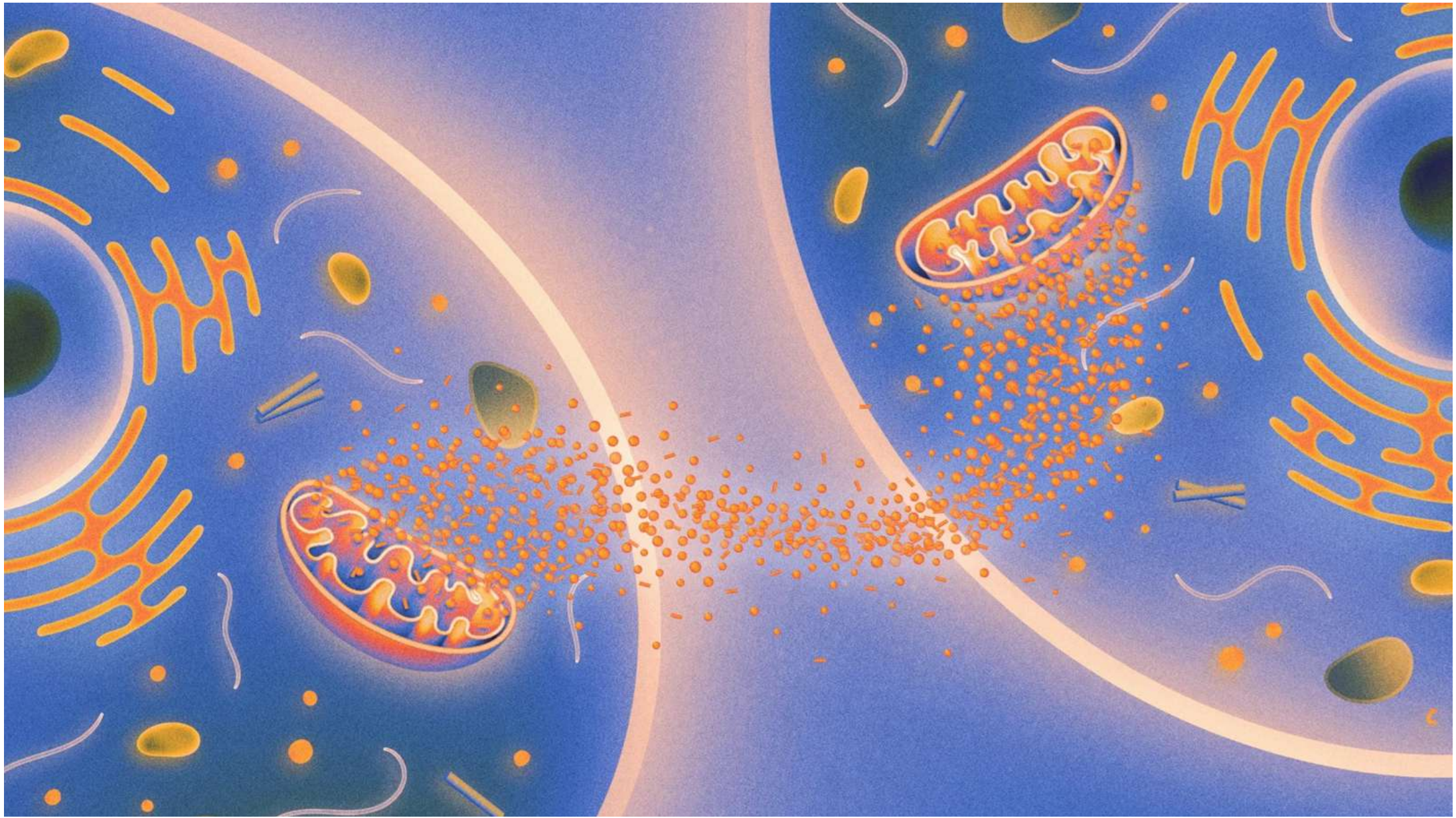
Cell Communication in Wound Healing

*Assist. Prof. MehmetAli Tibatan
İstanbul Zaim University
Molecular Biology and Genetics*



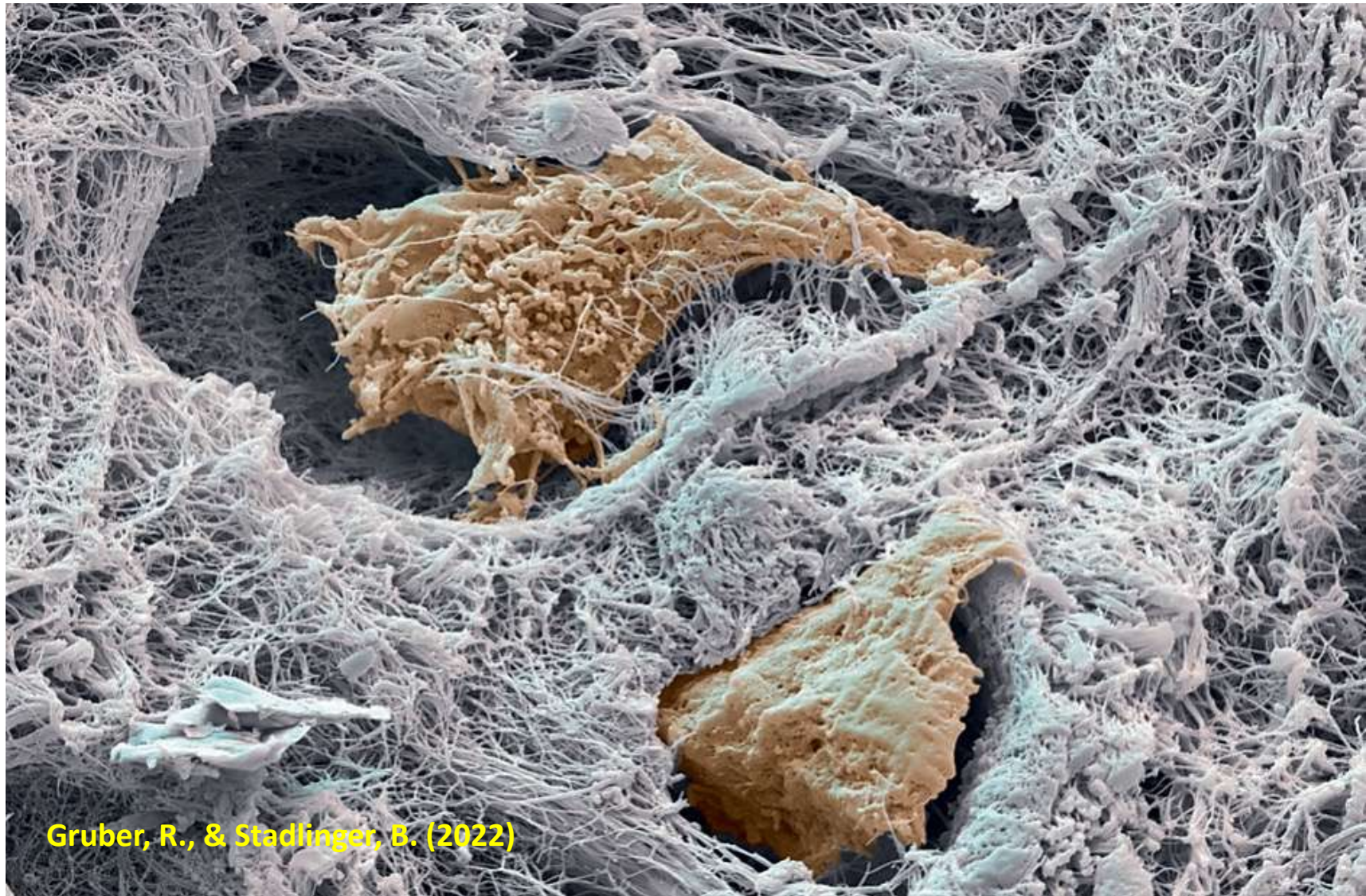
TEMAG

Textile Materials & Machinery
Research Group





Gruber, R., & Stadlinger, B. (2022)



Gruber, R., & Stadlinger, B. (2022)

Osteoclast destroying the lacuna
(bone tissue surrounding)
It is necessary for bone tissue
regeneration



Gruber, R., & Stadlinger, B. (2022). Cell-Atlas-Visual Biology in Oral Medicine. Quintessenz Verlag.

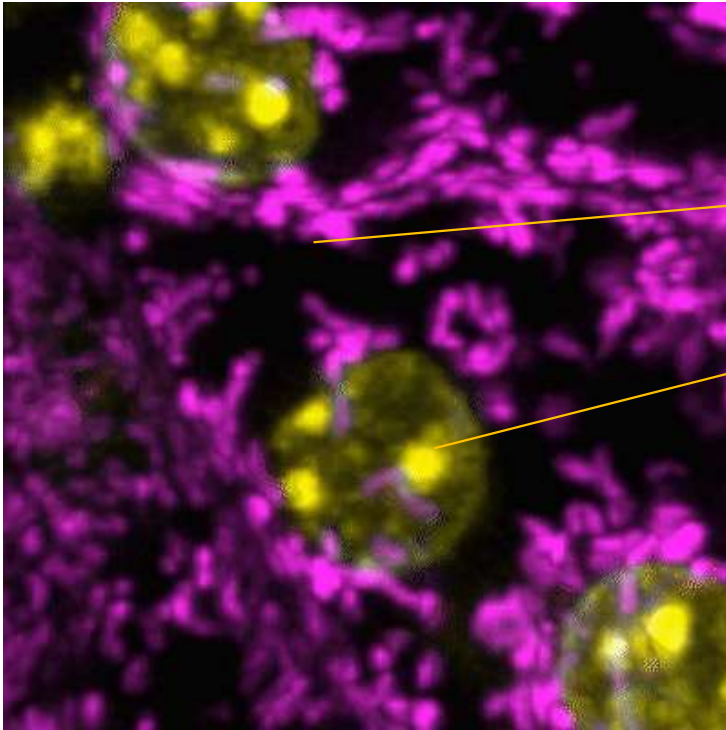
Gruber, R., & Stadlinger, B. (2022)

Swab sample from healthy oral mucosa of the cheek (buccal) contains several epithelial cells (*red-pink*). Bacterial cells (*green*) can naturally colonize the surface of the cells, in both healthy conditions and in disease.

Gruber, R., & Stadlinger, B. (2022). Cell-Atlas-Visual Biology in Oral Medicine. Quintessenz Verlag.



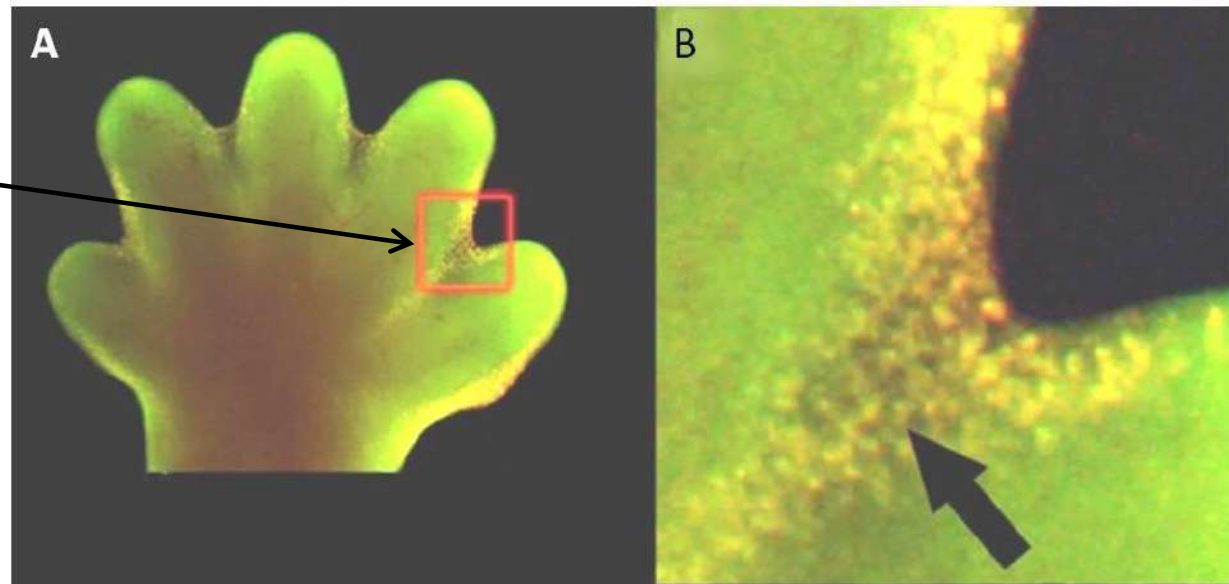
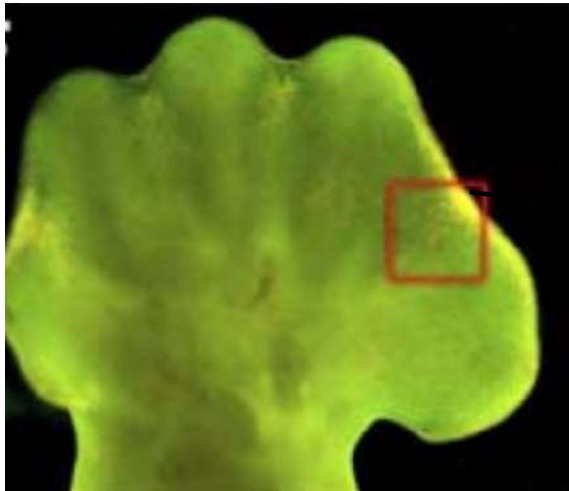
MITOCHONDRIA IS CONNECTED WITH NUCLEUS AND OTHER CELLS TOO



In these stained cells, the mitochondria appear magenta and the nuclei are yellow. Two populations of mitochondria can be distinguished by their behavior: Mitochondria near the cell membranes mostly stay in place; centrally positioned mitochondria are more motile

CELL COMMUNICATION CONTROLS APOPTOSIS

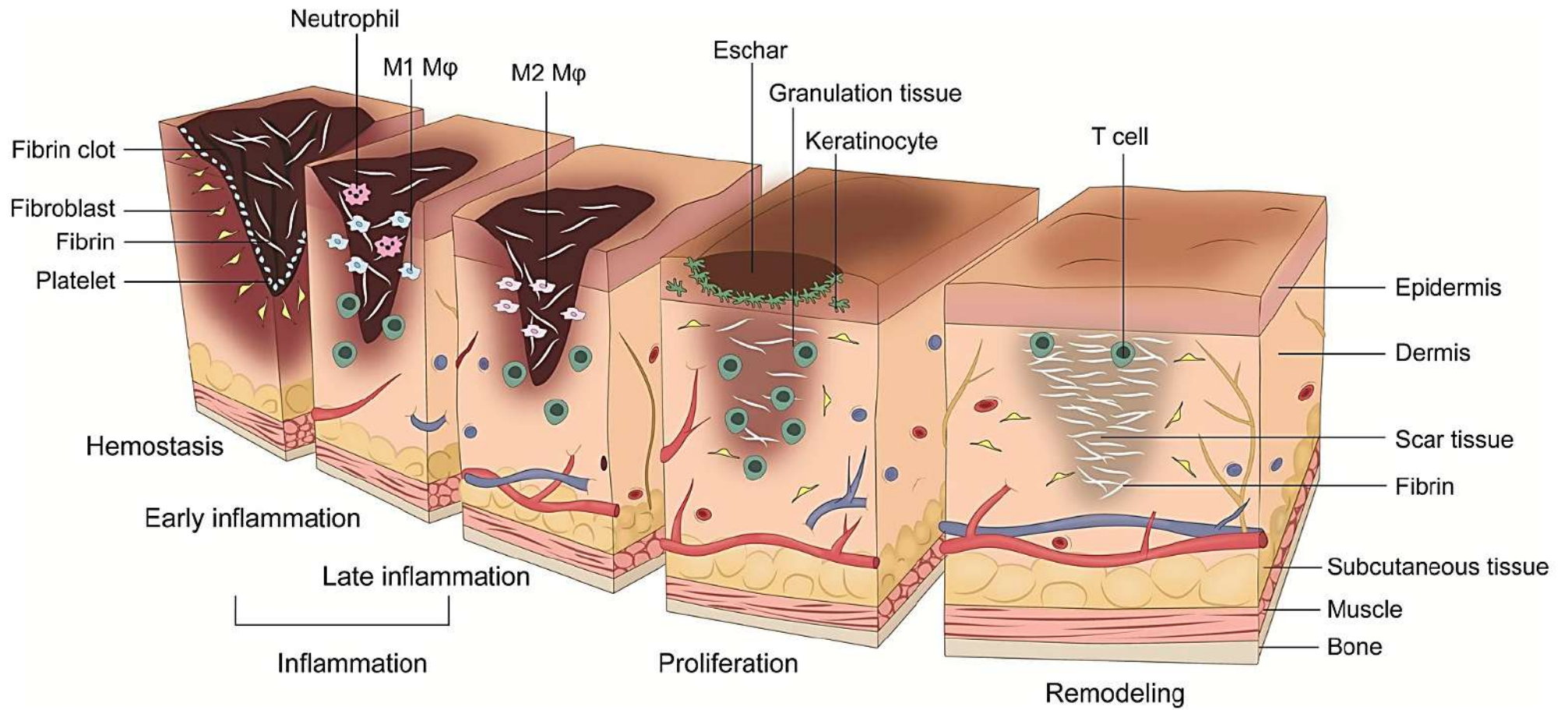
Bandyopadhyay et al., 2006

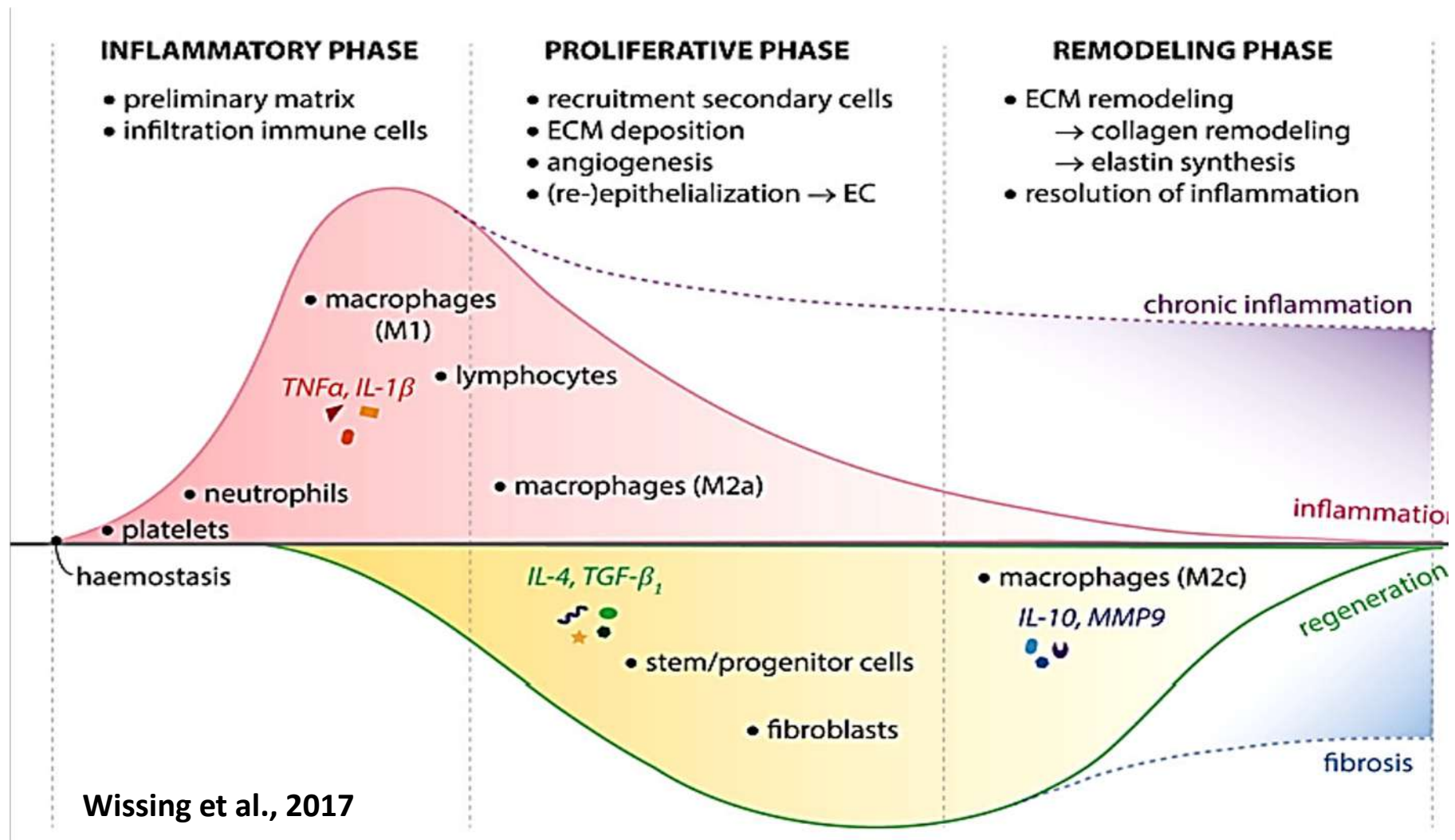


A: Apoptosis in a developing mouse paw.

B: An enlarged view of the boxed area, showing cells dying in the webbing between the digits.

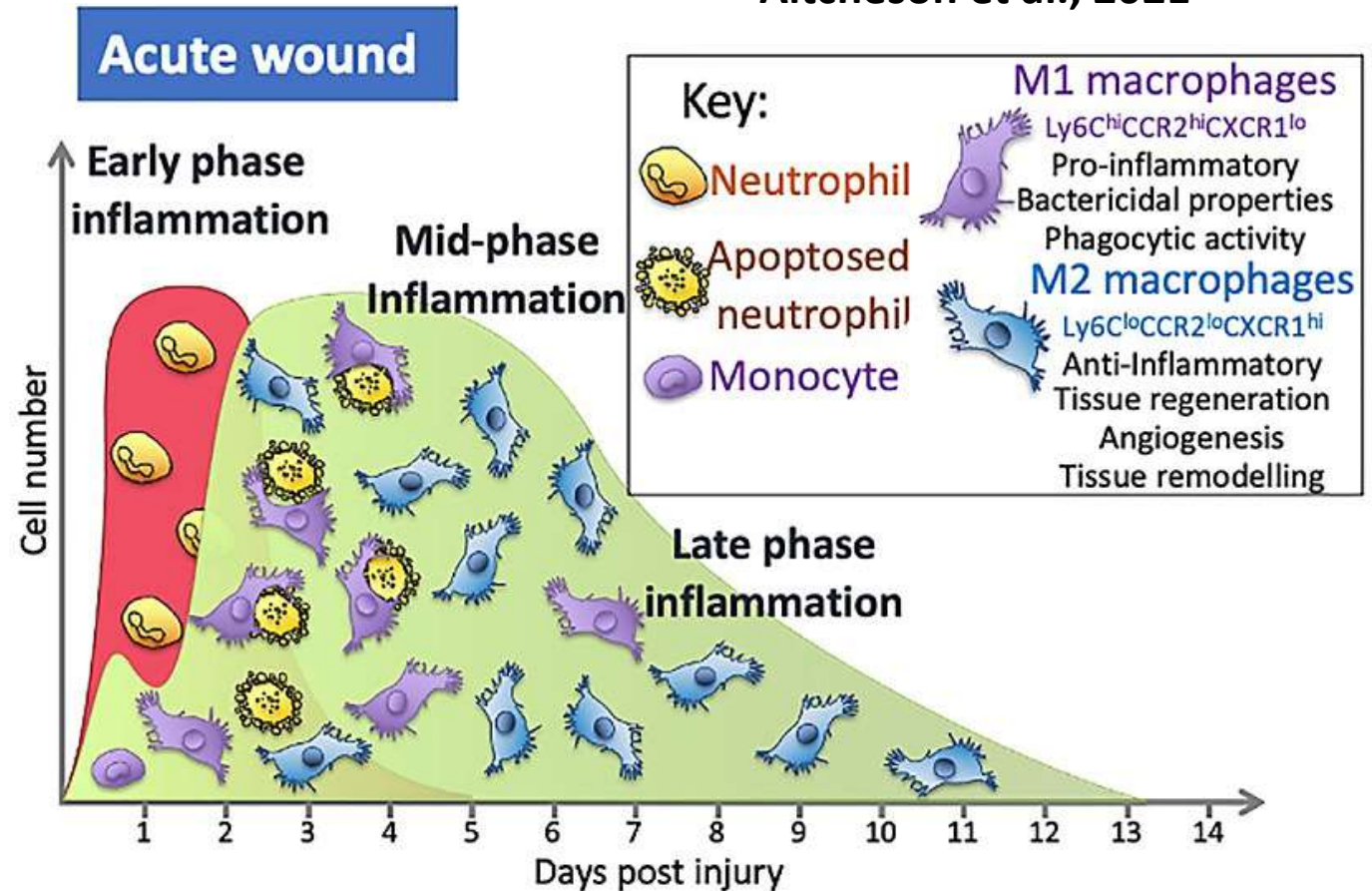
Bandyopadhyay, A., Tsuji, K., Cox, K., Harfe, B. D., Rosen, V., & Tabin, C. J. (2006). Genetic analysis of the roles of BMP2, BMP4, and BMP7 in limb patterning and skeletogenesis. *PLoS genetics*, 2(12), e216.



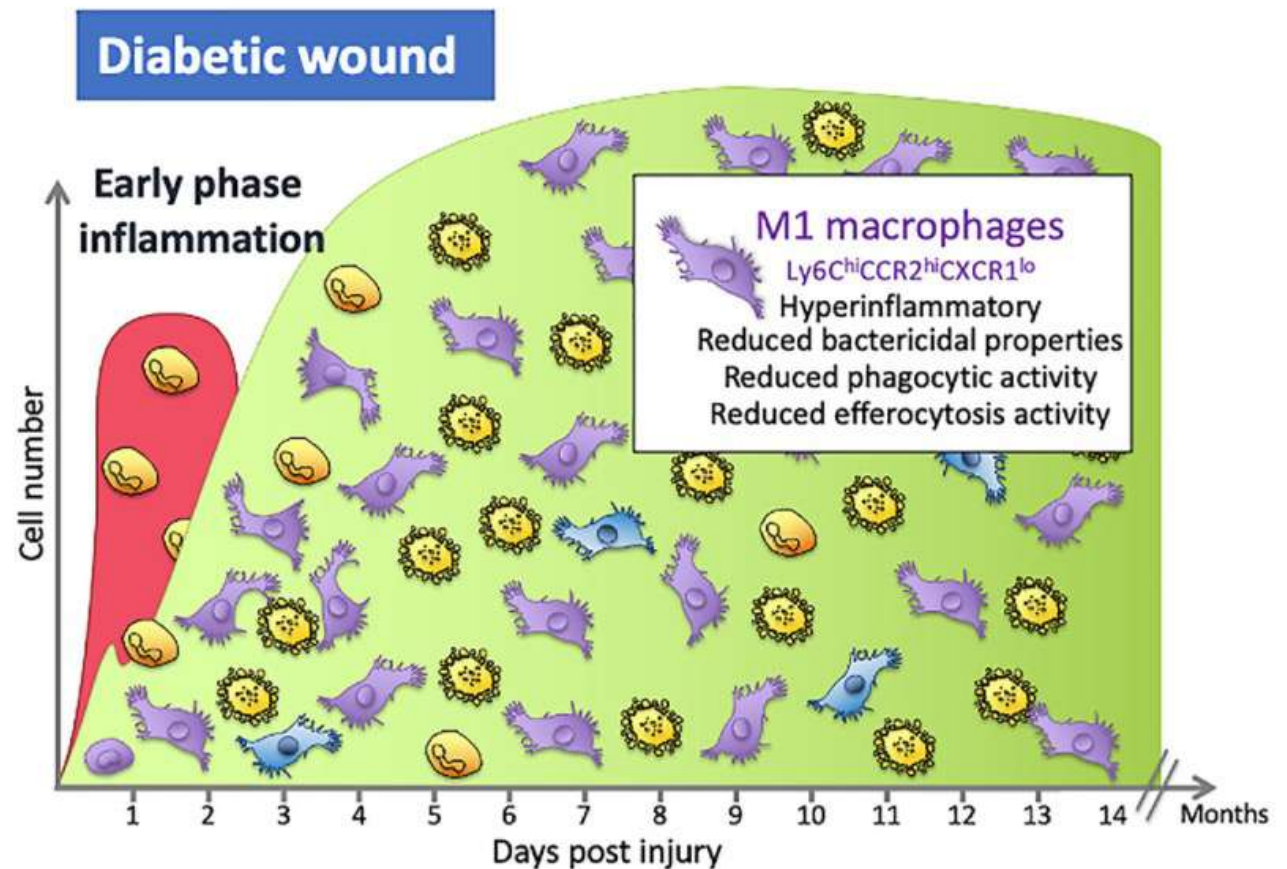


Cellular communication in wound area

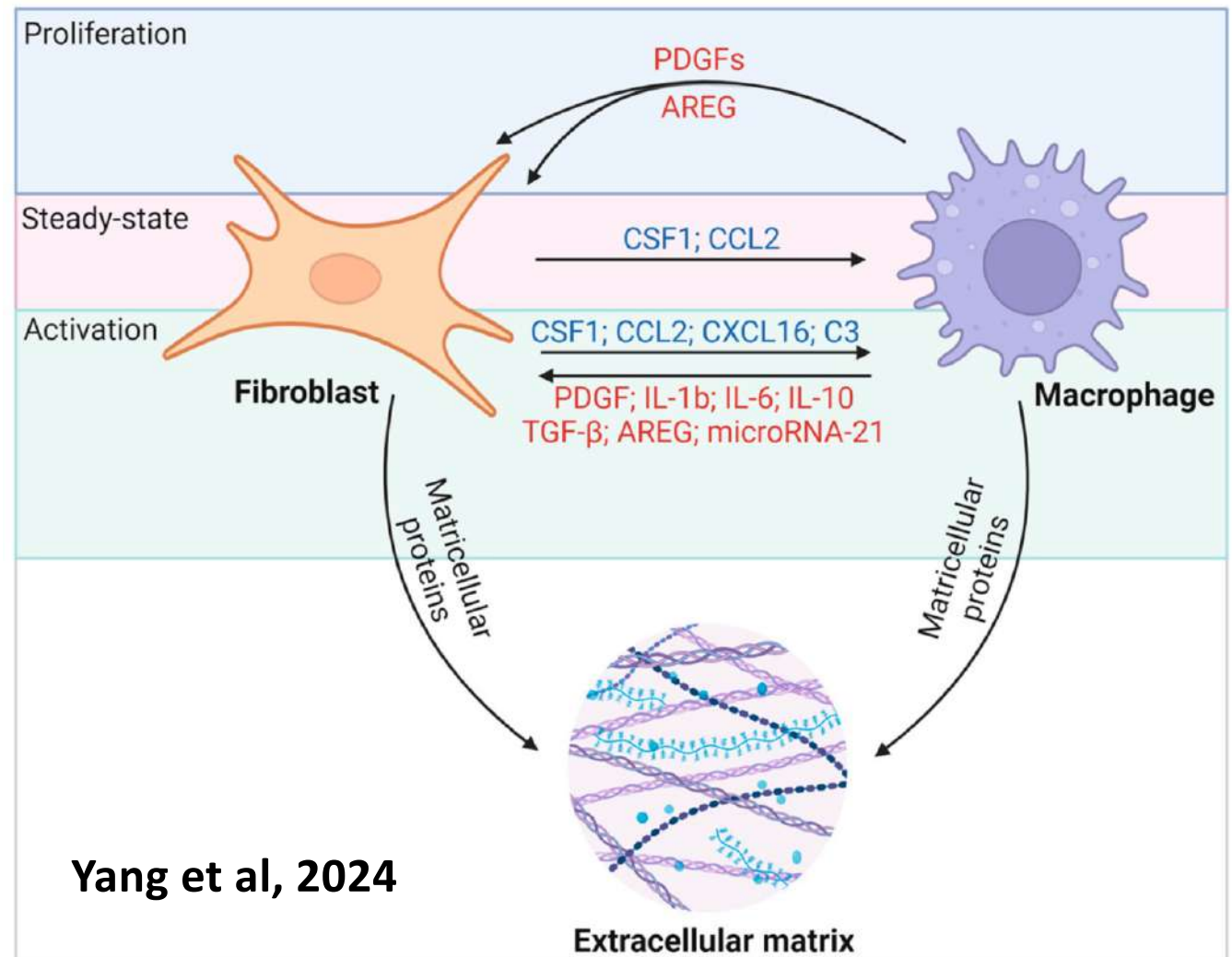
- During the early stages of inflammation in an acute wound, the wound is predominantly populated with M1 macrophages that are pro-inflammatory. A switch in the predominant phenotype is seen later in the inflammatory phase, where the majority of macrophages are M2.
- Normal process provides transition between healing stages as the immun system cell commune to each other.**

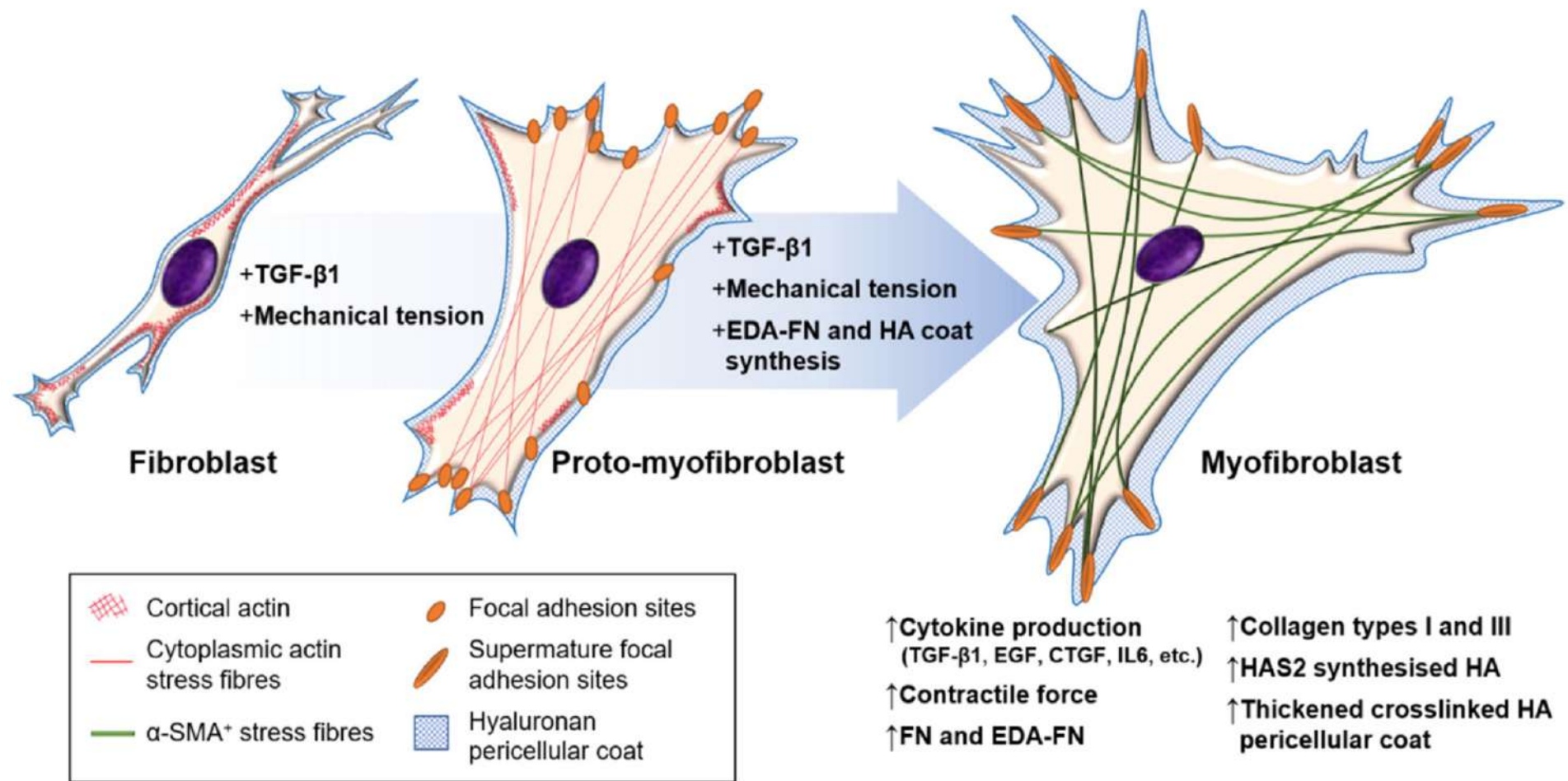


- In wounds of people with diabetes, macrophage numbers are altered and secrete more pro-inflammatory cytokines, have reduced phagocytic and **efferocytosis** abilities and are less likely to switch to the M2 phenotype in the mid- to late-inflammation phase that is as seen in normal acute wounds.
- **For this reason healing process never completed**



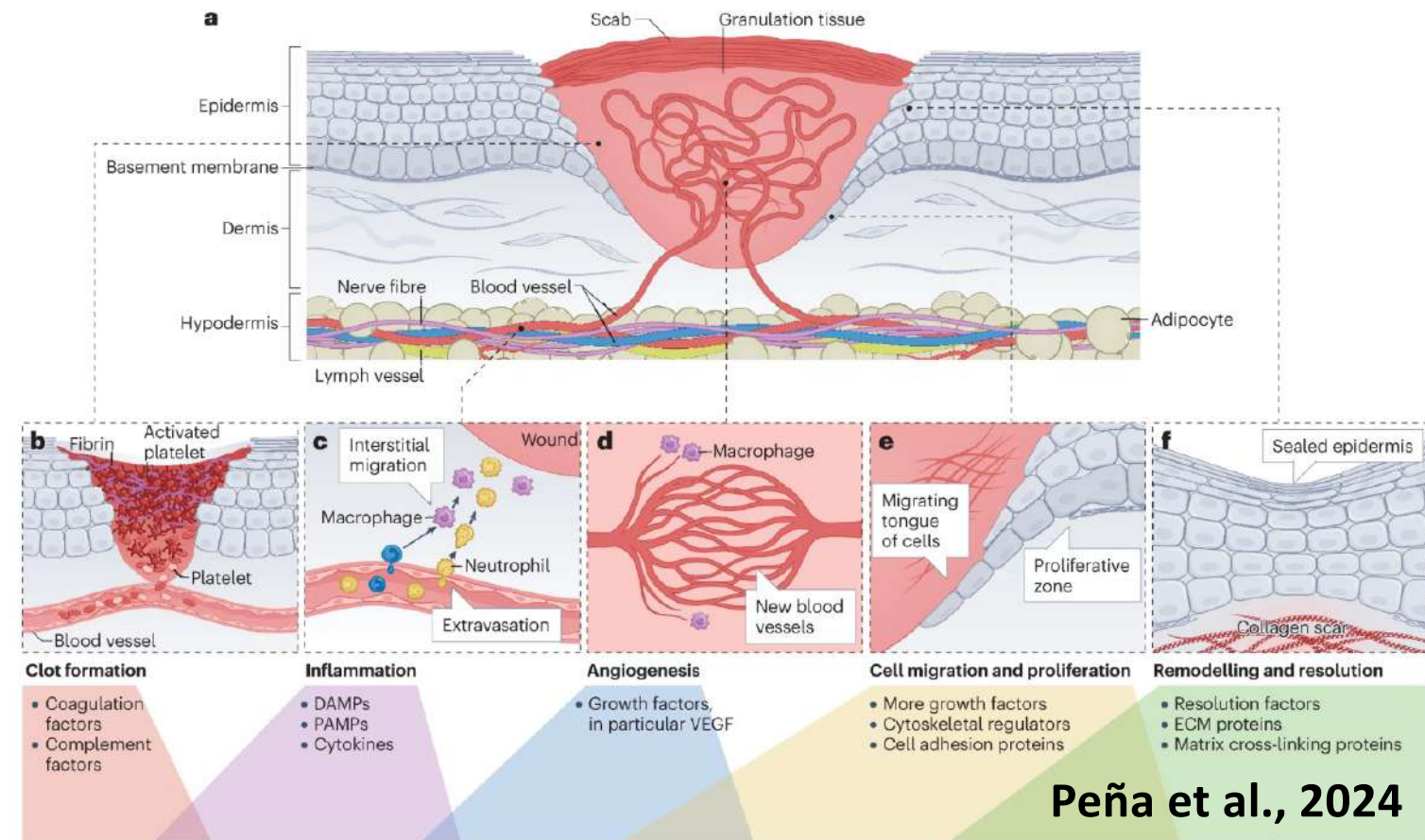
Cellular communication provides feedback mechanism to wound healing process

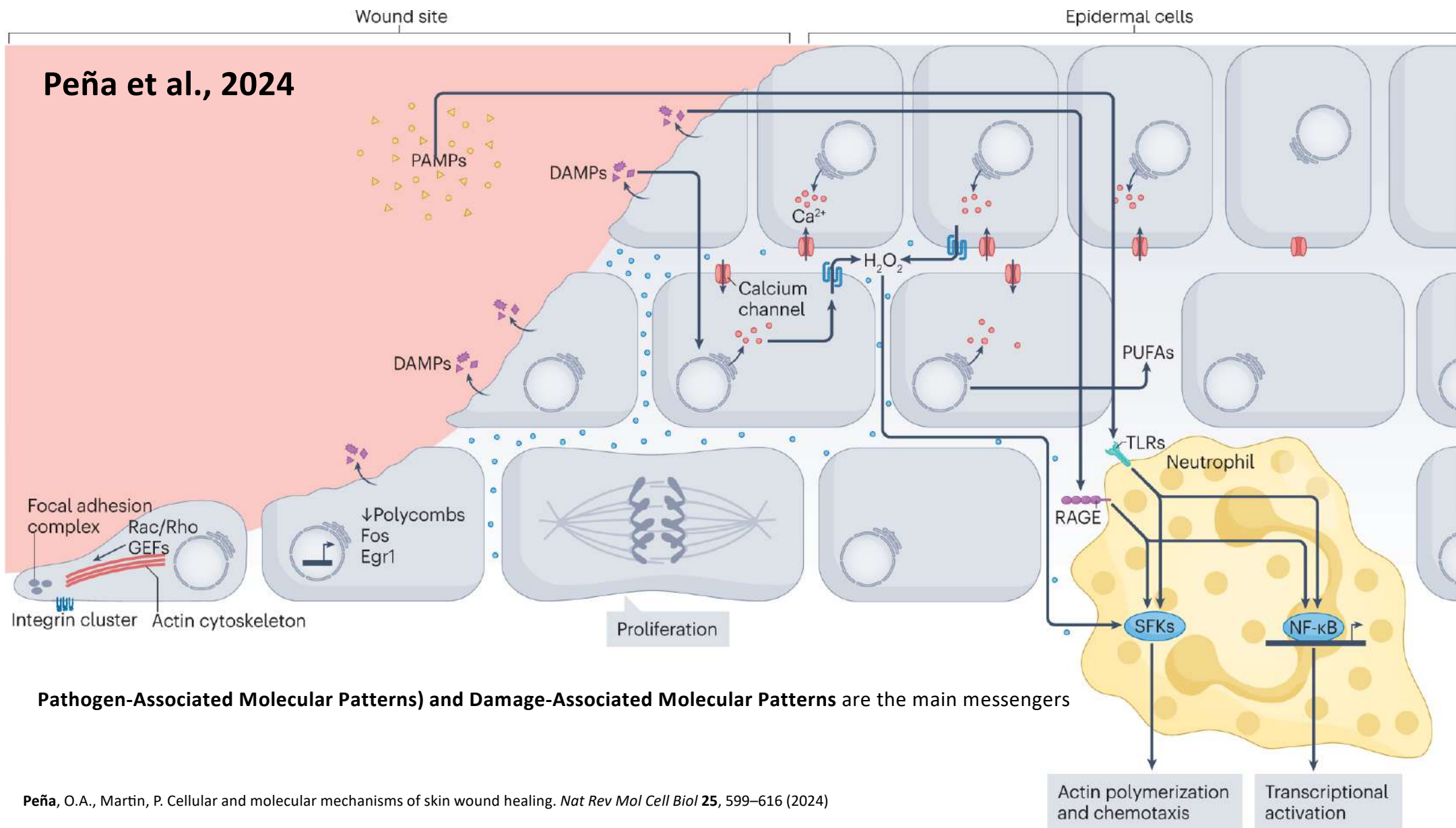




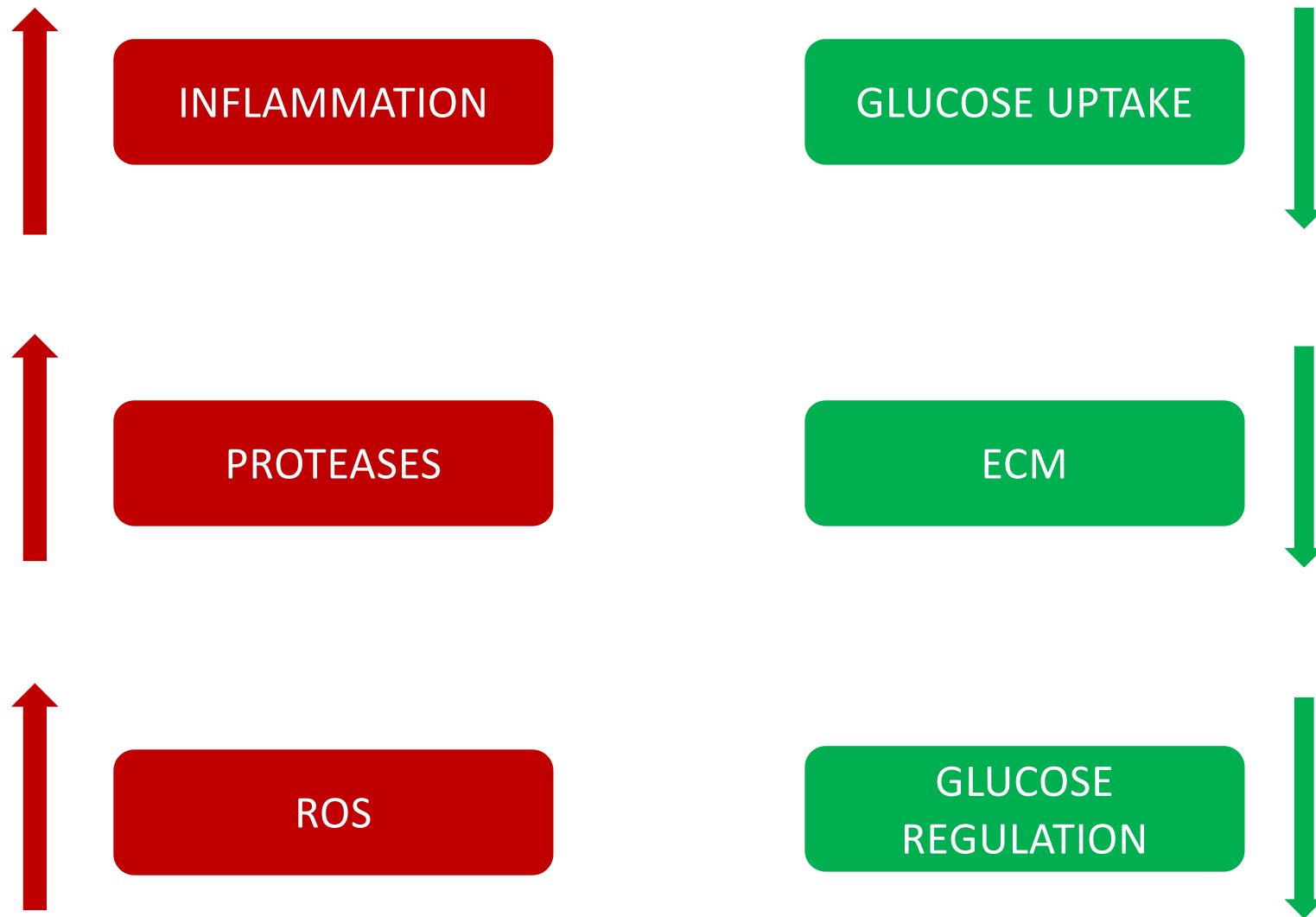
Tai, Y.; Woods, E.L.; Dally, J.; Kong, D.; Steadman, R.; Moseley, R.; Midgley, A.C. Myofibroblasts: Function, Formation, and Scope of Molecular Therapies for Skin Fibrosis. *Biomolecules* **2021**

Different layers and interconnecting cell types are required to be orchestrated for tissue homeostasis.





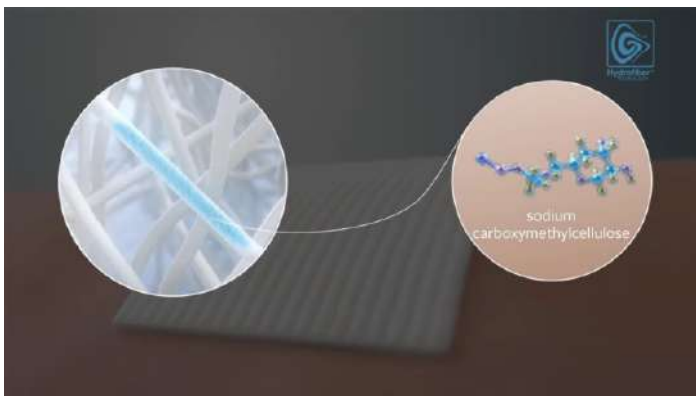
**There is A Cause-Effect Relation of Chronic
Wound in Type II Diabetes**



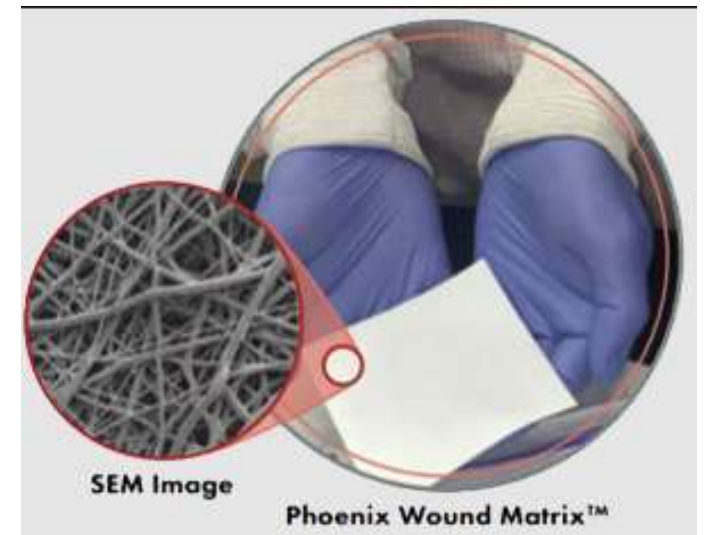
Wound dressing



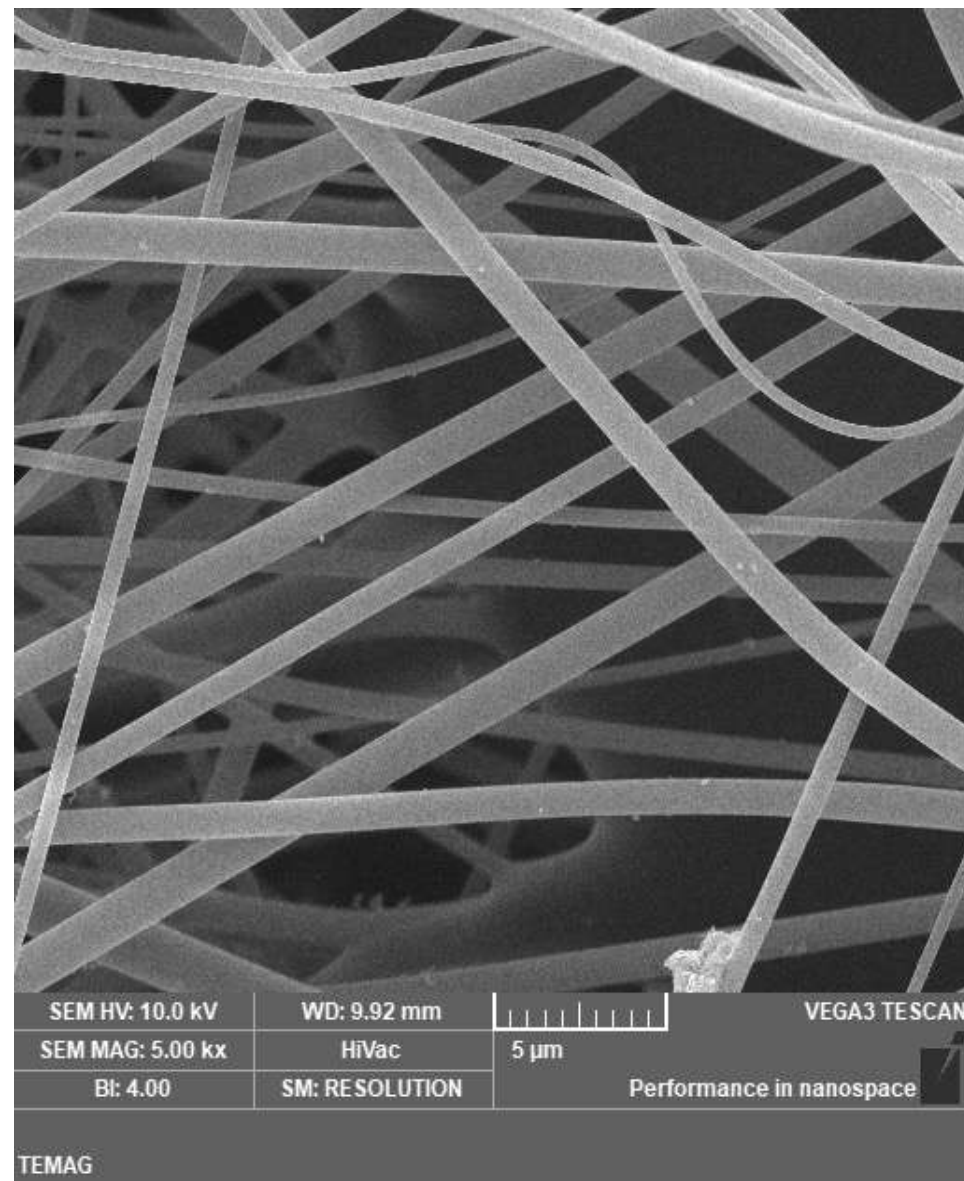
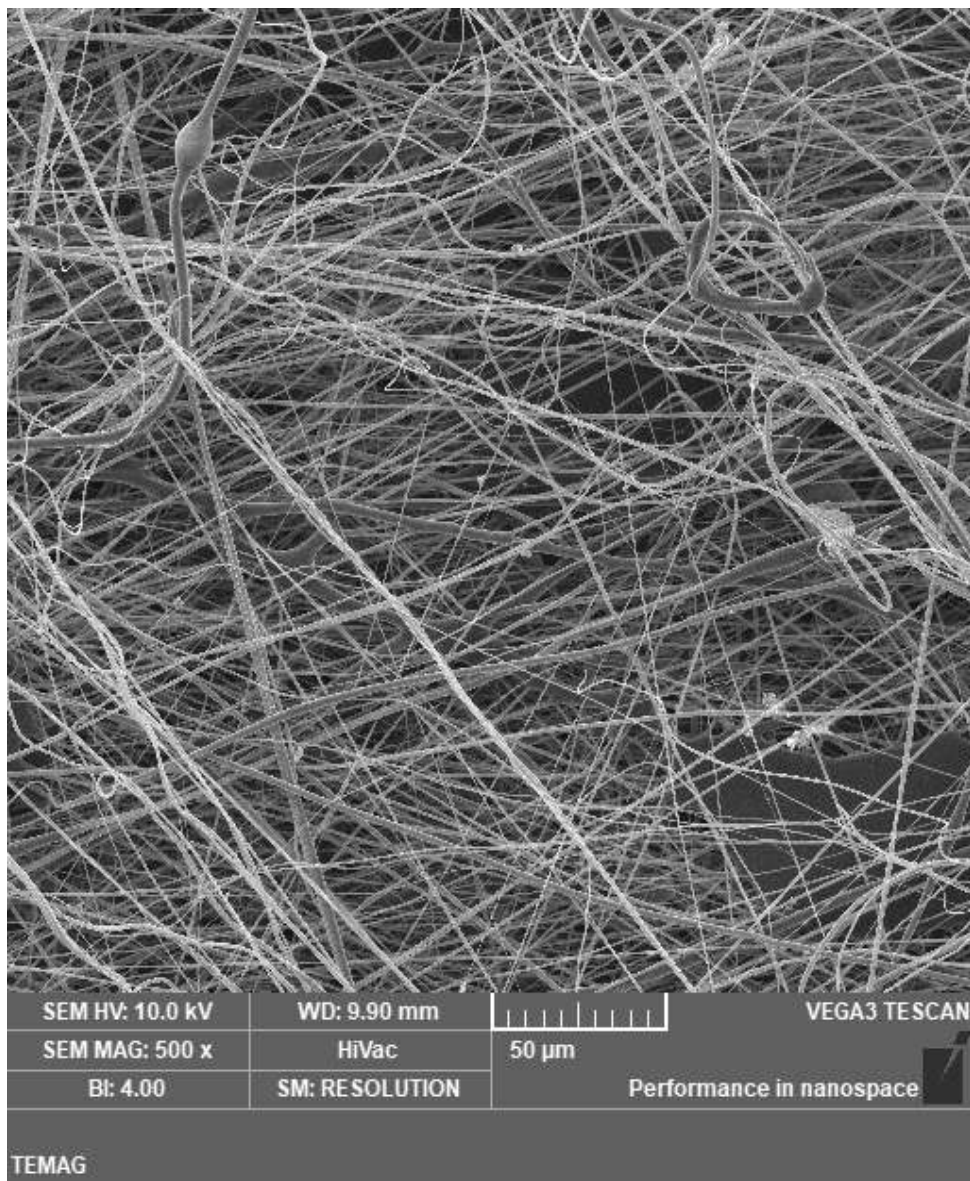
Integra



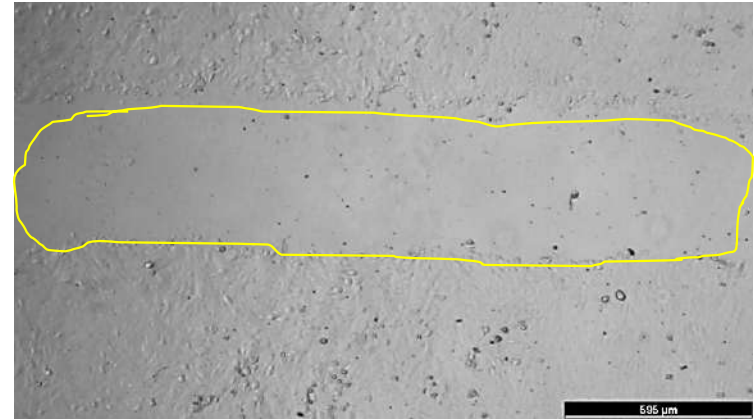
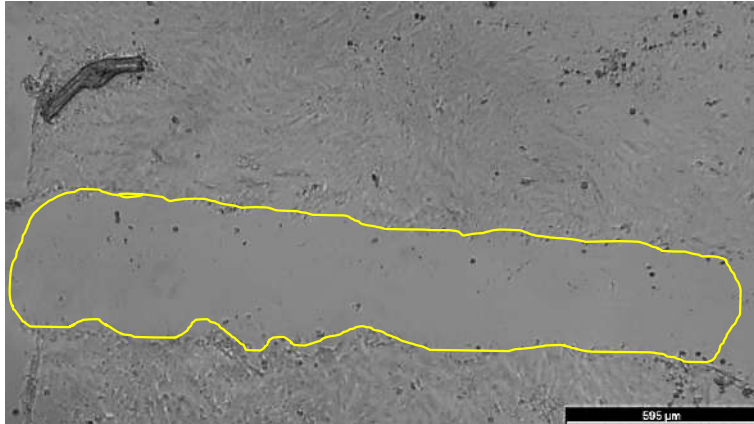
Aquacell



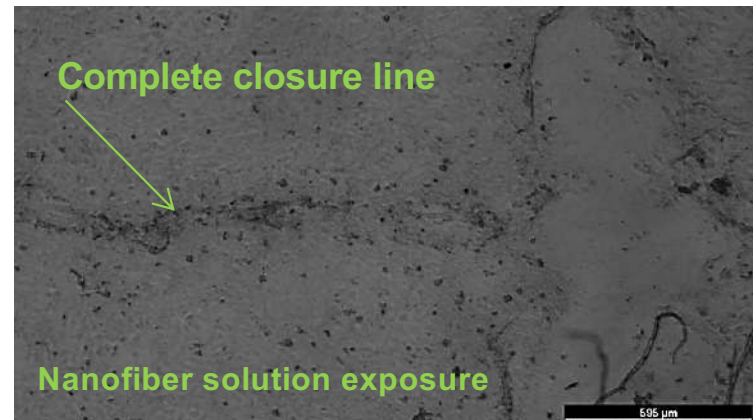
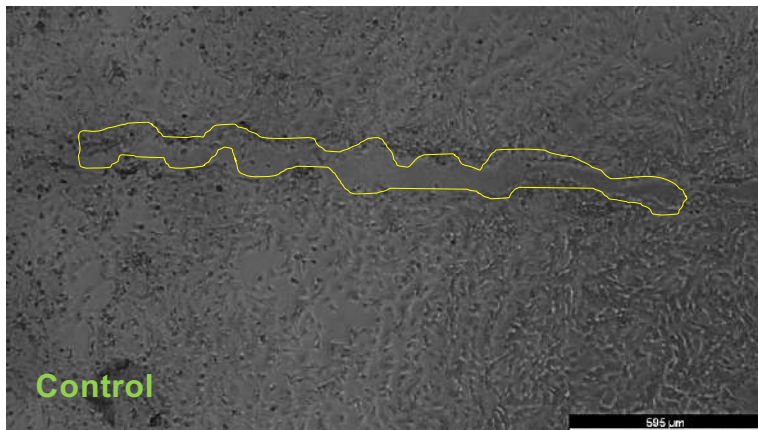
Renovoderm



Beginning



After 18h





16

ULUSLARARASI LİF VE POLİMER ARAŞTIRMALARI SEMPOZYUMU

16th INTERNATIONAL FIBER AND POLYMER RESEARCH SYMPOSIUM

Sürdürülebilir ve İşlevsel Lif ve Polimerler
Sustainable and Functional Fibers & Polymers



9-10 Mayıs 2025

İstanbul Teknik Üniversitesi
Gümüşsuyu Prof. Dr. Necmettin Erbakan Yerleşkesi

Istanbul Technical University
Gumussuyu Prof. Dr. Necmettin Erbakan Campus



16 ULUSLARARASI LİF VE POLİMER ARAŞTIRMALARI SEMPOZYUMU

16th INTERNATIONAL FIBER AND POLYMER RESEARCH SYMPOSIUM

SYMPOSIUM SCHEDULE

9 - 10 Mayıs 2025

İstanbul Technical University
Sürdürülebilir ve İşlevsel Lif ve Polimerler
Sustainable and Functional Fibers & Polymers

9 Mayıs 2025 Cuma | 9th May 2025 Friday

08:00 – 10:00

Sempozyum Karşılama, Kayıt & Çay/Kahve/İkramlar | Symposium Welcome, Registration & Tea/Coffee/Cookies
YER: İTÜ GÜMÜŞSUYU KAMPÜSÜ GİRİŞ KORIDORU | SESSION PLACE: İTÜ GUMUSSUYU BUILDING ENTRANCE HALL

10:00 – 12:30

AÇILIŞ TÖRENİ | OPENING CEREMONY
Protokol Konuşmaları ve Davetli Konuşmacılar | Protocol and Keynote Speeches

SALON | HALL OTURUM BAŞKANI | SESSION CHAIRMAN ORHAN ÖCALGIRAY KONFERANS SALONU | ORHAN ÖCALGIRAY CONFERENCE HALL
Prof. Dr. Ayşe BEDELOĞLU

| | | |
|---------------|---------------------------------------------------------------------------------------|------------------------------------------------------------------------------------------------|
| 10:00 – 10:08 | Prof. Dr. Ali DEMİR, Chairman of ULPAS | Opening Speech |
| 10:08 – 10:14 | Prof. Dr. Nevin Çiğdem GÜRSOY, Dean of İTÜ Faculty of Textile Technologies and Design | Welcoming Speech |
| 10:14 – 10:20 | Prof. Dr. Hasan MANDAL, Istanbul Technical University Rector | Welcoming Speech |
| 10:20 – 10:30 | Prof. Dr. Naci ÇAĞLAR, Bursa Technical University Rector | Welcoming Speech |
| 10:30 – 10:40 | Prof. Dr. İslam SHYHA | General Vision Talk: How I See ULPAS So Far and in the Future |
| 10:40 – 11:20 | KEYNOTE SPEECH: Prof. Dr. Alexander SEIFALIAN | Graphene and Butterfly-Inspired Fibre: A Revolution in Medical Devices and Textiles Industrial |
| 11:20 – 12:00 | KEYNOTE SPEECH: Prof. Dr. Nazmul KARIM | New material-based smart wearable electronic textiles |
| 12:00 – 12:40 | KEYNOTE SPEECH: Prof. Dr. Ahmad Mukifza HARUN | Effect of modified hydrothermal nanotitanium on the viability of Streptococcus Pneumoniae |

12:40 – 14:00

ÖĞLE ARASI & POSTER ZİYARETLERİ | LUNCH BREAK & POSTER SESSION

14:00 – 16:00

PARALEL OTURUMLAR 1 & 2 | PARALLEL SESSIONS 1 & 2

| | OTURUM 1 SESSION 1 | OTURUM 2 SESSION 2 |
|--------------------------------------------|-------------------------------------------------------------------------------------------------------------------------------------------------------------------------------------------------------------------------|-----------------------------------------------------------------------------------------------------------------------------------------------------------------------------------------------------------------------------------------------|
| SALON HALL OTURUM BAŞKANI SESSION CHAIRMAN | ORHAN ÖCALGIRAY KONFERANS SALONU ORHAN ÖCALGIRAY CONFERENCE HALL Assist. Prof. Dr. Aslı Nur POLAT | D331 NO'LU SALON ROOM D331 Assist. Prof. Dr. Ebru Yabaş |
| 14:00 – 14:30 | KEYNOTE SPEECH: The Role of Artificial Intelligence in Fiber Science, Prof. Dr. Melih GÜNAY | KEYNOTE SPEECH: Sustainability from the Perspective of Product and Process Innovation in Fiber and Yarn Spinning, Prof. Dr. Osman BABAARSLAN |
| 14:30 – 14:45 | Effect of unit cell geometry and wall thickness of auxetic structures on energy absorption capability under quasi-static compression, Ali İmran Ayten - Bekir Keskin - Ameen Tapa | Blown Üretim Teknolojisi ile Hafızalı ve İşlevsel Elastik Film Üretimi, İker Türkmen - Akif Dik |
| 14:45 – 15:00 | Superhydrophobic PVDF Nanofiber Piezoelectric Sensor Reinforced with Core-Shell ZnO@ZIF-8 Structure, Milad Atighi - Mahdi Hasanzadeh - Roohollah Bagherzadeh | Farklı modakrilik elyaf karışım oranına sahip kumaşların performans özelliklerinin incelenmesi, Gülşah Karakaya - Dilek Taprakaya Kut |
| 15:00 – 15:15 | Development of Gelatin-Chitosan Composite Nanofibers Incorporated with Corn-cob-Derived Cellulose Microcrystals, Salih Birhanu Ahmed - Beyza Soydan - Çiğdem Uçar - Emine Tekcan - Ali Toptaş - Harun Çuğ - Yasin Akgül | Spunbond dokusuz kumaş üretiminde bitim işlemi için yenilikçi bir prototip sisteminin geliştirilmesi, Gülistan Canlı - Halil İbrahim ÇELİK |
| 15:15 – 15:30 | The Effect of Ecocell™ Fiber on Some Performance Properties of Apparel Fabrics, Yasemin Dülek - İpek Yıldırım - Buğçe Sevinç - Hatice Salar - Tülin Kaya Nacarkahya - Şeyma Satıl - Cem Güneşoğlu | MicroEcocell ve Micromodal İpliklerin Karşılaştırmalı Analizi: Ring ve Vortex Eğirme Sistemlerinin İplik ve Kumaş Özelliklerine Etkisi, Şeyma SATIL - Tülin KAYA NACARKAHYA - Gonca BALCI KILIÇ - Asaf ÖZMEN - Burak AYYILDIZ - Servet ÖZTÜRK |
| 15:30 – 15:40 | An investigation study about LMF Co-PET fiber utilization on flat knitted automotive fabric structure, Osman AYDIN - Semih OYLAR - Ceyda UYANIKTIR | Fındık Kabuğu Dolgusunun EPDM Kauçuk Karışımlarının Mekanik, Kürlenme ve Fiziksel Özelliklerine Etkisi, Ayşe Çavuşoğlu - İdris Karagöz - Melih Fatih Geçgel - Filiz Memişoğlu Ölmez - Merve Oruç Karataş - Ümit Kaya |
| 15:40 – 15:50 | A STUDY ABOUT WATER REPELLENT AND SOIL RESISTANCE BEHAVIOR OF AUTOMOTIVE SEAT FABRICS, Benamir Fidanç - Selenay Elif İşler - Emir Baltacıoğlu | |
| 15:50 – 16:05 | SPONSOR SUNUMU - KİPAŞ | SPONSOR SUNUMU - R-B KARESİ |

| | | |
|--------------------------------------------------------|-----------------------------------------------------------------------------------------------------------------------------------------------------------------------------------------------------------------------------------------------------|--------------------------------------------------------------------------------------------------------------------------------------------------------------------------------------------------------------------------------|
| 16:00 – 16:30 | ÇAY-KAHVE MOLASI, POSTER ZİYARETLERİ TEA-COFFEE BREAK, POSTER SESSION | |
| 16:30 – 18:45 | PARALEL OTURUMLAR 3 & 4 PARALLEL SESSIONS 3 & 4 | |
| | OTURUM 3 SESSION 3 | OTURUM 4 SESSION 4 |
| SALON HALL OTURUM BAŞKANI SESSION CHAIRMAN | ORHAN ÖCALGİRAY KONFERANS SALONU ORHAN ÖCALGIRAY CONFERENCE HALL Prof. Dr. Aylin Toprakçı | D331 NO'LU SALON ROOM D331 Prof. Dr. Emel Onder Karaoglu |
| 16:30 – 17:00 | KEYNOTE SPEECH: Biomimicry in Textiles: Past, Present, and Potential, <i>Prof. Dr. Tushar Ghosh</i> | 16:30 – 17:10 KEYNOTE SPEECH: Enhancement of Textile Surfaces by Polymers: A Case Study, <i>Prof. Dr. Cem GÜNEŞOĞLU</i> |
| 17:00 – 17:15 | Optimization of nanofiber production from biodegradable PBS via electro-blowing method using Box-Behnken design, <i>Ali Toptaş</i> | 17:10 – 17:25 Effects of different processed bobbin structures on yarn and warp preparation performance in cotton spinning, <i>Gökhan Tandoğan - Kıymet Kübra Kaya Denge - Yasemin Korkmaz - Uğur Gündoğan - Sami Gizir</i> |
| 17:15 – 17:30 | Nanoclay reinforced nanofiber membranes for oilwater separation, <i>Ömer Tüylüce - Buse Girgin - Melike Deniz Bıçakcı - Züleyha Saraç - Çiğdem Taşdelen-Yücedağ</i> | 17:25 – 17:40 Effect of Surface-Active Agents on Liquid Transfer Properties of Hydroentangled Nonwoven Fabrics, <i>Ebru ÇELİK TEN - Mehmet DAŞDEMİR - Tülin KAYA NACAR KAHYA - Şeyma SATIL - Mehmet TOPALBEKİROĞLU</i> |
| 17:30 – 17:45 | Investigation of the usability of kaolin/agar biocomposite in the removal of U(VI) ions from aqueous solutions, <i>Pinar Aykin - Sabriye Yusan</i> | 17:40 – 17:55 Polymeric Superplasticizer Driven Concrete Strength Forecasting Using Ensemble Random Forests, <i>Uğur ÖZVEREN - Dicle EREN</i> |
| 17:45 – 18:00 | Production of facial sheet masks by adding green synthesized Ag nanoparticles with plant extracts and collagen to PCL composite nanofibers: Use in acne and wrinkle removal, <i>Ahmet Avcı - Cansu Güneş - Fatma Ahsen Öktemer - Edanur Korkmaz</i> | 17:55 – 18:10 Design of glitter-effect denim and non-denim surfaces with a novel coating material, <i>Gökhan GÜNEŞ - Osman BABAARSLAN</i> |
| 18:00 – 18:15 | Effects of Hemp fiber content on yarn quality for Ring and Vortex yarns, <i>Kübra Özşahin - Emel Çiçek - Hatice Kübra Kaynak</i> | 18:10 – 18:25 Amphiphilic Functional Polymers as Polypropylene Nonwoven Surface Treatment, <i>Mehmet Sinan Tübcü</i> |
| 18:15 – 18:30 | Identification of bisphenol A (BPA) sources in textile products and its contamination of wastewater, <i>Ayşe Ceren Şen - Hülya Kırık</i> | 18:25 – 18:40 Recovery of textile waste: The effect of recycled cotton fibers obtained from different fabric structures on yarn quality, <i>Kübra BAYKAN ÖZDEN - İbrahim Erkan EVRAN - Züleyha DEĞİRMENCİ</i> |
| 18:40 – 19:00 | POSTER SUNUMLARI POSTER SESSIONS | |
| 19:30 – 21:30 | GALA YEMEĞİ GALA DINNER FİLİZLER KÖFTE, ÜSKUDAR | |

10 Mayıs 2025 Cumartesi | 10th May 2025 Saturday

| | | | |
|--------------------------------------------------|--------------------------------------------------------------------------------------------------------------------------------------------------------------------------------------------------------------------------------------------------------------------------------------|-----------------------------------------------------------------------------------------------------------------------------------------------------------------------------------------------------------------------------------|--------------------------------------------------------------------------------------------------------------------------------------------------------------------------------------------------------------------------------------------------------------------|
| 08:00 – 10:00 | Sempozyum Karşılama, Kayıt & Çay/Kahve/İkramlar Symposium Welcome, Registration & Tea/Coffee/Cookies YER: İTÜ GÜMÜŞSUYU KAMPÜSÜ GİRİŞ KORİDÖRÜ SESSION PLACE: İTÜ GUMUSSUYU BUILDING ENTRANCE HALL | | |
| 10:00 – 12:00 | PARALEL OTURUMLAR 5, 6 & 7 PARALLEL SESSIONS 5, 6 & 7 | | |
| | OTURUM 5 SESSION 5 | OTURUM 6 SESSION 6 | OTURUM 7 SESSION 7 |
| SALON HALL OTURUM BAŞKANI SESSION CHAIRMAN | ORHAN ÖCALGIRAY KONFERANS SALONU ORHAN ÖCALGIRAY CONFERENCE HALL Assist. Prof. Dr. Yasin ALTIN | D331 NO'LU SALON ROOM D331 Prof. Dr. Alper Gursalsan | SÜREKLİ EĞİTİM MERKEZİ (SEM) CONTINUING EDUCATION CENTER Assist. Prof. Dr. Çiğdem Taşdelen-Yücedağ |
| 10:00 – 10:15 | INSPIRING PERSPECTIVE: Filtration: From Nature to Engineering, Assist. Prof. Dr. Mehmet Çalışır | 10:00 – 10:40 KEYNOTE SPEECH: Eco-Efficient Textile Dyeing: Leveraging Supercritical CO ₂ for Sustainable Innovation, Assoc. prof. Aminoddin HAJI | 10:00 – 10:40 KEYNOTE SPEECH: Electrospun Janus Fibrous Materials for Moisture Management Textiles, Assoc. Prof. Aijaz Ahmed Babar |
| 10:15 – 10:30 | INSPIRING PERSPECTIVE: Cell Communication in Wound Healing, Assist. Prof. Dr. Mehmet Ali Tıbban | 10:40 – 10:55 Surface Modification of Wool Fabrics with Metal-Organic Framework for Eco-Friendly Sustainable Natural Dyeing, Maryam Pishchvar - Motahareh Moradi - Aminoddin Haji - Mahdi Hasanazadeh | 10:40 – 10:55 Sound Absorption Performance of Three-dimensional Flexible Spacer Fabric Enhanced by Polyurethane Foam, Milad Atighi - Mohammad Davoudabadi Farahani - Mahdi Hasanazadeh |
| 10:30 – 10:50 | KEYNOTE SPEECH: Reinforcement of 3D Concrete Printed Buildings by Filament Yarns, Assoc. Prof. Seyedmansour Bidoki | 10:55 – 11:10 The Effect of Fiber Cross-section of Polyester Yarn on Dyeing Behavior of Microwave Assisted and Conventional Dyeing, Yosemin Dülek - İpek Yıldırım - Buğçe Sevinç - Esra Mert - Yosemin Özdemir - Cem Güneşoğlu | 10:55 – 11:10 Modified silica containing polyacrylonitrile Janus nanofiber membranes for environmental applications, Gülşah Gürbüz - Sedanur Öztürk - Melis Biliç - Yeldem Karabulut - Züleyha Saraç - Çiğdem Taşdelen-Yücedağ |
| 10:50 – 11:00 | In-Process Vertical Reinforcement of 3D Printed Concrete Structures, Seyedmansour BIDOKI - Mahsa Bidoki - Hasan Haroglu - Adil Kahwash Al-Tamimi - Ali Demir | 11:10 – 11:25 The Impact of Pigment Dyeing and Pigment Washing on the Mechanical Properties of 3D Knitted Fabrics, Arda DEVECI | 11:10 – 11:25 Effect of processing flaws on mechanical behaviour of graphene-epoxy nanocomposites, Osman Bayrak - Ayten Nur Yüksel Yılmaz - Yusuf İpek - Mertcan Işgör - Cantekin Kaykılarlı |
| 11:00 – 11:15 | Photocatalytic Activity of Ag-ZnO Structures Deposited onto Glass Fibers, Muhterem Damla YAĞMUR - Halil İbrahim AKYILDIZ | 11:25 – 11:40 Development of Air Pre-Filter Materials from Chicken Feather Fibers by Dry Laid Method, Emirhan Bay - Jan Sena Altınay - Mediha Demet Aysin - Sümeyye Üstüntağ | 11:25 – 11:40 Global and local positioning of seaweed fibers: A sustainable journey from fiber to fabric, Büşra Bozyer - Züleyha Değirmenci - Ersen Çatak |
| 11:15 – 11:30 | Fabrication of nanofibrous proton exchange membranes with significantly enhanced proton conductivity based on sulfonated polyether ether ketone/polydopamine-coated multi-walled carbon nanotubes, Zahra Esmailzadeh - Mohamad Karimi - Ahmad Mousavi Shoushtari - Mehran Javanbakht | 11:40 – 11:55 Towards Sustainable and Green Synthesis of Metal-Organic Frameworks (MOFs): A Pathway to Industrial Viability, Seif El Islam Lebouachera - Mahdi Hasanazadeh | 11:40 – 11:55 From manual methods to deep learning: evolution of image-based diameter analysis for fibers and particles, Muhammet Mahsun Çiğçi - Mehmet Durmuş Çalışır |
| 11:30 – 11:45 | LOI Prediction of Flame-Retardant Polypropylene Composites Using XGBoost, Uğur ÖZVEREN - Dicle EREN | 11:55 – 12:10 Curing Properties of Covalently Bonded Polyoxazoline-Imidazole Thermal Latent Curing Agents for One-Component Epoxy Resins, Ceren Özaltık - Asu Ece Atespare - Cume Ali Ucar - Bekir Dizman | 11:55 – 12:10 Investigation of the response of bio-organic material based biosensor to pesticide water solution at different concentrations by electrical characterization method, Burak TAŞ - Hüseyin Muzaffer ŞAGBAN - Ümit Hüseyin KAYNAR - Özge TÜZÜN ÖZMEN |

Best Papers Award of the 16th International Fiber and Polymer symposium (16th ULPAS)



CERTIFICATE Of Achievement

1

Fiber and Polymer Research Association
awards this price to

Yasin Altın

«Production and Characterization of Polyimide Nanofiber Yarns via Electrospinning»

For the best scientific study award as evaluated by Award Committee of ULPAS at the 16th International Fiber and Polymer Research Symposium held on-line and on-site on 9-10 November, 2025 with the kind hospitality of İstanbul Technical University, İstanbul Turkey.

Prof. Dr. Yusuf ULCAY

President of Fiber and Polymer Research Association

Doç. Dr. İdris KARAGÖZ

Award Committee Chair of 15th ULPAS

Prof. Dr. Ali DEMİR

Symposium Co-Chair

Prof. Dr. Levent ÖNAL

Symposium Co-Chair



CERTIFICATE Of Achievement

2

Fiber and Polymer Research Association
awards this price to

Seyedmansour Bidoki, Mahsa Bidoki, Hasan Haroglu, Adil Kahwash Al-Tamimi, Oguzhan Sahin, Ali Demir

«In-process vertical reinforcement of 3D printed concrete structures»

For the best scientific study award as evaluated by Award Committee of ULPAS at the 16th International Fiber and Polymer Research Symposium held on-line and on-site on 9-10 November, 2025 with the kind hospitality of İstanbul Technical University, İstanbul Turkey.

Prof. Dr. Yusuf ULCAY

President of Fiber and Polymer Research Association

Doç. Dr. İdris KARAGÖZ

Award Committee Chair of 15th ULPAS

Prof. Dr. Ali DEMİR

Symposium Co-Chair

Prof. Dr. Levent ÖNAL

Symposium Co-Chair



CERTIFICATE Of Achievement

3

Fiber and Polymer Research Association
awards this price to

Milad Atighi, Mahdi Hasanzade, Roohollah Bagherzadeh

«Superhydrophobic PVDF nanofiber piezoelectric sensor reinforced with core-shell ZnO@ZIF-8 structure»

For the best scientific study award as evaluated by Award Committee of ULPAS at the 16th International Fiber and Polymer Research Symposium held on-line and on-site on 9-10 November, 2025 with the kind hospitality of İstanbul Technical University, İstanbul Turkey.

Prof. Dr. Yusuf ULCAY

President of Fiber and Polymer Research Association

Doç. Dr. İdris KARAGÖZ

Award Committee Chair of 15th ULPAS

Prof. Dr. Ali DEMİR

Symposium Co-Chair

Prof. Dr. Levent ÖNAL

Symposium Co-Chair



CERTIFICATE Of Achievement

B

Fiber and Polymer Research Association
awards this price to

Maryam Kheirandish, Mohammad Reza Mohaddes Mojtahedi, Hossein Nazockdast

«Tailoring PET/PLA Film Properties Through Transesterification During Melt Processing»

For the best scientific study award as evaluated by Award Committee of ULPAS at the 16th International Fiber and Polymer Research Symposium held on-line and on-site on 9-10 November, 2025 with the kind hospitality of İstanbul Technical University, İstanbul Turkey.

Prof. Dr. Yusuf ULCAY

President of Fiber and Polymer Research Association

Doç. Dr. İdris KARAGÖZ

Award Committee Chair of 15th ULPAS

Prof. Dr. Ali DEMİR

Symposium Co-Chair

Prof. Dr. Levent ÖNAL

Symposium Co-Chair



CERTIFICATE Of Achievement



Fiber and Polymer Research Association
awards this price to

Muhammet Mahsun Çifçi, Mehmet D. Çalışır

«From manual methods to deep learning: evolution of image-based diameter analysis for fibers and particles»

For the best scientific study award as evaluated by Award Committee of ULPAS at the 16th International Fiber and Polymer Research Symposium held on-line and on-site on 9-10 November, 2025 with the kind hospitality of İstanbul Technical University, İstanbul Turkey.

Prof. Dr. Yusuf ULCAY

President of Fiber and Polymer Research Association

Doç. Dr. İdris KARAGÖZ

Award Committee Chair of 15th ULPAS

Prof. Dr. Ali DEMİR

Symposium Co-Chair

Prof. Dr. Levent ÖNAL

Symposium Co-Chair



CERTIFICATE Of Achievement



Fiber and Polymer Research Association
awards this price to

Ali Toptaş

«Optimization of nanofiber production from biodegradable PBS via electro-blowing method using Box-Behnken design»

For the best scientific study award as evaluated by Award Committee of ULPAS at the 16th International Fiber and Polymer Research Symposium held on-line and on-site on 9-10 November, 2025 with the kind hospitality of İstanbul Technical University, İstanbul Turkey.

Prof. Dr. Yusuf ULCAY

President of Fiber and Polymer Research Association

Doç. Dr. İdris KARAGÖZ

Award Committee Chair of 15th ULPAS

Prof. Dr. Ali DEMİR

Symposium Co-Chair

Prof. Dr. Levent ÖNAL

Symposium Co-Chair



CERTIFICATE Of Achievement



Fiber and Polymer Research Association
awards this price to

Gülşah Gürbüz, Sedanur Öztürk, Melis Bilgiç, Yeldem Karabulut, Züleyha Saraç, Çiğdem Taşdelen Yücedağ

«Modified silica containing polyacrylonitrile Janus nanofiber membranes for environmental applications»

For the best scientific study award as evaluated by Award Committee of ULPAS at the 16th International Fiber and Polymer Research Symposium held on-line and on-site on 9-10 November, 2025 with the kind hospitality of İstanbul Technical University, İstanbul Turkey.

Prof. Dr. Yusuf ULCAY

President of Fiber and Polymer Research Association

Doç. Dr. İdris KARAGÖZ

Award Committee Chair of 15th ULPAS

Prof. Dr. Ali DEMİR

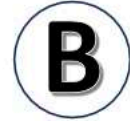
Symposium Co-Chair

Prof. Dr. Levent ÖNAL

Symposium Co-Chair



CERTIFICATE Of Achievement



Fiber and Polymer Research Association
awards this price to

Aysu Çavuşoğlu, İdris Karagöz, Melih Fatih Geçgel, Filiz Memiş Ölmez, Merve Oruç Karataş, Ümit Kaya

«Fındık Kabuğu Dolgusunun EPDM Kauçuk Karışımlarının Mekanik, Kürlenme ve Fiziksel Özelliklerine Etkisi»

For the best scientific study award as evaluated by Award Committee of ULPAS at the 16th International Fiber and Polymer Research Symposium held on-line and on-site on 9-10 November, 2025 with the kind hospitality of İstanbul Technical University, İstanbul Turkey.

Prof. Dr. Yusuf ULCAY

President of Fiber and Polymer Research Association

Doç. Dr. İdris KARAGÖZ

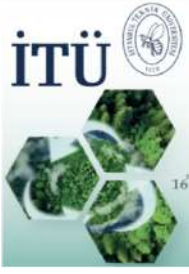
Award Committee Chair of 15th ULPAS

Prof. Dr. Ali DEMİR

Symposium Co-Chair

Prof. Dr. Levent ÖNAL

Symposium Co-Chair



16

ULUSLARARASI
LİF VE POLİMER
ARAŞTIRMALARI
SEMPOZYUMU

16th INTERNATIONAL FIBER AND POLYMER RESEARCH SYMPOSIUM

Sürdürülebilir ve İşlevsel Lif ve Polimerler
Sustainable and Functional Fibers & Polymers



BURSA
ULUDAĞ
ÜNİVERSİTESİ

9-10 Mayıs
May 2025

İstanbul Teknik Üniversitesi
Gümüşsuyu Prof. Dr. Necmettin Erbakan Yerleşkesi

Istanbul Technical University
Gumussuyu Prof. Dr. Necmettin Erbakan Campus



Best Posters Award of the 16th International Fiber and Polymer symposium (16th ULPAS)

CERTIFICATE

Of Achievement

1

This Certificate is Proudly Presented to

**Songül Özay, Ebru Erdal, Barış Batur, Gülben Akcan, Merve Bakıcı,
Hasret Tolga Şirin, Caner Bakıcı, Lokman Uzun, Murat Demirbilek**

«PBT-Based hard tissue implant»

For the best poster presentation award as evaluated by Award Committee of ULPAS at the
16th International Fiber and Polymer Research Symposium
held on-line and on-site on 9-10 November, 2025 with the kind hospitality of
İstanbul Technical University, İzmir, Turkey.

Prof. Dr. Yusuf ULCAI
President of Fiber and
Polymer Research Association



Assoc. Prof. Dr. İdris KARAGÖZ
Award Committee
Chair of 15th ULPAS



Prof. Dr. Ali DEMİR
Symposium Co-Chair



Prof. Dr. Levent ÖNAL
Symposium Co-Chair



CERTIFICATE

Of Achievement

2

This Certificate is Proudly Presented to

Sezin Demirci, Nalan Oya San Keskin

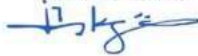
«Green synthesized selenium nanoparticles attached electrospun polycaprolactone nanofiber mats for fast photo degradation of dyes»

For the best poster presentation award as evaluated by Award Committee of ULPAS at the
16th International Fiber and Polymer Research Symposium
held on-line and on-site on 9-10 November, 2025 with the kind hospitality of
İstanbul Technical University, İzmir, Turkey.

Prof. Dr. Yusuf ULCA Y
President of Fiber and
Polymer Research Association



Assoc. Prof. Dr. İdris KARAGÖZ
Award Committee
Chair of 15th ULPAS



Prof. Dr. Ali DEMİR
Symposium Co-Chair



Prof. Dr. Levent ÖNAL
Symposium Co-Chair



CERTIFICATE

Of Achievement

B

This Certificate is Proudly Presented to

**Merve Açıksöz, Ayse Kalkanci, Ozlem Guzel Tunccan
Nalan Oya San Keskin**


**Development of high-efficiency polysulfone nanofiber filters for the removal of
Candida auris: Comparison of aligned and random morphology**

For the best poster presentation award as evaluated by Award Committee of ULPAS at the
16th International Fiber and Polymer Research Symposium
held on-line and on-site on 9-10 November, 2025 with the kind hospitality of
İstanbul Technical University, İzmir, Turkey.

Prof. Dr. Yusuf ULCAI
President of Fiber and
Polymer Research Association



Assoc. Prof. Dr. İdris KARAGÖZ
Award Committee
Chair of 15th ULPAS



Prof. Dr. Ali DEMİR
Symposium Co-Chair



Prof. Dr. Levent ÖNAL
Symposium Co-Chair



CERTIFICATE

Of Achievement

3

This Certificate is Proudly Presented to

**Aysu Çavuşoğlu, Tuana Orhun, Yasemin Balçık Tamer,
Harun Sepetçioğlu, İdris Karagöz**

**«Investigation of Mechanical Properties of Polycarbonate/ASA/Walnut
Shell Composites»**

For the best poster presentation award as evaluated by Award Committee of ULPAS at the
16th International Fiber and Polymer Research Symposium
held on-line and on-site on 9-10 November, 2025 with the kind hospitality of
İstanbul Technical University, İzmir, Turkey.

Prof. Dr. Yusuf ULCAI
President of Fiber and
Polymer Research Association



Assoc. Prof. Dr. İdris KARAGÖZ
Award Committee
Chair of 15th ULPAS



Prof. Dr. Ali DEMİR
Symposium Co-Chair



Prof. Dr. Levent ÖNAL
Symposium Co-Chair



CERTIFICATE

Of Achievement

B

This Certificate is Proudly Presented to

**Merve Açıksöz, Ayse Kalkanci, Ozlem Guzel Tunccan
Nalan Oya San Keskin**

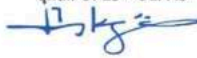
**Development of high-efficiency polysulfone nanofiber filters for the removal of
Candida auris: Comparison of aligned and random morphology**

For the best poster presentation award as evaluated by Award Committee of ULPAS at the
16th International Fiber and Polymer Research Symposium
held on-line and on-site on 9-10 November, 2025 with the kind hospitality of
İstanbul Technical University, İzmir, Turkey.

Prof. Dr. Yusuf ULCAI
President of Fiber and
Polymer Research Association



Assoc. Prof. Dr. İdris KARAGÖZ
Award Committee
Chair of 15th ULPAS



Prof. Dr. Ali DEMİR
Symposium Co-Chair



Prof. Dr. Levent ÖNAL
Symposium Co-Chair



CERTIFICATE

Of Achievement

B

This Certificate is Proudly Presented to

Sena Kardelen Dinc, Oznur Akbal Vural, Nalan Oya San Keskin

«From hydrophobic nanofibers to antimicrobial slippery liquid infused surfaces: A two-step surface strategy»

For the best poster presentation award as evaluated by Award Committee of ULPAS at the
16th International Fiber and Polymer Research Symposium
held on-line and on-site on 9-10 November, 2025 with the kind hospitality of
İstanbul Technical University, İzmir, Turkey.

Prof. Dr. Yusuf ULCAI
President of Fiber and
Polymer Research Association



Assoc. Prof. Dr. İdris KARAGÖZ
Award Committee
Chair of 15th ULPAS



Prof. Dr. Ali DEMİR
Symposium Co-Chair



Prof. Dr. Levent ÖNAL
Symposium Co-Chair



CERTIFICATE

Of Achievement

B

This Certificate is Proudly Presented to

Ayça Gül Özdağ, Nalan Oya San Keskin

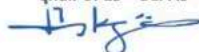
**«Evaluation of the microbial corrosion protection performance of
essential oilloaded nanofiber coatings on stainless steel»**

For the best poster presentation award as evaluated by Award Committee of ULPAS at the
16th International Fiber and Polymer Research Symposium
held on-line and on-site on 9-10 November, 2025 with the kind hospitality of
İstanbul Technical University, İzmir, Turkey.

Prof. Dr. Yusuf ULCAI
President of Fiber and
Polymer Research Association



Assoc. Prof. Dr. İdris KARAGÖZ
Award Committee
Chair of 15th ULPAS



Prof. Dr. Ali DEMİR
Symposium Co-Chair



Prof. Dr. Levent ÖNAL
Symposium Co-Chair



CERTIFICATE

Of Achievement

B

This Certificate is Proudly Presented to

Filiz Emiroğlu, Ayşe Çelik Bedeloğlu

«Investigation of the effect of bio-based finishing chemical on knitted fabric»

For the best poster presentation award as evaluated by Award Committee of ULPAS at the
16th International Fiber and Polymer Research Symposium
held on-line and on-site on 9-10 November, 2025 with the kind hospitality of
İstanbul Technical University, İzmir, Turkey.

Prof. Dr. Yusuf ULÇAY
President of Fiber and
Polymer Research Association



Assoc. Prof. Dr. İdris KARAGÖZ
Award Committee
Chair of 15th ULPAS



Prof. Dr. Ali DEMİR
Symposium Co-Chair



Prof. Dr. Levent ÖNAL
Symposium Co-Chair





16

16th INTERNATIONAL FIBER AND POLYMER RESEARCH SYMPOSIUM

ULUSLARARASI LİF VE POLİMER ARAŞTIRMALARI SEMPOZYUMU

Sürdürülebilir ve İşlevsel Lif ve Polimerler
Sustainable and Functional Fibers & Polymers



BURSA ULUDAĞ ÜNİVERSİTESİ

9-10 May 2025

İstanbul Teknik Üniversitesi
Gümüşsuyu Prof. Dr. Necmettin Erbakan Yerleşkesi

Istanbul Technical University
Gumussuyu Prof. Dr. Necmettin Erbakan Campus



BURSA TEKNİK ÜNİVERSİTESİ

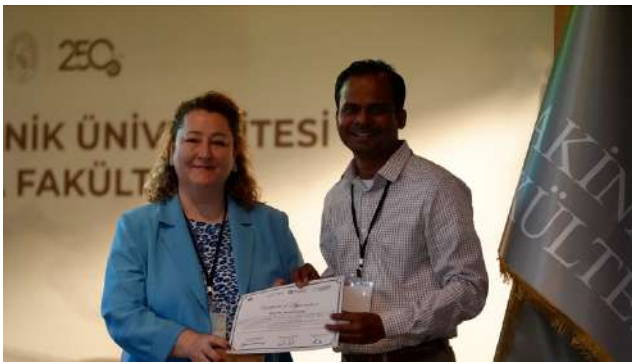
Photo Gallery of the 16th ULPAS





































After the 16th ULPAS

Dear Professors,
Dear Friends,

After months of preparation and intense work in the final weeks, we successfully and smoothly completed the 16th ULPAS on Friday and Saturday, May 9–10, 2025. Alhamdulillah.

We—the “ULPAS Organizing Committee”—accomplished this together. The group consists of 25 members. Except for 3, everyone worked diligently every week and with even greater enthusiasm and dedication during the symposium. I thank each and every one of my friends in this group again and again. I’m so glad you were with us, and I’m so glad you were part of this.

The excitement began on Monday, May 4, when we hung the large banner outside the building. On Thursday afternoon, May 8, we completed all preparations inside the building (posting banners, setting up roll-ups, pennants, poster stands, and tables).

On Friday morning, May 9, the registration desk was set up. Posters began to be mounted. Participants started arriving. With the arrival of Rector Prof. Dr. Hasan Mandal, things became very serious. Shortly after, BTU Rector Prof. Dr. Naci Çağlar arrived, and it was time for the symposium to begin. The goal was to start at 10:00. Thanks to Prof. Dr. Ayşe Bedeloğlu’s seriousness and efforts, the opening session started right on time.

Everything went smoothly. Following my opening speech, Dean Prof. Dr. Nevin Çiğdem Gürsoy, Rector Prof. Dr. Hasan Mandal, and BTU Rector Prof. Dr. Naci Çağlar gave their welcome remarks. With the visionary and vibrant talk by Prof. Dr. Islam Shyha, the message that “ULPAS should now take a flight” was clearly conveyed to the participants.

The hall was quite full—probably a 300-seat venue, and around 250 attendees were present. The three technical keynote speeches that followed were all rich in content and well-received.

After the first session, attendees were directed to the staff cafeteria for Friday lunch. As they walked past the posters to the cafeteria, they were immersed in a scientific symposium atmosphere while having lunch.

At 14:00 on Friday afternoon, parallel sessions began with great seriousness. Though the presentations inevitably went over their planned times, there were hardly any complaints. However, the most significant issue of the symposium may have been the inability to stick to scheduled presentation times. Still, there were no major delays overall. Perhaps large, visible clocks in each session room could help speakers and the audience manage time better. Other suggestions are welcome as well.

When the sessions in the conference hall and Room D331 ended at 18:30, the scientific satisfaction was visibly reflected in the participants’ eyes. It was time to take a joyful evening walk to Kabataş. The group gathered at the building entrance, and a group photo captured their

happiness and satisfaction. As we walked downhill, the beautiful Bosphorus view demanded another photo—this one turned out to be the best group shot of the event.

With great effort, Prof. Dr. Islam Shyha gathered the group, brought smiles, and helped take a memorable group photo. After a short ferry ride across the Bosphorus, we walked together along the Üsküdar coast, enjoying views of the Maiden's Tower and Topkapı Palace, and headed to Filizler Köftecisi.

Before entering the restaurant, another group photo was taken with the stunning Bosphorus view, once again turning the moment into a lasting memory.

The Gala Dinner was enjoyed in an atmosphere of both flavor and friendship. Everyone was extremely happy. Although not everyone may have heard the thank-you speeches after the meal, they certainly strengthened our bonds. Aside from Prof. Dr. Cem Gök twisting his ankle, all participants left satisfied. We wish Prof. Cem Gök a swift recovery.

On Saturday morning, May 10, at 10:00, sessions began on time in three rooms. The INSPIRING PERSPECTIVES talks, held for the first time at this symposium, offered deeply reflective insights. We extend our gratitude and appreciation to the young academics (Dr. Mehmet Çalışır and Dr. Mehmet Ali Tibatan) for their presentations.

The only online participation at the 16th ULPAS came from Prof. Dr. Amit Rawal. The session in Room D331, chaired by Prof. Dr. Levent Önal, went very smoothly. Prof. Rawal answered participants' questions from Sweden.

We completed the scientific sessions on Saturday with three parallel sessions, a coffee break, and two more parallel sessions.

The peak of the 16th ULPAS was the ÇİĞ KÖFTE Party that began at 14:30 on Saturday. Prepared with joy and care by Assoc. Prof. Dr. Ali Kılıç and Dr. Ali Toptaş, the çiğ köfte delighted all our guests.

During this event, the 16th ULPAS Science Awards were presented. Best Paper Awards, Best Poster Awards, and for the first time in this symposium:

- Honor Award – Lifetime Achievement: Prof. Dr. Hasabo Abdelbagi Mohamed
- Rising Scientist Award – Young Researcher: Dr. Ali Toptaş
- Loyalty and Contribution Award: Assoc. Prof. Dr. Ali Kılıç, Aysu Çavuşoğlu

With hopes, requests, and excitement to reunite at the 17th ULPAS, the symposium etched beautiful memories in our minds.

Prof. Dr. Ali Demir
May 12, 2025

16.ULPAS'ın Ardından

Değerli Hocalarım,

Değerli Arkadaşlarım,

Aylar süren hazırlık, son haftalardaki yoğun çalışmalar sonunda 9-10 Mayıs 2025 Cuma ve Cumartesi günleri 16. ULPAS'ı başarılı ve sorunsuz olarak tamamladık. Elhamdülillah.

Bunu bizler, bu "Ulpas Organizasyon Komitesi" grubu, başardı. Grupta 25 isim var. 3 isim dışında her hafta fiilen ve sempozyumda daha büyük heyecan ve özveri ile çalıştık ve başardık. Bu gruptaki her bir arkadaşımıza tekrar tekrar teşekkür ediyorum. İyi ki varsınız, iyi ki vardınız.

4 Mayıs Pazartesi büyük afiş kapının dışına asarak heyecanı başlattık.

8 Mayıs Perşembe öğleden sonra binadaki tüm hazırlıkları (afişlerin asılması, roll-upların, kırlangıçların, poster standlarının ve masaların yerleştirilmesi) yaptık.

9 Mayıs Cuma sabahı Kayıt masası kuruldu. Posterler asılmaya başladı. Katılımcılar gelmeye başladı. Rektör Prof. Dr. Hasan Mandal'ın binaya gelmesi ile iş çok ciddileşti. Hemen ardından da BTÜ Rektörü Prof. Dr. Naci Çağlar geldiğinde artık sempozyum başlayabilirdi. Hedef Saat 10.00'da sempozyumu başlatmak idi. Prof. Dr. Ayşe Bedeloğlu hocamın ciddiyeti ve gayreti ile açılış oturumu 10.00'da başladı. Her şey yolunda. Benim açılış konuşmam, Dekanımız Prof. Dr. Nevin Çiğden Gürsoy, Rektör Prof. Dr. Hasan Mandal ve BTÜ Rektörü Prof. Dr. Naci Çağlar'ın hoşgeldiniz konuşmaları ile sempozyum başladı. Prof. Dr. İslam Shyha'nın vizyoner, renkli konuşması ile artık Ulpas'ın uçuşması gerektiği mesajı katılımcılara verildi. Salon gayet dolu idi, Bu salon 300 kişilik sanırım. 250 kişi salonda vardı. Art arda gelen 3 teknik davetli konuşmaların hepsi de dolu doluydu ve katılanları memnun etti. İlk oturumun ardından, Cuma öğle yemeği için Personel Yemekhanesine yönlendirildi. Posterleri izleyerek yemekhaneye giden katılımcılar bir bilimsel sempozyum atmosferi ile öğle yemeklerini aldılar.

Cuma öğleden sonra Saat 14.00'de paralel oturumlar büyük bir ciddiyetle başladı. Kaçınılmaz olarak sunumlar planlanandan uzun sürmesine rağmen çok büyük bir şikayet olmadı. Ama bu sempozyumdaki en büyük sorun belki de sunumların planlandığı süre içinde bitirilememesiydi. Ancak toplamda çok büyük sarkmalar olmadı. Belki de her oturuma büyük, görünür bir saat yerleştirilerek konuşmacıları ve dinleyenlerin zamanın takip etmesi ve zamana uyması sağlanabilir. Başka öneriler de değerlendirmeye açıktır.

Konferans salonu ve D331'deki oturumlar 18.30'da bittiğinde katılımcıların gözlerinde bilimsel mutluluk görünür hale gelmişti. Artık güzel Mayıs akşamında büyük bir mutlulukla Kabataş'a yürüme vakti gelmişti. Bina girişinde toplanana grup, burada çekilen grup fotoğrafı ile mutluluğunu ve memnuniyetini kalıcı yaptı. Yokuş aşağı yürürken karşılaşılan güzel boğaz manzarasında fotoğraf çekmeden olmazdı ve en güzel grup fotoğrafı burada çekildi. Prof. Dr. İslam Shyha'nın büyük özverisi grubu topladı, gülümsetti ve güzel bir hatıra olacak toplu fotoğraf çekildi. Ve motorla kısa boğaz geçişinden sonra taklı bir meltem esintisi eşliğinde hep birlikte Üsküdar sahilinde Kız Kulesi, Topkapı Sarayı manzarası eşliğinde Filizler Köftecisi'ne yüründü. Köfteciye girmeden evvel yine güzel boğaz manzarasıyla çekilen toplu fotoğraflar bu günü bir kez daha kalıcı yaptı. Gala Yemeği, hem lezzet hem de dostluk atmosferi içinde yendi. Katılanların tamamı çok mutlu oldu. Yemek sonrası yapılan teşekkür konuşmaları belki tüm katılımcılar tarafından duyulmadı ama dostluğu pekiştirdi. Prof. Dr. Cem Gök hocamızın ayağının burkulmasından gayri tüm katılımcıların memnuniyeti ile gün tamamlandı. Cem Gök hocamıza şifalar diliyoruz.

10 Mayıs Cumartesi sabah 10.00'da oturumlar yine tam zamanında 3 salonda başladı. Bu sempozyum ilke kez yapılan INSPIRING PERSPECTIVE / İLHAM VEREN BAKIŞLAR konuşmaları derin düşündüren bakışlar oldu. Genç akademisyenlere (Dr. Mehmet Çalışır ve Dr. Mehmet Ali Tıbatan) bu sunumlarından dolayı teşekkür ve takdirlerimizi sunuyoruz. 16.ULPAS'daki tek on-line katılım Prof. Dr. Amit Rawal idi. Prof. Dr. Levent Önal hocamın oturum başkanlığı yaptığı D331 nolu salonaki on-line oturum da bir hayli sorunsuz ve başarılı gerçekleşti. Katılımcıların sorularına Amit Hoca İsveç'den cevap verdi. 3 paralel oturum, kahve arası ve iki paralel oturum ile Cumartesi günü bilimsel oturumları tamamladık.

16.ULPAS'ın zirvesi Cumartesi 14.30'da başlayan ÇİĞ KÖFTE Partisi oldu. Doç. Dr. Ali Kılıç ve Dr. Öğretim Üyesi Ali Toptaşı'nın mutluluk ve memnuniyetle yağurdıkları çiğ köfte tüm misafirleri mutlu etti. Bu esnada da 16.ULPAS Bilim Ödülleri takdim edildi. **En İyi Bildiri Ödülleri, En İyi Poster Ödülleri** ve bu sempozyum il kez verilen

- **Onur Ödülü – Yaşam Boyu Başarı:** Prof. Dr. Hasabo Abdelbagi Mohamed

- **Yükselen Bilim İnsanı Ödülü – Genç Araştırmacı:** Dr. Öğretim Üyesi Ali Toptaş

- **Vefa ve Katkı Ödülü:** Doç. Dr. Ali Kılıç, Aysu Çavuşoğlu

olarak sahiplerini buldu.

17.ULPAS'da yeniden buluşmak dilek, istek ve heyecanı ile sempozyum hafızalara güzel anılar nakşetti.

Prof. Dr. Ali Demir

12 Mayıs 2025



16th International Fiber and Polymer Research Symposium
9-10 May, 2025, Istanbul Technical University – Istanbul – Türkiye

16. Uluslararası Lif ve Polimer Araştırmaları Sempozyumu
9-10 Mayıs, 2025, İstanbul Teknik Üniversitesi, İstanbul,,Türkiye

Book of Proceedings

Editors/ Editörler

Prof. Dr. Yusuf Ulcay

Prof. Dr. Ali Demir

Assist. Prof. Ali Toptaş

Assoc. Prof. Dr. Seyedmansour Bidoki

Aysu Çavuşoğlu

ISBN: 978-975-561-665-0

16th International Fiber and Polymer Research Symposium (on-site)

16. Uluslararası Lif ve Polimer Araştırmaları Sempozyumu (on-site)

9-10 May, 2025 / 9-10 Mayıs, 2025

İTÜ



BURSA
ULUDAĞ
ÜNİVERSİTESİ



BURSA TEKNİK
ÜNİVERSİTESİ



16 ULUSLARARASI LİF VE POLİMER ARAŞTIRMALARI SEMPOZYUMU

16th INTERNATIONAL FIBER AND POLYMER RESEARCH SYMPOSIUM

Sürdürülebilir ve İşlevsel Lif ve Polimerler
Sustainable and Functional Fibers & Polymers

9-10 Mayıs 2025
May

İstanbul Teknik Üniversitesi
Gümüşsuyu Prof. Dr. Necmettin Erbakan Yerleşkesi
Istanbul Technical University
Gumussuyu Prof. Dr. Necmettin Erbakan Campus



Book of Proceedings

www.ulpas.org



ISBN: 978-975-561-665-0